OBJAVLJENI NAUČNI RADOVI

Dr Milana Dimitrijevića
(drugi deo)

Priredili: Dr Milan Dimitrijević
Dr Slaviša Milisavljević

Beograd, 2013

Teaching and Communicating Astronomy – JENAM'04
A. Ortiz-Gil and V. Martínez (eds)
EAS Publications Series, **16** *(2005) 35–43*

70 YEARS OF ASTRONOMICAL SOCIETY "RUDJER BOŠKOVIĆ" – AN INTERESTING EXPERIENCE IN ASTRONOMICAL EDUCATION, POPULARIZATION AND ORGANIZATION OF ASTRONOMER AMATEURS

M.S. Dimitrijević[1]

Abstract. The oldest organization of astronomers amateurs in Serbia is the Astronomical society "Rudjer Bošković" which in 2004. celebrates the 70th aniversary. The Society has People's observatory which in 2004 celebrates 40th jubilly, planetarium and publish the journal for astronomy "Vasiona" (Universe), which 50th aniversary has been celebrated in 2003. Here is given a review of the history and development of Society and an overview of its activities.

1 Foundation and First Years

The largest and the oldest organization of amateur-astronomers in Serbia is the Astronomical Society "Rudjer Bošković" in Belgrade (Kalemegdan, Gornji Grad 16, 11 000 Belgrade), which in the course of 70 years of its existence was spreading astronomical knowledge in our country. The founding meeting was held on 22 April 1934. The first Society's President was Djordje Nikolić (1934–1936) and the second Vojin Djuričić (1936–1941), the governer of the State Mortgage Bank.

In 1935 Society started publishing the first periodical for the popularization of science in Serbia "Saturn", "the periodical for astronomy, meteorology, geophysics and geodesy which purpose is to be useful to national culture", published in 12 issues per year up to the end of 1940. Editors in chief were Djordje Nikolić (1935), Vojislav Grujić (1936–1939) and Nenad Janković (1940).

Activity of the Society during this period was the organizing of a large number of popular lectures, with the aim to contribute to education and cultural life in our midst. Also Society organized occasional observational expeditions and observations for citizens.

[1] Astronomical Observatory, Volgina 7, 11160 Belgrade, Serbia and Montenegro

DOI: 10.1051/eas:2005060

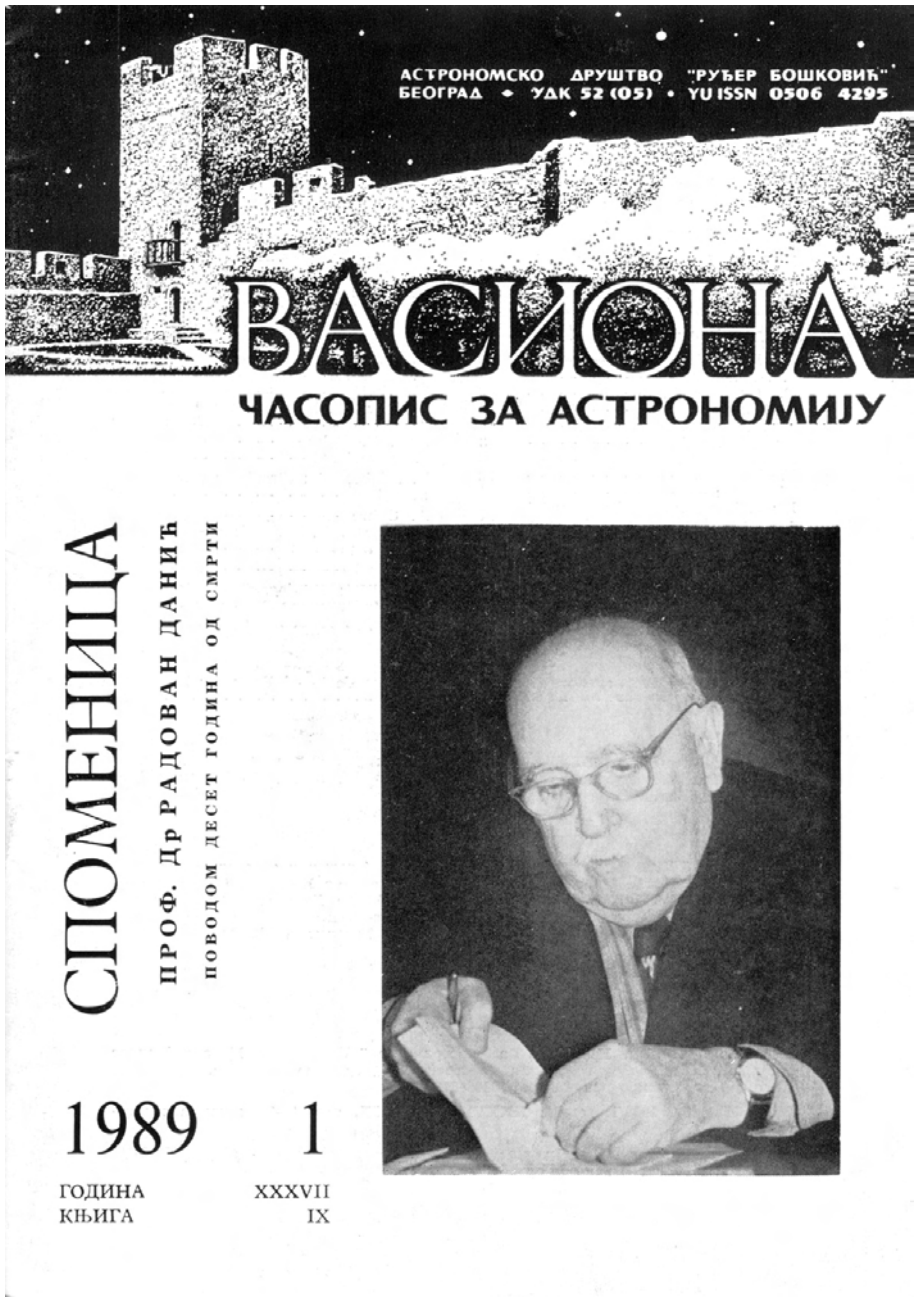

Fig. 1. Special issue of the astronomical journal "Vasiona" (Universe,) dedicated to Radovan Danić, president of Astronomical society "Rudjer Bošković (1952–1966), published to mark 10 years since he passed away.

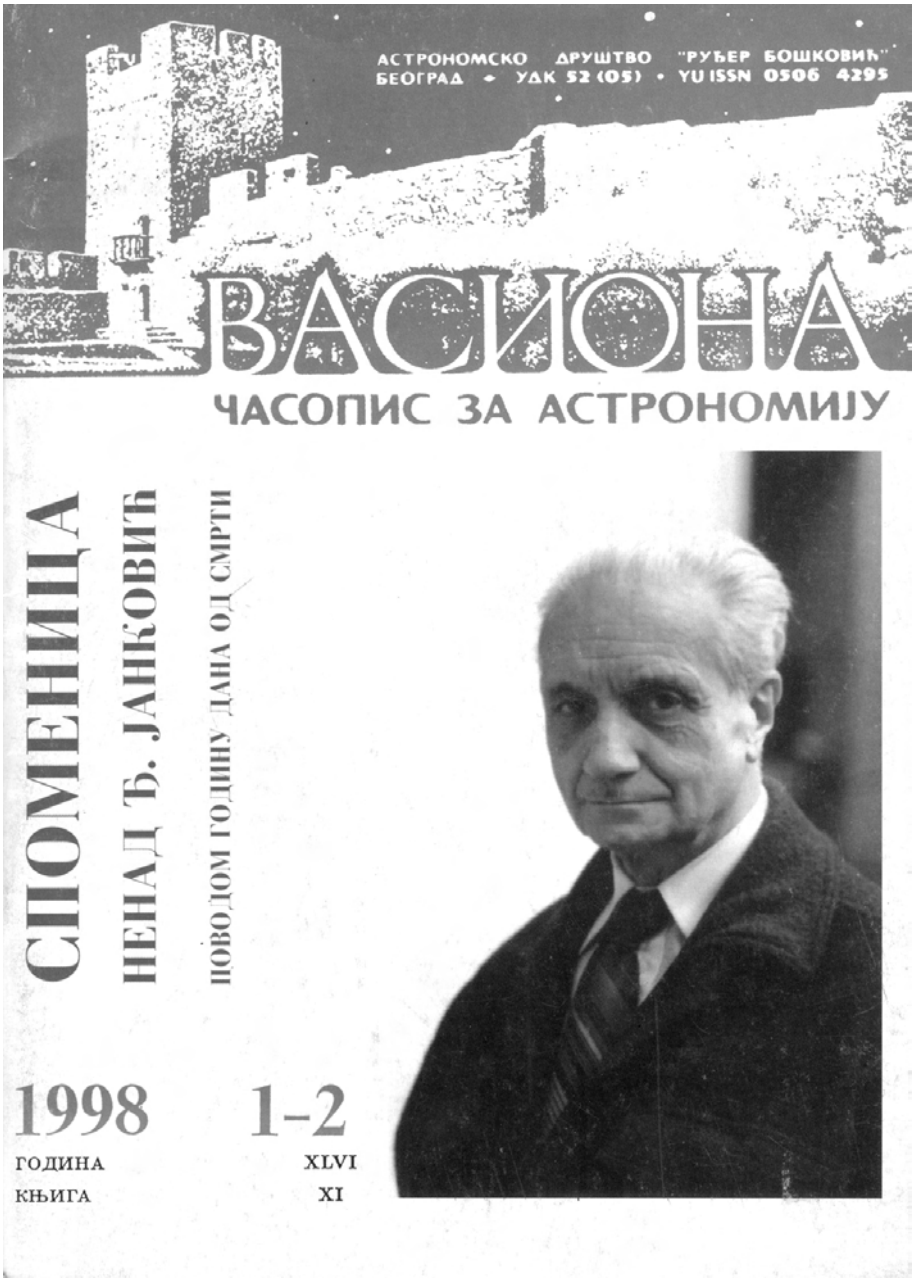

Fig. 2. Special issue of the astronomical journal "Vasiona" (Universe,) dedicated to Nenad Janković, its first Editor in chief (1953–1972), published to mark one years since he passed away.

Fig. 3. People's Observatory of the Astronomical Society "Rudjer Bošković, in Belgrade fortress on Kalemegdan, in the tower build by despot Stefan Lazarević in XV century.

2 The New Beginning after the World War II

After the War, on 9th December 1951 was held the founding meeting of the Belgrade Astronomical Club "Rudjer Bošković", re-registered next year into Astronomical Society "Rudjer Bošković". The founding meeting of the Society was held on 18 May 1952, Radovan Danić having been elected its President (1952–1966). Following him the Society' Presidents have been: Branislav Ševarlić (1966–1970), Pero Djurković (1970–1972), Nenad Janković (1972–1974), Božidar Popović (1974–1979), Zoran Knežević (1979–1982) Milan S. Dimitrijević (1982–2004) and from the 25th April 2004, Jelena Milogradov-Turin (Dimitrijević 2004a).

3 The Journal for Astronomy "Vasiona" (Universe)

In 1953 the Society, jointly with the Aeronautical Association of Yugoslavia, started publishing the periodical for astronomy and aeronautics (currently for astronomy) "Vasiona" (Universe). The first editor in chief of "Vasiona", was Nenad Dj. Janković (1953–1972). After him, the periodical's editors in chief were: Nenad Dj. Janković (1953–1972), Pero Djurković (1973–1974), Jelena Milogradov-Turin (1975–1982), Branislav Ševarlić (1983–1984) and Milan S. Dimitrijević (1985–2004), while Aleksandar Tomić is elected to be Editor in chief from the No. 1 for 2005. An analysis of the volumes issued during 50 years until the end of 2002 (Dimitrijević 2003) showed that within this period 5558 pages were published.

Fig. 4. After the session of the Editorial board of the "Vasiona" (Universe) journal, on 12th February 1992. *From the left*: Milan Vuletić, Milan Jeličić, Milan S. Dimitrijević, Jelena Milogradov-Turin, Luka Č. Popović, Aleksandar Tomić, Božidar Popović and Nenad Janković. Photo: Ljubiša Jovanović.

Impressive is also the number of 382 authors which published articles and larger contributions. If we add as well authors of smaller contributions, the total number of authors is 571. The complete of this journal represent a treasury, enabling the investigation of the history of astronomy in the past period, and particularly the study of the history and development of the Astronomical Society "Rudjer Bošković", as well as a very useful astronomical "library" and a real encyclopedia of the science approaching us to the stars.

4 People's Observatory and Planetarium

Thanks to the exertion of Pero Djurković, Radovan Danić and Nenad Janković with the authorities concerned, the Society obtained for itself the Despot Tower at Kalemegdan where, on 20 December 1964 was solemny opened the People's Observatory, whose regular activity started in June 1965. At the head of People's Observatory were Pero Djurković (1. VI 1965 – 1. XII 1965), Radovan Danić (1. XII 1965 – 6. X 1977), Aleksandar Tomić (6. X 1977 – 31. I 1991), Luka Č. Popović (1. IV 1991 – 31. V 1995), Jelena Milogradov - Turin (1. VI 1995 – 1. VI 1999) and again Luka Č. Popović (1. VI 1999 – 2004).

With the foundation of People's Observatory, Society obtained permanent offices and an observational post and also permanently employed staff, which largely

Fig. 5. Two telescopes on the terrace of People's Observatory. In the front is the older one refractor Zeiss (110/2040) and behind the newer one, the reflector TAL-200 K (200/2000). Photo by Vladimir Nenezić.

Fig. 6. Terrace of People's Observatory with four panoramic telescopes. Photo by Vladimir Nenezić.

Fig. 7. Projection of starry sky in the Planetarium of Astronomical Society "Rudjer Bošković" in Belgrade. Photo by Vladimir Nenezić.

improved conditions for its activities. Permanent offices enabled to start a regular astronomical seminar for the beginners and to organize a library.

For example LXXII spring seminar started on 7th March and terminated on 7th June 2003, and the LXXIII autumn seminar started on 26th September and

terminated on 13th December 003. On lectures were 79 attendants in average (Dimitrijević 2004b).

The Society managed also to procure a Zeiss planetarium, which was installed in an old spacious steam bath-house – Turkish Hamam – in the Kalemegdan Donji Grad. The Planetarium started operating in 1969, being formally opened on 27 February 1970. It is included in the educational system and around 15 000 pupils, students and other visitors per year, attend lectures and projections in it. The highest number of visitors was in 1982 – 18 297. May 2002 with 2046 visitors is also a record and the lecture with largest number of attendants is the lecture *Constelations* by Dragana Okolić, held on 15th March 1997 with 280 attendants (Stanić 2005).

5 Other Activities and Conclusion

The Society organized also VII National Conference of Yugoslav Astronomers on the occasion of its 50 years aniversary 1984, dedicated to the history of astronomy and astronomy in culture, the conference "Astronomy at Serbs" III 2004, and was the co-organizer of the IV Serbian-Bulgarian astronomical conference 2004.

It is worth to note the organization of the astronomical-astronautical exhibition in 1954, which after Belgrade was also in other cities and for example in Sombor was visited by around 7000 persons. This exhibition initiated the foundation of branches of the Society in other towns, and the most successful became in 1974 the Astronomical Society "Novi Sad", ADNOS.

In order to contribute to the education and to popularization of astronomy the Society organizes every year manifestations "The Belgrade astronomical weekend" in June and "The summer astronomical meetings" in August-September, occasional lectures on astronomy, observations of celestial objects and events, and special observational excursions out of Belgrade. Also People's Observatory is open for citizens on working days from 9 to 19 h, and during the weekend 12–22:30 h. For example in 2003, 29 010 visitors took a ticket. Stuff provides informations to media and citizens on astronomical events. For the journal "Politika", our Society daily provides data on the raise up and raise down of the Sun and Moon.

Enthusiasm always was the moving force of our astronomical society, unique from many aspects. All successes Society achieves by voluntary work of his members. Djordje Nikolić, Radovan Danić, Nenad Janković, Pero Djurković, Jelena Milogradov-Turin, Aleksandar Kubičela, Djordje Teleki, Aleksandar Tomić, Milan Jeličić, Milan Vuletić, Ninoslav Čabrić, Dušan Slavić, Ljubiša Jovanović, Sofija Sadžakov, Zoran Ivanović, Jovan Grujić and many others make a chain of enthusiasts without end, renewing permanently enabling to Society to be more than 70 years a source of knowledges on Universe, being for many young men the first step to the highest scientific achievements.

References

Dimitrijević, M.S., 2004a, Vasiona, 52(1), 1
Dimitrijević, M.S., 2004b, Vasiona, 52(1), 23
Dimitrijević, M.S., 2003, Vasiona, 51(4), 89
Stanić, N., 2005, Publ. Astron. Soc. "Rudjer Bošković" 6, in press

Question by Magda Stavinschi (Bucharest):
As I know, you are not amateur astronomer, you was even director of the Belgrade Observatory. Which is the official link between professional and amateur astronomy in your country?

The answer: as in other countries, in Serbia besides professional astronomers there is a much larger number of astronomers amateurs, which can help very much to professionals not only in work but also to spread astronomical knowledge in our midst and contribute that the public opinion is favorable for astronomical science. Amateurs are in Serbia organized in several societies. Besides two mentioned here in Belgrade and Novi Sad, such societies exist in Niš, Kragujevac, Valjevo, Zrenjanin, Prokuplje, Knjaževac, Novi Pazar and Leskovac. There are no official legal links with professionals, but in Belgrade practically all professional astronomers are also members of the Astronomical Society "Rudjer Bošković" and they dominate in all governing bodies, trying to organize the education of amateurs and direct their work to be useful for astronomy, education and cultural life in our country.

European Conference on Laboratory Astrophysics - ECLA
C. Stehlé, C. Joblin and L. d'Hendecourt (eds)
EAS Publications Series, **58** *(2012) 79–82*
www.eas.org

VIRTUAL LABORATORY ASTROPHYSICS: THE STARK-B DATABASE

S. Sahal-Bréchot[1], M.S. Dimitrijević[2,1] and N. Moreau[1]

Abstract. Stark broadening theories and calculations have been extensively developed for about 50 years. The theory can now be considered as mature for many applications, especially for accurate spectroscopic diagnostics and modelling. This requires the knowledge of numerous collisional line profiles, especially for very low abundant atoms and ions which are used as probes for modern spectroscopic diagnostics in astrophysics. Nowadays, the access to such data via an on line database becomes essential. STARK-B (http://stark-b.obspm.fr) is a collaborative project between the Astronomical Observatory of Belgrade and the Laboratoire d'Étude du Rayonnement et de la matière en Astrophysique (LERMA). It is a database of calculated widths and shifts of isolated lines of atoms and ions due to electron and ion collisions (impacts). It is devoted to modelling and spectroscopic diagnostics of stellar atmospheres and envelopes, laboratory plasmas, laser equipments and technological plasmas. Hence, the domain of temperatures and densities covered by the tables is wide and depends on the ionization degree of the considered ion. The STARK-B database is a part of VAMDC (Virtual Atomic and Molecular Data Centre, http://www.vamdc.eu), which is an European Union funded collaboration between groups involved in the generation and use of atomic and molecular data. VAMDC aims to build a secure, documented, flexible and interoperable e-science environment-based interface to existing atomic and molecular data.

1 Introduction

Pressure broadening of spectral lines arises when an atom or molecule which emits or absorbs light in a gas or a plasma, is perturbed by its interactions with the other particles of the medium. An atom or molecule may be neutral as well as charged.

[1] Observatory of Paris, LERMA, CNRS and University P. et M. Curie, LERMA, 5 place Jules Janssen, 92190 Meudon, France

[2] Astronomical Observatory, Volgina 7, 11060 Belgrade, Serbia

DOI: 10.1051/eas/1258012

Article published by EDP Sciences

The so-called Stark broadening is due to electron and ion colliders. It has been extensively developed for about 50 years and is currently used for spectroscopic diagnostics and modelling.

In fact, thanks to the considerable developments of the spectral resolution, of the sensitivity (high S/N) of the recent past years, and to large ground-based telescopes and space-born missions allow to observe in all ranges of wavelengths (from XUV to radio). For interpreting the spectra, the lines must be identified, and the atomic parameters responsible for their intensities and their profiles must be known. The development of realistic models of interiors and atmospheres of stars and the interpretation of their evolution and the creation of elements through nuclear reactions, requires the knowledge of numerous profiles, especially for trace elements. Chemical abundances are crucial parameters to be determined. This needs an accurate interpretation of the detailed line spectra of the stellar objects and thus extensive sets of atomic data, including collisional broadening and especially Stark broadening. In addition, spectroscopic diagnostics for laboratory plasmas, magnetic fusion plasmas (Tokamaks, *e.g.* ITER), inertial confinement fusion plasmas (*e.g.* laser LMJ) and technological plasmas (*e.g.* LED lamps) are also needed for many lines of many ions.

Hence, calculations based on a simple but enough accurate and fast methods are necessary for obtaining numerous results. Furthermore, the development of powerful computers also stimulates the development of atomic data on a large scale. Besides, the access to these atomic data via on line databases becomes essential.

This is the purpose of STARK-B (Sahal-Bréchot *et al.* 2012). It is a database of calculated widths and shifts of isolated lines of atoms and ions due to electron and ion collisions. This database is devoted to modelling and spectroscopic diagnostics of stellar atmospheres and envelopes, to laboratory plasmas, laser equipments and technological plasmas. It is a collaborative project between the Paris Observatory and the Astronomical Observatory of Belgrade and has been opened online since the end of 2008, though not complete and currently under development.

2 Calculations of Stark broadening and shifts and STARK-B

2.1 Calculations of Stark broadening and shifts

Stark broadening theory is based on the founding papers by Baranger (1958a–c). The impact approximation is the first basic one: the duration of a collision must be much smaller than the mean interval between two collisions. So the collisions between the radiating atom (or ion) act independently and are additive. It is quite always valid for electron collisions and is generally valid for collisions with positive ions in the conditions of stellar atmospheres (Sahal-Bréchot 1969a,b). The second basic approximation is the complete collision approximation: the radiating atom has no time to emit (or absorb) a photon during the collision process. In the line center, the impact approximation and the complete collision approximation are both valid, and the line broadening theory becomes an application of the theory of

collisions between the radiating atom and the surrounding perturbers. The present method is limited to the case of isolated lines: the levels of the studied transition broadened by collisions do not overlap with the neighbouring perturbing levels. So, hydrogen and hydrogenic ionic lines, some specific helium lines and some lines arising from Rydberg levels are excluded from our calculations and consequently from STARK-B. Therefore, the impact-complete collision-isolated lines approximation leads to a Lorentz line profile characterized by a width and a shift which depend on the physical conditions of the medium (temperature and density of the perturbers). Owing to the impact approximation, widths and shifts are proportional to the density. However, at high densities, the Debye screening effect can be important and is taken into account in our calculations. This decreases the width and the shift which thus become not proportional to the density.

Most of our calculations have been performed with the semiclassical-perturbation method (SCP) developed by Sahal-Bréchot (1969a,b) and further papers: Sahal- Bréchot (1974) for complex atoms, Fleurier *et al.* (1977) for inclusion of Feshbach resonances in elastic cross-sections of radiating ions, and by Mahmoudi *et al.* (2008) for very complex atoms. The numerical codes have been updated and operated by Dimitrijević and Sahal-Bréchot (1984) and further papers. The accuracy is about 20% for the widths but is worse for the shifts. The results of calculations made by Dimitrijević, Sahal-Bréchot, and co-workers are contained in more than 130 publications and enter STARK-B.

2.2 The Stark-B database: `http://stark-b.obspm.fr`

In this context, we are developing the STARK-B database. It is a collaborative project between the Astronomical Observatory of Belgrade and the Paris Observatory. The database is currently developed in Paris, and a mirror is planned in Belgrade. The domain of temperatures and densities covered by the tables is wide and depends on the ionization degree of the considered ion. The data are gradually implemented and the database is already on line though not yet complete. A graphical interface is provided. After clicking on the element in the Mendeleev periodic table and then on the ionization degree of interest, the user chooses the colliding perturber(s), the perturber density, the transition(s) by quantum numbers and the plasma temperature(s). Then a table displaying the widths and shifts is generated. Bibliographic references are given and linked to the publications via the SAO/NASA ADS Physics Abstract Service (`http://www.adsabs.harvard.edu/`) and/or within DOI. The papers can be freely downloaded if the access is not restricted. The widths and shifts data can be downloaded in ASCII. Request by domain of wavelengths instead by transitions, implementation of the remaining data, and fitting data are in progress. Fitting formulae as functions of temperatures and densities are also in progress. The current developments especially concern the compatibility of the output with the VO (Virtual Observatory) standards, which will be defined by VAMDC.

In fact, STARK-B is a part of VAMDC (Virtual Atomic and Molecular Data Centre, `http://www.vamdc.eu`). VAMDC, created in summer 2009 for the duration of three years, is an European Union funded collaboration between groups

involved in the generation and use of atomic and molecular data. The free exchange of atomic and molecular data requires the definition both of standards which model the data structure and of tools that implement these standards and that help to carry out science using these data. VAMDC aims to build a secure, documented, flexible and interoperable e-science environment-based interface to existing atomic and molecular data. In addition, there is a collaborative project of standardisation of lists of lines within the IVOA (International Virtual Observatory Alliance, http://www.ivoa.net/) consortium as well as a wider collaborative project of standardisation concerning many more processes of atomic and molecular data. Paris Observatory is a major partner in development of both standards and tools. All that is commented and described in more details in Dubernet *et al.* (2010), Rixon *et al.* (2011) and Dimitrijević *et al.* (2010).

3 Conclusion

The development of space born spectroscopy, building of giant telescopes of the new generation and increase of accuracy of computer codes for modelling of stellar atmospheres and envelopes, as well as laser equipments, laboratory, magnetic fusion and technological plasmas, has opened up a new era for obtaining new and numerous Stark broadening data. The continuation of the development and service of a powerful and constantly updated online database, easily accessible and easy to use has become indispensable. STARK-B should fulfil this purpose.

References

Baranger, M., 1958a, Phys. Rev., 111, 481

Baranger, M., 1958b, Phys. Rev., 111, 494

Baranger, M., 1958c, Phys. Rev., 112, 885

Dimitrijević, M.S., & Sahal-Bréchot, S., 1984, JQSRT, 31, 301

Dimitrijević, M.S., Sahal-Bréchot, S., Kovačević, A., Jevremović, D., & Popović, L.Č., 2010, JPCS, 257, 012032

Dubernet, M.L., Boudon, V., *et al.*, 2010, JQSRT, 111, 2151

Fleurier, C., Sahal-Bréchot, S., & Chapelle, J., 1977, JQSRT, 17, 5954

Mahmoudi, W., Ben Nessib, N., & Sahal-Bréchot, S., 2008, EPJD, 47, 7

Rixon, G., Dubernet, M.L., *et al.*, 2011, 7th International Conference on Atomic and Molecular Data and their Applications -ICAMDATA-2010, AIP Conf. Proc., 1344, 107

Sahal-Bréchot, S., 1969a, A&A, 1, 91

Sahal-Bréchot, S., 1969b, A&A, 2, 322

Sahal-Bréchot, S., 1974, A&A, 35, 319

Sahal-Bréchot, S., Dimitrijević, M.S., & Moreau N., 2012, Stark-B database, . Available: http://stark-b.obspm.fr

europhysics
conference
abstracts

EUROPEAN CONFERENCE ON ATOMIC PHYSICS

April 6-10, 1981, Ruprecht-Karls-Universität, Heidelberg

Book of Abstracts

Editors: J. Kowalski, G. zu Putlitz, H. G. Weber

Published by European Physical Society

Series Editor: Dr W. J. Merz, Zurich

Managing Editor: G. Thomas, Geneva

Volume
5 A
Part I

ELECTRON IMPACT BROADENED LINE WIDTHS IN A SUPERMULTIPLET

M.S.Dimitrijević
Institute of Applied Physics, P.O.Box 24, 11001 Beograd, Yugoslavia

From the analysis of the theoretical Stark broadening formulae [1] one may conclude that similarities between line widths within a given spectrum can be expected on the basis of the atomic physics aspects [2-4]. The widths (in angular frequency units) of all lines in a supermultiplet should be approximately equal, since within this larger group of lines the energy differences to the respective interacting levels do not vary considerably. One may argue with this conclusion on the basis of the analysis of the computed line widths for neutral and singly ionized atom lines [1,5-6], since in some cases differences within supermultiplet go up to factor of two. This is the consequence of the inconvenience of the used one electron model (only one energy level for each nℓ electron) for line widths within supermultiplets of complex spectra.

In order to demonstrate the similarities within a supermultiplet, we modified the computer code for Stark broadening parameters of singly charged ions, kindly supplied by H.R.Griem, taking into account properly every particular component of the supermultiplet. From numerical results, presented in table 1, one can conclude that line widths within the considered supermultiplet are approximately equal when atomic parameters are used properly. We can see also that the parameter $(\Delta S/S)_{JBG}$ demonstrating the completeness of the used set of energy levels [6] differs considerably within a supermultiplet, and the set of energy levels is practicaly the same for each particular component. This is an additional consequence of the faillure of the used model for the considered case.

1. H.R.Griem "Spectral Line broadening by Plasmas", Academic Press (1974)
2. W.L.Wiese, N.Konjević, Proc. VIII SPIG, Dubrovnik (1976) p.420

3. W.L.Wiese, N.Konjević, Proc. IX SPIG, Dubrovnik (1978) p.257

4. N.Konjević, M.S.Dimitrijević, Proc. V ICSLS Berlin (1980) (to be published)

5. S.M.Benett, H.R.Griem, University of Maryland Technical Report No. 71-097, College Park, Maryland (1971)

6. W.W.Jones, S.M.Benett, H.R.Griem, University of Maryland Technical Report No 71-128 (1971)

7. M.Platiša, M.V.Popović, N.Konjević, Astron.Astrophys. 45, 325 (1975)

Table 1

Comparison between calculated (W) widths (FWHM) of OII lines within a supermultiplet with other theoretical (W_{JBG}; Ref.6) and experimental(W_m; Ref. 7) results for electron density $N_e = 10^{17}cm^{-3}$ and temperature T = 25900K.

Designation	λ (Å)	$W \times 10^{-11}$ (s^{-1})	$\Delta S/S$	$W_{JBG} \times 10^{-11}$ (s^{-1})	$(\Delta S/S)_{JBG}$	$W_m \times 10^{-11}$ (s^{-1})
$3s^4P-3p^4D^o$	4652	2.80	-0.05	2.94	-0.03	1.99
$3s^4P-3p^4P^o$	4341	2.80	-0.05	2.38	-0.38	2.19
$3s^4P-3p^4S^o$	3736	3.00	-0.06	2.53	-0.49	2.75

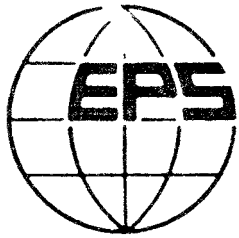

europhysics
conference
abstracts

EUROPEAN CONFERENCE ON ATOMIC PHYSICS

April 6-10, 1981, Ruprecht-Karls-Universität, Heidelberg

Book of Abstracts

Editors: J. Kowalski, G. zu Putlitz, H. G. Weber

Published by: European Physical Society

Series Editor: Dr. W. J. Merz, Zurich

Managing Editor: G. Thomas, Geneva

Volume
5 A
Part II

ELECTRON - HYDROGEN COLLISIONS IN A HOMOGENEOUS MAGNETIC FIELD : CLASSICAL CALCULATIONS

M. S. Dimitrijevic* and P. Grujic**
*Institute of Applied Physics, P.O.Box 24, Belgrade, Yugoslavia
**Institute of Physics, P.O.Box 57, Belgrade, Yugoslavia

In view of the rapidly growing interest in collision processes in an external magnetic field, which take place in a number of laboratory (e.g. MHD generators), geophysical and astrophysical conditions, we have undertaken classical investigations of the electron-hydrogen atom collisions. In this work the process :

$$e + H(|2p0\rangle) + \vec{B} \rightarrow \begin{cases} H(|n\ell m\rangle) + e + \vec{B}, & n \gg 1 \\ H^+ + 2e + \vec{B} \end{cases}$$

is examined. The initial target state can be prepared by a linearly polarized light beam [1]. Since the Coulomb interaction is weak in the asymptotic region, trajectories of the reaction products may be noticeably influenced by the magnetic field in the final state. The initial configuration is set up as shown in Fig. 1, with field $\vec{B}$ along Oz axis, as the impact velocity $\vec{v}$. As Oz axis lies in the initial atomic plane, the energy shift linear in B is zero, so that only the quadratic effect is present.

Calculations of the magnetic field contribution to $|2p0\rangle$ state energy as a perturbation along the Kepler orbit yields :

$$\bar{V}_B = B^2(1+\varepsilon)^3(A\cos^2\theta + D\sin^2\theta + C)$$

where constants A, D and C depend on the orbit eccenntricity ε, and θ is angle between Runge-Lenz vector and $\vec{B}$.

For magnetic field strength $B < 1$ au ($< 1.7\ 10^7$ G) the energy spread of the excited level is less than 1 %, so that a number of thre-

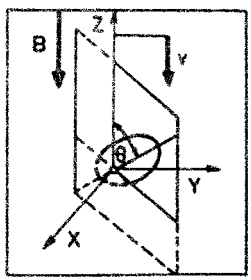

Figure 1. Initial configuration of system : $e + H(|n\ell 0\rangle) + \vec{B}$.

shold effects can be accuratelly treated. Because of the chosen orientation of the magnetic field, a process is determined by the probability of electron(s) passing through the planes : $z = \pm h$, spiraling along $\vec{B}$-lines [2].

Electron trajectories are computed by solving corresponding Newton equations :

$$M_i \frac{d^2\vec{R}_i}{dt^2} = \sum_j{}' Z_i Z_j \frac{\vec{R}_i - \vec{R}_j}{|\vec{R}_i - \vec{R}_j|^3} + Z_i \frac{B}{ic} (v_y^i \vec{i} - v_x^i \vec{j}), \quad i,j = 1,2,3$$

For that purpose the three-body classical computer code (e.g. [3]) has been modified and extended so as to account for the external field effects.

The computer program has been tested and calculations of some near ionization threshold processes, like the double escape probability, as function of the impact energy and B, are in progress. We hope to present numerical results at the Conference.

We acknowledge the financial support by RZN of Serbia.

[1] J. V. Hertel and W. Stoll, Adv. Atom. Molec. Phys., 13,113 (1977).

[2] A. Ohsaki, ISAS, Research Note 107, (1980).

[3] I. C. Percival, Comp. Phys. Comm., 6, 347 (1974).

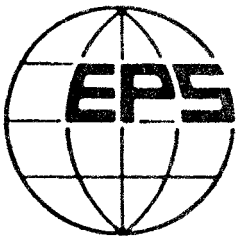

europhysics
conference
abstracts

EUROPEAN CONFERENCE ON ATOMIC PHYSICS

April 6-10, 1981, Ruprecht-Karls-Universität, Heidelberg

Book of Abstracts

Editors: J. Kowalski, G. zu Putlitz, H. G. Weber

Published by European Physical Society

Series Editor: Dr. W. J. Merz, Zurich

Managing Editor: G. Thomas, Geneva

Volume
5 A
Part II

ELASTIC e - He($2s^2$) SCATTERING : CLASSICAL TREATMENT

M. S. Dimitrijevic*, P. Grujic** and S. Vucic**
*Institute of Applied Physics, P.O.Box 24, Belgrade, Yugoslavia
**Institute of Physics, P.O.Box [illegible], Belgrade, Yugoslavia

Double excited atoms attract much attention presently, since they are typical systems where electron correlations play dominant role. A number of empirical and quantum mechanical formulae, in particular for the energies of Rydberg states, has been proposed, but s-states present considerable difficulties. In the case of two-electron atoms two types can be distinguished : (a) synchronous, (b) asynchronous electron motion models. In $\ell_1=\ell_2=0$ angular momenta case the first type appears as a degenerate extended Bohr's planetary model, with the eccentricity $\varepsilon=1$ [1], which is essentially hydrogenic system with the effective nuclear charge $Z_{eff}=Z-\frac{1}{4}$. On the other hand the asynchronous type is much more difficult to treat (see Fig. 1) and to our knowledge no analytical solution of the electrons motion has been obtained up to now.

In the present work equations of motion for the asynchronous (relativistic) model : $R_{1,2}=f(t+\delta_{1,2})$, have been evaluated numerically, with the total energy : $E(2s^2)=$ -62.475 eV taken equal to that of the synchronous type. This value differs from the quantum mechanically calculated result : -57.78 eV (e.g. [2]). The results show approximately that both electrons retain initially ascribed energies : [illegible], during the half-period T, so that, apart of the singularity at the origin : R = 0, the model appears to assure a full periodical motion : $\delta_1=\delta_2+\frac{1}{2}T$.

In order to test both models we have proposed to calculate differential cross section for low-energy electron excited helium atom elastic scattering, within the so called restricted four-body classical model. For that purpose a computer code, designed for e - H(ns) elastic scattering [3] is adapted. The program integrates the impact electron trajectory in the time-dependent potential of (undisturbed) dynamical

excited atomic system. The effect of the target distortion due to the impact electron electric field, which appears important for the small-angle scattering, can be also accounted for [3]. Differential cross section is then calculated in the Monte-Carlo method manner (e.g. [4]).

Both classical models will be discussed, in particular with their relation to corresponding quantum mechanical approaches (e.g. [5], [6]). Comparisons with other classical methods, especially with those by Gryzinski (e.g. [7]), will be made as well.

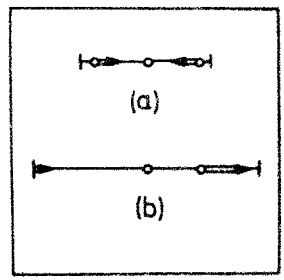

Figure 1. Classical $He(2s^2)$ models ; (a) synchronous, (b) asynchronous case.

The work is supported by RZN of Serbia.

[1] M. S. Dimitrijevic and P. Grujic, J. Phys. B : Atom. Molec. Phys., to be published.
[2] F. Gelebart, R. J. Tweed and J. Perresse, J. Phys. B : Atom. Molec. Phys., 9, 1739, (1976).
[3] P. Grujic, A. Tonic and S. Vucic, SPIG 1980, Dubrovnik, p. 1[illegible].
[4] I. C. Percival, Comp. Phys. Comm., 6, 347 (1974).
[5] C. E. Wulfman, Phys. Letters, 26A, 397 (1968).
[6] Herrick, Phys. Rev. A, 22, 1346 (1980).
[7] M. Gryzinski, J. Chem. Phys., 62, 2610 (1975).

Variations of the Solar irradiation of the Earth and Milutin Milankovic

M.S. Dimitrijevic

Astronomical Observatory, Volgina 7, 11160 Belgrade, Serbia (mdimitrijevic@aob.bg.ac.yu / Fax +381-11_2419-553 / phone: +381-64-297-8021)

One of the great scientific problems in the beginning of the twentieth century, was the occurence of the ice-ages in Europe in the Qartenary. Serbian scientist Milutin Milankovic (1879 - 1958) devoted his life to the solution of this mistery. He elaborated a mathematical theory of Earth's climate (applicable also to other planets) based on the calculation of variations of Solar irradiaton of Earth during the time.

In his capital work „Kanon der Erdbestrahlung und seine Anwendung auf das Eiszeitenproblem" (The Canon of the Earth's Irradiation and its Application to the Problem of Ice Ages), published in 1941, he collected the results of his longstanding researches, demonstrating the long-period cyclic changes in the Earth climate and the occurence of ice-ages as being a consequence of the variations of the Earth's irradiation by Sun, due to: (i) Changes of Earth's axis inclination with a 41 000 year period; (ii) Changes of the eccentricity of the Earth's orbit around the Sun with a 100 000 year period; (iii)Precession, affecting the duration of seasons with a 22 000 year periode.

With his famous curve of the cyclic variations of Solar irradiation of the Earth surface in last 600 000 years, he explained the occurence of ice-ages. Additionally, his theory, and the obtained curve of Solar irraditaion cyclicity, have numerous applications in Geophysics, Geology and Climatology of Earth and Mars.

In this paper we will review the Milankovic's theory of variation of Solar irradiation of Earth's (and other planets) surface with time, its role for the solution of the ice-ages problem, and its wider impact in Geophysics, Geology, Climatology and other scientific disciplines. Additionally, basic facts on the life and other scientific results and achievements of Milutin Milankovic and its applications will be reviewed.

Geophysical Research Abstracts, Vol. 9, 00275, 2007
SRef-ID: 1607-7962/gra/EGU2007-A-00275

Variations of the Solar irradiation of the Earth and Milutin Milankovic

M.S. Dimitrijevic

Astronomical Observatory, Volgina 7, 11160 Belgrade, Serbia (mdimitrijevic@aob.bg.ac.yu / Fax +381-11_2419-553 / phone: +381-64-297-8021)

One of the great scientific problems in the beginning of the twentieth century, was the occurence of the ice-ages in Europe in the Qartenary. Serbian scientist Milutin Milankovic (1879 - 1958) devoted his life to the solution of this mistery. He elaborated a mathematical theory of Earth's climate (applicable also to other planets) based on the calculation of variations of Solar irradiaton of Earth during the time.

In his capital work „Kanon der Erdbestrahlung und seine Anwendung auf das Eiszeitenproblem" (The Canon of the Earth's Irradiation and its Application to the Problem of Ice Ages), published in 1941, he collected the results of his longstanding researches, demonstrating the long-period cyclic changes in the Earth climate and the occurence of ice-ages as being a consequence of the variations of the Earth's irradiation by Sun, due to: (i) Changes of Earth's axis inclination with a 41 000 year period; (ii) Changes of the eccentricity of the Earth's orbit around the Sun with a 100 000 year period; (iii)Precession, affecting the duration of seasons with a 22 000 year periode.

With his famous curve of the cyclic variations of Solar irradiation of the Earth surface in last 600 000 years, he explained the occurence of ice-ages. Additionally, his theory, and the obtained curve of Solar irraditaion cyclicity, have numerous applications in Geophysics, Geology and Climatology of Earth and Mars.

In this paper we will review the Milankovic's theory of variation of Solar irradiation of Earth's (and other planets) surface with time, its role for the solution of the ice-ages problem, and its wider impact in Geophysics, Geology, Climatology and other scientific disciplines. Additionally, basic facts on the life and other scientific results and achievements of Milutin Milankovic and its applications will be reviewed.

European Journal of Science and Theology, *December 2005, Vol.1, No.4, 11-17*

'UN-TANGIBLE WORLD' AND MODERN PHYSICS

Emmanuel Danezis[1], Efstratios Theodosiou[1], Ioannis Gonidakis[1] and Milan S. Dimitrijevic[2*]

[1] *University of Athens, School of Physics, Department of Astrophysics, Astronomy and Mechanics, Panepistimiopolis, Zografos 15784, Athens, Greece*
[2] *Astronomical Observatory, Volgina 7, 11160 Belgrade, Serbia*

(Received 7 November 2005, revised 24 November 2005)

Abstract

The problem of the co-existence with the so-called 'tangible world' of a non-tangible one, inconceivable to human senses, was a point of disagreement and dispute between theology, philosophy and exact sciences. Here is discussed the evolution of this view from presocratic philosophers to modern physics. Arguments that are important for theologians in order to follow the achievements of modern Science are also given. This is particularly important for Antiretic-Objectionable Theology making an effort to confute the metaphysical views of the Christian Theology through ideas mainly based on the findings of the Exact Sciences.

Keywords: theology, modern physics, Universe, cosmology

1. Introduction

A problem that throughout the centuries was a point of disagreement and dispute between philosophers, theologians and exact sciences is the problem of the existence of an invisible to the human senses, but actual and objective, reality that co-exists with the so-called 'tangible world'. It is of interest to show that the existence of such 'un-tangible' world is not in collision with modern science, and to discuss the evolution of such idea.

We note here that a distinctive characteristic of the modern theological reality is the effort to confute the metaphysical views of the Christian Theology through the expression of ideas mainly based on the findings of Exact Sciences (Antiretic-Objectionable Theology). Today however, we know that the current scientific knowledge will be expanded, corrected, completed, and some 'truths' even annulled in the future under the pressure of new dramatic scientific discoveries. Thus, it is useful for theologians to study in detail the new Exact Sciences achievements. In fact, we suggest that they should follow the way of the Christian Church Fathers and become experts of the Exact Sciences of their epoch (like for example Saint Basil the Great [1]).

* Corresponding author: e-mail: mdimitrijevic@aob.bg.ac.yu

The question of 'un-tangible world' may be a good example in support of this statement.

2. Science and the un-tangible world

The concept of modern Physics and Astrophysics dramatically differs from the Science of earlier centuries.

When after the 'Copernican revolution' began the 'divorce' between Science and Theology, Science started to be based on Aristotelian, materialistic and positivistic ideas on the important role of *common sense*, '*matter' conceivable by our senses* and, the *Newtonian space* as a space where we are like in a 'room' without any interaction with it.

The human *common sense*, the logic developed through our senses, was at that time considered often as the scientific logic. Nowadays, the modern scientific thinking diverts from the 'human common sense'. For example the Newton's principle that a body will not change its state of motion without the acting of a force is now evident since for example space ships act in accordance with it. It was opposite however, to the Aristotelian opinion based on 'common sense' that without the acting of a force, the velocity of a body will decrease, and it will come finally in the state of absolute immobility on the immobile Earth based in the centre of the Universe.

The classical physics, based on Newton's 'principles' and the Newtonian–Euclidean space, was the basement of the disagreement between Science and Theology on the existence of the non-conceivable 'un-tangible' world. The triumph of Science was the discovery of a new planet – Neptune, discovered 'on the top of a pen'. Jean Jacques Urbain Le Verrier calculated its position, and when his friend Johan Galle looked through telescope it was on the predicted position [2].

At the beginning of the 20th century, it seemed that all problems of physics were solved and that on the 'crystal clear sky' of the Classical Physics there is only one small 'cloud' – the bizarre result of the Michelson-Morley's experiment, that the sum of the velocity of light and the velocity of Earth is in any direction equal to the velocity of light [3]. This result however, dramatically changed our view on space and time, showing that Newtonian Classical Physics is only the low velocity limit of a more general concept of the Nature.

As a matter of fact, the classical Newtonian Physics indicates that space could be fully described by Euclidean geometry. However, Einstein showed with the help of the General Relativity Theory, that space is not Euclidean but is described by another geometry, fundamentally different from the Euclidean one – the Riemann geometry forming the essential framework for this theory [4]. This would not be of great importance if one did not know the startling fact that images and shapes in the four dimensional Universe, can not be conceived in an adequate way by human senses. We know that our senses can only record and specify shapes that only occur in spaces up to three dimensions. Images and

shapes with more than three dimensions we can consider only with the help of theoretical models [5].

In fact, we can perceive only the projected shadows of four-dimensional shapes and figures on the three-dimensional space that is created through arbitrary intersections of the continuum and undivided universal time-space. What to say about the development of the Theory of cosmic strings, with the Universe with much more than four dimensions [6].

As mentioned by John Archibald Wheeler [7], a well-known American physicist and astronomer, "*The concepts of time and space do not represent the nature of reality, but representations of human conscience*". On the same subject, English astrophysicist Sir Fred Hoyle expresses the view that *everything exists.* "*Whatever previously existed or will exist in the future is inherent in the present. Only our conscience dissociates them and creates the feelings of historical inconsistency and time passing. Feelings though, are illusions, creations of our conscience, the way of understanding the world*." Similarly, describing the theories of Multiversum and parallel Universes, Max Tegmark [8] writes: *"One of the many implications of recent cosmological observations is that the concept of parallel Universes is no more metaphor. Space appears to be infinite in size. If so, than somewhere out there, everything that is possible becomes real, no matter how improbable it is. Beyond the range of our telescopes are other regions of space that are identical to ours. Those regions are a type of parallel Universe. Scientists can even calculate how distant these Universes are on average*."

Another old concept, overruled by the Physics of the 20th century, is that of the 'matter' as conceivable by our senses. With the discovery of spectral analysis, atomic and molecular structure and the development of the quantum physics, the opinion on the reality of the information obtained by human senses dramatically changed.

Charles Muses and A.M. Young [9] write in their book 'Consciousness and Reality': *"… a tree, a table, a cloud, a stone. All are dissolved under the influence of the 20th century science into something that consists of the same substance. That something is a medley of whirling particles that obey the laws of quanto-mechanics. This means that all the objects we can observe are simple, three-dimensional images that are formed by waves, under the influence of electromagnetic waves and nuclear processes".*

In the same way, matter, according to the theory of relativity, is not an unchangeable complex of molecules, but a condensation of an energy field. In the context of Einstein's space-time continuum, matter is not an entity on its own but a peculiarity of the field. A particle is nothing more than a moving, non-tangible whirl in space. According to modern Physics, what was perceived in earlier centuries as tangible and individualized matter, is only a false invention of our senses. In other words, we 'see' the ambient not as it is in reality, but as our senses allow us to perceive it.

What our senses are sensitive to are not the real images and shapes of the surrounding universe but their projections, their shadows. It is sufficient to see the photography of the Sun in X rays or some wavelengths insensitive for human eyes, to see the difference. It is obvious though that these projections (shadows) of the real images perceived by our senses, are not the actual world that can only be considered with the help of mathematical formulae. In other words, it should be understood that we live in a Universe that we cannot perceive through our senses and what we really see is just a 'shadow' of what really exists.

3. Theology and the un-tangible world

According to the modern Science together with the 'tangible' world, which we perceive with our senses, coexist the 'un-tangible' world of more than three dimensions. If we go toward the micro-world, we could conclude that we will also found in our three dimensions 'un-tangible' elements [10].

We could compare this view with the view of Great Father of the Christian Church Gregory of Nyssa (fourth century A.D.). His views are expressed by Elias Economou, professor at the Theological School of the University of Athens, in the book 'Theological Ecology' [11]:

"Aktistos (Uncreated) God willed and His will materialized into a tangible and a non-tangible Ktisis (Creation). One could classify the following realities:

1) *The reality of the Aktistos Trinitarian God.*
2) *The reality of the Ktisis as a result of the divine will, the materialization of God's will, which is divided in*
   a) *A non-tangible Ktisis of an invisible greatness.*
   b) *A tangible Ktisis of enormous extent, expanse, volume, variety and power.*
   c) *A mixed Ktisis of both tangible and non elements, the great and small human."*

It is interesting that such views concerning the existence of a non-tangible Creation has also been expressed by the ancient Greek philosophers. The world of senses for many of them was just an illusion, a deceptive image of the real, non-tangible world.

4. The un-tangible World of the pre-Socratic philosophers

Due to Aristotelianism, in earlier centuries the realism of the sensual world, and logics based on empiricism, often dominated. The incomprehensible by the senses, though real, world of Plato, the theory of its representation through a hylic (materialistic) tangible form, was opposite to the Aristotelian practical thinking, but without the scientific proofs to support it. Things have changed now and, apparently, Platonists could be satisfied. As already discussed, scholars know that the Universe is not tangible due to its property to be described by more than three dimensions. Images and shapes are just partial representations of true but not perceivable objects that we 'see' as 'shadows'.

The first hint concerning the relevance of truth for facts that can be conceived through human senses was made by Xenophanes who mentions:

"*No one knows and never finds out the truth about gods or everything I say, because even if one says the entire truth, they do not know it, for every issue there are only opinions."* [Extract 34, Sextus Empiricus, To Physicists VII, 49 and 110 prb Plutarch] Moreover,

"Let us consider that things resemble the truth." [Extract 35, Plutarch, Symposium Matters IX, 7, 746b]

A second hint is recorded by Heraclitus who seems to say:

"The real structure of things is usually hidden." [Extract 123, Themistius, Speeches 5, page 69D] and

"The invisible bond is stronger than the visible." [Extract 54, Hippolitus, El. IX, 9,5]

Apart from the previous abridgement, Sextus Empiricus is very persuasive that Heraclitus was completely aware of the illusive world of the human senses. He mentions:

"*Heraclite also believed that humans have two organs to achieve knowledge of truth, the sense and the 'word'. The former was considered to be deceitful, similarly to the previous physicists, the latter is accepted as the appropriate criterion.*" [Sextus Empiricus VII 126 (Heraclitus A16)] The 'word' here has its pre-Socratic meaning and it describes the result not obtained by the senses, the 'non-tangible'. The term 'word' used until now by the Christian Theology has the previous meaning, in order to define the meaning of God, considering Him through the expression 'non-tangible'.

According to Diogenes Laertius and Simplicius, the philosopher Parmenides also has such opinion concerning the illusion of the physical world as perceived by human senses. They state:

"*Parmenides believed that philosophy is two-fold; one of the patterns is consistent with the truth, while the other is only by guess. He determined as a criterion the 'word' since the senses are not accurate.*" [Diogenes Laertius IX 22 (Parmenides A1, 22)]

"Those people supposed two substances; one of the intelligible real being and another, that of the done and conceivable that they did not like to call 'being' but 'putative being'. Thus, they say that the truth is related to the real being, while for the changing being (the physical things) there is only presumption." [Simplicius Peri Uranou (De Coelum) 557, 20 (Parmenides B1)]

Empedocles, according to Sextus Empiricus, also conceived the idea of a false reality that our senses create.

"Others said that according to Empedocles, our senses are not the criteria for the truth, but only the 'right word' is. There are two kinds of the latter, the divine and the human. The divine 'word' is inexpressible (ineffable), while the human can be expressed." [Sextus Empiricus VII 122 (Empedocles B1)]

These points of view preceding Democritus, most probably constituted the starting point for Democritus and even Leucippus to formulate and justify their atomic theory. In more detail follow the views of Democritus on the 'truth' of the tangible Creation, as reported by Simplicius, Sextus Empiricus, Galenus, Aetius and Aristotle.

1. "*It is believed that there are two kinds of knowledge regarding the 'Rules', one through the senses and another through intellect. When retrieved through intellect is called pure, and is the most reliable for right judgment, while when retrieved through the senses, is called improper, without acknowledging its infallibility in the search of truth. Parts of the improper are the sight, the hearing, the smell, the taste and the touch. The other kind of knowledge is pure which is different to the improper.*" [Democritus, extract 11, Sextus Empiricus, *To physicists* VII, 138]

It is worth noticing that Democritus recognizes as improper the knowledge obtained by the human senses, which he states with their names. Another important point is that most of the pre-Socratic philosophers, including Democritus, refer to intellect as to a sixth sense, enabling to perceive the non-tangible, but existing and objective reality of the physical world. Thus, to realize the universal constitution as an objective reality, one should train the mind, avoiding that it becomes an in-objective sixth sense.

2. "*In Kratynteria, although [Democritus] promised that he would attribute to the senses the prestige of certainty, on the contrary he condemns them saying In reality we do not perceive anything certain, but only something that changes depending on the state of the body and the things that enter and exert pressure on it.*" [Democritus, extract 9, Sextus Empiricus, *To physicists* VII, 136]
3. "*… and again he says: It is obvious in several ways that in re ality one does not conceive reality, does not conceive how each thing should or not be.*" "*Humans should learn from this rule that they are separated from reality.*" "*This argument also shows that in reality we know nothing about things, but for each one of us there are their recreated patterns, faith.*" "*However, it should be very difficult to learn how each thing should appear in reality.*" [Democritus, extract 10 and 6-8, Sextus Empiricus, To physicists VII, 136]
4. "*Democritus sometimes refutes those obvious to our senses and says that none of them corresponds to reality, but only to human imagination.*" [Democritus, extract 9, Sextus Empiricus, To physicists VII, 135]
5. "*…Moreover, many healthy beings have the same things appearing different to how humans conceive them, even a human being does not always understand everything in the same way. Therefore, it is unknown which of these are actually real or fake, since the one is not more real than the other, but just as right. So, Democritus says that either nothing is real or (if it is) is invisible to us.*" (Aristotle, Met. Ã5, 1009b7)
6. "*…Miserable mind, you took the certainties from us (meaning the senses), now you reject us? Our rejection is your collapse.*" [Democritus, extract 125, Galenus, *About Medical Practice*, p. 113, Walzer]

Consequently, the views concerning the objective existence of a non-tangible world, are not coming only from the Christian theological mind, but this are views of different ancient civilizations as Greek, Indian, Babylonian, Egyptian and also South American. To be more precise, the existence of an 'unseen' world is discussed by the Greek pre-Socratic philosophers and for Christianity the assimilation and understanding of the ancient Greek testimonial logic was of great importance.

5. Conclusion

We can conclude that the modern Physics theoretically accepts the existence of a hyper-tangible universal and real space, as Theology also does. Michael Talbot highlights all the above in a characteristic way in his book 'Mysticism and Modern Science': " *According to New Physics, we can only dream of the real world. We dream of it mysteriously visible, omnipresent in space and constant in time. Despite the previous, we consciously approved ourselves in the false construction of illogical, loose and eternal intermissions [intersections] of its architecture, so one day one might see how false their initial frame is*". [12]

References

[1] E. Danezis, E. Theodossiou and M.S. Dimitrijevic, Romanian Astronomical Journal, (2005) in press.

[2] M. Littman, *Planets Beyond – Discovering the Outer Solar System*, John Willey and Sons Inc., New York, 1988, 46.

[3] P. Schwarz and J.H. Schwarz, *Special Relativity - From Einstein to Strings*, Cambridge University Press, Cambridge, 2004, 31.

[4] R. Penrose, *The Road to Reality – A Complete Guide to the Laws of the Universe*, Johnatan Cape, London, 2004, 49.

[5] E. Danezis and E. Theodossiou, *The Universe I loved - An Introduction to Astrophysics*, Diavlos Publications, Athens, 1999, 24.

[6] I. Antoniadis, *Physics with large extra dimensions,* in *2001: A Relativistic Spacetime Odyssey*, I. Ciufolini, D. Dominici, L. Lusanna (eds.), World Scientific, London, 2001, 43.

[7] J.A. Wheeler, *Superspace and the Nature of Quantum Geometrodynamics*, in *Batelle Rencontres 1967, Lectures in Mathematics and Physics*, M.C. de Witt and J.A. Wheeler (eds.), W.A. Benjamin, New York, 1968, 242.

[8] M. Tegmark, Sci. Am., **May** (2003) 30.

[9] C. Muses and A.M. Young, *Consciousness and Reality*, Outerbridge and Lazard, New York, 1972, 3.

[10] E. Theodossiou and E. Danezis, *To the Roots of I.X.T.H.Y.S. - History, Astronomy, Philosophy*, Diavlos Publications, Athens, 2000, 46.

[11] E. Economou, *Theological Ecology*, Ed. Mavromates, Athens, 1994, 56.

[12] M. Talbot, *Mysticism and Modern Science*, in Greek translation, Iamblichos Publications, Athens 1993, 71.

European Journal of Science and Theology, September 2010, Vol.6, No.3, 47-56

THE INCONVENIENT RELATION BETWEEN RELIGION AND SCIENCE: THE PREVALENCE OF THE HELIOCENTRIC THEORY

Efstratios Theodosiou[1], Vassilios Manimanis [1] and Milan S. Dimitrijevic[2*]

[1] *University of Athens, School of Physics, Department of Astrophysics, Astronomy and Mechanics, Panepistimiopolis, Zografos 15784, Athens, Greece*
[2] *Astronomical Observatory, Volgina 7, 11160 Belgrade, Serbia*

(Received 20 May 2010)

Abstract

The relation between religion and Science is discussed in this article on the example of attitude of Western Churches towards heliocentric theory. Also reasons of such attitude of the Church were considered.

In order to consider this relation, we will first note that in the case of a religious dogma, faith must be absolute. Dogma as a theory can be proved only through itself and its power is the absence of doubt. On the contrary, in the case of science, according to the philosophical view of Descartes, doubt should be present in any problem arising in order to avoid possible errors and prejudices; through doubt we can be led to the discovery of an indisputable truth.

The military and political power of the Holy See hindered for a long time the development of knowledge and hence Science. Giordano Bruno was accused and judged because, among other, he was teaching the infinite worlds of Metrodorus of Chios and of Epicurus (4th century BC). Similarly, Galileo stood trial on suspicion of heresy and he was condemned into house arrest because the heliocentric system he was supporting was at odds with the *Old Testament*, according to which Joshua ordered the Sun to stop – and not the Earth – during the Gibeon Battle of Israelites against Canaanites.

The heliocentric theory was not favored by the Western Church because it did not comply with the 'positions' of the *Bible* and the ancient Greek geocentric theory. When science contributed to the fall of the anthropocentric myth, first by showing that the Earth, the abode of man, is not at the center of the Universe and next by showing that even human itself is a product of evolution, then its separation from the Western Church was definite.

Therefore, a kind of war was waged against the heliocentrists, not just because the system they supported was at odds with what the Scriptures said, but also because the geocentric theory, which supported an absolutely motionless Earth, was in agreement with the celestial mechanics of the 'divine scientist' Aristotle. Since Aristotle had deeply influenced the mediaeval Catholic theology, the rejection of the geocentric theory would

[*] Corresponding author: e-mail: mdimitrijevic@aob.bg.ac.yu, Phone: +381-11-3089-072, Fax: +381-11-2419-553

diminish the authority of the great philosopher and consequently the theology of the Church. It thus became clear that the support of the geocentric theory was essentially an issue of Church authority.

Keywords: religion, science, religious dogma, Cartesian doubt, heliocentric theory

1. Introduction

Which is the relation between religion and Science? Or rather between religious dogma and Science? Convergence or opposition? Parallel or incompatible roads? Is this relation truly inconvenient?

In order to answer this question thoughtfully, we must first juxtapose these two primal notions.

In the case of a religious dogma, faith must be absolute. Dogma as a theory can be proved only through itself and its power is the absence of doubt.

On the contrary, in the case of Science, according to the philosophical view of Descartes, doubt should be present in any problem arising in order to avoid possible errors and prejudices; through doubt we can be led to the discovery of an indisputable truth. So the Cartesian doubt in the area of Science is the main methodological starting point, which leads us to the proof.

The difference between dogma and Science, or rather the difference of the religious beliefs from respective scientific theories, stems from exactly this point.

Religion is faith and absolute truth, while Science is doubt and falsifiability (or refutability). Karl R. Popper [1, 2], for example, was critical against the inductive methods used in Science. All inductive proofs are limited, he said, while he taught that falsifiability should replace the ability for verification as a criterion of the difference between the scientific and the non-scientific. Science is seen more in the frame of an unending search for objective knowledge, rather than in the frame of a knowledge system. The principle of falsifiability is for Popper the criterion for the scientific or non-scientific character of a given theory. Thus, for example, astrology or 'ufology' are classified as pseudosciences because of their incapability to be subjected to the application of the falsifiability principle. Within a religious structure there is no phenomenon that can refute the core of the theory and there is nothing that can make the foundations of the structure tremble.

In Science, when something new is discovered, anything that contradicts, even partially, to the prevailing scientific theory, then, sooner or later, the theory is replaced by a new theory. According to Popper, as cited in Theodossiou [3], scientists should rather try to disprove their theories than to verify them time and time again.

But let us consider our main topic, namely the prevalence of the heliocentric system and the controversy it created between Science and the Christian Church. When Galileo observed with his telescope the four large satellites of Jupiter, in 1609-1610, the geocentric theory suffered a fatal blow, in

spite of the reactions that followed by various scholars and the Roman Catholic Church, which had incorporated geocentric system as its favored one.

The fundamental difference between Science and religion we mentioned before was always rendering their relations inconvenient, especially in the West. For a certain period these relations were so tense that blood was shed in their sake; but it was rather the relation between the prevailing dogma and Reformation or the coming change that made that happen, and not the relation between religion and Science. The night of August 24th, 1572, is known in history as the Night of Saint Bartholomew because of the massacre of thousands of the Huguenots by fanatic Catholics in France. The kings of France were fighting violently Reformation, which was represented by Huguenots, because the alliance with the powerful Catholic Church allowed them better to hold their power steadily.

It is an indisputable fact that the military and political power of the Holy See hindered for a long time the development of knowledge and hence Science. Giordano Bruno was accused and judged because, among other, he was teaching the infinite number of worlds of Metrodorus of Chios and of Epicurus (4th century BC). Similarly, Galileo stood trial on suspicion of heresy and he was condemned into house arrest because the heliocentric system he was supporting was at odds with the *Old Testament*, according to which Joshua ordered the Sun to stop – and not the Earth – during the Gibeon Battle of Israelites against Canaanites; this reference means that the contemporary scholars were believing Earth was motionless and the Sun was revolving around it, i.e. into a genuine geocentric system.

2. The Gibeon Battle and other Scripture references

The ancient city Gibeon was to the northwest of Bethlehem; during the battle conducted there by Joshua against the Canaanites, Joshua asked God to cause the Sun and Moon to stand still, so that he could finish the battle in daylight and win it: *"and he said in the sight of Israel, Sun, stand thou still upon Gibeon; and thou, Moon, in the valley of Ajalon. And the Sun stood still, and the moon stayed, until the people had avenged themselves upon their enemies… …So the sun stood still in the midst of heaven, and hasted not to go down about a whole day"* (Joshua 10.12-13, The King James version).

The stillness of the Earth and the respective motion of the Sun is apparent also in other parts of the *Old Testament*, as in the *Psalms* and the *Ecclesiastes*: *"the world also is established, that it cannot be moved"* (Psalm 93.1), *"He appointed the moon for seasons: the sun knoweth his going down"* (Psalm 104.19), *"The sun also ariseth, and the sun goeth down, and hasteth to his place where he arose"* (Ecclesiastes 1.5).

3. Later incidents of opposition of the Church to the heliocentric theory

Nicolaus Copernicus (1473-1543) hid his fundamental work *De revolutionibus orbium coelestium* [4] for years, unwilling to publish it, exactly because he did not dare and did not want (as a priest himself) to clash with the Roman Catholic Church, to which he always belonged. His research was in support of the heliocentric system, contrary to the Church-supported geocentric system.

Even centuries later, Charles Darwin delayed in a similar way for several years the publication of his pioneering book *On the Origin of Species* [5] because he was either afraid of the power of the Church, or unwilling to oppose to it, although England was not subject to the Vatican authority!

In the 20th century it is known that some religious scholars and Church people even attempted to stop the translation of cuneiform writings from Mesopotamia and of the Dead Sea Scrolls because it was probable that they could reveal that our world is older than *circa* 6,000 years, an age they believed that can be calculated from the *Old Testament*. This calculation was originally made by the Archbishop of Armagh James Ussher (1581-1656), who concluded that the Earth was created on October 23rd, 4004 B.C.; others after him calculated similar chronologies that have been long ago rejected by modern sciences [6].

The revolution for the observation of the heavens came from Galileo in 1609, when for the first time in the history of astronomy he used a dynamic and pioneering for the times instrument, the telescope, which gave him the ability to discover wonderful things in the firmament: from the phases of Venus to the four large satellites of Jupiter, a miniature planetary system.

That year belonged to the first decade of the 17th century; a century that marked a period of multiple crisis. Philosophy, religion and Science itself found themselves into a maelstrom that shook the foundations of Western society. That maelstrom engulfed in its whirl the foundations of Astronomy, the science of the heavens. The ‘peaceful’ geocentric and at the same time egocentric system that was prevailing for many centuries gave its place to the correct heliocentric one.

A new physics appeared in the West in the 17th century, under the philosophical canopy of the Cartesian philosophy, the spirit of which had its deep influence on all his contemporary savants. This new physics, as was defined by Galileo and Kepler, was not interested in searching for purpose, but rather it was seeking for causes. The teleological model of understanding the Universe had now been fully unleashed from the bondage of Aristotelian philosophy. From the study of History and Philosophy of the sciences it can be said that this was the time the subject is placed as central entity on the philosophical stage; however, its place is not secured, in spite of the blows against the ‘traditional’ view on nature and human by the new science.

It may be that the crucial role for the liberation from Aristotelism, or for this revolution of the natural sciences, belongs to the dynamical appearance of the new astronomy, which put the Sun in the place of the Earth; however, several explanations have emerged based on a much wider understanding of the big change that took place in Italy and the Western Europe.

At least two to three centuries before 1609, the West was a boiling pot. Great scholars, such as Jean Buridan (Johannes Buridanus, ca. 1295-1358), Nicole d'Oresme (1323-1382), Nicolaus Cusanus (1401-1464), Copernicus (1473-1543) and many others in the natural sciences, centuries before Galileo and Kepler, based on the Pythagorean and pre-Socratic Greek natural philosophers, had added their small stone to the building of the new physics; at the same time, they had ignited the great change in Science and in the way to understand natural phenomena. A change that, stemming from the mentality shift in Astronomy, was now focusing attention to switching the European scientific thought from theory to practice, through experiment, observation and the use of Mathematics and their methods.

Galileo Galilei (1564-1642), the first physicist with the modern meaning of the term, rejected through his experiments the common perception for motion, setting the base for the modern mechanics, while Rene Descartes (1596-1650) generalized the re-explaining of everyday experience and proposed a new image of reality beyond experience. Descartes tried to show through his philosophy that nature's reality is not similar to what our senses present to us. Our world is not a finite wholeness with an impeccable internal structure, as it was presented in Aristotle's view of Cosmos and later in its slight alteration by Dante [7].

Things changed in new astronomy, too; scholars, liberated from the tightly closed and powerful crystal spheres, started to talk about an infinite Universe that didn't have or was controlled from a natural hierarchy, while its unity was a result of laws governing it, laws valid for all its parts.

4. Why the heliocentric theory proponents were persecuted?

The revivalist of the heliocentric theory, Copernicus, was according to Martin Luther '*the fool who wanted to overturn the Science of Astronomy'*. Later on, Giordano Bruno was burned for his views and ideas, while Galileo was put under house arrest. Why?

The answer lies in the indisputable fact that these scientists, by indicating the weakness of the geocentric theory were undermining in an essential way the egocentrism or the man-centred Universe, in other words a basic aspect of the Christian worldview, for which human is the centre and the reason for all Creation. Indeed, the German Neo-Kantianist philosopher and historian of Philosophy Wilhelm Windelband (1848-1915) assigned to the Christian worldview a 'human-centred character', because according to it (in contrast to the ancient Greek thought) human and human history become the reason for the Universe [8]. Yet, the human-centred view was inherent in all ancient astronomy, capitalized with the Ptolemaic view for the Cosmos (with the Earth

at the centre of it). To this the religious view that human is the central creature of the Creator and everything else revolves around him, dovetailed nicely.

The rare independence of thought combined with an integrated knowledge of Astronomy and Cosmology, knowledge not easily attainable at that period of time, were the necessary prerequisites for Copernicus, Giordano Bruno, Galileo and Kepler to expose persuasively the superiority of their heliocentric system version. That great proposition of Copernicus, which revived the heliocentric theory of Aristarchus of Samos not only paved the way towards modern Astronomy, but also helped to bring a decisive change in the way humans were facing the Universe. When people grasped that the Earth was not the centre of the Universe but instead just one of the Sun's planets, a member of the Solar System, the illusion of the central importance of humanity itself lost its support. Therefore, the heliocentric theory was not favoured by the Western Church because it did not comply with the 'positions' of the *Bible* and the ancient Greek geocentric theory. When Science contributed to the fall of the anthropocentric myth, first by showing that the Earth, the abode of man, is not at the centre of the Universe and next by showing that even human itself is a product of evolution, then its separation from the Western Church was definite.

Therefore, a kind of war was waged against the heliocentrists, not just because the system they supported was at odds with what the Scriptures said, but also because the geocentric theory, which supported an absolutely motionless Earth, was in agreement with the celestial mechanics of the 'divine scientist' Aristotle. Since Aristotle had deeply influenced the mediaeval Catholic theology, the rejection of the geocentric theory would diminish the authority of the great philosopher and consequently the Theology of the Church. It thus became clear that the support of the geocentric theory was essentially an issue of Church authority. This was the main reason Pope Urban VIII (1623-1644) moved the procedure against Galileo and included the work of Copernicus in the *Index Librorum Prohibitorum.*

The space of the Universe with the new astronomy and Physics departs from the set of the differentiated Aristotelian spaces and then it is identified with the space defined by Euclidean geometry, a homogeneous and isotropic space, to finally become, in the 19^{th} and 20^{th} centuries the space of non-Euclidean geometries.

Johannes Kepler, as a mystic and religious person, believed that the Universe was full of secret and transcendental forces. He was convinced that if he plugged the mystic mathematical harmonies into the study of the celestial sphere he could connect the planetary orbits with perfect geometrical solids. According to the German astronomer only the motions of the celestial bodies, eternal and perfect as they were, could be analyzed mathematically and geometrically, since he supported the view that Astronomy should be based on the principles of geometrical simplicity. However, Kepler was a Protestant and as such he never felt the pressure of Catholicism and the Inquisition [9, p. 266].

After the observations and the theoretical studies of these two great astronomers, Galileo and Kepler, the abdication of the Earth from its planetary throne was a reality. After thousands of years of reign for our small planet in the human thought, the heliocentric system prevailed and the Sun rightly occupied the position held by the Earth in the geocentric system. The eternal crystal spheres of the closed Aristotelian geocentric system with the perfect internal arrangement and the strict hierarchy gave place to a new cosmology that favoured an infinite Universe without any natural hierarchy.

Kepler, with his book *Astronomia nova* (1609) [10], came into conflict with the then prevailing ideas. The adoption of the material moving force he proposed was a blow against the divinely created cosmic order, imposed in the western thought by the Aristotelian physics.

As a conclusion we can state that Galileo with his pioneering observations and Kepler with his theoretical insight were the true founders of the new heliocentric system and the discoverers of the laws governing our planetary system; both in 1609, with the first telescopic observations of Galileo and the publication of *Astronomia nova*, which put on new bases the celestial science, since Kepler therein presented the two of the three basic laws governing planetary motions: The orbits of the planets are ellipses, the one focus of which is occupied by the Sun, and the line joining a planet and the Sun sweeps out equal areas during equal intervals of time. It can be said that the observational justification of the heliocentric theory began with Galileo and its mathematical foundations were laid exclusively by Johannes Kepler.

The heliocentric theory of Aristarchus and Copernicus was a blasphemy according to the Church, because it sowed the ideas for a science uncontrolled by Catholicism and the Inquisition. For this reason, in 1616 this theory was condemned by the Roman Catholic Church as irrational, impious and 'pseudo-scientific'. This condemnation lasted until 1820, when the heliocentric theory was regarded by the Church as rather 'proved' and 'scientific'; after that, the persecution against its supporters stopped.

5. Was there a solution?

A solution? Of course! The true solution to the problem of relations between Science and religion was and still is the separation of their roles. In any case, God is beyond the limits of Science; He reveals himself, He can't be calculated with equations or through theories; therefore, the scientific occupation of scientists with the divine is both dangerous and vain.

It must be noted that these questions are important not only because the terms 'science' and 'scientific' are present everywhere. The problem of the boundaries of Science is also of great social and political importance. We should not forget that in the late Soviet Union the communist party had the right to decide what science was and what was not, at any given case. Besides, the understanding of what is or is not science influences more or less the scientific

policy of the State, and this has consequences for the advancement or the stagnation of the scientific or the corresponding technological research.

For example, an empiricist's view on what is science favours the blind empirical research without the respective interest for its theoretical foundations: It is well-known in astronomical circles that the United States Air Force keeps an office responsible for the collection and analysis of information concerning the Unidentified Flying Objects (UFOs), which are normally reported to ignore the known laws of Physics and/or carry extraterrestrials! It is also known that several universities keep laboratories dedicated to 'paranormal research', which is at odds with the 'official' natural science and has up to now failed to give a single law for the 'paranormal phenomena'.

Of course, a certain answer to the question of what is science and what gives it its validity and effectiveness could be given – as in the Middle Ages – by resorting to some authority, such as the authority of Aristotle or some other ancient philosophers. But it seems that this solution causes problems. A tradition is known about the Pisa experiment conducted by Galileo: in order to disprove the Aristotelian belief that the heavier bodies fall faster than the lighter ones, Galileo climbed on the Leaning Tower of Pisa holding two objects, one light and one much heavier than the first, and he released them simultaneously to fall to the ground from the top of the Tower. The two objects reached the ground at the same moment, not caring for what Aristotle would say.

The wise professors of the University of Pisa, instead of acknowledging Aristotle's fallacy by means of the experiment, argued that the two bodies did not reach the ground simultaneously; while some that saw the truth thought that their eyes had played a trick to them, since Aristotle did not agree with that outcome. Therefore, the appeal to any authority does not offer necessarily a good answer to such questions; it rather creates more problems.

In the example of the above Pisa experiment tradition one can discern a widely held view of our age concerning what is science. It is the view of the empiricism: All knowledge is acquired through experience, which is the immediate perception of objects and phenomena through our senses. Galileo and Kepler were the first astronomers and physicists who escaped from the view that true knowledge can be acquired only through the study of the classic ancient texts as the writings of authorities, such as of that master of universal knowledge, Aristotle.

According to Alexandre Koyré [11], the scientific revolution of the 17th Century smashed the ancient Greek notion of Cosmos, of the Aristotelian vision, a world of first impressions, and replaced it with an Archimedean Universe of precision, of the 'geometrization' of space and of measure. The real world is not considered anymore a closed, finite and hierarchically structured wholeness, as limited by the mediaeval approach, which explained the world based on the *Bible* in accordance with the ancient Greek geocentric view; instead, it is an open, infinite and vague Universe, defined by the natural laws and by its fundamental components. The clash in the crucial field of Cosmology and the different way to approach and study nature was the point of transit to the final

theory of the Universe without an 'edge'. This clash was provoked by the works of great scientists and philosophers of the 16th and 17th centuries, including Copernicus, Tycho Brahe, Kepler, Galileo, Descartes and Newton.

As Bertrand Russell writes: "*Kepler and Galileo proceeded from the observation of separate events to the formulation of accurate quantitative laws; with their aid future events could be predicted in detail. They annoyed a lot their contemporaries, because not only their conclusions were in stark contrast to the beliefs of that period, but also the blind faith to an authority allowed the savants to limit their researches in the libraries and the professors were utterly upset by the idea that they would have to observe the world in order to learn exactly how it is*" [12].

In this passage Russell gives us the main characteristics attributed to Science by the so-called positivist philosophers, such as John Stuart Mill, Herbert Spencer, or the more recent ones Moritz Schlick, Otto Neurath, Kurt Gödel, Rudolf Carnap and others.

In very broad lines, for positivism science means sure and proved knowledge. Science provides the only method to reach absolute certainty. The scientific theories are built based on general and personal prepositions. According to positivism, we start from the partial, i.e. the personal propositions that describe observations, and we end up with the general, that is the universal propositions, which are the laws of Science.

The two basic principles of the original positivism are:

1. Every piece of knowledge that pertains to events-phenomena is based on the 'positive' elements of experience (the term 'positive' means affirmative);
2. Beyond the world of natural phenomena there is the world of pure Logic and pure Mathematics.

Positivism, as a main component of the physics mentality, is: secular, anti-theological and against Metaphysics; it sticks to the testimony of observation and experience – positive knowledge and experiment. Positivism, by rejecting Metaphysics helped to supersede preoccupations of the past and forwarded the development of the logical physical thought. In a positivistic world view, science is considered the way we can discover the truth and understand the world as good as possible, so that we will be able to predict it or change it [3, p. 94].

6. Conclusions

As a concluding remark, it should be stressed that our treatment of the topic is centred on the Western Christianity - Roman Catholic Church and Protestantism.

In the Orthodox tradition, in the words of theologian G.N. Filias [13], the two opposite trends characterizing the Western tradition – the clericalism of the Roman Church and the absence of clerical power in the Protestant denominations – can't be developed. This is probably why Orthodoxy did not experience situations like the Roman Catholic medieval society, in which

becoming a member of the clergy was considered something relative to the entrance in the mechanism of state (secular power).

Acknowledgements

This study formed part of the research at the University of Athens, Department of Astrophysics Astronomy and Mechanics, and we are grateful to the University of Athens for financial support through the Special Account for Research Grants.

References

[1] K.R. Popper, *The Logic of Scientific Discovery*, by Mohr Siebeck, Routledge Series, Taylor and Francis group Ltd, London, (The problem of Induction), 1959, 27.
[2] K.R. Popper, *Conjectures and Refutations: the growth of scientific knowledge*, reprinted (1st ed. 1963), Routledge Series, Taylor and Francis group Ltd, London, (Science as Falsification), 2004, 33-39.
[3] E. Theodossiou, *The Philosophy of Natural Sciences – From Cartesius to the Theory of Everything*. Diavlos Publ., (in Greek), Athens, 2008, 232.
[4] Nicolaus Copernicus, *De revolutionibus orbium coelestium* (*On the Revolutions of the Heavenly Spheres*), translation and commentary by Edward Rosen, Johns Hopkins University Press, Baltimore, 1992.
[5] C. Darwin, *On The origin of Species*, Oxford University Press, Oxford, 1998.
[6] E. Theodossiou, Astronomical and Astrophysical Transactions, **23** (2004), 75.
[7] E. Danezis and E. Theodossiou, *The Universe I loved – An Introduction to Astrophysics*, vol. II. Diavlos Publ., (in Greek), Athens, 1999, 231 & 237.
[8] W. Windelband, *A History of Philosophy: With Especial Reference to the Formation and Development of Its Problems and Conceptions*, transl. in English by James H. Tufts, Elibron Classics Series, Adamant Media Corporation, The MacMillan Company, New York, 2006, 4 & 466.
[9] E. Theodossiou, *The dethronement of the Earth – The dispute between the geocentric and the heliocentric system*, Diavlos Publ., (in Greek), Athens, 2007, 266.
[10] J. Kepler, *Astronomia nova seu. Physica coelestis*, tradita commentariis De motibus stellae martis, ex observationibus G.V. Tychonis Brahe, Pragae, 1609.
[11] A. Koyré, *From the close world to Infinite Universe*, Johns Hopkins University Press, Baltimore, (Preface), 1992, viii.
[12] B. Russell, *A History of Western Philosophy*, George Allen and Unwin Ltd, London, (The rise of Science), 1946, 551-556.
[13] G.N. Filias, Ephemerios. Publications of the Church of Greece, (in Greek), **58** (2009) 7.

European Journal of Science and Theology, December 2010, Vol.6, No.4, 57-69

THE CONTRIBUTIONS OF THE CHURCH IN BYZANTIUM TO THE NATURAL SCIENCES BYZANTINE ASTRONOMERS AND SCIENTISTS

Efstratios Theodosiou[1], Vassilios Manimanis [1] and Milan S. Dimitrijevic[2*]

[1] *University of Athens, School of Physics, Department of Astrophysics, Astronomy and Mechanics, Panepistimiopolis, Zografos 15784, Athens, Greece*
[2] *Astronomical Observatory, Volgina 7, 11160 Belgrade, Serbia*

(Received 15 September 2010)

Abstract

In this paper, the Natural sciences in Byzantium and the contribution of distinguished scholars are considered. Since they usually were monks, famous schools were in monasteries, and works of antiquity were preserved in monastic libraries, the importance of the Church in Byzantium for Natural sciences is analyzed and demonstrated.

Keywords: Orthodox Church, Eastern Church, Byzantium, Natural sciences, Byzantine monks, mathematicians, astronomers

1. Introduction

A large period of Greek history is occupied by the thousand-year Byzantine Empire. This empire was the Eastern Medieval Christian Empire, which Hélène Glykatzi-Ahrweiler calls *Empire of the Christian East* or *Greek Middle Ages Empire* [1].

The Byzantine period is the connecting link between Greek antiquity and the modern era, as in this period can be found the roots of the modern Greek nation and Orthodoxy. It is customarily approached mainly through Theology, religious art and religious literature; however, Byzantium was an empire whose scholars, mainly men of the Church, contributed also in the Natural sciences and Mathematics. In the following publications we will mention and examine in detail scientists of the Byzantine period and their work in Mathematics, Physics, Astronomy and generally in Science. In this work we shall mention some selected but still largely unknown scholars who cultivated and served the study of Science and especially Astronomy. We also want to underline the role of Church in Byzantium for Natural sciences of that tine, since, as we will

* Corresponding author: e-mail: mdimitrijevic@aob.bg.ac.yu, Phone: +381-11-3089-072, Fax: +381-11-2419-553

demonstrate in the following sections, practically all important scholars working in Mathematics, Astronomy and Physics, were monks, or in general men of Church and monasteries and monastic libraries were of greatest importance for activity of scholars, as well as for preserving the scientific legacy of antiquity.

According to modern Greek historian Anna Lazarou: "The contribution of Byzantium lies not so much in the increase of the corpus of knowledge delivered by Greek Antiquity, but rather in the preservation of many of its achievements, by both copying and saving ancient texts, and by their collection, writing of commentaries and interpreting them." [2]

The truth is that within the period from the 2nd century AD (the age of Claudius Ptolemy) to the 16th century (the age of Copernicus) the general progress of Science including Astronomy is standing rather than advancing. The reasons for such situation were basically the following three:

1. The tremendous authority, almost with a status of a religious dogma, of the two great scientific personalities: Aristotle, in all sciences, and astronomer Ptolemy. Their works, theories and unquestionable scientific presence were the quintessence of science for more than 15 centuries in both East and West. Whoever dared to question one of these two scientific authorities risked of being characterized as ignorant or illiterate, or of facing the mockery and open hostility of the whole scientific community and later on of the Christian Church.
2. The condemnation by the new religion of all who were practicing astrology and star-worship, whose borders with scientific Astronomy were often difficult to discern. So, scientific astronomy was hard to find a critical mass of followers in order to flourish.
3. The general orientation of Byzantium to theological studies rather than to scientific ones. The Byzantine savants preferred to study the teachings of Christianity and to try to pass over messages of tuning the human life according to the divine example of the life of Jesus.

Nevertheless, it is especially interesting to research and record the work of the Byzantine monks and other scholars who, despite the various difficulties discovered ways to cultivate Mathematics, Physics and Astronomy living in an empire that did not favour this kind of studies.

The study of Mathematics and Astronomy in particular experienced a growth during the last period of the empire, in the age of Paleologoi (1261-1453); however even before many scholars, whose names we can mention only selectively, dedicated a part of their time to the study of the sciences, collecting their material from the famous works of the ancient Greek mathematicians and astronomers that had been rescued and preserved in the libraries of the monasteries. At the same time, they were introducing and incorporating knowledge from other nations, by studying Indian, Persian or Arabic books, most of which were also based on ancient Greek sources.

The Byzantine scholars, often in monasteries, were successful in preserving and transmitting positive knowledge and this is the great and neglected contribution to the sciences and especially to Astronomy. They painstakingly studied, wrote commentaries, annotated, copied in new manuscripts in monasteries and finally they rescued and preserved the precious legacy of the ancient Greek philosophers and scientists. For this reason alone their contribution to the sciences would be worthy of every respect. The Byzantine Church and scholars, mainly connected with it, kept for the sake of all humankind the masterpieces of ancient Greek wisdom and science.

Of course there is the counterargument that the Eastern Orthodox Church impeded the research on Astronomy. This argument stems from the writings of the Fathers of the Church; they, however, mainly were expressing their opposition towards the astrologers and not to the mere observation of the celestial bodies. In reality the Orthodox Church depended on Astronomy and on the Alexandrine astronomers for the calculation of the Easter date, while a great number of Byzantine scholars, clergy members and monks were spending many hours on diverse kinds of arts and sciences, from Philosophy-Theology to Mathematics and Astronomy [3].

During the last few centuries of the Empire, Astronomy was cultivated to a great extent in both Constantinople and Trapezous (modern Trebizond); the echoes of the prominence of the Trapezous school of sciences reach our days [4].

It is probable that science was studied by some Byzantine monks and priests with a further aim to compose and to classify knowledge into a harmonic picture in order to serve spiritual cultivation and the exaltation-elevation of man towards God, a task for Theology as well. However, if we study more carefully the work of most scholars we notice that this knowledge, taken from ancient Greek philosophical writings with additions and commentaries by Byzantine savants, was directed towards the shaping of a unified science consisting of the 'septet of courses': Grammar, rhetoric and dialectics on one side and the quadrivium on the other, higher side: Arithmetic, Geometry, Astronomy and Music. All these should essentially serve Theology [5].

The interest and preference for Natural sciences and Mathematics in Byzantium should be placed in this framework. Commentaries were written for many works of ancient mathematicians, astronomers and natural philosophers, such as the Aristotelian *Meteorologics*, *De Caelo* and *Physica Minores*, the Euclidean *Elements* or the *Great Mathematical Syntaxis* of Claudius Ptolemy [6]. It is very probable that this explains the appearance of numerous scientific natural terms into historical (mainly) works, but also even in theological treatises. These terms refer to nature and the natural causes of phenomena such as thunderstorms, thunders, lightning, earthquakes and other [5, p. 219].

2. The philosophical schools and their representatives

The Alexandrine School excelled in sciences such as Medicine, Botany, pharmacology, zoology and agrarian science. Geography continued to be practically important for the Christians, as its knowledge was necessary for the determination of roads to the Holy Places and of the boundaries between ecclesiastical regions of jurisdiction. Thus, using as starting points the work of the ancient cartographer and geographer Marinos of Tyre (60-130 AD), and the famous *Geographike Hyphegesis* by Ptolemy [7] (2nd century AD), Byzantine scholars wrote their own treatises. Geographical studies were carried on almost exclusively in monasteries and the perceptions of Byzantine geographers about Earth (especially those of Cosmas Indicopleustes in the 6th century) were imaginary or copied by the Scriptures and religious ideas, while geographical books had been limited to lists of place names and city guides for school use, on the one hand, and written travelogues on the other; this clearly indicates the difference between ancient Greek geography and what the Byzantines were thinking of as 'geography'.

As a first Byzantine geographer appears the traveller, merchant, monk and author Cosmas Indicopleustes. As a monk, he wrote, on 547 AD, a 12 volumes book work under the title *Christian Topography* [8], in which he attempted to create a new geographical system that would be in accordance with the teachings of the *Bible*.

In Constantinople, a university was established immediately after the founding of the city itself. This institution was known under different names in various centuries, such as Mega or Ecumenical Didascaleion, School of Capitolium, Imperial Auditorium and Pandidacterion [9]. In the 5th century, due to the need for new church buildings, there was a development of Architecture and Civil engineering, something that led to the appearance of good mathematicians, geometricians and engineers, such as Anthemius of Tralles, Isidorus of Miletus and Isidorus of Miletus the Younger, who designed and constructed the famous church of Hagia Sophia (the Holy Wisdom of God) in Constantinople, while Eutocius (6th century AD) from Askalona of Palestine, student of Isidorus of Miletus, knew the first book of Heron's *Mechanics*, now lost [9, p. 175].

From the School of Constantinople emerged the noted Monophysite monk Ioannes (John) Philoponus (490-570), a religious author, philosopher, grammarian, mathematician, physicist, astronomer and one of the most distinguished scientists of the 6th century. Philoponus, who taught in Constantinople in the first half of the 6th century, developed original ideas in Physics, such as the notion of momentum, which opposed the then dominant Aristotelian positions; we will pursue a detailed investigation of his contribution to Physics in a future paper.

3. The Fathers of the Church and the wise bishops

From the 4th until the 8th century the thought of the Fathers of the Church was prevalent with the great Cappadocian Fathers who shaped Christian dogma: Saint Basil the Great, Gregorius of Nazianzos, Gregorius of Nyssa, Saint John Chrysostom; and then Epiphanius of Cyprus, Asterius of Amasseia, Cyril I of Alexandria, Caesarius, Nemesius (bishop of Emessa in Syria) and Dionysius Exiguus, who presented original work in the sciences while at the same time they fought against astrology and foretelling.

Selectively mentioning only Gregorius of Nyssa, we can say that he is considered an expert in the Mathematics and Astronomy of his age, as well as a great cosmologist; it is well known that he wrote that the origin of the Universe was a "seed-like power, offered (by God) towards the creation of everything" [10]. This "seed-like power" speaking in modern terminology, could very well be considered the ultra-dense mass of the Big Bang theory. Finally, the phrase "towards the creation of everything" hints at the dynamics of the cosmic explosion and the movement from the 'potentially' to 'empowered' [11].

In addition, as professor of Philosophy and author G. Zographides writes: "Many Christian church leaders were seeking the compatibility between Greek and Christian thought. To that end, they discovered a great number of passages from ancient texts that were compatible with the Christian teaching and they formulated the theory of the 'seed of the Word' i.e. the presence of seeds of the Christian truth in Greek philosophy." [12]

4. The science in the Alexandrine School

The School of Alexandria was still dominant in the first centuries of the Byzantine Empire, as the former 'world capital of science' in the Hellenistic and the Roman periods. There, scientists such as Serenus of Antinoopolis (Egypt) flourished, or mathematician Theon of Alexandria (330-395 AD), an astronomer who recorded all solar and lunar eclipses from 365 to 372 AD, wrote comments on what Aratos had written about lunar and solar halos, as well as a commentary on Ptolemy's *Mathematical Syntaxis*. This Theon was the father of mathematician, astronomer and philosopher Hypatia, whose student, later bishop of Cyrene Synesius, constructed an astrolabe following her advice.

In the Academia, the School of Athens, in the early 6th century, just before emperor Justinian closed its philosophical school, flourished Simplicius, the famous commentator of Aristotle [13, 14]. Simplicius also wrote commentaries and annotations to works of Euclid, while he rescued parts of works by Parmenides, Empedocles and Anaxagoras. In about the same period the works of Stephanus of Alexandria are placed [15].

5. The middle Byzantine period (610-1204 AD)

In the middle Byzantine period flourished Ioannes of Damascus or Chrysorrhoas (676-754), who knew well Aristotle's works and considered Philosophy as a knowledge that served Theology. From this idea stemmed the dominant perception in Western mediaeval thought that Philosophy is the servant of Theology.

According to the late professor of Astronomy at the University of Athens D. Kotsakis, Ioannes of Damascus occupied himself with Astronomy and the other natural sciences: "Ioannes of Damascus (1st half of VIII century) occupies himself with Astronomy and more general with Nature, while he fights against astrology and foretellers with great zeal." [16]

Ioannes of Damascus, in his work – as it has been treasured up in *Patrologia Greca* (volume 94) – offers excellent descriptions for various natural and celestial phenomena, such as the eclipses of the Sun and the Moon, which he describes in detail [6, vol. 94, p. 896]. At the same time he fights against astrology [6, vol. 94, p. 892-903], while he also describes natural phenomena like the thunderbolt, for which he offers a truly scientific description: "the thunderbolt is a helical spirit moving as fire, which travels downwards by flaming fire and lightning all around" [6, vol. 94, p. 1601]. However, the access to the natural phenomena and to their explanation was impossible. Basically in Byzantium the dominant way of thought was the theological one, which from its subject of study was directed towards the transcendental world. Ioannes of Damascus himself writes: "The things of nature seem senseless, because whatever relates to God is beyond nature, rational thinking and arguing. The knowledge of these things is knowledge of the soul and demon-like." [6, vol. 94, p. 895]

Essentially, this scholar leader of the Church with his previous views differentiated theological thought from apocryphal knowledge, which (Neo-Platonic in its essence) was based on the correspondence between the powers of a 'cosmic soul' (in which participates the human soul) and the powers of nature and material beings [2].

Of course, these views were based on the 'reborn' Platonism, which, as Neo-Platonism after the 4th century AD, offered the belief that life is not real and that God is by no means a part of this earthly world.

Leon the Philosopher or the Mathematician flourished as a scientist about 820-869 and later he became bishop of Thessalonica. Leon was a real polymath, with knowledge of Philosophy, Arithmetic, Geometry, Astronomy and Music, which he taught in Constantinople, while his fame reached the Caliph Al Mamoun in Bagdad, who invited him to teach in his capital [17]. Leon was an excellent teacher in many disciplines, so his contemporaries gave him the appellations 'the Philosopher', 'the Mathematician', 'the Geometrician' and 'the Astronomer', which they were using alternatively. He was also called 'the myriad-math among philosophers'.

This Leon constructed an optical telegraph or 'horonomium', which reinforced his reputation considerably. It was an optical mechanical system of information transmission that was used extensively by the Byzantine armed forces as a method of fast warning for Arab invasions in the empire. The horonomium, which today could be named 'optical military telegraphy', was based on synchronized clock mechanisms and a system of suitably located fire-signaling posts. Leon also constructed several automata that decorated the imperial palace. Also, we will pursue a detailed investigation of his contribution to Astronomy in a future paper.

During the Macedonian Dynasty, about 890, flourished Photios, the Patriarch. This was the period when the study of the holy books of Christianity is properly combined with the eternal texts of Greek antiquity. The scholars of the age discovered in monasteries the manuscripts of the classics and studied them, commented on them, copied them and classified them into codices. It was then that the first awakening of Science in the form of an official regeneration took place, with the polymath Photios, the author of *Myriobiblos*, as its main representative: when he became Ecumenical Patriarch with the support of his protector Caesar Vardas (†865), he re-established in Constantinople the study of ancient Greek philosophers. "The preparatory stage for metaphysics was offered by the writings of Plato, Plotinus and Proclus. In its final stage, the philosophical teaching of Metaphysics was reduced in Theology, the first philosophy." [18].

The monk and scholar Michael Psellus (1018-1078/1096) served as *logothetes* (minister) of the emperor, while his unsurpassed teaching at the university led to his characterization as the 'supreme philosopher'. His works were innumerable and of diverse content: philosophical, mathematical, geographical, medical, theological, and even about folklore. This polymath wrote also a historical work, the *Chronographia*, where he describes the events from 976 up to 1077 as they were interwoven around the lives of the emperors of that age [19].

Michael Psellus wrote a commentary on Aristotle's *Physica* and the meaning Psellus gave to the term 'physis' (nature) was followed by many subsequent philosophers. However, the restoration of a rationalistic spirit in the examination of natural phenomena did not accord with the dominant religious world view, for which the meteorological or other natural phenomena merely denoted God's intervention in the world. Of course here the philosophical thinking was more than necessary. According to Anna Lazarou: "The need for rational explanation led to the search for a scientific method, which could be offered only by the Greek philosophical tradition. According to Psellus, in order to explain things there was no other way apart from the search of their natural cause." [2]

This view resulted in Psellus following the Aristotelian practice, which stated that every being is governed by the laws of its own nature. In this point he was trying to reconcile the two different world views: while he did not want to abandon the Aristotelian position on the research of natural phenomena, he also did not want to question God's omnipotence upon the beings and the phenomena

of nature. Of course, this led him to Neo-Platonic principles, since Neo-Platonism accepted that nature is the last link of a continuous causal chain, which started with a transcendental first cause.

Both Michael Psellus and the scholar Joseph Bryennios (1350-1431), based on the texts of ancient Greek philosophers, are considered the first Greek folklorists, who attempted to record popular superstitions, to explain or to disapprove them. They were basically trying to relieve the world from superstition.

In Geography was distinguished the bishop of Thessalonica Efstathios Katafloros (1125-1194) with his work *Extensions (Parekvolai) to Dionysius the Traveler* (1170) and the monk Ioannes Fokas with his *Itinerary* (1177).

Professor Helias Pontikos writes that: "The prerequisite that favoured considerably the study of the natural phenomena, the study of Astronomy, Meteorology, Geography and Medicine, was the acceptance by Byzantine and Church-father tradition of the differentiation of human wisdom into three distinct parts: i) practical, aiming at the moral improvement of the individual, ii) natural, aiming at the study of nature as God's creation, and iii) theological, aiming at the enlightenment and the union of the individual with the divine." [20]

Astronomers in the 11th century were Symeon Seth or Sethes (2nd half of 11th century) and Eleftherios Zevelenos (he was born in 1040), while after them the prolific author Efstratios of Nice (1092-1120) wrote several philosophical works, mainly commentaries and annotations on Aristotle's *Analytics*, and the *Philosophical Definitions*. In his later works he turns his interest to the sciences, especially Meteorology and Astronomy; these works include a treatise on Natural sciences under the title *Meteorologics*. Both this treatise and his commentary on two books of Aristotle *The Nicomachean Ethics* [21] and two books on *Posterior Analytics* [22] were translated in the West and were known to both Albert the Great (1193 or 1206-1280) and Thomas Aquinas (1225-1274), while during 19th century the famous theologian and classical philologist Friedrich Ernst Daniel Schleiermacher (1768-1834) believed that they were an excellent piece of work [23].

Efstratios of Nice (1050-1120) and Michael of Ephesus (11th-12th century) – who wrote on Natural history and Zoology – represent the rationalistic movement of theologians-commentators of Aristotelian works, who used Aristotelian reasoning on theological problems. This movement influenced a lot the Western thought towards Aristotelian thought.

A great number of educated monks and priests who wrote on sciences follows, from Constantine Manasses (1130-1187), who describes in his work the 'horonomium', the invention of Leon the Mathematician that we have described already, to Prodromos Monachos (12th century).

Prodromos Monachos (*monachos* = monk) studied Mathematics and Astronomy in Constantinople. Then he moved to Bithynia, in Asia Minor, where he became a monk. Being a notable teacher, he founded a school in Scamander of the Trojan fame. Among his students – sometime after 1222 – we find the

great theologian, astronomer, mathematician, geographer and medical doctor Nicephoros Vlemmydes (1197-1272) with a pioneering work on the sciences and author of books such as the *Epitome of Physics* [24]. Louis Bréhier refers to him as "the most famous savant of his age" [25].

Then came Georgios Akropolites and his students Georgios of Cyprus (*c.* 1241-1290), who was subsequently ordained Patriarch under the name Gregory II, and Georgios Pachymeres (1242-1310), a teacher and philosopher who wrote rhetorical works, letters and above all his famous *Syntagma of the four courses, Arithmetic, Music, Geometry and Astronomy* or *Tetrabiblos* (Quadrivium). The late professor of Astronomy D. Kotsakis writes about this work and its author: *"This work alone would suffice to raise Pachymeres to the first grade of mathematicians of his age in both East and West, because it is written in a higher scientific spirit. Pachymeres easily uses the ancient and later authors, but he subjects their views in critic and stresses his personal views, which persuade the reader."* [26]

6. The 'new' Byzantine empire (1261-1453)

Contrary to the adverse political situation, the arts and letters flourish during the third and last Byzantine period, to the point that historians speak of a 'Paleologian Renaissance' in a severely territorially restricted empire. After the repatriation of 1261, emperor Michael VIII Paleologos ordered the restoration of all schools and appointed Georgios Akropolites as the director of the re-organized public university in the church of Hagia Sophia.

In this period flourished many savants, such as the scholar philologist, mathematician and astronomer Manuel Planoudis (1260-1310), who was born in Nicomedia of Bithynia (today Isnik) and was educated in Constantinople. Planoudis is considered one of the greatest philologists of his age and one of the Byzantine scholars who heralded the renaissance of classic studies in the West. In 1285, when he became a monk, he changed his name to Maximos and became known under this first name. Planoudis was teaching since the age of 20, in 1280, at two monastery schools in Constantinople. His Latin was excellent and he translated works of the Latin literature in Greek, works by Boethius (Boethius Anicius Manlius Torquatus Severinus), Cato the Elder, Ovid, Cicero, Julius Caesar, pseudo-Augustine, Thomas Aquinas, etc., starting with *De consolatione philosophiae* of Boethius, thus preparing the connection between the Byzantine civilization and the West.

Finally, Astronomy was served in that period by Theodoros Metochites (1260/61-1331), "one of the most important polymaths of the last centuries of the Byzantine empire" according to Karl Krumbacher [27]. He was succeeded by his student, Nicephoros Gregoras (1295-1360), arguably the greatest astronomer of all periods of the Byzantine empire [28]. Isaac Argyros (1310-1375), the student of Nicephoros Gregoras, is considered the most important expert on Ptolemy's astronomy. Both Gregoras and Argyros insisted on the need for a reformation of the Julian calendar. The contemporary astronomer

Theodoros Melitiniotes (1310-1388) is probably the second greatest Byzantine astronomer after Nicephoros Gregoras, with his work *Three Books on Astronomy* or *Astronomical Tribiblos* (*Tribiblos Astronomique* [29, 30]) being the most comprehensive and well-edited Byzantine astronomical work.

7. Scientific activity in Trapezous

In Trapezous a small tradition in Astronomy is created with Gregorios Chioniades (1240/50-1320), who knew Arabic and Persian astronomy and established the 'Trapezous Academy', Georgios Chrysococca, Constantinos Loukites or Lykites, Andreas Livadenos and the monk Manuel.

The late professor of History and Philosophy of Natural Sciences at the University of Athens Michael Stefanides mentions [31] Gregorios Chioniades as a 'myst' of the Persian astronomy together with Constantinos Loukites (1938, 217). The scholar Constantinos Loukites (13^{th}-14^{th} century) was professor at the Trapezous Academy. Appreciating his value and abilities, king Alexios II MegaComnenos (1297-1330) honored him with state offices.

Scholar Andreas Livadenos (14^{th} century) was honoured with the offices of *prototabularius* and *chartophylax* of the Trapezous Church. His work was mainly geographical, while he also wrote letters and poems. Both Livadenos and Loukites had a correspondence with Chioniades and Nicephoros Gregoras.

According to Herbert Hunger: *The monk and clergyman Manuel, who knew Farsi, is reported as the man who taught astronomy to Georgios Chrysococca* [32]. He became an astronomer by studying all the books on Physics, Mathematics, Astronomy and Medicine brought by Chioniades in Trapezous from Tabriz, a city in northwestern Iran that was then a centre of science.

In parallel monk Manuel taught in the schools of the monasteries of Saint Eugenios and Hagia Sophia in Trapezous. These 'schools' were probably the Trapezous Academy, which was hosted in the beginning in the monastery of Saint Eugenios, who was the patron saint of the city; this monastery was outside of the city's walls and after its destruction by fire (1340) the Academy was transferred in the Hagia Sophia monastery, about half an hour away from the city by foot [4, p. 365].

Finally, the Byzantine scholar, medical doctor and astronomer Georgios Chrysococca (14^{th} century), student of monk Manuel, published a famous astronomical work with the title *Synopsis tabularum persiacarum ex syntaxi Persarum Georgii medici Chrysococcae* (1347). It was published by Ishmael Bullialdus in Paris in 1645 [33]. R.H. Allen [34] refers to this work as 'Chrysococca's *Tables*.

8. The empire's last years

In the last decades of the Empire the view that the Earth is spherical is expressed by Georgios Yemistos or Plethon (1355-1452), who also proposed the introduction of a complete lunisolar calendar, not unlike the ancient Attic calendar, useful for the new religion he was preaching as suitable for the Greek (not Christian) nation, based on a Neo-Platonic morality.

The siege of Constantinople by the Ottoman Turks and finally its capture marks the start of a wave of emigration of scholars and scientists to the West. The Aristotelians Theodoros Gazis (1400-1476), Andronicos Callistos (1400-1486), Georgios of Trapezous (1396-1486), Theophanes of Medeia (†1480), as well as the Platonic Michael Apostolios (1420-1480), Ioannes Argyropoulos (1415-1487) and the subsequent Cardinal Bessarion (1403-1472) influenced in a positive way the Italian thought and the renaissance of sciences. Already Manuel Chryssoloras (1350-1415) had played a catalytic role by establishing in the University of Florence chair of Greek literature (1397-1400), the first such chair in the educational history of Europe. Manuel Chryssoloras is considered the first important pioneer of the Renaissance. In 1434 with the ascent of the House of Medici a new era begins in the intellectual life of Florence. Georgios Yemistos settled in this city and began to teach Plato, followed by Ioannes Argyropoulos, Demetrios Chalcocondyles (1423-1511), the Italian poet and humanist Angelo Politano (1454-1494), Janus Laskaris (1445-1534) and Michael Marullos of Tarchania (1499), who are the most well-known scholars who transferred in Italy not only the contest between Aristotelian and Platonic philosophers, but also a genuine intellectual activity, thus contributing to the Renaissance of the arts and letters in Italy and from there in the whole Western Europe.

All the above philosophers and scientists also contributed decisively to the so-called 'awakening of science' in the West; this element is added to the many others that indicate the important role Byzantine scholars played in 'firing' the Renaissance in Europe. Fortunately for the European civilization the intellectuality of Byzantium continued in the West and did not expire with the capture of its capital city. This way, through the Byzantine civilization a whole period. that of the Renaissance based its essence in the ancient Greek legacy. Moreover, the following centuries in Europe, even the 18th and the 19th, were immersed in the ancient Greek spirit.

At the same time, in the occupied by the Turks Greece the life of the nation was on the hands of the Church. Gennadios Scholarios, the first Ecumenical Patriarch after the Capture, an Orthodox 'Aristotelian' thinker and an admirer of the Western Scholasticism, was given by the capturer sultan Muhammad II the Church privileges over the captured nation that would save its identity.

The Orthodox Church would stay through all the following difficult centuries until the Greek independence as a steady column that covered not just the religious needs of the enslaved nation but also its cultural and educational needs. The independence, four centuries later, would also spring from within it.

Acknowledgements

This study formed part of the research at the University of Athens, Department of Astrophysics Astronomy and Mechanics, and we are grateful to the University of Athens for financial support through the Special Account for Research Grants. It is also supported by the Ministry of Science and Technological Development of Serbia through the project 146022 'History and Epistemology of Science'.

References

[1] H. Glykatzi-Ahrweiler, *Why Byzantium?*, in Greek, Ellinika Grammata Publ., Athens, 2009,10.
[2] A. Lazarou, Istorika Themata, **91** (2010) 60.
[3] E. Theodossiou and E. Danezis, *The Odyssey of the calendars,* Vol. II, in Greek, Diavlos Publ., Athens 1996, 160.
[4] S. Plakides, *Aktines*, **53** (1946) 318.
[5] F. Koukoules, *The life and civilization of the Byzantines*, vol. I, in Greek, Papademas Publ., Athens, 1948, 129.
[6] J.-P. Migne (ed.) *Patrologiae cursus completus, series graeca.* Typographi Brepols Editores Pontificii, Turnholti, 1857-1866.
[7] Ptolemy, *Klaudiu Ptolemaiou Geographike Hyphegesis*, translated in Latin by Karl Müller, Alfredo Didot, Paris, 1883.
[8] Cosmas Indicopleustes, J.W. McCrindle (ed.), *The Christian Topography of Cosmas Indicopleustes*, Hakluyt Society, city, (Reissued by Cambridge University Press, 2010), 1897.
[9] E. Theodossiou and E. Danezis, *At the years of Byzantium*, in Greek, Diavlos Publ., Athens, 2010, 130.
[10] Gregorius of Nyssa, *Apologetic speech about the Six-day Creation*, in *Patrologia Greca*, J.-P. Migne (ed.), vol. 44, Typographi Brepols Editores Pontificii, Turnholti (Turnhout), 1857-1866, 77D.
[11] G. Metallinos, Christianiki, **February 9** (2006) 5.
[12] G. Zographides, *Byzantine Philosophy,* in *Greek Philosophy and Science: From the Antiquity to the 20th century*, S. Virvidakis et al. (eds.), vol. I, Greek Open University, Patra, 2000, 347.
[13] Simplicius, *On the Heavens (De Caelo). Priores Commentaria*, Hermannus Diels (ed.), Typis et Impensis G. Reimeri, Berolini (Berlin), 1882-1895.
[14] Simplicius, *On Aristotle's Physics (In Aristotelis Physicorum, Libros IV)* 24, 13 (Z. 3-8 aus Theophrastus Phys. Opin. Fr. 2 Dox. 476), Priores Commentaria, Hermannus Diels (ed.), Typis et Impensis G. Reimeri, Berolini (Berlin), 1882.
[15] M. Papathanassiou, *The Apotelesmatiki Pragmateia or Islamic Horoscope of Stephanus of Alexandria*, in *The Sciences in the Greek area*, in Greek, Center for Modern Greek Studies of EIE. Trochalia Publ., Athens, 1977, 107.
[16] D. Kotsakis, Deltion Geographikis Ipiresias Stratou, **3/4** (1958) 8.
[17] P. Lemerle, *Le premier Humanisme byzantin, Notes et remarques sur enseignement et culture a Byzance des origines au X^{e} ciècle*, Presses Universitaires de France, Paris, 1971, 130.
[18] B.N. Tatakis, *La Philosophie byzantine*, Presses Universitaires de France, Paris, 1949, 164.

[19] M. Psellus, *Chronographia*, translated in English by E.R.A Sewter, Yale University Press, New Haven, 1953, available on line at http://www.fordham.edu/halsall/basis/psellus-chrono00.html.
[20] H. Pontikos, *The revival of Aristotle as a physicist in the 11th century in Byzantium*, in Greek, Dodone Publ., Athens, 1992, 83.
[21] Aristotle, *The Nicomachean Ethics*, with an English Translation by H. Tredenick. William Heinemann Ltd., Harvard University Press. London, 1968.
[22] Aristotle, *Posterior Analytics, Topica,* with an English Translation by H. Tredenick & E.S. Forster. William Heinemann Ltd., Harvard University Press., London, 1960.
[23] D.K. Georgoulis, *History of Hellenic Philosophy*, in Greek, Papademas Publ., Athens, 2007, 771.
[24] N. Vlemmydes, *Epitome of Physics*, in *Patrologia Greca*, J.-P. Migne (ed.), Typographi Brepols Editores Pontificii, Turnholti, 1857-1866, 1023.
[25] L. Bréhier, *La civilization Byzantine*, Editions Albin Michel, Paris, 1950, 479.
[26] D. Kotsakis, Deltion Geographikis Ipiresias Stratou, **3/4** (1956) 111.
[27] K. Krumbacher, *Geschichte der Byzantinischen Litteratur von Justinian bis zum Ende des oströmischen Reiches (527-1453)*, Nabu Press. Bookseller Inventory, München, 1891 und 1897, 288.
[28] E. Theodossiou, V. N. Manimanis, M. S. Dimitrijevic and E. Danezis, Astronomical and Astrophysical Transactions, **25** (2006) 105.
[29] R. Leurquin, *Théodore Méliténiote Tribiblos Astronomique*, Livre I (Corpus des Astronomes Byzantins 4), Gieben, Amsterdam, 1990.
[30] R. Leurquin, *Théodore Méliténiote Tribiblos Astronomique*, Livre II (Corpus des Astronomes Byzantins 5-6), Hakkert, Amsterdam, 1993.
[31] M. Stefanides, *An Introduction to history of Natural Sciences*, in Greek, Publications of the University of Athens, Athens, 1938.
[32] H. Hunger, *Die hochsprachliche profane Literatur der Byzantiner*, Beck, Munich, 1978, 57.
[33] I. Bullialdus (ed.), *Synopsis tabularum persiacarum ex syntaxi Persarum Georgii medici Chrysococcae* (1347), Astronomia Philolaica, Paris, 1645.
[34] R.H. Allen, *Star Names - Their Lore and Meaning*, Constable & Co., Dover edition, London, 1963, 121.

European Journal of Science and Theology, June 2011, Vol.7, No.2, 33-47

THE CONTRIBUTION OF BYZANTINE PRIESTS IN ASTRONOMY AND COSMOLOGY
I. THE CHURCH FATHERS: THE THREE BISHOPS ST. BASIL THE GREAT, ST. GREGORY OF NAZIANZUS AND ST. JOHN CHRYSOSTOM

Efstratios Theodosiou[1], Vassilios Manimanis [1] and Milan S. Dimitrijevic[2*]

[1] *National and Kapodistrian University of Athens, School of Physics, Department of Astrophysics, Astronomy and Mechanics, Panepistimiopolis, Zografos 15784, Athens, Greece*
[2] *Astronomical Observatory, Volgina 7, 11160 Belgrade, Serbia*

(Received 18 January 2011, revised February 2011)

Abstract

The life and work of the three Cappadocian bishops: Saint Basil the Great (330-379), Saint Gregory of Nazianzus (329-390) and Saint John Chrysostom (347-407), as well as their contribution to the Natural sciences, especially to Astronomy and Cosmology, have been examined and considered.

Keywords: Byzantium, Natural sciences, Cosmology, History of astronomy, Basil the Great, Gregory of Nazianzus, John Chrysostom

1. Introduction

On the opposite side of Emperor Julian and of the scholars who practiced astrology during the early Byzantine period, a number of Church Fathers ('Doctors of the Church') and bishops flourished and left a legacy in Philosophy and Science without belonging to a school, or representing one.

Some of these Church scholars were educated in the neo-Platonic school of Athens and they essentially formulated the Christian dogma, representing Christianity, since the Christian philosophy of that age was shaped on the basis of neo-Platonic and Aristotelian influences.

The main representatives of this current of thought in the early Byzantine period are above all others the three Church Fathers from Cappadocia: Saint Basil the Great, Saint Gregory of Nazianzus and Saint John Chrysostom.

[*] Corresponding author, e-mail: mdimitrijevic@aob.bg.ac.yu, Phone: +381-11-3089-072, Fax: +381-11-2419-553

These three were followed by the eminent bishops Saint Gregory of Nyssa, Epiphanius of Cyprus, Asterius of Amasseia, Cyril I of Alexandria, Synesius (who can be said to represent the school of Alexandria), Caesarius, Nemesius of Emessa (Syria) and finally the monk Dionysius Exiguus, who compiled *Easter Canons*.

This first paper on the Church Fathers and bishops deals with the Cosmology of the three great Cappadocian Fathers, the 'Three Prelates' as they are known in Greece; in a following paper we will examine the work of other eminent bishops and their contribution in the natural sciences.

2. The golden age of Theology and Ecclesiastical rhetorics

During the first century of its life, the Eastern Roman Empire, later called the Byzantine Empire by historians, struggled to discover and then to impose its new, Christian identity. In this context it was very important to construct the Christian dogma and a world view based on the Old Testament; on these two challenges were concentrated the efforts of the Christian scholars. This twin feat was achieved by the great Cappadocian bishops Saint Basil the Great (330-379), Saint Gregory of Nazianzus (329-390) and Saint Gregory of Nyssa, who was brother of Saint Basil. Thanks to them and to Saint John Chrysostom (347-407) the 4th century AD was called the 'Golden Age' of Theology and ecclesiastical rhetorics.

Professor Athanassios V. Vertsetis writes in his book *General Didactics* about the evolution of the art of teaching: *"The Fathers of the Church faced the issue of the methodology of teaching within the frame of the needs of Church rhetorics and catechism, and they examined the whole topic only relative to the monologic persuasive preaching. The Byzantine empire, as it is known, contributed nothing to the sciences; the Aristotelian dogmatism that prevailed during the whole Medieval period did not favor creative advances."* [1]

It is true that initially the position of the official Church, as a representative of a new and novel religion that was expanding to the point of prevalence, was quite negative towards the gentile science, since the latter was a product of the ancient pagan world. However, Astronomy was indispensable, because a calendar should be devised for the determination of the Christian holy days, especially of the date of the Easter. For this reason the wise bishops studied Astronomy and through this knowledge they approached the Cosmology and cosmogony of the *Old Testament*. Actually, in order to reconcile the astronomical views of their age with the cosmogony described in the Book of *Genesis*, they wrote treatises *On the Six-day Creation (Peri Hexahemerou* or *On Hexameron)* that became staple texts of the spiritual production of the 4th century [2]. As Th. Nikolaidis writes, *"The most important texts were the 'Homilies to the Six-day Creation' by Saint Basil the Great and those by his brother, Saint Gregory of Nyssa, treatises that exerted an especially strong influence, not only in the East but also in the West."* [3].

Most bishops were involved, in addition to their pastoral and theological work, in teaching and Astronomy, the science of time measurement and of the heavens, while they also wrote about Astronomy and cosmogony. Let us examine first the life and work of the three Cappadocian bishops: Saint Basil the Great, Saint Gregory of Nazianzus and Saint John Chrysostom.

3. Saint Basil the Great (330-379)

Basil (Vassilios) was born in Neocaesareia, on the Black Sea shore, in the year Constantinople was founded (330). His family was a pious Christian one; his father was Basil, a teacher of Rhetorics and his mother Emmeleia. His grandmother, Macrina, was a daughter of a martyr and she was taught the primal Christian theology by Gregory the Illuminator (c. 257–c. 331), the patron saint of Armenia.

After he received an elementary education in Neocaesareia, Basil continued his studies in Caesareia of Cappadocia, in Antioch, in Constantinople (under the gentile orator Livanius) and in the famous neo-Platonic school of Athens, where philosophers Imerius and Proaeresius were teaching. In these student years Basil became a friend of Gregory of Nazianzus, while he also met with Julian, the subsequent Emperor Julian the 'Renegade' (*Paravates*). When he returned in his homeland, Basil followed a monastic life for quite a while. In Caesareia Basil was ordained a deacon, a priest and later on he became a bishop (370-379). After his death he was elevated to the ranks of the saints of the Church due to his broad work as a philanthropist; his younger brothers Gregory of Nyssa and Peter of Sebasteia, and sister Macrina, were also sanctified.

During the several years of his studies Basil received a wide classical education. He studied Grammar, Rhetorics, Medicine, Philosophy, Geometry, Mathematics and Astronomy. However, as far as the study of Astronomy is concerned, Basil in his *Homilies to the Six-day Creation* (*The Hexæmeron,* 379 AD) writes: *"What is the meaning of Geometries and of the methods of Mathematics, of the stereometries and of the much-celebrated Astronomy, of all this multi-sided vanity, if all who ardently keep themselves busy with them made the thought that the world we see has the same origin with the Creator of everything God, thus equating in grandeur the limited and material world with the limitless and invisible nature?"* [4].

Nevertheless, it seems that when Basil the Great calls Astronomy a 'vanity' he most probably means what we now know as astrology. This view is supported by the fact that in other texts he considers the observation of the stars necessary, because through it, as he writes, we become acquainted with the divine wisdom and we receive important precept from its knowledge; but up to a certain point: one should not examine the stars beyond what is necessary. Indeed the polymath Father of the Church notes: *"What other does the moon teach us by becoming full and waning once again, except to avoid thinking great about the prosperities of life? I only suffice not to examine the signs that come from the stars beyond what is necessary."* [4].

Basil's classical culture enabled him to teach properly in his *Treatise towards the young* [5] on the issue of the place of the secular education in the Christian school and, in doing so, to influence the stance of the Church with respect to the classical education both then and during the Renaissance.

According to the late professor of Byzantine studies N. Tomadakis: "*While Basil the Great wrote a treatise on how children would benefit from the Greek texts, it should not be assumed that in this work the Church Father was advising the youth to adopt the thought of the classics; on the contrary. In books full of wrong beliefs and myths he was able to find several episodes that possessed a moral value and hence they could be used to form the character of the Christian children, nothing more. Basil and the other great Fathers studied of course excellent Greek in the Greek schools of Athens and of the East, however the influence of the Jewish spirit through the Scriptures was deep upon them… They studied the Greek authors for the favour of Rhetorics. The beautiful, the aesthetically good element, was of no interest to them when it was unrelated to the true and attached to the gentile element. And 'true' was only the revealed religion as a relation to God, while moral was only the teaching of Christianity.*" [6]

Basil studied Astronomy in Athens and his views on the cosmological visualization of our World are noteworthy, showing his effort to render the Greek and Hellenistic model of the Universe compatible with the Book of *Genesis*. According to G. Katsiampoura [7]: *"Basil was opposed with fervour to the view that the world is eternal ('aidius'), without a beginning or an end, an Aristotelian view already well-established in the 4th century. Without formulating a new personal cosmology, Basil adopts the cosmology of the Book of Genesis about the creation of the Universe out of nothing by the Christian Creator, as mentioned by V.N. Tatakis [8]. This perception, which will form the official cosmological view in the Medieval times, lies under the fact that Ptolemy's main cosmological work, the '*Hypotheseis Planomenon*', does not experience the dissemination of the respective astronomical work of the same author. On the other side, as far as the shape of the Earth and its place at the centre of the Universe are concerned, these are accepted by Basil as they are described by Aristotle and the Ptolemaic system without question. The only new element added by Basil with respect to the Universe is the existence of an additional sphere, that of the celestial waters, beyond the 8th sphere of the fixed stars described by Ptolemy. This ninth sphere separates the world of the material creation from the world of God. Much later, in the Medieval Age, even more spheres would be added. Nevertheless, the cosmological view expressed by Basil and adopted by the Church could coexist with the Ptolemaic system of the world; it is impossible to replace Ptolemy's astronomical system, because it is incomplete, interested more in the first cause of the Creation, cosmogony, than in the astronomical calculations of the Alexandrine savant and of his succeeding astronomers, as Th. Nikolaidis mentions [3]."*

4. The schools of Antioch and Alexandria

As a conclusion it can be said that Christian cosmology's foundation was laid by the work of Basil the Great, who, having studied in the gentile schools, was well acquainted with the principles of the Greek cosmology: The Earth was spherical, surrounded by a spherical sky and other spheres, the uppermost one being the vast 8th sphere of the fixed stars.

As a Christian priest, however, he also knew well the Jewish cosmology of the Book of *Genesis*. This cosmology is purely theological in its content, describing the Universe indirectly, through its creation by the omnipotent God within six days. According to this view of the world the Earth is supported by waters under it, the Sun is on the firmament along with the other (the fixed) stars and everything is surrounded by the universal waters, in accordance with the Babylonian model of the Universe [9].

We should not be impressed by this general view of the wise men of that era. Even today, during the Orthodox service of the Good Thursday it is chanted: "*… the One who suspended the Earth among the waters*."

In addition, according to the Judeo-Christian model of the Universe, this has one beginning: the moment of its creation by the creator God. It also has an end: during the Second Coming. All these should be coupled with the Greek/Hellenistic cosmology and some views should be eliminated ─ for example the fact that in the Greek cosmology of Aristotle and Ptolemy (2nd century AD) there was the sub-lunar destructible space and the space above the Moon, which was eternal and indestructible; this was an unacceptable view for a Christian thinker, since only God can be eternal and indestructible: if the space above the Moon had these properties, then the creation itself would be equally important with the creator God!

Following the description of the world's creation within six days, the Christian scholars, including Saint Basil the Great, entitled their works *On the Six-day Creation* (*Peri Hexahemerou* or *On Hexameron*). Essentially, despite the fact that Basil was educated in the Neo-Platonic school of Athens, his philosophy and ideology approaches more the views of Clement of Alexandria (c.150-211/216), Origen (185-251) and especially the theology of the Jewish scholar Philo of Alexandria (25 BC-40 AD). Through all these thinkers and subsequently by Augustine of Hippo (354-430), who was influenced a lot by the texts of both Saint Basil the Great and Saint Gregory of Nyssa, Platonic philosophy was introduced in the deeper theological core of the Christian Church [10].

Philo of Alexandria was the most important representative of the Alexandrine Jewish theology; he attempted to combine and reconcile Greek philosophy, especially the 'most holy Plato', with the wisdom of the Scripture (our *Old Testament*). His ideas stem from the notion of God as a clear, absolute, super-perfect and blissful entity, of whom we know only the existence, but not the essence.

The term *hexahemeros* ('six-day') occurs first in the writings of this Platonic philosopher and through Theophilus, the sixth bishop of Antioch (since 169) [11], was passed to the subsequent Fathers and was essentially established by Basil the Great with his famous *Nine Homilies to the Six-Day Creation* [12]. It is natural that here the views of two eminent Christian schools of thought slip into and are combined in this work. On the one side the worldview of the Antioch, which more or less interprets the Scriptures literally and expresses the Asian cosmological views (flat Earth and Universe of various shapes). On the other side the worldview of the Alexandria school, which due to its Greek and Hellenistic background interprets *Genesis* in a more metaphorical way in order to adapt it to the more advanced cosmological system of the Alexandrine natural philosophers, with its spherical Earth and a spherical Universe that has the Earth at its centre [13].

5. The heresies torment the Church

From the middle of the 4th century up to the 8th century various heresies and schisms trouble the Christian Church and more generally the Christian empire. The Church reacts through the Ecumenical Councils in its attempt to clarify and establish the Christian Faith. This had the effect that everything was centred through the topic and scope of the unity of the Church, which also reflected the unity of the empire. Therefore, it was very difficult for any scholar to think of and work on something different.

The great theological antitheses arising with these heresies, which were often oppositions between different cosmogony or cosmological views, lasted for about five centuries and they were recorded in the decisions of the Ecumenical Councils and in the texts of the Church Fathers. These differing views were often based upon different philosophical positions; for example the Nestorians, the followers of Nestorius of Constantinople, represented the Aristotelians of the Antioch school and they opposed to the Platonists of the Alexandrine school, led by Cyril I of Alexandria. Several heresies created a world model that was different from that of the Old Testament [14].

6. The works of Saint Basil the Great

Basil ended up as a very prolific author of the Church, a Father who struggled for Orthodoxy and against the heretical views of his period. First of all, he opposes to many views of the ancient Greek philosophy that do not agree with the Christian cosmological model; in addition he strongly opposes to certain Christian heretical views that also express or imply a world model different from that of the *Old Testament*.

For his tireless teaching and writing despite his fragile health, Basil was called by the Church 'Great' ecumenical Teacher. All of his works can be found in the *Patrologia Graeca* [15].

Basil's works can be divided into four broad categories: dogmatic, practical, homilies and epistulae (letters).

6.1. Dogmatic

- *Refutation of the Apology of the Impious Eunomius (Adversus Eunomium);*
- *On the Holy Spirit.*

6.2. Practical

- *Ascetics (Asketika),* of which the main genuine parts are the *Moralia*, the *Regulae tractatae* (in 55 + 80 chapters) [15, vol. 31, pp. 905-1052 and pp.1052-1306], works that were used as the basis of the monastic life in the East;
- *Address to Young Men on Greek Literature* (alternatively: *Address To Young Men On How They Might Derive Benefit From Greek Literature*), where he expands on his view that the Greek literature has a relative value, which is preparatory for the understanding of the Holy Scriptures, and therefore only those Greek texts that teach us virtue should be read;
- *Two Homilies on Baptism;*
- A *Divine Liturgy*, which is still performed by the Orthodox Church 10 times per year.

6.3. Homilies

- Hermeneutic, such as the *Nine Homilies to the Six-day Creation, On the Psalms, On Passages of the Scripture et a;*
- Moral, such as*: On Fasting, To the Rich, Against Anger, De humilitate;*
- Panygeric (Panygyric), to martyrs;
- Dogmatic: *Quod Deus non est auctor malorum (On that God is not the cause of Evil), De fide (On Faith), Contra Sabellianos et Arium et Anomœos (Against Savellians, Against Arius and the Unlawful), et al.*

6.4. Letters

About 350 letters are attributed to Saint Basil the Great.

Of special interest for those that study Theology, Philosophy and the History and philosophy of the sciences are the *Nine Homilies to the Six-Day Creation* and the letters, which show his broad and deep knowledge in Astronomy but also in Meteorology.

This is mentioned by professor K.D. Georgoulis: *"From a philosophical point of view, of special interest are the 'Nine Homilies to the Six-Day Creation'. In these Basil has incorporated his views in Physics, Cosmology and Anthropology. He exhibits a love towards nature and he appears to be a keen observer of natural phenomena and events… Nature is esteemed as a creation*

that was created by God through His wisdom… Basil the Great in these Homilies lays the foundations for the new stance of Christianity towards the physical reality. This work introduces him not only as a sharp observer but also as a connoisseur of the Aristotelian works on natural history." [16]

The *Nine Homilies to the Six-Day Creation* is a work rich in astronomical information and in the corresponding philosophical approaches of Cosmology; in the past our research team has made announcements on these thoughts and approaches of Basil the Great in international conferences of History and philosophy of astronomy and Natural sciences [17].

The *Nine Homilies* were translated for the first time in Latin by the Byzantine scholar and philosopher Ioannis Argyropoulos (1410-1490), who earned the seat of Greek studies at the University of Florence in 1456 and stayed there at least up to 1471.

The Emeritus professor of Astrophysics Sotirios N. Svolopoulos comments on Saint Basil's *Nine Homilies*: *"In two of these homilies much of Basil's astronomical knowledge appears. By analyzing the word 'beginning' (archè), he shows from the start an excellent use of dialectics, with the development of the mathematical notion of the point, of the impossibility of its subdivision, of the notion of time and of the beginning of time, coming to the conclusion of the impossibility of the existence of an infinite number of time beginnings. It would not be possible for time to exist before the creation of matter, for the notion of time is interwoven with the notion of change. Therefore, the Creation of the Universe was momentary and timeless (without time). And because the world has a beginning, Basil does not doubt that it will also have an end."* [18]

Basil the Great, bishop of Caesareia in Cappadocia and a saint of both the Eastern and the Western Christian Church, was explaining in a simple and understandable way in his first *Homily to the Six-Day Creation*, many centuries before the rise of modern science, that time as humans perceive it is not the same as motion, but it measures it through the effects of change and weathering it causes.

He also came through logical processes to the same conclusion modern Cosmology and Physics has arrived at: that time was born together with the Universe, i.e. along with the three-dimensional Euclidean space, giving an excellent philosophical explanation of the notion of the 'beginning' as far as the Creation is concerned.

More specifically, this great father of the Orthodox Church writes: *"The flow of time, which is always in a hurry, it rolls and leaves, never stops; or is not so? The past disappeared, the future has not yet come and the present slips out of our perception before we grasp it … …Therefore [time] was necessary for the bodies of animals and plants, which out of a necessity are bound to a flow and are joined by the motion that leads to the birth or to the decline, that causes them to be contained in the nature of time, which presents a special character according to the object or body that undergoes the change."* [4, p. 16]

In another passage of the *Nine Homilies to the Six-Day Creation* Basil mentions: *"Perhaps because the Creation was made in an instance and without the intervention of time, it was said that 'in the beginning He created'; for the beginning has no parts, nor dimensions. In the same way the beginning of the road is not road by itself and the beginning of the house is not house, the beginning of time is not time, not even the smallest time interval. If someone objects to this and supports the view that the beginning is time, let him know that he will need to divide it in the parts of time, which are beginning, the middle and the end. But to invent a 'beginning of a beginning' is absurd, and whoever bisects the beginning will produce two beginnings instead of one, or rather an infinite number of beginnings, for whatever gets divided this way it is divided ad infinitum to other parts."* [4, p. 18]

As a conclusion of the previous analysis, according to the views of Basil, the Universe was created outside of time. In other words the notion of the three spatial dimensions, of time and of the perceptible Euclidean space is a *result* of the creation of a perceptible Universe, i.e. what exactly is accepted by the modern Cosmology [11, p. 53].

About the *Nine Homilies to the Six-Day Creation* the professor of the School of Theology at the University of Athens father George D. Metallinos writes: *"Basil the Great offers with his 'Six-Day' (P.G. 29, 3-208) a classical example of Orthodox use of scientific knowledge. He achieves the connection of biblical and scientific facts through a continuous transcending of Science. He refutes the materialistic theories and the heretical faults by passing into the theological (and not metaphysical) explanation… Basil the Great himself, being affirmative to Science, as an omni scientist, he also accepts its god-centered character."* [19]

Basil, having studied the Greek pre-Socratic philosophers, Plato and Aristotle, and especially the latter's *Meteorologics* [20], offers in his works scientific explanations about the formation of the rainbow, of the rain itself, of the lightning, of the thunder and of other natural phenomena [5, vol. 29, p. 292].

As far as the triadic nature of God, Basil the Great accepts that the Father, the Son and the Holy Spirit as a set possess common characteristics: 'They' are infinite, impossible to be understood, indescribable and unbuilt (or inbuilt). Moreover, the clarification of the terms 'essence' ('ousia') and 'substance' ('hypostasis') by Basil not only formed the dogma of the Holy Trinity in an age when heresies tormented the Church, but also it served as a basis for the correct explanation of the relation between the two natures of the theanthrope Jesus Christ.

The Orthodox Church commemorates Saint Basil the Great, the first of the great ecumenical teachers and Church Fathers, on January 1, but also on January 30 together with Saint Gregory of Nazianzus and Saint John Chrysostom in the festival of the 'Three High Priests'. The Western Church celebrates his memory on June 14.

6.5. Some conclusions about the Homilies to the Six-Day Creation

Summing up, it can be said that Basil the Great:

1. Opposes the ancient Greek philosophy and certain Christian sects in that he does not accept the eternal and indestructible nature to the world above the Moon, since this world, too, had a beginning and so it will also have an end. According to Basil the eternal and immortal nature belongs only to God.
2. He accepts in general the ideas of the Greek and Alexandrian (Hellenistic) astronomy, i.e. the geocentric Ptolemaic system of the world. The spherical Earth lies at the centre of concentric spheres that reach up to the 8th sphere of the fixed stars. Consequently Basil does not accept the Asian cosmology, nor the ideas of the Antioch School; for this reason and because of his Greek education he reads *Genesis* in an allegorical way as far as the ordering and the motion of the world are concerned.
3. He adds another sphere, that of the celestial waters, beyond the 8th sphere of the fixed stars described by Claudius Ptolemy. This ninth sphere separates the world of the material creation from the world of God. He does so in order to agree with the biblical phrase *'above the seas He laid its foundations'* (meaning the Earth), a phrase he explains by writing that around the Earth there are waters everywhere, because there is the ninth sphere of the celestial waters.
4. Essentially, he attempts to create a compatibility and accordance between the Hellenistic astronomy (especially Ptolemy's *Great Syntaxis*) with the Judeo-Christian cosmology, to the extent of course that this feat is possible. He succeeds in separating the theoretical Hellenistic astronomy from cosmology by formulating a kind of 'personal school of thought' and generating a tradition that was followed by all subsequent Byzantine scholars to the age of Theodoros Metochites (1260/61–1331), who formulates scientific astronomy in the late Byzantine period [21].
5. He also interprets allegorically the verse of the *Psalm 75: "I bear up the pillars of it"*, which refers to the supporting of the Earth. He explains that these 'columns' are nothing more than the force that holds the Earth at the centre of the world (geocentric system).
6. Finally, to the verse of the *Genesis* that mentions that *"the Earth was formless and empty"*, which offered arguments to the heresy of the Gnostics [15] (they interpreted it to mean that Earth pre-existed before the Creation in the form of a formless matter) Basil gave a very simple interpretation: He suggested that the term 'empty' means that the Earth had not 'constructed' yet its natural world, i.e. the plant life, while the term 'formless' means that Earth was invisible because it was covered by the cosmic waters or because of the primordial darkness.

After Saint Basil the Great and his important philosophical and cosmological work, let us examine the other two bishops, who, in spite of their classical education and culture, are short of the cosmological background of Basil the Great.

7. Saint Gregory of Nazianzus (329-390)

Gregory was born in 329 in the small town of Arianzòs, near Nazianzòs of Cappadocia, hence he is called 'of Nazianzus' or **Nazianzen** (Greek: 'Nazianzinòs') from the wider area of his birth. Because of the power of his theological texts (mainly of the five theological treatises he wrote as bishop of Constantinople against the Arians) he is also called Gregory the Theologist. His father's name was also Gregory and he lived from 280 to 374; the father was a bishop of Nazianzòs and he is commemorated on January 1, along with Basil the Great's memory.

Gregory the younger received his basic education in Caesareia, where he was acquainted with Basil and the two adolescents continued their studies in Athens (the neo-Platonic school), where they received their secular education.

Gregory of Nazianzus became at first bishop of Sasima (372) and afterwards bishop of Constantinople (379). He was a profound and eminent orator, Church writer and poet. He is considered the best theologian of the Church after Saint John the Evangelist. In addition to his many theological works, which are the objects of study by other researchers, Gregory as the recipient of a very wide classical education presents in his texts a multitude of astronomical and cosmological topics that are of special interest to us, while at the same time he seeks for the harmonization of Christianity with the world.

Gregory of Nazianzus was the pioneer of an archaic-Christian humanism. In general his philosophy is influenced by Neo-Platonists, while his ascetic ideas were influenced by Stoicism. He is classified as a Neo-Platonic Church writer of the series of the Cappadocian Fathers of the Church, who formed the most important factor for the development of the Christian teaching on a philosophical basis.

Gregory himself wrote more than 245 *Letters* and 45 *Homilies*, where, *inter alia*, he presents the astronomy of his age. Of course, in his words, *"astronomy was considered a dangerous education subject"* [15, vol. 35, p. 761], he most probably means astrology, since in both his *Letters* and *Homilies* he refers to basic astronomical topics: to the stars, the Sun, the solar and lunar eclipses, the Milky Way Galaxy, the zodiac, and also to meteorological matters, such as the lightning and the thunders [15, vol. 36, p. 68]. His whole work can be found in the *Patrologia Graeca* [15, volumes 35-38], while still other works attributed to him by some sources, works generally considered as non-genuine, such as a treatise *Against astrologers*.

The Orthodox Church commemorates Saint Gregory of Nazianzus on January 25, but also on January 30 together with Saint Basil the Great and Saint John Chrysostom in the festival of the 'Three High Priests'.

8. Saint John Chrysostom (347-407)

John Chrysostom, the great Father of the Church, was born in Antioch of Syria in 347. His father was Secundus, a military officer, and his mother was the pious Anthoussa. He was educated in the schools of his hometown under the supervision of the philosopher Andragathius and the teacher of rhetorics Livanius; this way he was acquainted with the great orators of antiquity and the influence of classical studies is obvious in his whole work, which bears the seal of the ease in expressing himself.

Afterwards, following a prompt by the bishop Meletius of Antioch, John studied in the theological school of Antioch, whose director was Diodorus, the subsequent bishop of Tarsos. John was distinguished especially in the study of literature and in the classical studies, and became one of the greatest Fathers of the Church, an ecumenical teacher and the greatest orator of the Church: *'A Great initiator and leader into the great mysteries of God'*.

John was ordained a deacon in 380 in Antioch by bishop Meletius and a priest in 385 by Flavianus, the successor of Meletius. Finally, on December 15, 397, after the death of archbishop Nectarius, John was ordained bishop of Constantinople, assuming this throne on February 26, 398 AD, as *'the first great in essence ecumenical patriarch, before this title decorated the throne of the Queen of the Cities'*. In his sermons, John strictly criticized the life of eminent persons of the Empire and with his powerful personality he became a central figure of the public and social life of Constantinople. Being a great orator and proponent of Christian morality, he clashed with the highest social class and subsequently, in 402, the so-called '*epi Dryn*' (i.e. 'on the oak tree') Council unfrocked him with a fixed trial. However, the reaction of the people in favour of his worthy Church leader resulted in his call-back from the exile and in his return to the bishop's seat. Yet, in early 403, due to his unrelenting character, he clashed with the empress Eudoxia and the great logothetis Eutropius, a clash that led him to the exile, first in the city of Coucoussos in Armenia and afterwards (because with his correspondence he was still influencing his followers) further away, in the castle of Pityous near Caucasus. On his way to the latter he succumbed to the hardships and died in Comana of Pontos, on September 14, 407. He was buried there, in the church of Saint Basiliscus the martyr, while 31 years later, on January 27, 438 AD, his bones were transferred in Constantinople by his student Proclus, then bishop of the city.

John was an ardent orator and after the 6th century the adjective 'Chrysostom' (Greek *Chrysostomos*, meaning 'gold-mouth', i.e. that the speech was exiting as gold from his mouth) accompanies his name as a reminder of his speeches and sermons, as his rhetorical ability made his texts excellent specimens of Church literature. His work as a writer is enormous in volume and quality (he is the most prolific Father of the Church) and consists of *Treatises*, *Essays*, *Homilies* and *Letters*. In these he urges Christians to send their children to the monks in order to learn to read and write, using the *Scriptures* and the *Psalms* [15, vol. 47, p. 379], and not to the secular teachers, who were also

teaching ancient writers, because the study of the texts of the ancients increases, as he was saying, the thoughtlessness of the children [22].

The Byzantine people, as we know from historians of that age, believed generally in the 'birthday astrology' and therefore John Chrysostom warned: *"It is not the task of astronomy to learn from the stars about the people being born"* [15, vol. 57, pp. 61, 62]. This is evidence that he tried to strengthen the Christian faith, because he knew the culture of the Greek writers, and he wanted to combat astrology and not Astronomy.

John's treatise *About the Holy Orders* is considered especially eminent, while from his speeches of special importance are the 21 speeches *To the Statues* (prompted by the destruction of the emperors' statues by the Antiochians) and the two speeches *To Eutropius*.

Beyond these, the quality of John's astronomical knowledge is impressive and he has offered a deeply scientific (based on Astronomy) treatment on the issue of the nature of the Star of Bethlehem [11, p. 441, 442]. In it he demonstrates in detail that the Star of Bethlehem could not be, from its description, some strictly defined astronomical phenomenon [15, vol. 57, pp. 64, 65]. This means that according to him the existence of the historical Jesus and his divine character cannot be connected in any way with the apparition or the occurrence of some astronomical event in the period of his birth.

However, in spite of these correct astronomical views, it seems that John was supporting a system of the world that approached the views of the Antiochian school, which, as already mentioned, was interpreting *Genesis* word by word, i.e. they believed that the Earth was flat and that the Universe had many forms.

The Orthodox Church commemorates Saint John Chrysostom on November 13, on December 15, on January 27 (the transfer of his bones), but also on January 30 together with Saint Basil the Great and Saint Gregory of Nazianzus in the festival of the 'Three High Priests'.

9. Conclusions

It is very important to note that the 'Three High Priests' had a Greek education, a Greek culture and (therefore) a Greek mentality. Their whole philosophical outlook is expressed (although he often calls the ancient philosophy 'vain philosophy') by the famous text of Basil *'For the youth, as if they were benefited by Greek literature'*, where he develops the view that the Greek culture and education (poetry, History, rhetorics, Philosophy, music and Astronomy) can be proved very useful after all for a Christian pupil, for it exercises the mind of the pupils to discipline and assists the consolidation of the Christian principles, if of course a proper selection is done of authors and their texts, as Basil says.

Indeed, Christianity through the great Church Fathers assimilated many elements of the Greek civilization, creating the Graeco-Christian civilization with Alexandria, Antioch and Cappadocia as its centres.

This paper is the continuation of our previous work on the connections between spirituality and science [23, 24] and on the contribution of the Church in Byzantium to the natural sciences [25]. In our next paper in this series we shall examine the cosmological work and the contribution to the sciences of the following high priests (bishops): Saint Gregory of Nyssa, Epiphanius of Cyprus (315-403), Asterius of Amaseia (4th century), Cyril I of Alexandria (370-444), Synesius of Cyrene (370-414), Caesarius (4th century), Nemesius of Emessa (4th to 5th century) and Dionysius Exiguus (5th to 6th century). We shall especially analyze the work of Saint Gregory of Nyssa, the brother of Basil the Great, who wrote *Apologetic Speech to the Six-Day Creation* [15, vol. 44, pp. 61-124] and was elevated to the status of an eminent Christian cosmologist.

Acknowledgements

This study formed part of the research at the National and Kapodistrian University of Athens, Department of Astrophysics, Astronomy and Mechanics, and we are grateful to the University of Athens for financial support through the Special Account for Research Grants. It is also supported by the Ministry of Science and Technological Research of Republic of Serbia.

References

[1] A. Vertsetis, *General Didactica*, in Greek, vol. I, Athanasopoulos-Papadamis Publ., Athens, 2003, 21.
[2] E. Grant, *Physical Science in the Middle Ages*, Cambridge University Press, Cambridge, 1979, 8.
[3] T. Nikolaidis, Byzantiniaka, **11** (1991) 206.
[4] Basil the Great, *Homilies on Hexameron*, in Greek, Polytypo Publ., Athens, 1990, 14.
[5] Saint Basile, *Aux jeunes gens sur la manière de tirer profit des letters helléniques*, F. Boulenger (ed.), Les Belles Lettres, Paris, 1935.
[6] N. Tomadakis, *The Key of the Byzantine Philology - Introduction to the Byzantine Philology*, in Greek, 3rd edn., vol. I, Myrtidis Publ., Athens, 1965, 13.
[7] G. Katsiampoura, *Dialogue of two worlds: the ptolemaic thought in Byzantium*, Proceedings of the Conference: The aspects of the philosophers for the natural sciences. Hellenic Physicist Society, Xanthi, 2005, 145-163.
[8] V.N. Tatakis, *The contribution of Cappadoccia to the Christian thought*, in Greek, Publications of French Institute of Athens, Athens, 1960, 102.
[9] E. Danezis and E. Theodossiou, *The Cosmology of the Mind-Introduction to Cosmology*, in Greek, Diavlos Publ., Athens, 2003, 238.
[10] E. Theodossiou and E. Danezis, *To the traces of IXTHYS-Astronomy-History-Philosophy*, in Greek, Diavlos Publ., Athens, 2000, 111.
[11] Eusebius, *The church history of Eusebius*, English translation by A.C. Mcgiffert, T & T Clark Publ., Edinburgh, 1890, 25, available on line at http://www.ccel.org/ccel/schaff/npnf201.
[12] Bassile de Césarée, *Homelies sur l'Hexaémeron*, 2nd edn., Stanislas Giet, Sources Chretiennes 26 ^{bis}, Paris, 1968, 86.

[13] T. Nikolaidis, *Greek Astronomy and Christian cosmology*, Proceedings of the 4th Conference 'Aristarchus the Samian', in Greek, National Research Foundation of Greece, Samos, 2003, 183-184.
[14] E. Theodossiou, V.N. Manimanis, E. Danezis and M.S. Dimitrijevic, Transdisciplinarity in Science and Religion, **2** (2009) 47.
[15] ***, *Patrologiae Graecae cursus completus, series graeca*, J.-P. Migne (ed.), vol. 1-161, Centre for Patristic Publications, Athens, 2008.
[16] K.D. Georgoulis, *Hellenic Christian Philosophy*, in *Encyclopaedia of Helios*, in Greek, volumes 18, Helios Publ., Athens, 1957, vol. 7, 683.
[17] E. Danezis, E. Theodossiou and M. Dimitrijevic, *Cosmological Implications of the 'Hexameron' of Saint Basil the Great*. *Science and Orthodoxy-A necessary Dialogue*. Curtea Veche, Bucharest, 2005, 103-109.
[18] S. Sotirios, *Scientific consideration of the Homilies on Hexameron of Basil the Great*, in Greek, University of Ioannina Publ., Ioannina,, 1969, 1.
[19] G. Metallinos, Christianiki, **February 9** (2006) 5.
[20] Aristotle, *Meteorologica*, English translation by H.D. Lee, Heinemann, London, 1952.
[21] E. Theodossiou and E. Danezis, *At the Years of Byzantium – Byzantine scientists, physicians, chronologers and astronomers*, in Greek, Diavlos Publ., Athens, 2010, 475.
[22] F. Koukoules, *The life and civilization of the Byzantines*, in Greek, vol. I, Papademas Publ., Athens, 1948, 38 and 45.
[23] E. Danezis, E. Theodossiou, I. Gonidakis, M.S. Dimitrijević, Eur. J. Sci. Theol., **1(4)** (2005) 11.
[24] E. Theodossiou, V. Manimanis, M.S. Dimitrijević, Eur. J. Sci. Theol., **6(3)** (2010) 47.
[25] E. Theodossiou, V. Manimanis, M.S. Dimitrijević, Eur. J. Sci. Theol., **6(4)** (2010) 57.

European Journal of Science and Theology, December 2011, Vol.7, No.4, 25-45

THE CONTRIBUTION OF BYZANTINE PRIESTS IN ASTRONOMY AND COSMOLOGY II. GREAT CHURCH SCHOLARS IN THE EARLY BYZANTINE EMPIRE

Vassilios Manimanis [1], Efstratios Theodosiou[1] and Milan S. Dimitrijevic[2*]

[1] *National and Kapodistrian University of Athens, School of Physics, Department of Astrophysics, Astronomy and Mechanics, Panepistimiopolis, Zografos 15784, Athens, Greece*
[2] *Astronomical Observatory, Volgina 7, 11160 Belgrade, Serbia*

(Received 7 March 2011)

Abstract

In the present paper is analyzed the work of Saint Gregory of Nyssa, Epiphanius of Salamis, Asterius of Amaseia, Cyril I of Alexandria, Synesius, Caesarius of Nazianzus, Nemesius (the bishop of Emesa in Syria). Also, the monk Dionysius Exiguus, who introduced the BC/AD chronology, with emphasis in their contribution to the sciences, especially Astronomy. In particular, we present the cosmological views of Gregory of Nyssa and we comment upon them, as he is considered a great cosmologist and natural philosopher.

Keywords: Byzantium, Natural sciences, Cosmology, Gregory of Nyssa

1. Fourth century: the age of the great Church scholars

The 4th century AD, the first century of the Byzantine (Eastern Roman) Empire, is a period of prosperity for the Graeco-Christian theological philosophy, when the Christian doctrines were consolidated and efforts were made to interpret the cosmology of the *Old Testament*. Upon these topics, the work of the three Cappadocian Fathers: Saint Basil the Great (Basil of Caesarea, 330-379), Saint Gregory of Nazianzus (328-389) and Saint John Chrysostom (347-407), was examined in an earlier paper [1].

Besides the three Cappadocian bishops, the studies of many other leaders of the Church who left their mark not only in Theology but also in Science, mainly with their interesting cosmological and astronomical views are of interest.

* Corresponding author, e-mail: mdimitrijevic@aob.bg.ac.rs, Phone: +381-11-3089-072, Fax: +381-11-2419-553

These latter important figures that appeared at the age of the three great Cappadocian bishops or shortly after them, are the topic of the present paper. In rough chronological order they are: Saint Gregory of Nyssa, Epiphanius of Salamis (in Cyprus), Asterius of Amaseia, Cyril I of Alexandria, Synesius of Cyrene, Caesarius, Nemesius, the bishop of Emesa (Homs) in Syria and finally the monk (abbot) Dionysius Exiguus, who compiled Paschal (Easter) canons and introduced the BC/AD chronology.

During the first centuries of the appearance and propagation of Christianity the official stance of the leaders of the Christian Church was, as we have already mentioned in a previous paper [1], rather negative towards Science because they considered it as a product of the ancient pagan world. Nevertheless, the knowledge of Astronomy was necessary, since a calendar of the new religion's festivals should be devised, especially for the calendrical calculation of the Easter. For this reason the wisest bishops were educated in the 'gentile' culture with its trivium, i.e. Grammar, Rhetoric and Dialectics, and its quadrivium, i.e. Geometry, Arithmetic, Music and above all Astronomy; through Astronomy they studied the cosmology and cosmogony of the *Old Testament*. Actually, in order to reconcile the astronomical views of their age with the cosmogony described in the Book of *Genesis* they wrote treatises *On the Six-day Creation* (*Peri Hexahemerou* or *On Hexameron*) that were staple texts of the spiritual production of the 4th century [2]. As T. Nikolaidis writes, *"The most important texts were the "Homilies to the Six-day Creation" by St. Basil the Great and those by his brother, St. Gregory of Nyssa, treatises that exerted an especially strong influence, not only in the East but also in the West"* [3].

Indeed, Saint Gregory of Nyssa was an expert on the theories of the ancient Greek philosophers on cosmology, life and the Universe, and therefore through his work became one of the most capable judges of their beliefs.

2. Saint Gregory of Nyssa (335-394)

Gregory of Nyssa was the younger brother of Basil the Great (Basil of Caesarea) and he is considered one of the most important theologian of the Eastern Church. Gregory was born in Neocaesarea, on the Black Sea's southern shore, around 335 AD and he must have been educated mainly in Caesarea of Cappadocia having as a teacher his own brother Basil between the years 348 and 357, since he mentions only him as his teacher ([4], vol. 44, p. 125B; vol. 46, p. 1049A). Gregory initially worked as an orator and married Theosebeia; however, after her death he abandoned rhetoric following the advice of Gregory of Nazianzus and he followed the *'emphilosophos vios'* ('life that incorporates philosophy') of the monks and pursued theology studies [5].

He is known to us today as Gregory of Nyssa because he was ordained (by Basil himself) bishop of Nyssa in Cappadocia, a city strategically located on the road leading from Caesarea to Ankara, in order to relieve the latter from the tight grip of the influence of the followers of Arius, a cult leader. In the beginning Gregory had some problems with his diocese, however after the death of the

emperor Valens Flavius Augustus (364-378), a follower of Arius and supporter of his cult, he fully assumed his duties there and his actions from that point onwards is described in his work *To the life of the holy Macrina* [4, vol. 46, p. 960; 6]. Macrina was his sister. After the Council of Antioch in 378 Gregory visited Macrina and their younger brother Petros (Peter) in the place of their exercise on the southern shore of the Black Sea; his conversation with Macrina about the immortality of the soul is contained in his work *On the soul and the resurrection* [4, vol. 46, p. 12], also known for this reason as *The Macrineia.*

Gregory may be inferior to his brother as far as the bishop's actions and practical spirit are concerned; he may also be short of Gregory of Nazianzus in theological thought. However he clearly surpasses both of them in purely philosophical thought, as he was an expert on and researcher of the views of the Greek philosophers about life and the Universe. He also became a tremendous theoretical theologian, who used the teachings of Platonic and Stoic philosophy for the interpretation of the Christian faith [7].

Essentially the Fathers of the Church during that period were attempting to offer answers to core theological issues based on the pre-Socratic positive thought [8].

The work of Gregory of Nyssa, in which the perfect knowledge of Greek culture is evident, is multi-faceted: he wrote explanatory, dogmatic and practical treatises, speeches and letters. He also knew Mathematics and the Astronomy of his age, and he was a great cosmologist.

As a cosmologist, Gregory is known to support the view that the beginning of the Universe is *"seeding power spent [by God] towards the creation of everything"* [4, vol. 44, p. 77D]. This 'seeding power' can be identified in modern cosmological terms as the reason for the formation of the super-dense mass of the Big Bang theory. Also, the phrase *"towards the creation of everything"* shows the dynamic nature of the explosion and the movement from the potential to the naturally existing [9].

His view on Astronomy is that through it *"the intellect is excited towards virtue and the truth is understood through the numbers"* [4, vol. 46, p. 181]. Indeed, according to the late professor of Byzantine studies and academician F. Koukoules: *"The Byzantines knew of two kinds of mathematics: the scientific ones, whose teaching was allowed since, as Gregory of Nyssa writes* ... [the above passage is cited - 4, vol. 46, p. 181] *....and the occult ones, which were strictly forbidden. Astronomy, for example, as long as it examined the motions, the sizes and the distances between the celestial bodies, it was being taught; but when it turned into astrology by suggesting that the fate of humans depended on the stars, then it was considered despicable and its teaching was persecuted"* [10].

It can be said from the above that, while Gregory holds faith as the supreme criterion for the truth, he nevertheless does not despise the sciences and Astronomy in particular. The sciences, he informs us, are a jewel that the faithful Christian has to offer to the Church of Christ: "For we are ordered by the Leader of virtue to take ethical and natural philosophy, as well as Geometry and

Astronomy and the science of logic and all studies that those who are outside of the Church are engaged in, to take them from those who are rich in them and accept them in order to use them, because there are cases in which they are useful, when the divine temple of the sacrament must be embellished with the logical wealth. This can be observed to occur even now. The secular education is offered by many as a gift to the Church of God, by people like Basil the Great, who did the right thing during the years of his youth by preparing himself with a wealth of wisdom, comparable to that which Moses acquired living among the Egyptians, and with this wealth of the true wisdom he decorated the house of the Church." [4, vol. 44, p. 360]

Gregory of Nyssa wrote an *Apologetic [speech] on the Six-day Creation* [4, vol. 44, p. 61], in which he tackles cosmological topics found in Basil's *Nine Homilies to the Six-Day Creation* (*Peri Hexahemerou* or *On Hexameron*) [11]. The *Apologetic on the Six-day Creation* supplements both his work *On the construction of the human being* [4, vol. 44, p. 125] and Basil's *Nine Homilies*... In the *Apologetic on the Six-day Creation* Gregory attempts to harmonize the *Old Testament* with the scientific data of his period. However, in this work the influence by the theological positions of the Jewish philosopher Philo of Alexandria (25 BC - 40 AD) are obvious; Philo was the first who tried to combine Plato's philosophy and Biblical theology through his philosophical worldview.

Gregory of Nyssa, in addition to his other significant theological treatises, wrote a large number of *Epistulae* (*Letters*): Out of the 30 *Epistulae* that were saved and are attributed to him, the 28 are genuine, the 29th was written by the sophist Stagirius and the 30th was written by his younger brother, Petros (Peter), the bishop of Sevasteia, and is addressed to *"Gregory of Nyssa, his brother"*. In his *Epistulae* Gregory tackles, in addition to theological issues, astronomical and meteorological topics, such as the size and the number of the stars, the size of the Sun and the size of the celestial sphere. He also offers explanations about the solar and lunar eclipses, lightning, the thunders, the rain, the frost and other phenomena.

With his teaching Gregory continues the theology of Eirenaeus, Origenes, Saint Athanassios and other Fathers of the 4th century. In his *Homilies* are expressed his struggle against the heretical followers of Arius, the Pneumatomachi (or Macedonians followers of Macedonius) and the Apollinarists. In one of his *Letters* he writes that *"among the [members] of the Holy Trinity we find no difference at all."* This statement alone puts him on the opposite side of these heresies and especially the theories of Arius, who demoted the Son (Logos) to a mediator between God and the material Creation [12].

In cosmological issues Gregory of Nyssa generally did not follow the views of his brother Basil and this is the main reason he wrote the *Apologetic on the Six-day Creation* [4, vol. 44, p. 61-124]: to complement and explain certain passages in the corresponding work of Basil that had been misinterpreted. Through this work and from his views we understand that Gregory follows the worldview of Origenes and the Alexandrine School; this School, because of its

Greek and Hellenistic background, interprets the book of *Genesis* in an allegorical, symbolic way, in order to adapt it to the more advanced cosmological system of the Alexandrine natural philosophers: a spherical Earth and Universe, and a geocentric system of movements with the Earth at the centre of the Universe [13]. The *Apologetic on the Six-day Creation* was offered as a present to his brother Petros, later bishop of Sevasteia.

It is important to examine these views of Gregory, which are clearly influenced by the Physics and Cosmology of the pre-Socratic Greek natural philosophers, and how these views are sometimes juxtaposed to the views of Basil without being contrary to them; Gregory praises the work of his brother and regards it as very important.

In any way, as far as the Church Fathers are concerned, their texts reflect personalities highly educated and with a Greek culture; their cosmology is scholarly and scientific, utterly different from the simplistic cosmology of Cosmas Indicopleustes (6th century), which will be analyzed in a future paper.

The basic objections of Gregory of Nyssa are summarized in the following three points:

i) How is it possible that the Earth and the sky have been created from the beginning while at the same time the Earth appears formless and empty?
ii) How is it possible that the Sun appears to be created on the fourth day of the Creation while the light had already been created from the first day?
iii) How is it possible that there were other 'waters' above the firmament?

The answers to these questions are given in the following five points:

1. To the verse of *Genesis*: *"Now the Earth was formless and empty"*, which offered arguments to the Gnostics [14] (who were interpreting it as hinting that the Earth pre-existed before the Creation in a state of formless matter) Gregory gave a different interpretation from the one of his brother. Basil suggested that 'formless' means that the Earth had not yet 'form' its kingdom of plants, while 'empty' (in the Septuagint translation 'invisible') means that the Earth could not be seen either because it was covered by the cosmic waters or because of the original darkness [1]. On the contrary, Gregory suggested that the Earth was 'invisible' because the qualities of the elements that assign to matter its colour and various properties discernible with our vision had not been yet separated. Additionally, he was supporting the view that 'formless' means that matter was in a primeval state and had not yet acquire its proper density. Gregory, influenced by the natural philosophy of the Greek pre-Socratic philosophers, offers his own view: matter, when created, had initially a unified form and subsequently from this primeval matter were separated all these elements that composed the natural world as the latter was understood in that period.
   In the same passage of the *Apologetic*, the 'cosmologist' Gregory of Nyssa also answers another question: "*How the material world can be originated from the immaterial God*?" According to Professor of Theology Elias Moutsoulas: "Gregory stresses that matter was generated by the 'coming together' of 'qualities' such as the heavy, the light, the dense, the rarefied,

the humid, the dry, the bitter, the warm, the colour, the shape, which by themselves are notions and abstract meanings. Since the phrase 'in the beginning' means 'all at once', the verse 'in the beginning God created the heavens and the Earth' also includes the 'creation of all elementary ingredients of the beings that are known to us through our senses.'" [15]

By interpreting these first verses of *Genesis*, Gregory notes that right from the start the 'reasons and causes' for all beings were assigned to the Creation. Based on the cosmological views of his period, he attempts to describe how the world was produced gradually from the 'formless and empty Earth'. He stresses the contrast between Heaven and Earth, which is equivalent (according to the worldview of that age) to the distinction between motion and stillness and contributes to the generation and conservation of living beings. He especially stresses the connection and interrelation of all beings between them and with the 'really being' (the God), from whom they get the potential to exist [15, p. 377].

2. The light and darkness in the verse 1.3 of *Genesis*: *"And God said, Let there be light"* (*Genesis* 1.3) were discussed a lot within the frame of Christian cosmology, since from then on up to this day light is usually identified as representing God and good, while darkness often symbolizes demons and evil. The contrast light-darkness, which essentially is the duality good-evil through the views of Heraclitus and the Pythagoreans, was also an object of study for the Gnostic heretical groups. For example, the followers of Manes, the Manichaists, were attributing to darkness the power of the evil; they believed that darkness was an entity by itself and pre-existed the Creation in order to combat the benevolent nature of God [16].

   Basil the Great could not accept these views and regarded darkness not as a separate entity, but as a passive state of the environment or of the atmosphere, since there is darkness only when light is present somewhere else! The darkness, according to Basil, was created when God created the celestial dome, because in doing this he separated the existing terrestrial world from the divine light. The phrase of *Genesis* 1.3 means, according to him, that God instantaneously illuminated the world with the divine light, which exists since then beyond the firmament. Basil believes that beyond the terrestrial world there is a state of things similar to the one that prevailed before the Creation of the world by God: there the divine or 'uncreated' light prevails, which is not perceivable by the imperfect human senses.

   Gregory of Nyssa separates his position here as well, by suggesting that light during the Creation, a period when darkness prevailed, was not absent but it existed 'inside the particles of matter'. This 'hidden' light appeared with the order of God: *"And God said, Let there be light"*; in this way our world was illuminated.

3. Next in *Genesis* comes the passage: *"God saw the light, that it was good: and God divided the light from the darkness. And God called the light Day*

and the darkness he called Night" (*Genesis* 1.4-5). Astronomically thinking, we notice that this took place before the creation of the Sun and the stars in the firmament (*Genesis* 1.16). Therefore, the notion of the 'day' as the illuminated part of the 24-hour period and of the 'night' as the dark part of that period made no sense for the rationalistic ancient Greek astronomy.

Basil the great supports the view that this day and night, before the Sun, was not due to the revolution of the Sun around the Earth but due to light pulses, because of cycles of 'diffusion and contraction' of light, as God had ordered.

Gregory's explanation of this passage is once again different: being deeply influenced by Aristotelian physics, he believes that light presents a natural upward motion. Therefore, when it was ejected by the various elements, it immediately followed a motion towards the heavens ('upward'), where it concentrated. When it reached the spherical borders of the created world, in other words the ninth crystalline sphere, it assumed a circular motion. This way, as it followed its circular orbit on the ninth sphere, it illuminated the Earth from the one side, the 'day side', but as it continued its course the thicker part of the 'unformed Earth' was inserted between the light and our world, forming a shadow, i.e. the darkness of the night. This prevailed towards the opposite direction from the rays of the circularly moving light.

4. *Genesis* informs us that the 'two great lights' were made in the fourth day (1.16), when the Earth had already been created. Basil, who generally does never differentiate between the divine and the 'created' light, supports the view that in the fourth day the *carriers* of light were created, implying that all the celestial bodies are self-illuminated and that their differences in brightness are due only to their different sizes. Gregory of Nyssa on the other hand assumes that the celestial bodies are illuminated from the outside and that the Universe has tremendous size. He also believes that the stars have been formed by aggregations of particles; because these particles were not of the same nature, the stars differ in their properties. For example, the Sun was formed from brighter particles than the Moon, and for this reason it is much brighter than the latter.
5. Another intriguing passage in *Genesis* that created problems for the Greek-educated bishops was the following: "*Let there be a firmament in the midst of the waters, and let it divide the waters from the waters*" (Genesis 1.6). In other words, after the Creator God had made the Earth and the heavens, and after the creation of light and the separation of the day from the night, an 'expanse' or firmament was created in order to separate the celestial from the terrestrial waters. Here the Jewish world view prevails, according to which the Earth is surrounded by the universal waters; this in turn follows the most ancient Mesopotamian theory about the structure of the Universe (see Figure 1) [17]. Here appear together two cosmological elements totally alien to the classical Greek and Hellenistic astronomy: the expanse-firmament and the universal waters. Both Basil and Gregory use in their

explanation the celestial spheres of the Ptolemaic (Hellenistic) astronomy. Basil the Great thinks that the firmament is a solid sphere under the one that defines our world; the firmament keeps the universal waters – which are of the same nature as the terrestrial waters – in its upper side. In this way the firmament is identified with the eighth sphere of the fixed stars in the celestial sphere system of Claudius Ptolemy. Above it, according to Saint Basil the Great, there is the ninth sphere that forms the boundary of the created Universe and most probably is identified as the sphere of the 'primal cause' (the counterpart of the Primum Mobile of medieval and Renaissance astronomy). In the context of the Aristotelian and Ptolemaic view for the Universe, as it later reached the West, this ninth sphere is the 'second crystalline sphere' of the zodiac. In the West, of course, as in the Dante's *Divine Comedy* model, they proceeded further and considered the tenth sphere as the crystalline sphere of the Primum Mobile, placing beyond all these the ethereal heavens (see Figure 2) [18]. According to Basil, the water is extremely valuable; therefore, these 'universal waters' are a kind of celestial reservoir constructed by the providence of God in order to have enough water for his terrestrial creation until the end of the world.

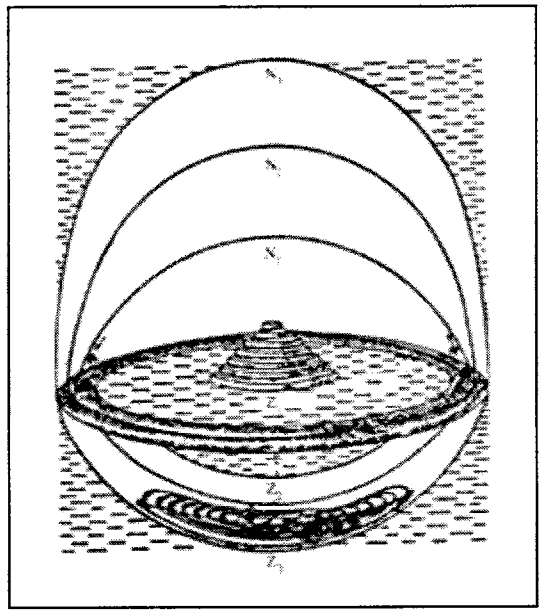

Figure 1. The Universe of the Babylonians. The three domes of the sky (N_1, N_2 and N_3) and the three zones of the Earth (Z_1, Z_2 and Z_3) can be seen. The uppermost terrestrial zone (Z_1) is dominated by the seven-terraced ziggurat, a religious building of the Babylonians.

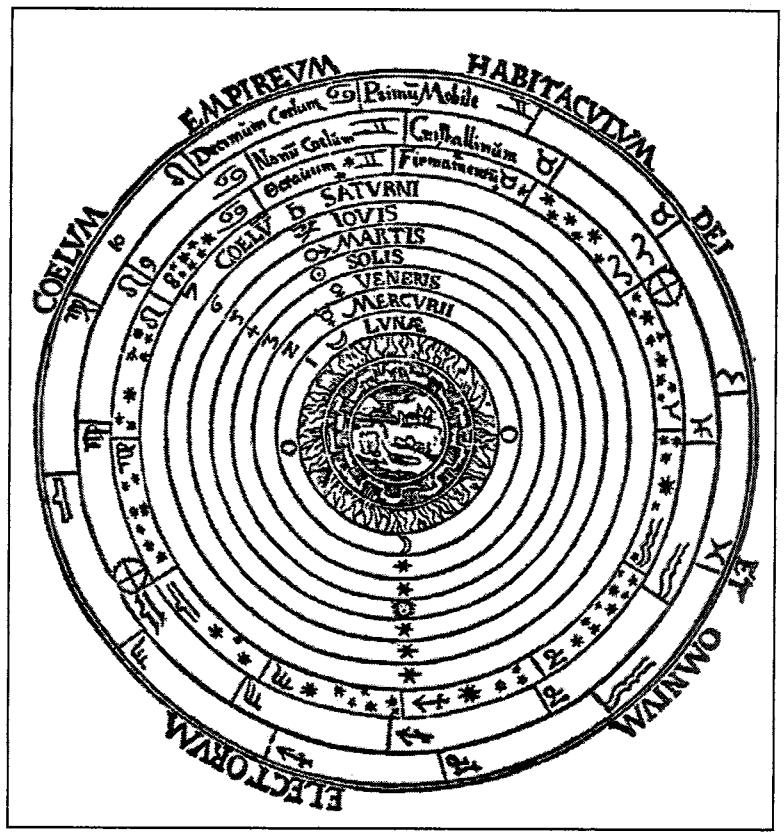

Figure 2: The Universe of Aristotle with the Latin names of the 'coeli' (heavens), as they were known in the West. In its centre are the Earth, the region of the air and the region of the fire. Going outwards we see the spheres of the seven 'planets' (Moon, Mercury, Venus, Sun, Mars, Jupiter and Saturn) and of the three zodiacs. The first sphere of the zodiac corresponded to the 8th 'coelum', that of the fixed stars; the second sphere corresponded to the 9th crystalline heaven and the third one to the 10th heaven of the Primum Mobile. Beyond these there are the ethereal heavens, the abode of the Divinity.

On the contrary, Gregory believes that the firmament is essentially the sphere of the created Universe itself and that it is not made from a solid material because this way the sphere would be too heavy and it would collapse. As for the celestial universal waters, these, according to the scholarly bishop, are 'spiritual': they do not belong to the created world, but to the transcendental world of God.

Gregory of Nyssa, beyond his cosmological explanations concerning our world, writes also about superstitions like the one he mentions about the Byzantine people of his time, that on the New Year's Day they were taking care so that they would first meet or have in their house (as the year's first guest) a person who would bring them good luck during the new year [19].

Of great philosophical value is Gregory's work *Great Catechism* (translated in English as *The Catechetical Oration of Gregory of Nyssa*) which has been translated in the major European languages. A central place in the works of Gregory is occupied by his teaching about man and his salvation. His work *On the Construction of Human* [4, vol. 44, p. 125-256] is an essay of Christian anthropology of the same level as the essay *De Natura Hominis* (*On the nature of man*) by Nemesius of Emesa [20]. In the work *On the Construction of Human* Gregory complements what Basil the Great exposed in his nine *Homilies On the Six-day Creation* (*Peri Hexahemerou* or *On Hexameron*), where he had omitted this topic.

According to theologian and professor of Theology V. Feidas: *"In the whole of his teaching, Theology is in perfect harmony with Anthropology and Cosmology, centred on the triadic God and His incarnation in Jesus Christ"* [21].

The basis of Gregory's philosophical thought is the metaphysical notion of existence. God is the 'one who really exists'. From this existence stems everything and humans also 'participate' in it, with the following essential difference: God has the 'Existence' by Himself, while man, as His creation, possesses the Existence 'through participation'. God creates the world/Universe from what does not exist through his Logos (logical speech or relation). The world was created from nothing with the will of triadic God alone [22]. The human being, the centre of the material world, is for Gregory a creation of God that lies on the boundary, as he writes, between the visible (or material) and the invisible (or spiritual) creation. Indeed, Plotinus, the 3rd century philosopher, placed Nous (mind) and the ideas between God and the soul, while Origenes identified Nous and the ideas with Logos, which in Christian thought took the meaning of the second person of the Holy Trinity. Gregory, however, does not accept the place of Nous as an intermediate and identifies it with the Father. In the position held by the ideas in the system of Plotinus and Origenes Gregory places the angels, who he regards, like the souls, creations of God, although they belong to the invisible or spiritual creation.

Finally, Gregory mentions that human, being the centre and the reason for the world, aims at the transition from 'in our image' to 'in our likenesses. Human's spiritual march, he writes, has no end, because humans are imperfect and God is infinite. Faith and knowledge are strictly separated. Through logical knowledge alone it is impossible to understand the divine being; also, our mind and thoughts act inside the frames of space and time, and they always 'see' things within frameworks or 'separations'. Thus, according to Gregory of Nyssa, we cannot approach the divine essence thought the way of the logical thought: God transcends our understanding (or perception) and the human vision, since He is the ultimate invisible and incomprehensible Being. Human wisdom, Gregory writes (transferring into a theological level the teaching of Socrates and Plato about ignorance) is *"the understanding of the incomprehensibility of the divine being"* [6, p. 686].

Scholar K. Gronau stresses in his work the influence of Poseidonius the Stoic upon both Basil the Great and Gregory of Nyssa; he writes that especially Gregory, in addition to Philo and Origenes, used as a direct stoic source the commentary on Plato's *Timaeus* by Posidonius (a disputed work), in which in an eclectic way are exposed views of the Pythagoreans, the Platonic and the Stoic philosophers [23].

According to Gregory the neoplatonic belief that the world originated from the essence of God and the Manichaean belief that the world was created by another, evil God, are both erroneous. Gregory states that the beings did not originate from the essence of God. The first and basic differentiation is the one between the 'one who really exists', which is uncreated (actiston), and all the created beings, which owe their origin to the former [15, p. 375]. Nevertheless, Gregory writes that he himself does not find great antithesis between Neoplatonism and Christianity; this probably explains why his work exerted a significant influence to both the Byzantine occult intellectuals and the Western Medieval one. Our personal opinion is that his work is worthy of further study and detailed research, in particular its cosmological ideas [12].

The whole work of Gregory of Nyssa has been included by J.-P. Migne in the volumes 44 to 46 of the *Patrologia Graeca* [4], while it was also published by Werner Jaeger [22], and its essay *On the Construction of Human* by J. Laplace [24]. In addition, emeritus professor of Theology at the University of Athens Elias D. Moutsoulas wrote the book *Gregory of Nyssa-Life, Works and Teaching*, where he writes in detail and full references all about the life, the works and the teaching of this great Church Father [15]. Gregory died after the Council of Constantinople (394), in which we know that he participated. The Third Ecumenical Council in 431 called him *"man second only to his brother in both word and manners"*, while the Seventh Ecumenical Council in 787 called him *"Father of Fathers"* [15, p. 53]. The Church sanctified Gregory; his memory is celebrated on January 10 by the Orthodox Church and on March 9 by the Catholic Church.

3. Epiphanius of Salamis or of Cyprus (315-403)

An important Church Father of the 4th century was the scholar Epiphanius, bishop of Constantia (the Salamis of the ancients) in Cyprus and archbishop of the whole island of Cyprus (367-403), hence the appellation *Kyprios* (Cypriot, of Cyprus).

This noted Church writer was a strong opponent of Origenism. He left a rich collection of theological works, including *Ancoratus* (the 'well anchored man', 374 AD), an epitome of the dogmatic teaching of the Church, especially about the Trinity dogma, and *Panarion* (meaning Medicine-chest) or *Adversus Haereses* (*Against the heresies*, 375 AD), where he analyzes and refutes all 80 heresies that had appeared up to his age [25]. In addition, he studied the issue of the celebration of the Easter, which is of historical interest to all astronomers; on this topic he disagreed with the great Cappadocian bishops, insisting on the

proto-Christian tradition of celebrating it on the first Sunday after the Jewish Passover.

Epiphanius was a polymath and could speak several languages: Greek, Hebrew, Syrian (Aramaic), Coptic-Egyptian and (less competently) Latin; for this reason Eusebius Hieronymus calls him *Pentaglossos* ('five-tongued') [26].

This Church scholar, aside from the polemics by which he is known, wrote in Greek two unusual books. The first one, composed in Constantinople for a Persian priest, was entitled *On Measures and Weights*, assumed its final form around 392 and covers a very wide range of subjects, from the geography of the Palestine to the measures and weights that are mentioned in the *Bible* and were used by the Jews [27]. It consists of three sections, the first one dealing with the canonical books and the translations of the *Old Testament*, the second one dealing with the measures and weights (that gave the title to the whole work) and the third one dealing with the geography of the Holy Land. It can therefore be characterized as a biblical encyclopaedia. It has been saved in its Syrian (Aramaic) translation and partly in its original Greek version. The texts appear not to have been given a polish but consist of rough notes and sketches, his modern editor, Allen A. Shaw, concluded; nevertheless Epiphanius' work on metrology was important in the history of measurement [27].

The second peculiar book by Epiphanius bears the title *Of the 12 stones in the decoration of Aaron*. It actually describes the gems and especially the twelve ones that decorated the diadem of the Jewish high priest Aaron.

Therefore, Epiphanius, whose memory is celebrated by the Orthodox Church on May 12, could be classified on behalf of these two works as one of the earlier Byzantine scientists. In addition, he was an ardent persecutor of astrology, which he denounced by the name of 'astronomy'.

In his philosophy, Epiphanius believes that humans have limited abilities for the understanding of the *Bible* and he considers the holy tradition as a necessary supplement to it; thus, the truth exists only in the Church, which accepts both the *Bible* and the holy tradition of Christianity.

The works of Epiphanius, in spite of their many errors, offer a wealth of data that would otherwise be unknown to us.

4. Asterius of Amaseia (4th century)

Asterius, the bishop of Amaseia of Pontos, succeeded as a bishop Eulalius in *circa* 385. He was contemporary of Basil of Caesarea and the other great Cappadocian Fathers. Asterius was distinguished especially for his theological and administrative work, and for his rhetorical ability, as well as for his occupation with the sciences.

From his work, 16 *Homilies* were saved and are included in *Patrologia Graeca* [4, vol. 40, p. 155-480], while Photios I of Constantinople in his renowned *Bibliotheca* or *Myriobiblon* mentions ten of them along with a summary of their content [4, vol. 104, p. 201-224]. These *Homilies* contain a wealth of mathematical and astronomical propositions, which indicate the level

of the respective knowledge in the 4th century AD. One example is offered by the professor of Byzantine studies and academician F. Koukoules: "According to Asterius of Amaseia [4, vol. 40, p. 301], the student could not understand astronomy if the teacher did not 'simulate the motion of the pole by turning knowingly his eyes'" [10, p. 131].

Thus, Asterius could be classified as a priest and religious author with parallel studies in Mathematics (Arithmetic and Geometry) and in Astronomy.

One of his best-known works is his *Homily to the celebration of Calendae* [4, vol. 40], which was delivered on the occasion of the January calendae, January 1 of the year 400 AD.

5. Cyril I of Alexandria (370-444)

Cyril I of Alexandria was born in Alexandria in either 370 or 376 and he received a significant education in his native city, which was the cultural capital of the empire. He was the nephew of the archbishop of Alexandria Theophilus (385-412) and thus he was from an early age associated with the Church of Alexandria. He became a monk and he went to stay in the desert along with Isidorus of Pelousion. He later returned in Alexandria, where he was ordained deacon and priest by his uncle. Finally, in 412, after his uncle's death, he succeeded him in the patriarchal throne. He was archbishop and patriarch for 32 years. He was a dynamic personality and his zeal often reached the borders of exaggeration.

Cyril I was the main opponent of Nestorius, the heretics and the Jews. He closed the temples of the Novateans and confiscated their property; he sealed the synagogues and confiscated their property, too. He clashed with the augustalius (commander) of Egypt Orestes because of these violent acts and because of the tragic death of the eminent mathematician and philosopher Hypatia in 415, since he was accused as the motivator of the angry mob of Catharoi or Paravalaneis.

Cyril I became a prolific author of the Eastern Church and the total of his work was included in *Patrologia Graeca* [4, vol. 68-77]. For example, the work *Against the Galileans* by the emperor Julian the Apostate is known only from its refutation by Cyril I. Cyril wrote mainly *Letters*, which are significant for both their theological content and their astronomical and historical value, since they contain astronomical information about the calculation of the Christian Easter date, probably as a continuation of the astronomical work *Paschal Canons* of Anatolius (late 3rd century).

Twenty nine out of Cyril's 100 *Letters* are on this topic, and they were probably used by the monk Dionysius Exiguus as the source for his own *Paschal Table*, from which he derived the date of the Easter starting from the birth of Jesus Christ. It is known that the responsibility for the calculation of the Easter date and for informing all the Christian churches had been assumed after the First Ecumenical Council (325) by the Church of Alexandria, because of the flourishment of astronomy studies in its schools. Cyril I compiled Paschal tables

starting from the age of Diocletian, which probably extended to the future up to the year 531 [28].

The rest 71 *Letters* by Cyril I are about the Christological question. Cyril I, who also was one of the leading organizers of the Third Ecumenical Council (431), was proclaimed a saint of the Orthodox Church and his memory is celebrated on January 18, along with the memory of Athanasius the Great, as well as on June 9.

6. Synesius (370-414)

Synesius, a famous Greek orator, poet, philosopher, astronomer and author, was born *circa* 370 to a prosperous family of gentiles in Cyrene. His family hired for him private tutors who taught him philosophy and the sciences. Subsequently, he went to Alexandria, where he completed his studies in Philosophy as a student (along with his brother Euoptius) of the famous philosopher, mathematician and astronomer Hypatia, with whom he was connected with a long friendship. It seems that he owed a lot to Hypatia, for he exalts her in certain letters by calling her *"mother and sister, most respected teacher, blissful lady, most divine soul and all that is honourable in both essence and name"* [4, vol. 66, p. 1352].

In Alexandria Synesius became acquainted with the Christian religion but he did not seek to be baptized, although Christians wanted him in the Church because of his education. Synesius could not understand the Christian dogma of the resurrection of the dead, since him, as a philosopher, favoured opposite beliefs, such as the pre-existence of the souls, the eternity of the Universe, etc., and he rejected the resurrection of the dead.

Eventually, because Synesius as a leading figure in Cyrene had saved Ptolemaïs from the looting raids of the barbarian tribes of Libya and he had succeeded (with a four-year mission-intercession to the emperor Arcadius) in decreasing the taxing of its population, the people of Ptolemaïs after the death of the their bishop asked that Synesius be ordained as his successor. Synesius refused, since he did not want to divorce his wife in order to become a bishop, neither to change his philosophical beliefs. When he spoke about these objections to the archbishop Theophilus of Alexandria, he recommended to him to be baptized and become a Christian without dissolving his marriage or renouncing his philosophical views; it would be enough just to avoid teaching these views. Celibacy was not imposed on the clergy back in that period, not even for bishops.

After these compromissorial propositions, Synesius was baptized and then Theophilus ordained him priest and then bishop of Cyrene's Ptolemaïs (410-413/14) without Synesius renouncing his philosophy.

Consequently, Synesius can be viewed as a characteristic figure of the transitional period of the expansion and the final prevalence of Christianity in Egypt and North Africa, a model of philosopher high priest of that age with tolerance towards the gentile culture. He taught as a follower of the ancient

Greek spirit who inserted his moral and ethical values into the Christian framework.

Synesius, as a polymath, composed hymns in the ancient Dorian dialect and wrote many treatises, essays and speeches (*Dio, sive de suo ipsius instituto*, *Aegyptus sive de providentia*, *Encomium calvitii*, *De regno* etc.). In addition, he studied Neoplatonic philosophy, Physics and Astronomy, while at the same time he was especially critical against astrologers. He is regarded as the philosopher who blends in his work Neoplatonic views with Christian positions to a greater extent than Plotinus (3rd century).

His major works are:

- His oration *De regno* (= *On Kingship*), which was addressed in 399 to the emperor Arcadius and it is considered a work that 'inaugurated' the period of the national anti-barbarian movement for the annihilation of the influence of the Goths in the army and the administration of the empire. According to Synesius, the ideal state must be based on rationalism and philosophy.
- The *De insomniis (On Dreams)*, addressed to his teacher Hypatia [4, vol. 66, p. 1432], from whom he asked advice regarding the construction of an astrolabe, an astronomical instrument that was used for the observation of the stars and the determination of their altitude above the horizon. His scientific interests are attested by this letter, in which occurs the earliest known reference to a hydrometer, and by a work on alchemy in the form of a commentary on pseudo-Democritus.

From his many works, the one entitled *Over the donated astrolabe* [4, vol. 66, p. 1577-1588] is addressed to his friend Paeonius in Constantinople, to whom he sends as a gift this astrolabe that he had constructed himself.

The loss of this speech is significant, as it included the full description of the instrument, which was made of silver and included a model of the celestial dome with one thousand stars; from this information it can be deduced that it should be quite large in size. The late professor of Geodesy and Astronomy at the National Technical University of Athens, I. Argyrakos, published in 1958 a relative *Study of the 'Astrolabe' of Synesius of Cyrene* [29]. According to that study, Synesius was most probably the first Greek astronomer we know of that he wrote a work about an astrolabe.

Finally, Synesius wrote more than 159 *Letters* on various subjects, which illuminate the history of his period. These *Letters* were admired in the Byzantine Empire for their excellent writing style – the *Suda* encyclopaedic dictionary describes them as 'admired letters'. These *Letters* were printed in Vienna in 1792 by Gregorios Konstantas from Pelion (as he is mentioned in this edition) along with a commentary by the Greek monk and ecclesiastical writer Neophytos Kafsokalybites (†1780).

Synesius, condemned astrology in these words: "So the savants foresee the future, some of them by observing the stars, others by observing torches and shooting stars, others by 'reading' the intestines, by hearing the noises, the sitting or the flying of the birds. For them the so-called symbols of future events

are obvious 'writings' and voices and comparisons done for other purposes that are considered as important for everything." [4, vol. 66, p. 1284]

In addition to all these, Synesius can be regarded as one of the most important ancient chemists, since according to R. Herschel [30] he invented a 'hydrometer' or 'areometer', which he called 'varyllion', as he wrote to his teacher Hypatia (*Epistulae* 15).

Synesius as the bishop of Cyrene waged from 410 a struggle against the oppressive commander of Cyrene Andronicus and then against the Africans who attacked the region with continuous raids. In this final struggle he fell on the battlefield as leader of the defence around 411, when Cyrene was lost forever for the Hellenistic civilization.

7. Caesarius of Nazianzus (4th century)

The Church author Caesarius (†369) was the younger brother of Gregory of Nazianzus (329-390) and his memory is celebrated by the Orthodox Church on March 9.

Caesarius studied Philosophy and Medicine in Alexandria. It is included in this study because a great geographical work is attributed to him. This work covers the Balkan Peninsula, Asia Minor, Syria and Palestine. Apart from the wealth of geographical information, this treatise, which is similar to a modern travel guide, contains several pieces of meteorological and astronomical knowledge and information.

In addition Caesarius gained a great fame as a medical doctor. Thus, when he moved to Constantinople, he became the chief-doctor of the emperor Constantius II (Flavius Julius Constantius) and then of his successor Julian the Apostate after a recommendation of the latter's friend and renowned doctor Oreivasius. Because he accepted this position and became the official doctor of an enemy of the Christians, Caesarius was reproved by his brother Gregory [12, p. 263]. Afterwards, emperor Vales appointed Caesarius as the 'overseer of treasures and paymaster of the public money' in Nicaea of Bithynia, where he died around 369.

Caesarius of Nazianzus is with a low probability the author of the significant theological work *Four Dialogues* [4, vol. 38, p. 852-1189].

8. Nemesius of Emesa (4th to 5th century)

The philosopher Nemesius, the bishop of Emesa (nowadays Homs of Syria) was contemporary to the great eastern Fathers of Church. Very few elements are known about his life. He flourished *circa* 400 AD, while he is better known to the historians of science from his famous work *De Natura Hominis* (*On the Nature of Human*), which is attributed by certain researchers to Gregory of Nyssa, due basically to its similarity with the latter's *On the Construction of Human*.

In this work Nemesius connects the Greek philosophers (Plato, Aristotle, Epicurus, the Stoics etc.), the physician Galenus and others with his contemporary Christian scholarly tradition in an effort to build an anthropological system in accordance with the Christian philosophy that was taking shape in his period. The philosophy of Nemesius is basically a Christian Neoplatonism with an Alexandrian overtone.

The whole text of *De Natura Hominis* is included in the *Patrologia Graeca* [4, vol. 40, p. 503-818] and could be described as the epitome of Christian anthropology: in this work the spiritual and material nature of human, the *"microcosm of the whole universal creation"* according to Nemesius, is described.

Author N.K. Laos in his book *Cognitive Science, Philosophy and Orthodox Theology*, writes: "Nemesius in this work studied the human being as a soul-and-body unity and wrote about the dialectic relation between body and mind. More specifically, this great Church Father writes that the soul is not body, it is not a material entity, but it is rather an essence 'independent and bodiless', 'an entity without size or volume or parts', that at the same time it is united with the body without any confusion." [31]

Geometry, Astronomy, time, Anthropology and Theology are inseparably connected in this work of Nemesius which is composed by 44 chapters. It deals with the generation and the essence of the soul, with its union with the body, with the power of the soul, with the freedom of the human being and with the divine providence in relation with the fate. It refutes the beliefs of the Manichaeists, the Eunomians (also known as the Anomœans) and the Apollinarists, who had adopted the fatalistic beliefs of the Greek philosophers. For all these the work of Nemesius occupies a high place in the Christian philosophy; it was esteemed by the subsequent bishops and it was used first by John of Damascus (7^{th} to 8^{th} century) in his *Exact Exposition of the Orthodox Faith* [4, vol. 94, p. 789-1228] and afterwards (9^{th} century) by the monk Melitius in his work *On the Construction Of Humans*.

Such a major work, as it was natural, was extensively translated: in Armenian (8^{th} century), in Latin (11^{th} and 12^{th} cent.) and afterwards many times in the West (Antwerp 1575, Oxford 1671, Halle 1800-1802, etc.). This work is valuable for its references in the history of time measurement (see e.g. G.J. Whitrow: *Time in History. Views of time from Prehistory to the present day* [32]), while it was used by the authors of this paper in a book [33] about the views of the Stoics on the re-creation of the Universe.

9. Dionysius Exiguus (5^{th} to 6^{th} century)

The abbot, Church author and chronologist-astronomer Dionysius Exiguus or Dionysius the Minor is more widely known to astronomers and chronologists as the introducer of the Christian chronology from the birth (incarnation) of Jesus. Very little is known about his life, mainly from what his contemporary monk Flavius Magnus Aurelius Cassiodorus (480-583) wrote in his work *De*

divinis Lectionibus (c. xxiii). A knowledgeable person who knew well Greek and Latin, Dionysius translated, *inter alia*, in Latin the letters and the *Paschal Table* of the bishop Cyril I of Alexandria, the treatise by Gregory of Nyssa *On the Construction of Human*, the life of Saint Pachomios and the Codex of Ecclesiastical Canons from the time of the Apostles to the Third Ankara Council (375).

The late Greek astronomer K. Khassapis [34] writes that Dionysius was a Greek monk from what is now the shores of Romania, the Scythia Minor of that period, hence he is called a Scythian. He made the voyage to Rome in 497 as a member of a mission from Constantinople and he stayed there becoming abbot of a monastery until 540. He became famous as both an ideal translator of the Greek Fathers of the Church and an author of his own works; he kept writing until his death in 546. His most important work is known as *Collectio Dionysiana* and contains two collections of religious canonical texts: the first collection consists of Greek texts with Latin translations and the second consists of Papal decisions. This work exerted a considerable influence in the West. The whole work of Dionysius, mainly his translations, is included in Migne's *Patrologia Latina* [35, vol. 67, p. 9-527].

Close to the beginning of the 6th century, Dionysius Exiguus started an attempt to determine with precision the date for the celebration of the Christian Easter. After he was prompted by Pope John I (523-526) and ordered by the emperor Justinian I (527-565), he tried to recalculate this date starting with the year of the birth of Jesus Christ. He based his calculations on the *Paschal Table* of the bishop Cyril I, which was numbering the years starting with the year of the emperor Diocletian.

Dionysius compiled new calendrical tables for the exact determination of the Easter Sunday. He was so absorbed by this huge task and the complicated calculations involved, that some minor mistakes slipped into these.

With the astronomical elements and the mathematical tools of that age he finally concluded that the year he finished his calculations was the year 248 of the Diocletian era our 532. It seems that the year he began constructing his Paschal Tables was 525. The fact that he ended in 532 may be related to the fact he knew that the Julian cycle of Easter 532 years long. Then Dionysius decided to count the years from the incarnation of Jesus Christ and thus our current numbering was introduced (Aera Christiani or Christian era). He calculated the Easter date for 95 years, from 532 to 626 by translating the *Paschal Table* of Cyril I (*De Ratione paschae*, *Argumenta pascalia*). His calculations for the year of Christ's birth are included in his work *Cyclus Decem Novennalis* and they were based on the texts of Clemens of Alexandria (150-229), who wrote that Jesus was born in the 28th year of the reign of Octavian Augustus. He then supposed that Jesus was born on December 25 of the year 754 from the building of Rome (754 A.U.C.) and not in the correct 749 A.U.C (= Ab Urbe Condita). He made the correspondence 754 AUC = 1 AD (primo anno Domini), not taking into consideration the introduction of a year '0' – he could not even think of it, since there was no zero in his age! [28, vol. II, p. 264]. Had he added such a year

in his chronology, Dionysius would have relieved us from the confusion regarding the celebration of the century change.

10. Conclusions

The contribution of the scholarly bishops of the early Byzantine period to the natural sciences is in our opinion a very important topic to study and research, as it is rather neglected. The cosmological views of Gregory of Nyssa are markedly influenced by the Physics and Cosmology of the pre-Socratic Greek natural philosophers, as he writes about them in his several writings. Of special interest are these views when they are juxtaposed with the views of Basil of Caesarea in his *Nine Homilies to the Six-Day Creation* (*Peri Hexahemerou*). In both views of the world, which were echoed in the subsequent works by Church Fathers, the celestial bodies are considered spherical, like the sky and the firmament. The motion of the celestial bodies is generally circular, although in no place in their texts is the constant speed circular motion mentioned, as it is described in Ptolemy's *Syntaxis (Almagest)*, a basic element of the Greek and Hellenistic astronomy. From this point of view the Christian cosmology tends to lift an obstacle for the refutation of the astronomical system, which was not so much the difference between heliocentric and geocentric system, but rather between circles and ellipses [13].

In any case, by studying the texts of the early Byzantine Church Fathers/scholarly bishops we easily realize that they were men of deep Greek culture and education. They study in detail the universal issues with a view based on the Greek and Hellenistic texts and it is at once scholarly and scientific, entirely different from the simplistic world views that appeared in the following centuries, such as the one of the monk Cosmas Indicopleustes (6^{th} century) with his *Christian Topography* [4, vol. 88, p. 445], which we shall examine in a future paper.

It should also be stressed that the works of the great Church scholars of the 4^{th} and 5^{th} centuries influenced to a large degree both their contemporary and the subsequent Western scholarly bishops. For example, Saint Augustine, bishop of Hippo (354-403) is influenced by Gregory of Nyssa in his view that in the human soul we discover traces of the properties of the Trinitarian God, as well as in his definition of time, which Gregory considers as 'dilation of the soul', division and tearing of the soul 'towards hope and memory' [33, p. 24].

According to author K.D. Georgoulis most modern theologians and philosophers exalt Gregory's contribution to the anthropological problem in relation with the incarnation and to the ontological 'transcendism' and existential starting point. Indeed, the fundamental metaphysical position of Gregory of Nyssa is not the essence, the 'what is this?', but rather the existence, the 'is', in other words the realization of the existence [7, p. 686].

It should be noted once more that, by reading the works by Gregory of Nyssa, the authors realized that it certainly needs further analysis and detailed research, especially its cosmology.

This paper is the continuation of our previous work on the connections between spirituality and science [36, 37] and on the contribution of the Church in Byzantium to the natural sciences [1, 38]. In our next paper in this series we shall examine the simplistic cosmology of Cosmas Indicopleustes (6th century) and his geographical aspects and writings.

Acknowledgements

This study formed part of the research at the National and Kapodistrian University of Athens, Department of Astrophysics, Astronomy and Mechanics, and we are grateful to it for financial support through the Special Account for Research Grants. It is also supported by the Ministry of Science and Technological Development of Serbia through the project III44002.

References

[1] E. Theodossiou, V.N. Manimanis and M.S. Dimitrijević, Eur. J. Sci. Theol., **7(2)** (2011) 57.
[2] E. Grant, *Physical Science in the Middle Ages*, Cambridge University Press, Cambridge, 1979, 8.
[3] T. Nikolaidis, Byzantiniaka, **11** (1991) 206.
[4] ***, *Patrologiae Graecae cursus completus, series graeca*, J.-P. Migne (ed.), vol. 1-161, Centre for Patristic Publications, Athens, 2008.
[5] K.D. Georgoulis, *Gregory of Nyssa*, in *Encyclopaedia of Helios*, in Greek, vol. 5, Helios Publ., Athens, 1957, 680.
[6] V.W. Callahan, J.P. Cavarnos and W. Jaeger (eds.), *Gregorii Nysseni Opera VIII, 1. Opera ascetica*, E.J. Brill, Leiden, 1952, 370.
[7] K.D. Georgoulis, *Hellenic Christian Philosophy,* in *Encyclopaedia of Helios*, in Greek, vol. 7, Helios Publ., Athens, 1957, 683.
[8] E. Danezis and E. Theodossiou, *The Future of our Past*, in Greek, Diavlos Publ., Athens, 2005, 72.
[9] G. Metallinos, Christianiki, **February 9** (2006) 5.
[10] F. Koukoules, *The life and civilization of the Byzantines*, in Greek, vol. I, Papademas Publ., Athens, 1948, 125.
[11] Basil the Great, *Homilies on Hexameron*, in Greek, Polytypo Publ., Athens, 1990.
[12] E. Theodossiou and E. Danezis, *At the Years of Byzantium – Byzantine scientists, physicians, chronologers and astronomers*, in Greek, Diavlos Publ., Athens, 2010, 254.
[13] T. Nikolaidis, *Greek Astronomy and Christian cosmology*, Proceedings of the 4th Conference 'Aristarchus the Samian', in Greek, National Research Foundation of Greece, Samos, 2003, 183-188.
[14] E. Theodossiou, V.N. Manimanis, E. Danezis and M.S. Dimitrijevic, Transdisciplinarity in Science and Religion, **2** (2009) 50.
[15] E.D. Moutsoulas, *Gregory of Nyssa - Life, Works and Teaching*, in Greek, Eptalophos Publ. A.B.E.E., Athens, 1997, 65.
[16] E. Theodossiou and E. Danezis, *To the traces of IXTHYS: Astronomy-History-Philosophy*, in Greek, Diavlos Publ., Athens, 2000, 309.

[17] E. Danezis and E. Theodossiou, *The Universe I loved - An Introduction to Astrophysics*, in Greek, Diavlos Publ., Athens, 1999, 229.
[18] E. Danezis and E. Theodossiou, *The Cosmology of the Mind - Introduction to Cosmology*, in Greek, Diavlos Publ., Athens, 2003, 245.
[19] E. Theodossiou and E. Danezis, *The year's Cicle-Astronomy and mysteries*, in Greek, Diavlos Publ., Athens, 2004, 153.
[20] Nemesius of Emesa, *Later Greek Religion*, E.R. Bevan (ed.), J.M. Dent & Sons, London, 1927.
[21] V. Feidas, *Gregory of Nyssa,* Encyclopaedia Papyros-Larousse-Britannica, in Greek, vol. 19, Papyros Publ., Athens, 1996, 249.
[22] W. Jaeger (ed.), *Gregorii Nysseni opera omnia*, Weidmann, Berlin and Leiden, 1921-1972, 62.
[23] K. Gronau, *Poseidonios und die judisch – christliche Genesisexegese*, Teubner Publ., Leipsig, 1914, 112.
[24] Grégoire de Nysse, *La creation de l'Homme*, J. Laplace and J. Danielou (eds.), Sources Chrétiennes, vol. 6, Aubier, Paris, 1944.
[25] ***, *The Panarion of Epiphanius of Salamis, Book I (Sects 1-46)* and *Book II and III (Sects 47-80, De Fide)*, translated in English by F. Williams, E.J. Brill, Leiden, 1987-1993.
[26] Eusebius Hieronymus, *Apologia Adversus Libros Rufini,* in J.-P. Migne, *Patrologiae Latinae,* Vol. 23, Book 2, Typographi Brepols Editores Pontificii, Turnholti, Paris, 22, available on line at http://www.documentacatholicaomnia.eu/02m/03470420,_Hieronymus,_Apologia_Adversus_Libros_Rufini,_MLT.pdf.
[27] A.A. Shaw, National Mathematics Magazine, **11** (1936) 3.
[28] E. Theodossiou and E. Danezis, *The Odyssey of the calendars*, vol. I, in Greek, Diavlos Publ., Athens, 1996, 160.
[29] I. Argyrakos, *A study of the 'Astrolabe' of Synesius of Cyrene (4^{th} AD century).* Vougioukas L., Athens, 1958.
[30] R. Herschel, *Epistolographi Graeci*, R.H. Didot, Paris, 1873.
[31] N.K. Laos, *Cognitive Science, Philosophy and Orthodox Theology*, in Greek, Diavlos Publ., Athens, 2005, 44.
[32] G.J. Whitrow, *Time in History. Views of time from Prehistory to the present day*, Oxford University Press, Oxford, 1989, 43.
[33] E. Theodossiou and E. Danezis, *Measuring the Timeless time – Time in Astronomy*, in Greek, Diavlos Publ., Athens, 2010, 22.
[34] K. Khassapis, *The Star of Bethlehem – An astronomical consideration*, in Greek, Karabias Publ., Athens, 1970, 1.
[35] ***, *Patrologiae Latinae (P.L.), Patrologiae cursus completus, series latina.* Turnholti, J.-P. Migne (ed.), vol. 1-221, Typographi Brepols Editores Pontificii, Parisiis (Paris), 1844-1865, available on line at http://e-homoreligiosus.blogspot.com/2010/11/mignes-patrologia-latina-on-line-pdf.html.
[36] E. Danezis, E. Theodossiou, I. Gonidakis, M.S. Dimitrijević, Eur. J. Sci. Theol., **1(4)** (2005) 11.
[37] E. Theodossiou, V. Manimanis, M.S. Dimitrijević, Eur. J. Sci. Theol., **6(3)** (2010) 47.
[38] E. Theodossiou, V. Manimanis, M.S. Dimitrijević, Eur. J. Sci. Theol., **6(4)** (2010) 57.

European Journal of Science and Theology, *June 2012, Vol.8, No.2, 7-24*

ASTROLOGY IN THE EARLY BYZANTINE EMPIRE AND THE ANTI-ASTROLOGY STANCE OF THE CHURCH FATHERS

Efstratios Theodossiou[1], Vassilios Manimanis[1] and Milan S. Dimitrijevic[2*]

[1] National and Kapodistrian University of Athens, School of Physics, Department of Astrophysics, Astronomy and Mechanics, Panepistimiopolis, Zografos 15784, Athens, Greece
[2] Astronomical Observatory, Volgina 7, 11160 Belgrade, Serbia

(Received 7 March 2011)

Abstract

The peoples of the Roman Empire in the 4th century AD were very superstitious. Sorcery and astrology were widespread in the early Byzantine period. Astrologers, guided by Ptolemy's *Tetrabiblos*, were compiling horoscopes and dream-books, while a common literature were the *seismologia*, *selenodromia* and *vrontologia*, with which people tried to predict the future. It was natural that in this environment many astrologers were famous and they flourished especially in the court of the Emperor Julian (361-363). The Fathers of the Church, however, were clearly against astrology and they were condemning those who wanted to learn about the future events from astrology and other occult practices and pseudo-sciences. Here are presented astrologers Maximus of Ephesus, Paul of Alexandria, Hephaestion of Thebes, Ioannis Laurentius of Lydia and Rhetorius of Byzantium, as well as the Emperor Julian the Apostate, together with the condemnation of astrology by Emperor Honorius and Church Fathers Basil the Great of Cesarea, Gregory of Nyssa, Gregory of Nazianzus, John Chrysostom, the bishop of Jerusalem Cyril I, Epiphanius of Cyprus, Eusebius of Alexandria, Nemesius of Emesa, and Synesius of Cyrene.

Keywords: astrology, occult, Byzantine Empire, Tetrabiblos, foretelling, Emperor Julian

1. Introduction

In the first century of the Byzantine (i.e. the Eastern Roman) Empire astrology was an extremely common activity. Claudius Ptolemy's *Tetrabiblos* (= 'Four-book work') was the basic work of reference for all persons who practiced astrology [1]. This astrological opus, which still forms the basis of the modern 'Western' astrology, defends the usefulness of predicting the future through the

[*] Corresponding author, e-mail: mdimitrijevic@aob.bg.ac.rs, Phone: +381-11-3089-072, Fax: +381-11-2419-553

observation of the stars – the 'prediction through Astronomy'. In this work Ptolemy presents the Hellenistic horoscope astrology in a detailed and systematic manual, the first complete manual of astrology, which of course was based on the geocentric system as it is described in the *Almagest*. This great astronomer, however, seems to consider astrological predictions rather as a probabilistic tool than as an infallible guide. Besides, he rejected other common types of prediction, such as numerology. In addition to *Tetrabiblos* the Byzantine astrologers were inspired and influenced by the works of the Neoplatonist philosopher Porphyrius of Tyros (232/233 - 305?), Iamblichus Chalcidensis (250-326) and later on by some Arabic works.

Thus, the early Byzantine astrologers were compiling horoscopes, oracles based on natural phenomena, dream-books, other kinds of oracles and other. This was the heyday of the so-called *seismologia* ('earthquake guides') *selenodromia* ('moon-phase books') and *vrontologia* ('thunder guides'), texts that were 'explaining' how one could prophesize e.g. the death of an eminent person or the outcome of a war through the sound of thunders. These special books, as the late professor of Byzantine studies and academician F. Koukoules writes [2], had their roots most probably in Aristotle's *Meteorologica* [3], where the 'thunder-prediction' is expressly mentioned.

It is an indisputable fact that in the first centuries of the Byzantine Empire its subjects were very superstitious and that sorcery and astrology were very widespread. Koukoules writes [2, p. 43]: *"The superstitious parents were taking care to learn, among other things, which day was the most appropriate for their children to start courses; as we know from astrological texts, appropriate dates were thought to be the first day of the moon and also the seventh, the tenth, the eleventh, the eighteenth, the twenty-seventh and the twenty-eighth days. They were also observing in which zodiacal sign was the moon; the astrological texts considered appropriate the dates on which the moon was residing in Pisces, Gemini, Leo, Capricorn or Virgo, as they are listed in the 'Catalogus codicum astrologorum graecorum'* ([4])*."*

In this *Catalogus codicum astrologorum graecorum* were given even the appropriate dates to end a baby's breast-feeding [4, Book 2, p. 19, Book 5, p. 3, 94, 96, Book 6, p. 22].

Astrology was so commonplace in the Byzantine 4th and 5th centuries that even the hunters were consulting its directions. According to these guidelines: *"When the moon is in Gemini it favors hunting and when it is in Libra it favors hunting using falcons"* [4, Book 5, p. 94 and 95].

Astrology, in other words, occupied an eminent place in the everyday life in the early empire, and its importance persisted even in its subsequent periods. One should not forget that legend has it that during the founding of Constantinople Emperor Constantine ordered the astrologer Vales to predict its future and its longevity [5].

In the early Byzantine Empire, while the Christian religion was struggling with the old one – especially during the short reign of Julian – a famous astrologer, Maximus of Ephesus, is mentioned among the consultants of Julian

in the emperor's effort to revive the ancient Graeco-Roman religion. In the 4th century another famous astrologer is mentioned: Paul of Alexandria, who was flourishing around 378 AD and wrote a treatise entitled *Eisagogica [eis tin apotelesmatikin]*, i.e. *Introduction [to the effective]*, meaning the power and the 'effective' energy of the stars and the signs. In the same period flourished Hephaestion of Thebes, who wrote the *Apotelesmatika* (= *The effective ones*) around 415. Finally, as Herbert Hunger reports in his *Byzantine Literature* [6], a few decades later we have Ioannis of Lydia, who wrote the treatise *On Diosemeia* (the divine signs or miracles) during the reign of Justinian [7].

The division of the zodiac into 12 parts, the so-called signs, is mentioned in texts of the Church Fathers; more specifically it is mentioned by Basil the Great [8], by Caesarius (the brother of Gregory of Nazianzus) [8, vol. 38, p. 938] and by Procopius of Gaza [8, vol. 87, p. 96]; all three of them condemn astrology, as all Fathers of the Church did.

Let us present now certain eminent astrologers of the first two centuries of the Byzantine Empire along with the scholar emperor Julian.

2. Maximus of Ephesus (4th century)

Maximus of Ephesus was a famous Neoplatonist philosopher of the 4th century. Some researchers suggest that he was born in Ephesus, hence his surname, yet others believe that he was born in Smyrna and he moved to Ephesus after completing his studies in the Neoplatonist School of Pergamus. He was a student of both Iamblichus (250-326) and Aedesius (†335). Maximus exerted a strong influence on the religious policy of Emperor Julian (361-363): he was his friend, his teacher and his spiritual advisor. It seems likely that when he moved to the capital city of Constantinople Maximus took the surname 'Byzantius', for in the literature he is also mentioned as Maximus Byzantius: it is most probable that Maximus of Ephesus and Maximus Byzantius is one and the same person.

Maximus, following the general philosophical views of Plotinus (204/205-269/270), studied sorcery, astrology and Logic. It is believed that he contributed a lot to the Emperor Julian's hostility towards Christianity, since he initiated him into the Chaldean rites as well as into the worship of the Sun and Mithra. According to the author K. Tsopanis: *"A central teaching of Maximus was the theory about the universal affinity, which manifests itself in above-the-Earth secret cycles, such as the solar cycles. According to this theory, every living creature (but also every object in the world) bears inside it a 'divine spark' that brings it into direct 'magical' contact with the Sun. According to Maximus, even the statues of the gods were 'soaked' as the years passed through worship and rituals by outflows of the divine essence, resulting in their ability to perform miracles."* [9]

As it was natural, after Julian's death in 363 Maximus of Ephesus was accused as astrologer and an enemy of Christianity, as well as for participation against the new emperor Valens Flavius Augustus (364-378). For all these

charges he suffered persecutions and humiliations, and finally he was executed by Phestus, the vice-consul of Asia, in 371. Maximus is the probable author of two philosophical treatises entitled *On unresolved antitheses* and *Commentary to Aristotle*. The latter work comments on Aristotle's *Analytics*, while it seems that Maximus also wrote a commentary on the Aristotelian work *Categories*. He also wrote astrological poems, such as *Peri katarchon* (= *On the beginnings* or *On commencing the sacrifices*), as well as astrological treatises such as the *Peri arithmon* (= *On numbers*). He probably wrote some other treatises addressed to the Emperor Julian, which were lost [7, p. 225]. Julian is examined separately in the following section, as he favoured astrology in his effort to revive the ancient Graeco-Roman religion.

3. The Emperor Julian the Apostate

Flavius Claudius Julianus was born in 331 AD in Constantinople, to the royal family of Flavii; he was the son of Flavius Julius Constantius, the half brother of Constantine the Great. His mother Basilina died only months after Julian's birth, an event that influenced decisively his character. In any case, he lived a tragic childhood, witnessing from a tender age a number of murders in his environment so that claims to the throne would not arise. After the death of Constantine the Great, in May 337, the six-year-old Julian was saved from the imperial purges of Constantius II, the son of Constantine the Great, thanks to his uncle Eusebius. Eusebius was Basilina's brother, a bishop of Nicomedeia and later the archbishop of Constantinople (339-341), the leader of the sect of Arius in the capital, who was then under the favor of Emperor Constantius II during the specific period of time. Julian and his brother Gallus continued to be protected by Eusebius until the bishop's death, in 342. Julian, still an eleven-year-old child then, was first educated by Mardonius, a teacher of Greek from Thrace, who inspired him his love for the ancient Greek world, while his religious education was in the hands of Eutropius, a fanatic monk and follower of the heresy of Arius. Later Julian studied in both Nicomedeia and Athens, where he was indoctrinated with the views of Neoplatonism. In the philosophical School of Pergamus he had Aedesius as his teacher, who in turn was a student of Iamblichus. Julian was also taught by Nicocles and by the Christian sophist Ekevolius, while he became acquainted with the teaching of Livanius the orator (314-390?) through notes kept by his students.

Aedesius, being then in an old age (and hence probably being more respectable in the eyes of his students) brought Julian into contact with his best four students in Pergamus: Maximus of Ephesus, Priscus – who is known as a Neoplatonist philosopher– from Thesprotia, Chrysanthius from Sardis and Eusebius of Caria or Emesa, the so-called 'silent philosopher' or Pittacàs. All four, but mainly Maximus as we have already mentioned, contributed decisively to the separation of Julian from the Christian religion and to his turn towards the old religion [7, p. 226].

Julian continued his studies in Athens under the two famous teachers of rhetoric: Imerius of Proussa and Prohaeresius from Caesarea or Armenia, a Christian scholar who died in 368. It was in Athens that Julian met Saint Basil the Great (Basil of Caesarea) and Gregory of Nazianzus, who were also there as students.

Subsequently Julian was married Helen, the daughter of Constantine the Great and sister of emperor Constantius II. This marriage probably saved him from the second round of purges, as his brother Gallus was executed in 355 under imperial orders. However, the young Julian was also protected by the clever and educated Flavia Aurelia Eusebia (†360), the second wife of Constantius II (337-360).

In 350 Julian was appointed as commander in Galatia by the emperor. There, showing considerable ability and decisiveness, he expelled the Franks and the Alamanni by winning a series of battles at the north-western borders of the Roman Empire, in Danube, Argentoratum (Battle of Strasbourg, 357) and in other places. He also revived the economy of the region, while he became known as a just person. Finally, as the last survivor of the dynasty of Constantine the Great, but also being especially popular in the army and the populace, Julian became Emperor after the death of childless Constantius II (November 3, 361 AD), on December 11, 361, and returned to Constantinople.

As an emperor, Julian imposed the appropriate reforms in the fields of the administration and economic policy that relieved the people: he reduced the inflation, and stopped some fruitless spending in the imperial court, regulated the prices of food and reorganized the taxing system and the public services. These actions made Julian more popular, while in parallel he increased the wealth of the state treasuries [7, p. 227].

On the other side, Julian's admiration for the ancient Greek civilization led him to an effort to replace the Christian religion with the ancient Graeco-Roman one as the state's official faith. During his reign (361-363), Julian stopped the state subsidies towards the Church, while he removed the Christians from the upper public offices of the Empire and the positions of philosophy teachers with the justification that it was unfit for people who did not believe in the gentile gods to teach and to interpret the works of the gentile authors, which were full of references to these gods. From this edict was excluded his teacher Prohaeresius, who, however, refused to accept this special treatment and he resigned in 362.

In addition, with the edict of February 4, 362, Julian re-established the gentile worship, imposing the reopening of the temples of the gentiles that had been closed and restarting of the sacrifices on the altars.

Julian with his actions aimed to utterly vanish the new religion and he knew that these actions would bring divisions in the Church so that the divided Church would not represent a major threat for paganism any more [10]. These actions were met with remorse by the Christians and due to them Julian was called by the Church 'Apostate' ('Renegade') and by the lay Christians, mockingly, 'Adonaeus'.

It is, however, probable that he just wanted to equilibrate the situation in order to either establish a state without a preference towards a specific religion or to create a *syncretic* (mixed) 'state religion', which would accept the ancient gods, it would had a priesthood composed from priests of all religions without discrimination and its head would be the Emperor as Pontifex Maximus. This plan would be opposed by both Christians and devout gentiles, since they would see it as an attack against both religions and absurd [7, p. 228].

Julian's friend, the Latin historian of Greek descent Ammianus Marcellinus (330–400), wrote: *"Although Julian was more inclined towards the worship of the gentile deities since his youth and as he gradually grew older he was burning with the zeal to practice it, yet, because he had several reasons to be afraid, he did whatever pertinent to this worship he did with the greatest possible secrecy. But when his fears vanished and he realized that the time had come to freely materialize his wish, he revealed the secrets of his heart and with clear and explicit edicts he ordered the opening of the idolatry's temples, to resume sacrifices upon the altars and, in general, to restore the worship of the idols"* [11].

In reality, the ancient religion had closed its life cycle. Among Julian's friends was a medical doctor, Oreivasius (325-403), who, when Julian became emperor, was appointed chief doctor and treasurer in Constantinople. According to the tradition, he was the emissary of Julian to the Oracle of Delphi. He had been sent in order to receive prophesy on whether the ancient religion could be revived. The literary tradition saved the oracle given by Pythia to Oreivasius, according to the legend: *"Tell to the king: everything has collapsed, Apollo has no roof over his head anymore, neither foretelling bay leaf, nor speaking spring – the speaking water has also dried"* [12, 13].

This oracle, either uttered by Pythia or, more probably, being a creation of tradition, expresses an indisputable truth: the ancient religion was vanishing and along with it the famous sanctuary of Apollo was also perishing. It seems that the Olympian gods had decided to retreat from the stage of history and to silence themselves. Their allocated time in the history has passed [14].

3.1. Emperor Julian and the heliocentric system

Julian was a scholar and cultivated person, an emperor who was also a philosopher and an author, and became the source of inspiration, according to Robert Browning, for eminent literary figures and intellectuals [15]. From a passage in his texts he even appears as a forerunner of Copernicus more than eleven centuries earlier! He believed that the planets revolve around the Sun, following circular orbits in well-defined distances. This passage (from the *Hymn to King Helios*) reads: "*For the planets round about him (the Sun), as though he were their king, lead on their dance, at appointed distances from him pursue their orbits with the utmost harmony; they make, as it were, pauses; they move backwards and forwards (terms by which those skilled in Astronomy denote these properties of the stars)*" [16].

This means that Julian was thinking of the Earth as a planet, which revolves following a circular orbit around the Sun and along with it all the other planets, which revolved around the Sun in well-defined orbits and intervals, i.e. spaced by well-defined distances between them. This quote shows that in the fourth century AD the heliocentric theory of Aristarchus of Samos (310-230 BC) was not forgotten, and that it still had its supporters.

Perhaps in the Neoplatonic School of Athens, where Julian studied and shaped his scientific opinions, the heliocentric theory of Aristarchus was being taught.

3.2. The death of Emperor Julian

Julian was mortally wounded by the spear of an unknown knight in 363 during a battle near Ctesiphon against the king of Persians Sappor II (310-379), and he died in the evening of June 26 to 27.

Figure 1. Saint Mercurius mortally wounds Emperor Julian (*Meteora, Monastery of Saint Stephanos, photograph by the authors*).

It should be noted that the theory of chronographer Ioannis Malalas [17] (also reproduced by Ioannis of Nikiou [18]) that Julian was killed by the spear of Saint Mercurius, is totally groundless. Mercurius had suffered martyrdom during the reign of Decius (249-251) or of Valerian (251-259) and therefore he is

totally out of date; yet, the tradition has it that this was done after a request of Saint Basil. However, since Basil was a fellow student and a friend of Julian, it is impossible that he made an entreaty to a Saint to 'murder' Julian. However, this legend is alive in the Greek Iconografy (see, for example, the icon of Saint Mercurius from Meteora – Figure 1).

Livanius the orator (314-393) supported the view that Julian's fatal injury was the result of an act by a fanatic Christian [19] and Sozomenus, the Christian writer of the early 5th century, agrees with this opinion [20]. Both are based on the fact that no Persian soldier appeared to state that he wounded Julian with his spear, in spite of the huge reward the Persian king had promised to the one who would exterminate his opponent.

Julian was emperor from November 3, 361, to June 26, 363, i.e. less than two years. After his reign the character of the Byzantine Empire would be strictly Christian and in Astronomy geocentric. The emperor's last evening is described by the historian Ammianus Marcellinus as follows: *"And because all who were present were crying, he, still retaining his grandeur, admonished them by saying that it was improper to lament for a sovereign who would become one with the sky and the stars. Then everybody fell silent and Julian started a complicated conversation with philosophers Maximus and Priscus about the nobility of the soul. Suddenly, the wound on his rib opened, the blood pressure cut his breath and, after he drank cool water he had asked for, departed calmly from this life in the darkness of the night at the age of 32."* [11, p. 15].

Julian's cousin Procopius asked from the new emperor Flavius Claudius Jovianus (Jovian, 363-364) the permission to bury his body in Tarsus, which was given to him immediately.

Jovianus ordered that the following words be carved on Julian's tomb: *"Here, next to the rich waters of Tigris, lies Julian, a good king and at the same time a valiant warrior"* [21].

From the works of Julian, which are considered masterpieces of style, the following ones are saved:

- *Panegyric in honor of Constantius,*
- *The heroic deeds of Constantius,*
- *Panegyric in honor of Queen Eusebia,*
- *Hymn to King Helios [Addressed to Sallust],*
- *Antioch's speech* or *Beard-Hater* (ed. C. Lacombrade), a speech against the Christians of Antioch who jeered at the Emperor's beard, which he used to keep long according to trait of the philosophers of that age.
- *The Caesars* or *Symposium,*
- *Apologies,*
- *Epistulae (Letters).*

From all these works the *Hymn to King Helios* contains the clear reference that supports the heliocentric system we already mentioned. There is also another work that was only partially saved (one book out of three), entitled *Against the Galileans*, i.e. against the Christians [22]. This work was refuted by

the Byzantine scholar and priest Philip of Side (4th to 5th century), the successor of Didymus the Blind in the School of Alexandria.

Figure 5. Julian pictured on a golden coin (solidus) of Antioch.

After the years of Julian astrology continued to flourish. It seems that never lost its grip on the Byzantine populace. After Paul of Alexandria, Hephaestion of Thebes and Ioannis of Lydia we find as the last astrologer of the early Byzantine period the sixth-century foreteller Rhetorius of Byzantium. Let us examine their work and personality one by one.

4. Paul of Alexandria (4th century)

Paul of Alexandria flourished in Alexandria around the year 378. He is regarded as the author of an astrological treatise entitled *Eisagogica [eis tin apotelesmatikin]*, i.e. *Introduction [to the effective]*, meaning the power and the 'effective' energy of the stars and the signs upon the persons and their actions.

This work was present in the library of Leon the Wise or the Mathematician (780-869), who in his *Codex* about astrology writes: *"The secret principles of Phoebus' art of foretelling I was taught by Paul, the eminent astrologer"* [6, p. 38].

5. Hephaestion of Thebes (4th to 5th century)

Hephaestion, an eminent Graeco-Egyptian astrologer of the 4th and 5th centuries, was born in Thebes of Egypt and flourished in Alexandria around 380; he wrote a treatise in three books that are entitled: *Astronomical principles*, *Birthday lore*, *Catarchae* or *Apotelesmatika* (= *The effective ones*).

In the first book, Hephaestion writes about the general principles of astronomy. In the second book he deals with birthday astrology, while in the third book, which is the main part of his treatise, he deals with the choice of the appropriate time to start any important work.

The work of Hephaestion influenced all subsequent Byzantine scholars who delved in astrology and can be found today in its entirety in the National Library in Paris and in libraries of several Italian cities. It is important for an additional reason: from certain passages of it we learn about significant scientists of that age, such as Thrasyllus, Critodemus, Apollinarius, Antigonus and others, for which it is the sole source of information [7, p. 233].

6. Ioannis Laurentius of Lydia (490-565)

The historian-archaeologist, scholar, astronomer and astrologer Ioannis Laurentius of Lydia was born in Philadelphia of Lydia. He followed law studies in the Pandidakterion (University) of Constantinople and his knowledge of Law and History helped him to rise to eminent offices of the empire. One of his teachers was Agapius, a philosopher and scholar who in turn was a student of Proclus.

Ioannis (John) worked initially in the tachygraphy service; subsequently he became a state officer by being promoted to the post of the service's director by the emperor Anastasius I (491-518). Finally, the emperor Justinian I (527-565) appointed him as a teacher of Latin in the Pandidakterion, from which he resigned after he fell into disfavour in 552, in order to pursuit full-time writing.

His work was not restricted to History as he gave it a rather encyclopaedic character; it is composed by three treatises, of which the larger one is the Law treatise *On the Powers* or *On the magistrates of the Roman State*. This work follows the evolution of the Roman offices from the beginning of the Roman Empire up to Justinian I. It offers us rich information about the history of the institutions and also about the actions of Ioannis Cappadoces, a Justinian's supreme officer of the praetorians. In addition, Ioannis Laurentius analyzes the administration of the empire and gives information on his personal life and career. This information, although it reveals a tendency for personal show-off, is illuminating as far as the character of education and the operation of the administration in the middle of the 6^{th} century are concerned.

This treatise was used as a source by the Byzantine author, historian and law specialist Theophylact Simocatta (6^{th} to 7^{th} century) in his *Ecumenical History* (an opus of 8 books) [23] and by the bishop of Lepanto Constantinos Manassis (1130-1187), in his verse work *Synopsis of Time* [8, vol. 127]. The treatise *On the Powers* by Ioannis of Lydia was published in Leipzig in 1903 by R. Wünsch [24].

The other two treatises by Ioannis Laurentius of Lydia are entitled *On months* and *On Diosemeia*. The first one contains a wealth of historical information about the Roman calendar and festivals, and about the various customs observed in certain dates. For this reason it is a very interesting book for those who study calendrical issues and historical folklore; it also deals with the associated legends.

Finally, the second treatise refers to methods of weather forecasting based on astrological connotations. Its name refers to the 'signs of Dias' (the divine signs or miracles) after the Greek god Zeus (Días-Diòs), because the ancient lore attributed all atmospheric phenomena to him. *On Diosemeia* contains a multitude of references to meteorological omens and weather phenomena. It describes these phenomena (thunderstorms, thunders, rain, lightning) but also earthquakes and the phases of the moon, lunar and solar eclipses, the apparitions of comets and other phenomena associated with oracles and the religion of both the Roman and the Etruscan civilization. In other words, this treatise deals with all the kinds of celestial omens. Both this and *On months* were published by August Immanuel Bekker [25].

As a writer, Ioannis Laurentius is uncritical and superstitious; nevertheless, his works are significant, as they offer a wealth of information.

7. Rhetorius of Byzantium (6th century)

The last significant astrologer of the early Byzantine empire was Rhetorius of Byzantium, who was also an astronomer, widely considered as the author of the opus *Description And Explanation Of the Entire Art Of Astronomy*, which consists of 120 books.

Unfortunately, it is difficult to find more about his life and his written works. It is very probable, however, that he is the same person with the astrologer Rhetorius of Egypt who lived in the same century and whose work is a mixture of older books on the subject (such as those by Vetius Vales of Antioch, Claudius Ptolemy, Paul of Alexandria and others). Most of his work has been saved [4].

It should also be noted that the famous philosopher Proclus (410-485), inspired by Ptolemy's *Tetrabiblos*, wrote an astrological work that essentially is a rephrasing of *Tetrabiblos*. This work is known as *Paraphrasis to the Tetrabiblos of Ptolemy* [26]. Although its genuineness has been doubted because in several points it makes mistakes in interpreting the Ptolemaic text (which is difficult and rather vague, anyway) and these mistakes are incompatible with the tremendous interpreting capacity Proclus shows in his commenting of other texts, especially Platonic ones, nevertheless the *Paraphrasis* was especially valued during the Middle Ages and the Renaissance as a basic manual for the interpretation of the Ptolemaic text; apart from its mistakes, in other passages it gives appropriate and correct interpretations, following faithfully the original text, clarifying it and smoothing its language. One of the manuscripts that contain the *Paraphrasis*, the Vatican No. 1453, is dated from the 10th century and thus it is older than any saved manuscript of the *Tetrabiblos* itself.

Finally, Heliodorus the Neoplatonist (5th to 6th century), the brother of the philosopher, astronomer and mathematician Ammonius (†510), is considered by many to be the author of the astrological treatise *Eisagoge eis ta apotelesmatika*, probably influenced by the work of the astrologer Paul of Alexandria [7, p. 173].

8. The condemnation of astrology by Honorius and the Church Fathers

During the first century of the Byzantine (Eastern Roman) Empire, as we already mentioned, the flourishing of astrology was so great that even emperors like Honorius (the son of Theodosius I the Great and his successor in the western part of the empire), issued a decree that condemned the practice of astrology in Rome. Indeed, as Karl Krumbacher (1856-1909) writes: *"Honorius issued a law for the the 'mathematicians' from Rome and the burning of their books"* [27].

Subsequently the larger part of the burden of the struggle against astrology and astrologers (who were casually called mathematicians) fell on the shoulders of the Church Fathers and the scholarly bishops. Because of the intensity of the clash between the bishops and the astrologers, the impression is often created that all bishops were opposed to the cultivation of Science and to the research of the celestial phenomena rather than to that apocryphal art. However, the reality was different; the leaders of the Church with their writings and other actions were condemning not the science of Astronomy but the quackery, the omens and all those who claimed that they could predict the future from the relative positions of the celestial bodies, the 'earthquake guides' the 'moon-phase books' and the 'thunder guides'.

Basil of Caesarea, for example, in his homilies *On the Six-day Creation* (*Peri Hexahemerou* or *On Hexameron*, circa 379) writes with respect to the study of Astronomy: *"What is the meaning of Geometries and of the methods of Mathematics, of the stereometries and of the much-celebrated Astronomy, of all this multi-sided vanity, if all who ardently keep themselves busy with them made the thought that the world we see has the same origin with the creator of everything God, thus equating in grandeur the limited and material world with the limitless and invisible nature?"* [28].

However, it seems that when Basil calls astronomy a 'vanity' he most probably means what we now know as *astrology*. This view is supported by the fact that in other texts he considers the observation of the stars necessary, because through it, as he writes, we become acquainted with the divine wisdom and we receive important precept from its knowledge; but up to a certain point: one should not examine the stars beyond what is necessary. Indeed the polymath Father of the Church notes: *"What other does the Moon teach us by becoming full and waning once again, except to avoid thinking great about the prosperities of life? It only suffices not to examine the signs that come from the stars beyond what is necessary."* [8, vol. 29, p. 9]

Basil's classical culture enabled him to teach properly in his *Treatise towards the young* [29] on the issue of the place of the secular education in the Christian school and, in doing so, to influence the stance of the Church with respect to the classical education both then and during the Renaissance. In other words, the attack of Basil and other Church Fathers is not directed against the scientific research of the celestial bodies and events, but rather against all those who proceed beyond the information gained through the observation and the experience, and want to infer conclusions from the stars.

The late professor of Astronomy Demetrios Kotsakis (1909-1986) suggested that both Basil of Caesarea and his brother Gregory of Nyssa were strong adversaries to all those who tried to predict future events based on the stellar positions and constellations in the sky; in a relative paper entitled '*Saint Basil the Great against astrologers*' writes: *"It is important to hear the views (in short) as well as the reasoning of two brothers and scholars: Basil the Great and Gregory of Nyssa. Basil, commenting on the method of the astrologers, who scrutinize things to determine with an accuracy not just of degrees but of arc minutes and arc seconds the positions of the stars, in order to predict with purported absolute certainty the future life of various persons, demonstrates that it is impossible to determine with high absolute precision the positions of planets or of fixed stars and hence it is impossible to predict this or that future evolution of a child* [8]. *Gregory of Nyssa in his speech 'Against fate', in order to refute the belief that wars, earthquakes and various disasters are caused by 'peculiar forces of the stars' cites various biblical events* [8, vol. 45, p. 165], *such as Noah's Flood, the burning of Sodom and the destruction of the Egyptians in the Red Sea, in order to refute in the end the faults of the astrologers by a crushing argument."* [30]

Gregory of Nyssa was not against the science of Astronomy; for example, he wrote that through the science of the heavens *"the intellect is excited towards virtue and the truth is understood through the numbers"* [8, vol. 46, p. 181].

In addition to Basil of Caesarea, Gregory of Nazianzus writes that *"astronomy was considered a dangerous teaching"* [8, vol. 35, p. 761] meaning astrology, since in a homily he argued that: *"... and Asia was the school of impiety, to the extent it relates wonders about astronomy and the births and fancies of predictions, and about the art of witchcraft that follows these"* [8, vol. 36, p. 557].

Here it is obvious that the scholarly bishop does not accuse Astronomy but astrology, thinking of Asia as the place it was developed. Also, in his letters and homilies he mentions in positive terms the topics of cosmography, the study of the solar and lunar eclipses, the Sun, the stars, the Galaxy (Milky Way), the ecliptic and of meteorological phenomena such as lightning, thunders, etc. [8, vol. 36, p. 68].

Finally, in his funeral oration for his brother Caesarius, Gregory mentions that Caesarius avoided: *"... the dangerous teachings of astronomy that suggest that all things and events depend on the stars"* [8, vol. 35, p. 761]. In a more general context he argues that: *"At least from geometry and astronomy and the learning that is dangerous to the other people, he [i.e. Caesarius] had chosen the useful part, which is the admiration of the Creator from the celestial harmony and order, while he escaped the harmful part – by not attributing the beings and the events to the course of the stars, like those that put the material creation (which is subordinate like them) above the Creator, but by assigning their motions to God, as it is natural, along with everything else."* [8, vol. 36, p. 761]

The populace in the empire, as it is known from the historians of that period, generally believed in the foretelling power of the stars, which was also known as *genethliology* ('birthday-logy'), i.e. birthday astrology, since it was said to predict the future of every child from the moment of its birth. In addition, often the future parents of the baby asked the Byzantine astrologers about its sex before tackling birthday astrology: *"before [the birth], when it was asked to make known the sex of the child, since as they argued, the time of the conception defined the sex of the child to be born"* [2, vol. I, Book 2, p. 141]. For this reason John Chrysostom taught that: *"It is not the job of astronomy to know from the stars about the people who are being born"* [8, vol. 57, p. 61]. Once again here he means astrology and not the science of astronomy. He also wrote: "*Do not pay attention to genealogies, oracles and astrologies… …which you inherited by the Greeks and the Jews"* [8, vol. 59, p. 564].

From John's writings it is evident that he attempted to consolidate the Christian faith since he was a connoisseur of the culture of the ancient Greek authors himself and he wanted to condemn astrology and not Astronomy.

The late professor of Astronomy at the University of Athens D. Kotsakis writes in another work: *"The experts in this foretelling art used a special instrument called the astrolabe or horoscope in order to determine with precision the positions of the planets and the stars on the celestial sphere. Needless to say, they mostly observed the constellations of the zodiac, the so-called signs, the positions of the planets and the positions and the phases of the Moon. The development of the pseudo-science of astrology assisted in certain periods the development of astronomy, however in other periods it was a motive for the defamation and the persecution of the purely astronomical and, more generally, the scientific research."* [31]

Indeed, according to F. Koukoules: *"The Byzantines knew of two kinds of mathematics: the scientific ones, whose teaching was allowed since, as Gregory of Nyssa writes, 'the intellect is excited towards virtue and the truth is understood through the numbers' and the occult ones, which were strictly forbidden. Astronomy, for example, as long as it examined the motions, the sizes and the distances between the celestial bodies, it was being taught; but when it turned into astrology by suggesting that the human fate depended on the stars, then it was considered despicable and its teaching was persecuted."* [2, vol. I, Book 1, p. 125]

Similarly, the other Fathers of the Church condemned astrology. The bishop of Jerusalem Cyril I (348-386?) was a strong opponent of astrology and superstition, writing: *"Do not pay attention neither to astrologies, nor to bird omens, nor to other superstitions; do not even listen to the mythical oracles of the Greeks, the use of potions, the singing prophesies and the most unlawful things of the necromancers"* [8, vol. 33, p. 501].

Also, Epiphanius of Cyprus (315-403) was an eminent persecutor of astrology, which he condemned by writing: *"Magic and potion drinking, astronomy, the cledonism"* [8, vol. 24, p. 3], meaning of course 'astrology' by writing 'astronomy'. Eusebius of Alexandria (444-451), in his *Homilies* on

moral, ascetic and dogma issues also accuses *"the mythologists and curious people and astronomers"* [8, vol. 86A, p. 422]. Nemesius of Emesa (Syria, c. 400) writes about all the believers of astrology: *"Those who attribute the cause for all events to the revolution of the stars do not only combat common sense, but also they render useless all state justice. For the laws are out of place and the courts are unnecessary when they punish those who are responsible for nothing. But the stars, too, are unjust in cleansing the fornicators and the murderers; and prior to the stars their creator God mentioned the reason."* [8, vol. 40, p. 761]

Synesius of Cyrene (370-414), bishop of Ptolemaïs in Cyrene, condemned astrology in these words: *"So the savants foresee the future, some of them by observing the stars, others by observing torches and shooting stars, others by 'reading' the intestines, by hearing the noises, the sitting or the flying of the birds"* [8, vol. 66, p. 1284].

Finally, according to the *Codex Justinianus* in the paragraph it deals with *"maleficis et mathematicis et ceteris similibus"* [32], the practice of 'mathematics' was forbidden; this stipulation was in force and was repeated in the following centuries. The books of 'mathematics' were burned and their teachers were removed from the city [2, vol. I, Book 2, p. 144]. In this case, however, once again the term means astrology, since astrologers were also called 'mathematicians'. Besides, the *Teaching of the Twelve Disciples* suggests the same: *"My child, do not become a bird observer… …nor a mathematician… …because from all these stems idolatry (paganism)"* (Chapter III). In addition, the 36th canon of the Council of Laodikeia prohibits the practice of mathematics (i.e. astrology) by clergy members: *"It is forbidden for priests to be magicians or mathematicians, or to construct the so-called amulets, which are prisons of their souls"* [33].

9. Conclusions

Astrology was extremely widespread during the early Byzantine years and emperors such as Julian favored its dissemination by keeping astrologers in their court as advisors. The parents were asking for the advice of astrologers not only for the future of their children, but also for the appropriate dates for them to start courses. Even hunters were asking astrologers about the best days for hunting and the best method to use for a particular day or week.

The Church Fathers, however, and most of the educated bishops were indisputably against astrology and they were condemning all astrologers, foretellers and magicians who boasted that they could tell the future by using astrology or other occult practices. The Church Fathers were by no means against scientific research or against Astronomy and Mathematics, however, they were struggling against those who proceeded beyond the simple observation and knowledge of the phenomena, i.e. beyond the data of science, and wanted to extrapolate them with vague and unscientific methods where they could not possibly be applied, i.e. to the prediction of the future and the fate of

human beings. Their polemic was against oracle giving, bird watching and astrology – often called 'mathematics' or 'astronomy', hence the misunderstanding. The practitioners of these techniques were trying to predict the future by observing the intestines of the sacrificed animals, by hearing the thunders or by observing the positions and motions of the Sun and the planets through the zodiac. After Julian's death the official state also was against these charlatans: According to the *Codex Justinianus* the practice of 'mathematics' (i.e. of astrology) was forbidden, while as professor F. Koukoules writes, their occult books were being burned and they were driven away from the cities.

However, because the simple priests were sometimes influenced and tempted by the pseudo-science of astrology, a canon of the Council of Laodikeia prohibited the practice of mathematics (i.e. astrology) by clergy members.

Nevertheless, the practice of astrology persisted in the Byzantine Empire throughout its middle (610-1204) and late (1204-1453) periods. There were certain time intervals during which many scholars, even emperors like Manuel I Comnenus (1143-1180), dealt with it. Present article follows our previous work on the spirituality and science [34, 35] and on the contribution of the Church in Byzantium to the natural sciences [36, 37]. The scholars who studied astrology will be examined in more detail in a future paper.

Acknowledgements

This study formed part of the research at the National and Kapodistrian University of Athens, Department of Astrophysics, Astronomy and Mechanics, and we are grateful to it for financial support through the Special Account for Research Grants. It is also supported by the Ministry of Science and Technological Development of Serbia through the project III44002.

References

[1] Ptolemy, *Tetrabiblos*, The Loeb Classical Library No. 435, English translation, Cambridge University Press, London, 1940.
[2] F. Koukoules, *The life and civilization of the Byzantines*, in Greek, vol. I, Papademas Publ., Athens, 1948, 219.
[3] Aristotle, *Meteorologica*, The Loeb Classical Library; English translation Cambridge University Press, London, 1952, Book 1, 8.
[4] ***, *Catalogus codicum astrologorum graecorum. Codices hispanienses*, Book 3, C.O. Zuretti and H. Lamertin (ed.), Bruxelles 1898 (reprinted 1932), 34.
[5] ***, *Ioannis Zonarae Epitomae historiarum libri XVIII 1-3*, Corpus Scriptorum Historiae Byzantinae, Th. Büttner-Wobst (ed.), Bonn, 1841-1897, Book 13, 3.
[6] H. Hunger, *Die hochsprachliche profane Literatur der Byzantiner*, C.H. Beck, München, 1978, 31.
[7] E. Theodossiou and E. Danezis, *At the Years of Byzantium – Byzantine scientists, physicians, chronologists and astronomers*, in Greek, Diavlos Publ., Athens, 2010, 134.
[8] ***, *Patrologiae Graecae cursus completus, series graeca*, J.-P. Migne (ed.), vol. 29, Centre for Patristic Publications, Athens, 2008, 129.

[9] K. Tsopanis, Crypto, **7** (2005) 9.
[10] A.A. Vasiliev, *History of the Byzantine empire, 324-1453*, The University of Wisconsin Press, Madison, 1952, 72.
[11] ***, *Ammiani Marcellini Rerum gestarum libri qui supersunt* [*Res gestae*], Book XXV, § 3, Rec. V. Gardthausen. Stereotypa Editionis, Stutgardiae, 1874**,** 22.
[12] ***, *Anthologiae Graecae Appendix*, E. Cougny (ed.), Didot, Paris, 1890, 122, 1-3.
[13] ***, *Georgius Cedrenus (Synopsis Historiarum) and Ioannis Scylitzae ope.*, vol. I, I. Bekker (ed.), Corpus Scriptorum Historiae Byzantinae, Bonn, 1838, 532.
[14] I.K. Tsentos, *Julian the Apostate-Apostate of Christianity and Renegade of Hellenism*, in Greek, Tenos Publ., Athens, 2004, 117.
[15] R. Browning *The emperor Julian*, Weidenfeld and Nicolson, London 1976, 228.
[16] ***, *L'empereur Julien. Oeuvres complètes*, C. Lacombrade (ed.), vol. 2.2, Les Belles Lettres, Paris 1964, 226, available on line at http://www.tertullian.org/fathers/julian_apostate_1_sun.htm.
[17] Ioannis Malalae, *Chronographia*, vol. I., Corpus Scriptorum Historiae Byzantinae, L. Dindorf (ed.), Bonn 1831, 333.
[18] Ioannis of Nikiou, *Chronikon*, English translation by R.H. Charles, Book LXXX, Williams and Norgate, London and Oxford, 1916, 19-26.
[19] Libanii, *Opera*, Speech IH (18), 274.1-275.9, Richard Foerster (ed.), B.G. Teubner, Lipsiae (Leipzig), 1903–1927.
[20] Sozomenos, *Ekklesiastike historia/Ecclesiastical History*, *Histoire Ecclesiastique*, Y΄ 1, 14.4.-16.5, Greek text of the edition by J. Bidez, translation in French by Andre-Jean Festugiere, annotation by Guy Sabbah, Editions du Cerf-Paris Sources Chretiennes, no 306, Paris, 1983.
[21] C. Fouquet and P. Grimal, *Julien, La mort du Monde Antique*, Les Belles Lettres, Paris, 1985, 235.
[22] Emperor Julian, *Against the Galilaeans*, *Juliani imperatoris librorum contra Christianos quae supersunt*, C.J. Neumann (ed.), B.G. Teubner, Lipsiae (Leipzig), 1880.
[23] Theophylact Simocatta, *Ecumenical History*, C. de Boor (ed.) rev. by P. Wirth, B.G. Teubner, Stuttgart, 1972.
[24] Ioannis Lydi, *(Peri arhon) De magistratibus populi Romani libri tres*, R. Wünsch (ed.), B.G. Teubner, Lipsiae (Leipzig), 1898.
[25] ***, *Corpus Scriptorum Historiae Byzantinae*, August Immanuel Bekker (ed.), G. Reimer Berolini, Berlin, 1837.
[26] ***, *Proklou tou Diadochou Parafrasis eis tēn tou Ptolemaiou Tetrabiblon* (*Procli Diadochi Paraphrasis in Ptolemaei libros IV*), in Greek, Kaktos Publ., Athens, 2009.
[27] K. Krumbacher, *Geschichte der Byzantinischen Litteratur von Justinian bis zum ende des ostromischen reiches (527-1453)*, C.H. Beck (ed.), Book II, Series Handbuch der klassischen Altertums-Wissenschaft, München, 1891, p. 442.
[28] Basil the Great, *Homilies on Hexameron*, in Greek, Polytypo, Athens, 1990, 14.
[29] Saint Basile, *Aux jeunes gens sur la manière de tirer profit des letters helléniques*, F. Boulenger (ed.), Les Belles Lettres, Paris, 1935.
[30] D. Kotsakis, Aktines, **63** (1955) 18.
[31] D. Kotsakis, Epeteris of Byzantine Studies, **KA(21)** (1954) 215.
[32] P. Krueger, *Corpus Juris Civilis- Codex Iustiniani*, Book 9, §18, Apud Weidmann, Berlin, 1889, 2, available on line at http://www.archive.org/details/corpusiuriscivi00schogoog)

[33] G. Rallis and M. Potlis, *Syntagma of divine and holy Canons*, vol. 3, in Greek, Typografia G. Hartophylax Publ., Athens, 1852-1859, 203.
[34] E. Danezis, E. Theodossiou, I. Gonidakis, M.S. Dimitrijević, Eur. J. Sci. Theol., **1(4)** (2005) 11.
[35] E. Theodossiou, V. Manimanis, M.S. Dimitrijević, Eur. J. Sci. Theol., **6(3)** (2010) 47.
[36] E. Theodossiou, V. Manimanis, M.S. Dimitrijević, Eur. J. Sci. Theol., **6(4)** (2010) 57.
[37] E. Theodossiou, V.N. Manimanis and M.S. Dimitrijević, Eur. J. Sci. Theol., **7(2)** (2011) 57.

European Journal of Science and Theology, December 2012, Vol.8, No.4, 23-40

THE GEOGRAPHERS OF THE EARLY BYZANTINE PERIOD

Vassilios Manimanis [1], Efstratios Theodosiou[1] and Milan S. Dimitrijevic[2*]

[1] *National and Kapodistrian University of Athens, School of Physics, Department of Astrophysics, Astronomy and Mechanics, Panepistimiopolis, Zografos 15784, Athens, Greece*
[2] *Astronomical Observatory, Volgina 7, 11160 Belgrade, Serbia*

(Received 8 January 2012)

Abstract

In Byzantine empire the knowledge of Geography was considered necessary for locating the Holy Land and for setting the boundaries of the dioceses. Essentially, Geography was studied by monks in the monasteries; the perception of the Earth by Byzantine geographers – especially by the monk Cosmas Indicopleustes – was to a large extent imaginary and influenced by the Scriptures and religious ideas.
Here are considered geographers of the early Byzantine period: Éthicus Istriote, Marcian of Heracleia, Caesarius, Palladius of Helenopolis, Agathodaemon, Christodorus, Hierocles the Grammarian, Procopius of Caesarea, Corippus the African, Stephen of Byzantium, Nonnosus, Priscianus the Grammaticus, Marcellinus the Illyrian and John of Gaza.

Keywords: Byzantium, Geography, Byzantines geographers, Natural Sciences

1. Introduction

During the early Byzantine period the knowledge of Geography was considered necessary for locating the Holy Land and for setting the boundaries of the dioceses. Thus, starting with the work of the ancient cartographer and geographer Marinus of Tyre (ca. 60/70 - 130 AD), and with the renowned *Geography* (also known as *Geographia*, *Cosmographia*, or *Geographike Hyphegesis*) [1] of the classical astronomer, mathematician and geographer Claudius Prolemy, the Byzantine scholars wrote their own treatises on the subject.

Essentially, only monks in the monasteries were studying Geography; the perception of the Earth by Byzantine geographers – especially by Cosmas Indicopleustes – was to a large extent imaginary and influenced by the Scriptures and religious ideas, while the geographical works were limited to lists

* Corresponding author, e-mail: mdimitrijevic@aob.bg.ac.rs, Phone: +381-11-3089-072, Fax: +381-11-2419-553

of names and city guides for school use, as well as travel narrations and descriptions, a fact that clearly delineates the difference between the ancient Greek geography and Geography as it was understood in Byzantium.

The capital of the Eastern Roman Empire (commonly known as the Byzantine Empire), Constantinople, had in the Byzantine period its own University, known as the *Pandidacterion*, which was the re-organized Roman Auditorium. It was also known as the *Magna aula* school, from the building it housed it, a section of the *Questor sacri palatii* (palace) complex built by Constantine the Great. The Pandidacterion itself was established by emperor Theodosius II the Younger (*Flavius Theodosius Junior*) on February 27, 425 AD, after he was persuaded in doing so by his wife, the educated daughter of the philosopher Leontius, Athenaïs, who was baptized as an adult, taking the Christian name Eudocia. The organization of the Pandidacterion, which is widely considered the first European university, provided for 31 professors: ten for the Greek grammar, five for the Greek rhetorics, ten for the Latin grammar, three for the Latin rhetorics, two for the Law studies and one for Philosophy [2]. Unfortunately, only one instructor was teaching Arithmetic, Astronomy and their branches, *"i.e. physics, which in turn included geography and animal history"* [3]. Consequently, the teaching of geography was *de facto* limited.

The Pandidacterion was also called 'Ecumenical Teachers College' and the instructors bore the title of the 'ecumenical teacher' or that of the 'teacher of teachers'.

2. The Natural Sciences and Geography during the early Byzantine period

The Natural Sciences as we perceive them today did not experience the growth it would be expected in the Byzantine Empire. The Byzantines were concentrating their efforts on the study of the works of the eminent ancient Greek philosophers and on the popularization and dissemination of the already present knowledge on Physics and Mechanics. This effort was directed towards the practical application both in everyday life and for military purposes. The publication of a form of encyclopaedias was a significant means for achieving this aim. In the Byzantium the teaching and the detailed study of the sciences was always combined with the corresponding philosophical systems in such a way that essentially it was a continuation of the teachings of the two main philosophical schools, those of Athens and Alexandria. A few basic subjects were taught in both elementary and higher education. Physics was taught along with Natural history, Zoology, Botany and Geography.

There was no scientific research, nor any novelty. A reason is that the sciences require the proper conditions for their development. In the Byzantine Empire one of these conditions did not exist: the proper mentality of the scholars. Sciences were approaching the reality of the natural world in a way that was not acceptable by the religious dogma (the prevalent factor that shaped people's thought in that period), while they were bringing in mind the pagan culture and hence paganism itself. The late historian Sir Steven Runciman

(1903-2000) described the scientific knowledge of the Byzantines in Geography and the natural phenomena not during the early Byzantine period, since he considers it negligible, but during the later period, that of Constantine VII Porphyrogennetos and Anna Komnena: *"Constantine Porphyrogennetos makes very few geographical mistakes, ... Anna Komnena is full of information, usually correct, about the currents and the prevailing winds... However, the various natural phenomena were not understood correctly. Kekaumenos attempts to explain the thunder and he realizes that the sound and the lightning are generated at the same moment. And Acropolites knows the cause of the eclipses. But the perception that these phenomena were warnings or punishments coming from 'above' was so extended that their explanation seemed to be more moral than natural."* [4]

During the early Byzantine period, Geography was served by the scholars Éthicus or Aethicus Istriote (4th century), Marcian of Heracleia (Marcianus Heracleensis, 4th - 5th century), Caesarius (4th century), Palladius (368-430), Agathodaemon (early 5th century?), Christodorus (5th century) and Hierocles (482-565), who is considered the author of a treatise under the title *Synecdemus* or *Synekdemos*, in which 64 provinces (eparchies) and 912 cities of the Empire are described.

In the 6th century the best-known persons in the field were the historian Procopius of Caesarea with his work *Buildings of Justinian*, Flavius Cresponius Corippus (Corippus the African), Stephen (Stephanus) of Byzantium, Nonnosus, Priscianus Caesariensis, Marcellinus the Illyrian, John (Ioannis) of Gaza and finally Cosmas Indicopleustes, who wrote a geographical treatise entitled *Christian Topography* and he will be examined in detail in a future paper of our team.

3. The main geographers of the early Byzantine period

Let us now examine in detail the work of these geographers in the following paragraphs in chronological order.

3.1. Éthicus Istriote (4th century)

The geographer and scholar Éthicus or Aethicus from Istria of Illyria (hence his appellation Istriote) lived during the first decades of the empire. He is the most probable author of a *Cosmographia* in Greek, which contains much geographical and historical information. Although his work is characterized by an off-hand attitude, omissions and inaccuracies, it is useful in many ways, since it contains valuable data, especially about the countries and the tribes of Northern Europe. The manuscripts of *Cosmographia* were discovered in such a bad condition that they are unintelligible, however an adaptation of its text written in Latin is saved in good condition; it is attributed to Saint Hieronymous. However, the specialists in manuscripts believe that the Latin adaptation does not render the lost Greek prototype with accuracy [2, p. 202].

This adaptation was first published in 1852 by Marie Armand Pascal d'Avezac [5]. In the next year, Heinrich Wuttke (1818-1878), based on the Leipsig code (*Codex Lipsiensis*), published a summary of the Latin adaptation, again in Latin, under the title *Cosmographiam Aethici Istrici ab Hieronymo ex graeco in latinum breviarium redacta* [6]. In 1854, Heinrich Wuttke in another work [7] supported the view that *Cosmographia* was indeed a prototype work by Éthicus, rejecting the theory of some researchers that its first part was a just copy of the *Cosmography* written by Julius Honorius while the second part was an elaboration upon a portion of *Historiarum adversus paganos, libri VII* by Paulus Orosius (5th century) [2, p. 203].

In any case, the value of Éthicus' *Cosmographia*, unlike its originality, is not a subject of debate, since it offers a wealth of useful information.

3.2. Marcian of Heracleia (4th-5th century)

Marcian of Heracleia (Latin form: Marcianus Heracleensis) was a Greek geographer from Heracleia of Pontos, where he was born *circa* 400 AD; as he himself wrote: *"I am Roman by name, while by nationality, language and education I am a Greek"* [2, p. 203]. His main works are:

- *Circumnavigation of the Outer Sea in two books*, of which the second one is incomplete;
- *Epitome of the eleven [books] of the geography of Artemidorus of Ephesus*, a work also consisting of 11 books, which was lost;
- *On the distances of the main cities of the World from Rome*, of which some fragments are saved;
- *Epitome of the circumnavigation work by Menippos of Pergamon in three books*, of which also some fragments are saved;
- Finally, to our author are attributed with probability the works *Preface* and *Circumnavigation of both Seas of Bithynia.*

The best edition of Marcian works is the one of 1855 by K. Müller (ed.) and the publishing house of Ambroise-Firmin Didot, at the end of the first volume of *Geographi Graeci Minores* [8].

The saved works of Marcian are considered valuable for their distance determinations and they testify to the profundity and diligence of this capable geographer.

3.3. Caesarius (4th century)

The Church author and medical doctor Caesarius (†369) was the younger brother of Saint Gregory of Nazianzus, being the son of Gregory, bishop of Nazianzòs, and Saint Nonna. Caesarius received an education on Philosophy and Medicine in Alexandria. He is included in this paper because to him is attributed an eminent geographical work that covers the entire region of the Balkan Peninsula, Asia Minor, Syria and Palestine with a wealth of geographical

information. In addition to this information, this treatise –a kind of traveller's guide – contains a lot of meteorological and astronomical data.

On the other hand, Caesarius acquired a great reputation as a medical doctor. After his Alexandrine studies, he settled down in Constantinople, where, because of his reputation, he became the palace doctor. His brother Gregory, after the end of his own studies in Athens, travelled to Constantinople between the years 358 and 360, where he met Caesarius and from there they went together in Nazianzòs. Then, Caesarius returned to the capital, where he became the chief-doctor of emperor Constantius II and then (proposed by medical doctor Oreivasius) of the emperor Julian, something for which he was reprimanded by his brother Gregory, as he accepted a position offered to him by a prosecutor of Christianity. Subsequently, the next emperor Valens Flavius Augustus offered him the office of 'overseer of treasures and paymaster of the public money' in Nicaea of Bithynia, where he died peacefully around 369 after he had survived as by a miracle the terrible earthquake of 368 [2, p. 262].

Caesarius of Nazianzus is with a low probability the author of the significant theological work *Four Dialogues* [9]. His brother, Saint Gregory, mentions in his works and orations the prudency and devotion of Caesarius to the Christian faith, as he was not influenced at all by emperor Julian's prompts to renounce his faith. The Eastern Orthodox Church elevated Caesarius to the ranks of its saints and honours his memory on March 9 [*Synaxari* (The book of the lives of Christian saints), online at http://www.agiooros.net/modules.php?name=GCalendar&file=viewday&y=2011&m=3&d=9&e=108].

3.4. Palladius of Helenopolis (364-431 or 368-430)

The scholar, Church author and monk Palladius was born in Galatia. A disciple of Evagrius of Pontus and an admirer of Origen, he became a monk in a young age. He acquired a rich monastic experience in Jerusalem around 380 and later on in the major monastic centres of Palestine, Syria and Egypt, where he stayed in the Nitrian desert and met Evagrius of Pontus (346-399), with whom he was nine years. Subsequently, he was ordained priest in Egypt by the bishop of Hermoupolis, Dioscurus, one of the famed 'Long Brothers'. After the death of Evagrius, Palladius returned in Palestine and then he travelled to Constantinople seeking Saint John Chrysostom's protection against the enmity of the archbishop of Alexandria Theophilus against the 'Long Brothers'. There Chrysostom became his close friend and ordained him bishop of Helenopolis in Bithynia (400-406). When Chrysostom was exiled, Palladius, also accused as an Origenist, went to Rome in 405 in order to communicate the issue to Pope Innocent I. The Western emperor Honorius sent Palladius back to Constantinople as a member of a mission sent to the Eastern emperor Arcadius (395-408) in favour of the banished patriarch. However, Arcadius sent Palladius in exile, to Syene in Upper Egypt; there from 406 to 408, Palladius as a student of Saint John Chrysostom narrated the life of his teacher and friend in his

Dialogue with deacon Theodore about the life and manners of John Chrysostom (*Dialogus de vita Sancti Joannis Chrysostomi*), which is our primary source about Chrysostom's life.

Palladius lived in Thebaid, Egypt, for four years, in Antinoe or Antinoopolis, and he returned to Palestine in 412, when Theophilus died and so the reaction against Chrysostom came to an end. Then he went to Galatia, where he lived in the house of a priest called Philoramus and in 417 he was ordained bishop of Aspuna in Galatia. Then we wrote (*circa* 419-420) his other major work, *The Lausiac History* (*Historia Lausiaca*). Its name comes from the dedication to Lausos, a chamberlain of Theodosius II (408-50), and it is also known as *He pros Lauson historia* and then shortly *Lausiakon* or *Lausaikon* [9, vol. 34, 1156C- 1161A].

So, Palladius wrote two important works: *The Lausiac History* [10] and the *Dialogue... ...about the life of Saint John Chrysostom* [11]. In the *Lausiac History* he describes the lives of monks in Egypt and Palestine who lived in the first Christian centuries and he offers in a simple language a portrait of the Egyptian ascetism, describing the ascetic ideal. *The Lausiac History* is an interesting text of the end of the ancient period for both theologians and historians who examine this specific period. Now, a part of it concerning the history of the monks of Egypt is more of a narration than a history or a collection of biographies; it has the form of the description of a voyage along the Nile, and so it could be classified as a geographical work, as well. It was included by J.-P. Migne in his *Patrologia Latina* [12]. This form is probably a literary imitation of the Hellenistic novels. However, Palladius's visit to Upper Egypt must be a literary fiction. At one time the entire *Lausiac History* was considered a compilation of imaginary legends (see Weingarten, *Der Ursprung des Mönchtums*, Gotha, 1877 [13], and others). Later research has very considerably rehabilitated Palladius; the chief authorities now (Butler, Preuschen) consider the *Lausiac History* to be in the main a serious historical document as well as an invaluable picture of the lives and ideas of the earliest Christian monks.

Yet, most important from a geographical point of view is his work *On the nations and the Brahmans of India* (*Epistola de Indicis Gentibus et de Bragmanibus*), which contains original material both from personal experiences and from the descriptions of Egyptian travellers to India [14]. According to Beverley Berg Palladius describes Sri Lanka, which was also described by Cosmas Indicopleustes in his *Christian Topography* [15]. Palladius, however, describes in addition places that are to the east of Sri Lanka [16]. It seems very probable that Palladius actually made a journey to India at a date which cannot be definitely ascertained.

3.5. Agathodaemon (early 5th century)

Geography in Alexandria was served by the Alexandrine geographer and engineer Agathodaemon, who most probably lived around the year 400. Some

researchers think that he was contemporary of Claudius Ptolemy, while others think he lived centuries after him; in any case, he can't be considered as posterior of the 5th century. From his works are saved 27 geographical maps ('tables') – the 26 of them showing various regions and one depicting the whole Earth. These maps are adapted to the manuscripts of Ptolemy's *Geographical Hyphegesis* (Codices *Vindobonensis* and *Veneticus*) and bear the signature: *"from the eight geographical books by Claudius Ptolemaeus, Agathodaemon of Alexandria depicted the whole œcumene"* [2, p. 204].

3.6. Christodorus (5th century)

The epic poet Christodorus from Egypt can be regarded as a geographer in the wide meaning of the word. He is mostly known for the poem he wrote about the victory of the Byzantine emperor Anastasios I (491-518) over the Isaurs in 497, for another work about the students of Proclus and for a singular opus entitled *Description of the statues in the public gymnasium called Zeuxippos* (in Constantinople) [17]. However, he is mentioned here because of his *Patria*, a set of narrations in verse about numerous cities, such as Constantinople, Thessaloniki, Miletus, Aphrodisias and Tralles in Asia Minor, which can be considered a geographical work. Yet, this work has been lost; the only work of this poet that was saved is the *Description of the statues in the public gymnasium called Zeuxippos*.

3.7. Hierocles the Grammarian (482-565)

In the age of Justinian I (527-565) flourished the famed historian, geographer and general author Hierocles (also written as Hierokles), who bore the epithet 'Grammarian' as a distinction from two earlier scholars: the Alexandrine philosopher Hierocles (5th century) and the veterinarian and law expert Hierocles who wrote the work *On the therapies of horses* and lived in the 4th century AD.

Hierocles the Grammarian presented what is probably the leading work of its kind: an opus of political and ecclesiastical administrative geography written most probably in 535, which bears the title *Synekdemos* (= *[Travel] Companion)*.

Synekdemos is essentially a work of statistical geography and a list of 64 provinces (eparchies) and 912 cities of the Empire, being the most important source for the administrative and political geography of the Byzantine Empire (Eastern Roman Empire) prior to the Arab raids. This is what it is written in its preface: *"There are all provinces and cities under the King of Romans in Constantinople, 64 provinces and 912 cities"*. Hierocles also gives a wealth of numerical and geographical elements.

The *Synekdemos* (or *Synecdemus*) of Hierocles, a real guide and statistical survey of the Eastern Roman Empire assumed to have been based on state documents, was the best his period could offer and formed in turn the basis of

the Byzantine political geography. It was the most important source about the administrative and political geography of the Empire prior to raids of the Arabs. It contains the 'official' list of the cities of the provinces of the Balkan peninsula in the period from 500 AD to the coronation of Justinian I (527) and a list of the cities of the 22 provinces of Asia Minor in the period from the late 5th to the early 6th century, with the names of 427 cities in Asia Minor.

Like the *Geoponics* of his contemporary Cassianos Vassos, the *Synekdemos* of Hierocles along with the work by Stephanus Byzantius were used by the emperor Constantine VII Porphyrogennetos as his main source of information on geographical issues and formed the basis upon which this emperor wrote his treatise *About the Provinces* (*De thematibus*) in the 10th century.

This very important work, which is considered to be the only source for the study of the ecclesiastical geography (Church administration geography) of the early Byzantine period, was first printed in Amsterdam in 1735 by Peter Wesseling [18] (reprint. 1840 in Bonn [19]) and then by Gustav Parthey (*Hieroclis Synecdemus*) in Berlin (1866) [20], and Amsterdam [21] and in a corrected text by A. Burckhardt in the Teubner series (*Hieroclis Synecdemus*, Leipzig, 1893) [22]. The last and most authoritative edition is E. Honigmann's *Le Synekdèmos d'Hiéroklès et l'opuscule géographique de Georges de Chypre* (Brussels 1939) [23]. Finally, the *Synekdemos* of Hierocles had been included already since 1864 in L.-P. Migne's *Patrologia Greca* [9, vol. 113, 141-156].

3.8. Procopius of Caesarea (490/507-562)

The historian Procopius of Caesarea (Latin: *Procopius Caesarensis*) was born in the city Caesarea of Palestine *circa* 500 AD to a rich and noble family. As a result of this, he received the best possible education for his time. He studied law and rhetoric ('*an orator and sophist*', according to the *Suda* encyclopaedic dictionary) in the renowned school of Beirut, while he also learned several foreign languages by private tutors: apart from Latin, he was especially fluent in Syrian (Aramaic) and had a working knowledge of Farsi and Gothic. His broad education and deep classical culture along with his proficiency in languages assisted him in becoming a famous historian, the 'Thucydides of the 6th century' as he was called ([2, p. 206], commonly held to be the last major historian of the ancient world.

After concluding his education, Procopius settled in Constantinople, where he worked as a lawyer. He proceeded to occupy administrative posts (*councillor, assessor* and *signer*) in the staff of General Belisarius, whom he followed in his military campaigns against the Persians (527-531), against the Vandals in Africa (533-534) and against the Goths in Italy until 540. From all these wars, Procopius collected valuable historical material. After 542 he worked as *illustrius* and *praefector* in Constantinople. A modern historiography for Procopius was written by Anthony Kaldellis [24].

Procopius, living on the border between the late Antiquity and the Middle Age, wrote three main works: *On the Wars [of Justinian]* (*De Bellis*), the *Apocryphal* or *Secret History* (*Historia Arcana* or *Anecdota*) and *About Buildings* (Greek: *Peri Ktismaton*; Latin: *De aedificiis*) all of which are valuable first-hand sources about the times and the actions of emperor Justinian I and for his period's history. As a historical author, Procopius attempts to imitate Thucydides, while he makes references to Herodotus, Xenophon, Polybius and also to Aeschylus, Aristotle, Strabo and others. The first work, *Eight Books On the Wars*, or just *Histories* [25], is a narration of the wars of Justinian I, mostly the campaigns of Belisarius in which he participated; it also contains valuable information about ethnography, cultural history, the Nika riots or revolt, and more generally about the political and socioeconomic state of the Empire in his period. He also describes the plague in Constantinople in 542.

The second book, the *Apocryphal* or *Secret History* [26], is a kind of a 'secret diary' or libel that was published after the death of Justinian I and contains unflattering details about the life in the imperial Court and his staff, from the emperor and his wife Theodora to general Belisarius and his own wife.

However, from all the works of Procopius the most interesting from a geographical point of view is the one *About Buildings* (*De Aedificiis*), a treatise in six books that was written *circa* 553-555 and praises the political and legislative activity of Justinian I along with his constructional achievements throughout the empire (castles, city walls, reservoirs, churches) [27].

As he describes in detail the buildings of the empire, Procopius proceeds to the description of their regions and cities; this way he offers a wealth of geographical, topographical and economical information, while he became a very significant source on the empire's internal and local history. This work most probably was written in parts during different time periods; in any case it seems that it was finished before the collapse of the dome of Saint Sophia on May 7, 558. The six books or 'Logoi' of the *De Aedificiis* offer a detailed exposition by region of the numerous public works that were constructed by Justinian I up to the year 550. Starting with the capital Constantinople (Logos 1), Procopius describes subsequently the region of the borders with Persia (Logos 2), then Armenia (Logos 3), Europe (Logos 4), Asia Minor and Palestine (Logos 5) and finally North Africa, from Alexandria to Gibraltar (Logos 6). The whole opus is a testimony to the extent of the emperor's efforts to fortify vital positions and, by doing this, to stop the stream of the barbarian raids against the regions of the empire. With this work Procopius made an 'official' account of the huge program of building and other public construction activities designed and materialized by the emperor and his staff from the one edge of the empire to the other; Procopius mentions significant Justinianian works in such remote places as Sinai, Jerusalem and Bethlehem, Egypt, Ravenna in Italy, in the Greek mainland and other places. His motto was founding, renovation or re-erection + renovation of old castles, erection of new fortifications and even founding of new cities. The *De Aedificiis* is a vital source about the works of the emperor in the Balkans, as well as about the history and geography of cities and castles. For

example, in Epirus we know from the *De Aedificiis* that Justinian I built walls around Nikopolis, while he renovated the walls of the cities Photike, Phoenice and Adrianopolis, which he renamed into Justinianopolis ('City of Justinian', nowadays Edirne in Turkey). Later, he erected walls at both Thermopylae and the Isthmus of Corinth in order to protect Peloponnese from the raids of the barbarians. Procopius, who – as a senior administrative officer – had access to the official documents, gives a list of 570 cities and fortifications in the Balkan Peninsula, a key region of Justinian's constructive activity. Similarly, in the 4th book of *De Aedificiis* the author mentions by name 56 cities or towns that were either renovated or built as new in Asia Minor.

For these reasons Procopius, is classified not only as a great historian, but also (perhaps involuntarily) as a great geographer, with sources that are totally reliable. It should be noted that in the *De Aedificiis* he reveals an exceptional ability in the description of the architectural monuments. This shows his broad and deep culture. Although he attempts to imitate Thucydides and Herodotus, his style is more sinewy and plain. This eminent historian and geographer, like all the scholars of his period, lived in an age that forms the exact border between two distinct periods in history: from the one side stands the ancient Greek/Graeco-Roman pagan world and from the other side the novel Byzantine Christian Empire. This becomes evident in both the works by Procopius and those of other authors of that period from the fact that often the ancient ideas and beliefs intermingle and alternate with the corresponding Christian teachings.

The entire work of Procopius was published by H.B. Dewing in seven volumes from 1914 to 1940 [28], and by J. Haury in 1964 [29].

3.9. Corippus the African (6th century)

Flavius Cresponius Corippus was a Latin grammarian and epic poet from North Africa, hence his surname 'African'. He lived initially in Carthage and later he became an officer of the imperial court of the Byzantine Empire in the years of Justinian I (527-565) and of his successors.

As a poet, Corippus wrote in Latin two poems of historical content in hexameter verse. The first one, entitled *Iohannidos seu De bellis Libycis libri 8* (*Of John or About the Libyan Wars in 8 Books*) is an epic poem of 5,000 verses in 8 books, which was composed in 549-550 AD in honour of Justinian's Byzantine general Ioannis Troglites, who stifled the rebellion of the Moorish in Africa (546-548). Corippus emerges as a competent geographer in this work, since he adds valuable material on the geography, topography and the ethnic background of the northern Africa. This poem was published in 1970 by James Diggle and Francis Richard David Goodyear [30].

In his second poem, entitled *In laudem Justini Augusti minoris* (*In praise of the younger Justin*), which was composed in 567 in four books, Corippus narrates in pompous style the ascending of Justin II (565-578) to the throne, as well as the first events of his period. It is also a very important work, because it presents facts about the imperial Court of that period [31].

3.10. Stephen of Byzantium (6th century)

Stephen of Byzantium or Stephanus Byzantius was a renowned scholar and geographer who flourished in the early 6th century, most probably during the reign of Justin I (518-527). Stephen wrote the *Ethnica* or *On Cities and Boroughs*, a unique great geographical dictionary in which he used all the geographical knowledge of the ancient Greek historians and geographers; this work's first title stems from the fact that in it the cities are mentioned with their ethnikà (gentile, old) names [32]. Indeed, it was a dictionary of Geography and names consisting of 55 books in which Stephen exposes valuable information about the geography of the ancient world. The sources for the compilation of this opus were the works of the great geographers, savants and historians of the antiquity, from Anaximander, Hecataeus of Miletus, Herodotus, Polybius and Pausanias to the Phoenician grammarian Philo Erennius (1st century AD), who had written a work under the same title (*On Cities And On the Glorious Persons Each Of Them Has Offered)*, and to Claudius Ptolemy (2nd century AD). For this reason the *Ethnica* contains a lot of important pieces of information (historical, religious, mythological, on linguistics and etymology, etc.) about the whole period from the antiquity to the author's century [33].

It should be noted that the ancient Greek historian, geographer and speech writer Hecataeus of Miletus (560-480 B.C.) in his work *Perihegesis* (*Tour of Earth*) compiled a 'world map' improving on that by Anaximander. In the new map (which was restored based on text from his written work) the eastern view about the world prevailed, i.e. that the Earth has the shape of a flat circular disk, with the land occupying the disk's central part and the Ocean surrounding the whole surface of the land.

Stephen's *Ethnica* geographical dictionary included also elements of the so-called mathematical geography. For the correct spelling of the place names and of their derivatives Stephen used as a source the famed grammarian Aelius Herodianus, whose work partly rescued. In this way, Stephen of Byzantium succeeded in writing an excellent encyclopaedic dictionary in both geographical and linguistic aspects.

This dictionary became particularly known and popular from an epitome written by a certain Hermolaus, a scholar and grammarian who dedicated it to emperor Justinian I (527-565). This epitome was circulated widely in the empire and became very popular; it is mentioned as being of great value by Theophanes, by the emperor Constantine VII Porphyrogennetos and by others, and rightly so, because even as an epitome, the *Ethnica* is of enormous value for the geography, the history and the evolution of language during the early Byzantine period. The full work formed the main source for the *De thematibus* by Constantine VII Porphyrogennetos.

Daniel Demetrio Magnes in his own dictionary (1834) writes the following about the *Ethnica*: "*This dictionary writes about Cities and Boroughs, and of the generation of the gentile names. Of this very useful Dictionary only a few fragments are saved and the Epitome written a certain grammarian*

Hermolaus from Constantinople during the reign of Justinian. The most complete edition of this work is the Greek and Latin of Lugdunum of 1694, which contains many and significant comments and Notes." [34]

The last full edition of this work was done by Augustus Meineke in 1849, in Berlin [35], and by convention references to the text use Meineke's page numbers. A new completely revised edition in German is in preparation by Margarethe Billerbeck.

The chief fragments remaining of the original work are preserved in *De administrando imperio*, ch. 23 (the article *Iberiae dio*) and *De thematibus*, ii. 10 (an account of Sicily); the latter includes a passage from the comic poet Alexis on the *Seven Largest Islands*. Another respectable fragment, from the article '*Dyme*' to the end of letter Delta, exists in a manuscript of the Fonds Coislin, the library formed by Pierre Séguier.

3.11. Nonnosus (6th century)

In the same age with Stephen of Byzantium flourished the polymath, scholar and speaker of many eastern languages Nonnosus. He was born to a family of diplomats, so he became an ambassador himself and during the reign of Justinian I he participated, as Photius writes in his *Bibliotheca* [36], in several missions-embassies to various nations, such as to the Ethiopians (553), to the Saracens (557) and others.

Nonnosus is mentioned as the author of various treatises, which originated in notes taken during his embassies to the Arabs, to the Red Sea nations and to the Axumites. The special interest in his work stems from the fact that it contains much reliable geographical and ethnographic information collected from the author's personal experience and impressions. For example, in the year 557 he personally led an embassy to the Saracens ('then a most powerful nation') and wrote down his impressions to a text, a passage of which was saved in Photius' *Bibliotheca* along with other fragments from his works about his diplomatic missions [36, Cod. 3: I 2]. In addition, from his work *Historia* only fragments exist today [37].

The work of Nonnosus was an important information source for the subsequent historians John Malalas (6th century), Theophanes (6th century) and those who continued the work of Theophanes (6th and 7th century), Photius (9th century) and George Cedrenus (11th century) [2, p. 210].

An example of Nonnosus from Photius follows: *"He tells us that most of the Saracens, those who live in Phoenicon as well as beyond it and the Taurenian mountains, have a sacred meeting-place consecrated to one of the gods, where they assemble twice a year. One of these meetings lasts a whole month, almost to the middle of spring, when the sun enters Taurus; the other lasts two months, and is held after the summer solstice. During these meetings complete peace prevails, not only amongst themselves, but also with all the natives; even the animals are at peace both with themselves and with human beings. Other strange, more or less fabulous information is also given.*

He tells us that Adulis[1] is fifteen days' journey from Axumis. On his way there, he and his companions saw a remarkable sight in the neighbourhood of Aue (Ave), midway between Axumis and Adulis; this was a large number of elephants, nearly 5000. They were feeding in a large plain, and the inhabitants found it difficult to approach them or drive them from their pasture. This was what they saw on their journey.

We must also say something about the climatic contrarieties of summer and winter between Ave and Axumis. When the sun enters Cancer, Leo, and Virgo, it is summer as far as Ave, as with us, and the atmosphere is extremely dry; but from Ave to Axumis and the rest of Ethiopia, it is severe winter, not throughout the day, but beginning from midday, the sky being covered with clouds and the country flooded with violent rains. At that time also the Nile, spreading over Egypt, overflows and irrigates the land. But when the sun enters Capricornus, Aquarius, and Pisces, the atmosphere, conversely, floods the country of the Adulites as far as Ave, while it is summer from Ave to Axumis and the rest of Ethiopia, and the fruits of the Earth are ripe.

During his voyage from Pharsan[2], Nonnosus, on reaching the last of the islands, had a remarkable experience. He there saw certain creatures[3] of human shape and form, very short, black-skinned, their bodies entirely covered with hair. The men were accompanied by women of the same appearance, and by boys still shorter. All were naked, women as well as men, except for a short apron of skin round their loins. There was nothing wild or savage about them. Their speech was human, but their language was unintelligible even to their neighbours, and still more so to Nonnosus and his companions. They live on shell-fish and fish cast up on the shore. According to Nonnosus, they were very timid, and when they saw him and his companions, they shrank from them as we do from monstrous wild beasts."

[1] A seaport town, generally identified with modern Thulla or Zula in Annesley Bay on the West shore of the Red Sea.

[2] Town in Ethiopia.

[3] The Pygmies

3.12. Priscianus the Grammaticus (6th century)

Priscianus, commonly known as Priscian, was a noted Latin grammarian, hence his nickname 'Grammaticus'. Because he was from Caesaria of Mauritania, he is also known as Priscianus Caesariensis. He flourished *circa* 500 AD in Constantinople as a professor of grammar and rhetorics, a fact known from a speech he wrote and dedicated to the emperor Anastasius I (Prisciani Grammatici, *De laude imperatoris Anastasii et de ponderibus et mensuris carmina*) [38].

However, he is better known from his 18-book opus on grammar entitled *Institutiones grammaticae* (*Grammatical Foundations*) [39]. In addition to some other works he wrote on Mathematics and Science, such as *De Figuris numerum*, *De metris fabularum Terentii* (*The Meters of the Plays of Terence*)

etc., Priscian should probably be also mentioned separately as a geographer. This is because he translated in Latin and disseminated in the Western Empire the geographical poem *Ecumenes Periegesis* (*Tour of the World*) by Dionysius the Traveler (*Periegesis de Dionysio*) [40] a work of 1,187 hexameter verses. This Dionysius had flourished during the Roman imperial times, in the age of the emperor Hadrianus, and for his poem he used as prime sources works by eminent geographers such as Eratosthenes, Poseidonius, Metrodorus, Alexander of Ephesus and others.

3.13. Marcellinus the Illyrian (6th century)

Marcellinus was born in the western part of Illyria. He was a scholarly writer of considerable education. From his work is saved only a *Chronicle* (*Annales*) in Latin, with which he continues the work of Hieronymus and covers the period from 379 to 534 AD [41]. In his *Annales* Marcellinus offers precious facts concerning the history of the empire's eastern part. He lived in Constantinople during the reign of the emperor Justinian I (527-565); Marcellinus was chancellor to Justinian, so when Justinian ascended to the throne his chancellor remained in favor and obtained various high places in the government and the title of 'Count' (*Comes*) [42]. Otherwise little or nothing is known of his life. Marcellinus died apparently soon after 534.

Marcellinus is of interest as far as Geography is concerned because of his lost work *Odoiporikon*, a 'most exact description of the cities of Constantinople and Jerusalem in four little books' with geographical and topographical information, which is mentioned by Cassiodorus the monk (Flavius Magnus Aurelius Cassiodorus Senator, *c.*485-*c.*585) in his *Institutiones Divinarum et Saecularium Litterarum* (*Institutes of Divine and Secular Literature*, 543-555) [43].

3.14. John of Gaza (Ioannis Gazaios, 6th century)

John was a renowned scholar, poet and geographer from Gaza of Palestine, that's why he is known as Gazaios. John also flourished under the reign of Justinian I (527-565).

From John's works was saved a poetic geographical description composed in 700 hexameter verses (with introductions in trimeter verse) under the title *Ecphrasis tou Cosmikou Pinakos* (*Expression of the World Table*). It is reported that John was inspired to compose this work from 'a painted map of the World' located in Gaza's winter baths with a mixture of Christian and pagan elements. According to the standard edition of Johns' poem by P. Friedländer [44] these are the baths Choricius of Gaza refers to as in course of construction at Gaza in 535 or 536 [45].

In his *Ecphrasis* John of Gaza imitates the literary, poetic and metric style of Nonnus of Panopolis (fl. *c* 450 AD). John also wrote poems on various topics and epigrams.

4. Other authors of Geography

After the age of the previous geographers and geographical authors, early Byzantine period followed various 'itineraries' or travelogues with much geographical information, especially about the Holy Land, since they were of practical use for the pilgrims.

Of noted significance are the itineraries written by John Phocas, Andreas Livadenos and Daniel, the bishop of Smyrna. Also, in the 7th century appeared the geographical work by George of Cyprus, which was of similar style with the work by Hierocles.

Essentially, aside from various patriarchal documents that contain many historical-geographical elements, cities and towns of their age, as 'real' historical-geographical sources can be classified the *Synecdemos* of Hierocles the grammarian (6th century), the Greek Codex No. 1155a of the 8th century (now in the French National Library, in Paris), the treatise *De thematibus* (*About the Provinces*) by the emperor Constantine VII Porphyrogennetos (10th century), as well as two works by foreign travellers-geographers: The first by the Arab traveller Abu Abdullah Muhammad ibn Ash Sharif al Idrisi (or Edrisi, 1106-1166), entitled *Kitab Nuzhat al-mushtaq fi'khtiraq al-'afaq* (= *The book of pleasant journeys into faraway lands* or *The pleasure of him who longs to cross the horizons*, 12th century), and the second by the Jewish Rabbi Benjamin of Tudela (1130-1173) under the title *Travels in the Middle Ages* [46]. It should be noted that the French expert of Byzantine studies Raymond Janin (1882-1972) dedicated his life to the history of the ritual of the eastern Churches and to the geography of the Byzantine Empire [http://openlibrary.org/authors/OL132622A/Raymond_Janin].

5. Conclusions

The early Byzantine period extends from about 300 AD to the 6th century and is characterized by the efforts to consolidate the Christian religion and make it the prevalent one in the empire. Therefore, anything that was in contradiction with the Holy Scripture should conform to it in any possible way. For this reason, and because geographical information often was not in agreement with the text of Scripture (and since the *Bible* could not be wrong), Geography according to the current way of thinking had to be adapted to the holy texts of Christianity. This task was overtaken by the Nestorian Christian monk Cosmas, the so-called Indicopleustes (6th century), who will be the subject of our subsequent paper. Cosmas wrote a *Christian Topography*, a work through which he attempted to create a novel system of Geography in the sense of a representation of the World in a way that would be compatible with the text of the Holy Scriptures.

We note here as well, that this paper is the continuation of our previous work on the connections between spirituality and Science [47, 48], on the contribution of the Church in Byzantium to the Natural sciences [49-51] and on the anti-astrology stance of the Church Fathers [52].

Acknowledgements

This study formed part of the research at the National and Kapodistrian University of Athens, Department of Astrophysics, Astronomy and Mechanics, and we are grateful to it for financial support through the Special Account for Research Grants. It is also supported by the Ministry of Science and Technological Development of Serbia through the project III 44002.

References

[1] ***, *Ptolemy's Geography: An Annotated Translation of the Theoretical Chapters*, English translation by J.L. Berggren and A. Jones, Princeton University Press, Princeton, New Jersey, 2001.
[2] E. Theodossiou and E. Danezis, *At the Years of Byzantium – Byzantine scientists, physicians, chronologers and astronomers*, in Greek, Diavlos, Athens, 2010, 134.
[3] F. Koukoules, *The life and civilization of the Byzantines*, vol. I, in Greek Papademas, Athens 1948, 125.
[4] S. Runciman, *Byzantine Civilization*, Arnold Publ., London, 1933, 266.
[5] M.A.P. d'Avezac, Mémoires de l'Académie des inscriptions, **2** (1852) 230.
[6] H. Wuttke, *Die Kosmographie des Istrier Aithikos im lateinischen Auszuge des Hieronymus*, Dyk'sche Buchhandlung, Leipzig, 1853.
[7] H. Wuttke, *Die Aechtheit des Auszugs aus der Kosmographie des Aithikos*, Dyk'sche Buchhandlung, Leipzig, 1854.
[8] K. Müller (ed.), *Geographi Graeci minores*, vol. 1, A.F. Didot, Paris, 1855.
[9] J.-P. Migne (ed.), *Patrologia Graeca cursus completus*, vol. 38, Centre for Patristic Publications, Athens, 2008, 852-1189.
[10] E.C. Butler, *The Lausiac History of Palladius: A Critical Discussion Together with Notes on Early Egyptian Monachism*, Elibron Classics, Adamant Media Corporation, New York, 2001, on line at http://www.touregypt.net/documents/lausiacindex.htm or at http://users.sch.gr/npavlou/lafsaikon.htm (original in Greek).
[11] Palladius of Helenopolis, *Historia Lausiaca*, vol. II, *The Life of St. John Chrysostom*, in Greek, Tenos, Athens, 1990, on line at http://books.google.gr/books?id=DKo4AAAAIAAJ&pg=PR38&lpg=PR38&dq=Dialogus+de+vita+Sancti+Joannis+Chrysostomi&source
[12] J.-P. Migne (ed.), *Patrologiae Latinae. Patrologiae cursus completus, series latina.* Turnholti, vol. 21, Typographi Brepols Editores Pontificii, Parisiis (Paris), 1848, 381-462, online at http://e-homoreligiosus.blogspot.com/2010/11/mignes-patrologia-latina-on-line-pdf.html.
[13] H. Weingarten Hermann, *Der Ursprung des Monchtums im nachconstantinischen Zeitalter*, F.A. Perthes, Gotha, 1877.
[14] J. Derett, Classica et Medievalia, **21** (1960) 77.

[15] ***, *Cosmas Indikopleustês, Topographie Chrétienne*, English translation by W. Wolska-Conus, Sources Chrétiennes, vol. 2, Les Editions du Cerf, Paris, 1968, 141, 159, 197.
[16] B. Berg, Byzantion, **44** (1974) 5.
[17] ***, *Palatine Anthology*, The Loeb Classical Library, vol. 67, E.H. Warmington (ed.), Harvard University Press, London, 1916, 59, online at http://www.ancientlibrary.com/greek-anthology/0072.html.
[18] P. Wesseling (ed.), *Hieroclis Grammatici Synecdemus,* Wetstenium and Smith, Amsterdam, 1735, 632-734.
[19] P. Wesseling (ed). *Hierocleous Grammatikou Synekdemos*. Corpus Scriptorum Byzantinae Historiae (CSBH, 3), Weber, Bonn, 1840, 379-532.
[20] G. Parthey (ed.), *Hieroclis Synecdemus et notitiae Graecae episcopatuum*; *acedunt nili doxapatrii notitia patriarchatuum et locorum nomina immutata*, Berliner Byzantinische Arbeiten, Berlin, 1866.
[21] G. Parthey (ed.), *Hieroclis Synecdemus et notitiae Graecae episcopatuum*; *acedunt nili doxapatrii notitia patriarchatum et locorum nomina immutata*, A.M. Hakkert, Amsterdam, 1967.
[22] A. Burckhardt, *Hieroclis Synecdemus*, Teubner, Leipzig, 1893.
[23] E. Honigmann (ed.), *Le Synekdèmos d'Hiéroklès et l'opuscule géographique de Georges de Chypre*, Editions de l'Institut de Philologie et d'Histoire Orientales et Slaves, Brussels, 1939.
[24] A. Kaldellis, *Procopius of Caesarea: Tyranny, History and Philosophy at the End of Antiquity*, University of Pennsylvania Press, Philadelphia, 2004.
[25] Procopius, *History of the Wars; The Secret History; Buildings*, English translation by H.B. Dewing, 7 vols., Harvard University Press, Cambridge, 1924-1940.
[26] Procopius, *The Secret History*, English translation by A. Kaldellis. Hackett Publishing, Indianapolis, 2010.
[27] G. Downey, Transactions and Proceedings of the American Philological Association, **78** (1947) 171.
[28] H.B. Dewing (ed.), *Procopius*, 7 vols., Loeb Classical Library, Harvard University Press, London, 1914-1940.
[29] J. Haury (ed.), *Procopii Caesariensis opera omnia*, 3 vols., Teubner, Leipzig, 1964.
[30] J. Diggle and F.R.D. Goodyear (eds.), *Flavii Cresponii Corippi Iohannidos seu De bellis Libycis libri 8*, Cambridge University Press, London, 1970.
[31] A. Cameron, *Flavius Cresponius Corippus: In laudem Iustini Augusti minoris* (*In praise of Justin II*), The Athlone Press, London, 1976.
[32] Stephanus Byzantius, *Ethnica*, 2 vols., in Greek, Series: Ancient Greek Literature ('The Greeks'), Kaktos, Athens, 2004.
[33] D. Whitehead (ed.), *From political Architecture to Stephanus Byzantius*, Sources for the Ancient Greek Polis, *Historia Einzelschriften* 87, Franz Steiber Verlag, Stuttgart, 1994.
[34] D.D. Magnes, *Lexicon Istorikomythikon kai Geographikon*, in Greek, Venice, 1834 (reprinted by the Society for the Study of Greek History, Athens, 2003), 355.
[35] A. Meineke (ed.), *Stephani Byzantii: Ethnicorum Quae Supersunt*, G. Reimerus, Berlin, 1849.
[36] Photius, *The Bibliotheca*, R. Pearse (ed.), Les Belles Lettres, Paris, 1959, Cod. 3: I 2, online at http://www.ccel.org/ccel/pearse/morefathers/files/photius_03 bibliotheca.htm.
[37] K. Müller (ed.), *Fragmenta Historicorum Graecorum*, vol. IV, A.F. Didot, Paris, 1851, 178.

[38] Prisciani Grammatici, *De laude imperatoris Anastasii et de ponderibus et mensuris carmina*, P.J. Schalbacher et Socios, Vindobonae, Vienna, 1828.
[39] Prisciani Grammatici, *Institutiones grammaticae*, Teubner, Lipsiae (Leipsig), 1859, online at http://www.worldcat.org/identities/np-priscianus$caesariensis.
[40] G. Bernhardy (ed.), *Dionysius Periegetes [opera omnia] graece et latine cum vetustis commentariis et interpretationibus*. Vol. 1 of Geographi graeci minores. Weidmann, Lipsiae (Leipsig), 1828.
[41] B. Croke, *Count Marcellinus and his Chronicle*, Oxford University Press, Oxford, 2001, 101.
[42] A. Fortescue, *Marcellinus Comes*, in *Catholic Encyclopedia*, Robert Appleton Company, New York, 1913, online at http://en.wikisource.org/wiki/Catholic_Encyclopedia_(1913)/Marcellinus_Comes.
[43] Cassiodorus, *Institutiones divinarum et saecularium litterarum* (*Institutions of divine and secular learning*), in *De Historici Christianis*, vol. XVII, Herder, Freiburg, 2003, online at http://www.intratext.com/IXT/LAT0482/.
[44] P. Friedländer: *Johannes von Gaza und Paulus Silentiarius*, Kunstbeschreibungen justinianischer Zeit, Habilitationsschrift publ., Leipzig und Berlin, 1912, 111.
[45] A. Cameron, The Classical Quarterly, New Series, **43(1)** (1993) 348, online at http://www.jstor.org/stable/639482.
[46] Benjamin of Tudela, *The Itinerary of Benjamin of Tudela: Travels in the Middle Ages*, English translation by M.N. Adler, Publications Joseph Simon Pangloss Press, Malibu, California, 1993.
[47] E. Danezis, E. Theodossiou, I. Gonidakis and M.S. Dimitrijević, Eur. J. Sci. Theol., **1(4)** (2005) 11.
[48] E. Theodossiou, V.N. Manimanis and M.S. Dimitrijević, Eur. J. Sci. Theol., **6(3)** (2010) 47.
[49] E. Theodossiou, V.N. Manimanis and M.S. Dimitrijević, Eur. J. Sci. Theol., **6(4)** (2010) 57.
[50] E. Theodossiou, V.N. Manimanis and M.S. Dimitrijević, Eur. J. Sci. Theol., **7(2)** (2011) 57.
[51] V.N. Manimanis, E. Theodossiou and M.S. Dimitrijević, Eur. J. Sci. Theol., **7(4)** (2011) 25.
[52] E. Theodossiou, V.N. Manimanis, M.S. Dimitrijević, Eur. J. Sci. Theol., **8(2)** (2012) 25.

European Journal of Science and Theology, April 2013, Vol.9, No.2, 19-29

THE CONTRIBUTION OF BYZANTINE MEN OF THE CHURCH IN SCIENCE COSMAS INDICOPLEUSTES (6TH CENTURY)

Vassilios N. Manimanis[1], Efstratios Theodosiou[1] and Milan S. Dimitrijevic[2*]

[1]*National and Kapodistrian University of Athens, School of Physics, Department of Astrophysics-Astronomy and Mechanics, Panepistimiopolis, Zographos 15784, Athens, Greece*
[2]*Astronomical Observatory, Volgina 7, 11060 Belgrade, Serbia*

(Received 15 February 2012)

Abstract

The first Christian centuries in the Byzantine Empire, from the 3rd one to the 6th one, comprise a period in which the Christian religion had to consolidate its place as the dominant religion. Therefore, everything that seemed to contradict the Scriptures had to be adapted to them by any means. For this reason, since Geography did not agree in several instances with the holy texts, and because the Scriptures could not be in error, the Geography of the times had to be harmonized with the holy texts of the new religion. This task was undertaken by the 6th century Nestorian Christian monk Cosmas the 'Indicopleustes'. Cosmas wrote the *Christian Topography*, a work through which he attempted to create a new system of geography or a representation of the World that would fit to the information contained in the Holy Scripture. His work and life are considered here.

Keywords: Byzantium, geography, Cosmas Indicopleustes, Christian topography

1. Introduction

The study of geography in the Byzantine Empire was considered essential and useful, because this knowledge was necessary for the determination of the location of the Holy Land, as well as for setting the borders between the bishoprics. Therefore, having as starting points the work of the ancient cartographer and geographer Marinus of Tyre (ca. 60/70-130 AD) and the famous opus *The Geography* (also known as *Geographia*, *Cosmographia*, or *Geographike Hyphegesis*) [1] by the great astronomer, mathematician and geographer Claudius Ptolemy (2nd century AD), Byzantine scholars composed their own geographical treatises.

* Corresponding author; e-mail: mdimitrijevic@aob.bg.ac.rs, phone: +381-11-3089-072, fax: +381-11-2419-553

To be exact, geographical studies and the study of the works of the ancient geographers were taking place mainly, almost exclusively, in the monasteries. The beliefs of the early Byzantine geographers about the Earth, especially those of Cosmas Indicopleustes, were rather imaginary, heavily influenced by the Holy Scripture and its ideas on cosmogony, while the main five geographical works of that period are in their majority mere catalogues of names and city guides for use by the school pupils, students and the visitors of the cities.

The fact that the geographical works of the early Byzantine centuries were basically written travelogues and travel-oriented descriptions indicates the clear difference between the Geography of the Greek antiquity and Geography as it was perceived in the early Byzantine period.

The first Christian centuries in the Empire, from the 3rd one to the 6th one, were those in which the 'new' Christian religion had to consolidate its place as the dominant religion. Therefore, everything that seemed to contradict the Scriptures had to either disappear and be forgotten, or to be adapted to them. Therefore, since Geography of the Greek and Hellenistic periods did not agree in several instances with the holy texts, and because the Scriptures could not be in error, Geography as it was perceived at the time had to be harmonized with the holy texts of the new religion. This task was undertaken by a 6th-century Nestorian (heretic) Christian merchant, traveller and later monk in the Monastery of Saint Catharine of Mount Sinai. His name was Cosmas, the so-called 'Indicopleustes', i.e. the one who had sailed to India.

2. The life of Cosmas Indicopleustes

Cosmas was of Greek origin and he became famous from the work he authored in the Monastery of Saint Catharine around 547 AD. When he was still young, *circa* 520, he travelled as a merchant to the region around Egypt, i.e. the Red Sea (and to the east up to the Persian Gulf) ([2], Book II, 29), the Kingdom of Axum and its vicinity (the region of the modern countries Ethiopia, Eritrea and Somalia) ([2, p. 159], Book II, 30), the Palestine and the Sinai peninsula ([2, p. 197], Book V, 8, 14, 51, 52).

After these first voyages and for about 15 years during the reign of Justinian I (527-565), Cosmas travelled in the Black Sea, east Africa and he sailed along the shore of the Indian Ocean, reaching India and Sri Lanka. For this reason he was later called 'Indicopleustes', not in the manuscripts about his work but around the 11th century [3].

Finally, our voyager returned to Alexandria and retreated to the famous Monastery of Saint Catharine on Mount Sinai, where he became a monk in 535 and started to write down impressions and descriptions from his voyages around a large part of the then known world: He authored a geographical work entitled *Topographia Christiana* (*'Christian Topography'*) or simply *Cosmographia*, which consisted initially of five books, later of six and finally of twelve. With his *Christian Topography* Cosmas attempted to create a new system of geography, or just a representation of the World, in such a way that it would be

in harmony with the teachings of the Holy Scripture. It is not absolutely certain that the name 'Cosmas' was his real one; it is generally used because it is written in just one of the copies of *Topographia Christiana*, the one kept in Florence (*Laurentianus Plutei IX. 28*).

It seems that the writing of the *Topographia Christiana* was completed in the middle of the 6th century. According to Roger Pearce: *"The date of the work is fairly certain. In book 2, Cosmas tells us that it is 25 years since he was in Axum, and he was there when Elesbaas was preparing his expedition against the Homerites. That expedition probably took place in 525 AD, or possibly 522 AD. At the beginning of book 6, he refers to two eclipses, giving the dates as Mechir 12 and Mesori 24: these would seem to be the eclipses of 6 Feb. 547 and 17 Aug. 547. The logical inference is that the work was written around 550 AD."* [Cosmas Indicopleustes, *Christian Topography*. Preface to the online edition, 2003, http://www.tertullian.org/fathers/cosmas_12_book12.htm].

It should be noted that Mechir and Mesori are, respectively, the 6th and the 12th month, of the ancient Egyptian solar calendar, which had Thoth as the first month of its year [4].

3. Topographia Christiana

In the 12-book version of the *Christian Topography* [5], many useful pieces of geographical information are contained, which were correctly recorded by Cosmas as an *in situ* collector of information. He describes the places he visited himself, but also all what he heard about them by both the sailors and the inhabitants of these places. In addition, he drew many maps of these places and sketches of the peculiar animals he saw there. In parallel, he records valuable historical information of his age, since it is certain that he happened to 'be there' when historical events were taking place, such as the military preparations of the king of the Axumites, ***Elesba(a)s*** (or Kaleb or Chaleb) against the Jewish people of Yemen (the Homerites). Elesba(a)s, or Elesboas or Kaleb is honoured by the Ethiopian Church as a blessed person: his feast is on May 15. As a king of Axum (Aksum) in Ethiopia, he fought in 525 against the Jewish ruler Dhu-Nawas, who persecuted the Christians in Nedjran, a town in South-Arabia. Also, Emperor Justinian asked Elesbaas for his help against the Persians. Elesbaas lost a battle against an opponent, and retired to a cell near Axum. He died about 555. Elesbaas sent legates to Palestine in *c.* 550 [6].

Cosmas had not received any special education [2, Book II, 1], and so it is natural that his work contains some very naïve cosmographical views, which contradict the worldview of the great astronomer and geographer of the 2nd century Claudius Ptolemaeus (Ptolemy). Cosmas outright condemns these views as 'false'.

The content of *Topographia Christiana*, being a compilation of various topics, does not really correspond to its title, but as a whole it does have an underlying aim: to set the foundations for a novel system of natural geography that would be totally based on the *Bible*. To this end, the polymath scholar and

patriarch Photius I (820-895) of Constantinople calls *Topographia Christiana* a simplistic transfer of the descriptions of the *Pentateuch* and he characterizes Cosmas with some scorn as "*closer to myth rather than to truth*" [3]. Because his language is simple, Photius accuses him of "*ignoring the Greek language*" and concludes his mention to this work and its author by asserting that "*[Cosmas] also writes some other, bizarre things*" [3, p. 212].

4. The cosmological views of Cosmas Indicopleustes

Essentially, Cosmas is a zealot heretical (Nestorian) Christian, who has a tremendous zeal to defend the simple cosmology of the Jewish tradition. By combining his empirical geographical observations with certain Biblical references he accepts that, contrary to the then accepted Ptolemaic system, the shape of the Earth is not spherical, but flat, long and narrow, like the tabernacle, the house of worship described to Moses by God during the Jewish Exodus from Egypt. In other words, according to Cosmas the Earth is a flat rectangular region – rectangular parallelogram. Similarly, the Universe is a two-floor rectangular parallelepiped box of vast volume, similar to the Arc of the Covenant, having the Earth as its base and the 'first heaven' (the highest one) as its cover. This heaven is the one identified as the Heavenly Kingdom and it rests upon the firmament. The firmament in turn forms the 'second heaven', which is the heaven of the mortals, in other words the kingdom of the Earth. In essence, this is a belief rooted in the ancient Egyptian cosmogony. The whole system is supported on its four edges, which, in the form of columns, rest upon the four 'corners of the Earth', which, as we mentioned already, is believed by Cosmas to be a flat parallelogram area covered by the celestial dome, the firmament and surrounded by the ocean of the waters, beyond which the paradise is located. Cosmas believes that the flat Earth sits upon the bottom of the motionless Universe, which is also non-spherical: it is presented as a huge cubical chamber with a curved (concave) ceiling. Around a bell-shaped mountain towards the North, revolve the Sun, the Moon and the stars, tracing circular orbits, always in accordance with God's orders, who at any given moment can stop and redefine their course, as in the book of Isaiah, where the Sun moved backwards by 10 degrees: "*I will make the shadow cast by the sun go back the ten steps it has gone down on the stairway of Ahaz'. So the sunlight went back the ten steps it had gone down.*" (*Isaiah* 38.8)

... and as happened in Gibeon, when Joshua, holding his hands outstretched during the battle of the Israelites with the Amorites, stopped the course of the Sun: "*On the day the Lord gave the Amorites over to Israel, Joshua said to the Lord in the presence of Israel: 'O sun, stand still over Gibeon; O moon, over the valley of Aijalon.' So the sun stood still, and the moon stopped, till the nation avenged itself on its enemies, as it is written in the book of Jashar? The sun stopped in the middle of the sky and delayed going down about a full day.*" (*Joshua* 10.12-13)

The Sun approaches alternatively the peak and the base of the bell-shaped mountain. This way Cosmas explains the succession of day and night. When the Sun shines and illuminates our part of the Earth, we have day, yet the tall bell-shaped mountain in the north prevents the rays of sunlight to shine on the regions of the Earth that are beyond the other side of the mountain, so darkness prevails upon these lands.

In summer, according to Cosmas, the Sun revolves around the narrow peak of the mountain, and therefore disappeared from our view only for a short time span, since this part of the revolution was short; but in winter the Sun revolves around the wide base of the mountain and so the winter nights are longer than the days, since the revolution of the Sun around the huge base of the mountain lasts for a much longer time span.

In addition, Cosmas writes that the stars and the planets do not move by themselves, but they are moved by the 'planetary angels', a belief that reached even the 17th century, the age of Johannes Kepler, the 'law giver of the skies'.

5. The theological views of Cosmas and the heresies of his period

As far as the theological ideas contained in the *Christian Topography* are concerned, Cosmas Indicopleustes, being a Nestorian heretic, adopts several views from the works by the earlier Christian bishops Diodorus of Tarsus (? – in office from 378, passed away in 392) and Theodorus of Mopsuhestia (350-429), who expressed Nestorian views. Nestorians, named after Nestorius (386-450), who was archbishop of Constantinople for three years (428-431), separated the two natures of Jesus and stressed the specific content of each of these two natures, which were clearly different from each other. They believed that, if the unification of these two natures was ever possible, this could be only 'moral'. According to their beliefs, the Virgin Mary did not give birth to the pre-existing Logos and Son of God, but just to the human Jesus. Mary, being a human herself, could not generate a God, but only a man, with whom the God-Logos was united later on. Nestorius, along with other representatives of Antiochean theology, such as Theodore of Mopsuhestia, Diodorus of Tarsus and others, used to call Mary *Anthropotokos* (man-bearer) and *Christotokos* (Christ-bearer) instead of *Theotokos* (God-bearer). Nestorius and his teachings were condemned as heretical by the Third Ecumenical Council, which was held in Ephesus in 431. The Council's decision was that Christ had two natures, the divine one and the human one, which were truly and absolutely united in His person, therefore the adjective *Theotokos* is valid for Virgin Mary [7].

Cosmas, in the 5th book of his *Christian Topographia*, mentions three other sects, those of Manicheans, Marcionists [2, Book V, 178] and Montanists [2, Book V, 252]. This fact indicates that these heresies were active and they had followers in Alexandria at the time Cosmas was writing *Topographia.*

Manichaeism was named after the Persian Manes (216-277), who emphasized the eternal struggle between Good and Evil, believing that Jesus was created by the spirit of Good and that his Crucifixion was the work of Satan.

Manichaeism was characterized by the intensity of the clash between Good and Evil and the duality Light-Darkness [7, p. 303].

Marcionism was named after Marcion, a Gnostic from Sinope who taught during the 2nd century. His teaching's main points are the existence of a benevolent-supreme God-Father, the Highest God, who is superior to the God-Creator, who is merely just. The Highest God is perfect and benevolent, while the Creator (who created the World) is just but not benevolent: he is the God of the *Old Testament*, while the God of the *New Testament* is the benevolent Highest God [7, p. 303].

Finally, Montanism was named after Martinus Montanus, a former priest of Cybele, who in 172 AD formulated his theory about a Century of the Father (*Old Testament*), a Century of the Son (*New Testament*) and a Century of the Spirit, the one announced by Montanus himself. He assigned a paramount position to the *Gospel of John*: "*But when the Counselor (Paracletos) comes, whom I shall send to you from the Father, even the Spirit of truth, who proceeds from the Father, he will bear witness to Me*" (John 15.26). So, in *John's Gospel*, Montanus detected the promise of the coming of Paracletos [7, p. 306].

All these sects are mentioned in the work by Cosmas, who at the same time rejects the Greek science and keeps a hostile stance against the 'gentile' education.

6. Cosmas Indicopleustes as a geographer

A central point in the main work of Cosmas is his attempt to prove that the Greek geographers were wrong in writing that the Earth is spherical, while in his opinion it is flat. However, this particular view of the flat Earth was of small acceptance even in his day; it was not accepted by the Byzantine scholars, nor by the educated Christian priests.

Nevertheless, despite its naïve character and its extravagant statements, the *Topographia* was and still is important, not for his beliefs about the nature of the world, but for the valuable geographical, cultural and historical information it contains, which is based on his own experiences as an 'eye witness' of the countries he travelled.

His views and information were discussed and commented upon by several subsequent scholars, while his popular writing style made the *Christian Topography* [5] a favourite reading among the less educated Byzantines, since it agreed with their daily experience.

However, his near-contemporary eminent Christian philosopher John Philoponus (490-570), who had Monophysitic tendencies, was quick to reject *Topographia Christiana*, along with most of the Byzantine scholars, in the name of the Aristotelian-Ptolemaic Universe. For this reason (see *on line Christian Topography*) parts of the 11th and even more the 12th book of the *Topographia* seem rather disconnected from the work's main topic (geography or topography): Instead, in the 12th book Cosmas tries to counter the criticism of other scholarly monks and the Christian Byzantine savants, who did not agree

with his views. In the 11th book he describes certain ports of India's west coast, where ships were loading pepper, and he also offers significant information about Sri Lanka, which he calls Taprobane: He explains its significance for commerce and he notes that on this island there existed a community of Nestorian Christians. Sri Lanka is also mentioned by Palladius of Helenopolis (364-431 or 368-430, see our previous paper [8]), in his famous work *Epistola de Indicis Gentibus et de Bragmanibus* (*On the nations and Brahmans of India*), where he exploits original material from his personal experience but also from descriptions by Egyptian travellers to India [9].

7. Existing copies and editions of *Topographia Christiana*

The work of Cosmas, *Topographia Christiana*, is saved in three basic copies. One is in the Vatican, it is the code *Vaticanus Graecus 699*, and it was written in the 9th century in Constantinople; it contains only the first ten books, i.e. the two books that are rather irrelevant to the work's main topic (the 11th and the 12th, see previous paragraph) are omitted.

The other two existing copies of the *Topography* contain all 12 books. They were both dated in the 11th century. The first one is an illustrated manuscript kept in the Monastery of Saint Catharine on Mount Sinai (*No. 1186*), yet it is considered to be a copy written in Cappadocia. The second one, the code *Laurentianus Plutei IX. 28*, is kept in Florence, but it was written in the Iviron Monastery of Mount Athos.

It should be noted that a fourth complete copy of *Topographia Christiana*, which is an exact transcription of the one kept in Florence, dated from 1682, was in England (*Phillips 2581*) but it has been lost and it is not known whether it was destructed or it is kept in some unknown library or in the archive of some secretive collector.

However, there are many more (at least 20) manuscripts that contain minor parts of the *Topographia*. These partial manuscripts contain mainly illustrations: 1) Paris Suppl. Gr. 844, 18th century. Contains only copies of some of the pictures in L. 2) Paris Gr. 2426 (P). 16th century. On ff. 112 ff, contains a copy of most of book 11, copied by Nicholas de la Torre, possibly from the archetype of Z, although it contains more of this book than Z did. The text is handled freely, and seems to relate to the Smyrna manuscript: 3) Smyrna B-8 (Z), ca. 1100 AD, described by Papadopoulos Kerameus in an 1877 catalogue. Selections appear on pp.156-192, under the name of Maximus (written over a shorter name that has been erased). Just a collection of pictures with short bits of text attached to it. 4) Vienna Theol. 9 (W). Selections. Bought in Constantinople by A. Busbeck. Copied from S, or more likely an Ms. similar to S. 5) Vat. Gr. 363 (R2), 10th century. 6) Oxford, Bodleian Library: Ms. Cromwell 15, 11th century. Bought on Mount Athos in 1727. 7) Bodleian Arch. Selden 29. AD 1338, fol. 116 has a catena on Luke, ascribed to *Cosmas Indicopleustes*. 8) Vat. Gr. 342. 12th century, fol. 7v. 9) Vat. Gr. 525. 12th century. fol. 1. 10) Venice, Marcianus Gr. 498. 14th century. fol. 270. 11) Bodleian, Baroc. 15, 12th

century. fol. 22. 12) Turin B. I. 10. 13) Milan, Ambrosian. B. 106. 10th century. 14) Moscow 358, 11th century. 15) Vat. Gr. 1747. 16) Paris Gr. 2743. Once Colbertinus 1476, 16th century, copied by J. Diassorinos. This is mentioned by Montfaucon, and also by Omont, both of whom lead the reader to suppose Cosmas was the author of a commentary on the *Psalms* preserved herein. In fact it contains only the usual chunk of book 5, followed by material from other authors. 17) Paris Gr. 169 (Mazarin-Reg. 3450), 14th century. A similar Ms., with the paragraph expanded by adding a following section from other authors. 18) Vallicellianus C. 4. 16th century. ff. 434-5. Also with the expanded paragraph from book 5. 19) Paris Gr. 3179, 16th century. Copied by Bigot. Also with the expanded paragraph from book 5. 20) Vat. Gr. 711. fol. 196. (More details in the complete list exist in the Preface of the online edition by Roger Pearce, 2003).

As far as printed editions of the work are concerned, *Topographia Christiana* was published for the first time in the West in 1707 by the French scholar and critic Bernard de Montfaucon (1645-1741) in *Collectio nova patrum et scriptorum graecorum* [10]. In 1806 it was included in the 88th volume of *Patrologia Graeca* by J.-P. Migne [5], while as a separate book it was published in London, translated by J. Mac Crindle under the title *The Christian Topography of Cosmas, an Egyptian Monk* (Hakluyt Society Publications, no. 98, London 1897, pages 365) [11] and in Cambridge, England, by E.O. Winsted, as *The Christian Topography of Cosmas Indicopleustes* [12].

The views of Cosmas Indicopleustes as expressed in his *Topographia Christiana* were studied by Wanda Wolska-Conus, who published a pertinent treatise entitled *La Topographie chrétienne de Cosmas Indikopleustès - Théologie et Science au VI siecle* (Paris 1962) [13]. A voluminous work on him was published by Redin [14] as well. In Serbian, *Christian Topography* was translated in 1649, by monk Gavrilo Troičanin, in the Monastery of Holy Trinity, and illustrated by Andrija Raičević [15]. On the influence it had on the formation of erroneous comprehensions, witness the manuscript where Cosmas is named the Saint [16], as well as some icons and frescoes in Serbian monasteries where the Earth is represented as a flat tablet with a conus like mountain according to Cosmas [15, p. 37].

Nowadays the text of *Topographia Christiana* is available on line in the Internet, both the prototype (in Greek) [http://www.hs-augsburg.de/~harsch/graeca/Chronologia/S_post06/Cosmas/cos_ipro.html], and translated in English.

Cosmas also wrote other works, such as *Geographia* (*Cosmographia*) and *Astronomia* (astronomical tables), but these were lost; however, besides *Topographia Christiana*, there is one more work by Cosmas that was saved: this is the *Description of the Plants and Animals of India* [17] (contained in Thevenot's *Relation des divers Voyages curieux*). This work was compiled from first-hand information and it was published in Paris by Melchisédec Thévenot (1663).

8. Conclusions

In the middle of the 6th century AD the Hellenistic antiquity reaches its end. In this age of the early Byzantine period the Near and the Middle East become Christian at a fast pace. However, the struggle between the two worlds, the old 'gentile' one and the emerging Christian one, is intense and it appears both indirectly, through ancient philosophical elements in the dogmas of Christian sects, and directly, in the form of the confrontation between the last scholars of the ancient world and the bishops and priests of the Church.

In this contest comes to participate a dynamic Nestorian monk, 'Cosmas the Indicopleustes', an uneducated but much travelled man. Armed with the practical knowledge he amassed from his distant voyages, he writes the *Christian Topography*, a work that essentially stands against the correct theories of the Greek astronomers and geographers of antiquity, who wrote and taught about the sphericity of the Earth.

For Cosmas the secular wisdom is of no value whatsoever; he elaborates on another logic, in which everything is explained with the use of the sacred texts and especially with the *Old Testament*. His views about the world are based on the theory of the flat Earth, which, in general, is supported by a literal interpretation of the holy texts of all three major monotheistic religions (Judaism, Christianity and Islam). Thus, a considerable part of the work written by Cosmas has as its deeper purpose to lay the foundations of a system of natural geography based on the *Bible*. For this reason, the scholarly patriarch Photius (810-891) labels *Topographia Christiana* as a naïve interpretation of the *Pentateuch*'s contents and he looks down on Cosmas, writing about him rather scornfully.

In reality, Cosmas does not represent the Christian Church, since he is just a Nestorian (heretic) monk and his views were not accepted by the educated priests or the leaders of the Church. Neither does he represent some scientific or cultural or spiritual or ideological current inside the Church. However, he considerably influenced the simple, uneducated members of the lower priesthood, as well as the naïve, uneducated laypersons in the Byzantine Empire, because his *Christian Topography* was an original and interesting work that contained a wealth of information of travel-oriented geographical and commercial interest given in a simple language, a fact that made it an easy-to-read and interesting work. While in its age it captivated its readers with its descriptions of exotic places and animals, which always fascinate the wider populace, it is still of interest to modern research scholars and scientists, since the *Christian Topography* continues to be a valuable source for the history of science, commerce and the sea routes of that remote period.

It should not be overlooked that the voyage of an average person to the kingdoms of east Africa, the Red Sea, the Palestine, to Mount Sinai, to the Arabian kingdoms, the Persian Gulf, and especially to India and Sri Lanka was an almost impossible feat.

The *Topography* of Cosmas, apart from its simplistic cosmology, is a significant opus, since it allows the modern reader to take a look upon the world of the sixth century, or at least upon a large part of it, through the pen of an 'eye witness' who lived 15 centuries ago, complete with maps, sketches and drawings that decorate and strengthen the text.

On the other side, it can be said that *Topographia Christiana* was one of the earlier Byzantine works that indicate the results of the abandonment of the ancient secular education, which had started from the previous centuries. Apart from natural sciences such as astronomy, cosmology and geography, the classic medicine as the legacy of the great doctors of Greek and Hellenistic antiquity gradually retreats during the same period, without losing its representatives: the populace begins to assign metaphysical causes of the diseases and to consider them as merely a form of divine punishment, a belief that can be find even nowadays, especially in the Third World countries. In this way, in the Byzantine Empire after the 7th century the medical doctor was gradually replaced by the monk or the equivalent of the Russian *starets*, who was called in order to drive away the disease, or rather the demons that caused it, by reading prayers, giving their blessing and burning incense [18].

Only centuries later, in the period of the Palaiologean Dynasty (1261-1453) a relative Renaissance of the sciences and culture happened in the Byzantine Empire, however it was too late for a true revival of sciences as the Empire was then in permanent political and territorial decline and the fall of the capital Constantinople to the Ottoman Turks was near (1453).

This paper is the continuation of our previous work on the connections between spirituality and science [19, 20], on the contribution of the Church in Byzantium to the Natural sciences [21-23], the anti-astrology stance of the Church Fathers [24] and on the contribution of the Church in Byzantium to Geography [8].

Acknowledgements

This study formed part of the research at the National and Kapodistrian University of Athens, Department of Astrophysics, Astronomy and Mechanics, and we are grateful to the University of Athens for financial support through the Special Account for Research Grants. It is also supported by the Ministry of Education and Science of the Republic of Serbia, through the project III44002.

References

[1] ***, Ptolemy's Geography: An Annotated Translation of the Theoretical Chapters, English translation, Princeton University Press, Princeton, 2001.

[2] Cosmas Indikopleustês, Topographie Chrétienne, French translation, Sources Chrétiennes, vol. I, Les Editions du Cerf, Paris, 1968, 141.

[3] E. Theodossiou and E. Danezis, At the Years of Byzantium – Byzantine scientists, physicians, chronologers and astronomers, in Greek, Diavlos Publ., Athens, 2010, 211.

[4] E. Theodossiou and E. Danezis, *The Odyssey of the calendars*, vol. I: *Searching for the roots of Knowledge*, in Greek, Diavlos Publ., Athens, 1996, 68.
[5] J.-P. Migne (ed.), *Patrologia Graeca cursus completus*, vol. 88, Centre for Patristic Publications, Athens, 2008, 445.
[6] A. Mertens, *Encyclopedia: Who was a Christian in the holy land?*, *Elesba(a)s*, Studium Biblicum Franciscanum (SBF), Jerusalem, 1980, online at http://www.christusrex.org/www1/ofm/sbf/escurs/wwc/e.html.
[7] E. Theodossiou and E. Danezis, *To the traces of IXTHYS: Astronomy-History-Philosophy*, in Greek, Diavlos Publ., Athens, 2000, 314.
[8] V. Manimanis, E. Theodossiou and M.S. Dimitrijević, Eur. J. Sci. Theol., **8(4)** (2012) 23.
[9] J. Derett, Classica et Medievalia, **21** (1960) 77-135.
[10] Bernard de Montfauco, *Collectio nova patrum et scriptorum graecorum*: *Eusebii Caesariensis, Athanasii, & Cosmae Aegyptii*, C. Rigaud Publ., Paris, 1707, online: http://openlibrary.org/works/OL1086644W/Collectio_nova_patrum_et_scriptorum_graecorum.
[11] J.W. McCrindle (ed.), *The Christian Topography of Cosmas, an Egyptian Monk,* Hakluyt Society Publications, London, 1897.
[12] E.O. Winstedt, (ed.), *The Christian Topography of Cosmas Indicopleustes*, Cambridge University Press, Cambridge, 1909.
[13] W. Wolska-Conus, *La Topographie chrétienne de Cosmas Indikopleustês - Théologie et Science au VIe siècle,* vol. 3, Bibliothèque Byzantine. Presses Universitaires de France, Paris, 1962.
[14] E.K. Redin, *Christian Topography of Cosmas Indicopleustes according to Greek and Russian manuscripts I*, in Russian, Typography of G. Lissner and D. Sobko, Moscow, 1916.
[15] N.D. Janković, *Astronomy in old Serbian manuscripts*, in Serbian, Serbian Academy of Sciences and Arts, Particular editions, Vol. DXC, Department of natural-mathematical sciences, book 64, Belgrade, 1989, 34.
[16] L. Stojanović, *Catalogue of National library in Belgrade IV*, Manuscript No. 497, in Serbian, Royal Serbian State Printing Office, Belgrade, 1903.
[17] M. Thévenot, *Relations de divers Voyages curieux,* Thomas Moette, Paris, 1663.
[18] I. Anagnostakis, *Food poisoning in Byzantium*, Proc. of the Symposium 'Food and Cooking in Byzantium', D. Papanikola-Bakirtzi (ed.), Archaeological Receipts Fund-Publications of Ministry of Culture, Athens, 2005, 17-30.
[19] E. Danezis, E. Theodossiou, I. Gonidakis and M.S. Dimitrijević, Eur. J. Sci. Theol., **1(4)** (2005) 11-17.
[20] E. Theodossiou, V.N. Manimanis and M.S. Dimitrijević, Eur. J. Sci. Theol., **6(3)** (2010) 47-56.
[21] E. Theodossiou, V.N. Manimanis and M.S. Dimitrijević, Eur. J. Sci. Theol., **6(4)** (2010) 57-69.
[22] E. Theodossiou, V.N. Manimanis and M.S. Dimitrijević, Eur. J. Sci. Theol., **7(2)** (2011) 57-71.
[23] V.N. Manimanis, E. Theodossiou and M.S. Dimitrijević, Eur. J. Sci. Theol., **7(4)** (2011) 25-45.
[24] E. Theodossiou, V.N. Manimanis and M.S. Dimitrijević, Eur. J. Sci. Theol., **8(2)** (2012) 25-45.

EPJ D
www.epj.org
Atomic, Molecular, Optical and Plasma Physics

Eur. Phys. J. D (2008) DOI: 10.1140/epjd/e2008-00128-9

Temperature dependence of atomic spectral line widths in a plasma

B. Zmerli, N. Ben Nessib and M.S. Dimitrijević

EDP SCIENCES
Società Italiana di Fisica
Springer

Eur. Phys. J. D (2008)
DOI: 10.1140/epjd/e2008-00128-9

THE EUROPEAN PHYSICAL JOURNAL D

Temperature dependence of atomic spectral line widths in a plasma

B. Zmerli[1], N. Ben Nessib[1], and M.S. Dimitrijević[2,a]

[1] Groupe de Recherche en Physique Atomique et Astrophysique, Institut National des Sciences Appliquées et de Technologie, Centre Urbain Nord, BP 676, 1080 Tunis Cedex, Tunisia
[2] Astronomical Observatory, Volgina 7, 11160 Belgrade, Serbia

Received 14 November 2007 / Received in final form 13 February 2008
Published online 25 June 2008 –

Abstract. We investigated here temperature dependence of Stark widths for neutral atom spectral lines in order to find a more precise method for scaling with temperature than sometimes used dependence $T^{-1/2}$, which is often inadequate particularly for Stark broadening of neutral emitter lines. We found here an analytical scaling with temperature within simplified semiclassical approaches of Freudenstein and Cooper and Dimitrijević and Konjević. For analysis of the temperature dependence, lines of HeI were used.

PACS. 32.70.Jz Line shapes, widths, and shifts – 32.60.+i Zeeman and Stark effects – 52.20.Fs Electron collisions

1 Introduction

Stark broadening is of particular interest for a large number of problems which concern laboratory plasma spectroscopy and astrophysics as well. Consequently, a number of experimental and theoretical papers have dealt with Stark broadening of neutral atom spectral lines, due to their importance for plasma diagnostics. Moreover, the existing critical reviews of experimental data ([1] and references therein), facilitate testing of various theoretical approximations.

In order to compare experimental data for Stark width of non hydrogenic atom-, and ion-lines obtained at various plasma conditions, different methods for scaling with temperature are used. Among them, sometimes is used that the Stark width w depends on T as $T^{-1/2}$, which is often good for ionized atoms. For example Griem [2] says on the temperature dependence of Stark widths of multiply ionized atoms that most of "measurements are consistent with the simple $T^{-1/2}$ dependence". Namely in the case of charged emitters, if one looks for example at the simple semiempirical formula, Stark width is proportional to the $T^{-1/2}$ (coming from the average velocity since the Stark width w is proportional to the product of perturber density (electrons), their average velocity and the averaged sum of cross sections for different collisional processes populating and depopulating the upper and lower level of the optical electron transition) and to the Gaunt factors summed up over all the perturbing levels. If the energy of the perturbing electron is less than twice the energy difference between the perturbing levels, the Gaunt factors are nearly independent of temperature, and the dependence is as $T^{-1/2}$. On the other side, at high temperatures the temperature dependence of different Gaunt factors will be combined with factor $T^{-1/2}$ thus giving often more or less a temperature independent or slowly decreasing Stark width. Such $T^{-1/2}$ dependence of Stark line width is so commonly assumed, especially in astrophysics, that some databases used for modelling of stellar spectra like for example Vienna atomic line data base (VALD) [3] provide for Stark broadening parameters only the values for $T = 10\,000$ K, assuming an interpolation to other temperatures as $T^{-1/2}$ (or, eventually as a constant within a smaller temperature interval).

The principal aim of this paper is to draw attention, especially to astrophysicists using such values at $T = 10\,000$ K and extrapolating them to other temperatures as $T^{-1/2}$, on the uncertainties of such method, especially for Stark broadening of neutral atom lines, where cross sections for inelastic collisions have a more pronounced part increasing with energy, and to propose a better method. Namely, the use of such dependence without additional checks might be inadequate, especially for spectral lines of neutral atoms. For example, in [4], empirical relations for Stark width dependences on temperature, different from $T^{-1/2}$, are obtained for a number of particular cases of neutral atom spectral lines. With the selected

[a] e-mail: mdimitrijevic@aob.bg.ac.yu

ratios of measured w_m, and theoretical Stark widths w_t, the linear best fit formula $w_m/w_t = A+BT$ is determined and given for studied lines or multiplets. Also, in order to present results for synthetic spectrum calculations in [5], all data on FWHM (W) were fitted with the expression $W = A_0 T^{A_1}$. Instead of the commonly adopted temperature dependence, Šćepanović and Purić used functions of the form $f(T) = A + BT^{-C}$ [6]. A general form of that dependence in the case of the particular transition array, in function of the rest core charge Z of the emitter as seen by the electron undergoing the transition, is $W = N_e f(T)/Z^D$.

In order to demonstrate the deviations from the $T^{-1/2}$ dependence for neutral atom lines, we will derive here the explicit temperature dependence for two particular cases: the simplified formulae of Freudenstein and Cooper [7] and Dimitrijević and Konjević [8]. We note that the present study on the Stark broadening of neutral atom lines is the continuation of our previous ones for ions in various stages of ionization [9–14].

For neutral atoms, the variation of the Stark width with electron density N_e was studied in [15,16] while now the Stark width temperature dependence investigation will be presented.

In [17], Table IV, most Stark widths are decreasing with temperature but someones (e.g. $2s^1\mathrm{S}-2p^1\mathrm{P}^\circ$) are increasing. Namely, cross sections for inelastic electron – neutral atom collisions, have an increasing and a decreasing part so that when temperature corresponds to the dominantly increasing part of particular contributions to the Stark width, it may not only decrease but increase as well. To take into account such variation with temperature, we performed the analysis of the Stark HWHM (half width at half intensity maximum), w, dependence on temperature, using several neutral helium multiplets. For Stark width calculations and the analysis of the temperature dependence, methods of Freudenstein and Cooper [7] and Dimitrijević and Konjević [8] were used and the obtained temperature trends are compared and checked with other theoretical results in [17] and [18].

2 Theory

Freudenstein and Cooper [7] approximated the expression for electron-impact width of neutral atom isolated lines obtained within the semiclassical method [19], assuming that the perturbation of the respective closest perturbing level is dominant for the initial (i), as well as for the final (f) state of the considered transition. Then Stark HWHM (w) of an isolated, non hydrogenic, neutral atom spectral line may be expressed as [7]

$$w = \frac{c_1}{\sqrt{T}} \left[R_{ii}^2 f_w \left(\eta_{ii'} R_{ii'}\right) + R_{ff}^2 f_w \left(\eta_{ff'} R_{ff'}\right) \right] \qquad (1)$$

where i' and f' are the corresponding closest perturbing levels,

$$c_1 = \left(\frac{32}{27}\right)^{\frac{1}{2}} N_e \pi \left(\frac{E_H}{k}\right)^{\frac{1}{2}} \left(\frac{\hbar a_0}{m}\right), \qquad (2)$$

m and N_e are the electron mass and electron density respectively. k is Boltzmann constant, T temperature, E_H hydrogen atom ionization energy and a_0 Bohr radius.

$$R_{jj}^2 = \frac{n_j^{*2}}{2Z^2}[5n_j^{*2} + 1 - 3\ell_j(\ell_j+1)], j = i, f, \qquad (3)$$

here, n_j^* and ℓ_j are effective principal, and orbital quantum numbers of the atomic energy level j and Z charge "seen" by the optical electron ($Z = 1$ for neutrals, 2 for singly charged ions...). The dipole matrix element (in units of the Bohr radius a_0^2) ${R_{jj'}}^2$ is expressed as

$${R_{jj'}}^2 = f_{jj'} \times \frac{\lambda_{jj'}(\text{Å})}{303.7}, \qquad (4)$$

$f_{jj'}$ is the oscillator strength for a transition between levels j and j', $\lambda_{jj'}$ the corresponding wavelength and

$$\eta_{jj'} = \frac{\triangle E_{jj'}}{3kT} = \frac{|E_j - E_{j'}|}{3kT}, \qquad (5)$$

where E_j and $E_{j'}$ are energies of the corresponding atomic levels. The function $f_w(\eta_{jj'}R_{jj'})$ is an approximate fitted expression proposed in [7] as

$$f_w\left(x\right) = e^{-1.33x} \ln\left(1 + \frac{2.27}{x}\right) + \frac{0.487x}{0.153 + x^{\frac{5}{3}}} + \frac{x}{7.93 + x^3} \qquad (6)$$

where

$$x = \eta_{jj'} R_{jj'} = \frac{\triangle E_{jj'} R_{jj'}}{3kT} = \frac{T_0^{jj'}}{T} \qquad (7)$$

where

$$T_0^{jj'} = \frac{R_{jj'} \triangle E_{jj'}}{3k}. \qquad (8)$$

For ηR much larger than one or

$$T \ll T_0^{jj'}, \qquad (9)$$

the function $f_w(\eta_{jj'}R_{jj'})$ may be approximated as [7]

$$f_w(\eta_{jj'}R_{jj'} \gg 1) \approx \frac{1}{2}\left[3\pi^2/32\left(\eta_{jj'}R_{jj'}\right)^2\right]^{1/3}$$

$$\approx 0.487(\eta_{jj'}R_{jj'})^{-2/3}. \qquad (10)$$

For such a case, we present an explicit function f_w which depends on T as

$$f_w \approx B_{jj'} T^{2/3} \qquad (11)$$

$$B_{jj'} = \frac{1}{2}\left(\frac{27}{32}\right)^{1/3} \left(\pi k/\triangle E_{jj'} R_{jj'}\right)^{2/3}. \qquad (12)$$

Finally, w may be expressed as an explicit function of T as

$$w(T \ll T_0^{jj'}) \approx \frac{C}{\sqrt{T}} T^{2/3} \approx C T^{1/6} \qquad (13)$$

$$C = c_1 \left(B_{ii'} R_{ii}^2 + B_{ff'} R_{ff}^2\right). \qquad (14)$$

For ηR much smaller than one or

$$T \gg T_0^{jj'}, \tag{15}$$

the function $f_w(\eta_{jj'}R_{jj'})$ may be approximated as [7]

$$f_w(\eta_{jj'}R_{jj'} \ll 1) \approx \ln\,(2.27/\eta_{jj'}R_{jj'}). \tag{16}$$

For this case we can also express explicitly the dependence of w on T, since

$$f_w \approx \ln\,(D_{jj'}T) \approx \ln\,(T) + \ln\,(D_{jj'}), \tag{17}$$

$$D_{jj'} = 2.27 \times 3k/\triangle E_{jj'}R_{jj'} \tag{18}$$

and

$$w(T \gg T_0^{jj'}) \approx \frac{1}{\sqrt{T}}\left[F_1 + F_2\,\ln\,(T)\right] \approx F_2\frac{\ln\,(T)}{\sqrt{T}}, \tag{19}$$

$$F_1 = c_1\left[R_{ii}^2\,\ln\,(D_{ii'}) + R_{ff}^2\,\ln\,(D_{ff'})\right], \tag{20}$$

$$F_2 = c_1\left(R_{ii}^2 + R_{ff}^2\right). \tag{21}$$

Dimitrijević and Konjević [8] generalized the theory of Freudenstein and Cooper for the case of more than one important perturbing level and also derived analogous formula for the shift. With such generalization (1) becomes

$$w = \frac{c_1}{\sqrt{T}}\left[\sum_{i'\neq i} R_{ii'}^2 f_w(\eta_{ii'}R_{ii'}) + \sum_{f'\neq f} R_{ff'}^2 f_w\,(\eta_{ff'}R_{ff'})\right]. \tag{22}$$

For this case, the temperature dependence described by (13) and (19) is also valid, but the corresponding quantities C, F_1 and F_2 become

$$C = c_1\left(\sum_{i'\neq i} B_{ii'}R_{ii'}^2 + \sum_{f'\neq f} B_{ff'}R_{ff'}^2\right), \tag{23}$$

$$F_1 = c_1\left[\sum_{i'\neq i} R_{ii'}^2 \ln\,(D_{ii'}) + \sum_{f'\neq f} R_{ff'}^2 \ln\,(D_{ff'})\right], \tag{24}$$

$$F_2 = c_1\left(\sum_{i'\neq i} R_{ii'}^2 + \sum_{f'\neq f} R_{ff'}^2\right). \tag{25}$$

Our objective here is to demonstrate that the $T^{-1/2}$ dependence for scaling widths with temperature is often inadequate, particularly for Stark broadening of neutral emitter lines. Consequently, we have shown that within theoretical approaches of Freudenstein and Cooper [7] in (1), and Dimitrijević and Konjević [8] in (22), an explicit temperature dependence of line widths, different from $T^{-1/2}$, can be obtained at low and high temperature limit.

It is convenient to write (6) as a function of the temperature T, $(T/T_0^{jj'} = 1/x)$, in order to analyze the intermediate region:

$$f_w = \mathrm{e}^{-1.33\frac{T_0^{jj'}}{T}}\,\ln\,\left(1 + 2.27\frac{T}{T_0^{jj'}}\right) + \frac{0.487\left(T/T_0^{jj'}\right)^{2/3}}{1 + 0.153\left(T/T_0^{jj'}\right)^{5/3}} + \frac{\left(T/T_0^{jj'}\right)^2}{1 + 7.93\left(T/T_0^{jj'}\right)^3}. \tag{26}$$

Therefore, the expression for atom-lines Stark widths (w) in function of initial and final levels may be expressed as an explicit function composed of three components as:

$$w = w(T) = \sum_{n=1}^{3} w_n(T) \tag{27}$$

where

$$w_n(T) = \sum_{j=i,f} w_{jn}(T) = w_{in}(T) + w_{fn}(T) \tag{28}$$

such as

$$w_{j1}(T) = \frac{c_1}{\sqrt{T}}\sum_{j'\neq j} R_{jj'}^2\left[\mathrm{e}^{-1.33\frac{T_0^{jj'}}{T}}\,\ln\,(1 + 2.27\frac{T}{T_0^{jj'}})\right] = \frac{c_1}{\sqrt{T}}\sum_{j'\neq j} R_{jj'}^2 f_1, \tag{29}$$

$$w_{j2}(T) = \frac{c_1}{\sqrt{T}}\sum_{j'\neq j} R_{jj'}^2\left[\frac{0.487(T/T_0^{jj'})^{2/3}}{1 + 0.153(T/T_0^{jj'})^{5/3}}\right] = \frac{c_1}{\sqrt{T}}\sum_{j'\neq j} R_{jj'}^2 f_2, \tag{30}$$

$$w_{j3}(T) = \frac{c_1}{\sqrt{T}}\sum_{j'\neq j} R_{jj'}^2\left[\frac{(T/T_0^{jj'})^2}{1 + 7.93(T/T_0^{jj'})^3}\right] = \frac{c_1}{\sqrt{T}}\sum_{j'\neq j} R_{jj'}^2 f_3. \tag{31}$$

We can see that the temperature dependence may be very complicated if the contribution of several perturbing levels is similar. If T is much larger than all $T_0^{jj'}$ corresponding to $\eta_{jj'}R_{jj'} \ll 1$,

$$w(T \gg T_0^{jj'}) \approx w_{j1}(T) \tag{32}$$

is given by (19), (24), (25) and for low temperature $T \ll T_0^{jj'}$ corresponding to $\eta_{jj'}R_{jj'} \gg 1$,

$$w(T \ll T_0^{jj'}) \approx w_{j2}(T) \tag{33}$$

is given by (13), (23).

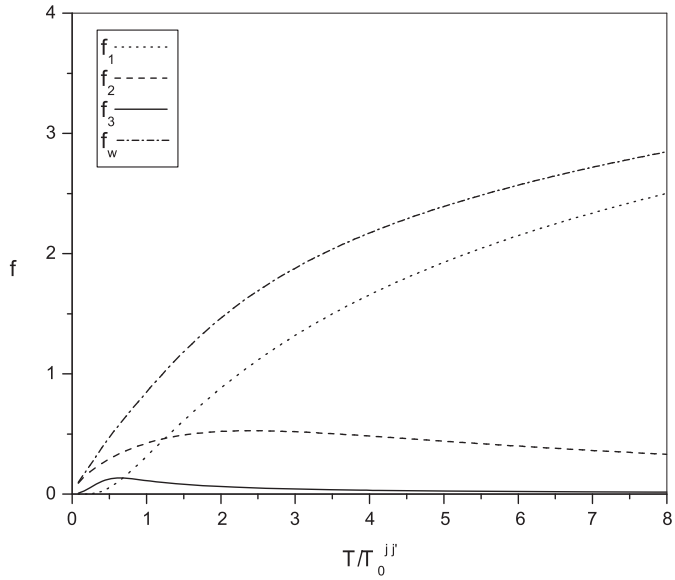

Fig. 1. A plot of the functions f_1, f_2, f_3 and f_w versus the reduced temperature $T/T_0^{jj'}$.

In both cases, where T is much smaller or much higher than $T_0^{jj'}$, the temperature dependence deviates from $T^{-1/2}$. For the intermediate case, only if the function f_w may be assumed to be constant the width dependence on T is $T^{-1/2}$. If there are several important perturbing levels it is very difficult to find such a case. Consequently, in general, the dependence of Stark width w on temperature is not simple and may be very different from $T^{-1/2}$. In Figure 1, where functions f_1, f_2, f_3 and f_w are presented as functions of T, one can see that f_3 and consequently w_{j3} are of importance only within a very limited range at low temperatures.

To study the influence of temperature in the broadening of spectral lines, we analyze also the strong and the weak collisions separately [19]:

$$w = w_{strong} + w_{weak} \tag{34}$$

where

$$w_{strong} = \frac{4\pi}{3} N_e \left(\frac{\hbar}{m}\right)^2 \int \frac{f(v)}{v} dv \times \left\{ \sum_{j' \neq j} R_{jj'}^2 \frac{1}{2} \left[A^2(z_{jj'}^m) + B^2(z_{jj'}^m)\right]^{1/2} \right\} \tag{35}$$

and

$$w_{weak} = \frac{4\pi}{3} N_e \left(\frac{\hbar}{m}\right)^2 \int \frac{f(v)}{v} dv \left\{ \sum_{j' \neq j} R_{jj'}^2 a(z_{jj'}^m) \right\}. \tag{36}$$

The argument $z_{jj'}^m$ of Stark broadening functions is related with the minimum impact parameter ρ_m, the difference of energy $\Delta E_{jj'}$ and the electron velocity v by:

$$z_{jj'}^m = \frac{\Delta E_{jj'} \rho_m}{\hbar v}. \tag{37}$$

Using the approximate velocity average, w_{strong} can be written as [17]:

$$w_{strong} = N_e \overline{v} \pi \rho_m^2 \tag{38}$$

where ρ_m is the minimum impact parameter (Weisskopf radius)

$$\rho_m = \left(\frac{2}{3}\right)^{1/2} \left(\frac{\hbar}{m\overline{v}}\right) \left| \sum_{j' \neq j} R_{jj'}^2 \left[A(z_{jj'}^m) + iB(z_{jj'}^m)\right] \right|^{1/2}. \tag{39}$$

The properties of Stark broadening functions $a(z_{jj'}^m)$, $A_(z_{jj'}^m)$ and $B(z_{jj'}^m)$ permits to simplify w_{strong} and w_{weak} at high and low temperatures. For high temperatures $A_(z_{jj'}^m) \approx 1$, $B(z_{jj'}^m) \approx 0$ and $a(z_{jj'}^m) \approx \ln\left(\frac{1}{z_{jj'}^m}\right)$ so (39) becomes:

$$\rho_m^2 \approx \left(\frac{2}{3}\right) \left(\frac{\hbar}{m\overline{v}}\right)^2 \sum_{j' \neq j} R_{jj'}^2 \tag{40}$$

then

$$\rho_m \approx \left[\left(\frac{2}{3}\right) \left(\frac{\hbar}{m}\right)^2 \left(\frac{m}{3k}\right) \sum_{j' \neq j} R_{jj'}^2 \right]^{1/2} T^{-1/2} \approx G_{jj'}^0 T^{-1/2} \tag{41}$$

and the width will be:

$$w_{strong}(T \gg T_0^{jj'}) \approx G_{jj'} T^{-1/2}, \tag{42}$$

where

$$G_{jj'} = \left(\frac{2}{3}\right) N_e \pi \left(\frac{\hbar}{m}\right)^2 \left(\frac{m}{3k}\right)^{1/2} \sum_{j' \neq j} R_{jj'}^2 \tag{43}$$

and

$$w_{weak}(T \gg T_0^{jj'}) \approx 2 G_{jj'} \frac{\ln(T)}{T^{1/2}}. \tag{44}$$

For low temperatures $A_(z_{jj'}^m) \approx 0$, $B(z_{jj'}^m) \approx \frac{\pi}{4z_{jj'}^m}$ and $a(z_{jj'}^m) \approx \frac{\pi}{2} e^{-2z_{jj'}^m}$ so (39) becomes:

$$\rho_m^2 \approx \left(\frac{1}{6}\right) \left(\frac{\hbar}{m\overline{v}}\right)^2 \sum_{j' \neq j} R_{jj'}^2 \frac{\pi \hbar \overline{v}}{\Delta E_{jj'} \rho_m} \tag{45}$$

then

$$\rho_m \approx \left[\left(\frac{\pi\hbar}{6\Delta E_{jj'}}\right) \left(\frac{\hbar}{m}\right)^2 \left(\frac{m}{3k}\right)^{1/2} \sum_{j' \neq j} R_{jj'}^2 \right]^{1/3} T^{-1/6} \approx I_{jj'}^0 T^{-1/6} \tag{46}$$

and the width will be:

$$w_{strong}(T \ll T_0^{jj'}) \approx I_{jj'} T^{1/6}, \tag{47}$$

where

$$I_{jj'} = N_e \pi \left(\frac{3k}{m}\right)^{1/6} \left[\frac{\pi\hbar}{6\Delta E_{jj'}} \left(\frac{\hbar}{m}\right)^2 \sum_{j' \neq j} R^2_{jj'}\right]^{2/3} \quad (48)$$

and

$$w_{weak}(T \ll T_0^{jj'}) \approx \pi G_{jj'} \frac{e^{-\alpha_{jj'} T^{-2/3}}}{T^{1/2}}, \quad (49)$$

where

$$\alpha_{jj'} \approx \left(\frac{2}{\hbar}\right) \left(\frac{m}{3k}\right)^{1/2} I^0_{jj'} \Delta E_{jj'}. \quad (50)$$

Therefore one can conclude that weak collisions are dominant for high temperatures and strong collisions for low temperatures:

$$\begin{aligned} w(T \ll T_0^{jj'}) &= w_{strong} + w_{weak} \\ &\approx I_{jj'} T^{1/6} + \pi G_{jj'} \frac{e^{\alpha_{jj'} T^{-2/3}}}{T^{1/2}} \\ &\approx I_{jj'} T^{1/6} \end{aligned} \quad (51)$$

and

$$\begin{aligned} w(T \gg T_0^{jj'}) &= w_{strong} + w_{weak} \\ &\approx G_{jj'} T^{-1/2} + 2G_{jj'} \frac{\ln(T)}{T^{1/2}} \\ &\approx 2G_{jj'} \frac{\ln(T)}{T^{1/2}}. \end{aligned} \quad (52)$$

We can see that the dependence of Stark width on temperature for $w(T \ll T_0^{jj'})$ (51) and $w(T \gg T_0^{jj'})$ (52) for $w_{strong} + w_{weak}$ is the same as derived previously (Eqs. (13) and (19)) respectively, as expected.

3 Results and discussion

We will choose the simplest non hydrogenic element HeI to analyze and discuss the temperature dependence of Stark widths, and will try to show when the neutral atom line Stark width increases with temperature (e.g. $2s^1\mathrm{S}-2p^1\mathrm{P}^\circ$ in the Griem's Tab. IV – in the appendix p. 322 of [17]) and when decreases (e.g. $2s^1\mathrm{S}-3p^1\mathrm{P}^\circ$ in the same reference).

In Tables 1 and 2, we present results for the partial widths $w_1(T)$, $w_2(T)$, $w_3(T)$ and the HWHM (w_{DK}) calculations according to the formula in [8] for the two lines cited previously, using the 3-level model. For the transition 20 581.3 Å ($2s^1\mathrm{S}-2p^1\mathrm{P}^\circ$), we use $3d^1\mathrm{D}$ as a perturbing level for the $2p^1\mathrm{P}^\circ$ atomic energy level as well as for the $3p^1\mathrm{P}^\circ$ level in the transition 5015.7 Å ($2s^1\mathrm{S}-3p^1\mathrm{P}^\circ$).

When we compare the maximal value of the function $w_i(T)$ for these two transitions having the same final level $2s^1\mathrm{S}$, we found that this function, which is the sum of the $w_{i1}(T)$, $w_{i2}(T)$ and $w_{i3}(T)$ ((29), (30) and (31)), has a maximal value corresponding to the critical temperature which for the first line (20 581.3 Å) is $T_0^{jj'} = 98\,267.25$ K (corresponding to $R_{jj'}\Delta E_{jj'} = 59\,120.24$). Consequently the width is increasing until $T_0^{jj'}$ and all values in the Griem's Table IV [17] are increasing.

Table 1. Calculations of w_1, w_2, w_3 and $w_{DK} = w_1 + w_2 + w_3$ (HWHM calculated according to Dimitrijević and Konjević formula [8]) for the 3-level model of HeI 20 581.3 Å ($2s^1\mathrm{S}-2p^1\mathrm{P}^\circ$) line as a function of temperature T. Electron density $N_e = 10^{22}$ m^{-3}. Note that the 3-level model for this line is adequate only to analyze the temperature dependence. Multilevel-model calculations using Dimitrijević and Konjević formula [8] give w'_{DK} – 0.408, 0.458, 0.514, 0.550 and 0.577 Å for T = 5000, 10 000, 20 000, 30 000 and 40 000 K respectively.

T [K]	$w_1(T)$ $\times 10^{-2}$[Å]	$w_2(T)$ $\times 10^{-2}$[Å]	$w_3(T)$ $\times 10^{-2}$[Å]	w_{DK} $\times 10^{-2}$[Å]
5000	0.008	6.291	1.237	7.500
10 000	0.399	6.934	2.706	10.000
20 000	3.015	7.362	2.720	13.100
30 000	5.904	7.319	1.817	15.000
40 000	8.204	7.052	1.249	16.500
80 000	12.900	5.402	0.459	18.800
100 000	14.000	4.637	0.3293	18.900
120 000	14.600	3.992	0.2508	18.800
150 000	15.100	3.228	0.1796	18.500
200 000	15.400	2.355	0.1167	17.800
400 000	14.700	0.966	0.0413	15.700
800 000	13.000	0.359	0.0146	13.400

For the second line (5015.7 Å), the critical value of temperature is $T_0^{jj'} = 1523.65$ K (corresponding to $R_{jj'}\Delta E_{jj'} = 916.68$) so that the width is decreasing because the plasma temperatures used in Griem's Table IV [17] (5000−40 000 K) are higher than $T_0^{jj'}$.

For the first line we also calculated widths for higher temperatures and one can see that the widths decrease after $T_0^{jj'}$ (see Tab. 1). We can predict the increasing or decreasing with temperature because for the first line $R_{jj'}\Delta E_{jj'}$ is much higher than for the second one. We remark also, in these two previous cases, that the partial width w_1 is less than w_2 when the temperature is less than $T_0^{jj'}$ and the partial width w_1 is higher than w_2 for temperature higher than $T_0^{jj'}$.

In the case of the multi-level model (22), the temperature dependence is more complicated since we have a sum of contributions for a number of perturbing levels with various $T_0^{jj'}$. However, on the basis of previous analysis, some general predictions of increasing or decreasing of Stark widths with temperature may be done and in the case of one or two dominant perturbing levels, temperature scaling by using (26), (27) is possible. As an example, in Table 2, we present Stark HWHM (w_G, w_{DSB}, w'_{DK}) for the HeI 5015.7 Å ($2s^1\mathrm{S}-3p^1\mathrm{P}^\circ$) line calculated using the multi-level model. Our results are compared with the semiclassical values of Griem [17] and Dimitrijević and Sahal-Bréchot [18]. For all results, the width is decreasing versus the temperature because we are in the high temperature conditions. One can see that the temperature

Table 2. Electron-impact HWHM of HeI 5015.7 Å ($2s^1\mathrm{S}-3p^1\mathrm{P}^\circ$) line as a function of temperature T: w_G – semiclassical results of Griem [17] w_{DSB} – semiclassical results of Dimitrijević and Sahal-Bréchot [18], w'_{DK} – our calculations according to Dimitrijević and Konjević formula [8] for the multi-level model. w_1, w_2, w_3 and $w_{DK} = w_1 + w_2 + w_3$ – our calculations according to Dimitrijević and Konjević formula [8] for the 3-level model for an electron density of $N_e = 10^{22}$ m^{-3}.

T [K]	w_G $\times 10^{-2}$[Å]	w_{DSB} $\times 10^{-2}$[Å]	w'_{DK} $\times 10^{-2}$[Å]	$w_1(T)$ $\times 10^{-2}$[Å]	$w_2(T)$ $\times 10^{-2}$[Å]	$w_3(T)$ $\times 10^{-2}$[Å]	w_{DK} $\times 10^{-2}$[Å]
5000	37.8	31.7	46.6	30.9	2.646	0.117	33.6
10 000	35.9	30.0	44.9	27.9	1.000	0.041	28.9
20 000	33.4	28.6	41.9	23.8	0.364	0.015	24.2
30 000	–	27.6	39.4	21.3	0.199	0.008	21.5
40 000	30.6	26.8	37.4	19.6	0.130	0.005	19.7
80 000	–	24.7	32.0	15.8	0.046	0.002	15.8

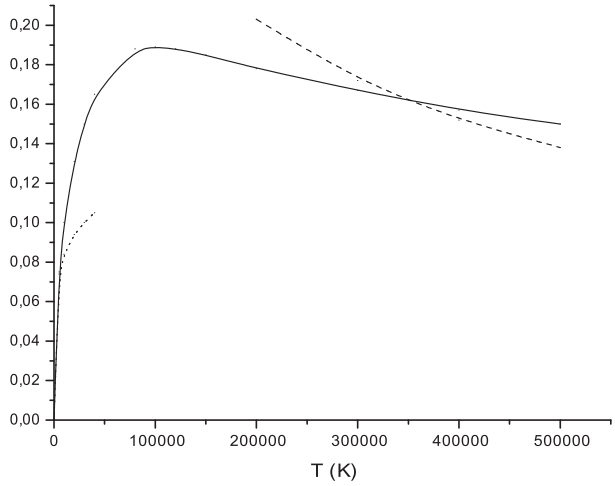

Fig. 2. A plot of the Stark width for the $2s^1\mathrm{S}-2p^1\mathrm{P}^\circ$ transition of helium spectral lines (20 581.3 Å) as a function of temperature T and its asymptotic limits: dot line – as calculated from (51) for low temperatures, and dashed line – as calculated from (52) for high temperatures.

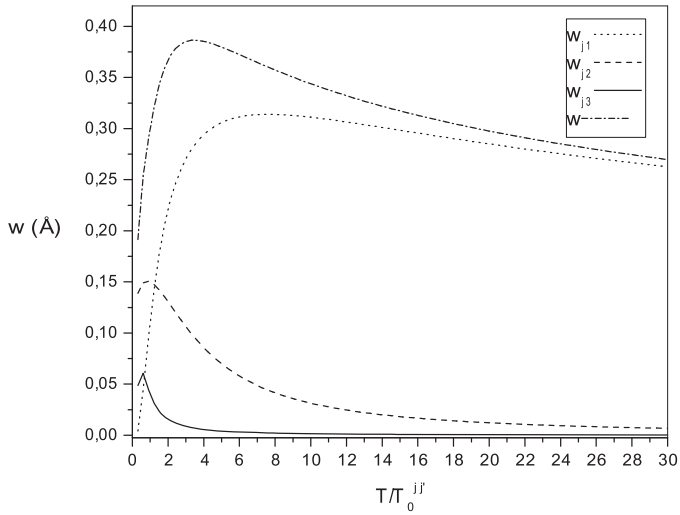

Fig. 3. A plot of the functions w_{j1}, w_{j2}, w_{j3} and w versus the reduced temperature $T/T_0^{jj'}$ calculated for the 3-level model of HeI 5015.7 Å line, for the temperature range $[0-50\times10^3$ K]. The critical temperature $T_0^{jj'}$ is 1523.65 K.

dependence is similar in our approximate and more sophisticated semiclassical calculations. Consequently, the simple approach used here, might be used to predict the temperature trend when more sophisticated results are missing or to extrapolate with temperature, for example, experimental values.

We notice as well that in general for neutral emitters, the width increases until a certain temperature and then decreases (see Figs. 2 and 3).

We show in Figure 4 that the Stark line width w dependence on $\ln(T)/T^{1/2}$ may be well approximated by a straight line for $T \gg T_0^{jj'}$. Consequently, we can say that, at high temperature limit, the Stark width dependence on temperature is $\ln(T)/T^{1/2}$ (see Fig. 4).

In Figure 5 for HeI 5015.7 Å, and Figure 6 for HeI 20 581.3 Å, the differences between the extrapolation of a Stark width value obtained at one temperature to another one with the proposed here temperature dependence (Eqs. (51) and (52)) and $T^{-1/2}$ are illustrated. Assume that you have an experimental value obtained say at 20 000 K and that you want to compare it with values

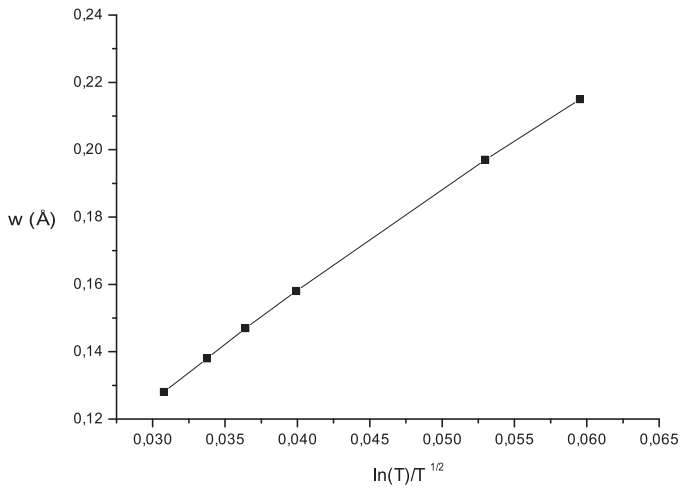

Fig. 4. Stark width (HWHM) w_{DK} versus $\ln(T)/T^{1/2}$ calculated for the 3-level model of HeI 5015.7 Å line, for the temperature range $[3\times10^4-15\times10^4$ K]. The critical temperature $T_0^{jj'}$ is 1523.65 K.

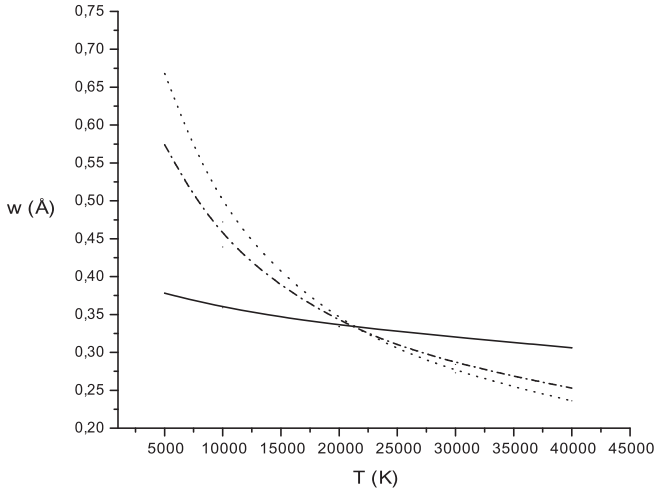

Fig. 5. Stark widths for the $2s^1\mathrm{S}-3p^1\mathrm{P}^\circ$ transition of helium spectral lines (5015.7 Å) as a function of temperature T for an electron density $N_e = 10^{22}$ m^{-3}. Solid line – results of Griem [17], dashed line – our calculations according to (19) and dot line – our calculations using the $T^{-1/2}$ dependence.

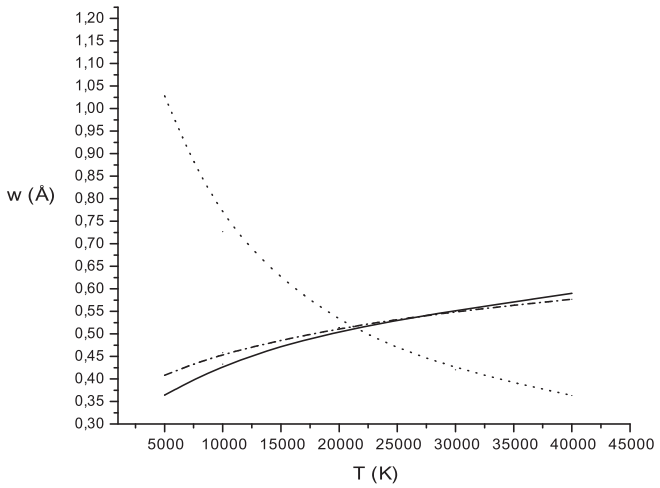

Fig. 6. Stark widths for the $2s^1\mathrm{S}-2p^1\mathrm{P}^\circ$ transition of helium spectral lines (20 581.3 Å) as a function of temperature T for an electron density $N_e = 10^{22}$ m^{-3}. Solid line – semi-classical results of Griem [17], dashed line – our calculations according to (13) and dot line – our calculations using the $T^{-1/2}$ dependence.

obtained for 5000 K and 40 000 K. In order to do so we took the corresponding w_G values at $T = 20\,000$ K and extrapolated them, using (Eqs. (52) and (51)) and $T^{-1/2}$ scaling, within the range 5000−40 000 K. We can see in Figures 5 and 6 the dimensions of the possible mistake which might be introduced by $T^{-1/2}$ scaling and the advantages of the method proposed here.

4 Conclusion

We have found a clear influence of the temperature effects on Stark line widths, and the simple 3-level model calculations performed here explain, in general, their temperature dependence. Using the simplified theories of Freudenstein and Cooper [7] and Dimitrijević and Konjević [8] for determination of Stark width of an isolated, non-hydrogenic, neutral atom spectral line, we have derived the explicit temperature dependence, and demonstrated that it is in general different from the often used scaling as $T^{-1/2}$.

The proposed temperature scaling with the three level model (27)–(31) may be useful for more realistic comparison of experimental values obtained at different temperatures, and extrapolations of a single value to other needed temperatures, e.g. for the synthesis of stellar spectra.

This work is a part of the project (146 001), supported by the Ministry of Science of Serbia. We are grateful to the referees for carefully reading the manuscript and their valuable comments and suggestions

References

1. N. Konjević, A. Lesage, J.R. Fuhr, W.L. Wiese, J. Phys. Chem. Ref. Data **31**, 3 (2002)
2. H.R. Griem, Spectral Line Shapes, edited by R.M. Herman, AIP Conf. Proc. **467**, 3 (1999), Vol. 10
3. N.E. Piskunov, F. Kupka, T.A. Ryabchikova, W.W. Weiss, C.S. Jeffery, Astron. Astrophys. Suppl. Ser. **112**, 525 (1995)
4. N. Konjević, Phys. Rep. **316**, 339 (1999)
5. L.Č. Popović, M.S. Dimitrijević, T. Ryabchikova, Astron. Astrophys. **350**, 719 (1999)
6. M. Šćepanović, J. Purić, J. Quant. Spectr. Rad. Trans. **78**, 197 (2003)
7. S.A. Freudenstein, J. Cooper, Astrophys. J. **224**, 1079 (1978)
8. M.S. Dimitrijević, N. Konjević, Astron. Astrophys. **163**, 297 (1986)
9. N. Ben Nessib, M.S. Dimitrijević, S. Sahal-Bréchot, Astron. Astrophys. **423**, 397 (2004)
10. H. Elabidi, N. Ben Nessib, S. Sahal-Bréchot, J. Phys. B: At. Mol. Opt. Phys. **37**, 63 (2004)
11. H. Elabidi, N. Ben Nessib, M.S. Dimitrijević, New Astron. **64**, 70 (2006)
12. W.F. Mahmoudi, N. Ben Nessib, S. Sahal-Bréchot, Physica Scripta **70**, 142 (2004)
13. W.F. Mahmoudi, N. Ben Nessib, M.S. Dimitrijević, Astron. Astrophys. **434**, 773 (2005)
14. W.F. Mahmoudi, N. Ben Nessib, S. Sahal-Bréchot, Physica Scripta **71**, 190 (2005)
15. H. Ben Chaouacha, N. Ben Nessib, S. Sahal-Bréchot, Astron. Astrophys. **419**, 771 (2004)
16. H. Eleuch, N. Ben Nessib, R. Bennaceur, Eur. Phys. J. D **29**, 391 (2004)
17. H.R. Griem, *Spectral Line Broadening by Plasmas* (Academic Press, New York, 1974)
18. M.S. Dimitrijević, S. Sahal-Bréchot, Astron. Astrophys. **82**, 519 (1990)
19. H.R. Griem, M. Baranger, A.C. Kolb, G.K. Oertel, Phys. Rev. **125**, 177 (1962)
20. M.S. Dimitrijević, S. Sahal-Bréchot, Astron. Astrophys. **136**, 289 (1984)

March 2009 Vol. 5 No. 1 ISSN 1841 - 0464

European Journal of Science and Theology

Editor-in-Chief: Iulian Rusu

Academic Organisation for Environmental Engineering and Sustainable Development

BOOK REVIEW

The Universe as communion
Towards a Neo-Patristic synthesis of Theology and Science

Alexei V. Nesteruk
T&T Clark, London and New York (2008), 286 pp, £ 75.00
ISBN (10): HB: 0-567-03327-9,
ISBN (13): HB: 978-0-567-03327-7

The new monograph, 'The Universe as Communion', is a valuable and interesting contribution of Alexei Nesteruk to the hotly debated topic of possibilities and ways of dialogue between Science and Religion.

Nesteruk is a lecturer in Mathematics, Philosophy of Science and Science and Theology at the University of Portsmouth, writer and researcher in Science and Theology and Philosophy of Science, who has published a number of articles on the subject of this monograph, and the book 'Light from the east; Theology, Science and the Eastern Orthodox Tradition' (Fortress Press, 2003), revealing how the Orthodox tradition deeply rooted in the thought of Greek Fathers, can lead to a different approach to the natural sciences from that of Western Church.

The present monograph is a continuation and extension of that one, where the discussion on relations and possibilities for dialogue between Theology and Science was based on comparison of modern scientific views with patristic legacy, without contemplation of internal life of human subjectivity and its relation to the revelation of the world and the sense of communion with God. Here, Nesteruk considers the dialogue between Theology and Science within the framework of the phenomenological analysis to understand further "the sense of the continuing embodiment of the human spirit in the world through faith, knowledge and technology". The author underlines that his objective is "to explore the ways of manifestation of being-in-the-world through studying the relationship between Theology and Science".

The monograph has introduction and five chapters, each divided in a number of subtopics, and include a large and informative bibliography and useful index, having in total 286 pages. Bibliography covers the subject and corresponding Patristic writers, allowing the reader to easily locate the original sources for further reading and research of the topic discussed, which is invaluable, especially for beginning researchers and students.

In the introduction is provided a discussion of the delimiters of the dialogue between Theology and Science. Nesteruk sees the problem of such dialogue, as a problem of disunity of the human spirit. He says that the contemporary Science – Religion dialogue is doubtfully meaningful outside of the "traditional and historical aspect of Theology" and "the philosophical tradition of the Science." If one places the Theology and Science at the same intellectual level, "the mystical and ecclesial dimensions of Theology are being eliminated and both are under ascendancy of reason".

As the objective of this monograph, Alexei Nesteruk states the advancement of the dialogue between Science and Theology by using ideas of the early Church Fathers, who defended Christianity in an agnostic and atheistic environment like today. Author sees the way for this dialogue in a new synthesis of Patristic and modern Theology with modern Philosophy and scientific ideas, in the so called 'Neo-Patristic Synthesis', advocated by the known Russian Orthodox theologian George Florovski, with the idea that Greek patristic legacy is important "for the catholicity of faith and existential implication not only in the Orthodox context, but also in Western Christianity".

In Chapter 1 'A Neo-Patristic Ethos in the Dialogue between Theology and Science', subdivided in nine subtopics, starting with the citation of Dumitru Staniloae that "... the most important problem of the Orthodox Theology of tomorrow, will be to reconcile the cosmic vision of the Fathers with a vision which grows out of the results of the natural sciences...", Nesteruk discussed Florovsky's appeal to a neo-Patristic synthesis in Theology, claiming that the 'patristic era', when fundamental Christian doctrines were fixed by the Fathers of the Church, never ended in a sense, that many later writers may also be considered as 'Fathers'. Moreover, since we live in the same historical reality of agnostic environment in which the Fathers lived, in this sense "our age can still be considered as the age of the Fathers".

Author considers further a neo-Patristic synthesis, the modern Orthodox Theology and the reintegration of the human spirit, as well as disintegration between East and West as seen through a different attitude to Science. Nesteruk emphasizes that sciences and secular philosophy were used for the exploration of environment implying that they do not transgress the boundaries of the present world. In the western civilization, they predict things beyond this world and age. like Theology, so that they were lifted up to the same level.

But if reason attempts to go beyond "the sphere of its legitimate domain in the world" it must be changed. This "transformation or transfiguration of reason or change of mind", under the pressure of new realities which it attempts to conceive, is called *metanoia* and, the lack of it in scholastic thinking is an obstacle for successful dialogue. Author considers the significance of metanoia in the collision of Faith and Knowledge and the relevance of a Patristic insight, particularly analyzing the need for 'change of mind' in scientific research and changes in the human life and views introduced by technology.

Namely, technology extends the boundary of human's contact with the world, providing new capacities for knowledge and truth. Extending the human subjectivity beyond the limits that existed earlier, technology has anthropological and cosmic dimension. As a way, suggested by a neo-patristic synthesis, for the relation between the scientific progress and technology of the West, and Theology, Nesteruk proposes "to transfigure the vision of Science into prophetic and para-Eucharistic activity in order to reveal in Science the presence of the gift of God to humanity to explore the world and thus praise God for his good creation," stating that "knowledge of earthly things, which is attained in Science, needs to be sanctified through faith, repentance and love".

Starting from the words of Max Planck, who compares scientific research and religious experience with two parallel lines which have a common point of intersection in infinity, the eschatological unity of Science and Religion is discussed in detail, speculating that Science and its applications in Technology, making life easier "stops in humans the access to transcending as a leap towards experience of eschatological presence".

Nesteruk analyzes the inadequacy of the dialogue between Science and Theology from the scientific point of view "within the natural attitude" without metanoia, since if Theology is transformed into a set of views and formal teachings, it loses "its existential meaning and its transcendent and mystical origin in communion with God". On the other hand, the objective of neo-patristic synthesis of Theology and Science is not to treat some contemporary scientific views using the legacy of the Greek Fathers, but to bring Science in the heart of Theology - "the voice of the Church".

In Chapter 2, subdivided into six subtopics, are discussed the lines of convergence between neo-Patristic synthesis and existential Phenomenology, in particular the Hellenistic roots and tradition, views of Husserl and Heidegger and a neo-Patristic synthesis as the 'anticipation' of the past. In the era of Fathers, Theology and Christianity were in a constant dialogue with contemporary philosophy and according to Nesteruk, we should learn from them to prepare and conduct such a dialogue now. Patristic Theology "is a synthesis of Gospel message with Hellenistic culture" of dogma, liturgy and icons, "which all points to the age to come", encoding the "*telos* of created humanity".

In Chapter 3, subdivided into introduction and nine subtopics, are considered Theology and Phenomenological attitude, the human condition, existential faith and transcendence, especially Theology as experience of God and Faith, and its relations with Anthropology.

Nesteruk discuss various explanations of the term *Theology*, introduced into Christianity by Clement of Alexandria, as the organized exposition of Christian doctrine, demonstrated faith, prayer, communion with God and the "last and the highest 'stage' of spiritual development in man, that is, the accomplishing mode of a Christian's experience of deification".

Considering the relation between Theology and Science in the epoch of Fathers, he emphasizes that they made a clear distinction between empirical, natural knowledge or knowledge of things, which is relative, and spiritual, intellectual knowledge, which "transcends the natural realm and aims to apprehend intelligible realities and the realm of the Divine ('supernatural knowledge')".

In order to show the distinction between the modes of subjectivity in Theology and Science, Nesteruk concludes that while the Science deal with the objects of surrounding world, Theology is turned to the primary fact of "human existence and to its internal conscious life".

In Chapter 4, subdivided in introduction and eleven subtopics, the human-centred dialogue between Theology and Science, as opposed to the nature-centred is considered, in particular the paradox of human subjectivity and its relations to the Theology, existence, scientific objectivity, incarnation. Also relations between Nature and Mathematics, and the mathematization of Nature are discussed, tracing a way from the mathematization of Nature to the world of Persons as a condition for the meeting of Science and Theology.

Nesteruk explains that in Scientific, natural attitude, the criterion of objectivity is based on the principle of quantity. Whatever can be "quantified and mathematised according to certain rules is objective by definition". The world possesses a rationality that can be fully understood. A paradox implicitly present in this view is that the world is describing by human beings. Since the man feels nature through his senses and thinks about it with his intelligence, a natural consequence is its mathematization. Author underlines that with extreme scientific mathematization of nature "no reasonable and justified dialogue between Science and Theology is possible". Consequently, Nesteruk demands to "enquire the roots of mathematization with the purpose to 'deconstruct' it and restore the lost image of humanity".

The Chapter 5, 'The Universe as Communion: Apophatic Cosmology, Personhood and Transcendence', is subdivided in introduction, ten subtopics and conclusion, In this Chapter, the link of Science and Theology by ascension from Cosmology to God via human persons is considered. According to Nesteruk, the Universe as a medium of person's facticity, reveals itself as a mode of communion with God. He argues that transcendence in Cosmology "is only possible through articulating the conditions of communion with the Universe, which inevitably leads to human persons as existential events of disclosure and then to communion with God as the pillar and ground of facticity of all".

Nesteruk considers in detail the paradox of human subjectivity from the notion of presence in absence of personhood, with particular relation to Science, and to the personhood as Communion. He underlines that Physics deals with particles, fields, space-time, planets and galaxies, but there is no place for human subjectivity. When a scientific fact or theory enters in the Science, it is unnecessary to enter in communion with the person of scientist.

As an example Nesteruk gives the Theory of Relativity. While reading the corresponding texts, one can contemplate the presence of Einstein in his spatial

and temporal absence, but for the Physics in general, the presence of its personhood is not necessary, when the relativistic view of the world once entered in Science. Author makes the conclusion that Science is not able to account for personhood, showing that its functioning is only possible "in the conditions of presence in absence of personhood."

Discussing the identity of the Universe, Nesteruk note that it can only be contemplated through communion and participation as a "direct experience of belonging *to* and unity *with"* it. He underlines that the Universe can not be an object since it can not be removed from human experience because this imply the removal of consciousness. So the conscious life imply the communion with the Universe. This is drastically different from the scientific Cosmology considering the Universe as a "structured and complex system dominated with its domains of non-human", since "only those areas from which life is stripped off can be described by Physics with a great efficiency".

Any description of the Universe in terms of its gradual changes is irrelevant, according to Nesteruk, in the sense that the entirety of the Universe is co-present to human subjectivity and 'transcendent' to all object-like visions of its parts and phases of development. He parallels such communion with the Universe, as co-inherence and simultaneity with the totality of one's life, with the communion with a person, which is present in absence. Nesteruk emphasizes, that with such attitude, the question of the origin of the Universe does not arise since it is not an object but communion.

Finally, Alexei Nesteruk discusses some similarities between Cosmology and Religion, namely their apophatic character. In Theology, apophaticism is the consistency of religious beliefs in their limitations, dogmas – boundaries of faith that can not be demonstrated from outside. So the apophaticism is freedom of expression of faith within the dogmatic system, representing its boundaries. Similarly, one can not test the initial conditions of the Universe from the outside, and cosmological theories, like in Theology, rely on the coherence of its own statements and assumptions. Consequently, different theories can explain the Universe independently of their correspondence with the truth, giving to Cosmology an apophatic meaning like in Theology.

The monograph of Alexei Nesteruk 'The Universe as Communion' is an important and interesting contribution to discussion and consideration of essential question on relation between human being and the Universe and enlighten from several different aspects the differences and common points between Science and Theology, the complex question of the dialogue between them and interesting and valuable analysis of the possibilities for their new synthesis which existed in the era of Fathers of the Church.

Dr. Milan S. Dimitrijević

Research Professor
Belgrade Astronomical Observatory (Serbia)

Eur. Phys. J. Appl. Phys. **50**, 30701 (2010)
DOI: 10.1051/epjap/2010047

THE EUROPEAN PHYSICAL JOURNAL APPLIED PHYSICS

Regular Article

Spectroscopic estimation of electron temperature and density of zinc plasma open air induced by Nd:YAG laser

R. Qindeel[1,a], M.S. Dimitrijević[2], N.M. Shaikh[3], N. Bidin[1], and Y.M. Daud[1]

[1] Advanced Photonic Science Institute, Faculty of Science, University of Teknologi Malaysia, Skudai 81310 Johor, Malaysia
[2] Astronomical Observatory, Volgina 7, 11060 Belgrade-34, Serbia
[3] Institute of Physics, University of Sindh, Jamshoro 76080, Pakistan

Received: 2 October 2009 / Accepted: 8 March 2010
Published online: 23 April 2010 –

Abstract. The spectroscopic emission of zinc plasma along with CCD imaging profile has been studied. The zinc target has been irradiated with a Q-switched Nd:YAG laser (1064 nm, 290 mJ, 10 ns, 29 MW) in air at atmospheric pressure. The plasma emission is recorded with 100 ns integration time. Boltzmann plot method and Stark broadening profile of the transition line has been used to estimate the electron temperature (T_e) and electron density (N_e) respectively. Estimated values of T_e and N_e is in the range of (5700–6756) K and $(1.6 \times 10^{15} - 3.39 \times 10^{15})$ cm^{-3} at three laser shots respectively.

1 Introduction

The laser plasma studies for material processing are increasing now a day. In the laser produced plasmas the electron temperature (T_e) and the electron density (N_e) are very essential to predict plasma chemistry. Laser-induced breakdown spectroscopy (LIBS) is a useful technique for a variety of applications like environmental monitoring, material analysis and thin film deposition [1]. In this technique a high intensity laser pulse interacts with a target leading to the formation of micro-plasma. During the nanosecond (ns) laser pulse interaction with a solid surface, the material evaporation taken place with in the few tens of the picoseconds the rest of the laser pulse is absorbed in the plasma by the inverse bremsstrahlung (IB) absorption [2]. This technique can be easily combined with other optical techniques such as Raman spectroscopy to extract elemental, mineralogical, and biological information. The analytical performance of the LIBS depend on several laser parameters such as pulse duration, pulse irradiance, laser wavelength and fluence), sample characteristics (thermal conductivity, surface reflectivity, thermal diffusivity, optical absorption coefficient, etc.), and the ambient conditions [3–5].

There are many experimental studies reported in the literature about the effects of laser parameters on the evaporation process, plume and plasma characteristics of the zinc plasma. The spatial and temporal behavior of Li, Zn and Li-Zn alloy plasma under vacuum using XeCl excimer laser at 308 nm has been studied by Gogić and Milošević [6]. They observed the atomic and ionic lines of Zn, Li and Li-Zn alloy. The ablation of Li-Zn alloy showed faster decay of the Zn spectral features than of the Li spectral lines. Al impurity in zinc alloy in the environment of air, vacuum and Ar, using an Nd:YAG laser at 105 mJ pulse energy with 3 ns pulse width was analyzed by Kim et al. [7]. In order to investigate, analyze and model various plasmas, different diagnostic techniques are used to find their characteristics. The key parameters of laser ablated plumes are density and temperature. Konjević [8] has studied the plasma broadening and shifting effects of non hydrogenic neutral atom and positive ion spectral lines in detail. In this study the plasma-broadened and shifted spectral line profiles have also been studied which is non-interfering plasma diagnostic method.

In the present work, we have investigated the spectroscopic properties of the zinc plasma in air at atmospheric pressure produced by 1064 nm Nd:YAG laser. The optical emission has been spatially resolved by scanning the plume along its area. The electron temperature T_e and density N_e has been observed by the spectroscopic study of Zn plasma.

2 Experimental setup

A schematic diagram of the experimental setup is shown in Figure 1. The laser beam from a Q-switched Nd:YAG laser with pulse duration of 10 ns, 1064 nm wavelength, pulse energy 290 mJ and power density of 4×10^{10} W cm^{-2} was used to irradiate the Zn target. Laser spot diameter was 2 mm. He-Ne laser was coaxial with IR laser for an ease of alignment. The irradiated sample images were recorded via CCD camera for morphological and structural analysis. Each emission spectrum of the zinc plasma

[a] e-mail: qindeel.plasma@gmail.com

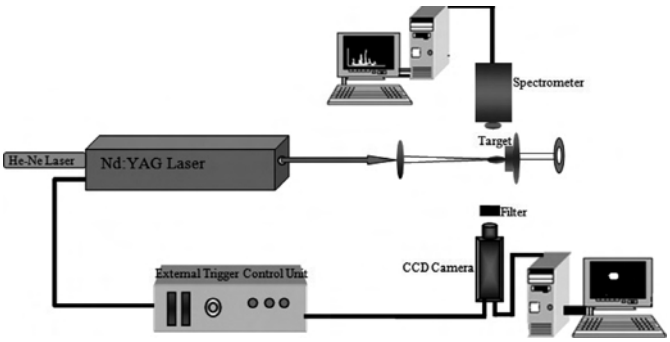

Fig. 1. Schematic diagram of experimental setup.

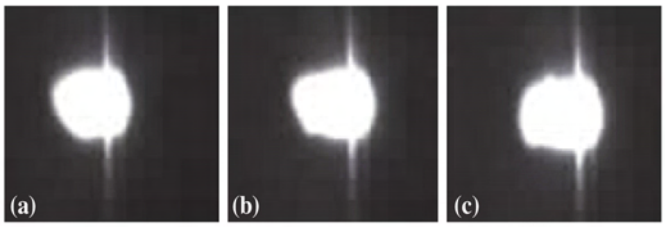

Fig. 2. CCD Image of Zn plasma formation recorded at integration time of 100 ns produced by the 1064 nm Nd:YAG laser. (a) First laser shot, (b) second laser shot, (c) third laser shot.

was recorded with 100 ns integration time. The laser beam was focused through a 20 cm quartz lens on the Zn target in air. The target was slowly rotated to avoid surface damage, minimize the local heating and to make the laser pulse fall on a fresh target surface. The emission from the plume was registered by spectrometer with the covering range between 350 nm and 650 nm. In order to record the emission spectrum from the plume, the spectrometer is interfaced with computer and Q-switched Nd:YAG laser was synchronized with external trigger unit to emit single shot pulse. Zinc target was placed at a fixed distance 20 cm and in-situ CCD imaging, and emission spectroscopy of laser ablated zinc target was also explored. The acquired emission data by Ophir WaveStar spectrometer (CCD laser spectrum analyzer) have been stored in a PC using WaveStar 1.05 software for subsequent analysis.

3 Results and discussion

3.1 CCD imaging

The in situ CCD image profile was recorded to study the surface chemistry and physical interaction of the laser with the target. Some results of CCD images are shown in Figure 2. The CCD image frame of every laser shot was recorded by the PULNIX TM–6EX CCD video camera with a Matrox Inspector image grabbing interfaced with a computer. The structure of the laser plume does not have the circular nature which can be clearly observed in Figure 2. The vertical line at the right hand side of the image frame represents the position of Zn target. The direction of laser is from left to the right of each frame and the bright image of the dark background shows the formation of plasma plume accompanied by a shock wave to increase the emission intensity. The plasma was expanding supersonically towards the laser beam. The emission enhancement mechanisms are due to change in the plasma properties and increased quantity of ablated mass. The engraved semi spherical shape pits of CCD images give information of depth profile.

3.2 Optical emission spectroscopy

In situ emission spectroscopic data were acquired by PC interfaced spectrometer WaveStar 1.05 software for subsequent analysis. Three sets of data were recorded in which three emission lines of Zn were only observed with a slight variation of wavelengths with the same instrument under the same conditions. Three emission spectra of zinc plasma are illustrated in Figures 3a– 3c. All emission spectra were recorded in the spectral range 360–630 nm. These lines belonging to neutral zinc have been observed in the spectral range 450–490 nm. The values of spectroscopic parameters of the emission lines of neutral zinc plasma data used in the Boltzmann plot are tabulated in Table 1. More over the schematic diagram of energy levels for emission lines of neutral zinc are shown in Figure 4. The Boltzmann plots of the three shots (mentioned above) have been sketched in Figures 5a– 5c in which the linear fit of the data is also shown.

3.3 Shifting of wavelength

In these open air laser shots the variation in intensity and wavelength was also observed. The assignment of these lines is straightforward as the levels belonging to the lower and upper state configurations are well known and tabulated in the NBS (NIST) database [9]. At the three different laser shots, besides the variation in the intensity of the zinc triplet we have also observed the shift in the peak value of the emission line. The estimated value of the shift in the transition lines toward the longer wavelength was about 0.01 nm. This shift in the transition lines may be due to the Stark effect due to the micro electric field, because the radiating atom at a distance r from an ion or electron is perturbed by the electric field. This interaction is described by the Stark effect. The linear Stark effect ($\sim E$) exists only for hydrogen, for all other atoms the interaction is quadratic ($\sim E^2$ and $\sim 1/r^4$). The shift is usually towards the red and is same for ions as for electrons (E^2 dependence) [10]. The other cause of this phenomenon may be absorption of laser heat during initial laser shot due to joule heating of the target surface. Since in the initial shot Figure 3a the intensity of emission was too low because a part of laser energy was used in heating the target but in the third shot Figure 3c the intensity was high because the target was preheated during the initial two shots. The comparison of wavelength shifting of the emission lines of neutral Zn plasma is shown in Table 2.

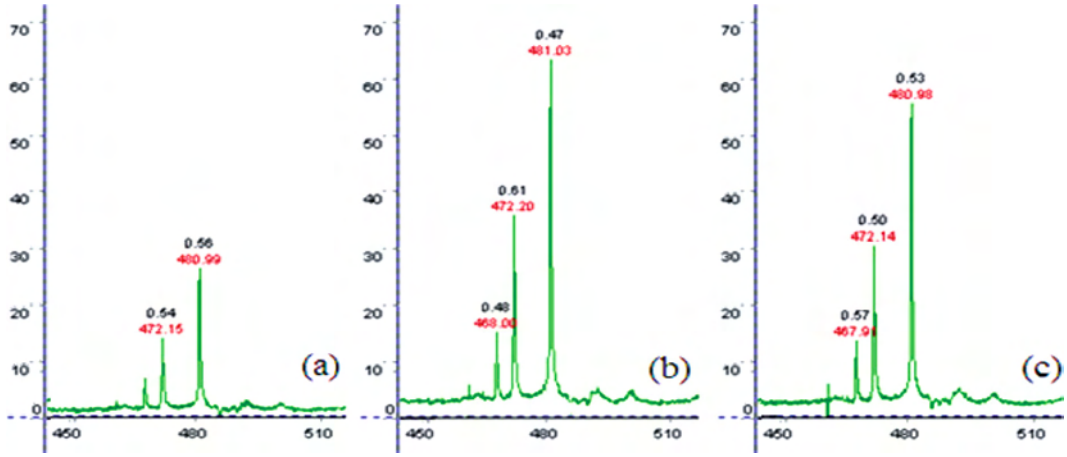

Fig. 3. (Color online) The emission spectra of Zn is at integration time of 100 ns, generated by 1064 nm laser. (a) First laser shot, (b) second laser shot, (c) third laser shot. On abscissa is wavelength in nm and in ordinate intensity in arbitrary units.

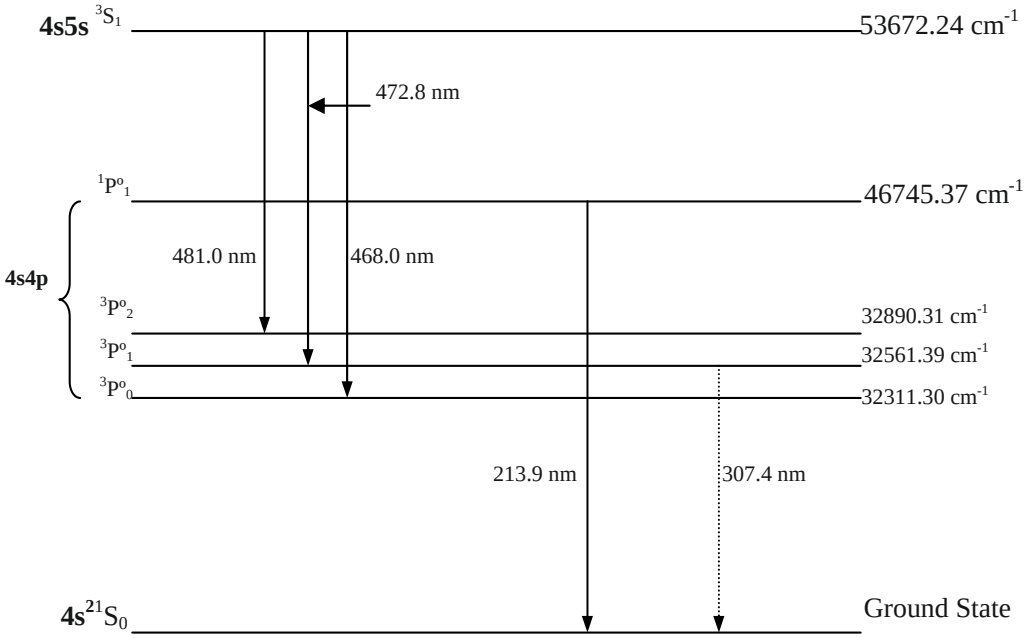

Fig. 4. Energy level diagram of neutral zinc showing all the prominent transitions observed in the present experiment.

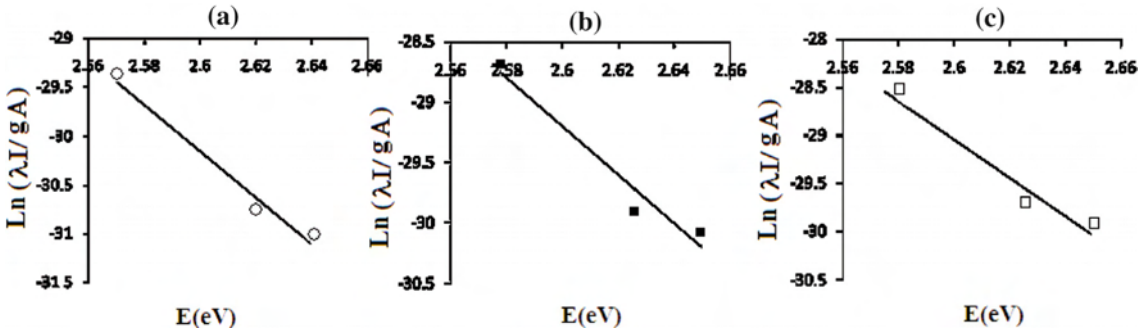

Fig. 5. Three Boltzmann plots of the transition lines registered at time integral of 100 ns, (a), (b) and (c) are sketched to determine electron temperature of Zn plasma. The slope of the plotted curves yields electron temperatures as 5700 K, 6756 K and 6677 K respectively. On abscissa is energy in eV.

Table 1. Spectroscopic parameters of the observed zinc lines in the plasma.

SET	Wavelength λ(nm)	Transition		Statistica weight		Transition probability $A_{ij}(s^{-1})$	Energy of the lower level observed	Energy of the upper level
A	λ(nm)			g_i	g_k	$A_{ij}(\mathrm{s}^{-1})$	$E_i(\mathrm{cm}^{-1})$	$E_k(\mathrm{cm}^{-1})$
	468.0	$4s5s^3\mathrm{S}_1$	$\rightarrow 4s4p^3\mathrm{P}^0$	1	3	1.55×10^7	21367.5	53672.24
	472.15	$4s5s^3\mathrm{S}_1$	$\rightarrow 4s4p^3\mathrm{P}^0_1$	3	3	4.58×10^7	21179.5	53672.24
	480. 99	$4s5s^3\mathrm{S}_1$	$\rightarrow 4s4p^3\mathrm{P}^0_2$	5	3	7.00×10^7	20790.5	53672.24
B								
	467.94	$4s5s^3\mathrm{S}_1$	$\rightarrow 4s4p^3\mathrm{P}^0$	1	3	1.55×10^7	21370.3	53672.24
	472.14	$4s5s^3\mathrm{S}_1$	$\rightarrow 4s4p^3\mathrm{P}^0_1$	3	3	4.58×10^7	21180.2	53672.24
	480.98	$4s5s^3\mathrm{S}_1$	$\rightarrow 4s4p^3\mathrm{P}^0_2$	5	3	7.00×10^7	20790.9	53672.24
C								
	468.06	$4s5s^3\mathrm{S}_1$	$\rightarrow 4s4p^3\mathrm{P}^0$	1	3	1.55×10^7	21364.8	53672.24
	472.2	$4s5s^3\mathrm{S}_1$	$\rightarrow 4s4p^3\mathrm{P}^0_1$	3	3	4.58×10^7	21177.5	53672.24
	481.03	$4s5s^3\mathrm{S}_1$	$\rightarrow 4s4p^3\mathrm{P}^0_2$	5	3	7.00×10^7	20788.7	53672.24

Table 2. (Color online) Wavelength shifting of the emission lines of neutral zinc plasma and electron densities measurement by Stark broadening equation (3) (* positive shift, ** negative shift).

SET	Wavelength λ(nm)	Intensity	FWHM $\lambda_{1/2}$(nm)	Shift observed λ(nm)	Electron density N_e
A	λ(nm)		$\lambda_{1/2}$(nm)	λ(nm)	(cm^{-3})
	468.0	5	0.52	0^*	3.09524×10^{15}
	472.15	14	0.54	0.05^*	1.71975×10^{15}
	480. 99	28	0.56	0.01^*	1.69697×10^{15}
B					
	467.94	13	0.57	0.06^*	3.39286×10^{15}
	472.14	30	0.50	0.06^*	1.59236×10^{15}
	480.98	56	0.53	0.06^*	1.60606×10^{15}
C					
	468.06	15	0.48	0.06^{**}	1.86047×10^{15}
	472.2	37	0.61	0^{**}	2.54167×10^{15}
	481.03	64	0.47	0.03^{**}	2.55435×10^{15}

3.4 Plasma characterization

3.4.1 Bremsstrahlung process and inverse bremsstrahlung absorption

In the nanosecond laser matter interactions the material evaporation taken place with in the few tens of picosecond the rest of the laser pulse is absorbed in the plasma via inverse bremsstrahlung (IB) absorption process, that is the dominant process for the longer wavelength [3,4]. The IB absorption α_{ib} via free electron is estimated from the expression

$$\alpha_{ib}(\mathrm{cm}^{-1}) = 1.37 \times 10^{-35} \lambda^3 N_e^2 {T_e}^{-1/2}.$$

In this expression, λ is the wavelength of the laser photon in μm, N_e (cm^{-3}) is the electron density and T_e (eV) is the electron temperature. In case of fundamental 1064 nm laser used in this experiment, IB absorption is approximately equal to 1.96×10^{-5} cm^{-1} at the laser irradiance of 5.6×10^{10} W cm^2.

On the other hand, is plasma optically thin, has been verified using the criteria mentioned in [11] by checking are the intensity ratios of the zinc triplets consistent with the ratios of the statistical weights of their upper level (1:3:5). One can see from Table 1 that these differences for the ratio of the strongest and the weakest line in the multiplet are 12% for the set A, 14% for the set B and 15% for the set C, indicating that it is a reasonable approximation to consider the plasma as optically thin. We should note

that if the observed intensity of the strongest line in the multiplet is reduced relative to the weakest one, indicates that self absorption, resulting in broader line, is present.

This result indicates that the plasma was optically thin according to a procedure described previously by Simeonsson and Miziolek [12]. For optically thin plasma, the reabsorption effects of plasma emission are negligible, so the emitted spectral line intensity I is a measure of the population of the corresponding energy level of this element in the plasma. In our laser plasma experiments, the decrease in temperature may be due to expansion in velocities and the surface of the target constantly absorbs radiation during the time interval of laser pulse. In the image profile of Figure 2, these behaviors somehow support this trend.

3.4.2 Electron temperature measurement

Laser-induced plasma the state of local thermodynamic equilibrium exists then the analyzed intensity is proportional to the relative population of the levels and follows the Boltzmann distribution. Using the ratio of the relevant intensities of spectral lines, electron temperature can be estimated. In this study also the Boltzmann plot method was applied to calculate electron temperature. In the case of an air plasma populations of the atomic states are given by the Boltzmann equation, so that line intensities I_{ij} are proportional to the Boltzmann factor described as [7]:

$$I_{ij} \propto g_j A_{ij} \exp\left(-\frac{E_j}{kT}\right), \quad (1)$$

where g_j is the statistical weight of the upper level, A_{ij} is the transition probability, E_j is the energy of the upper level, I_{ij} are used for two spectral lines of the same element under consideration, T is the temperature, and k is the Boltzmann constant. A logarithmic plot of $\lambda I/gA$ versus E results in straight lines which slope is inversely proportional to the temperature. The electron temperature is calculated from the slope $S = -1/kT_e$ and the values of the transition probabilities for emission line have been used from NIST [9]. The electron temperature and electron number density contains about 10% uncertainties due to the uncertainties in the width measurement, the instrumental width de-convolution integrated intensity of the transition line, transition probability and the electron impact parameter.

The estimated values of the T_e of these three shots were obtained 5700 K, 6756 K and 6677 K respectively.

3.4.3 Electron density measurement

In LIBS, two spectroscopic methods are commonly used to determine the N_e. The first method requires the measure of the population ratio of two successive ionization states of the same element and the second requires measure of the Stark broadening of the spectral lines. The emission spectral lines of the laser produced plasma are noticeably broadened therefore N_e can be extracted from the widths of the spectral lines. There are two important line broadening mechanisms in the laser plasma i.e. Stark broadening and Doppler broadening.

The Stark line broadening appears due to collisions of emitting atom with charged species and this is the primary mechanism influencing these emission spectra [13,14]. The electron density was determined from Stark broadening of emission lines.

3.4.4 Doppler broadening measurements

Doppler broadening based on the Maxwellian distribution law can be used to estimate the half width FWHM by a simple equation as [3,7]:

$$\Delta\lambda_{1/2} = 2\lambda\sqrt{2kT\ln 2/mc^2}, \quad (2)$$

where λ (m) is the wavelength, k (J K^{-1}) is the Boltzmann constant, T (K) is the absolute temperature, m (kg) is the atomic mass and c (m s^{-1}) is the speed of light. In the plasma the Stark broadening, induced by collisions with charged particles, is dominant in comparison with Doppler one. At a temperature of 5700 K, the Doppler width is estimated ≈0.0031 nm for the transition at 468 nm. This width is too small to be detected in the present studies, therefore it is neglected.

3.4.5 Stark-broadening measurements

Stark broadened spectral line widths depend on the electron density N_e. The electron number density N_e (cm^{-3}) could be determined from the full width at half maximum (FWHM) of the neutral zinc lines. If we have determined experimentally the Stark width (FWHM) $\Delta\lambda_{1/2}$, and we have calculated or found in literature the theoretical Stark width (ω), which is for neutral atoms usually tabulated for $N_e = 10^{16}$ cm^{-3}, we can obtain the electron density N_e from the relation [13–18]:

$$\Delta\lambda_{1/2} = 2\omega\left(\frac{N_e}{10^{16}}\right) + 3.5A\left(\frac{N_e}{10^{16}}\right)^{1/4}\left[1-\frac{3}{4}N_D^{-1/3}\right]\omega\left(\frac{N_e}{10^{16}}\right). \quad (3)$$

Here is assumed that the line is isolated and broadened by collisions with electrons and ions. Also one should take into account that in literature Stark widths are sometimes given as FWHM and sometimes as half half-widths or half widths at half-intensity maximum (HFHM). In equation (3) ω is HFHM and if the theoretical width is FWHM coefficients for the first and second term will be 1 and 1.75 instead of 2 and 3.5. The quantity A in equation (3) is ion-broadening parameter also assumed that it is given or calculated for $N_e = 10^{16}$ cm^{-3}, and the parameter N_D the number of particles in the Debye sphere. In equation (3) for electrons is used impact approximation and for ions

used quasistatic one due to their much larger mass. Comparing the electron and ion mass we can also conclude that the contribution of ion-broadening is much smaller in comparison with electron-broadening in considered plasma as $m_e \ll m_i$ so the $V_e \gg V_i$ where m_e, m_i, V_e and V_i denote the masses and velocities of both electron and ion respectively. The value of ion-broadening parameter is several percent and the reasonable approximation is to neglect it. So neglecting in equation (3) the second term describing ion-broadening contribution, one obtains for N_e the following expression:

$$N_e = \left(\frac{\Delta\lambda_{FWHM}}{2\omega}\right) \times 10^{16}, \quad (4)$$

where $\Delta\lambda_{FWHM}$(nm) is the half width (FWHM) observed in neutral zinc line, N_e (cm^{-3}) is the electron density and ω is the electron-impact half width (HWHM) (Stark width value from literature). Substituting the values of Stark broadening impact-width parameter ω from [19], in equation (4), the electron densities for zinc plasma are in the range 1.6×10^{15} cm^{-3} to 3.39×10^{15} cm^{-3} and it is tabulated in Table 2.

3.4.6 McWhirter criterion for the validity of LTE

For the plasma to be in LTE, atomic and ionic states should be populated and depopulated predominantly by collisions rather than by radiation. This requires that the electron density has to be high enough to ensure a high collision rate. The corresponding lower limit of electron density is given by the McWhirter's criterion [20]:

$$N_e \geq 1.6 \times 10^{12} \Delta E^3 T^{1/2}, \quad (5)$$

where N_e (cm^{-3}) is electron density, ΔE (eV) is the largest energy transition for which the condition holds and T (K) the plasma temperature. It is only at later times that the electron density values converge toward this lower limit. This means that, in principle, LTE conditions should prevail over the major part of plasma duration. However, one should note that the McWhirter's criterion is, according to the author himself, a necessary but not sufficient condition for LTE. By knowing the electron density and the plasma temperature one can determine whether the local thermodynamic equilibrium (LTE) assumption is valid using the criterion proposed by McWhirter [20]. The lower limit for electron density for which the plasma will be assumed in LTE is given in the inequality shown in equation (5).

In the present case, the variation of energy of transition ΔE is 2.56 eV for Zn and the value of lower limit of electron density as given by equation (5) is 2.0×10^{15} cm^{-3}. The electron densities obtained for the considered plasma are near this value or greater, which is consistent with the assumption that the LTE prevails in the plasma.

In the laser produced plasma, the plasma plume properties rapidly changes with space and time, so the detector position, detection delay time and integration time plays an important role in the study of plume dynamics. The variation in the plasma properties such as excitation temperature is attributed to the fact that the thermal energy is rapidly converted in to the kinetic energy, with the plasma attaining maximum expansion velocities and hereby causing temperature to drop as the plasma expands and decrease of N_e is mainly due to recombination between electrons and ions in the plasma. The most likely processes in laser produced plasma are the radiative recombination and the three-body recombination. In our case we have select the optimum integration time of 100 ns to record the well defined zinc plasma emission spectrum.

4 Conclusion

In summary, we have carried out optical characterization of laser induced zinc plasma. In situ emission spectroscopy and CCD imaging techniques have been successfully applied on three shots of zinc plasmas. The electron densities and electron temperatures have been estimated for pure zinc plasma in front of metal target.

The obtained results indicate that the estimated values of the plasma parameters (T_e, N_e) are consistent with the reported results and almost have the same values for the three shots with minor difference. In perspective of laser plasma diagnostics the physical properties of the target also play an important role and affect the values of the laser ablated plasma temperature T_e and electron density N_e. In situ CCD imaging performed here will be focused in later studies which might be helpful to understand the physical effects and surface topology of the target.

The authors would like to thank the Sciences, Research Alliance Enabling Science & Nanotechnology (ESciNano), administration of Universiti Teknologi Malaysia for encouragement and generous support. We are also grateful Prof. Dr. M. Aslam Baig for providing information about the subject.

References

1. D.M. Bubb, M.R. Papantonakis, B. Toftmann, J.S. Horwitz, R.A. McGill, D.B. Chrisey, R.F. Haglund Jr, J. Appl. Phys. **91**, 9809 (2002)
2. P. Stavropoulos, C. Palagas, G.N. Angelopoulos, D.N. Papamantellos, S. Couris, Spectrochim. Acta Part B **59**, 1885 (2004)
3. N.M. Shaikh, B. Rashid, S. Hafeez, Y. Jamil, M.A. Baig, J. Phys. D: Appl. Phys. **39**, 1384 (2006)
4. R.K. Singh, Narayan, Phys. Rev. B **41**, 8843 (1990)
5. N.M. Shaikh, S. Hafeez, M.A. Baig, Spectrochim. Acta Part B **62**, 1311 (2007)
6. S. Gogić, S. Milošević, Fizika A **7**, 37 (1998)
7. D.E. Kim, K.J. Yoo, H.K. Park, K.J. Oh, D.W. Kim, Appl. Spectrosc. **51**, 22 (1997)
8. N. Konjević, Phys. Rep. **316**, 339 (1999)

9. J.E. Sansonetti, W.C. Martin, J. Phys. Chem. Ref. Data **34**, 1559 (2005)
10. I.B. Gornushkin, L.A. King, B.W. Smith, N. Omenetto, J.D. Winefordner, Spectrochim. Acta Part B **54**, 1207 (1999)
11. Y. Walid Tawfik Mohamed, A. Askar, Prog. Phys. **1**, 46 (2007)
12. J.B. Simeonsson, A.W. Miziolek, Appl. Opt. **32**, 939 (1993)
13. H.R. Griem, *Principles of Plasma Spectroscopy* (Cambridge University Press, 1997)
14. C. Colon, A. Alonso-Medina, C. Herran-Martinez, J. Phys. B: At. Mol. Opt. Phys. **32**, 3887 (1999)
15. G. Befeki, *Principles of laser plasmas* (Wiley-Interscience, New York, 1976)
16. B. Le Drogoff, J. Margot, M. Chakaer, M. Sabsabi, O. Barthélemy, T.W. Johnston, S. Laville, F. Vidal, Y. von Kaenel, Spectrochim. Acta Part B: At. Spectrosc. **56**, 987 (2001)
17. J.A. Aguilera, C. Aragon, Appl. Phys. A (Suppl.) **69**, S475 (1999)
18. I.B. Gornushkin, L.A. King, B.W. Smith, N. Omenetto, J.D. Winefordner, Spectrochim. Acta Part B: At. Spectrosc. **54**, 1207 (1999)
19. M.S. Dimitrijević, S. Sahal-Bréchot, A&AS **140**, 193 (1999)
20. R.W.P. McWhirter, *Plasma Diagnostic Techniques*, edited by R.H. Huddlestone, S.L. Leonard (Academic Press, New York, 1965), Chap. 5

Eur. Phys. J. D **27**, 209–213 (2003)
DOI: 10.1140/epjd/e2003-00278-2

THE EUROPEAN PHYSICAL JOURNAL D

Transition probabilities in Kr II and Kr III spectra

S. Djeniže[1,2,a], V. Milosavljević[1,b], and M.S. Dimitrijević[3,c]

[1] Faculty of Physics, University of Belgrade, P.O.B. 368, Belgrade, Serbia
[2] Hungarian Academy of Sciences, Budapest, Hungary
[3] Astronomical Observatory, 11160 Belgrade, Volgina 7, Serbia

Received 22 February 2003 / Received in final form 16 June 2003
Published online 16 September 2003 –

Abstract. On the basis of the relative line intensity ratio (RLIR) method, transition probability values of the spontaneous emission (Einstein's A values) of 14 transitions in the singly (Kr II) and 7 transitions in doubly (Kr III) ionized krypton spectra have been obtained relatively to the reference A values related to the 435.548 nm Kr II and 324.569 nm Kr III, the most intensive transitions in the Kr II and Kr III spectra. Our Kr III transition probability values are the first data obtained experimentally using the RLIR method. A linear, low–pressure, pulsed arc operated in krypton discharge was used as an optically thin plasma source at a 17 000 K electron temperature and 1.65×10^{23} m^{-3} electron density. Our experimental relative A values are compared with previous experimental and theoretical data.

PACS. 52.70.Kz Optical (ultraviolet, visible, infrared) measurements – 32.70.Cs Oscillator strengths, lifetimes, transition moments – 32.70.Fw Absolute and relative intensities

1 Introduction

Due to the development of space born astronomical techniques and devices such as Goddard high resolution spectrograph on the Hubble space telescope, the spectral lines of trace elements, such as krypton, are observed and the corresponding atomic data are of the increasing interest. On the basis of the recent investigation of Planetary Nebulae spectra [1] it was found that krypton is one of the most abundant elements in the cosmos with $Z > 32$. Krypton has been detected also in the spectra of the interstellar medium [2]. Moreover, krypton is present in many light sources and lasers as the working gas. Thus, the singly (Kr II) and doubly ionized (Kr III) krypton spectral lines are very useful for plasma diagnostical purposes. For the modeling or diagnostics of cosmic and laboratory plasmas it is necessary to know the transition probability values (Einstein's A values) [3]. A significant number of papers are dedicated to this topic [4] (and references therein), especially in the case of the Kr II A values. However, the existing experimental and theoretical Kr II A values show evident mutual scatter. In the case of the Kr III A values the situation is similar, but with a considerably smaller number of experimental and theoretical studies dedicated to the investigation of Kr III A values.

This work presents 14 Kr II and 7 Kr III A values obtained on the basis of accurately measured spectral line intensities using the step-by-step technique by the line profile recording [5] and our deconvolution procedure [6] which allows accurate measurements of the line intensities. The well-known [7–9] relative line intensity ratio (RLIR) method was used for the A values determination applied by us already in case of the Ar III, Ar IV, O II, Ne II, N III, N IV, N V and Si III spectra [10–15].

The experimental $A^{\rm exp}$ values are obtained relatively to reference A values for the 435.548 nm Kr II and 324.569 nm Kr III lines, the most intense among the investigated lines in the Kr II and Kr III spectra. Our Kr III transition probability values are the first data obtained experimentally using the RLIR method. Our experimental A values have been compared with the transition probabilities from the references which contain A data corresponding to our chosen reference Kr II and Kr III transitions only.

2 Experiment

A modified version of the linear low pressure pulsed arc [5,10,12–17] has been used as an optically thin plasma source. A pulsed discharge was driven in a Pyrex discharge tube of 5 mm inner diameter and plasma length of 7.2 cm. A capacitor of 14 μF was charged up to 1.5 kV. The working gas was krypton (99.99% purity) at 130 Pa filling pressure mountained by a constant flux. The spectral line profiles recording procedure together with the used experimental set–up system are described in references [13,14,18]. Two recorded Kr III line profiles, as an example, are shown in Figure 1.

[a] e-mail: steva@ff.bg.ac.yu
[b] e-mail: vladimir@ff.bg.ac.yu
[c] e-mail: mdimitrijevic@aob.bg.ac.yu

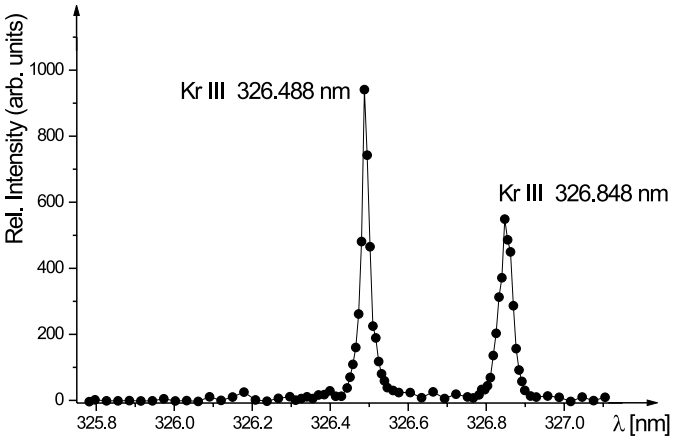

Fig. 1. Recorded Kr III spectral lines at a plasma temperature of 17 000 K and an electron density of 1.65×10^{23} m^{-3}.

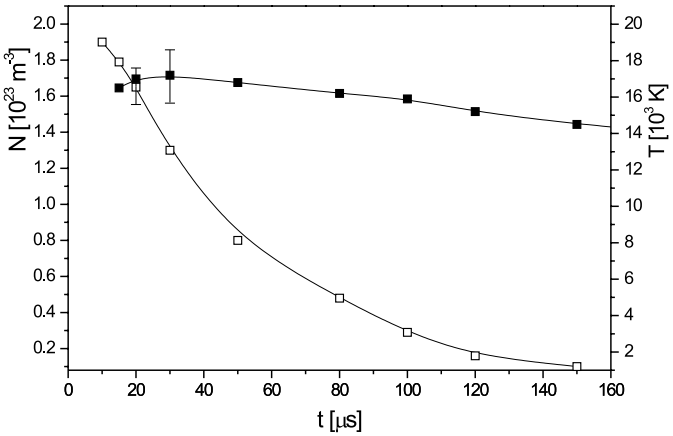

Fig. 2. Temporal evolution of the electron temperature (close symbols) and electron density (open symbols) in the decaying plasma.

One can notice that the investigated spectral lines are well isolated while the continuum is very close to zero within the wavelength range of interest. These facts are important for an accurate determination of line intensities and, correspondingly, for a reliable determination of A values.

The plasma was monitored by the Kr II line radiation and by the discharge current. Variations of the latter were found to be within 4%. All investigated Kr II and Kr III lines are recorded by the same experimental arrangement.

The measured profiles were of the Voigt type due to the convolution of Lorentzian profile from Stark broadening with Gaussian profile from Doppler and instrumental broadening. Line intensities were extracted from the experimental data by fitting convoluted line profiles [6] to the measured spectra. The line intensity (I) corresponds to the area under the line profile and was obtained within 3–5% accuracy from the fit. Great care was taken to minimize the influence of self–absorption on the line intensity determinations. Using a technique described in reference [10] the absence of self-absorption was obtained in the case of the investigated Kr II and Kr III spectral lines.

The plasma parameters were determined using standard diagnostic methods [7–9]. Thus, the electron temperature was determined from the ratios of the relative intensities (Saha equation) of nine Kr II spectral lines (435.548, 457.721, 461.529, 461.917, 463.388, 465.888, 473.900, 476.574 and 483.208 nm) to the five Kr I spectral lines (435.136, 436.264, 446.369, 557.028 and 587.091 nm) with an estimated error of ±9%, assuming the existence of LTE, according to the criterion from references [7,9]. All the necessary atomic data were taken from references [4,19]. The electron temperature decay is presented in Figure 2. The electron density decay was measured using a well-known single laser interferometry technique for the 632.8 nm He–Ne laser wavelength with an estimated error of ±7%. The electron density decay is also presented in Figure 2.

Table 1. Our relative (dimensionless) experimental ($A^{\rm rel}_{\rm exp}$) transition probability values in the Kr II spectrum. Wavelengths, transitions and upper-level energies ($E_{\rm u}$ in eV), are taken from references [4,19]. Transitions are ranged following increasing $E_{\rm u}$ values.

Transition	λ (nm)	$E_{\rm u}$	$A^{\rm rel}_{\rm exp}$
$5s\ ^4\mathrm{P}_{5/2}$–$5p\ ^4\mathrm{P}^o_{5/2}$	473.900	16.60	$0.83 \pm 9\%$
$5s\ ^4\mathrm{P}_{5/2}$–$5p\ ^4\mathrm{P}^o_{3/2}$	465.888	16.65	$0.69 \pm 9\%$
$5s\ ^4\mathrm{P}_{3/2}$–$5p\ ^4\mathrm{P}^o_{1/2}$	483.208	16.83	$0.89 \pm 8\%$
$5s\ ^4\mathrm{P}_{5/2}$–$5p\ ^4\mathrm{D}^o_{7/2}$	435.548	16.83	$1.00 \pm 3\%$
$5s\ ^4\mathrm{P}_{3/2}$–$5p\ ^4\mathrm{D}^o_{5/2}$	476.574	16.87	$0.78 \pm 8\%$
$4d\ ^4\mathrm{D}_{5/2}$–$5p\ ^4\mathrm{D}^o_{3/2}$	556.865	17.16	$0.04 \pm 12\%$
$5s\ ^2\mathrm{P}_{3/2}$–$5p\ ^2\mathrm{P}^o_{1/2}$	484.661	17.24	$0.73 \pm 10\%$
$5s\ ^2\mathrm{P}_{3/2}$–$5p\ ^2\mathrm{P}^o_{3/2}$	461.529	17.37	$0.58 \pm 11\%$
$5s\ ^2\mathrm{P}_{3/2}$–$5p\ ^2\mathrm{D}^o_{5/2}$	461.917	17.37	$0.72 \pm 11\%$
$5s'\ ^2\mathrm{D}_{3/2}$–$5p'\ ^2\mathrm{F}^o_{5/2}$	463.388	18.48	$0.85 \pm 18\%$
$5s'\ ^2\mathrm{D}_{5/2}$–$5p'\ ^2\mathrm{F}^o_{7/2}$	457.721	18.56	$1.15 \pm 18\%$
$5s'\ ^2\mathrm{D}_{5/2}$–$5p'\ ^2\mathrm{P}^o_{3/2}$	447.501	18.62	$0.92 \pm 19\%$
$5s'\ ^2\mathrm{D}_{5/2}$–$5p'\ ^2\mathrm{D}^o_{5/2}$	408.833	18.88	$0.97 \pm 21\%$
$5p\ ^4\mathrm{D}^o_{7/2}$–$5d\ ^4\mathrm{F}_{9/2}$	378.310	20.11	$2.97 \pm 30\%$
$5p\ ^4\mathrm{D}^o_{5/2}$–$5d\ ^4\mathrm{F}_{7/2}$	377.809	20.15	$2.70 \pm 30\%$

3 Transition probability measurements

When the plasma remains at LTE the well–known formula [7–9]

$$(I_1/I_2)_{EXPT} = (A_1 g_1 \lambda_2 / A_2 g_2 \lambda_1) \exp(\Delta E_{21}/kT) \quad (1)$$

can be used for a comparison between measured relative line intensity ratios and corresponding calculated values, taking into account the validity of the Boltzmann distribution for the population of the excited levels in the emitters. In this expression I denotes the measured (EXPT) relative intensity, λ the wavelength of the transition, A the transition probability of the spontaneous emission, ΔE the difference in the excitation energy, and g the corresponding statistical weight. T is the electron temperature of the plasma in LTE and k is the Boltzmann constant.

Table 2. Relative (dimensionless) Kr II transition probability values. $A^{\rm rel}_{\rm exp}$ represent our experimental values. A_N denote tabulated values in NIST atomic spectra data base [4] where absolute and relative values (normalized to a 435.548 nm transition) are mutually equal. Other relative (dimensionless) experimental transition probability values: $A^{\rm rel}_K$, [21]; $A^{\rm rel}_L$, [20]; $A^{\rm rel}_D$, [22]; $A^{\rm rel}_M$, [25]; $A^{\rm rel}_B$, [24]; $A^{\rm rel}_{FC}$, [23]; $A^{\rm rel}_{BR}$, [26]; $A^{\rm rel}_{SCH}$, [31]; $A^{\rm rel}_{MH}$, [33]; $A^{\rm rel}_F$, [34] and $A^{\rm rel}_{MK}$, [32]. Data in brackets denote absolute A values of the reference 435.548 nm transition (in 10^8 s^{-1}).

λ (nm)	$A^{\rm rel}_{\rm exp}$	A_N	$A^{\rm rel}_K$	$A^{\rm rel}_L$	$A^{\rm rel}_D$	$A^{\rm rel}_M$	$A^{\rm rel}_B$	$A^{\rm rel}_{FC}$	$A^{\rm rel}_{BR}$	$A^{\rm rel}_{SCH}$	$A^{\rm rel}_{MH}$	$A^{\rm rel}_F$	$A^{\rm rel}_{MK}$
473.900	0.83	0.76	0.72		0.94	1.50	0.64	0.83	1.35	0.88	1.04	1.02	0.92
465.888	0.69	0.65	0.63	0.84	0.87	1.12	0.63	0.80	1.06			0.80	0.89
483.208	0.89	0.73		0.55	0.86	1.46		0.87	1.39				0.89
		(1.00)	(1.02)	(9.1)	(1.30)		(1.15)	(1.43)	(1.20)	(1.39)	(1.25)	(1.15)	(1.38)
435.548	1.00	1.00	1.00	1.00	1.00	1.00	1.00	1.00	1.00	1.00	1.00	1.00	1.00
476.574	0.78	0.67	0.66			1.21	0.65			0.72	0.84	1.14	
556.865	0.04												
484.661	0.73					1.75	0.78		2.00				
461.529	0.58	0.54				0.87			1.29				
461.917	0.72	0.81	0.79		0.94	1.47	0.71	0.87	1.35	0.90		0.98	
463.388	0.85	0.71	0.70	0.73	0.86	1.24	0.70	0.78	2.17		0.89	0.77	0.84
457.721	1.15	0.96	0.94	0.76	0.92	1.54	0.69	0.86	2.30		0.96	1.05	
447.501	0.92				1.22	1.12		1.06				1.14	
408.833	0.97				1.10	0.84		1.03	0.91			1.16	
378.310	2.97											1.64	
377.809	2.70											1.34	

On the basis of the measured relative line intensity ratio and electron temperature equation (1) yields ratio of the corresponding transition probabilities or conversely, the transition probability of a particular transition relative to a selected reference A value. As reference A values the transition probabilities of the 435.548 nm Kr II and 324.569 nm Kr III transitions have been chosen. These lines are the most intense and have the highest reproducibility among the investigated Kr II and Kr III spectral lines. Our experimental relative A values ($A^{\rm rel}_{\rm exp}$) are presented in Tables 1 and 4 with estimated accuracies which contain the uncertainties of the line intensity and electron temperature determinations and the uncertainties of the calibration procedure. $A^{\rm rel}_{\rm exp}$ represent averaged values obtained during plasma decay in a time interval for which the criterion of the existence of the LTE is fulfilled. Our $A^{\rm rel}_{\rm exp}$ values provide the possibility for a future comparison with absolute data as well as with data presented in relative form.

4 Results and discussion

Our experimentally obtained $A^{\rm rel}_{\rm exp}$ values are given in Tables 1, 2, 3 and 4.

On the basis of Tables 1–4 one can conclude: first of all, it must be remarked that absolute A values, taken from various references, corresponding to our reference 435.548 nm Kr II and 324.569 nm Kr III transitions lie in a wide range (1.00−1.64; for Kr II and 1.59−3.33; for Kr III) excluding unrealistically high Kr II A (9.1×10^8 s^{-1}) value from reference [20].

Fortunately, the absolute A value of the reference 435.548 nm Kr II transition tabulated by NIST [4] is 1.00×10^8 s^{-1} making the absolute and relative NIST A_N values mutually equal (in the case of our experiment). Our $A^{\rm rel}_{\rm exp}$ values agree well (within ±12%, on average) with 8 Kr II A_N values, especially in the case of the 465.888, 473.900 and 461.917 nm transitions.

Our Kr II $A^{\rm rel}_{\rm exp}$ values show tolerable agreement with previously experimental results by: reference [21] (6 transitions within ±14% on average), reference [22] (8 transitions within ±17% on average), reference [23] (8 transitions within ±14% on average), reference [24] (7 transitions within ±17% on average). In the case of the Kr III transitions the best agreement was found with $A^{\rm rel}_F$ values (6 transitions within ±26% on average).

The experimental Kr II $A^{\rm rel}_M$ [25] and $A^{\rm rel}_{BR}$ [26] values are significantly larger than our and other experimental values. Although the $A^{\rm rel}_L$ [20] values are reasonable, it should be pointed out that their reference value is extremely large (9.1×10^8 s^{-1}).

Our $A^{\rm rel}_{\rm exp}$ values are in a good agreement with theoretical values ($A^{\rm rel}_{FC}$ and $A^{\rm rel}_{MRT}$) predicted on the basis of the LS coupling approximation performed in reference [23] (8 transitions within ±12% on average) and in reference [27] (8 transitions within ±14% on average), and with $A^{\rm rel}_{SG}$ values predicted on the basis of the effective operator formalism presented in reference [28] (11 transitions within ±15% on average).

Theoretical Kr II $A^{\rm rel}_{SC}$ values [29] calculated on the basis of the LS coupling approximation lie far below all cited experimental and theoretical data. The $A^{\rm rel}_{KT}$ values calculated in reference [30] lie below other $A^{\rm rel}$ data except

Table 3. Same as in the Table 2. Relative theoretical Kr II transition probability values: $A^{\rm rel}_{MRT}$, [27]; $A^{\rm rel}_{KT}$, [30]; $A^{\rm rel}_{SG}$, [28]; $A^{\rm rel}_{SC}$, [29]; $A^{\rm rel}_{B}$, [24] and $A^{\rm rel}_{FC}$, [23].

λ (nm)	$A^{\rm rel}_{\rm exp}$	A_N	$A^{\rm rel}_{MRT}$	$A^{\rm rel}_{KT}$	$A^{\rm rel}_{SG}$	$A^{\rm rel}_{SC}$	$A^{\rm rel}_{B}$	$A^{\rm rel}_{FC}$
473.900	0.83	0.76	0.81	0.75	0.76	0.62	0.55	0.76
465.888	0.69	0.65	0.79	0.65	0.62	0.09	0.37	0.68
483.208	0.89	0.73	0.74	0.56	0.69	0.45		0.79
		(1.00)	(1.47)	(1.64)	(1.64)	(1.30)	(1.32)	(1.45)
435.548	1.00	1.00	1.00	1.00	1.00	1.00	1.00	1.00
476.574	0.78	0.67		0.42	0.69	0.31	0.56	
556.865	0.04							
484.661	0.73				0.64	0.007	0.28	
461.529	0.58	0.54		0.48	0.45	0.10		
461.917	0.72	0.81	0.71	0.47	0.75	0.25	0.94	0.84
463.388	0.85	0.71	0.99		0.71		0.78	0.78
457.721	1.15	0.96	0.80		0.86		0.87	0.82
447.501	0.92		0.91		1.12			0.87
408.833	0.97		1.21		1.04			1.11
378.310	2.97							
377.809	2.70							

Table 4. Our relative (dimensionless) experimental ($A^{\rm rel}_{\rm exp}$) transition probability values in the Kr III spectrum and those of the other authors: $A^{\rm rel}_{F}$, [34]; $A^{\rm rel}_{KPA}$, [37] and $A^{\rm rel}_{R}$, [38]. Wavelengths, transitions and upper-level energies ($E_{\rm u}$ in eV), are taken from references [4,19]. Data in brackets denote absolute transition probability values of the 324.569 nm Kr III reference transition (in 10^8 s^{-1}). Transitions are ranged following increasing $E_{\rm u}$ values.

Transition	λ (nm)	$E_{\rm u}$	$A^{\rm rel}_{\rm exp}$	$A^{\rm rel}_{F}$	$A^{\rm rel}_{KPA}$	$A^{\rm rel}_{R}$
$5s\ ^5\mathrm{S}^o_2$–$5p\ ^5\mathrm{P}_1$	335.193	21.76	$0.94 \pm 6\%$	0.86	1.11	0.89
$5s\ ^5\mathrm{S}^o_2$–$5p\ ^5\mathrm{P}_2$	332.575	21.79	$0.98 \pm 6\%$	0.90	1.02	0.89
				(1.59)	(3.33)	(2.80)
$5s\ ^5\mathrm{S}^o_2$–$5p\ ^5\mathrm{P}_3$	324.569	21.88	$1.00 \pm 3\%$	1.00	1.00	1.00
$5s\ ^3\mathrm{S}^o_1$–$5p\ ^3\mathrm{P}_2$	350.742	22.32	$1.22 \pm 9\%$	1.16	0.85	0.75
$5s'\ ^3\mathrm{D}^o_2$–$5p'\ ^3\mathrm{D}_2$	343.946	23.89	$1.68 \pm 18\%$	1.34	0.86	1.13
$5s'\ ^3\mathrm{D}^o_1$–$5p'\ ^3\mathrm{F}_2$	326.848	24.03	$1.59 \pm 20\%$	1.10	0.97	0.08
$5s'\ ^3\mathrm{D}^o_3$–$5p'\ ^3\mathrm{F}_4$	326.481	24.26	$1.60 \pm 21\%$	0.92	0.92	0.88
$5s'\ ^3\mathrm{D}^o_3$–$5p'\ ^3\mathrm{P}_2$	302.445	24.56	$1.02 \pm 23\%$		1.32	0.80

transitions 473.900 and 465.888 nm in the $5s\ ^4\mathrm{P}$–$5p\ ^4\mathrm{P}^o$ Kr II multiplet.

Experimental Kr II $A^{\rm rel}_{SCH}$ [31], $A^{\rm rel}_{MK}$ [32] and $A^{\rm rel}_{MH}$ [33] values agree with our $A^{\rm rel}_{\rm exp}$ values within the noticed experimental accuracies in the cited experiments and our work.

The experimental Kr II $A^{\rm rel}_{F}$ values lie above our $A^{\rm rel}_{\rm exp}$ data by about 20%, on average. Exceptions are the transitions of 378.310 and 377.809 nm in the high lying $5p\ ^4\mathrm{D}^o$–$5d\ ^4\mathrm{F}$ multiplet.

The transition 556.865 nm designated in reference [19] as $4d\ ^4\mathrm{D}_{5/2}$–$5p\ ^4\mathrm{D}^o_{3/2}$, belongs to the poorly investigated Kr II transitions and we have no other $A^{\rm rel}$ values for comparison. Absolute A values of this transition, observed experimentally, are presented in references [35,36].

It should be pointed out that in the recent study [35] the authors have found satisfactory agreement among their experimental A values and calculated Kr II transition probabilities in reference [28]. Their A data show good agreement with those from reference [24].

Finally, it turns out that in the studies [35,36,39–48] a number of the Kr II and Kr III A values have been obtained, but without ones corresponding to our chosen transitions so that the comparison with our $A^{\rm rel}_{\rm exp}$ data is impossible.

5 Conclusion

On the basis of the accurately obtained spectral line intensities we have obtained 14 Kr II and 7 Kr III transition probability values relatively to the reference transitions

at 435.548 nm and 324.569 nm, respectively. The comparison among all available $A^{\rm rel}$ values (except extremely high or small values) and here presented data show agreement (within ±15%) between $A^{\rm rel}$ values corresponding to the 463.388 and 408.833 nm Kr II and 335.193 and 332.575 nm Kr III transitions. Thus, they can be recommended as useful atomic data with accurate $A^{\rm rel}$ values, related to the chosen Kr II and Kr III reference transitions needed in plasma diagnostic or modeling.

This work is a part of the projects "Determination of the atomic parameters on the basis of the spectral line profiles" (OI1228) and "Influence of collision processes on astrophysical plasma lineshapes" (GA1195) supported by the Ministry of Science, Technologies and Development of the Republic of Serbia. S. Djeniže is grateful to the Foundation "Arany János Közalapitvány" Budapest, Hungary.

References

1. H.L. Dinerstein, Astrophys. J. **550**, L223 (2001)
2. J.A. Cardelli, D.M. Meyer, Astrophys. J. **477**, L57 (1997)
3. C. Zeippen, Phys. Scripta **58**, 43 (1995)
4. NIST — Atomic Spectra Data Base Lines (wavelength order) — `http://physics.nist.gov/cgi-bin/AtData/main-asd` (2003)
5. V. Milosavljević, S. Djeniže, Eur. Phys. J. D **15**, 99 (2001)
6. V. Milosavljević, G. Poparić, Phys. Rev. E **63**, 036404 (2001)
7. H.R. Griem, *Plasma Spectroscopy* (McGraw-Hill Book Company, New York, 1964)
8. W.L. Wiese, *Methods of Experimental Physics*, edited by Bederson, W.L. Fite (Academic Press, New York, 1968), Vol. 7B
9. R. Rompe, M. Steenbeck, *Ergebnisse der Plasmaphysik und der Gaselektronik* (Akademie Verlag, Berlin, 1967), Band 1
10. S. Djeniže, S. Bukvić, Astron. Astrophys. **365**, 252 (2001)
11. A. Srećković, V. Drinčić, S. Bukvić, S. Djeniže, Phys. Scripta **63**, 306 (2001)
12. A. Srećković, S. Djeniže, S. Bukvić, Phys. Scripta **65**, 359 (2002)
13. S. Djeniže, V. Milosavljević, M.S. Dimitrijević, Astron. Astrophys. **382**, 359 (2002)
14. S. Djeniže, A. Srećković, S. Bukvić, Eur. Phys. J. D **20**, 11 (2002)
15. S. Djeniže, M.S. Dimitrijević, A. Srećković, S. Bukvić, Astron. Astrophys. **396**, 331 (2002)
16. J. Purić, S. Djeniže, A. Srećković, J. Labat, Lj. Ćirković, Phys. Rev. A **35**, 2111 (1987)
17. S. Djeniže, A. Srećković, J. Labat, R. Konjević, L.Č. Popović, Phys. Rev. A **44**, 410 (1991)
18. V. Milosavljević, S. Djeniže, M.S. Dimitrijević, Phys. Rev. E **68**, 016402 (2003)
19. R.A. Striganov, N.S. Sventickij, *Tablicy Spektraln'ykh Linij* (Atomizdat, Moskva, 1966)
20. M.A. Levchenko, Sov. Phys.–JETP **14**, 1445 (1971)
21. H.W. Keil, Diplomarbeit Universitat Kiel, unpublished, in [24], 1973
22. K.E. Donnelly, P.J. Kindlmann, W.R. Bennett Jr, J. Opt. Soc. Am. **65**, 1359 (1975)
23. V. Fonseca, J. Campos, J. Phys. B **15**, 2349 (1982)
24. T. Brandt, V. Helbig, K.P. Nick, J. Phys. B **15**, 2139 (1982)
25. M.H. Miller, R.A. Roig, R.D. Bengtson, J. Opt. Soc. Am. **62**, 1027 (1972)
26. G. Bertucceli, H.O. Di Rocco, Spectrosc. Lett. **24**, 1039 (1991)
27. H. Marantz, R.I. Rudko, C.L. Tang, IEEE J. Quant. Electron. **QE-5**, 38 (1969)
28. N. Spector, S. Garpman, J. Opt. Soc. Am. **67**, 155 (1976)
29. Th.M. El Sherbini, Z. Phys. A **276**, 325 (1976)
30. S.H. Koozekanani, G.L. Trusty, J. Opt. Soc. Am. **59**, 1281 (1969)
31. W. Schade, Z.W. Stryla, V. Helbig, Phys. Scripta **39**, 246 (1989)
32. K.A. Mohamed, G.C. King, J. Phys. B **12**, 2809 (1979)
33. J.E. Le Mond, C.E. Head, Nucl. Instrum. Meth. Phys. Res. B **24/25**, 309 (1987)
34. U. Fink, S. Bashkin, W.S. Bickel, J. Quant. Spectrosc. Radiat. Transfer **10**, 1241 (1970)
35. F. Rodriguez, J.A. Aparicio, A. de Castro, J.A. del Val, V.R. González, S. Mar, Astron. Astrophys. **372**, 338 (2001)
36. V. Podbiralina, Y.M. Smirnov, N.V. Stegnova, Opt. Spektrosk. **34**, 467 (1973)
37. J.A. Kernahan, E.H. Pinnington, W. Ansbacher, J. Opt. Soc. Am. B **4**, 1130 (1987)
38. M. Raineri, J.G. Reyna Almados, F. Bredice, M. Gallardo, A.G. Trigueiros, S.-G. Pettersson, J. Quant. Spectrosc. Radiat. Transfer **60**, 25 (1998)
39. T.M. El Sherbini, A.A. Farrag, J. Phys. B **9**, 2797 (1976)
40. H. Smid, J.E. Hansen, J. Phys. B **16**, 3339 (1983)
41. F. Bredice, M. Raineri, M. Gallardo, A.G. Trigueros, J. Phys. B **29**, 5643 (1996)
42. A. de Castro, J.A. Aparicio, J.A. del Val, V.R. González, S. Mar, J. Phys. B **34**, 3275 (2001)
43. F.J. Coetzer, P.B. Kotzé, P. van der Westhuizen, Z. Phys. A **306**, 19 (1982)
44. M.B. Das, J. Quant. Spectrosc. Radiat. Transfer **57**, 237 (1997)
45. R.E. Mitchell, S.D. Rosner, T.J. Scholl, R.A. Holt, Phys. Rev. A **45**, 4452 (1992)
46. G. Langhans, W. Schade, V. Helbig, Phys. Lett. A **183**, 205 (1993)
47. F.J. Coetzer, P.B. Kotzé, T.C. Kotzé, P. van der Westhuizen, Spectrochim. Acta B **39**, 1021 (1984)
48. K.B. Blagoev, J. Phys. B **14**, 4743 (1981)

FACTA UNIVERSITATIS
Series: **Philosophy, Sociology, Psychology and History** Vol. 10, N°1, 2011, pp. 89 - 99

THE COSMOLOGICAL THEORIES OF THE PRE-SOCRATIC GREEK PHILOSOPHERS AND THEIR PHILOSOPHICAL VIEWS FOR THE ENVIRONMENT*

UDC 1(38)

Efstratios Theodossiou[1], Vassilios N. Manimanis[1], Milan S. Dimitrijević[2]

[1]Department of Astrophysics-Astronomy and Mechanics, School of Physics, National and Kapodistrian University of Athens, Greece
E-mail: etheodos@phys.uoa.gr
[2]Astronomical Observatory of Belgrade, Belgrade, Serbia
E-mail: mdimitrijevic@aob.bg.ac.rs

Abstract. *In this paper the views related to nature, Mother-Earth and the natural environment in the ancient Greek world are discussed, from the Orphic Hymns and the Homeric world, through the works of Hesiod and Sophocles, and the theories and works of the pre-Socratic philosophers, the Ionian School, Thales, Anaximander, Anaximenes, Heraclitus, Pythagoras and the Pythagoreans, Empedocles, Socrates, Plato, Aristotle, the Stoics and Neo-Platonists, with a particular emphasis on Plotinus. The common elements in the teaching of the pre-Socratic Ionian philosophers and of the latter ancient Greek natural philosophers were the observation of living environment and nature, the corresponding relations, changes and cyclic periodic variations. We note the attempts of Anaximander to formulate the need for the conservation of a dynamical equilibrium in nature and in ecosystems; also, his views on evolution of the leaving creatures and the humans.*

Key words: *history of science, natural philosophy, pre-Socratic philosophers, environment.*

1. INTRODUCTION

The views of the ancient Greek pre-Socratic philosophers from Ionia opened new paths for the study of nature using human logic. Starting from the worship of the Earth as a goddess, they proceeded to examine its position in the Cosmos, proposing a spherical

Received March 02, 2011
* **Acknowledgements**. This study formed part of the research at the University of Athens, Department of Astrophysics Astronomy and Mechanics, and we are grateful to the University of Athens for financial support through the Special Account for Research Grants. It is also supported by the Ministry of Education and Science of Serbia through the project III44002

shape for our planet. They pioneered the unifying approach for the physical world, assuming one element as the basis for everything in the Universe – this element was water for Thales, infinity for Anaximander, air for Anaximenes, fire for Heraclitus. The genesis and the decay of worlds succeed one another eternally. Anaximenes believed, like Anaximander, that our world was not the only one that existed. Heraclitus believed that, of the vast richness of the natural creation with its unpredictable changes, nothing remains stable and motionless. There is no constancy, only an eternal flow, a perpetual motion. This is similar to what we accept today in quantum physics; the apparent stability and immobility is an illusion of our limited senses. According to Heraclitus, as Diogenes Laertius writes, matter is constantly transformed (Diogenes Laertius 1935: IX, 7-8, Theodossiou 2007: 72).

The views and the theories of the ancient philosophers indicate the relation of the antique Greek world with the mother Earth and the natural environment, an international issue of first priority nowadays, regarding the need for its immediate protection.

In this work we examine the development of the notions of living environment from the *Orphic Hymns* and the Homeric world, through the pre-Socratic philosophers, Socrates, Plato, Aristotle, Stoics and Neo-Platonists, with a particular accent on Plotinus, in order to follow the development of ideas like the need for the protection of the dynamical balance of an ecosystem, and the apprehension of the living environment, nature and mother Earth, which, as a kind of travel back to the primal sources, has much to reveal to us concerning our modern worries.

2. FROM MYTH TO REASON

The pre-Socratic philosophers of Ionia were carefully observing in the 6th century BC the natural phenomena and their contribution to the challenging of myths was crucial. They attempted to extract all possible conclusions from the observation of nature by using mainly their logic (Theodossiou 2007: 44)

Ancient Greek natural philosophers were preoccupied by the ‘cosmic riddle’, i.e. the questions of the origins, the structure and the construction of our Universe. At the same time, a sudden and rather unexpected shift took place, from mysticism and religious worldview towards reasoning thought, which was the greatness of the ancient philosophy; a switch with very deep consequences for humanity.

Of course, most pre-Socratics were natural ‘monist’ philosophers, in the sense that they were interested in defining the ultimate substance or principle, the primal element from which all things of our world originated. So they created philosophical systems through which they would be able to explain in a rational way the relation between humans and nature. This is the reason that their philosophical thought is relevant today and that the natural component of pre-Socratic philosophy is of such a great importance.

For the first time in the history of the world, with the pre-Socratic views it was expressed the total decoupling of myth from the rational intellect. Here it will be shown how from myth physical environmental thought appeared and was shaped during the first scientific revolution in Ionia, in the 6th century BC. Then philosophers tried to answer two basic questions they were preoccupied with: the first was on the origins of the world and the second was on its structure or form. This was the reason they became the founders of philosophical thought and of science itself.

3. The place of the Earth in worship and inside the Cosmos

The worship of the Earth

A starting point could be the worship of the mother-Earth. In parallel to the primal worship of the Sun, a prominent place in religion was held by mother-Earth, the universal mother. The philosophy of the Greek pre-Socratic philosophers reflected views that respected Nature as the feeding mother of men and their attitude towards 'her' was the one expected towards a living and respectable deity.

In a sense Earth was the supreme goddess, and for this reason Greeks called her –the word for 'earth' in Greek language is of the feminine gender– *Hypertatan* (Supreme) Earth. It should be noted, however, that Gaia (the Earth) was never worshipped as a celestial body or as anthropomorphic deity, but rather as *gaia-chthon*, as the nature with its ground, soil and interior, where humans live and get their food from. Man is 'accused' by the tragic poet Sophocles (5th Century BC) as the creature daring to annoy the supreme goddess, not hesitating to inflict pain on her:

> *"by ploughing her with his plough, trenching it ceaselessly year after year"*
> (Sophocles *Antigone* 1994: verse 330).

The conversion of earth-nature to an omnipotent goddess-mother most probably took place when the agricultural societies developed, along with their agricultural festivals-mysteries, pertaining to the eternal cycle of life (sprouting, bearing fruits, ripening, decline and death, seed, sowing, rebirth). Beginning from the depths of antiquity, it can be said that the primitive human from his first cognitive observations of life on Earth understood that, like him, the rest of animal and plant life forms were also tied to the triptych life-development-death. Man's survival was connected with the terrestrial vegetation, since, like the rest of the animals, was eating what was available in nature (Eliade 1978).

Our primitive ancestors, observing carefully the life cycle of the plants, with the seed, its planting inside Mother-Earth and its transformation into new life, discovered over the centuries the corresponding primal cycle of animal sexual reproduction. The sperm (in Greek the word 'sperm' means 'seed') was im-planted by the male into the womb of female, in an exact analogy with the seed of a plant; and from the maternal organism a new life was created. From the 'lifeless' seed, Earth was producing life, exactly as the animal females. Therefore, Earth should also be a living creature and, in order to give birth, she should come into contact with a male element. For this reason, our primitive ancestors personified Earth as a female form, while the fertilizing male was the Sky with his rain, or some large river, such as the divine Nile in Egypt.

Earth (*Gaia*) and Sky (*Ouranos*) constitute the first divine couple, united by cosmogonic orphic Eros (Kern, *Orphic. Fragm* 1922: 1); in this symbolism of erotic cosmogony the Sky (*Ouranos*) embraces and fertilizes Earth with 'his' rain. Their union is therefore presented as an extremely powerful force of reproduction, which united and multiplied the deities, an aspect revered and sung by mythical Orpheus as product of the original Chaos or Erebus and the illuminated part of the day. This union is also symbolized by the love affair of Semele, which represents the Earth, and Zeus (Jupiter), a celestial god who fertilizes his beloved woman with his thunders, harbingers of the precious rain. Similar is the way Zeus fertilizes the earthly Danae, after he is transformed into golden rain in order to penetrate into her subterranean cell. Symbolically, the sky god softens with his beneficial waters the dried from the drought body of the Earth in order to grow life in it.

4. THE PLACE OF EARTH IN THE COSMOS

Earth in the Homeric Universe was considered as a circular flat disc surrounded by a vast circular 'river', the Ocean. This model appears for the first time in the *Homeric Hymn*: *"Incense to Pan - various"* (*Panos thymiama, poikila*): *"And the Ocean encircles the Earth in its waters"* (*Homeric Hymns* 1914).

The Sky rises upon Earth. In the Orphic Hymns (1981) the Sky is mentioned as the master of the World (Cosmos), encompassing the Earth as a sphere (our Celestial Sphere). The Sky is the abode of the blissful gods and it moves in rotations, spinning (*Orphic Hymn* 4: *Incense to Ouranos*).

According to the ancient Greek traditions the Sky was a metallic canopy made of copper or iron, supported by very tall columns; in other traditions the Sky was a giant. Homer combines these two views by having the giant Atlas supporting the columns himself (*Odyssey* 1919: 1:53-54). Hesiod writes that his fate of supporting the sky was assigned to him by Zeus (*Theogony* 2006: 517). So, in ancient Greece the Sky was thought to be made of a solid, metallic, material. For this reason, in the Homeric poems is referred as *chalcous* that means of copper (*Iliad* 1924: 17:424) and *polychalcus* that is made of much copper (*Iliad* 1924: 5:504, *Odyssey* 1919: 2:458, 3:2, 16:364, 19:351), or as *siderous* – of iron (*Odyssey* 1919: 15:329, 17:565).

The space between the Sky and the Earth, according to the beliefs registered by Homer, was filled with the (comparatively dense) air in its part towards the Earth (*Iliad* 1924: 14:288). Towards the Sky this intermediate space was filled with the clean and transparent *aether* (the ether), a kind of 'light air'. Beyond the ether there was the starry Sky.

Of course, one must not believe that the Sky was a bare metallic dome. It was, as Homer mentions, full of life, a life offered by the stars that decorate it. Because of this it was called *asteroeis*, i.e. full of stars (*Iliad* 1924: 6:108, 15:371, *Odyssey* 1919: 9:527). On this celestial dome travels the Sun (*Odyssey* 1919: 1:7-9), hence called *ouranodromos* (running on the sky).

Homer in his poems, dated *circa* 900 to 800 BC, describes the Earth as flat and circular with the Ocean around it, a model first appearing in the *Orphic Hymn* "X. TO PAN, *The Fumigation from Various Odors*", verse 15: *"Old Ocean too reveres thy high command, whose liquid arms begirt the solid land"*, while Hesiod in his *Theogony* describes the Universe as spherical, divided in two parts by the plane of the flat Earth.

The great philosopher Pythagoras (6^{th} Century BC) is generally credited as the first supporter of the idea of the spherical Earth. He expressed the opinion that, since the Sun and the Moon are spherical in form, the same should be the case with the Earth, which was sitting motionless in the center of the Universe! Pythagoras was teaching that Earth was spherical, isolated and inhabited; it should be noted that Anaximander also supported that the Earth was isolated, while Empedocles stated that the Earth floats freely in space. Thus, Pythagoras and the Pythagorean philosophers were supporting the spherical shape of the Earth mainly for symmetry reasons, since they regarded sphere as the most perfect form a solid body can take. The same views were upheld by Parmenides in the 5^{th} century BC, who declared with certainty that the Earth was spherical.

Influenced and probably persuaded by the thoughts of Pythagoras and his School, many other major Greek philosophers and astronomers adopted similar views, such as Aristotle, Hipparchus, Crates of Miletus and others. Aristotle dedicates a significant por-

tion of his book *On the Heavens* to the support and propagation of this view, stating that *"the Earth has a spheroid shape, as is necessary to her"* (*On the Heavens* 1956: B, 297b, 18-19).

However, as with many other pioneering views, ideas and theories of the ancient Greek philosophers –e.g. the heliocentric system of Aristarchus– the hypothesis of the spherical shape of Earth was forgotten with the decline of ancient Greece and the rise of the practical Roman spirit during the times of the Roman Empire. It was therefore natural for the simpler view to conquer the Byzantine East and the mediaeval West, and this was the flat Earth theory. The teachings of scholars who tried to restore the old view for the shape of the Earth were intensely fought by simpler people, who basically were arguing that it would be impossible for the Earth to be spherical, because in such a case the people living at the antipodes, i.e. the diametrically opposite point of the Earth would stand upside down and would inevitably fall into the abyss.

Of course it must be stressed that accepting a spherical shape for Earth would mean not only abandoning the 'obvious' flat shape of our world, but the deeply entrenched notion in the mind of mediaeval people that in space there is one absolutely defined direction: the 'up' and 'down' one. This was an age without physics and the seemingly easy for us to comprehend idea that all material bodies are attracted towards the center of the Earth was even for educated people of that period utterly incomprehensible!

From the 15th century on, when the scholars of the age had a better look at the Aristotelian text, the debate on the shape of the Earth started again. It must not be forgotten that, probably based on this view of Aristotle (and of the other Greek philosophers) and guided by the writings of Ptolemy on Geography (*Geografike Hyphegesis* 1883, Berggren and Jones 2000) Christopher Columbus dared his voyage to the West in order to discover another way to India.

5. The pre-Socratic environmental approaches

In the 6th Century BC, with the philosophers from Miletus and the rest of Ionia, a real revolution took place in philosophy and science. The scientific philosophy was born, its theory, notions and objective physical-mathematical science, the great accomplishment of the Greek spirit even to this day (Theodossiou 2007: 40).

At first, Thales of Miletus, the founder of Monism, proposed that the basis of everything was water. Then, Anaximander proposed infinity, Anaximenes the air, while Heraclitus of Ephesus proposed the fire as the primal element. The variety of their answers to the question of the basic element characterizes their philosophy.

A common element in the thought of all natural pre-Socratic Greek philosophers was the observation of the environment, of the rates and the mutations of the natural elements, and of the cyclical, periodically repeated natural processes.

Thales, the founder of the Ionian School and the first theoretician of geometry and astronomy, was the first to express the opinion that the polymorphic world of natural phenomena has single base, originating from one only creative common natural entity, the water according to him.

Water was for Thales the essential component of all things, beyond any divine interventions; all entities in nature were mutations of that original material. For Thales water was representing the primal essence from which all forms of matter were emerging and to

which they were returning time and time again. According to Thales beings have a common natural origin and reason, water, and all physical entities are created as transformations of that original element through 'condensation' or diluting. Water (*hydor*) is the element that expanding through its evaporation creates the air, while with its contraction and condensation produces the earth; this can be verified, Thales believed, with the appearance of alluvial deposits from the rivers.

Not only our planet, but the whole Universe according to Thales was based on water and it had the form of a hemisphere. Its interior was full of air, while its surface was the sky, the celestial dome. On the plane of its base there was the stationary Earth, which he thought it was floating on water: *"floating as a piece of wood or something similar"* (Aristotle, *On the Heavens* 1956: B, 297b, 28).

Anaximander believed that in the Universe there is a kind of natural law, a cosmic 'justice' that keeps the balance among the four principal elements, which always are in a state of antagonism due to their different essence and texture. Their natural relation, according to Anaximander, should be conserved in eternity, so that no one of the four basic elements could subordinate the rest. Anaximander was rejecting the idea of his teacher Thales that the basic element was the water, because if this were the case the natural balance of 'justice' among the four elements would be disturbed. If one of the elements had an advantage over the others, then it would have absorbed the rest, and the Universe would be not only entirely different, but it would be headed for its final destruction.

The following phrase is attributed to Anaximander by the neo-Platonic philosopher Simplicius (6th century):

> *"Anaximander had said that the origin of all beings is infinity, from which all heavens were created and all the worlds that exist within them; and that their birth came from infinity and to infinity they end through their wearing. In this way they compensate one another for the injustices that took place as time passed"* (*Simplicius in Physicorum* 1895: 24, 13).

This passage indicates the belief that the opposites, through the successive prevalance of one upon the other, are the agents of evolution and change. The 'passing of time' denotes most probably a universal law that checks the deadlines for the justification to come along, which will correct for the 'injustices'.

This principle can be proved to apply in the equilibria among ecosystems. In the ecosystems there are no one-sided and monopolic processes; all exist in a state of dynamical equilibrium. Destruction, decomposition, creation and regeneration are continuous and periodically alternating processes. New organisms are born only when the old forms die, because the material for the composition of the new creatures comes from the material of their dissolution. This state of dynamical equilibrium (whose great importance was realized by environmental scientists only in the second half of the 20th century) is subject, according to Anaximander, to a 'procession of time'. In other words, they are subject to periods of time. This observation applies to the currently observed biorhythms and biological cycles of the ecosystems, since inside each open biological system there are periods in the increase and decrease of the populations it contains. By extending this principle we could argue that probably the ignorance of its power led the Western civilization to invest on energy and time to one-sided selections, such as the choice of fossil fuels as its main energy source, overlooking the fact that the cycle of the terrestrial fossil fuels is of the order of many million

years. Consequently, the need for a dynamical equilibrium in nature is urgent, a fact that can be extracted as a conclusion by the above proposition of Anaximander.

Anaximander was the first cartographer who dared to draw the known world. He also proposed a most intriguing origin for the human species; according to it the first humans were created from fish-like beings. Other pre-Socratic Ionian philosophers, like Empedocles, had made such conjectures concerning the origin from dead matter or the various transformations of the first life forms; for Empedocles they had disappeared because of lack of adapting ability. These first attempts to formulate a theory of natural history and a reasonable explanation of the phenomenon of life were agreeing in a 'spontaneous creation', and not in the creation of life by some Creator God, as Plato supported later in his *Timaeus* (Plato 1929).

As it can be deduced from the above, the idea that no life form is eternally unchanged, but it evolves in its attempt to adapt to an equally changing environment did not originate with Charles Darwin (*The origin of species* 1998) but with Anaximander.

Anaximenes also accepted (as the rest of the Ionian philosophers) the basic principle of monism common to the Ionian School that everything stems from one origin and finally goes back to it. According to his views, the origin of everything was the air, which for Anaximenes was infinite, that is indeterminate and eternal. The air was the vast material mass to which everything was or could be reduced.

The air of Anaximenes was constantly moving, exactly as Anaximander's infinity. Out of this perpetual motion of the air all the variety of things and phenomena was finally created. Fire originated from the air through thinning, while the condensation of the air created the waters and the Earth.

The genesis and the decay of worlds succeed one another eternally. Anaximenes believed, like Anaximander, that our world was not the only one that existed; he also supported the idea that the vast mass of the air incorporated innumerable worlds that were being created and died all the time, emerging from and returning back to the initial infinity.

Heraclitus considered fire as the originating essence of our world. He believed that, of the vast richness of the natural and celestial/Universal creation with its unpredictable changes, nothing remains stable, motionless and granted. There is not constancy, but only an eternal flow, a perpetual motion.

This is exactly what we accept today for the world of quantum physics; the apparent stability and immobility is an illusion and is due to our limited senses. According to Heraclitus, matter is constantly transformed, while in our finite Universe the elements 'fire', 'air' and 'earth' are just different states of one and only material.

All the ancient natural philosophers of Ionia distanced God the Creator from nature and history, keeping always a deep respect for the beliefs of their fellow people; most probably they, too, kept a form of God in some area of their minds and souls, in his spiritual and moral dimension.

After the natural philosophers of Ionia, in Socrates we see the rejection of the distinction man-animal kingdom, while in Plato we find a philosophical treatment of the Earth and the celestial bodies. Plato also mentions some environmental problems in ancient Attica. In Plato's *Dialogues*, especially in *Gorgias*, we find the following philosophical position: *"Society keeps together sky and earth and gods and men…"* (1925: 508A), while in the cosmological *Timaeus* (1929: 77a) Socrates tackles, as we mentioned, our relation with the animal and plant kingdoms:

> *"Blending it with other shapes and senses they engendered a substance akin to that of man, so as to form another living creature: such are the cultivated trees and plants and seeds which have been trained by husbandry and are now domesticated amongst us; but formerly the wild kinds only existed" (Timaeus* 1929: 77a*).*

Socrates concludes that there is no essential difference among the three broad categories of living creatures (humans-animals-plants): *"… Thus, both then and now, living creatures keep passing into one another in all these ways, as they undergo transformation by the loss or by the gain of reason and unreason."* (*Timaeus*, 1929, 92b-c), and: *"there were two kinds of living beings, the human race and a second one, a single class, comprising all the beasts"* (*Statesman* 1925: 263c).

In addition, from the study of Aristotle's works it is evident that in his teaching sciences, philosophy and the world that surrounds us are all correlated and interdependent. Setting out from the description of this conception of him, the great philosopher creates the term 'energy' (Aristotle 1933: *Metaphysics*, I, 982b, 7, 1072a - 8, 1073a).

6. STOICISM AND NEO-PLATONISM

In the following centuries we witness the continuation of the Platonic tradition in the Stoics. Professor P. Damaskos, starting from the views of several scholars (e.g. Sambursky 1959, Long 1986, Brennan 2005), writes:

> *"Stoicism elevates to the status of a basic principle the decision to live in accordance with Nature and the co-existing Logos. These notions are not explained; they are taken as known. Besides, Stoicism is not famous for dwelling on theoretical forms and mental analyses on cosmological and metaphysical matters. However, even in its moral teachings we can discern its respect for the Whole, the brotherly coexistence of all beings and the respect for the nature of each species." (The problem of ecology in the Stoics,* 27 March 2009).

In the chain of philosophical schools Neo-Platonicism comes next; neo-Platonists returned to the theoretical, rather dogmatic Platonic tradition and in this form is represented by the significant philosopher Plotinus. The classic Greek philosophy owes much to the renovating thought and penetrating mind of Plotinus, to its knowledge, but also to his dialectic attempt to develop Platonic dogmatic views and at the same time to combine them with the theories of Stoics and of the Peripatetic School, as well as with Aristotelian views.

Klaus Oehler notes that:

> *"Neo-Platonicism, without a doubt a feat of systematic meditation, is the last product of the methodical and systematical character that was inherent to the philosophical schools already from the beginning of the Hellensitic age and up to its period*." (2000, p. 6).

According to theologian Dr. Ioannis Lilis (2006: 583), Plotinus also uses the term 'energy' (*energia*) to describe his own cosmic view. More specifically, Plotinus suggests that the entire reality consists of the En (The One – God), the Nous (Mind), the Psyche (Soul of the World), nature and matter. The universe "comes out" from God not by free and

willing creation but by constant "emanation". Through these emanations the "God-substance" becomes common to all other degrees of reality (Pantheism). God transcends the world, yet the world-stuff is God-stuff. The emanations are the *Nous*, the world Soul, and nature and matter. The first emanation is the *Nous*, i.e. the intelligence, and the second emanation is the world Soul, the *Psyche*. It proceeds from the Nous as the Nous proceeds from the *En* and it is therefore inferior to the Nous. The third emanation, proceeding from Nous and Psyche forms the nature and the matter; matter, as the final step, has no form, while nature perceptible through our senses does have form. Plotinus, stressing that Nous is emanating from En, and that Psyche is one within the unified reality, since has two kinds of activities, contemplative (beyond matter and time) and plastic (in forming the particular things of the Universe according the ideas contemplating in the Nous), calls Nous and Psyche "*from energy, not potentially*". He stresses that everything was created by the Essence or Quantity and together with it: "*If it is maintained that the continuous is a Quantity by the fact of its continuity, then the discrete will not be a Quantity. If, on the contrary, the continuous possesses Quantity as an accident, what is there common to both continuous and discrete to make them quantities*?" (Plotinus 1991: *The Enneads* 6, 4, 4).

In addition, *The Enneads* contain a beautiful passage about the personified Nature: *"If one asked: For what reason does her create? And if Nature heard the question and wanted to answer, she would certainly say: You should not ask me but instead you should understand by yourself, in silence like me, for I do not speak often. So, what should you understand? That my creation is an object of viewing made by me, the silent one, an object that resulted by nature and has received by me (I was also resulted by such a viewing) the property to be viewed. And my viewing creates the viewed object, just like mathematicians can draw only when they can view. And, while I do not draw but I just watch, the borderlines of the bodies result somewhat like the rainfall. Nothing different happens with me than what happens with my parents; they, too, resulted from such a viewing"* (*The Enneads*: 3, 8,4).

In other words, nature, personified in this passage by Plotinus presents herself, her origins and her work.

7. Conclusions

In this work the views related to nature, mother Earth and the natural environment in the ancient Greek world were examined, from the *Orphic Hymns* and the Homeric world, through works of Hesiod and Sophocles, and theories and works of the pre-Socratic philosophers, the Ionian School, Thales, Anaximander, Anaximenes, Heraclitus, Pythagoras and the Pythagoreans, Empedocles, Socrates, Plato, Aristotle, Stoics and Neo-Platonists, with a particular emphasis on Plotinus. The way such views evolved to physical studies, reflection and theories during the first scientific revolution in Ionia in the 6th century BC, has been discussed from a mythological point of view the development of such theories and some of their possible implications in later centuries, like the idea of spherical Earth of Pythagoreans and the idea of Columbus to search for a new way to India.

We can conclude that the common elements in the teaching of pre-Socratic Ionian philosophers and latter ancient Greek natural philosophers were the observation of living environment and nature, the corresponding relations, changes and cyclic periodic variations.

We also emphasize the attempts of Anaximander to formulate the need for the conservation of a dynamical equilibrium in nature and in ecosystems and his views on evolution of the living creatures and the humans, which all witness that in works of Greek antiquity one could find several interesting views and reflections on our modern worries.

REFERENCES

1. Aristotle (1933) *Metaphysics*. Books I-IX, transl. by Hugh Tredennick. The Loeb Classical Library (reprinted 1936, 1947, 1956, 1961, 1968, 1975, 1980, 1989, 1996). London: Heinemann.
2. Aristotle (1956) *On the Heavens* (*De Caelo*). transl. by W.K.C. Guthrie. The Loeb Classical Library (reprinted 1936, 1947, 1953, 1956). London: Heinemann.
3. Brennan, T. (2005) *The Stoic Life*. Oxford: Oxford University Press.
4. Damaskos, P. (2009, March 27) *The problem of Ecology in the Stoics*. Symposium Hellenic Physicist Society, Rethymno, Creta [in Greek].
5. Berggren, J. L. and Jones, A. (2000) *Ptolemy's Geography*: *An Annotated translation of the theoretical Chapters*. Princeton: Princeton University Press,.
6. Darwin, C. R. (1998) *The Origin of Species.* Oxford World's Classics. Oxford, New York: Oxford University Press.
7. Diogenes Laertius (1935) *Lives of Eminent Philosophers*. transl. by R.D. Hicks. Two volumes. Loeb Classical Library, London: W. Heinemann.
8. Eliade, M. (1978) *A History of Religious Ideas*, vol. I, *From the Stone Age to the Eleusinian Mysteries.* transl. by W. Trask, Chicago: University of Chicago Press.
9. Hesiod (2006) volume I, *Theogony*. *Works and Days*. *Testimonia*. Ed. & transl. by Glenn W. Most. The Loeb Classical Library, No. 57N, London: W. Heinemann.
10. Homer (1924) *The Iliad*. transl. by A.T. Murray (reprinted 1954), The Loeb Classical Library, London: W. Heinemann.
11. Homer (1919) *The Odyssey*. transl. by A.T. Murray, revised by G.E. Dimock (reprinted 1954 and 1995). The Loeb Classical Library, London: Heinemann.
12. *Homeric Hymns*. (1914) transl. by Hugh G. Evelyn-White, Cambridge, M.A., Harvard University Press. London: Heinemann.
13. Kern, O. (1922) *Orphicorum Fragmenta*. Berlin: Weidmann.
14. Long, A. A. (1986) *Hellenistic Philosophy: Stoics, Epicureans, Skeptics*. 2nd edition, London: Duckworth.
15. Lilis I. (2006) "The presence of ancient Hellenic philosophy during the first Byzantine centuries", *Orthodoxy*, period 2, year 13, July-September, pp. 577-596. Ecumenical Patriarchate, Constantinople [in Greek].
16. *Orphic Hymns* (*The Hymns of Orpheus*). (1981) transl. from the original Greek text by Thomas Taylor, Introduction preface by Manly Hall, The Philosophical Research Society INC., Los Angeles, California.
17. Oehler K. (2000) "The continuation of Hellenic Philosophy from the end of Ancient Times to the fall of Byzantine Empire". Linos Benakis (edit.), Medieval Philosophy. Modern research and Anticipations, *Parousia*, Athens, p. 6. [in Greek].
18. Plato (1929) *Timaeus, Critias, Cleitophon, Menexenus, Epistles*. transl. by R.G. Bury (reprinted 1942, 1952, 1961, 1966, 1975, 1981, 1989, 1999). The Loeb Classical Library No. 234 (v. 9). Harvard University Press. London: Heinemann.
19. Plato (1925) *Lysis. Symposium. Gorgias*. transl. by W.R.M. Lamb (reprinted 1932, 1939, 1946, 1953, 1961, 1967, 1975, 1983, 1991, 1996). The Loeb Classical Library No. 166. Harvard University Press. London: Heinemann.
20. Plato (1925) *Statesman, Philebus, Ion*. transl. by H.N. Foweler & W.R.M. Lamb. The Loeb Classical Library No. 164. Harvard University Press. London: Heinemann.
21. Plotinus (1991) *The Enneads.* transl. by Stephen MacKenna and John Dillon. Penguin, London & *The Six Enneads*, transl. by S. Mackenna and B.S. Page. The Internet Classics Archive at MIT. classics.mit.edu/Plotinus/enneads.html
22. Ptolemy (1883) *Klaudiu Ptolemaiou Geographike Hyphegesis*. trans. in Latin by Karl Müller, Editore Alfredo Didot, Paris.
23. Sambursky, S. (1959) *The Physics of the Stoics*. London: Routledge.
24. *Simplicius in Physicorum*. (1895) Libros VVIII, in *Commentaria* in *Aristotelem Graeco*, Editit Hermannus Diels, Typis et Impensis G. Reimeri. Vol. X. Berolini.

25. Sophocles (1994) Vol. II. *Antigone*. *The women of Trachis. Philoctetes. Oedipus at Colonus*. Edit. & trans. by W.H.S. Jones, The Loeb Classical Library No. 21. Harvard University Press. London: Heinemann.
26. Theodossiou, E. (2007) *The dethronement of the Earth – The dispute between geocentric and heliocentric systems*. Athens: Diavlos Publ. [in Greek].

KOSMOLOŠKE TEORIJE GRČKIH PRESOKRATOVSKIH FILOZOFA I NJIHOVI FILOZOFSKI POGLEDI NA ČOVEKOVU ŽIVOTNU SREDINU

Efstratios Theodossiou, Vassilios N. Manimanis, Milan S. Dimitrijević

U ovom radu razmatraju se pogledi u antičkom grčkom svetu na prirodu, Majku Zemlju i čovekovu životnu sredinu, od Orfičkih himni i homerovskog sveta, preko radova Hezioda i Sofokla,i teorija i radova presokratovskih filozofa, Jonske škole, Talesa, Anaksimandra, Anaksimena, Heraklita, Pitagore i Pitagorejaca, Empedokla, Sokrata, Platona, Aristotela, Stoika i Neoplatonista sa posebnim naglaskom na Plotina. Zajednički elementi u učenju presokratovskih jonskih filozofa i kasnijih starogrčkih filozofa prirodnjaka bili su posmatranje čovekove životne sredine i prirode, odgovarajućih veza, promena i cikličkih i periodičkih varijacija. Naglašavamo pokušaje Anaksimandra da formuliše potrebu za očuvanjem dinamičke ravnoteže u prirodi i ekosistemima, kao i njegove poglede na evoluciju živih bića i ljudi.

Ključne reči: *istorija nauke, prirodna filozofija, presokratovski filozofi, životna sredina.*

FACTA UNIVERSITATIS
Series: **Philosophy, Sociology, Psychology and History** Vol. 11, N°2, 2012, pp. 211 - 221

THE NOTION OF CHAOS: FROM THE COSMOGONICAL CHAOS OF ANCIENT GREEK PHILOSOPHICAL THOUGHT TO THE CHAOS THEORY OF MODERN PHYSICS

UDC 113+124.1

Efstratios Theodossiou[1], Konstantinos Kalachanis[1], Bassilios N. Manimanis[1], Milan S. Dimitrijević[2]

[1]Department of Astrophysics-Astronomy and Mechanics, School of Physics, University of Athens, Panepistimioupolis, Athens, Greece
E-mail: etheodos@phys.uoa.gr
[2]Astronomical Observatory, Belgrade, Serbia

Abstract. *Due to the importance of modern science, the appearance of the notion of Chaos in ancient Greek cosmogonies and philosophical thought and the evolution of its meaning has been studied in this paper. In addition, a comparison has been made with the meaning of this important notion in modern Theory of Chaos.*

Key words: *Orpheus, Phanes, Cosmogony, chaos, Chaos Theory, fractals.*

1. INTRODUCTION-COSMOLOGICAL VIEWS

In the ancient Greek civilization where the first philosophers attempted to explain the creation of the Universe, the hymns of mysticist Orpheus proved to be of significant importance, by introducing the term 'Chaos'. According to Orpheus, Chaos condenses into the giant Cosmic Egg, whose rupture resulted in the creation of Phanes and Ouranos and of all the gods who symbolize the creation the Universe.

Later, Greek philosophers supported the view that chaos describes the unformed and infinite void, from which the Universe is created. So, this void in ancient Greek thought is not just an abstract term, but a kind of empty space with cosmogonical characteristics.

In modern physics, the term 'chaotic' describes systems whose parameters consist of many hidden laws, which are difficult to describe and can be changed any time. Due to the importance of the notion of *Chaos* in modern science, it is of interest to consider its appearance in ancient Greece and the evolution of its meaning, which is the aim of this paper.

Received May 06, 2012

During the early period of development of the first human civilizations, the refined thought of pioneer priests, astronomers and philosophers – through religious faith and empirical thought – attempted to explain the 'first beginning', through which the Universe came into being. According to Aristotle "*For it is owing to their wonder that men both now begin and at first began to philosophize*" (Aristotle, *Metaphysics*: 982b: 12-13). It is obvious that the first philosophers attempted to explain the origin of natural phenomena. In this context, wise people who originate from eastern civilizations supported the existence of gods. According to these people, there are two contingents which resulted in the creation the universe: a) The universe was created through divine energy, a theory which is known as *ex nihilo creation*, and b) There was an eternal matter as substrate, which finally was formatted by a God or Gods. A major point in this case is the fact that the creation of the Universe depends on the mixing and combination of cosmic elements (Theodossiou, 2007: 31).

In ancient Greece, the teaching of mysticist Orpheus (13th century B.C.) evolved, which proved to be the initial form of Greek religion, and consisted of poems and hymns of significant literary value (*Orphica*, 1805, *Orphicorum fragmenta*, 1922, *Orphic Hymns*, 2007).

Orpheus, picture on an ancient column crater from Gela.
(ca. 450 BC, Staatliche Museen, Berlin)

2. ORPHIC COSMOGONY

According to the orphic cosmogony, initially the *ageraos* (never getting old) Chronos (Time) emerged. Once Chronos was created, he gave birth to the duality of Aether and Chaos. Then Chronos and Aether created the *cosmic silver Egg*, which through its fertilization, brought into being the second divine triad: the *protogonos* (the first to appear) Eros or Phanes, God of Light, Metis, the Goddess of wisdom, skill and craft and finally the life-giving Herikepeos. In the ancient tradition, it is claimed that Herikepeos had two genders, both the male and female.

The sixth Orphic Hymn '6. *Protogonos*' speaks of Chaos which condenses into the giant Cosmic Egg. After the egg was ruptured, its upper part created Ouranos (the Sky), while the Earth was created from the bottom part. From the central part of the Egg, *Protogonos* (first created) or Phanes took form, whose name also means *luminous.*

Orpheus
Picture from an ancient Greek vessel segment

> 6. *I invoke Protogonus, of a double nature, great, wandering through the ether, Egg-born, rejoicing in the golden wings, having the countenance of a bull, the procreator of the blessed gods and mortal men.*

It would be useful to note that in ancient Greek philosophy and astronomy, Eros symbolizes the spiritual power of nature that creates the Universe.

Then, Phanes with his sister Nyx (Nychta = Night) gave birth to Ouranos (Uranus), whose role was dominant among the Gods and Earth: *he was the king of the Gods after mother Night.* It is worth noting that the consecutive birth of Gods according to orphic cosmogony is similar to the version which is proposed by poet Hesiod in his poem *Theogony*. So, Ouranos is displaced by his son Cronus (Saturn), who was also displaced by Zeus, the creator and ruler of the world. An important person which appears in the orphic cosmogony is Dionysus Zagreus, son of Zeus and Persephone, whose birth marks the end of creation of divine beings in the world.

The Titans sliced and ate Dionysus Zagreus, but goddess Athena saved his heart, through which Zeus resurrected him. This unholy and desecrating action was punished by Zeus by striking them with a thunderbolt. The ash of the Titans was the matter through which God created human beings. But the fact that the ash of the Titans also included the ash of Dionysus, the human race consists of two natures: 1) the evil or *Titanic* nature, 2) the divine/spiritual nature.

Clemens Romanus, the third Bishop of Rome **(**88-97 or 92-101), in his '*Epistulae'* compares the hesiodic cosmogony to that of Orpheus "*Orpheus likens Chaos to an Egg, in which all the first elements can be found mixed. Hesiod perceives this Chaos as a substrate, called by Orpheus as Egg (Cosmic Egg), a creation that emerged from formless matter…".*

3. PHANES THE GOD IN THE RELIEF OF THE MUSEUM OF MODENA IN ITALY

In this relief of god Phanes, which on display in the Modena Museum in Italy, the god of light, truth and justice is depicted surrounded by the ecliptic, with the twelve signs of the Zodiacal constellations. In the four angles of the relief the winds of the four cardinal points are depicted, which correspond to the four initial elements: fire, earth, air and water. Inside the ecliptic we can see the Cosmic Egg divided into two parts. In the middle of the relief, Phanes appears through the flames in the form of a man with wings on his shoulders, since he is the creator Eros. Behind him the crescent of Selene, the Moon is displayed. Also, Phanes holds a scepter, as the ruler of the world (Phanes and Herikepeos), while in his right hand he holds lightning, just like Zeus, the father of gods and men (Cook 1925: 1051).

Herikepeos - Phanes - Metis: the Cosmic Egg in its triadic status, the light of Phanes, Mitis's wisdom and Herikepeos's life. A snake huddled around the body of Phanes, which reaches the top of his head, symbolizes the Earth (Gaia). He has animal hindquarters, just like the ancient god Pan, who is a Pancosmic (Universal) god (Theodossiou 2007: 33).

The God Phanes
Modena Museum, 2nd c. A.D.

On Phanes's body three animal heads appear: of the ram, lion, and goat. Professor M. Papathanasiou claims here, that "*The heads of the ram and goat symbolize the astronomical phenomena which appeared during the construction of the relief in the 2nd century AD, when the vernal equinox was in the constellation of Aries, while the winter solstice was in the constellation of Capricorn. But the lion head displayed in the center under the chest is a remnant of ancient astronomical phenomena of the 2nd and 3rd millennium BC, when the vernal equinox was in the constellation of Taurus, the summer solstice in the constellation of Leo, and the winter solstice in the constellation of Aquarius*" (Papathanassiou, 2009: 296).

Inside the elliptical egg there is a faded inscription: [E]YPHROSY[NE ET] FELIX. Below, outside the ellipsis and above the heads of the winds, there are two capital letters 'P': P(ecunia) P(osuit) and below, at the edges of the rectangular sculpture we can see there is an inscription: FELIX PATER (sacrorum), according to Cook (1925: 1052).

4. THE MEANING OF THE COSMIC EGG

It is important to note that the meaning of the Cosmic Egg in all cosmological myths symbolizes the unity from which the whole Universe emerges. Also, the Cosmic Egg that symbolizes the creation appears in the Orphic Hymns, in Hinduism, in Finnish legends (Theodossiou 2007: 33) and also in the tradition of the primitive tribe of Dogon, in the Mali of Western Africa (Griaule, M. and G. Dieterlen 1965).

The Cosmic Egg is the matrix which includes the sperm of cosmic creation. Almost all ancient legends refer to the Cosmic Egg, because, except for the fact that the egg is the symbol of creation, it is also the symbol of birth and new life (Danezis and Theodossiou 2003: 228-248).

After the ancient Orphic Hymns, which were probably recorded in the 2nd century AD and also in Hesiod's *Theogony*, the creation of the world is one of the main subjects that philosophers and poets deal with. Let us see how Hesiod describes the first cosmogonic principles: *"Verily at first Chaos came to be, but next the wide-bosomed Earth, the ever-sure foundations of all (4) the deathless ones who hold the peaks of snowy Olympus, and dim Tartarus in the depth of the wide-pathed Earth, and Eros (Love)."* (*Theogony* 1914: lyr: 116-123)

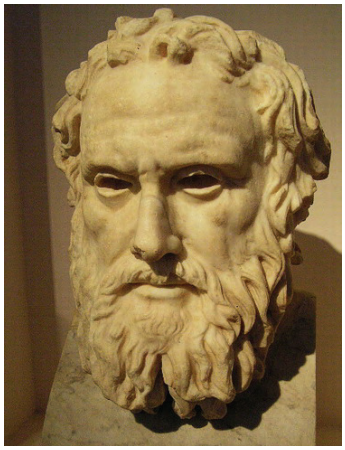

Hesiod
National Archaeological Museum of Athens (Roman copy).

Also, Aristophanes (448-380 BC) in his comedy named *Aves* (*The Birds*, 414 BC) writes: *"At the beginning there was only Chaos, Night, dark Erebus and deep Tartarus. The earth, the air and heaven did not exist. First, the black-winged Night laid a germless egg in the bosom of the infinite deeps of Erebus, and from this, after the revolution of long ages, sprang the graceful Eros with his glittering golden wings, swift as the whirlwinds of the tempest. He mated in deep Tartarus with dark Chaos, winged like himself, and thus hatched forth our race, which was the first to see the light. That of the Immortals did not exist until Eros had brought together all the ingredients of the world and from their marriage Heaven, Ocean, Earth and the imperishable race of blessed gods sprang into being."*

[Aristoph. *Av.* 693 (Chor der Vögel)]

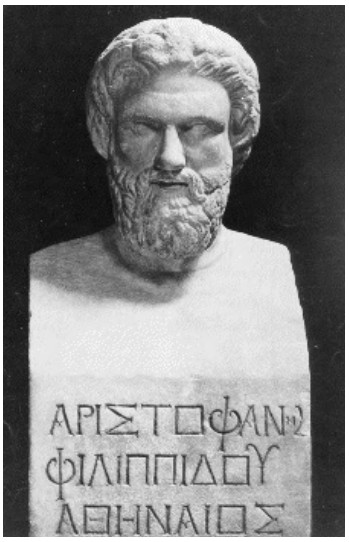

Aristophanes

The great comedian also mentions Chaos in his comedy *Nebulae* (*Nephelae).* In this comedy, Aristophanes aims to squib Socrates and the *Sophists.* So, he describes the teachings in which Socrates initiates the naïve peasant Strepsiades. Socrates orders him to *claim as gods* only *Chaos, Language, and Nebulae* (Aristophanes, *Nebulae*: 423).

5. THE MEANING OF CHAOS IN THE ANCIENT GREEK PHILOSOPHICAL THOUGHT

It seems that the meaning of the term 'Chaos' – from the Greek root 'cha' (Polites 2004, 24) – which is the original situation of the cosmic matter before the creation of the universe, describes the unformed and infinite void. This void in ancient Greek thought is not just an abstract term, but a kind of empty space that consists of nebulae and darkness. Theoretically, Chaos is the infinite space that included, in the form of 'seeds', all the elements which were about to create the universe. Moreover, Chaos was the only creative principle through which everything emerged. Certainly, this unformed space between the Earth and the sky has no eternal being, but it was created at some time in the past. This conclusion originates from Hesiod's text.

In his poem *Theogony*, Hesiod claims that Chaos was not present in the beginning of creation, but that it was created in the beginning, followed by Erevus and Earth. This means that Hesiod did not intend to answer the question of what existed initially, but what was created first. So, he does not speak about an eternal first cause of creation.

According to Jaeger (1953: p. 23), Hesiod does not by-pass the question of the first cause because of his unwillingness to give an answer, but because in his era, this philosophical question had not arisen. In ancient cosmogonies there is no 'before', because of the eternal existence of the universe. Even the Pre-Socratic philosophers, as well as Plato and Aristotle, were in favor of the idea of the eternal existence of cosmic matter. It is important to note that only the Christian Church Fathers and philosophers spoke of the *ex nihilo* creation of the universe.

So, the question of what existed before Chaos has no meaning for Hesiod.

In this context, in the *Old Testament* we can read that *in the beginning when God created the heavens and the earth* (*Gen.* A, 1), there is no reference to what existed before the creation of the universe by God, because the question of what existed before the first cause has no meaning.

Certainly for Hesiod the Heaven and the Earth are the basic elements of the visible universe, but they are not the first causes of cosmic creation. This cause is, according to Hesiod, Chaos. In fact, we can see in Hesiod's poems and in all ancient Greek cosmogonies that there is no reference of any kind to a 'personal God' who creates the universe, but rather what first takes place and what continues to happen later (through the whole cosmogony) happens by its own power. This reflects the period in which the Pre-Socratic philosophers (6th century BC) separated completely the myth from reason.

As we have already seen, *Erevus* and *Nyx* who have emerged from Chaos, generated *Aether* and *Imera* (Day). Chaos also generated Eros, whose sense is definitely cosmological. Nyx was also an important cosmological power, towards which even Zeus showed great respect. Homer writes that Nyx was a consultant of Zeus in the creation of the universe (Homer, *Iliad* 1919: XIV 259). Her power resulted from her old age and her clairvoyance.

So, in *Theogony* Chaos, Earth and Eros were the three primal basic elements through which the universe came into being. Chaos is the receptor of every creation, while Earth symbolizes the solid ground of all living creatures. Eros' nature is totally different, because he is the force which leads everything to its regeneration.

Gigon (1968: 26) claims that the meaning of Eros is not just cosmological, because he is a basic factor not only of human life, but of the entire cosmos. The late professor of Philosophy at the University of Athens, Theophilos Veikos claims that the "*human in the*

early Greek thought is not an isolated part of the universe, but an integral part of the whole cosmos" (Veikos 1988: 20).

In the Pre-Socratic philosophical thought several versions of expressing what existed before the cosmic creation can be found. For example, Leucipus and Democritus believed in the existence of a void. Anaxagoras spoke in favor of the existence of a mixture containing the matter of the universe, while Anaximander spoke about the *infinite.* Also, the lyric poet Alcman (7th century BC) claims that Chaos, keeping its original mythical characteristics, takes form in the name of matter that gives birth to Thetis, the creator of the universe (Kirk et al. 1983: 34, Danezis and Theodossiou 1999: 125-130).

Also, a very interesting aspect of the creation of the universe has been put forward by Plato, who in spite of the fact that he does not speak clearly about Chaos, although he describes the primitive situation of matter as chaotic, which was formatted by the *craftsman* "*He was good and the good can never be jealous of anything. And being free from jealousy, he desired that all things should be as similar to him as they could be. This is in the truest sense the origin of creation and the world as we shall do well to believe in the testimony of wise men. God decided that all things should be good and nothing bad, so far as this was attainable. Wherefore also finding the whole visible sphere not at rest, but moving in an irregular and disorderly fashion, out of disorder he drew order, considering that this was in every way better than the other*" (Plato 1902, 30a, 2-6). So, the cosmic creation consists of the change of matter from disorder into order (Kalachanis 2011: 89-90). Aristotle just repeats the teachings of Hesiod about the creation of the universe from Chaos (Aristotle *Metaphysics*, 984b, 28). Ovidius (Publius Ovidius Naso, 43 BC-17 AD) also considers Chaos *"a raw confused mass, nothing but inert matter, badly combined discordant atoms of things, confused in one place"* (Ovidius, 2002: lyr. 5-8).

Those cosmogonical aspects of ancient savants and also the meaning of the term "chaos" have contributed to the perception of chaos as an infinite space, an abyss, or as unformed matter, from which the universe evolved. The Professor Emeritus of Astronomy at the University of Thessaloniki, Nicolaos Spyrou, claims that *"a universe that emerges from Chaos represents the belief of ancient Greeks in an unpredictable Nature which is ruled by eccentric gods. However, during the 6th century BC in Ionia a new world view evolved, according to which the Universe is understandable, because of its inner order; inside nature there are regularities, which allow the exploration of its secrets and its operating principles. Nature is not completely unpredictable, because of its regularities, the rules which it must obey. This orderly and admirable aspect of the Universe was called Cosmos by the ancient Greeks, which means ornament, decoration"* (Spyrou 1998: 85).

6. Theory of Chaos and Fractal Geometry

The late Ilya Prigogine (1917-2003), the 'father' of chaos theory and complexity wonders whether there are any laws within chaos. So, is chaos non-predictable by definition?

Awarded the Nobel Prize in chemistry (1977) for his research in thermodynamics, he considers that it is possible to include chaos in the laws of nature. So, he does not agree with the view of chaos as a kind of a non-predictable disorder. According to the classic view, physical law is deterministic, while the time is 'reversible', something which means that the future and past play the same role.

Chaos expands our perception of the physical law by implying the importance of 'possibility" and 'irreversibility'. This radical change forces us to check again our basic description of nature. Deterministic laws produce seemingly random results. Or maybe God 'by playing dice' creates a deterministic universe governed by order. Using chaos theory results in the development of a new branch of physics, which deals not only with laws, but with a science that does not deny the evolution of modern scientific theories.

According to Barry Parker (1999), the Universe inspires admiration and a spontaneous desire for research. We do not know whether we will be able to provide satisfactory answers or not. Chaos Theory reminds us that unpredictability is a characteristic of our dynamic Universe. Chaos Theory along with Quantum theory and the theory of relativity are among the most important scientific discoveries of the 20th century.

Attempts to describe the universe based on a deterministic model are opposed to the physics of the 20th century, because determinism was refuted by Einstein's theory of relativity or by Heisenberg's uncertainty principle. Scientists could not describe the physical reality because of many chaotic parameters. Some examples of these parameters can be seen in meteorological systems, in the eddies of the rivers, even in artificial systems, like the stock exchange. In contrast with Laplace (Theodossiou 2008: 144), who claimed that everything in nature is predictable provided that we know all the basic elements of physical procedures, the scientists of the 20th century admitted that they could not predict phenomena like these. It is obvious that in such systems it is very difficult to know all the parameters, which can change at any time, as well as the hidden laws of nature. This is the simple definition of a chaotic situation. However, the Greek word is used in a different way in several cases. Thus, the term chaos has a different interpretation in Greek philosophy than in everyday life or in Modern Greek (chaos means confusion or disorder), or in its image of Mandelbrot sets (Mandelbrot, 1982). Also, the interpretation of chaos in science is quite different.

Thus, chaos theory was developed, considered the third scientific revolution of physics in the 20th century, after relativity theory and quantum mechanics. Chaos theory is a mathematical concept explaining that it is possible to get very different results from very similar initial conditions of a system. The main precept behind this theory is the underlying notion of small occurrences significantly affecting the outcomes of seemingly unrelated events. The new state that is being assumed by the chaotic system depends on the mathematical concept of *attractor*. However, this new *locus*, in which the system will be 'settled' by the attractor, has parameters whose predictability cannot be described with eternal deterministic laws. This concept of disorder has been the subject of scientific study since the 1970s'.

Physicists, astronomers, mathematicians, meteorologists, biologists, chemists and economists have been looking for connections among different types of non-normality. After the first surprising results from the study of chaotic models, scientists attempted to explain the chaotic movements of everyday life, such as weather conditions, the population of wild animal species and fluctuations in stock prices. They recreated those uncontrollable phenomena with non-linear differential equations on computers. That is how scientists discovered the hidden order that rules them, confirming the Pre-Socratic philosopher Heraclitus, according to whom *hidden harmony is better than obvious harmony* (Diels & Kranz, 1966, B 54, 1).

Nowadays we know that chaos theory is based on the fact that chaos and uncertainty are not due to the inability of technology, because they are basic characteristics of the universe. Chaotic systems are very sensitive, because a tiny and difficult to observe detail may cause a significant result, like the 'butterfly effect', according to which a butterfly in China may cause a storm on the western coast of USA. Another example of a chaotic system is the set of mathematical values of the four interactions of Universe (gravity, electromagnetism, strong and weak nuclear forces). In the case that these values differed minimally, the Universe would be extremely different. So, nature is a dynamical system which could not be described by linear equations. Also, in the field of astronomy it is admissible that chaos played an important role in the creation of the solar system. So, scientists started examining the chaotic systems not just in theory, but as applied sciences.

Peculiar movements in chaotic systems create an odd mixture of tracks and swirls which does not seem completely irregular. The American topologist Stephen Smale claimed that *the most significant feature of a dynamic system is its long time asymptotic behavior. This system chooses, through the entire system, a simpler set of movements* (as cited in Ian Stewart, 1998: 131). This repetitive behavior of a system finally creates a rudimentary geometric form, called a 'strange attractor' by mathematicians.

The support of chaos theory presupposed the proper mathematical model. This model was finally created by *fractal geometry*, developed by the mathematician Benoit B. Mandelbrot (1924-2010).

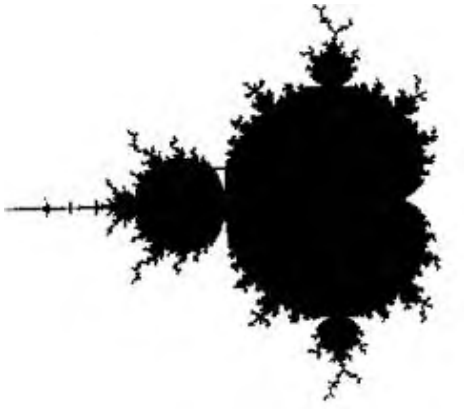

A typical Mandelbrot fractal

Such an object's basic feature is self-similarity, because it contains small patterns of itself, in any scale it is examined. Observing the object at different scales, we see the original object unfolded. Still, starting from a simple original object – just like a triangle – and applying a simple geometric transformation continuously, we come to a fractal object of great complexity which is obviously chaotic. Suddenly, chaos acquires order. Fractal geometry proves to be very useful, to put order into chaos. Fractal structures were discovered in seemingly chaotic systems, like the buffering of wind and snow, in galactic structures, in human organs such as lungs, brain and kidneys. Other examples of fractal systems include the distribution of forests on the Earth's surface, in the shape of the coastline, in the formation of the bronchi of the lungs and also in the music of famous compos-

ers, like Bach and Mozart. So, scientists speak now not of chaos and order, but of a super-order, in which random and chaotic is everything we cannot describe or identify. Those physical laws that rule such systems remain unknown. Therefore, according to Plutarch, the oracle of Delphi correctly supported the view: *"that God eternally geometrizes"* (Plutarch, *Symposiakon* 718 B, 8).

REFERENCES

1. Aristophanes (1928), *Aves*, ed. V. Coulon and M. van Daele, vol. 3, Les Belles Lettres, Paris
2. Aristophanes (1968), *Clouds*, ed. K.J. Dover, Clarendon Press (repr. 1970), Oxford.
3. Aristotle, *Metaphysics*, 1924, ed. W.D. Ross, 2 vols. Oxford, Clarendon Press (repr. 1970).
4. Cook Arthur Bernard (1925), *Zeus: A study in ancient religion*, Cambridge University Press, vol. II, Appendix G, Cambridge, p. 1051-1053.
5. Danezis, E., Theodossiou E., et al. (1999), "A presocratic Cosmological Proposal", *Journal of the History and Heritage of Astronomy* (*JAH2*) 2(2):125-130.
6. Danezis, E. and Theodossiou, E. (2003), *The Cosmology of the mind – An Introduction to Cosmology*, Diavlos Publications, Athens, pp. 228-248 [in Greek].
7. Diels, H. and Kranz, W. (1966). *Die Fragmente der Vorsokratiker*, vol. 1, Weidman, Berlin.
8. Gigon, O. (1968), Der Ursprung der griecheischen Philosophie von Hesiod bis Parmenides, Basel, Stuttgard.
9. Griaule, M. and Dieterlen, G. (1965), *Le Renard Pâle*. Vol. I, 1, 544. Institut d'Ethnologie. Musée de l'Homme, Palais de Chaillot, Paris.
10. Hesiod (1914), *The Homeric Hymns and Homerica* (*Theogony*). The Loeb Classical Library; English translation by Hugh G. Evelyn-White, Heinemann, London (reprinted 1954).
11. Hesiod (1914), *Theogony of Hesiod*, Heinemann, The Loeb Classical Library; English translation by Hugh G. Evelyn-White, London (reprinted 1954).
12. Homer (1924), *The Iliad*. The Loeb Classical Library; English translation by A.T. Murray, Heinemann, London (reprinted 1954).
13. Homer (1919), *The Odyssey*. The Loeb Classical Library; English translation by A.T. Murray, revised by G.E. Dimock, Heinemann, London (reprinted 1995).
14. Jaeger, W. (1953), *Die Theologie der frühen griecheischen Denker*, Kohlhammer verlag, Stuttgard, p. 23.
15. Kalachanis, K. (2011), *On the Paradigm and the Icon in the work of John Philoponus*, PhD Thesis, Department of Philosophy, Paedagogics and Psychology, Department of Philosophy, University of Athens [in Greek].
16. Kirk, G.S., Raven, J.E. and Schofield, M. (1983), *The Presocratic Philosophers. A critical History with a selection of Texts*, Cambridge University Press, First printed (reprinted 1995), p. 34.
17. Mandelbrot, B. Benoit (1982), *The fractal geometry of nature*, W.H. Freeman, New York.
18. Orpheus (2007), *Hymns*, Ideotheatron Publications, Athens [in Greek].
19. *Orphica* (1805), Ed. G. Hermannus, Fritsch, Lipsiae.
20. *Orphicorum Fragmenta* (1922), Ed. O. Kern, Weidmann, Berlin.
21. Ovidius (2002), Metamorhoses, translated in Greek from Latin voice, by the monk Maximus Planoudes, Academy of Athens, Greek Library, Athens.
22. Papathanasiou M. (October 2009), Phanes of Modena relief, *Uranus*, vol. 73: 296, [in Greek].
23. Parker, B. (1999), *Chaos and Astronomy, the impressive complexity of the universe*, Trans by Theophanes Grammenos, Travlos Publications, Athens.
24. Plato (1902). *Timaeus*, Clarendon Press, Oxford (repr: 1968).
25. Polites, N.G. (2004), *Philosophimata*, Athens [self-edited], [in Greek].
26. Spyrou, N. (June 1998), Ionian Philosophy and Cosmic Science, *Apoplous* (Special edition), pp. 83-106 [in Greek].
27. Stewart, I. (1998), *Does God play dice?*, Travlos Publications, Athens [in Greek].
28. *The Holy Bible* (1979), The Gideons International. National Publishing Company, U.S.A.
29. Theodossiou, E. (2007), The dethronement of the Earth – The dispute between geocentric and heliocentric system. Diavlos Publications, Athens, p. 31 [in Greek].
30. Theodossiou, E. (2008), *Philosophy of Physics-From Descartes in the Theory of Everything*, Diavlos Publications, Athens, p. 144, [in Greek].
31. Veikos Th. (1988), *The Presocratic Philosophers*, I. Zacharopoulos Publications, Athens [in Greek].

POJAM HAOSA: OD KOSMOGONIJSKOG HAOSA U STAROJ GRČKOJ FILOSOFSKOJ MISLI DO TEORIJE HAOSA U MODERNOJ FIZICI

Evstratije Teodosiju, Konstantin Kalahanis, Vasilije N. Manimanis, Milan S. Dimitrijević

Razmotren je nastanak pojma haos u starim grčkim kosmogonijama i filosofskoj misli i evolucija njegovog značenja. Takođe je značenje ovog važnog pojma upoređeno sa onim u modernoj Teoriji haosa.

Ključne reči: *Orfej, Fanes, Kosmogonija, haos, Teorija haosa, fraktali.*

МУЗЕЈ НАУКЕ И ТЕХНИКЕ

Phlogiston®

Часопис за историју науке

Journal of the History of Science

ISSN 0354-6640 — БРОЈ 16 ISSUE NO — Година 2008

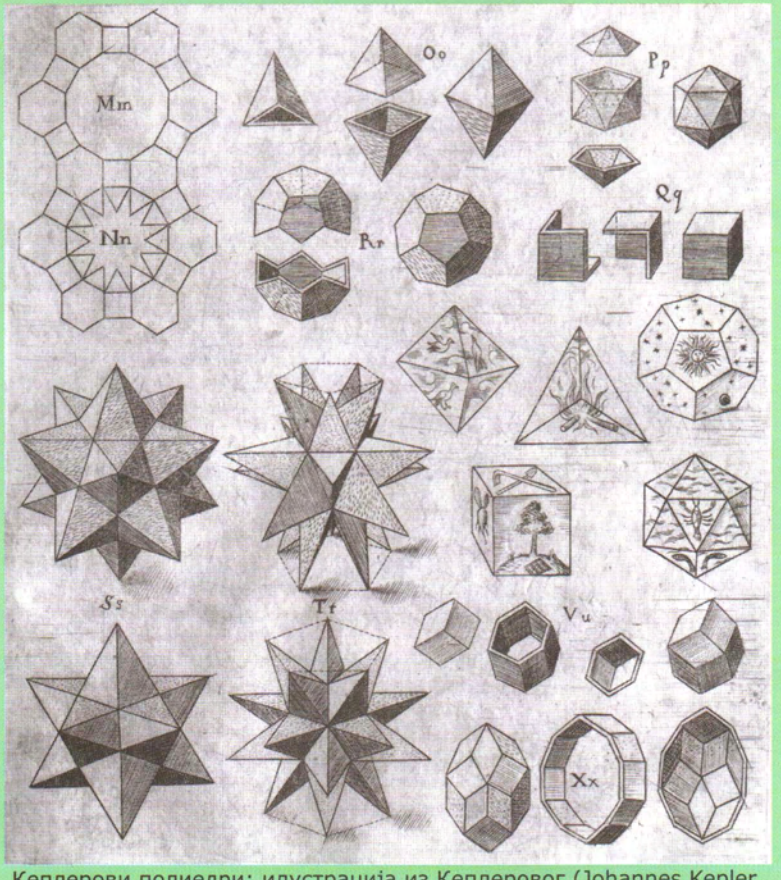

Кеплерови полиедри: илустрација из Кеплеровог (Johannes Kepler, 1571–1630) дела *Хармоније света* (Harmonices mundi) из 1619. године.

НАУЧНА ПОЛЕМИКА

Efstratios Theodossiou[1],
Aris Dacanalis[1],
Milan S. Dimitrijevic[2],
Petros Z. Mantarakis[3]

ORIGINS OF THE HELIOCENTRIC SYSTEM

Abstract: The evolution of the heliocentric theory in the Antiquity has been analyzed, from the first seeds in Orphic Hymns to the emperor Julian, also called "the Apostate" in the 4th century A. D. In particular were analyzed Orphic Hymns, views of Pythagoreans, the heliocentric ideas of Philolaus of Croton, Icetas, Ecphantus, Heraclides of Pontos, Anaximander, Seleucus of Seleucia, Aristarchus of Samos and Emperor Julian.

INTRODUCTION

Since early antiquity, philosophers and astronomers pondered the question of which of the heavenly bodies occupied the center of the known world. The geocentric system, in accordance with its anthropocentric formulation, placed our small planet in the center of the world. Enjoying the favor of the majority of the philosophers and astronomers, it was the dominant theory for centuries. However, there were also opposing views in

[1]Department of Astrophysics, Astronomy and Mechanics
Physics Faculty – University of Athens
[2]Astronomical Observatory of Belgrade
[3]Chatsworth, California, USA

favor of the heliocentric theory. Aristarchus of Samos (c. 310 B. C.– c. 230 B. C.) is generally credited with being the first to postulate a non-earthcentric system. But, centuries before him, seeds of the heliocentric theory can be traced back to the Orphic Hymns and to the teachings of Anaximander and the Pythagoreans. Initially, due to the weight of Aristotle's views, and later on due to those of the great astronomer Claudius Ptolemy (2^{nd} century A. D.), the heliocentric theory did not prevail.

Yet the heliocentric system had not been entirely forsaken. During the 4^{th} century A. D., Emperor Julian – also called "the Apostate" – the last emperor of the first Byzantine dynasty, became a fervent supporter. Julian held the Earth as a planet which, like all other planets, went around the sun in a circular orbit. Thus, Aristarchus' theory had not been forgotten during the first centuries A. D., but even enjoyed strong advocacy.

ORPHIC HYMNS

The ancient teachings of Orpheus are considered to be the basis of the first mystic Greek religion. The Orphic Hymns consist of 87 hexametric poems or 1200 verses in total, which have survived under the title *Hymns of Orpheus to Musaeus*.

The hymns contain a breadth of astronomical information, partly obscured by the use of a strongly poetic language, as well as interesting ideas for the creation and the supreme being. This last piece of information tells us that the hymns belong to a monotheistic cult, since the creation of the Universe is ascribed to a single supreme force. We also discover the interesting concepts of *chaos* and the *cosmic egg*, which led to the creation of "Phanes", the protogonus god, who is not only radiant but the primal generator of life.

From eyes obscure thou wip'st the gloom of night, all-spreading splendour, pure and holy light. Hence Phanes call'd, the glory of the sky, on waving pinions thro' the world you fly.
[V TO PROTOGONUS, *The Fumigation from Myrrh*, verse 15]

Nearly all of the ancient Greek sages and writers drew inspiration from themes found in the Orphic Hymns, and were thus influenced while formulating their unique theories and teachings.

It should be noted that in the Orphic Hymns, "*chaos*" stands for what we would now call space. "Gaia" represented the earth-mother (and not the planet); whereas "Eros" (love), stood for the creational force. In the same hymn, we find a praise to *chaos* which spans the ether ("aether"), and was born from the cosmic egg:

O Mighty first-begotten [Protogonos], hear my pray'r, two-fold, egg-born, and wand'ring thro' the aether...
[V TO PROTOGONUS, *The Fumigation from Myrrh*, verse 1]

In Homeric times, the Earth was perceived as a circular flat disk which was surrounded by a vast circular river, the Ocean. This notion is made evident in the following verse:

Old Ocean [Okeanos] too reveres thy high command, whose liquid arms begirt the solid land.
[X TO PAN, *The Fumigation from Various Odors, verse* 15]

The hymns mention Heaven being the ruler of the world, revolving around the Earth:

Great Heav'n [Ouranos], whose mighty frame no respite knows... Hear, world ruler,..., forever whirling as a sphere around this earth
[III TO HEAVEN: *The Fumigation from Frankincense,* verse 1]

Another verse suggests that the origins of the heliocentric system seem to be located in the Orphic Hymns, as has been previously stressed by Constanstinos Chassapis (1967), the late Greek astronomer, and Maria Papathanassiou (1978, 1980), assistant professor of Mathematics at the University of Athens:

Hear golden Titan! Glowing like gold, you who strides above, oh heavenly light...
...you who combines the epochs ...You are the world ruler...
With your golden lyre, draw on the harmonious path of the world...
... [you] who wanders through fire and moves around in a circle
[VIII TO THE SUN, verse 2]

The phrase "[you who attracts] *draw on the harmonious path of the world*" is striking since this could be a seminal idea of the harmonious movement of the planets around the Sun, a notion which was commonly used for at least the first five centuries B. C. If the planets are to be included in the notion of the world, then the "golden" Sun could be seen as the attractive center of their harmonious orbits. One may therefore make the assumption that the seeds of a heliocentric theory can be traced in the Orphic Hymns.

Furthermore, on hymn (34): To Apollo, we find the following:

Loxias, the pure! ... You mixed in equal parts winter and summer...
[XXXIV TO APOLO, verse 6,... and 20]

Thus, the "Loxias" Sun (meaning "tilted") mixed the components of the year and divided it in two equal parts, the summer and the winter. This is a very important chronological detail which has drawn some attention from the astronomical community, because it has been linked to the dating of the Orphic Hymns. If we take this statement literally, and look back in time when the summer and winter were of exactly equal length we find that the Orphic Hymns probably originated near the following dates: 1841 B. C. or 1366 B. C. (C. Chassapis, 1967 and M. Papathanassiou, 2003). This view however, requires the assumption that ancient Greece possessed very capable astronomers in early antiquity, an idea with little evidence to support it.

Another excerpt which, although referring to Hestia, goddess of the hearth, seems to add to the heliocentric aspect of the hymns, is Hymn (84) [To Hestia]:

You who occupies the center of the home of the greatest and eternal fire.
[LXXXIV TO HESTIA, verse 2]

In *Orphicorum Fragmenta*, a fragment tells us about the rotation of the Earth. This section states that Musaeus knew the path of the star and the movement of the sphere around the Earth, as this round Earth rotates in equal time period around its axis (Fr. 247 v. 24–26, pp. 261–262). Thus, all the elements of a heliocentric system – a central sun, revolving celestial objects and a rotating Earth – were touched upon in the Orphic Hymns.

THE PYTHAGOREANS

The philosopher and mathematician Pythagoras founded his School at Croton in lower Italy, in c. 540 B. C. He and his followers held the view that the most important cosmological principles were based on numbers and

that this was the ultimate reality. The Pythagorean School laid the foundation for mathematics and physics, by relating order and the harmony of sound to the harmony of the Universe.

Virtually all of the students of Pythagoras were trained in astronomy, but their studies of the motion and the distances of the planets were carried out with a rather mystical approach. They believed in mystical and sacred relations between the numbers and the phenomena they described. In the Pythagorean view, the planetary distances were analogous to a heavenly musical rhythm, which was created by harmonious sounds. They believed that this harmony was constantly created, being an eternal expression – of the highest order – of the unique divine harmony.

It is interesting, and somewhat provocative, that 2500 years after the Pythagoreans, contemporary science has come up with ideas very similar to theirs. For example, modern String Theory holds that everything on a microscopic level is a combination of oscillating, multidimentional strings. The Pythagoreans, developers of the "music and harmony of the spheres", would have seen particles as microscopic strings whose rhythmical vibrations create other particles, i.e. "the musical notes". These notes, in turn, create the music of the heavenly spheres. Thus though their eyes, our whole world would seem like a musical symphony, composed with these notes.

Pythagoras' School was a brotherhood, with various degrees of initiation, and may have been founded after the manner of the Orphic religious communities. Its contribution to geometry, music, arithmetic and astronomy was the building block essential for the evolution of scientific thought. Through geometry, as well as the harmony of sound and numbers, the Pythagoreans developed the notion of perfection in the Universe, and coined an appropriate word to describe it: "Cosmos". The etymology of the word comes from either "cosmo" which means "to orderly arrange", or from "cosmema" which means "jewel" (ornament). Pythagoras himself appears to be the

first to use the word "Cosmos", according to the doxographer Aetius: "Pythagoras was the first to name the place of all things Cosmos, due to its orderly nature" [Aetius, *De Vestutis Placitis,* II, 1, 1 (D. 327, 8)].

The Pythagorean School held that the essence of all things was the "number", a rather abstract notion, which could not be perceived through one's senses, but only through intellect. In this manner, the proponents of this school of thought equated infinity with those material elements which could not be subject to measurement or definition.

Some elements of the Pythagorean cosmology have come to us via one of Aristotle's books, namely *Metaphysics*. According to the Pythagoreans, the Cosmos was created after the "One" initially came into being. The "one" – or "en" in Greek – served as the first principle, attracted the "infinite" (*apeiron*) to its own self, and bestowed on it with the "limit" (*peras*). These last two notions, the "limit" and the "infinite", have not survived, but it has been speculated that they could be referring to the prime and even numbers.

Aristotle also mentions the following: "The elements of number, according to them, are the Even and the Odd. Of these the former is limited and the latter unlimited; Unity consists of both (since it is both odd and even) [note of trans: either because by addition it makes odd numbers even and even numbers odd (Alexander, Theo Smyrnaeus) or because it was regarded as the principle of both odd and even numbers (Heath)]. Number is derived from Unity; and numbers, as we have said, compose the whole sensible universe" [Aristotle, *Metaphysics*, A5, 986, 15].

Aristotle provides us with a further comment on the Pythagorean concepts: "It is absurd also, or rather it is one of the impossibilities of this theory, to introduce generation of things which are eternal. There is no reason to doubt whether the Pythagoreans do or do not introduce it; for they clearly state that when the One had been constituted – whether out of planes of superficies or seed or of

something that they cannot explain – immediately the nearest part of the Infinite began to be drawn in and limited by the Limit [note of trans: if numbers are eternal, it is absurd that they should be generated]. [Aristotle, *Metaphysics*, 1091a, 14].

Another cosmological notion that the Pythagorean School of thought held was that the Creation began from a unique single point, which continuously expanded to infinity. One can conclude that the Pythagoreans believed that the Universe evolved from a spherically expanding infinitesimal core.

Another idea that Pythagoras believed in was that the Earth was spherical and immobile in the centre of the Cosmos, which was spherical as well. „... the water, earth and air; these elements interchange and turn into one another completely and combine to produce a universe animate, intelligent, spherical, with the earth at its centre, the earth itself too being spherical and inhabited round about" [Diogenes Laertius, *Lives of Eminent Philosophers*, VIII, 25, 8–10].

Many Pythagoreans held an identical view of a spherical Earth, placed in the center of the world, *without being supported by anything*. This was a novel idea in its time, and demonstrates a clear progress when compared to assumptions that were previously held by other Greek philosophers.

According to the late professor of astronomy, Demetrios Kotsakis, "Pythagoras was the first who taught that the apparent motion of the sun on the celestial sphere from the east to the west, could be analyzed in to two distinct motions: One daily from East to West, parallel to the equator, and one yearly from West to East on the ecliptic" (Kotsakis, D., 1976, p. 28).

In the 6th century B. C., some students and followers of Pythagoras, and most importantly Philolaus of Croton, Heraclides of Pontus, Ecphantus of Syracuse as well as others, believed in a "pyrocentric" theory. This means that they accepted that the element of fire was the "first principle" of the Cosmos. They believed that after

the Creation, the element of fire accumulated in the center of the Cosmos and its attraction to its neighboring parts was part of the creation, formation and formulation of the various bodies that made up the spherical Universe.

THE THEORIES OF PHILOLAUS OF CROTON

Philolaus of Croton (c. 480 B. C. – c. 385 B. C.), spread the Pythagorean ideas concerning the "first principle", by organizing and writing a synopsis of Pythagorean philosophy. It appears that he was the primary creator of the philosophical notions of the "limit", the "infinite" and the harmony between the two, which, according to his views, was achieved due to the "number". He believed that the Cosmos is unique and began its creation from the center, which was occupied by fire. Around it, he placed the "Anticthon", (or Counter–earth – a hypothetical invisible Earth), the Earth, the Moon, the Sun, the five planets known at the time (Mercury, Venus, Mars, Jupiter and Saturn), and the sphere of the fixed stars. Thus, ten heavenly bodies "danced" around the central fire, a number which the Pythagoreans held as sacred. It has been speculated that the Anticthon was introduced exactly for this reason, namely to raise the number of the celestial bodies to the sacred number ten.

According to some accounts, Archippus, Lysias and few others, survived a bloody revolt against the Pythagoreans in Croton. Cylon, an ex-student of Pythagoras, who had been sent away from the school for failing to comply with its principles initiated the attack while all the followers were gathered together. It is certain that the teachings of Pythagoras and his students, their innovative theories, their mysticism, as well as their aristocratic political tendencies caused the violent reaction of their democratic adversaries, who either killed or exiled many of them: "Cylon of Croton ... and those allied with him,

hunted (killed) the Pythagoreans down to the man." (Iamblichus *Vita Pythagorii* (V. P.) 248–249 ff).

One of the survivors, Lysias, eventually became the teacher to Philolaus of Croton. According to some other accounts, the teacher of Philolaos is not Lysias but Pythagoras and Philolaos survived the revolt of Cylon together with other Pythagoreans as Lysias (or Lyssis) and Archippus.

Philolaus taught Pythagorean philosophy and wrote the books *Bachae* and *On Nature* A, B and C (Cosmos, Nature and Soul respectively). An extant fragment from his first book reads: "The world is uniform, it began its creation from the center, and from the center it expanded uniformly upwards and downwards, keeping equal distances from the center" (Diels-Kranz, 1996, *Die Fragmente der Vorsokratiker*).

Several sources provide information on some of his cosmological thoughts: "The initial One, the beginning of the creation of the Universe, is called Hestia" [*On Nature*, fragment 7, Stob. *Eclogae* I 21, 8 (p. 189, 17 W)].

Diogenes Laertius mentions: "According to Demetrius, in his work "on men of the same name", Philolaus was the first to publish pythagorean treatises, to which he gave the title "On Nature", beginning as follows: Nature in the ordered universe was composed of unlimited and limiting elements, and so was the whole universe and all that is therein" [Diogenes Laertius, *Lives of Eminent Philosophers*, 85 (A1 I 398, 20)].

The doxographer Aetius (Aet. I 3, 10), informs us (citing Theophrastus) of the following: "Philolaus believes that there is fire around the center of the Universe, which he calls "hestia of all" and "house of Zeus", "mother of the Gods", "altar, constraint and measure of nature". There is another fire which dwells in the outer region of the Universe. The center, he says, came first by nature, and around it dance ten heavenly bodies: The sphere of fixed stars, then the five planets, then the Sun, then the Moon, followed by the Earth and Anticthon, and after all these the fire of "hestia", which lies around the center. The outer

region, which surrounds the whole Universe, is a place where the elements are in their pure state, unmixed, and that place he calls "Olympus". All that lies beneath Olympus, namely the part where the five planets along with the Sun and the Moon lie, he calls "cosmos", while the area beneath those, the sublunar space ...he calls "heaven". Wisdom is relevant with the order which holds in the heavenly bodes, while virtue is relevant with the disorder of the things which are subject to birth. The first is perfect while the second is imperfect." [Aet. *De Vetustis Placitis*, II 7, 7 (D. 336, vermutlich Theophrast. im Poseidonios--Excerpt)].

The above are mentioned once again by Aetius: "The Pythagorean Philolaus places the fire in the center (for it is the Universe's focal point), secondly he places the Anticthon, then, our habitat, the Earth comes third, placed opposite [from the Antictchon] and moving in a circle, that being the reason for the beings of the Anticthon being invisible to the beings of the Earth. The ruling power of the Universe lies in the central fire, which God placed, like a keel, to base the foundation of the sphere that makes up the world". [Aet. III 11, 3 (D. 337 from Theophrastus)].

From all of the above we can sum up that, according to Philolaus, everything in "Olympus" and the "Cosmos" never changed, while in the areas up to the Moon, every being gifted with life was born, changed and finally died. The Earth and all the other planets were rotating around Hestia with the same direction but at different levels and with different speeds. Hestia was invisible because it shed its light to the antipodes of the Earth, which were impossible to get to. The Sun did not have its own light, but accepted and accumulated the fire of Hestia.

Philolaus, through his questioning of the traditional geocentric cosmology, set the foreground for Aristarchus' heliocentric theory, which would clearly dispute the central role of our small planet in the Universe. Even though he did not specifically place the Sun in the center, the idea of the "central fire" certainly served as a basis for the

heliocentric theory. Stavros Plakides (1983–1990), a late Greek professor of Astronomy at the University of Athens, speculated that Philolaus, after having experienced the violence in southern Italy, avoided placing the Sun in the center of the Universe. Fear for his life may have been the motive for adopting the milder approach of placing the "central fire" instead (1974).

Diogenes Laertius, an important source from which we draw the views of Philolaus, mentions that opinions were divided as to who claimed first that the Earth is indeed moving: "It is told that he [Philolaus] was the first to claim that the Earth moves in a circle, while others ascribe it to Icetas of Syracuse" [Diog.Laert. *Lives of Eminent Philosophers* VIII, 84, 85)].

Aetius, another source, informs us that concerning the motion of the Earth Philolaus taught the following: "Others believe that the Earth is immobile. Philolaus on the contrary, believes that the earth is moving in a circle around the fire, tracing a tilted circle, just like the Sun and the Moon does" [Aet. *De Vestutis Placitis* III, 13, 1. 2. (D 378)]. Therefore, Philolaus came at a disagreement with his master, and taught that the earth was not immobile in the center of the world, but was circling the "Central Fire".

Diogenes Laertius also informs us that Plato bought a copy of the work of Philolaus for, what was at that time, a very high price: "Some authorites, amongst them Satyrus, say that he wrote to Dion in Sicily instructing him to purchase three Pythagorean books from Philolaus for 100 mnae" [Diog. Laertius, *Lives of Eminent Philosophers,* III 9].

Plato, according to Plutarch, studied the work of Philolaus very carefully, and, nearing the end of his life, was convinced that the Earth is indeed moving around the Sun: "As Theophrastus informs us, Plato, near the end of his days had regrets for his older opinion, by which he unfittingly placed the Earth at the center of the Universe" [*Platonicae Quaestiones* H1 915, vol. $XIII_1$, 76-78]. The study of Philolaus may have been the reason for another change in the views of Plato: In *Republic* he identifies the

celestial equator with the ecliptic, an idea which was different from that expressed in *Timaeus*.

Aristotle, in his book *On the Heavens* (*De Caelo*), provided us with some commentary on a few pythagorean views: "These affirm that the centre is occupied by fire and that the Earth is one of the stars, and creates night and day as it travels in a circle about the centre" [Aristotle, *On the Heavens* B, 13, 293a, 21–23]. Also, "The Pythagoreans make a further point. Because the most important part of the Universe – which is the centre – ought more than any to be guarded, they call the fire which occupies this place the Watch-tower of Zeus, as if it were the centre in an unambiguous sense, being at the same time the geometrical centre and the natural centre of the thing itself... For this reason there is no need for them to be alarmed about the universe, nor to call in a guard for its mathematical centre; they ought rather to consider what sort of thing the true centre is, and what is its natural place" [Aristotle, *On the Heavens* B, 13, 293b, 1–10].

The late professor of Astronomy at the University of Athens Demetrios Cotsakis (1976) mentions that the creation of the world–view which Philolaus describes was indeed revolutionary for the scientific thought of the time. He specifically mentions the views of the Italian astronomer Giovanni Schiaparelli (1835–1910), who wrote, as cited in Cotsakis (1976), the following, concerning the views of the Pythagoreans and the system proposed by Philolaus: "The system of Philolaus was not a fruit of some restless imagination, but came through the torque and pull of one who sets the outcomes of observation in accordance with a predetermined principle, which exists above the nature of things ... Appreciating this, and combining it to the fundamental theorems of the Pythagorean Philosophy ,the system of Philolaus naturally appears as one the most wonderful creations of human genius. His critics are incapable of appreciating the power of research, which was necessary, in order to unify the ideas of the roundness of the Earth, its levitation in space, and its motion. Indeed, without these ideas, there would have

been no Copernicus, neither Kepler, nor Galileo or Newton" [1976, p. 30].

THE VIEWS OF ICETAS, ECPHANTUS AND HERACLIDES OF PONTUS

Beyond the theories of Philolaus of Croton, there were other students of Pythagoras, like Icetas and Ecphantus of Syracuse as well as Heraclides of Pontus (c. 5th century BC), who put forward novel ideas.

Icetas of Syracuse claimed that the Heaven, the Sun, the Moon and the stars were immobile, and the only thing that moved was the Earth. Concerning his views, Cicero mentions the following: "As Theophrastus says, Icetas of Syracuse was of the opinion that the heaven, the Sun, the moon and the stars (i.e. the planets) and all that is high above are immobile, and nothing in the world is moving, apart from the Earth. But as it rotates around its axis with the greatest possible speed, its motion causes all these phenomena to appear, which would have appeared were the Earth immobile and heaven rotated instead of it" [Cicero, *Academica priora II,* xxxix, 123].

It appears that this theory was embraced by both Ecphantus and Heraclides as well, both of which believed that the Earth rotated in space, just like a wheel around its axis.

Therefore, the students of Pythagoras were the ones to reduce our planet to its real place and motions, while at the same time holding a pyrocentric planetary theory, which certainly assisted Aristarchus of Samos (310–230 B. C.) to formulate his novel heliocentric theory.

According to Hippolytus, the Pythagorean Ecphantus appears to have also followed an "atomic theory" of Pythagorean inspiration, by "giving body" to units, which were directed and governed by some divine force, "nous" (the mind). He also mentions that Ecphantus believed that the Earth spins around its axis with an eastern direction,

but does not change its place in space. [Hippol. *Ref.* I 15 (D. 566W. 28)]. These last two pieces of information are also mentioned by the doxographer Aetius, who finds Heraclides in agreement with Ecphantus. [Aet. *De Vetustis Placitis*, III, 13, 3 (D. 378)].

Heraclides in particular appears to have modified the atomic theory of Leucippus and Democritus, proposing that the first material elements were molecules and not atoms. According to him, the universe was composed of small material molecules which did not share any connection.

THE VIEWS OF OTHER PHILOSOPHERS

Anaximander and Seleucus

So far we have mentioned the views of the Pythagoreans concerning the motion of the Earth. However, even before the Pythagoreans, during the 6th century B. C., Anaximander, was most likely the first Greek philosopher-astronomer to talk about the motion of our planet around the center of the world, which may have been the Sun. He was a fastidious astronomer who produced detailed maps of the heavens and proposed that the earth was a rotating disk that was separated from the apeiron ("detachment of the Earth"). This information can be found in the work *Expositio rerum mathematicarum ad legendum Platonem utilium* of Theon Smyrnaus (70–135 A. D.), who lived during the reign of Emperor Adrian.

Anaximander's views were adopted by later philosophers like Empedocles of Agrigentum (490–430 B. C.), Parmenides of Elea (early 5th century B. C.), Aristarchus of Samos, Cleomedes (2nd or 3rd century B. C.) and several Pythagoreans.

Another philosopher, Seleucus of Seleucia (*c.* 2nd century B. C.), was an astronomer of the hellenistic period from Anatolia, who supported a heliocentric theory of his own. Fragments of his work are found in the works of

Plutarch, Strabo, Aetius and Hippolytus. Hippolytus informs us that the Earth was indeed moving, and that the Moon played a part in its axial rotation as well as in its orbit around the Sun. [*Philosophoumena,* Book C, 897C, 14–16]. The same source also informs us that he believed that the Cosmos was infinite [*Philosophoumena,* Book B, 886C, 6].

Plutarch mentions a few of his other astronomical ideas [*Platonicae Quaestiones* H1 915, vol. XIII$_1$, 76–78], but unfortunately, all of the original work of Seleucus has been lost.

Aristarchus of Samos

After the Pythagoreans, appeared the great astronomer Aristarchus of Samos (310–230 B. C.), the foremost originator of the heliocentric theory as we know from the book of Archimedes *Arenarius* [I 4–6 (3, 180–182), manuscript 2, Cod. Laurent. Gr. 28].

Plutarch, also, writes about the heliocentric theory of Aristarchus of Samos [*De placitis philosophorum* II, 24 (7, 355a)].

Aristarchus' hypothesis was original and quite bold for its time. For this reason Plutarch mentions that he was accused of atheism [*De facie in orbe lunae*, 923A (15, vol. XII, p. 54)]. Aristarchus, according to Aetius was helped to escape in Alexandria by his teacher Straton of Lampsacus (Aetius, *Placitorum Compositione* book 7, 313b, 16–17).

It is thus apparent that there were several Greek thinkers whose philosophical thoughts disputed the validity of the geocentric system and its fervent followers.

Unfortunately, overcoming the objections of the heliocentrists, the geocentric system, as was formulated by Claudius Ptolemy (2nd century A. D.), reigned for centuries, seconded by the weight of the views of Aristotle, whose work was held as indisputable during the Dark Ages.

EMPEROR JULIAN

The heliocentric theory was not completely forgotten however. During the 4th century A. D. emperor Julian (336–363 A. D.) studied with care the works of the ancient Greek philosophers, which he held in deep regard. His studies took place in the philosophical schools of Athens. Enchanted by the beauty of the ancient Greek spirit, he wished to revitalize it. He believed that the Earth's world order was influenced by a heavenly and divine hierarchy, in which everything originated from the unique God, the illuminating Sun.

He was interested in philosophy as well as astronomy, and rose as a fervent supporter of the heliocentric system. In his book *Hymn to King Helios dedicated to Sallust* (*Hymn to the king Sun dedicated to Sallust*), he writes: "For that the planets dance about him as their king, in certain intervals, fired in relation to him, and revolve in a circle with perfect accord, making certain halts, and pursuing to and fro their orbit, as those who are learned in the study of the spheres call their visible motions; and that the light of the moon waxes and wanes varying in proportion to its distance from the Sun, is I think, clear to all" [*Hymn to King Helios dedicated to Sallust*, 135b, 1–6].

Therefore, Julian held the Earth, as a planet, revolved in a circular orbit around the Sun. He believed that all the planets revolved in circular orbits around the Sun, in determined intervals (i.e. constant distances). The above clearly show that the theory of Aristarchus hadn't been forgotten, but during the 4th century A. D. enjoyed advocacy.

CONCLUSION

Beyond the seed of the heliocentric theory that we saw in the Orphic Hymns, several scholars of Ancient Greece supported this "heretical" view. Its main introdu-

cers were the Pythagorean philosophers Philolaus, Icetas, Ecphantus, Heraclides and foremost Aristarchus of Samos, who gave the Sun its rightful place in the Pythagorean "central fire".

The heliocentric theory did not prevail, however, and instead, the geocentric model, elaborated by the great astronomer Claudius Ptolemy, reigned for centuries in the West, supported by the weight of Aristotle's agreement with it.

Yet, the heliocentric theory had not perished, since in the 4th century A. D. the Emperor Julian, a believer in the divinity of the Sun, became a fervent supporter. In the end, the heliocentric system faded away until the 16th century when the great Polish clergyman and astronomer Mikolaj Kopernik (Nicolaus Copernicus 1473–1543 A. D.), brought it back to light (1995). The hypotheses of Aristarchus of Samos and the preparation of the Pythagoreans were the foundations for the great Polish astronomer's thoughts.

Signatures for illustrations (find in Serbian text):

No 1 / p. 83 – Phanes: God of light, truth and justice. Here he is depicted within an egg–shaped ecliptic with the zodiacal signs and the four basic elements. Above and below him are two halfs of the cosmic egg, and Phanes is depicted with wings like Eros. In his right hand he holds thunder (like Zeus does) and a scepter in his left, signifying his kingly place on the world. The curled snake on him symbolizes the Earth, the cup stands for water, the wings for air and the torch for fire. Its legs are shaped like a fork, just like those of the god Pan.

No 2 / p. 84 – The Homeric Universe: In the Universe of Homer's times, the mountains can be seen to rise over the surface of the great disk of the Earth, the Ocean spreading

around them, while the center is dominated by Mount Olympus which rises up to heaven. In its highest peak, the all-seeing Zeus is seated, supervising both immortal gods and mortal men, sometimes rewarding and sometimes punishing them. Beyond Olympus spreads Heaven, supported by the pillars of Atlas. In heaven we can locate the Moon, the stars and the constellations.

In particular, in this figure we can distinguish – but not referred to by Homer – the constellations of Hydra, Corvus, Crater, Cancer, Leo, Gemini, Taurus as well as the Pleiades open cluster(as cited in D. Cotsakis, 1976, p. 18).

No 3 / p. 91 – Anticthon: The hypothetical invisible Earth, which according to the Pythagoreans occupied the antipodes of the Earth.

No 4 / p. 94 – The world view of Philolaus.
In the world view of Philolaus, the center is occupied by the Central Fire, Anticthon (Counter-Earth, CE), The Earth, the Moon (M), the Sun, and beyond those lie the spheres of the five planets and that of the fixed stars. The crystalline spheres around the Central Fire are 10 (= 1+2+3+4), equal to the sum of the first four numbers.

No 5 / p. 99 – The coin of the emperor Julian, known as Julian Apostate from the collection of Sergije Dimitrijević. This roman emperor was born in 332 in Constantinople. His relative Constantius II proclamed him in Mediolanum for cesar of the West on the 6th of November 355. The army proclamed him for the emperor (august) in February in Paris. After the death of Constantius II, on the 3rd of November 361, he became the unique emperor of the whole Roman empire. He passed away on the 26th of June 363, because of the wound obtained in the war against Sassanide empire. He was a philosopher and a writer who attempted to return the pagan religion.

МУЗЕЈ НАУКЕ И ТЕХНИКЕ

Phlogiston®

Часопис за историју науке

Journal of the History of Science

ISSN 0354-6640 — БРОЈ 16 ISSUE NO — Година 2008

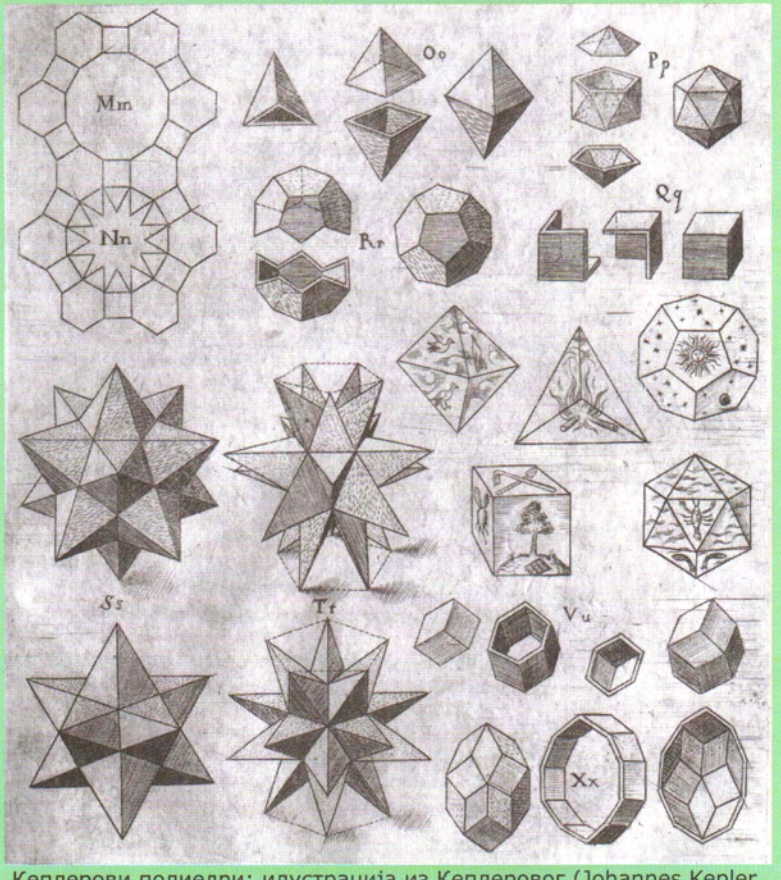

Кеплерови полиедри: илустрација из Кеплеровог (Johannes Kepler, 1571–1630) дела *Хармоније света* (Harmonices mundi) из 1619. године.

НАУЧНА ПОЛЕМИКА

 UDK: 523(38) ; 113(38)

Ефстратије Теодосиу, Ари Даканалис[1],
Милан С. Димитријевић[2], Петрос Мантаракис[3]

ПОРЕКЛО ХЕЛИОЦЕНТРИЧНОГ СИСТЕМА

Апстракт: Анализирана је еволуција хелиоцентричне теорије у античком свету, од њених почетака у *Орфичким химнама* до цара Јулијана Апостате у четвртом веку. Посебно су разматране Орфичке химне, погледи питагорејаца, хелиоцентричне идеје Филолаја из Кротона, Хикете, Екфанта, Хераклида Понтијског, Анаксимандра, Селеука из Селеукије, Аристарха са Самоса и цара Јулијана.

УВОД

Још у раној антици, филозофи и астрономи су били обузети питањем које од небеских тела заузима централно место у познатом свету. Геоцентрични систем, у складу са антропоцентричним погледом, поставио је нашу малу планету у центар универзума. Уживајући наклоност већине филозофа и астронома, вековима је била доминантна теорија. Ипак, било је и

[1] Департман за астрофизику, астрономију и механику, Физички факултет, Атински универзитет, Атина
[2] Астрономска опсерваторија, Београд
[3] Чатсворт, Калифорнија, САД

супротних ставова у корист хелиоцентричне теорије. Обично се сматра да је Аристарх са Самоса (око 310. пре н. е. – око 230. пре н. е.) први замислио један негеоцентрични систем. Али, први трагови хелиоцентричног система могу се наћи вековима пре њега, још у *Орфичким химнама* и учењима Анаксимандра и питагорејаца. У почетку, захваљујући значају који је придаван Аристотеловим погледима, а касније, захваљујући мишљењу великог астронома Клаудија Птоломеја (2. век), хелиоцентрична теорија није превладала.

Али, хелиоцентрични систем није био у потпуности заборављен. У току 4. века, цар Јулијан, назван такође Апостата (отпадник), постао је његов велики поборник. Јулијан је сматрао да је Земља планета која се, као и остале, окреће око Сунца по кружној орбити. Дакле, Аристархова теорија није била заборављена у првим вековима нове ере, него је имала и следбенике.

ОРФИЧКЕ ХИМНЕ

Стара учења Орфеја су сматрана основом прве грчке мистичне религије. *Орфичке химне* се састоје од 87 песама у хексаметру или 1200 стихова укупно, које су дошле до нас под насловом *Химне Орфеја Мусеју*, митском Орфејевом ученику или сину.

Химне садрже опширне астрономске информације, делимично сакривене употребом песничког језика, као и интересантне идеје о Стварању и Врховном бићу. Ово последње говори да химне припадају монотеистичком култу, пошто се стварање универзума приписује јединственој врховној сили. Такође, ту налазимо занимљиве појмове *Хаоса* и *космичког јајета*, које је довело до стварања „Фанеса", прворођеног бога, који није само онај који зрачи, него и првобитни творац живота:

„Из очију си обрисао тамни мрак ноћи, свеширећи сјају и чиста света светлости. Тако је Фанес звао славу неба, машући крилима по свету где лети.“ [V Прворођеном, *Кађење миром*, стих 15]

Сл. 1 – Фанес бог светлости, истине и правде. Овде је представљен у еклиптици у облику јајета са зодијачким знацима и четири основна елемента. Изнад и испод њега су две половине космичког јајета, а сам Фанес је представљен са крилима као и Ерос. У десној руци држи муњу (као Зевс), а у левој скиптар који означава његов краљевски положај на овом свету. Змија омотана око њега симболизује Земљу, чаша означава воду, крила ваздух, а бакља ватру. Ноге су му рачваст као код Пана.

Готово сви старогрчки мудраци и писци налазили су инспирацију у темама *Орфичких химни*, и под њиховим утицајем су стварали своје јединствене теорије и учења.

Напоменимо да у *Орфичким химнама* „Хаос“ представља оно што би данас звали пространство, „Геа“ је мајка-земља (а не планета), док је „Ерос“ (љубав) стваралачка сила. У већ наведеној химни на-

лазимо молитву Хаосу, који премошћава етар, а рођен је из космичког јајета:

„О Моћни прворођени [Protogonos], чуј моју молитву, двоструки, рођени из јајета, и лутајући кроз етар..."
[V Прворођеном, *Кађење миром*, стих 1]

Сл. 2 – Хомеров универзум: У васељени хомеровских времена, могу се видети планине како се дижу са површине великог диска Земље, Океан се шири око њих, док у средишту доминира планина Олимп, која се диже до неба. На његовом највишем врху, столује свевидећи Зевс, надгледајући како бесмртне богове тако и смртне људе, које некада награђује, а некада кажњава. Поред Олимпа су небеса подржана Атласовим стубом. На небу можемо да видимо Месец, звезде и сазвежђа.
На овој слици можемо да уочимо – мада их Хомер не помиње – сазвежђа Хидру (Hydra), Гаврана (Corvus), Пехар (Crater), Рака (Cancer), Лава (Leo), Близанце (Gemini), Бика (Taurus) и отворено јато Плејаде [наведено према Cotsakis, 1976, стр. 18].

У хомеровско време, сматрано је да је Земља равна кружна плоча, око које је река, Океан. Овај појам је очигледан из следећег стиха:

„Стари Океане такође дубоко поштују твоју врховну наредбу, којом течне руке окружују чврсту земљу."

[X Пану, *Кађење различитим мирисима,* стих 15]

Химне помињу Небо које је владар света, и окрећс се око Земље:

„Велико Небо [Ouranos], чији моћни оквир не зна за починак... Чуј, владару света,..., који се као сфера заувек окрећеш око земље."
[III Небу, *Кађење тамјаном,* стих 1]

Један други стих сугерира да су почеци хелиоцентричног система изгледа у *Орфичким химнама*, као што је раније нагласио грчки астроном Константин Хасапис (Constanstinos Chassapis, 1967), и Марија Папатанасију (Maria Papathanassiou, 1978., 1980), доцент на Математичком факултету Атинског универзитета:

„Чуј златни Титану! Сијајући као злато идеш горе, дугачким кораком, о небеска светлости...
...ти [Сунце] који спајаш епохе ...Ти си владар света...
Са златном лиром, црташ хармоничну путању света...
...[ти] који луташ кроз ватру и крећеш се наоколо по кругу."
[VIII Сунцу, стих 2]

Израз „[ти који привлачиш] *црташ хармоничну путању света*" је изненађујући пошто то може бити клица идеје о хармоничном кретању планета око Сунца, појам који је широко коришћен најмање првих пет векова пре наше ере, а можда и раније. Ако укључимо планете у појам света, онда се златно Сунце може сматрати као привлачно средиште њихових хармоничних путања. Можемо дакле претпоставити да се зачетак хелиоцентричне теорије може наћи у *Орфичким химнама.*

Даље у химни (34) Аполону, налазимо следеће:

„Локсијасу, чисти! ... Помешао си у једнаким деловима зиму и лето..."
[XXXIV Аполону, стих 6,... и 20]

Дакле, „Локсијас" Сунце (у смислу „нагнут") помешао је годишња доба и поделио их у два једнака дела, лето и зиму. То је веома значајан астрономски детаљ који је скренуо пажњу астрономске јавности, зато што је повезан са временом настанка *Орфичких химни*. Ако ову информацију схватимо дословно, и погледамо уназад, када су лето и зима били потпуно исте дужине, закључићемо да су *Орфичке химне* вероватно настале близу следећих датума: 1841. пре н. е. или 1366. пре н. е. (Chassapis, 1967. и Papathanassiou, 2003). Овај закључак тражи претпоставку да су стари Грци имали веома способне астрономе у раној антици, у прилог чему имамо мало чињеница.

Још један одломак, мада се односи на Хестију, богињу огњишта, изгледа да доприноси хелиоцентричном аспекту Химни. То је химна (84) [Хестија]:

„Ти која заузимаш центар дома највеће и вечне ватре."
[LXXXIV Хестији, стих 2]

У *Orphicorum Fragmenta* један одломак нам говори о ротацији Земље. У том делу се каже да је Мусеј знао путању звезде и кретање сфере око Земље, пошто се ова округла Земља обрће у једнаким временским периодима око своје осе (Фр. 247, стих 24–26, стр. 261–262). Дакле, у *Орфичким химнама* су дотакнути сви елементи хелиоцентричног система – централно Сунце, небески објекти који се крећу по својим путањама и ротирајућа Земља.

ПИТАГОРЕЈЦИ

Филозоф и математичар Питагора је основао своју школу у Кротону у јужној Италији око 540. године пре н. е. Он и његови следбеници сматрали су да су најважнији космолошки принципи засновани на бројевима и да је то основна реалност. Питагорејска школа поставила је темеље филозофије математике и физике, повезујући поредак и хармонију звука са хармонијом универзума.

Практично сви Питагорини ученици обучавани су у астрономији, али су њихова проучавања кретања и растојања планета извођена прилично мистичним прилазом. Веровали су у мистичне и свете односе између бројева и појава које они описују. У питагорејском учењу, планетарна растојања била су аналогна небеској музичкој хармонији, коју су стварали хармонични звуци. Сматрали су да се ова хармонија непрестано ствара, те да је вечни израз – највишег реда – јединствене божанске хармоније.

Занимљиво је и помало провокативно да 2500 година после питагорејаца, савремена наука долази до идеја веома сличних њиховим. На пример, модерна теорија струна сматра да је све на микроскопском нивоу комбинација вибрирајућих, мултидимензионалних струна. Питагорејци, који су развили концепт „музике и хармоније сфера", видели би честице као микроскопске струне чије ритмичке вибрације стварају друге честице, то јест „музичке ноте". Ове ноте, са друге стране, стварају музику небеских сфера. Дакле, сходно њиховим погледима, цео наш свет би изгледао као музичка симфонија, компонована од ових нота.

Питагорина школа била је братство, са различитим степенима иницијације, а вероватно је била заснована попут Орфичких религијских заједница. Њен допринос геометрији, музици, аритметици и астрономији био је веома значајан за развој људске

мисли. Преко геометрије, као и хармоније звукова и бројева, питагорејци су развили појам савршенства у универзуму, и сковали одговарајућу реч да га опишу: „Космос“. Ово име је изведено или од речи „космо“ са значењем „поређати у ред“ или од речи „космема“ што значи „драги камен – украс“. Сам Питагора је, изгледа, први користио реч „Космос“ према доксографу Аетију: „Питагора је био први који је именовао место свих ствари Космосом, захваљујући његовој уређеној природи“ [Aetius, *De Vetustis Placitis,* II, 1, 1 (D. 327, 8)].

Питагорејска школа сматрала је да је суштина свих ствари „број“, прилично апстрактан појам, који се не може опажати чулима, већ само помоћу разума. На тај начин, следбеници ове филозофске школе изједначавали су бесконачност са оним материјалним елементима који се нису могли измерити или дефинисати.

Неки елементи питагорејске космологије дошли су до нас преко Аристотелових књига, односно *Метафизике*. Према питагорејцима, Космос је настао пошто је „Један“ дошао у постојање. „Један“ или „хен“ на грчком – служио је као први принцип и привукао је „бесконачно“ (апеирон) властитој суштини, и успоставио му границу (limit – перас). За њих јасно значење ова два појма, „ограничено“ и „бесконачно“, није дошло до нас, али се претпоставља да се могу односити на просте и парне бројеве.

Аристотел нам преноси следеће: „Елементи бројева, према њима, су Парно и Непарно. Од њих прво је ограничено а друго неограничено; Јединица се састоји од оба (јер поседује и непарност и парност) [напомена: или пошто додавањем претвара парни број у непарни, а непарни у парни (Александар, Теон из Смирне) или зато што је сматрана као принцип и парних и непарних]. Број је изведен из Јединице; а бројеви, као што смо рекли, сачињавају цео универзум доступан чулима“ [Aristotle, *Metaphysics*, A5, 986, 15].

Аристотел нам је оставио и друге коментаре питагорејских идеја: „Такође је апсурдно, или је то пре

једна од немогућности ове теорије, да се уведе стварање ствари које су вечне. Нема разлога да се сумња да ли су их питагорејци увели или не; они јасно изјављују да када се „Један" успоставио – било из равни површина или семена или из нечега што они не могу да објасне – одмах је најближи део Бесконачног почео да се креће у њега и био ограничен Границом [напомена: ако су бројеви вечни, апсурдно је да треба да су створени]" [Aristotle, *Metaphysics*, 1091a, 14].

Још један космолошки појам који је усвојила Питагорејска школа био је да је Стварање почело из једне јединствене тачке, која се непрекидно ширила до бесконачности. Може се закључити да су питагорејци веровали да је универзум еволуирао од инфинитезималног језгра које се сферично ширило.

Друга идеја у коју су питагорејци веровали била је да је Земља округла и непокретна у центру Космоса, који је такође сферичан: „...вода, земља и ваздух; ови елементи се смењују и прелазе један у други потпуно и комбинују се да створе продуховљен, интелигентан, сферичан универзум са земљом у средишту а земља је и сама округла и настањена" [Diogenes Laertius, *Lives of Eminent Philosophers*, VIII, 25, 8–10].

Многи питагорејци имали су истоветан став о округлој Земљи, која се налази у средишту универзума, *а да је ништа не придржава.* То је у оно време била нова идеја, и јасан је показатељ напретка када се упореди са претпоставкама које су пре тога имали различити грчки филозофи.

Према професору астрономије Деметриосу Коцакису (Demetrios Kotsakis): „Питагора је био први који је учио да привидно кретање Сунца на небеској сфери са истока на запад, може бити анализирано као два различита кретања: једно дневно са истока на запад, паралелно екватору, и једно годишње са запада на исток, дуж еклиптике" [Kotsakis, D., 1976, p. 28].

У шестом веку пре н. е. неки ученици и следбеници Питагоре, од којих су најважнији Филолај из Кротона, Хераклид из Понта, Екфант из Сиракузе, као

и други, веровали су у „пироцентричну“ слику света. То значи да су прихватали да је елемент ватра био „први принцип“ Космоса. Веровали су да се после Стварања, елемент ватра нагомилао у средишту Космоса и да је његово привлачење суседних делова било део стварања и обликовања различитих тела што је начинило сферични универзум.

ИДЕЈЕ ФИЛОЛАЈА ИЗ КРОТОНА

Филолај из Кротона (450–500 пре н. е.), ширио је питагорејске идеје у односу на „први принцип“, организујући и пишући преглед питагорејске филозофије. Изгледа да је био главни стваралац филозофских појмова „ограничености“ и „бесконачности“ и склада међу њима, који је, према његовим погледима, био постигнут захваљујући „броју“. Веровао је да је Космос јединствен и да је настао стварањем из средишта, где се налазила ватра. Око ње је сместио „Антихтон“ (или Антиземљу – хипотетичку невидљиву Земљу), Земљу, Месец, Сунце, пет планета познатих у то доба (Меркур, Венера, Марс, Јупитер и Сатурн), и сферу непокретних звезда. Дакле, десет небеских тела „играло“ је око средишњег огња, број који су питагорејци сматрали светим. Размишљало се да је Антихтон уведен управо из тог разлога, наиме да се број небеских тела повећа до светог броја десет.

Према неким подацима Архип, Лисија и неколико других, преживели су крваву буну против питагорејаца у Кротону. Килон, бивши Питагорин ученик, који је избачен из школе зато што није хтео да се сагласи са њеним принципима, подстакао је напад, када су сви следбеници били окупљени. Извесно је да су учења Питагоре и његових ученика, њихове иновативне теорије, мистицизам и аристократске политичке тенденције изазвале силовиту реакцију њихових демократских противника који су многе од њих или убили

или прогнали: „Килон из Кротона... и његови савезници, гонили (убијали) су Питагорејце до последњег човека“ [Iamblichus, *De vita Pythagorica* (V. P.) 248–249 ff].

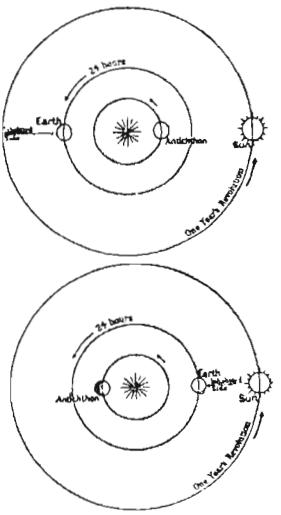

Сл. 3 – Антихтон: Хипотетичка невидљива Земља, која је према питагорејцима антипод Земље

Један од преживелих, Лисија, можда је постао учитељ Филолаја из Кротона. Према другим подацима, његов учитељ није Лисија него Питагора, и Филолај је преживео Килонову буну заједно са другим питагорејцима као што су Лисија (или Лисис) и Архип.

Филолај је поучавао питагорејску филозофију и писао књиге *Bachae* и *О природи* A, B и C (Космос, Природа, Душа). Један постојећи одломак из његове прве књиге каже: „Свет је униформан, почиње својим стварањем из средишта, и из средишта се равномерно ширио према навише и наниже, одржавајући једнако растојање до центра“ [Diels–Kranz, 1996, *Die Fragmente der Vorsokratiker*].

Неколико извора пружају информацију о неким његовим космолошким погледима: „Првобитно Један, почетак стварања Универзума зове се Хестија“ [*On*

Nature, fragment 7, Stob. *Eclogae* I 21, 8 (стр. 189, 17 W)].

Диоген Лаертије напомиње: „Према Деметрију, у његовом раду *О људима истог имена*, Филолај је био први који је објављивао питагорејске расправе, којима је дао наслов *О природи*, почињући овако: 'Природа се у уређеном универзуму састоји од неограничених и ограничавајућих елемената, и такав је био цео универзум и све што је у њему'" [Diogenes Laertius, *Lives of Eminent Philosophers*, 85 (A1 I 398, 20)].

Доксограф Аетије (Aetius, I 3, 10), обавештава нас (наводећи Теофрастуса) о следећем: „Филолај верује да је око центра Универзума ватра, коју назива „хестија свега" и „Зевсова кућа", „мајка богова", „олтар, ограничење и мера природе". Постоји и друга ватра која се налази у спољашњој области Универзума. Центар, каже он, је природно настао први, и око њега игра десет небеских тела: Сфера непокретних звезда, онда пет планета, Сунце, Месец, праћен Земљом и Антихтоном, и после свега тога огањ „хестије" који лежи око средишта. Спољашња област, која окружује цео Универзум, је место где се елементи налазе у чистом стању, непомешани, и ово место он назива „Олимп". Све што лежи испод Олимпа, наиме део где се налазе пет планета са Сунцем и Месецом, он назива „космос", а област испод ове, сублунарни простор ...назива „небо". Мудрост је релевантна за поредак који важи међу небеским телима, док је врлина релевантна за неред онога што је подвргнуто рађању. Прво је савршено а друго несавршено" [Aet., *De Vetustis Placitis*, II 7, 7 (D. 336, vermutlich Theophrast. im Poseidonios–Excerpt)].

Горе речено је још једном поменуо Аетије: „Питагорејац Филолај ставља огањ у средиште (а то је жижна тачка Универзума), затим ставља Антихтон, онда наше станиште, Земља долази на треће место супротно [од Антихтона] и креће се по кругу, због чега је Антихтон невидљив за становнике Земље. Сила која управља светом налази се у централној ватри, коју је

Бог поставио, као кобилицу брода, да заснива основицу сфере, која чини свет“ [Aet., III 11, 3 (D. 337 из Теофрастуса)].

На основу свега реченог можемо закључити да се, према Филолају, ништа на „Олимпу“ и у „Космосу“ никада не мења, док се у областима до Месеца, свако биће коме је дарован живот, рађа, мења и на крају умире. Земља и све друге планете окрећу се око Хестије у истом смеру, али на разним нивоима и различитим брзинама. Хестија је невидљива зато што сјаји своју светлост антиподима Земље, Сунце нема сопствену светлост него прима и акумулира Хестијин огањ.

Филолај је, својим довођењем под сумњу традиционалне геоцентричне космологије, поставио основе за Аристархову хелиоцентричну теорију, која је јасно довела у питање централну улогу у Универзуму наше мале планете. Мада није поставио Сунце у центар, идеја „средишње ватре“ сигурно је послужила као основа за хелиоцентричну теорију. Ставрос Плакидес, професор астрономије на Атинском универзитету, претпоставио је да је Филолај, пошто је искусио насиље у јужној Италији, избегавао да постави Сунце у средиште Универзума. Страх за сопствени живот можда је био мотив да усвоји блажи прилаз, стављајући ту „централни огањ“ уместо њега [Plakides, 1974].

Диоген Лаертије, важан извор одакле добијамо погледе Филолаја, помиње да су подељена мишљења о томе ко је први устврдио да се Земља заиста креће: „Говори се да је он [Филолај] био први који је тврдио да се Земља креће по кругу, док други то приписују Хикети из Сиракузе“ [Diog. Laert., *Lives of Eminent Philosophers* VIII, 84, 85)].

Аетије, други извор, обавештава нас да је Филолај о кретању Земље подучавао следеће: „Други верују да је Земља непокретна. Насупрот томе, Филолај сматра да се Земља креће по кругу око огња, описујући нагнуту кружницу, управо као Сунце и Месец“ [Aet., *De Vestutis Placitis* III, 13, 1. 2. (D 378)].

Дакле, Филолај се не слаже са својим учитељем, и сматра да Земља није непокретна у центру света, него кружи око „средишњег огња".

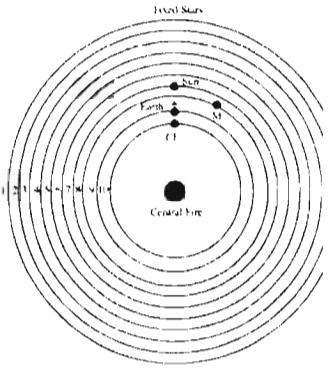

Сл. 4 – Филолајева слика света.
У Филолајевој слици света, средиште заузима Централни огањ. Око њега круже Антихтон (Против-Земља – Counter-Earth, CE), Земља, Месец (M), Сунце, а иза њих леже сфере пет планета и сфера непокретних звезда. Око средишњег огња има 10 (= 1+2+3+4) кристалних сфера, што је једнако збиру прва четири броја.

Диоген Лаертије нас такође обавештава да је Платон купио примерке Филолајевих радова за, у оно време, изузетно велику цену: „Неки ауторитети, међу њима Сатирус, кажу да је Диону са Сицилије написао упутство да му купи три питагорејске књиге Филолаја за 100 мина" [Diog. Laertius, *Lives of Eminent Philosophers*, III 9].

Платон је, према Плутарху, веома пажљиво проучавао радове Филолаја, и после темељног читања, пред крај живота, постао убеђен да се Земља заиста креће око Сунца: „Како нас обавештава Теофраст, Платон је пред крај својих дана зажалио због свог старог мишљења, по коме је неприкладно ставио Земљу у средиште Универзума" [*Platonicae Quaestiones* H1 915, vol. XIII$_1$, 76–78]. Проучавање Филолаја можда је било разлог и за једну другу промену Платонових погледа, наиме у *Држави* он поистовећује не-

бески екватор са еклиптиком, што је идеја коју је изменио у *Тимеју*.

Аристотел, у својој књизи *О небу* (*De Caelo*), даје коментаре неких питагорејских погледа: „Они потврђују да се у средишту налази огањ и да је Земља једна од звезда, и ствара ноћ и дан како путује по кругу око центра" [Aristotle, *On the Heavens* B, 13, 293a, 21–23]. Такође, „Питагорејци изводе даљи закључак. Зато што најзначајнији део Универзума – односно центар – највише треба да буде чуван, они називају ватру која се налази на овом месту Зевсова кула-стражара, као да је то недвосмислено центар, истовремено и геометријско и природно средиште саме ствари... Због тога, за њих нема потребе да се узнемиравају због Универзума, нити да позивају на заштиту његовог математичког центра; пре треба да разматрају шта је у ствари прави центар, и које је његово природно место" [Aristotle, *On the Heavens* B, 13, 293b, 1–10].

Деметриос Коцакис, професор астрономије на Атинском универзитету (Cotsakis, 1976), сматра, да је стварање погледа на свет које описује Филолај било заиста револуционарно за научну мисао тога доба. Посебно помиње уверења италијанског астронома Ђованија Скјапарелија (Giovanni Schiaparelli, 1835–1910), који је, како наводи Коцакис (Cotsakis, 1976), коментарисао на следећи начин погледе питагорејаца и систем који је предложио Филолај: „Филолајев систем није био плод немирне маште, већ је резултат довијања и натезања некога ко доводи исходишта посматрања у склад са претходно одређеним принципом, који постоји изнад природе ствари... Ценећи ово, и комбинујући га са основним теоремама питагорејске филозофије, Филолајев систем се природно јавља као једна од најчудеснијих креација људског генија. Његови критичари су неспособни да цене истраживачку снагу која је била потребна, да би се објединиле идеје округлости Земље, њеног лебдења у простору и кретања. Заиста, без ових идеја, не би било ни Копер-

ника, као ни Кеплера, Галилеја или Њутна“ [Cotsakis, 1976, стр. 30].

ПОГЛЕДИ ХИКЕТЕ, ЕКФАНТА И ХЕРАКЛИДА ПОНТИЈСКОГ

Осим теорија Филолаја из Кротона, било је и других Питагориних ученика који су ширили нове идеје, као Хикета и Екфант из Сиракузе и Хераклид из Понта.

Хикета из Сиракузе је тврдио да су Небо, Сунце, Месец и звезде непокретни и да је једино небеско тело које се креће Земља. О његовим погледима Цицерон напомиње следеће: „Како каже Теофраст, Хикета из Сиракузе био је мишљења да су небо, Сунце, Месец и звезде (тј. планете) непокретне као и све што је високо горе, и да се ништа у свету не креће осим Земље. Али како се она окреће око своје осе са највећом могућом брзином, њено кретање је узрок свих феномена који се запажају а који би се појавили када би Земља била непокретна а небеса се обртала уместо ње“ [Cicero, *Academica priora II,* XXXIX, 123].

Показало се да су ову теорију прихватили Екфант и Хераклид; обојица су веровала да се Земља креће окрећући се у простору управо као точак око своје осовине.

Дакле, Питагорини ученици су довели нашу планету на њено право место и стање кретања, заступајући истовремено пироцентричну планетарну теорију, која је свакако помогла Аристарху са Самоса (310–230 пре н. е.) да формулише нову хелиоцентричну теорију.

Према Хиполиту, изгледа да је Питагорејац Екфант, такође, био следбеник једне „атомистичке теорије“ питагорејске инспирације, „дајући телесност“ јединицама, које су биле вођене и управљане неком божанском силом, „нусом“ (разумом). Такође, напо-

мање да је Екфант сматрао да се Земља обрће око своје осе у источном правцу, али да не мења положај у простору [Hippol., *Ref.* I 15 (D. 566W. 28)]. Ова два последња става помиње и доксограф Аетије, који налази да је Хераклид у сагласности са Екфантом [Aet., *De Vetustis Placitis*, III, 13, 3 (D. 378)].

По свему судећи Хераклид је изменио атомску теорију Леукипа и Демокрита, предлажући да су основни елементи материје молекули, а не атоми. Према њему, Универзум је састављен од малих материјалних молекула који не деле никакву везу.

ПОГЛЕДИ ДРУГИХ ФИЛОЗОФА

Анаксимандар и Селеук

До сада смо изнели погледе питагорејаца у односу на кретање Земље. Ипак, чак и пре њих, у шестом веку пре наше ере, велики филозоф Анаксимандар, био је највероватније први грчки филозоф–астроном који је говорио о кретању наше планете око центра света, који је можда Сунце. Био је одличан астроном, који је направио детаљне карте неба и предложио да је Земља диск који ротира а одвојен је од апејрона (њена „одвојеност“ у простору, од небеског свода). Ово се може наћи у делу *Expositio rerum mathematicarum ad legendum Platonem utilium* Теона из Смирне (70–135), који је живео за време цара Хадријана.

Ставове филозофа Анаксимандра усвојили су каснији филозофи као Емпедокле из Агрићента (490–430 пре н. е.), Парменид из Елеје (рани 5. век пре н. е.), Аристарх са Самоса, Клеомед (2. или 3. век пре н. е.) и неколико питагорејаца.

Други филозоф, Селеук из Селеукије (око 2. века пре н. е.), био је хеленистички астроном из Анатолије, који је ширио своју сопствену хелиоцентричну теорију. Одломци његовог дела налазе се у делима Плутарха, Страбона, Аетија и Хиполита. Хиполит нас

обавештава да се Земља заиста креће и да Месец има улогу у њеном обртању око осе, као и окретању око Сунца [*Philosophoumena,* Book C, 897C, 14–16]. Исти извор нам каже да је сматрао да је Космос бесконачан [*Philosophoumena,* Book B, 886C, 6].

Плутарх помиње мало и друге његове астрономске идеје [*Platonicae Quaestiones* H1 915, vol. $XIII_1$, 76-78]; нажалост целокупно Селеуково дело је изгубљено и немамо сазнања о његовој хелиоцентричној теорији.

Аристарх са Самоса

После питагорејаца, појавио се велики астроном Аристарх са Самоса (310–230 пре н. е.), који је, како знамо из Архимедове књиге *Arenarius* [I 4–6 (3, 180–182), манускрипт 2, Cod. Laurent. Gr. 28], први увео хелиоцентричну теорију.

Плутарх, такође, пише о хелиоцентричној теорији Аристарха са Самоса [*De placitis philosophorum* II, 24 (7, 355a)].

Аристархова хипотеза била је оригинална и веома смела за то доба. Због тога је, како помиње Плутарх, био оптужен за безбожништво [*De facie in orbe lunae*, 923A (15, vol. XII, стр. 54)]. Аристарху је, према Аетијусу, његов учитељ, Стратон из Лампсакуса, помогао да побегне из Александрије [Aetius, *Placitorum Compositione* књига 7, 313b, 16–17].

Очигледно је да је било неколико грчких мислилаца који су оспоравали исправност геоцентричног система света.

Нажалост, прелазећи преко примедби хелиоцентричара, геоцентрични систем, како га је формулисао Клаудије Птолемеј (2. век), владао је вековима, подржаван ауторитетом који су имали Аристотелови погледи, о чијем се делу, током Доба таме, није могло расправљати.

ЦАР ЈУЛИЈАН

Вера у хелиоцентрични систем још није била напуштена. Током 4. века цар Јулијан (332–363) је пажљиво проучавао радове старих грчких филозофа, које је дубоко поштовао. Ова изучавања одвијала су се у филозофским школама Атине. Одушевљен лепотом старог грчког духа, желео је да га обнови. Веровао је да је место Земље у Универзуму под утицајем небеске и божанске хијерархије, у којој све потиче од јединственог бога сјајног Сунца.

Сл. 5 – Новац цара Јулијана познатог као Јулијан Апостат (одступник) из збирке Сергија Димитријевића. Овај римски цар рођен је 332., у Константинопољу. Његов рођак Констанције II прогласио га је 6. новембра 355. у Медиолануму (Милано) за цезара Запада, а војска га је фебруара 360. у Паризу прогласила за цара (августа). После смрти Констанција II, 3. новембра 361. године постаје јединствени император целог Римског царства. Умире 26. јуна 363. од ране задобијене у рату против Сасанидске империје. Био је филозоф и писац који је покушао да врати паганску религију.

Интересовала га је филозофија и астрономија, и био је велики поборник хелиоцентричног система. У својој књизи *Химна краљу Сунцу посвећена Салусту*, пише: „Због тога планете играју око њега као око свога краља, на сигурним растојањима, подстакнуте односом са њим, и окрећу се око њега у круг у савршеном складу, застајкујући повремено и идући амо тамо својим путањама, како они који су знalци у проучавању сфера, зову њихова видљива кретања; а и

месечева светлост се повећава и ишчезава, мењајући се сразмерно његовом растојању од Сунца што је мислим јасно" [Julian the Emperor, 1954: *Hymn to King Helios dedicated to Sallust*, 135b, 1–6].

Према томе, Јулијан је сматрао да је Земља планета, која се по кружној орбити окреће око Сунца. Сматрао је да се све планете крећу око Сунца по кружним путањама, на одређеним размацима, то јест на сталним растојањима. Ово јасно показује да Аристархово учење није било заборављено, него је у току четвртог века уживало и подршку.

ЗАКЉУЧЦИ

Осим клице хелиоцентричног погледа на свет коју смо уочили у *Орфичким химнама*, неколико учених људи старе Грчке подржавало је овај, за њихово време „јеретички" став. Најзначајнији, који су га заступали, били су питагорејски филозофи Филолај, Хикета, Екфант, Хераклид и најважнији Аристарх са Самоса, који је Сунцу дао право место у питагорејском „средишњем огњу".

Хелиоцентрична теорија ипак није преовладала, и геоцентрични систем који је разрадио велики астроном Клаудије Птолемеј, владао је вековима на западу, подржаван ауторитетом Аристотела, који га је усвојио.

Ипак, хелиоцентрична идеја није пропала, пошто је у 4. веку цар Јулијан Апостата, који је веровао у божанственост Сунца, постао њен убеђени присталица. На крају, хелиоцентрични систем је ишчезнуо док га у 16. веку, велики пољски астроном и човек цркве Николај Коперник (Nicolaus Copernicus, 1473–1543), није поново изнео на светлост дана (Copernicus, 1995). Теорија Аристарха са Самоса и припремни радови питагорејаца, биле су основа за размишљања великог пољског астронома.

Захвалница

Овај рад је урађен у оквиру пројекта „Астрономија, историја и филозофија", потписаног између Астрономске опсерваторије у Београду и Катедре за астрономију, астрофизику и механику, Школе за физику, Универзитета у Атини. Такође је део пројекта „Историја и епистемологија природних наука", при Министарству за науку и технолошки развој Републике Србије.

ЛИТЕРАТУРА / REFERENCES

Aetius, *Placitorum Compositione* (*De Vetustis Placitis*), vol. IV 9, 8. in Diels Hermann: *Doxographi Graeci*. Berolini. Apud Walter De Gruyter et Socios, Editio Quarta, 1879 (reprinted 1965).

Archimedes, *Arenarius* in *Opera Omnia*, Bibliotheca Scriptorum Graecorum et Romanorum Teubneriana. Ed. I. L. Heiberg, vol. II corrigenda Adiecit E. S. Stamatis. Stutgardiae in Aedibus MCMLXXII.

Aristotle, *The Metaphysics,* vol. I–IX, The Loeb Classical Library, Book XVII with an English Translation by H. Rackham. London: William Heinemann Ltd. Cambridge, Massachusetts: Harvard University Press, 1956.

Aristotle, *On the Heavens* (*De Caelo*), The Loeb Classical Library, with an English Translation by W. K. C. Guthrie. M. A. London. William Heinemann Ltd. Cambridge, Massachussets: Harvard University Press, MCMLIII (First printed 1933., reprinted 1936., 1947., 1956).

Cicero, *Academica Priora,* with an English Translation by H. Rackham, M. A. The Loeb Classical Library. London. William Heinemann LtD. Cambridge, Massachussetes: Harvard University Press, MCMLXI (First printed 1933., reprinted 1951., 1956. and 1961). pr. 11, 12, 3.

Cicero Marcus Tullius, *Academica,* Publ. Lubrecht & Cramer, Ltd. October 1984.

Copernicus Nicolaus, *De Revolutionibus Orbium Coelestium, libri VI. On the Revolution of Heavenly Spheres*, Trans. By Charles Glenn Wallis, Prometheus Books, October 1995.

Cotsakis Demetrios, *The pioneers of Science and the creation of the World,* Ed. Zoe, Athens, 1976.

Die Fragmente der Vorsokratiker von Hermann Diels, Herausgegeben von Walther Kranz, Ester und Zweiter Band, Weidmann, Zürich, 1996.

Diogenes Laertius, *Lives of Eminent Philosophers,* vol. II, IX 34–35, pp. 3, 441–445. Heinemann, London, 1925., The Loeb Classical Library; English translation by R. D. Hicks, revised and reprint 1959.

Hippolytus, *A Refutation of All Heresies*: *Refutationis Omnium Haeresium* (*Filosofoumena*), Patrologia Greca (P. G.) 16, In Origenes, Liber VII, 404–405, 339. Typographi Brepols Editores Pontificii, Parisiis 1857–1866.

Iamblichus, *De vita Pythagorica* (V. P.) *Life of Pythagoras*, with the English translation by Thomas Taylor in 1881, J. M. Watkins, 1965, p. 248–249 ff.

Iuliani Imperatoris, *Oratio* IV (*To King Helios*), Vol I, 143 B. 146 D., Lipsiae Teubner, 1875.

Orphic Hymns, Ed. Ideotheatro, Athens [in Greek, sine anno].

Orphicorum Fragmenta, Ed. O. Kern, Weidmann, 1922.

Papathanassiou Maria, *Cosmological and cosmogonical aspects in Greece during 2nd millennium B. C.,* PhD. Thesis, University of Athens [self edited], Athens, 1978 [in Greek].

Papathanassiou Maria, „Aristarchus the Samian", *Mathematical Review* 20, Editions of the Hellenic Mathematical Society, 1980, p. 91-120 [in Greek].

Papathanassiou Maria, „Primordial astronomical learning", *Elefterotypia-Historica*, Athens, January 2, 2003, p. 6–12 [in Greek].

Petrides S., *The Orphic Hymns, Astronomy in the Age of Ice* [self edited], Athens, 2002 [in Greek].

Plakides Stavros, „The Geocentric and the Heliocentric Theory", *Parnassos* 16, Athens 1974 [in Greek].

Plutarch Chaeronsis, *Scripta Moralia,* Graece et Latine, Tomus Secundus, De placitis Philosophorum Libri quinque, Parisiis, Editore Ambrosio Firmin Didot MDCCCXLI.

Stobaei Ioanni, *Eclogae,* Wachsmuth Dox. 336 B 20–337 B 10 and Bibliotheca of the ancient Greek writers, Ed. Georgiades, Athens [sine datum].

Theonis Smyrnaei, *Philos. Platonici,* Ed. Hiller. Lipsiae 1878, p. 198, 14–19.

Theon of Smyrna, *Mathematics useful for understanding Plato or Pythagorean Arithmetic, Music, Astronomy, Spiritual Disciplines,* Trans. by Christos Toulis, Wizards Bookshelf, 1979.

„The Orphic Hymns through astronomical view", *Pravda Online*, February 20, 2007.

The works of the emperor Julian. The Orations of Julian, IV. Hymn to king Helios dedicated to Sallust, The Loeb Classical Library, Trans. By Wilmer Cave Wright, Ph.D., William Heinemann Ltd. Cambridge, Massachusetts: Harvard University Press MCMLIV (First printed 1923, reprinted 1930, 1954).

Chassapis Constantinos, *The Greek Astronomy of the 2nd millennium B. C. according the Orphic Hymns,* PhD. Thesis, University of Athens [self edited], Athens 1967 [in Greek].

МУЗЕЈ НАУКЕ И ТЕХНИКЕ

Phlogiston®

Часопис за историју науке

Journal of the History of Science

ISSN 0354-6640 — БРОЈ 18/19 ISSUE NO — Година 2010/2011

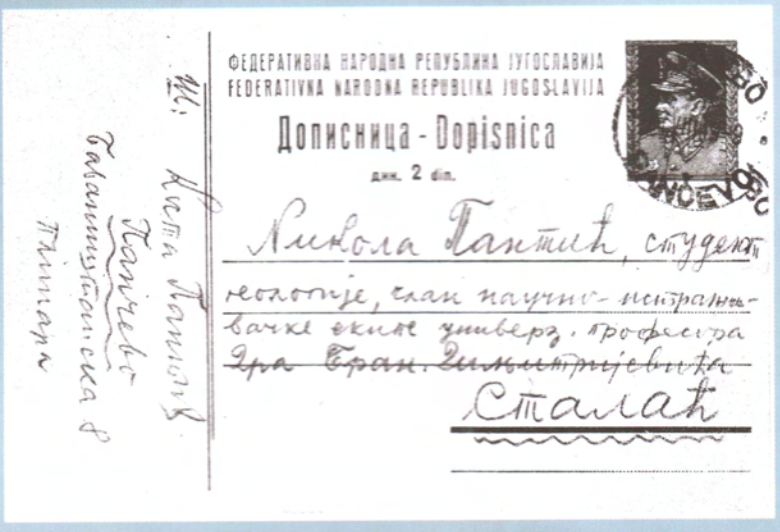

Дописница Николе К. Пантића са летње праксе

ИЗ ИСТОРИЈЕ НАУКЕ И ТЕХНИКЕ
ФИЛОЗОФИЈА НАУКЕ
ОРГАНИЗАЦИОНЕ НАУКЕ И КУЛТУРА
ДОКУМЕНТИ
ПОЛЕМИКЕ

Оригиналан научни рад UDK: 524.86:929 Лезбиос Б.

Ефстратије Теодосију, Василије Н. Маниманис*,
Милан С. Димитријевић**

„ТЕОРИЈА СВЕГА" БЕНЏАМИНА ЛЕЗБИОСА

Апстракт: Бенџамин Лезбиос или Бенџамин са Лезбоса био је свештеник и научник грчког просветитељства. Будући под очигледним утицајем духа западноевропског просветитељства, Бенџамин је од стране званичника православне цркве био оптужен због новог учења о природи. Био је утицајан филозоф и поставио је теорију *пантахекинетона*, уједињујућу теорију природе.
Кључне речи: Бенџамин Лезбиос, теорија пантахекинетона.

1. Елементи биографије

Млађи савременик Руђера Бошковића, Бенџамин Лезбиос, као и наш велики научник, формулисао је једну унифицирану „теорију свега", што пружа могућности за различита упоређивања и паралеле. Рођен је у старом Пломарију, на острву Лезбос, 1759. или 1762. године. Био је син Амирисе и Јоаниса Георгантиса или Георгантелиса или Кареа. Крштено име му је вероватно било Василије и основно образовање је до-

* Универзитет у Атини, Одељење астрофизике – астрономија и механика, Школа физике
** Астрономска опсерваторија, Београд

био у своме селу. Када је имао 17 година, дошао је на Атос и закалуђерио се у манастиру Пантократор; тада је добио име свога ујака Бенџамина.

Године 1790. уписао се на Универзитет у Пизи а затим на Екол Политекник у Паризу, где му је између осталих предавао Антоан-Лоран Лавоазје (Argyropoulou, 1983: 49). Упоредо са основним студијама природних наука и филозофије, Бенџамин је проучавао дела представника европског просветитељства. Пошто је у Паризу остао неколико година, ушао је у кругове учених Грка у дијаспори и упознао се са Адамантиосом Кораисом. Бенџамин је почео да пише чланке за часопис *Λοΐιος Хермес*. Пошто је завршио циклус студија у Паризу, 1798. одлази на годину дана у Енглеску, на чувену Гриничку опсерваторију где се налази телескоп Виљема Хершела (Valetas, G., 1974: 280).

Године 1799, Бенџамин се вратио у Кидониес (Ајвалик) и тамо почео да предаје у школи, која је 1803. реорганизована и названа „Академија Кидониеса". Бенџамин је предавао филозофију (етику и метафизику), алгебру, геометрију, физику и астрономију, а нарочито је наставу физике допуњавао извођењем експеримената (ΕΕΕ, 1983: 239). Његова предавања доприносила су ширењу славе Академије као високе наставне институције, у коју су долазили многи студенти са Балкана, чији је број премашивао шест стотина.

Садржај и методи његове наставе изазвали су реакције, које су, оснажене личним антагонизмом нарочито Атанасиоса Париоса, довеле до оптужби против Бемџамина у Васељенској патријаршији у Константинопољу и од стране Патријарха Калиника IV.

Оптужбе су биле да Бенџамин предаје: да се Земља креће а Сунце стоји непомично, да су небеска тела настањена другим бићима и да је Сунце тамно и осветљено рефлексијом.

Године 1803, Бенџамина је Синод Васељенске патријаршије осудио *in absentia* да се одрекне својих теорија (Argyropoulou 1983: 59). Услед интервенције утицајних пријатеља – међу осталима ефеског владике

Дионисија Калиархеса, те фанариотског хегемона Александроса Мурузиса и његовог брата Деметриоса – осуда Патријаршије никада није спроведена.

Након избијања грчког рата за независност прелази у Ајвалик да би, заједно са Папафлесасом, набавио муницију за борбу против отоманске власти. У лето 1821, путује на грчко копно преко острва Псаре, Хидре и Спецеса и настањује се на Пелопонезу. Ту учествује у раду Прве Народне скупштине у Епидаурусу (децембар 1821), као један од 20 представника пелопонеског Сената. Године 1822, као члан Егејске комисије, Бенџамин обилази грчка острва организујући отпор, а у исто време сакупља новац за финансирање борбе. На Другој Народној скупштини у Астросу (март - април 1823) Бенџамин је изабран у деветочлану комисију за израду нацрта привременог Кривичног закона, а следеће године учествује у плановима за стварање више школе у Аргосу (ΕΕΕ, 1983: 239). Активност му је прекинута у септембру 1824, када у Науплиону на Пелопонезу умире од тифуса.

2. *Дела Бенџамина са Лезбоса*

Дела Бенџамина Лезбиоса могу се разврстати у три главне групе: филозофски радови, радови из физике и астрономије, математички радови (Houzaios, G. M., 2009, 7). Детаљније то су:

А) Филозофска дела:

1. *Apologia [...] pros tas sykofantias tou neou philosophou* (*Извињење због клеветања новог филозофа)*, без датума, 1-12.

2. *Stoicheia ethikis* (*Елементи моралне филозофије*). У почетку необјављено, публиковано је post-mortem са уводом и коментарима Р. Аргиропулоса, Центар за модерна грчка истраживања, Национална фондација за истраживања, Атина 1994, 1-302.

3. *Stoicheia tis metaphysikis* (*Елементи метафизике*). Беч, Аустрија, објавио Johannes Schneirer, 1820, 1-471.

Б) Дела из физике и астрономије:

1. *Physiki*, објављено постхумно.

2. *Meteorologika* и *Astronomia*, Лицеј у Волосу, 1991.

В) Математичка дела:

1. *Stoicheia arithmitikis* (*Елементи аритметике*), том I, Беч, Аустрија, објавио Johannes Schneirer, 1818, стр. xiv + 197.

2. *Geometrias Euclidou Stoicheia* (*Елементи Еуклидове геометрије*), том II, Беч, Аустрија, објавио Johannes Schneirer, 1820, 1-255.

3. *Stoicheia Algebras* (*Елементи алгебре*). Необјављено.

4. *Trigonometria* (*Тригонометрија*). Необјављено.

Бенџамин Лезбиос је писао углавном уџбенике за предмете које је предавао у Кидониесу (Ајвалику). У све три претходне групе присутне су филозофске и научне теорије просветитељства, под лупом његовог личног критичког прилаза. Језик који користи је уобичајени говорни облик грчког, али не оклева да уведе сопствени систем интерпункције и да се врати старом грчком да би изразио научне термине. Због оваквих иновација, био је оптужен да је „неписмени филозоф" (Argyropoulou, 1983:55).

3. Пантахекинетон теорија

Садржај Бенџаминових рукописа пажљиво је проучавао физичар др Антонис Н. Андриотис, који је написао књигу на ову тему, неку врсту коментара под насловом: *„Пантахекинетон" теорија Бенџамина са*

Лезбоса: Од картезијанског етера до универзалности и дуалности феномена преноса енергије (2009).

Али зашто „од картезијанског"? Интерес за природни свет поново се рађа после италијанске ренесансе; полет му даје развој експерименталних наука у 16. и 17. веку. Први велики филозоф, следбеник ове еволуције, био је Рене Декарт или Cartesius (René Descartes, 1596-1650). Две основице његове филозофије, како је описао у своме делу *Расправа о методи* (*Discours de la méthode*, 1637), су сумња и логичка мисао. Није хтео да се ослања на божанско откровење, али истовремено није прихватао без оклевања оно што нам нуде чула; то је оно што га је вероватно довело до чувене изреке: 'cogito ergo sum'.

Према Хајзенбергу, његов првенствени допринос теоријским и експерименталним наукама је то што је омогућио физичарима да описују свет без помињања Бога, а то је напредак који је пружио велико поверење у науку. *Ускоро се показало да је ова основа била готово неопходна општа претпоставка за све експерименталне науке.*

Представимо сада Пантахекинетон теорију. Бенџамин одбацује Њутнов закон [универзалне] гравитације и уводи појам *пантахекинетона*, флуидног супстратума који се слободно креће у свим правцима и узрок је свих природних и духовних појава (Valetas, 1974: 282). Према С. Куманудису (1988): „пантахекинетон, извесни флуид, постоји у природи према Бенџамину Лезбиосу и стимулише чула и осећања".

Можда је Бенџаминов најважнији цитат: „Пантахекинетон је флуид који непрекидно тече од једног тела ка другом, а његов долазећи и одлазећи флукс је пропорционалан запремини тела" (*Physics*, §6). У следећем пасажу пише, (*Physics*, §64): „Тако сам овом флуиду дао назив Пантахекинетон; и његово постојање може бити само пука хипотеза, ипак од сада ће сва пракса физике бити да докаже његово постојање и својства" (Andriotis 2009, p. 45). На основу Бенџаминових идеја у *Физици* и *Елементима метафизике* може

се закључити да је *пантахекинетон* смело предложен као узрок свих појава у природи и души. Етимологија појма настаје од речи *пантахе* = свугде и *кинетон* = кретање (*Dictionary of Greek language*, Papyros ed., Athens, 2008).

Садржај Бенџаминове *Физике* је двострук. Најпре, то је уџбеник и енциклопедија физике, од античких времена до његовог доба, који представља *пантахекинетон* теорију, унифицирани модел за представљање различитих природних појава.

Пажљиво проучавање Бенџаминовог дела показује да он није био пуки преводилац западних идеја у физици; имао је слободан и пионирски дух.

Бенџамин не оклева да додирне сам садржај метафизичких исходишта. На основу *пантахекинетон теорије*, покушава да објасни 'зао поглед' и разне друге феномене помешане духовне и телесне природе; али пре свега настоји да научи о ствараоцу објеката, Богу: „Али пошто знање духовне природе захтева знање ствараоца бића, односно Бога, очигледно је да је неопходно учити о Богу" (тема коју додирује у *Physiki Theologia* = *Теолоџија Природе*, то јест метафизика).

Као што је Андриотис (2009) писао о *пантахекинетон* теорији читајући Бенџаминову *Физику* постаје очигледно да је то добро урађен физички модел са консолидованом унутрашњом структуром и савршеном самоусаглашеношћу. Штавише, *пантахекинетон* теорија може да пружи одговоре на експерименталне резултате оног доба. *Пантахекинетон* теорија покушава да објасни природне појаве заједно са неким метафизичким на сличан начин, пошто су за њега психички феномени *епекеина* (продужетак) природних појава. Андриотис карактерише овај модел као „семи-космолошки".

Бенџамин помиње погледе античких пресократовских грчких филозофа, мада подржава хелиоцентрички систем. Проблем настаје са новим физичким астрономским идејама и језиком који користи. Због тога је називан „неписмени и безбожник", пошто је дово-

дио у сумњу библијску космологију, па је на крају био присиљен да напусти Ајвалик.

4. *Теорије о етеру*

Пантахекинетон по својој природи има карактер сличан етеру, мада се описује као нешто есенцијалније. Бенџамин наводи теорије о преносу енергије помоћу таласа, гравитације, магнетизма, електрицитета, светлости, топлоте и звука, да би лоцирао њихове слабе тачке, које остављају место за развој савршенијег или фундаменталнијег новог предлога за описивање ових појава.

Бенџамин са Лезбоса увек прво наводи тадашње погледе и теорије, онда их коментарише и на крају даје сопствено објашњење засновано на *пантахекинетон* хипотези, када је могуће.

Дакле Бенџаминова *Физика* је истовремено јасна и конзистентна презентација прихваћених модела у физици његовог доба, као и модела који су доминирали у прошлости, на пример у антици.

5. *Сукоб између две „школе"*

Бенџаминов рад у физици одражава сукоб између две школе мишљења: Њутнове, која прихвата деловање сила на даљину; и картезијанске, која сматра да је потребан утицај медијума (као што је етар) да би сила деловала; ова школа уводи механицистичке моделе да би то објаснила.

У том контексту, *пантахекинетон* се јавља као сложени медијум са мултифункционалним особинама; он посредује у преносу гравитационог и електромагнетног међудејства, у преносу надражаја преко неурона и утиче на простирање светлости.

Полазећи од таласне природе простирања светлости, Бенџамин са Лезбоса, на основу погледа Ро-

берта Бојла (који сматра да је светлост лонгитудинални талас у етеру, као звук у ваздуху), изражава мишљење да је *пантахекинетон* носиоц звука.

Андриотис (2009) повезује Бенџаминове погледе са научним знањем у физици његовог доба, са модерним унификационим теоријама 20. века, као и са питагорејским теоријама о „*олкос* сфери", Аристотеловском теоријом о етеру и картезијанском теоријом о вртложном кретању.

У четвртом поглављу *Физике* Бенџамин пише о гравитацији, критикујући Њутнове ставове. Износи своје гледиште да је гравитација резултат притиска фине, невидљиве супстанце, док је у контексту *пантахекинетон* теорије појам „односити са" употребљен за објашњење гравитације и електричних и магнетних сила.

Бенџамин наставља са појмом „тежине" у *пантахекинетон* теорији, називајући „куфа" тела она која немају „тенденцију" да гравитирају.

У параграфу 93 *Физике* помиње се инерција, која се, мада пропорционална маси, разликује од гравитације, пошто делује у сваком правцу.

Затим следе теорије о магнетном (магнетизму) и електричном (електрицитету) флуиду. Андреотис напомиње да је појам „истицања" електричног флуида последица његове идентификације са *пантахекинетоном*.

Затим у рукопису следи теорија светлости, где се помиње Касинијев резултат о растојању од осам светлосних минута између Сунца и Земље. Бенџамин ту даје и објашњење поларне светлости помоћу *пантахекинетон* теорије.

У петом поглављу је приказано гравитационо привлачење у светлу *пантахекинетон* теорије: „Дакле, с обзиром на постојање пантахекинетона, овде је дато како гравитационе појаве треба да буду објашњене."

Постоје и одељци са насловима: *Моћ одржавања на површини и пантахекинетон, Инерција и пантахекинетон, Структура материје и пантахекине-*

тон, Однос магнетног флуида (магнетизма) и пантахекинетона. А увек следе и друкчији погледи: *Теорије Декарта и Халеја о земљином магнетном пољу.*

У магнетној теорији, Бенџамин са Лезбоса прво доказује да се, према *пантахекинетон* теорији, Земља понаша као џиновски магнет, па је њено магнетно поље (геомагнетно поље) као код обичног магнета: „Како се чини, Декартова хипотеза је хипотеза траженог. Пошто је питање шта је магнет, а Декарт је претпоставио да је Земља магнет" (*Физика*, §574).

Андриотис (2009) напомиње да описана интеракција између два обична портабл магнета има заједничке црте са Бенџаминовим објашњењем гравитационог привлачења (*Физика*, §65). Механизам привлачења је истоветан.

Коначно, Бенџамин пише о статичкој густини пантахекинетона и његовом току. После много година, налазимо да је „флукс поља" природна величина, која се односи на интензитет поља (Гаусов закон). Према Бенџамину са Лезбоса „термогоно" (топлота) нити је материјална супстанца (као што се распростањено сматрало у његово доба), нити појава; то је „флуид" исте природе као сунчеви зраци (*Физика*, §980). О ватри, топлоти и светлости пише: "Ватра и топлота се не налазе у порама тела него у њиховим молекулима" (§987). А осим тога: ...„како нас чула обавештавају, сунчеви зраци нису ништа друго него топлота" (*Физика*, §1019).

У оквиру *пантахекинетон* теорије, дат је и поступак одбијања светлости: „Долази до диференцијације између сунчевог и земаљског флуида" (*Физика*, §1316).

6. Закључак

Пантахекинетон теорија је заснована на дубоком разумевању познатих експерименталних провера својстава гравитације, електрицитета, магнетизма, оп-

тичких појава, топлоте и звука. Не избегавајући указивање на озбиљне недостатке ове теорије, закључујемо да је „ингениозан предлог“ Бенџамина Лезбиоса довољан да га идентификујемо као веома важну особу за историју покушаја унифицираног описа природе, што се данас често назива потрага за „теоријом свега“.

(Списак литературе дат је иза енглеске верзије текста)

Original Scientific Paper UDK: 524.86:929 Lesbios B.

Efstratios Theodossiou, Vassilios N. Manimanis,*
Milan S. Dimitrijević**

THE THEORY OF PANTACHEKINETON OF BENJAMIN LESBIOS

Abstract: Benjamin Lesbios or Benjamin of Lesbos was a scholar monk of Greek enlightenment. Clearly influanced by the spirit of Western European enlightenment, Benjamin was accused by Orthodox Church officials for teaching the new natural world knowledge. He was an important philosophical mind and introduced the *Pantachekineton*, a pioneering unifying natural theory.
Keywords: Benjamin Lesbios, theory of Pantachekineton

1. Biographical elements

The younger contemporaneous of „Rudjer Bošković", Benjamin Lesbios or Benjamin of Lesbos, as our great scientist, has formulated one unified theory „of everything", which gives oportunity for different comparations and parallels. He was born in the old Plomari, in the Lesbos island, in the year 1759 or 1762. He was the son of Amyrissa and Ioannis Georgantis or Georgantellis or Karre. His given name was most probably Vassilios and he received some elementary education in his village. When

* University of Athens, Department of Astrophysics – Astronomy and Mechanics, School of Physics
** Astronomical Observatory, Belgrade

he was 17 years old, he went to Hagio Oros (Athos, the monastic state) and was ordained a monk at the Pantocrator Monastery; then he received the name of his maternal uncle, abbot or prior Benjamin.

In 1779, young Benjamin was sent as a sacristan to the monastery's branch of Hagios Nicolaos (St. Nicholas) in Kydonies, now Ayvalik in Turkey, where his uncle Benjamin was staying (Argyropoulou, 1983: 47). There, he attended courses in the flourishing School of Ioannis Economos (Dimitrakellis) for approximately one year; then, prompted by Economos, and after he was ordained a deacon and a priest, he left for the island of Patmos to study there. He stayed there until 1786; for the next three years he studied in the then famous School of Chios (1786-1789), where he attended, among other teachers, Athanassios Parios, while he became a friend of Dorotheos Proios (afterwards a bishop) (EEE, 1983: 239).

Still a young man, father Benjamin returned in Ayvalik in 1789 or 1790; there he taught for a while in the Economos School. Ioannis Economos mediated to secure for his former student the financial support of wealthy members of the local society in order to send him for further studies in Europe. In 1790, following a suggestion by Proios, Benjamin of Lesbos enrolled at the University of Pisa and then at École Polytechnique in Paris, where he was taught, among others, Antoine-Laurent Lavoisier (Argyropoulou, 1983: 49). In parallel with his main studies in natural sciences and philosophy, Benjamin also studied the works of representatives of European Enlightenment. As he stayed in Paris for several years, he entered the cycles of the Greek scholars of diaspora and he was acquainted with Adamantios Korais. Benjamin started to write articles in the *Logios Hermes* magazine. Having finished a cycle of courses in Paris, in 1798 he went for approximately one year in England, at the famous Greenwich Observatory, where he saw William Herschel's telescope (Valetas, G., 1974: 280).

In late 1799, Benjamin rejected the proposal of the Chios Commissioners to teach in the School of Chios

under Athanassios Parios; instead, he returned to Kydonies (Ayvalik) and worked in the School there, which in 1803 was reorganized and called the "Academy of Kydonies". There Benjamin taught philosophy (ethics and metaphysics), algebra, geometry, physics and astronomy, while especially in the case of physics he complements his teaching with the conduction of experiments (EEE, 1983: 239). He had been supplied with a part of the necessary experimental devices and relative manuals by Korais in Paris. He taught based on manuscripts and following contemporary teaching methods, with frequent use of teaching aids and experiments. His teaching contributed in the spread of the Academy's fame as a higher education institute, attracting many students from the Balkans with a total student number of more than 600.

However, both the content and the methods of his teaching caused reactions, which, reinforced by personal antagonisms, especially in the case of Athanassios Parios, led to charges brought against Benjamin in the Ecumenical Patriarchate in Constantinople and Patriarch Callinicus IV.

The charges were that Benjamin was teaching: i) that the Earth moves and the Sun stays motionless, ii) that the celestial bodies are inhabited by other creatures and iii) that the Sun is dark and is illuminated by reflection.

In 1803 Benjamin was condemned *in absentia* by the Synod of the Ecumenical Patriarchate to revoke his theories (Argyropoulou 1983: 59). Yet, with the intervention of influential friends – among others the bishop of Ephesus Dionysius Caliarches and the Phanariot hegemon Alexandros Mourouzis along with his brother Demetrios – the patriarchal condemnation was never carried out. Finally, Benjamin Lesbios, with the support of his students and of the middle class of Kydonies (Ayvalik), continued to teach in the Academy until 1812 (Valetas, 1974: 283). However, he himself had expressed since 1808 his will to resign and leave the city due to continuing reactions by conservatives-archaists and the problems these reactions were causing to the operation of the School.

In 1812 Benjamin Lesbios was invited to direct no other than the Patriarchal School in Constantinople (Istanbul)! He finally rejected this invitation, deciding to settle to his native island of Lesbos and to establish his own school there (EEE, 1983: 239). However, despite the support of the islanders and several of his students from Kydonies, his plans did not succeed and he decided to move to Istanbul. There he was offered the hospitality of medical doctor Georgios Desyllas, in the house of which he worked as a private tutor. In this period he is invited to become schoolmaster in Kurutsesme and at a school in Athens, which had been just established by the 'Philomoussos Society' (Argyropoulou, 1983: 64–68). Having rejected these proposals, Benjamin accepts in 1817 an invitation by the hegemon (ruler) of Wallachia Ioannis Karatzas to reorganize the Academy of Bucharest. In this work he found a collaborator: Alexandros Mavrocordatos, the ruler's nephew (EEE, 1983: 239). Nevertheless, his work there was soon interrupted, after the fall of Karatzas in September 1818, and Benjamin went to Jassy (Iasi). He will stay in Moldova for the next two years under the protection of ruler Alexandros Callimachis and during this time he will become a member of Philiki Etaireia ('Society of the Friends'), the secret organization for the liberation of Greece (Valetas, 1974: 288). From this point onwards, Benjamin's work as a teacher will be combined with efforts for the independence of Greece from the Ottoman rule.

In this context, Benjamin of Lesbos is found in September 1820 in Izmir (Smyrna), teaching in 'Evangeliki' School, the higher education school in the city, while at the same time he acts as the local agent of Philiki Etaireia (EEE, 1983: 239). After the break of the Greek War of Independence, Benjamin moves to Ayvalik in order to gather ammunition for the struggle against the Ottomans, together with Papaflessas. In the summer of 1821 he travels to the Greek mainland, passing from the naval islands of Psara, Hydra and Spetses, and settling in Peloponnese. There he participated in the First National

Assembly of Epidaurus (December 1821) as one of the 20 representatives of the Peloponnesian Senate, where he supported politically his old collaborator Alexandros Mavrocordatos. In 1822, as a member of the Aegean Commission, Benjamin tours the Greek islands organizing the revolt there, while at the same time he collects money for financing the struggle. In the Second National Assembly of Astros (March–April 1823) Benjamin is elected in the nine-member drafting commission for a temporary penal code and next year he participates in making the plans for the creation of a higher School in Argos (EEE, 1983: 239). His actions were interrupted in September 1824, when he died in Nafplio, Peloponnese, from typhus.

2. Works by Benjamin of Lesbos

The works of Benjamin Lesvios can be classified into three main categories: A) Philosophical works. B) Works of physics and astronomy. C) Mathematical works (Houzaios, G.M., 2009, σελ. 7). In more detail:

A) Philosophical works

1. *Apologia [...] pros tas sykofantias tou neou philosophou* (*Apology to the calumny of the new philosopher*), s.d., pp. 12
2. *Stoicheia ethikis* (*Elements of moral philosophy*). Initially unpublished, it was published postmortem with an introduction and comments by R. Argyropoulou. Center of Modern Greek Research, National Research Foundation, Athens 1994, pp. 302.
3. *Stoicheia tis metaphysikis* (*Elements of metaphysics*). Vienna, Austria, publ. by Johannes Schneirer, 1820, pp. 471.

B) Works of physics and astronomy

1. *Physiki*, published postmortem.

2. *Meteorologika* and *Astronomia* (*Astronomy*). 1st Lyceum of Volos, 1991.

C) Mathematical works

1. *Stoicheia arithmitikis* (*Elements of arithmetic*), vol. I. Vienna, Austria, publ. by Johannes Schneirer, 1818, pp. xiv + 197.

2. *Geometrias Euclidou Stoicheia* (*Elements of Euclid's Geometry*), vol. II. Vienna, Austria, publ. by Johannes Schneirer, 1820, pp. 255.

3. *Stoicheia Algebras* (*Elements of Algebra*). Unpublished.

4. *Trigonometria* (*Trigonometry*). Unpublished.

Benjamin Lesvios authored mainly textbooks for the courses he was teaching in Kydonies (Ayvalik). In all three previous categories, the philosophical and scientific theories of Enlightenment are presented, under the lens of his own critical approach. As for his general thoughts about sciences and philosophy, he recognizes in mathematics the basis of even empirical science and a starting point for philosophical thought; he considers natural philosophy an extension of metaphysics and includes in it, among others, chemistry, astronomy and cosmology. As for the language he uses, it is the common spoken form of Greek, while he doesn't hesitate to introduce his own punctuation system and to resort to ancient Greek in order to render scientific terms. For these innovations, Benjamin was accused as being an 'illiterate philosopher' (Argyropoulou, 1983: 55).

3. The Pantachekineton theory

The texts of Benjamin's manuscripts were assiduously studied by physicist Dr. Antonis N. Andriotis, chief researcher in the Foundation of Research and Technology, who wrote a book on the topic, a kind of commentary, under the title: *The theory of 'Pantachekineton'*

of Benjamin of Lesvos: From the ether of the Cartesians to universality and duality of the phenomena of energy transfer (2009).

But why 'from the Cartesians'? Here it is essential to interpolate: The interest for the natural world experiences a revival after the Italian Renaissance; it is boosted by the great developments in experimental science during the 16th and 17th centuries. And the first major philosopher who followed this evolution is Cartesius (René Descartes, 1596–1650). The two bases supporting his philosophy, as they are described in his opus *Discourse about the Method* (*Discours de la méthode*, 1637), are: doubt and logical thought. He doesn't want to rely on Divine Revelation, but at the same time he does not accept without hesitation what the senses offer to us; this is what will lead him eventually to his famous dictum: 'cogito ergo sum'.

At this point, it should be noted the discrimination Heisenberg makes between the pre-Socratic philosophers and Descartes:

1. The pre–Socratics searched for the fundamental essence or first principle from which came (and probably still comes) the Universe; all of them were starting from the ontological problem.

2. For Descartes, the basis is the search for the fundamental knowledge. The *cogito* is of a purely nature-of-knowledge κατηγορίας.

However, it is rather inaccurate to state that Descartes gave with his novel philosophical method a new direction to human thought. His prime contribution to both theoretical and experimental science (despite all his mistakes and contrivances, such as the distinction between *res cogitans* and *res extensa*, that mark his philosophy) is, according to Heisenberg, that he gave to physicists the medium to describe the world without speaking about God or the Ego, an advancement which gave a great thrust to science. *It soon turned out that this base was the almost necessary general presupposition for all experimental sciences.*

Let us now present the *Pantachekineton* theory. Benjamin rejects Newton's law of [universal] gravity and he introduces the notion of *'pantachekineton'*, a fluid essence that moves freely towards all directions and is the cause of all natural and soul phenomena (Valetas, 1974: 282). According to S. Coumanoudis: *"pantachekineton, a certain fluid that, according to Benjamin Lesvios, exists in nature and stimulates our senses and sentiments"* 1998.

Probably this was his most important passage: *"The pantachekineton is a fluid that flows incessantly from one body to another, whose influx and outflux is proportional to the body's volume"* (*Physics*, §6). In a subsequent passage, Benjamin writes (*Physics*, §64): *"So, to this fluid I give the name Pantachekineton; and now its existence may be a mere hypothesis, however from this point on the whole practice of physics will be a proof of its existence and properties"* (Andriotis 2009, p. 45). Based on the ideas of Benjamin in his *Physics* and *Elements of metaphysics* it can be concluded that *pantachekineton* is boldly proposed as the cause of all phenomena of nature and soul. The etymology of the word originates from the words *pantache* = everywhere and *kineton* = moving (*Dictionary of Greek language*, Papyros ed., Athens, 2008).

Is this metaphysics? Those that studied the work of Benjamin Lesvios –the most significant publication on the subject remains the Ph.D. dissertation of R. Argyropoulou, 1983 – regard that, apart from the improbability or not of this original theory, this cosmological model is rooted on physics rather than on metaphysics. As Benjamin himself has stated, he proceeded because his 'natural curiosity' did not allow him to stop at the results, but *'dragged him to search for the causes'*.

By studying the manuscripts of both volumes of Benjamin's *Physics*, which are kept in good condition in the Leimon Monastery, in Callone of Lesbos, and in the library of the Plomari Club 'Benjamin o Lesvios' (which has published them in photostatic reproduction), Andriotis (2009) isolated and presented the main points of the

pantachekineton theory in his work, after thirty years of research and studies; he characterizes *pantachekineton* as an 'ether-like element' with such properties that allowed qualitative approaches for most of physics topics known at the age the Lesbos savant was teaching.

The *pantachekineton* theory can be applied to almost all basic phenomena and quantities of physics, as opposed to the then prevailing theories of that age.

A basic search line for Dr. Andriotis was to see if there are any elements of the *pantachekineton* theory that persist in modern physics, and therefore would justify a deeper study of this topic; Andriotis believes that this theory is an important building block in the development of scientific knowledge.

The late Professor of astronomy D. Kotsakis (1940) believed that the *pantachekineton* theory is 'unfortunate'. However, according to Andriotis (2009) Benjamin proposes improvements of old theories at the same time he states new ideas, in a procedure not unlike that followed by modern papers and review papers, in which the proposed theories are systematically compared point-by-point with the corresponding older ones.

The in-depth understanding of the *pantachekineton* theory requires a careful analysis of Benjamin's arguments and their correlation with the current prevailing theories in physics of his age.

Andriotis studied the two-volume opus *Physics* by Benjamin, which consists of 1450 paragraphs and 758 pages, rescued it because it transcribed it, and after studied it he thinks that is as easy-to-read as e.g. the *Astronomy* by Th. Kairis (Mavrommatis 1989).

The content of Benjamin's *Physics* is double: i) It is a textbook and an encyclopaedia of the physics, from the ancient times to his age. ii) It presents the *pantachekineton* theory, the unified model for the explanation of the various natural phenomena.

The careful study of Benjamin's work shows that he was not a mere translator of the Western ideas on physics; he has a free and pioneering thought. According

to him, God is not of the same 'texture' (synaidios) with matter, but instead He is the Creator of matter *ex nihilo* (Kavarnos, 1964). God is omnipotent (*pantodynamos*) and not 'of great power' (*megalodynamos*); the human soul is an essence independent of the body and not a form or *eidos* of the body, as Aristotle has written.

Benjamin of Lesbos responds creatively to the new way of thought, which in the West results in a purely axiomatic and abstract treatment of everything, while he also caters to educational needs of his nation.

Benjamin does not hesitate to tackle metaphysical issues in the same context. Based on the *pantachekineton* theory, he attempts to explain 'evil eye' and various other phenomena of mixed spiritual and bodily nature; but above all he attempts to learn about the creator of entities, God: *"But because the knowledge of the soul's nature requires the knowledge of the creator of beings, that is of God, hence it is evident that it is necessary to learn about God* (a topic he tackles in his *Physiki Theologia* = *Theology of Nature*, that is metaphysics).

As Andriotis (2009) writes about the *pantachekineton* theory, by reading Benjamin's *Physics* it became evident that he was in front of a well-done and well-worked model of physics, with a consolidated internal structure and perfect self-consistency. Moreover, the *pantachekineton* theory could offer answers to the experimental findings of his age. *Pantachekineton* theory attempts to explain natural phenomena along with several metaphysical ones in a similar way, as psychic phenomena are for him *epekeina* (extensions) of natural phenomena. Andriotis characterizes this model as "semi-cosmological".

Benjamin mentions the views of pre-Socratic ancient Greek philosophers, although he is a supporter of the heliocentric system. However, problems arise with the novel physical/astronomical ideas and with the language he uses. This is why he was called 'illiterate and an atheist', as he doubts Scriptural cosmology, and was finally forced to leave Ayvalik.

In the same time period with Benjamin of Lesbos, physics was being taught in Greece by Eugenios Voulgaris, Athanassios Psallidas, Nikephoros Theotokis, Sergios Macraeos, Constantinos Koumas, Constantinos Vardalachos, Dimitrios Darvaris and his student, Theophilos Kairis; in other words there was a real current of 'enlighters' in the occupied by the Ottomans Greece.

5. Theories about ether

Pantachekineton by its own nature has an ether-like character, although it is identified as something much more essential than ether. Benjamin continues by citing theories about energy transfer by waves, gravity, magnetism, electricity, light, heat, and sound, in order to locate their weak points, which leave room for the development of more perfect or fundamentally new propositions for the descriptions of the above phenomena, as he believes.

Benjamin of Lesbos always gives first the current views and theories, then he comments on them and finally gives his own explanation based on the *pantachekineton* hypothesis, where this is possible.

Therefore, Benjamin's *Physics* is at the same time a clear and concise presentation of the prevailing models in the physics of his age, as well as of models that prevailed in the past, e.g. in antiquity.

6. The conflict between two 'schools'

Benjamin's work in physics reflects the conflict between two schools of thought:

1. The Newtonian, which accepts the action of forces from a distance.
2. The Cartesian, which thinks that the intervention of a medium (like the ether) is necessary for a force to act; this school introduces mechanistic models in order to explain these actions.

In this context, *pantachekineton* theory emerges as a complex medium with multifunctional properties; it mediates in the transmission of gravitational and electromagnetic interactions, in the transfer of stimuli through neurons and affects the propagation of light.

As far as the wave nature of light propagation, Benjamin of Lesbos, based on the view of Robert Boyle (who believes light is a longitudinal wave in the ether, like sound waves in the air), expresses the view that *pantachekineton* is the carrier of sound.

Andriotis (2009) correlates Benjamin's views with the scientific knowledge of his age in physics, with the modern unified theories of the 20th century, but also with the Pythagorean theories about the '*olkos* sphere', the Aristotelian theory of ether and the Cartesian theory about whirling motion.

In the fourth chapter of his *Physics* Benjamin writes about gravity, criticizing the Newtonian view. He expresses his view that gravity is the result of the pressure of some fine and invisible material, while in the context of the *pantachekineton* theory the notion of 'carrying away with' is employed for the explanation of gravity and of the electric and magnetic forces.

Benjamin continues with the notion of 'weight' in the *pantachekineton* theory, calling 'koúfa' the bodies that do not have the 'tendency' to gravitate.

In paragraph 93 of the *Physics*, there is a mention of inertia, which, although proportional to mass, differs from gravity, as it acts towards any direction.

The theories about the magnetic fluid (magnetism) and the electric fluid (electricity) follow in the manuscript. Andriotis conjectures that the notion of the 'outflow' of electric fluid is a consequence of its identification with *pantachekineton*.

Several major natural scientists of the 18th century and older are mentioned and their views compared with those of Benjamin in the study by Andriotis (2009), exhausting this topic, such as Descartes, Huygens, Newton, O. Roemer, Snell [or Snellius], R. Hooke, astronomer

J. Bradley, T. Young, astronomer E. Halley (called 'Allius' by Benjamin), Jean-Antoine Nollet (called 'Doxa Noletou', that is 'Glory of Nolletus'), B. Franklin (called 'Glory of Franklee'), etc.

According to Benjamin's manuscript, after the sound theory there is a reference to the term *'diachoresis'*, in the section about 'thermogono' (heat). It can be inferred that *diachoresis* means heat capacity, while *'krasis'* means temperature (*thermo–krasia* in modern Greek). The theory of light follows in the manuscript and there Cassini's finding about the 8 light-minutes from the Sun to the Earth is mentioned. Finally, Benjamin of Lesbos gives an explanation for aurora borealis with the *pantachekineton* theory.

In the fifth chapter there is a presentation of gravitational attraction according to the *pantachekineton* theory: *"Therefore, given the existence of pantachekineton, here it is how the gravitational phenomena should be explained."*

Sections exist under the titles: Buoyancy and pantachekineton, Inertia and pantachekineton, structure of matter and Pantachekineton, Relation of magnetic fluid (magnetism) and pantachekineton. And always a critic follows: the theories of Descartes and Halley about the terrestrial magnetic field.

In his magnetic theory, Benjamin of Lesbos first proves that the Earth behaves as a giant magnet according to the pantachekineton theory and therefore its magnetic field (the geomagnetic field) is like that of a common magnet: *"The hypothesis of Descartes, as it seems, is a hypothesis of the wanted. Because, the question is what is a magnet and Descartes hypothesized that the Earth is a magnet"* (*Physics*, §574).

Andriotis (2009) discerns that the described interaction between two common portable magnets has common features with the explanation of the gravitational attraction given by Benjamin (*Physics*, §65). The mechanism of attraction is identical.

Finally, Benjamin writes about the static density of pantachekineton and about its flow. After many years, we find the 'field flux' to be the natural quantity related with the intensity of the field (Gauss law). According to Benjamin of Lesbos, 'thermogono' (heat) is neither a material substance (as was widely believed in his time), nor an event; instead, it is a 'fluid' of the same nature with sunlight rays (*Physics*, §980). About fire, heat and light he writes: *"The fire and the heat do not dwell in the pores of the bodies, but in their molecules"* (§987). And moreover:

"... the solar rays as our senses themselves inform us, are not something else but heat" (*Physics*, §1019).

There is also the treatment of the reflection of light according to the *pantachekineton* theory: *"There is a differentiation between the solar and the terrestrial fluid"* (*Physics*, §1316).

7. Conclusion

Andriotis (2009) in his epilogue (p. 182) reports: *"My conclusions allow me to describe the pantachekineton theory as a very intelligent and fruitful combination of the worldviews of the Cartesian and Newtonian schools of thought. The pantachekineton theory includes many original elements, which elevate Benjamin of Lesbos to the status of the father of the concept of dual nature of light and energy in general (wave-particle), and of the unified description of all natural phenomena."*

The theory of *pantachekineton* is founded upon a deep understanding of the then known experimental verifications of the properties of gravity, electricity, magnetism, optical phenomena, heat and sound. Without avoiding stressing the serious gaps of this theory, we conclude along with Andriotis that the 'ingenious proposition' of Benjamin of Lesbos suffices to identify him as a very important person for the history of attempts of the unified description of nature, which are today often named as the search for "the theory of everything".

Literature

Andriotis, Antonios, 2009, *The theory of "Pantachekineton" of Benjamin Lesvios: From the ether of the Cartesians to universality and duality of the phenomena of energy transfer*, published by the author, Irakleio [in Greek].

Argyropoulou, Roxanne, 1983, *Benjamin Lesvios and the European thought of 18th century*, Ph.D. dissertation, Institute of Modern Greek Studies of the National Research Foundation (E.I.E.) (reprinted in 2003) [in Greek].

Descartes, René, 1637, *Discours de la méthode*, Laurence J. Lafleur trans.: *Discourse on Method and Meditations*, New York: The Liberal Arts Press, 1960.

EEE: *Ekpaideftiki Elliniki Enkyklopedia – Pagosmio Viografiko Lexiko (Greek Educational Encyclopedia – World Biographical Dictionary)*, 1983, Ekdotiki Athinon, vol. 2, Athens [in Greek].

Houzaios, G.M., 2009, *Benjamin Lesvios and Contemporary Physics*, reprint from the 20th volume of the journal *Lesviakà* of the Society of Lesbian Studies, Mytilene [in Greek].

Kavarnos, K.P., 1964, *Symbols and indications of immortal life*, Astir publ., Athens [in Greek].

Kitromilidis, Paschalis, 1999, *Modern Greek Enlightenment – The political and social ideas*, Morfotiko Idrima Ethnikis Trapezis (MIET), Athens [in Greek].

Kotsakis, Dimitrios, 1940, *The study of Astronomy in Greece during the 18th century*, published by the author [in Greek].

Koumanoudis, Stefanos, 1998, *Compilation of New Words – invented by scholars from the fall of Constantinople up to this day,* Series: Modern Greek studies; series supervisor: F. Iliou. Hermes publ., Athens [in Greek].

Lexiko tis ellinikis glossis, 2008, Papyros publ., Athens [in Greek].

Mavrommatis, Konstantinos, 1989, *The Astronomy of Theophilos Kairis*, 1st Volos High School edition, Thessaloniki [in Greek].

Valetas, G., 1974, "The persecutions against Benjamin and his turbulent struggle to enlighten the nation", *Aeolika Grammata* 4, p. 283-288. Kallithea [in Greek].

Highlights of Astronomy, Volume 14
IAU XXVI General Assembly, 14-25 August 2006
Karel A. van der Hucht, ed.

doi:10.1017/S1743921307010083

Joint Discussion 4
UV astronomy: stars from birth to death

Ana I. Gómez de Castro[1] and Martin A. Barstow[2] (eds.)

[1]Instituto de Astronomía y Geodesia (CSIC-UCM), Facultad de Matemáticas, Universidad Complutense de Madrid, Madrid, Spain
email: aig@mat.ucm.es
[2]Department of Physics and Astronomy, University of Leicester, University Road, Leicester LE1 7RH, UK
email: mab@star.le.ac.uk

Abstract. The scientific program is presented as well a the abstracts of the contributions. An extended account is published in *"The Ultraviolet Universe: stars from birth to death"* (Ed. Gómez de Castro) published by the Editorial Complutense de Madrid (UCM), that can be accessed by electronic format through the website of the Network for UV Astronomy (www.ucm.es/info/nuva).

There are five telescopes currently in orbit that have a UV capability of some description. At the moment, only *FUSE* provides any medium- to high-resolution spectroscopic capability. *GALEX*, the *XMM* UV-Optical Telescope (UVOT) and the *Swift*. UVOT mainly delivers broad-band imaging, but with some low-resolution spectroscopy using grisms. The primary UV spectroscopic capability of *HST* was lost when the Space Telescope Imaging Spectrograph failed in 2004, but UV imaging is still available with the *HST*-WFPC2 and *HST*-ACS instruments.

With the expected limited lifetime of sl FUSE, UV spectroscopy will be effectively unavailable in the short-term future. Even if a servicing mission of *HST* does go ahead, to install COS and repair STIS, the availability of high-resolution spectroscopy well into the next decade will not have been addressed. Therefore, it is important to develop new missions to complement and follow on from the legacy of *FUSE* and *HST*, as well as the smaller imaging/low resolution spectroscopy facilities. This contribution presents an outline of the UV projects, some of which are already approved for flight, while others are still at the proposal/study stage of their development.

This contribution outlines the main results from Joint Discussion 04 held during the IAU General Assembly in Prague, August 2006, concerning the rationale behind the needs of the astronomical community, in particular the stellar astrophysics community, for new UV instrumentation. Recent results from UV observations were presented and future science goals were laid out. These goals will lay the framework for future mission planning.

Keywords. ultraviolet-general, ultraviolet-solar system, ultraviolet-stars, ultraviolet-ISM, space vehicles-instruments

1. Preface

This joint discussion was organized to provide a forum during the IAU General Assembly where the accomplishments of UV astrophysics could be highlighted and a new road map for the future discussed.

The UV range is of prime interest for astrophysics since the resonance lines of the most abundant atoms and ions at temperatures between 3 000 K and 300 000 K, together with the electronic transitions of the most abundant molecules (H_2, CO, OH, CS, S_2, CO_2^+, C_2, O_2, O_3, ...) are at UV wavelengths. After enjoying more than 30 years of continuous access to this range, the astronomical community has been facing uncertain times and provision during the decade 2010–2020 remains so. Coordination is required to define the science goals for the future and the resulting requirements for future UV instrumentation.

density, the Full Width at Half Maximum (FWHM), the absorbed and the emitted energy of the independent regions of matter which produce the main and the satellites components of the studied spectral lines.
Discussion: We point out that the new and important aspect of our study is the values' calculation of the above parameters, their time scale variations and their variations as a function of spectral subtype,using the DACs or SACs theory. Our results are a successful test of this theory and of Danezis *et al.* proposed method. This study is a part of a Ph.D. Thesis.

9.6. *Study of Hα regions in 120 Be-type stars, and the complex structure of the Si IV 1393.755, 1402.77 Å regions of 68 Be-type stars*

Evaggelia Lyratzi, E. Danezis, Antonios Antoniou, D. Nikolaidis, L.C. Popovic, and M.S. Dimitrijevic: As it is already known, the spectra of many Oe- and Be-type stars present Discrete Absorption Components (DACs) which, due to their profiles' width as well as the values of the radial velocities, create a complicated profile of the main spectral lines. In this poster paper we detect the presence of this phenomenon (DACs or SACs) in the shape of Hα line in the spectra of 120 Be-type stars, and in the Si IV resonance lines in the spectra of 68 Be-type stars of all the spectral subtypes and luminosity classes.
Method: In our study we apply the method proposed by Danezis *et al.* on the stellar spectrographs of 120 Be-type stars which were taken by Fehrenbach and Andrillat (resolution 5,5 and 27 Å with the telescope of 152 cm in the Observatory of Haute Provence), and on the spectra of 68 Be stars observed with *IUE*, and we examine the variations of the physical parameters, stated below, as a function of spectral subtype and luminosity class.
Results: We find that in the Be-type stellar atmospheres, there are two regions that can produce the Hα Satellite Absorption Components (SACs or DACs). The first one lies in the chromosphere and the second one in the cool extended envelope. With the above method we calculate: (*a*) For the chromospheric absorption components we calculated the optical depth as well as the rotational and radial velocities of the independent regions of matter which produce the main and the satellites components. *b*) For the emission and absorption components which are created in the cool extended envelope we calculated the FWHM, the optical depth and the radial velocities of the independent regions of matter which produce the main and the satellites components.
We find that the absorption atmospherical regions where the Si IV resonance lines originated may be formed of one to five independent density layers of matter which rotate with different velocities, producing one to five Satellite Absorption Components (SACs or DACs). With the above method we calculate the values of the apparent rotational and radial velocities, as well as the optical depth of the independent regions of matter which produce the main and the satellites components of the studied spectral lines.
Discussion: We point out that the new and important aspect of our study is the values' calculation of the above parameters and their variations as a function of spectral subtype and luminosity class, using the DACs or SACs theory. Our results are a successful test of this theory and of Danezis *et al.* (2003, 2005) proposed method. This study is a part of a Ph.D. Thesis.

9.7. *A new approach for DACs and SACs phenomena in the atmospheres of hot emission-line stars*

D. Nikolaidis, E. Danezis, Evaggelia Lyratzi, L.C. Popovic, M.S. Dimitrijevic, Antonios Antoniou, and E. Theodossiou: As it is already known, the spectra of

many Oe- and Be-type stars present Discrete Absorption Components (DACs) which, due to their profiles' width as well as the values of the radial velocities, create a complicated profile of the main spectral lines. This fact is interpreted by the existence of two or more independent layers of matter, in the region where the spectral lines are formed. Such a structure is responsible for the formation of a series of satellite components (DACs or SACs) for each spectral line (Bates & Halliwell, 1986, Danezis *et al.* 2003, 2005).
Method: In this paper we present a mathematical model reproducing the complex profile of the spectral lines of Oe-type and Be-type stars that present DACs or SACs. This model presupposes that the regions, where these spectral lines are formed, are not continuous but consist of a number of independent absorbing or emitting density layers of matter and an external general absorption region. In this model we assume that the line broadening is due to the random motion of the ions and the rotation of the density regions that produce the spectral line and its satellite components. With this method we can calculate the values of the apparent rotational and radial velocities, the Gaussian standard deviation of the random motions of the ions, the random velocities of these motions, as well as the optical depth, the Full Width at Half Maximum (FWHM), the absorbed and the emitted energy and finally the column density of the independent regions of matter which produce the main and the satellites components of the studied spectral lines.
Results: In order to check the above spectral line function, we calculated the rotational velocity of He I 4387.928 Å absorption line in the spectra of five Be-type stars, using two methods, the classical Fourier analysis and our model. The values of the rotational velocities, calculated with Fourier analysis, are the same with the values calculated with our method.
Discussion: We point out that the new and important aspect of this method is the values' calculation of the above parameters using the DACs or SACs theory.

9.8. *Eta Carinae: what we have learned from HST-STIS in the UV*

Theodore R. Gull: The Luminous Blue Variable η Carinae is revealing many answers to its mysteries by high spatial resolution in the visible and the ultraviolet. Studies with the *HST*-STIS from 1998.0 to 2004.3 show major changes in the stellar and nebular spectra that track with the 2024-day period first noted by A. Damineli in the visible and followed by M. Corcoran via *RXTE* x-ray monitoring. We will show examples of the stellar and nebular spectra indicating changes in the central source, likely a massive binary system and indicating the response of the nebular ejecta, which is the $> 12\,M_\odot$ Homunculus, the $0.5\,M_\odot$ Little Homunculus, both bipolar structures, with intervening skirts. Within the interior skirt are located the Weigelt blobs, B, C and D, plus the Strontium Filament, all of which respond to the strong UV emission originating from the hot, less massive companion. Narrow-line absorption systems correlate with the Homunculus and Little Homunculus and are seen in hundreds of metal lines. For the Homunculus, the metal energy level populations correspond to 760 K, but the OH, CH, NH and CH+ to 60 K, while nearly a thousand H_2 lines are visible during the broad maximum. The Little Homunculus has a kinetic temperature of $\sim$6400 K during the broad maximum, but drops to 5000 K during the short minimum. Much is being learned about the N-rich, C,O-poor chemistry of this ejecta from a massive star in the late stages of CNO-processing. Recent GRB spectra show similar hot metal absorption gases likely being the ejecta from progenitor stars. Were they Wolf-Rayet stars?

9.9. *High resolution echelle spectrograph NES for visible and groundbased UV regions*

Vladimir E. Panchuk, Valentina G. Klochkova, I.D. Najdenov, and Maxim V. Yushkin: We present the high-resolution echelle spectrograph NES of the 6 m telescope.

MEASURED AND CALCULATED STARK PARAMETERS FOR SEVERAL AR I SPECTRAL LINES

Vladimir Milosavljević[a,1], Milan S. Dimitrijević[b] and Stevan Djeniže[a]

[a]*Faculty of Physics, University of Belgrade, P.O.B. 368, Belgrade, Serbia*

[b]*Astronomical Observatory, Belgrade, Volgina 7, Serbia*

[1]vladimir@ff.bg.ac.yu

Abstract: On the basis of the precisely recorded five neutral argon (Ar I) line shapes (in the 4s-5p transition) we have obtained the separate electron (W_e) Stark width. Moreover, we have determined as well and ion (W_i) contributions to the total Stark width, not measured previously for these lines. Also, we have calculated Stark parameters for these five neutral argon lines within the semiclassical-perturbation formalism.

We have tested also recently published line deconvolution procedure which enables to determine beside line broadening parameters, electron temperature (T) and electron density (N). An excellent agreement has been found among plasma parameters, obtained parameters by well established techniques and the examined method, which recommends proposed deconvolution procedure for diagnostic purposes.

Key words: Plasmas, Line: profiles, Atomic data

1. Introduction

In this paper we present the measured Stark broadening parameters of the 415.86 nm, 416.42 nm, 419.83 nm, 420.07 nm and 426.63 nm Ar I spectral lines (in the 4s-5p transition) at about 16 000 K electron temperature and at about 7.0×10^{22} m^{-3} electron density. The used T values are typical for many laboratory and cosmic light sources. Our total, electron-impact and ion widths (FWHM) W_t, W_e, W_i and parameter A characterizing quasistatic ion broadening have been compared to all available theoretical and experimental Stark broadening parameters.

In our work we applied the line deconvolution procedure of Ref. [1] to the five precisely recorded Ar I line profiles. Plasma parameters have been measured (T^{exp} and N^{exp}) using independent, well-known, experimental diagnostical techniques. Moreover the basic plasma parameters, i.e. electron temperature (T^D) and electron density (N^D) have been obtained also, using the new line deconvolution procedure [1], in the case of three various plasmas created in a linear, low-pressure, pulsed arc discharge in helium-argon and hydrogen-argon mixtures.

2. Experiment

The modified version of the linear low pressure pulsed arc [2-6] has been used as a plasma source. Pulsed discharge was performed in a quartz discharge tube. The working gases were helium-argon (28% He + 72% Ar) and hydrogen-argon (3% H_2 + 97% Ar) mixtures. The used tube geometry and corresponding discharge conditions are presented in Table 1.

Table 1. Various discharge conditions: C-bank capacity (in μF), U-bank voltage (in kV), H-plasma length (in cm), Φ-tube diameter (in mm), P-filling pressure (in Pa). N^{exp} (in 10^{22} m^{-3}) and T^{exp} (in 10^3 K) denote experimental electron density and temperature, respectively obtained at the moment when the line profiles were recorded. N^D (in 10^{22} m^{-3}) and T^D (in 10^3 K) represent averaged electron density and averaged electron temperature obtained by using the line deconvolution procedure [1]. Estimated accuracies of the measurements: ±11% for T^{exp}, ±7% for N^{exp} and ±12% for N^D and T^D.

Working gas	Exp.	C	U	H	Φ	P	N^{exp}	N^D	T^{exp}	T^D
72% Ar + 28% He	a	14	1.5	7.2	5	133	6.7	6.9	15.6	15.8
97% Ar + 3% H_2	b	14	1.5	7.2	5	67	7.0	7.3	16.0	16.2
97% Ar + 3% H_2	c	14	1.5	7.2	5	133	7.1	7.4	16.2	16.5

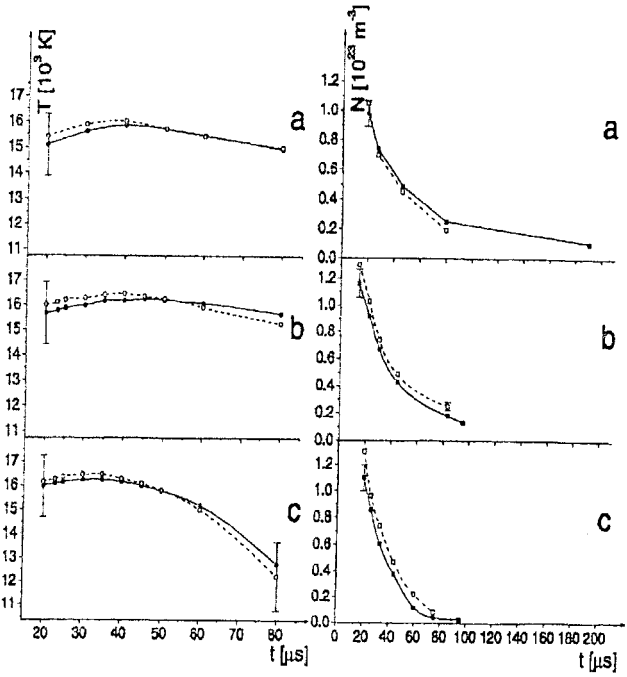

The plasma parameters were determined using standard diagnostic methods. The electron temperature was determined from the ratios of the relative line intensities of 7 Ar I spectral lines to the 5 Ar II spectral lines with an estimated error of ±11%, assuming the existence of the LTE [7].

Fig. 1 - Electron temperature (T) and density (N) decays. ____ measured data using independent experimental techniques. - - - - - data obtained using the line deconvolution procedure in various plasmas (see a, b and c in Table 1). Error bars represent estimated accuracies of the measurements (±11% and ±7% for T and N, respectively) and deconvolutions (±12%).

The necessary atomic data have been taken from Ref. [8]. The electron density decay was measured using a well-known single wavelength He-Ne laser interferometer technique for the 632.8 nm transition with an estimated error of ±7%. The electron densities (N^{exp}) and temperatures (T^{exp}), obtained at the moment when the line profiles were recorded, are presented in Table 1 together with the N^D and T^D values obtained using the deconvolution procedure.

3. Method of calculation

The description of the semiclassical perturbation formalism is given in Refs. [9-11]. Using this method we have calculated electron- and proton- impact line widths for 5 spectral lines of neutral argon. The obtained results are shown in Table 3, for perturber density of 10^{22} m^{-3} and temperatures T = 2500 - 50000 K.

4. Applications of the Deconvolution procedure

The used deconvolution procedure in its details is described in Refs. [1, 12]. It includes an advanced numerical procedure for deconvolution of theoretical asymmetric convolution integral of a Gaussian and a plasma broadened spectral line profile. This method, when applicable, gives complete information on the plasma parameters from a single recorded spectral line. The method determines W_t, W_e, W_i, A and D (characterizing the ion dynamics), as well as N and T, self-consistently and directly from the shape of spectral lines. All one needs to know additionally is the instrumental width of the spectrometer. The measured profiles are a convolutions of the Lorentzian Stark and Gaussian profiles caused by Doppler and instrumental broadenings [7]. Van der Waals and resonance broadenings were estimated to be negligible in comparison to Stark, Doppler and instrumental ones. The deconvolution procedure was performed using the least Chi-square function [1]. The absence of self-absorption was checked using the method presented in Ref. [13].

The total line Stark FWHM (W_t) is a function of W_e and W_i (the electron and ion contributions, respectively). The W_t may be calculated, within the quasistatic approximation for ion broadening [7, 14, 15] as $W_t \approx W_e \cdot (1 + 1.75 \cdot AD(1 - 0.75 \cdot R))$, i.e. one can considered that $W_t = W_e + W_i$. The R is the ratio of the mean ion separation to the Debye length (see Eq. (2.7) in Ref. [1]), A is the quasi-static ion broadening parameter (see Eq. (224) in Ref. [7]) and D is a coefficient of the ion-dynamical contribution defined and explained in Ref. [1], see Eqs. (2.14) and (2.15). When D = 1 the influence of the ion-dynamic is negligible and the line shape may be treated using the quasi-static ion approximation, described by Ref. [1, and references therein], with the help of the function

$$K(\lambda) = K_0 + K_{max} \cdot \int_{-\infty}^{+\infty} \exp(-t^2) \cdot \left\{ \int_0^{\infty} \frac{H_R(\beta)}{1 + \left(2 \frac{\lambda - \lambda_0 - \frac{W_G}{2\sqrt{\ln 2}} \cdot t}{W_e} - \alpha \cdot \beta^2 \right)^2} \cdot d\beta \right\} \cdot dt \quad .$$

Here K_0 is the baseline (offset) and K_{max} is the maximum intensity (for $\lambda=\lambda_0$) [1]. $H_R(\beta)$ is an electric microfield strength distribution function of normalized field strength $\beta=F/F_0$, where F_0 is the Holtsmark field strength. The parameter α is $A^{4/3}$.

For the purpose of the deconvolution iteration process we need to know the value of K as a function of λ for every group of parameters (K_{max}, λ_0, W_e, W_G, R, A). Gauss width W_G is defined e.g. by Eq. (2.3) in Ref. [1]. The used numerical procedure for solution of K-function is described in earlier publications [1, 12, 16].

From set of equations in Ref. [1] it is possible to obtain the plasma parameters (N and T) and the line broadening characteristics measured and calculated (W_t, W_e, W_i, A and D). One can see that the ion contribution, expressed in terms of the A and D parameters directly determine the ion width (W_i) component in the total Stark width, if quasistatic aproximation for ion broadening is applicable.

This sophisticated deconvolution method, which, when applicable, allows direct determining of all six parameters by fitting theoretical K-profile on experimental data, requires sufficient number of experimental points per line, obtained with small statistical errors. The minimal requirements for the application of this method are minimum twenty experimental points per line (the border of line is $-3/2W_e+\lambda_0<\lambda<+3/2W_e+\lambda_0$), and maximal statistical uncertainty in intensity determination is 5% at every experimental point. Experimental measurements with poor accuracy lead to non-applicability of this method. This has been concluded by testing the sensitivity of the algorithm by generating random statistical noise with Gaussian distribution in every point involved by theoretical profiles. The fitting procedure has been also tested with the K convolution integral using other experimental data. The K convolution integral is used for the analysis of our new data for many spectral lines of neutral rare gases. By comparing our different spectral lines obtained under the same plasma conditions, we tested "the physical stability" of the deconvolution procedure. The obtained parameters, which are related to plasma conditions, such as T^D and N^D, are independent from the analyzed lines. Our calculated values of temperature from each spectral line and values obtained by Boltzmann and Saha equations are in very good agreement, within ±7% . The electron density

calculated from each spectral line shows even better agreement with the values measured by interfeometry, the agreement being within ±5%.

Taking into account the uncertainties of the line profile measurements and above mentioned, we estimated errors to be ±12% for the W_e and W_i, ±15% for the A and ±20% for D.

5. Results and Discussion

The Stark broadening parameters (W_t^{exp}, W_e^{exp} and W_i^{exp}) obtained using the deconvolution procedure of the recorded line profiles at measured N^{exp} and T^{exp} values are presented in Table 2 together with those of other authors. The A^{exp} and D^{exp} have been presented in Ref. [17]. The ratio of experimental data and theoretical predictions in Ref. [7], denoted with *G*, and present theoretical results (*Tw*) are also given.

Table 2. The Ar I line broadening characteristics. Measured: total Stark FWHM (W_t^{exp} in pm within ±12% accuracy), electron Stark width W_e^{exp} in pm within ±12% accuracy) at measured electron temperature (T^{exp} in 10^3 K) and electron density (N^{exp} in 10^{22} m^{-3}). Under Ref. are sources of experimental data: with (Tw) are denoted the present data. Other notations: KM, [18]; B, [19]; G, [20]; J, [21]; HW, [22]; A, [23]; P, [24]; MM, [25]; JP, [26]; M, [27]; Ch, [28]; Gr, [29]. The index G and Tw denote theoretical data taken from Ref. [7] and this work (Table 3) at a given T and N, respectively.

Multiplet	λ(nm)	T^{exp}	N^{exp}	W_t^{exp}	W_e^{exp}	W_i^{exp}	Ref.	W_e^{exp}/W_e^{G}	W_e^{exp}/W_e^{Tw}
$[3/2]_1^0$-	419.83	15.6	6.7	130	112	18	Tw	0.50	0.69
$[1/2]_0$		16.0	7.0	137	117	20	Tw	0.50	0.69
		16.2	7.1	139	119	30	Tw	0.50	0.69
		11.1	0.4		3.3		KM	0.27	0.35
		12.4	7.3		120		B	0.52	0.70
		14.0	1.0		23		G	0.71	0.97
$[3/2]_2^0$-	415.86	15.6	6.7	132	114	18	Tw		1.00
$[3/2]_2$		16.0	7.0	139	119	20	Tw		0.99
		16.2	7.1	143	122	21	Tw		1.00
		11.9	6.2	148*	121	27*	J		1.20
		11.9	6.2	137*	112	25*	HW		1.12
		13.5	10.0		246		A		1.48
		12.7	9.4		173		B		1.12
		11.4	4.6		110		G		1.48

Multiplet	λ(nm)	T^{exp}	N^{exp}	W_t^{exp}	W_e^{exp}	W_i^{exp}	Ref.	W_e^{exp}/W_e^{G}	W_e^{exp}/W_e^{Tw}
$[3/2]_2^0$-	415.86	14.0	1.0		18.3		P		1.10
$[3/2]_2$		12.5	9.2		190		MM		1.27
		11.9	6.2	151*	123	28*	JP		1.22
		13.4	4.5		107		M		1.43
$[3/2]_2^0$-	416.42	15.6	6.7	126	109	17	Tw		0.95
$[3/2]_1$		16.0	7.0	134	115	19	Tw		0.96
		16.2	7.1	134	115	19	Tw		0.94
		11.9	6.2	127*	97	30*	HW		0.96
		13.8	14.5		332		Ch		1.37
		11.1	0.4		3.7		KM		0.56
		12.7	9.4		171		B		1.11
		11.4	4.6		100		G		1.35
		14.0	1.0		18.1		P		1.08
		10.6	2.6		59.6		MM		1.44
		11.5	5.1		96		M		1.17
$[3/2]_1^0$-	426.63	15.6	6.7	127	110	27	Tw		0.92
$[3/2]_2$		16.0	7.0	130	113	27	Tw		0.90
		16.2	7.1	136	118	28	Tw		0.92
		11.9	6.2	145*	126	19*	HW		1.19
		11.4	4.6		110		G		1.41
		14.0	1.0		17.9		P		1.02
		12.6	9.9		240		M		1.41
$[3/2]_2^0$-	420.07	15.6	6.7	138	119	19	Tw	0.77	1.05
$[5/2]_3$		16.0	7.0	143	123	20	Tw	0.76	1.04
		16.2	7.1	147	126	21	Tw	0.76	1.04
		13.8	14.5		324		Ch	1.00	1.35
		11.1	0.4		2.8		KM	0.34	0.44
		12.7	9.4		155		B	0.76	1.01
		11.4	4.6		100		G	1.03	1.36
		12.6	9.2		180		Gr	0.90	1.22
		13.4	4.5		94		M	0.95	1.26

NOTE - Asterisk denote Stark widths calculated by us on the basis of the given W_e^{exp} and A^{exp} values for plasma parameters presented in Refs. [21, 22, 26] using Eqs. (1-3).

Table 3. Calculated Ar I Stark FWHM (W^{Tw} in pm) for electrons (a), protons (b) and helium ions (c) as perturbers for various temperatures (T) at 10^{22} m^{-3} perturber density.

λ [nm]		T [10^3 K]					
		2.5	5.0	10.0	20.0	30.0	50.0
419.83	a	18.0	20.6	22.7	25.1	26.7	29.0
	b	*5.66	*6.05	*6.43	6.85	7.16	7.58
	c	-	*5.51	*5.81	*6.13	*6.33	4.48
415.86	a	12.0	13.8	15.7	18.1	19.7	22.1
	b	*4.64	*4.85	5.04	5.26	5.40	5.61
	c	4.36	*4.60	*4.75	*4.90	5.00	5.14
416.42	a	12.0	13.7	15.6	18.0	19.6	22.1
	b	*4.62	*4.82	5.01	5.22	5.36	5.58
	c	*4.34	*4.57	*4.73	*4.87	4.97	5.10
426.63	a	12.6	14.6	16.5	19.0	20.7	23.3
	b	*4.88	*5.10	5.30	5.53	5.68	5.91
	c	*4.58	*4.84	*5.00	*5.16	5.26	5.41
420.07	a	12.0	13.7	15.6	18.0	19.7	22.3
	b	*4.52	*4.73	4.92	5.13	5.28	5.49
	c	*4.25	*4.48	*4.63	*4.78	4.88	5.01

NOTE - With asterisk are denoted case for which the collision volume multiplied by the perturber density (the condition for validity of the impact approximation) lies between 0.1 and 0.5.

In order to make the comparison among the separated measured (W_e^{exp}) and calculated (W_e^{G} and W_e^{Tw}) electron width values easier, the ratio W_e^{exp}/ W_e^{G} and W_e^{exp}/ W_e^{Tw} dependence on the electron temperature is presented graphically in Figures 2 and 3. The W_e^{G} values are from Ref. [7] and W_e^{Tw} from Table 3.

We note that Stark broadening parameters (W_i^{exp}) measured here are for electron temperatures from 15600 K up to 16200 K while all other experiments are for T≤14000 K.

The comparison of our experimental values with theoretical data [7] was possible for only two transitions. One can see in Figure 2 and 3 that the agreement of experimental and theoretical values is better for present calculations. Generally, our experimentally found electron contribution to the total Stark width is about 85% (on average) at about 16000 K electron temperature.

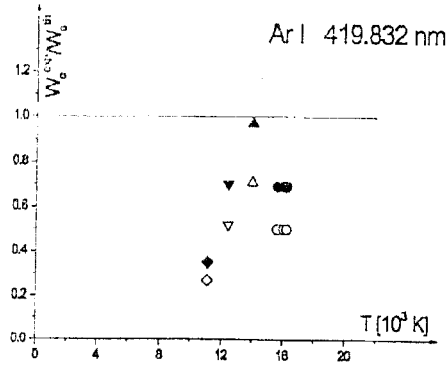

Fig. 2. - Ratios of the experimental electron Stark FWHM (W_e^{exp}) to the theoretical (W_e^{G}) predictions [7] (empty symbol) and (W_e^{Tw}) predictions from this work (full symbol) vs. electron temperature for λ=419.832 nm. Circle, diamond, nabla and triangle represent our experimental data and those from Refs. [22], [23] and [24], respectively.

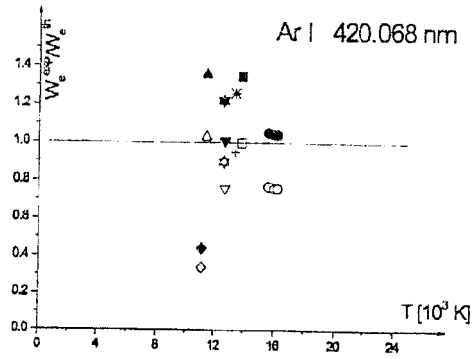

Fig. 3. - Ratios of the experimental electron Stark FWHM (W_e^{exp}) to the theoretical (W_e^{G}) predictions [7] (empty symbol and *) and (W_e^{Tw}) predictions from this work (full symbol and +) vs. electron temperature for λ=420.068 nm. Circle, square, diamond, nabla, triangle and star represent our experimental data and those from Refs. [28], [22], [23], [24] and [29], respectively, also with * and + are represent [27].

Acknowledgments. This work is a part of the projects OI1228 "Determination of the atomic parameters on the basis of the spectral line profiles" and GA1195 "Influence of collision processes on astrophysical plasma lineshapes" supported by the Ministry of Science, Technologies and Development of the Republic of Serbia.

References

[1] Milosavljević V. and Poparić G., *Phys. Rev. E* **63**, 036404 (2001).

[2] Djeniže S., Srećković A., Labat J., Konjević R. and Popović L. Č., *Phys. Rev. A* **44**, 410 (1991).

[3] Djeniže S., Milosavljević V. and Srećković A., *JQSRT* **59**, 71 (1998).

[4] Djeniže S., Milosavljević V. and Dimitrijević M. S., *A&A* **382**, 359 (2002).

[5] Milosavljević V., Djeniže, S., Dimitrijević M. S. and Popović L. Č., *Phys. Rev. E* **62**, 4137 (2000).

[6] Milosavljević V., Dimitrijević M. S. and Djeniže S., *Astrophys. J. Supp. Ser.* **135**, 115 (2001).

[7] Griem H. R., *Spectral Line Broadening by Plasmas* (New York: Acad. Press), 1974.

[8] NIST - *Atomic Spectra Data Base Lines* (wavelength order) - **http://physics.nist.gov** (2003).

[9] Sahal-Bréchot S., *A&A* **1**, 91 (1969).

[10] Sahal-Bréchot S., *A&A* **2**, 322 (1969).

[11] Dimitrijević M. S. and Sahal-Bréchot S., *JQSRT* **31**, 301 (1984).

[12] Milosavljević V., *PhD Thesis*, University of Belgrade, Faculty of Physics, Belgrade (unpublished), 2001.

[13] Djeniže S. and Bukvić S., *A&A* **365**, 252 (2001).

[14] Barnard A. J., Cooper J. and Smith E. W., *JQSRT* **14**, 1025 (1974).

[15] Kelleher D. E., *JQSRT* **25**, 191 (1981).

[16] Milosavljević V., *Monograph*, pub. Zadužbina Andrejević, ISBN 86-7244-270-9, Belgrade, 2002.

[17] Milosavljević V. and Djeniže S., *A&A* **405**, 397 (2003).

[18] Kusz J. and Mazur D., in *Spectral line shapes*, vol. **9**, ed. M. Zoppi, Lorenzo Ulivi, p.323, Firenze (1996).

[19] Bues L., Haag T. and Richter J., *A&A* **2**, 249 (1969).

[20] Gericke W. E., *Z. Astrophys.* **53**, 68 (1961).

[21] Jones D. W., Wiese W. L. and Woltz A. L., *Phys. Rev. A* **34**, 450 (1986).

[22] Hahn D. T. and Woltz A. L., *Phys. Rev. A* **42**, 1450 (1990).

[23] Aparicio J. A., Pérez C., del Val J. A., Gigosos M. A., de la Rosa M. I. and Mar S., *J. Phys. B* **31**, 4909 (1998).

[24] Powell W. R., *Diss. Abstr. B***29**, 3030 (1969).

[25] Musielok B., Musielok J. and Wujec T., *Zesz Nauk. Wyzsz. Szk. Pedagog. Opolu.*, Fiz. No. 17, 63 (1976).

[26] Jones D. W., Pichler G. and Wiese W. L, *Phys. Rev. A* **35**, 2585 (1987).

[27] Musielok J., *Acta Phys. Pol. A* **86**, 315 (1994).

[28] Chapelle J., Cabanne Sy. A., Cabanners F. and Blandin J., *JQSRT* **8**, 1201 (1967); *C.R.H. Acad. Sci. Ser. B* **264**, 853 (1967).

[29] Griem H. R., *Phys. Rev.* **128**, 515 (1962).

JOURNAL DE PHYSIQUE IV
Colloque C1, supplément au Journal de Physique II, Vol. 1, mars 1991

SEMICLASSICAL CALCULATIONS OF STARK BROADENING PARAMETERS

M.S. DIMITRIJEVIĆ and SAHAL-BRÉCHOT*

Astronomical Observatory, Volgina 7, 11050 Beograd, Yugoslavia
**Observatoire de Paris-Meudon, F-92195 Meudon Cedex, France*

Resume - On présente ici une revue des calculs des largeurs et des déplacements des raies élargis par l'éffet Stark, obtenus a l'aide du formalisme semiclassique-perturbations. On compare les résultats des calculs obtenus par les programmes de (i) Jones, Benett et Griem, (ii) Sahal-Bréchot et (iii) Bassalo, Cattani et Walder, et aussi, on discute la comparaison avec les résultats expérimentaux.

Abstract - A review of semiclassical calculations of Stark broadening parameters is presented. We compare the results obtained by using computer codes due to (i) Jones, Benett and Griem, (ii) Sahal-Brechot and (iii) Bassalo, Cattani et Walder. The comparison with experimental results has also been discussed.

1 - INTRODUCTION

In order to perform the calculation of a Stark Broadened line profile, the three principal ways to describe a radiating (absorbing) system are widely used, i.e. the quantum mechanical, the semiclassical or the classical approach. In the pure quantum mechanical approach, we have usually a system of non-interacting cells, containing the radiating atom and N perturbers and, we consider the whole cell as a giant molecule. However, to perform a pure quantum mechanical strong coupling calculation is very difficult and only few such calculations exist. For example the strong coupling method is used for Li I (2s - 2p) /1/, Ca II (4s-4p, and 3d - 4p) /2 and 3/, Mg II (3s - 3p) /3,4/ and Be II (2s - 2p) /5/ lines. Recently, Seaton performed close coupling calculations for 42 transitions in Li-like ions C III, O V, Ne VII, Be II, B III, C IV, O VI, Ne VIII /6/ and for the transitions $2s^2\ ^1S - 2s2p\ ^1P^o$, $2s2p\ ^3P^o - 2p^2\ ^3P$, and $2s2p\ ^1P^o - 2p^2\ ^1D$ and ^1S in C III /7/. These results, obtained as solutions of the close coupling problem which uses truncated expansions, are assumed to be correct probably within 10 percent /7/.

In spite of the existence of more refined quantum mechanical method, the semiclassical approach is still the most widely used technique for the calculation of line broadening data Moreover, in a lot of cases such as e.g. complex spectra, heavy elements or transitions between more excited energy levels, the sophisticated quantum mechanical approach is very difficult or even practically impossible to use and, in such cases, the semiclassical approach remains the most efficient method for Stark broadening calculations.

2 - SEMICLASSICAL METHOD

Within the semiclassical model, the radiating (absorbing) atom is described quantum mechanically while perturbers are classical particles with well defined velocity (v) and impact parameter (ρ). The system of classical perturbers acts on the quantum mechanical atom via classical, time dependent interaction potential. The Schrödinger equation which is satisfied by the atomic wave functions is usually solved using the second order non stationary perturbation theory.

The existing large scale calculations of Stark broadening parameters were performed by using three different computer codes developed by (i) Jones, Benett and Griem /8-10/: (ii) Sahal-Bréchot /11,12/ and (iii) Bassalo, Cattani and Walder /13/.

Within the frame of the semiclassical theory, half half width (w) and shift (d) of an isolated line may be expressed via S matrix as /e.g. 10/

$$w + id = N \int_0^\infty v f(v) dv \int_0^\infty 2\pi\rho\, d\rho \left(1 - S_{ii}(\rho,v) S_{ff}^{-1}(\rho,v)\right)_{Av} \qquad (1)$$

Here, N is the electron density: f(v) is the Maxvellian velocity distribution function for electrons: i and f denote the initial and final atomic energy levels: and i' and f' are their corresponding perturbing levels, while $(...)_{Av}$ denotes the angular average over the directions of the colliding electron.

If one express the relevant inelastic and elastic cross sections via corresponding S matrix elements which are proportional to the transition probability $P_{jj'}$ /11,12/ one obtains the formulae which enter the computer code of Sahal-Brechot

$$2w = N \int_0^\infty v f(v) dv \left[\sum_{i' \neq i} \sigma_{ii'}(v) + \sum_{f' \neq f} \sigma_{ff}(v) + \sigma_{el}\right], \qquad (2)$$

$$d = N \int_0^\infty v f(v) dv \int_{R_3}^{R_D} 2\pi\rho\, d\rho \sin 2\phi_p \qquad (3)$$

with

$$\sum_{j' \neq j} \sigma_{jj'}(v) = \frac{1}{2}\pi R_1^2 + \int_{R_1}^{R_D} 2\pi\rho\, d\rho \sum_{j' \neq j} P_{jj'}(\rho,v), \qquad (4)$$

$$\sigma_{el} = 2\pi R_2^2 + \int_{R_2}^{R_D} 8\pi\rho\, d\rho \sin^2(\phi_p + \phi_q)^{1/2}. \qquad (5)$$

The phase shifts ϕ_p and ϕ_q due respectively to the polarization potential (r^{-4}) and to the quadrupolar potential (r^{-3}) part, are given in the part 3 of Section 2 in the Ref. /11/. All the cutoffs R_1, R_2, R_3 and R_D are described in the part 1 of Section 3 of the Ref. /12/. The contribution of resonances in the elastic cross sections is taken into account in the ion-line-width calculations according to Ref. /14/. The formulae for the ion impact broadening are analogous but inelastic collisions are negligible.

In the computer code of Bassalo, Cattani and Walder, so called convergent theory, originally developed by Vainshtein and Sobel'man /15/ has been used. Using the similarity between the Dyson series for S matrix perturbational developement and Taylor series for exponential function, this method avoid the divergence in the integration over impact parameter when ς tends to 0 /15/.

Comprehensive calculations of Stark broadening parameters of non-hydrogenic neutral and singly ionized atom lines (helium through calcium and cesium) using the computer code of Jones, Benett and Griem, were published in 1971 and later in 1974 /8-10/. Using the same code /10/ and the version adapted by Dimitrijević for the case of multiply charged ions, data for Br I, Ge I, Hg I, Pb I, Rb I, Cd I, Zn I /16/, O II /17/, O III /18/, C III /19/, C IV /19,20/, N II, N III, N IV /21/, S III, S IV, Cl III /22/ and Ti II, Mn II /23/ have been published. Semiclassical calculations based on the method developed by Sahal-Bréchot /11,12/ exist for light elements such as C, N, Mg, Si (without the contribution of resonances /see e.g. 24 and References therein/. Data for alkali-like ions Be II, Mg II, Ca II, Sr II, Ba II may be found in Ref. /14/, while in Ref. /25/ the semiclassical and experimental data for the low-excitation Si II lines have been compared. Recently, using the same computer code, extensive calculations for 79 neutral helium multiplets /26-30/, 62 sodium /31-33/ and 51 potassium multiplets /34,35/ for perturber densities 10^{13} - $10^{19}cm^{-3}$ become available. Data for F I /36/, Ar II /37/, Ga II, Ga III /38/ also exist. Using this code Lanz et al /39/ published recently a set of the Si II Stark broadening parameters required for stellar analysis.

Stark width values obtained by the code of Sahal-Bréchot are in general smaller than those obtained using the code according to Griem /10/, due to the symmetrization procedure used by Sahal-Bréchot and to different lover cut-offs. This difference becomes smaller if the contribution of resonances is taken into account. In the case of the Mg II resonance lines, the experimental data of Goldbach et al /40/, chosen after the critical analysis /41/ as very reliable, agree better with the results obtained using the procedure of Sahal-Bréchot, as well as a number of experimental data in the case of the Si II multiplet 1 /25/ (see Fig. 1). However, a general conclusion is difficult to obtain /see e.g. Ref. 28/ since different assumptions involved in these two versions of the semiclassical method have different validity conditions.

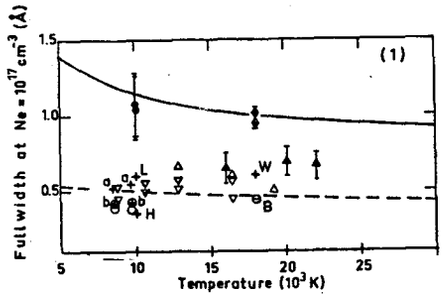

Fig. 1 - Line widths for Si II multiplet 1 at electron density $10^{17}cm^{-3}$ vs temperature. Experimental data: ▲, Lesage et al /25/; ○, Konjević et al /42/; ▽, ▼, △, Purić et al /43-45/; ●, Lesage et al /46/; ⊕, Chiang and Griem /47/. Theoretical data: (i) Semiclassical calculations: —— Griem /10/; - - - Sahal-Bréchot /in Ref. 46/; (ii) Distorted wave calculations: ⊖ Blaha

/in Ref. 47/; (iii) Semiempirical calculations: Konjević et al /42/ treating perturbing levels together (+a) and individually (+b)*; Lesage et al /46/ (+L)*; Hey /48/ (+H)*; Jones /49/ (+W).

Extensive calculations by Bassalo,Cattani and Walder obtained using the convergent semiclassical method exist for He I lines.

All three methods have been compared with critically selected experimental data for 13 He I multiplets /28/. In order to estimate the average accuracy of different methods, ratios of experimental and theoretical values have been averaged first in multiplet and then over the number of multiplets. Obtained results are presented in Table 1

Table 1 - Average accuracy of different theoretical methods compared to Stark width (W_m) and shift (d_m) experimental data for helium lines. The results in parentheses are obtained by excluding the $2p^3D$ - $3d^3D$ line which exibits a strong unexplained difference between d_m and and the calculated shift (especially for d_{DSB} and d_{BG}). With DSB are denoted the data from Ref. /26/, with BCW the data from Ref. /13/ and with BG the data from Ref. /8/ (also in Ref. /10/).

	All experiments included	Experiments with *C* and *D* accuracy excluded
$(W_m/W_{DSB})_{av}$	1.17±0.04	1.17±0.02
$(W_m/W_{BCW})_{av}$	1.07±0.04	1.07±0.04
$(W_m/W_{BG})_{av}$	0.92±0.04	0.93±0.02
$(d_m/d_{DSB})_{av}$	1.20±0.13 (1.07±0.04)	1.13±0.03
$(d_m/d_{BCW})_{av}$	1.23±0.08 (1.27±0.07)	1.34±0.09
$(d_m/d_{BG})_{av}$	1.14±0.07 (1.07±0.04)	1.14±0.03

One can see that the agreement between experimental and all three semiclassical calculations is within the limits of ±20%, what is the predicted accuracy of the semiclassical method /10/. This is also well illustrated in Table 2 where average ratios of measured Stark widths and shifts to the calculated ones by using Griem's code are given.

Table 2 - Average ratios of measured and calculated linewidths (W_M/W_{th}) for various emitters in the case of various calculations according to Ref. /10/. Values in Table are from Ref. /50/ in the case of neutrals and singly charged ions and from Ref. /51/ in the case of doubly charged ions. Number of data for W and d are given under n_W and n_d ($n \geqslant 5$).

Element	W_M/W_{th}	d_M/d_{th}	n_W	n_d
He I	0.93	1.11	14	14
C I	0.88	1.00	18	9
N I	0.96	0.82	49	26
O I	0.93	1.03	7	5
F I	0.93	1.15	9	8

Element	W_M/W_{th}	d_M/d_{th}	n_W	n_d
Ne I	0.84	1.55	17	6
Si I	1.09	0.90	6	8
P I	1.00		10	
S I	1.09		5	
Cl I	1.10		6	
Ar I	0.86	0.81	21	15
Cs I	1.15		19	
C II	1.14		5	
N II	1.09		8	
O II	0.93		13	
Ne II	1.14		12	
Mg II	0.78	1.01	6	6
Al II	1.08		5	
Si II	0.99		6	
S II	1.03		10	
Ar II	1.00	1.15	34	26
Ca II	0.79	0.65	9	7
Ge II	1.05		7	
C III	0.76		7	
O III	0.72		6	
S III	0.73		16	
Cl III	0.74		15	

One can see that for doubly charged ions the agreement is less satisfactory and the results are consistently larger than experimental values as well as the quantum mechanical results /6,7/. If we look at a particular spectrum, the semiclassical results are of lower accuracy for first one or two lines, since in this case the possibilities of the semiclassical approach are not so good due to the significant contribution of resonances, especially in the case of charged emitters, as well as to the influence of strong and elastic collisions. In the case of singly charged ions the discrepancies between Jones, Benett and Griem's calculations /9,10/ and experimental values for Mg II and Ca II resonance lines are reason for lower (W_M/W_{th}) ratios in Table 2.

3 - MULTIPLY CHARGED IONS

With the increase of the ionization degree, increases the importance of the short range effects since perturbers come closer to the emitter due to larger Coulomb attraction making the validity of the classical path approximation more questionable. The comparison /53/ of different experimental and theoretical results is presented for 2s - 2p C IV multiplet in Fig. 2 and for 3s - 3p C IV line (λ = 5801.3Å) in Table 3. One can see that the agreement is not so good as in the case of neutrals and singly charged ions. However, the agreement becomes better for higher temperatures. This can be explained by the fact that the distance between the perturbing levels and the initial and final levels is larger for multicharged ions than in the case of singly charged iones. Therefore, elastic collisions are more important than inelastic ones, and elastic collisions are due to close interactions which are not well treated by the perturbation theory. At high temperatures or for excited levels, inelastic collisions become important: they are due to more distant interactions and the perturbation theory may give correct results. It can be noticed that quantum close coupling calculations become difficult to perform for high levels, owing to the number of involved channels.

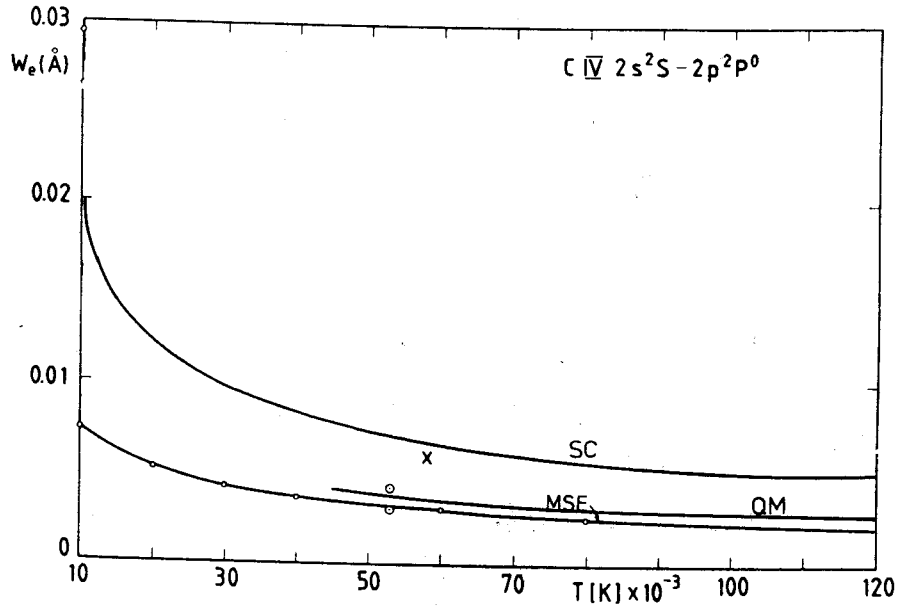

Figure 2 - Theoretical and experimental Stark widths (FWHM) for C IV $2s^2S$ - $2p^2P^o$ multiplets as function of temperature: SC=Semiclassical calculations, Dimitrijević, Sahal-Bréchot (1990) /52/; QM=Quantum close coupling calculations, Seaton (1988) /6/; MSE=Modified semiempirical calculations, Dimitrijević, Konjević (1980) /53/; Experimental data : X=Bogen (1972) /54/; ⊙=El-Farra, Hughes (1983) /55/.

Table 3 - Experimental (W_M) and calculated (W_{th}) Stark widths (FWHM) for the transition C IV, $3s^2S_{1/2}$ - $3p^2P^o_{3/2}$ (λ = 5801.3Å) at an electron density of 1.8 $10^{18}cm^{-3}$ and kT = 12.5 eV.

W_M(Å)	W_{th}(Å)	Reference
10.0		/56/
	7.38	/52/
	7.98	/10/
	6.01	/53/
	5.45	/57/
	6.09	/58/
	10.80	/59/
	5.32	/6/

Therefore the two methods are complementary: at low temperatures and for lines between low levels, quantum close coupling calculations are necessary if one needs a good accuracy: the semiclassical approximation can not give better than a factor of two. At high temperatures or for lines originating from high levels the semiclassical approximation can give correct results when close coupling calculations become unoperative.

With the increase of the ionization degree the contribution of the ion-impact broadening also decrease. In astrophysical investigations broadening by the radiator interaction with protons is the most important and also, such results give an upper limit since the proton collisions are the most effective in comparison with the heavier ionic species. In Table 4 the validity condition of the impact approximation for proton-impact broadening in the case of the O V (1371Å) $2p^2\ ^1D$ - $2s2p\ ^1P$ line /60/ is presented. We can see that only for the plasma conditions $N_e = 10^{22}cm^{-3}$ and $T = 2$ and $3x10^5K$ the validity of impact approximation becomes questionable in the line center.

Table 4 - The validity of the impact approximation for proton collisions in the case of O V (1371Å) $2p^2\ ^1D$ - $2s2p\ ^1P$ line /60/. (The time of interest for line broadening/the line width) $\ll 1$ (see Refs. /11,12/).

N_e (cm^{-3}) \ T (K)	$1.2x10^5$	$2x10^5$	$3x10^5$
10^{18}	$0.9x10^{-4}$	$1.3x10^{-4}$	$1.4x10^{-4}$
10^{20}	$0.9x10^{-2}$	$1.3x10^{-2}$	$1.3x10^{-2}$
10^{22}	0.1	0.6	0.9

In Table 5 the semiclassical calculations /60/ of widths are compared for the same O V line. One can see that the proton width is very small compared to the electron width. This is due to the Coulomb repulsion which increases with the radiating ion charge.

Table 5 - The electron- and proton-impact widths (FWHM) for O V (1371Å) $2p^2\ ^1D$ - $2s2p\ ^1P$ line at $N_e = 10^{20}cm^{-3}$ and at different temperatures.

Temperature (K)	$8.0x10^4$	$1.2x10^5$	$2.0x10^5$	$3.0x10^5$
Electron-impact width (Å)	4.6	3.8	3.0	2.5
Proton-impact width (Å)	0.06	0.1	0.17	0.22

A quasistatic calculation in the wings /60/ shows that the proton contribution becomes completely negligible. In the examined case the Franck-Condon turning point falls inside the classical - ly forbidden region determined by the Coulomb repulsion /60/.

4 - CONCLUDING REMARKS

Generally, the width data are more reliable than the shift data, since shift calculations are more sensitive to the small variations of various parameters. The reason is because shifts are smaller than widths and produced in average by more distant collisions. Roberts /61/ performed an analysis of the width and shift values convergence as a function of the number of perturbing levels, demonstrating that in the case of the shift, even the sign may be changed if an unsufficient number of perturbing levels is used.

This is also illustrated in Figs. 3 and 4 (from Ref. /1/). Here, we have sums of relative contributions to width and shift for the various angular momenta ℓ of the colliding electron.

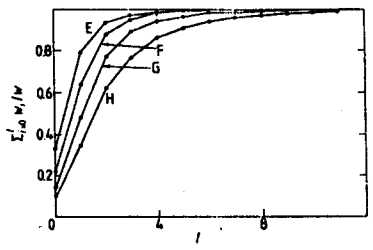

Fig. 3 - Convergence of the sum $\sum_{i=1}^{\ell} W_i/W$ in the semiclassical approximation as a function of ℓ. The curves E, F, G and H refer to temperatures of 2500, 5000, 10000 and 20000 K respectively.

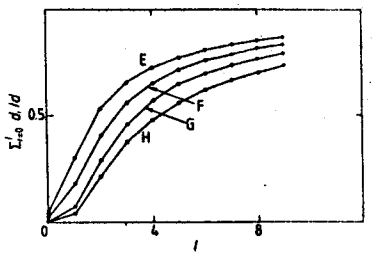

Fig. 4 - Convergence of the sum $\sum_{i=1}^{\ell} d_i/d$ in the semiclassical approximation as a function of ℓ. Otherwise the same notation.

We can see that in the case of the shift the convergence is not so good as in the case of the width. Consequently, larger computational efforts are needed in order to obtain a good accuracy for the shift.

REFERENCES

/1/ Dimitrijević, M.S., Feautrier, N. and Sahal-Bréchot, S., J.Phys.B 14 (1971) 2559.
/2/ Barnes, K.S. and Peach, G., J.Phys.B 3 (1970) 350.
/3/ Barnes, K.S., J.Phys.B 4 (1971) 1377.
/4/ Bely, O. and Griem, H.R., Phys.Rev.A 1 (1970) 97.
/5/ Sanchez, A., Blaha, M. and Jones, W.W., Phys.Rev.A 8 (1973) 774.
/6/ Seaton, M.J., J.Phys.B 21 (1988) 3033.
/7/ Seaton, M.J., J.Phys.B 20 (1987) 4631.
/8/ Benett, S.M. and Griem, H.R., Calculated Stark Broadening Parameters for Isolated Spectral Lines from the Atom Helium through Calcium and Cesium, Univ. Maryland, Techn.Rep. No 71-097, College Park, Maryland (1971).
/9/ Jones, W.W., Benett, S.M. and Griem, H.R., Calculated Electron Impact Broadening Parameters for Isolated Spectral Lines from Singly Charged Ions Lithium through Calcium, Univ. Maryland Techn.Rep. No 71-128, College Park, Maryland (1971).
/10/ Griem, H.R., Spectral Line Broadening by Plasmas, Academic Press, New York (1874).
/11/ Sahal-Bréchot, S., Astron.Astrophys. 1 (1969) 91.
/12/ Sahal-Bréchot, S., Astron.Astrophys. 2 (1969) 322.

/13/ Bassalo, J., Cattani, M. and Walder, V.S., J.Quant.Spectrosc.Radiat.Transfer 28 (1982) 75.
/14/ Fleurier, C., Sahal-Bréchot, S. and Chapelle, J., J.Quant.Spectrosc.Radiat.Transfer 17 (1977) 595.
/15/ Vainshtein, L.A. and Sobel'man, I.I., Opt.Spektrosk. 6 (1959) 279.
/16/ Dimitrijević, M.S. and Konjević, N., J.Quant.Spectrosc.Radiat.Transfer 30 (1983) 45.
/17/ Dimitrijević, M.S., Astron.Astrophys. 112 (1982) 251.
/18/ Dimitrijević, M.S., Publ.Astr.Obs. Sarajevo 1 (1980) 215.
/19/ Dimitrijević, M.S., V ESCAMPIG, Dubrovnik (1980) p. 90.
/20/ Dimitrijević, M.S., Bull.Obs.Astron.Belgrade 139 (1988) 31.
/21/ Dimitrijević, M.S. and Konjević, N., J.Quant.Spectrosc.Radiat.Transfer 25 (1981) 387.
/22/ Dimitrijević, M.S. and Konjević, N., J.Quant.Spectrosc.Radiat.Transfer 27 (1982) 203.
/23/ Dimitrijević, M.S., in Sun And Planetary System, eds. W.Fricke, G.Teleki, D.Reidel P.C., Dordrecht (1982) p. 101.
/24/ Sahal-Bréchot, S. and Segrè, S., in Highlights of Astronomy 2, ed. C. de Jager (1971) p. 566.
/25/ Lesage, A., Rathore, B.A., Lakićević, I.S. and Purić, J., Phys.Rev.A 28 (1983) 2264.
/26/ Dimitrijević, M.S. and Sahal-Bréchot, S., J.Quant.Spectrosc.Radiat.Transfer 31 (1984) 301.
/27/ Dimitrijević, M.S. and Sahal-Bréchot, S., Astron.Astrophys. 136 (1984) 289.
/28/ Dimitrijević, M.S. and Sahal-Bréchot, S., Phys.Rev.A 31 (1985) 316.
/29/ Dimitrijević, M.S. and Sahal-Bréchot, S., Astron.Astrophys.Suppl.Series (1990) in press.
/30/ Dimitrijević, M.S. and Sahal-Bréchot, S., Bull.Obs.Astron.Belgrade 141 (1989) in press.
/31/ Dimitrijević, M.S. and Sahal-Bréchot, S., J.Quant.Spectrosc.Radiat.Transfer 34 (1985) 149.
/32/ Dimitrijević, M.S. and Sahal-Bréchot, S., J.Quant.Spectrosc.Radiat.Transfer (1990) in press.
/33/ Dimitrijević, M.S. and Sahal-Bréchot, S., Bull.Obs.Astron.Belgrade 142 (1990) in press.
/34/ Dimitrijević,M.S. and Sahal-Bréchot,S., J.Quant.Spectrosc.Radiat.Transfer 38 (1987) 37.
/35/ Dimitrijević, M.S. and Sahal-Bréchot, S., Bull.Obs.Astron.Belgrade (1990) in press.
/36/ Vujnović, V., Vadla, Č., Lokner, V. and Dimitrijević, M.S., Astron.Astrophys. 123 (1983) 249.
/37/ Dimitrijević, M.S. and Truong-Bach, Z.Naturforsch. 41a (1986) 772.
/38/ Dimitrijević, M.S. and Artru, M.-C., XIII Symp.Phys.Ioniz.Gases, Šibenik (1986) p.317.
/39/ Lanz, T., Dimitrijević, M.S. and Artru, M.-C., Astron.Astrophys. 192 (1988) 249.
/40/ Goldbach,C., Nollez, G., Plomdeur, P. and Zimmermann, J.P., Phys.Rev.A 25 (1982) 2596.
/41/ Konjević, N., Dimitrijević, M.S. and Wiese, W.L., J.Phys.Chem.Ref.Data, 13 (1984) 649.
/42/ Konjević, N., Purić, J., Ćirković, Lj. and Labat, J., J.Phys.B 3 (1970) 999.
/43/ Purić, J., Djeniže, S., Labat, J. and Ćirković, Lj., Z.Phys. 267 (1974) 71.
/44/ Purić, J., Djeniže, S., Labat, J., Ćirković, Lj. and Lakićević, I., VIII SPIG, Dubrovnik (1976).
/45/ Purić, J., Lesage, A. and Knežević, V., IX SPIG, Dubrovnik (1978).
/46/ Lesage, A., Sahal-Bréchot, S. and Miller, M.H., Phys.Rev.A 16 (1977) 1617.
/47/ Chiang, T. and Griem, H.R., Phys.Rev.A 18 (1978) 1169.
/48/ Hey, J.D., J.Quant.Spectrosc.Radiat.Transfer 18 (1977) 425.
/49/ Jones, W.W., Phys.Rev.A 7 (1973) 1826.
/50/. Konjević, N., in The Physics of Ionized Gases (SPIG-1982, Invited Lectures), ed. G.Pichler, Institute of Physics of the University, Zagreb (1982) p. 417.
/51/ Dimitrijević, M.S., in The Physics of the Ionized Gases (SPIG-1982, Invited Lectures), ed. G.Pichler, Institute of Physics of the University, Zagreb (1982) p. 397.
/52/ Dimitrijević, M.S. and Sahal-Brechot, S., Annales de Physique (Proc. Coll. Collisions et Rayonnement) (1990) in press.

/53/ Dimitrijević, M.S. and Konjević, N., J.Quant.Spectrosc.Radiat.Transfer 24 (1980) 451.
/54/ Bogen, P., Z.Naturforsch. 27a (1972) 210.
/55/ El-Farra, M.A. and Hughes, T.P., J.Quant.Spectrosc.Radiat.Transfer 30 (1983) 335.
/56/ Bötcher, F., Breger, P., Hey, J.D. and Kunze, H.J., Phys.Rev.A 38 (1988) 2690.
/57/ Hey, J.D. and Breger, P., J.Quant.Spectrosc.Radiat.Transfer 24 (1980) 349.
/58/ Hey, J.D., and Breger, P. J.Quant.Spectrosc.Radiat.Transfer 23 (1980) 311, S.Afr.J.Phys. 5 (1982) 111.
/59/ Baranger, M., in Atomic and Molecular Processes, ed. D.R. Bates, Academic Press, New York (1962).
/60/ Sahal-Bréchot, S., to be published.
/61/ Roberts, D.E., J.Phys.B 1 (1968) 53.

JOURNAL DE PHYSIQUE
Colloque C1, supplément au n°1, Tome 50, janvier 1989

ELECTRON-IMPACT BROADENING OF Cu IV LINES FOR THE DIAGNOSTIC OF THE ARC PLASMA OF ELECTRODYNAMIC MACRO-PARTICLE ACCELERATOR

M.S. DIMITRIJEVIĆ, Z.D. JURIĆ* and A.A. MIHAJLOV*

Astronomical Observatory, Volgina 7, YU-11050 Beograd, Yugoslavia
**Institute of Physics, PO Box 57, YU-11001 Beograd, Yugoslavia*

RESUME En utilisant une méthode modele pour la simulation des pertes sur les surfaces limites, on a calculé la temperature et la composition du plasma de l'arc dans l'accélérateur électrodynamique des macro particules, initié par l'évaporation d'une plaque du cuivre. La largeur stark diagnostique de plasma de l'arc, on été calculées en utilisant la méthode semiempirique modifiée.

ABSTRACT Using a model method of loss energy simulation on the boundary surfaces, temperature and composition of an electrodynamic macroparticle accelerator arc plasma created by the evaporation of a Cu foil, have been calculated. Stark widths for Cu IV lines of interest for the arc plasma diagnostic have been calculated also, by using the modified semiempirical method.

1.INTRODUCTION

Investigation of the electron-impact broadening of atomic and ionic lines is important for a number of physical and astrophysical problems. Here, we present the Cu IV Stark line width calculations for the electrodynamic accelerator of macroparticles, arc plasma diagnostics. Such plasma is especially interesting since this is an example of very dense plasma at relatively low temperatures. More over, up to now the diagnostic of such a plasma is very difficult. Our results are suitable for the far arc-tail plasma diagnostics.

2.ELECTRODYNAMIC MACROPARTICLE ACCELERATOR ARC PLASMA

The electrodynamic accelerators of macroparticles enable the creation of extremely dense plasmas at relatively low temperatures. An example of such apparaturs (based on the conductor acceleration in the circuit's magnetic field) consists of an electrical power source and two parallel metal rails between which the macroparticle move /1/. The circuit is closed by the electrical arc created between the rails. The arc plasma (formed by the evaporated metal foil through which the discharge is

initiated) is accelerated by the magnetic field, and its hydrodynamic pressure accelerates the macroparticle- projectile.

Using a model method /2/ of loss energy simulation on the boundary surfaces, we calculated arc plasma characteristics (temperature, composition) for rectangular geometry. It is assumed, like in Ref.1, that the arc plasma is created by the evaporation of a Cu foil. Results obtained are presented in Table 1. Our results show that in the arc plasma electron density is $10^{24}m^{-3}$ in the arc tail and increase monotonically in the main arc part. The electron temperature vary from 25000K to 70000K.

Table 1. Plasma composition on the axis of arc. x is the position on the axis (x=0 is the front). N is the ground state density for ions in the respective ionization stage and
Ne is the electron density (in units of $10^{26}m^{-3}$).

x	T(K)	Ne	NII	NIII	NIV
0.0	25597	1.73	1.66-1	1.95-2	4.09-9
0.01	44625	1.27	7.24-2	3.52-2	3.81-6
0.04	54221	1.07	1.85-3	2.67-2	1.59-5
0.09	61464	9.42-1	7.48-4	2.11-2	3.48-5
0.16	66736	8.48-1	3.95-4	1.73-2	5.47-5
0.25	69181	7.66-1	2.78-4	1.49-2	6.44-5
0.36	67700	6.85-1	2.55-4	1.36-2	5.49-5
0.49	61544	5.86-1	3.19-4	1.30-2	2.94-5
0.64	51159	4.43-1	5.86-4	1.18-2	7.13-6
0.81	37736	2.31-1	1.47-3	7.45-3	3.09-7
0.99	29588	1.79-3	1.57-6	7.50-5	6.05-9

The arc plasma contains mainly Cu III ions. However, Cu IV ions also present and their lines are more convenient for diagnostic purposes due to the less influence of selfabsorption. For such a reason, we performed also the calculation of electron-impact broadening parameters for selected Cu IV lines.

3.STARK BROADENING

For the calculation, the modified semiempirical approach /3/ has been used. Electron-impact full halfwidth W_{SEM} can be calculated from the following expression:

$$W_{SEM} = 2(2\pi\hbar/3m)^2(6m/\pi kT)^{1/2}N\Big\{\sum_{\substack{j,j'=\\ i,i',f,f'}}\Big[\hat{R}^2_{\ell_j,\ell_{j+1}}\tilde{g}(E/\Delta E_{\ell_j,\ell_{j+1}}) + \hat{R}^2_{\ell_j,\ell_{j-1}}\tilde{g}(E/\Delta E_{\ell_j,\ell_{j-1}}) + \sum_{j'}(\hat{R}^2_{jj'})_{\Delta n\neq 0}\tilde{g}(3kTn_j^8/4Z^2E_H)\Big]\Big\},$$

$$\tilde{g}(x) = 0.7 - 1.1/Z + g(x),$$

$$\check{R}^2_{\ell,\ell'} = (3n/2Z)^2 \left[\max(\ell,\ell')/(2\ell+1)\right]\left[n^2 - \max^2(\ell,\ell')\right]\phi^2,$$

$$\sum_{j'} (\check{R}^2_{jj'})_{\Delta n \neq 0} = (3n_j/2Z)^2 (n_j^2 + 3\check{\ell}_j^2 + 3\ell_j + 11)/9.$$

Here, i and f designate initial and final energy levels, n is the effective principal quantum number, Z-1 is the ionic charge, ϕ the Bates and Damgaard factor (see e.g. Ref.3) and E = 3kT/2. Atomic energy level data are taken from Ref.4.

Electron-impact full halfwidths for six Cu IV multiplets are given in Table 2. The results are presented for the standard electron density $10^{17}cm^{-3}$ (far arc plasma tail condition) but for higher densities across the arc plasma axis electron-impact width will be large.

Table 2. Electron-impact full halfwidths (W_{SEM}) in Angströms for Cu IV lines for different temperatures (T) and at electron concentration $10^{17}cm^{-3}$.

Ion	Transition λ(Å)	T(K)	W_{SEM}(Å)
Cu IV	$3d^7(^4F)4s\ ^3F$-	10 000	1.44-2
	$-3d^7(^4F)4p\ ^3D$	20 000	1.02-2
	λ = 1381.6Å	30 000	8.34-3
		50 000	6.46-3
		80 000	5.11-3
		100 000	4.57-3
		150 000	3.75-3
Cu IV	$3d^7(^4F)4s\ ^3F$-	10 000	1.57-2
	$-3d^7(^4F)4p\ ^3F$	20 000	1.11-2
	λ = 1435.6Å	30 000	9.08-3
		50 000	7.03-3
		80 000	5.56-3
		100 000	4.97-3
		150 000	4.10-3
Cu IV	$3d^7(^4F)4s\ ^3F$-	10 000	1.60-2
	$-3d^7(^4F)4p\ ^3G$	20 000	1.13-2
	λ = 1445.8Å	30 000	9.22-3
		50 000	7.14-3
		80 000	5.65-3
		100 000	5.05-3
		150 000	4.17-3

(Table 2)

Cu IV	$3d^7(^4F)4s\ ^5F$-	10 000	1.33-2
	$-3d^7(^4F)4p\ ^5G$	20 000	9.41-3
	λ = 1359.5Å	30 000	7.68-3
		50 000	5.95-3
		80 000	4.71-3
		100 000	4.21-3
		150 000	3.45-3
Cu IV	$3d^7(^4F)4s\ ^5F$-	10 000	1.37-2
	$-3d^7(^4F)4p\ ^5D$	20 000	9.70-3
	λ = 1378.4Å	30 000	7.92-3
		50 000	6.14-3
		80 000	4.85-3
		100 000	4.34-3
		150 000	3.56-3
Cu IV	$3d^7(^4F)4s\ ^5F$-	10 000	1.47-2
	$-3d^7(^4F)4p\ ^5F$	20 000	1.04-2
	λ = 1422.5Å	30 000	8.49-3
		50 000	6.58-3
		80 000	5.20-3
		100 000	4.65-3
		150 000	3.83-3

REFERENCES

/1/ POWELL, J.D., BATTEH, J.H., J.Appl.Phys. 52 (1981) 2717

/2/ DJURIĆ, Z.,MIHAJLOV, A.A., to be published in Cont.Pl.Phys. (1988)

/3/ DIMITRIJEVIĆ, M.S., KONJEVIĆ, N., JQSRT, 24 (1980) 457

/4/ SCHRÖDER, J.F., VAN KLEEF, TH.A.M., Physica, 49 (1970) 388

Journal of Applied Spectroscopy, Vol. 72, No. 3, 2005

STARK BROADENING OF F III LINES IN LABORATORY AND STELLAR PLASMA

Z. Simić,[a] M. S. Dimitrijević,[a,b*] L. Č. Popović,[a] and M. D. Dačić[a] UDC 533.9.082.5

Using a semiclassical approach, we have considered electron-, proton-, and ionized helium-impact line widths and shifts for the F III $2p^3\ ^4S^o$–$3s\ ^4P$ resonant line. Moreover, for 10 F III multiplets where the full semiclassical perturbation approach is not applicable in an adequate way due to the lack of reliable atomic data, electron-impact line widths have been calculated within the modified semiempirical approach. Results are obtained as a function of temperature for perturber density of 10^{17} cm^{-3}. The theoretical data obtained have been used to consider the influence of Stark broadening for A-type star atmosphere conditions.

Keywords: *Stark broadening of spectral lines, semiclassical approach, line profiles, atomic processes, A-type stars.*

Introduction. From the Stark broadening parameters, it is possible to obtain the basic plasma parameters such as the electron temperature and electron density, which are essential for modeling the plasma considered, so that such data are of interest for diagnostics and investigation of various laboratory, astrophysical, and technological plasmas. For example, hydrogen fluoride has been detected in sunspots [1], on α Orioni [2], in red giants [3], and in interstellar media [4]. Stark broadening data for fluorine spectral lines are also of interest for the design and development of, e.g., HF and similar lasers.

The first experimental consideration of the Stark broadening of F III spectral lines was published in 1961 [5], and two unique reliable quantitative experimental determinations are given in [6–7]. Theoretical determinations of Stark broadening of F III spectral lines have been performed in [8–10] by using the modified semiempirical method [11] for $3s\ ^4P_6$–$3p\ ^4P^o_6$, $3s\ ^4P$–$3p\ ^4D^o$, $3s\ ^2P_4$–$3p\ ^2P^o_4$, $3s\ ^2P$–$3p\ ^2D^o$ and $3p'\ ^2D^o$–$3d''\ ^2D$ transitions.

Experimental Stark widths [6] of the 3113.62 Å spectral line from the multiplet $3s\ ^4P$–$3p\ ^4D^o$ and the 3154.39 Å line from the multiplet $3p'\ ^2D^o$–$3d''\ ^2D$ have been compared in [6] with the calculations in [8], performed within the modified semiempirical approach [11]. The corresponding ratios of the measured and theoretical values are 1.17 and 1.13, which is also an indicator for results presented here, since there are no experimental data for the spectral lines considered in this work.

In order to make the set of Stark broadening data for F III as complete as possible, we have used the semiclassical perturbation formalism [12, 13] (see also [14–20]) to determine electron-, proton-, and ionized helium-impact line widths and shifts for the F III $2p^3\ ^4S$–$3s\ ^4P$ resonant line. For an additional ten F III multiplets, where the full semiclassical perturbation approach is not applicable in an adequate way due to the lack of reliable atomic data, electron-impact line widths have been calculated within the modified semiempirical approach [8, 11, 21–24]. The theoretical results obtained will be used here also to consider the influence of Stark broadening in A-type star atmosphere conditions.

Results and Discussion. The semiclassical perturbation formalism used [12, 13] and all innovations and optimizations of the computer code have been discussed, e.g., in [20], while the modified semiempirical method employed [8, 11, 21–23], along with all of its applications, has been reviewed in detail in [24]. The atomic energy levels needed for calculations have been taken from [25]. Oscillator strengths have been calculated by using the method of Bates and Damgaard [26, 27]. For higher levels, the method described in [28] has been used. The results obtained

*To whom correspondence should be addressed.

[a]Astronomical Observatory, Belgrade, Serbia and Montenegro, Volgina 7, 11160; e-mail: mdimitrijevic@aob.bg.ac.yu; [b]IHIS-Chemical Power Sources Institute, Belgrade-Zemun, Serbia and Montenegro. Published in Zhurnal Prikladnoi Spektroskopii, Vol. 72, No. 3, pp. 412–415, May–June, 2005. Original article submitted December 7, 2004.

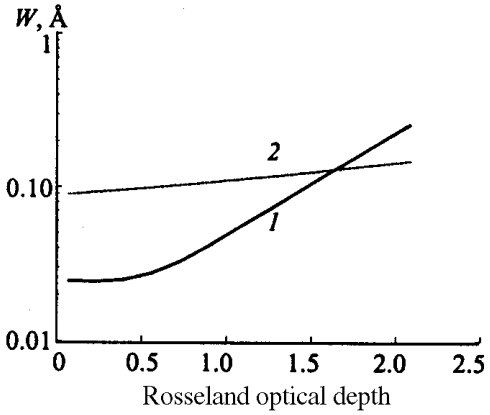

Fig. 1. Stark (1) and Doppler widths (2) for F III $4s\ ^4P$–$4p\ ^4D^o$ (λ = 8890 Å) as functions of the Rosseland optical depth τ_{Ross}, for an A-type stellar atmosphere model with T_{eff} = 10,000 K and log g = 4 [31].

TABLE 1. Electron-, Proton-, and Ionized Helium-Impact Broadening Parameters (full width at half maximum W and shift d) Obtained within the Semiclassical Perturbation Approach [13, 14] for the F III $2p^3\ 4S^o$–$3s\ ^4P$ Resonant Line (λ = 315.4 Å, $C = 0.32 \cdot 10^{19}$) for a Perturber Density of 10^{17} cm^{-3} and Temperatures from 10,000 up to 300,000 K

T, K	Electron		Proton		He II	
	W, Å	d, Å	W, Å	d, Å	W, Å	d, Å
10,000	$0.123 \cdot 10^{-2}$	$0.143 \cdot 10^{-3}$	0.714·10–6	0.858·10–5	0.188·10–5	0.846·10–5
20,000	$0.771 \cdot 10^{-3}$	$0.648 \cdot 10^{-4}$	0.442·10–5	0.175·10–4	0.579·10–5	0.163·10–4
50,000	$0.465 \cdot 10^{-3}$	0.635·10–4	0.195·10–4	0.324·10–4	0.183·10–4	0.286·10–4
100,000	$0.341 \cdot 10^{-3}$	0.681·10–4	0.352·10–4	0.443·10–4	0.327·10–4	0.367·10–4
150,000	$0.291 \cdot 10^{-3}$	0.669·10–4	0.441·10–4	0.492·10–4	0.385·10–4	0.410·10–4
300,000	$0.230 \cdot 10^{-3}$	0.615·10–4	0.588·10–4	0.591·10–4	0.489·10–4	0.490·10–4

Note. When dividing C by the corresponding full width at half maximum [17], we obtain an estimate for the maximum perturber density for which the line may be treated as isolated and tabulated data may be used.

within the semiclassical perturbation method [12, 13] for the Stark widths (full width at half maximum) and shifts of the F III $2p^3\ ^4S$–$3s\ ^4P$ resonant line due to electron-, proton-, and ionized helium impacts are shown in Table 1 for a perturber density of 10^{17} cm^{-3} and temperatures from 10,000 K up to 300,000 K. The data on spectral-line Stark widths for ten F III transitions obtained within the modified semiempirical approach are shown in Table 2 for the same perturber density and temperatures.

For the resonant-line semiclassical results, we also specify a parameter C [17]; when divided by the corresponding full width at half maximum, it gives an estimate of the maximum perturber density such that the line may be treated as isolated. The standard accuracy of the semiclassical results is within the limit of 30% and 50% for the modified semiempirical ones.

In the case of A-type stars, where the role of Stark broadening, as demonstrated many times (see, e.g., [29]), may be significant, our temperatures correspond to the deep photospheric and subphotospheric layers. Seaton [30] has drawn attention to the importance of Stark broadening for their modeling and investigation. Consequently, compared in Fig. 1 are F III $4s\ ^4P$–$4p\ ^4D^o$ (λ = 8890 Å) line widths due to Stark and thermal Doppler broadening mechanisms as functions of Rosseland optical depth corresponding to the 10,000–30,000 K temperature range, for an A-type star at-

TABLE 2. F III Electron-Impact Broadening Parameters (Full width at half maximum W) Obtained by the Modified Semiempirical Method [11] for Perturber Density of 10^{17} cm^{-3} and Temperatures from 10,000 up to 300,000 K

Transition	T, K	W, Å	Transition	T, K	W, Å
2473 Å	10,000	0.0886	874 Å	10,000	0.0348
	20,000	0.0627		20,000	0.0246
	50,000	0.0396		50,000	0.0178
$3s\ ^4P–^3p\ ^4S^o$	100,000	0.0298	$3s\ ^4P–^4p\ ^4S^o$	100,000	0.0159
	200,000	0.0253		200,000	0.0148
	300,000			300,000	0.0141
904 Å	10,000	0.0339	911 Å	10,000	0.0343
	20,000	0.0240		20,000	0.0242
	50,000	0.0172		50,000	0.0174
$3s\ ^4P–4p\ ^4P^o$	100,000	0.0151	$3s\ ^4P–4p\ ^4D^o$	100,000	0.0154
	200,000	0.0139		200,000	0.0142
	300,000	0.0134		300,000	0.0136
1723 Å	10,000	0.1130	1560 Å	10,000	0.0905
	20,000	0.0795		20,000	0.0640
	50,000	0.0576		50,000	0.0465
$4s\ ^4P–3p\ ^4S^o$	100,000	0.0507	$4s\ ^4P–3p\ ^4P^o$	100,000	0.0409
	200,000	0.0462		200,000	0.0374
	300,000	0.0438		300,000	0.0354
1504 Å	10,000	0.0838	6286 Å	10,000	2.72
	20,000	0.0593		20,000	1.93
	50,000	0.0431		50,000	1.43
$4s\ ^4P–3p\ ^4D^o$	100,000	0.0380	$4s\ ^4P–4p\ ^4S^o$	100,000	1.31
	200,000	0.0347		200,000	1.22
	300,000	0.0329		300,000	1.16
8263 Å	10,000	4.43	8890 Å	10,000	5.11
	20,000	3.13		20,000	3.61
	50,000	2.32		50,000	2.68
$4s\ ^4P–4p\ ^4P^o$	100,000	2.09	$4s\ ^4P–4p\ ^4D^o$	100,000	2.43
	200,000	1.94		200,000	2.26
	300,000	1.86		300,000	2.15

mosphere model with $T_{\rm eff}$ = 10,000 K and log g = 4 [31]. One should take into account that, due to differences between the Lorentz (Stark) and Gauss (Doppler) line intensity distributions, Stark broadening may be more important on line wings in comparison with the thermal Doppler one, even when it is smaller in the central part.

In closing, we can note that the obtained Stark broadening parameters also contribute to the creation of a set of such data for no matter how large the number of spectral lines, which is of significance for a variety of problems in research into laboratory, technological, and astrophysical plasmas.

Acknowledgements. This work is part of the project GA-1195 "Influence of collisional processes on astrophysical plasma line shapes," supported by the Ministry of Science, Technologies, and Development of Serbia.

REFERENCES

1. D. N. B. Hall and R. W. Noyes, *Astrophys. Lett.*, **4**, 143–148 (1969).
2. H. Spinrad, L. D. Kaplan, P. Connes, J. Connes, V. G. Kunde, and J. P. Maillard, in: G. W. Lockwood and H. M. Dyck (Eds.), *Proc. Conf. Late Type Stars* KPNO, Tucson (1970), pp. 59–75.
3. A. Jorissen, V. V. Smith, and D. L. Lambert, *Astron. Astrophys.*, **261**, 164–187 (1992).
4. D. A. Neufeld, J. Zmuidzinas, P. Schilke, and T. G. Phillips, *Astrophys. J.*, **488**, L141–L144 (1997).
5. M. B. Sarma, *Proc. Phys. Soc. London*, **77**, 665–668 (1961).
6. J. Purić, A. Srećković, S. Djeniže, and M. Platiša, *Phys. Rev. A*, **37**, 4380–4386 (1988).

7. S. Djeniže, J. Labat, A. Srećković, O. Labat, M. Platiša, and J. Purić, *Physica Scripta*, **44**, 148–150 (1919).
8. M. S. Dimitrijević and N. Konjević, in: B. Wende (Ed.), *Spectral Line Shapes*, W. de Gruyter, New York (1981), pp. 211–239.
9. M. S. Dimitrijević, *Astron. Astrophys. Suppl. Ser.*, **76**, 53–59 (1988).
10. M. S. Dimitrijević, *Bull. Obs. Astron. Belgrade*, **139**, 31–58 (1988).
11. M. S. Dimitrijević and N. Konjević, *J. Quantum Spectrosc. Rad. Transfer*, **24**, 451–459 (1980).
12. S. Sahal-Bréchot, *Astron. Astrophys.*, **1**, 91–123 (1969).
13. S. Sahal-Bréchot, *Astron. Astrophys.*, **2**, 322–354 (1969).
14. S. Sahal-Bréchot, *Astron. Astrophys.*, **35**, 319–321 (1974).
15. C. Fleurier, S. Sahal-Bréchot, and J. Chapelle, *J. Quantum Spectrosc. Rad. Transfer*, **17**, 595–604 (1977).
16. S. Sahal-Bréchot, *Astron. Astrophys.*, **245**, 322–330 (1991).
17. M. S. Dimitrijević, S. Sahal-Bréchot, and V. Bommier, *Astron. Astrophys. Suppl. Ser.*, **89**, 581–590 (1991).
18. M. S. Dimitrijević and S. Sahal-Bréchot, *Physica Scripta*, **52**, 41–51 (1995).
19. M. S. Dimitrijević and S. Sahal-Bréchot, *Physica Scripta*, **54**, 50–55 (1996).
20. M. S. Dimitrijević, *Zh. Prikl. Spektrosk.*, **63**, 810–815 (1996).
21. M. S. Dimitrijević and N. Konjević, *Astron. Astrophys.*, **172**, 345–349 (1987).
22. M. S. Dimitrijević and V. Krsljanin, *Astron. Astrophys.*, **165**, 269–274 (1986).
23. M. S. Dimitrijević and L. Č. Popović, *Astron. Astrophys. Suppl. Ser.*, **101**, 583–586 (1993).
24. M. S. Dimitrievich and L. Ch. Popovich, *Zh. Prikl. Spektrosk.*, **68**, 685–690 (2001).
25. S. Bashkin and J. O. Stoner, Jr., *Atomic Energy Levels and Grotrian Diagrams*, Vol. 1, Amsterdam, North Holland (1975).
26. D. R. Bates and A. Damgaard, *Trans. Roy. Soc. London*, Ser. A, **242**, 101–122 (1949).
27. G. K. Oertel and L. P. Shomo, *Astrophys. J. Suppl. Ser.*, **16**, 175–218 (1968).
28. H. Van Regemorter, Hoang Binh Dy, and M. Prud'homme, *J. Phys. B*, **12**, 1053–1062 (1979).
29. M. S. Dimitrijević. T, Ryabchikova, L. Č. Popović, D. Shylyak, and V. Tsymbal, *Astron. Astrophys.*, **404**, 1099–1106 (2003).
30. M. J. Seaton, *J. Phys. B*, **20**, 6363–6378 (1987).
31. R. L. Kurucs, *Astrophys. J. Suppl. Ser.*, **40**, 1–340 (1979).

Journal of Astronomical History and Heritage, 14(3), 180-189 (2011).

SIRIUS IN ANCIENT GREEK AND ROMAN LITERATURE: FROM THE ORPHIC *ARGONAUTICS* TO THE *ASTRONOMICAL TABLES* OF GEORGIOS CHRYSOCOCCA

Efstratios Theodossiou[1], Vassilios N. Manimanis[1], Milan S. Dimitrijević[2] and Peter Z. Mantarakis[3]

[1]Department of Astrophysics-Astronomy and Mechanics, School of Physics, National and Kapodistrian University of Athens, Panepistimioupolis, Zographos 157 84, Athens, Greece.

E-mail: etheodos@phys.uoa.gr; vmaniman@phys.uoa.gr

[2]Astronomical Observatory of Belgrade, Volgina 7, 11060 Belgrade, Serbia.

E-Mail: mdimitrijevic@aob.bg.ac.rs

[3] 22127 Needles St, Chatsworth, California, USA

E-mail: zanispetros@socal.rr.com

Abstract: The brightest star of the night sky, is Sirius, Alpha Canis Majoris (α CMa). Due to its intense brightness, Sirius had one of the dominant positions in ancient mythology, legends and traditions. In this paper the references of the many ancient classical Greek and Roman authors and poets who wrote about Sirius are examined, and the problem of its 'red' color reported in some of these references is discussed.

Keywords: Seirios, Sirius, Dog Star, Canis Major, scorching star, Maira

1 INTRODUCTION

Sirius, Alpha Canis Majoris (α CMa), is the brightest star in the night sky. It is visible throughout Greece on clear winter nights, and for this reason occupies a significant place in ancient mythology, legends and traditions. The original Greek name, 'Seirios', meant 'sparking', 'shining', 'fiery' or 'burning'.

In this work, ancient Greek and Roman and some Byzantine references to Sirius will be considered, which led to the popularization of its name in the Greco-Roman literature. The same is true for the myths and classical traditions associated with it; the classical folklore associated with Sirius became known and was enriched through the work of the main Latin authors. In this way, both the name and the myths were long established in Western culture and thus survived. We will also examine and discuss the problem of the 'red' color of Sirius, which arises from references of some ancient authors.

2 SIRIUS IN THE CONSTELLATION CANIS MAJOR

Canis Major is an average-sized southern constellation with 95 stars visible to the naked eye. Its brightest star, Sirius, is almost four times brighter than any other star visible from the latitude of Athens (38°, central Greece). One must go further south than 37° N, to Rhodes or Crete, in order to observe the next brightest star, Canopus, which is half as bright as Sirius (Canopus is the brightest star of the constellation Carina, and is Alpha Carinae).

We now know that Sirius is one of the closest stars to the Earth at a distance of just 2.64 parsecs (8.60 light years), and it has an apparent magnitude $m = -1.46$. This is 20 times brighter than our Sun would be at the same distance. Canopus is at a much greater distance of 96 pc (313 l.y.) and shines with an apparent magnitude of -0.72.

Of all visible celestial objects, only the Sun, the Moon, Venus, Jupiter and Mars appear brighter than Sirius; actually, Mars is brighter than Sirius only when it is close to opposition, approximately once every two years.

Sirius (α CMa), Procyon (α CMi, the brightest star in the constellation Canis Minor) and Betelgeuse (α Ori, the brightest star in the constellation Orion) form a large triangle in the January-to-March sky, the so-called, 'Winter Triangle', which is almost equilateral. Today, Sirius first appears in the dawn skies several weeks later than it did in ancient times (10 August versus near the summer solstice). This is because of the precession of the equinoxes due to the 26,000-year wobble of the Earth's axis.

Sirius is in fact a triple star system. The companion star, Sirius B, is a white dwarf about the size of the Earth; most of its mass is compressed so much that a cubic cm of this material would weigh on Earth a few tons (and hundreds of tons on the surface of the white dwarf). Sirius B shines eighty times fainter than the naked-eye theoretical limit, but even if it reached that limit the intense glow from the adjacent Sirius A would render its companion invisible. This is the reason that Sirius B was only indirectly detected in 1844 from the perturbations it caused in the position of Sirius. The discovery was made by the German astronomer Friedrich Wilhelm Bessel. It was first optically observed in 1862 by the American astronomer and telescope-maker Alvan G. Clark during the testing of a refracting telescope of exquisite quality. In 1994 Daniel Benest and Jean-Louis Duvent (1995) from the O.C.A. Observatoire de Nice in France suggested the existence of a second companion to Sirius, Sirius C.

Because of its great brightness, Sirius occupied a prominent position in mythology, legends and traditions of most people, and especially of the ancient Greeks. Its very name, ***Seirios***, in Greek means 'sparking', 'fiery' or 'burning', 'flamboyant', 'scorching star' or 'scorcher' (Table 1); this epithet dates from at least the sixth century BC, as it was recorded in the Orphic *Argonautics* (Demetrakos, 1964: Volume 13).

Claudius Ptolemaeus (= Ptolemy, second century AD) mentions Sirius as "… the one in the mouth [of the dog], most bright, is called Dog and ***hypokirros***." (Ptolemy, 1903: 142).[1] In a small differentiation, Johann Bayer in his *Uranometria* places the bright star on the greater dog's snout (see Bayer, 1603: Leaf 38).

Sirius can be seen from every inhabited region of the Earth's surface. The best time of the year to view it in our epoch is around 1 January, when it reaches the meridian at true midnight. In 500 BC this happened around 11 December.

3 SIRIUS IN GREEK AND ROMAN MYTHOLOGY

Canis Major probably depicts the faithful dog of Orion the Hunter, Laelaps. Orion is a nearby constellation. Indeed, Sirius can be located on the celestial sphere if we extend the line formed by the three stars of 'Orion's Belt' to the east.

In a tale of Greek mythology, Orion was in love with the goddess Artemis—the Greek equivalent of Diana. However, Apollo, in order to cancel the union of mortal Orion with his twin sister, sent a huge scorpion—represented now by the constellation Scorpius—that killed the unlucky hunter. After Orion's death, his beloved Artemis donated his exquisite hound to Procris, daughter of Erechtheus and one of Artemis' following nymphs. Procris later gave Laelaps to her husband Cephalus, who also was a famous hunter.

> In early classical days it was simple Canis, represented the dog Laelaps, the hound of Actaeon, or that of Diana's nymph Procris, or the one given to Cephalus by Aurora and famed for the speed that so gratified Jove as to cause its transfer to the sky. (Allen, 1963: 117).

Table 1: Greek names for Sirius.

Greek Name	Translit-eration	Latin spelling	Translation
Σείριος	Seirios	Sirius	Sparking
Αστροκύων	Astrokyon	Aster Cyon	The Dog Star

According to Eratosthenes' *Catasterismoi* (1997; cf. Eratosthenis, 1897), Laelaps is the dog given as a gift by Zeus to Europa. Their son, Minos, King of Crete, gave it later on to Procris because she healed him of some illness. Procris again donated it to her husband Cephalus. After Cephalus accidentally killed Procris, Zeus placed his dog in the homonymous constellation.

Less known versions refer to Sirius in connection with Cerberus, the wild three-headed dog that guarded the gates of the underworld (Hades), or with one of the hunting dogs of Actaeon, a renowned hunter and hero from Thebes, who, had the misfortune of wandering onto Artemis' bathing site. After this dog saw Artemis naked, she turned him into a deer and made his own dogs kill him.

Seirios was variously identified in myth. Some say that it was Maira, a daughter of the Titan Atlas, or that, according to the Roman poet Ovid (43 BC–AD 17), it was Maira, the faithful dog of King Ikarios—represented by Boötes.

Sirius may also have been associated with Orthros (= the morning twilight), hound of Geryon,[2] the giant of the West. The dog-star was probably also associated with the dog-goddess Hecate, daughter of the Titans Perses and Asteria.

It was also considered to represent Orion's hunting dog, pursuing Lepus the Hare or helping Orion fight Taurus the Bull; and is referred to in this way by Aratus, Homer and Hesiod (Theodossiou and Danezis, 1990: 114).

The ancient Greeks refer only to one dog, but by Roman times, Canis Minor appears as Orion's second hound (Allen, 1963: 132). According to Richard H. Allen (1963: 118), in Rome two additional names of Canis Major were

> Custos Europae [which] is in allusion to the story of the Bull who, notwithstanding the Dog's watchfulness, carried off that maiden; and Janitor Lethaeus, the Keeper of Hell, [who] makes him a southern Cerberus the watch-dog of the lower heavens, which in early mythology were regarded as the abode of demons.

4 SIRIUS IN ANCIENT GREEK AND ROMAN LITERATURE

4.1 The Ancient Greek References

In the Orphic *Argonautica*, in the scene where Zeus mates with Alcmene (Hercules' mother) it states: "… when the Sun was losing his Sirius-like triple lumenescence in his course and the black night was spreading from everywhere …" (Apollonius Rhodius, 1962: verse 121); or: "… just when for three consecutive days lost its light the flamboyant Sun ('Seirios Sun') …" (Petrides, 2005: 49).

Homer mentions Sirius in the *Iliad* (1924, V: 1-5, XXI: 25-32) and *Odyssey* (1919: v 4) as 'oporinós', the star of autumn, and as Orion's dog:

> Then Athena gave power and courage to Diomedes, so that excellently amidst the Greek multitudes he would be glorified and take shining fame everywhere. From his helmet and shield a flame was visible, which pours light without sleeping, as the autumn star, bathed in the Ocean, shines with its full light. (Homer, 1924, V: 1-5).

The 'autumn star' is actually Sirius, and appears every year, for the geographical latitude of Greece, in the predawn sky in late July or early August. This is mentioned also by Allen, who writes:

> Homer alluded to it in the *Iliad* as *Οπωρινός*, the Star of Autumn; but the season intended was the last days of July, all August, and part of September—the latter part of summer. The Greeks had no word exactly to our "autumn" until the 5th century before Christ, when it appeared in writings ascribed to Hippocrates. Lord Derby translated this celebrated passage: "A fiery light. There flash'd, like autumn's star, that brightest shines. When newly risen from his ocean bath …" (Allen, 1963: 120).

In *Iliad's* rhapsody XXII both Orion and Sirius are mentioned. The brightest star, Sirius, is referred to as Orion's dog. Homer presents Sirius as an ominous sign in the sky, as every summer it is connected with the so-called 'dog burnings':

> … like the star that comes to us in autumn, outshining all its fellows in the evening sky – they call it Orion's dog, and though it is the brightest of all stars it bodes no good bringing much fever, as it does, to us poor mortals. (Homer, 1924: Ch. 22, v 25-31ff).

At about the same time, or slightly later, Hesiod (1914), in his famous book *Works and Days*, discusses all the stars and constellations mentioned by Homer, with a special reference to Sirius. Indeed, he mentions Sirius in three different passages. In the first of these he gives some advice to his brother Perses about grape-gathering:

> But when Orion and Sirius are come into mid-heaven, and rosy-fingered Eoς [Dawn] sees Arcturus, then cut

> off all the grape-clusters, Perses,[3] and bring them home. (Hesiod, 1914: v 609ff).

In the other two passages he speaks about the dog burnings: "For then the star Sirius passes over the heads of men, who are born to misery, only a little while by day and takes greater share of night …" (ibid.: 417) and "… for Sirius dries the head and the knees and the body is dry from the heat." (ibid.: 587).

Another work by Hesiod, ***Aspis Irakleous*** (***The Shield of Hercules***), is to a certain extent an imitation of ***Aspis Achilleos*** (***The Shield of Achilles***) as it is described in the ***Iliad*** (Homer, 1924). In this work, too, Hesiod mentions Sirius twice:

> Their souls passed beneath the earth and went down into the house of Hades; but their bones, when the skin is rotted about them, crumble away on the dark earth under parching Sirius. (Hesiod, 1914: v 139ff).

> And when the dark-winged whirring grasshopper, perched on a green shoot, begins to sing of summer to men—his food and drink is the dainty dew—and all day long from dawn pours forth his voice in the deadliest heat, when Sirius scorches the flesh, then the beard grows upon the millet which men sow in summer. (ibid.: v 391).

The ancient Greek lyric poet Alcaeus (seventh-sixth century BC) states the following about Sirius:

> Wet your lungs with wine: the dog star, Seirios, is coming round, the season is harsh, everything is thirsty under the heat, the cicada sings sweetly from the leaves ... the artichoke is in flower; now are women most pestilential, but men are feeble, since Seirios parches their heads and knees. (Alcaeus, 1982, 1993; cf. Alcaeus, 1922; Alcée, 1999).

Theognis (570–480 BC), a significant elegy poet from Megara, wrote several symposium poems, distinguished for their dignity and their respect for the gods. He even gave a rule for wine drinking, adding some information for the period around the rise of Sirius, calling it 'astrokyon' in Greek (Table 1): "Witless are those men, and foolish, who don't drink wine even when the Dog Star is beginning …" (Wender, 1984: 1039-1040).

The tragic poet Aeschylus (525–456 BC), in his tragedy ***Agamemnon*** (Aeschylus, 1955: v 966-968), also mentions Sirius, as 'seirios dog', while Euripides (480–406 BC) in both his tragedies ***Hecuba*** (2008) and ***Iphigenia at Aulis*** (1999; 2003; 2004) mentions it by its name, Seirios proper. Here are the relevant verses in their English translations:

> For while the stock is firm the foliage climbs, Spreading a shade, what time the Dog-star (seirios kynos) glows; And thou, returning to thine hearth and home, Art as a genial warmth in winter hours. (Aeschylus, 1955: v 967).

> Where Orion and Sirius dart from their eyes a flash as of fire … (Euripides, 2008: v 1104).

> Sirius, still shooting o'er the zenith on his way near the Pleiads' sevenfold track … (Euripides, 2004: 1A8).

The poet Lycophron of the Alexandrine 'Pleias'[4] (third century BC), in his only surviving poem, wrote of Cassandra's prophecy for the fall of Troy in which he referred to a 'Seirian ray', meaning more probably a solar ray (Scheer, 1958: Frag. 397).

The renowned Greek astronomical poem, ***Phaenomena***, written by Aratus of Soloi in the Court of Antigonos Gonatas, the King of Macedonia (270 BC), refers to Seirios calling it 'Star of the Dog', 'Poikilos' (most probably meaning 'changing in color') and 'Seirios':

> A star that keenest of all blazes with a searing flame and him men call Seirios. When he rises with Helios (the Sun), no longer do the trees deceive him by the feeble freshness of their leaves. For easily with his keen glance he pierces their ranks, and to some he gives strength but of others he blights the bark utterly. Of him too at his setting are we aware. (Aratus of Soloi, 1921: 326-340).

Aratus also appended an adjective to the name, calling Sirius μέγας (= big, great); according to Allen. With this adjective he wanted only to characterize the brilliancy of the star, and not to distinguish it from the Lesser Dog. The Greeks did not know of the two Dogs at that time, nor did the comparison appear until the latter days of Vitruvius (Allen, 1963: 117). However, Allen does not mention the use of the same adjective (big, great) for Sirius by Eratosthenes.

Eratosthenes (276–194 BC) in his work ***Astrothesiai*** or ***Catasterismoi*** (Eratosthenes, 1997a; 2001) writes about the Dog, which he calls both ***Isis*** and ***Seirios***, describing it as "… great and bright." However, he also uses the word ***seirios*** as an adjective, writing for example: "Such stars are called 'seirioi' by astronomers due to the quivering motions of their light." ('Seirioi' is the plural of 'seirios').

Apollonius of Rhodes (third century BC) in his ***Argonautica***, a major epic poem that remolds in poetic form the mythical expedition of the Argonauts from Thessaly to Colchis on the Black Sea, also mentions Sirius in connection to the unbearable summer heat:

> But when from heaven Sirius scorched the Minoan Isles, and for long there was no respite for the inhabitants … (Apollonius Rhodius, 1962, Book II: 517).

Also, in another passage:

> But soon he appeared to her longing eyes, striding along loftily, like Sirius coming from ocean's depths, which rises fair and clear to see, but brings unspeakable mischief to flocks … (Apollonius Rhodius, 1962, Book III: 956-958).

Diodorus Siculus (ca. 80–20 BC), a Greek historian of Agyrium in Sicily, wrote forty books on world history, called ***Library of History***, in three parts: mythical history of peoples (both non-Greek and Greek) up to the Trojan War; history up to Alexander's death (323 BC); and history up to 54 BC. From his writings we have complete Books I-V (Egyptians, Assyrians, Ethiopians, Greeks) and Books XI-XX (Greek history 480-302 BC); and fragments of the rest. He was an uncritical compiler, but used good sources and reproduced them faithfully. He is valuable for details that are not recorded elsewhere, and as evidence for works now lost, especially the writings of Ephorus, Apollodorus, Agatharchides, Philistus and Timaeus. Diodorus Siculus writes in ***The Library of History***:

> A plague [i.e. a pestilence arising in a time of drought] prevailed throughout Greece … [and] the sacrifice he offered there was on behalf of all the Greeks. And since the sacrifice was made at the time of the rising of the star Seirios, which is the period when the Etesian winds customarily blow, the pestilential diseases, we are told, came to an end. Now the man who ponders upon this event may reasonably marvel at the strange

> turn which fortune took; for the same man [Aristaios] who saw his son [Aktaion] done to death by the dogs likewise put an end to the influence of the star which, of all the stars of heaven, bears the same name [i.e. Seirios, which was known as the dog-star] and is thought to bring destruction upon mankind, and by so doing was responsible for saving the lives of the rest. (Diodorus Siculus, 1939, IV: 81.1).

Satirical author Lucian of Samosata (AD 120−190) mentions Sirius in his fantasy novel ***Trips to the Moon*** (original title: ***A True Story***), where he narrates the imaginary war between earthlings with the dog-faced inhabitants of Sirius, who are called Cynobalani:

> Near them were placed the Cynobalani [88b] about five thousand, who were sent by the inhabitants of Sirius; these were men with dog's heads, and mounted upon winged acorns: some of their forces did not arrive in time; amongst whom there were to have been some slingers from the Milky Way, together with the Nephelocentauri; [88c] they indeed came when the first battle was over, and I wish [88d] they had never come at all: the slingers did not appear, which, they say, so enraged Phaëton that he set their city on fire. (Lucian, 2010).

Apart from this work, which probably could be considered as the first science fiction novel, Lucian mentions Sirius in other works, as 'the Dog of Orion': "For this reason the poet, in order to praise the Dog of Orion, called it lion-tamer." (Lucian, 1911: Volume 6).

In ***The Almagest***, Ptolemy (1903: Books VII and VIII) called Sirius *Αστροκύων* (***Astrokyon*** = Dog star; see Table 1), writing that it was a red star like Antares (Alpha Scorpionis) and Aldebaran (Alpha Tauri). Ptolemy

> … and his countrymen knew it by Homer's title, and often as *Αστροκύων*, although it seems singular that the former never used the word *Σείριος*. (Allen 1963: 118).

Ptolemy used Astrokyon as the location for the celestial globe's central meridian.

In the same century, Plutarch writes in his work ***De Iside et Osiride*** that the constellation of the Dog was dedicated to goddess Athena-Isis:

> And the ship that Greeks call 'Argo' was built in the form of the ship of Osiris; it was enlisted among the constellations as an honor and it moves not far from the constellations of Orion and of the Dog, from which the former is dedicated by the Egyptians to Horus, while the latter is dedicated to Isis. (Plutarch, 1932: 354c-359f).

According to Allen (1963: 120),

> Plutarch called it *Προόπτης*, the Leader, which well agrees with its character and is an almost exact translation of its Euphratean, Persian, Phoenician, and Vedic titles; but *Κύων, Κύων σείριος, Κύων αστήρ, Σείριος αστήρ, Σείριον άστρον*, or simply *το άστρον*, were its names in early Greek astronomy and poetry.

According to the architect and author Nikolaos V. Litsas (2008: 40):

> Plutarch in his opus ***'De Iside et Osiride'*** (354c and 366a) writes that Isis, which he identifies with Athena, is Sirius, the well-known star of the Dog. This is why Parthenon, the temple of Athena in the Acropolis of Athens is oriented in such a way that once per year, on July 2 [modern date], when the Sun passes above Sirius, the rays of the rising Sun penetrate in the sacrosanct of the sanctuary.

Quintus Smyrnaeus was a Greek epic poet who flourished in Smyrna in the late fourth century AD. His only surviving work is a fourteen-book epic entitled the ***Fall of Tro***y (or ***Posthomerica***). This poem covers the period of the Trojan War from the end of Homer's ***Iliad*** to the final destruction of Troy. Quintus is believed to have drawn heavily from works of the poets of the Epic Cycle, including such now-lost works as the ***Aethiopis*** and the ***Little Iliad***:

> From the ocean's verge upsprings Helios (the Sun) in glory, flashing fire far over earth - fire, when besides his radiant chariot-team races the red star Seirios, scatterer of woefullest diseases over men. (Quintus Smyrnaeus, 1913, 8: 30ff).

In the same period (fourth century AD) we have Anonymous, perhaps Pamprepius of Panopolis, referring to Seirios, as the dog-star (***kynos astraios***):

> The snow-white brightness of blazing Phaethon [the Sun] is quenched by the liquid streams of rain clouds, and the fiery … [lacuna]... of the dog-star [(kynos astraios)] is extinguished by the watery snowstorms. (Anonymous, 1950: No. 140).

Nonnus, a Greek epic poet of the fifth century AD from the Egyptian city of Panopolis, writes in his ***Dionysiaka*** twice about the dog burnings of Sirius:

> He sent an opposite puff of winds to cut off the hot fever of Sirius. (Nonnus, 1940, 5: 275ff).
>
> He [Aristaios] had not yet migrated to the island formerly called Meropis [Kos]: he had not yet brought there the life breathing wind of Zeus the Defender [the Etesian Winds], and checked the fiery vapour of the parched season; he had not stood steel clad to receive the glare of Seirios, and all night long repelled and clamed the star's fiery heat—and even now the winds cool him with light puffs, as he lances his hot parching fire through the air from glowing throat. (ibid. 13: 253 ff).

4.2 The Ancient Latin and Byzantine References

According to Allen (1963), the Romans adopted their Canis from the Greeks and kept that name forever, sometimes in its even diminutive form ***Canicula*** (with the adjective ***candens***, meaning 'shining'). There are also the names 'Erigonaeus' and 'Icarius' from the fable of the dog 'Maera'—which by itself means 'Shining'. In the fable, the dog's mistress, Erigone, is transformed into Virgo, her master, Icarius, is transformed into Boötes, and Maera becomes Sirius. According to Allen (1963: 118), Ovid alluded to this in his ***Icarii stella proterva canis*** [***Amor***. II.16.4]; and Statius mentioned the ***Icarium astrum***, although Hyginus [***Fab***. 130] had ascribed this to the Lesser Dog.

From the Latin authors and poets, Virgil in his ***Georgics***, tragic poet Seneca (2003) in his ***Oedipus***, epic poet Valerius Flaccus in his ***Argonautica*** (1934) and poet Statius in his ***Silvae*** (2003), all refer to Sirius mostly as the 'star of the dog'.

Virgil (first century BC) writes:

> The time when the sultry Dog Star [Canis] splits the fields that gape with thirst … (Virgil, 1916: ***Georgics*** 2, 353 ff).
>
> And now Sirius (the Dog Star), fiercely parching the thirsty Indians, was ablaze in heaven, and the fiery Sun had consumed half his course; the grass was withering and the hollow streams, in their parched throats, were

> scorched and baked by the rays down to the slime. (ibid. 2: 425 ff).

Virgil also writes in *Aeneid's* Books III and X about Sirius:

> Just as when comets glow, blood-red and ominous in the clear night, or when fiery Sirius, bringer of drought and plague to frail mortals, rises and saddens the sky with sinister light. (Virgil, 2002: Book X: v 271-273).

> They relinquished sweet life, or dragged their sick limbs around: then Sirius blazed over barren fields: the grass withered, and the sickly harvest denied its fruits (Virgil, 2002: Book III: v 140-142).

Seneca writes in his Roman tragedy *Oedipus* (first century BC):

> [Thebes was plagued by drought and] … No soft breeze with its cool breath relieves our breasts that pant with heat, no gentle Zephyrus blows; but Titan [Helios, the Sun] augments the scorching dog-star's [Seirios'] fires, close-pressing upon the Nemean Lion's [i.e. Leo, zodiac of mid-summer] back. Water has fled the streams, and from the herbage verdure. Dirce[5] is dry, scant flows Ismenus' stream, and with its meagre wave scarce wets the naked sands. (Seneca, 2004: *Oedipus*, 37 ff).

The Roman Valerius Flaccus writes in his epic *Argonautica* (first century BC):

> When Sirius in autumn sharpens yet more his fires, and his angry gold gleams in the shining tresses of night, the Arcadian [planet Mercury] and great Jupiter [the planet] grow dim; fain are the fields that he would not blaze so fiercely in heaven, fain too the already heated waters of the streams. (Valerius Flaccus, 1934, 5: 370 ff).

Horace (Quintus Horatius Flaccus) mentions Sirius in his *Satires* (Horace, 1870: V). Finally, Statius in *Silvae* (Roman poetry, first century AD) refers to Sirius:

> T'was the season when the vault of heaven bends its most scorching heat upon the earth, and Sirius the Dog-star smitten by Hyperion's [the Sun's] full might pitilessly burns the panting fields. (Statius, 2003: 3, 1, 5).

According to Allen (1963: 118), Sirion and Syrius occasionally appeared with the best Latin authors; and the *Alfonsine Tables* of 1521 had Canis Syrius.

Arab astronomers, influenced by Ptolemy and the other Greek astronomers, called Sirius 'Al Shiʿrã', which means 'the shining one', because of its extreme brightness (Allen, 1963: 121).

The scholar and Byzantine Princess, Anna Comnena (Komnene), in her large work *Alexias* (1148) mentions the 'star of the Dog':

> … even though it was summer and the sun had passed through Cancer and was about to enter Leo – a season in which, as they say, the star of the Dog rises … (Anna Comnena, 1928, 1969: I, Book 3, XII.4).

Finally, the Byzantine scholar, medical doctor and astronomer Georgios Chrysococca (fourteenth century) mentions Sirius as *Siaèr Jamanè* in his astronomical work *Synopsis tabularum persiacarum ex syntaxi Persarum Georgii medici Chrysococcae* (Chrysococca, 1645: 1347). Allen refers to this work as 'Chrysococca's *Tables*'. It was published by Ismael Bullialdus in Paris in 1645.

As a general observation, it can be noted that the ancient Greeks and Romans generally did not distinguish the constellation Canis Major from the star Sirius by name, but often called both simply 'Dog' (Ceragioli, 1996: 121).

5 MAIRA

Sirius in the annual period from its heliacal rising to 22 August was also called 'Maira', a word coming from the ancient Greek verb ***marmairo***, which means 'to shine' (*Palatine or Greek Anthology*, 1917, 9: 55). As a name, Maira (or Maera) therefore became the star-goddess of the scorching dog-star Seirios, whose rising in conjunction with the Sun brought on the scorching heat of midsummer. Like the Pleiades and Hyades, Maira was a starry daughter of the Titan Atlas. She married a mortal King, the Arcadian Tegeates, the son of King Lycaon and the eponymous founder of the Arcadian town of Tegea. The precise location of her tomb was not known, and both Tegea and Mantineia laid claim to it. Pausanias (1935, VIII: 12, §4; 48, §4; 53, §1) thinks that Maira was the same as the Maira whom Odysseus saw in Hades (Pausanias: "[Odysseus sees the ghosts of heroines in the Underworld:] I saw Maira too." (Homer, 1919: 11, 326 ff).

In his *Description of Greece*, the Greek traveller Pausanias (second century AD) writes about the story of the nymph Maira, and reports all the mythical and historical information associated with her:

> There are also tombs [in Tegea, Arcadia] of Tegeates, the son of Lykaon, and of Maira, the wife of Tegeates. They say Maira was a daughter of Atlas, and Homer makes mention of her in the passage where Odysseus tells to Alkinous his journey to Hades, and of those whose ghosts he beheld there. (Pausanias, 1935: 8.48.6).

> The ruins of a village called Maira, with the grave of Maira … For probably the Tegeans, and not the Mantineans, are right when they say that Maira, the daughter of Atlas, was buried in their land. (ibid.: 8.12.7).

> Apollon and Artemis, they say, throughout every land visited with punishment all the men of that time who, when Leto was with child and in the course of her wanderings, took no heed of her when she came to their land [Tegea in Arcadia]. So when the divinities came to the land of Tegea, Skephros, they say, the son of Tegeates, came to Apollon and had a private conversation with him. And Leimon [= water-rich meadow], who also was a son of Tegeates, suspecting that the conversation of Skephros contained a charge against him, rushed on his brother and killed him. Immediate punishment for the murder overtook Leimon, for he was shot by Artemis. At the time Tegeates and Maira sacrificed to Apollon and Artemis, but afterwards a severe famine fell on the land, and an oracle of Delphi ordered mourning for Skephros (ibid.: 8.53.2).

5.1 Maira/Maera as a Dog in Greek and Roman Mythology

Maera was the faithful hound of Icarius, an Athenian King, and follower of the wine-god Dionysus. Icarius was the father of the maiden Erigone.

This is the whole story, according to the Roman mythographer Hyginus (second century AD): Dionysus had taught Icarius how to make wine. One day, Icarius was travelling on the road in a wagon, when he met some shepherds. Icarius shared his wineskin. The shepherds fell into a drunken stupor and when they woke up they thought Icarius had tried to poison them, so they killed him and buried him under a tree.

Concerned for her father's whereabouts, Erigone set off with Maera to find him, and Maera led the maiden to the grave. The hound howled in its grief, before leaping off the cliff to its death. Erigone was also distraught over her father's death, and hanged herself from the tree above her father's grave.

Taking pity on his followers and the hound, Dionysus placed them in the sky as the constellations Boötes (Icarius), Virgo (Erigone), and Maera as the constellation with the star Sirius. So, Maira was closely identified with the *Kyon Ikarion*, the dog of Icarius, which along with her star formed the constellation Canis Major. Others say the constellation Canis Major or Canis Minor was Maera.

Dionysus did not let the shepherds escape for murdering Icarius. Dionysus caused madness in Athens, where all the maidens hanged themselves. The Athenians found out from the oracle what had caused this phenomenon so they captured the murderers and hanged them. From that time onwards, the Athenians held an annual festival in honour of Icarius and his daughter during the grape harvest, where the girls swung on trees in swings. In a different version, the shepherds found refuge in the land of the Keans (i.e. on the island of Kea).

5.2 Maira as the Star Seirios

Callimachus, the Hellenistic poet of the third century BC, writes:

> The [Kean] priests of Zeus Aristaios Ikmaios (the Lord of Moisture): priests whose duty is upon the mountain-tops to assuage stern Maira [Seirios] when she rises. (Callimachus, 1958: *Aetia Fragment* 3. 1).

The Greeks believed that the constellation Canis Minor and the Dog Star (Sirius) heralded the coming of a drought.

In the words of Hyginus:

> Jupiter [Zeus], pitying their misfortune, represented their forms among the stars … The dog, however, from its own name and likeness, they have called Canicula. It is called Procyon by the Greeks, because it rises before the greater Dog. Others say these were pictured among the stars by Father Liber [Dionysus].
>
> [The constellation] … Canicula rising with its heat, scorched the land of the Keans, and robbed their fields of produce, and caused the inhabitants, since they had welcomed the killers to be plagued by sickness, and to pay the penalty to Icarus with suffering. Their king, Aristaeus, son of Apollo and Cyrene, and father of Actaeon, asked his father by what means he could free the state from affliction. The god bade them expiate the death of Icarus with many victims, and asked from Jove that when Canicula rises he should send wind for forty days to temper the heat of Canicula. This command Aristaeus carried out, and obtained from Jove [Zeus] the favour that the Etesian winds should blow … (Pseudo-Hyginus, 1960).

It should be noted that the brightest star in the constellation of Canis Minor, Alpha Canis Minoris, is called Procyon (from the Greek words *pro* = before and *kyon* = dog) because it rises just before Sirius (the Great Dog).

The epic poet Nonnus of Panopolis (previously mentioned in Section 3.1) also calls Sirius 'Maira's star' in his *Dionysiaka* (Nonnus, 1940, Book 5: v. 220-222).

6 'DOG BURNINGS' AND 'DOG DAYS'

In antiquity the heliacal rise of Sirius had been connected with a period of the year of extremely hot weather, *κυνικά καύματα* (kynica kavmata, canine burnings). This period corresponded to late July, August and early September in the Mediterranean region. The Romans also knew these days as *dies canicullariae*, the hottest days of the whole year, associated with the constellation of the Great Dog. Ancient Greeks theorized the extra heat was due to the addition of the radiation of bright Sirius to the Sun's radiation.

In ancient Greek folklore, people referred to the summer days after the heliacal rise of Sirius as 'dog burnings'. The term has no relation to the Dog-star or the constellation, but rather to dogs in general, thinking that only dogs were crazy enough to go outside when it was so hot. This idea persisted through the centuries and can be found in modern Greek folklore as the belief that during the hot days of July and August, and especially between 24 July and 6 August, dog bites are infectious (Theodossiou and Danezis, 1990: 115).

According to an ancient myth, the inhabitants of the island Kea were dying from a famine caused by a drought brought on by the dog burnings around 1600 BC. Then, the god Apollo made a prophesy that Phthia[6] Aristaeus, the god's son, could be summoned to help them. Upon arriving on Kea, Aristaeus performed rituals, cleansings and sacrifices to Zeus Ikmaeus, the lord of the rains and the skies, and to Apollo the Dog.

Both gods listened to his pleas and they sent the Etesian Winds, northern winds that have blown ever since across the Aegean Sea during mid-summer, so that people could survive the unbearable heat. After that, the people of Kea, incited by Aristaeus, made sacrifices to the constellation of Canis Major and to Sirius; in order to remember his beneficence, they honored Aristaeus as 'Aristaeus Apollo' and pictured his head on the one side of their coins, while on the other side they depicted Sirius crowned with rays (Wendel, 1935: 168.8-12). Indeed, ancient coins retrieved from the island and dating to the third century BC feature dogs or stars with emanating rays, highlighting Sirius' importance (Holberg, 2005). From then on, the islanders of Kea used to predict from the first appearance of Sirius (its heliacal rising) whether the following year would be healthy or not: if it rose clear, it would portend good fortune; if it was misty or faint then it foretold (or emanated) pestilence.

According to Allen (1963: 126), even the 'father of Medicine', Hippocrates, writing *circa* 460 BC, stressed in his *Epidemics* and *Aphorisms* the influence of Sirius on the weather and on the physical aspect of humans; the same he believed for Arcturus. Some minor doctors in antiquity were arguing that the 'dog star' played some role in the appearance of cases of rabies (Ideler, 1841).

In ancient poetry Sirius is mentioned as a star with a particularly negative influence, a belief that is evident in the Homeric verse "… the most bright one, yet it bodes no good to us poor mortals." (Homer, 1924: XXII: 25-31).

Socrates appears to swear to Apollo, the Dog, in his *Apology* (and not to curse, as some have argued): "…

and, by the Dog, oh men of Athens – for I must tell you the truth." (Plato, 2002: 22a-22b). Similarly, Plato (*Platonis opera*, 1900-1907) in *Gorgias* swears to the god Kyna (Dog) that what he writes is true: "By the Dog, Gorgias, a lengthy conversation is needed about how these things are, so that we can analyze them in extent." [461b].

It should be noted that Kynas (Sirius) is one of the numerous appellations of Apollo, the god of solar and spiritual light, and of music.

Professor Pericles Theochares (1995) writes about the Kea island myth:

> This myth alludes to the relation of Sirius with the Earth. The sacrifices were made to Zeus Meilichius,[7] a god of the weather, of the sun and rain, and to Sirius, who causes the dog burnings on Earth; they believed that not only the Sun is responsible for the great heat of the summer, but also Sirius when standing next to the Sun. This was probably the belief of the builders of the Argolis pyramids, orienting their entrance corridors towards the azimuth of Sirius.

Also, for Manilius (1977: 5.208) the Dog-star is, in effect, a fiery mad dog that "… raves with its own fire."

On the influence of Sirius on 'dog burnings' Geminus (1898: 17.26) writes in *Isagoge*:

> For everyone assumes that the star has a peculiar power and is the cause of the intensification of summertime heat, when it rises with the sun.

7 THE RED COLOR OF SIRIUS

It is an interesting fact that the star's color is mentioned by most ancient authors as red, while today, we know it is a star of spectral type A1 V, and is white.

In essence, there is a series of ancient references about Sirius from different civilizations that describe it as a red star (Allen 1963: 128). In the fourth century AD epic poet Quintus Smyrnaeus (1913: 8. 30ff) mentions the 'red star' Sirius in the *Fall of Troy*.

From the Roman literary figures, Horace (1870) refers to Sirius as a red star (*rubra*), while Seneca (2004) writes (ca. AD 35) that: "… when the air is clear, then Sirius appears more red than planet Mars." (Whittet, 1999: 335).

In 1927, T.J.J. See reported on references to the color of Sirius from the second century AD to the tenth century AD:

> Many classical literature artists – Cicero, Horatius and Seneca to name a few – mention Sirius as a red star. Ptolemy goes even further in his description and claims that Sirius is fire-red in color. On the other hand, the Arabian Astronomer Abd-al Rahman Al-Sufi contradicts them and classifies Sirius as a white star in his catalogue dating around 925 BC, 850 years after Ptolemy. Also in *Carmina Burana*, based on the pastoral songs of the 13th century, the whiteness of Sirius is compared to that of ivory. Geoffrey Chaucer, in 1391, relates that the Arabians call Sirius Al-Habur, the beautiful white star. Chinese Astronomer and Historian Simaquian (91 BC), Roman artists Hyginus, Manilius and Avienus, (360 BC), and Archbishop Saint Isidore of Seville all support the opinion that Sirius is a white star.

According to Holberg (2007: 157),

> One of the most contentious and long-running mysteries regarding Sirius originated in the 2nd century AD with what appears to be a casual comment made by the Alexandrine astronomer/astrologer Claudius Ptolemy (Chapter 3). Books VII and VIII of Ptolemy's *Almagest* contain one of the earliest and most famous of the ancient star catalogues, in which Ptolemy lists the positions and brightness of some 1022 stars. He comments on the color of only six of these stars – Betelgeuse, Aldebaran, Pollux, Arcturus, Antares, and Sirius – and assigns the color red to each. In particular, for Sirius in the constellation Canis Major, he states its location, on the dog's mouth, as well as its relative brightness and color: bright and red.

Besides the references already mentioned, Horace (first century BC), Seneca (first century AD) and Aratus (third century BC) also described Sirius as being red in color. Various early translations of their works, including those by Cicero and Germanicus, drew no concern from anyone about Sirius' redness. In fact, it was not until 1760 (after a translation by Samuel Johnson) that anyone voiced skepticism about the observations.

There is a quote from Hephaestion of Thebes (Ceragioli, 1996) describing how the star's color upon rising was inspected as an omen. Curiously, he mentions that the star is 'white' (*lefkòs*). This agrees with Hyginus' description of Sirius as being remarkable for its 'candor', which is usually—from the context—interpreted as 'brightness', but almost certainly implies a white color. Add to these Manilius and Avienus, who explicitly describe the star Sirius as blue or perhaps blue-white.

Since we can see that there was an awareness and assumed meaning in the color of Sirius, perhaps Ptolemy's (1903) characterization of the star as 'hypokirros' is a guess at the star's 'actual' color, since we do not know if he shared an assumption with Seneca that celestial bodies have no inherent color. There is very little context to make a guess, although several astronomers (most notably See) took up the task and piled up dubious citations leading ultimately to the conclusion that the ancients saw Sirius as a 'fiery red' star all the time. So probably the correct question to ask here is not really 'Was Sirius red in antiquity?', but rather 'Did Sirius sometimes appear to be red, or was it sometimes described as red (or other colors) in antiquity, and if so what did this mean?'.

The certain thing is that the impression Sirius currently gives to a visual observer is of a 'cold white' star (i.e. with a lightly bluish tint) when it is high enough above the horizon, an impression which agrees with its modern spectral classification as an A1 star.

Another explanation involves the modern finding that Sirius is part of a binary star system. The fainter star of the pair (the companion), Sirius B, is a white dwarf. This means that it started with the larger mass of the two stars of the system, as it evolved faster and became a stellar remnant after it first passed from the evolutionary stage of the red giant. In that stage the fiery red light of Sirius B would dominate over the cold white light of Sirius A, thus causing all the ancient color descriptions mentioned in the previous paragraphs. Of course, the main weakness of this explanation scheme is that the time needed for a star to pass from the stage of a bright red giant to that of a clear white dwarf is, according to theoretical astrophysics, much longer than a few thousand years, so this can not be the reason for the ancient 'red color' of Sirius.

A more plausible explanation is that perhaps some interstellar cloud in the space between the Solar System and Sirius was absorbing the shorter wavelengths of the Sirian light, thus causing its ancient red appearance. This is not so probable, though, due to the relatively small distance of Sirius, only 2.64 parsecs. A much more feasible explanation is that the ancient tradition was created by the color of Sirius when it was very low in the sky, near the horizon. In this position Sirius—like other stars—appeared to twinkle, to move rapidly around a mean position and to change its color in tenths of a second, exhibiting a variety of very intense nuances more intense than its true color. All three phenomena are caused by the Earth's atmosphere. Moreover, Sirius is only a few times fainter than Venus in the terrestrial sky, and it is known that Rayleigh scattering of Venus' light—which is a function of the light's wavelength—reddens it considerably when the planet is near the horizon (the phenomenon of course is much better known and is more impressive in the case of the Sun and the Moon). Now Sirius, as we saw earlier, was intensely observed by the ancient Greeks when it first appeared in its heliacal rising, that is, when it was just above the eastern horizon during the last hour of the night. So, unlike today, the most frequently-observed image of Sirius in antiquity was when it was very close to the horizon. Hence, this explanation is by far the most probable.

8 CONCLUSIONS

In this paper we have only studied ancient Greek, Roman and Byzantine references to Sirius.

The name ***seirios***, which means sparking, fiery or burning, flamboyant, scorching star or scorcher, turned out to be very ancient in the form of an adjective, as it occurred in the Orphic ***Argonautics***, even though it did not relate to a specific star. Homer, also, did not use ***seirios*** for the star, preferring to call it the 'autumnal star' and 'Orion's Dog'. Hesiod, writing at about the same time (circa 800 BC) in two different works, calls this particular bright star ***Seirios***, which is a most important turning point in the star's lore. Additional references to Sirius and its various names were in the works of Aratus and Eratosthenes.

After the two great epic poets (Homer and Hesiod), the Greek lyrical poet Alcaeus (seventh to sixth centuries BC) also mentioned the star as ***Seirios*** and the 'Dog's star'. Theognis of Megara (570–480 BC) refers to it in a single-word form (***Astrokyon***).

Next came the tragic poets Aeschylus and Euripides; the former with his 'seirios dog', while the latter used just Seirios as a proper name.

Lykophron of Alexandria (third century BC), a well-known poet of that period, wrote of a 'seirian ray' (most probably meaning sunray). Eratosthenes (third century BC) in his famous ***Catasterismoi***, calls the star both ***Isis*** and ***Seirios***, still using, however, the word ***seirios*** as an adjective; the use of the word as a name for the specific star had nevertheless been widespread by then, as is evident by the ***Argonautics*** of Apollonius of Rhodes during the same years (two different passages), and by Diodorus Siculus in ***The Library of History***.

Passing to the AD years, Lucian of Samosata mentioned Sirius by that name in his ***True Story*** or ***Trips to the Moon***. The leading astronomer of the time, Ptolemy, followed the older tradition by calling the star ***Astrokyon***. Plutarch called it *Προόπτης*, the Leader; but *Κύων*, *Κύων σείριος*, *Κύων αστήρ*, *Σείριος αστήρ*, *Σείριον άστρον*, or simply *το άστρον* ('the star') were its names in early Greek astronomy and poetry.

Also considered were works from the fourth century AD, of epic poet Quintus Smyrnaeus and Pamprepius of Panopolis. One century later, epic poet Nonnus of Panopolis, in his main work ***Dionysiaka***, wrote twice about Sirius and the 'dog burnings'.

The Latin authors and poets who mentioned the star are Virgil in his ***Georgics*** and the ***Aeneid*** (Books III and X), Seneca in his ***Oedipus***, and Valerius Flaccus in his ***Argonautica***, and the poet Statius in his ***Silvae*** (3.1.5).

According to Allen (1963: 118): "***Sirion*** and ***Syrius*** occasionally appeared with the best Latin authors; and the ***Alfonsine Tables*** of 1521 had ***Canis Syrius.***"

In the mid-twelfth century, Byzantine Princess Anna Comnena (Komnene) in her opus ***The Alexiad*** (1148) also mentioned Sirius as the 'Dog's star'. Finally, the Byzantine scholar, medical doctor and astronomer Georgios Chrysococca, two centuries later, in his astronomical work ***Synopsis tabularum*** …, mentioned Sirius as ***Siaèr Jamanè***.

An important additional element is that Sirius from its heliacal rising up to 22 August bore the special appellation Maira, both a Greek word stemming from the verb ***marmairo***, which means 'to shine', and the name of a dog from Greco-Roman mythology. The name Maira appears for Sirius in poems by Callimachus in the third century BC and Nonnus (as 'Maira's star') eight centuries(!) later.

Mythology associated with the star and its constellation is also plentiful, a fact that indicates their significance. Thus, according to Eratosthenes, Sirius is Laelaps, the faithful dog of Orion the Hunter. Another legend puts in its place Cerberus, the horrid three-headed dog that guarded the World of the Dead, or with one of the hunting dogs of Actaeon, a renowned hunter and hero from Thebes.

The myths about Sirius also involve Orthrus (the dog of Geryon the giant), Maira (the faithful dog of Icarius, placed in the sky by the god Dionysus according to Ovid and Hyginus), and Hecate, the goddess protecting dogs, who was the daughter of the Titans Perses and Asteria.

A Roman myth refers to Canis Major as Custos Europae, the dog guarding Europa; and as Janitor Lethaeus, the watch-dog of the 'lower heavens', i.e. the Keeper of Hell.

The significance of the brightest star in the sky which emerges from all of these references is evident. As for the traditional ancient characterization of Sirius as 'red', this most likely arose from the custom of watching the star on the nights of its heliacal rising, when it was very low in the sky.

10 NOTES

1. All translations into English in this paper were made by the authors.
2. Geryon, son of Chrysaor and Callirrhoe and grand-

son of Medusa, was a giant on the island of Erytheia (Hesiod, 1914: 979 ff) in the far west of the Mediterranean. According to Hesiod (1914: 287 ff), Geryon had one body and three heads, whereas the tradition followed by Aeschylus (1955: 869 ff) gave him three bodies. He owned a herd of magnificent red cattle, guarded by a two-headed hound named Orthrus, which was the brother of Cerberus. In the ***Bibliotheke*** of Pseudo-Apollodorus (1913: 2. 5. 10) the tenth labour of Heracles was to obtain the Cattle of Geryon.

3. Perses was the brother of Hesiod. He is mentioned several times in the ***Works and Days***.
4. Pleias is a 'group of seven stars' and refers to the seven tragic poets who wrote at Alexandria under Ptolemy Philadelphus in the third century BC: Alexander Aetolus, Philiscus, Sositheus, Homerus, Aeantides, Sosiphanes and Lycophron.
5. In Greek Mythology, Dirce was the wife of the Theban King, Lycus. She was devoted to the god Dionysus, who caused a spring to flow where she died, near Thebes (Tripp, 1970: стр. 213).
6. Phthia (Greek: Φθία or Φθίη; transliterations: Fthii (modern), Phthíē (ancient)) in ancient Greece was the southernmost region of ancient Thessaly, on both sides of the Othrys Mountain. It was the homeland of the Myrmidones tribe, who took part in the Trojan War under Achilles (Hornblower, 2004).
7. Meilichius is the surname of Zeus, the protector of those who honored him with propitiatory sacrifices.

11 ACKNOWLEDGEMENTS

This study forms part of the research at the University of Athens, Department of Astrophysics, Astronomy and Mechanics, and we are grateful to the University for financial support through the Special Account for Research Grants. This research is also supported by the Ministry of Science and Technological Development of Serbia through the project 146022 "History and Epistemology of Science".

12 REFERENCES

Aeschylus, 1955. *Agamemnon*. Edited by G. Murray, *Aeschyli Tragoediae, Second Edition*. Oxford, Clarendon Press (reprinted 1960).

Alcée, 1999. *Fragments* (Collection des Universités de France publiée sous le patronage de l'Association Guillaume Budé). Edited and translated by G. Liberman. Paris, Les Belles Lettres [in French].

Alcaeus, 1922. *Lyra Graeca, Volume I.* Translated by J.M. Edmonds. The Loeb Classical Library, Harvard University Press. London, Heinemann.

Alcaeus, 1982. *Greek Lyric I. Fragment 347*. Translated D.A. Campbell. The Loeb Classical Library No. 142, Harvard University Press. London, Heinemann.

Allen, R.H., 1963. *Star Names - Their Lore and Meaning*. London, Constable & Co. (Dover edition).

Anna Comnena (Komnene), 1928. *The Alexiad*. Edited and translated by E.A. Dawes. London, Routledge, Kegan, Paul.

Anna Comnena (Komnene), 1969. *The Alexiad*. Edited and translated by E.R.A. Sewter. Harmondsworth. Penguin Books.

Anonymous, 1950. *Two Poems – Fragments. Volume 3, Select Papyri III, Greek Poetry 4th Century AD. Literary Papyri, Poetry (LCL 1950)*. Text, translation and notes by D.L. Page. The Loeb Classical Library, No. 140. London, Heinemann.

Apollonius Rhodius, 1962. *Argonautica*. Translated by R.C. Seaton. The Loeb Classical Library, Harvard University Press. London, Heinemann.

Aratus of Soloi, 1921. *The Fall of Troy*. In *Callimachus: Hymns and Epigrams, Lykophron: Alexandra, Aratus of Soloi: Phaenomena.* Translated by A.W. Mair. The Loeb Classical Library No. 129. London, Heinemann.

Bayer, Johann, 1603. *Uranometria*. Augsburg, Christoph Mang (Linda Hall Library of Science, Engineering & Technology e-edition, 2005).

Benest, D., and Duvent, J.-L., 1995. Is Sirius a triple star? *Astronomy & Astrophysics*, 299, 621-628.

Callimachus, 1958. *Aetia, Iambi, Hecale, and Other Fragments, Fragment 3.1, from Oxyrhynchus Papyri 7*. Translated by C.A. Trypanis. The Loeb Classical Library. London, Heinemann.

Campbell, D.A., 1991. *Greek Lyric Poetry*. London, Bristol Classical Press.

Ceragioli, R.C., 1996. Solving the puzzle of 'red' Sirius. *Journal for the History of Astronomy*, 27, 93-128.

Chrysococca, G., 1645. *Synopsis Tabularum Persiacarum ex Syntaxi Persarum Georgii Medici Chrysococcae*. Edited by Ismael Bullialdus. Paris, Astronomia Philolaica [in Latin].

Demetrakos, D.B., 1964. *Mega Lexicon of the Whole Greek Language*. Edited by Tegopoulos, X., and Asimakopoulos, B. Athens, Dome [in Greek].

Diodorus Siculus, 1939. *The Library of History*. Translated by C.H. Oldfather. The Loeb Classical Library. London, Heinemann.

Eratosthenes, 1878. *Catasterismorum Reliquiae*. Edited by Karl Robert. Berlin, Weidmann [in Latin].

Eratosthenes, 1997. *Catasterismoi*. Translated by Theony Contos. In *Star Myths of the Greeks and Romans: A Sourcebook*. Grand Rapids, Phanes Press.

Eratosthenes, 2001. *Le Ciel: Mythes et Histoire des Constellations; les Catastérismes d'Eratosthènes*. Text Traduit, Présenté et Commenté par Pascal Charvet et Arnaud Zucker. Paris, NIL éditions [in French].

Eratosthenis, 1897. *Pseudo-Eratosthenis Catasterismoi = Mythografi Graeci Vol. 3, fasc. 1*. Edited by A. Olivieri. Leipzig, Teubner [in Greek].

Euripides, 1999. *Iphigenia at Aulis - Iphigenia at Tauris*. Translation and supervision by D. Goudis. Athens, Papadimas Publications [in Greek].

Euripides, 2003. *Bacche, Iphigenia at Aulis, Rhesus*. Edited and translated by D. Kovacs. The Loeb Classical Library No. 495. London, Heinemann.

Euripides, 2004. *Iphigenia at Aulis*. Translated by E.P. Coleridge. eBooks@Adelaide.

Euripides, 2008. *Hecuba*. Series: *Ancient Greek Dramatic Poetry*. Thessaloniki, Zetros Publications [in Greek].

Geminus, 1898. *Isagoge*. In C. Manitius (ed.). *Gemini Elementa Astronomiae*. Leipzig, B.G. Teubner [in Latin].

Hesiod, 1914. *The Homeric Hymns and Homerica (Theogony)*. Translated by H.G. Evelyn-White. The Loeb Classical Library. London, Heinemann (reprinted 1954).

Hesiod and Apollonius of Rhodes, 2005. *Theogony, Works and Days, Shield of Hercules, Argonautica*. Thessaloniki, Zetros Publications [in Greek].

Holberg, J.B., 2005 How degenerate stars came to be known as white dwarfs. *Bulletin of the American Astronomical Society*, 37, 1503.

Holberg, J.B., 2007. *Sirius - Brightest Diamond in the Night Sky*. New York, Springer Praxis.

Homer, 1919. *The Odyssey*. Translated by A.T. Murray; revised by G.E. Dimock. The Loeb Classical Library. London, Heinemann (reprinted 1995).

Homer, 1924. *The Iliad*. Translated by A.T. Murray. The Loeb Classical Library. London, Heinemann (reprinted 1954).

Homer, 1950. *The Iliad.* Translated by E.V. Rieu. London,

Penguin Classics.
Homer, 1998. *The Odyssey*. Translated by W. Shewring. Oxford, Oxford University Press.
Horace, 1870. *The Satires, Epistles and Art of Poetry of Horace*. Translated by J. Conington. London, Bell and Dadly.
Hornblower, Simon, 2004. *Thucydides and Pindar: Historical Narrative and the World of Epinikian Poetry*. Oxford, Oxford University Press.
Hyginus, 1993. *Fabulae. Editio Altera*. Edited by P.K. Marshall. Munich, K.G. Saur (corrected edition 2002) [in Latin].
Ideler, L. (ed.), 1841. *Physici e Medici Graeci Minores*. Berlin, Reimer (Amsterdam, reprint 1963) [in Latin].
Litsas, N.B. (ed.), 2008. The alchemists from the Pre-Socratic philosophers to Plato. *Archeology and Arts*, 106, (March), 38-51 [in Greek].
Lucian, 1911. *The Complete Works*. Translated by Ioannis Kondylakis. Athens, Fexis [in Greek].
Lucian, 2010. *Trips to the Moon*. Edited by H. Morley; translated by Th. Francklin. On-line version at: http://pospapendix.blogspot.com/2010/06/lucians-trips-to-moon..html
Manilius, 1977. *Astronomica*. Edited and translated by G.P. Goold. The Loeb Classical Library No. 469. Cambridge (Mass.), Harvard University Press.
Nonnus, 1940. *Dionysiaca*. *Volume I, Books 1-15*. Translated by W.H.D. Rouse. The Loeb Classical Library No. 344. London, Heinemann.
Palatine or Greek Anthology. *Volume III, Book 9* (1917). Translated by W.R. Paton. The Loeb Classical Library No. 84, Harvard University Press. London, Heinemann.
Pausanias, 1935. *Description of Greece*. *Volume IV*: *Arcadia*, *Boeotia*, *Phocis and Ozolian Locri*, *Books 8.22-10*. Translated by W.H.S. Jones. The Loeb Classical Library No. 297. London, Heinemann.
Petrides, S., 2005. *Orpheus' Argonautica – A Dissertation on Seafaring of the Late Pleistocene*. Athens, published by the author.
Plato, 2002. *The Apology of Socrates*. *Introduction*. Translation and comments by N.E. Tzirakis. Athens, Patakis Publications [in Greek].
Platonis Opera. I-V (1900-1907). Edited by J. Burnet. Oxford, Clarendon Press (republished 1967-1968).
Plutarch, 1932. *Moralia Vol. 2*, *Fasc. 3*: *De Iside et Osiride*. Edited by W. Sieveking. Leipzig, B.G. Tuebner [in Latin].
Pseudo-Apollodorus, 1913. *Bibliotheke (Library)*. Edited by J.G. Frazer. The Loeb Classical Library No. 121. Harvard University :Press. London, Heinemann.
Pseudo-Hyginus, 1960. *Astronomica 2. 4*. In *The Myths of Hyginus*. Edited and translated by Mary Grant. Lawrence, University of Kansas Press (University of Kansas Publications in Humanistic Studies, No. 34).
Ptolemy, 1903. *Claudi Ptolemaei Opera quae Extant Omnia. Syntaxis Mathematica*. Leipsig, J.L. Heiberg [in Latin].
Quintus Smyrnaeus, 1913. *The Fall of Troy*. Translated by A.S. Way. The Loeb Classical Library Volume 19. London, Heinemann.
Scheer, E. (ed.), 1958. *Lycophronis Alexandra. Vol 2 Scholia Continens*. Berlin, Weidmann [in Latin].
See, T.J.J., 1927. Historical researches indicating a change in the color of Sirius between the epochs of Ptolemy, 138, and of Al Sûfi, 980, A.D. *Astronomische Nachrichten*, 229, 245-272.
Seneca, 2004. *Tragedies* II: *Oedipus*, *Agamemnon*, *Thyestes*, *Hercules on Oeta*, *Octavia*. Edited and translate by J.G. Fitch. The Loeb Classical Library. London, Cambridge University Press.
Statius, 2003. *Silvae.* English and Latin edition, translated by D.R. Shackleton Bailey. The Loeb Classical Library No. 206. Harvard University Press. London, Heinemann.
Theochares, P., 1995. *The Pyramids of Argolis and their Dating*. 11th Panhellenic Conference, May 12-13. Nafplio, Foundation of the Peloponnesian Studies [in Greek].
Theodossiou, E., and Danezis, E., 1990. *The Stars and Their Myths — Introduction to Uranography*. Athens, Diavlos Publications [in Greek].
Theognis, 1997. *Lyrical Poems III*. Athens, Epikairotita Publications [in Greek].
Tripp, Edward, 1970. *Crowell's Handbook of Classical Mythology*, New York, Thomas Crowell Press.
Valerius Flaccus, 1934. *Argonautica*. Translated by J.H. Mozley. The Loeb Classical Library No. 286. Harvard University Press. London, Heinemann.
Virgil, 1916. *Eclogues*, *Georgics*, *Aeneid*, *I-VI*. Edited and translated by H.R. Fairclough; revised by G.P. Goold. The Loeb Classical Library No. 63. Harvard University Press. London, Heinemann.
Virgil, 2002. *Aeneid*. *Boo*k *III & X*. Translated by A.S. Kline. Online: http://www.poetryintranslation.com/index.html
Wendel, C. (ed.)., 1935. *Scholia in Apollonium Rhodium Vetera*. Berlin, Weidmann [in Latin].
Wender, D., 1984. *Hesiod and Theognis*. New York, Penguin Books.
Whittet, D.C.B., 1999. A physical interpretation of the 'red Sirius' anomaly. *Monthly Notices of the Royal Astronomical Society*, 310, 335-359.

Dr Efstratios Theodossiou is an astronomer, and an Associate Professor of History and Philosophy of Astronomy and Physical Sciences in the School of Physics at the University of Athens. His scientific interests include observational astronomy and astrophysics, satellite spectrophotometry of Be stars and history and philosophy of astronomy. He has published more than 200 scientific papers in international refereed journals and proceedings of astronomical conferences, 300 articles in Greek newspapers and journals and sixteen books on history and philosophy of astronomy and physics. He is a member of IAU Commission 41.

Dr Vassilios N. Manimanis is a post-doctoral researcher in the School of Physics at the University of Athens. His scientific interests include observational astronomy and astrophysics, photometry of cataclysmic variable stars, history and philosophy of astronomy and sciences, popularization of astronomy and bioastronomy. He has published 25 research papers in international refereed journals and many articles in popular magazines.

Dr Milan S Dimitrijević is an astronomer at the Belgrade Astronomical Observatory. His scientific interests include spectroscopy of astrophysical and laboratory plasma, stellar astrophysics, collisions and their influence on spectral lines, and history and philosophy of astronomy. He has published several books, around 200 papers in international journals and several hundred contributions in conference proceedings and newspapers.

Petros Z. Mantarakis received a B.S. in astronomy from the California Institute of Technology, and an M.S. in astronomy from the University of Arizona. He worked in industry for thirty years, where he attained the level of President of several companies. He has 20 patents, and has published two books and numerous articles. He lives in Los Angeles, California, where he continues to write and do consulting work.

ЖУРНАЛ ПРИКЛАДНОЙ СПЕКТРОСКОПИИ

V.63 , N 5 JOURNAL OF APPLIED SPECTROSCOPY September-October 1996

STARK BROADENING OF Se I SPECTRAL LINES

M.S.Dimitrijević[a]* and S.Sahal-Bréchot[б]

[a]*Astronomical Observatory, Volgina 7, 11050 Belgrade, Serbia, Yugoslavia*
[б]*Laboratoire "Astrophysique, Atomes et Molécules", Département Atomes et Molécules en Astrophysique, Unité associée au C.N.R.S. N 812, Observatoire de Paris-Meudon, 92190 Meudon, France*

(Поступила 28 марта 1996)

С использованием полуклассического приближения рассчитаны ударное уширение и сдвиги линий за счет электронов, протонов и ионов аргона для 31 мультиплета Se I, необходимые для теоретических и экспериментальных исследований спектральных линий нейтрального селена.

Using a semiclassical approach, we have calculated electron-, proton-, and ionised argon-impact line widths and shifts for 31 Se I multiplets, in order to provide Stark broadening data for theoretical and experimental investigations of neutral selenium lines.

Key words: spectral line widths and shifts, semiclassical approach, multiplets.

Introduction. In order to try to provide an as much as possible more complete set of semiclassical Stark-broadening parameters needed for research of astrophysical, laboratory and laser produced plasma we obtained such data for large number of different emitter lines (see Ref. [1] and references therein). Such set of data is not only of interest e.g. for plasma diagnostic, opacity calculations or the investigation/modelling of a particular line or emitter spectrum but as well for different examinations of regularities and systematic trends for e.g. homologous atoms [2] or in general [3]. Moreover, we do not know *a priori* the chemical composition of a star and with the development of space born techniques, the astrophysically importance of up to now often astrophysically meaningless lines increases.

By using the semiclassical-pertubation formalism [4, 5], we have calculated electron-, proton-, and ionised argon-impact line widths and shifts for 31 multiplets of neutral selenium. The obtained results will be presented and discussed here.

Method of calculation. The semiclassical perturbation method has been discussed in detail in Refs. [4, 5] and a brief summary is given in Ref. [6]. Consequently, only the most important details including the innovations regarding the mentioned references will be given here. Within the semiclassical perturbation formalism [4—6] the full width of an isolated spectral line broadened by electron impacts, can be expressed in terms of cross sections for elastic and inelastic processes as

$$W = N\int vf(v)dv\Big(\sum_{i'\neq i}\sigma_{ii'}(v) + \sum_{f'\neq f}\sigma_{ff'}(v) + \sigma_{el}\Big) + W_R, \qquad (1)$$

$$d = N\int vf(v)dv\int_{R_3}^{R_p} 2\pi\rho d\rho \sin 2\phi_p \quad , \qquad (2)$$

Here, $f(v)$ is the Maxwellian velocity distribution function for electrons and ρ denotes the impact parameter of the incoming electron. The inelastic cross section $\sigma_{jj}(v)$ can be expressed by an integration over the impact parameter of the transition probability $P_{jj}(\rho,v)$

$$\sum_{i' \neq i} \sigma_{jj'}(v) = \frac{1}{2}\pi R^2 + \int_{R_1}^{R_D} \sum_{j \neq j'} P_{jj'}(\rho, v), \; j = i, f \tag{3}$$

and the elastic cross section is given by

$$\sigma_{el} = 2\pi {R_2}^2 + \int_{R_2}^{R_D} 8\pi\rho d\rho \sin^2 \delta \; , \tag{4}$$

$$\delta = ({\phi_p}^2 + {\phi_q}^2)^{1/2} \; . \tag{5}$$

The phase shifts ϕ_p and ϕ_q due respectively to the polarisation potential (r^{-4}) and to the quadrupolar potential (r^{-3}) are given in Section 3, of Chapter 2 in Ref. [5]. The contribution of the Feshbach resonances is given by W_R [7]. Here, R_D is the Debye radius. All the cut-offs R_1, R_2, R_3 are described in Section 1 of Chapter 3 in Ref. [4]. For multiply charged ions (the ionisation degree larger than one), the cut-off R_1 can become smaller than the mean atomic radii $<r_j>$, $<r_{j'}>$. In such a case we have used the cut-off for excitation of ions by electron impacts [8, 9] adapted in Ref. [10] for Stark broadening purposes

$$\sum_{j' \neq j} \sigma_{jj'} = \sum_{j' \neq j} \int_{\mathrm{Max}(<r_j>, <r_{j'}>)}^{R_D} 2\pi\rho d\rho P_{jj'}(\rho, v) \; , \tag{6}$$

where $R_1 < \mathrm{Max}(<r_j>, <r_{j'}>)$.

As the difference with Refs. [3, 4], where only the elastic contribution has been taken into account for ion-impact broadening, the formulae for the ion-impact broadening parameters here are completely analogous with formulae for electron-impact broadening ones.

Results and discussion. Energy levels for Se I lines have been taken from Ref. [11]. Oscillator strengths have been calculated by using the method of Bates and Damgaard [12, 13]. For higher levels, the method described in Ref. [14] has been used. For $4p^4\,{}^3P - 4p^3({}^4S^0)5s\,{}^3S^0$, $4p^4\,{}^3P - 4p^3({}^2D^0)5s'\,{}^3D^0$ and $4p^4\,{}^3P - 4p^3({}^2P^0)5s'\,{}^3P^0$ have been used the oscillator strengths calculated in Ref. [15], by using a semiempirical approximation based on the intermediate coupling scheme and the quantum defect method [15]. In addition to electron-impact full halfwidths and shifts, Stark-broadening parameters due to proton- and ionised-argon impacts have been calculated. Our results are shown in Table 1 for a perturber density of 10^{16} cm^{-3} and temperatures T= =2,500—50,000 K. We also specify a parameter c [16] which, when it is divided by the corresponding electron-impact full width at half maximum, gives an estimate for the maximum perturber density for which the line may be treated as isolated. For each value given in Table 1, the collision volume (V) multiplied by the perturber density (N) is much less than one and the impact approximation is valid [4, 5]. Values for $0.1<NV<0.5$ are denoted with an asterisk. When the impact approximation is not valid, the ion-broadening contribution may be estimated by using quasistatic estimations [17, 18]. The accuracy of the results obtained decreases when broadening by ion interactions becomes important. At high densities, the results are no longer linear with density due to Debye screening. This effect is more important for the shift than for the width.

With the help of regularities and systematic trends the Stark width and resonant Se I $4p^4\,{}^3P - 4p^3({}^4S^0)5s\,{}^3S^0$ multiplet have been estimated to be W=0.058 Å and $|d|$=0.033 Å for T=20,000 K and an electron density of 10^{17}

Table 1. This table shows electron-, proton-, and ionised argon-impact broadening parameters for Se I for a perturber density of 10^{16} cm^{-3} and temperatures from 2,500 up to 50,000 K. Transitions and averaged wavelengths for the the multiplet (in Å) are also given. If one divides c value with the linewidth value, we obtain an estimate for the maximum perturber density (in cm^{-3}) for which the line may be treated as isolated and tabulated data may used. The asterisk identifies cases for which the collision volume multiplied by the perturber density (the condition for validity of the impact approximation) lies between 0.1 and 0.5

PERTURBERS ARE:		ELECTRONS		PROTONS		IONIZED ARGON	
TRANSITION	T(K)	WIDTH(Å)	SHIFT(Å)	WIDTH(Å)	SHIFT(Å)	WIDTH(Å)	SHIFT(Å)
1	2	3	4	5	6	7	8
$4P-5S$	2500	0.249E-02	0.256E-2	0.786E-03	0.690E-03	0.457E-03	0.377E-03
1997.9 Å	5000	0.352E-02	0.298E-02	0.882E-03	0.796E-03	0.513E-03	0.446E-03
C = 0.39E+19	10000	0.418E-02	0.350E-02	0.990E-03	0.910E-03	0.575E-03	0.516E-03
	20000	0.466E-02	0.395E-02	0.111E-02	0.103E-02	0.645E-03	0.591E-03
	30000	0.481E-02	0.406E-02	0.119E-02	0.111E-02	0.690E-03	0.637E-03
	50000	0.508E-02	0.387E-02	0.129E-02	0.121E-02	0.752E-03	0.699E-03
$4P-6S$	2500	0.117E-01	0.851E-02	0.263E-02	0.206E-02	*0.152E-02	*0.101E-02
1522.6 Å	5000	0.137E-01	0.103E-01	0.295E-02	0.249E-02	*0.171E-02	*0.132E-02
C=0.69E+18	10000	0.153E-01	0.121E-01	0.331E-02	0.292E-02	*0.192E-02	*0.160E-02
	20000	0.161E-01	0.125E-01	0.372E-02	0.337E-02	0.216E-02	0.189E-02
	30000	0.168E-01	0.121E-01	0.398E-02	0.364E-02	0.231E-02	0.206E-02
	50000	0.175E-01	0.105E-01	0.433E-02	0.401E-02	0.251E-02	0.228E-02
$4P-7S$	2500	0.411E-01	0.293E-01	*0.886E-02	*0.553E-02		
1409.5 Å	5000	0.474E-01	0.344E-01	*0.999E-02	*0.741E-02		
C=0.23E+18	10000	0.506E-01	0.382E-01	*0.112E-01	*0.917E-02		
	20000	0.549E-01	0.375E-01	*0.126E-01	*0.109E-01		
	30000	0.560E-01	0.332E-01	*0.135E-01	*0.119E-01		
	50000	0.614E-01	0.278E-01	0.147E-01	0.132E-01	*0.851E-02	*0.741E-02
$5P-6S$	2500	1.36	0.904	0.323	0.215	*0.233	*0.108
16773.0 Å	5000	1.57	1.11	0.351	0.258	*0.251	*0.138
C=0.84E+20	10000	1.79	1.19	0.384	0.302	*0.267	*0.167
	20000	2.13	1.17	0.421	0.347	*0.286	*0.195
	30000	2.36	1.02	0.446	0.375	0.298	0.213
	50000	2.76	0.849	0.479	0.412	0.314	0.235
$5P-7S$	2500	1.64	1.13	*0.350	*0.218		
8905.4 Å	5000	1.88	1.40	*0.394	*0.291		
C=0.92E+19	10000	2.01	1.43	*0.442	*0.360		
	20000	2.19	1.40	*0.496	*0.427		
	30000	2.35	1.22	*0.530	*0.467		
	50000	2.65	1.03	0.577	0.519	*0.337	*0.290
$4P-4D$	2500	0.433E-03	-0.160E-02	0.186E-02	-0.405E-03	*0.177E-02	-0.222E-03
1553.6 Å	5000	0.458E-02	-0.185E-02	0.188E-02	-0.468E-03	*0.183E-02	-0.262E-03
C=0.10E+19	10000	0.500E-02	-0.192E-02	0.189E-02	-0.534E-03	*0.185E-02	-0.303E-03
	20000	0.561E-02	-0.178E-02	0.190E-02	-0.606E-03	0.186E-02	-0.347E-03
	30000	0.603E-02	-0.157E-02	0.192E-02	-0.652E-03	0.187E-02	-0.374E-03
	50000	0.656E-02	-0.134E-02	0.193E-02	-0.712E-03	0.187E-02	-0.410E-03

1	2	3	4	5	6	7	8
$4P-5D$	2500	0.150E-01	-0.643E-02	*0.627E-02	-0.156E-02		
1424.9Å	5000	0.168E-01	-0.629E-02	*0.647E-02	-0.188E-02		
C=0.31E+18	10000	0.195E-01	-0.451E-02	0.659E-02	-0.220E-02		
	20000	0.235E-01	-0.311E-02	0.669E-02	-0.253E-02		
	30000	0.258E-01	-0.278E-02	0.675E-02	-.0.273E-02	*0.644E-02	-0.155E-02
	50000	0.282E-01	-0.218E-02	0.685E-02	-0.300E-02	*0.648E-02	-0.171E-02
$4P-6D$	2500	0.806E-01	0.541E-01				
1371.7 Å	5000	0.910E-01	0.535E-01				
C = 0.73E+17	10000	0.106	0.448E-01				
	20000	0.125	0.350E-01	*0.274E-01	*0.195E-01		
	30000	0.133	0.300E-01	*0.288E-01	*0.215E-01		
	50000	0.139	0.220E-01	*0.308E-01	*0.241E-01		
$5P-5D$	2500	0.769	-0.359	*0.300	-0.815E-01		
9556.1 Å	5000	0.866	-0.394	*0.310	-0.986E-01		
C=0.14E+20	10000	1.01	-0.389	0.317	-0.116		
	20000	1.22	-0.335	0.323	-0.134		
	30000	1.35	-0.305	0.327	-0.144	*0.308	-0.817E-01
	50000	1.50	-0.259	0.333	-0.159	*0.310	-0.905E-01
$5P-6D$	2500	2.47	1.54				
7583.5 Å	5000	2.80	1.60				
C=0.22E+19	10000	3.27	1.27				
	20000	3.90	0.952	*0.837	*0.591		
	30000	4.16	0.807	*0.881	*0.653		
	50000	4.39	0.559	*0.941	*0.732		
$5S-5P$	2500	0.187	0.117	0.795E-01	0.293E-01	*0.738E-01	*0.158E-01
10347.4 Å	5000	0.207	0.139	0.813E-01	0.342E-01	*0.762E-01	*0.189E-01
C=0.50E+20	10000	0.240	0.130	0.833E-01	0.392E-01	*0.774E-01	*0.221E-01
	20000	0.297	0.112	0.858E-01	0.447E-01	0.783E-01	0.255E-01
	30000	0.347	0.929E-01	0.875E-01	0.481E-01	0.789E-01	0.275E-01
	50000	0.417	0.740E-01	0.900E-01	0.527E-01	0.796E-01	0.302E-01
$5S-6P$	2500	0.303	0.203	*0.100E+00	*0.447E-01		
5372.3 Å	5000	0.349	0.243	*0.106	*0.560E-01		
C=0.44E+19	10000	0.390	0.255	*0.112	*0.670E-01		
	20000	0.441	0.244	0.119	0.781E-1		
	30000	0.476	0.210	0.124	0.848E-01	*0.990E-01	*0.475E-01
	50000	0.529	0.177	0.130	0.936E-01	*0.102	*0.530E-01

1	2	3	4	5	6	7	8
$5S - 7P$	2500	0.594	0.376				
4534.9 Å	5000	0.683	0.454				
C=0.16E+19	10000	0.779	0.448	*0.212	*0.117		
	20000	0.897	0.415	*0.225	*0.140		
	30000	0.983	0.348	*0.234	*0.154		
	50000	1.08	0.296	*0.245	*0.171		
$6S - 6P$	2500	10.2	6.40	*3.60	*1.35		
33469.4 Å	5000	11.9	6.09	*3.77	*1.66		
C=0.17E+21	10000	14.8	5.58	3.92	1.97		
	20000	19.3	4.14	4.07	2.28		
	30000	22.4	3.59	4.18	2.47	*3.63	*1.39
	50000	25.9	3.20	4.33	2.72	*3.69	*1.55
$6S - 7P$	2500	6.87	4.15				
15564.0 Å	5000	7.89	4.73				
C=0.19E+20	10000	9.29	4.80	*2.43	*1.31		
	20000	11.1	3.83	*2.58	*1.56		
	30000	12.5	3.31	*2.67	*1.71		
	50000	14.0	2.92	*2.80	*1.91		
$4D - 5P$	2500	1.50	0.730	0.536	0.187		
21505.7 Å	5000	1.69	0.863	0.550	0.220	*0.514	*0.121
C=0.20E+21	10000	1.94	1.01	0.563	0.254	*0.525	*0.143
	20000	2.23	1.07	0.578	0.291	*0.532	*0.165
	30000	2.41	1.04	0.589	0.313	0.535	0.179
	50000	2.64	0.949	0.605	0.343	0.540	0.197
$4D - 6P$	2500	6.27	3.89	*1.97	*0.861		
23256.7 Å	5000	7.24	4.66	*2.10	*1.08		
C=0.82E+20	10000	8.17	5.15	*2.22	*1.29		
	20000	9.18	5.02	2.34	1.51		
	30000	9.84	4.72	2.43	1.64		
	50000	10.8	4.02	2.55	1.81	*2.01	*1.02
$4D - 7P$	2500	4.99	3.02				
12924.7 Å	5000	5.75	3.59				
C=0.13E+20	10000	6.56	3.79	*1.74	*0.957		
	20000	7.54	3.54	*1.85	*1.15		
	30000	8.23	3.20	*1.92	*1.26		
	50000	9.05	2.66	*2.02	*1.40		
$5S - 5P$	2500	0.130	0.884E-01	0.523E-01	0.218E-01	*0.480E-01	*0.117E-01
8972.6 Å	5000	0.143	0.101	0.538E-01	0.254E-01	*0.494E-01	*0.141E-01
C=0.33E+20	10000	0.165	0.939E-01	0.555E-01	0.291E-01	0.503E-01	0.164E-01
	20000	0.202	0.771E-01	0.576E-01	0.331E-01	0.510E-01	0.189E-01
	30000	0.235	0.628E-01	0.591E-01	0.357E-01	0.515E-01	0.204E-01
	50000	0.279	0.491E-01	0.612E-01	0.391E-01	0.522E-01	0.224E-01

1	2	3	4	5	6	7	8
$5S - 6P$	2500	0.275	0.189	*0.798E-01	*0.401E-01		
4737.1 Å	5000	0.311	0.234	*0.861E-01	*0.508E-01		
C=0.25E+19	10000	0.341	0.222	*0.923E-01	*0.611E-01		
	20000	0.375	0.200	0.995E-01	0.716E-01		
	30000	0.400	0.172	0.104	0.778E-01	*0.774E-01	*0.434E-01
	50000	0.433	0.143	0.111	0.860E-01	*0.803E-01	*0.486E-01
$5S - 7P$	2500	0.750	0.483				
4013.9 Å	5000	0.824	0.557				
C=0.73+18	10000	0.889	0.555				
	20000	0.963	0.451				
	30000	1.02	0.385	*0.261	*0.199		
	50000	1.06	0.319	*0.280	*0.223		
$6S - 6P$	2500	10.2	6.90	*3.03	*1.42		
30275.8 Å	5000	11.6	6.57	*3.24	*1.77		
C=0.10E+21	10000	13.6	5.88	*3.44	*2.12		
	20000	17.1	4.32	3.66	2.47		
	30000	19.3	3.94	3.82	2.69	*2.98	*1.50
	50000	21.5	3.18	4.04	2.96	*3.07	*1.68
$6S - 7P$	2500	9.14	6.00				
14072.2 Å	5000	10.0	6.36				
C=0.89E+19	10000	11.0	6.19				
	20000	12.2	4.70				
	30000	13.2	4.08	*3.16	*2.39		
	50000	13.9	3.20	*3.38	*2.68		
$5P - 6S$	2500	0.940	0.615	0.222	0.150	*0.161	*0.762E-01
15010.7 Å	5000	1.11	0.744	0.242	0.180	*0.172	*0.964E-01
C=0.74E+20	10000	1.29	0.855	0.264	0.209	*0.184	*0.116
	20000	1.54	0.865	0.290	0.240	0.196	0.135
	30000	1.69	0.783	0.307	0.259	0.205	0.147
	50000	1.94	0.649	0.330	0.285	0.216	0.163
$5P - 7S$	2500	0.990	0.674	*0.209	*0.139		
8122.8 Å	5000	1.14	0.837	*0.234	*0.180		
C=0.96E+19	10000	1.24	0.886	*0.263	*0.218		
	20000	1.39	0.859	0.294	0.257	*0.173	*0.141
	30000	1.50	0.760	0.315	0.280	*0.185	*0.156
	50000	1.72	0.637	0.342	0.310	*0.201	*0.174

1	2	3	4	5	6	7	8
$5P - 5D$	2500	0.886	-0.442	*0.244	-0.108		
9038.9 Å	5000	0.962	-0.552	*0.258	-0.134		
C=0.90E+19	10000	1.04	-0.558	0.272	-0.159		
	20000	1.13	-0.500	0.288	-0.185		
	30000	1.18	-0.456	0.299	-0.200	*0.242	-0.113
	50000	1.23	-0.387	0.315	-0.221	*0.248	-0.125
$5P - 6D$	2500	1.44	0.305				
7033.1 Å	5000	1.89	0.459	*0.366	*0.552E-01		
C=0.22E+19	10000	2.38	0.498	*0.374	*0.649E-01		
	20000	2.86	0.496	*0.378	*0.752E-01		
	30000	3.11	0.471	*0.379	*0.826E-01		
	50000	3.35	0.395	0.380	0.908E-01		
$5P - 7D$	2500	3.02	0.377				
6304.3 Å	5000	3.94	0.672				
C=0.93E+18	10000	4.92	0.849				
	20000	5.85	0.740				
	30000	6.31	0.707	*0.700	-0.185		
	50000	6.70	0.609	*0.707	-0.295		
$4D - 5P$	2500	1.93	0.997	0.572	0.254	*0.510	*0.133
24689.4 Å	5000	2.16	1.18	0.593	0.298	*0.532	*0.163
C=0.25E+21	10000	2.40	1.36	0.616	0.344	*0.545	*0.193
	20000	2.65	1.40	0.644	0.393	0.555	0.223
	30000	2.78	1.34	0.663	0.424	0.562	0.242
	50000	2.96	1.19	0.691	0.465	0.572	0.266
$4D - 6P$	2500	3.83	2.45	*1.05	*0.522		
16907.4 Å	5000	4.36	2.88	*1.13	*0.663		
C=0.31E+20	10000	4.79	3.08	*1.22	*0.800		
	20000	5.23	2.91	1.31	0.936		
	30000	5.51	2.69	1.37	1.02		
	50000	5.86	2.28	1.46	1.13	*1.06	*0.636
$4D - 7P$	2500	5.04	3.17				
10290.4 Å	5000	5.55	3.70				
C=0.48E+19	10000	5.98	3.78				
	20000	6.47	3.26				
	30000	6.81	2.83	*1.73	*1.31		
	50000	7.11	2.22	*1.85	*1.47		

cm^{-3}. Our calculations give W=0.047 Å and $|d|$=0.040 Å, which is an encouraging agreement.

We hope that the presented Stark broadening data will be of help for the consideration of various scientific problems.

Acknowledgements. This work is a part of the project "Physics and dynamics of celestial bodies", supported by Ministry of Science and Technology of Serbia.

References

1. **M.S.Dimitrijevic.** Zh. P.S in press
2. **M.S.Dimitrijevic and M.M.Popović.** Astron. Astrophys., **217** (1989) 201
3. **J.Purić, M.S.Dimitrijević and A. Lesage.** Astrophys. J., **382** (1991) 353
4. **S.Sahal-Bréchot.** Astron. Astrophys., **1** (1969) 91
5. **S.Sahal-Bréchot.** Astron. Astrophys., **2** (1969) 322
6. **M.S.Dimitrijevic, S.Sahal-Bréchot and V.Bommier.** Astron. Astrophys. Suppl. Series, **89** (1991) 581
7. **C.Fleurier, S.Sahal-Bréchot and J.Chapelle.** JQSRT, **17** (1977) 595
8. **M.J.Seaton.** Proc. Phys. Soc., **79** (1962) 1105
9. **D. Burges.** Proceedings of the Symposium on Atomic Collision Processes in Plasmas Culham, England (1964)
10. **N.Feautrier.** Ann. d'Astrophys., **31** (1968) 305
11. **C.E.Moore.** Atomic Energy Levels, Vol. II, NSRDS-NBS 35, U. S. Govt. Print. Office, Washington (1971)
12. **D.R.Bates and A.Damgaard.** Trans. Roy. Soc. London, Ser. A, **242** (1949)101
13. **G.K.Oertel and L.P.Shomo.** Astrophys. J. Suppl. Series, **16** (1968) 175
14. **H.Van Regemorter, Hoand Binh Dy and M.Prud'homme.** J. Phys. B, **12** (1979) 1073
15. **M.S.Dimitrijević and S.Sahal-Bréshot.** JQSRT, **31** (1984) 301
16. **P.F.Gruzdev.** Opt. Spectrosc., **27** (1969) 301
17. **H.R.Griem.** Spectral Line Broadening by Plasmas, New York: Academic Press (1974)
18. **S.Sahal-Bréchot.** Astron. Astrophys., **245** (1991) 322

STARK BROADENING OF F III LINES IN LABORATORY AND STELLAR PLASMA

Z. Simić [a], M. S. Dimitrijević [a,b*], L. Č. Popović [a], M. D. Dačić [a]

[a] *Astronomical Observatory, Belgrade, Serbia and Montenegro, Volgina 7, 11160; e-mail: mdimitrijevic@aob.bg.ac.yu*
[b] *IHIS-Chemical Power Sources Institute, Belgrade-Zemun, Serbia and Montenegro*

Using a semiclassical approach, we have considered electron-, proton-, and ionized helium-impact line widths and shifts for the F III $2p^3\,{}^4S^o$—$3s\,{}^4P$ resonant line. Moreover, for 10 F III multiplets where the full semiclassical perturbation approach is not applicable in an adequate way due to the lack of reliable atomic data, electron-impact line widths have been calculated within the modified semiempirical approach. Results are obtained as a function of temperature, for perturber density of 10^{17} cm^{-3}. Obtained theoretical data have been used to consider the influence of Stark broadening for A type star atmospheres conditions.

***Keywords**: Stark broadening of spectral lines, semiclassical approach, line profiles, atomic processes, A type stars.*

ШТАРКОВСКОЕ УШИРЕНИЕ ЛИНИЙ F III В ЛАБОРАТОРНОЙ И ЗВЕЗДНОЙ ПЛАЗМЕ

З. Симич [a], М. С. Димитриевич [a,б*], Л. Ч. Попович [a], М. Д. Дачич [a]

УДК 533.9.082.5

[a] *Астрономическая обсерватория, Сербия и Черногория, 11160, Белград, Волгина, 7; e-mail: mdimitrijevic@aob.bg.ac.yu*
[б] *Институт источников химической энергии, Белград-Земун, Сербия и Черногория*

(Поступила 7 декабря 2004)

С использованием полуклассического приближения определены значения ширины и сдвига резонансной линии F III $2p^3\,{}^4S^o$—$3s\,{}^4P$ для случаев столкновения с электронами, протонами и ионами гелия. Для десяти мультиплетов F III, к которым применение полного полуклассического приближения теории возмущений было бы некорректным из-за отсутствия надежных данных по атомным характеристикам, величину обусловленного электронными столкновениями уширения рассчитывали в рамках модифицированного полуэмпирического подхода. Результаты получены в виде температурной зависимости для плотности возмущающих частиц 10^{17} $см^{-3}$. Полученные теоретические данные использованы при анализе влияния штарковского уширения в условиях атмосферы звезд спектрального класса А.

***Ключевые слова:** штарковское уширение спектральных линий, полуклассическое приближение, профили линий, атомные процессы, звезды класса А.*

Introduction. From the Stark broadening parameters, it is possible to obtain the basic plasma parameters such as the electron temperature and electron density, essential for modeling a plasma considered, so that such data are of interest for diagnostics and investigation of various laboratory, astrophysical and technological plasmas. For example, hydrogen fluoride has been detected in sunspots [1], on α Orioni [2], red giants [3], and in interstellar medium [4]. Stark broadening data for fluorine spectral lines are also of interest for the design and development of e.g. HF and similar lasers.

The first experimental consideration of the Stark broadening of F III spectral lines has been published in 1961 [5], and two unique reliable quantitative experimental determinations are in Refs. [6—7]. Theoretical determinations of F III spectral lines Stark broadening have been performed in Refs. [8—10] by using the modified semiempirical method [11] for $3s\,{}^4P_6$—$3p\,{}^4P_6{}^o$, $3s\,{}^4P$—$3p\,{}^4D^o$, $3s\,{}^2P_4$—$3p\,{}^2P_4{}^o$, $3s\,{}^2P$—$3p\,{}^2D^o$ and $3p'\,{}^2D^o$—$3d'\,{}^2D$ transitions.

Experimental Stark widths [6] of the 3113.62 Å spectral line from the multiplet $3s\ ^4P—3p\ ^4D^o$ and the 3154.39 Å line from the multiplet $3p'\ ^2D^o—3d'\ ^2D$ have been compared in Ref. [6] with the calculations in Ref. [8], performed within the modified semiempirical approach [11]. The corresponding ratios of the measured and theoretical values are 1.17 and 1.13, which is also an indicator for results presented here, since there is no experimental data for the spectral lines considered in this work.

In order to make a set of Stark broadening data for F III as complete as possible, we have used the semiclassical perturbation formalism [12, 13] (see also Refs. [14—20]) to determine electron-, proton-, and ionized helium-impact line widths and shifts for the F III $2p^3\ ^4S—3s\ ^4P$ resonant line. For additional 10 F III multiplets, where the full semiclassical perturbation approach is not applicable in an adequate way due to the lack of reliable atomic data, electron-impact line widths have been calculated within the modified semiempirical approach [8, 11, 21—24]. Obtained theoretical results will be used here also to consider the influence of Stark broadening in A type star atmospheres conditions.

Results and Discussion. The semiclassical perturbation formalism used [12, 13] and all innovations and optimizations of the computer code have been discussed e.g. in Ref. [20], while the modified semiempirical method employed [8, 11, 21—23], along with all its applications, has been reviewed in detail in Ref. [24]. Atomic energy levels needed for calculations have been taken from Ref. [25]. Oscillator strengths have been calculated by using the method of Bates and Damgaard [26, 27]. For higher levels, the method described in Ref. [28] has been used. The results obtained within the semiclassical perturbation method [12, 13] for the Stark widths (full width at half maximum) and shifts of the F III $2p^3\ ^4S—3s\ ^4P$ resonant line due to electron-, proton-, and ionized helium-impacts, are shown in Table 1 for perturber density of 10^{17} cm^{-3} and temperatures from 10000 K up to 300000 K. The data on spectral line Stark widths for ten F III transitions obtained within the modified semiempirical approach, are shown in Table 2 for the same perturber density and temperatures.

Table 1. Electron-, proton-, and ionized helium-impact broadening parameters (full width at half maximum W and shift d) obtained within the semiclassical perturbation approach [13, 14] for the F III $2p^3\ ^4S^o—3s\ ^4P$ resonant line ($\lambda = 315.4$ Å, $C = 0.32 \cdot 10^{19}$) for perturber density of 10^{17} cm^{-3} and temperatures from 10000 up to 300000 K

T, K	Electron		Proton		He II	
	W, Å	d, Å	W, Å	d, Å	W, Å	d, Å
10000	$0.123 \cdot 10^{-2}$	$0.143 \cdot 10^{-3}$	$0.714 \cdot 10^{-6}$	$0.858 \cdot 10^{-5}$	$0.118 \cdot 10^{-5}$	$0.846 \cdot 10^{-5}$
20000	$0.771 \cdot 10^{-3}$	$0.648 \cdot 10^{-4}$	$0.442 \cdot 10^{-5}$	$0.175 \cdot 10^{-4}$	$0.579 \cdot 10^{-5}$	$0.163 \cdot 10^{-4}$
50000	$0.465 \cdot 10^{-3}$	$0.635 \cdot 10^{-4}$	$0.195 \cdot 10^{-4}$	$0.324 \cdot 10^{-4}$	$0.183 \cdot 10^{-4}$	$0.286 \cdot 10^{-4}$
100000	$0.341 \cdot 10^{-3}$	$0.681 \cdot 10^{-4}$	$0.352 \cdot 10^{-4}$	$0.443 \cdot 10^{-4}$	$0.327 \cdot 10^{-4}$	$0.367 \cdot 10^{-4}$
150000	$0.291 \cdot 10^{-3}$	$0.669 \cdot 10^{-4}$	$0.441 \cdot 10^{-4}$	$0.492 \cdot 10^{-4}$	$0.385 \cdot 10^{-4}$	$0.410 \cdot 10^{-4}$
300000	$0.230 \cdot 10^{-3}$	$0.615 \cdot 10^{-4}$	$0.588 \cdot 10^{-4}$	$0.591 \cdot 10^{-4}$	$0.489 \cdot 10^{-4}$	$0.490 \cdot 10^{-4}$

Note. When dividing C by the corresponding full width at half maximum [17], we obtain an estimate for the maximum perturber density for which the line may be treated as isolated and tabulated data may be used.

For the resonant line semiclassical results, we also specify a parameter C [17]; when divided by the corresponding full width at half maximum, it gives an estimate for the maximum perturber density such that the line may be treated as isolated. The standard accuracy of the semiclassical results is within the limit of 30 per cent and 50 per cent for the modified semiempirical ones.

In the case of A type stars, where the role of Stark broadening, as demonstrated many times (see e.g. Ref. [29]), may be significant, our temperatures correspond to the deep photospheric and subphotospheric layers. Seaton [30] draws attention to the importance of Stark broadening for their modeling and investigation. Consequently, compared in Fig. 1 are F III $4s\ ^4P—4p\ ^4D^o$ ($\lambda = 8890$ Å) line widths due to Stark and thermal Doppler broadening mechanisms as functions of Rosseland optical depth corresponding to 10000—30000 K temperature range, for an A type star atmosphere model with $T_{\rm eff} = 10000$ K and $\log g = 4$ [31]. One should take into account that due to differences between Lorentz (Stark) and Gauss (Doppler) line intensity distributions, Stark broadening may be more important on line wings in comparison with the thermal Doppler one, even when it is smaller in the central part.

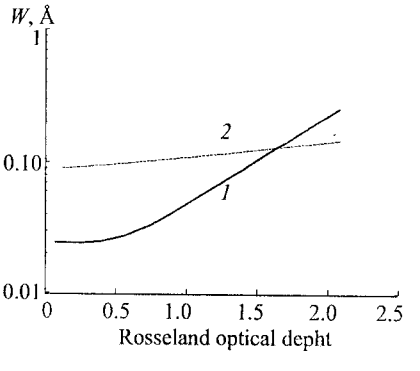

Figure 1. Stark (1) and Doppler widths (2) for F III $4s\ ^4P—4p\ ^4D^o$ ($\lambda = 8890$ Å) as functions of the Rosseland optical depth $\tau_{\rm Ross}$, for an A type stellar atmosphere model with $T_{\rm eff} = 10000$ K and $\log g = 4$ [31]

Table 2. F III electron-impact broadening parameters (full width at half maximum W) obtained by the modified semiempirical method [11] for perturber density of 10^{17} cm^{-3} and temperatures from 10000 up to 300000 K

Transition	T, K	W, Å	Transition	T, K	W, Å
	10000	0.0886		10000	0.0348
2473 Å	20000	0.0627	874 Å	20000	0.0246
	50000	0.0396		50000	0.0178
$3s\ ^4P$—$3p\ ^4S^\circ$	100000	0.0298	$3s\ ^4P$—$4p\ ^4S^\circ$	100000	0.0159
	200000	0.0253		200000	0.0148
	300000	0.0242		300000	0.0141
	10000	0.0339		10000	0.0343
904 Å	20000	0.0240	911 Å	20000	0.0242
	50000	0.0172		50000	0.0174
$3s\ ^4P$—$4p\ ^4P^\circ$	100000	0.0151	$3s\ ^4P$—$4p\ ^4D^\circ$	100000	0.0154
	200000	0.0139		200000	0.0142
	300000	0.0134		300000	0.0136
	10000	0.1130		10000	0.0905
1723 Å	20000	0.0795	1560 Å	20000	0.0640
	50000	0.0576		50000	0.0465
$4s\ ^4P$—$3p\ ^4S^\circ$	100000	0.0507	$4s\ ^4P$—$3p\ ^4P^\circ$	100000	0.0409
	200000	0.0462		200000	0.0374
	300000	0.0438		300000	0.0354
	10000	0.0838		10000	2.72
1504 Å	20000	0.0593	6286 Å	20000	1.93
	50000	0.0431		50000	1.43
$4s\ ^4P$—$3p\ ^4D^\circ$	100000	0.0380	$4s\ ^4P$—$4p\ ^4S^\circ$	100000	1.31
	200000	0.0347		200000	1.22
	300000	0.0329		300000	1.16
	10000	4.43		10000	5.11
8263 Å	20000	3.13	8890 Å	20000	3.61
	50000	2.32		50000	2.68
$4s\ ^4P$—$4p\ ^4P^\circ$	100000	2.09	$4s\ ^4P$—$4p\ ^4D^\circ$	100000	2.43
	200000	1.94		200000	2.26
	300000	1.86		300000	2.15

In closing we can note that the obtained Stark broadening parameters contribute also to the creation of a set of such data for no matter how large number of spectral lines, which is of significance for a variety of problems in research into laboratory, technological and astrophysical plasmas.

Acknowledgements. This work is a part of the project GA-1195 "Influence of collisional processes on astrophysical plasma line shapes", supported by the Ministry of Science, Technologies and Development of Serbia.

[1] **D.N.B.Hall, R.W.Noyes.** Astrophys. Lett., **4** (1969) 143—148
[2] **H.Spinrad, L.D.Kaplan, P.Connes, J.Connes, V.G.Kunde, J.P.Maillard.** Proc. Conf. Late Type Stars, Eds. G.W.Lockwood, H.M.Dyck, Tucson, KPNO (1970) 59—75
[3] **A.Jorissen, V.V.Smith, D.L.Lambert.** Astron. Astrophys., **261** (1992) 164—187
[4] **D.A.Neufeld, J.Zmuidzinas, P.Schilke, T.G.Phillips.** Astrophys. J., **488** (1997) L141—L144
[5] **M.B.K.Sarma.** Proc. Phys. Soc. London, **77** (1961) 665—668
[6] **J.Purić, A.Srećković, S.Djeniže, M.Platiša.** Phys. Rev. A, **37** (1988) 4380—4386
[7] **S.Djeniže, J.Labat, A.Srećković, O.Labat, M.Platiša, J.Purić.** Physica Scripta, **44** (1991) 148—150
[8] **M.S.Dimitrijević, N.Konjević.** In "Spectral Line Shapes", Ed. B.Wende, New York, W. de Gruyter (1981) 211—239
[9] **M.S.Dimitrijević.** Astron. Astrophys. Suppl. Ser., **76** (1988) 53—59
[10] **M.S.Dimitrijević.** Bull. Obs. Astron. Belgrade, **139** (1988) 31—58
[11] **M.S.Dimitrijević, N.Konjević.** J. Quantum Spectr. Radiat. Transfer, **24** (1980) 451—459
[12] **S.Sahal-Bréchot.** Astron. Astrophys., **1** (1969) 91—123
[13] **S.Sahal-Bréchot.** Astron. Astrophys., **2** (1969) 322—354
[14] **S.Sahal-Bréchot.** Astron. Astrophys., **35** (1974) 319—321
[15] **C.Fleurier, S.Sahal-Bréchot, and J.Chapelle.** J. Quantum Spectr. Radiat. Transfer, **17** (1977) 595—604
[16] **S.Sahal-Bréchot.** Astron. Astrophys., **245** (1991) 322—330
[17] **M.S.Dimitrijević, S.Sahal-Bréchot, and V.Bommier.** Astron. Astrophys. Suppl. Ser., **89** (1991) 581—590
[18] **M.S.Dimitrijević, S.Sahal-Bréchot.** Physica Scripta, **52** (1995) 41—51
[19] **M.S.Dimitrijević, S.Sahal-Bréchot.** Physica Scripta, **54** (1996) 50—55
[20] **M.S.Dimitrijević.** Журн. прикл. спектр., **63** (1996) 810—815

[21] **M.S.Dimitrijević, N.Konjević.** Astron. Astrophys., **172** (1987) 345—349
[22] **M.S.Dimitrijević, V.Kršljanin.** Astron. Astrophys., **165** (1986) 269—274
[23] **M.S.Dimitrijević, L.Č.Popović.** Astron. Astrophys. Suppl. Ser., **101** (1993) 583—586
[24] **М.С.Димитриевич, Л.Ч.Попович.** Журн. прикл. спектр., **68** (2001) 685—690
[25] **S.Bashkin, J.O.Stoner, Jr.** Atomic Energy Levels and Grotrian Diagrams, Vol. 1, North Holland, Amsterdam (1975)
[26] **D.R.Bates, A.Damgaard.** Trans. Roy. Soc. London, Ser. A, **242** (1949) 101—122
[27] **G.K.Oertel, L.P.Shomo.** Astrophys. J. Suppl. Ser., **16** (1968) 175—218
[28] **H.Van Regemorter, Hoang Binh Dy, M.Prud'homme.** J. Phys. B, **12** (1979) 1053—1062
[29] **M.S.Dimitrijević, T.Ryabchikova, L.Č.Popović, D.Shylyak, V.Tsymbal.** Astron. Astrophys., **404** (2003) 1099—1106
[30] **M.J.Seaton.** J. Phys. B, **20** (1987) 6363—6378
[31] **R.L.Kurucs.** Astrophys. J. Suppl. Ser., **40** (1979) 1—340

Journal of Applied Spectroscopy, Vol. 68, No. 6, 2001

MODIFIED SEMIEMPIRICAL METHOD

M. S. Dimitrijević and L. Č. Popović*

UDC 533.9.082.5

A review of the application, during the years 1980 to 2000, of the modified semiempirical method developed by Dimitrijević and Konević in 1980 for calculating the parameters of Stark broadening is given and the possibility of using this method to calculate the Stark width and, in some cases, the shift of a large number of spectral lines of various atoms and a number of ions is shown.

Keywords: *line profile, Stark broadening, plasma.*

Introduction. More than twenty years have elapsed since the formulation of the modified semiempirical (MSE) approach [1] to calculation of the Stark broadening parameters for nonhydrogenic ion spectral lines. During these decades, the method has been found to be useful in solving various problems in physics and astrophysics.

In comparison with the fully semiclassical perturbation approach [2–4] and Griem's (1968) semiempirical approach [5], which need practically the same set of atomic data as the more sophisticated semiclassical one, the modified semiempirical approach requires a considerably smaller number of such data. In fact, if there are no perturbing levels that strongly violate the approximation made, then, e.g., for the line width calculations, we need only the energies of the levels with $\Delta n = 0$ and $l = l_{i,f} \pm 1$, since all perturbing levels with $\Delta n \neq 0$, needed for a full semiclassical investigation or an investigation within Griem's semiempirical approach [5], are lumped together and estimated approximately. Here, n is the principal and l the orbital angular momentum quantum numbers of the optical electron, with i and f denoting the initial and final state of the transition considered.

Owing to the considerably smaller set of needed atomic data in comparison with the complete semiclassical [2–4] or Griem's semiempirical [5] methods, the MSE method is particularly useful for stellar spectroscopy depending on a very extensive list of elements and line transitions with their atomic and line broadening parameters where it is not possible to use a sophisticated theoretical approach in all of the cases of interest.

The MSE method is also very useful whenever line broadening data for a large number of lines are required, and the high precision of every particular result is not so important as, e.g., for opacity calculations or plasma modeling. Moreover, in the case of more complex atoms or multiply charged ions, the lack of accurate atomic data needed for more sophisticated calculations makes the reliability of the semiclassical results decrease. In such cases, the MSE method might be very interesting as well.

The Modified Semiempirical Method. According to the modified semiempirical approach [1, 6–9], for electron impact broadening, the full width at half maximum of the spectral line of wavelength λ is given as

*To whom correspondence should be addressed.

Astronomical Observatory, 7 Volgin Str., Belgrade, 11160, Serbia, Yugoslavia; e-mail: mdimitrijevic@aob.bg.ac.yu. Translated from Zhurnal Prikladnoi Spektroskopii, Vol. 68, No. 6, pp. 685–690, November–December, 2001. Original article submitted January 31, 2001.

0021-9037/01/6806-0893$25.00

$$W_{\mathrm{MSE}} = N \frac{8\pi}{3} \frac{\hbar^2}{m^2} \left(\frac{2m}{\pi kT} \right)^{1/2} \frac{\pi}{\sqrt{3}} \frac{\lambda^2}{2\pi c} \left\{ \sum_{l_i \pm 1} \sum_{A_{i'} J_{i'}} \overrightarrow{\mathfrak{R}}^{\,2} [n_i l_i A_i J_i, n_i (l_i \pm 1) A_{i'} J_{i'}] \, \tilde{g} (x_{l_i, l_i \pm 1}) + \right.$$

$$+ \sum_{l_f \pm 1} \sum_{A_{f'} J_{f'}} \overrightarrow{\mathfrak{R}}^{\,2} [n_f l_f A_f J_f, n_f (l_f \pm 1) A_{f'} J_{f'}] \, \tilde{g} (x_{l_f, l_f \pm 1}) + \left(\sum_{i'} \overrightarrow{\mathfrak{R}}_{ii'}^{\,2} \right)_{\Delta n \neq 0} g (x_{n_i, n_i + 1}) +$$

$$\left. + \left(\sum_{f'} \overrightarrow{\mathfrak{R}}_{ff'}^{\,2} \right)_{\Delta n \neq 0} g (x_{n_f, n_f + 1}) \right\}, \tag{1}$$

and the corresponding Stark shift as

$$d_{\mathrm{MSE}} = N \frac{4\pi}{3} \frac{\hbar^2}{m^2} \left(\frac{2m}{\pi kT} \right)^{1/2} \frac{\pi}{\sqrt{3}} \frac{\lambda^2}{2\pi c} \left\{ \sum_{A_{i'} J_{i'}} \sigma_{J_i J_{i'}} \overrightarrow{\mathfrak{R}}^{\,2} [n_i l_i A_i J_i, n_i (l_i + 1) A_{i'} J_{i'}] \, \tilde{g}_{\mathrm{sh}} (x_{l_i, l_i + 1}) + \right.$$

$$- \sum_{A_{i'} J_{i'}} \sigma_{J_i J_{i'}} \overrightarrow{\mathfrak{R}}^{\,2} [n_i l_i A_i J_i, n_i (l_i + 1) A_{i'} J_{i'}] \, \tilde{g}_{\mathrm{sh}} (x_{l_i, l_i - 1}) - \sum_{A_{f'} J_{f'}} \sigma_{J_f J_{f'}} \overrightarrow{\mathfrak{R}}^{\,2} [n_f l_f A_f J_f, n_f (l_f + 1) A_{f'} J_{f'}] \, \tilde{g}_{\mathrm{sh}} (x_{l_f, l_f + 1}) +$$

$$+ \sum_{A_{f'} J_{f'}} \sigma_{J_f J_{f'}} \overrightarrow{\mathfrak{R}}^{\,2} [n_f l_f A_f J_f, n_f (l_f - 1) A_{f'} J_{f'}] \, \tilde{g}_{\mathrm{sh}} (x_{l_f, l_f - 1}) + \left(\sum_{i'} \overrightarrow{\mathfrak{R}}_{ii'}^{\,2} \right)_{\Delta n \neq 0} g_{\mathrm{sh}} (x_{n_i, n_i + 1}) - \tag{2}$$

$$- 2 \sum_{i' (\Delta E_{ii'} < 0)} \sum_{A_{i'} J_{i'}} \overrightarrow{\mathfrak{R}}^{\,2} (n_i l_i A_i J_i, n_{i'} l_{i'} A_{i'} J_{i'} \, g_{\mathrm{sh}} (x_{l_i, l_{i'}}) - \left(\sum_{f'} \overrightarrow{\mathfrak{R}}_{ff'}^{\,2} \right)_{\Delta n \neq 0} g_{\mathrm{sh}} (x_{n_f, n_f + 1}) +$$

$$\left. + 2 \sum_{f' (\Delta E_{ff'} < 0)} \sum_{A_{f'} J_{f'}} \overrightarrow{\mathfrak{R}}^{\,2} (n_f l_f A_f J_f, n_{f'} l_{f'} A_{f'} J_{f'} \, g_{\mathrm{sh}} (x_{l_f, l_{f'}}) + \sum_k \delta_k \right\}.$$

Here, the initial level is denoted by i and the final one by f, and the square of the matrix element is

$$\overrightarrow{\mathfrak{R}}^{\,2} [n_k l_k A_k J_k, n_k (l_k \pm 1) A_{k'} J_{k'}] = \frac{L_>}{2 J_k + 1} Q [l_k A_k, l_k \pm 1) A_{k'}] \, Q (J_k, J_k') \left[R_{n_k l_k}^{* \, n_k^* (l_k \pm 1)} \right]^2, \tag{3}$$

where $k = i, f$; $l_> = \max (l_k, l_k \pm 1)$, and

$$\left(\sum_{k'} \overrightarrow{\mathfrak{R}}_{kk'}^{\,2} \right)_{\Delta n \neq 0} = \left(\frac{3 n_k^*}{2Z} \right)^2 \frac{1}{9} \left(n_k^{*2} + 3 l_k^2 + 3 l_k + 11 \right). \tag{4}$$

In Eqs. (1) and (2),

$$x_{l_k, l_{k'}} = \frac{E}{\Delta E_{l_k, l_{k'}}}, \quad k = i, f,$$

where $E = (3/2)kT$ is the electron kinetic energy and $\Delta E_{l_k,l_{k'}} = \left| E_{l_k} - E_{l_{k'}} \right|$ is the energy difference between the levels l_k and $l_k \pm 1$ ($k = i, f$),

$$x_{n_k,n_k+1} \approx \frac{E}{\Delta E_{n_k,n_k+1}},$$

where, for $\Delta n \neq 0$, the energy difference between energy levels with n_k and $n_k + 1$ is estimated as $\Delta E_{n_k,n_k+1} \approx 2Z^2 E_H/(n_k^*)^3$ and $n_k^* = [EHZ2/(E_{ion} - E_k)]^{1/2}$ is the effective principal quantum number, Z is the residual ionic charge (for example, Z = 1 for neutral atoms), and E_{ion} is the appropriate spectral series limit.

In Eqs. (1) and (2), the sums

$$\sum_{l_k \pm 1} \sum_{A_{k'}J_{k'}} \vec{\mathfrak{R}}^{\,2} [n_k l_k A_k J_k, n_k (l_k \pm 1) A_{k'} J_{k'}] \, \tilde{g} (x_{l_k,l_k \pm 1}),$$

$$\sum_{A_{k'}J_{k'}} \sigma_{J_k J_{k'}} \vec{\mathfrak{R}}^{\,2} [n_k l_k A_k J_k, n_k (l_k + 1) A_{k'} J_{k'}] \, \tilde{g}_{sh} (x_{l_k,l_k+1}),$$

$$\sum_{A_{k'}J_{k'}} \sigma_{J_k J_{k'}} \vec{\mathfrak{R}}^{\,2} [n_k l_k A_k J_k, n_k (l_k - 1) A_{k'} J_{k'}] \, \tilde{g}_{sh} (x_{l_k,l_k-1}), \quad k = i, f,$$

represent contributions of the allowed dipole transitions for $l_k \to l_k + 1$ and $l_k \to l_k - 1$ for $\Delta n = 0$. In the case of the shift, where particular contributions have different signs, all transitions with $\Delta n \neq 0$ are first summed, with the squared matrix elements lumped together. From the sum obtained, the group of transitions with $\Delta E_{kk'} < 0$, $k = i, f$, is subtracted so that in Eq. (2) the sums

$$\sum_{k'(\Delta E_{kk'}<0)} \sum_{A_{k'}J_{k'}} \vec{\mathfrak{R}}^{\,2} n_k l_k A_k J_k, n_{k'} l_{k'} A_{k'} J_{k'}) \, g_{sh} (x_{l_k,l_{k'}})$$

would be present. In both equations, (1) and (2), the sums $(\Sigma_{k'} \mathfrak{R}^2_{kk'})_{\Delta n \neq 0}$ represent the combined contributions for the energy levels with $\Delta n \neq 0$.

If we know the oscillator strength, e.g., from the literature, the corresponding squared matrix element may be calculated as

$$\vec{\mathfrak{R}}^{\,2}_{kk'} \approx 3 \frac{E_H}{E_{k'} - E_k} f_{k'k}, \quad E_{k'} > E_k, \quad k = i, f,$$

or

$$\vec{\mathfrak{R}}^{\,2}_{kk'} \approx 3 \frac{E_H}{E_k - E_{k'}} \frac{2k' + 1}{2k + 1} f_{kk'}, \quad E_{k'} < E_k, \quad k = i, f,$$

where $f_{k'k}$ and $f_{kk'}$ are the oscillator strengths, E_H is the hydrogen ionization energy, and $2k + 1$ is the statistical weight for the level k.

The ultimate configuration mixing may be taken into account (see, e.g., [9]) if one represents $\mathfrak{R}^2_{\alpha\beta}$ as

$$\vec{\mathfrak{R}}^{\,2}_{\alpha\beta} = K_\alpha \vec{\mathfrak{R}}^{\,2}_{\alpha\alpha'} + K_\beta \vec{\mathfrak{R}}^{\,2}_{\beta\beta'},$$

where K_α and K_β are the mixing coefficients for the two configurations and $K_\alpha + K_\beta = 1$.

In Eqs. (1)–(4), N and T are the electron density and temperature, respectively, whereas $Q(lA, l'A')$ and $Q(J, J')$ are the multiplet and line factors. The value of A depends on the coupling approximation (see, e.g., [10]): $A = L$ for LS coupling, $A = K$ for jK coupling, and $A = j$ for jj coupling. $\left[R^{n_k^* l_k \pm 1}_{n_k^* l_k}\right]$ is the radial integral; and $g(x)$ [5], $\tilde{g}(x)$ [1] and $g_{\rm sh}(x)$ [5], $\tilde{g}_{\rm sh}(x)$ [8] denote the corresponding Gaunt factors for the width and the shift, respectively. The factor $\sigma_{kk'} = (E_{k'} - E_k)/|E_{k'} - E_k|$, where E_k and $E_{k'}$ are the energies of the level being considered and of the level perturbing it. The sum $\Sigma_k \delta_k$ is different from zero only if there are perturbing levels with $\Delta n \neq 0$ strongly violating the assumed approximations, so that they should be taken into account separately. The δ_k, $k = i, f$, may be evaluated as

$$\delta_i = \pm \vec{\Re}^2_{ii'} \left[g_{\rm sh}\left(\frac{E}{\Delta E_{i,i'}}\right) \mp g_{\rm sh}\,(x_{n_i, n_i+1}) \right] \tag{5}$$

for the upper level, and

$$\delta_f = \mp \vec{\Re}^2_{ff'} \left[g_{\rm sh}\left(\frac{E}{\Delta E_{f,f'}}\right) \mp g_{\rm sh}\,(x_{n_f, n_f+1}) \right] \tag{6}$$

for the lower level. In Eqs. (7) and (8), the lower sign corresponds to $\Delta E_{kk'} < 0$, $k = i, f$.

Simplified Modified Semiempirical Formula. For astrophysical purposes, of particular interest might be the simplified semiempirical formula [7] for the Stark widths of the isolated lines of singly and multiply charged ions. It is appreciable in the cases where the nearest atomic energy level ($j' = i'$ or f') from which a dipolarly allowed transition can occur from or to the initial (i) or final (f) energy level of the considered line, is so far that the condition $x_{jj'} = E/|E_{j'} - E_j| \leq 2$ is satisfied. In such cases, the full width at half maximum is given by the expression [7]

$$W\,[\mathring{\rm A}] = (2.2151 \cdot 10^{-8}) \frac{\lambda^2\,[\rm cm]\, N\,[\rm cm^{-3}]}{T^{1/2}\,[\rm K]} \left(0.9 - \frac{1.1}{Z}\right) \sum_{j=i,f} \left(\frac{3n_j^*}{2Z}\right)^2 (n_j^{*2} - l_j^2 - l - 1)\,. \tag{7}$$

Here, N and T are the electron density and temperature, respectively, $E = 3kT/2$ is the energy of a perturbing electron, $Z - 1$ is the ionic charge, and n^* is the effective principal quantum number. This expression is of interest for abundance calculations and also for stellar atmosphere research, since its validity conditions are often satisfied for stellar plasma conditions.

Similarly, in the case of the shift

$$d\,[\mathring{\rm A}] = (1.1076 \cdot 10^{-8}) \frac{\lambda^2\,[\rm cm]\, N\,[\rm cm^{-3}]}{T^{1/2}\,[\rm K]} \left(0.9 - \frac{1.1}{Z}\right) \frac{9}{4Z^2} \sum_{j=i,f} \frac{n_j^{*2}\varepsilon_j}{2l_j + 1} \times$$

$$\times \left\{ (l_j + 1)\,[n_j^{*2} - (l_j + 1)^2] - l_j\,(n_j^{*2} - l_j^2) \right\}. \tag{8}$$

If all the levels $l_{i,f} \pm 1$ exist, an additional summation may be performed in Eq. (10) to obtain

$$d\,[\mathring{\rm A}] = (1.1076 \cdot 10^{-8}) \frac{\lambda^2\,[\rm cm]\, N\,[\rm cm^{-3}]}{T^{1/2}\,[\rm K]} \left(0.9 - \frac{1.1}{Z}\right) \frac{9}{4Z^2} \sum_{j=i,f} \frac{n_j^{*2}\varepsilon_j}{2l_j + 1} (n_j^{*2} - 3l_j^2 - 3l_j - 1)\,,$$

where $\varepsilon = +1$ if $j = i$ and -1 if $j = f$.

Applications. The modified semiempirical approach has been tested several times on numerous examples [11]. In order to test this method, selected experimental data for 36 multiplets (7 different ion species) of triply charged ions were compared with theoretical linewidths. The averaged values of the ratios of measured to calculated widths are as follows [1]: for doubly charged ions 1.06 ± 0.32 and for triply charged ions 0.91 ± 0.42. The adopted accuracy of the MSE approximation is at about ±50%, but it has been shown in [12] and [13] that the MSE approach, even in the case of emitters with very complex spectra (e.g., Xe II and Kr II), gives very good agreement with experimental measurements (in the interval ±30%). For example, for the 6*s*–6*p* transitions of Xe II the averaged ratio between the experimental and theoretical widths of the lines is 1.15 ± 0.5 [12].

In order to complete as much as possible the needed Stark broadening data, the Belgrade group (Milan S. Dimitrijević, Luka Č. Popović, Vladimir Kršljanin, Dragana Tankosić, and Nenad Milovanović) used the modified semiempirical method to obtain the Stark width and, in some cases, shift data for a large number of spectral lines for various atoms and a number of ions. Up to now the following transitions have been calculated: 6 Fe II [14], 4 Pt II [15], 16 Bi II [9], 12 Zn II, 8 Cd II [16], 18 As II, 10 Br II, 18 Sb II, 8 I II [17], 20 Xe II [12, 18], 138 Ti II [19], 3 La II [20], 16 Mn II [21, 22], 14 V II [23, 24], 6 Eu II [20], 37 Kr II [13], 6 Y II, 6 Sc II [18, 25], 4 Be III, 4 B III [1, 6, 26, 27], 13 S III [28], 8 Au II [29, 30], 8 Zr II [18, 25, 31], 53 Ra II [32], 3 Mn III, 10 Ga III, 8 Ge III [21, 22], 4 As III, 3 Se III [33], 6 Mg III [34], 6 La III [20], 5 Sr III [35], 8 V III [23, 24], 210 Ti III [19], 9 C III, 7 N III, 11 O III, 5 F III, 6 Ne III, 8 Na III, 10 Al III, 5 Si III, 3 P III, 16 Cl III, 6 Ar III [1, 6, 26, 27], 30 Zr III [31], 2 B IV [1, 6, 26, 27], Cu IV [36], 30 V IV [23, 24], 14 Ge IV [21, 22], 7 C IV, 4 N IV, 4 O IV, 2 Ne IV, 4 Mg IV, 7 Si IV, 3 P IV, 2 S IV, 2 Cl IV, 4 Ar IV [1, 6, 26, 27], 3 C V, 50 O V, 12 F V, 9 Ne V, 3 Al V, 6 Si V, 11 N VI, 28 F VI, 8 Ne VI, 7 Na VI, 15 Si VI, 6 P VI, and 1 Cl VI [37]. The shift data have been calculated for the following transitions: 16 Bi II [9], 12 Zn II, 8 Cd II [16], 18 As II, 10 Br II, 18 Sb II, 8 I II [17], 20 Xe II [12], 5 Ar II [38, 39], 6 Eu II [20], 14 V II [23, 24], 8 Au II [29, 30], 14 Kr II [40], and 138 Ti II [19]. Moreover, 286 Nd II Stark widths have been calculated [41] within the simplified modified semiempirical approach.

For comparison with experimental data or testing the theory, calculations within the modified semiempirical approach have been performed also for the Stark width for the following transitions: 14 Al I, 46 Al II, 12 Al III [42], 1 C IV, 1 N V, 1 O VI [43, 44], 1 Ne VIII [44], 3 N III, 3 O IV, 3 F V, 2 Ne VI [45], 12 C IV [46], 4 C II, 5 N II, 3 O II, 4 F II, 3 Ne II [47], 1 N II [48], 8 S II [49], 2 Ne VII [50], 4 N III, 2 F V [51], 2 Ne III, 2 Ar III, 2 Kr III, 2 Xe III [52], 3 Si III [53], 3 Ne III, 2 Ar III, 2 Kr III, and 2 Xe III [54]. Moreover, in [55] the Stark widths and shifts for the 2 Cl II and 6 Ar III lines have been calculated.

In [56–59], reviews of the modified semiempirical approach are given. In addition to the investigation of the Stark broadening of specific spectral lines in laboratory and astrophysical plasmas, the considered method has been successfully applied, e.g., to the study of elemental abundances in early *B*-type stars [60], normal late-*B* and HgMn stars [61], and hot white dwarfs [62], investigations of abundance anomalies in stars [63], elemental abundance analyses with DAO spectrograms for 15-Vulpeculae and 32-Aquarii [64], calculation of radiative acceleration in stellar envelopes [65–69], consideration of radiative levitation in hot white dwarfs [62, 70], quantitative spectroscopy of hot stars [71], non-LTE calculations of silicon-line strengths in *B*-type stars [72], calculation and study of stellar opacities [73–79], investigations of atmospheres and winds of hot stars [80], Ga II lines in the spectrum of Ap stars [81], design and development of new lasers [82–87], spectroscopic diagnostics of railgun plasma armatures [88], investigations of 3*d* photoabsorption in Zn III, Ge V [89], Zn II, Ga III, and Ge IV [90], research of Stark broadening parameter regularities and systematic trends [91–99], calculations of radiative emission coefficients for thermal plasmas [100, 101], considerations

of plasma-wall contact [102, 103], and examination of particle-velocity distribution and expansion of a surface flashover plasma in the presence of magnetic fields [104].

The modified semiempirical method has also entered in computer codes, as, e.g., the OPAL opacity code [75], handbooks [105, 106] and monographs [59, 107, 108].

As can be seen, over the coarse of twenty years a large number of Stark broadening parameter data, calculated within the modified semiempirical approach has been provided to plasma physicists and astrophysicists. In order to make the application and use of these data easier, we are now organizing them in a database, BELDATA.

REFERENCES

1. M. S. Dimitrijević and N. Konjević, *J. Quant. Spectrosc. Radiat. Transfer*, **24**, 451–459 (1980).
2. S. Sahal-Bréchot, *Astron. Astrophys.*, **1**, 91–123 (1969).
3. S. Sahal-Bréchot, *Astron. Astrophys.*, **2**, 322–354 (1969).
4. H. R. Griem, *Spectral Line Broadening by Plasmas*, Academic Press, New York (1974).
5. H. R. Griem, *Phys. Rev.*, **165**, 258–266 (1968).
6. M. S. Dimitrijević and N. Konjević, in: B. Wende (ed.), *Spectral Line Shapes*, W. de Gruyter, Berlin–New York (1981), pp. 211–239.
7. M. S. Dimitrijević and N. Konjević, *Astron. Astrophys.*, **172**, 345-349 (1987).
8. M. S. Dimitrijević and V. Krŝljanin, *Astron. Astrophys.*, **165**, 269-274 (1986).
9. M. S. Dimitrijević and L. Č. Popović, *Astron. Astrophys. Suppl. Ser.*, **101**, 583–586 (1993).
10. I. I. Sobel'man, *Atomic Spectra and Radiative Transitions*, Springer–Verlag, Berlin (1979).
11. M. S. Dimitrijević, in: R. Wehrse (ed.), *Accuracy of Element Abundances from Stellar Atmospheres*, Lecture Notes in Physics, **356**, Springer, Berlin–Heidelberg (1990), pp. 31–44.
12. L. Č. Popović and M. S. Dimitrijević, *Astron. Astrophys. Suppl. Ser.*, **116**, 359–365 (1996).
13. L. Č. Popović and M. S. Dimitrijević, *Astron. Astrophys. Suppl. Ser.*, **127**, 295–297 (1998).
14. M. S. Dimitrijević, in: R. Viotti, A. Vitone, M. Friedjung, and D. Reidel (eds.), *Physics of Formation of Fe II Lines Outside LTE*, Dordrecht–Boston–Lancaster–Tokyo (1988), pp. 211–216.
15. M. Š. Dimitrijević, *Astrophys. Lett. Commun.*, **28**, 385–388 (1993).
16. L. Č. Popović, I. Vince, and M. S. Dimitrijević, *Astron. Astrophys. Suppl. Ser.*, **102**, 17–23 (1993).
17. L. Č. Popović and M. S. Dimitrijević, *Physica Scripta*, **53**, 325–331 (1996).
18. L. Č. Popović and M. S. Dimitrijević, *Bull. Astron. Belgrade*, **155**, 159–164 (1997).
19. D. Tankosić, L. Č. Popović, and M. S. Dimitrijević, *Atomic Data and Nuclear Data Tables*, **77**, 277–310 (2001).
20. L. Č. Popović, M. S. Dimitrijević, and T. Ryabchikova, *Astron. Astrophys.*, **350**, 719–724 (1999).
21. L. Č. Popović and M. S. Dimitrijević, *Astron. Astrophys. Suppl. Ser.*, **128**, 203–205 (1998).
22. L. Č. Popović and M. S. Dimitrijević, *Bull. Astron. Belgrade*, **156**, 173–178 (1997).
23. L. Č. Popović and M. S. Dimitrijević, *Serb. Astron. J.*, **157**, 109–114 (1998).
24. L. Č. Popović and M. S. Dimitrijević, *Physica Scripta*, **61**, 192–199 (2000).
25. L. Č. Popović and M. S. Dimitrijević, *Astron. Astrophys. Suppl. Ser.*, **120**, 373–374 (1996).
26. M. S. Dimitrijević, *Bull. Obs. Astron. Belgrade*, **139**, 31–58 (1988).
27. M. S. Dimitrijević, *Astron. Astrophys. Suppl. Ser.*, **76**, 53–59 (1988).
28. M. Š. Dimitrijević, S. Djeniže, A. Srećković, and M. Platiša, *Physica Scripta*, **53**, 545–548 (1996).
29. L. Č. Popović, M. S. Dimitrijević, and D. Tankosić, *Astron. Astrophys.*, **139**, 617–623 (1999).
30. L. Č. Popović, M. S. Dimitrijević, and D. Tankosić, *Serb. Astron. J.*, **159**, 59–64 (1999).
31. L. Č. Popović, N. Milovanović, and M. S. Dimitrijević, *Astron. Astrophys.*, **365**, 656–659 (2001).
32. D. Tankosić, L. Č. Popović, and M. S. Dimitrijević, *Physica Scripta*, **63**, 54–61 (2001).

33. L. Č. Popović and M. S. Dimitrijević, *Publ. Astron. Obs. Belgrade*, **50**, 105–106 (1995).
34. L. Č. Popović and M. S. Dimitrijević, *Publ. Astron. Obs. Belgrade*, **54**, 39–41 (1996).
35. L. Č. Popović and M. S. Dimitrijević, *Publ. Astron. Obs. Belgrade*, **60**, 71–73 (1998).
36. M. S. Dimitrijević, Z. Djurić, and A. A. Mihajlov, *J. Phys. D: Appl. Phys*., **27**, 247–252 (1994).
37. M. S. Dimitrijević, *Astron. Astrophys. Suppl. Ser*., **100**, 237-241 (1993).
38. V. Kršljanin and M. S. Dimitrijević, *Bull. Obs. Astron. Belgrade*, **140**, 7–14 (1989).
39. V. Kršljanin and M. S. Dimitrijević, *Z. Phys. D*, **14**, 273–280 (1989).
40. V. Milosavljević, S. Djeniže, M. S. Dimitrijević, and L. Č. Popović, *Phys. Rev. E*, **62**, 4137–4145 (2000).
41. L. Č. Popović, S. Simić, N. Milovanović, and M. S. Dimitrijević, *Astrophys. J*., **135**, 109–114 (2001).
42. D. J. Heading, J. S. Wark, R. W. Lee, R. Stamm, and B. Talin, *Phys. Rev. E*, **56**, 936–946 (1997).
43. F. Böttcher, P. Breger, J. D. Hey, and H.-J. Kunze, *Phys. Rev. A*, **38**, 2690–2693 (1988).
44. S. Glenzer, N. I. Uzelac, and H.-J. Kunze, *Phys. Rev. A*, **45**, 8795–8802 (1992).
45. S. Glenzer, J. D. Hey, and H.-J. Kunze, *J. Phys. B: At. Mol. Opt. Phys*., **27**, 413–422 (1994).
46. U. Ackermann, K. H. Finken, and J. Musielok, *Phys. Rev. A*, **31**, 2597–2609 (1985).
47. B. Blagojević, M. V. Popović, and N. Konjević, *Physica Scripta*, **59**, 374–378 (1999).
48. V. Milosavljević, R. Konjević, and S. Djeniže, *Astron. Astrophys. Suppl. Ser*., **135**, 565–569 (1999).
49. S. Djeniže, A. Srećković, M. Platiša, R. Konjević, J. Labat, and J. Purić, *Phys. Rev. A*, **42**, 2379–2384 (1990).
50. Th. Wrubel, S. Glenzer, S. Büscher, H.-J. Kunze, and S. Alexiou, *Astron. Astrophys*., **306**, 1023–1028 (1996).
51. B. Blagojević, M. V. Popović, N. Konjević, and M. S. Dimitrijević, *Phys. Rev. E*, **54**, 743–756 (1996).
52. R. Konjević, *Publ. Obs. Astron. Belgrade*, **50**, 87–90 (1995).
53. M. S. Dimitrijević, *Astron. Astrophys*., **127**, 68–72 (1983).
54. N. Konjević and T. L. Pittman, *J. Quant. Spectrosc. Radiat. Transfer*, **37**, 311–318 (1987).
55. R. Kobilarov and N. Konjević, *Phys. Rev. A*, **41**, 6023–6031 (1990).
56. M. S. Dimitrijević, *Zh. Prikl. Spektrosk*., **63**, 810–815 (1996).
57. L. Č. Popović and M. S. Dimitrijević, in: B. Vujičić, S. Djurović, and J. Purić (eds.), *The Physics of Ionized Gases*, Institute of Physics, Novi Sad (1977), pp. 477–486.
58. M. S. Dimitrijević, *Astrophys. Space Sci*., **252**, 415–422 (1997).
59. N. Konjević, *Phys. Rep*., **316**, 339–401 (1999).
60. D. R. Gies and D. L. Lambert, *Astrophys. J*., **387**, 673–700 (1992).
61. K. S. Smith, *Astron. Astrophys*., **276**, 393–408 (1993).
62. P. Chayer, S. Vennes, A. K. Pradhan, P. Thejll, A. Beauchamp, G. Fontaine, and W. Wesemael, *Astrophys. J*., **454**, 429–441 (1995).
63. G. Michaud and J. Richer, in: M. Zoppi and L. Ulivi (eds.), Proc.9th AIP Cond. "*Spectral Line Shapes*," **386** (1992), pp. 397–410.
64. C. Bolcal, D. Kocer, and S. J. Adelman, *Month. Not. Roy. Astron. Soc*., **258**, 270–276 (1992).
65. J. F. Gonzales, M.-C. Artru, and G. Michaud, *Astron. Astrophys*., **302**, 788–796 (1995).
66. J. F. Gonzales, F. LeBlanc, M.-C. Artru, and G. Michaud, *Astron. Astrophys*., **297**, 223–226 (1995).
67. G. Alecian, G. Michaud, and J. Tully, *Astrophys. J*., **411**, 882–890 (1993).
68. F. LeBlanc and G. Michaud, *Astron. Astrophys*., **303**, 166–174 (1995).
69. M. J. Seaton, *Month. Not. Roy. Astron. Soc*., **289**, 700–720 (1997).
70. P. Chayer, G. Fontaine, and F. Wesemael, *Astrophys. J. Suppl. Ser*., **99**, 189–221 (1995).
71. R. Kudritzki and D. G. Hummer, *Ann. Rev. Astron. Astrophys*., **28**, 303–345 (1990).
72.

D. J. Lennon, A. E. Lynas-Gray, J. F. Brown, and P. L. Dufton, *Month. Not. Roy. Astron. Soc.*, **222**, 719–729 (1986).
73. C. A. Iglesias and F. J. Rogers, *Rev. Mexicana Astron. Astrofis.*, **23**, 161–170 (1992).
74. C. A. Iglesias, F. J. Rogers, and B. G. Wilson, *Astrophys. J.*, **360**, 221–226 (1990).
75. F. J. Rogers and C. A. Iglesias, in: S. J. Adelman and W. L. Wiese (eds.), *ASP Conf. Ser. "Astrophysical Applications of Powerful New Databases,"* **78** (1995), pp. 31–50.
76. M. J. Seaton, in: W. W. Weiss and A. Baglin (eds.), *137 IAU Colloq., Astron. Soc. of the Pacific Conf. Ser.*, **40** (1993), pp. 222–235.
77. A. N. Mostovych, L. Y. Chan, K. J. Kearney, D. Garren, C. A. Iglesias, M. Klapisch, and F. J. Rogers, *Phys. Rev. Lett.*, **75**, 1530-1533 (1995).
78. F. J. Rogers and C. A. Iglesias, *Space Sci. Rev.*, **85**, 61 (1999).
79. F. J. Rogers and C. A. Iglesias, *Astrophys. J. Suppl. Ser.*, **79**, 507–568 (1992).
80. K. Butler, in: S. J. Adelman and W. L. Wiese (eds.), *ASP Conf. Ser. "Astrophysical Applications of Powerful New Databases,"* **78** (1995), pp. 509–525.
81. T. Lanz, M.-C. Artru, P. Didelon, and G. Mathys, *Astron. Astrophys.*, **272**, 465–476 (1993).
82. C. D. Decker and R. A. London, *Phys. Rev. A*, **57**, 1395–1399 (1998).
83. E. E. Fill and T. Schoning, *J. Appl. Phys.*, **76**, 1423–1430 (1994).
84. B. E. Lemoff, C. P. J. Barty, and S. E. Harris, *Opt. Lett.*, **19**, 569–571 (1994).
85. B. E. Lemoff, G. Y. Yin, C. L. Gordon, C. P. J. Barty, and S. E. Harris, *Phys. Rev. Lett.*, **74**, 1574–1577 (1995).
86. B. E. Lemoff, G. Y. Yin, C. L. Gordon, C. P. J. Barty, and S. E. Harris, *J. Opt. Soc. Am. B, Opt. Phys.*, **13**, 180–184 (1996).
87. P. A. Norreys, J. Zhang, G. Cairns, A. Djaoui, L. Dwivedi, M. H. Key, R. Kodama, J. Krishnan, C. L. S. Lewis, D. Neely, D. O. Neill, G. J. Pert, S. A. Ramsden, S. J. Rose, G. J. Tallents, and J. Uhomoibhi, *J. Phys. B*, **26**, 3693–3699 (1993).
88. V. Bakshi, B. D. Barett, T. D. Boone, Jr., and W. C. Nunnally, *IEEE Trans. on Magnetics*, **29**, 1097–1101 (1993).
89. F. O'Reilly and P. Dunne, *J. Phys. B*, **31**, L141–L145 (1998).
90. F. O'Reilly and P. Dunne, *J. Phys. B*, **31**, 1059–1068 (1998).
91. S. Glenzer, N. I. Uzelac, and H.-J. Kunze, *Phys. Rev. A*, **45**, 8795–8802 (1992).
92. S. Glenzer, J. D. Hey, and H.-J. Kunze, *J. Phys. B*, **27**, 413–422 (1994).
93. T. Wrubel, I. Ahmad, S. Buscher, and H.-J. Kunze, *Phys. Rev. E*, **57**, 5972–5977 (1998).
94. J. Purić, A. Srećković, S. Djeniže, and M. Platiša, *Phys. Rev. A*, **36**, 3957–3963 (1987).
95. J. Purić, S. Djeniže, A. Srećković, M. Platiša, and J. Labat, *Phys. Rev. A*, **37**, 498–503 (1988).
96. J. Purić, S. Djeniže, A. Srećković, M. Čuk, J. Labat, and M. Platiša, *Z. Phys. D*, **8**, 343–347 (1988).
97. J. Purić, S. Djeniže, J. Labat, M. Platiša, A. Srećković, and M. Čuk, *Z. Phys. D*, **10**, 431–436 (1988).
98. J. Purić, A. Srećković, S. Djeniže, and M. Platiša, *Phys. Rev. A*, **37**, 4380–4386 (1988).
99. J. Purić, *Zh. Prikl. Spektrosk.*, **63**, 816–830 (1996).
100. J. Menart, J. Heberlein, and E. Pfender, *J. Quant. Spectrosc. Radiat. Transfer*, **56**, 377–398 (1996).
101. J. Menart, J. Heberlein, and E. Pfender, *Plasma Chem. Plasma Processing*, **16**, S245–S265 (1996).
102. N. K. Berezhetskaya, V. A. Kop'ev, I. A. Kossyi, I. I. Kutuzov, and B. M. Tiit, *Zh. Tekh. Fiz.*, **61**, No. 2, 179–184 (1991).
103. H. Ehrich, J. Kaplan, and K. G. Muller, *IEEE Trans. Plasma Sci.*, **PS-14**, 603–608 (1986).
104. Y. Maron, E. Sarid, O. Zahavi, L. Perelmutter, and M. Sarfaty, *Phys. Rev. A*, **39**, 5842–5855 (1989).
105. G. Peach, in: G. W. F. Drake (ed.), *Atomic, Molecular, and Optical Physics. Handbook*, AIP Press, Woodbury–New York (1996), pp. 669–680.

106. H. H. Vogt (ed.), in: *Stellar Atmospheres: Atomic and Molecular Data, Astronomy and Astrophysics*, Extension and Suppl. to Vol. 2, Subvol. B, *Stars and Star Clusters*, Landolt–Boernstein, Group VI: *Astron. Astrophys*., Vol. 3, Springer (1996), p. 57.
107. D. F. Gray, *The Observation and Analysis of Stellar Photospheres*, Cambridge University Press, Cambridge (1992).
108. H. R. Griem, *Principles of Plasma Spectroscopy, Cambridge Monographs of Plasma Physics* **2**, Cambridge University Press, Cambridge (1997).

Journal of Applied Spectroscopy, Vol. 70, No. 4, 2003

STARK BROADENING OF Ne II AND Ne III SPECTRAL LINES

M. S. Dimitrijević

UDC 533.9.082.5

Using a semiclassical approach, the widths and shifts of the spectral lines of three Ne II and six Ne III multiplets caused by collisions with electrons, protons, and helium ions at a density of perturbing particles of 10^{17} cm^{-3} and different temperatures have been calculated. The results obtained have been compared with the known experimental and theoretical data.

Keywords: *Stark broadening of spectral lines, semiclassical approach, impact width of spectral line, shift of spectral line.*

Introduction. Knowledge of the Stark broadening parameters of the Ne II and Ne III spectral lines is of interest for diagnostics, modeling, and investigation of laboratory, astrophysical, and technological plasmas. Namely, from the Stark broadening parameters, it is possible to obtain basic plasma parameters such as the electron temperature and electron density, essential for modeling the plasma considered. Moreover, neon is present in many light sources, lasers, and different plasma devices as the working gas. Neon is also the most abundant element in the universe after hydrogen, helium, oxygen, and carbon, and it is, for example [1], one of the products of hydrogen and helium burning in orderly evolution of stellar interiors. Moreover, after the hydrogen-, helium-, and carbon-burning periods come to an end in massive stars, neon burning begins.

From the first investigation of the influence of the Stark broadening effect on the Ne II spectral lines [2, 3], the Ne II Stark broadening parameters have been investigated in several experiments (see [4] and references therein and [5–16]) and theoretically in [6, 7, 9, 12, 15–18]. Also, estimation of Ne II Stark broadening using regularities and systematic trends has been performed in [19–21]. The Ne III Stark widths have been measured in [11, 12, 15, 22, 23] and the results of theoretical calculations have been presented in [12, 15, 22–27]. In [15] electron-impact widths for twenty two Ne II, five Ne III, and two Ne IV multiplets have been calculated within the semiclassical perturbation formalism [28, 29] (see also [30–36]) and in [16] electron-impact shifts for twenty two Ne II multiplets. Due to the significance of neon for laboratory, astrophysical, and technological plasmas, it is of interest to provide corresponding Stark broadening data, especially for resonance lines and for lines originating from low-lying energy terms. In order to complete this research, which provides complete data for the Ne II spectral lines where it is possible to do with our standard accuracy, this paper presents the results of calculations, within the semiclassical formalism of perturbations [28, 29] caused by electron-, proton-, and ionized helium impacts of line widths and shifts for an additional three Ne II and six Ne III multiplets of interest for laboratory, laser-produced fusion, and astrophysical plasma research. The results obtained are compared with available experimental [9, 11, 14] and theoretical [9, 18, 19, 26, 27] data.

Results and Discussion. The semiclassical perturbation formalism used here [28, 29] and all innovations and optimizations of the computer code have been discussed, for example, in [36] and will not be repeated here. The atomic energy levels needed for calculations, not found in [37, 38] (or revised later), were taken from [39] for Ne II and from [40] for Ne III. The corresponding ionization potential for Ne III was also taken from [40]. Oscillator strengths have been calculated by using the method of Bates and Damgaard [41, 42]. For higher levels, the method described in [43] has been used. The results for three Ne II multiplets for the Stark broadening due to electron-, proton-, and ionized helium impacts are shown in Table 1. It should be noted that the electron-impact width for the $3s\ ^5S^o–3p^5P$ and $3s\ ^3S^o–3p^3P$ multiplets are taken from [15] and here are given in order to complete the data.

Astronomical Observatory, 7 Volgina Str., Belgrade, 11160, Serbia, Yugoslavia. Translated from Zhurnal Prikladnoi Spektroskopii, Vol. 70, No. 4, pp. 439–443, July–August, 2003. Original article submitted September 4, 2002.

0021-9037/03/7004-0493$25.00

TABLE 1. Electron-, Proton-, and Ionized Helium Impact Broadening Parameters for the Ne II and Ne III Spectral Lines for a Perturbing Density of 10^{17} cm^{-3} and Different Temperatures as well as Transitions and Corresponding Wavelengths (in Å)

Transition, λ, Å	*T*, K	Perturbing particles					
		electron		proton		helium ions	
		width	shift	width	shift	width	shift
Ne II							
$2p^5{}^2P–3s^2P$	5000	$0.292\cdot10^{-2}$	$0.110\cdot10^{-2}$	$0.484\cdot10^{-5}$	$0.281\cdot10^{-4}$	$0.695\cdot10^{-5}$	$0.270\cdot10^{-4}$
446.6	10,000	$0.206\cdot10^{-2}$	$0.843\cdot10^{-3}$	$0.210\cdot10^{-4}$	$0.540\cdot10^{-4}$	$0.250\cdot10^{-4}$	$0.496\cdot10^{-4}$
$C = 0.56\cdot10^{19}$	20,000	$0.142\cdot10^{-2}$	$0.656\cdot10^{-3}$	$0.520\cdot10^{-4}$	$0.834\cdot10^{-4}$	$0.509\cdot10^{-4}$	$0.732\cdot10^{-4}$
	30,000	$0.115\cdot10^{-2}$	$0.546\cdot10^{-3}$	$0.754\cdot10^{-4}$	$0.102\cdot10^{-3}$	$0.730\cdot10^{-4}$	$0.858\cdot10^{-4}$
	50,000	$0.944\cdot10^{-3}$	$0.468\cdot10^{-3}$	$0.106\cdot10^{-3}$	$0.119\cdot10^{-3}$	$0.930\cdot10^{-4}$	$0.990\cdot10^{-4}$
	100,000	$0.769\cdot10^{-3}$	$0.380\cdot10^{-3}$	$0.140\cdot10^{-3}$	$0.143\cdot10^{-3}$	$0.119\cdot10^{-3}$	$0.119\cdot10^{-3}$
$3s^2P–3p^2S$	5000	0.317	$-0.447\cdot10^{-3}$	$0.583\cdot10^{-2}$	$-0.299\cdot10^{-3}$	$0.824\cdot10^{-2}$	$-0.298\cdot10^{-3}$
3507.9	10,000	0.230	$-0.145\cdot10^{-2}$	$0.100\cdot10^{-1}$	$-0.650\cdot10^{-3}$	$0.123\cdot10^{-1}$	$-0.629\cdot10^{-3}$
$C = 0.35\cdot10^{21}$	20,000	0.168	$-0.189\cdot10^{-2}$	$0.140\cdot10^{-1}$	$-0.119\cdot10^{-2}$	$0.154\cdot10^{-1}$	$-0.110\cdot10^{-2}$
	30,000	0.144	$-0.180\cdot10^{-2}$	$0.154\cdot10^{-1}$	$-0.155\cdot10^{-2}$	$0.166\cdot10^{-1}$	$-0.134\cdot10^{-2}$
	50,000	0.126	$-0.219\cdot10^{-2}$	$0.169\cdot10^{-1}$	$-0.198\cdot10^{-2}$	$0.181\cdot10^{-1}$	$-0.172\cdot10^{-2}$
	100,000	0.112	$-0.197\cdot10^{-2}$	$0.188\cdot10^{-1}$	$-0.249\cdot10^{-2}$	$0.195\cdot10^{-1}$	$-0.208\cdot10^{-2}$
$3p^4S–4s^4P$	5000	0.668	0.271	$0.130\cdot10^{-1}$	$0.155\cdot10^{-1}$	$0.139\cdot10^{-1}$	$0.130\cdot10^{-1}$
3414.8	10,000	0.468	0.207	$0.227\cdot10^{-1}$	$0.242\cdot10^{-1}$	$0.232\cdot10^{-1}$	$0.203\cdot10^{-1}$
$C = 0.97\cdot10^{20}$	20,000	0.345	0.155	$0.338\cdot10^{-1}$	$0.325\cdot10^{-1}$	$0.304\cdot10^{-1}$	$0.268\cdot10^{-1}$
	30,000	0.314	0.141	$0.393\cdot10^{-1}$	$0.364\cdot10^{-1}$	$0.345\cdot10^{-1}$	$0.300\cdot10^{-1}$
	50,000	0.291	0.116	$0.462\cdot10^{-1}$	$0.421\cdot10^{-1}$	$0.405\cdot10^{-1}$	$0.348\cdot10^{-1}$
	100,000	0.271	0.0911	$0.551\cdot10^{-1}$	$0.490\cdot10^{-1}$	$0.467\cdot10^{-1}$	$0.405\cdot10^{-1}$
Ne III							
$3s^5S–3p^5P$	20,000	$0.916\cdot10^{-1}$	$-0.108\cdot10^{-2}$	$0.173\cdot10^{-2}$	$-0.527\cdot10^{-3}$	$0.244\cdot10^{-2}$	$-0.510\cdot10^{-3}$
2593.1	50,000	$0.594\cdot10^{-1}$	$-0.114\cdot10^{-2}$	$0.326\cdot10^{-2}$	$-0.111\cdot10^{-2}$	$0.395\cdot10^{-2}$	$-0.982\cdot10^{-3}$
$C = 0.26\cdot10^{21}$	100,000	$0.450\cdot10^{-1}$	$-0.167\cdot10^{-2}$	$0.436\cdot10^{-2}$	$-0.156\cdot10^{-2}$	$0.465\cdot10^{-2}$	$-0.135\cdot10^{-2}$
	200,000	$0.361\cdot10^{-1}$	$-0.144\cdot10^{-2}$	$0.500\cdot10^{-2}$	$-0.196\cdot10^{-2}$	$0.524\cdot10^{-2}$	$-0.163\cdot10^{-2}$
	300,000	$0.324\cdot10^{-1}$	$-0.147\cdot10^{-2}$	$0.539\cdot10^{-2}$	$-0.218\cdot10^{-2}$	$0.555\cdot10^{-2}$	$-0.182\cdot10^{-2}$
	500,000	$0.288\cdot10^{-1}$	$-0.137\cdot10^{-2}$	$0.581\cdot10^{-2}$	$-0.250\cdot10^{-2}$	$0.581\cdot10^{-2}$	$-0.204\cdot10^{-2}$
$3p^5P–3d^5D$	20,000	$0.712\cdot10^{-1}$	$-0.103\cdot10^{-3}$	$0.262\cdot10^{-2}$	$0.738\cdot10^{-6}$	$0.340\cdot10^{-2}$	$0.738\cdot10^{-6}$
2162.6	50,000	$0.469\cdot10^{-1}$	$-0.687\cdot10^{-5}$	$0.437\cdot10^{-2}$	$0.191\cdot10^{-5}$	$0.493\cdot10^{-2}$	$0.191\cdot10^{-5}$
$C = 0.17\cdot10^{21}$	100,000	$0.360\cdot10^{-1}$	$0.277\cdot10^{-5}$	$0.517\cdot10^{-2}$	$0.382\cdot10^{-5}$	$0.557\cdot10^{-2}$	$0.381\cdot10^{-5}$
	200,000	$0.294\cdot10^{-1}$	$0.446\cdot10^{-4}$	$0.582\cdot10^{-2}$	$0.754\cdot10^{-5}$	$0.617\cdot10^{-2}$	$0.739\cdot10^{-5}$
	300,000	$0.268\cdot10^{-1}$	$0.217\cdot10^{-4}$	$0.616\cdot10^{-2}$	$0.109\cdot10^{-4}$	$0.636\cdot10^{-2}$	$0.104\cdot10^{-4}$
	500,000	$0.242\cdot10^{-1}$	$0.233\cdot10^{-4}$	$0.640\cdot10^{-2}$	$0.160\cdot10^{-4}$	$0.656\cdot10^{-2}$	$0.147\cdot10^{-4}$
$2p^4{}^3P–2s^3S$	20,000	$0.738\cdot10^{-3}$	$0.598\cdot10^{-4}$	$0.355\cdot10^{-5}$	$0.152\cdot10^{-4}$	$0.482\cdot10^{-5}$	$0.143\cdot10^{-4}$
313.4	50,000	$0.438\cdot10^{-3}$	$0.584\cdot10^{-4}$	$0.169\cdot10^{-4}$	$0.287\cdot10^{-4}$	$0.158\cdot10^{-4}$	$0.252\cdot10^{-4}$
$C = 0.37\cdot10^{19}$	100,000	$0.318\cdot10^{-3}$	$0.619\cdot10^{-4}$	$0.304\cdot10^{-4}$	$0.396\cdot10^{-4}$	$0.289\cdot10^{-4}$	$0.329\cdot10^{-4}$
	200,000	$0.245\cdot10^{-3}$	$0.585\cdot10^{-4}$	$0.448\cdot10^{-4}$	$0.475\cdot10^{-4}$	$0.385\cdot10^{-4}$	$0.395\cdot10^{-4}$
	300,000	$0.213\cdot10^{-3}$	$0.565\cdot10^{-4}$	$0.519\cdot10^{-4}$	$0.528\cdot10^{-4}$	$0.440\cdot10^{-4}$	$0.437\cdot10^{-4}$
	500,000	$0.182\cdot10^{-3}$	$0.526\cdot10^{-4}$	$0.611\cdot10^{-4}$	$0.601\cdot10^{-4}$	$0.526\cdot10^{-4}$	$0.492\cdot10^{-4}$
$2p^4{}^3P–2d^3D$	20,000	$0.191\cdot10^{-2}$	$0.260\cdot10^{-4}$	$0.116\cdot10^{-3}$	$-0.964\cdot10^{-4}$	$0.129\cdot10^{-3}$	$-0.837\cdot10^{-4}$
229.1	50,000	$0.146\cdot10^{-2}$	$0.383\cdot10^{-5}$	$0.177\cdot10^{-3}$	$-0.141\cdot10^{-3}$	$0.170\cdot10^{-3}$	$-0.117\cdot10^{-3}$
$C = 0.13\cdot10^{18}$	100,000	$0.122\cdot10^{-2}$	$0.287\cdot10^{-5}$	$0.218\cdot10^{-3}$	$-0.169\cdot10^{-3}$	$0.202\cdot10^{-3}$	$-0.140\cdot10^{-3}$
	200,000	$0.103\cdot10^{-2}$	$0.104\cdot10^{-4}$	$0.265\cdot10^{-3}$	$-0.198\cdot10^{-3}$	$0.230\cdot10^{-3}$	$-0.162\cdot10^{-3}$
	300,000	$0.933\cdot10^{-3}$	$0.194\cdot10^{-4}$	$0.300\cdot10^{-3}$	$-0.216\cdot10^{-3}$	$0.245\cdot10^{-3}$	$-0.175\cdot10^{-3}$
	500,000	$0.822\cdot10^{-3}$	$0.216\cdot10^{-4}$	$0.330\cdot10^{-3}$	$-0.233\cdot10^{-3}$	$0.270\cdot10^{-3}$	$-0.196\cdot10^{-3}$

TABLE 1. (Continued)

Transition, λ, Å	T, K	Perturbing particles					
		electron		proton		helium ions	
		width	shift	width	shift	width	shift
Ne II							
$3s^3S$–$3p^3P$	20,000	0.106	$-0.118\cdot10^{-2}$	$0.221\cdot10^{-2}$	$-0.558\cdot10^{-3}$	$0.307\cdot10^{-2}$	$-0.540\cdot10^{-3}$
2679.0	50,000	$0.688\cdot10^{-1}$	$-0.128\cdot10^{-2}$	$0.404\cdot10^{-2}$	$-0.118\cdot10^{-2}$	$0.485\cdot10^{-2}$	$-0.104\cdot10^{-2}$
$C = 0.27\cdot10^{21}$	100,000	$0.525\cdot10^{-1}$	$-0.176\cdot10^{-2}$	$0.524\cdot10^{-2}$	$-0.165\cdot10^{-2}$	$0.561\cdot10^{-2}$	$-0.143\cdot10^{-2}$
	200,000	$0.424\cdot10^{-1}$	$-0.159\cdot10^{-2}$	$0.598\cdot10^{-2}$	$-0.208\cdot10^{-2}$	$0.630\cdot10^{-2}$	$-0.173\cdot10^{-2}$
	300,000	$0.382\cdot10^{-1}$	$-0.160\cdot10^{-2}$	$0.643\cdot10^{-2}$	$-0.232\cdot10^{-2}$	$0.665\cdot10^{-2}$	$-0.193\cdot10^{-2}$
	500,000	$0.339\cdot10^{-1}$	$-0.152\cdot10^{-2}$	$0.686\cdot10^{-2}$	$-0.265\cdot10^{-2}$	$0.688\cdot10^{-2}$	$-0.217\cdot10^{-2}$
$3p^3P$–$3d^3D$	20,000	$0.645\cdot10^{-1}$	$-0.938\cdot10^{-3}$	$0.372\cdot10^{-2}$	$-0.292\cdot10^{-2}$	$0.414\cdot10^{-2}$	$-0.254\cdot10^{-2}$
1248.1	50,000	$0.486\cdot10^{-1}$	$-0.676\cdot10^{-3}$	$0.558\cdot10^{-2}$	$-0.427\cdot10^{-2}$	$0.535\cdot10^{-2}$	$-0.354\cdot10^{-2}$
$C = 0.40\cdot10^{19}$	100,000	$0.405\cdot10^{-1}$	$-0.613\cdot10^{-3}$	$0.679\cdot10^{-2}$	$-0.510\cdot10^{-2}$	$0.631\cdot10^{-2}$	$-0.422\cdot10^{-2}$
	200,000	$0.342\cdot10^{-1}$	$-0.310\cdot10^{-3}$	$0.816\cdot10^{-2}$	$-0.599\cdot10^{-2}$	$0.707\cdot10^{-2}$	$-0.487\cdot10^{-2}$
	300,000	$0.311\cdot10^{-1}$	$0.708\cdot10^{-5}$	$0.917\cdot10^{-2}$	$-0.646\cdot10^{-2}$	$0.769\cdot10^{-2}$	$-0.533\cdot10^{-2}$
	500,000	$0.275\cdot10^{-1}$	$0.120\cdot10^{-3}$	$0.999\cdot10^{-2}$	$-0.705\cdot10^{-2}$	$0.851\cdot10^{-2}$	$-0.593\cdot10^{-2}$

Note. By dividing the value of C by the corresponding full width at half-maximum [33], we obtain an estimate for the maximum perturbing density of charged particles, for which the line may be treated as isolated and tabulated data may be used.

Also the parameter C [33] has been specified; it gives an estimate for the maximum density for which the line may be treated as isolated, when it is divided by the corresponding full width at half-maximum. When the impact approximation is not valid, the ion broadening contribution may be estimated by using a quasistatic approach [17, 32]. In the intermediate region, where neither of these two approximations is valid, a unified type theory should be used. For example, in [44] a simple analytical formula for such a case is given. The accuracy of the results obtained decreases when broadening by ion interactions becomes important.

In Table 2 our semiclassical results are compared with available experimental data [9, 11, 14]. In [14] the measurements of the Ne II Stark widths were performed in a pure discharge lamp working with the continuous flow of a pure neon gas. In [11] a linear pinch plasma source with neon as a working gas was used and in [9] it was a low pressure pulsed arc Z-discharge filled with pure neon or a gas mixture consisting of 25% Ne and 75% N_2. In Table 2, full line widths at half-maximum due to impacts with Ne and N ions are also shown and the differences are negligible. Our results are in good agreement with the experimental values of [11] for the Ne III 2163.8 Å line. For Ne II, our results are higher than the experimental ones except for the 3481.96 Å line where agreement is good. However, if we look at the difference in the experimental values of [11] for the 3481.96 Å (0.15 Å) and 3557.84 Å (0.10 Å) lines within the same Ne II $3s^2P$–$3p\ ^2S^o$ multiplet, we cannot find a theoretical explanation. Namely, if the positions of atomic energy levels are regular and the difference between the energy levels within the $3s\ ^2P$ and $3p\ ^2S^o$ terms is much smaller than the distance to the closest perturbing terms (which is the case here), the line widths within such a multiplet should be similar. Consequently, a new experimental determination of Stark widths for these lines is of interest.

In [9] the semiempirical [46] calculations for the Ne II 3557.84 Å line were performed and the ratio of measured and calculated values is 1.71, while this ratio with our results is 0.73. In [9] the ratio of measured values and semiclassical values from [18], equal to 1.20, is also given. The dependence of the Stark widths and shifts of the resonance spectral lines on atomic polarizability was determined in [18] and used to estimate the width of the Ne II $2p^5\ ^2P^o$–$3s^2P$ multiplet. For the electron temperature T = 10,000 K and electron density $n_e = 10^{17}$ cm^{-3} the estimated value is 0.00194 Å, while our result is 0.00142 Å, which is in reasonable agreement. In [16, 27], the Stark widths of the Ne III lines were calculated by using the modified semiempirical approach of [47]: W_{MSE}; the Griem's semiempirical approach [46]; the Griem's approximate semiclassical method (see [17], Eq. 526). W_G; and its modification

TABLE 2. Theoretical Results for Stark Full Widths at Half Maximum Due to Electron- (W_e), Nitrogen- (W_N), and Neon Ions (W_{Ne}) Collisions Compared with Experimental Values of W_m

Transition	Wavelength, Å	n_e, 10^{17} cm^{-3}	T, K	W_e, Å	W_N, Å	W_{Ne}, Å	W_m, Å
Ne II							
$3s^2P$–$3p^2S$	3481.96	1.0	40,000	0.132	0.0183	0.0184	0.150 [14]
	3557.84	1.0	40,000	0.132	0.0183	0.0184	0.100 [14]
		1.39	28,000	0.205	0.0240	0.0242	0.149 [9]
$4s^4P$–$3p^4S$	3442.12	1.0	40,000	0.298	0.0343	0.0431	0.170 [14]
Ne III							
$3p^5P$–$3d^5D$	2163.8	2.18	59,000	0.0955	0.0117	0.0118	0.080 [11]

[47]: W_{GM}. For example, for the Ne III $3p\,^5P_7$–$3d\,^5D^o_9$, 2163.8 Å line at T = 20,000 K and $n_e = 10^{17}$ cm^{-3}, W_{MSE} = 0.0484 Å; W_{GM} = 0.0606 Å, W_G = 0.0760 Å and our result is 0.0712 Å, so that the best agreement is observed with the results obtained with the Griem's approximate semiclassical method.

Conclusions. The Stark broadening parameters presented here contribute not only to our knowledge of Stark broadening in the Ne II and Ne III spectra but also to the creation of a large set of reliable semiclassical Stark broadening data of significance for a number of problems in laboratory, technological, and astrophysical plasma research.

This work is a part of the project "Influence of collisional processes on astrophysical plasma line shapes" supported by the Ministry of Science, Technologies, and Development of Serbia.

REFERENCES

1. V. Trimble, *Astron. Astrophys. Rev*., **3**, 1–46 (1991).
2. W. E. Pretty, *Proc. Phys. Soc. London*, **43**, 279–304 (1931).
3. L. I. Maissel, *Proc. Phys. Soc. London*, **74**, 97–100 (1959).
4. S. L. Mandel'shtam, in: *Optik und Spektroskopie aller Wellenlängen*, Akademie Verlag, Berlin (1962), pp. 372–378.
5. S. L. Mandel'shtam, M. A. Mazing, I. I. Sobel'man, and I. A. Vainshtein, in: *Proc. VI Int. Conf. on Ionized Phenomena in Gases*, Vol. 3, S.E.R.M.A, Paris (1963), pp. 331–334.
6. M. A. Mazing and N. A. Vrublevskaya, *Opt. Spektrosk.*, **13**, 308–312 (1962).
7. M. Platiša, M. S. Dimitrijević, and N. Konjević, *Astron. Astrophys*., **67**, 103–105 (1978).
8. T. L. Pittman and N. Konjević, *J. Quant. Spectrosc. Radiat. Transfer*, **35**, 247–253 (1986).
9. N. Konjević and T. L. Pittman, *J. Quant. Spectrosc. Radiat. Transfer*, **35**, 473–477 (1986).
10. J. Purić, S. Djeniže, A. Srećković, J. Labat, Lj. Ćirković, *Phys. Rev. A*, **35**, 2111–2116 (1987).
11. J. Purić, S. Djeniže, A. Srećković, M. Ćuk, J. Labat, and M. Platiša, *Z. Phys. D*, **8**, 343–347 (1988).
12. N. I. Uzelac, S. Glenzer, N. Konjević, J. D. Hey, and H. J. Kunze, *Phys. Rev. E*, **47**, 3623–3630 (1993).
13. B. Blagojević, M. V. Popović, and N. Konjević, *Physica Scripta*, **59**, 374–378 (1999).
14. J. A. del Val, J. A. Aparicio, and S. Mar, *Astrophys. J*., **536**, 998–1004 (2000).
15. V. Milosavljević, M. S. Dimitrijević, and S. Djeniže, *Astrophys. J. Suppl. Ser*., **135**, 115–124 (2001).
16. S. Djeniže, V. Milosavljević, and M. S. Dimitrijević, *Astron. Astrophys*., **382**, 359–367 (2002).
17. H. R. Griem, *Spectral Line Broadening by Plasmas*, Academic Press, New York (1974).
18. W. W. Jones, S. M. Bennet, and H. R. Griem, *Calculated Electron-Impact Broadening Parameters for Isolated Spectral Lines from the Singly Charged Ions: Lithium through Calcium*, University of Maryland Tech. Report No. 71–128, College Park, Maryland (1971).
19. J. Purić, I. S. Lakićević, and V. Glavonjić, *J. Quant. Spectrosc. Radiat. Transfer*, **26**, 65–70 (1981).
20. D. Bertucelli and H. O. Di Rocco, *Physica Scripta*, **47**, 747–750 (1993).
21. S. Djeniže, A. Srećković, J. Labat, and M. Platiša, *Physica Scripta*, **59**, 98–104 (1999).
22. N. Konjević and T. L. Pittman, *J. Quant. Spectrosc. Radiat. Transfer*, **37**, 311–318 (1987).

23. B. Blagojević, M. V. Popović, and N. Konjević, *J. Quant. Spectrosc. Radiat. Transfer*, **67**, 9–20 (2000).
24. M. S. Dimitrijević and N. Konjević, in: B. Wende and W. de Gruyter (eds.), *Spectral Line Shapes*, New York (1981), pp. 211–239.
25. M. S. Dimitrijević and N. Konjević, *Astron. Astrophys*., **172**, 345–349 (1987).
26. M. S. Dimitrijević, *Astron. Astrophys. Suppl. Series*, **76**, 53–59 (1988).
27. M. S. Dimitrijević, *Bull. Obs. Astron*. Belgrade, **139**, 31–58 (1988).
28. S. Sahal-Bréchot, *Astron. Astrophys*., **1**, 91–123 (1969).
29. S. Sahal-Bréchot, *Astron. Astrophys*., **2**, 322–354 (1969).
30. S. Sahal-Bréchot, *Astron. Astrophys*., **35**, 319–321 (1974).
31. C. Fleurier, S. Sahal-Bréchot, and J. Chapelle, *J. Quant. Spectrosc. Radiat. Transfer*, **17**, 595–604 (1977).
32. S. Sahal-Bréchot, *Astron. Astrophys*., **245**, 322–330 (1991).
33. M. S. Dimitrijević, S. Sahal-Bréchot, and V. Bommier, *Astron. Astrophys. Suppl. Ser*., **89**, 581–590 (1991).
34. M. S. Dimitrijević and S. Sahal-Bréchot, *Physica Scripta*, **52**, 41–51 (1995).
35. M. S. Dimitrijević and S. Sahal-Bréchot, *Physica Scripta*, **54**, 50–55 (1996).
36. M. S. Dimitrijević, *Zh. Prikl. Spektrosk.*, **63**, 810–815 (1996).
37. C. E. Moore, *Atomic Energy Levels*, Vol. I, Nat. Stand. Ref. Data Ser., **35**, NBS, Washington (1971).
38. S. Bashkin and J. O. Stoner, Jr., *Atomic Energy Levels and Grotrian Diagrams*, Vol. 2, North Holland, Amsterdam (1978).
39. P. Quinet, P. Palmeri, and E. Biémont, *Physica Scripta*, **49**, 436–445 (1994).
40. W. Persson, C. G. Wahlström, and I. Jönsson, *Phys. Rev. A*, **43**, 4791–4823 (1991).
41. D. R. Bates and A. Damgaard, *Trans. Roy. Soc. London, Ser. A*, **242**, 101–122 (1949).
42. G. K. Oertel and L. P. Shomo, *Atrophys. J. Suppl. Ser*., **16**, 175–218 (1968).
43. H. Van Regemorter, Hoang Binh Dy, and M. Prud'homme, *J. Phys. B*, **12**, 1053–1062 (1979).
44. A. J. Barnard, J. Cooper, and E. W. Smith, *J. Quant. Spectrosc. Radiat. Transfer*, **14**, 1025–1077 (1974).
45. W. L. Wiese and N. Konjević, *J. Quant. Spectrosc. Radiat. Transfer*, **28**, 185–198 (1982).
46. H. R. Griem, *Phys. Rev*., **165**, 258–266 (1968).
47. M. S. Dimitrijević and N. Konjević, *J. Quant. Spectrosc. Radiat. Transfer*, **24**, 451–459 (1980).

Available online at www.sciencedirect.com

ScienceDirect

Advances in Space Research xxx (2013) xxx–xxx

ADVANCES IN SPACE RESEARCH (a COSPAR publication)

www.elsevier.com/locate/asr

Stark broadening of B IV lines for astrophysical and laboratory plasma research ☆

Milan S. Dimitrijević [a,b,*], Magdalena Christova [c], Zoran Simić [a], Andjelka Kovačević [d], Sylvie Sahal-Bréchot [b]

[a] Astronomical Observatory, Volgina 7, 11060 Belgrade 38, Serbia
[b] Laboratoire d'Étude du Rayonnement et de la Matière en Astrophysique, Observatoire de Paris, UMR CNRS 8112, UPMC, 5 Place Jules Janssen, 92195 Meudon Cedex, France
[c] Department of Applied Physics, Technical University-Sofia, 1000 Sofia, Bulgaria
[d] Faculty of Mathematics, University of Belgrade, 11000 Belgrade, Serbia

Abstract

Stark broadening parameters for 36 multiplets of B IV have been calculated using the semi-classical perturbation formalism. Obtained results have been used to investigate the regularities within spectral series and temperature dependence.

Keywords: Atomic data; Atomic processes; Line: profiles; Stars: atmospheres

1. Introduction

The study presents Stark broadening parameters (widths and shifts) of B IV spectral lines which have been determined using the semi-classical perturbation formalism (Sahal-Bréchot, 1969a,b). Data on boron lines are of interest in astrophysics, astrochemistry, and cosmology, in technological plasma research, for thermonuclear reaction devices, and for laser produced plasma investigations. For abundance determinations of boron and modelling, and analysis of stellar plasma it is necessary to have reliable atomic and spectroscopic data, including Stark broadening parameters. This enables to provide data on the astrophysical processes that can both produce and destroy this rare element. Namely, the light elements lithium, beryllium, and boron (LiBeB) are sensitive probes of stellar models due to the fact that the stable isotopes of all three consist of nuclei with small binding energies that are destroyed easily by (p, a) reactions at modest temperatures (Cunha and Smith, 1999). The origin and evolution of boron are of special interest because it is hardly produced by the standard big bang nucleosynthesis (BBN), and cannot be produced by nuclear fusions in stellar interiors (Tankosić et al. et al., 2003). The cosmic abundance of ^{11}B is of major importance for the model of Galactic chemical evolution (GCE) (Ritchey et al., 2011). Ritchey et al. (2011) concluded that a major portion of the cosmic abundance of ^{11}B can be attributed to neutrino nucleosynthesis. Thus, it is necessary to accurately describe the stellar evolution, and the formation of elements, which are closely connected. To make progress in these developments chemical abundances are crucial parameters to be determined. This needs an accurate interpretation of the detailed line spectra of the stellar objects. In order to provide the data needed in astrophysics, laboratory-, technological-, fusion-, and laser produced-plasma research, our aim is to determine here Stark broadening parameters (full widths

☆ This template can be used for all publications in Advances in Space Research.

* Corresponding author at: Astronomical Observatory, Volgina 7, 11060 Belgrade 38, Serbia. Tel.: +381 642978021; fax: +381 2419553.
E-mail addresses: mdimitrijevic@aob.rs (M.S. Dimitrijević), mchristo@tu-sofia.bg (M. Christova), zsimic@aob.bg.ac.rs (Z. Simić), andjelka@matf.bg.ac.rs (A. Kovačević), sylvie.sahal-brechot@obspm.fr (S. Sahal-Bréchot).

0273-1177/$36.00 © 2013 COSPAR. Published by Elsevier Ltd. All rights reserved.
http://dx.doi.org/10.1016/j.asr.2013.08.021

Table 1
Stark broadening parameters for singlet B IV multiplets for a perturper density of 10^{17} cm^{-3} and temperatures from 20,000 to 500,000 K. The width (FWHM) W and shift d (a positive shift is towards the red) values from different perturbers are given in (Å) for 36 multiplets. The ratio of the included parameter C versus the corresponding Stark width gives an estimate of the maximal pertuber density for which the line may be treated as isolated. The asterisks indicate that the impact approximation reaches the limit of validity. W_e – electron-impact width, d_e – electron-impact shift, W_p – proton-impact width, d_p – proton-impact shift, W_{He+} – singly charged helium ion-impact width, d_{He+} – singly charged helium ion-impact shift.

Transition	T (K)	W_e (Å)	d_e(Å)	W_p (Å)	d_p (Å)	W_{He+}(Å)	d_{He+} (Å)
B IV 2p-3d	20,000	0.244E−02	0.677E−04	0.735E−04	0.159E−03	0.898E−04	0.147E−03
418.7 Å	50,000	0.160E−02	0.111E−03	0.209E−03	0.275E−03	0.204E−03	0.241E−03
C = 0.24E+18	100,000	0.122E−02	0.117E−03	0.348E−03	0.349E−03	0.297E−03	0.295E−03
	200,000	0.953E−03	0.106E−03	0.487E−03	0.421E−03	0.387E−03	0.353E−03
	300,000	0.832E−03	0.100E−03	0.586E−03	0.468E−03	0.455E−03	0.390E−03
	500,000	0.710E−03	0.849E−04	0.739E−03	0.522E−03	0.550E−03	0.430E−03
B IV 2p−4d	20,000	0.581E−02	0.221E−03				
308.4 Å	50,000	0.451E−02	0.308E−03				
C = 0.17E+16	100,000	0.369E−02	0.288E−03				
	200,000	0.298E−02	0.365E−03				
	300,000	0.262E−02	0.303E−03				
	500,000	0.222E−02	0.222E−03				
B IV 2p−5d	20,000	0.130E−01	0.506E−03				
274.9 Å	50,000	0.104E−01	0.616E−03				
C = 0.97E+15	100,000	0.856E−02	0.585E−03				
	200,000	0.692E−02	0.854E−03				
	300,000	0.607E−02	0.665E−03				
	500,000	0.512E−02	0.457E−03				
B IV 2p−6d	20,000	0.251E−01	0.804E−03				
259.6 Å	50,000	0.203E−01	0.102E−02				
C = 0.62E+15	100,000	0.168E−01	0.985E−03				
	200,000	0.136E−01	0.165E−02				
	300,000	0.119E−01	0.121E−02				
	500,000	0.101E−01	0.806E−03				
B IV 2p−7d	20,000	*0.411E−01	*0.111E−02				
251.2 Å	50,000	0.344E−01	0.133E−02				
C = 0.20E+15	100,000	0.290E−01	0.139E−02				
	200,000	0.237E−01	0.223E−02				
	300,000	0.209E−01	0.165E−02				
	500,000	0.177E−01	0.115E−02				
B IV 3p−4d	20,000	0.116	0.607E−02				
1190.5 Å	50,000	0.889E−01	0.723E−02				
C = 0.25E+17	100,000	0.727E−01	0.677E−02				
	200,000	0.591E−01	0.761E−02				
	300,000	0.521E−01	0.636E−02				
B IV 3p−5d	20,000	0.126	0.514E−02				
809.7 Å	50,000	0.999E−01	0.657E−02				
C = 0.84E+16	100,000	0.822E−01	0.622E−02				
	200,000	0.666E−01	0.841E−02				
	300,000	0.585E−01	0.662E−02				
	500,000	0.495E−01	0.469E−02				
B IV 3p−6d	20,000	0.186	0.623E−02				
689.8 Å	50,000	0.150	0.808E−02				
C = 0.44E+16	100,000	0.124	0.779E−02				
	200,000	0.101	0.124E−01				
	300,000	0.886E−01	0.917E−02				
	500,000	0.749E−01	0.621E−02				
B IV 3p−7d	20,000	*0.269	*0.758E−02				
633.2 Å	50,000	0.224	0.928E−02				
C = 0.12E+16	100,000	0.189	0.953E−02				
	200,000	0.155	0.148E−01				
	300,000	0.137	0.110E−01				
	500,000	0.116	0.776E−02				

Please cite this article in press as: Dimitrijević, M.S., et al. Stark broadening of B IV lines for astrophysical and laboratory plasma research. J. Adv. Space Res. (2013), http://dx.doi.org/10.1016/j.asr.2013.08.021

Table 1 (*continued*)

Transition	T (K)	W_e (Å)	d_e(Å)	W_p (Å)	d_p (Å)	W_{He+}(Å)	d_{He+} (Å)
B IV 4p–5d	20,000	1.50	0.745E−01				
2567.3 Å	50,000	1.18	0.906E−01				
C = 0.84E+17	100,000	0.973	0.846E−01				
	200,000	0.789	0.104				
	300,000	0.693	0.840E−01				
	500,000	0.587	0.610E−01				
B IV 4p–6d	20,000	1.17	0.455E−01				
1655.2 Å	50,000	0.938	0.568E−01				
C = 0.25E+17	100,000	0.775	0.541E−01				
	200,000	0.629	0.793E−01				
	300,000	0.552	0.600E−01				
	500,000	0.467	0.416E−01				
B IV 4p–7d	20,000	*1.31	*0.419E−01				
1363.1 Å	50,000	1.09	0.500E−01				
C = 0.58E+16	100,000	0.915	0.504E−01				
	200,000	0.749	0.741E−01				
	300,000	0.661	0.561E−01				
	500,000	0.560	0.399E−01				
B IV 3d–4p	20,000	0.105	−0.806E−02	0.122E−01	−0.128E−01	*0.115E−01	*−0.104E−01
1163.5 Å	50,000	0.768E−01	−0.845E−02	0.193E−01	−0.181E−01	*0.163E−01	*−0.151E−01
C = 0.76E+18	100,000	0.615E−01	−0.783E−02	0.255E−01	−0.222E−01	*0.205E−01	*−0.184E−01
	200,000	0.496E−01	−0.691E−02	0.324E−01	−0.252E−01	0.251E−01	−0.210E−01
	300,000	0.438E−01	−0.613E−02	0.377E−01	−0.271E−01	0.281E−01	−0.226E−01
	500,000	0.375E−01	−0.500E−02	0.448E−01	−0.300E−01	0.330E−01	−0.254E−01
B IV 3d–5p	20,000	0.121	−0.989E−02				
798.8 Å	50,000	0.911E−01	−0.103E−01	*0.302E−01	−0.265E−01		
C = 0.18E+18	100,000	0.737E−01	−0.921E−02	*0.391E−01	−0.314E−01		
	200,000	0.596E−01	−0.881E−02	*0.474E−01	−0.357E−01	*0.367E−01	−0.305E−01
	300,000	0.526E−01	−0.749E−02	*0.524E−01	−0.394E−01	*0.404E−01	−0.315E−01
	500,000	0.448E−01	−0.601E−02	*0.662E−01	−0.429E−01	*0.466E−01	−0.361E−01
B IV 3d–6p	20,000	0.174	−0.138E−01				
682.5 Å	50,000	0.137	−0.146E−01				
C = 0.77E+17	100,000	0.113	−0.133E−01				
	200,000	0.925E−01	−0.140E−01				
	300,000	0.817E−01	−0.118E−01				
	500,000	0.697E−01	−0.923E−02				
B IV 3d–7p	20,000	*0.257	*−0.183E−01				
627.3 Å	50,000	0.210	−0.197E−01				
C = 0.40E+17	100,000	0.177	−0.191E−01				
	200,000	0.146	−0.224E−01				
	300,000	0.129	−0.187E−01				
	500,000	0.110	−0.141E−01				
B IV 4d–6p	20,000	1.11	−0.843E−01				
1635.6 Å	50,000	0.877	−0.907E−01				
C = 0.47E+17	100,000	0.727	−0.828E−01				
	200,000	0.594	−0.893E−01				
	300,000	0.524	−0.748E−01				
	500,000	0.446	−0.580E−01				
B IV 4d–7p	20,000	*1.27	*−0.883E−01				
1350.9 Å	50,000	1.04	−0.962E−01				
C = 0.32E+17	100,000	0.873	−0.929E−01				
	200,000	0.719	−0.110				
	300,000	0.637	−0.917E−01				
	500,000	0.544	−0.686E−01				
B IV 5d–6p	20,000	*11.0	*−0.749				
4623.4 Å	50,000	8.80	−0.830				
C = 0.27E+18	100,000	7.30	−0.762				
	200,000	5.95	−0.873				

(*continued on next page*)

Please cite this article in press as: Dimitrijević, M.S., et al. Stark broadening of B IV lines for astrophysical and laboratory plasma research. J. Adv. Space Res. (2013), http://dx.doi.org/10.1016/j.asr.2013.08.021

Table 1 (*continued*)

Transition	T (K)	W_e (Å)	d_e(Å)	W_p (Å)	d_p (Å)	W_{He+}(Å)	d_{He+} (Å)
	300,000	5.24	−0.718				
	500,000	4.45	−0.543				
B IV 5d−7p	20,000	*6.68	*−0.436				
2897.7 Å	50,000	5.46	−0.484				
C = 0.11E+18	100,000	4.60	−0.467				
	200,000	3.78	−0.568				
	300,000	3.34	−0.469				
	500,000	2.84	−0.347				
B IV 3d−4f	20,000	0.522E−01	0.145E−03				
1170.9 Å	50,000	0.395E−01	−0.224E−03				
C = 0.24E+17	100,000	0.319E−01	−0.401E−03				
	200,000	0.258E−01	−0.114E−02				
	300,000	0.228E−01	−0.793E−03				
	500,000	0.196E−01	−0.228E−03				
B IV 3d−5f	20,000	0.817E−01	0.691E−03				
800.6 Å	50,000	0.679E−01	0.109E−03				
C = 0.21E+16	100,000	0.568E−01	0.175E−03				
	200,000	0.464E−01	−0.965E−03				
	300,000	0.409E−01	−0.573E−03				
	500,000	0.347E−01	0.297E−04				
B IV 3d−6f	20,000	0.140	0.139E−02				
683.2 Å	50,000	0.119	0.553E−03				
C = 0.10E+16	100,000	0.996E−01	0.536E−03				
	200,000	0.813E−01	−0.148E−02				
	300,000	0.716E−01	−0.640E−03				
	500,000	0.607E−01	0.244E−03				
B IV 3d−7f	20,000	*0.220	*0.170E−02				
627.7 Å	50,000	0.190	0.148E−02				
C = 0.67E+15	100,000	0.162	0.133E−02				
	200,000	0.133	0.301E−03				
	300,000	0.118	0.872E−03				
	500,000	0.998E−01	0.103E−02				
B IV 4d−5f	20,000	1.08	−0.507E−02				
2530.1 Å	50,000	0.900	−0.156E−01				
C = 0.21E+17	100,000	0.753	−0.134E−01				
	200,000	0.615	−0.304E−01				
	300,000	0.542	−0.225E−01				
	500,000	0.460	−0.116E−01				
B IV 4d−6f	20,000	0.920	0.264E−02				
1639.7 Å	50,000	0.775	−0.399E−02				
C = 0.59E+16	100,000	0.651	−0.334E−02				
	200,000	0.532	−0.173E−01				
	300,000	0.468	−0.107E−01				
	500,000	0.396	−0.358E−02				
B IV 4d−7f	20,000	*1.10	*0.394E−02				
1352.8 Å	50,000	0.943	0.187E−02				
C = 0.31E+16	100,000	0.802	0.170E−02				
	200,000	0.661	−0.457E−02				
	300,000	0.583	−0.760E−03				
	500,000	0.495	0.137E−02				
B IV 5d−6f	20,000	9.65	−0.507E−01				
4657.0 Å	50,000	8.08	−0.137				
C = 0.48E+17	100,000	6.77	−0.128				
	200,000	5.52	−0.301				
	300,000	4.85	−0.208				
	500,000	4.10	−0.109				
B IV 5d−7f	20,000	*5.91	*−0.114E−01				
2906.0 Å	50,000	5.06	−0.328E−01				

Please cite this article in press as: Dimitrijević, M.S., et al. Stark broadening of B IV lines for astrophysical and laboratory plasma research. J. Adv. Space Res. (2013), http://dx.doi.org/10.1016/j.asr.2013.08.021

Table 1 (*continued*)

Transition	T (K)	W_e (Å)	d_e(Å)	W_p (Å)	d_p (Å)	W_{He+}(Å)	d_{He+} (Å)
$C=$ 0.14E+17	100,000	4.29	−0.320E−01				
	200,000	3.52	−0.841E−01				
	300,000	3.10	−0.509E−01				
	500,000	2.63	−0.250E−01				
B IV 4f–5d	20,000	1.23	0.315E−01				
2532.0 Å	50,000	0.990	0.483E−01				
$C=$ 0.82E+17	100,000	0.817	0.468E−01				
	200,000	0.662	0.737E−01				
	300,000	0.582	0.563E−01				
	500,000	0.492	0.367E−01				
B IV 4f–6d	20,000	1.05	0.262E−01				
1640.5 Å	50,000	0.855	0.385E−01				
$C=$ 0.25E+17	100,000	0.708	0.380E−01				
	200,000	0.574	0.663E−01				
	300,000	0.505	0.483E−01				
	500,000	0.426	0.313E−01				
B IV 4f–7d	20,000	*1.23	*0.276E−01				
1353.1 Å	50,000	1.03	0.372E−01				
$C=$ 0.57E+16	100,000	0.866	0.392E−01				
	200,000	0.710	0.650E−01				
	300,000	0.626	0.479E−01				
	500,000	0.530	0.328E−01				
B IV 5f–6d	20,000	*10.3	*0.189				
4661.8 Å	50,000	8.45	0.304				
$C=$ 0.72E+17	100,000	7.04	0.294				
	200,000	5.72	0.550				
	300,000	5.03	0.397				
	500,000	4.25	0.248				
B IV 5f–7d	20,000	*6.34	*0.117				
2907.4 Å	50,000	5.34	0.168				
$C=$ 0.26E+17	100,000	4.51	0.176				
	200,000	3.69	0.306				
	300,000	3.26	0.224				
	500,000	2.76	0.150				

at half intensity and shifts) for 36 B IV multiplets. Obtained results will be also used for the consideration of regularities within spectral series and temperature dependence of Stark broadening parameters.

2. Theory of Stark broadening in the impact approximation

Pressure broadening of spectral lines arises when an atom, ion, or molecule which emits or absorbs light in a gas or plasma, is perturbed by its interactions with the other particles of the medium. Interpretation of this phenomenon is currently used for modelling of the medium and for spectroscopic diagnostics, since the broadening of the lines depends on the temperature and density of the medium. The physical conditions in the Universe are very various, and collisional broadening with charged particles (Stark broadening) appears to be important in many domains. For example, at temperatures around 10^4 K and densities 10^{13}–10^{15} cm^{-3}, Stark broadening is of interest for modelling and analysing spectra of A and B type stars: see e.g. (Lanz et al., 1988; Popović et al., 2001a,b, 1999a,b; Tankosić et al. et al., 2003; Simić et al., 2005; Sahal-Bréchot, 2010). Especially in white dwarfs, Stark broadening is the dominant collisional line broadening mechanism in all important layers of the atmosphere (Popović et al., 1999b; Tankosić et al. et al., 2003; Simić et al., 2006, 2009; Hamdi et al., 2008; Dimitrijević et al., 2011; Dufour et al., 2011; Larbi-Terzi et al., 2012). The theory of Stark broadening is well applied, especially for accurate spectroscopic diagnostics and modelling. This requires the knowledge of numerous profiles, especially for trace elements, as boron in this case, which are used as useful probes for modern spectroscopic diagnostics. Interpretation of the spectra of white dwarfs, which are very faint, allows understanding the evolution of these very old stars, which are close to death. The results for Stark broadening parameters of 36 BIV multiplets have been calculated using the semi-classical perturbation formalism (Sahal-Bréchot, 1969a,b). Within this theory the full half width (W) and the shift (d) of an isolated line originating from the transition between the initial level i and the final level f is expressed as:

$$W = n_e \int_0^{+\infty} v f(v) dv \left[\sum_{i' \neq i} \sigma_{ii'}(v) + \sum_{f' \neq f} \sigma_{ff'}(v) + \sigma_{el} \right], \qquad (1)$$

$$d = n_e \int_0^{+\infty} v f(v) dv \int_{R_3}^{R_D} 2\pi\rho d\rho \sin 2\phi_p, \quad (2)$$

where i' and f' are perturbing levels, n_e and v are the electron density and the velocity of perturbers respectively, and $f(v)$ is the Maxwellian distribution of electron velocities.

The inelastic cross sections $\sigma_{ii'}(v)$ (respectively $\sigma_{ff'}(v)$) can be expressed by an integration of the transition probability Pii' over the impact parameter ρ:

$$\sum_{i' \neq i} \sigma_{ii'}(v) = \frac{1}{2}\pi R_1^2 + \int_{R_1}^{R_D} 2\pi\rho d\rho \sum_{i' \neq i} P_{ii'}(\rho, v). \quad (3)$$

The elastic collision contribution to the width is given by:

$$\sigma_{el} = 2\pi R_2^2 + \int_{R_2}^{R_D} 8\pi\rho d\rho \sin^2 \delta + \sigma_r, \quad (4)$$

$$\delta = (\phi_p^2 + \phi_q^2)^{1/2}. \quad (5)$$

The phase shifts ϕ_p and ϕ_q are due to the polarization and quadruple potential respectively. The cut-off parameters R_1, R_2, R_3, the Debye cut-off R_D and the symmetrization procedure are described in the above mentioned papers.The contribution of Feshbach resonances, σ_r is described in Fleurier et al. (1977). In the following, the collisions of emitters with electrons, protons and ionized helium are examined, and the contribution of different perturbers in total Stark broadening parameters are discussed.

3. Results and discussion

In this paper, Stark broadening widths (FWHM) and shifts for 36 BIV multiplets have been calculated using the semiclassical perturbation formalism (Sahal-Bréchot, 1969a,b) and presented in Table 1. Since the Stark broadening widths and shifts are the same for spectral lines within a multiplet when expressed in angular frequency units for a simple spectrum like the B IV one, it is easy to obtain their values in Angströms or nanometers (see e.g. Eqs. 7 and 8 in Hamdi et al., 2013). In particular, the spectral line broadening due to interactions of the emitters with electrons, protons and singly charged helium ions as perturbers has been examined.

Calculations have been performed using experimental values of energy levels in Kramida et al. (2008). The oscillator strengths have been calculated using the Coulomb approximation method (Bates and Damgaard, 1949) and the tables of Oertel and Shomo (1968), while for higher levels, the method described by Van Regemorter et al. (1979) has been applied. The asterisks in Table 1 indicate that the impact approximation reaches the limit of validity.

The temperature dependences of Stark widths and shifts for the $1s2p^1P^o - 1s3s^1S$, $1s2p^1P^o - 1s3d^1D$, $1s3p^1P^o - 1s4s^1S$ and $1s3p^1P^o - 1s4d^1D$ transitions at an electron density of

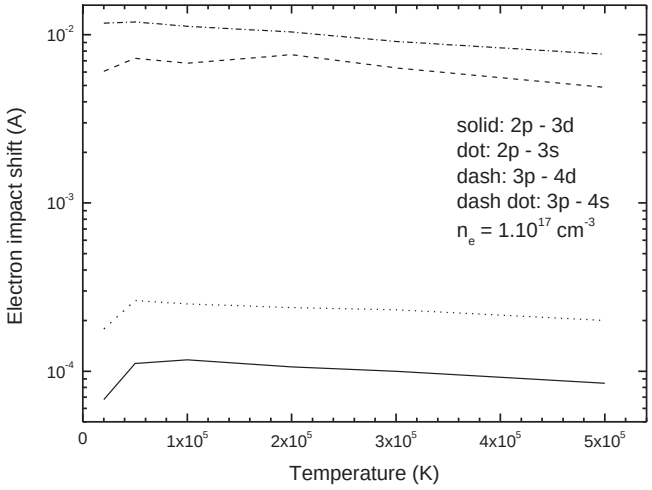

Fig. 2. Temperature dependence of the electron impact shift for $1s2p^1P^o - 1s3s^1S$, $1s2p^1P^o - 1s3d^1D$, $1s3p^1P^o - 1s4s^1S$ and $1s3p^1P^o - 1s4d^1D$ transitions at an electron density of 1.10^{17} cm^{-3}.

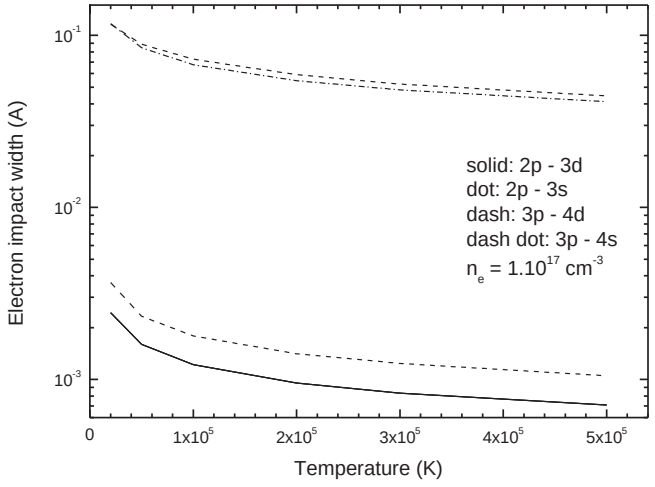

Fig. 1. Temperature dependence of the electron impact width for B IV $1s2p^1P^o - 1s3s^1S$, $1s2p^1P^o - 1s3d^1D$, $1s3p^1P^o - 1s4s^1S$ and $1s3p^1P^o - 1s4d^1D$ transitions at an electron density of 1.10^{17} cm^{-3}.

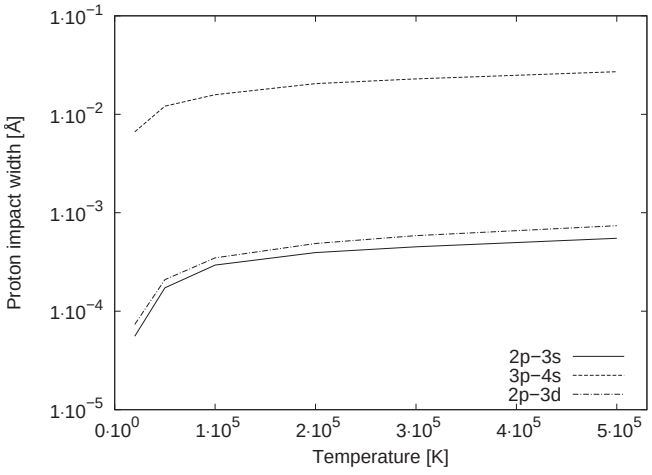

Fig. 3. Temperature dependence of the proton impact width for $1s2p^1P^o - 1s3s^1S$, $1s2p^1P^o - 1s3d^1D$, $1s3p^1P^o - 1s4s^1S$ and $1s3p^1P^o - 1s4d^1D$ transitions at an electron density of 1.10^{17} cm^{-3}.

Please cite this article in press as: Dimitrijević, M.S., et al. Stark broadening of B IV lines for astrophysical and laboratory plasma research. J. Adv. Space Res. (2013), http://dx.doi.org/10.1016/j.asr.2013.08.021

10^{17} cm^{-3} have been presented in Figs. 1 and 2, respectively. The first two transitions have the same lower energy level $2p$ where both, the width and shift of $2p-3s$ are larger than the Stark parameters of $2p-3d$. For the other transitions with the same $3p$ lower energy level, $3p-4d$ transition has larger width, while $3p-4s$ has larger shift. For all of them, the width and shift due to electrons decrease slowly for temperature values above 100, 000 k.

In Figs. 3 and 4, the temperature dependences of proton-impact widths and shifts, respectively, are shown. One can see that both widths and shifts slowly increase with the temperature. For proton-impact broadening for B IV $3p-4d$ transition the impact approximation is not valid at an electron density of 10^{17} cm^{-3} within the whole interval of the considered temperatures and they are not included in the figures.

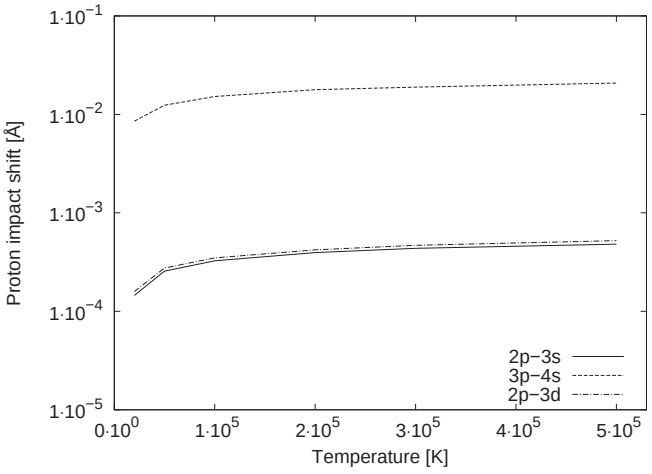

Fig. 4. Temperature dependence of the proton impact shift for $1s2p^1P^o-1s3s^1S$, $1s2p^1P^o-1s3d^1D$, $1s3p^1P^o-1s4s^1S$ and $1s3p^1P^o-1s4d^1D$ transitions at an electron density of 1.10^{17} cm^{-3}.

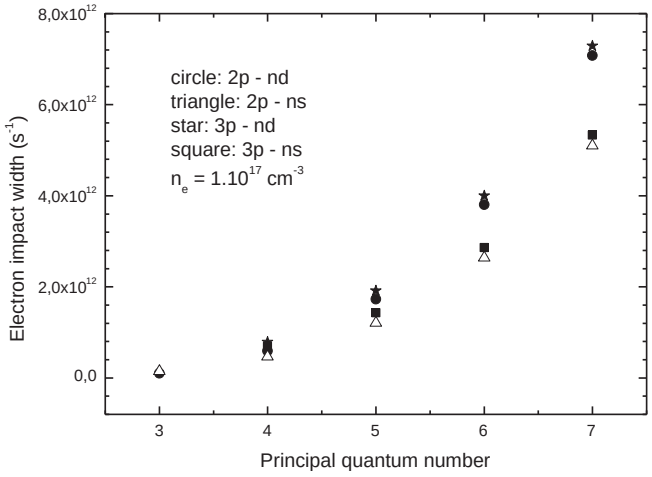

Fig. 5. Principal quantum number dependence of the electron-impact width for transitions within $1s2p^1P^o-1sns^1S$, $1s2p^1P^o-1snd^1D$, $1s3p^1P^o-1sns^1S$ and $1s3p^1P^o-1snd^1D$ spectral series at an electron density of 1.10^{17} cm^{-3} and $T=200{,}000$ K.

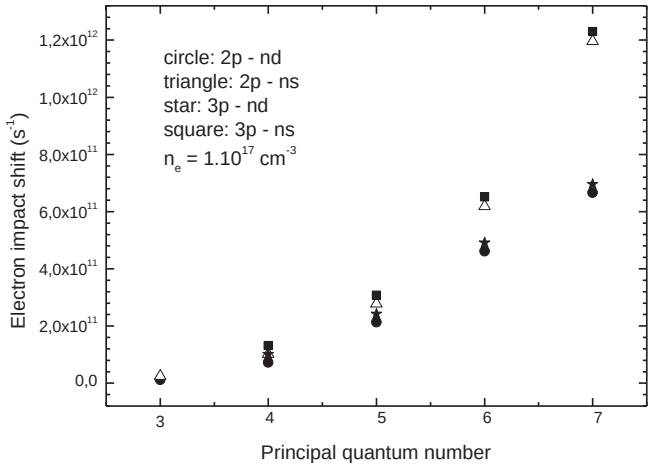

Fig. 6. Principal quantum number dependence of the electron-impact width for transitions within $1s2p^1P^o-1sns^1S$, $1s2p^1P^o-1snd^1D$, $1s3p^1P^o-1sns^1S$ and $1s3p^1P^o-1snd^1D$ spectral series at an electron density of 1.10^{17} cm^{-3} and $T=200{,}000$ K.

The dependence of the broadening parameters of spectral lines due to impacts with charged particles versus principal quantum number within a spectral series is an important information. If we know the trend of Stark broadening parameters within a spectral series, it is possible to interpolate or extrapolate the eventually missing values within the considered series. The regular behavior of Stark broadening widths and shifts versus principal quantum number within spectral series is presented in Figs. 5 and 6. The both parameters increase with principal quantum number which reflects the decrease of the distance to the nearest perturbing levels with the increase of the principal quantum number.

4. Conclusion

New Stark broadening parameters for 36 multiplets of B IV have been determined within the frame of the semi-classical perturbation formalism.The results for Stark broadening parameters of boron lines could be applicable for the adequate interpretation of the observed spectra in astrophysics, astrochemistry, and cosmology, in technological plasma research, for thermonuclear reaction devices, and for laser produced plasma investigation. We also note that the Stark broadening data obtained in the present research, will be inserted in the STARK-B database (Sahal-Bréchot et al., 2012, 2013), which is a part of Virtual Atomic and Molecular Data Center (VAMDC – Dubernet et al., 2010; Rixon et al., 2010).

Additionally, it has been confirmed that the behaviour of Stark broadening parameters within B IV spectral series is regular, enabling the interpolation and extrapolation of new data.

Please cite this article in press as: Dimitrijević, M.S., et al. Stark broadening of B IV lines for astrophysical and laboratory plasma research. J. Adv. Space Res. (2013), http://dx.doi.org/10.1016/j.asr.2013.08.021

Acknowledgments

This paper is within the projects 176002 and III44022 of Ministry of Education, Science and Technological Development of Republic of Serbia. It is also the result of Short term Scientific Mission CM0805 within COST programme on The Chemical Cosmos: Understanding Chemistry in Astronomical Environments. Partial financial support from project No 6572-20 Technical University – Sofia within Euroatom Programme is also acknowledged. One of us (MSD) acknowledges the support of the LABEX PLAS@PAR.

References

Bates, D.R., Damgaard, A., 1949. The calculation of the absolute strengths of spectral lines. Trans. R. Soc. London Ser. A 242, 101–122.

Cunha, K., Smith, V.V., 1999. A determination of the solar photospheric boron abundance. ApJ 512, 1006–1013.

Dimitrijević, M.S., Kovačević, A., Simić, Z., Sahal-Bréchot, S., 2011. Baltic Astron. 20, 580–586.

Dubernet, M.L., Boudon, V., Culhane, J.L., et al., 2010. Virtual atomic and molecular data center. J. Quant. Spectrosc. Radiat. Tranfer 111, 2151–2159 (<http://www.vamdc.eu>).

Dufour, P., Ben Nessib, N., Sahal-Bréchot, S., Dimitrijević, M.S., 2011. Stark broadening of carbon and oxygen lines in hot DQ white dwarf stars: recent results and applications. Baltic Astron. 20, 511–515.

Fleurier, C., Sahal-Bréchot, S., Chapelle, J., 1977. Stark profiles of some ion lines of alkaline earth elements. JQSRT 17, 595–603.

Hamdi, R., Ben Nessib, N., Dimitrijević, M.S., Sahal-Bréchot, S., 2013. Stark broadening of Pb IV spectral lines. MNRAS 431, 1039–1047.

Hamdi, R., Ben Nessib, N., Milovanović, N., Popović, L.Č., Dimitrijević, M.S., Sahal-Bréchot, S., 2008. Atomic data and electron-impact broadening effect in DO white dwarf atmospheres: SiVI. MNRAS 387, 871–882.

Kramida, A.E., Ryabtsev, A.N., Ekberg, J.O., Kink, I., Mannervik, S., Martinson, I., 2008. Additions to the spectrum and energy levels and a critical compilation of helium-like and hydrogen-like boron, B IV and B V. Phys. Scr. 78 (p. 025302 (1–8)).

Lanz, T., Dimitrijević, M.S., Artru, M.C., 1988. Stark broadening of visible SI II lines in stellar atmospheres. A&A 192, 249–254.

Larbi-Terzi, N., Sahal-Bréchot, S., Ben Nessib, N., Dimitrijević, M.S., 2012. Stark-broadening calculations of singly ionized carbon spectral lines. MNRAS 423, 766–773.

Oertel, G.K., Shomo, L.P., 1968. Tables for the calculation of radial multipole matrix elements by the coulomb approximation. ApJS 16, 175–218.

Popović, L.Č., Dimitrijević, M.S., Ryabchikova, T., 1999a. The electron-impact broadening effect in CP stars: the case of La II, La III, EU II, and EU III lines. A&A 350, 719–724.

Popović, L.Č., Dimitrijević, M.S., Tankosić, D., 1999b. The stark broadening effect in hot star atmospheres: AU I and AU II lines. A&AS 139, 617–623.

Popović, L.Č., Milovanović, N., Dimitrijević, M.S., 2001a. The electron-impact broadening effect in hot star atmospheres: the case of singly– and doubly-ionized zirconium. A&A 365, 656–659.

Popović, L.Č., Simić, S., Milovanović, N., Dimitrijević, M.S., 2001b. Stark broadening effect in stellar atmospheres: Nd II lines. ApJS 135, 109–114.

Ritchey, A.M., Federman, S.R., Sheffer, Y., Lambert, D.L, 2011. The abundance of boron in diffuse interstellar clouds. ApJ 728 (70 (13–7)).

Rixon, G., Dubernet, M. L., Piskunov, N. et al., 2010. "virtual atomic and molecular data centre" and astrophysics: level 2 release, seventh international conference on atomic and molecular data and their applications – ICAMDATA-2010, Vilnius, (Lithuania), 21–24 September 2010, AIP Conf. Proc. 1344, pp. 107–115.

Sahal-Bréchot, S., 1969a. Impact theory of the broadening and shift of spectral lines due to electrons and ions in a plasma. A&A 1, 91–123.

Sahal-Bréchot, S., 1969b. Impact theory of the broadening and shift of spectral lines due to electrons and ions in a plasma (continued). A&A 2, 322–354.

Sahal-Bréchot, S., 2010. Case studies on recent Stark broadening calculations and STARK-B database development in the framework of the European project VAMDC (Virtual Atomic and Molecular Data Center). J. Phys.: Conf. Ser. 257 (p. 012028 (1–10)).

Sahal-Bréchot, S., Dimitrijević, M.S., Moreau, N., 2013. STARK-B Database. <http://stark-b.obspm.fr>.

Sahal-Bréchot, S., Dimitrijević, M.S., Moreau, N., 2012. Virtual Laboratory Astrophysics: the STARK-B database for spectral line broadening by collisions with charged particles and its link to the European project VAMDC. J. Phys.: Conf. Ser. 397, 012019–012026.

Simić, Z., Dimitrijević, M.S., Kovačević, A., 2009. Stark broadening of spectral lines in chemically peculiar stars: Te I lines and recent calculations for trace elements. New Astron. Rev. 53, 246–251.

Simić, Z., Dimitrijević, M.S., Milovanović, N., Sahal-Bréchot, S., 2005. Stark broadening of Cd I spectral lines. A&A 441, 391–393.

Simić, Z., Dimitrijević, M.S., Popović, L.Č., Dačić, M., 2006. Stark broadening parameters for Cu III, Zn III and Se III lines in laboratory and stellar plasma. New Astron. 12, 187–191.

Tankosić, D., Popović, L.Č., Dimitrijević, M.S., 2003. The electron-impact broadening parameters for Co III spectral lines. A&A 399, 795–797.

Van Regemorter, H., Hoang, Binh Dy, Prud'homme, M., 1979. Radial transition integrals involving low or high effective quantum numbers in the Coulomb approximation. J. Phys. B 12, 1053–1061.

Available online at www.sciencedirect.com

ScienceDirect

Advances in Space Research xxx (2013) xxx–xxx

ADVANCES IN SPACE RESEARCH (a COSPAR publication)

www.elsevier.com/locate/asr

The STARK-B database as a resource for "STARK" widths and shifts data: State of advancement and program of development

Sylvie Sahal-Bréchot [a,*], Milan S. Dimitrijević [a,b], Nicolas Moreau [a], Nabil Ben Nessib [c]

[a] *Laboratoire d'Étude du Rayonnement et de la Matière en Astrophysique, Observatoire de Paris, UMR CNRS 8112, UPMC, 5 Place Jules Janssen, 92195 Meudon Cedex, France*

[b] *Astronomical Observatory, Volgina 7, 11060 Belgrade, Serbia*

[c] *Department of Physics and Astronomy, College of Science, King Saud University, Riyadh 11451, Saudi Arabia*

Abstract

"Stark" broadening theories and calculations have been extensively developed for about 50 years and can now be applied to many needs, especially for accurate spectroscopic diagnostics and modeling. This requires the knowledge of numerous collisional line profiles. Nowadays, the access to such data via an online database becomes essential. STARK-B is a collaborative project between the Astronomical Observatory of Belgrade and the Laboratoire d'Étude du Rayonnement et de la matière en Astrophysique (LERMA). It is a database of calculated widths and shifts of isolated lines of atoms and ions due to electron and ion collisions (impacts). It is devoted to modeling and spectroscopic diagnostics of stellar atmospheres and envelopes, laboratory plasmas, laser equipments and technological plasmas. Hence, the domain of temperatures and densities covered by the tables is wide and depends on the ionization degree of the considered ion. STARK-B has been fully opened since September 2008 and is in free access.

The first stage of development was ended in autumn 2012, since all the existing data calculated with the impact semiclassical-perturbation method and code by Sahal-Bréchot, Dimitrijević and coworkers have now been implemented. We are now beginning the second stage of the development of STARK-B. The state of advancement of the database and our program of development are presented here, together with its context within VAMDC. VAMDC (Virtual Atomic and Molecular Data Center) is an international consortium which has built a secure, documented, flexible interoperable platform e-science permitting an automated exchange of atomic and molecular data.

Keywords: Databases; Atomic data; Atomic processes; Line: profiles; Stars: atmospheres

1. Introduction

Broadening of spectral lines due to perturbation of emitting or absorbing atoms, ions, or molecules, by their interactions with the surrounding particles in a plasma or gas is called pressure broadening. If perturbers are charged particles, electrons or ions, such broadening mechanism is called Stark broadening. Data on Stark broadening are of interest for plasma diagnostic and modeling, as well as for spectra analysis and synthesis in many domains for research of different kinds of plasma in laboratory, inertial fusion investigations, for lasers and laser produced plasmas and especially in astrophysics, since thanks to space missions, large space observatories like Hubble, Chandra, Spitzer, Lyman, and to ground-based telescopes of the ten meters class, spectra with very high resolution could be obtained from X to radio wavelength ranges.

In stellar astronomy, Stark broadening data are of particular importance for white dwarfs, where Stark broadening is the dominant collisional line broadening mechanism (Popović et al., 1999b; Tankosić et al., 2003; Simić et al., 2006; Hamdi et al., 2008; Simić et al., 2009; Dimitrijević

* Corresponding author. Tel.: +33 15077442; fax: +33 1 45077100.
E-mail addresses: sylvie.sahal-brechot@obspm.fr (S. Sahal-Bréchot), mdimitrijevic@aob.bg.ac.rs (M.S. Dimitrijević), nicolas.moreau@obspm.fr (N. Moreau), nbennessib@ksu.edu.sa (N. Ben Nessib).

0273-1177/$36.00 © 2013 COSPAR. Published by Elsevier Ltd. All rights reserved.
http://dx.doi.org/10.1016/j.asr.2013.08.015

et al., 2011; Dufour et al., 2011; Larbi-Terzi and Sahal-Bréchot, 2012). Such data are also of significance for interpretation, analysis and synthesis of A and B type star spectra (see e.g. Lanz et al., 1988; Popović et al., 2001a,b, 1999a,b; Tankosić et al., 2003; Simić et al., 2005; Sahal-Bréchot et al., 2010). Modern codes for stellar atmosphere modeling, like e.g. PHOENIX (Baron et al., 1998; Hauschildt et al., 1999; Short et al., 1999) require the knowledge of atomic data for as much as possible transitions, especially for trace elements, so that the access to such atomic data, including Stark broadening ones, via online databases becomes very important.

The database STARK-B (Sahal-Bréchot et al., 2013), which contains Stark broadening parameters, namely calculated line widths and shifts of isolated lines of atoms and ions due to collisions with electrons, protons and different ions, first of all ionized helium as the most important after electrons and protons for stellar atmospheres, is not useful only for modeling and spectroscopic diagnostics of stellar atmospheres and envelopes, but also for laboratory plasmas, inertial fusion plasma, laser equipments and technological plasmas. This is a common project where participants are from the Paris Observatory and the Astronomical Observatory of Belgrade. The database STARK-B has been opened online since September 2008, and is in free access. The objective of the first phase of database development, was to implement all the existing data calculated with the impact semiclassical-perturbation method and code by Sahal-Bréchot, Dimitrijević and coworkers. We are now working on the second stage and the state of advancement of the database STARK-B will be presented here, as well as our program of development. We note also that STARK-B enters in Virtual Atomic and Molecular Data Center – VAMDC (Dubernet et al., 2010; Rixon et al., 2010), a secure, documented, flexible, interoperable platform based on e-science, which permits an optimized search and exchange of atomic and molecular data. The relation between STARK-B database and VAMDC was discussed in Sahal-Bréchot et al. (2012).

2. STARK-B database

Within the impact-complete collision-isolated line approximation, the profile of an isolated spectral line is the Lorentz one, characterized by a width at half maximum of intensity and a shift, so called Stark broadening parameters, depending on temperature T and density N of perturbers. For not too high densities, due to the impact approximation, widths and shifts are linearly proportional to the density of perturbers. But at high densities, due to the Debye screening effect which decreases the width and the shift, and which for such conditions can become significant, the dependence of Stark broadening parameters as a function of perturber density may decline from the linear one. This is taken into account in majority of our calculations, so that for many of atoms and ions the Stark broadening parameters for a grid of perturber densities are implemented in STARK-B.

In the first stage of STARK-B development, we implemented in STARK-B Stark broadening parameters determined with the semiclassical-perturbation method (SCP) developed by Sahal-Bréchot (1969a,b) and updated in further papers by Sahal-Bréchot (1974) for more complex atoms, by Fleurier et al. (1977) for inclusion of Feshbach resonances in elastic cross-sections for the line widths for ion emitters, and by Mahmoudi et al. (2008) for the particular cases of very complex atoms. The numerical codes have been also updated by Dimitrijević and Sahal-Bréchot (1984) and in further papers. The accuracy is about 20% for the widths of simpler spectra but is worse for the shifts and very complex spectra, particularly when configuration mixing is present in description of energy levels. The results of Stark broadening parameters determination performed by Dimitrijević, Sahal-Bréchot, and co-workers using the semiclassical-perturbation method are contained in more than 130 publications and now have been implemented in the STARK-B database.

STARK-B is devoted for modeling and spectroscopic diagnostics of various plasmas in astrophysics, laboratory physics, technology and other topics, so that the range of temperatures and densities in the tables is wide and vary with the ionization degree of the considered ion. The temperatures in tables vary from several thousands Kelvins for neutral atoms to several millions for highly charged ions. Also the perturber densities vary from 10^{12} cm^{-3} to several 10^{22} cm^{-3}. The presentation of data, in particular the definition of configurations, terms and atomic energy levels is in accordance with the VAMDC standards, in order to allow interoperability with other atomic databases included in the Virtual Atomic and Molecular Data Center. We note also that the wavelengths in STARK-B are usually calculated from the energy levels that are used as input data for the determination of Stark broadening parameters. Consequently, the tabulated wavelengths are most often different from the measured ones, especially if the used energy levels are theoretically calculated. For the identification of the lines, the configurations, terms and levels are included in tables as well as the multiplet number from NIST database (Kramida et al., 2012).

If one opens the homepage, proposed menus are “Introduction”, “Data Description”, “Access to the Data”, “Updates” and “Contact”. In “Introduction” methods of Stark broadening parameter calculations and different approximations which are adopted are briefly explained. “Data Description” describes the data which are tabulated. “Access to the Data” provides a graphical interface enabling to the visitor to click on the needed element in the Mendeleev periodic table and then on the corresponding ionization degree. For elements in yellow cells, which symbols are additionally enhanced by boldface, Stark broadening data exist in the database, and for other cells, which have the color a little bit lighter than the background, there is no data. After choosing the needed

Please cite this article in press as: Sahal-Bréchot, S., et al. The STARK-B database as a resource for “STARK” widths and shifts data: State of advancement and program of development. J. Adv. Space Res. (2013), http://dx.doi.org/10.1016/j.asr.2013.08.015

ionization stage, the user with several clicks chooses the colliding perturber(s), the perturber density, the transition(s) by quantum numbers and the plasma temperature(s). A query by domain of wavelengths instead by transitions is also possible. Then a table containing the Stark full widths at half maximum of intensity and shifts is generated. In our tables, a positive shift is towards the red and a negative one towards the blue. At the beginning, before the table, an instruction how to cite the use of STARK-B, and bibliographic references for the data in the table below are given and linked to the publications via the SAO/NASA ADS Physics Abstract Service (http://www.adsabs.harvard.edu/) and/or within DOI, if available. The widths and shifts data can be downloaded as an ASCII table or in format adapted for Virtual Observatories – VOTable format (XML format).

Actually (1st of July 2013) in the STARK-B are Stark broadening parameters for 79 transitions of He, 61 Li, 29 Li II, 19 Be, 30 Be II, 27 Be III, 1 B II, 12 B III, 148 C II, 1 C III, 90 C IV, 25 C V, 1 N, 7 N II, 2 N III, 1 N IV, 30 N V, 4 O I, 12 O II, 5 O III, 5 O IV, 19 O V, 30 O VI, 14 O VII, 8 F I, 5 F II, 5 F III, 2 F V, 2 F VI, 10 F VII, 25 Ne I, 22 Ne II, 5 Ne III, 2 Ne IV, 26 Ne V, 20 Ne VIII, 62 Na, 8 Na IX, 57 Na X, 270 Mg, 66 Mg II, 18 Mg XI, 25 Al, 23 Al III, 7 Al XI, 3 Si, 19 Si II, 39 Si IV, 16 Si V, 15 Si VI, 4 Si XI, 9 Si XII, 61 Si XIII, 114 P IV, 51 P V, 6 S III, 1 S IV, 34 S V, 21 S VI,2 Cl, 10 Cl VII, 18 Ar, 2 Ar II, 9 Ar VIII,51 K, 4 K VIII, 30 K IX, 189 Ca, 28 Ca II, 8 Ca V, 4 Ca IX, 48 Ca X, 10 Sc III, 4 Sc X, 10 Sc 11,10 Ti IV, 4 Ti XI, 27 Ti XII,26 V V, 33 V XIII, 9 Cr I, 7 Cr II, 6 Mn II, 3 Fe II, 2 Ni II, 9 Cu I, 32 Zn, 18 Ga, 11 Ge, 11 Kr, 1 Kr II, 6 Kr VIII, 24 Rb, 33 Sr, 32 Y III, 3 Pd, 48 Ag, 70 Cd, 1 Cd II, 18 In II, 20 In III, 4 Te, 4 I, 14 Ba, 64 Ba II, 6 Au, 7 Hg II, 2 Tl III and 2 Pb IV.

We will continue to implement the new results and under the menu "Updates" is the description of newly added data with the date of importation. Also all updates with the date of the first importation and the importation of revised data are noted. Moreover, for further enquiries or user support, there is the menu "Contact" with the possibility to send an e-mail with questions to the corresponding persons.

3. Fitting formulae as functions of temperature

The first step of the stage two of STARK-B development was the implementation of possibility to fit the tabulated data with temperature. The theory of Stark broadening shows that the dependence of line widths with temperature is proportional to $T^{-1/2}$ at low temperature and to $\log(T)/T^{1/2}$ at high temperatures. This was checked many times, for example in Elabidi et al. (2009). However, in astrophysics, especially for the modeling of stellar atmospheres, this is not sufficient, since fitting formulae and coefficients as functions of temperature for the whole line are needed, since such fitting coefficients are easier to be imported to the computer codes for stellar atmosphere modeling than data with tabulated widths and shifts for a set of temperatures.

Consequently, in order to enable the better and more adequate use of STARK-B for stellar atmospheres modeling, we have derived (Sahal-Bréchot et al., 2011) a simple and accurate fitting formula based on a least-square method, which is logarithmic and represented by a second degree polynomial:

$$\log(w) = a_0 + a_1 \log(T) + a_2(\log(T))^2, \qquad d/w = b_0 + b_1 \log(T) + b_2(\log(T))^2. \tag{1}$$

One can be noted that Dimitrijević et al. (2007) proposed the fitting formula $w = C + AT^B$, but the present one is more accurate, due to the second degree term of the expansion. It should be noted also that none of them have a real physical sense.

Now in STARK-B, for each table with widths and shifts is added a complementary table with coefficients a_0, a_1, a_2 and b_0, b_1, b_2 for the corresponding fitting with the temperature using Eq. (1), so that it is easier to include the corresponding Stark broadening parameters in computer codes for stellar atmospheres modeling. We plan also to develop the fitting formulae as functions of perturber densities in order to make easier the use of data on high densities needed for white dwarf atmospheres and sub photospheric layers modeling.

4. The further development of STARK-B, stage 2

As the next step in STARK-B development is planned the implementation of Stark broadening data obtained with the Modified semiempirical method (Dimitrijević and Konjević, 1980; Dimitrijević and Kršljanin, 1986; Dimitrijević and Popović, 2001). We use this approach for emitters where atomic data are not sufficiently complete to perform an adequate semiclassical perturbation calculation. Stark line widths and in some cases also shifts of the following emitters spectral lines were calculated up to now:

Ag II, Al III, Al V, Ar II, Ar III, Ar IV, As II, As III, Au II, B III, B IV, Ba II, Be III, Bi II, Bi III, Br II, C III, C IV, C V, Ca II, Cd II, Cl III, Cl IV, Cl VI, Co II, Cu III, Cu IV, Eu II, Eu III, F III, F V, F VI, Fe II, Ga II, Ga III, Ge III, Ge IV, I II, Kr II, Kr III, La II, La III, Mg II, Mg III, Mg IV, Mn II, N II, N III, N IV, N VI, Na III, Na VI, Nd II, Ne III, Ne IV, Ne V, Ne VI, O II, O III, O IV, O V, P III, P IV, P VI, Pt II, Ra II, S II, S III, S IV, Sb II, Sc II, Se III, Si II, Si III, Si IV, Si V, Si VI, Sn III, Sr II, Sr III, Ti II, Ti III, V II, V III, V IV, Xe II, Y II, Zn II, Zn III, and Zr II.

Another future step is the implementation of our quantum data in STARK-B. Also, our plans concerns the development of additional fittings along principal quantum number for a given multiplet, charge of the ion collider along isoelectronic sequences, of the radiating ion, homologous ions in order to enable to estimate by interpolation

Please cite this article in press as: Sahal-Bréchot, S., et al. The STARK-B database as a resource for "STARK" widths and shifts data: State of advancement and program of development. J. Adv. Space Res. (2013), http://dx.doi.org/10.1016/j.asr.2013.08.015

and extrapolation the data that are missing in STARK-B database.

Acknowledgments

The support of Ministry of Education, Science and Technological Development of Republic of Serbia through projects 176002 and III44022 is acknowledged. A part of this work has been supported by VAMDC. VAMDC is funded under the Combination of Collaborative Projects and Coordination and Support Actions Funding Scheme of The Seventh Framework Program. Call topic: INFRA-2008-1.2.2 Scientific Data Infrastructure. Grant Agreement number: 239108. This work has also been supported by the cooperation agreements between Tunisia (DGRS) and France (CNRS) (project code 09/R 13.03, No.22637), and by the Programme National de Physique Stellaire (INSU-CNRS). The support of the French LABEX Plas@Par (UPMC, PRES Sorbonne Universties) is also acknowledged.

References

Baron, E., Hauschildt, P.H., 1998. Parallel implementation of the PHOENIX Generalized Stellar Atmosphere Program. II. Wavelength parallelization. ApJ 495, 370–376.

Dimitrijević, M.S., Konjević, N., 1980. Stark widths of doubly- and triply-ionized atom lines' in the references 'Dimitrijević and Konjević (1980)' and 'Dimitrijević, Kršljanin (1986)', 'Dimitrijević et al. (2007)'. JQSRT 24, 451–459.

Dimitrijević, M.S., Kršljanin, V., 1986. Electron-impact shifts of ion lines – modified semiempirical approach. A&A 165 (24), 269–274.

Dimitrijević, M.S., Popović, L.Č., 2001. Modified semiempirical method. J. Appl. Spectr. 68, 893–901.

Dimitrijević, M.S., Sahal-Bréchot, S., 1984. Stark broadening of neutral helium lines. JQSRT 31, 301–313.

Dimitrijević, M.S., Ryabchikova, T., Simić, Z., Popović, L.Č., Dačić, M., 2007. The influence of Stark broadening on Cr II spectral line shapes in stellar atmospheres. A&A 469, 681–686.

Dimitrijević, M.S., Kovačević, A., Simić, Z., Sahal-Bréchot, S., 2011. Baltic Astron. 20, 580–586.

Dubernet, M.L., Boudon, V., Culhane, J.L., et al., 2010. Virtual atomic and molecular data center. JQSRT 111, 2151–2159 <http://www.vamdc.eu>.

Dufour, P., Ben Nessib, N., Sahal-Bréchot, S., Dimitrijević, M.S., 2011. Stark broadening of carbon and oxygen lines in hot DQ White Dwarf stars: recent results and applications. Baltic Astron. 20, 511–515.

Elabidi, H., Ben Nessib, N., Sahal-Bréchot, S., 2009. Quantum Stark broadening of 3s–3p spectral lines in Li-like ions; Z-scaling and comparison with semi-classical perturbation theory. Eur. Phys. J. 54, 51–64.

Fleurier, C., Sahal-Bréchot, S., Chapelle, J., 1977. Stark profiles of some ion lines of alkaline earth elements. JQSRT 17, 595–603.

Hamdi, R., Ben Nessib, N., Milovanović, N., Popović, L.Č., Dimitrijević, M.S., Sahal-Bréchot, S., 2008. Atomic data and electron-impact broadening effect in DO white dwarf atmospheres: SiVI. MNRAS 387, 871–882.

Hauschildt, P.H., Allard, F., Baron, E., 1999. The NextGen model atmosphere grid for $3000 \leqslant T_{eff} \leqslant 10,000$ K. ApJ 512, 377–385.

Kramida, A., Ralchenko, Yu., Reader, J., NIST ASD Team 2012. NIST Atomic spectra database (ver. 5.0), National Institute of Standards and Technology, Gaithersburg, MD, Available from: http://physics.nist.gov/asd [2013, May 3].

Lanz, T., Dimitrijević, M.S., Artru, M.C., 1988. Stark broadening of visible Si II lines in stellar atmospheres. A&A 192, 249–254.

Larbi-Terzi, N., Sahal-Bréchot, S., Ben Nessib, N., Dimitrijević, M.S., 2012. Stark-broadening calculations of singly ionized carbon spectral lines. MNRAS 423, 766–773.

Mahmoudi, W.F., Ben Nessib, N., Sahal-Bréchot, S., 2008. Stark broadening of isolated lines: calculation of the diagonal multiplet factor for complex configurations ($n_1l_1^n\ n_2l_2^m\ n_3l_3^p$). Eur. Phys. J. D. 47, 7–10.

Popović, L.Č., Dimitrijević, M.S., Ryabchikova, T., 1999a. The electron-impact broadening effect in CP stars: the case of La II, La II i, EU II, and EU II i lines. A&A 350, 719–724.

Popović, L.Č., Dimitrijević, M.S., Tankosić, D., 1999b. The Stark broadening effect in hot star atmospheres: Au I and Au II lines. A&AS 139, 617–623.

Popović, L.Č., Milovanović, N., Dimitrijević, M.S., 2001a. The electron-impact broadening effect in hot star atmospheres: the case of singly- and doubly-ionized zirconium. A&A 365, 656–659.

Popović, L.Č., Simić, S., Milovanović, N., Dimitrijević, M.S., 2001b. Stark broadening effect in stellar atmospheres: Nd II lines. ApJS 135, 109–114.

Rixon, G., Dubernet, M.L., Piskunov, N., et al., 2010. Virtual atomic and molecular data centre and astrophysics: level 2 release, 7th international conference on atomic and molecular data and their applications – ICAMDATA-2010, Vilnius, (Lithuania), 21–24 September 2010. AIP Conf. Proc. 1344, 107–115.

Sahal-Bréchot, S., 1969a. Impact theory of the broadening and shift of spectral lines due to electrons and ions in a plasma. A&A 1, 91–123.

Sahal-Bréchot, S., 1969b. Impact theory of the broadening and shift of spectral lines due to electrons and ions in a plasma (continued). A&A 2, 322–354.

Sahal-Bréchot, S., 1974. Stark broadening of isolated lines in the impact approximation. A&A 35, 319–321.

Sahal-Bréchot, S., 2010. Case studies on recent Stark broadening calculations and STARK-B database development in the framework of the European project VAMDC (Virtual Atomic and Molecular Data Center). J. Phys.: Conf. Ser. 257 (012028), 1–10.

Sahal-Bréchot, S., Dimitrijević, M.S., Ben Nessib, N., 2011. Comparisons and comments on electron and ion impact profiles of spectral lines. Baltic Astron. 20, 523–530.

Sahal-Bréchot, S., Dimitrijević, M.S., Moreau, N., 2012. Virtual Laboratory Astrophysics: the STARK-B database for spectral line broadening by collisions with charged particles and its link to the European project VAMDC. J. Phys.: Conf. Ser. 397, 012019–012026.

Sahal-Bréchot, S., Dimitrijević, M.S., Moreau, N., 2013. STARK-B Database. <http://stark-b.obspm.fr>.

Short, I.C., Hauschildt, P.H., Baron, E., 1999. Massive multispecies, multilevel non-LTE model atmospheres for novae in outburst. ApJ 525, 375–385.

Simić, Z., Dimitrijević, M.S., Milovanović, N., Sahal-Bréchot, S., 2005. Stark broadening of Cd I spectral lines. A&A 441, 391–393.

Simić, Z., Dimitrijević, M.S., Popović, L.Č., Dačić, M., 2006. Stark broadening parameters for Cu III, Zn III and Se III lines in laboratory and stellar plasma. New Astron. 12, 187–191.

Simić, Z., Dimitrijević, M.S., Kovačević, A., 2009. Stark broadening of spectral lines in chemically peculiar stars: Te I lines and recent calculations for trace elements. New Astron. Rev. 53, 246–251.

Tankosić, D., Popović, L.Č., Dimitrijević, M.S., 2003. The electron-impact broadening parameters for Co III spectral lines. A&A 399, 795–797.

Journal of Astronomical History and Heritage, 14(1), 22-30 (2011).

ASTRONOMY AND CONSTELLATIONS IN THE *ILIAD* AND *ODYSSEY*

E. Theodossiou and V.N. Manimanis
Department of Astrophysics-Astronomy and Mechanics, School of Physics, National & Kapodistrian University of Athens
Panepistimioupolis, Zographos 157 84, Athens, Greece.
E-mail: etheodos@phys.uoa.gr

P. Mantarakis
22127 Needles St, Chatsworth, California, U.S.A.
E-mail: zanipetros@socal.it.com

and

M.S. Dimitrijevic
Astronomical Observatory of Belgrade, Volgina 7, 11060 Belgrade, Serbia.
E-mail: mdimitrijevic@aob.bg.ac.rs

Abstract: The *Iliad* and the *Odyssey*, in addition to their supreme status as cornerstones of world literature, are a rich source of information about the scientific and technological knowledge of ancient Greeks in both pre-Homeric and Homeric times. The two Homeric epic poems, which we date to the 8th century BC, include, *inter alia*, a wealth of astronomical elements, informing about the Earth, the sky, the stars, constellations and asterisms such as the Pleiades and the Hyades. They also offer a more erudite image of Homer, which reflects the cosmological views of his period. The model of the Universe that is presented is continuous and has three levels: the lower level corresponds to the underworld, the middle one to the Earth and the upper one to the sky. But the key point of this paper is to illuminate the fact that the ancient Greek appellations for many of the stars and constellations have remained the same even after three millennia.

Keywords: *Iliad, Odyssey*, Homeric cosmological model

1 INTRODUCTION

The *Iliad* and the *Odyssey* are not only of supreme literary importance, but are, as well, a rich source of historical, scientific, technological and astronomical knowledge of the ancient Greeks in pre-Homeric and Homeric times. These two epic poems, which we date to the 8th century BC, include a wealth of information about the Earth, the sky, the stars (e.g. Sirius), constellations such as Ursa Major, Boötes and Orion, and star clusters like the Pleiades and the Hyades. They therefore offer us the possibility of seeing the more general cosmological views of that time.

A large number of authors have considered different astronomical aspects, facts and allusions in the *Iliad* and the *Odyssey* (e.g. see Walker, 1872; Schoch, 1926a; 1926b; 1926c; Neugebauer, 1929; Lorimer, 1951; Dicks, 1970; Trypanis, 1975; Gendler, 1984; Lovi, 1989; Genuth, 1992; Kirk, Raven and Schofield, 1995; Konstantopoulos, 1998; Wood and Wood, 1999; Flanders, 2007; Baikouzis and Magnasco, 2008; Minkel, 2008; and Varvoglis, 2009). This illustrates the continuing interest in this attractive subject. It is our aim here to analyze the astronomical data and allusions in the Homeric epics in order to better understand the cosmological model of the Universe that would prevail for a millennium after the Trojan War.

D.R. Dicks (1970: 10) has stated that: "We can't form a clear idea about the shape and the position of the Earth with respect to heavens and the underworld from the Homeric epics." Strictly speaking, this may be true. However, we wish to explore the prospect that it is in fact possible to ascertain a cosmological model from the passages and astronomical information contained in the *Iliad* and the *Odyssey*. We will investigate which constellations and celestial phenomena were known to Greeks of that era, and how these were woven into a complex model of the Universe. We will also consider the names of the stars and constellations, several of which are exactly the same today as in Homeric times.

2 THE POSITION OF THE OCEAN, THE EARTH AND THE SKY IN THE HOMERIC UNIVERSE

2.1 The Ocean and the Earth

The ancient teachings of Orpheus (dating as far back as the 13th Century BC) are considered to be the basis of the first mystic Greek religion, with poems and hymns of great beauty. Nearly all of the ancient Greek sages and writers drew inspiration from themes found in the Orphic Hymns, and were thus influenced in formulating their individual theories and teachings.

Besides the Orphic Hymns (Petrides, 2002), the Homeric epics are a rich source of historical and technological facts. Indeed, an astronomer who studies in detail the descriptions in the *Iliad* and the *Odyssey* will discover a treasure-trove of astronomical information. It is generally believed that Homer lived in the Iron Age (a period roughly spanning 1200 to 550 BC), but told stories that occurred in the Late Bronze Age (ca. 12th century BC).

As Emile Mireaux (1959: 9) writes:

> The Iliad and the Odyssey contain elements from the old Mycenean civilization; basically, however, although they refer to events of the 12th century BC, the lives of their heroes (social, political economical and family), their laws and customs ... all reflect the way of life witnessed by the poet who composed the epic.

The two epic poems took their definite form in the Ionic cities of Anatolia in the 9th or 8th century BC;

first came the *Iliad* and later the *Odyssey* (Trypanis, 1975). The poems describe the culture, religious beliefs, general knowledge and habits of Greek populations during this period. They also describe the cosmological model that would prevail for the next millennium, i.e. up to the time of Ptolemy and his *Almagest.*

The Earth of the Homeric Universe was a circular flat disk surrounded by a huge circular river, the Ocean, a model first appearing in the Orphic Hymn "X. To Pan, The Fumigation from Various Odors", verse 15: "Old Ocean [Okeanos] too reveres thy high command, whose liquid arms begirt the solid land."

This mythical 'river' is different from the seas: it is something that defines the boundaries of the terrestrial world. Above all, Ocean is the primal and original creative element, the starting point of all things: "I can put the currents to sleep and, if you wish, of the river Ocean, which was the beginning of everything." (*Iliad*: XIV, 245-246).[1] Ocean is the male ancestor of the gods, who had Tethys as his spouse during the Creation: "I shall go to the ends of the Earth to find the father of all gods, the Ocean and Tethys the mother." (*Iliad*: XIV, 200).

This mythical 'river' has no sources, nor estuary; it is "apsorroos", i.e. cyclically moving or backward-flowing. Its current goes back to where it started in a ceaseless and eternal motion. From this Ocean, mentioned 19 times in the *Iliad* and 14 in the *Odyssey*, all other waters on Earth were created: seas, rivers and lakes. This is mentioned in the *Iliad*: "The all-powerful Ocean, the deep-current one, from whom all sea, river, source and fountain springs, and every deep well." (*Iliad*: XXI, 195-197).

In the *Odyssey*, the Ocean is described as terrible and fearful: "...'cause he has deep currents and large rivers in his midst, which no one without a fast ship can pass across." (*Odyssey*: XI, 160). However, we are not given a definite description of the exact shape or size of the Ocean; we just learn about its watery structure.

Although Dicks is correct that we cannot get a clear idea about the position of the Earth in the cosmos, it can certainly be said that in the Homeric cosmological model, the Earth is between the sky and the underworld. Its precise structure and shape are not known, we just suppose it is a circular disk since it is surrounded by the circular watery Ocean. In the *Iliad*: (VIII, 13-16), a contrary view about Tartarus (a 'deep place' below sky, Earth and the sea) is given when Zeus threatens the gods that he will send them there:

> ... or I shall throw him down with my own hands, in the darkness of Tartarus, long away to the depths of the world, that has iron gates and copper threshold, under the Hades as far as the heavens are from the Earth. (*Iliad*: VIII, 13-16).

In parallel, Homer imagines Hades in the depths of the Earth:

> ... and if you go to the ends of the Earth and the sea, where Japetus and Cronus reside, and winds do not blow on them, nor the sunlight shines on them and deep Tartarus surrounds them from everywhere. (*Iliad*: VIII, 480).

One can conclude Homer believes that a) Hades is below the Earth and surrounded by Tartarus; b) the Earth is the center of the Universe and of life; and c) the starry sky is supported by the Earth (*Odyssey*: ix, 534). This is depicted in Figure 1.

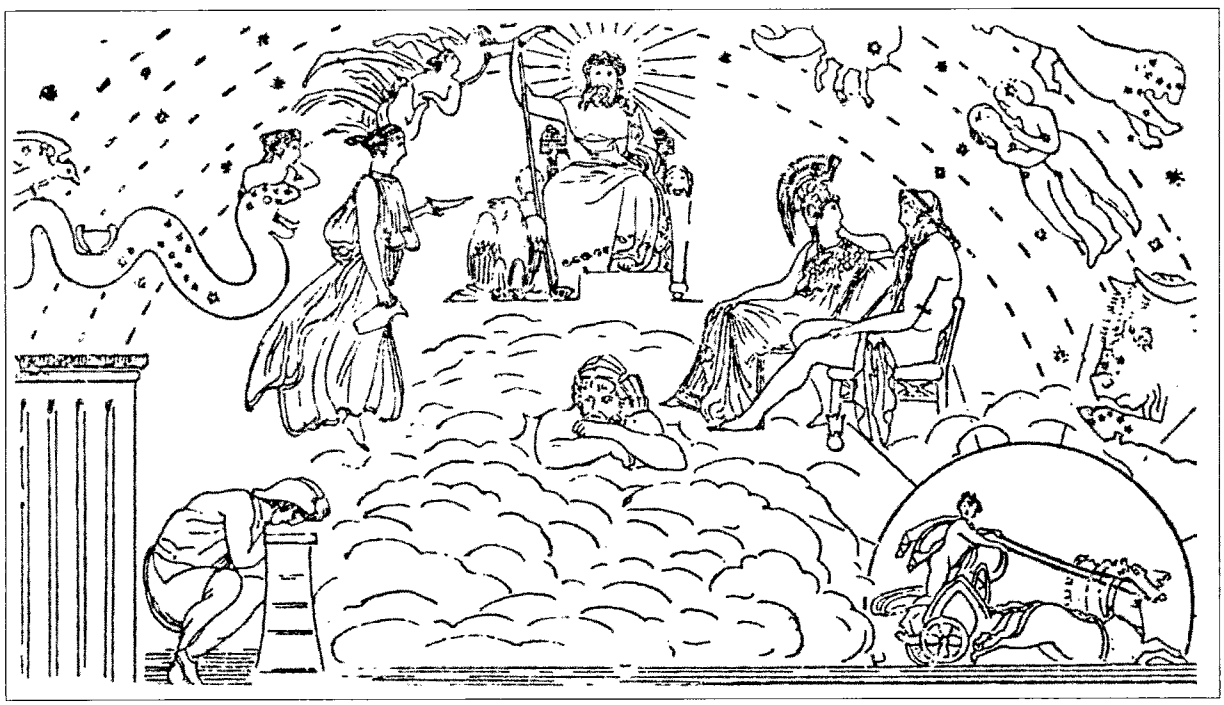

Figure 1: The Homeric Universe. In the Universe of Homer's times, the mountains can be seen to rise over the surface of the great disk of the Earth, the Ocean spreading around them, while the center is dominated by Mount Olympus which rises up to heaven. In its highest peak, the all-seeing Zeus is seated, supervising both immortal gods and mortal men, sometimes rewarding and sometimes punishing them. Beyond Olympus spreads Heaven, supported by the pillars of Atlas. In heaven we can locate the Moon, the stars and the constellations. In particular, in this figure we can distinguish the Pleiades open cluster and the constellations of Hydra, Corvus, Crater, Cancer, Leo, Gemini, Taurus as well – these constellations are not specifically referred to by Homer (after Cotsakis, 1976: 18).

2.2 The Sky

Heaven, with its luminous stars, is depicted as a hemispherical dome exactly covering the flat Earth (*Odyssey*: xi, 17). That is, the cosmos of this time was envisioned as a celestial dome over a disk-like Earth floating on water. The view of this age as recorded in the *Odyssey* is that the sky rests upon the Earth with the columns that keep the whole world in equilibrium held up by the mythical Atlas: "The daughter of the Atlas, of the one who knows the depth of every sea and he alone lifts the tall columns that divide Heaven and Earth in two." (*Odyssey*: i, 53-54).

For the ancient Greeks, the sky was a dome made of solid matter, iron or copper, held up there by tall columns or, according to another view, by some giant. Homer combines these two views by having Atlas supporting the columns. Hesiod in *Theogony* (1988: 517) writes that Zeus was the one who had assigned this duty to Atlas.

For Homer the sky was, more specifically, made of copper, as described in the *Iliad*: "... the Achaeans, white in dust to the top, for the horses were lifting it up to the copper sky with their feet." (V, 504). Or, in another passage: "They were fighting there and the iron noise was thundering up to the copper sky through the air." (XVII, 424-425). In another "polychalcus", that is "... of much copper." (*Iliad*: V, 504, *Odyssey*: iii, 2; *Iliad*: II, 458; XVI, 364; XIX, 351). There are also references to an iron sky in the *Odyssey*: (xv, 329 and xvii, 565), but it is not known whether this was meant metaphorically or in some other context.

We thus conclude that the sky was perceived by the ancient Greeks as something solid though unreachable. Its unimaginable distance was often used in similes to confer vastness. For example, the glory of Nestor's golden shield reached the skies: "... and then we shall take the shield of Nestor, whose glory has reached the stars." (*Iliad*: VIII, 192-193). Similarly, the glory of Penelope, which also was reaching the wide skies (*Odyssey*: xix, 108).

The space between sky and Earth was filled firstly by the dense air: "... up to the air its vast branches extended." (*Iliad*: XIV, 288), and over this layer and towards the direction of the sky there was the clean and transparent 'aether', lighter than the air. Aether is essentially the 'higher air', through which the heavens can be seen:

> ... and up to the stars, which twinkle in windless aether, charming around the luminous moon – every peak, every edge, every side is visible, as a vast aether opened by the sky, which made visible all the stars to the joy of the shepherds. (*Iliad*: VIII, 554-559).

Above the aether, on the peaks of Olympus that reach the sky, the gods dwell: "... and he offered a lot of sacrifices to the gods that dwell in heavens." (*Odyssey*: i, 68-69), and "Without the opinion of the gods, who dwell in heavens ... but now he is like the gods who enjoy the heavens." (*Odyssey*: vi, 242-245). The gods are described either as "Olympians" or "heavenly gods", because the tallest peaks of Olympus seemed to touch the heavens: "Our father, son of Cronus, first of the heavenly ones ..." (*Odyssey*: i, 46). Finally, it is mentioned that above the aether there was the "polychalcus" sky (*Iliad*: II, 458; XVI, 364; XIX, 351).

Of course, one should not assume that the Homeric sky was a barren metallic dome; it was, as Homer sings, full of life, the life of the stars and the constellations. Thus, the ancient Greeks were calling the sky "... full of stars." ("asteroeis") (*Iliad*: VI, 108; XV, 371), and star-decorated (*Odyssey*: ix, 535), as was natural for a people living in a country with few cloudy nights.

On this celestial dome, Helios, the god of the Sun, travels on its path, so he is described with the adjective 'ouranodromos' (sky-running): "For they were perished due to their own fault, the impious, who ate the oxen of the sky-running Helios and he deprived them of the day of their homecoming." (*Odyssey*: i, 7-9). This is only one out of 119 references to the Sun in the Homeric epics: there are 42 references in the *Iliad* and 77 in the *Odyssey*. As a god, Helios appears 34 times (8 in the *Iliad* and 26 in the *Odyssey*). In stark contrast, for the Moon (Selene) there are only three references in the *Iliad*: (VIII, 554; XVII, 367; XVIII, 484) and only two in the *Odyssey*: (iii, 46 and ix, 144). Besides, the Moon appears under its archaic name, "Mene" one more time in the *Iliad*: (XIX, 374). A possible explanation for the scarcity of lunar references is that the main events in the *Iliad*—that is, the battles—took place only during the daylight, whereas in the *Odyssey* the Moon was usually hidden behind the clouds: "For it was thick darkness around and the moon, hidden in clouds, didn't shine in the skies." (*Odyssey*: ix, 144).

Before moving on to examine the stars and constellations in the epics, it is interesting to present some meteorological and climatologic elements as they appear in the *Iliad* and the *Odyssey*. The air between the sky and the Earth is traversed by the winds and the clouds, through which the omnipotent Zeus covers the sky, sends the rains onto the Earth and throws his lightning and thunders (*Iliad*: XVI, 364-365; XII, 25-26; *Odyssey*: v, 303; xxiii, 330).

As is mentioned in Rhapsody V in the *Iliad*, the gates of both Heaven and Olympus are formed by dense clouds. Their guards are the Orae (Hours), goddesses of the seasons who regulate the weather conditions:

> ... and Hera moves the horses violently with the whip; the gate of Heaven thunders open in front of them, which the guardians of the vast Sky and Olympus, the Hours, block with the cloud or remove it. (*Iliad*: V, 749-751).

3 THE STARS AND THE CONSTELLATIONS IN THE *ILIAD* AND THE *ODYSSEY*

Let us now examine closely all the Homeric references to the constellations, the stars and the planet Venus, as they appear in the two epics.

Homer mentions in the *Iliad* the "autumnal" star:

> Then Athena gave power and courage to Diomedes, so that excellently amidst the Greek multitudes he would be glorified and take shining fame everywhere. From his helmet and shield a flame was visible, which pours light without sleeping, as the autumn star, bathed in the Ocean, shines with its full light. (*Iliad*: V, 1-5).

The "autumn star" is actually Sirius, the brightest fixed star of the night sky. Sirius appears every year, for the geographical latitude of Greece, in the night

sky in late July or early August. This is mentioned also by Richard H. Allen, who writes (1963: 120):

> Homer alluded to Sirius in the Iliad as Οπωρινός, the star of Autumn; but the season intended was the last days of July, all August, and part of September – the latter part of summer. The Greeks had no word exactly to our 'autumn' until the 5th century before Christ, when it appeared in writings ascribed to Hippocrates. Lord Derby translated this celebrated passage: A fiery light. There flash'd, like autumn's star, that brightest shines. When newly risen from his ocean bath.

Although it cannot be supported with certainty, the Homeric man, perceiving the Earth as a flat circular disk surrounded by the Ocean, considered that the Sun, the Moon and most stars rose from the Ocean and set back in it. The idea of a spherical Earth appeared much later, with the Pythagorean philosophers in the 5th century BC.

In the *Iliad*: (XVIII, 478-488) it is mentioned that on the shield of Achilles, which was constructed by the god Hephaestos (Vulcan) after an order by Thetis (Achilles' mother), were depicted all of the constellations (Figure 2):

> And he made first a powerful and large shield, all with art and triple circle around. With five bendings this shield was made and upon it various images he designed with his wise knowledge: The earth, the sky, the sea he drew, the untiring sun, the full moon, the stars that crown from everywhere the sky, Orion's power, the Hyades, the Pleiades, the Bear, also called the Wagon, which rotates always at the same place, watching Orion, the only one that doesn't experience the bathing in the Ocean.

Wood and Wood (1999) have speculated on how the sky during Homeric times may have appeared. Although interesting in its approach, their work is considered unproven and controversial.

The Hyades and the Pleiades, which are actually two open clusters, were called 'constellations' by the ancient Greeks—today they are both included in the constellation Taurus. Taurus is not mentioned by Homer, although he mentions the adjacent constellation Orion, and with the stressing phrase "Orion's power". This is exactly the way Orion is mentioned by Hesiod (West, 1988: 598, 615, 619). Both authors refer to the constellation's "power", alluding to its apparent brightness.

Homer ends his stellar reference with the circumpolar constellation Ursa Major, which does indeed 'watch' Orion. Ursa Major does not "... experience the bathing in the Ocean ...", i.e. it never 'contacts' the sea, because its position near the North Celestial Pole keeps it away from the horizon as the Earth rotates.

The Hyades and the Pleiades are mentioned together with the other star asterisms as 'constellations' in their own right, in both the *Iliad* and the *Odyssey* (v, 272-277). The Pleiades are mentioned just once in the first poem, together with the Hyades (in the passage above, XVIII, 485), and once in the *Odyssey*: (v, 272). Indeed, in the *Odyssey* there are references to all of the above-mentioned star clusters and constellations:

> Then he set sail, a joyful Odysseus (Ulysses), and, sitting at the helm, was steering artfully; and no sleep closed his eyes as he was staring at the Pleiades, and the Shepherd, who is late to set, and the Bear, also called the Wagon by many, which rotates always at the same place, watching the Hunter, the only one that doesn't bathe in the Ocean's wave. For Calypso had told him to keep that star on his left hand while sailing. (*Odyssey*: v, 270-277).

As R.H. Allen (1963: 96) writes: "Homer characterized the constellation of Boötes as 'οψέ δύων', meaning late in setting, a thought and expression [that has] now become hackneyed by frequent repetition."

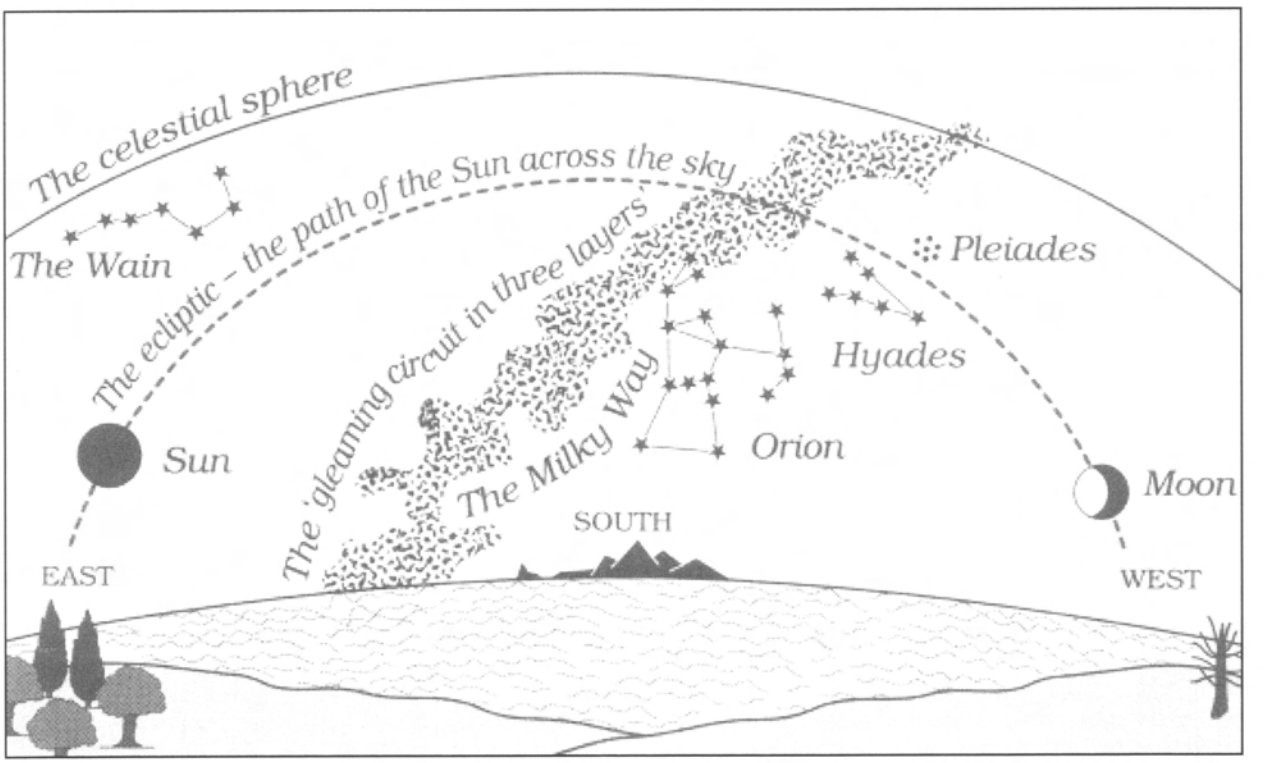

Figure 2: The Homeric Universe as it was depicted on the shield of Achilles (after Wood and Wood, 1999: 199).

Homer states that the constellation Boötes is late/ slow in setting, and Aratos that it "... lingers more than half the night ..." (since it is very long and narrow with its long side oriented north-south on the celestial sphere). So Boötes rises 'on his side', all at once, and sets nearly vertically (starting from its right lower corner for the sky of Athens, and becoming more and more vertical), feet setting first, then his waist, and his upper body setting last, therefore taking only a short time to rise but a very long time to set.

It must also be noted in the cited verses that, for the first and only time in the epics, there is a reference to the use of constellations for orientation in the sea. Calypso advises Ulysses that, in order to keep the right course, he must keep always on his left the Bear (Ursa Major). Of course, this means that, having on his left a northern constellation, he would travel eastwards. So Homer was placing Ogygia, the island of Calypso, somewhere to the west of all Greece, since Ithaca, where he was bound, was in the western part of Greece itself.

As Homer believed that the Earth was a flat circular disk surrounded by the Ocean, he was certain that the Sun, the Moon and the stars rise from the Ocean and set in it; only Ursa Major did not set for ancient people living on the northern shores of the Mediterranean Sea. In Greek mythology, Zeus lusted after a nymph named Callisto. Hera, Zeus' wife, out of jealousy turned Callisto into a bear. Zeus later swept her, and her son Arcas, into the sky forming the constellation of Ursa Major. Aristotle mentions that the bear is the only animal that, because of its thick fur can dauntlessly roam the icy northern polar regions. The circumpolar character of Ursa Major is in our age only partial, but in protohistoric times, when Alpha Draconis (Thuban) was the 'Pole Star', all seven of the brightest stars in Ursa Major never set. Today, due to the precession of the Earth's axis, Alkaid (Eta Ursae Majoris, the last star in the tail) remains under the northern horizon of Athens, Ithaca and central Greece in general, for approximately three hours. Only in northern Greece and in places with a geographical latitude higher than $\varphi = 40.1°$ are all of Ursa Major's brightest stars circumpolar. Allen (1963: 419) states: "Sir George Cornewall Lewiss writes – for Homer's line Arctos, sole star that never bathes in th' ocean wave (by reason of precession it then was much nearer to the pole than it now is)." The difference in the declination of Alkaid (η UMa) between Homeric times and today is >15°, so in antiquity all of Ursa Major was circumpolar even from the southernmost tip of Greece.

Homer, however, does not mention explicitly the Great Bear, so a modern commentator could argue that Ursa Minor (the Lesser Bear), is meant, or even a combination of both. Most probably, though, he meant the Great Bear, as it has much brighter stars, it is a much larger and more impressive constellation, and, most important, Ursa Minor was (according to the tradition) introduced to the Greeks by Thales of Miletus in the 6th century BC—that is, two centuries after Homer. Ursa Minor is still a totally circumpolar constellation as seen from Europe.

The last constellation mentioned in the *Odyssey* is Orion the Hunter. Its appearance in the night sky each year coincided with the start of the rainiest and stormiest part of the year; therefore Orion is called "stormy" and destructive. Both Hesiod and Aristotle mention that the rising of Orion was a certain warning for sailors that storms are coming (Hesiod, *Works and Days*: 598, 615, 619; Aristotle, *Meteorology*: 2.5.4).

In *Iliad's* Rhapsody XXII, both Orion and Sirius are mentioned. The brightest fixed star, Sirius, is referred to as Orion's dog. Today, Sirius is known as Alpha Canis Majoris, the brightest star in the constellation of Canis Major (the Great Dog). Homer presents Sirius as an ominous sign in the sky, as every summer it is connected with the so-called "dog burnings" (*The Iliad*, 1950: Chapter 22, verses 25-31):

> ... like the star that comes to us in autumn, outshining all its fellows in the evening sky – they call it Orion's dog, and though it is the brightest of all stars it bodes no good bringing much fever, as it does, to us poor mortals.

3.1 'Dog burnings' and 'Dog days'

In antiquity the heliacal rise of Sirius was connected with a period of the year of extremely hot weather, "*κυνικά καύματα*"("kynica kavmata", canine burnings). This period corresponded to late July, August and early September in the Mediterranean region. Romans also knew these days as "dies canicularіae", the hottest days of the whole year, associated with the constellation of the Great Dog, the hunter's (Orion's) dog Sirius. Ancient Greeks theorized the extra heat was due to the addition of the radiation of bright Sirius to the Sun's radiation.

In ancient Greek folklore, people called the summer days after the heliacal rise of Sirius "dog burnings" without correlating them with the Dog star or the constellation, but with dogs in general, thinking that only dogs were so crazy as to go outside when it was so hot. This belief has persisted through the centuries and can be found in modern Greek folklore in the belief that during the hot days of July and August, and especially between July 24 and August 6 dog bites are infectious (Theodossiou and Danezis, 1991: 115).

According to an ancient myth, the inhabitants of the island Kea were dying from a famine caused by the drought brought on by the dog burnings around 1600 BC. Then, the god Apollo gave an oracle to call Aristaeus, the god's son, from the region of Phthia, in order to help them. Upon arriving on Kea, Aristaeus performed rituals, cleansings and sacrifices to Zeus Ikmaeus, the lord of the rains and the skies, and to Kyon Apollo, that means to Apollo the Dog. Both gods listened to his pleas and they sent Etesian Winds, the northern winds blowing over the Aegean Sea every mid-summer for forty days, so that people could survive the unbearable heat. After that, the people of Kea, incited by Aristaeus, made sacrifices to the constellation of Canis Major and to Sirius. In order to remember his beneficence, they honored Aristaeus as "Aristaeus Apollo" and pictured his head on one side of their coins, while on the other side they depicted Sirius crowned with rays.

The late Professor and Academician of the National Technical University of Athens, Pericles S. Theochares (1995: 183) wrote:

> This myth alludes to the relation of Sirius with the Earth. The sacrifices were made to Zeus Meilichius, a god of the weather, of the sun and rain, and to Sirius, who causes the dog burnings on Earth; they believed

that not only the Sun is responsible for the great heat of the summer, but also Sirius when standing next to the Sun. This was probably the belief of the builders of the Argolis pyramids, orienting their entrance corridors towards the azimuth of Sirius.

In ancient poetry Sirius is mentioned as a star with especially negative influence, something obvious in the Homeric verse "... it bodes no good ... to us poor mortals." (*Iliad*: XXII, 25-31). Because the Greeks of that era had noticed that people tended to become sluggish during the dog days, they had consolidated the belief that Sirius was exerting a halting influence on human activities. For this reason, even Hippocrates refers to the bad influence of this star on humans. Hippocrates made much, in his *Epidemics* and *Aphorisms*, of this star's power over the weather, and the consequent physical effect upon mankind (Allen, 1963: 126).

3.2 The Planet Venus

Venus is mentioned in both the *Iliad* and the *Odyssey*. In *Iliad*'s Rhapsody XXII (verse 317) Homer mentions Hesperus, the Evening Star, and in XXIII (verse 226) Eosphorus (Lucifer in Latin), the Morning Star that brings the light of dawn. In both cases Venus is the object really mentioned, although Homer considers them most probably as two different stars:

And as amidst the stars the evening star proceeds bright, that most beautiful among the stars of the sky, likewise the lance was shining, which was thrown by his right hand with malevolent purpose towards divine Hector, watching to find an uncovered part of his soft body. (*Iliad*: XXII, 317-321).

Similarly in the second passage: "When Lucifer heralds the light and golden Eos (the Dawn) emerges from the sea's depths, the fire was fading and flames stopped." (*Iliad*: XXIII, 226-228).

In Homer's *Odyssey* the passage brings us once again to the sea: "As the all-bright star emerged that comes first to herald the light of the night-born Dawn, then the foam-happy ship was nearing the island." (*Odyssey*: xiii, 98-100). It means that Ulysses reaches Ithaca before dawn, the time Venus appears, as the brightest star 'coming' before dawn.

3.3 Solstices

Also in the *Odyssey*, there is a clear reference to the solstices as "turnings of the Sun": "Syria they call an island – if you ever heard of it – higher than Ortygia, to the turning of the Sun." (*Odyssey*: xv, 403-404).

3.4 Other Ancient Authors about the Stars, Constellations and Sirius

Homer's epics assuredly influenced other ancient Greek poets and authors who mentioned the stars and the constellations of the sky. The most references are to the brightest star, Sirius.

Due to its bright apparent magnitude (–1.46), Sirius had a special place in the mythology, legends and traditions of most peoples of the Earth. Its very name means in Greek "sparking", "fiery" or "burning"", or "flamboyant"; this name is most ancient, as it occurs in the Orphic *Argonautics*: "... just when for three consecutive days lost its light the flamboyant sun." (*Argonautics*: 121-122; Petrides, 2005), as well as in Homer (*Iliad*: XXII, 25-32 and *Odyssey*: v, 4).

In about the same period as Homer, or slightly later, Hesiod in his famous book, *Works and Days*, mentions several constellations that the farmer needs to watch for his daily work as well as three references to the solstices. For example, Hesiod suggests that the harvest should start when the Pleiades rise (heliacal rise), while seeding should start when they are about to set. Hesiod spoke of all the stars and constellations mentioned by Homer, with a special reference to Sirius. Indeed, he mentions Sirius in three different passages. In the first one he gives some advices to his brother Perses about grape-gathering: "And when Orion and Sirius reach the middle of the sky and the rose-fingered Dawn watches Arcturus, then, Perses, gather all grapes and bring them to the house." (Hesiod, 1988: 609-610), while in the other two he speaks about the dog burnings: "Then Sirius, the star proceeds a little more over the head of the mortal men each day and takes a larger part of the night." (ibid.: 417) and "For Sirius dries the head and the knees and the body is dry from the heat." (ibid.: 587).

Another work by Hesiod, *Aspis Irakleous* (*Shield of Hercules*), is to a certain extent an imitation of "Aspis Achilleos" (the Shield of Achilles) as it is described in the *Iliad*: (XVIII, 468-817). In this work, too, Hesiod mentions the bright star Sirius twice (Hesiod, 1988: 391):

'Their souls descend into Hades to be dressed with earth, while their bones, when the skin around them is melted by fiery Sirius, get rotten in the black earth.' (Shield of Hercules, 151). And: 'When the noisy, blue-winged cicada, sitting on a green branch in summer, starts singing to people, and his food and drink is the soft dew, and all day long, starting from the dawn, pours its voice in the most terrible heat, when Sirius burns the body, then primes start appearing on the millets that are sowed in summer'.

The poet Aeschylus (525-456 BC) in his tragedy *Agamemnon* also mentions Sirius the dog (verse 967).

Apollonius of Rhodes (3rd century BC) wrote his *Argonautics*, a major epic poem remolding in a poetic form the mythical expedition of the Argonauts from Thessaly to Colchis of the Black Sea. Apollonius also mentions Sirius in connection with the unbearable heat of the summer (Apollonius, 1988: Song III, v. 517):

When Minoan islands were heated from the sky by Sirius and for a long time their dwellers didn't find any treatment to this ... [And later on] 'He appeared again like Sirius, which rises to the heights from Ocean's edge.' (ibid.: Song III, v. 956).

Theognis (570–480 BC), a significant elegy poet from Megara, wrote several symposium poems, distinguished for their dignity and their respect of the gods. He even gives a rule for wine drinking, adding some information for the period around the rise of Sirius: "Witless are those men, and foolish, who don't drink wine even when the Dog Star is beginning ..." (Wender, 1984: 1039-1040).

Eratosthenes (276-194 BC) uses the word "sirios" as an adjective, writing for example: "Such stars are called sirios by astronomers, due to the quivering motions of their light." (Eratosthenes, 1997: 34).

Nonnus, a Greek epic poet of the 5th century AD from the Egyptian city of Panopolis, writes in his *Dionysiaka* about the dog burnings of Sirius: "He sent

an opposite puff of winds to cut off the hot fever of Sirius." (Nonnus, *Dionysiaka*: V 275).

In the Byzantine period, Princess Anna Comnene [Komnene, or latinized Comnena, according to Wikipedia] writes in her *Alexias*: "... even though it was summer and the sun had passed through Cancer and was about to enter Leo – a season in which, as they say, the star of the Dog rises." (Comnene, 2005: Book 3, XII.4).

4 DESCRIPTION OF A TOTAL SOLAR ECLIPSE IN THE *ODYSSEY*

In Rhapsody XX of the *Odyssey* there is the following passage: "The entrance and all the yard is full from shadows of the dead, who run in the dark. The Sun disappeared from the sky, and a thick dimness fell everywhere." (XX, 356-357).

This passage probably describes an astronomical phenomenon, possibly the most ancient Western record of a total solar eclipse. As totality is a relatively rare astronomical event for a given place, occurring on the average once every 360 years, if the area of totality is restricted then a very probable date could be determined for that eclipse (Varvoglis, 2009).

Although no solar or lunar eclipses are directly mentioned in a Homeric text, the previous verses motivated two astronomers, Constantinos Baikouzis from the Laboratory of Mathematical Physics at The Rockefeller University in New York and Marcelo Magnasco from the Proyecto Observatorio, Secretaría de Extensión, Observatorio Astronómico de La Plata, to attempt a precise determination of the date Ulysses returned to Ithaca. They hypothesized (2008) that in the *Odyssey*: XX, 356-357 Homer refers to a total eclipse of the Sun that occurred on the day Penelope's suitors were exterminated.

A prediction of an event like this is included in the literature, as the oracle Theoclymenus had warned the suitors that "The Sun will be obliterated from the sky, and an unlucky darkness will invade the world when the householder comes back and blood will be found in their dishes." (*Odyssey*: XX, 350-355).

This quotation was correlated by Baikouzis and Magnasco with other references to ancient solar eclipses in ancient texts, and certain similarities were found. Moreover, in the Homeric text there are another four astronomical 'markers' concerning the return of Ulysses to Ithaca.

The first one is the phase of the Moon: Homer notes more than once that it was the time of New Moon, so the prime prerequisite for a solar eclipse is satisfied, according to Baikouzis and Magnasco (2008).

The second has to do with Venus, which six days before the slaughter of the suitors was visible high in the sky: "As the all-bright star emerged that comes first to herald the light of the night-born Dawn, then the foam-happy ship was nearing the island." (*Odyssey*: xiii, 98-100).

The third 'marker' is about the stars and constellations Ulysses was seeing when he left the island of Calypso: 29 days before the day in question, the Pleiades were visible after sunset, as well as the constellation Boötes.

The fourth is the reference to the god Hermes (Mercury) who "... flies westwards ..." of the Ogygia island 33 days before the eclipse. According to Baikouzis and Magnasco (2008) this is a reference to the planet Mercury appearing low in the sky before sunrise. The planet undergoes retrograde motion once every 116 days, around the eastern edge of its apparent orbit.

Haris Varvoglis (2009), Professor of Astronomy at the University of Thessaloniki, notes that if we suppose that this last passage refers to the planet Mercury, then its western elongation (to the west of the Sun) and its turn to the east, along with the position of the Pleiades over the western horizon after sunset, and the simultaneous visibility of Boötes and with the apparition of Venus as 'Morning Star', all coincide once every 2000 years. Since it is known from the archaeological excavations of Troy that its destruction occurred around 1190 BC, it is clear that, if in the decades before or after that year such an astronomical coincidence happened, this can not be anything other than an independent confirmation of the year of Troy's destruction (Varvoglis, 2009: 3).

Knowing the probable year of Troy's destruction, combining all the previous astronomical information in Homer, and considered 1684 New Moons between 1250 and 1125 BC, Baikouzis and Magnasco used planetarium software to research the astronomical past of the Ionian Sea region. They discovered that a total solar eclipse occurred in 1178 BC and was visible as such from Ithaca. After a more precise calculation, they verified the exact date on the Julian calendar: 16 April in 1178 BC. They set this date as the day the suitors were exterminated. If this is true and the wanderings of Ulysses indeed covered ten years, as Homer states, then the capture and destruction of Troy should have happened in 1188 BC.

Baikouzis and Magnasco say that their research may not prove beyond a doubt the timing of the return of Ulysses to Ithaca, but it at least proves that Homer knew of certain astronomical phenomena that occurred centuries before his own age. If they are right and Homer 'tied' that date to astronomical events that can be verified, then this fact can help historians to date the fall of Troy with far greater precision.

A possible counter-argument to that position is that Homer, who is presumed to have lived in the 8th century BC, would have found it difficult to describe astronomical events that occurred more than four centuries earlier. Also, although the words of Theoclymenus seem to describe a solar eclipse, the poet may have merely wanted to give a general image in fitting with the dark fate of Penelope's suitors. Science journalist J.R. Minkel (2008) reports in *Scientific American*:

> Researchers say that references to planets and constellations in the Odyssey describe a solar eclipse that occurred in 1178 B.C., nearly three centuries before Homer is believed to have written the story. If correct, the finding would suggest that the ancient poet had a surprisingly detailed knowledge of astronomy ... Greek scholars Plutarch and Heraclitus advanced the idea that Theoclymenus's speech was a poetic description of an eclipse. They cited references in the story that the day of the prophecy was a new moon, which would be true of an eclipse. In the 1920s researchers speculated that Homer might have had a real eclipse in mind, after

calculating that a total solar eclipse (in which the moon blocks out the sun) would have been visible on April 16, 1178 BC over the Ionian Islands, where Homer's poem was set. The idea languished, however, because the first writings on Greek astronomy did not come until centuries later.

Minkel's reference to "... some researchers in the 1920s ..." includes a link to an article by C. Schoch (1926a), who first determined 16 April 1178 B.C. as the date of the total solar eclipse connected with the words of Theoclymenus (but see, also, Schoch, 1926b; 1926c; and Neugebauer, 1929).

5 CONCLUSIONS

The cosmological model of Homer, which records the views of his age, and perhaps older views as well, survived in Ionia for centuries after his death.

Writing most probably in the 8th century BC, Homer presents the Earth as a disk surrounded by the watery Ocean on all sides. The starry sky is a solid vault that must be supported in order not to fall, while Hades, an underworld, exists below Earth, being as far from the Earth as the sky.

Not all of the planets known in antiquity were mentioned in the Homeric poems, but there is persuasive evidence that their characteristics and the correlation of the state of the sky with the passage of time on Earth were widely known after a great number of empirical observations had been carried out.

In conclusion, it can be said that the Homeric references show that certain constellations and certain celestial phenomena were known to the Greeks of that age. A number of stars had been named, and they were so familiar that they were used in similes regarding gods and humans. Another interesting point is that Homer mentions some stars and several constellations under exactly the same names as used today.

Beginning with the *Iliad*, the first reference to a star occurs in the 5th Rhapsody (V, 5), where Sirius is presented as an autumnal star; it seems natural that the first star mentioned is the brightest one of the night sky. A richer astronomical reference is in the description of the shield of Achilles (XVIII, 478-488). Homer states that upon it were depicted Orion, the Hyades, the Pleiades and the Bear or Wagon, "... which rotates always at the same place, watching Orion ..." and without ever touching the Ocean. This seems to be a clear implication that this constellation is circumpolar and always visible from the northern latitudes where the epic's story is taking place. This fact makes the Bear suitable as an easily-seen navigator's aid, so its inclusion in a popular poem would be of practical use for the society. Towards the end of the *Iliad* Homer again mentions Sirius, calling it Orion's dog (XXII, 29).

In the *Odyssey* there is again a reference to circumpolar stars and to the usual constellations (v, 279-287), but this time Boötes is added.

So, in total, Homer mentions three constellations (the circumpolar Ursa Major, Orion and Boötes); two open clusters, which were then known as constellations (the Pleiades and the Hyades); the bright star Sirius indirectly (as the autumn's star and the 'bad star' bringing the dog's burnings to people); and the planet Venus as a star with its ancient Greek names for the Evening Star and the Morning Star.

There is a 'star' mentioned without a name in the *Odyssey* (V, 286): "For she told him to keep that star on his left hand when sailing in the sea." The mathematician Konstantinos Mavrommatis (2000) suggests that this is probably the Pole Star of that age. Also, the astronomer Chariton Tomboulidis (2008) mentions that in the *Iliad* goddess Athena is likened to a 'spark' star: "From the peaks of Olympus she dashed as the star that Cronides threw as a sign to humans ... a bright star and infinite the sparks that are thrown." (IV, 75-78). Probably Homer alludes here to a shooting star or meteor, as such 'stars' would be more often observed back then in the very dark skies of ancient Greece.

In the *Odyssey* there is also a very clear reference to solstices (xv, 403-404) and a probable one to the phenomenon of stellar scintillation (xii, 318).

Finally, although solar or lunar eclipses are not explicitly mentioned in the Homeric epics, it has been suggested (Schoch, 1926a; Baikouzis and Magnasco, 2008) that in the *Odyssey* (XX, 356-357) Homer alludes to a total solar eclipse from which even a specific date for the arrival of Ulysses in Ithaca can be extracted. However, caution should be taken in this instance not to confuse poetic metaphors with real astronomical events, as Homer lived approximately four centuries after the mooted eclipse of 16 April 1178 BC.

It is a fact that there is only one case of using stars or constellation(s) for orientation purposes in Homeric texts (*Odyssey*: v, 271-277). The task of teaching practical applications of astronomy was undertaken by Hesiod half a century later, with his opus *Works and Days*, which offered to Greek people the first calendar for agricultural works, a guide of seasonal activities based on the heliacal rising or setting of various stars, constellations or of the Pleiades open cluster.

The Homeric astronomical literary tradition was followed by several ancient Greek authors, such as Hesiod with his books *Works and Days* and *Shield of Hercules*, the tragic poet Aeschylus in his tragedy *Agamemnon*, Apollonius of Rhodes with his *Argonautics*, Eratosthenes of Cyrene with his *Catasterismoi*, Nonnus with his *Dionysiaca* and even the Byzantine Princess Anna Comnene with her *Alexias*.

All these references indicate that at least since Greek antiquity, starting with the Orphic Hymns (2006) and subsequently Homer's epic poems, and up to this day, certain stars and the surviving constellations retain exactly the same names.

6 NOTES

1. All the English translations from the *Illiad* and the *Odyssey* in this paper are from the Loeb editions, unless otherwise noted.

7 REFERENCES

Aeschylus, 2000. *Agamemnon*. Athens, Daedalus-Zacharopoulos Publications [in Greek].

Allen R.H., 1963. *Star Names - Their Lore and Meaning*. London, Constable.

Apollonius of Rhodes, 1988. *Argonautics*. Athens, Kardamitsa Publications [in Greek].

Aristotle, 1952. *Meteorologica*. London, Heinemann (The

Loeb Classical Library; English translation by H.D.P. Lee).

Baikouzis, C., and Magnasco, M.O., 2008. Is an eclipse described in the Odyssey? *Proceedings of the National Academy of Sciences*, 105, 8823-8828.

Comnene, A., 2005. *Alexias*, Books I to XV. Athens, Agra Publications [in Greek].

Cotsakis, D., 1976. *The Pioneers of Science and the Creation of the World*. Athens, Zoe Publications [in Greek].

Dicks, D.R., 1970. *Early Greek Astronomy to Aristotle*. London, Thames and Hudson.

Eratosthenes, 1997. *Catasterismoi*. Translated by Theony Contos in *Star Myths of the Greeks and Romans: A Sourcebook*. Grand Rapids, Phanes Press.

Flanders, T., 2007. Did the Greeks, in Homer's time, name a constellation or asterism after Achilles? *Sky and Telescope*, 114(8), 82.

Gendler, J.R., 1984. Jupiter-Saturn conjunctions in Homer's Odyssey and Iliad. *Bulletin of the American Astronomical Society*, 16, 489-490.

Genuth, S.S., 1992. Astronomical imagery in a passage of Homer. *Journal for the History of Astron*omy, 23, 293-298.

Hesiod, 1914. *The Homeric Hymns and Homerica (Theogony)*. London, Heinemann (The Loeb Classical Library; English translation by Hugh G. Evelyn-White; reprinted 1954).

Hesiod, 1988. *Theogony and Works and Days*. Oxford University Press (Oxford World's Classics; translation, Introduction and notes by M.L. West; reprinted 1999).

Homer, 1924. *The Iliad*. London, Heinemann (The Loeb Classical Library; English translation by A.T. Murray).

Homer, 1950. *The Iliad*. New York, Penguin Books (English translation by E.V. Rieu).

Homer, 1919. *The Odyssey*. London, Heinemann (The Loeb Classical Library; English translation by A.T. Murray, revised by G.E. Dimock; reprinted 1995).

Kirk, G.S., Raven, J.E., and Schofield, M., 1995. *The Presocratic Philosophers: A Critical History with a Selection of Texts*. Cambridge, Cambridge University Press (First printed 1883).

Konstantopoulos, P., 1998. *Homeric Greeks*. Two Volumes. Athens, Metron Publications [in Greek].

Lorimer, H.L., 1951. Stars and Constellations in Homer and Hesiod. *The Annual of the British School in Athens*, 46, 86-101.

Lovi, G., 1989. Stargazing with Homer. *Sky and Telescope,* 77(1), 57.

Mavrommatis, K., 2000. Astronomical elements in Homer's Odyssey. *Ouranos,* 35, 112-114 [in Greek].

Minkel, J.R., 2008. Homer's Odyssey said to document 3,200 year-old eclipse – clues in the text hint that the poet knew his astronomy. *Scientific American* (http://www.scientificamerican.com/article.cfm?id=homers-odyssey-may-document-eclipse).

Mireaux, E., 1959. *Daily Life in the Time of Homer*. New York, The Macmillan Company (English translation by Iris Sells).

Nonnus, *Dionysiaca*, (s.d.). Athens, Georgiades-Elliniki Agoge Publications (translated by E. Darviri) [in Greek].

Neugebauer, P.V., 1929. *Astronomische Chronologie*, Berlin, Walter de Gruyter.

Orphic Hymns, 2006. Athens, Ideotheatro Publications [in Greek].

Petrides, S., 2002. *The Orphic Hymns – Astronomy in the Age of Ice*. Athens, privately published.

Petrides, S., 2005. *Orpheus' Argonautica – A Dissertation on Seafaring of the Late Pleistocene*. Athens, privately published.

Schoch, C., 1926a. The eclipse of Odysseus. *The Observatory*, 49, 19-21.

Schoch, C., 1926b. Die Datierung des Trojanischen Krieges und der Irrfahrten des Odysseus. *Die Sterne*, 6, 88.

Schoch, C., 1926c. *Die sechs griechischen Dichter-Finsternisse*. Berlin, Steglitz, Selbstverlag.

Theochares, P., 1995. *The Pyramids of Argolis and their Dating*. 11th Panhellenic Conference, Nafplio [in Greek].

Theodossiou, E., and Danezis, E., 1991. *The Stars and their Myths – Introduction to Uranography*, Athens, Diavlos Publications [in Greek].

Theognis, 1997. *Lyrical poems III*. Athens, Epikairotita Publications [in Greek].

Tomboulidis, C., 2008. Homer's astronomical elements. *Ouranos*, 67, 130-133 [in Greek].

Trypanis, K.A., 1975. *The Homeric Epics*. Athens, Prometheus-Hestia Publications [in Greek].

Varvoglis, H., 2009, Pharmacology and astronomy in Odyssey. *BemaScience*, History, p. 3 [in Greek].

Walker, G.J., 1872. Astronomical allusions in Homer, Dante, Shakespeare and Milton. I. *Homer. The Astronomical Register*, 10, 229-237.

Wender, D., 1984. *Hesiod and Theognis*. New York, Penguin Books.

West, M.L. (ed.), 1988. *Works and Days*. Oxford, Oxford University Press.

Wood F., and Wood, K., 1999. *Homer's Secret Iliad: The Epic of the Night Skies Decoded*. London, John Murray.

Dr Efstratios Theodossiou is an astronomer, and an Associate Professor of History and Philosophy of Astronomy and Physical Sciences in the School of Physics at the University of Athens. His scientific interests include observational astronomy and astrophysics, satellite spectrophotometry of Be stars and history and philosophy of astronomy. He has published more than 200 scientific papers in international refereed journals and proceedings of astronomical conferences, 300 articles in Greek newspapers and journals and sixteen books on history and philosophy of astronomy and physics. He is a member of IAU Commission 41.

Dr Vassilios N. Manimanis is a post-doctoral researcher in the School of Physics at the University of Athens. His scientific interests include observational astronomy and astrophysics, photometry of cataclysmic variable stars, history and philosophy of astronomy and sciences, popularization of astronomy and bioastronomy. He has published 25 research papers in international refereed journals and many articles in popular magazines.

Petros Z. Mantarakis received a B.S. in astronomy from the California Institute of Technology, and an M.S. in astronomy from the University of Arizona. He worked in industry for thirty years, where he attained the level of President of several companies. He has 20 patents, and has published two books and numerous articles. He lives in Los Angeles, California, where he continues to write and do consulting work.

Dr Milan S Dimitrijević is an astronomer at the Belgrade Astronomical Observatory. His scientific interests include spectroscopy of astrophysical and laboratory plasma, stellar astrophysics, collisions and their influence on spectral lines, and history and philosophy of astronomy. He has published several books, around 200 papers in international journals and several hundred contributions in conference proceedings and newspapers.

J. Phys. B: Atom. Molec. Phys., Vol. 10, No. 15, 1977. Printed in Great Britain.

Stark broadening of Si III and Si IV lines

M Platiša, M Dimitrijević, M Popović and N Konjević
Institute of Physics, 11001 Beograd, PO Box 57, Yugoslavia

Received 4 April 1977, in final form 2 June 1977

Abstract. The halfwidths of seven Si III and four Si IV lines have been measured in a pulsed arc. The electron density of $5{\cdot}8 \times 10^{16}$ cm^{-3} was determined by laser interferometry, while the electron temperature of 25600 K was measured from a Boltzmann plot of the relative intensities of the Cl III lines. The experimental Si III and Si IV Stark-profile halfwidths were compared with calculated values obtained from Baranger's semiclassical and Griem's semiempirical approaches. The agreement between experiment and semiempirical results is within 15%.

1. Introduction

A recently published critical review and tables of selected data (Konjević and Wiese 1976) indicate that there are only a few reliable measurements of the Stark-broadening parameters of multiply ionised atom lines. In order to supply more data, we have performed a number of experiments to investigate the Stark broadening of the prominent spectral lines of Ar III and Ar IV (Platiša *et al* 1975a), N III (Popović *et al* 1975), O III (Platiša *et al* 1975b) and Cl III (Platiša *et al* 1977). These data were also compared with the theoretical results in order to verify the application of various approximations (Platiša *et al* 1975a, 1977, Hey 1976).

From a plasma diagnostic point of view, there is constant interest in the lines of different elements and their ion species as these can be used for the determination of the plasma electron density. Since silicon is frequently present as an impurity in laboratory plasmas, the Stark-broadening parameters of multiply ionised silicon lines may be of particular interest. Therefore, we have performed an experiment to investigate the Stark broadening of Si III and Si IV lines, and the results for some prominent lines are given in this paper. The experimental results are compared with the theoretical results calculated using two approaches (Baranger 1962, Griem 1968).

2. Calculation of the linewidths

For the theoretical evaluation of the linewidths, we have used two basically similar theoretical approaches: Baranger's semiclassical approach and Griem's semiempirical approach. Most of the detail of the theoretical calculations can be found elsewhere (Baranger 1962, Griem 1968, 1974) and therefore only a few details will be given here for completeness.

The semiclassical theory of Baranger (1962) uses second-order perturbation theory, and treats an electron–atom collision as the time-dependent perturbation of an atom by an electron moving along a hyperbolic path. In this theory, line broadening is caused only by weak inelastic transitions. If one neglects quadrupole and higher-order interactions (treating a collision as a monopole–dipole interaction), the Stark half-width of an isolated line of a radiating ion is given by

$$W = \int_0^\infty vf(v)\,\mathrm{d}v\,\frac{4\pi}{3}N_e\lambda\!\!\!^{-2}\sum_{jj'}\boldsymbol{R}_{jj'}^2\,\frac{9}{32\pi^2}f_{E_1}(\xi_{jj'})\exp(2\pi|\xi_{jj'}|) \qquad jj' = ii', ff' \tag{1}$$

where N_e, v and $\lambda\!\!\!^{-} = \hbar/mv$ are the electron density, velocity and reduced de Broglie wavelength respectively. $f(v)$ is the velocity distribution function (Maxwellian), and $\boldsymbol{R}_{jj'}^2$ is the square of the matrix element of the atomic-electron position vector $\boldsymbol{r}$ in units of the Bohr radius for upper level i and lower level j and corresponding perturbing levels i', j':

$$\boldsymbol{R}_{jj'}^2 = \frac{|\langle j|\,\boldsymbol{r}\,|j'\rangle|^2}{g_j}. \tag{2}$$

Here g_j is the statistical weight which, in the case of LS coupling, has a value for the multiplet of

$$g_j = (2L_j + 1)(2S_j + 1). \tag{3}$$

The Coulomb excitation function f_{E_1} is tabulated by Alder *et al* (1956) and in the classical limit is given by

$$\frac{9}{32\pi^2}\exp(2\pi|\xi_{jj'}|)f_{E_1}(\xi_{jj'}) = \exp(\pi\xi_{jj'})\xi_{jj'}K_{i\xi}(\xi_{jj'})K'_{i\xi}(\xi_{jj'}) \tag{4}$$

where $K_{i\xi}(\xi)$ are Hankel functions (Alder *et al* 1956, Abramowitz and Stegun 1964) and

$$\xi_{jj'} = \frac{Ze^2}{\hbar}\left(\frac{1}{v'} - \frac{1}{v}\right) \qquad \tfrac{1}{2}mv^2 = \tfrac{1}{2}mv' + \hbar\omega_{jj'} \tag{5}$$

where Z is the ionisation stage and $\omega_{jj'}$ is the angular frequency separation of levels j and j'. Argument $\xi_{jj'}$ is symmetrised with respect to the perturber velocity before (v) and after (v') an inelastic collision. Integration of the velocity in equation (1) starts at a threshold, i.e. $f_{E_1} = 0$ if $v^2 < 2\hbar\omega_{jj'}$. The right-hand side of equation (4) is equal to the Stark-broadening function $a_2(\xi, \epsilon_{\min})$ (see e.g. Griem 1974), where ϵ is the eccentricity of the hyperbolic path for $\epsilon_{\min} = 1$.

For evaluation of the linewidths, we used Griem's (1968) semiempirical approach, with the semiempirical Gaunt factor g extrapolated below the threshold for an inelastic process. This approach gives for the line halfwidth:

$$w = \frac{4\pi}{3}N_e\frac{\hbar^2}{m^2}\left(\frac{1}{v}\right)_{av}\sum_{jj'}\boldsymbol{R}_{jj'}^2\,\frac{\pi}{\sqrt{3}}\,\bar{g}\left(\frac{3kT}{2\hbar\omega_{jj'}}\right) \tag{6}$$

where

$$(1/v)_{av} = (2m/\pi kT)^{1/2}.$$

This method is based on the quasiclassical Gaunt factor obtained in the first Born approximation, using the Bethe formula for the inelastic cross section. Then, the theoretical Gaunt factor is replaced by the semiempirical one with the value 0·2 at the threshold. This value below the threshold also makes an allowance, in some way, for the contribution of the elastic collisions.

The Coulomb excitation functions are expressed through the Gaunt factor

$$\frac{9}{32\pi^2}\exp(2\pi|\xi_{jj'}|)f_{E_1}(\xi_{jj'}) = \frac{\pi}{\sqrt{3}}g(\xi_{jj'}). \tag{7}$$

In the high-energy limit, $g(\xi_{jj'})$ obtained from Coulomb excitation theory is equivalent to the quasiclassical Gaunt factor obtained in the first Born approximation, but in the adiabatic limit $g(\xi_{jj'})$ tends to unity. This is a very crude value and all attempts to improve the calculations have usually been concerned with introducing cut-off multiplicators in the electron velocity integration (Seaton 1962). On the other hand, the value $g = 0{\cdot}2$ at threshold is too low for multiply ionised atoms, as was indicated by some experimental results (Platiša *et al* 1975a, 1975b, 1977) and pointed out by Hey (1976). This also follows from recent calculations by Hayes (1975). Still, with the value $g = 0{\cdot}2$, theory (Griem 1968) gives much better agreement with experiment than with $g = 1$.

For both theoretical approaches (Baranger 1962, Griem 1968) it is necessary to evaluate the square of the matrix element of the electron position vector $|\langle j|r|j\rangle|^2$, which was taken from Bates and Damgaard (1949) and Oertel and Shomo (1968), and to perform the calculation for each particular line.

3. Experiment

The plasma source was a low-pressure pulsed arc (Konjević *et al* 1971). It consisted of a pyrex tube of 24 mm internal diameter with the distance between electrodes equal to 20 cm. At the centre of both electrodes, holes of 1 mm diameter were located for laser interferometric measurements and for end-on plasma observations. The discharge was driven by a 150 μF condenser bank charged to 1·4 kV. It was first necessary to pre-ionise the gas in the discharge tube and later discharge the main condenser bank via the ignitron. In order to obtain a uni-directional current plasma decay, a second ignitron placed in parallel with the discharge was fired after 25 μs (discharge current ringing frequency 10 kHz). During the experiment a continuous flow of an argon–silicon tetrafluoride–dichlorodifluoromethane mixture was sustained at a pressure of 0·15 Torr.

The light from the pulsed arc was observed end-on by an EMI 6255B photomultiplier–monochromator system (1 m McPherson, inverse linear dispersion 4·16 Å mm^{-1}). This instrument has, with 10 μm slits, a measured instrumental half-width of 0·047 Å. The relative spectral response of the photomultiplier–monochromator system was calibrated against a standard tungsten 'coiled-coil' quartz–iodine lamp. During the scanning of the line, great care was always taken to ensure that measurements were taken in the region of the linear response of the photomultiplier and amplifier. The output of the photomultiplier together with the current waveform were recorded on a dual-beam oscilloscope. Scanning of the Si III and Si IV lines was accomplished by repeated pulsing of the arc while advancing the monochromator

in 0·02 Å wavelength steps. All signals were analysed at the maximum electron concentration.

4. Determination of line profiles

The experimental line profiles are, in fact, the result of the superposition of a Stark profile, an instrumental profile and the profiles induced by other broadening mechanisms. To assess the importance of different broadening processes apart from electron impact Stark broadening, table 1 gives calculated linewidths for various multiplets of Si III and Si IV.

Table 1. Calculated full halfwidths of spectral lines of different multiplets of Si III and Si IV. The results are given in ångströms.

		Broadening				
Ion	Multiplet	Natural†	Doppler	Resonance‡	van der Waals‡	Ion§
Si III	4s ^{3}S–4p ^{3}P°	0·0048	0·098	0·0	$1{\cdot}9 \times 10^{-21} N_{Ar}$	0·0011
Si III	4p ^{3}P°–4d ^{3}D	0·0036	0·082	0·0	$1{\cdot}6 \times 10^{-21} N_{Ar}$	0·0015
Si IV	4s ^{2}S–4p ^{2}P°	0·0089	0·090	$2 \times 10^{-21} N_{SiIV}$	$1{\cdot}4 \times 10^{-21} N_{Ar}$	0·0006

Experimental conditions: $N_e = 5{\cdot}8 \times 10^{16}\,\mathrm{cm}^{-3}$, $T_{ion} = 25600$ K.
† Transition probabilities taken from Wiese *et al* (1969).
‡ Evaluated from Griem (1964), equations (4.104) and (4.113).
§ Evaluated from Griem (1974), equation (2186).

From table 1 it is easy to conclude that, apart from electron impact broadening (typical full halfwidth 0·15 Å), Doppler broadening makes the largest contribution to the experimental linewidth. If one takes into account the initial pressure of neutral argon (0·15 Torr) and the corresponding concentration of Si (<0·01 Torr), resonance and van der Waals broadenings are found to be negligible. The same conclusion can be drawn for ion broadening which, in all cases, is less than 1% of the experimental linewidth. However, it is interesting to note that natural line broadening is not completely negligible, in particular for the Si IV multiplet.

Therefore, the experimental line profile consists of two parts: dispersion (caused mainly by electron impact and natural broadening) and Gaussian (caused by Doppler and instrumental broadening). To obtain the Stark profile from the measured one, it was first necessary to use a deconvolution procedure for the dispersion and Gaussian profiles (Davies and Vaughan 1963). If the natural linewidth is known, it is straightforward to deduce the Stark linewidth from the dispersion profile. However, the natural linewidths did not exceed 7% of the dispersion profile linewidth.

As we knew the instrumental width, it was possible to deduce the ion temperature from the Gaussian part of the linewidth. It was found that the ion temperature and measured electron temperature are the same (within the limits of the experimental errors) for the present experimental conditions at the peak of the electron density. If we also take into account the relatively high electron concentration ($\sim 5 \times 10^{16}\,\mathrm{cm}^{-3}$), we can use the assumption of excitation and ionisation LTE for the determination of the electron temperature in our plasma (Griem 1964). An example of experimental measurements fitted with the corresponding Voigt profile

is given in figure 1. This figure illustrates, at the same time, the typical scatter in the experimental data.

The greatest care was taken to ensure that line self-absorption did not affect our lineshape determinations. This was achieved by careful examination of the line intensities and lineshapes as functions of the experimental conditions and by checking the optical depth of the strongest lines by measuring the intensity ratios within each multiplet. The experimental ratios were then compared with theoretical predictions based on *LS* coupling.

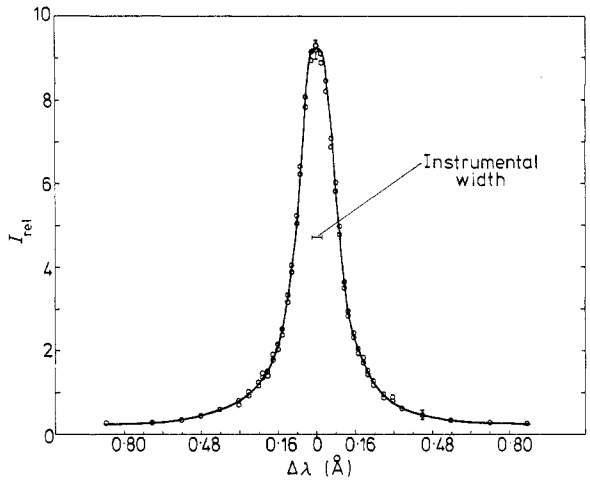

Figure 1. Experimental data (○) for the 4088·8 Å Si III line fitted with corresponding Voigt profile (——). The electron density was $5{\cdot}8 \times 10^{16}$ cm^{-3}, and the electron temperature 25 600 K.

The ratio SiF_4:Ar = 1:40 (or 1:20) was determined after a number of experiments in which SiF_4 was diluted gradually. Two criteria were used to determine the time at which to stop further dilution: (*a*) the line intensities within a multiplet should agree to within 5% with the values derived from transition probability data (Wiese *et al* 1969), and (*b*) the line intensity should start to decrease while the linewidth remains constant for the strongest lines in the spectrum investigated. It should be mentioned here that, at high dilution ratios, the plasma parameters (electron density and temperature) at constant pressure do not change within the limits of the experimental errors.

Finally, it should be noted that the experimental results presented later in table 2 were obtained end-on from the discharge in the argon–silicon tetrafluoride–dichlorodifluoromethane mixture. Traces of the third gas (CCl_2F_2) were introduced for plasma thermometric purposes, so that the relative intensities of the Cl III lines could be used to measure the electron temperature. Most of the Si III and Si IV lines were investigated in the mixture with the ratio SiF_4:Ar = 1:40, while the Si III lines 4574·76 and 3230·50 Å and the Si IV line 4116·10 Å were investigated with a mixture of ratio 1:20. The total initial pressure was 0·15 Torr.

5. Plasma diagnostics

A helium–neon laser interferometer with a plane external mirror was used to determine the axial electron density. Interferometric fringes at 6328 Å were detected by a photomultiplier placed behind the monochromator to separate the signal from the plasma radiation. The peak electron density was $5{\cdot}8 \times 10^{16}\,\mathrm{cm}^{-3}$ with an estimated error not exceeding $\pm 7\%$.

The electron temperature of 25600 K $\pm$ 10% was determined from the Boltzmann plot of the relative intensities of the Cl III lines (3191·45, 3289·80, 3393·45, 3530·03, 3612·85 and 3748·81 Å), assuming thermal equilibrium (Griem 1964); the transition probabilities were taken from Wiese *et al* (1969).

Both quoted values, for the electron density and the temperature, were taken at the peak of the electron density where all the measurements of the line profiles were performed.

6. Results and conclusions

The experimentally determined, full halfwidths of seven Si III and four Si IV lines (in ångströms) at an electron concentration of $5{\cdot}8 \times 10^{16}\,\mathrm{cm}^{-3}$ and an electron temperature of 25600 K are given in table 2. The estimated errors of these linewidths are typically $\pm 15\%$. The estimated errors do not include the uncertainty in the electron density and temperature measurements.

For the same experimental conditions, two sets of theoretical data were calculated and are also given in table 2. The semiclassical results for the linewidths according to the theory of Baranger (1962) with hyperbolic trajectories for the perturber paths are introduced in the table under W_B. The results obtained from Griem's (1968)

Table 2. Experimental Si III and Si IV full halfwidths W_M in ångströms, compared with theoretical values calculated for the same experimental conditions from Baranger's (1962) semiclassical W_B and Griem's (1968) semiempirical W_{SE} approach. $\Delta S/S$ is defined by equation (8).

Ion	Transition array	Designation (multiplet number)	Wavelength	W_M	W_B	W_{SE}	$\Delta S/S$
Si III	3s4s–3s(^{2}S)4p	^{3}S–^{3}P°	4552·62	$0{\cdot}18_0$	0·142	0·152	0·045
		(2)	4567·82	$0{\cdot}18_1$	0·142	0·152	0·045
			4574·76	$0{\cdot}17_6$	0·142	0·152	0·045
	3s4p–3s(^{2}S)4d	^{3}P°–^{3}D	3791·41	$0{\cdot}20_4$	0·157	0·176	−0·016
		(5)					
	3s4p–3s(^{2}S)5s	^{3}P°–^{3}S	3241·61	$0{\cdot}18_6$	0·151	0·173	−0·035
		(6)	3233·95	$0{\cdot}18_6$	0·151	0·173	−0·035
			3230·50	$0{\cdot}18_2$	0·151	0·173	−0·035
Si IV	4s–4p	^{2}S–^{2}P°	4088·85	$0{\cdot}12_5$	0·092	0·101	−0·017
		(1)	4116·10	$0{\cdot}12_3$	0·092	0·101	−0·017
	4p–4d	^{2}P°–^{2}D	3165·71	$0{\cdot}13_8$	0·075	0·097	0·006
		(2)	3149·56	$0{\cdot}13_7$	0·075	0·097	0·006

Experimental conditions: $N_e = 5{\cdot}8 \times 10^{16}\,\mathrm{cm}^{-3}$, $T_e = 25600$ K.

semiempirical approach are shown in the table under W_{SE}. Here it should be noted that, using a semiempirical approach, we did not lump together dipole matrix elements as was recommended by Griem (1968, 1974). The necessary condition for this simplification (Griem 1968, 1974) was not fulfilled since the Gaunt factors for the several perturbing levels are far away from the threshold value of 0·2. For example, if one uses for Si IV 4p ^{2}P°–4d ^{2}D (multiplet number 2) the sum of the dipole matrix elements for all perturbing transitions, a full halfwidth of 0·128 Å is obtained which is about 30% larger than the corresponding value in table 2.

In order to illustrate the completeness of the sets of perturbing energy levels, with regard to the dipole matrix elements, for each particular line in table 2, the parameter $\Delta S/S$ is introduced (Jones *et al* 1971)

$$\frac{\Delta S}{S} = \frac{\Sigma_{i'} R^2_{ii'} + \Sigma_{f'} R^2_{ff'} - \langle i|r^2|i\rangle - \langle f|r^2|f\rangle}{\langle i|r^2|i\rangle + \langle f|r^2|f\rangle} \tag{8}$$

where

$$\langle j|r^2|j\rangle = \frac{n^{*2}}{2Z^2}[5n^{*2} + 1 - 3l(l+1)]$$

$$n^{*2} = Z^2 \frac{E_H}{E_\infty - E_j}.$$

Here E_H is the ionisation energy of the hydrogen atom and E_∞ is the energy of the state to which the term of the level investigated converges. From the data for $\Delta S/S$ in table 2, one can conclude that sufficiently complete sets of energy levels (Moore 1965) were taken into account.

Both theoretical approaches (Baranger 1962, Griem 1968) give values which are smaller than the measured ones, although the semiempirical method is closer to the experimental data. It is possible to explain, at least qualitatively, why the values calculated from Baranger's (1962) approach are smaller. This theory does not take into account the contribution of elastic collisions, while Griem's (1968) semiempirical method takes care of elastic collisions through the integration of the perturber velocity below the threshold energies. For higher ionisation stages, typical energy-level separations are increased, so it is not correct to neglect the contribution from elastic collisions. In order to assess the importance of elastic collisions, we have calculated the dipole polarisation term for elastic collisions in the second Born approximation according to Bréchot and Van Regemorter (1964). For the Si III lines in table 2, the magnitude of the contribution of the elastic collision term is about 50% of the measured linewidths W_M, while for Si IV it is even greater than 50%. For example, for Si IV 4s ^{2}S–4p ^{2}P° (multiplet number 1) the elastic dipole polarisation term is 0·120 Å.

From the comparison between theory and experiment (table 2), one can conclude that there is agreement to within 15% with the semiempirical results (Griem 1968), although the theoretical data are systematically smaller. The results obtained from the semiclassical approach (Baranger 1962) are also systematically smaller, but the agreement is worse, in particular for the Si IV lines. The discrepancy would be decreased if one took into account the contribution of the elastic collisions to the linewidth. However, the semiempirical results obtained with a Gaunt factor of 0·2 at a threshold still agree better with experiment.

To our knowledge there is only one experimental result for the Si III 4552·62 Å line (Purić *et al* 1974) which can be used for comparison with our data and it has been obtained in a reflected shock-wave plasma at an electron temperature of 16400 K. A halfwidth of 0·36 Å is given (Purić *et al* 1974) for an electron density of $1 \times 10^{17}\,\mathrm{cm}^{-3}$. If one normalises the result for the same line in table 2 to the electron density $1 \times 10^{17}\,\mathrm{cm}^{-3}$, a full halfwidth of 0·31 is obtained. The agreement is within the limits of the experimental errors of both experiments.

References

Abramowitz M and Stegun J (ed) 1964 *Handbook of Mathematical Functions; NBS Appl. Math. Ser., No* 55 (Washington, DC: NBS)

Alder K, Bohr A, Huss T, Mottelson B and Winther A 1956 *Rev. Mod. Phys.* **28** 432–542

Baranger M 1962 *Atomic and Molecular Processes* ed D R Bates (New York: Academic Press) chap 13

Bates D R and Damgaard A 1949 *Phil. Trans. R. Soc.* A **242** 101–21

Bréchot S and Van Regemorter H 1964 *Ann. Astrophys.* **27** 739–58

Davies J T and Vaughan J M 1963 *Astrophys. J.* **137** 1302–5

Griem H R 1964 *Plasma Spectroscopy* (New York: McGraw-Hill)

——1968 *Phys. Rev.* **165** 258–66

——1974 *Spectral Line Broadening by Plasmas* (New York: Academic Press)

Hayes M A 1975 *J. Phys. B: Atom. Molec. Phys.* **8** L8–11

Hey J D 1976 *J. Quant. Spectrosc. Radiat. Transfer* **16** 575–7

Jones W W, Benett S and Griem H R 1971 *University of Maryland, Technical Report* 71–128

Konjević N, Platiša M and Purić J 1971 *J. Phys. B: Atom. Molec. Phys.* **4** 1541–7

Konjević N and Wiese W L 1976 *J. Phys. Chem. Ref. Data* **5** 259–308

Moore C E 1965 *Selected Tables of Atomic Spectra* NSRDS-NBS3 (Washington, DC: US Govt Printing Office)

Oertel G K and Shomo L P 1968 *Astrophys. J. Suppl. Ser.* **16** 175–91

Platiša M, Dimitrijević M, Popović M and Konjević N 1977 *Astron. Astrophys.* **54** 837–40

Platiša M, Popović M, Dimitrijević M and Konjević N 1975a *Z. Naturf.* **30a** 212–5

Platiša M, Popović M V and Konjević N 1975b *Astron. Astrophys.* **45** 325–7

Popović M V. Platiša M and Konjević N 1975 *Astron. Astrophys.* **41** 463–5

Purić J. Djeniže S. Labat J and Ćirković Lj 1974 *Z. Phys.* **267** 71–5

Seaton M J 1962 *Atomic and Molecular Processes* ed D R Bates (New York: Academic Press) chap 11

Wiese W L, Smith M W and Miles B M 1969 *Atomic Transition Probabilities* NSRDS-NBS22, vol 2 (Washington, DC: US Govt Printing Office)

J. Phys. B: Atom. Molec. Phys., Vol. 12, No. 11, 1979. Printed in Great Britain

On mutual angle and energy distributions near ionisation thresholds for electron–ion collisions

M S Dimitrijević† and P V Grujić‡

† Institute of Applied Physics, PO Box 24, 11001 Belgrade, Yugoslavia
‡ Institute of Physics, PO Box 57, 11001 Belgrade, Yugoslavia

Received 6 November 1978

Abstract. Angular correlations between the escaping electrons after ionising collisions between an electron and single-, double- and triple-charged hydrogenic ions have been examined in the vicinity of the ionisation thresholds. Numerical investigations indicate, within a restricted classical model, an increasing spread of the mutual-angle distribution with an increase of the ion charge, but do not reveal the total disappearance of all angular correlations for an ion nuclear charge $Z \geqslant 3$, as predicted by Rau. The increase in the total spread of the mutual angle with the nuclear charge has been fitted by a $Z^{0.56}$ power law. Dependence of the angular spread on the total energy has been examined for e–Li^{2+} and excellent agreement with the analytical prediction of Vinkalns and Gailitis has been obtained. The final energy distribution generally appears to be uniform, as in the case of electron–neutral-atom collisions, but in some cases it deviates from this simple behaviour when $Z \geqslant 3$. The relation between the regular non-uniform distributions and those suggested by Temkin and Rau has been discussed.

1. Introduction

The advance of experimental techniques and the extensive use of powerful computers have renewed interest in near-threshold ionisation processes for electron–atom collisions. Apart from the threshold law, derived analytically as early as 1953 by Wannier and confirmed both experimentally (e.g. McGowan and Clarke 1968, Cvejanović and Read 1974) and numerically (e.g. Banks *et al* 1969, Peterkop and Tsukerman 1970, Grujić 1972), some other features, peculiar to near-zero total energy processes, have attracted the attention both of experimenters and theoreticians. In particular, the mutual-angle distribution function for e–He ionisation has been investigated experimentally by Cvejanović and Read (1974) and numerically for e–H collisions (Grujić 1976). Both measurements (Cvejanović and Read 1974) and computer calculations for e–H (e.g. Grujić 1972) and e–He^+ (Cvejanović and Grujić 1974, Boesten *et al* 1976) of the total energy partition between the escaping electrons agree with the numerical analysis of Vinkalns and Gailitis (1967), which was the first to indicate that every partition of the available energy between the outgoing electrons should be equally probable (see, however, Temkin 1974).

Of particular importance to the present work are three analytical approaches by (i) Vinkalns and Gailitis (1967), (ii) Peterkop (1971) and (iii) Rau (1971). In (i) a purely classical approach was employed, though different from the original Wannier one. Besides re-deriving Wannier's threshold law, these authors found that the spread of the

$\theta_{12}-\pi$ distribution function should decrease with a decrease of the total energy E as $E^{1/4}$, for $Z \leqslant 2$, and as

$$E^{1/4-\nu/2} \qquad \nu = \tfrac{1}{2}[(4Z-9)/(4Z-1)]^{1/2} \qquad \text{for } Z \geqslant 3 \tag{1}$$

Z being the charge of the nucleus of the hydrogenic target (atomic units are used throughout). It was argued that only a full quantum mechanical calculation in the innermost region (of the order of the dimensions of the target) could yield the proper form of the differential cross section. The Wannier part of the phase-space of the electron–hydrogen-atom system has been investigated semiclassically by Peterkop (1971), who derived a constant differential cross section, in the vicinity of the saddle point of the potential (method (ii)). Finally, Rau (1971) carried out a quantum mechanical analysis in the same (Wannier) region and also confirmed Wannier's results (method (iii)). Later the same author (Rau 1976) expanded his analysis and found that, in the first approximation to $\theta_{12}-\pi$, the angular distribution function should be Gaussian in shape.

It is worth emphasising the following common features of the above calculations: (i) the authors restricted themselves to the Coulomb zone, where all important correlation effects persist; (ii) the energy dependence of the spread of the distribution functions for $Z = 1, 2$ is that quoted in Vinkalns and Gailitis (1967). The latter result has been corroborated by the measurements of Cvejanović and Read (1974), but the experiment was unable to provide the shape of the angular distribution.

Besides taking actual measurements, one can investigate collision phenomena by making use of computer simulations of a real experiment. This can be done in several ways, e.g. by applying a Monte Carlo method (see, e.g. Suzukawa and Wolfsberg 1978). These procedures, however, are not suitable for the investigation of near-threshold behaviour, because the ionisation probability is extremely small in that energy region. In this case one must resort to a combined graphical and non-random integration method, which has already been used in some previous calculations. However, whilst being successful in providing the threshold law, this method is of only limited value in investigating distribution functions. Nevertheless, it can give an insight into some general features of near-threshold phenomena, in particular into the angular and energy distributions, as indicated earlier (Grujić 1976). This method is used here in order to study some properties of the angular and energy distributions in the vicinity of the threshold in He^{+}, Li^{2+} and Be^{3+}.

In the next section we give a brief description of the classical three-body computer program, together with some details of the numerical procedures employed. Numerical results are presented in § 3 and then discussed in § 4.

2. Numerical procedure

As in previous calculations, the computer program developed by Abrines *et al* (1966) has been used, with a modified Runge–Kutta subroutine due to Banks and Wilson (private communication). The program is based on the classical three-body system, which in our case consists of the incident electron and a hydrogenic ion with a nuclear charge Z. For the purpose of our calculations, the program has been modified in three respects: (i) non-random integration is adopted, at variance with the original Monte Carlo procedure; (ii) asymptotic initial-state Coulomb interaction between the impinging electron and the ion has been accounted for by inserting a subroutine which

evaluates the initial position and moment of the incident particle, from given values at infinity; (iii) the code has been converted into double precision so that a typical accuracy of 99% has been achieved.

The classical three-body model describes the target ion by a nucleus (practically) at rest in the laboratory system, with an electron moving around it along a Kepler orbit, and the incident electron moving along the $0z$ axis from infinity. The entire system can be defined (at a fixed total energy E) by six parameters: the total angular momentum (L); the angular momentum of the target (l); the Euler angles of the Kepler orbit (ϕ, θ, ψ); and the position of the atomic electron on the orbit, defined by the time parameter t. Obviously, a full statistical treatment of any near-threshold distribution function would be a formidable computational task. Even disregarding the time needed to find out ionisation intervals, a complete treatment of the angular distribution would mean calculations of N^6 trajectories, where N is the number of values of a particular parameter. Adopting $N = 10$ and taking an average computing time of 1 min/orbit (a typical value), it is obvious that this kind of approach would not be feasible even with the help of the very powerful computers available at present. Consequently, one has to resort to a more restricted model which will not give the exact shape of any differential cross section.

We have chosen the following (plane case) model: $L = 0$, $l^2 = 0{\cdot}5$, $\theta = \frac{1}{2}\pi$, $\psi = \frac{1}{2}\pi$ (see figure 1). Values of l^2 being uniformly distributed within a microcanonical ensemble (see e.g. Abrines *et al* 1966), the choice of $l^2 = \langle l^2 \rangle = 0{\cdot}5$ is aimed at a partial compensation for the omitted variation. (This choice seemed more appropriate than that of $l^2 \simeq 0{\cdot}8$ (Grujić 1972).)

The general computational procedure is as follows. For a fixed value of ϕ, the time parameter t is varied over the whole interval $(0, \tau)$, where the orbit period τ is given by

$$\tau = (2\pi/\mu)(n^3/Z^2) \tag{2}$$

where μ is the electron–nucleus reduced mass, and n the principal quantum number (in our case $n = 1$). The program calculates the final energy of the impact electron as a function of t (see figure 2) so that ionisation intervals are determined by means of graphical interpolations. The largest of these intervals is examined further by computing trajectories within the interval. The accuracy of the final computed values is checked by comparing conserved quantities, the total energy and the total angular momentum of the system, before and after the collision.

3. Results

3.1. Angular distributions

We first examined the case of e–He^+, i.e. $Z = 2$. A typical electron final-energy curve is plotted in figure 2 against the time parameter t. The ionisation intervals, defined by E_1^f, $E_2^f > 0$ are determined by the intersections of E_1^f (E_2^f) with $E^f = 0$ and $E^f = E$ (see figure 3). Generally, one of these intervals is much larger than the others. In the particular case shown in figure 2, this is the interval furthest left, which has been shown in more detail in figure 3. The final electron energy, as seen in figure 3, is a strictly linear function of t, showing that the energy distribution function

$$F_t(E_1^f) = \text{const}\ \mathrm{d}t/\mathrm{d}E_1^f \tag{3}$$

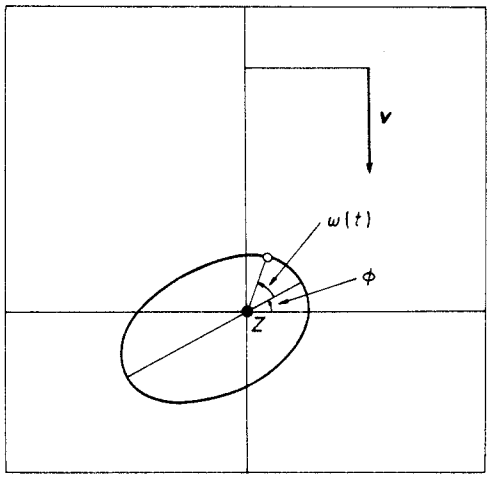

Figure 1. The initial (schematic) configuration for an electron–hydrogenic-ion collision, for the plane case $L = 0$ (see text).

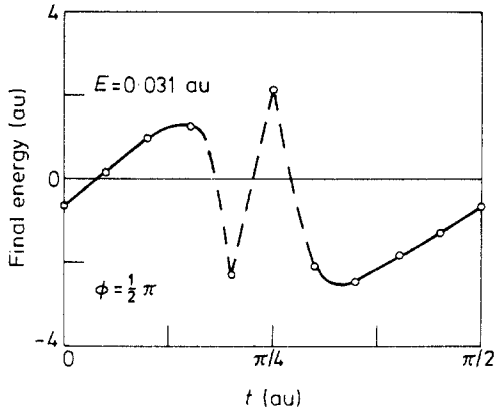

Figure 2. Final energy of one of the electrons as a function of the initial time parameter t (see text), for e–He^+ collisions.

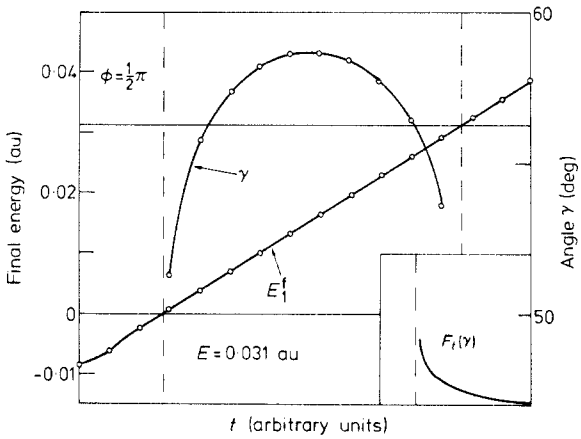

Figure 3. Electron final energy and mutual angle parameter $\gamma(=\pi-\theta_{12})$ in the ionisation interval, for e–He^+ collisions. The angular distribution, corresponding to the γ curve is sketched in the lower right-hand corner (see text).

is constant over the entire ionisation interval. The corresponding distribution function for the mutual angle θ_{12}

$$F_t(\theta_{12}) = \text{const}\ \mathrm{d}t/\mathrm{d}\theta_{12} \tag{4}$$

indicated at the lower right-hand corner of figure 3, is strongly peaked at the particular (minimum) angle and can be approximated well by a delta-function. Repeating computations for different ϕ values, we have obtained a set of $\gamma = \pi - \theta_{12}^{\min}$ (ϕ) values, as shown in figure 4. One point computed for $l^2 = 0{\cdot}8$ is presented for the sake of comparison. Making use of the curve in figure 4 one could calculate the distribution $F_\phi(\gamma) = \text{const}\ \mathrm{d}\phi/\mathrm{d}\gamma$, as was done in the case of $Z = 1$ (Grujić 1976), but we shall dispense with that here, sketching only the general shape of this function in the upper

right-hand corner of figure 4. What is, however, of importance here is the total spread of $F_\phi(\gamma)$, which is given by the length of the interval $[0, \gamma(\frac{3}{4}\pi)]$, as seen from figure 4. Another important feature of $F_\phi(\gamma)$ is that its maximum is well removed from $\gamma = 0$, in accordance with the findings for e–H collisions, where the maximum is situated at $\theta_{12} = \pi$ only for much smaller total energies (Grujić 1976). Hence, if the actual distribution is to be Gaussian, it must be at $E \ll 0{\cdot}03$ au, according to the model adopted here. Analogous computations have been carried out for e–Li^{2+} collisions, and the results are shown in figure 5. Comparing curves from figures 4 and 5 one sees: (i) the simple, almost linear, form of $\gamma(\phi)$ for He^+ disappears; (ii) the total spread is again determined by $\gamma(\frac{3}{4}\pi)$.

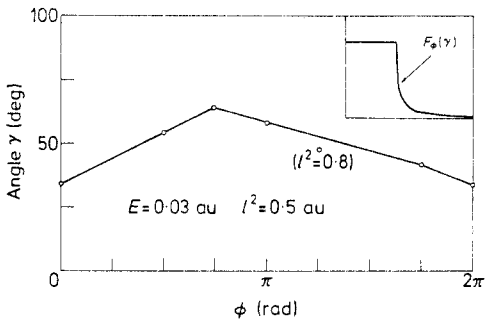

Figure 4. Mutual angle parameter $\gamma(=\pi-\theta_{12}^{\min})$ versus the initial orientation of the Kepler orbit ϕ, for e–He^+ collisions. The angular distribution, derived from the γ function is sketched in the upper right-hand corner (see text).

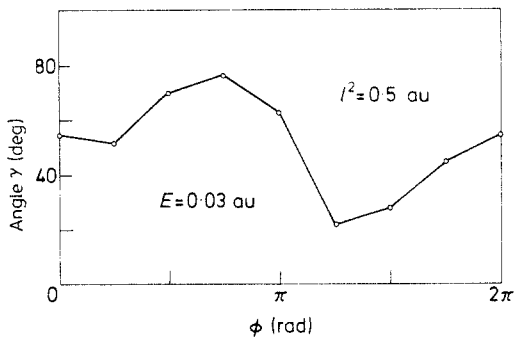

Figure 5. Same as for figure 4 but for e–Li^{2+} collisions.

Assuming that (ii) is a common feature for $Z \geqslant 3$ (although this assumption is not a crucial one), we carried out computations for e–Be^{3+} at $\phi = \frac{3}{4}\pi$ only, since as the nuclear charge increases the curves $E_1^f(t)$ become more oscillatory and generally the computations become much more involved.

In order to see how the spread of $F_\phi(\gamma)$ depends on Z, we have plotted $\gamma(\phi = \frac{3}{4}\pi)$ versus the nuclear charge Z, as shown in figure 6. As can be seen, the angle γ increases monotonically with Z, and no radical change is observed in passing from $Z = 2$ to $Z = 3$. In order to test this monotonic behaviour of γ further, the value for the $Z = 1$ case has also been plotted (note, however, that the latter had been calculated with $l^2 = 0{\cdot}8$ au). The point calculated from the results for e–H (Grujić 1976) fits the general behaviour well.

In order to test the analytically derived formula for the spread of the angular distribution (Vinkalns and Gailitis 1967), we carried out computations of $\gamma(\phi = \frac{3}{4}\pi)$ for e–Li^{2+} collisions at two more energies. The results are presented in table 1, together with the best fit function of the form $\gamma = \alpha E^\beta$ (second and third columns). As can be seen from the third column in table 1, the best fit β exponent is in excellent agreement with the analytically derived (Vinkalns and Gailitis 1967) value of $\beta = 0{\cdot}1195$. Judging from the dispersion of the computed points, this almost exact coincidence is however somewhat fortuitous.

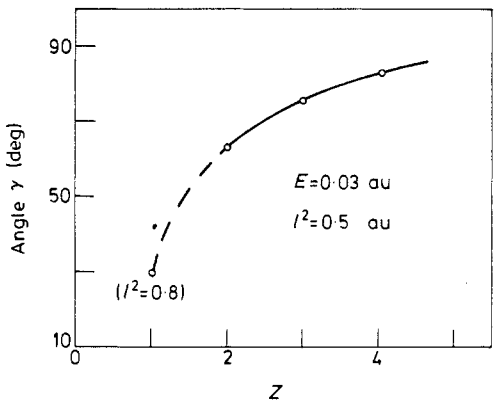

Figure 6. The spread of the angular distribution, at $\phi = \frac{3}{4}\pi$, versus the ion charge Z (see text).

Table 1. Mutual angle parameter $\gamma = \pi - \theta_{12}^{\min}$ and ionisation intervals Δt (second and fourth columns) and corresponding best-fit values (third and fifth columns) at different total energies E in the case of e–Li^{2+} collisions (see text).

E (au)	γ (deg)	$117{\cdot}1\,E^{0{\cdot}1196}$	$\Delta t \times 10^5$ (au)	$284\,E^{1{\cdot}033}$
0·0064	64·33	64·01	1·65	1·539
0·0316	76·58	77·48	8·04	8·007
0·0615	84·50	83·91	15·9	15·93

3.2. Energy distributions

As already mentioned, all numerical investigations up to now and the only measurements carried out (Cvejanović and Read 1974) do not reveal any deviation from energy uniformity in the final (ionised) state near the threshold. However, it was argued by Rau (1976) that, taking the second-order correction to the differential cross section $\beta^2\gamma^2$ ($\beta = \frac{1}{4}\pi - \tan^{-1}(r_2/r_1)$) there should be a non-uniformity in the β distribution at relatively large values of γ, for $Z = 1, 2$. We looked for deviations in the linear dependence of E_1^f (E_2^f) on t, for e–He^+, and did not find any, even for $\gamma > 50°$. For instance, at $\gamma = \gamma(\frac{3}{4}\pi) \simeq 64°$ the linearity persists in the E_1^f energy band for an order of magnitude beyond the total energy E. However, we found that in a few particular cases (i.e. at a specific ϕ value) of e–Li^{2+} collisions, the energy distribution does deviate from uniform. The function $E_1^f(t)$ within the ionisation interval for $\phi = \frac{3}{4}\pi$ and $E = 0{\cdot}0064$ au ($\gamma = 56{\cdot}4°$) is shown in figure 7. No attempt has been made to extract an energy distribution $F_t^f(E_1) = \text{const}\ dt/dE_1^f$, but it is evident from figure 7, that F_t has a minimum near the centre of the ionisation interval, i.e. at small β values. This is opposite to Rau's (1976) analysis for $Z = 1, 2$. One can interpret this result with the following simple considerations. If the escaping electrons share the available energy unequally, i.e. if $\beta \neq 0$, then γ may be relatively large, since the electron mutual distance can still be large ($r_1 \gg r_2$), in contrast to the case of $r_1 \simeq r_2$ when the 'harmonic-oscillator force' imposes strict correlation in θ_{12} on the motion. In other words, if $E_1 \gg E_2$ the outgoing electrons may follow each other and still both escape.

If this interpretation is correct, then the 'non-linearity effect' might be present whenever γ is large. We examined the ionisation interval for e–Be^{3+}, where $\gamma = 83{\cdot}3°$ ($\phi = \frac{3}{4}\pi$) and found an energy dependence quite analogous to that in figure 7.

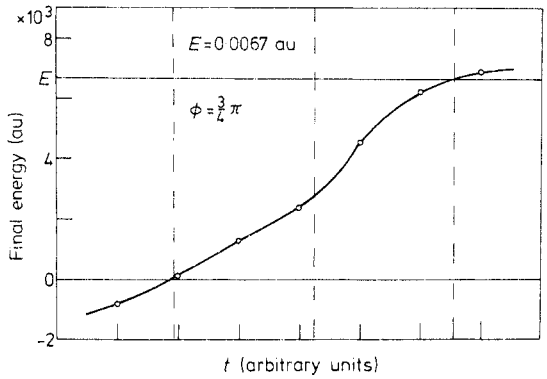

Figure 7. Final energy of one of the electrons, for e–Li^{2+} collisions.

Generally, present calculations reveal that energy distribution does not follow the usual pattern corresponding to $Z<3$ for $Z\geqslant 3$. In one particular case of e–Li^{2+}, $E = 0{\cdot}0064$ ($\phi = \frac{3}{4}\pi$) the $E^{f}_{1(2)}(t)$ functions are quite irregular and show an undulatory character in the ionisation interval. In order to check if this ionisation interval can be used in deriving the threshold law, we calculated the lengths of three ionisation intervals, and the results are shown in table 1 (fourth column), together with values obtained from the best fit to aE^{b} function. As can be seen from table 1, computed values are in fair agreement with the Wannier threshold behaviour $E^{1{\cdot}036}$, particularly considering Δt (0·0064) was rather poorly determined. Consequently, the uniformity of energy distribution does not seem to be crucial in determining the threshold law for the ionisation cross section.

4. Discussion

The present calculations have revealed a gradual increase in the spread in the mutual-angle differential cross section as the ionic targets become more charged and this was as expected. As the influence of the remaining ion nucleus increases, the role of electron correlation diminishes. That this change in the spread as a function of Z can be regarded as an actual representation of the change in the complete angular distribution has been corroborated by the high level of agreement between the total spread behaviour, as a function of E, and the analytically derived law. Our numerical results conform more to Peterkop's (1971) expressions than to those of Rau (1971). It should be noticed that the present approach is in a sense complementary to treatments (i)–(iii) quoted earlier: we have confined ourselves to a plane, but our treatment covers the entire range of r_1, r_2, while the analytical treatments mentioned employ a full three-dimensional space, but remain outside the inner zone, i.e. $r_1^2 + r_2^2 > R^2$.

The energy distribution behaviour in the case of Li^{2+} and Be^{3+} turned out to be irregular, ranging from a simple uniform distribution to quite complicated forms.

Generally, we conclude that, as the ion charge increases, the energy differential cross section may become inhomogeneous. As Wannier's threshold law turns into a linear function for $Z \gg 1$, since all correlation effects die out, the uniform energy distribution may disappear for the same reason. Whether this effect would be measurable depends on the relative frequency of the 'irregular' ionisation intervals. Hence, in the case of $Z \geqslant 3$ a numerical derivation of an actual energy distribution may require a full 'six-parameter statistical treatment', just as in the case of the mutual-angle distribution.

The present numerical investigations have not revealed the predicted $Z = 2 \rightarrow Z = 3$ 'jump' in the mutual-angle distribution, but have indicated that the jump may appear in the energy distribution. It is interesting to notice that a non-uniform distribution was put forward by Temkin (1974) for any value of Z. We can say that in a number of cases examined in this work, our findings are not inconsistent with the distribution which he proposed.

As for possible experimental investigation, it would be of interest to perform measurements with double- and triple-charged ions and see whether the features calculated numerically are dominant or, at least, noticeable. As was done by Cvejanović and Read (1974) with He, both angular and energy distributions could be checked in a single experimental arrangement.

Acknowledgments

The present work has been accomplished with financial support from RZN SR Serbia. We would like to thank Professor I Percival and Drs N Valentine and D Banks for the three-body classical computer program. Useful discussions with Dr S Cvejanović are also acknowledged.

We are indebted to the Federal Hydro-meteorological Centre, Belgrade, for providing us with computing facilities.

References

Abrines R, Percival I and Valentine N 1966 *Proc. Phys. Soc.* **89** 515–23
Banks D, Percival I C and Valentine N 1969 *Proc. 6th Int. Conf. on Physics of Electronic and Atomic Collisions* (Cambridge, Massachusetts: MIT Press) pp 215–6
Boesten L G J, Heideman H G M, Bonsen T F M and Banks D 1976 *J. Phys. B: Atom. Molec. Phys.* **8** L1–4
Cvejanović S and Grujić P 1974 *Proc. Symp. on Ionized Gases* (Rovinj: Institute of Physics of the University, Zagreb) pp 65–7
—— 1975 *J. Phys. B: Atom. Molec. Phys.* **8** L305–9
Cvejanović S and Read F H 1974 *J. Phys. B: Atom. Molec. Phys.* **7** 1841–52
Grujić P 1972 *J. Phys. B: Atom. Molec. Phys.* **5** L137–9
—— 1976 *Proc. Symp. on Physics of Ionized Gases* (Dubrovnik: J Stefan Institute, Ljubljana) pp 70–3
McGowan J W and Clarke E 1968 *Phys. Rev.* **167** 43–51
Peterkop R 1971 *J. Phys. B: Atom. Molec. Phys.* **4** 513–21
Peterkop R and Tsukerman P B 1970 *Zh. Eksp. Teor. Fiz.* **58** 699–705
Rau A R P 1971 *Phys. Rev.* A **4** 207–20
—— 1976 *J. Phys. B: Atom. Molec. Phys.* **9** L283–8
Suzukawa H H Jr and Wolfsberg M 1978 *J. Chem. Phys.* **68** 1423–5
Temkin A 1974 *J. Phys. B: Atom. Molec. Phys.* **7** L450–3
Vinkalns I and Gailitis M 1967 *Latvian Academy of Science Report* No 4 (Riga: Zinatne) pp 17–34
Wannier G H 1953 *Phys. Rev.* **90** 317–25

J. Phys. B: At. Mol. Phys. **14** (1981) 1663–1674. Printed in Great Britain

Electron–helium double ionisation near the threshold: numerical investigations

M S Dimitrijević† and P Grujić‡

† Institute of Applied Physics, PO Box 24, Belgrade, Yugoslavia
‡ Institute of Physics, PO Box 57, Belgrade, Yugoslavia

Received 21 August 1980, in final form 12 December 1980

Abstract. The classical trajectory method is applied to the investigation of low-energy $e + He \rightarrow He^{2+} + 3e$ collisions. In contrast to the hydrogenic case numerical calculations appear unable to derive the ionisation threshold law by varying one or two initial parameters. Final electron energies appear as linear functions of the initial time parameter and it is conjectured that the energy distribution should be uniform within the total energy interval: $0.544 \leq E \leq 6.75$ eV. Calculated angular correlations between the three escaping electrons conform to the full central symmetry at very small energies, but go over to axially symmetric configurations as the energy rises. The final angular momenta acquire large values, with dramatic enhancement at the edges of an ionisation interval, where momentum exchange becomes particularly strong. Finally, the applicability of the classical model to non-hydrogenics is discussed, as well as some stochastic effects encountered.

1. Introduction

Since renewed interest in the classical theory of atomic collisions was initiated by Gryzinski (1959), much work has been done, both analytically and numerically, concerning charged-particle–atom(ion) collisions within the classical picture (see e.g. Burgess and Percival 1968). However, the classical approach to atomic processes has been used either for charged-particle–hydrogenic collisions (such as e–H scattering) or 'hydrogen situations' (e.g. electron–Rydberg-atom collisions), which reduce essentially to a three-body problem (see e.g. Percival and Richards 1975). Another approach, adopted by Gryzinski (see e.g. Gryzinski 1979), which treats the atomic target as a dynamical stationary system, reduces to particle—time-dependent-potential scattering.

All numerical calculations based on the classical trajectory method, since the appearance of the three-body computer code of Abrines and Percival (1966), have been, in fact, dealing with hydrogenic systems, regardless of the processes considered. Bonsen and Banks (1971) did some computations for p–He ionisation, but the approximation they used reduced the classical scattering model to the binary encounters approach, which is essentially a quasi-three-body problem. In the case of the near threshold processes this is not a serious drawback, since in the ionisation volume (and its close vicinity) of the phase space all atoms behave as quasi-single-electron systems (e.g. Cvejanović and Grujić 1975). However, in the case of processes where more than one active atomic electron takes part, as in case of a multiple ionisation, the problem of setting up a reasonable classical many-electron atomic system must be directly faced.

0022-3700/81/101663+12$01.50

This is not a trivial extension of the hydrogen model, since, as is well known, it is the failure of the old quantum theory to provide an adequate non-hydrogenic model (see e.g. Percival 1980) that led to quantum mechanics.

The aim of this paper is twofold. Firstly, we want to examine how effective a purely classical two-electron atomic model can be in describing a class of electron–atom processes, such as the near-threshold double ionisation of He. Secondly, unlike the single-ionisation threshold processes, when all theoretical and experimental data agree on the threshold law (see e.g. Grujić 1972, and references therein), there is disagreement between the analytical calculations (Wannier 1955, Klar and Schlecht 1976) and the unique experimental results (Brion and Thomas 1968). Besides this principal aim, numerical investigation of the energy and angular distributions and angular momenta behaviour are also of interest. Unfortunately, it turned out that the procedure of varying only one (or two) parameter, which was successful in the case of hydrogenics, does not work in the case of a three-electron system as far as the threshold law is concerned. On the other hand, the study of angular distributions and angular momenta behaviour have revealed some new interesting features.

In § 2 the physical model adopted for e–He collisions is set up and discussed, as well as the computer code used in the numerical calculations. Calculations of the ionisation threshold law, the energy and mutual angle distributions, and of the angular momenta of the escaping electrons, are presented in § 3. Finally, the capability of the classical trajectory method in describing many-electron threshold effects is disucssed in the last section, together with some intrinsic computational difficulties met.

2. Calculations

2.1. e–He classical model

The helium model we have adopted is based on the so-called Bohr's model (see Leopold and Percival 1980, for this and some other classical set-ups), which consists of two electrons revolving around the nucleus along the common (circular) orbit. The model assumes elliptical rather than circular orbits (see figure 1), but it preserves the original symmetry with regard to both radius and velocity vectors of the electrons. This

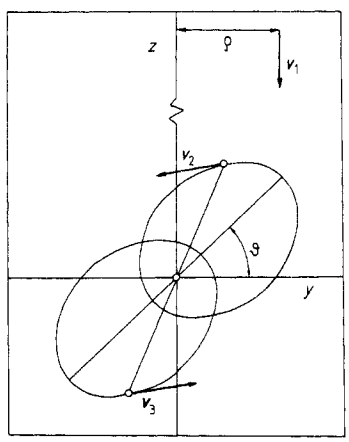

Figure 1. Electron–helium scattering classical model (initial configuration).

symmetry is important in numerical calculations, as it ensures a reasonable stability of the atomic system. Further, the model provides a fairly good ground state energy: −3.063 au, as compared with the actual value: −2.9037 au.

Hence, our collision model consists of an impact electron moving along the Oz axis, with an impact parameter ρ and the quasi-hydrogenic helium target in the same plane, as shown in figure 1. The computer program used is based essentially on the code developed by Abrines *et al* (1966) for three-body classical-trajectory Monte-Carlo calculations. The code is modified and extended for the purpose of dealing with quasi-four-body systems. Besides removing all statistical features of the code (see Dimitrijević and Grujić 1979, to be referred to as I) essential modifications to the program are:

(*a*) The code has been converted into double precision (14 significant figures). This change is imposed by the greater complexity of the system, and particularly by the nature of the physical process under consideration, since the double-ionisation intervals were expected to be much smaller than those for single ionisation. This double-precision conversion has been carried out in two stages: (i) first only the Runge–Kutta integration routine has been rewritten, the rest of the program being left in single precision. This ensured an accuracy better than 99% in the total energy calculated value as well as in the total angular momentum numerical results; (ii) when the total energy was decreased below 0.08 au, the entire code was put into double precision, so that the input data were determined very accurately, too. The importance of this improvement will be disucssed in the last section.

(*b*) We have set the target nucleus to be at rest at the origin, so that the system consists of three (identical) particles moving in the Coulomb field (quasi-three-body problem). The program then solves the corresponding Newton equations (cf Percival 1973) (atomic units are used throughout).

$$\frac{\mathrm{d}^2\boldsymbol{r}_i}{\mathrm{d}t^2}=-\frac{2}{r_i^2}+\sum_{j\neq i}\frac{\boldsymbol{r}_i-\boldsymbol{r}_j}{|\boldsymbol{r}_i-\boldsymbol{r}_j|^3} \qquad i,j=1,2,3. \tag{1}$$

(*c*) The exit routine, which checks if a final configuration has been achieved, had to be extended considerably, the number of possible 'channels' in the final configurations being enlarged by introducing the third electron. Since in the final channel the two-electron bound state is (classically) inaccessible (cf Cvejanović and Grujić 1975), the computing proceeds until at least two electrons reach the free state; this inevitably prolongs the computing time per orbit†.

For the fixed helium (ground) state energy and the total angular momentum $L=0$, the system can be described initially by the parameters: ε (eccentricity), θ (orientation of the major axis), t (time parameter) and the impact energy E_e. The primary goal is to find an ionisation interval by varying at least one of the quantities: ε, θ and t (with E_e fixed). Once the ionisation interval is localised, the quantities of interest, like the final energies, angular momenta, etc, are calculated, within and around it, as functions of the initial parameter varied. The initial values of the parameters varied are distributed equidistantly and, where necessary, a graphical interpolation is employed so as to save computational time, which was typically 2 min per orbit, within or close to an ionisation interval. The program calculates the final energies, angular momenta and mutual angles (in case of triple escape).

† We are indebted to Dr S Cvejanović for help in developing the exit routine.

3. Results

3.1. Threshold Law

3.1.1. Review of analytical and experimental investigations. The first conjecture of the possible threshold behaviour of the double ionisation cross sections was made by Wannier (1955), who concluded, on the basis of simple geometrical considerations, that electron–atom multiple ionisation should follow the power law

$$\sigma_I^{(n)} \propto (\sigma_I^{(1)})^n \tag{2}$$

where $\sigma_I^{(1)}$ is the cross section for the single ionisation (double escape) and n is the degree of ionisation. Further, following his previous classical study of single ionisation near threshold (Wannier 1953) he suggested that the double ionisation threshold law should read, approximately:

$$\sigma_I^{(2)} \propto E^{2.254} \tag{3}$$

where E is the total energy, i.e. the exponent should be somewhat larger than 2, the value corresponding to the no-correlation case.

In their analytical quantum mechanical study of the multiple escape of electrons from a Coulomb field Klar and Schlecht (1976) found that the dominant contribution to the ionisation probability close to threshold comes from the doublet quantum state, and that the exponent (cf equation (3)) has the value 2.270†.

To our knowledge, the only experiment performed to derive the double ionisation threshold behaviour was done by Brion and Thomas (1968) by measuring the intensity of the $^3He^{2+}$ ion current. Although the electron energy resolution quoted (50 meV) was sufficient to reveal a deviation from the square law, they fitted the results to E^2 behaviour in the energy region (0–25 eV) above the double ionisation threshold. This is to be regarded as more disturbing in view of their $e + He \rightarrow He^+ + 2e$ results, which they found definitely in accordance with the $E^{1.127}$ power law in the region 0–12 eV. However, it is to be noted that, in general, the low-energy ionisation cross section curve goes over to the no-correlation case if either the impact electron energy spread is too large or the total energy interval considered is too wide. It is the latter case which seems to have affected the results for the double ionisation and more elaborate investigations in the energy range 0–5 eV are needed (in particular, experimental set-ups of the type due to Cvejanović and Read (1974) are desirable).

3.1.2. Numerical search for the threshold law. In searching for the ionisation intervals we have adopted the same strategy as in I, keeping the θ and ε parameters constant and varying the positions of the atomic electrons on their Kepler orbits *via* the time parameter t (see figure 1). In the energy region $2.4 \leqslant E \leqslant 6.75$ eV the following values have been used: $\theta = 297.5°$, $\varepsilon \simeq 0.8$, the latter meaning that $l_1 = -1.4$ au, $l_2 = l_3 = 0.7$ au (the initial values of the electron angular momenta). An ionisation interval is determined by the requirement that the final energies of all three electrons are positive: $E_1^f, E_2^f, E_3^f > 0$ ($E_1^f + E_2^f + E_3^f = E = \text{constant}$). In figure 2 an ionisation interval at $E = 0.1682$ au (4.6 eV) is shown. This has the typical energy dependence on t of all 'high-energy' intervals ($E > 2$ eV), with the impact electron energy curve running

† Interestingly, though the latter authors quote Wannier's theory for the single ionisation, no mention of his work of 1955 has been made. On the other hand, Klar and Schlecht's results for the multiple ionisation (p 1709) have been, in our opinion, misinterpreted in the review by Burke and Williams (1977, p 345).

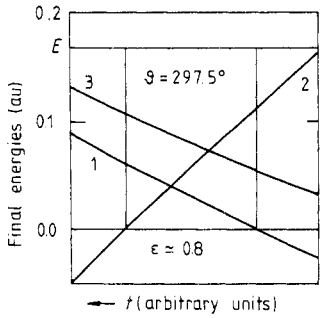

Figure 2. Double-ionisation interval at $E = 0.1682$ au; θ, initial orientation of the orbit (see figure 1); ε, eccentricity.

parallel to one of the atomic electron's final energy. The length of the interval turns out to be very small indeed, being typically 10^{-4} of the range of t $(0, T \simeq 2$ au). The accuracy of E_j^f calculations was typically better than 99%, achieved by putting an error parameter, which governs the integration step length, EPSILN = 0.1.

Following our earlier procedure (see Grujić 1972) we computed a number of intervals at different values of E, in order to establish their dependence on the energy. However, unlike the hydrogenic cases, it turned out that no simple power law could be fitted to the values calculated, the curves computed exhibiting no monotonic behaviour at all. Starting at $E = 6.75$ eV with a finite length it reached a maximum at $E = 2.55$ eV, and then decreased more or less monotonically until it disappeared at $E = 2.15$ eV. We have been unable to find it for lower E without changing one of the parameters (kept constant for $E > 2.15$ eV). A single interval was detected at $E = 0.088$ au with θ slightly changed to $\theta = 296.9°$. The corresponding electron energy configurations are shown in figure 3, which exhibits a different pattern compared with the 'high-energy' region (cf figure 2). Attempts to locate this interval at some nearby energy points have failed, indicating apparently irregular behaviour of the whole system in the final configuration, as in the case for higher E.

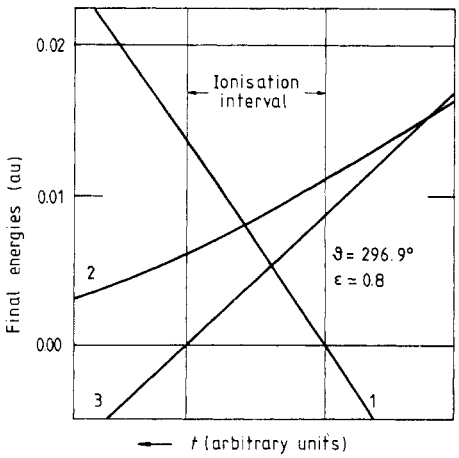

Figure 3. Triple-escape interval at $E = 0.02$ au (lower energy region, see text).

The possibility of deriving a threshold law from the behaviour of a single parameter interval comes from the fact that in hydrogenic case an appropriate choice of the system parameters may reduce the corresponding phase-space volume contraction, as E decreases, to reduction along a single direction (Wannier 1953).

In general, this need not be the case and the full extent of this phase-space volume should be calculated (in which case not only the threshold law, but the absolute cross section would be obtained). Hence, one possible way out would be to compute not ionisation intervals, but manifolds of higher dimensions as eventual representatives of the threshold behaviour. A tentative choice would be a determination of magnitudes of surfaces in a two-parameter subspace. Thus a trial was made by changing both the θ and t parameters. (This kind of approach was used in calculating $e + H(n = 1) \rightarrow e + H(n = 2)$ excitation function behaviour (Grujić 1973).) We have computed the quantities

$$\sigma_\varepsilon = \int_{\text{Vol}} \delta(\varepsilon - 0.8)\, d\varepsilon\, d\theta\, dt$$

at two energies: 2.67 and 5.15 eV; it provided the power law: $\sigma_\varepsilon \sim E^{4.069}$, with the exponent twice as large as that expected. Apparently, the ionisation phase-space volume is not fixed, or/and it does not preserve its shape as the energy varies. The possibility that a homotetic contraction takes place must be ruled out, since in such a case ionisation intervals for every parameter should conform to a power law, as can be easily shown. Hence it appears that an evaluation of the full volume in the configuration subspace spanned by ε, θ and t would be necessary. This, however, would require prohibitive computing time.

3.2. The energy distribution

Unlike the hydrogenic case where it is sufficient to examine the final energy of only one of the escaping electrons (see figure 4 in I), the energy curves being symmetrical about $E/2$, in the triple escape case it is more convenient to plot all three energy functions, as was done in figures 2 and 3. As can be seen from these figures, the functions are linear in t, as a general case, in near-threshold processes (see, however, figure 7 in I), but a derivation of the corresponding energy distribution among the escaping particles is not straightforward here.

We consider first the higher energy region. From the energy conservation law and shapes of $E_j^f(t)$ (see figure 2) we have (approximately), with superscript f omitted

$$\left|\frac{dt}{dE_1}\right| = \left|\frac{dt}{dE_3}\right| = 2\left|\frac{dt}{dE_2}\right|. \tag{4a}$$

Now in view of the complexity of the electron trajectories in the strong interaction region, it is reasonable to assume that all configurations have equal statistical weights. Then there is a set $\{\theta, \varepsilon\}$ which yields the same energy dependence as in figure 2 with curves 2 and 3 interchanged. This quasi-ergodic hypothesis is corroborated by figure 2, where it is the impact electron final energy (curve 1) that runs parallel to that of electron 3, rather than the other atomic electron (curve 2). Therefore we may write, for some other initial configuration, an analogous set of equations:

$$\left|\frac{dt}{dE_1}\right| = \left|\frac{dt}{dE_2}\right| = 2\left|\frac{dt}{dE_3}\right|. \tag{4b}$$

From the first equations of equations (4*a*) and (4*b*) we conclude that, *statistically*,

$$\left|\frac{dt}{dE_1}\right| = \left|\frac{dt}{dE_2}\right| = \left|\frac{dt}{dE_3}\right| = \text{constant}. \tag{5}$$

This, however, still does not imply that it corresponds to a uniform energy distribution, unlike the hydrogenic case; for the latter to hold equations (5) must be valid in the entire possible range: $0 \leqslant E_j^f \leqslant E$, $j = 1, 2, 3$. To get a proper energy distribution a sample of the graphs of the type of figure 2 would be necessary for a number of different sets $\{\theta, \varepsilon\}$, in contrast to the hydrogenic case (cf I). One can infer, however, some qualitative features of the actual distribution, without going into extensive computations. We see from figure 2 that neither of the electron energies come close to E. In order to do that curve 3 would have to move upwards, decreasing at the same time its slope, curve 1 following this decrease so as to remain parallel to curve 3. (Actually, this sort of behaviour is found, at a fixed $\{\theta, \varepsilon\}$ set, as the energy E increases.). A decrease of slope would mean, on the other hand, an increase of the probability of finding an electron within the corresponding energy interval, and consequently the overall balance would be shifted to the energies close to E. However, it can be shown that the statistical weight of the curves $E_j(t) \simeq \text{constant} \leqslant E$ is smaller than those with $E_j(t) \simeq E/2$, for example. Let us consider two representative cases:

$$E_1 \ll E_2 \ll E_3 \leqslant E \tag{6a}$$

$$E_1 \ll E_2 < E_3 < E. \tag{6b}$$

The number of occurrences of the last inequality of (6*a*) depends on the number of possible arrangements of E_1 and E_2, within the very small interval $(0, E-E_3)$, which itself will be relatively small, too. In contrast to this, in case (6*b*) this number would be considerably larger, for, say, $E_3 = \frac{2}{3}E$, and consequently, the statistical weight of the latter, accordingly greater. With these two competing effects, i.e. the increase of $|dt/dE_3|$ and diminishing statistical significance of $E_3 \leqslant E$ points, a conjecture that the overall energy distribution remains uniform seems reasonable.

As for the lower energy region (see figure 3), the situation is somewhat more complicated since no correlations (apart from the conservation law) appear among $E_j(t)$. However, the same sort of analysis is applicable here, too. For instance, keeping the E_3 curve fixed, the E_1 curve may move its left-hand side towards E, while E_2 curve would correspondingly approach the E_3 line. Hence, we estimate that the final energy distribution may be uniform, just as was the case with hydrogenic targets.

3.3. Angular distribution

As the analytical calculations, based on Wannier's theory, suggest (Klar and Schlecht 1976, see also Rau 1976), configurational symmetry in the final state found in the double escape case, should be the principal 'carrier' of other multiple escapes, with the equilateral triangle configuration in case of double ionisation, tetrahedron for fourfold escape, etc. These symmetrical arrangements are to be compared with the planetary model of bound states (Bohr 1913) (plane case), where the exact angular (central) symmetry is assumed, too, but the energy distribution is a singular function (δ distribution), in contrast to an ionisation channel, which possesses only configurational, but not the velocity, symmetry (uniform energy distribution).

We have examined angular configurations for a number of the ionisation intervals computed and found that these configurations fall into two distinct classes, depending on the energy region considered. In figure 4 we present the numerical results for the mutual angles between three escaping electrons from the ionisation interval from figure 3, at $E = 0.020$ au. As can be seen the mutual angles are close to the completely symmetrical case ($\theta_{ij} = 120°$). However, one can notice a sort of dynamical symmetry, which appears axial rather than central: while the velocity v_2 remains almost constant within the interval, v_1 and v_3 change noticeably in direction and considerably in magnitude (cf figure 5).

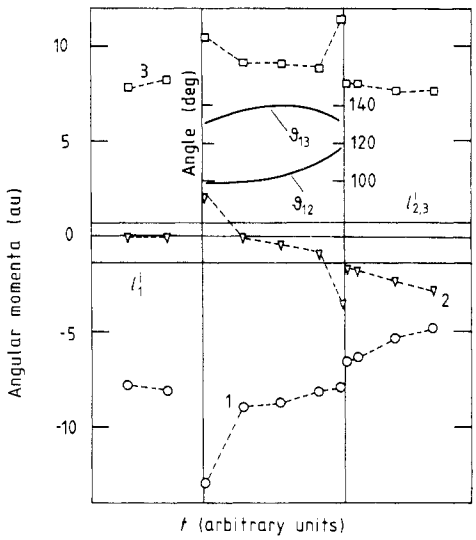

Figure 4. Angular momenta at $E = 0.02$ au; l^i_j, initial value of jth electron; θ_{ij}, mutual angles of escaping electrons.

The axial symmetry, in fact, appears to a fuller extent as one moves to higher energies. Namely, it turns out that the most significant mutual angles are 90° and 180°, as can be infered from figure 5, at $E = 0.098$ au, where $\theta_{12} = 89°$ and $\theta_{13} = 170°$ are calculated in the middle of the ionisation interval. Hence, one has a hydrogenic double escape, followed (or preceded) by a single escape perpendicularly to the double escape direction. This finding might be of interest for a possible experimental investigation of the double ionisation processes. Namely, at energies larger than 2 eV above the threshold, it would be sufficient to detect (in coincidence) two escaping electrons, with their energy measured, in an experimental set-up similar to that from Cvejanović and Read (1974).

3.4. Angular momenta

Since Fano's conjecture (1974) about an enhanced exchange of the electron angular momenta in the threshold vicinity, much attention has been paid to the behaviour of the final state momentum (see Grujić 1979, and references therein). In view of the more

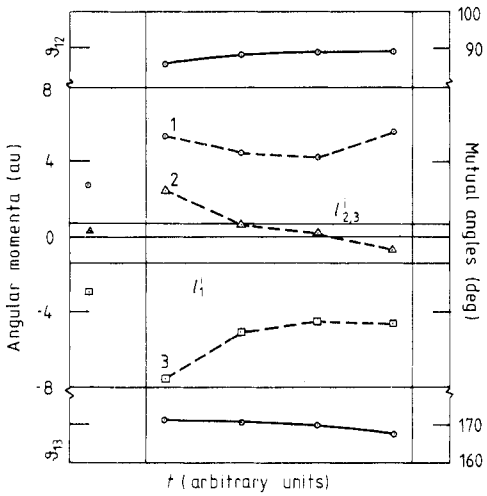

Figure 5. The same as in figure 4 at $E = 0.098$ au.

complex system we are dealing with here, it is of interest to see if the electrons within and close to the ionisation intervals acquire large angular momenta, too, and how they behave as the energy of the system goes to zero. In figure 5 computed individual angular momenta, at $E = 0.098$ au, are shown and compared with their initial values (horizontal lines). As found before in the hydrogenic cases, the angular momenta are largely enhanced by the combined attractive force of the remaining ion and the mutual repulsion due to other electrons, as can be seen in figure 5 (cf figure 1 from Grujić 1979). Angular momenta become particularly large as the edges of an ionisation interval are approached. This effect is especially prominent at small energies, as is evident in figure 4 for $E = 0.02$ au. At the boundary where an electron bound state goes over the continuum, the many-body features appear crucial for the angular momenta exchange. In the case of the hydrogenic target it was the nucleus which ceases to play the role of a spectator and takes over a great amount of the momentum. In the present case motion of the nucleus has been suppressed, but the third electron, introduced into the system, takes over its role. (In the particular case shown in figure 4 it is electron 2; cf figure 1 from Grujić 1979.) Note, also, the abrupt changes of the momenta as one enters the ionisation interval; they take different forms: a step in case of electron 1 (at the right-hand edge), pole-like behaviour for electron 2 (left-hand edge) and mixed features in other cases shown. From figure 4 we see that the step corresponds to 'recombination' of the impact electron, with atomic electrons flying away (single ionisation *via* the exchange). It is interesting to note, comparing right-hand edge effects in figures 3 and 4, that a change of sign of the impact electron energy gives rise to a dramatic change of the angular momenta of the other two electrons, but not of their energies. The situation looks rather similar at the left-hand edge, with the roles of electrons 1 and 3 interchanged. This edge effect indicates a rather peculiar (classical) mechanism and deserves the attention of an analytical study.

Another point of interest, raised by Fano's (1974) considerations, concerns the energy dependence of the electron angular momenta. However, as it was the case with the energy distribution (see § 3.2), the situation is complicated by the presence of three-body correlations here. Thus it would not be very instructive to follow the change

of a single angular momentum, say of electron 1, as shown in figure 6. The magnitude of the momentum (taken from the middle of the corresponding intervals, where momenta acquire, approximately, stationary values) exhibits a monotonic decrease as for the hydrogenics, but no attempt has been made here to fit the numerical results to a power law. (Note that $l_1(E = 0.02)$ has a different sign from the rest; this ionisation interval was calculated at a slightly different θ value, which might have affected numerical results to an unknown extent; see the discussion in the last section.)

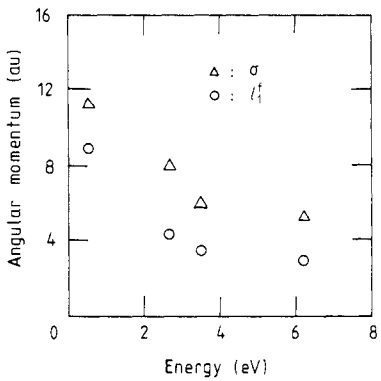

Figure 6. Energy dependence of the angular momenta; note that the lowest energy momentum corresponds to a (slightly) different θ value. $l_j^{i(f)}$, initial (final) angular momentum of jth electron.

As a more appropriate measure of the energy behaviour of the angular momenta, we have calculated the quantity

$$\sigma^2 = \sum_{j=1}^{3} (l_j^i - l_j^f)^2 \tag{7}$$

which has been plotted in figure 6, as well. As can be seen, $\sigma(E)$ follows closely $l_1(E)$. Hence the exchange effect does play an increased role as zero energy is approached in case of a three-electron system, in accordance with Fano's prediction for single ionisation.

4. Concluding remarks and discussion

An extension of the electron–hydrogen three-body problem to the e–He system is not a trivial task. Although the latter is a quasi-four-body system, one should bear in mind that, except for the angular momentum edge effect, discussed in the previous section, the e–H system is also a quasi-three-body problem. Further, though conceptually a straightforward extension of the e–H system, numerical difficulties met in the computation reported here turned out to be considerably more serious and in some respects formidable. Since it seems to be an inherent feature for the non-hydrogenic case, these difficulties deserve particular considerations. We shall discuss two rather distinct energy regions: higher energy (2.0–6.0 eV) and lower energy (0–0.6 eV) intervals,

which we examined numerically. Although both sets of calculations were carried out with the same accuracy in the trajectory integrations, they differed in the accuracy of the input data, the first region using a single-precision mode (6 reliable significant figures), the other one 13 figures (double precision). The numerical error in both cases was below 1%. However, in the single-precision input data calculations the final results turned out not to be reproducible, to the extent that the final energy curves were shifted, and thus the corresponding ionisation interval, too. This translation in the 'energy space' affected computed lengths of the ionisation intervals to a much smaller extent, so that the irregular behaviour of the latter could not be attributed to the observed 'motion' of the final data.

This effect was particularly prominent in the lower energy region, so that we had to convert the entire code to the double-precision mode. The instability has been thereby considerably suppressed, though small shifts still persisted. On the other hand, as the structure of the final energy curves becomes progressively more complicated, pushing the ionisation intervals further towards zero energy turned out not to make much sense, as the computation at $E = 0.017$ au showed. To appreciate the numerical complexity of the problem in this region, let us quote that, when the error parameter EPSILN was changed from 0.1 to 0.2, the error in the total energy rose from 10^{-2} to 10^{4}. However, this is not to be confused with the quasi-erratic behaviour of the trajectory due to (small) changes of the initial conditions (irreproducibility). The latter has, in fact, become the subject of an extensive study, both analytically and numerically, within the problem of the dynamical stability of the classical systems. There are, in fact, two aspects of the stability problem. One is related to small perturbations of the (conservative) classical systems (see Whiteman 1977, and references therein) and concerns, in our case, the stability of the classical helium model (see, e.g., Percival 1979a). This problem, on the other hand, is related (from the point of view of the numerical treatment of a particular classical dynamical system) to the instability due to a small displacement of the volume of the phase space for the initial conditions (Percival 1979b), which is surely relevant to the problem of e–He collisions, as our computations have shown. The quasi-erratic behaviour in the case studied appears as a noticeable (and even substantial) displacement and distortion of the final phase-space volume when the volume for the initial parameters is slightly changed. In the higher energy region the latter is effected by the (random) change of the seventh figure of the values of the initial parameter whereas in the lower energy part even the fourteenth figure turned out to be of importance.

According to the present results the e–He collision appears as a true many-body system, even within the restricted problem we consider—near-threshold Wannier's phase space. It is, possibly, the most complex system which can be treated by the classical-trajectory method and, in some aspects as discussed, is even too complex. On the other hand, apart from both the numerical and analytical problems of stability, there remains the problem of the procedure for numerical derivation of the double ionisation threshold law *via* Wannier's theory. A further elaboration of Wannier's approach for triple escape should at least clarify the difficulty we have met in the present work.

Acknowledgments

The authors thank Dr S Cvejanović for clarifying discussions concerning the experimental situation and for his contribution in developing the computer code. We are grateful to Professor I C Percival and Drs N Valentine and D Banks for supplying us

with their original version of the code. Useful discussions with Professor I Percival are also acknowledged with pleasure.

The work reported has been partially supported by RZN of Serbia.

References

Abrines R and Percival I C 1966 *Proc. Phys. Soc.* **88** 861–72
Abrines R, Percival I and Valentine N 1966 *Proc. Phys. Soc.* **89** 515–23
Bohr N 1913 *Phil. Mag.* **26** 1 (reprinted: 1967 *The Old Quantum Theory* ed D ter Haar (Oxford: Pergamon)
Bonsen T F M and Banks D 1971 *J. Phys. B: At. Mol. Phys.* **4** 706–14
Brion C E and Thomas G E 1968 *J. Mass. Spectrom. Ion. Phys.* **1** 25–39
Burgess A and Percival I C 1968 *Adv. At. Mol. Phys.* **4** 109–41
Burke P G and Williams J F 1977 *Phys. Rep.* **34** 326–69
Cvejanović S and Grujić P 1975 *J. Phys. B: At. Mol. Phys.* **8** L305–9
Cvejanović S and Read F H 1974 *J. Phys. B: At. Mol. Phys.* **7** 1841–52
Dimitrijević M and Grujić P 1979 *J. Phys. B: At. Mol. Phys.* **12** 1873–80
Fano U 1974 *J. Phys. B: At. Mol. Phys.* **7** L401–4
Grujić P 1972 *J. Phys. B: At. Mol. Phys.* **5** L137–9
—— 1973 *J. Phys. B: At. Mol. Phys.* **6** 268–99
—— 1979 *J. Phys. B: At. Mol. Phys.* **12** L131–4
Gryzinski M 1959 *Phys. Rev.* **115** 374
—— 1979 *J. Physique* **40** *Suppl.* 7 C171–7
Klar H and Schlecht W 1976 *J. Phys. B: At. Mol. Phys.* **10** 1699–711
Leopold J G and Percival I C 1980 *J. Phys. B: At. Mol. Phys.* **13** 1037–47
Percival I C 1973 *Comput. Phys. Commun.* **6** 347–57
—— 1979a *J. Phys. A: Math. Gen.* **12** L57–60
—— 1979b *Proc. R. Soc.* A **366** 129–41
—— 1980 *Phys. Bull.* **31** 160–1
Percival I C and Richards D 1975 *Adv. At. Mol. Phys.* **11** 1–82
Rau A R P 1976 *J. Phys. B: At. Mol. Phys.* **9** L283–8
Wannier G H 1953 *Phys. Rev.* **90** 817–25
—— 1955 *Phys. Rev.* **100** 1180–1
Whiteman K J 1977 *Rep. Prog. Phys.* **40** 1033–69

J. Phys. B: At. Mol. Phys. **14** (1981) 2559–2568. Printed in Great Britain

Comparison between quantum and semiclassical calculations of the electron impact broadening of the Li I resonance line

M S Dimitrijevic†, N Feautrier and S Sahal-Bréchot
Observatoire de Paris, 92190 Meudon, France

Received 23 December 1980, in final form 2 March 1981

Abstract. We present quantum mechanical calculations of Stark broadening parameters for the Li I 2s ^{2}S–2p ^{2}P line. Semiclassical calculations have also been performed and both have been compared with other available results. A detailed analysis of Stark broadening parameters as functions of the impact electron angular momentum quantum number and of the temperature is carried out. The influence of the polarisation potential and of the completeness of the set of energy levels on the Stark broadening parameters is investigated. The low temperature behaviour of the half width is discussed too.

1. Introduction

In spite of the existence of very successful semiclassical treatments (e.g. Sahal-Bréchot 1969a, b, Griem 1974) for electron collisional broadening parameters, it is interesting to perform sophisticated quantum mechanical calculations. Our purpose is in fact to provide a quantitative check of the different approximations which are made in the usual semiclassical perturbation treatments. We have chosen the case of a neutral atom. As a matter of fact, whereas the dominant angular momentum of the colliding electron varies between 3 and 15 for ion emitters because of the long range of the Coulomb field, for neutrals it lies typically between 1 and 5 (Bely *et al* 1963). Therefore, short-range effects are more important and this will facilitate the discussion concerning this important aspect of the semiclassical treatment (cut off and strong-collisions terms). Moreover, the effect of the exchange should be more important for neutrals and this is typically a quantum process. We have chosen the resonance line of Li I (2s ^{2}S–2p ^{2}P) because the polarisability of Li is very large both in the fundamental and excited states and therefore the importance of the polarisation potential, which is also a short-range effect, will be easier to discuss.

Thus we have computed the impact Stark width and shift of the Li I resonance line, both quantum mechanically and semiclassically. For the quantum calculation, we have used the K-matrix elements of Burke and Taylor (1969a, b). These are close-coupling calculations with exchange including only the 2s and 2p levels. By using the same atomic structure (wavefunctions of Weiss (1963)) and the same set of energy levels, we have performed the semiclassical calculations by means of the computer code of Sahal-Bréchot (1969a, b). In a second stage, we have included the 3s, 4s, 3d, 4d and 5d

† Present address: Institute of Applied Physics, PO Box 24, 11001 Beograd, Yugoslavia.

0022-3700/81/152559+10$01.50

levels in the semiclassical calculations in order to test the importance of these higher levels, and in particular their influence on the polarisation potential effect. We have also included this effect in the quantum calculation by introducing polarisation potentials in the coupled equations (Damburg and Karule 1967, Feautrier *et al* 1971) and we have compared the results step by step. This is detailed in the following sections.

2. Quantum and semiclassical methods

On the basis of the Baranger (1958a, b, c) general quantum mechanical pressure broadening theory, Bely and Griem (1969) have derived an expression suitable for Stark broadening of isolated lines of non-hydrogenic atoms and ions, which takes into account the influence of different components within a multiplet. A similar formula, which neglects fine structure, has been developed by Barnes and Peach (1970). We adopted the last approach, since in the case of the Li I 2s ^{2}S–2p ^{2}P line fine-structure effects can be neglected. Let the initial atomic level i have quantum numbers L_i, S_i and final state f have quantum numbers L_f, S_f. For an allowed transition in LS coupling, we shall write $S_i = S_f = S$. According to Barnes and Peach (1970), the half-half width w and shift d of an isolated non-hydrogenic line can be evaluated in terms of the scattering matrix elements S_i and S_f in the following manner:

$$w + \mathrm{i}d = \frac{\pi N \hbar^2}{m^2} \sum_{\substack{L_i^{\mathrm{T}} L_f^{\mathrm{T}} S^{\mathrm{T}} \\ ll'}} (-1)^{l+l'} \frac{2S^{\mathrm{T}}+1}{2(2S+1)} (2L_i^{\mathrm{T}}+1)(2L_f^{\mathrm{T}}+1) \begin{Bmatrix} L_i & L_i^{\mathrm{T}} & l \\ L_f^{\mathrm{T}} & L_f & 1 \end{Bmatrix}$$
$$\times \begin{Bmatrix} L_i & L_i^{\mathrm{T}} & l' \\ L_f^{\mathrm{T}} & L_f & 1 \end{Bmatrix} \int_0^\infty \frac{f(v)}{v} \mathrm{d}v \left(\delta_{ll'} - S_i(L_i S l' \tfrac{1}{2} L_i^{\mathrm{T}} S^{\mathrm{T}}, L_i S l \tfrac{1}{2} L_i^{\mathrm{T}} S^{\mathrm{T}})\right.$$
$$\left. \times S_f^*(L_f S l' \tfrac{1}{2} L_f^{\mathrm{T}} S^{\mathrm{T}}, L_f S l \tfrac{1}{2} L_f^{\mathrm{T}} S^{\mathrm{T}})\right) \tag{1}$$

where the summation is taken over the total angular momenta L_i^{T} and L_f^{T} of the system (atom + perturber) in the initial and final states of the transition, the total spin S^{T} of the system and the perturber angular momenta l and l' respectively before and after the collision. The coefficients in the curly brackets are 6-j symbols, N is the electron density, $f(v)$ is the velocity distribution function for electrons. For a Maxwellian distribution of velocity at temperature T

$$f(v) = 4\pi \left(\frac{m}{2\pi kT}\right)^{3/2} v^2 \exp\left(-\frac{mv^2}{kT}\right). \tag{2}$$

Owing to the conservation of energy, S_i is evaluated at total energy $\varepsilon_i + \frac{1}{2}mv^2$ and S_f evaluated at total energy $\varepsilon_f + \frac{1}{2}mv^2$, ε_i and ε_f being the energy of the initial and final levels of the line.

In the case of the 2s ^{2}S–2p ^{2}P Li I line, the formula (1) can be considerably simplified. We have $L_i = 1$, $L_f = 0$ and $l = l' = L_f^{\mathrm{T}}$ so that expression (1) becomes

$$w = \mathrm{i}d = (\pi N \hbar^2/m^2) \sum_{L_i^{\mathrm{T}} S^{\mathrm{T}} l} \tfrac{1}{4}(2S^{\mathrm{T}}+1)\tfrac{1}{3}(2L_i^{\mathrm{T}}+1)$$
$$\times \int_0^\infty f(v) v^{-1} \mathrm{d}v \left(1 - S_i(l, L_i^{\mathrm{T}}, S^{\mathrm{T}}) S_f^*(l, l, S^{\mathrm{T}})\right) \tag{3}$$

where the following notation is used:

$$S_i(l, L_i^T, S^T) = S_i(1\tfrac{1}{2}l\tfrac{1}{2}L_i^T S^T, 1\tfrac{1}{2}l\tfrac{1}{2}L_i^T S^T)$$

and

$$S_f(l, l, S^T) = S_f(0\tfrac{1}{2}l\tfrac{1}{2}lS^T, 0\tfrac{1}{2}l\tfrac{1}{2}lS^T).$$

We can sum over L_i^T, obtaining the final formula

$$\begin{aligned} w + \mathrm{i}d = N \int_0^\infty vf(v)\,\mathrm{d}v \frac{\pi\hbar^2}{m^2v^2} \sum_l (2l+1)\Bigg(\sum_{S^T=0}^{1} \frac{(2S^T+1)}{12(2l+1)} \\ \times[(2l+3)(1 - S_i(l, l+1, S^T)S_f^*(l, l, S^T)) \\ + (2l-1)(1 - S_i(l, l-1, S^T)S_f^*(l, l, S^T)) \\ + (2l+1)(1 - S_i(l, l, S^T)S_f^*(l, l, S^T))]\Bigg). \end{aligned} \tag{4}$$

For several open channels, the S matrix can be expressed in terms of the reactance K matrix in the usual manner

$$S = (1 + \mathrm{i}K)/(1 - \mathrm{i}K). \tag{5}$$

Below the 2p threshold, S reduces to $S = \exp(2\mathrm{i}\delta)$.

The connection with semiclassical theory can be made by replacing the summation over l by an integration over the impact parameter ρ of the perturbing classical particle, i.e.

$$l \to \rho k \quad \text{with } k = mv. \tag{6}$$

The equivalent semiclassical formula (e.g. Sahal-Bréchot 1969a) is

$$w + \mathrm{i}d = N \int_0^\infty vf(v)\,\mathrm{d}v \int_0^\infty 2\pi\rho\,\mathrm{d}\rho (1 - S_{ii}(\rho, v)S_{ff}^{-1}(\rho, v))_{\mathrm{Av}} \tag{7}$$

S is here the equivalent semiclassical S matrix. The angular average $(\ )_{\mathrm{Av}}$ over the directions of the colliding electron is expressed by a summation over the magnetic quantum numbers of the radiating atom

$$\begin{aligned} \sum_{\substack{M_iM_f \\ M_i'M_f' \\ \mu}} (-1)^{2L_i+M_i+M_i'} \begin{pmatrix} L_f & 1 & L_i \\ M_f' & \mu & -M_i' \end{pmatrix} \begin{pmatrix} L_f & 1 & L_i \\ M_f & \mu & -M_i \end{pmatrix} \langle L_i S M_i' | S | L_i S M_i \rangle \\ \times \langle L_f S M_f | S^{-1} | L_f S M_f' \rangle. \end{aligned}$$

The formulae which enter the computer code of Sahal-Bréchot are as follows

$$2w = N \int_0^\infty vf(v)\,\mathrm{d}v \Bigg(\sum_{j \neq i} \sigma_{ij}(v) + \sum_{j' \neq f} \sigma_{ff'}(v) + \int_0^\infty 8\pi\rho\,\mathrm{d}\rho \sin^2\delta \Bigg) \tag{8}$$

$$\delta = \varphi_p^2 + \varphi_q^2$$

$$d = N \int_0^\infty vf(v)\,\mathrm{d}v \int_0^\infty 2\pi\rho\,\mathrm{d}\rho \sin 2\varphi_p. \tag{9}$$

The inelastic cross section $\sigma_{ij}(v)$ can be expressed by an integration over the impact parameter of the transition probability

$$\sigma_{ij}(v) = \int_0^\infty 2\pi\rho \, \mathrm{d}\rho \, P_{ij}(\rho, v) \quad \text{with } P_{ij}(\rho, v) = S_{ij}^2(\rho, v)$$

$$i = 2\mathrm{p}\ ^2\mathrm{P} \qquad f = 2\mathrm{s}\ ^2\mathrm{S} \qquad j, j' = nl\ ^2L.$$

The phaseshifts φ_p and φ_q due respectively to the polarisation potential (r^{-4}) and to the quadrupolar potential (r^{-3}) part are given in § 3 of chapter 2 of Sahal-Bréchot (1969a).

All the cut-off and symmetrisation procedures in the inelastic cross sections are described in § 1 of chapter 3 of Sahal-Bréchot (1969b). We only recall that the cut-offs R_2, R_3 in the elastic-collision contribution are chosen so that

$$\sin^2 \delta(R_2) = \tfrac{1}{2}$$

and thus

$$\int_0^\infty 8\pi\rho \, \mathrm{d}\rho \sin^2 \delta = 2\pi R_2^2$$

and

$$\int_0^{R_3} 2\pi\rho \, \mathrm{d}\rho \sin 2\varphi_\mathrm{p} = 0 \qquad 2\varphi_\mathrm{p}(R_3) = 1$$

(cf § 2 of chapter 3 of Sahal-Bréchot 1969b).

In order to exhibit the contributions to the line width and shift of a given l, we have defined the equivalent semiclassical Stark broadening parameters w_l^{sc} and d_l^{sc} in the following manner

$$w_l + \mathrm{i}d_l = N \int_0^\infty v f(v) \, \mathrm{d}v \int_{l/k}^{(l+1)/k} 2\pi\rho \, \mathrm{d}\rho (1 - S_{ii}(\rho, v) S_{ff}^{-1}(\rho, v))_{\mathrm{Av}}. \qquad (10)$$

This procedure will allow us to check the validity of the semiclassical approximation by comparing step by step $w_l^{\mathrm{sc}} + \mathrm{i}d_l^{\mathrm{sc}}$ with $w_l^{\mathrm{cc}} + \mathrm{i}d_l^{\mathrm{cc}}$.

3. Results and discussion

In the present paper, we are primarily concerned with the validity of the semiclassical approximation. If this is valid, formula (10) and the quantum treatment must give the same results. Thus the comparison of these results will give us a check of the semiclassical approach. In the first two calculations (A and B) the 2s ^{2}S and 2p ^{2}P terms have been included either in a quantum approach (A) or in a semiclassical approximation (B). Moreover, quantum calculations including the polarisation of ^{2}S and ^{2}P terms by means of coupled polarised orbitals (Feautrier *et al* 1971) were made (C) and higher levels 3s, 4s, 3d, 4d and 5d have been added in the semiclassical calculation (D) in order to show the importance of the polarisation of the 2p ^{2}P term. For this last result (D), it is important to notice that terms in de-excitation contribute to the polarisability of excited states as was proved theoretically by Damburg (1968). Indeed, in the quantum calculations, these terms do not have to be included in the polarisability because they are already taken into account in the close-coupling formalism. Malinovsky and Sahal

(1970) have shown the importance of these terms in the semiclassical calculation of the shift of some caesium and oxygen lines.

The atomic data (Wiese *et al* 1966) used are consistent in semiclassical and quantum calculations, in order to obtain a reliable comparison. The set of energy levels and the atomic data used are listed in table 1. For the quantum calculations, we used equation (3) with data from Burke and Taylor (1969b) for the phaseshifts and the K-matrix elements, and we have calculated data at three extra values of the energy. The close-coupling solutions of Burke and Taylor have been obtained using a two-state approximation, in which the levels 2s and 2p of Li have been explicitly included. As we are concerned with a line broadening problem, we have calculated the data for the decoupled channel corresponding to the 2p level: they were not calculated by Burke and Taylor who were only interested in the excitation collision problem. We have also calculated the data for higher l values ($l \leqslant 20$) in the two-state close-coupling approximation without exchange, using the Li wavefunction from Weiss (1963) and the code of Seaton and Wilson (1972). Also the K-matrix elements are calculated in the close-coupling approximation taking into account the total polarisation of the 2p state. The solutions of Burke and Taylor are calculated at only a few energies and we calculated the missing data at the same values of the energies. For the integration over the velocity distribution for several temperatures requiring a large number of values of the energy, we adopted a least-squares interpolation and extrapolation procedure which produces a loss of accuracy.

Table 1. Atomic data.

(*a*) Term i	E_i (cm^{-1})	$\bar{r}_i(a_0)$	$\bar{r}_i^2(a_0^2)$
2s ^{2}S	0	3.80	—
2p ^{2}P	14904	4.75	27.5
3s ^{2}S	27206	10	—
4s ^{2}S	35012	21	—
3d ^{2}D	31283	10	—
4d ^{2}D	36623	21	—
5d ^{2}D	39095	34	—

(*b*) Transition $i \rightarrow j$	Oscillator strength ($i \rightarrow j$)
2s ^{2}S → 2p ^{2}P	0.753
2p ^{2}P → 3s ^{2}S	0.115
2p ^{2}P → 4s ^{2}S	0.0125
2p ^{2}P → 3d ^{2}D	0.667
2p ^{2}P → 4d ^{2}D	0.122
2p ^{2}P → 5d ^{2}D	0.0453

We have evaluated the contributions w_l and d_l of the various angular momenta l to the semiclassical half width w and shift d of the Li I 2s ^{2}S–2p ^{2}P, 6707 Å line, as given by equation (10). Results for $T = 2500$, 5000, 10 000 and 20 000 K are given in figures 1 and 2. From both figures one can see that the importance of higher l values increases with temperature and that higher l values are more important for the shift, produced by weak elastic collisions, than for the width. Also, one can see that perturbing electrons with $l = 1$ are the most important for the line width at $T < 20\,000$ K and for line shift at

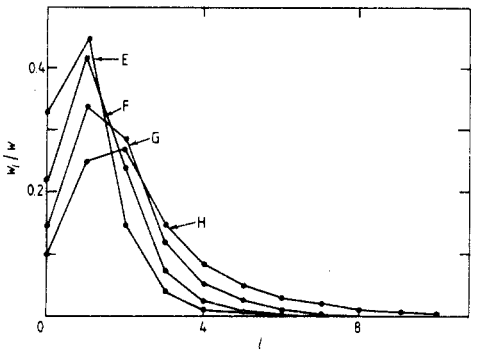

Figure 1. Relative contributions, w_l/w, of the various angular momenta l of the colliding electron for the semiclassical half half widths at different temperatures. The curves E, F, G and H refer to temperatures of 2500, 5000, 10 000 and 20 000 K respectively.

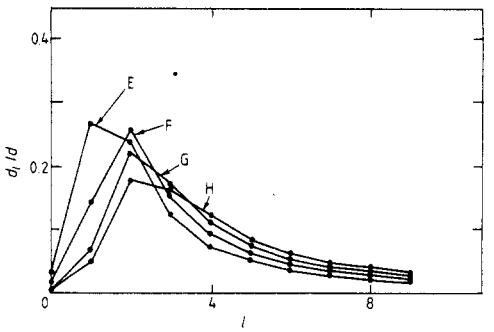

Figure 2. Relative contributions, d_l/d, of the various angular momenta l of the colliding electron for the semiclassical shift at different temperatures. Otherwise the same notation as in figure 1.

$T < 5000$ K. For higher temperatures electrons with $l = 2$ are more effective. This is in accordance with the conclusions of Bely *et al* (1963), that for neutrals typical l values for the incident electron are between 1 and 5.

Figures 3 and 4 show the convergence of the sums $\Sigma_{i=0}^{l} w_i/w$ and $\Sigma_{i=0}^{l} d_i/d$ for various temperatures. We can see that 80% of the width is given by $l \leqslant 1$ at low temperature (5000 K) whereas at high temperature $l \leqslant 1$ contribute to only 30% of the width. For the shift, the convergence is slower: even for $T = 5000°$, a summation up to $l = 10$ is necessary to obtain 80% of the result.

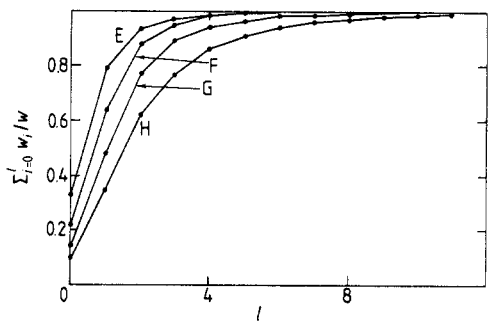

Figure 3. Convergence of the sum $\Sigma_{i=0}^{l} w_i/w$ in the semiclassical approximation as a function of l. The curves E, F, G and H refer to temperatures of 2500, 5000, 10 000 and 20 000 K respectively.

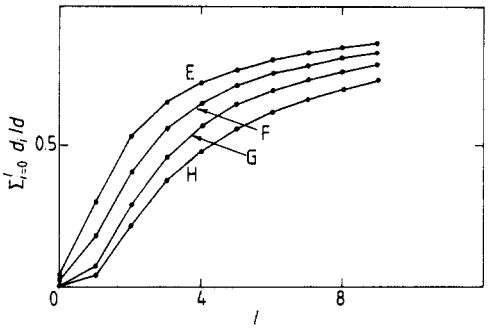

Figure 4. Convergence of the sum $\Sigma_{i=0}^{l} d_i/d$ in the semiclassical approximation as a function of l. Otherwise the same notation as in figure 3.

In figures 5 and 6 (2s, 2p) close-coupling quantum mechanical calculations (curve A) of w and d, respectively, are presented, together with quantum mechanical calculations with total polarisation of the 2p state (curve C). As was expected, we can see that the effect of polarisation is important for low l values, especially for the shift, where the inclusion of this effect can even change the sign of d_l. Semiclassical results which include

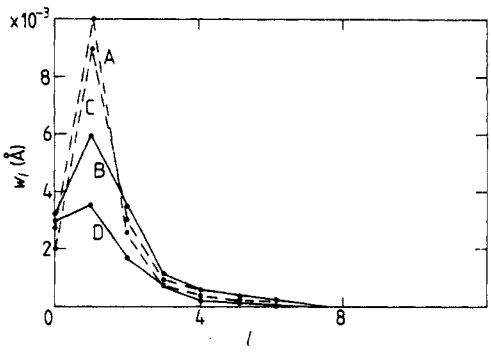

Figure 5. Comparison between quantum mechanical and semiclassical half half width calculations for different l values. The broken lines (A and C) refer to quantum results and the full lines (B and D) to semiclassical results; curves A and B correspond to the inclusion of the 2s and 2p levels only, and full polarisation of the 2p and 2s levels is included in curves C and D.

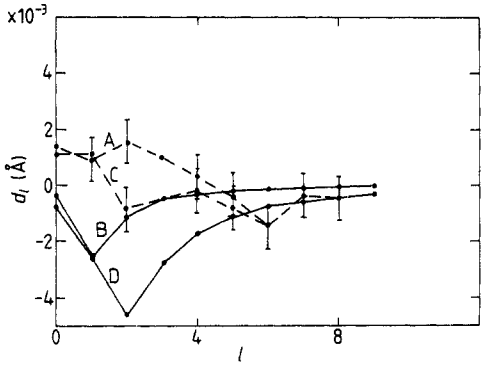

Figure 6. Same as in figure 5, but for the shift. The vertical bars represent the estimated inaccuracies of the quantum calculations.

2s and 2p states (curve B) and all perturbing levels (curve D), are also given in figures 5 and 6.

At low temperatures the inelastic collisions are quite negligible. Therefore the inclusion of all perturbing levels in the semiclassical approximation is equivalent to a semiclassical inclusion of the total polarisation of the 2p state. Thus, one can see by comparing A and C and B and D respectively that the inclusion of the total polarisation of the 2p state has a more important influence on the semiclassical calculations than on the close-coupling calculations. Since there is roughly a factor of two between the quantum and semiclassical calculations, this is an indication that additional effects which cannot be taken into account by the semiclassical calculations are much more important. This remark is to be connected to that of the end of this section: at low temperatures the predominant contribution to the width is given by the quantum elastic 2s–2s cross section. This cross section is then dominated by low-energy resonances in the S and P waves and this is typically a quantum effect. As a matter of fact one can see that the difference between quantum mechanical and semiclassical calculations is most prominent for the lowest l values, while with the increase of l the results converge as expected. We can also see that for line width calculations the most important partial contribution is for $l = 1$. When l increases, the relative accuracy of the quantum calculations decreases because the K matrix elements become smaller and smaller and thus the interpolation procedures diminish the accuracy. Since the convergence of the contribution of various l is slower for the shift, the latter becomes very sensitive to the interpolation procedures. Because of this it is not possible to obtain reliable quantum mechanical results for the shift for angular momenta higher than 5.

If one takes into account the inaccuracies of the quantum calculations, one can see from figures 5 and 6 that the semiclassical and the close-coupling calculations converge together at around $l = 3$ for the width and $l = 4$ for the shift.

We then investigated the influence of the cut-off on the semiclassical calculations (figures 7 and 8). At the chosen test temperature of 5000 K, the contribution of the inelastic collisions is quite weak and therefore the influence of a change in the

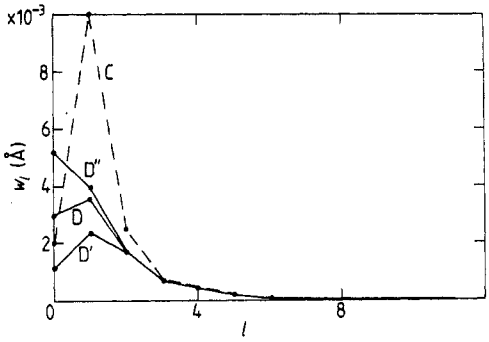

Figure 7. Influence of the change of the cut-off on the half half width. Curve C shows the quantum results (cf figure 5), curves D, D', D'' are the semi-classical results obtained for the cut-offs R_2, R_2' and R_2'' such that the corresponding phase shift $\delta(R_2') = \frac{1}{2}\delta(R_2)$ and $\delta(R_2'') = 2\delta(R_2)$.

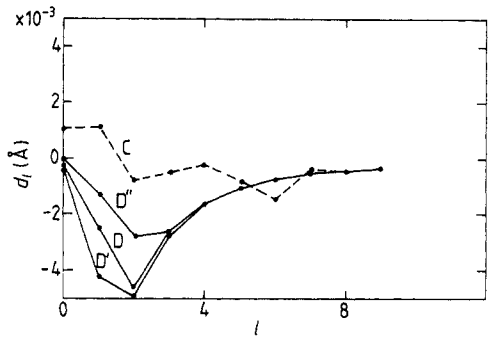

Figure 8. Same as in figure 7, but for the shift.

corresponding cut-off is negligible on the total half width. On the other hand, a change in the cut-off for the elastic-collision contribution (R_2 for the width, R_3 for the shift, cf preceding section) is only important for $l = 0, 1$ for the width and $l = 0, 1, 2$ for the shift. This is an interesting result because we have chosen a rather low temperature and a neutral atom in order to increase short-range and quantum close-coupling effects, and, in spite of that, our results show that the semiclassical perturbational treatment is valid for smaller l values than theoretically expected.

The above analysis explains the features and the variations reported in table 2 (width) and table 3 (shift). Firstly, one can recall that the MMM (model microfield method) calculation (Mazure and Nollez 1978) is, in the particular case of lithium, equivalent to a close-coupling dipolar semiclassical treatment because non-impact effects are negligible. The results of Bennet and Griem (1971) should be equivalent to our perturbational semiclassical treatment: the main differences come from the choice of the cut-offs and the symmetrisation procedure which is ignored and from the set of levels and atomic data. Comparison between lines 2, 3 and 6 shows that the coupling and short-range quantum effects decrease when the temperature increases as expected. The difference between the semiclassical and quantum calculations which attains a

Table 2. Li I $2s\,^2S$–$2p\,^2P$, $\lambda = 6707.8$ Å: half half widths in Å for $N_e = 10^{16}$ cm^{-3} as a function of the temperature. The experiment of Purić *et al* (1977) would give $W = 0.019$ Å, $d = -0.0042$ Å and $W = 0.023$ Å, $d = -0.0039$ Å at 17 500 and 26 500 K respectively, for the same density.

T (K)	2500	5000	10 000	20 000
(1) *A*	0.022	0.017	0.014	0.015
(2) *B*	0.015	0.016	0.018	0.020
(3) *C*	0.021	0.017	0.015	0.015
(4) *D*	0.010	0.011	0.012	0.016
(5) Bennet and Griem (1971)	—	0.0099	0.014	0.020
(6) Mazure and Nollez (2s–2p) (1978)	0.012	0.014	0.016	—
(7) Mazure and Nollez all levels (1978)	0.0087	0.012	0.015	0.021

Table 3. As in table 2, but for the shift; a positive shift is red.

T (K)	2500	5000	10 000	20 000
(2)	−0.016	−0.018	−0.021	−0.024
(4)	−0.0056	−0.0066	−0.0071	−0.0068
(5)		−0.0043	−0.0044	−0.0042
(6)	−0.019	−0.020	−0.022	—
(7)	−0.0044	−0.0044	−0.0043	−0.0041

factor two at 2500° is only 20% at 10^4 K. Quantum calculations at 20 000 K are not presented because of the lack of accuracy due to the necessary interpolation procedures at high energies. The importance of the short-range polarisation effects for the width is exhibited by comparing lines (1)–(3) and (2)–(4). In our case of the lithium resonance line, owing to the polarisation effect, the width decreases and the shift becomes less blue: this is due to the fact that the inclusion of the polarisation of the $2p\ ^2P$ level by higher terms shifts this level to the red and in our case this effect has a large influence. We have preferred not to give the quantum results of the shift because of the inaccuracies in the matrix elements for high l values which are predominant.

Concerning the variation of the width with temperature, we can see that the behaviour of the half width is qualitatively different in the quantum mechanical and semiclassical cases. In all semiclassical calculations, the half width increases with temperature, whereas the quantum mechanical results are a decreasing function of temperature. This difference is connected with the behaviour of the quantum elastic 2s–2s cross section which gives the predominant contribution to the width at low temperatures. In fact, Burke and Taylor (1969a) have shown that the cross section peaks within 0.1 eV of the 2s threshold due to the presence of low-energy resonances in the S and P waves. As can be seen from table 4, the contribution $w_l \leqslant 1$ of these two waves is predominant at low energies, $w_{l\leqslant 1}$ is a decreasing and $w_{l\geqslant 1}$ an increasing function of temperature. It is evident that w is a decreasing function for lower and increasing for higher temperatures with a turning point between 10 000 and 20 000 K. Semiclassical calculations cannot take resonances into account, therefore the elastic cross section does not peak at low energy and the width increases with temperature for all temperatures. The only existing experiment (Purić *et al* 1978) has been performed at too high temperatures and does not allow a check of these quantum effects.

Table 4. Comparison between quantum mechanical half half widths for $l=0$ and $l=1$, $w_{l\leqslant 1}$ (Å) and $l>1$, $w_{l>1}$ (Å), $N_e = 10^{16}$ cm^{-3}.

T (K)	2500	5000	10 000	20 000
$w_{l\leqslant 1}$ (Å)	0.016 95	0.011 83	0.008 03	0.005 87
$w_{l>1}$ (Å)	0.004 75	0.005 07	0.006 37	0.009 53

4. Conclusion

The present results show that, for all the plasma conditions considered, the contributions from the first l values are decisive for evaluating Stark broadening parameters and

for their temperature dependence. The importance of higher l values increases with temperature. Also, for the same plasma conditions, higher l values are more important for shift than for width. The temperature dependence for low temperatures is determined by the elastic part of the total cross section of e–Li scattering, which, within the framework of the semiclassical approximation, can be less accurately calculated than the inelastic contribution, especially for low temperatures, where strong collisions are important. We have shown the different behaviour of the semiclassical and close-coupling calculations with temperature. This can be explained entirely by the importance of the quantum effects and especially of the resonances which are predominant at low angular momenta. It would be interesting to perform experiments at a lower temperature in order to check these results.

Acknowledgments

We are indebted to J Dubau, A Mazure, C Goldbach and G Nollez for useful discussions, and H van Regemorter for interesting comments.

One of us (MSD) would like to acknowledge the financial support of RZN of Serbia and of the Observatoire de Meudon.

References

Baranger M 1958a *Phys. Rev.* **111** 481
—— 1958b *Phys. Rev.* **111** 494
—— 1958c *Phys. Rev.* **112** 855
Barnes K S and Peach G 1970 *J. Phys. B: At. Mol. Phys.* **3** 350
Bely O and Griem H R 1969 *Phys. Rev.* **1** 97
Bely O, Tully J and van Regemorter H 1963 *Ann. Phys., Paris* **8** 303
Bennet S M and Griem H R 1971 *Technical Report No 71-097* University of Maryland
Burke P G and Taylor A J 1969a *J. Phys. B: At. Mol. Phys.* **2** 869
—— 1969b *Theoretical Physics Division AERE Harwell* H1 63/2392
Damburg R J 1968 *J. Phys. B: At. Mol. Phys.* **1** 1001
Damburg R J and Karule E 1967 *Proc. Phys. Soc.* **90** 937
Feautrier N, van Regemorter H and Vo Ky Lan 1971 *J. Phys. B: At. Mol. Phys.* **4** 670
Griem H R 1974 *Spectral Line Broadening by Plasmas* (New York: Academic)
Malinovsky M and Sahal S 1970 *C.R. Acad. Sci., Paris* **270** 1409
Mazure A and Nollez G 1978 *Z. Naturf.* **33a** 15, 75 and private communication
Purić J, Labat J, Ćirković Lj, Lakićević I and Djeniže S 1977 *J. Phys. B: At. Mol. Phys.* **10** 2375
Sahal-Bréchot S 1969a *Astron. Astrophys.* **1** 91
—— 1969b *Astron. Astrophys.* **2** 322
Seaton M J and Wilson P M H 1972 *J. Phys. B: At. Mol. Phys.* **5** L1
Weiss A W 1963 *Astrophys. J.* **138** 1262
Wiese W L, Smith M W and Glennon B N 1966 *Atomic Transition Probabilities* NSRDS-NBS4, vol 1 (Washington, DC: US Govt Printing Office)

J. Phys. B: At. Mol. Phys. **16** (1983) 297–305. Printed in Great Britain

The classical trajectory study of $e^+ + A \rightarrow A^+ + e^- + e^+$ reaction near the threshold†

M S Dimitrijević‡ and P Grujić§

‡ Institute of Applied Physics, PO Box 58, 11071 Belgrade, Yugoslavia
§ Institute of Physics, PO Box 57, 11001 Belgrade, Yugoslavia

Received 14 April 1982, in final form 2 July 1982

Abstract. Numerical investigations of the positron–atom ionisational collisions near the threshold have been carried out within the classical trajectory method. It is found that for an infinitely heavy target the threshold law reads: $I \sim E^{2.49}$, whereas recent analytical calculations predict a value of 2.65 for the exponent. However, in the case of a hydrogen-atom target, the value 1.64 has been obtained, indicating that the resting target mass assumption, as employed in all previous analytical investigations of $e^{\pm}$–A processes near the ionisation threshold, breaks down in the case of the positron–light-atom collisions.

The energy distribution of the outgoing particles appears non-zero and uniform in larger parts of available energy regions: $e^+[E/2, E]$, $e^-[0, E/2]$, but turns out, surprisingly, to be zero around $E/2$. The calculated energy dependence of the mutual angle is consistent with the analytically predicted $\theta_{+-} \sim E^{1/4}$ behaviour.

1. Introduction

Numerical investigations of near-threshold processes serve a twofold purpose: firstly, they check the internal consistency of the classical calculations, usually involving dynamical approximations and secondly, they supplement classical analytical studies with additional information, like some distribution functions, usually not uniquely determined by various analytical examinations. The present computational study of positron–atom ionisation near the threshold has been motivated by: (i) the general rise of interest in processes where positrons are participating, due to the recent improvement in the experimental facilities (see, e.g. Griffith 1979) and in theoretical advances in modifying the methods designed for $e^- + A$ processes (e.g. Humberston 1979), (ii) recent analytical derivations of the threshold law for positron–atom ionisation, by Klar (1981), making use of his WKB theory, and by Grujić (1982b) via a generalised classical method due to Vinkalns and Gailitis (1967). The law derived theoretically reads: $I \sim E^{2.65}$, where E is the total energy of the system. This differs considerably from $e^- + A$ case, when the exponent attains the value of 1.127 (Wannier 1953).

Recently it has been suggested (Temkin 1982a) that ionisation by positrons need not follow a power threshold law similar to previous conjectures about electron impact ionisation (see Temkin 1982b, and references therein). In particular, a non-uniform energy distribution has been predicted within that approach.

† This work has been dedicated to Professor M J Seaton, on the occasion of his 60th birthday.

0022-3700/83/020297+09$02.25

Both Klar's (semiclassical) and Grujić's (classical) calculations were based on the same Wannier model for the near-zero double escape: outgoing particles move approximately along a common direction, not far away from the saddle point of the interaction potential surface, leaving the target ion at rest at the origin. Thus the model reduces the three-body problem to the quasi-two-body system: two light particles moving in the Coulomb potential of an (infinitely) heavy ion. This dynamical approximation had no effect in the case of an electron impact, due to the highly symmetrical configuration in the final ionisation state. On the other hand, as discussed by Grujić (1982b, to be referred to as I), since e^- and e^+ move in the same direction while escaping from the remaining ion, the finite-ion-mass effect may be noticeable near the threshold. We have, therefore, carried out two sets of computations: set A, for e^+–H collisions, and set B, for the e^+–A system, where the target A is a hydrogen-like atom with the nucleus mass: $M_A = 10^{10} m_e$. As we shall see, the finiteness of the proton mass resulted in a striking difference in the threshold behaviour of the ionisation cross sections.

In § 2 some of the relevant analytical results and the numerical method are briefly given and the results of the present numerical calculations are then presented in § 3. The computed data are compared with the corresponding analytically derived results and discussed in the last section.

2. Theoretical and computational preliminaries

2.1. Wannier's model for the near-threshold ionisation

Though explicitly designed for electron–atom (ion) collisions, Wannier's theory can be easily extended to cover positron–atom (ion) ionisation, as shown in I, where the approach due to Vinkalns and Gailitis (VG) was adopted. Here we point out some of the important features of the model.

Because of the attractive $e^- + e^+$ interaction, the positron pulls out the target electron and they can escape from the ion, moving in the same direction, by two possible ways: the electron remains between the ion and the positron (ionisation) all the time or forms a bound system with the positron (positronium). In the case of ionisation, double escape proceeds around the saddle point, defined by: θ_{+-} (mutual angle) $= 0$, $r_+/r_- = 2.153\,72$, where r_+, r_- are the distances from the origin (where the ion is supposed to reside) of the positron and the electron, respectively. Further, the total angular momentum of the system is assumed to be zero (this is not a crucial approximation and can be easily relaxed). As the total energy E decreases, escaping trajectories which do not cluster tightly around the saddle point gradually disappear. As shown in I, a typical mutual angle θ_{+-} tends to zero as $E^{1/4}$ as the threshold is approached. Further, on the basis of the form of the (semiclassical) wavefunction for the escaping $e^\pm$ pair, Klar (1981) concluded that the energy distribution between the outgoing particles should be uniform, as was the case with ionisation by electrons (see Dimitrijević and Grujić 1979 and references therein).

2.2. Numerical procedure

Since it has been given in more details elsewhere (see, e.g. Dimitrijević and Grujić 1979), we only outline the main features of the computer code used here and quote

the parameters adopted for the present computations. A modified, double-precision version of the original computer three-body code by Abrines *et al* (1966) has been employed for calculating classical trajectories of all charged particles—the nucleus, electron and positron. The motion has been confined to $0yz$ plane, for the sake of numerical accuracy. The Kepler orbit eccentricity was chosen to be 0.316 23 and the major axis was directed along the $0z$ axis. All computations have been carried out with the error parameters (see Abrines *et al* 1966 for their definitions): $\varepsilon = 0.05$, $\gamma = 0.12$ and $\delta = 0.05$, except in a part of the A-set computations (described in the next section), where a larger δ value had to be adopted.

Positron–atom collisions are notorious for numerical difficulties. This can be understood on the basis of an electron–positron attraction, so that they may come very close to each other during collision. Within the classical trajectory method it means that $e^{\pm}$ paths can be very complicated and a large numerical error can be accumulated; this actually turned out to be the case with trajectories in the ionisation intervals of the A-set computation. Computing time per orbit appeared to be consistently larger than for electron impacts and was typically a few minutes per collision. In A-set calculations the typical error in calculating the total energy was about 10%, whereas in B-set computations (see § 3.2) it was considerably less than 1%.

As was shown in I, the derivation of the threshold law for $e^+ + A$ can be reduced, as it was the case with $e^- + A$, to the variation of a single system parameter. As in previous numerical investigations of the near-threshold processes, we decided to vary the position of the atomic electron on its Kepler orbit, defined by the time parameter t (see, e.g. figure 1 in Dimitrijević and Grujić 1979). An ionisation interval is determined by the final energies: $0 < E_+ < E$, $0 < E_- < E$. Unlike $e^- + H$ collisions, a charge transfer is also possible, leading to positronium formation. As we shall see, this channel greatly influences the length of an ionisation interval. Another (unstable) system may be formed during the positron–hydrogen collision, namely autodetaching states of the e^+–H (see Grujić, 1982a), but this process is precluded here, since we shall deal with the continuum ($E > 0$) only. We note here only that in these autoionising states one also has: $r_+/r_- = 2.153\,72$, so that an ionisation interval may be viewed as a continuation of the autoionisation metastable states.

3. Results

3.1. A-set calculations

Here we investigate the process: $e^+ + H \rightarrow p^+ + e^- + e^+$, at three total energies: $E = 0.026, 0.036, 0.046$ (atomic units are used throughout). By varying t within the atomic ground state period $(0, T)$, final energies of all three particles are computed. In figure 1 a typical plot of $e^{\pm}$ final energies is given, for the energy $E = 0.036$ au. As can be seen in the figure, single-particle energy curves enter the first (left) ionisation interval with steep slopes, as t increases (the two curves meet at $E_{+-} = E/2$). For larger t values, the electron attains too large a velocity and catches up with the outgoing positron (positronium interval). Since the particle energies are calculated in the laboratory reference system, instantaneous values are considerably scattered around the mean values, as can be seen in figure 1 (so much so that the positron finds itself occasionally in the negative energy region, as exemplified by the rightmost point). The charge exchange channel ends up within another (right) ionisation interval (much narrower than the left one), and finally direct scattering emerges again.

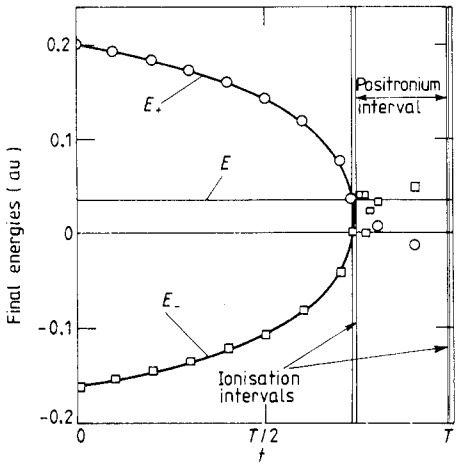

Figure 1. Positron (E_+) and electron (E_-) final energies for $e^+ + H$ collisions plotted against the initial time parameter at the total energy $E = 0.036$ au; ○: positron and □: electron points.

Both ionisation intervals are subsequently examined in more detail, so information on their length, energy distribution and mutual angle and angular momentum behaviour may be obtained. It turned out that the numerical error in large parts of the ionisation intervals was too large, so that we were forced to reduce the computing time (i.e. the number of steps) per orbit, by letting the orbit integration finish somewhat before a final state is definitely reached, by increasing the value of the δ parameter. This mainly affected the final values for the electron, but still allowed us to determine lengths of the intervals quite accurately (checks for the points near the interval edges confirmed that the free states are reasonably well attained; see Abrines *et al* 1966 for the relevant criterion). In table 1 numerical values for the ionisation intervals are presented, together with least-square fits to the analytical function: aE^{λ}. The best fit has been obtained, for both interval sets, with $\lambda = 1.64$. The fact that both sets yield the same exponent, together with the quality of the fits, as can be inferred from figure 2, convinces us that λ has been accurately computed. As another check, we computed the length of the left ionisational interval at $E = 0.056$ au, but with $\delta = 0.05$ (final state definitely reached; at higher energies the number of steps is not excessively big). As can be seen in figure 2, the point lies close enough to the fitting curve. We

Table 1. Ionisation intervals for $e^+ + H$ collisions. The figures in brackets indicate the power of ten by which the corresponding value is to be multiplied.

	Left interval		Right interval	
Energy (au)	Δt_{num} (au)	$0.0823E^{1.64}$	Δt_{num} (au)	$0.0269E^{1.64}$
2.6 (−2)	2.00 (−4)	2.07 (−4)	7.05 (−5)	6.766 (−5)
3.6 (−2)	3.43 (−4)	3.53 (−4)	1.15 (−4)	1.154 (−4)
4.6 (−2)	5.37 (−4)	5.276 (−4)	1.72 (−4)	1.724 (−4)
5.6 (−2)†	7.75 (−4)	7.315 (−4)		

† The check point; left interval only. Final state fully achieved (see text).

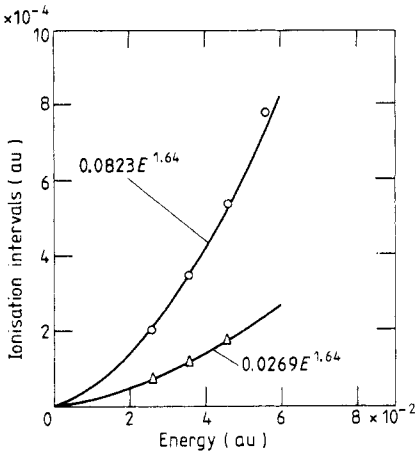

Figure 2. Numerical results for the lengths of the ionisation intervals and the best-fit curves: aE^{λ}, for $e^+ + H$ collisions. ○: left interval; △: right interval.

therefore conclude that the threshold law for positron–hydrogen ionisation reads

$$I_{\text{ion}} \sim E^{1.64}. \tag{1}$$

This deviates remarkably from the analytically predicted behaviour, as quoted above.

Because of insufficient accuracy in computing $l_+(l_-)$ and θ_{+-}, no attempt has been made to estimate typical $l_+(E)$ and $\theta_{+-}(E)$ behaviour. The values obtained are, nevertheless, found to be consistent with theoretically predicted ones. Thus, l_+, l_- appear much larger than the corresponding initial values (angular momentum exchange), while θ_{+-} is sufficiently small to indicate a preferential common direction. As for the energy distribution, it could be inferred from the present results, but since the curves $E_+(t)$, $E_-(t)$ are computed much more accurately in the B-set calculations, we shall present the derivation later on.

3.2. B-set calculations

By setting the mass of a hydrogen-like atom nucleus: $M_A = 10^{10} m_e$ we investigate a model system: $e^+ + A \rightarrow A^+ + e^+ + e^-$ which consists of the $e^{\pm}$ pair in the Coulomb field of the resting $Z = 1$ au charge. Computations have been carried out at energies: $E \simeq 0.016$, 0.026 and 0.036 au. For the last energy numerical results are given in figure 3, where the final energies $E_{+,-}$, positron angular momentum l_+ and mutual angle θ_{+-} are plotted against the initial time parameter t. Also, the mock angle: $\alpha = \tan^{-1} 2.153\,72 - \tan^{-1}(r_+/r_-)$ is shown. The last data measure departure from the saddle point in radial direction (see Wannier 1953).

3.2.1. Energy distribution. This can be deduced from the plot of E_+ and E_- in figure 3. As indicated in the upper right corner in the same figure, the distribution for e^+ appears non-zero in the region: $\xi E/2 < E_+ < E$, $\xi \leqslant \frac{3}{4}$ and zero otherwise. This rather surprising result demonstrates a marked difference between the motion of two escaping electrons and the $e^{\pm}$ pair. When r_+/r_- approaches asymptotically the value 1.179 80, the quasi-free $e^{\pm}$ pair configuration abruptly collapses into a bound state (positronium). The effect can be explained by the fact that both interacting particles are very light

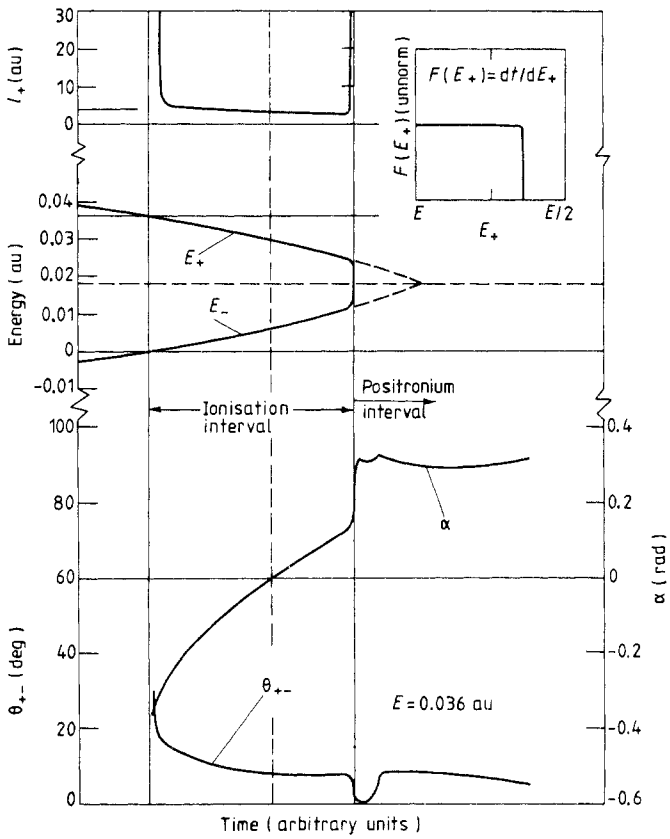

Figure 3. Final energies E_+, E_-, mutual angle θ_{+-}, positron angular momentum l_+ and the mock angle $\alpha = \tan^{-1} 2.153\,72 - \tan^{-1}(r_+/r_-)$, for the model hydrogen-like target: $M_A = 10^{10} m_e$. In the insert positron energy distribution is sketched.

and when the positron starts slowing down, the following electron is speeded up at the same rate to form a bound state with the former. As a consequence, no free particles are expected to be detected within, approximately, one third of the total energy interval $(0, E)$, around $E/2$.

3.2.2. Threshold law. Computed lengths of the ionisation intervals are presented in table 2, together with the least-square fit values. The fitting gives a value of 2.49 for the exponent, which is to be compared with the analytically derived value of 2.65.

Table 2. Results for the model (set B) calculations, with $M_A = 10^{10} m_e$. The figures in brackets as in table 1.

Energy (au)	Δt_{num} (au)	$0.668E^{2.49}$	$l_+(\alpha = 0)$ (au)	$\theta_{+-}(\alpha = 0)$ (rad)	$\Delta t(\alpha = 0)/\Delta t$
1.593 (−2)	2.3 (−5)	2.23 (−5)	12	0.175	0.58
2.599 (−2)	7.75 (−5)	7.545 (−5)	3	0.227	0.57
3.605 (−2)	1.695 (−4)	1.704 (−4)	4.1	0.148	0.59

The difference is fairly small, but in view of the rather small dispersion of the computed data, as evident from figure 4, one could expect even better agreement. From the present result we conclude that for a real atom A, the break-up process: $e^+ + A \rightarrow A^+ + e^+ + e^-$ near the threshold has the following energy dependence of the cross section:

$$I_{\text{ion}} \sim E^{\lambda} \qquad 1.64 \leq \lambda \leq 2.65 \tag{2}$$

where the analytical value for the upper limit of the exponent is adopted.

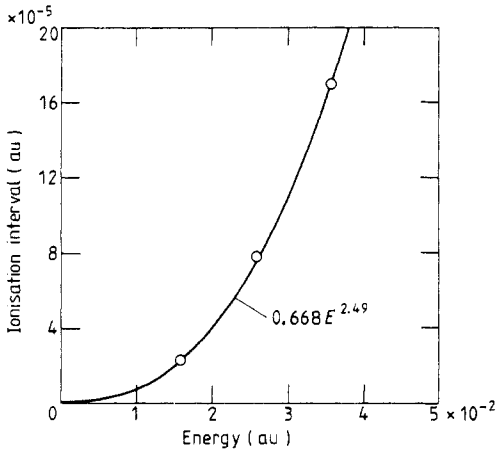

Figure 4. Numerical results for the lengths of the left ionisation intervals for $e^+ + A$ collisions, $M_A = 10^{10} m_e$, with the best-fit curve: aE^{λ}.

3.2.3. Angular momenta. These attain rather large values in the final channel, as seen in figure 3 (note that initially either of the particles can have an angular momentum less than one). It is interesting to note, also, that near the very edges of an ionisation interval, angular momenta increase enormously. This effect has been observed before (see, e.g. Dimitrijević and Grujić 1981, and references therein). The present calculations, however, reveal that this effect can arise solely due to the angular momentum exchange between the light, outgoing, particles, since in the present case the nucleus is only a spectator, apart of its Coulomb field.

The present computations have not provided a reliable estimate of the threshold behaviour of the final individual angular momenta (cf Grujić 1979 and references therein).

3.2.4. Mutual angles. Computed saddle-line $\theta_{+-}(\alpha = 0)$ values are shown in table 2. As can be seen from the table, the scatter of the computed data appears very large. Nevertheless, we have fitted the data to the analytical form

$$\theta_{+-} = aE^{1/4} \tag{3}$$

with a single adjustable parameter a. Computed results provide $a = 0.46$ and appear consistent with this theoretically predicted threshold behaviour (see ref I), but other exponents are admissible too. As for the angular distribution, it appears highly peaked

at a specific angle (close to the saddle-line value) within an ionisation interval, but this angle may vary from one interval to the other at the same E. Therefore, no effort has been made to calculate the distribution within an ionisation interval.

4. Discussion and concluding remarks

Since an experimental investigation of the near-threshold ionisation by positrons is still beyond our technical feasibility, a numerical study of the threshold phenomena seems at present indispensable. On the other hand, these computational examinations appear, as expected, much more involved and considerably less accurate than corresponding calculations for electron–atom collisions. However, while, apart from minor unexpected effects (see Dimitrijević and Grujić 1979), the numerical study tended to corroborate all the main analytical results for electron–atom (ion) collisions close to threshold, the present calculations have revealed two unexpected effects. Firstly, an abrupt cut-off in the energy distribution, giving rise to a hole around $E/2$, and secondly, the breakdown of the infinite-mass assumption for an asymmetric final state, as encountered in the positron–atom collisions. One might conjecture that if the energy distribution cut-off were absent (see the corresponding broken line continuations of E_+, E_- in figure 3) one would obtain a different threshold law. However, since E_+, E_- curves are not exactly straight lines, it is not possible to infer which threshold behaviour would arise by extrapolation of the present results. On the other hand, one could make use, not of an entire ionisation interval, but only of the parts from the left (right) edges of the left (right) intervals up to the $\alpha = 0$ point. As shown in the last column of table 2, the length of this segment is proportional to the total computed length, indicating 'stability' of the saddle point. Hence, it appears that it is the finite mass which makes the threshold law deviate from the analytically predicted behaviour, rather than the observed collapse of the energy distribution. Finally, we note that more detailed information about the angle distribution could be obtained by a complete simulation of a real experiment by Monte-Carlo calculations (see e.g. Percival 1973), but this would require prohibitive computer time.

Acknowledgments

It is a pleasure for one of us (PG) to express his gratitude to Professor M J Seaton for introducing him to the classical theory of atomic collisions. We are indebted to Professor I C Percival, Dr N Valentine and Dr D Banks for supplying us with their computer code. This work has been supported by RZN of SR Serbia. The computing was carried out on an IBM 360/44, at the Institute of Mathematics, Belgrade.

References

Abrines R, Percival I and Valentine N 1966 *Proc. Phys. Soc.* **89** 515–23
Dimitrijević M and Grujić P 1979 *J. Phys. B: At. Mol. Phys.* **12** 1877–80
—— 1981 *J. Phys. B: At. Mol. Phys.* **14** 1663–74
Griffith T C 1979 *Adv. At. Mol. Phys.* **15** 135–66
Grujić P 1979 *J. Phys. B: At. Mol. Phys.* **12** L131–4

Grujić P 1982a *J. Phys. B: At. Mol. Phys.* **15** L195–9
—— 1982b *J. Phys. B: At. Mol. Phys.* **15** 1913–28
Humberston J W 1979 *Adv. At. Mol. Phys.* **15** 101–33
Klar H 1981 *J. Phys. B: At. Mol. Phys.* **14** 4165–70
Percival I C 1973 *Comput. Phys. Commun.* **6** 347–57
Temkin A 1982a *J. Phys. B: At. Mol. Phys.* **15** L301–4
—— 1982b *Comm. At. Mol. Phys.* **11** 287–95
Vinkalns I and Gailitis M 1967 *Latvian Academy of Science Report* No 4 (Riga: Zinatne) pp 17–34
Wannier G H 1953 *Phys. Rev.* **90** 817–25

J. Phys. B: At. Mol. Phys. **17** (1984) L283–L287. Printed in Great Britain

LETTER TO THE EDITOR

The trajectory effect in calculations of the phaseshift for binary collisions and broadening of neutral atom lines

Milan S Dimitrijević

Institute of Physics, PO Box 57, 11001 Beograd, Yugoslavia

Received 14 December 1983

Abstract. The trajectory effect for a $C_n r^{-n}$ ($n=2, 3$ and 4) potential is estimated and compared with the results obtained according to the approximate method of Vallée *et al*, based on the use of effective rectilinear trajectories.

Within the semiclassical and the classical formalism for the calculation of neutral atom spectral line shapes within the impact approximation, the trajectory of the perturber is commonly represented by a straight line. At low temperatures the effect of back reaction of the neutral emitter on a perturbing particle may become noticeable and consequently deviations of the perturber motion from the uniform one should be taken into account (Roueff and Suzor 1974, 1975, Vallée *et al* 1976, Berard and Lallemand 1978, Dimitrijević and Grujić 1978, 1979). Here, the phaseshifts due to collisions with a perturbing particle moving in a $\pm C_n r^{-n}$ ($n=2, 3$ and 4) potential ($-$ is for an attractive and $+$ for a repulsive potential) are evaluated. The results are compared with the phaseshifts calculated taking into consideration the average effect of the trajectory (Vallée *et al* 1976) and their applicability in the adiabatic line broadening theories (see e.g. Lindholm 1945, Foley 1946, Allard and Kielkopf 1982 and references therein).

Using polar coordinates, the motion of the perturbing particle is described by (Goldstein 1950):

$$\dot{\theta} = \rho v / r^2$$
$$\dot{r} = v\left(1 - \frac{\rho^2}{r^2} - \frac{2V(r)}{Mv^2}\right)^{1/2}. \tag{1}$$

Here, M represents the reduced mass, v the relative velocity of the particles at infinity and ρ the impact parameter. The phaseshift is

$$\eta = \frac{2C_n}{v}\int_{r_m}^{\infty} \frac{\mathrm{d}r}{r^n(r^2-\rho^2-r^2V(r)/E_0)^{1/2}} \tag{2}$$

where r_m is the largest of the positive roots of the denominator. If the potential $V(r)$ is small compared with the kinetic energy $E_0 = Mv^2/2$, the term $r^2V(r)/E_0$ in equation (2) can be neglected and hence the trajectory can be considered to be rectilinear. In such a case equation (2) becomes (see e.g. Lang 1974)

$$\eta^0 = \frac{\sqrt{\pi}\Gamma[(n-1)/2]C_n}{\Gamma(n/2)v_0\rho^{n-1}}. \tag{3}$$

0022-3700/84/090283+05$02.25

Let us suppose that we retain the term $r^2V(r)/E_0$, but attribute to it an average constant value during the collision (Vallée *et al* 1976), in order to obtain an average effect of the real trajectory. This hypothesis (Vallée *et al* 1976) means that we take an effective rectilinear trajectory with a new impact parameter

$$\beta = \rho\left(1+\frac{V(\lambda\rho)}{2E_0}\right) \tag{4}$$

where $V(\lambda\rho)/2E_0$ is always very small compared with unity and the value of λ is calculated from the average potential $V(\lambda\rho) = (1/\tau)\int V(r)dt$ (for $n = 2, 3, 4$, and 6 the value of λ is 0.564, 0.794, 0.893 and 0.973 respectively). Here, τ is the average collision time. Within this approximation the phaseshift η' is (Vallée *et al* 1976):

$$\eta' = \eta^0[1+(2-n)V(\lambda\rho)/2E_0]. \tag{5}$$

In some cases integration in equation (2) may be performed easily. For the considered potential $V(r) = \pm C_n r^{-n}$ and for $n = 2$ (the linear Stark effect):

$$\eta = \eta^0\left(1+\frac{C_2}{\rho^2 E_0}\right)^{-1/2} \qquad \eta' = \eta^0. \tag{6}$$

The case $n = 3$ corresponds to the resonance broadening (also called self-broadening). This kind of interaction is usually present together with the van der Waals interaction ($n = 6$) but in special cases (e.g. discharge in helium at liquid nitrogen temperature, Damaschini and Vergès 1981) the resonance interaction is the principal line broadening mechanism. For the case $n = 3$ the solution of equation (2) can be obtained in the following form:

$$\eta = \eta^0 \frac{2\rho^2}{b[a(b-c)]^{1/2}}\left[K(k)+\left(\frac{b}{a}-1\right)\Pi(k^2, k)\right] \tag{7}$$

$$k^2 = \frac{b(a-c)}{a(b-c)}.$$

Here, K and Π are the complete elliptic integrals of the first and third kind, respectively (Gradshtein and Ryzhik 1965) and $a = (2\rho/\sqrt{3})\cos(\phi/3)$; $b = (2\rho/\sqrt{3})\cos[(\phi+4\pi)/3]$; $c = (2\rho/\sqrt{3})\cos[(\phi+2\pi)/3]$; $a > b > c$ are roots of the denominator in the integral in equation (2), and:

$$\cos\phi = -(\rho_c/\rho)^3$$

$$\rho_c = \sqrt{3}(C_3/Mv)^{1/3}. \tag{8}$$

Since the potential is attractive, if the impact parameter of the incoming electron is smaller than ρ_c, the atoms 'fall' into each other. In such a case one must resort to a more realistic emitter–perturber potential which accounts for a number of short-range effects.

Damaschini and Vergès (1981) have measured the resonance broadening of the He I 2^1P–2^1S, $\lambda = 2.06\ \mu$m line and have reported a considerable discrepancy between experiment and calculations using straight-line trajectories. The experiment was performed in helium at liquid nitrogen temperature ($T = 77$ K). For these conditions, ρ_c (from equation (8)) is $896a_0$, the perturbative approach as well as the very concept of a classical trajectory becomes questionable and a more refined theory is needed.

For $n=4$ (the quadratic Stark effect) the potential may be attractive or repulsive, depending on the sign of the quadratic Stark constant C_4 of the target.

For the attractive case one has:

$$\eta = \eta^0 \frac{4\rho^3}{\pi ab^2}(K(k)-E(k))$$

$$a, b = (\rho^2/2)\{1 \pm [1-(1/\tilde{\rho})]^{1/2}\}$$

$$\tilde{\rho} = (\rho/\rho_c)^4$$

$$k = b/a$$

$$\rho_c = (8|C_4|/v^2)^{1/4} \tag{9}$$

where $E(k)$ is the complete elliptic integral of the second kind.

For the repulsive case (Dimitrijević and Grujić 1979)

$$\eta = \eta^0 \frac{16}{\pi}\tilde{\rho}\sqrt{\beta}\left(E(k)-\frac{\beta+1}{2\beta}K(k)\right)$$

$$\beta^2 = 1+\tilde{\rho}^{-1} \qquad k^2 = \frac{\beta-1}{2\beta}. \tag{10}$$

As we can see, in the case of a repulsive potential the introduction of a non-uniform motion of the perturbing electron eliminates the problem of the minimum impact parameter, a crucial difficulty in the low-temperature region. We note that influence of the near-atom region (where the simple multipole form of the potential is not justified) is not of critical importance in such a case even at low temperatures.

For $n=6$ the integration in equation (2) is also straightforward but the solution is so cumbersome that numerical integration appears easier.

As an example we consider here the He I (3^1P°–2^1S), $\lambda = 5017$ Å (multiplet 4) line, which has a large and negative quadratic Stark constant for the upper state of the transition: $C_4(3^1P) = -5.275\times10^4$ au (Dimitrijević and Grujić 1979). In figure 1 the e–He(3^1P) scattering phaseshifts obtained from equations (3), (5) and (9) are presented. One can see that for $\rho > \rho_c$ the approximate treatment of Vallée *et al* (1976) is in good agreement with the exact solution of equation (2), but differs considerably in the region $\rho < \rho_c$, where the proposed approximation is not applicable. In the case considered the potential is repulsive due to the negative quadratic Stark constant, and the phaseshift (η) does not diverge for small impact parameters. Consequently, in the adiabatic impact theory of Stark broadening (see e.g. Allard and Kielkopf 1982) where the integration over ρ is needed in order to obtain the line width (w) and shift (d), the large discrepancy between η' and η for $\rho < \rho_c$ may be a problem.

In the case considered, the broadening of the lower level as well as the influence of the quadrupole interaction may be neglected (Dimitrijević and Grujić 1979). The half–half width and the shift of a line within the adiabatic impact approximation (e.g. Allard and Kielkopf 1982) are given by the following formula

$$w - id = 2\pi N_e v \int [1-\exp(i\eta)]\rho d\rho \tag{11}$$

with v meaning the mean electron velocity for a Maxwellian distribution (the use of v as a representative velocity instead of the average over the velocity distribution is

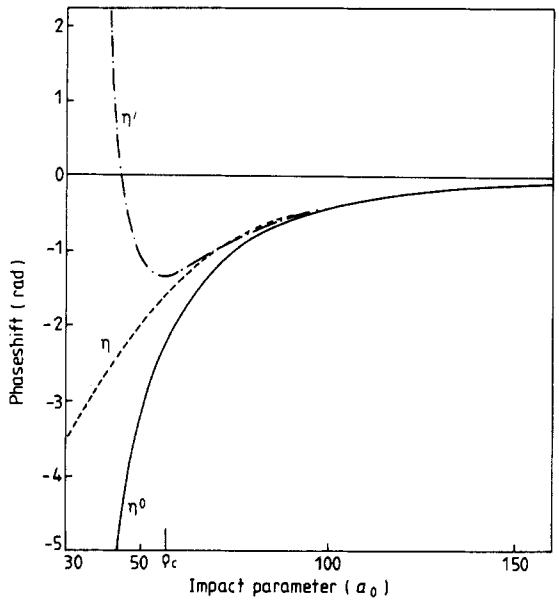

Figure 1. e–He(3^1P) scattering phaseshift for plasma at $T = 5000$ K.

justified at low temperatures, where the trajectory effect is most pronounced). For the He I (3^1P^o–2^1S) line for $T = 5000$ K and electron density $N_e = 10^{16}$ cm^{-3}, Dimitrijević and Grujić (1979) have obtained for the half-half width: $w = 0.400$ Å, using the exact solution of equation (2) (i.e. equation (9)) whereas the ordinary adiabatic theory calculations (Griem 1974) with straight-line perturber paths provide the value 0.367 Å, and using the approximate solution (5) we obtain the value $w = 0.206$ Å. The semiclassical method (Griem 1974) yields 0.378 Å. If we compare the half-half widths obtained using the exact and the approximate solutions of equation (2) ($w = 0.400$ Å and $w = 0.206$ Å respectively) we can see that the error introduced in our calculations by using an average velocity is negligible in comparison with the difference between results obtained.

In the cases when integration over all values of impact parameter is needed the approximate solution (5) may be used only for $\rho > \rho_c$. Finally we can conclude that in the region $\rho < \rho_c$ equation (5) is not applicable. This is especially important for the repulsive potential, since in such cases the contribution of the perturbers with $\rho < \rho_c$ is substantial.

References

Allard N and Kielkopf J 1982 *Rev. Mod. Phys.* **54** 1103
Berard M and Lallemand P 1978 *J. Quant. Spectrosc. Radiat. Transfer* **19** 387
Damaschini R and Vergès J 1981 *Spectral Line Shapes* ed B Wende (Berlin: de Gruyter) p 857
Dimitrijević M S and Grujić P 1978 *J. Quant. Spectrosc. Radiat. Transfer* **19** 407
—— 1979 *Z. Naturf.* **34a** 1362
Folley H M 1946 *Phys. Rev.* **69** 616
Goldstein H 1950 *Classical Mechanics* (London: Addison-Wesley)
Gradshtein I S and Ryzhik I W 1965 *Tables of Integrals, Series and Products* (New York: Academic)

Griem H R 1974 *Spectral Line Broadening by Plasmas* (New York: Academic)
Lang K R 1974 *Astrophysical Formulae* (Berlin: Springer)
Lindholm E 1945 *Ark. Math. Astron. Phys.* **32A** 1
Roueff E and Suzor A 1974 *J. Physique* **35** 727
—— 1975 *J. Phys. B: At. Mol. Phys.* **8** 2708
Vallée O, Ranson P and Chapelle J 1976 *J. Phys. B: At. Mol. Phys.* **9** L289

J. Phys. B: At. Mol. Opt. Phys. **22** (1989) 3845-3850. Printed in the UK

On the influence of Debye shielding on the Stark broadening of ion lines within the classical model

M S Dimitrijević†, A A Mihajlov‡, Z Djurić‡ and B Grabowski§

† Astronomical Observatory, Volgina 7, 11050 Beograd, Yugoslavia
‡ Institute of Physics, Maksima Gorkog 118, 11080 Zemun, Yugoslavia
§ Institute of Physics, Pedagogical University, Oleska 48, Pl-45052 Opole, Poland

Received 25 April 1989, in final form 6 July 1989

Abstract. The influence of Debye shielding on the Stark lineshift to width ratio is demonstrated in the case of ion lines. The Coulomb cut-off potential, especially suitable for a non-ideal plasma and for higher densities, has been used.

1. Introduction

The Stark lineshift to width ratio obtained within the classical model is important for the modern Stark broadening theory (Griem 1974, Griem *et al* 1962) as its constitutional part. Namely, within the GBKO (Griem *et al* 1962) theory for Stark broadening of neutral atom lines, the classical theory of Lindholm (1945) and Foley (1946) is used as the adiabatic limit. The same is done in the case of singly-charged ion lines (Griem 1974), where a numerical coefficient is introduced in the semiclassical theory in order to obtain at the adiabatic limit the same line shift (d) to width (w) ratio as within the classical model (Roberts and Davis 1967).

Moreover, the adiabatic limit is important for the Stark broadening theory since strong collisions, which are roughly speaking adiabatic (Caby-Eyraud *et al* 1975), are often of the same importance as weak collisions or even dominant. Also, in the semiclassical perturbation formalism of Sahal-Bréchot (1969a, b) the elastic collision contribution is estimated using the adiabatic theory. Moreover, when the impact approximation for ion broadening is valid, an adiabatic approach is commonly used.

The classical adiabatic approach for Stark broadening of ion lines was developed by Roberts and Davis (1967) from the theory of Lindholm (1945) and Foley (1946), with the assumption that Debye screening is not important. However, for higher densities, as well as for lines originating from more excited atomic states, such an assumption is often not justified. The aim of this paper is to obtain the frequency shift and the ion line Stark shift to width ratio (d/w) within the classical model (assumed to be correct at the adiabatic limit (Griem 1974)), taking into account Debye screening and to investigate how this screening influences the d/w ratio.

2. Phaseshifts

2.1. Coulomb cut-off potential

In Stark broadening investigations, electrostatic screening in a plasma is often taken into account by an upper cut-off ρ_{max} in the integral over impact parameter ρ (see

0953-4075/89/233845+06$02.50

Griem 1974). In order to determine ρ_{max} one must know the Debye radius r_D and, for the sake of simplicity, we will assume hereafter that $\rho_{max} = r_D$. We will describe the electron–ion interaction using the Coulomb cut-off potential, suitable especially in the case of a non-ideal plasma. Such a potential is continuous in the region $0 \leq r < \infty$, where r is the instantaneous electron distance:

$$V(r) = \begin{cases} -1/r + 1/r & r \leq r_c \\ 0 & r > r_c \end{cases} \tag{1}$$

where r_c is the cut-off parameter playing the role of the radius of screening in this model (we will assume that $r_c = r_D$). Electron scattering on the potential (1) was investigated by Suchy (1964) and Mihajlov *et al* (1987, 1989) in order to determine the electroconductivity of a non-ideal plasma. One possible application of such an approach is to obtain the correspondence between the electrical and the optical properties of such a plasma. Such a correspondence is obviously possible if (e.g. for the interpretation of measured data) one assumes that the same r_c value determines the electroconductivity of the investigated plasma, as well as the broadening and shift of spectral lines. Moreover, Kraeft and Mihajlov (1983) demonstrated that for electron kinetic energies of $1/r_c$ or greater, electron scattering on the Coulomb cut-off potential (1) may be treated classically.

2.2. Phaseshifts for binary collisions

For a number of problems in atomic and plasma physics, especially for atomic collision and lineshape investigations in the adiabatic limit the frequency phaseshift is often used (Peach 1981, Dimitrijević 1989). This quantity is also important in impact theories of spectral lineshapes for the calculation of the elastic processes. Within quasistatic theories, frequency shift in the emitted radiation caused by each perturber may be used to obtain the distribution of frequencies in the line directly (Peach 1982).

Using polar coordinates (ϑ, r) and atomic units, the motion of the perturbing particle is described by (Goldstein 1950):

$$\dot{\vartheta} = \rho v / r^2 \tag{2}$$

$$\dot{r} = v(1 - \rho^2/r^2 - 2V(r)/v^2)^{1/2} \tag{3}$$

where v is the perturber velocity. Introducing the quantity $\rho_0 = (C_4/v)^{1/3}$ (proportional to the Weiskopf radius ρ_W ($\rho_0 = \text{const}\,\rho_W$), where C_4 is the quadratic Stark constant), $z = 1/\rho_0 v^2$ (a measure of the ratio of perturber potential energy to kinetic energy), $k = \rho/\rho_0$ and $k_D = r_D/\rho_0$, the phaseshift induced during the collision becomes:

$$\eta = 2\rho_0^3 \int_{r_0}^{r_D} \frac{dr}{r^3(Rr^2 + 2z\rho_0 r - k^2\rho_0^2)^{1/2}} \tag{4}$$

where r_0 is the largest of the positive roots of the denominator and $R = 1 - 2z/k_D$.

The solution of equation (4) is:

$$\eta = \eta_4^0 \left[R + \frac{2}{\pi}\left(R + \frac{3z^2}{k^2}\right) \tan^{-1} \frac{zk_D - k^2}{k(k_D^2 - k^2)^{1/2}} + \frac{3z^2}{k^2} + \frac{2}{\pi}\left(\frac{k}{k_D} + \frac{3z}{k}\right)[1 - (k/k_D)^2]^{1/2} \right] \qquad k \leq k_D \tag{5}$$

$$\eta_4^0 = \pi/2k^3. \tag{6}$$

For $r_D \to \infty$ equation (5) becomes identical with the solution of Robert and Davis (1967):

$$\eta = \eta_4^0\left[1+\frac{2}{\pi}\left(1+\frac{3z^2}{k^2}\right)\tan^{-1}\left(\frac{z}{k}\right)+\frac{3z^2}{k^2}+\frac{6z}{\pi k}\right]. \tag{7}$$

In the high-temperature limit ($v \to \infty$, i.e. $z \to 0$ and $\rho_0 \to 0$) equation (5) reduces to the Lindholm-Foley result for straight-line trajectories, $\eta = \eta_4^0$, while in the low-velocity limit:

$$\eta = \frac{3\pi z^2}{k^5}\left[1+\frac{k}{\pi}\left(\frac{2\rho_0}{r_D z}\right)^{1/2}\right] \simeq \frac{3\pi z^2}{k^5}. \tag{8}$$

In figures 1-3 are plotted frequency shifts as a function of k for $k_D = 2, 10, 100$ and ∞ and for $z = 0.01, 0.1$ and 0.5, respectively. One can see that the differences are more pronounced for larger values of z; i.e. for higher plasma densities and/or lower plasma temperatures. We can see also that collisions with electrons outside the Debye sphere do not produce a frequency shift, as expected (i.e. the function becomes zero for the corresponding k values).

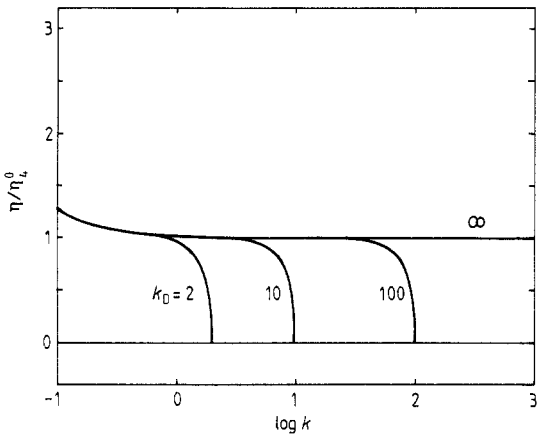

Figure 1. The phaseshift η/η_4^0 as a function of k and k_D for $z = 0.01$.

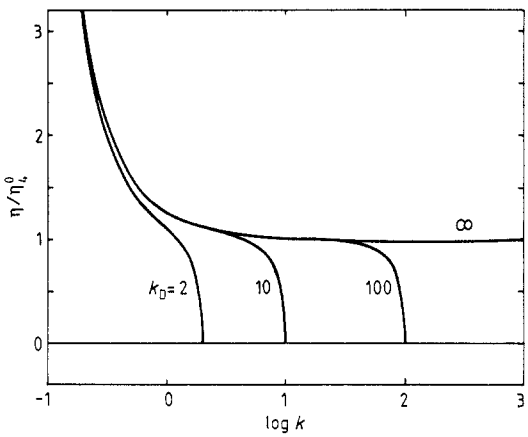

Figure 2. Same as figure 1 but for $z = 0.1$.

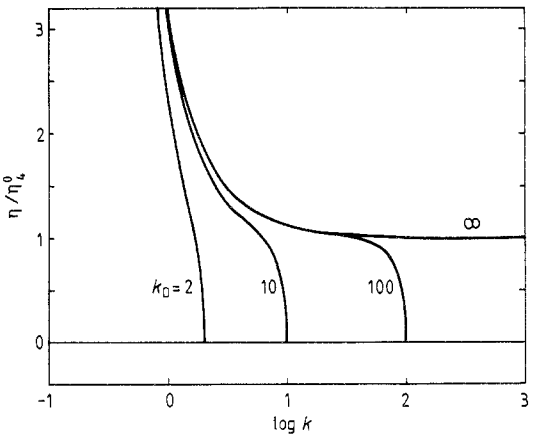

Figure 3. Same as figure 1 but for $z = 0.5$.

3. Lineshapes

In the semiclassical approximation, half half width (w) and shift (d) can be expressed via elements of the scattering matrix S:

$$w + \mathrm{i}d = N_e \int \nu f(\nu)\, \mathrm{d}\nu \int 2\pi\rho\, \mathrm{d}\rho [1 - S_{ii}(\rho, \nu) S_{ff}^{-1}(\rho, \nu)]_{\mathrm{Av}} \tag{9}$$

where the angular average (Av) is to be performed over the directions of the colliding electron.

In the classical adiabatic limit:

$$[1 - S_{ii}(\rho, \nu) S_{ff}^{-1}(\rho, \nu)]_{\mathrm{Av}} = \exp[-\mathrm{i}\eta(\rho, \nu)]. \tag{10}$$

Moreover, for lower temperatures one can use the mean electron velocity v for Maxwellian distribution.

The Stark width w and shift d can be expressed now as:

$$w(z, k_D) + \mathrm{i}d(z, k_D) = 2\pi N_e v \rho_0^2 \int_0^{k_D} \{1 - \exp[-\mathrm{i}\eta(z, k, \rho_0, r_D)]\} k\, \mathrm{d}k. \tag{11}$$

If one expresses the integral over k as $\int_0^\infty - \int_{k_D}^\infty$, and one makes a rough estimate of the second integral, one obtains in the high-temperature limit ($z \to 0$; $k, k_D \to \infty$; $\rho_0 \to 0$):

$$\begin{aligned} w + \mathrm{i}d &= 2\pi N_e v \rho_0^2 \left[\frac{1}{3} \left(\frac{\pi}{2} \right)^{2/3} \frac{\pi \exp(\mathrm{i}\pi/3)}{\sin(2\pi/3)\Gamma(5/3)} - \frac{\pi^2}{48 k_D^6} - \mathrm{i} \frac{\pi}{6 k_D^3} \right] \\ \frac{d}{w} &= \frac{1}{k_D} \frac{k_D^3 - a_1}{k_D^2/3^{1/2} - (\pi/8) a_1} \\ a_1 &= \tfrac{1}{2}(2/\pi)^{2/3} \Gamma(\tfrac{5}{3}) = 0.40988 \\ d/w &\to 3^{1/2} \qquad \text{if } k_D \to \infty. \end{aligned} \tag{12}$$

In figure 4 is represented the shift to width ratio (d/w) as a function of z for $k_D = 2, 10, 100$ and ∞. We can see that the d/w ratio is now a function of k_D and z

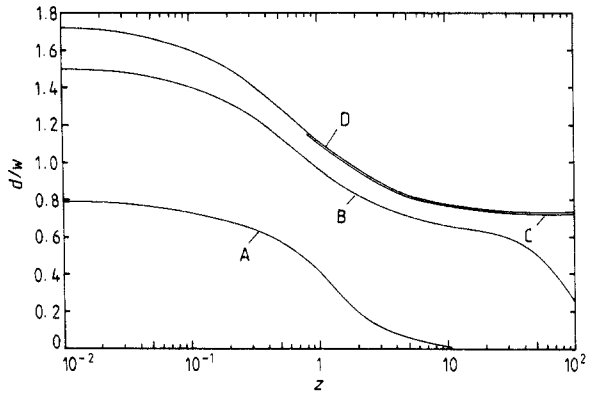

Figure 4. The shift to width ratio (d/w) as a function of z and k_D: curve A is for $k_D = 2$, B for $k_D = 10$, C for $k_D = 100$ and D for $k_D = \infty$.

and particularly at higher densities (small k_D) and towards the adiabatic limit ($v \to 0$, i.e. $z \to \infty$) deviates considerably from the $r_D = \infty$ case.

4. Conclusions

The influence of Debye shielding on the Stark lineshift to width ratio has been examined using the Coulomb cut-off potential suitable especially for a non-ideal plasma and for higher densities. The results obtained show that the d/w ratio is a function of the Debye radius also and that towards the adiabatic limit deviates considerably from the low-density case.

The analytical solution for the frequency phaseshift has also been obtained. The differences from the $r_D = \infty$ case are more pronounced for smaller electron velocities, higher plasma densities and/or lower temperatures.

Acknowledgments

This work is financially supported by RZN of SR Serbia. Also, this is a part of the project 'Atomic molecular and plasma spectroscopy' and enters in the Yugoslav-Polish collaboration through the project 'Radiation and atomic collision processes in astrophysical and laboratory plasmas'.

References

Caby-Eyraud M, Coulaud G and Nguyen Hoe 1975 *J. Quant. Spectrosc. Radiat. Transfer* **15** 593
Dimitrijević M S 1989 *Classical Dynamics in Atomic and Molecular Physics* (Singapore: World Scientific)
Foley H M 1946 *Phys. Rev.* **69** 616
Goldstein H 1950 *Classical Mechanics* (London: Addison-Wesley)
Griem H R 1974 *Spectral Line Broadening by Plasmas* (New York: Academic)
Griem H R, Baranger M, Kolb A C and Oertel G K 1962 *Phys. Rev.* **125** 177
Kraeft W D and Mihajlov A A 1983 *Physica* **120A** 263
Lindholm E 1945 *Ark. Mat. Astron. Phys.* **32A** 1

Mihajlov A A, Dimitrijević M S, Djordjević D, Luft M and Kraeft W D 1987 *Contrib. Plasma Phys.* **27** 1
Mihajlov A A, Djordjević D, Popović M M, Mayer T and Kraeft W D 1989 *Contrib. Plasma Phys.* in press
Peach G 1981 *Adv. Phys.* **30** 367
Roberts D E and Davis J 1967 *Phys. Lett.* **25A** 175
Sahal-Bréchot S 1969a *Astron. Astrophys.* **1** 91
—— 1969b *Astron. Astrophys.* **2** 322
Suchy K 1964 *Beitr. Plasmaphys.* **4** 71

J. Phys. B: At. Mol. Opt. Phys. **23** (1990) 1641-1653. Printed in the UK

Small-energy three-body systems: IV. Classical trajectory calculations for the near-threshold behaviour of collision-induced dissociation

M S Dimitrijević†, P Grujić‡, G Peach§ and N Simonović‡

† Astronomical Observatory, Volgina 7, 11050 Belgrade, Yugoslavia
‡ Institute of Physics, PO Box 57, 11000 Belgrade, Yugoslavia
§ University College London, Department of Physics and Astronomy, Gower Street, London WC1E 6BT, UK

Received 7 August 1989, in final form 8 January 1990

Abstract. Near-threshold collision-induced dissociation is simulated numerically for the process $Xe+Xe_2 \rightarrow 3Xe$ by carrying out detailed classical trajectory calculations. A static model of the target is chosen and the system is assumed to have zero total angular momentum. Then by varying a single parameter, the threshold law $\sigma \sim E^{1.6}$ for the cross section is derived, and this is consistent with analytical results obtained previously. We also consider the distributions of energy, mutual angles and individual angular momenta in the final channel.

1. Introduction

This paper is a sequel to the previous one (Grujić and Simonović 1988, hereafter referred to as III), where the method for treating break-up processes in Coulombic systems in the near-threshold region (see Simonović and Grujić 1987), was extended to the general case of inverse-power law interaction potentials. For a system of three identical particles, it was found that in the cases where the classical model of Wannier (1953) holds, the exponent κ in the threshold law

$$\sigma \sim E^{\kappa} \qquad E \rightarrow 0 \tag{1}$$

where E is the total energy of the three-body system, is given by

$$\kappa = \mathrm{Re}[(2k-4+(k+2)\{(1+4\lambda)^{1/2}+[1-4\lambda/(k+1)]^{1/2}\})/4k]$$
$$\lambda = \frac{3k(k+1)}{2(1+\frac{1}{2}k)^2}\frac{2^{k+1}}{1+2^{k+1}} \qquad k=1,2,3,\ldots, \tag{2}$$

if the total interaction potential in the final state can be written as

$$V_T(R_{12}, R_{23}, R_{31}) = -C_k\left(\frac{1}{R_{12}^k}+\frac{1}{R_{23}^k}+\frac{1}{R_{31}^k}\right). \tag{3}$$

In equation (3), the position of particle i relative to particle j is specified by $\boldsymbol{R}_{ij}$ and C_k is a positive constant. For the case of the Van der Waals interaction, $k=6$, and equations (2) yield $\kappa = 1.693$ as a universal result for processes of the type

$$A+A_2 \rightarrow 3A. \tag{4}$$

However, as distinct from the purely Coulomb case where at least two particles repel each other, the Van der Waals interactions are all attractive, and hence it is possible

0953-4075/90/101641+13$03.50

for any two of the three particles to form a bound state in the final channel. This makes the near-threshold problem two-dimensional and hence two parameters should be varied in order to derive the threshold law numerically.

Numerical calculations complement analytical theory and serve to: (i) check the internal consistency of the model used, and (ii) provide additional quantities that are often difficult or impossible to obtain analytically. Also by simulating a complete collision process one goes beyond the restriction of a final-state analysis, cf Grujić (1983) and Read (1984). In this way one can test a number of assumptions inherent in the model of Wannier (1953), such as the unimportance of the short-range interaction for the actual threshold law, or the validity of the quasi-ergodic hypothesis. In this sense, numerical studies of collision-induced dissociation or equivalently triatomic photodissociation, correspond to ionisation of complex or non-hydrogenic atoms, rather than to the multiple ionisation of atoms that eventually leaves a bare nucleus. The dimensions of atomic systems determine the range of energy where a threshold law holds (cf Klar 1981), and sometimes means that the classical model cannot be applied (see III).

Collision-induced dissociation is a real three-body problem and from the numerical point of view corresponds to double ionisation (cf Dimitrijević and Grujić 1981), rather than to a double-escape process, where the remaining nucleus, a bare ion, plays the role of a spectator. As we shall see later, many of the advantages of the Wannier model (see for example, Vinkalns and Gailitis 1967), are severely diminished. Nevertheless we are able to extract a number of relevant quantities without using a full statistical analysis (see for example, Wetmore and Olson 1986).

In the next section we present the physical model used in the classical treatment of collision-induced dissociation and give some details of the numerical procedure. In sections 3 and 4 numerical results for the threshold law and for the distributions of energy, angular momenta and mutual angles are presented. Finally a brief discussion of the results is given in section 5.

2. Model and numerical procedure

Over fifty years ago, Hirschfelder *et al* (1936) published pioneering work on the dynamics of the $H+H_2$ system. Subsequently, Karplus *et al* (1965) integrated the classical equations of motion in order to study exchange reactions in collisions between H and H_2, but they did not study the energy region in which collision-induced dissociation could take place. A classical model for three bodies interacting through purely Coulombic forces was originally constructed by Abrines *et al* (1966). This model was subsequently modified in order to account for the internal structure of the interacting atomic subsystems by Peach *et al* (1985), that is deviations from pure Coulombic interactions were included. Here, the three-body classical model is adapted to describe collision-induced dissociation, and then some details are given of the numerical procedure used in deducing the near-threshold behaviour of the system.

2.1. The model for collision-induced dissociation

The principal problem in applying the classical trajectory method to processes of molecular fragmentation is the construction of a classical model for a molecular system. Obviously it is very difficult, if not impossible, to construct a classical counterpart of

the chemical bonds that hold a molecular target together. We adopt a model for the two-body interaction which describes the medium-range interaction reasonably accurately and the tail of the potential, which is usually well known, with the best possible accuracy. If the actual threshold law for fragmentation does not depend noticeably on the short-range interactions, see section 3.2 in III, the detailed form of the model potential in this region will prove to be unimportant. On the other hand, the interatomic potential should be described by as simple an analytical expression as possible, so as not to burden the numerical calculations with unnecessary computational effort. The model which satisfies both these requirements is the Lennard-Jones potential

$$V(R) = \varepsilon_0 \left[\left(\frac{R_0}{R} \right)^{12} - 2 \left(\frac{R_0}{R} \right)^{6} \right] \tag{5}$$

where R is the interatomic separation and R_0 and $-\varepsilon_0$ give the position and value of the minimum in $V(R)$. Equation (5) for $V(R)$ contains the correct Van der Waals term, and in order to preserve the internal consistency of the model, we shall confine ourselves to those diatomic systems which have their bound states determined by a Lennard-Jones potential, rather than by a chemical binding force. This choice restricts us to inert-gas dimers. The total interaction between the three identical atoms A, say, is then given by

$$V_T(R_{12}, R_{23}, R_{31}) = V(R_{12}) + V(R_{23}) + V(R_{31}) \tag{6}$$

and this potential takes the form given in (3) for large internuclear separations, where

$$C_6 = 2\varepsilon_0 R_0^6. \tag{7}$$

The question as to whether $V(R)$ supports a bound state or not (as is the case with models for He_2 for example) is of no importance here, at least as long as one is mainly concerned with the threshold behaviour. The model must provide reasonable initial conditions for the numerical integration of the classical equations of motion, but equations (2) and (3) indicate that the magnitude of C_6 is not expected to influence the value of κ in the threshold law. Of course for other quantities such as the distribution functions, we must have a reasonably realistic representation of the real interaction.

2.2. The validity of the classical approximation

If the energies E_1, E_2 and E_3 of the atoms, A, in the final channel are calculated using the centre of mass O of the three bodies as the origin of the reference system, then

$$E = E_1 + E_2 + E_3. \tag{8}$$

In this reference frame, the energies of atoms that occupy two-body bound states may be positive, but if we use the centre of mass O′ of the pair of atoms, A+A, as the origin, the energy, ε, of A+A will be negative if a bound state of A_2 has been formed as a final product of the reaction. The diatomic system A_2 can also have non-zero angular momentum l and so the effective potential for the system is defined by

$$V_{\text{eff}}(R) = V(R) + \frac{l^2}{2\mu R^2} \qquad \mu = \tfrac{1}{2}m \tag{9}$$

where m is the mass of atom A and μ is the reduced mass of A_2.

The validity of the classical approximation can be examined by considering the configuration in which the three atoms are collinear. This is because such a configuration is expected to correspond to the minimum energy of the system, see section 2.1

in III, and hence by decreasing the total energy E the system is forced to evolve along a straight line. If atom 1 is stationary at the centre of mass of the whole system, and atoms 2 and 3 are moving symmetrically outwards, each with an energy $E/2$,

$$\boldsymbol{R}_{13} = -\boldsymbol{R}_{12} = \tfrac{1}{2}\boldsymbol{R}_{23} \equiv \boldsymbol{R} \tag{10}$$

say. Following the analysis of section 2.2 in III, atoms 2 and 3 are each subject to the interaction potential $V_2(R)$ defined by

$$V_2(R) = V(R) + \tfrac{1}{2}V(2R) \tag{11}$$

where $V(R)$ is given by (5). If in addition atoms 2 and 3 each have angular momentum l_2, the associated effective potential is given by

$$V_{2\,\mathrm{eff}}(R) = V_2(R) + \frac{l_2^2}{2mR^2}. \tag{12}$$

In the region where the atoms are in close contact, the classical approximation breaks down, but it is possible to define a separation $R = R_{\mathrm{sc}}$ that specifies the radius of the so-called 'strong correlation zone' and beyond which classical mechanics is valid. R_{sc} can be estimated by requiring that

$$\tfrac{1}{2}E = \zeta V_2(R_{\mathrm{sc}}) \tag{13}$$

where ζ is to some extent arbitrary, but is assumed to be in the range $0.1 \leqslant \zeta \leqslant 0.5$. The range of validity of E is given by

$$\tfrac{1}{2}E = \zeta |V_2(R)|_{\max} \tag{14}$$

where $|V_2(R)|_{\max}$ is the maximum of the absolute value of $V_2(R)$ in the classical region. Another criterion for the validity of the classical approximation is that the spread in the wavepacket corresponding to atom 2 or 3 is small, so that

$$\mathrm{d}\lambda\!\!\!^{-}/\mathrm{d}R \ll 1 \tag{15}$$

where $\lambda\!\!\!^{-}$ is the reduced de Broglie wavelength defined by

$$\lambda\!\!\!^{-} = \hbar[2m(\tfrac{1}{2}E - V_{2\,\mathrm{eff}}(R))]^{-1/2}. \tag{16}$$

The application of these criteria to the case of A = Xe is considered in section 3.

2.3. Numerical procedure

The computer code of Abrines *et al* (1966) has been used for a great number of classical trajectory calculations where the interactions are Coulombic, see for example Grujić (1986) and references therein. This code has now been modified to account for forces derived from the potential (5). The structure of the computer program has been described elsewhere and we just outline its main features here.

The program solves Newton's equations for the system (see equation (28) in III), using the Runge–Kutta method and evaluates particle trajectories for given sets of initial conditions. The code uses a variable step length during execution and checks to see if a final state is achieved. For a fixed target energy, the energy of the incident particle is varied within the threshold region, and by varying an appropriate number of system parameters, the properties of the constituent fragments in the final channel are obtained. A special procedure identifies the final channels and then the required quantities, evaluated in the reference system with its origin at O, are printed or plotted.

The code correctly identifies two-body bound states even if the atomic energies are positive and the quasi-bound states discussed in section 2.2 are classified as free states as physically they must be.

A feature peculiar to near-threshold studies is the quasi-statistical character of the calculations, because of the high improbability of the fragmentation process (4) for small values of the total energy E. Consequently, the corresponding phase-space volumes are very small, and an ordinary statistical approach such as Monte Carlo would be very time consuming. Therefore a special strategy is adopted for evaluating the relevant quantities and is described in the next section.

3. The process $Xe + Xe_2 \rightarrow 3Xe$

We first establish the adequacy of the classical model that depends crucially on the strength of the interaction specified by C_6, and on the mass m of each atom. We then consider the actual quasi-statistical method used. Note that throughout the sections that follow, all quantities are expressed in atomic units.

3.1. The classical approximation

The Lennard-Jones potential (5) for Xe_2 and the associated effective potential $V_{\text{eff}}(R)$ in (9) are specified by

$$m = 2.3935 \times 10^5 \qquad \varepsilon_0 = 3.75 \times 10^{-4} \qquad R_0 = 8.41 \tag{17}$$

see Radcig and Smirnov (1980). We choose ζ in (13) and (14) to have the value 0.1 throughout this section, and then condition (14) shows that the numerical value of ε_0 determines the upper limit of the threshold region, i.e.

$$0 < E < 7.5 \times 10^{-5}. \tag{18}$$

In figure 1, $V_{\text{eff}}(R)$ is illustrated for several different values of l, the angular momentum of Xe_2. The position and height of each maximum is listed in table 1. In table 2, the radius of the strong correlation zone, R_{sc}, is given for different values of the energy and the position and value of the maximum in $d\lambda/dR$ are also listed for different values of l_2. The asymptotic region where $R > R_{\text{sc}}$ can be seen to start at about $R = 10$ which is a little larger than the equilibrium internuclear separation R_0. The maximum values of $d\lambda/dR$ occur in the asymptotic region, and the classical condition (15) is clearly satisfied except for low values of E and high values of l_2, where the classical approximation fails because of the high centrifugal barrier.

3.2. The quasi-statistical method

The initial configuration for the $Xe + Xe_2$ system is shown in figure 2. For the sake of computational simplicity we have chosen a static model of the Xe_2 target by assuming (i) $R_{23} = R_0$ see figure 2, and (ii) no rotation of the initial configuration of the target. Further, we assume (iii) zero impact parameter, which implies in combination with (i) and (ii) that the total angular momentum of the system, $L = 0$. The problem is thus reduced to one of motion in a plane, and the initial orientation ϕ of the molecular axis with respect to the direction of velocity of the incident Xe atom is the single free

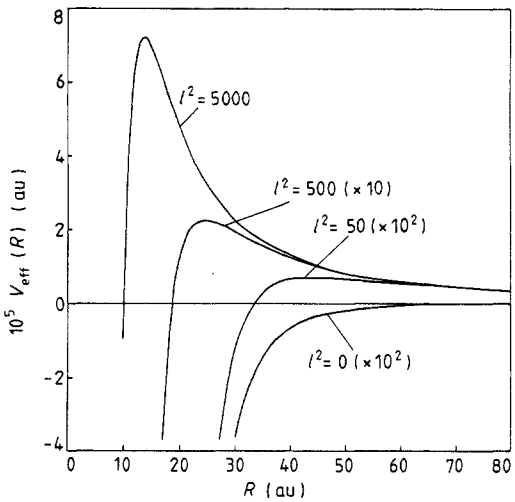

Figure 1. The medium- and long-range parts of the effective potential for the Xe-Xe interaction; $V_{\text{eff}}(R)$ is defined by equation (9). The factor by which $V_{\text{eff}}(R)$ is multiplied is given in brackets for $l^2 \leqslant 500$.

Table 1. Some characteristic quantities of the classical model for the effective potential $V_{\text{eff}}(R)$ defined by equation (9). All quantities are in atomic units.

l^2	50	500	5000
$R_{\max}$	44.2	24.8	13.8
$V_{\text{eff}}(R_{\max})$	7.13×10^{-8}	2.26×10^{-6}	7.22×10^{-5}

Table 2. Some characteristic quantities of the classical model for the effective potential $V_{2\,\text{eff}}(R)$ defined by equation (12). All quantities are in atomic units.

E	10^{-6}	3×10^{-6}	5×10^{-6}	10^{-5}	3×10^{-5}
R_{sc}	19.4	16.1	14.8	13.1	10.8
$l_2^2 = 0$					
$R_{\max}$	23.1	19.3	17.7	15.8	13.3
$\mathrm{d}\lambda/\mathrm{d}R\|_{\max}$	0.097	0.067	0.057	0.045	0.030
$l_2^2 = 50$					
$R_{\max}$	23.6	19.5	17.8	15.9	13.3
$\mathrm{d}\lambda/\mathrm{d}R\|_{\max}$	0.107	0.070	0.058	0.046	0.031
$l_2^2 = 100$					
$R_{\max}$	24.2	19.7	18.0	16.0	13.3
$\mathrm{d}\lambda/\mathrm{d}R\|_{\max}$	0.121	0.074	0.061	0.047	0.031
$l_2^2 = 500$					
$R_{\max}$	—	21.9	19.3	16.6	13.6
$\mathrm{d}\lambda/\mathrm{d}R\|_{\max}$	—	0.146	0.88	0.057	0.34
$l_2^2 = 1000$					
$R_{\max}$	—	—	22.4	17.6	13.8
$\mathrm{d}\lambda/\mathrm{d}R\|_{\max}$	—	—	0.463	0.085	0.039

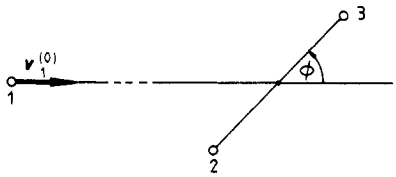

Figure 2. A schematic representation of the initial configuration for the $Xe+Xe_2$ collision.

parameter. The angle ϕ is varied and atomic trajectories calculated until the atoms attain some final configuration. The possible final channels are

$$E_1>0,\ E_2,\ E_3<0 \qquad \text{(direct scattering)} \tag{19a}$$

$$E_1,\ E_{2(3)}<0,\ E_{3(2)}>0 \qquad \text{(exchange)} \tag{19b}$$

$$E_1,\ E_2,\ E_3>0 \qquad \text{(fragmentation)} \tag{19c}$$

where $E>0$. We plot the final-state quantities as functions of ϕ and then derive a number of features of the near-threshold break-up process.

The computations have been carried out using the Vax 11/750 at the Institute of Physics and the Cray X-MP/48 at the Rutherford-Appleton Laboratories. The positions of break-up intervals are first located and then the structure is examined in more detail. In general, a single fragmentation interval is sufficient for the derivation of the threshold law, but the distribution functions cannot be usually inferred from an analysis of a single interval as will be seen in section 4.

4. Numerical results

Preliminary results of the calculations have already been reported by Dimitrijević *et al* (1988). Because of the symmetry of the initial configuration, it is sufficient to consider the interval $0\leqslant\phi\leqslant\pi/2$, see figure 2. In figure 3 we show individual final energies E_1, E_2 and E_3 as functions of ϕ, for the total energy $E=2.466\times10^{-5}$. Here we cover the range $0\leqslant\phi\leqslant\pi$ in order to demonstrate this symmetry and to indicate, via the symmetry of the figure with respect to the reflection in the $\phi=\pi/2$ axis, the overall accuracy of computations. The energies are defined with respect to the centre of mass O of the whole system and the final-energy curves contain large oscillations due to induced rotational motion. This can be seen in the left-hand part of figure 3, where one of the bound atoms has positive energy, due to the collinearity of the motion and the motion of the two-body system to which it belongs. As the rotation speeds up, this oscillatory behaviour becomes prominent because both atoms in the molecule change their energies rapidly from positive to negative and vice versa. This spurious kinematic effect disappears when we consider the fragmentation process (19*c*).

The next step is to locate a 'well behaved' fragmentation interval, to represent the break-up process. This means that we require the interval not only to be large enough, but also to preserve its global structure as the energy E decreases. In figure 4, two intervals A and B are shown that both satisfy the first condition, but only interval B turns out to meet our second requirement. As our calculations show, interval A splits up into a combination of metastable states and true dissociation intervals as E is decreased. In general, for a given energy an interval can be found that contains only

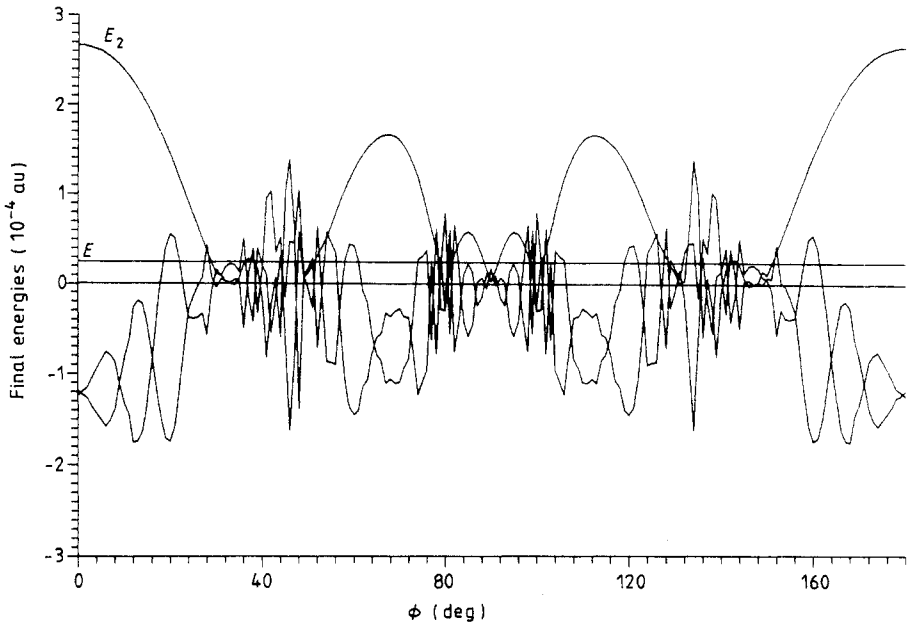

Figure 3. The final energies of the atoms relative to the centre of mass of the whole system, O; note the symmetry with respect to $\phi = \pi/2$, see figure 2.

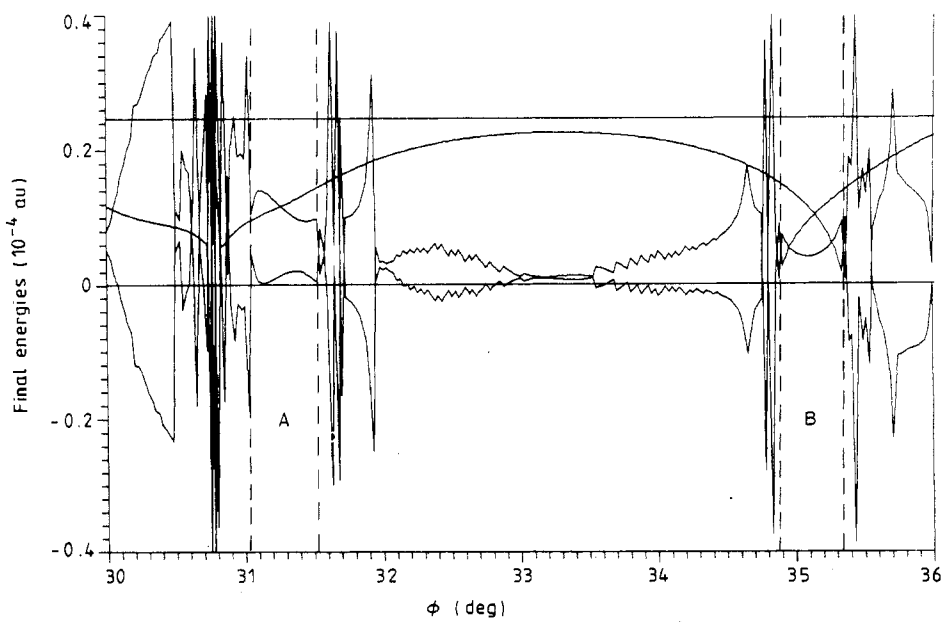

Figure 4. The final energies of the atoms relative to the centre of mass of the whole system, O; note the fragmentation intervals A and B.

metastable states. Further, region (19*c*) is normally situated between regions (19*a*) and (19*b*). If both these intervals are large enough, then region (19*c*) is well behaved. If however, the neighbouring intervals are of the same type, either (19*a*) or (19*b*), the study of process (19*c*) turns out to be very difficult, if not impossible.

4.1. The fragmentation threshold law

In table 3 the break-up intervals B are given for five energies. As can be seen they are very narrow, they shrink as E decreases and slowly change in position. In figure 5 we plot $\ln(\Delta\phi)$ against $\ln E$ and the slope of the most probable straight-line fit gives $\kappa = 1.6$ in equation (1). This is in good agreement with the result $\kappa = 1.693$ derived analytically (see equation (70) in III).

One of the principal features of the quasi-statistical approach to near-threshold studies is the assumption that any fragmentation interval can be taken to be representative of the relevant phase-space change with total energy. It is convenient to choose

Table 3. Fragmentation intervals B in the threshold region. The angles ϕ are quoted in degrees.

Number	E	ϕ	$\Delta\phi$
1	0.2462×10^{-4}	34.873 – 35.343	0.470 ± 0.002
2	0.1796×10^{-4}	34.6785 – 34.9625	0.284 ± 0.001
3	0.1129×10^{-4}	34.4915 – 34.6285	0.137 ± 0.001
4	0.7956×10^{-5}	34.400 38 – 34.476 88	0.0765 ± 0.0003
5	0.4622×10^{-5}	34.3073 – 34.3348	0.0275 ± 0.0001

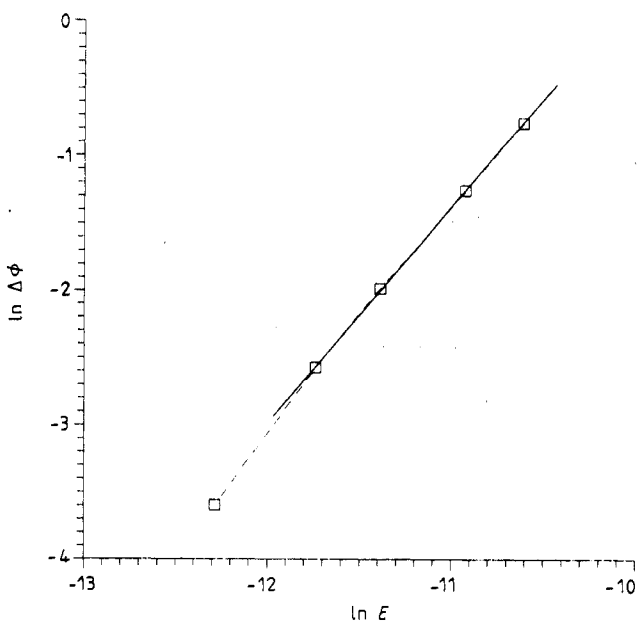

Figure 5. The most probable fit to the data obtained from interval B to obtain the power law given in equation (1).

a large break-up interval, for two reasons; firstly, they are easier to analyse and secondly, they should be statistically dominant. Nevertheless it is wise to examine at least one other interval to see if the assumption of 'coherent scaling' holds. Therefore we have also analysed intervals A and if we ignore the segments occupied by metastable states, the shrinking of the true dissociation interval can be followed in the same manner as for interval B in table 3. Below the energy $E = 1.5 \times 10^{-5}$, the shrinking of interval A is monotonic and numerical values are given in table 4.

Table 4. Fragmentation intervals A in the threshold region. The angles ϕ are quoted in degrees.

Number	E	ϕ	$\Delta\phi$
1	0.1466×10^{-4}	31.915 – 32.151	0.236 ± 0.002
2	0.1133×10^{-4}	32.1955 – 32.3335	0.138 ± 0.001
3	0.799×10^{-5}	32.438 75 – 32.510 75	0.072 ± 0.0005
4	0.599×10^{-5}	32.5685 – 32.6165	0.048 ± 0.001

By fitting the numerical results from intervals A we obtain $\kappa = 1.8$, and thus the values of κ derived from intervals A and B are equally compatible with the analytic result. However, we have more confidence in the result derived from interval B because firstly, it is pure without any metastability admixture and secondly, it appears to be regular within the entire energy region examined so that a more reliable fit to the numerical data can be made.

4.2. Distribution functions

The distributions of various final-state quantities may depend crucially on the detailed structure of the short- and medium-range interaction potential and/or on the accuracy with which one follows the system's evolution within the strong-interaction region. Only if the final-state results follow a unique and preferably simple pattern as is the case with the Coulombic interaction and its energy distribution (see for example, Cvejanović and Grujić 1975, Grujić 1983) can this restricted quasi-statistical treatment work (see however Cvejanović 1988). Otherwise a full statistical treatment is required in order to obtain the real distribution function.

4.2.1. Energy distributions. In figure 6 we show the final energies of the individual atoms for $E = 1.8 \times 10^{-5}$. The corresponding energy distribution as a function of ϕ is given by the ratio of the final energy density to the initial phase-space density (cf Vinkalns and Gailitis 1967). In the inset we show distributions $P(E_1)$ and $P(E_2)$ deduced from the graphs, and we see from figure 6 that $P(E_3)$ is very similar to $P(E_1)$. Clearly the distributions are not uniform, as distinct from the Coulomb case. Further, by comparing the patterns in intervals A and B in figure 4, it is obvious that these vary from one interval to another, and this precludes any reliable derivation of the actual distribution within this restricted quasi-statistical treatment.

Nevertheless figure 6 shows some characteristics of the energy sharing in the final states. In contrast to the problem of ionisation by electrons where the heavy residual ion remains at rest and the outgoing electrons share the available energy equally, here the middle atom takes on some residual energy, and the other two particles move

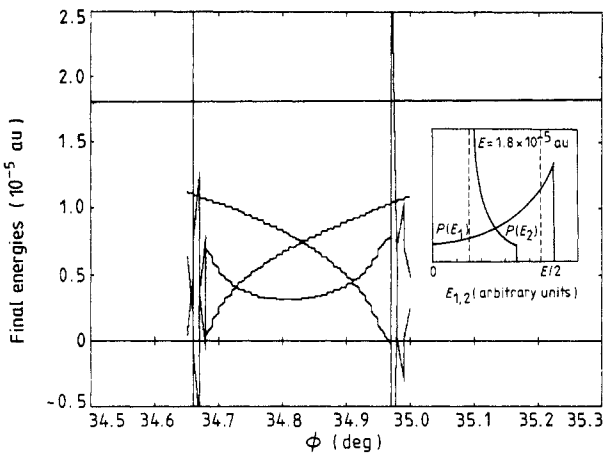

Figure 6. The final energies of the atoms relative to the centre of mass of the whole system, O, for the fragmentation interval B. The corresponding energy distributions $P(E_1)$ and $P(E_2)$ are shown in the inset.

symmetrically on average, throughout the dissociation interval. Note that for a minimum distribution all three curves in figure 6 would have to be linear, with the same absolute value of slope. In the case of a linear leading trajectory, which ideally is expected here, a semi-uniform partition would require $P(E_2) = \delta(E_2)$ and curves for E_1 and E_2 in figure 6 to be symmetrically crossing rectilinear lines.

4.2.2. Mutual angle distributions. The distributions for the mutual angles θ_{ij}, $i \neq j = 1, 2, 3$ are shown in figure 7. If the final configuration were truly collinear, the distributions $P(\theta_{ij})$ would be delta functions around angles 0 and π. The actual situation is indeed close to that in the middle of the break-up interval B. It is interesting to note that at the interval boundaries there is strict collinearity, and here the distributions go to zero. This behaviour is almost identical to that found in the case of the

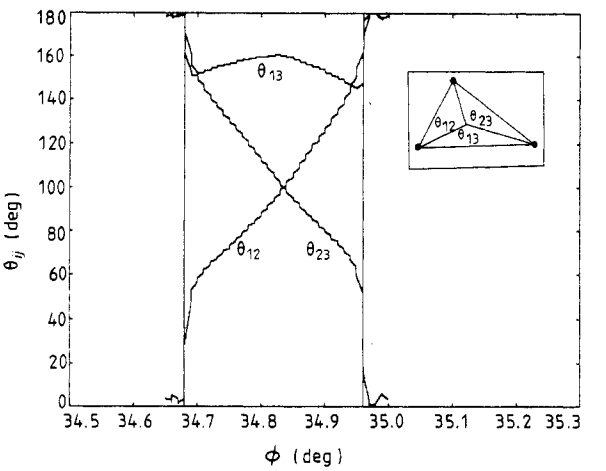

Figure 7. The final configurations for interval B of the mutual angles θ_{12}, θ_{23} and θ_{31} which are shown in the inset.

ionisation of hydrogen by electrons (Grujić 1976). Judging from the rather flat character of the potential-energy surface, see figure 1 in III, one may expect that the actual partition function is very broad.

4.2.3. The angular momenta. In figure 8, typical final angular momenta of the particles are shown. The outer particles acquire large angular momenta, as does the middle atom close to the interval boundaries. Since at this energy particles cannot overcome the centrifugal barriers, see figure 1, they obviously gain these angular momenta only after reaching safe distances from the centre of mass. Near-threshold processes generally are capable of producing states with large angular momenta that are either bound or in the continuum (see, for example, Read 1984), and the case of Van der Waals interactions is no exception.

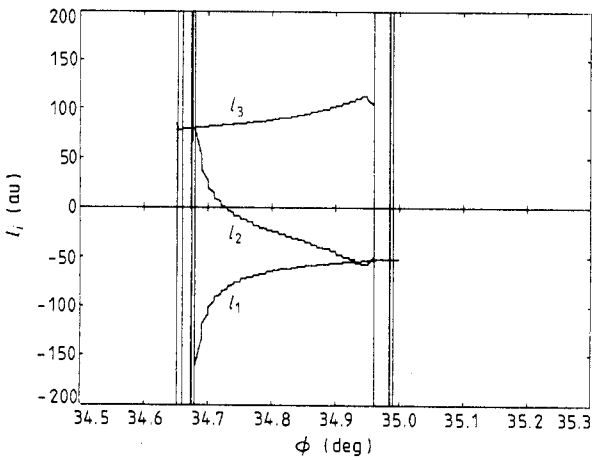

Figure 8. Individual angular momenta in the final state for interval B, relative to the centre of mass of the whole system, O.

The appearance of large angular momenta in the final state and the agreement with the analytically derived threshold law confirms the validity of our assumption that the role of the centrifugal force need not be crucial in the case of a Van der Waals interaction (see the appendix of III). At the same time, it justifies *a posteriori* the assumption that any reasonable choice of the total angular momentum should yield essentially the same threshold behaviour as that obtained for $L=0$. The agreement between the value of κ deduced from our numerical calculations and the analytic result obtained in III, verifies that the short-range part of the Lennard-Jones potential (5) does not significantly affect the threshold law.

5. Concluding remarks

Our restricted quasi-statistical calculations have confirmed all the principal assumptions inherent in Wannier's approach to near-threshold processes, but for an interaction potential that is short range by comparison with the Coulomb case. We consider this as another significant argument in favour of the Wannier model having wider validity than was previously thought. Of course, our results mainly lend support to the

self-consistency of the classical approach, and it remains to be seen whether experiments will support our conclusions. As far as we know, no measurements have been reported of collision-induced dissociation or of processes of an equivalent type for near-threshold regions.

No simple pattern emerges for the distribution functions from our analysis of single fragmentation intervals, and so partition functions cannot be deduced. Obviously, one needs a reasonably extended statistical treatment, involving the variation of extra parameters. In our model of the process, vibrational and/or rotational degrees of freedom can be introduced and the whole procedure repeated for a number of total angular momenta. We plan to carry out such calculations in the near future.

Acknowledgments

We thank the referees for some very helpful suggestions. This work has been partially supported by RZN of Serbia and is also a part of a British Council project, ALIS link no 198.

References

Abrines R, Percival I C and Valentine N A 1966 *Proc. Phys. Soc.* **89** 515-23
Cvejanović S 1988 *Electronic and Atomic Collisions* ed H Gilbody, W R Newell, F H Read and A C H Smith (Amsterdam: Elsevier) pp 767-74
Cvejanović S and Grujić P 1975 *J. Phys. B: At. Mol. Phys.* **8** L305-9
Dimitrijević M S and Grujić P 1981 *J. Phys. B: At. Mol. Phys.* **14** 1663-74
Dimitrijević M S, Grujić P, Peach G and Simonović N 1988 *Int. Conf. on Classical Dynamics in Atomic and Molecular Physics (Brioni, Yugoslavia)* (Belgrade: Institute of Physics) Abstracts p 48
Grujić P 1976 *Proc. Symp. on Physics of Ionised Gases* (Dubrovnik: J Stefan Institute, Ljubljana) pp 70-3
—— 1983 *J. Phys. B: At. Mol. Phys.* **16** 2567-76
—— 1986 *Comment. At. Mol. Phys.* **18** 47-74
Grujić P and Simonović N 1988 *J. Phys. B: At. Mol. Opt. Phys.* **21** 1845-59
Hirschfelder J, Eyring H and Topley B 1936 *J. Chem. Phys.* **4** 170-7
Karplus M, Porter R N and Sharma R D 1965 *J. Chem. Phys.* **43** 3259-87
Klar H 1981 *J. Phys. B: At. Mol. Phys.* **14** 3255-65
Peach G, Willis S L and McDowell M R C 1985 *J. Phys. B: At. Mol. Phys.* **18** 3921-37
Radcig A A and Smirnov B M 1980 *Handbook of Atomic and Molecular Physics* (Moscow: Atomizdat) (in Russian)
Read F H 1984 *J. Phys. B: At. Mol. Phys.* **17** 3965-86
Simonović N and Grujić P 1987 *J. Phys. B: At. Mol. Phys.* **20** 3427-36
Vinkalns I and Gailitis M 1967 *Latvian Academy of Sciences Report no 4* (Riga: Zinatne) pp 17-34 (in Russian)
Wannier G H 1953 *Phys. Rev.* **90** 817-25
Wetmore A E and Olson R E 1986 *Phys. Rev.* A **34** 2822-9

J. Phys. B: At. Mol. Opt. Phys. **25** (1992) 5121-5127. Printed in the UK

Influence of ion–atom collisions on the recombination of electrons

A A Mihajlov†, N N Ljepojević‡ and M S Dimitrijević§

† Institute of Physics, PO Box 57, 11001 Beograd, Yugoslavia
‡ Department of Applied Mathematics and Theoretical Physics, University of Cambridge, Cambridge CB3 9EW, UK
§ Astronomical Observatory, Volgina 7, 11050 Beograd, Yugoslavia

Received 7 February 1992, in final form 22 June 1992

Abstract. We show that for the study of recombination of ions and electrons in weakly ionized low-temperature hydrogen plasmas, the processes $H+H^++e\rightarrow H+H^*(n)$ and $H_2^++e\rightarrow H+H^*(n)$ must both be considered since their contributions are comparable. A simple method for the calculation of the corresponding rate coefficients is presented.

1. Introduction

The parallel study of processes in plasma involving diatomic molecular ions and colliding atom-atomic-ion complexes has already been demonstrated to be useful for the study of electromagnetic radiation in a plasma (Mihajlov and Dimitrijević 1986, 1992). In addition to the interaction between diatomic molecular ions and colliding atom-atomic-ion complexes with radiation in a plasma, their interaction with free electrons is also important. In this paper we report on the latter study of the processes, i.e.

$$A_2^++e\rightarrow A+A^*(n) \tag{1a}$$

$$A+A^++e\rightarrow\begin{cases}A+A^*(n)\\A^*(n)+A\end{cases} \tag{1b}$$

where A denotes a neutral atom in the ground state, A^+ and A_2^+ atomic and molecular ions, $A^*(n)$ an atom excited to the level with the principal quantum number n, and e denotes an electron. Processes $(1a)$ and $(1b)$ are important recombination channels in weakly ionized low-temperature plasmas.

Ion-atom collision creates the quasimolecular complex A^++A, whose electronic state can be well described as a superposition of the ground and first excited electronic state of molecular ion A_2^+, during a certain period of time. This is known from the theory of resonant charge exchange caused by symmetrical ion-atom collisions. Consequently, processes $(1a)$ and $(1b)$ become similar since both represent the same dielectronic recombination. These processes are dielectronic processes, because both the free electron and the electronic shell of the atomic subsystem change their states (Bates and Dalgarno 1962, Smirnov 1981). Namely, the ion-atomic subsystem (A_2^+ in the $(1a)$ case, or the collisional complex $A+A^+$ in the $(1b)$ case) is excited from the ground state to the first excited state, and the free electron is captured by one of the atomic

0953-4075/92/235121+09$07.50

particles. The difference between processes $(1a)$ and $(1b)$ is that in the $(1a)$ case the ion–atom subsystem (A_2^+) is in the ground state with the probability equal to one and in the $(1b)$ case the considered subsystem $(A+A^+)$ is in the ground state with the probability $\frac{1}{2}$.

The process $(1b)$ was first considered by Mihajlov and Ljepojević (1982). However, its contribution to the recombination has so far been neglected in the literature (see e.g. Flannery 1990 or Schneider *et al* 1991). The process $(1b)$ should not be mixed up with the process of three-particle recombination $A^+ + B + e \rightarrow A^* + B$ where the third particle is a neutral atom B (Pitajevskij 1962). The latter process occurs at very large distances between A^+ and B, so that A^+ and B do not form a molecular complex and there is no energy exchange between the free electron and the electronic component of the subsystem $A^+ + B$.

Our first aim in this paper is to draw attention to the recombination channel $(1b)$, i.e. *electron–ion recombination during the scattering of free electrons on collisional* symmetrical ion–atom complexes. For partially ionized plasma, this channel always exists parallelly with the well known channel $(1a)$, i.e. with the channel of dissociative recombination. We will show that the contribution of the channel $(1b)$ is not only comparable with the contribution of channel $(1b)$ but even dominant within a wide range of electron densities and temperatures. Consequently, our objective is to find the ratio between the recombination rate coefficients for the channel $(1b)$ and for channels $(1a)$ and $(1b)$ together. In order to do this we will present here a simple method for the calculation of the corresponding rate coefficients for the case $n \geqslant 4$, n being the principal quantum number. The method is derived within the semiclassical approximation, using the resonant energy transfer model within the electronic components of the atomic system considered (Mihajlov and Janev 1981) and the results obtained by Mihajlov and Dimitrijević (1986). The rate coefficients are calculated assuming that the following conditions are fulfilled.

(i) The energy distribution function for the free atoms and ions is Maxwellian with the temperature T_a.

(ii) The energy distribution of bound states of the molecular ion A_2^+ is Boltzmannian with the temperature T_a.

(iii) The energy distribution of the free electrons is Maxwellian with the temperature $T_e \geqslant T_a$.

The presented method will be applied to the hydrogen case.

2. Theory and discussion

Let $R_n^{(a,b)}$ be the number of recombinations per unit time in a unit volume,

$$R_n^{(a,b)} = K_{r,n}^{(a,b)} N_A N_e N_{A^+} \tag{2}$$

where the N denote number density. If we denote by $f_e(\varepsilon)$ the electron energy distribution function, satisfying the normalization condition

$$\int f_e(\varepsilon)\varepsilon^{1/2}\,\mathrm{d}\varepsilon = 1 \tag{3}$$

and the electron energy ε is calculated in the $A+A^+$ complex centre of mass reference frame, $k_{r,n}^{(a,b)}(T_a, \varepsilon) f_e(\varepsilon)\varepsilon^{1/2}\,\mathrm{d}\varepsilon$ will be the differential recombination rate coefficient

(i.e. recombination rate coefficient for electron energy interval ε, $\varepsilon+\mathrm{d}\varepsilon$), depending only on ε and the temperature T_a of the ion–atom component.

The recombination rate coefficient $K_{r,n}^{(a,b)}$ for the processes $(1a)$ and $(1b)$ is written as

$$K_{r,n}^{(a,b)} = \int k_{r,n}^{(a,b)}(T_a, \varepsilon) f_e(\varepsilon) \varepsilon^{1/2}\, \mathrm{d}\varepsilon. \tag{4}$$

Equation (4) determines the recombination rate coefficient for any electron energy distribution function, but in this paper we limit ourselves to the case of Maxwellian distribution function $f_e(\varepsilon)$ with electron temperature T_e. (We note that T_e is not in a general case equal to the atom temperature T_a.)

Now the problem is reduced to the determination of $k_{r,n}^{(a,b)}(T_a, \varepsilon)$. In order to determine $k_{r,n}^{(a,b)}(T_a, \varepsilon)$ we will concern ourselves for the moment with the processes inverse to the processes $(1a)$ and $(1b)$, i.e. to the ionization processes

$$\mathrm{A} + \mathrm{A}^*(n) \rightarrow \mathrm{A}_2^+ + \mathrm{e} \tag{5a}$$

$$\mathrm{A} + \mathrm{A}^*(n) \rightarrow \mathrm{A}^+ + \mathrm{A} + \mathrm{e}. \tag{5b}$$

Processes $(5a)$ and $(5b)$ have been investigated in detail within the semiclassical approximation in Janev and Mihajlov (1980) and Mihajlov and Janev (1981). Let $I_{i,n}^{(a,b)}$ be the number of ionizations per unit time in a unit volume. In a fashion similar to equation (2), $I_{i,n}^{(a,b)}$ may be expressed as

$$I_{i,n}^{(a,b)} = K_{i,n}^{(a,b)} N_A N_{A^*}. \tag{6}$$

The corresponding ionization rate coefficient $K_{i,n}^{(a,b)}$ may be expressed in terms of the differential ionization rate coefficient $k_{i,n}^{(a,b)}$ (i.e. the ionization rate coefficient in the electron energy interval ε, $\varepsilon+\mathrm{d}\varepsilon$) as

$$K_{i,n}^{(a,b)} = \int k_{i,n}^{(a,b)}(T_a, \varepsilon)\, \mathrm{d}\varepsilon. \tag{7}$$

In the case of LTE, i.e. for $T_e = T_a$, the balance equation must be satisfied at the differential level, i.e.

$$[k_{r,n}^{(a,b)}(T_a, \varepsilon) f_e(\varepsilon, T_e) \varepsilon^{1/2} N_e N_A N_{A^+}]_{T_e=T_a}\, \mathrm{d}\varepsilon \equiv [k_{i,n}^{(a,b)}(T_a, \varepsilon) N_A N_{A^*}]_{T_e=T_a}\, \mathrm{d}\varepsilon. \tag{8}$$

Since $k_{i,n}^{(a,b)}$ is determined in an analytical form (Mihajlov and Janev 1981), equation (8) gives us the possibility to obtain $k_{r,n}^{(a,b)}$ in the form

$$k_{r,n}^{(a,b)}(T_a, \varepsilon) = \frac{k_{i,n}^{(a,b)}(T_a, \varepsilon)}{[f_e(\varepsilon)\varepsilon^{1/2}]} \left[\frac{N_{A^*}}{N_A}\right] \left[\frac{N_e N_A^+}{N_A}\right]^{-1}$$
$$k_{i,n}^{(a,b)}(T_a, \varepsilon) = \langle v_a\, \mathrm{d}\sigma_{i,n}^{(a,b)}/\mathrm{d}\varepsilon \rangle \tag{9}$$

where $\mathrm{d}\sigma_{i,n}^{(a,b)}/\mathrm{d}\varepsilon$ is the differential ionization cross section for the $(5a)$ and $(5b)$ reactions, v_a the initial relative atom–atom velocity in the input channels for the reaction given by equation (5), and $\langle \ldots \rangle$ denotes the averaging over the Maxwellian function with $T = T_a$. The expressions in square brackets are determined assuming LTE with $T \equiv T_a$ by the Boltzmann equation which relates N_{A^*} and N_A, and the Saha equation which relates N_{A^+}, N_A and N_e. Consequently, the expressions in square brackets are known functions of T_a. We assume here that the plasma is weakly non-ideal in such degree that one can neglect the lowering of the ionization potential. In the opposite case, equation (9) will become the function of an additional parameter (density or pressure).

Equation (9) is a consequence of the principle of thermodynamical balance and describes processes (1*a*, *b*) rather successfully. In the case of a symmetrical ion–atom system $d\sigma_{i,n}^{(a,b)}/d\varepsilon$ attains a simple analytical form determined in Mihajlov and Janev (1981). Using this simple analytical form, Saha and Boltzmann equations, Maxwellian functions and expressing incomplete gamma functions through the error function (Mihajlov and Dimitrijević 1986) it is simple to obtain $K_{r,n}^{(a,b)}$ in the form

$$K_{r,n}^{(a,b)}(T_a, T_e) = C_n(T_a, T_e) \int_{\varepsilon_n}^{\varepsilon_{max}} \frac{e^{-\varepsilon/kT_e}}{\varepsilon} R_\varepsilon^4 \, e^{-U_1(\varepsilon)/kT_a} X^{(a,b)}(\varepsilon, T_a) \, d\varepsilon \tag{10}$$

where

$$\begin{aligned} C_n(T_a, T_e) &= \frac{8\pi^{5/2}}{3(6^{1/2})} [\gamma n^3 (kT_e)^{3/2}]^{-1} \exp(|\varepsilon_n|/kT_e) \\ X^{(a)}(\varepsilon, T_a) &= \Phi(Z^{1/2}) - 2\pi^{-1/2} Z^{1/2} \exp(Z) \\ X^{(b)}(\varepsilon, T_a) &= 1 - X^{(a)}(\varepsilon, T_a) \\ Z &= -U_1(R_\varepsilon)/(kT_e) \end{aligned} \tag{11}$$

where Φ is the error function (Abramowitz and Stegun 1972), and all quantities in equations (10)–(11) are in atomic units. The internuclear distance R_ε as a function of ε is determined from the equation

$$\varepsilon = U_2(R_\varepsilon) - U_1(R_\varepsilon) \tag{12}$$

where it is assumed that the electron recombination occurs in the close vicinity of the resonant internuclear distance R_ε. Here ε is the energy difference between the final (repulsive) and the initial (attractive) electronic states with energies U_2 and U_1 of the ion–atom subsystem (molecular ion), $U_1(R_\varepsilon)$ is the energy of the initial state of A_2^+ ($U_1(R) < 0$) and ε_n the ionization energy of the atomic state $A^*(n)$. The quantity γ in equation (11) is defined as

$$\gamma = |d \ln \varepsilon(R)/dR|_{R=R_\varepsilon}. \tag{13}$$

Equation (13) may be successfully approximated as $\gamma \approx \gamma_A(1 - O(\delta/\gamma_A R))$; $\gamma_A^2/2 = I_A(\text{au})$; $\delta = (2/\gamma_A) - 1$; where I_A is the ionization potential of A. For $R_\varepsilon > R_{min}$ (R_{min} corresponds to the minimum of the molecular potential U_1, $\gamma \approx \gamma_A = \text{const}$ ($\gamma = 1$ for H and 1.345 for He). The square of the corresponding dipole matrix element is in equation (10) approximated as $\sim e^2 R_\varepsilon^2/4$ (for details see appendix A in Mihajlov and Popović (1981) and the corresponding discussion in Mihajlov and Dimitrijević (1992)). The maximal energy, ε_{max} in equation (10) corresponds to the maximal difference in equation (12). In the case of hydrogen, the R_ε corresponding to ε_{max} is equal to zero (in Mihajlov and Ljepojević (1982), the calculations were performed under the assumption that $\varepsilon_{max} = \infty$, since the corresponding analytical approximations for the expression under the integral were used).

The total rate coefficient for process (1), i.e. (1*a*)+(1*b*) (we omit the subscript *r* for simplicity)

$$K_n(T_a, T_e) = K_n^{(a)}(T_a, T_e) + K_n^{(b)}(T_a, T_e) \tag{14}$$

is given by the expression

$$K_n(T_a, T_e) = C_n(T_e) \int_{\varepsilon_n}^{\varepsilon_{max}} \frac{e^{-\varepsilon/kT_e}}{\varepsilon} R_\varepsilon^4 \, e^{-U_1(\varepsilon)/kT_a} \, d\varepsilon. \tag{15}$$

The present method is correct when in the output channels for the reactions (1*a*) and (1*b*) the interaction between the $A^*(n)+A$ and $A^+ + A^-$ system terms may be neglected. In the hydrogen case, the electron affinity is $\varepsilon^{(-)}=0.75$ eV (Massey 1976). Therefore, the proposed method is correct for $n>4$ in this case. However, the $n=4$ case can be included since the interaction of the $H^*(n=4)+H$ and $H^+ + H^-$ system terms occurs for $R \geqslant 10$ au. In the case of $n=4$, this region is not of importance. Consequently we may conclude that the present method is valid for $n \geqslant 4$ in the hydrogen case.

3. Results and conclusion

As an example, we show the results of calculations for $n=4$–10 for hydrogen. Now, U_1, U_2 correspond to the Σ_g^+ and Σ_u^+ electron states of H_2^+ and were taken from Bates *et al* (1953). Results for $K_n(T_a, T_e)$ and $K_n^{(a)}(T_a, T_e)/K_n(T_a, T_e)$ as functions of T_a and T_e are presented in tables 1 and 2.

For $n>10$ one may use the following approximation. On the basis of the analytical expression for $\varepsilon(R)$ (Greenland 1982) for large R

$$\varepsilon(R)=4R\exp[-(R+1)][1+O(1/R)] \tag{16}$$

one can obtain the following approximate expressions for R_ε, suitable in our case for $n>10$

$$R_\varepsilon=\ln(4/e\varepsilon)+\ln[\ln(4/c\varepsilon)] \tag{17}$$

where $c=2.718$. Moreover, for $n>10$ one can use for U_1 the approximate expression (Herring 1962):

$$U_1=-\frac{\varepsilon}{2}-\frac{\alpha_H}{2R^4} \tag{18}$$

where α_H is the polarizability of hydrogen ($\alpha_H=4.5$ au).

Using the tabulated values for $n=10$ one can calculate the $K_n(T_a, T_e)$ for $n>10$ with the following approximate expression

$$K_n(T_a, T_e)=\frac{1000}{n^3}\exp\left(\frac{\varepsilon_n-\varepsilon_{10}}{kT_e}\right)K_{10}(T_a, T_e)+6.104\times10^{-24}n^{-3}\gamma^{-1}T_e^{-3/2}$$
$$\times\exp\left(\frac{3.1578\times10^5}{2n^2T_e}\right)R_\varepsilon^4\sum_{k=m+1}^{n}1/k. \tag{19}$$

We have checked the agreement between results obtained by using equations (19) and (15) up to $n=100$ and found that convergence is very good. For $n=11$ maximal differences are of the order of several per cent and for higher n results are the same. In such a way, using tables 1 and 2 and the relations (16)–(19), one can obtain in a simple manner the required recombination coefficients for higher n. In tables 1 and 2 the results are presented starting from $T_a=1000$ K, since for the process (1*a*) for lower T_a the proposed method breaks down. At low T, the nucleus motion in the molecular ion A_2^+ cannot be treated classically with success. Namely, at low temperatures the A_2^+ ion is mostly in one of the lowest vibrational states, where the nucleus motion is quantum mechanical. However, in the case of the process of recombination on col-

Table 1. Recombination rate coefficient $K_n(T_a, T_e)$ ($cm^6 s^{-1}$) for $n = 4$–10 for hydrogen as a function of atomic temperature T_a and electron temperature T_e.

T_e (K) \ T_a (K)	1000	1500	2000	3000	4000	5000	6000	7000	8000
$N=4$	1 000	0.432E−25							
	3 000	0.269E−24	0.718E−26	0.182E−26	0.528E−27				
	5 000	0.126E−22	0.208E−25	0.251E−26	0.502E−27	0.249E−27	0.167E−27		
	7 000	0.248E−21	0.824E−25	0.434E−26	0.532E−27	0.231E−27	0.147E−27	0.110E−27	0.899E−28
	10 000	0.394E−20	0.444E−24	0.103E−25	0.631E−27	0.223E−27	0.130E−27	0.930E−28	0.740E−28	0.627E−28
	20 000	0.146E−18	0.640E−23	0.607E−25	0.111E−26	0.233E−27	0.107E−27	0.674E−28	0.498E−28	0.401E−28
	30 000	0.452E−18	0.160E−22	0.122E−24	0.148E−26	0.237E−27	0.939E−28	0.546E−28	0.383E−28	0.299E−28
	40 000	0.726E−18	0.236E−22	0.163E−24	0.165E−26	0.229E−27	0.832E−28	0.458E−28	0.311E−28	0.237E−28
$N=5$	1 000	0.795E−26							
	3 000	0.457E−25	0.194E−26	0.683E−27	0.278E−27				
	5 000	0.318E−23	0.569E−26	0.857E−27	0.236E−27	0.139E−27	0.104E−27		
	7 000	0.763E−22	0.257E−25	0.149E−26	0.236E−27	0.122E−27	0.858E−28	0.690E−28	0.594E−28
	10 000	0.142E−20	0.159E−24	0.378E−26	0.272E−27	0.112E−27	0.720E−28	0.553E−28	0.464E−28	0.408E−28
	20 000	0.625E−19	0.274E−23	0.260E−25	0.493E−27	0.112E−27	0.555E−28	0.373E−28	0.289E−28	0.242E−28
	30 000	0.206E−18	0.729E−23	0.553E−25	0.681E−27	0.114E−27	0.481E−28	0.295E−28	0.216E−28	0.175E−28
	40 000	0.340E−18	0.111E−22	0.764E−25	0.778E−27	0.112E−27	0.426E−28	0.245E−28	0.173E−28	0.137E−28
$N=6$	1 000	0.294E−26							
	3 000	0.146E−25	0.867E−27	0.375E−27	0.186E−27				
	5 000	0.125E−23	0.238E−26	0.424E−27	0.146E−27	0.959E−28	0.763E−28		
	7 000	0.335E−22	0.114E−25	0.709E−27	0.137E−27	0.795E−28	0.601E−28	0.506E−28	0.450E−28
	10 000	0.675E−21	0.761E−25	0.184E−26	0.150E−27	0.691E−28	0.480E−28	0.387E−28	0.336E−28	0.304E−28
	20 000	0.328E−19	0.144E−23	0.137E−25	0.267E−27	0.646E−28	0.342E−28	0.241E−28	0.194E−28	0.167E−28
	30 000	0.112E−18	0.396E−23	0.300E−25	0.374E−27	0.653E−28	0.289E−28	0.185E−28	0.141E−28	0.117E−28
	40 000	0.188E−18	0.609E−23	0.421E−25	0.432E−27	0.638E−28	0.253E−28	0.152E−28	0.111E−28	0.898E−29

$N=7$	1 000	0.153E−26								
	3 000	0.651E−26	0.494E−27	0.246E−27	0.139E−27					
	5 000	0.625E−24	0.125E−26	0.254E−27	0.102E−27	0.724E−28	0.601E−28			
	7 000	0.179E−22	0.611E−26	0.405E−27	0.916E−28	0.577E−28	0.458E−28	0.397E−28	0.361E−28	
	10 000	0.379E−21	0.427E−25	0.105E−26	0.951E−28	0.479E−28	0.351E−28	0.293E−28	0.261E−28	0.240E−28
	20 000	0.195E−19	0.857E−24	0.814E−26	0.162E−27	0.417E−28	0.233E−28	0.171E−28	0.142E−28	0.125E−28
	30 000	0.676E−19	0.240E−23	0.182E−25	0.229E−27	0.414E−28	0.191E−28	0.127E−28	0.997E−29	0.848E−29
	40 000	0.115E−18	0.373E−23	0.258E−25	0.266E−27	0.402E−28	0.165E−28	0.103E−28	0.772E−29	0.640E−29
$N=8$	1 000	0.962E−27								
	3 000	0.351E−26	0.323E−27	0.178E−27	0.110E−27					
	5 000	0.360E−24	0.753E−27	0.171E−27	0.771E−28	0.576E−28	0.492E−28			
	7 000	0.108E−22	0.369E−26	0.258E−27	0.664E−28	0.445E−28	0.365E−28	0.324E−28	0.298E−28	
	10 000	0.235E−21	0.265E−25	0.659E−27	0.658E−28	0.356E−28	0.271E−28	0.233E−28	0.210E−28	0.196E−28
	20 000	0.126E−19	0.553E−24	0.526E−26	0.107E−27	0.290E−28	0.169E−28	0.129E−28	0.109E−28	0.973E−29
	30 000	0.441E−19	0.157E−23	0.119E−25	0.151E−27	0.282E−28	0.136E−28	0.932E−29	0.747E−29	0.646E−29
	40 000	0.754E−19	0.245E−23	0.169E−25	0.175E−27	0.272E−28	0.116E−28	0.740E−29	0.570E−29	0.481E−29
$N=9$	1 000	0.678E−27								
	3 000	0.214E−26	0.231E−27	0.137E−27	0.903E−28					
	5 000	0.228E−24	0.496E−27	0.123E−27	0.610E−28	0.473E−28	0.413E−28			
	7 000	0.701E−23	0.242E−26	0.178E−27	0.507E−28	0.357E−28	0.300E−28	0.271E−28	0.252E−28	
	10 000	0.157E−21	0.177E−25	0.445E−27	0.483E−28	0.277E−28	0.218E−28	0.190E−28	0.174E−28	0.164E−28
	20 000	0.861E−20	0.378E−24	0.360E−26	0.750E−28	0.212E−28	0.129E−28	0.101E−28	0.866E−29	0.785E−29
	30 000	0.305E−19	0.108E−23	0.820E−26	0.105E−27	0.202E−28	0.101E−28	0.712E−29	0.582E−29	0.511E−29
	40 000	0.523E−19	0.170E−23	0.117E−25	0.122E−27	0.194E−28	0.848E−29	0.558E−29	0.438E−29	0.376E−29
$N=10$	1 000	0.514E−27								
	3 000	0.141E−26	0.175E−27	0.110E−27	0.760E−28					
	5 000	0.155E−24	0.348E−27	0.937E−28	0.498E−28	0.398E−28	0.353E−28			
	7 000	0.485E−23	0.168E−26	0.129E−27	0.403E−28	0.294E−28	0.252E−28	0.230E−28	0.216E−28	
	10 000	0.110E−21	0.124E−25	0.316E−27	0.370E−28	0.222E−28	0.179E−28	0.159E−28	0.147E−28	0.139E−28
	20 000	0.616E−20	0.271E−24	0.258E−26	0.547E−28	0.162E−28	0.102E−28	0.810E−29	0.709E−29	0.648E−29
	30 000	0.219E−19	0.778E−24	0.591E−26	0.761E−28	0.151E−28	0.777E−29	0.562E−29	0.468E−29	0.415E−29
	40 000	0.378E−19	0.123E−23	0.849E−26	0.887E−28	0.143E−28	0.646E−29	0.435E−29	0.348E−29	0.302E−29

Table 2. Relative participation of process (1*a*) $[K_n^{(a)}(T_a, T_e)/K_n(T_a, T_e)]$ for $n = 4$–10 for hydrogen as a function of atomic temperature T_a and electron temperature T_e.

	T_a (K) / T_e (K)	1000	1500	2000	3000	4000	5000	6000	7000	8000
$N=4$	1 000	0.981								
	3 000	0.999	0.960	0.879	0.707					
	5 000	1.00	0.990	0.935	0.774	0.641	0.549			
	7 000	1.00	0.998	0.970	0.828	0.689	0.589	0.519	0.471	
	10 000	1.00	1.00	0.990	0.886	0.749	0.639	0.560	0.503	0.463
	20 000	1.00	1.00	0.999	0.963	0.861	0.749	0.655	0.583	0.529
	30 000	1.00	1.00	1.00	0.981	0.907	0.805	0.709	0.632	0.571
	40 000	1.00	1.00	1.00	0.987	0.928	0.836	0.743	0.663	0.599
$N=5$	1 000	0.921								
	3 000	0.993	0.892	0.761	0.576					
	5 000	1.00	0.975	0.869	0.659	0.533	0.460			
	7 000	1.00	0.996	0.941	0.736	0.588	0.500	0.445	0.410	
	10 000	1.00	0.999	0.983	0.827	0.664	0.555	0.486	0.441	0.410
	20 000	1.00	1.00	0.999	0.948	0.817	0.688	0.592	0.524	0.476
	30 000	1.00	1.00	1.00	0.974	0.880	0.759	0.657	0.578	0.521
	40 000	1.00	1.00	1.00	0.984	0.909	0.800	0.697	0.614	0.551
$N=6$	1 000	0.831								
	3 000	0.984	0.815	0.662	0.495					
	5 000	1.00	0.955	0.801	0.575	0.467	0.411			
	7 000	1.00	0.993	0.910	0.661	0.520	0.446	0.403	0.377	
	10 000	1.00	0.999	0.975	0.773	0.599	0.499	0.440	0.403	0.379
	20 000	1.00	1.00	0.998	0.933	0.777	0.639	0.545	0.482	0.439
	30 000	1.00	1.00	0.999	0.968	0.855	0.721	0.614	0.537	0.483
	40 000	1.00	1.00	1.00	0.980	0.892	0.768	0.658	0.575	0.514
$N=7$	1 000	0.740								
	3 000	0.973	0.744	0.588	0.444					
	5 000	1.00	0.934	0.742	0.518	0.427	0.382			
	7 000	1.00	0.990	0.880	0.604	0.474	0.412	0.377	0.355	
	10 000	1.00	0.999	0.967	0.727	0.551	0.460	0.409	0.378	0.358
	20 000	1.00	1.00	0.998	0.919	0.743	0.600	0.509	0.451	0.412
	30 000	1.00	1.00	0.999	0.963	0.833	0.687	0.579	0.505	0.454
	40 000	1.00	1.00	1.00	0.977	0.875	0.740	0.626	0.543	0.485
$N=8$	1 000	0.660								
	3 000	0.960	0.685	0.534	0.412					
	5 000	1.00	0.914	0.694	0.478	0.400	0.363			
	7 000	1.00	0.987	0.852	0.561	0.443	0.389	0.359	0.340	
	10 000	1.00	0.999	0.959	0.689	0.515	0.432	0.387	0.360	0.342
	20 000	1.00	1.00	0.997	0.907	0.713	0.568	0.480	0.426	0.391
	30 000	1.00	1.00	0.999	0.957	0.812	0.659	0.550	0.479	0.431
	40 000	1.00	1.00	1.00	0.974	0.860	0.715	0.598	0.516	0.461
$N=9$	1 000	0.596								
	3 000	0.947	0.637	0.496	0.390					
	5 000	1.00	0.894	0.653	0.449	0.381	0.349			
	7 000	1.00	0.984	0.827	0.528	0.419	0.371	0.345	0.328	
	10 000	1.00	0.999	0.952	0.656	0.487	0.410	0.370	0.346	0.329
	20 000	1.00	1.00	0.997	0.894	0.687	0.541	0.457	0.407	0.374
	30 000	1.00	1.00	0.999	0.952	0.793	0.633	0.525	0.456	0.411
	40 000	1.00	1.00	1.00	0.971	0.846	0.692	0.573	0.494	0.440

Table 2. (continued)

T_e (K) \ T_a (K)		1000	1500	2000	3000	4000	5000	6000	7000	8000
$N = 10$	1 000	0.547								
	3 000	0.934	0.599	0.467	0.374					
	5 000	1.00	0.876	0.620	0.427	0.366	0.337			
	7 000	1.00	0.982	0.804	0.501	0.401	0.357	0.333	0.317	
	10 000	1.00	0.998	0.945	0.629	0.464	0.393	0.356	0.333	0.318
	20 000	1.00	1.00	0.997	0.883	0.663	0.518	0.438	0.390	0.359
	30 000	1.00	1.00	0.999	0.947	0.776	0.611	0.504	0.438	0.395
	40 000	1.00	1.00	1.00	0.968	0.833	0.671	0.552	0.474	0.422

lisional ion–atom complexes (1*b*), the derived expressions are valid down to room temperature.

One can see that for our plasma conditions the process (1*b*) of recombination on collisional quasi-molecular complexes and the dissociative recombination process (1*a*) are competitive. The method presented offers a possibility for the determination of their relative participation and for the calculation of the corresponding rate coefficients.

The transition to the more complex symmetrical atomic systems of the type $A+A^+$ may be done by replacing $R_\omega^2/4$ in the preceding equations with the square of the modulus of the corresponding dipole matrix element and by introducing the corresponding $\varepsilon(R)$.

References

Abramowitz M and Stegun I 1972 *Handbook of Mathematical Functions* (New York: Dover)

Bates D R and Dalgarno A 1962 *Atomic and Molecular Processes* ed D R Bates (New York: Academic) ch 7, section 2

Bates D R, Ledsham K and Stewart A L 1953 *Phil. Trans. R. Soc.* **246** 215

Flannery M R 1990 *Proc. 10th Eur. Sect. Conf. on Atomic and Molecular Physics of Ionized Gases (Orleans)* (Geneva: European Physics Society) p 18

Greenland P T 1982 *Phys. Rep.* **81** 133

Herring C 1962 *Rev. Mod. Phys.* **34** 631

Janev R K and Mihajlov A A 1980 *Phys. Rev.* A **21** 819

Massey H 1976 *Negative Ions* (Cambridge: Cambridge University Press)

Mihajlov A A and Dimitrijević M S 1986 *Astron. Astrophys.* **155** 319

—— 1992 *Astron. Astrophys.* **256** 305

Mihajlov A A and Janev R K 1981 *J. Phys. B: At. Mol. Phys.* **14** 1639

Mihajlov A A and Ljepojević N N 1982 *Proc. Symp. on Physics of Ionized Gases (Dubrovnik, 1982)* (Zagreb: Institute of Physics of the University of Zagreb) contributed papers p 385

Mihajlov A A and Popović M M 1981 *Phys. Rev.* A **23** 1679

Pitajevskij L P 1962 *Zh. Eksp. Teor. Fiz.* **42** 1326

Schneider I F, Dulieu O and Giusti-Suzor A 1991 *J. Phys. B: At. Mol. Opt. Phys.* **24** L289

Smirnov B M 1981 *Usp. Fiz. Nauk* **133** 569

J. Phys. B: At. Mol. Opt. Phys. 27 (1994) 5717–5730. Printed in the UK

Small-energy three-body systems: V. Threshold laws when Wannier theory fails

M S Dimitrijević†, P V Grujić†‡ and N S Simonović‡

† Astronomical Observatory, Volgina 7, 11050 Belgrade, Yugoslavia

‡ Institute of Physics, PO Box 57, 11000 Belgrade, Yugoslavia

Received 17 May 1994, in final form 21 July 1994

Abstract. We investigate cases of Coulombic systems near the break-up threshold for which the Wannier model holds, but not Wannier theory. Making use of the classical trajectory method, we derive threshold laws for a model system of fractional charge ($Z = \frac{1}{4}$ au) nucleus and electrons, and a real (though perhaps impractical) system of two beryllium nuclei and an antiproton. For the first system we find the threshold law of the form $\exp(-\lambda/\sqrt{E})$, where E is the total energy, and for the second one a number of characteristic features above the classical threshold have been obtained. Finally we investigate numerically a realistic case of an electron and two beryllium nuclei and discuss some general features of the ionization probability above the classical threshold.

1. Introduction

We continue with investigations of three-body systems near the break-up thresholds. This paper is a sequel to the first one in the series (Simonović and Grujić 1987, hereafter referred to as I), where a general case of the near-threshold behaviour of the Coulombic systems with arbitrary masses and charges has been treated. We are interested in finding out the threshold law for the process when a charged particle impinges on a binary system itself consisting of two charged particles. As usual, one assumes the threshold law in the form

$$\sigma \sim E^{\kappa} \qquad E \to +0 \tag{1}$$

where σ is the break-up cross section, E is the total energy of the system and κ is the threshold law exponent to be found out. In the case of a symmetric system, when the two wing (outgoing) particles are identical, one has for the exponent (equation (38) of I) (atomic units are used throughout)

$$\kappa = \frac{3}{4}\left(1 + \frac{16}{9}\frac{1 + 2m_3/m_1}{1 + q_3/4q_1}\right) - \frac{1}{4} \tag{2}$$

where m_3 $(= m_2)$ and q_3 $(= q_2)$ are the masses and charges of the wing particles respectively, with particle 1 (with a charge q_1 opposite in sign to the outer ones) staying in the middle. If $m_3 \ll m_1$ and $q_3 < -4\,q_1$ one recovers the standard Wannier result (Wannier 1953). In particular, for $q_1 = 1$ and $q_3 = -1$, one has $\kappa = 1.126\,89$, a well known value for the case of ionization of hydrogen by electrons.

Looking at (2) as it stands, one observes two important points: (i) formally, the exponent assumes real values only outside the region: $-\frac{1}{4} < q_1/q_2 < -\frac{9}{100}$; (ii) approaching the right

0953-4075/94/235717+14$19.50

border of this region from the right, the exponent tends to infinity. The latter case arises, for instance, in the process

$$Be^{4+} + Be^{3+} \rightarrow Be^{4+} + e + Be^{4+}. \tag{3}$$

Two questions impose themselves, however, in a situation like this. First, what would be the meaning of an infinite exponent in (1), and second whether this case belongs to the Wannier model of the near-threshold processes. As we shall see immediately, cases which lead to an unphysical value of κ may still be described by the Wannier model, but not within Wannier theory (see, e.g. Grujić 1986).

In the next section we examine applicability of the Wannier theory to these non-standard situations and in the following sections we present our numerical calculations of the exponent κ for the following cases: the model case of type (3), but with a different choice of masses and charges (equation (11)), then the process (3) with e replaced by an antiproton, and finally the realistic case described by (3) is discussed. Motivation for this particular choice will be explained in the course of calculations. Finally, we present a brief discussion of the results obtained and of further possible extensions of the present approach.

2. Wannier model of double escape

The classical Wannier model has been discussed in a number of review articles (see, e.g. Read 1985, Grujić 1986) and here we shall content ourselves with a brief sketch of the simplest case of (identical particle) double escape process. In this case the most important (classical) configuration appears to be the rectilinear one (collinear motion), with particles of charge of the same sign repelling each other and moving from that with opposite charge (central particle) to infinity, if the process is endothermal (total energy positive). For very small total energy E the double escape probability appears to be a subtle interplay of two competing interactions—an attraction towards the central body and mutual repulsion of the wing particles. The central construct of the model is the so-called *leading trajectory*, a straight line along which particles move at $E = 0$ (note that kinematically there is an innumerable number of trajectories realizing the same geometrical configurations). Strictly speaking, the leading trajectory is a unique point in the corresponding phase space (apart from a physically unimportant rotational degree of freedom), with

$$r_2(t) = -r_3(t) \tag{4}$$

which implies the same relation for derivatives with respect to time t (equal, antiparallel velocities). Now, if the net force acting on outgoing (wing) particles along the leading trajectory is attractive, Wannier theory is applicable. This is essentially a peturbative approach, which leads in the borderline case (see equation (11a) in I, free motion case) to

$$q_1/q_3 = -\tfrac{1}{4} \tag{5}$$

for motion along the Wannier ridge (4)

$$r_i(t) = r(t) = \left(\frac{E}{m_3}\right)^{1/2} \cdot t + C \qquad i = 2, 3 \tag{6}$$

with the usual choice $C = 0$. In the limit $E \to 0$ and for $C > 0$ both wing particles would remain at rest all the time, the system being in an unstable equilibrium (unstable fixed point, see, e.g., Percival and Richards 1985). For the non-zero velocity ($E > 0$) one has the so-called *dynamic equilibrium* (symmetrical configuration), with the total mutual screening of the constituent particle charges. Now the equation for small radial perturbations with respect to the leading configuration (4), (see, e.g. (39) in I) reads

$$\frac{d^2\Delta}{dt^2} = \frac{K_\Delta \Delta}{t^3} \tag{7a}$$

$$K_\Delta = \frac{-2q_1q_3M\sqrt{m_3}}{m_1E^{3/2}} \qquad M = m_1 + m_2 + m_3 \tag{7b}$$

and similarly for the transverse deviations

$$\frac{d^2\delta}{dt^2} = \frac{K_\delta \delta}{t^3} \qquad K_\delta = -\tfrac{1}{2}K_\Delta. \tag{8}$$

Note that K_Δ is positive for $E > 0$ and that, unlike the standard Wannier case, equations (*7a*) and (8) are not of Euler type and cannot be solved analytically. As a consequence, further analytical derivation of threshold law, as in Wannier (1953), is not possible and this justifies the term *non-Wannier* employed for the present calculations. On the other hand, all physical assumptions underlying Wannier's derivations remain valid and the whole approach is based on the Wannier model.

Let $rF_i(r)$ $i = 1, 2$ (with t substituted by r according to (6)) be particular solutions of (*7a*), then one can write the geneal solutions as

$$\Delta/r = C_1F_1(r) + C_2F_2(r) \tag{9a}$$

$$\delta/r = C_3F_3(r) + C_4F_4(r) \tag{9b}$$

where C_i are arbitrary constants. However, unlike the standard Wannier case, since r depends explicitly on E, so do F_i. On the other hand, as the similarity transformations (e.g. (31) in I) leave the left-hand side of (*9a, b*) intact, it follows that C_i must be E-dependent. This precludes, consequently, a standard derivation of threshold law from an explicit form of F_i (Vinkalns and Gailitis 1967). This need not be of crucial importance provided that one can infer from (*9a, b*) whether some of the terms appear divergent in the limit $r \to \infty$. The total number of diverging terms determines the dimensionality of the total phase-space subspace volume which shrinks as the energy goes to zero, what determines threshold law. In the standard Wannier case, it turns out that only one of the RHS terms diverges and thus a single C_2 determines near-threshold behaviour (single-parameter theory). In our case, in the absence of analytical solutions, only numerical calculations can provide an answer to the relevant dimensionality and yield the threshold law.

3. Numerical calculations

Generally speaking there are two approaches to deriving double-escape threshold laws: (i) by simulating full-time-scale collisions, varying a proper number of initial parameters, by solving corresponding classical equations, as has been done in a number of investigations up to now; and (ii) by examining numerically the system evolution in the final configuration

(the so-called *half-collision* method, cf Read (1985)). (We note in passing that with a couple of exceptions all analytical approaches belong to half-collision class of study of near-threshold behaviour.) The latter approach would correspond to solving numerically equations (7) and (8), instead of e.g. Newton equations (see, e.g. (10) in I). But whichever approach is adopted, the problem concerning the number of parameters to be varied remains.

An investigation of the small-energy behaviour of a system by the classical trajectory method can be very involved, as the case with process (3) shows. First, because of the extremely slow motion of the impinging paticle (or, alternatively, very fast motion of the target electron) a very large number of integration steps is needed. Further, owing to the enormous difference in the masses of the electron and the Be nuclei, the ionization interval is expected to be extremely small indeed, which requires a proportionally large number of trajectories to run, in order to find out the ionization region. But besides these practical difficulties, there is another conceptual one, which makes a proper numerical full-collision study intractable, if both colliding systems are charged with the same sign.

One of central assumptions of near-threshold studies, not only within the Wannier model, is the notion of compound state, which the colliding particles form temporarily, before the final-state fragments emerge. For this to happen, the colliding particles must approach each other closely enough for the so-called quasiergodic hypothesis to hold (Wannier 1953). Consider now two charged atomic particles, like those in (3), in the initial channel. Beside the direct collisions, when the target electron remains bound to the same nucleus two other processes may occur. One is charge exchange, when the target loses its electron to the scattered impinging ion, and the other is ionization, with the free electron in the final state. The latter process can proceed via two different final configurations. In one case all three particles move in the final state in noticeably different directions (direct ionization). The second type of fragmentation evolves essentially along the common straight line, what is called capture into the continuum. In either case if ionization is to happen the particles should approach each other at least within a distance $R_{12}^{\min} = \gamma d_0$, where γ is of order unity and d_0 is the diameter (or the major axis) of the target Kepler orbit. If target constituent charges are Z_1 and Z_2 and the projectile charge is Z_3, one has for the impinging energy $E_{\text{imp}} \equiv \beta U_{\text{ion}}$, with ionization potential $U_{\text{ion}} = \mu Z_1^2 Z_2^2/2$, and μ is the reduced mass

$$\frac{R_{12}^{\min}}{d_0} \approx \frac{Z_3(Z_1+Z_2)}{\beta}. \tag{10a}$$

If the target is neutral ($Z_1 = -Z_2$), dominant interaction is of the monopole–dipole type (e.g. Grujić 1973) $V_{\text{dip}} = DR_{12}Z_3/2R_{12}^3$ and (10a) goes into

$$\frac{R_{12}^{\min}}{d_0} \approx (Z_1 Z_2)(Z_3 D)^{1/2} \tag{10b}$$

where D is the classical mean dipole moment of the target. We note in passing that quantum mechanically it is a polarization potential which counts and since it is always attractive, no $R_{12}^{\min}$ appears. For reaction (3) one has the RHS of (10*a*) near the threshold ($\beta \approx 1$) equal approximately 10. Consequently, only at relatively high impact energies ($\beta \geqslant 10$) can reaction (3) proceed classically, what moves the process away from the threshold. Quantum mechanically, of course, one has an underbarrier penetration and ionization does start at the true threshold, though with a reduced probability due to the tunnelling effect.

Within the full-collision approach we employ the usual numerical procedure for detecting ionization volume intervals (e.g. Dimitrijević *et al* 1990), by varying the initial

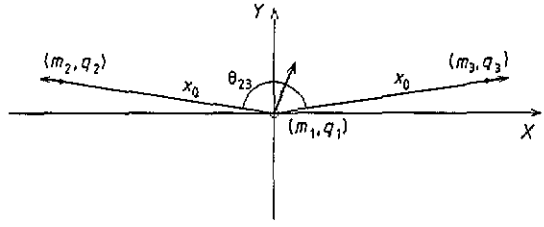

Figure 1. Initial configuration (schematic) for the half-collision calculations.

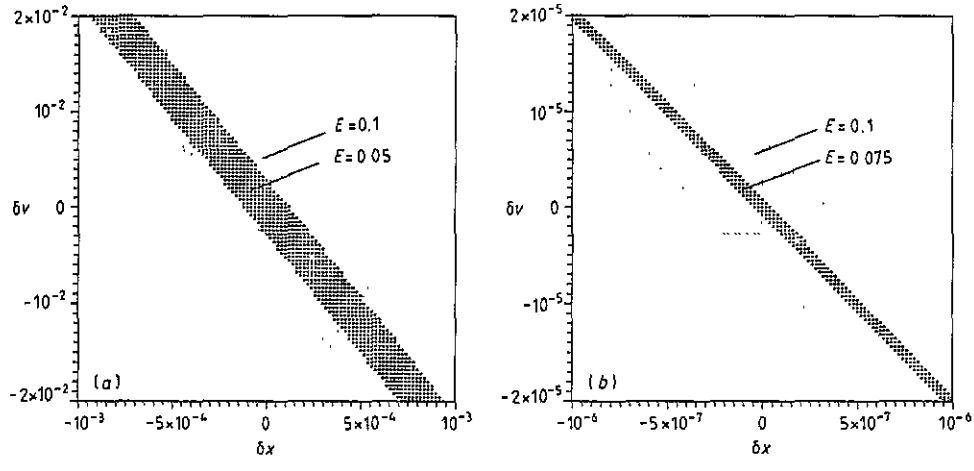

Figure 2. Ionization regions for the half-collision computations (two parameter variations, collinear case, see text): (*a*) $Z = 1$, Wannier case; (*b*) $Z = \frac{1}{4}$.

orientation of the target binary system, with the constituents moving around each other along Keplerian orbits. Then the particle final energies are evaluated by numerically integrating Newton equations and regions where all three particles fly away with positive energies are determined. Repeating the procedure for a number of total energies E and finding the corresponding break-up regions one obtains the threshold law by fitting numerical results to an analytical expression.

In order to get insight into the physical side of the problem, we have chosen to treat a model case of type (3) first, more precisely with fractional charges of the nuclei, and then we move to more realistic, but numerically more involved cases.

3.1. Model-system calculations

We treat the process ($m_A = \infty$)

$$e^- + [A^{+1/4} + e^-] \rightarrow e^- + A^{+1/4} + e^-. \tag{11}$$

Computations have been carried out first within the half-collision arrangement, that is by following only the evolution of the RHS of (11), solving the corresponding Newton equations

$$m_i \frac{d^2 r_i}{dt^2} = \sum_{i \neq j} q_i q_j r_{ij}/r_{ij}^3 \qquad i = 1, 2, 3 \tag{12}$$

with obvious notation.

3.1.1. Half-collision approach. We start with the collinear final-state configuration ($\theta_{23} = \pi$, see figure 1), with electrons symmetrically spaced with respect to the positive heavy ion at the origin. In order to test the reliability of the approach, we first carry out computations for the charge of the central ion $Z = 1$ (Wannier case). Two sets of computations have been done: (a) by varying small velocity deviations from the symmetrical ones, with fixed symmetrical initial positions; (b) by varying both positions and velocities simultaneously. In case (a) the best-fit calculations, for four different energies $0.01 \leqslant E \leqslant 0.1$ provide $\kappa = 1.1254$, which compares well with the analytically derived value, according to (2), 1.1269. The set (b) computations were carried out for the same four total energies. In figure 2(*a*) we show the corresponding phase-space double-escape regions for three different total energies. The fit to the form (1) yields the exponent value 1.1214.

It should be noted here that a two-parameter half-collision treatment does not imply two-dimensionality of the Wannier theory. In fact, a one-parameter full-collision approach implies many-parameter half-collision treatments, for it is an initial configuration for a complete scattering process which defines (physical) parameters of the problem. Nevertheless, it is a comfortable assurance that the final-state approaches yield the same threshold law for different numbers of varied parameters (cf Read 1984).

Table 1. Half-collision calculated velocity intervals δv and the best-fit values for three analytical expressions for reaction (11) ($x_0 = 0.1$).($x.x - yy$ stands for $x.x\ 10^{-yy}$).

E	δv	$1433.5E^{8.2517}$	$1.8797 \times 10^{-3}e^{-0.5645/E}$	$6.8307e^{-4.3465/\sqrt{E}}$
0.050	2.465 – 08	2.634 – 08	2.350 – 08	2.469 – 08
0.075	8.778 – 07	7.457 – 07	1.0126 – 06	8.742 – 08
0.100	7.311 – 06	8.030 – 06	6.6467 – 06	7.330 – 06
RMS		2.436 – 07	6.6467 – 06	6.3375 – 09

Now we proceed with non-Wannier parameters $Z = \frac{1}{4}$. Corresponding areas for case (b) are shown in figure 2(*b*). In table 1 numerical data for the single parameter variations (case (a)) are shown, with δv velocity double-escape intervals. Numerical results are then fitted to the additional two (beside that in (1)) analytical forms : (i) $A\exp(-\lambda/E)$; (ii) $A\exp(-\lambda/\sqrt{E})$. Corresponding best-fit values are shown in table 1, also, together with RMS values. Evidently, form (ii) appears the best choice.

These computations have been carried out with the electron initial positions $x_0 = 0.1$. In order to check the independence of the final results from the choice of initial distance from the origin, we have repeated computations with three different choices of x_0, and compared with the form (ii). In table 2 we show one set of the results for $x_0 = 1$, for an extended range of total energy.

Note that different initial positions dictate different minimum values for E. These results are in accordance with an important property of Coulombic systems, *similarity transformations (scaling laws)* (e.g Wannier 1953), as can be checked by direct inspection.

$$r \to \vartheta r \qquad E \to E/\vartheta \qquad v \to v/\sqrt{\vartheta} \qquad \vartheta > 0 \tag{13}$$

which in our case reads

$$\delta v = \frac{1}{\sqrt{x_0}} f(x_0 E). \tag{14}$$

Table 2. Half-collision calculated numerical results and the best-fit values, for $x_0 = 1$, for reaction (11). ($x.x - yy$ stands for $x.x\ 10^{-yy}$).

E	δv	$1.817\exp(-1.364/\sqrt{E})$
2.5 – 03	2.325 – 12	2.530 – 12
3.5 – 03	1.710 – 10	1.734 – 10
5.0 – 03	7.791 – 09	7.544 – 09
7.5 – 03	2.776 – 07	2.602 – 07
1.0 – 02	2.312 – 06	2.148 – 06
1.5 – 02	2.817 – 05	2.626 – 05
2.5 – 02	3.383 – 04	3.235 – 04
3.5 – 02	1.253 – 03	1.230 – 03
5.0 – 02	3.986 – 03	4.050 – 03
7.5 – 02	1.168 – 02	1.241 – 02
1.0 – 01	2.204 – 02	2.419 – 02
RMS	2.0873 – 04	

Hence, one has for the threshold law for the case at hand the following general formula

$$\sigma \sim e^{-\lambda/\sqrt{x_0 E}}. \tag{15}$$

According to our numerical findings one can ascribe a numerical value to the scale-independent constant $\lambda = 1.364$ in (15).

The Wannier model predicts not only collinear final double-escape configurations, but also final state trajectories which cluster around the collinear ones, within a pencil of a small aperture. We have repeated computations for the final electron positions and velocities making a mutual angle $\theta_{12} = 170°$ instead of 180°. Computations corroborate formula (15) again, but with a somewhat worse fit than in the strictly collinear case. A plot of outgoing particle trajectories shows an oscillatory (around a collinear line) angular motion, just as in the case of the Wannier system (cf e.g. Vinkalns and Gailitis 1967).

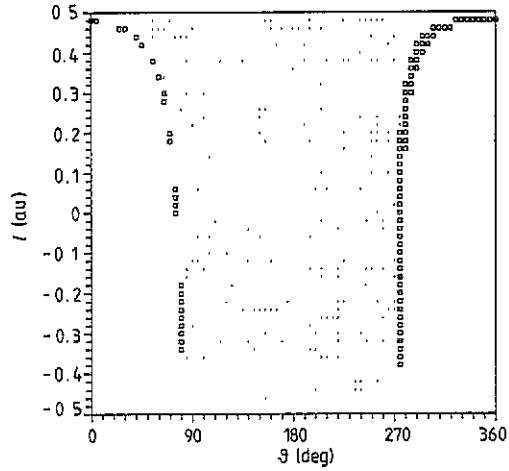

Figure 3. Ionization regions (squares) for the full-collision calculations for reaction (11), at $E = 0.01$ au.

3.1.2. Full-collision treatment. This approach is more in the spirit of real experiments. We employed the standard three-body computer code used previously for three-body classical trajectory calculations (see, e.g. Grujić 1973), but this time the accuracy has been considerably improved by implementing the *regularization*, as described by Aarseth and Zare (1974, see also Richter and Wintgen 1990). An initial configuration consists of a charged particle impinging on the two-body Keplerian system (see, e.g. figure 2 in Grujić 1973). With a fixed (ground state) target energy and total system angular momentum ($L = 0$, plane case), we choose to vary two parameters: (i) the orbit eccentricity; (ii) orientation of the orbit (ϑ). We chose, in fact, to vary the eccentricity via the semiclassical angular momentum quantum number ℓ, defined by

$$\epsilon = \left[1 - \left(\frac{\ell + \frac{1}{2}}{n}\right)^2\right]^{1/2} \tag{16}$$

where n is the bound system principal quantum number. Thus by varying ℓ within the interval $(-\frac{1}{2}, \frac{1}{2})$, eccentricities from 0 to 1 are covered. In figure 3 we show results for process (11) for the total energy $E = 10^{-2}$ au.

The total number of trajectories was 3723, with double-escape events numbering 89. For other total energies similar figures are obtained. However, it turns out that the width of an ionization strip varies considerably faster than its height. This implies that a good representative of the total area change, as the energy E varies, would be the width variation at a particular ℓ value. Thus the problem is again reduced to a single-parameter variation. We choose the simplest case possible—the circular orbit ($\ell = -\frac{1}{2}$). We note that in the limit $\ell = -\frac{1}{2}$ the initial definition of ϑ becomes meaningless. In fact ϑ now determines the electron position on the circular Keplerian orbit, which we designate by the corresponding time variable τ and vary within the total period T. The initial distance of the impinging electron was 300 a_0, with zero total angular momentum ($L = 0$). In table 3 we give numerical values of the ionization intervals for the first ten total energies. Before discussing these results, a few remarks concerning some characteristic features of the calculation are in order. First, the final results depend rather crucially on the numerical accuracy. We kept the total energy (one of two integration integrals) accurate up to four significant figures. Less accurate integrations tend to change noticeably both the positions and lengths of the ionization intervals. Further, numerical integrations confirmed that the ionization intervals disappear below some energy $E = E_0$. In our case $E_0 < 2.4 \times 10^{-3}$. It should be emphasized that this disappearence means an absence of the electron exchange, rather than a zero value of the ionization interval (which might otherwise have something to do with the numerical accuracy achieved). This latter feature led us to carry out fitting procedure by a somewhat different analytical function compared with that in (15), with E replaced by $E - E_0$. As shown in table 3 our best-fit value was $E_0 = 2.175 \times 10^{-3}$. This should be compared with the potential-barrier threshold, which according to the estimate (10*a*) is expected to be around 8×10^{-3} au.

Inclusion of the next point at $E = 4 \times 10^{-3}$ (not shown in table 3) resulted in much worse fit, with RMS larger for two orders of magnitude, while not changing the value of E_0 and negligibly changing the fit with the first 10 points. As can be seen from table 3 the fit to the analytical formula appears excellent. We also tried unsuccessfully a fit to the Wannier expression (1). A fit with $E_0 = 0$ failed, with κ assuming a value of several tens and the A value went beyond the range of our PC. A non-zero E_0 value improved the fit, but it remained far worse than that quoted in table 3 for the exponential form. We conclude

Table 3. Full-collision calculated values for the ionization intervals $\Delta\vartheta$. $\lambda = 0.330\,698$, $A = 1.875\,67 \times 10^3$, for reaction (11) ($x.x - yy$ stands for $x.x\,10^{-yy}$).

E	$(\delta\vartheta)_{\text{num}}$	$a\,e^{-\lambda/\sqrt{E-E_0}}$
0.240 00 – 02	0.500 00 – 06	0.499 43 – 06
0.250 00 – 02	0.200 00 – 04	0.202 55 – 04
0.260 00 – 02	0.207 00 – 03	0.202 56 – 03
0.275 00 – 02	0.191 00 – 02	0 192 21 – 02
0.285 00 – 02	0.553 40 – 02	0.556 17 – 02
0.300 00 – 02	0.187 70 – 01	0.187 47 – 01
0.310 00 – 02	0.355 31 – 01	0.355 59 – 01
0.325 00 – 02	0.780 10 – 01	0.781 23 – 01
0.335 00 – 02	0.121 10 + 00	0.121 15 + 00
0.350 00 – 02	0.213 17 + 00	0.212 62 + 00
RMS		5.655 – 05

therefore that the full-collision approach is compatible with the half-collision treatment. Incidentally, a semiqualitative analysis of the full-collision results reveals that the most appropriate value for x_0 in the half-collision arrangement would be $\langle x_0 \rangle \approx 17\ a_0$.

As for the non-zero E_0 value, we have tried to implement the same correction to the half-collision results, but with no improvement. Evidently, there exists a barrier between the initial configurations in the full- and half-collision arrangements, which lifts up the reaction threshold, as discussed above.

3.2. Real system collisions

A real system is much more difficult to deal with, since here the wing particles are heavy and collision processes evolve slowly in time. In the case of the half-collision arrangement the total energy is distributed over all three particle and the small-energy numerical calculations appear less straightforward than with the electrons. If the full collisions are simulated, computing time per orbit becomes very large and smaller statistics can be afforded. We start with a more realistic, though still somewhat artificial, true three-body system.

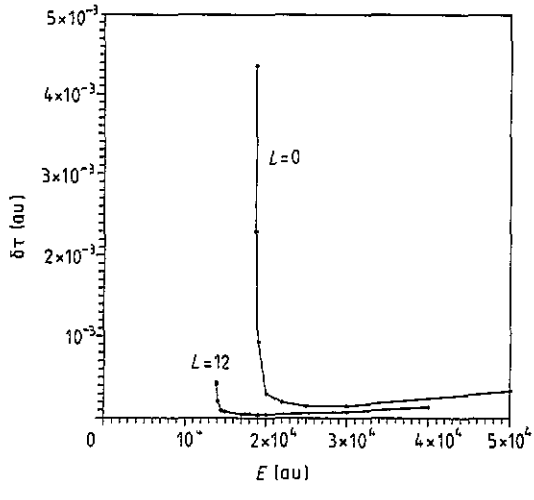

Figure 4. Break-up interval functions for reaction (17), for two values of the total angular momentum L.

3.2.1. Beryllium antiprotonic ion. We examine numerically the process

$$Be^{4+} + [Be^{3+} + p^-] \rightarrow Be^{4+} + p^- + Be^{4+}. \tag{17}$$

This reaction appears much more convenient for a numerical analysis because of the large antiproton mass, which considerably increases the ionization probability at small energies. We have carried out computations for $L = 0$ total angular momentum, employing the same procedure as above. The classical breakup threshold appears somewhere immediately below $E_{imp} \approx 31\,892$ au ($E \approx 18\,670$ au), as compared with the ionization potential $U_{ion} = 13\,222.04$ au. In figure 4 results are shown for the energy interval (0, 50 000). We started computations from the $E = 20\,000$ au point, following an ionization interval, moving to smaller and larger energies. One notices the sharp rise of the ionization probability as the (classical) threshold is approached from above. We have been unable to detect any point left from the first one in figure 4, where the curve presumably sharply drops to zero. In order to check if the observed behaviour is peculiar to the $L = 0$ configuration, we have repeated computations for $L = 12$ and the results are also shown in figure 4. This choice of angular momentum yields the impact parameter of the order of the target equivalent orbit diameter. As can be seen from figure 4 the break-up process starts somewhat earlier (immediately below $E = 13\,870$ au and the ionization intervals appear smaller, compared with $L = 0$ data. Otherwise the general behaviour turns out much the same.

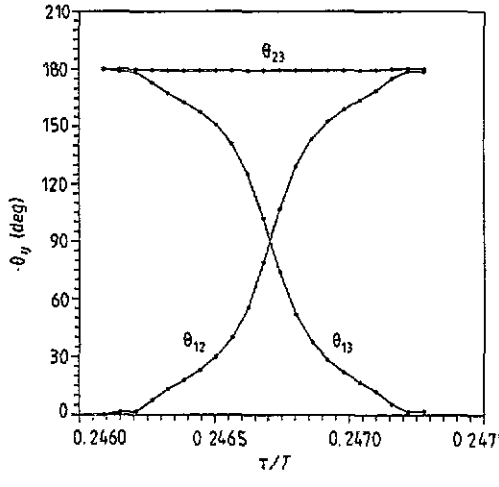

Figure 5. Final-state mutual-angle functions for $L = 0$, $E = 19\,001.2$ au, for reaction (17).

In figure 5 we plot the final state mutual angles of the outgoing particles, in the CMS, for $L = 0$ partial configuration. As can be seen from figure 5, heavy particles Be^{4+} move approximately along a straight line through the centre of mass, whereas the antiproton changes its final direction from following the parent nucleus ($\theta_{23} \approx 0°$), through the escape along a perpendicular direction, around the middle of the breakup interval ($\theta_{3i} \approx 90°$, $i = 1, 2$), and finally starts trailing the impact particle ($\theta_{23} \approx 180°$—capture to the continuum). Though we have not carried out a full-scale collision simulations (such as the Monte Carlo method, e.g. Olson 1986), which would provide data for various final-state distributions, one can infer from data like those in figure 5 a number of characteristic

features of a real distribution. We notice in figure 5 that the (mutual) angle distribution, defined as

$$P_{ij} = c\frac{\mathrm{d}\tau}{\mathrm{d}\theta_{ij}} \tag{18}$$

where c is a normalization constant and τ is the system parameter varied in the case at hand (e.g. Dimitrijević and Grujić 1979), appears uniform in the central region and at the wings, with distribution function assuming somewhat larger value at the latter part of the break-up interval. This feature suggests that the perpendicular escape should be less probable than those by trailing the nuclei.

In a series of papers Ovchinnikov and Solov'ev (1988), Ovchinnikov (1990) and Pieksma and Ovchinnikov (1991) carried out detailed analyses of an ionization mechanism of a bare nucleus collision on a single-electron target. Though their model does not cover our singular ($Z_1 = Z_2 = 4$) system, it seems instructive to compare our numerical results with their study. According to these analyses one can define two sets of intermediate states *via* which an ionization process evolves quantum mechanically. One series (so-called *S-series*) promotes the electron by means of the centrifugal barrier around the closely separated nuclei, and should be absent for s-states. Classically, this series is associated with unstable electron trajectories on the top of the centrifugal barrier and the electron moves asymptotically along the internuclear axis. The other, so-called *T-series*, promotes the electron escape starting from the middle between the receding nuclei (*saddle-point electrons*). Their classical trajectories end asymptotically perpendicular to the internuclear axis. Pieksma and Ovchinnikov (1991) conclude that the saddle-point mechanism contributes significantly to the ionization probability, in the energy region studied (5–20 keV amu^{-1}) for p + H collisions. Our numerical results suggest that the saddle-point mechanism appears prominent in process (17), too, though its contribution might be somewhat smaller than in the case of single-electron Wannier systems.

The analysis of the final-state evolution can help also in understanding the rather peculiar behaviour of the break-up interval in figure 4. At energies not too close to the (classical) break-up threshold ionization appears as a intermediate process between direct and exchange (antiproton capture) collisions. Right above the threshold, however, the exchange is surpressed. The impact particle does not approach the target sufficently close and the lighter target constituent cannot reach the potential barrier top, but presumably starts moving back towards the parent nucleus. It is this turning point which enhances the length of an ionization interval, as evident from the steep rise of the latter in figure 4. Also, this effect should be more prominent at head-on collisions (small L), when radial motion is dominant, as also illustrated in figure 4. At even smaller energy the velocity of the target nucleus is insufficient to run away and the returning antiproton catches it up and recapture takes place. This explains the abrupt drop of the ionization probability to zero, immediately before the left parts of the curves in figure 4. Because of this uncertain position of the threshold we have not plotted zero-valued ionization intervals in the same figure.

Since the threshold positions as well as the magnitudes of different partial configuration intervals differ, it is not possible to infer from our computations an exact position of the classical break-up threshold. On the other hand, it would be reasonable to expect that the overall ionization probability should be small below the impact energy $E_{\mathrm{imp}} \approx 31\,000$ ($\approx$ 840 keV), since in this region ionization takes place exclusively *via* the tunnelling effect through the Coulomb barrier in the initial channel. Only after this barrier has been surmounted can a (quasi)compound state be formed and a break-up initiated in the final channel.

3.2.2. Beryllium ion. Reaction (3) describes a truly two-centre problem. For $Z < 4$ calculations, both numerical (Olson 1983, 1986) and analytical (Ovchinnikov 1990, Pieksma and Ovchinnikov 1991) have been carried out. Standard Wannier-type calculations yield (Simonović and Grujić 1987) a power threshold law of (1), whereas calculations for H + p-type collisions, within the WKB approximation provide ionization probability small-energy behaviour in the form

$$P = A\left[\frac{E}{(\ln E)^4}\right]^{\alpha} \tag{19}$$

$$A = \left[c_0\beta'\left[\ln(c_0\beta')\right]^4\right]^{\alpha}\exp\left[-\sqrt{\gamma'/c_0}\right] \tag{20}$$

$$\alpha = c_1\sqrt{2\mu/c_0} \tag{21}$$

$$c_0 = (\sqrt{Z_2} + \sqrt{Z_3})^2 - Z_2Z_3 \tag{22}$$

$$c_1 = \frac{(\sqrt{Z_2} + \sqrt{Z_3})^2}{(4Z_2Z_3)^{1/4}} \tag{23}$$

where $Z_{2,3}$ are the charges of the wing (heavy) particles, μ their reduced mass and β', γ' are numerical constants. Ovchinnikov's analysis is essentially a first-order perturbation theory with respect to the small parameter $1/\mu$, where μ is the atomic reduced mass. Exponent α coincides approximately with threshold exponent κ in (1). For (p+e+p) system $\alpha = 69.975$ (69.735 according to (2)), as compared to (e+p+e) system, with $\kappa = 1.127$. Because of the large numerical value of the threshold exponent for the two-centre problem, the logarithmic term in (19) changes radically small-energy behaviour of the fragmentation process. Thus in the case of (p + e + p) system, for which one has the threshold region approximately (0, 0.05), according to (19)

$$\frac{P(0.04)}{P(0.02)} \approx 5.9063 \times 10^{44} \tag{24}$$

what makes (19) practically a Heaviside-like (unit) function. Besides, it appears inappropriate for the singular case: $Z_2 = Z_3 \to 4$ when one has $c_0 \to 0$, $\alpha \to \infty$, $A \to 0$, as in standard Wannier theory.

As in the beryllium–antiprotonic case, numerical analysis of the final-state system evolution, via the half-collision approach, appears inconvenient. We have thus carried out computations by simulating the full-collision process, for $L = 0$. According to (10*a*) the process should start at $E_{\text{imp}} \approx 12$ au. Our computations reveal the beginning of the exchange reaction at $E \approx 75.3$ au, which corroborates the analytical estimate. However, the lengths of the corresponding ionization intervals turn out to be extremely small, different from the analogous antiprotonic case. In the region $80 < E < 200$ au these lengths turned out beyond the double-precision accuracy of our PC, that is $\Delta\tau/T < 10^{-14}$. These findings indicate that the saddle-point configuration is so unstable that the probability of a promotion into the continuum is practically zero. The electron moves so fast that the heavy wing particles cannot run away and (re)capture takes place quickly. An eventual triple-escape configuration evolves presumably with the electron moving perpendicular to the internuclear axis, but we have been unable to 'get into' an ionization interval, and could only locate its position.

This effect appears more general than the singular system studied here. We have repeated computations for $He^{2+} + He^{+}$ collisions ($L = 0$), for which (10*a*) suggests $E_{\text{min}} \approx 3$ au. Computations at $E = 30$ au detect intervals smaller than 10^{-14} T. Evidently, ionization probabilities for nuclear charges greater than 1 turn out negligible in every respect, even above the classical barrier.

4. Concluding remarks

An extension of the simple Wannier process, like electron impact ionization of a neutral or charged target, to heavy ion collisions is not a trivial task, neither analytically nor numerically. Analytically, difficulties appear both within the classical and quantum mechanical approaches, though of formally diferent nature. The singular case of complete screening in the final state on the leading trajectory (or equivalently in the final channel in the (semi)quantum mechanical theory) poses additional complications. Our attempts to resolves these difficulties by a detailed numerical analysis (without involving massive computations) have been only partially successful. The model systems designed to separate formal singular features of these non-Wannier processes from undesirable properties of real physical systems, have enabled us to estimate an exponential near-threshold behaviour, as opposed to the simple power law for the standard Wannier processes. It is interesting to note that the same kind of the exponential function appears as a factor of the near-threshold behaviour of the break-up processes with two charged and one neutral particle in the final channel (Hart *et al* 1957). (Note, however, the minus sign in front of the exponent '$\frac{1}{2}$' is missing in the corresponding equation (28*a*), se e.g. Grujić and Koledin 1993.) This sort of exponential law also appears muchalike the far-from-threshold behaviour of the (partial) probability function for ionization by heavy ions, within the semiclasical theory (e.g. Solov'ev 1989).

As for experimental evidence, no measurements for the singular systems have been reported up to now. Even for standard cases, such as $H^+ + H$ collisions, experiments have been carried out in the keV region only (e.g. Shah *et al* 1987). The same holds for theoretical investigations, such as those by coupled-states quantum mechanical calculations due to Fritsch and Lin (1983) (see, e.g. Pieksma and Ovchinnikov 1991 and references therein). Our numerical computations have shown that the low-energy ionization probability must be extemely small, even above the classical threshold. This means that the standard classical Monte Carlo calculations would be quite inefficient in this energy region and thus inappropriate for studying near-threshold behaviour for charged particle collisions.

One way to circumvent theoretical difficulties in the non-Wannier case mentioned above would be an *ab initio* quantum mechanical, or semiclassical approach, with singularity in the leading final-state configuration accounted for from the very begining. Since this case appears the only one not covered by the analytical theory up to now, it should be worth trying this sort of calculation.

Finally, in response to a referee's suggestion, we comment on the role of correlations in the fragmentation near the threshold. As mentioned above, if the wing particles are of the same charge, radial correlations govern double escape, via the threshold exponent κ in equation (2). For the singular ('resonant') charge ratio $q_1/q_3 = -\frac{1}{4}$ the type of correlations change, causing a new kind of near-threshold behaviour. For $q_1/q_3 > -\frac{1}{4}$ another sort of correlation should set in and this would surely bring about yet another threshold law. Similarly for the angular correlations. Although for the particular distribution of the (signs of) charges at hand the fragmentation probability does not depend on these correlations, the angular distribution and its spread do, via the corresponding parameter κ_δ. In the general case this exponent depends on charges and masses (see equation (30) in Simonović and Grujić (1987), where κ_δ is designated as $\mathcal{K}_2^\delta$). In the simple Wannier case of two escaping electrons and residual ion charge Z, there is a borderline charge value $Z = \frac{9}{4}$ at which $\mathcal{K}_2^\delta$ changes from real ($Z > \frac{9}{4}$) to complex values ($Z < \frac{9}{4}$). This change indicates the presence of different types of angular correlations, which causes different distribution-spread behaviour—equation (36) in Simonović and Grujić (1987) (but note that $\mathcal{K}_2^\Delta$ in equation

(36) should read K_2^{δ}). Since radial and transversal strengths of forces differ greatly, the corresponding borderline values of charge ratios may differ considerably too, as is the case with the above Wannier system (by a factor of nine).

Acknowledgments

This work was supported by the Ministry of Science and Technology of Serbia.

References

Aarseth S J and Zare K 1974 *Celest. Mech.* **10** 185
Dimitrijević M S and Grujić P V 1979 *J. Phys. B: At. Mol. Phys.* **12** 1873
Dimitrijević M S, Grujić P V, Peach G and Simonović N 1990 *J. Phys. B: At. Mol. Opt. Phys.* **23** 1641–53
Fritsch W and Lin C D 1983 *Phys. Rev.* A **27** 3361–4
Grujić P 1973 *J. Phys. B: At. Mol. Phys.* **6** 286–99
—— 1986 *Comment. At. Mol. Phys.* **18** 47–74
Grujić P and Koledin D 1993 *Z. Phys.* D **28** 183
Hart R W, Gray E P and Guier W H 1957 *Phys. Rev.* **108** 1512–22
Olson R E 1983 *Phys. Rev.* A **27** 1871
—— 1986 *Phys. Rev.* A **33** 4397
Ovchinnikov S Y 1990 *Phys. Rev.* **42** 3865–77
Ovchinnikov S Y and Solov'ev E A 1988 *Comment. At. Mol. Phys.* **22** 69
Percival I and Richards D 1985 *Introduction to Dynamics* (Cambridge: Cambridge University Press)
Pieksma M and Ovchinnikov S Y 1991 *J. Phys. B: At. Mol. Opt. Phys.* **24** 2699–718
Read F H 1984 *J. Phys. B: At. Mol. Phys.* **17** 3965–86
—— 1985 *Electron Impact Ionization* ed T D Mark and G H Dunn (New York: Springer) p 42
Richter K and Wintgen D 1990 *J. Phys. B: At. Mol. Opt. Phys.* **23** L197–201
Shah M B, Elliott D S and Gilbody H B 1987 *J. Phys. B: At. Mol. Phys.* **20** 2481–5
Simonović N and Grujić P 1987 *J. Phys. B: At. Mol. Phys.* **20** 3427–36
Solov'ev E A 1989 *Sov. Phys.–Usp.* **32** 228
Vinkalns I and Gailitis M 1967 *Latvian Academy of Science Report* No 4 (Riga: Zinatne) pp 17–34 (in Russian)
Wannier G H 1953 *Phys. Rev.* **90** 817–25

INSTITUTE OF PHYSICS PUBLISHING JOURNAL OF PHYSICS B: ATOMIC, MOLECULAR AND OPTICAL PHYSICS

J. Phys. B: At. Mol. Opt. Phys. **37** (2004) 2713–2724 PII: S0953-4075(04)79539-5

Electron and ion contributions to the Ne I spectral line broadening

V Milosavljević[1], S Djeniže[1] and M S Dimitrijević[2]

[1] Faculty of Physics, University of Belgrade, PO Box 368, Belgrade, Serbia
[2] Astronomical Observatory, 11160 Belgrade, Volgina 7, Serbia

E-mail: vladimir@ff.bg.ac.yu

Received 3 April 2004
Published 11 June 2004
Online at stacks.iop.org/JPhysB/37/2713
doi:10.1088/0953-4075/37/13/009

Abstract

On the basis of the experimentally determined 26 prominent neutral neon (Ne I) line shapes (in the 3s–3p, 3s–3p′, 3s′–3p′, 3s′–3p and 3p–3d transitions) we have obtained electron (W_e) and ion (W_i) contributions to the total Stark width (W_t). Stark widths are also calculated using the semiclassical perturbation formalism for electrons and protons as perturbers up to 50 000 K electron temperatures. We made comparison of our measured and calculated W_e data and compared both of them with available experimental and theoretical W_e values.

1. Introduction

In thermal plasmas at local thermodynamic equilibrium (LTE), and for temperatures of about 1–2 eV (an electron density of about 1×10^{23} m^{-3}), the dominant pressure broadening mechanism is caused by collision processes with electrons and ions. Stark broadening in plasmas is important not only for theoretical understanding, but also for experimental methods, e.g. as a diagnostic tool. Plasma broadened and shifted spectral line profiles have been used for a number of years as a basis of an important non-interfering plasma diagnostic technique. Numerous theoretical and experimental efforts have been made to provide reliable data for such applications. This technique becomes, in some cases, the most sensitive and sometimes the only possible plasma diagnostic tool.

Classical emission laboratory plasmas spectroscopy has been mainly applied to optically thin plasma where absorption of the emitted radiation is negligible. Investigation of line profiles of atomic neon in medium dense plasmas, at about 1×10^{23} m^{-3}, is of particular interest for verifying predictions of theoretical approximations. Since neon is a constituent of laboratory plasmas the Ne I spectral line shapes represent important sources of information about the physical conditions in the place of birth of the radiation.

Stark broadening of spectral lines is the dominant pressure broadening mechanism also in some astrophysical objects such as chemically peculiar A-type stars and white dwarf atmospheres. Moreover, even for cooler stars such as Solar-type ones, the Stark broadening data are needed also for the analysis and modelling of subphotospheric layers [1]. Consequently knowledge of the Stark broadening parameters of spectral lines is of interest for diagnostic, modelling and consideration of astrophysical, laboratory and technological plasmas. Particularly, from such data, it is possible to obtain the basic plasma parameters, such as the electron temperature and electron density.

In order to underline the astrophysical importance of neon data one should say that neon is the most abundant element in the universe after hydrogen, helium, oxygen and carbon, and it is for example [2] one of the products of hydrogen and helium burning in the orderly evolution of stellar interiors.

Stark broadening of neutral neon (Ne I) spectral lines has been studied experimentally several times [3–16]. The most complete existing calculation is in [17]. Also in [18] calculations have been performed for the Ne I 650.7 nm (3s–3p) spectral line using five different theoretical approaches. Results [18] are presented graphically and it is not easy to use them for detailed comparison. In [19] the quasistatic Stark broadening constant C_4 was calculated and some theoretical estimates exist also in [10].

Due to large uncertainties of the theoretically determined Stark broadening parameters (e.g. $\pm 30\%$ for the semiclassical method as estimated in [17]), the mutual agreement of experimental values independently obtained in various laboratories permits us to single out some lines as particularly reliable and suitable for diagnostic purposes.

Since the dependence of Stark broadening parameters on temperature is still not known with a large accuracy, it is of interest also to have experimental results in a wide temperature range.

Our experimental $W_{\mathrm{e}}^{\mathrm{exp}}$ and $W_{\mathrm{i}}^{\mathrm{exp}}$ values, presented here for 26 Ne I lines, are separated from the measured total Stark width using the line deconvolution procedure described in [20–22] which has already been applied for some He I [23–25], Ar I [26] and Kr I [27] lines. We note as well that in [28, 29] static (A) and dynamic (D) ion parameters, respectively, have been determined for a number of the Ne I lines considered here.

Using the semiclassical perturbation formalism (SCPF) (updated several times) [30–35], we have calculated $W_{\mathrm{e}}^{T_{\mathrm{w}}}$ values for 25 Ne I lines and also the $W_{\mathrm{i}}^{T_{\mathrm{w}}}$ values, generated by protons which are the main component in the astrophysical plasmas. Our values are compared with available experimental and theoretical data.

The basic plasma parameters, i.e. electron temperature (T^{D}) and electron density (N^{D}), have been obtained by using the line deconvolution procedure directly from the Ne I line profiles and also measured (T^{exp} and N^{exp}) using independent, well-known, experimental diagnostical techniques. Excellent agreement was found among the two sets of the obtained parameters (T^{D} and T^{exp}; and N^{D} and N^{exp}). Such a method is applicable for optically thin plasmas. For optically thick plasmas, the situation is more complicated due to weak asymmetry of the spectral line profile caused by self-absorption [17, 36].

2. Experiment and deconvolution procedure

A modified version of the linear low pressure pulsed arc [37–40] has been used as a plasma source. A pulsed discharge was driven in a pyrex tube of 5 mm inner diameter and effective plasma length of 7.2 cm (figure 1 in [38]). The working gas was neon (99.9% purity) at 133 Pa filling pressure in flowing regime. A capacitor of 14 μF was charged up to

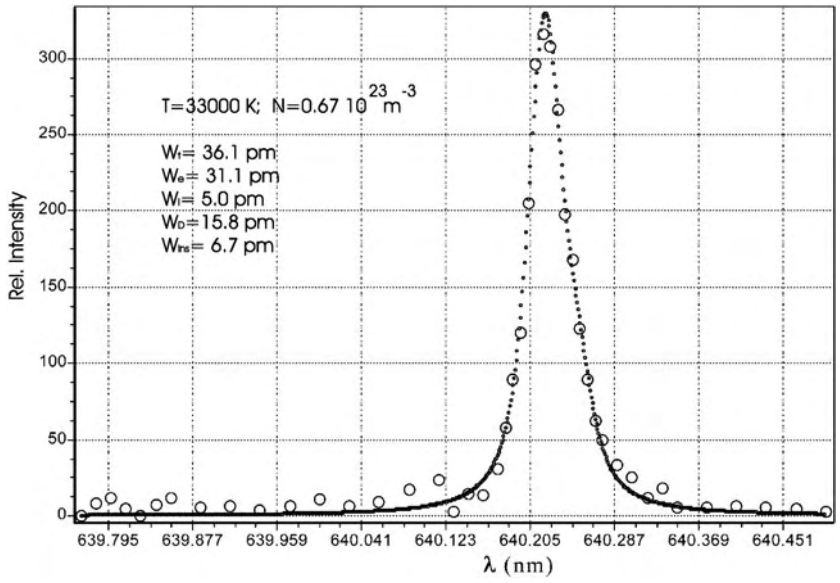

Figure 1. The recorded Ne I 640.225 nm line profile (o) with its fitting *K* function (dotted line) in the 25th μs after the beginning of the discharge at $U = 1.5$ kV bank voltage and $P = 133$ Pa gas pressure. This figure is an extension of figure 3.4.2 in [21]. W_t, W_e and W_i denote measured total, electron and ion Stark widths. W_D is the Doppler width determined at a measured T and N. W_{ins} is the instrumental width.

1.5 kV (experiment a) and 2.5 kV (experiment b), respectively. The complete experimental procedure with the set-up system used is described in [40]. Recorded Ne I spectral line profile with deconvolution fitting function, as an example, is shown in figure 1.

The absence of self-absorption was checked using the method described in [41]. The electron temperature (T^{exp}) was determined from the Boltzmann plot of the relative intensities of 14 Ne II spectral lines (331.98 nm, 336.06 nm, 337.18 nm, 341.48 nm, 341.69 nm, 341.77 nm, 350.36 nm, 356.83 nm, 366.41 nm, 369.42 nm, 429.04 nm, 439.19 nm, 440.93 nm and 441.32 nm) within energy interval of 7.1 eV for corresponding upper levels, with an estimated error of $\pm 6\%$, assuming the existence of LTE, according to the criterion from [36]. All necessary atomic data were taken from [42–44]. The electron temperature decays are presented in figure 2. The electron density (N^{exp}) decay was measured using a well-known single laser interferometry technique [45] for the 632.8 nm He–Ne laser wavelength with an estimated error of $\pm 7\%$. The electron density decays are presented also in figure 2. The T^D and N^D values obtained by deconvolution procedure [20] are also presented in figure 2. The experimental W_e^{exp}, W_i^{exp} and W_t^{exp} values are obtained using the deconvolution procedure.

The total line Stark FWHM (full-width at a half intensity maximum, W_t) is a function of W_e and W_i i.e.

$$W_t = f(W_e, W_i), \tag{1}$$

where W_e and W_i are the electron and ion contributions, respectively. For a non-hydrogenic, isolated neutral atom line the ion broadening is not negligible and the line profiles are described by an asymmetric *K* function (see equation (3) and [20, 26]). The

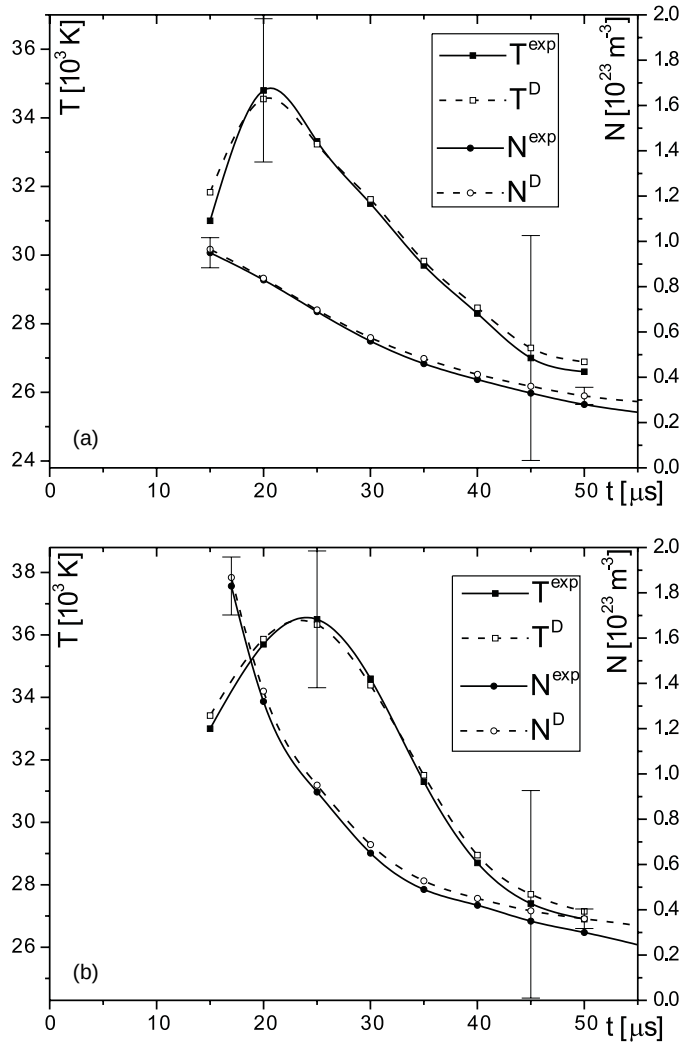

Figure 2. Electron temperature (T) and density (N) decays. Full lines represent measured data using independent experimental techniques. Dashed lines represent plasma parameters obtained using our line deconvolution procedure in different plasmas ((a) for 1.5 kV bank energy, (b) for 2.5 kV bank energy). Error bars represent estimated accuracies of the measurements (±6% and ±7% for T and N, respectively) and deconvolutions (±12%).

total Stark width with dynamic ion contribution $\left(W_{\mathrm{t}}^{\mathrm{dyn}}\right)$ and with static ion contribution ($W_{\mathrm{t}}^{\mathrm{st}}$; $W_{\mathrm{t}}^{\mathrm{st}} = W_{\mathrm{t}}^{\mathrm{dyn}}$ for $D = 1$) [17, 46, 47] may be calculated from the equation:

$$W_{\mathrm{t}}^{\mathrm{dyn}} \approx W_{\mathrm{e}}[1 + 1.75AD(1 - 0.75R)], \tag{2}$$

where R is the ratio of the mean ion separation to the Debye length. A is the quasi-static ion broadening parameter (see equation (224) in [17]) and D is a coefficient of the ion-dynamic contribution [26].

When $D = 1$ the influence of the ion-dynamical effect is negligible and the line shape is treated using the quasi-static ion approximation. From equations in [20, 26] it is possible to

obtain the plasma parameters (N and T) and the line broadening characteristics (W_t, W_e, W_i, A and D). One can see that the ion contribution, expressed in terms of the A and D parameters, directly determines the ion width (W_i) component in the total Stark width (equations (1) and (2)).

$$K(\lambda) = K_o + K_{max} \int_{-\infty}^{\infty} \exp(-t^2) \cdot \left[\int_0^{\infty} \frac{H_R(\beta)}{1 + \left(2\frac{\lambda - \lambda_o - \frac{W_G}{2\sqrt{\ln 2}}t}{W_e} - \alpha\beta^2\right)^2} \mathrm{d}\beta \right] \mathrm{d}t. \tag{3}$$

Here W_G is the Gaussian FWHM width given by (4) (i.e equation (2.3) in [20]).

$$W_G = 2\sqrt{\frac{2\ln 2kT}{m}}\frac{\lambda_o}{c}. \tag{4}$$

Where T is the emitter equivalent kinetic temperature, m is its mass, and k and c are the Boltzmann constant and velocity of light, respectively.

All other details about the asymmetric K function (3) and the complete numerical procedure for deconvolution of recorded spectral lines are described in earlier publications [20–22, 26, 29].

3. Method of calculation

A description of the semiclassical perturbation formalism used here is given in [30–35, 48]. For electrons hyperbolic paths due to the attractive Coulomb force were used, while for perturbing ions the paths are different since the force is repulsive. The expected accuracy of the semiclassical perturbation approach is ±30%.

Within the semiclassical perturbation formalism, we have calculated electron- and proton-impact line widths for 25 spectral lines of neutral neon. Energy levels have been taken from [49]. Oscillator strengths have been calculated by using the method of Bates and Damgaard [50, 51]. For higher levels, the method described in [52] has been used. The results obtained for Stark widths (FWHM) of 25 spectral lines of neutral neon are shown in table 2, for perturber density of 10^{22} m^{-3} and temperatures T = 2500–50 000 K.

For each value given in table 2, the collision volume (V) multiplied by the perturber density (N) is much less than 1 and the impact approximation is valid [17, 30–35, 48]. When the impact approximation is not valid, the ion broadening contribution may be estimated by using the quasi-static approach ([17] or [53]).

In the region where neither of these two approximations is valid, a unified type theory should be used. For example, in [46], simple analytical formulae for such a case are given. The accuracy of the results obtained decreases when broadening by ion interactions becomes important.

4. Results and discussion

Our experimentally obtained W_t^{exp}, W_e^{exp} and W_i^{exp} data are shown in table 1 together with the ratios W_e^{exp}/W_e^{G} and $W_e^{exp}/W_e^{T_w}$ where G and T_w denote theoretical values from [17] and this work (see table 2), respectively.

Calculated Stark FWHM values (W^{T_w}) generated by electrons and protons for 25 Ne I lines in the 3s–3p, 3s–3p′, 3s′–3p′, 3s′–3p and 3p–4d transitions using semiclassical perturbation formalism are presented in table 2.

The measured N^{exp} and T^{exp} decays are presented in figure 2 together with the averaged (within 26 Ne I lines) N^{D} and T^{D} values obtained using the line profile deconvolution procedure

Table 1. Measured total Stark FWHM (W_t^{exp} in pm within ±12% accuracy), electron and ion (Ne^+, Ne^{2+}, ...) Stark widths (W_e^{exp} and W_i^{exp} in pm within ±12% accuracy) at measured electron temperatures T^{exp} (in 10^3 K) and electron densities N^{exp} (in 10^{22} m^{-3}). The indices G and T_w denote theoretical data taken from [17] and this work (see table 2), respectively at a given T^{exp} and N^{exp}.

Transition	Multiplet	λ (nm)	T^{exp}	N^{exp}	W_t^{exp}	W_e^{exp}	W_i^{exp}	W_e^{exp}/W_e^G	$W_e^{exp}/W_e^{T_w}$
3s–3p	$[3/2]_2^0$–$[1/2]_1$	703.241	3.30	6.7	44	39	5	0.86	1.10
			3.65	8.8	56	50	6	0.81	1.03
	$[3/2]_1^0$–$[1/2]_1$	724.517	3.30	6.7	46	43	3	0.87	1.14
			3.65	8.8	61	52	9	0.77	1.00
	$[3/2]_1^0$–$[1/2]_0$	607.434	3.30	6.7	34	31	3		0.88
			3.65	8.8	44	40	4		0.84
	$[3/2]_2^0$–$[3/2]_2$	614.306	3.30	6.7	37	32	5		0.97
			3.65	8.8	47	41	6		0.91
	$[3/2]_2^0$–$[3/2]_1$	621.728	3.30	6.7	43	39	4		1.16
			3.65	8.8	53	48	5		1.04
	$[3/2]_1^0$–$[3/2]_2$	630.479	3.30	6.7	37	32	5		0.92
			3.65	8.8	51	44	7		0.93
	$[3/2]_1^0$–$[3/2]_1$	638.299	3.30	6.7	30	27	3		0.76
			3.65	8.8	40	34	6		0.70
	$[3/2]_2^0$–$[5/2]_3$	640.225	3.30	6.7	36	31	5	0.72	0.92
			3.65	8.8	45	38	7	0.65	0.83
	$[3/2]_2^0$–$[5/2]_2$	633.443	3.30	6.7	35	30	5		0.91
			3.65	8.8	41	34	7		0.75
	$[3/2]_1^0$–$[5/2]_2$	650.653	3.30	6.7	36	33	3	0.74	0.95
			3.65	8.8	45	41	4	0.67	0.86
3s–3p′	$[3/2]_2^0$–$[1/2]_1$	588.190	3.30	6.7	29	25	4		0.83
			3.65	8.8	37	31	6		0.75
	$[3/2]_1^0$–$[1/2]_1$	603.000	3.30	6.7	37	32	5		1.01
			3.65	8.8	48	41	7		0.94
	$[3/2]_2^0$–$[3/2]_2$	594.483	3.30	6.7	32	27	5	0.72	0.90
			3.65	8.8	43	37	6	0.73	0.90
	$[3/2]_2^0$–$[3/2]_1^0$	597.553	3.30	6.7	40	36	4		1.18
			3.65	8.8	50	44	6		1.05
	$[3/2]_1^0$–$[3/2]_2$	609.616	3.30	6.7	30	28	2	0.70	0.88
			3.65	8.8	39	35	4	0.64	0.81
	$[3/2]_1^0$–$[3/2]_1$	612.846	3.30	6.7	26	22	4		0.69
			3.65	8.8	36	30	6		0.68
3s′–3p′	$[1/2]_1^0$–$[1/2]_1$	659.895	3.30	6.7	36	31	5		0.81
			3.65	8.8	50	43	7		0.82
	$[1/2]_1^0$–$[1/2]_0$	585.249	3.30	6.7	42	35	7		0.88
			3.65	8.8	54	45	9		0.84
	$[1/2]_0^0$–$[1/2]_1$	616.359	3.30	6.7	32	28	4		0.85
			3.65	8.8	44	38	6		0.84
	$[1/2]_1^0$–$[3/2]_2$	667.828	3.30	6.7	41	37	4	0.73	0.97
			3.65	8.8	55	50	5	0.73	0.96
	$[1/2]_1^0$–$[3/2]_1$	671.704	3.30	6.7	39	36	3		0.93
			3.65	8.8	50	46	4		0.87
	$[1/2]_0^0$–$[3/2]_1$	626.650	3.30	6.7	35	31	4	0.74	0.92
			3.65	8.8	46	41	5	0.72	0.89
	$[1/2]_0^0$–$[3/2]_1$	653.288	3.30	6.7	36	30	6	0.65	0.82
			3.65	8.8	44	37	7	0.59	0.74

Table 1. (Continued.)

Transition	Multiplet	λ (nm)	$T^{\exp}$	$N^{\exp}$	$W_{\mathrm{t}}^{\exp}$	$W_{\mathrm{e}}^{\exp}$	$W_{\mathrm{i}}^{\exp}$	$W_{\mathrm{e}}^{\exp}/W_{\mathrm{e}}^{\mathrm{G}}$	$W_{\mathrm{e}}^{\exp}/W_{\mathrm{e}}^{T_{\mathrm{w}}}$
3s′–3p	$[1/2]_1^0$–$[3/2]_2$	692.947	3.30	6.7	38	35	3	0.62	0.84
			3.65	8.8	50	45	5	0.59	0.79
	$[1/2]_1^0$–$[5/2]_1$	717.394	3.30	6.7	42	39	3		0.92
			3.65	8.8	53	49	4		0.85
3p–4d	$[3/2]_2$–$[5/2]_3^0$	597.463	3.30	6.7	42	36	6		
			3.65	8.8	53	45	8		

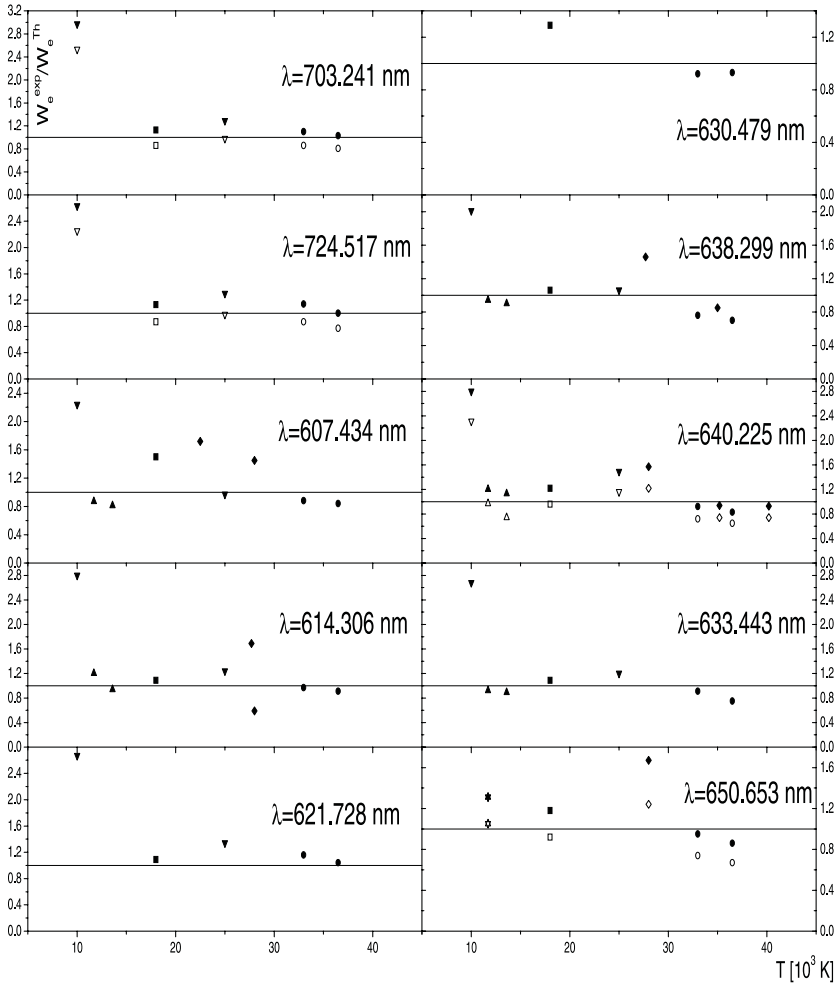

Figure 3. Ratios of the experimental $W_{\mathrm{e}}^{\exp}$ and theoretical $W_{\mathrm{e}}^{\mathrm{Th}}$ electron Stark widths versus electron temperature (T) for the Ne I lines in the 3s–3p transition (see also table 1). Empty and filled symbols are related to the Griem's (1974) (G) theoretical values and ones calculated by us (T_{w}) taken from table 2. ○, our experimental results and those of other authors: △, [6]; ✡, [7]; ▽, [11]; ◇, [12] and □, [16].

Table 2. Our calculated Ne I Stark FWHM (W^{T_w} in pm) for electrons (a) and protons (b) as perturbers for various temperatures (T) at 10^{22} m^{-3} perturber density.

		T ($\times 10^3$ K)					
λ (nm)		2.5	5.0	10.0	20.0	30.0	50.0
703.241	a	2.89	2.93	3.23	4.18	5.05	6.34
$3s[3/2]^0_2$–$3p[1/2]_1$	b	1.58	1.59	1.59	1.59	1.59	1.59
724.517	a	3.04	3.09	3.43	4.47	5.41	6.80
$3s[3/2]^0_1$–$3p[1/2]_1$	b	1.68	1.68	1.68	1.68	1.69	1.69
607.434	a	2.76	2.95	3.30	4.21	5.05	6.36
$3s[3/2]^0_1$–$3p[1/2]_0$	b	1.53	1.54	1.55	1.56	1.57	1.59
614.306	a	2.60	2.74	3.06	3.93	4.76	6.03
$3s[3/2]^0_2$–$3p[3/2]_2$	b	1.47	1.48	1.48	1.49	1.50	1.51
621.728	a	2.59	2.71	3.03	3.93	4.78	6.06
$3s[3/2]^0_2$–$3p[3/2]_1$	b	1.47	1.48	1.49	1.49	1.50	1.51
630.479	a	2.70	2.84	3.19	4.15	5.06	6.42
$3s[3/2]^0_1$–$3p[3/2]_2$	b	1.55	1.55	1.56	1.57	1.57	1.58
638.299	a	2.68	2.81	3.17	4.16	5.08	6.45
$3s[3/2]^0_1$–$3p[3/2]_1$	b	1.55	1.56	1.57	1.57	1.58	1.58
640.225	a	2.57	2.67	3.01	3.95	4.84	6.15
$3s[3/2]^0_2$–$3p[5/2]$	b	1.49	1.50	1.50	1.51	1.51	1.51
633.443	a	2.57	2.68	3.01	3.94	4.81	6.11
$3s[3/2]^0_2$–$3p[5/2]$	b	1.49	1.49	1.50	1.50	1.50	1.51
650.653	a	2.67	2.78	3.16	4.18	5.13	6.51
$3s[3/2]^0_1$–$3p[5/2]$	b	1.57	1.57	1.58	1.58	1.58	1.59
588.190	a	2.39	2.50	2.78	3.59	4.35	5.51
$3s[3/2]^0_2$–$3p'[1/2]_1$	b	1.34	1.34	1.35	1.36	1.36	1.37
603.000	a	2.47	2.58	2.91	3.78	4.61	5.85
$3s[3/2]^0_1$–$3p'[1/2]_1$	b	1.40	1.41	1.42	1.42	1.43	1.43
594.483	a	2.37	2.47	2.77	3.59	4.37	5.53
$3s[3/2]^0_2$–$3p'[3/2]_2$	b	1.34	1.35	1.35	1.36	1.36	1.37
597.553	a	2.37	2.46	2.76	3.59	4.37	5.55
$3s[3/2]^0_2$–$3p'[3/2]_1$	b	1.34	1.35	1.35	1.36	1.36	1.37
609.616	a	2.46	2.56	2.89	3.79	4.63	5.88
$3s[3/2]^0_1$–$3p'[3/2]_2$	b	1.41	1.42	1.42	1.42	1.43	1.43
612.846	a	2.46	2.55	2.88	3.79	4.64	5.89
$3s[3/2]^0_1$–$3p'[3/2]_1$	b	1.41	1.42	1.42	1.43	1.43	1.43
659.895	a	3.17	3.36	3.70	4.63	5.49	6.83
$3s'[1/2]^0_1$–$3p'[1/2]_1$	b	1.69	1.70	1.71	1.73	1.74	1.75
585.249	a	3.36	3.75	4.21	5.07	5.75	6.85
$3s'[1/2]^0_1$–$3p'[1/2]_0$	b	1.65	1.68	1.71	1.75	1.77	1.81
616.359	a	2.84	3.02	3.29	4.04	4.72	5.84
$3s'[1/2]^0_0$–$3p'[1/2]_1$	b	1.48	1.49	1.50	1.52	1.53	1.54
667.828	a	2.92	3.04	3.45	4.56	5.59	7.10
$3s'[1/2]^0_2$–$3p'[3/2]_2$	b	1.69	1.70	1.70	1.71	1.71	1.72
671.704	a	2.92	3.03	3.45	4.57	5.61	7.12
$3s'[1/2]^0_1$–$3p'[3/2]_1$	b	1.70	1.70	1.71	1.71	1.71	1.72
626.650	a	2.64	2.74	3.05	3.92	4.77	6.04
$3s'[1/2]^0_0$–$3p'[3/2]_1$	b	1.48	1.49	1.49	1.50	1.50	1.51
653.288	a	3.03	3.20	3.51	4.40	5.22	6.50
$3s'[1/2]^0_0$–$3p'[3/2]_1$	b	1.62	1.63	1.64	1.66	1.66	1.68
692.947	a	3.22	3.39	3.83	5.02	6.14	7.80

Table 2. (Continued.)

		T ($\times 10^3$ K)					
λ (nm)		2.5	5.0	10.0	20.0	30.0	50.0
$3s'[1/2]_1^0$–$3p[3/2]_2$	b	1.87	1.87	1.88	1.89	1.90	1.91
717.394	a	3.47	3.64	4.00	5.06	6.04	7.56
$3s'[1/2]_1^0$–$3p[5/2]_1$	b	1.89	1.90	1.91	1.92	1.94	1.95

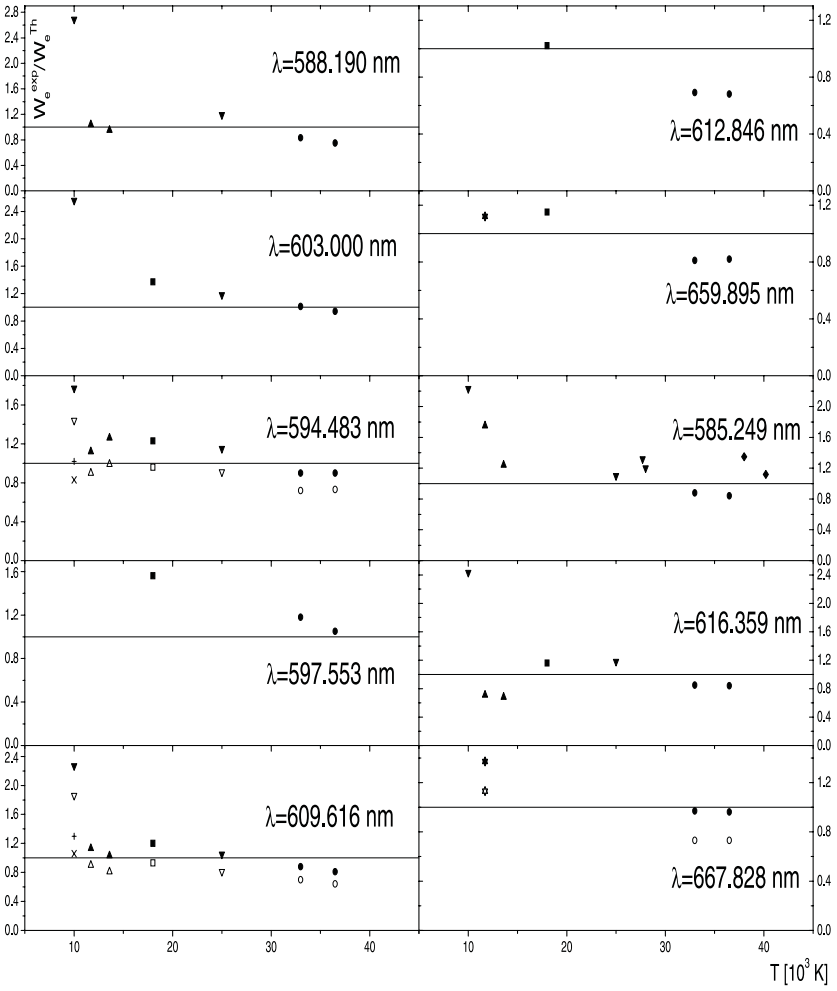

Figure 4. Same as in figure 3 but for the Ne I lines in the 3s–3p′ and 3s′–3p′ transitions. In addition: +, for the ratios of experimental data from [15] related to the Griem's (1974) (G) theoretical values; and ×, for their ratios related to our calculated (T_w) values.

for Ne I lines. One can conclude that the agreement between N^{exp} and N^D values is excellent (within 3% on average) in the two plasmas investigated. This fact confirms homogeneity of the investigated plasma in the linear part of our light source (see figure 1 in [38]). In the case of the electron temperature the situation is similar. The agreement between the two sets of the electron temperature decays (T^{exp} and T^D) is also excellent (within 2% on average).

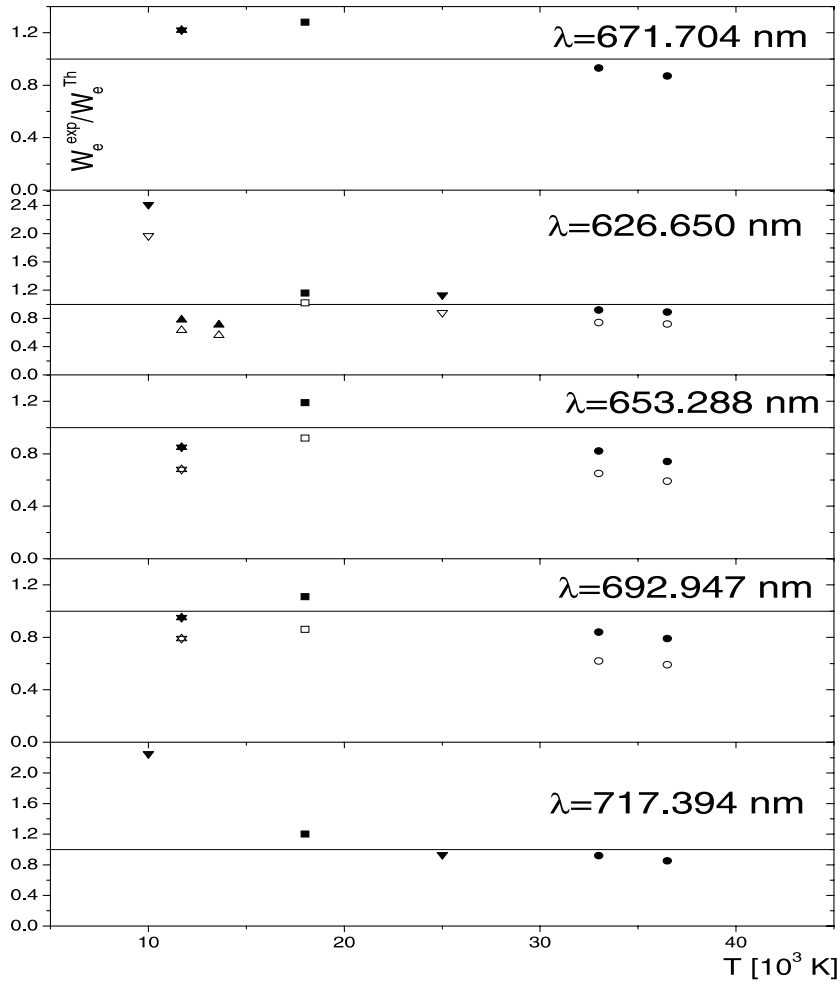

Figure 5. Same as in figure 3 but for the Ne I lines in the 3s′–3p′ and 3s′–3p transitions.

In order to make the comparison between the measured $\left(W_{\mathrm{e}}^{\mathrm{exp}}\right)$ and calculated $\left(W_{\mathrm{e}}^{\mathrm{Th}}\right)$ electron width values easier, the dependence of the ratio $W_{\mathrm{e}}^{\mathrm{exp}}/W_{\mathrm{e}}^{\mathrm{Th}}$ on the electron temperature is presented graphically in figures 3–5. Experimental $W_{\mathrm{e}}^{\mathrm{exp}}$ data are related to the Griem's (1974) (G) and our calculated (T_{w}) values taken from table 2.

We have found that the widths generated by protons show weak dependence on the electron temperature and are about three times smaller than the widths generated by electrons (see table 2) at $T = 30\,000$ K.

All our measured $W_{\mathrm{e}}^{\mathrm{exp}}$ values lie below Griem's (1974) $W_{\mathrm{e}}^{\mathrm{G}}$ values at about 29% (averaged through 10 lines). The greatest disagreement between them was found for the case of the 653.288 nm and 692.947 nm Ne I lines. Most of the $W_{\mathrm{e}}^{\mathrm{exp}}$ values of the other authors lie also below Griem's data (see figures 3–5).

All calculated $W_{\mathrm{e}}^{T_{\mathrm{w}}}$ values (see table 2), generated by electrons, are smaller than $W_{\mathrm{e}}^{\mathrm{G}}$ values at about 20%, but these are also higher than our measured ones. Within estimated experimental accuracy of $\pm 12\%$ our $W_{\mathrm{e}}^{\mathrm{exp}}$ values agree with our calculated ones $\left(W_{\mathrm{e}}^{T_{\mathrm{w}}}\right)$ for the ten Ne I lines and all obtained ratios of our experimental and theoretical values are within

1.0 ± 0.3 interval which is less than combined experimental ($\pm 12\%$) and theoretical ($\pm 30\%$) error.

We have found that the electron contribution $\left(W_{\mathrm{e}}^{\mathrm{exp}}\right)$ to the total Stark widths is about 82%. At our plasma parameters the neon ions (Ne II, Ne III, ...) contribute about 18% (on average) to the total Stark widths.

The $W_{\mathrm{e}}^{\mathrm{exp}}$ values from [11] (∇ in figures 3–5) obtained at 10 000 K electron temperature are about 2.5 times higher from other experimental data. This is, probably, caused by unreliable measured electron density. We have excluded these values from all comparisons. Our $W_{\mathrm{e}}^{\mathrm{exp}}$ and $W_{\mathrm{e}}^{T_{\mathrm{w}}}$ values are within $\pm 20\%$ on average in agreement with recently published [16] data for 19 Ne I lines.

Very good agreement was found among all existing $W_{\mathrm{e}}^{\mathrm{exp}}$ and $W_{\mathrm{e}}^{T_{\mathrm{w}}}$ values for the 626.650, 671.704, 717.394, 703.241, 724.517, 633.443, 588.190, 609.616 and 616.359 nm Ne I spectral lines in a wide range of electron temperatures.

5. Conclusion

It has been found that the electron contribution to the total Stark widths is about 82% and the neon ions contribute 18% (on average) to the total Stark widths. Generally, our measured and calculated electron Stark widths are smaller than those presented in [17] by about 20% on average.

In the electron temperature range between 10 000 K and 40 000 K very good agreement has been found among all existing $W_{\mathrm{e}}^{\mathrm{exp}}$ and our $W_{\mathrm{e}}^{T_{\mathrm{w}}}$ values for the 626.650, 671.704, 717.394, 703.241, 724.517, 633.443, 588.190, 609.616 and 616.359 nm Ne I spectral lines.

Acknowledgments

This work is a part of the projects OI1228 ‘Determination of the atomic parameters on the basis of the spectral line profiles’ and GA1195 ‘Influence of collision processes on astrophysical plasma lineshapes’ supported by the Ministry of Science, Technologies and Development of the Republic of Serbia.

References

[1] Seaton M J 1987 *J. Phys. B: At. Mol. Phys.* **20** 6363
[2] Trimble V 1991 *Astron. Astrophys. Rev.* **3** 1
[3] Mazing M A and Mandel’shtam S L 1957 *Opt. Spektrosk.* **2** 276
[4] Moo-Young G A, Greig J R and Griem H R 1970 *Phys. Rev.* A **2** 1617
[5] Miller M H and Bengston R D 1970 *Phys. Rev.* A **1** 983
[6] Nubbemeyer H, Stuck D and Wende B 1970 *Z. Phys.* **234** 29
[7] Miller M H, Roig R A and Moo-Young G A 1971 *Phys. Rev.* A **4** 971
[8] Im T D, Kazantsev A P, Routian S G, Saprykin E G and Shalagin A M 1974 *Sov. J. Quantum Electron.* **4** 234
[9] Im T D, Kochanov V P, Routian S G, Saprykin E G and Shalagin A M 1974 *Opt. Spectrosk. (USSR)* **36** 125
[10] Im T D, Kochanov V P, Routian S G, Saprykin E G and Shalagin A M 1976 *Sov. J. Quantum Electron.* **6** 283
[11] Purić J, Ćuk M and Rathore B H 1987 *Phys. Rev.* A **35** 1132
[12] Purić J, Srećković A, Djeniže S, Labat J and Ćirković Lj 1988 *Phys. Lett.* A **126** 280
[13] Deinezhenko A L and Protasevich E T 1988 *Opt. Spektrosk. (USSR)* **65** 303
[14] Windholz L and Neureiter C 1988 *Phys. Rev.* A **37** 1978
[15] Döhrn A and Helbig V 1996 *Phys. Rev.* E **53** 6581
[16] del Val J A, Aparicio J A and Mar S 1999 *Astrophys. J.* **513** 535
[17] Griem H R 1974 *Spectral Line Broadening by Plasmas* (New York: Academic)
[18] Syrkin M I 1981 *Opt. Spektrosk. (USSR)* **51** 431
[19] Krylova S I, Luizova L A, Solyanikova V A and Khakhaev A D 1971 *J. Appl. Spektrosk. (USSR)* **14** 676

[20] Milosavljević V and Poparić G 2001 *Phys. Rev.* E **63** 036404
[21] Milosavljević V 2001 *PhD Thesis* Faculty of Physics, University of Belgrade, Belgrade (unpublished)
[22] Milosavljević V 2002 *Monograph* (Belgrade: Zadužbina Andrejević)
[23] Milosavljević V and Djeniže S 2002 *Astron. Astrophys.* **393** 721
[24] Milosavljević V and Djeniže S 2002 *New Astron.* **7–8** 543
[25] Milosavljević V and Djeniže S 2003 *Eur. Phys. J.* D **23** 385
[26] Milosavljević V and Djeniže S 2003 *Astron. Astrophys.* **405** 397
[27] Milosavljević V, Djeniže S and Dimitrijević M S 2003 *Phys. Rev.* E **68** 016402
[28] Milosavljević V and Djeniže S 2002 *Phys. Lett.* A **305/1–2** 70
[29] Milosavljević V and Djeniže S 2003 *Astron. Astrophys.* **398** 1179
[30] Sahal-Bréchot S 1969 *Astron. Astrophys.* **1** 91
[31] Sahal-Bréchot S 1969 *Astron. Astrophys.* **2** 322
[32] Sahal-Bréchot S 1974 *Astron. Astrophys.* **35** 321
[33] Dimitrijević M S and Sahal-Bréchot S 1984 *J. Quant. Spectrosc. Radiat. Transfer* **31** 301
[34] Dimitrijević M S and Sahal-Bréchot S 1985 *Phys. Rev.* A **31** 316
[35] Dimitrijević M S, Sahal-Bréchot S and Bommier V 1991 *Astron. Astrophys. Suppl. Ser.* **89** 581
[36] Griem H R 1964 *Plasma Spectroscopy* (New York: McGraw-Hill)
[37] Djeniže S, Srećković A and Labat J 1992 *Astron. Astrophys.* **253** 632
[38] Djeniže S, Milosavljević V and Srećković A 1998 *J. Quant. Spectrosc. Radiat. Transfer* **59** 71
[39] Milosavljević V, Djeniže S, Dimitrijević M S and Popović L Č 2000 *Phys. Rev.* E **62** 4137
[40] Milosavljević V, Dimitrijević M S and Djeniže S 2001 *Astrophys. J. Suppl. Ser.* **135** 115
[41] Djeniže S and Bukvić S 2001 *Astron. Astrophys.* **365** 252
[42] NIST—Atomic Spectra Data Base Lines (wavelength order) 2003 Online at http://physics.nist.gov
[43] Wiese W L, Smith M W and Glennnon B M 1966 *Atomic Transition Probabilities, vol I Hydrogen Through Neon* (Washington, DC: US Department of Commerce, National Bureau of Standards) (NSRDS-NBS4)
[44] Striganov R A and Sventickij N S 1966 *Tablicy Spektral'nykh linij* (Moskva: Atomizdat)
[45] Ashby D E T F, Jephcott D F, Malein A and Raynor F A 1965 *Appl. Phys. B: Photophys. Laser Chem.* **36** 29
[46] Barnard A J, Cooper J and Smith E W 1974 *J. Quant. Spectrosc. Radiat. Transfer* **14** 1025
[47] Kelleher D E 1981 *J. Quant. Spectrosc. Radiat. Transfer* **25** 191
[48] Fleurier C, Sahal-Bréchot S and Chapelle J 1977 *J. Quant. Spectrosc. Radiat. Transfer* **17** 595
[49] Bashkin S and Stoner J J Jr 1975 *Atomic Energy Levels and Grotrian Diagrams* vol 1 (Amsterdam: North-Holland)
[50] Oertel G K and Shomo L P 1968 *Astrophys. J. Suppl. Ser.* **16** 175
[51] Bates D R and Damgaard A 1949 *Trans. R. Soc.* A **242** 101
[52] Van Regemorter H, Hoang Binh Dy and Prud'homme M 1979 *J. Phys. B: At. Mol. Phys.* **12** 1053
[53] Sahal-Bréchot S 1991 *Astron. Astrophys.* **245** 322

ISSN 1450-6998 | UDC 930.85(3)(082)

ЗБОРНИК

МАТИЦЕ СРПСКЕ ЗА КЛАСИЧНЕ СТУДИЈЕ

JOURNAL OF CLASSICAL STUDIES MATICA SRPSKA

14

НОВИ САД
NOVI SAD
2012

UDC 821.14’02-13.09 Homeros

Ефстратије Теодосију[1], *Василије Н. Маниманис*[1],
Петрос Мандаракис[2], *Милан С. Димитријевић*[3]
[1] Department of Astrophysics-Astronomy and Mechanics, School of Physics, University of Athens, Panepistimioupolis, Zographos 157 84, Athens–Greece

АСТРОНОМИЈА И САЗВЕЖЂА У ХОМЕРОВОЈ *ИЛИЈАДИ* И *ОДИСЕЈИ*

АПСТРАКТ: *Илијада* и *Одисеја* су, осим највишег статуса стожера светске литературе, и богат извор информација о научном и технолошком знању старих Грка у прехомерска и хомерска времена. Две Хомерове епске песме, које потичу из 8. века пре н.е., укључују, *inter alia*, богатство астрономских елемената, те нам пружају податке о Земљи, небу, звездама и сазвежђима, као што су Ursa Major, Boötes, Орион, Сиријус, Плејаде и Хијаде. Такође нам нуде представу о много образованијем Хомеру, који одражава козмолошке погледе свога доба. Модел Универзума који описује је непрекидан али има три нивоа: доњи, који одговара подземном свету, средњи Земљи и горњи небу. У раду су размотрени козмолошки модел и астрономски елементи у *Илијади* и *Одисеји*.

КЉУЧНЕ РЕЧИ: историја астрономије, Хомер, античка козмологија.

УВОД

Илијада и *Одисеја* немају само изузетан литерарни значај, него су такође и богат извор података о историји и научним, технолошким и астрономским знањима старих Грка у прехомерска и хомерска времена. Ова два епска дела, настала у 8. веку пре н.е., укључују драгоцене информације о Земљи, небу, звездама и сазвежђима, као што су Ursa Major, Boötes (Βοώτης), Орион, Сиријус, Плејаде и Хијаде, и дају могућност да се шире сагледају општији козмолошки погледи тога доба.

Велики број аутора је разматрао различите астрономске аспекте, чињенице и алузије у *Илијади* и *Одисеји*, као на пример Walker

(1872), Schoch (1926a, b, c), Neugebauer (1929), Lorimer (1951), Dicks (1970), Trypanis (1975), Gendler (1984), Lovi (1989), Genuth (1992), Konstantopoulos (1998), Wood и Wood (1999), Flanders (2007), Baikouzis и Magnasco (2008), Minkel (2008), Varvoglis (2009). Све то сведочи о непрекидном интересовању за ову привлачну тему, па је наш циљ да анализирамо астрономске податке и алузије у Хомеровим еповима, да бисмо боље сагледали модел Универзума, чији су елементи тамо дати, козмолошки модел који ће потрајати миленијум после Тројанског рата. На пример Д. Р. Дикс каже: „На основу Хомерових епова не можемо да обликујемо јасну идеју о облику и положају Земље у односу на небеса и подземни свет“ (Dicks 1970, стр. 10). Желимо да размотримо да ли нека идеја о томе ипак може да се обликује и да, на основу одговарајућих пасажа и астрономских података из *Илијаде* и *Одисеје*, утврдимо која су сазвежђа и небеске појаве били познати у то доба старим Грцима, као и да анализирамо имена звезда и сазвежђа, од којих су нека данас потпуно иста као и у хомерска времена.

ПОЛОЖАЈ ОКЕАНА, ЗЕМЉЕ И НЕБА У ХОМЕРСКОМ УНИВЕРЗУМУ

Океан и Земља

Сматра се да су стара учења Орфеја основа прве мистичне грчке религије, са песмама и химнама велике лепоте. Готово сви стари грчки мудраци и писци црпели су инспирацију из тема у *Орфичким химнама*, и тако су били под њиховим утицајем при формулисању својих јединствених теорија и учења.

Осим *Орфичких химни*, Хомерови епови су богат извор историјских и технолошких чињеница. Заиста, астроном који детаљно проучава описе у *Илијади* и *Одисеји* открије ризницу астрономских информација. Сматра се да је Хомер живео у гвозденом добу (период који се грубо протеже од 1200. до 550. пре н.е.), а његова прича се одиграва на крају бронзаног доба (око 12. века пре н.е.).

Како пише Емил Миро:

> *Илијада* и *Одисеја* садрже елементе старе Микенске цивилизације; у основи, оне се односе на догађаје из 12. века пре н.е., животе њихових јунака (друштвене, политичке, економске и породичне), њихове законе и обичаје... ... Све то одражава начин живота, о коме сведочи песник који је створио еп (Mireaux 1959, стр. 9).

Две епске поеме су добиле коначни облик у јонским градовима Анадолије у 9. или 8. веку пре н.е.; прво *Илијада* а касније *Оди-*

ceja (Tryparis 1975, стр. 92). Поеме описују културу, религиозна веровања, опште знање и навике грчког становништва током овог периода. Такође описују космолошки модел који ће преовладавати следећи миленијум.

Земља хомерског Универзума била је кружни, раван диск окружен огромном реком, Океаном – модел који се први пут појавио у Орфичкој химни Х. ПАНУ, *Кађење различӣтим мирисима*, стих 15: „Стари Океане, такође дубоко поштују твоју врховну наредбу, којом течне руке окружују чврсту земљу“.

Ова митска „река“ разликује се од мора: то је нешто што дефинише границе земаљског света. Пре свега, Океан је првобитни и оригинални стваралачки елемент, полазна тачка свих ствари: „Могу да успавам токове и, ако хоћете, реку Океан, која је била почетак свега“. (*Илијада*, XIV 245–246). Океан је мушки предак богова, чија је супруга, током Стварања, била Тетија: „Ићи ћу до крајева Земље да нађем оца свих богова, Океан и мајку Тетију“ (*Илијада*, XIV 200) [Сви коришћени енглески преводи су из Loeb Classical Library издања, ако није другачије речено].

Ова митска „река“ нема извор ни ушће, она је „апсороос“ (ἀψόρροος), тј. кружно се креће. Њен ток се враћа, где је и почео, у непрекидном и вечном кретању. Од Океана, поменутог 33 пута у Хомеровим делима (19 пута у *Илијади* и 14 у *Одисеји*), настале су све друге воде на Земљи: мора, реке и језера. То се помиње у *Илијади*: „Свемоћни Океан, дубоког тока, од кога су сва мора, реке, извори и сваки дубоки кладенац“ (*Илијада*, XXI 195–197).

У *Одисеји*, Океан се описује као ужасан и застрашујући: „...зато што има дубоке токове и велике реке које нико не може прећи без брзог брода“ (*Одисеја*, xi 160). Ипак, није дат коначни опис тачног облика или величине Океана, само смо сазнали да је од воде.

Д. Р. Дикс пише: „На основу Хомерових епова не можемо да обликујемо јасну идеју о облику и положају Земље у односу на небеса и подземни свет“ (Dicks 1970, стр. 10). Мада је то истина, може се рећи да је у хомерском космолошком моделу Земља између неба и подземног света. Њена тачна структура и облик нису познати, само претпостављамо да је то кружни диск пошто је окружен циркуларним воденим Океаном. У *Илијади* (VIII 13–16) је дато супротно виђење Тартара („дубоког места“ испод неба, Земље и мора), када Зевс прети боговима да ће их тамо послати: „или ћу га бацити доле сопственим рукама, у мрак Тартара, далеко у дубине света, који има челичне капије и бакарни под, под Хадом далеко као што је небо од Земље“ (*Илијада*, VIII 13–16).

Паралелно, Хомер замишља Хад у дубинама Земље: „и ако идеш на крај Земље и мора, где Јапет и Хронос бораве, и ветрови

не дувају на њих, осветљава их сунчева светлост а дубоки Тартар окружује са свих страна“ (*Илијада*, VIII 480). Може се закључити да Хомер сматра да а) Хад је испод Земље, окружен Тартаром, б) Земља је центар Универзума и живота, и в) Земља подржава звездано небо (*Одисеја*, ix 534).

Небо

Небо, са сјајним звездама, представљено је као полусферна купола, која тачно покрива равну Земљу (*Одисеја*, xi 17). То јест, Космос оног времена био је замишљен као небески свод преко Земљиног диска који плива на води. Тада се сматрало, како је саопштено у

Τὸ Σύμπαν τῆς Ὁμηρικῆς ἐποχῆς. Ἐπὶ τῆς περιφερείας τοῦ μεγάλου δίσκου τῆς Γῆς ὑψοῦνται τὰ ὄρη, γύρω δὲ εἶναι ὁ Ὠκεανός, ἐνῷ εἰς τὸ μέσον ὁ Ὄλυμπος, φθάνων μέχρι τοῦ Οὐρανοῦ. Εἰς τὴν ὑψίστην κορυφὴν κάθεται ὁ Ζεὺς καὶ ἐπιβλέπει τοὺς θνητοὺς καὶ τοὺς ἀθανάτους, ἀμείβει ἢ τιμωρεῖ αὐτούς. Ἐπάνω ἐκτείνεται ὁ Οὐρανός — ποὺ στηρίζεται εἰς τὰς στήλας τοῦ Ἄτλαντος — ὁ ὁποῖος ἔχει τοὺς ἀστέρας, τὴν Σελήνην, τὸν Ὠρίονα, τὰς Πλειάδας (κ. Πούλια), τὸν Σείριον, τὴν «ἅμαξαν», δηλαδὴ τὴν Μεγάλην Ἄρκτον, ἡ ὁποία τότε δὲν ἐλούετο εἰς τὸ κῦμα τοῦ Ὠκεανοῦ.

Слика 1: Хомеров Универзум. У Универзуму хомерских времена, могу се видети планине које се уздижу са површине великог диска Земље и Океан који се шири око њих, а центром доминира планина Олимп, која се диже до небеса. На највишем врху је свевидећи Зевс на престолу, који надгледа како бесмртне богове тако и смртне људе, и с времена на време их награђује или кажњава. Изван Олимпа шире се небеса, која држе Атласови стубови. На небу су Месец, звезде и сазвежђа (али не према Хомеру): Hydra, Corvus, Crater, Cancer, Leo, Gemini, Taurus, као и отворено звездано јато Плејаде (цитирано у Cotsakis 1976, стр. 18).

Одисеји, да небо, наслоњено на стубове, носи Земља, а њих, који одржавају цео свет у равнотежи, држи и чува митолошки Атлас: „Ћерка Атласа, који познаје дубину сваког мора и сам диже високе стубове који деле Земљу и Небо на двоје“ (*Одисеја*, I 53–54).

За старе Грке, небо је било купола начињена од чврстог материјала, гвожђа или бакра, коју су придржавали високи стубови или, по друкчијем виђењу, неки џин. Хомер комбинује ова два погледа тако што Атлас придржава стубове. Хесиод у *Теогонији* (517e) пише да је Зевс дао ову дужност Атласу.

За Хомера небо је направљено од бакра, како је описано у *Илијади*: „Ахајци, до темена бели од прашине, коју су коњи својим стопама дизали до бакарног неба“ (V 504).

Или други пасаж: „Борили су се онде и гвоздена бука грмела је кроз ваздух до бакарног неба” (XVII 424–425). У другим деловима хомерских дела, небо се такође назива „полихалкис“, тј. „од много бакра“ (*Илијада*, V 504; *Од.* III 2; *Илијада*, II 458, XVI 364, XIX 351). У *Одисеји* (xv 329 и xvii 565) помиње се и гвоздено небо, али се не зна да ли је оно употребљено као метафора или у неком другом контексту.

Закључујемо дакле да је код старих Грка представа о небу била да је оно нешто чврсто и недостижно. Његова незамислива удаљеност често је коришћена у поређењима да дочара огромност. На пример, слава Несторовог златног штита досеже небеса: „и тада ћемо узети Несторов штит, чија слава досеже звезде“ (*Илијада*, VIII 192–193). Слично, Пенелопина слава такође допире до широког неба (*Од.* xix 108).

Простор између неба и Земље на почетку је био испуњен густим ваздухом: „до ваздуха су се протезале његове огромне гране“ (*Илијада*, XIV 288).

Преко овог слоја и у правцу неба био је чисти и прозирни „етар“, лакши од ваздуха. Етар је есенцијално „виши ваздух“, кроз који се може видети небо: „и до звезда, које трепере у етру без ветра, очаравајући око светлог Месеца – сваки врх, свака ивица, свака страна је видљива, као простран етер отворен небом, који чини видљивим све звезде на радост пастира“ (*Илијада*, VIII 554–559).

Изнад етра, на врховима Олимпа који допиру до неба, бораве богови: „и принео је много жртава боговима који столују на небесима“ (*Од.* i 68–69), и: „Без мишљења богова који бораве на небу ..., али сада је попут богова који уживају небеса“ (*Од.* vi 242–245). Богови се описују као „олимпијски“ или „небески“, зато што се чини да највиши врх Олимпа додирује небо: „Наш отац, син Хрона, први од небесника“ (*Од.* i 46). Коначно, помиње се да је изнад етра „полихалкис“ небо (*Илијада*, II 458, XVI 364, XIX 351).

Свакако, не треба претпоставити да је хомерско небо пуста метална купола; оно је, како Хомер пева, пуно живота, живота звезда и сазвежђа. Тако су стари Грци небо називали „пуним звездама“ (’астероис’, ἀστερόεις) (*Илијада*, VI 108, XV 371), и украшено звездама (*Од.* ix 535), што је природно за људе који живе у земљи са малим процентом облачних ноћи. Небеским сводом путује Хелиос, бог Сунца, тако да се описује придевом „уранодромос“ (по небу путујући): „Страдали су због свога дрског злочинства, грешници, јели су говеда Хелиоса путујућег по небу (Хипериона), који им је одузео дан за повратак дому“ (*Од.* i 7–9). То је само једно од 119 помињања Сунца у хомерским еповима: 42 пута у *Илијади* и 77 у *Одисеји*. Као бог, Хелиос се јавља 34 пута (8 у *Илијади* и 26 у *Одисеји*). То је у великој супротности са Месецом (Селене) који се у *Илијади* (VIII 554, XVII 367, XVIII 484) помиње само три а у *Одисеји* (iii 46 и ix 144) два пута. Још једном, Месец се помиње у *Илијади* (XIX 374) под својим архаичним именом „мене“. Могуће објашњење ретког помињања Месеца је да се главни догађаји у *Илијади*, тј. битке, одигравају током дана. У *Одисеји* пак месец је обично сакривен иза облака: „Јер била је густа тама наоколо и месец, сакривен у облацима, није сијао на небу“ (*Од.* ix 144).

Пре него што пређемо на разматрање звезда и сазвежђа код Хомера, занимљиво је да се представе неки метеоролошки и климатолошки елементи како се јављају у *Илијади* и *Одисеји*. Ваздухом између неба и Земље пролазе ветрови и облаци, помоћу којих свемогући Зевс покрива небо, шаље кишу на Земљу и баца муње и громове (*Илијада*, XVI 364–365, XII 25–26; *Од.* 303, xxiii 330).

Како се помиње у Певању V *Илијаде*, капије неба и Олимпа начињене су од густих облака. Њихови чувари су Хоре (Часови), богиње годишњих доба, које подешавају временске услове: „и Хера силно бичем тера коње; пред њима се уз грмљавину отвара капија неба, коју Хоре, чувари огромног неба и Олимпа, запречавају облацима или их уклањају“ (*Илијада*, V 749–751).

ЗВЕЗДЕ И САЗВЕЖЂА У *ИЛИЈАДИ* И *ОДИСЕЈИ*

Сада ћемо ближе испитати сва Хомерова помињања сазвежђа, звезда и планете Венере.

У *Илијади*, Хомер помиње „јесењу“ звезду: „Тада Атина даде снагу и храброст Диомеду, тако да би у грчком мноштву био изванредно хваљен и свуда сијао славом. Са његовог шлема и штита видео се пламен, који је без одмора исијавао светлост, попут јесење звезде, што се купа у Океану и сија пуном светлошћу“ (*Илијада*, V 1–5).

„Јесења звезда“ је у ствари Сиријус, најсјајнија звезда на ноћном небу. На географској ширини Грчке, сваке године се појављује крајем јула или почетком августа. О томе пише и Ричард Х. Ален:

> Хомер је у *Илијади* наговестио Сиријус као Ὀπωρινός, Јесењу звезду; али одговарајућа сезона су последњи дани јула, цео август и део септембра – каснији део лета. Грци нису имали тачну реч за нашу „јесен“ до 5. века пре н.е., када се појавила у списима приписаним Хипократу. Лорд Дерби је превео овај чувени пасаж: Жестока светлост синула је онде, као јесења звезда, која најсјајније сија када се наново диже са свог океанског купања (Allen 1963, стр. 120).

Мада се не може тврдити са сигурношћу, хомерски човек је поимао Земљу као раван кружни диск окружен Океаном, сматрао је да се Сунце, Месец и већина звезда издижу из Океана и поново залазе у њега. Идеја о сферној Земљи појавила се много касније, са питагорејским философима (5. век пре н.е.).

У *Илијади* се помиње да су по наредби Ахилејеве мајке Тетиде, на његовом штиту, који је начинио бог Хефест (Вулкан), била насликана сазвежђа: „И прво је направио моћан и велики штит, вештином и троструки круг около. Овај штит је направљен са пет превоја а на њему је нацртао различите слике својим мудрим знањем: Земљу, небо, море је нацртао, неуморно сунце, пун месец, звезде које са свих страна крунишу небо, снагу Ориона, Хијаде,

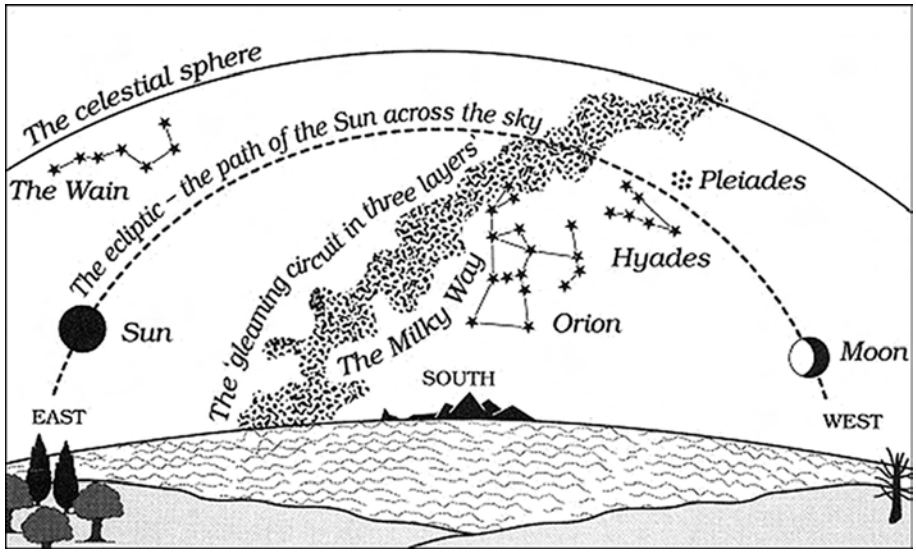

Слика 2: Хомерски Универзум према Флоренс и Кенету Вуду чији су астрономски елементи насликани на Ахилејевом штиту. Извор: Florence & Kenneth Wood (1999). Homer's Secret Iliad: *The Epic of the Night Skies Decoded*. London: John Murray, Albemarle Street, стр. 199.

Плејаде, Медведа, који такође зову Кола, што стално се окреће на истом месту, гледајући Ориона, јединог који се не купа у Океану“ (*Илијада*, XVIII 478–488).

Хијаде и Плејаде, које су у ствари два отворена јата, стари Грци су звали „сазвежђа“ – данас су оба укључена у сазвежђе Бика. Њега Хомер не помиње, мада говори о суседном Ориону, са наглашеним исказом „Орионова снага“. То је управо начин како Ориона помиње Хесиод (*Works and Days*, 598, 615, 619). Оба аутора упућују на „снагу“ сазвежђа, алудирајући на његов привидан сјај.

Хомер завршава са звездама, циркумполарним сазвежђем Ursa Major, које заиста „гледа“ на Орион. Ursa Major се не купа у Океану, тј. никада не „додирује“ море, пошто га положај близу северног небеског пола држи даље од хоризонта док се Земља окреће.

Хијаде и Плејаде се помињу заједно са другим звезданим формацијама, као што су и сама „сазвежђа“, како у *Илијади* тако и у *Одисеји* (272–277). У првом епу Плејаде су поменуте само једном, заједно са Хијадама (у горњем пасажу, XVIII 485), и једном у *Одисеји* (272).

Заиста, у *Одисеји* се помињу све више наведене звезде и сазвежђа: „Тада је радосни Одисеј поставио једра, и седећи за крмом, вешто је крманио; сан му није затварао очи док је гледао Плејаде, Пастира, који касни у залажењу, и Медведа, који многи зову и Кола, што се окреће увек на истом месту и гледа на Ловца, једини који се не купа у таласима Океана јер му је Калипсо казала да увек ту звезду држи са леве стране док плови“ (*Од.* 270–277).

Како Р. Х. Ален (1963, стр. 96) пише:

> Хомер је сазвежђе Boötes карактерисао као ‘οψέ δύων’, са значењем касни у залажењу, мисао и израз који су постали обични због честог понављања. Арат је то користио: „И када је заморен преко дана, задржава се више од пола ноћи“.

Хомер каже да сазвежђе Boötes „касни у залажењу“, односно споро залази, а Арат да се „развлачи више од пола ноћи“, пошто је веома дугачко, релативно уско и дугом страном је оријентисано у правцу север–југ на небеској сфери. Зато Boötes излази „својом дугом страном“, одједном цело, а залази готово вертикално (полазећи, за небо Атине, од доњег десног угла и постајући све вертикалније); прво залазе ноге, па струк и на крају горњи део тела, тако да му треба кратко време да изађе, а веома дуго да зађе.

Треба напоменути да се у овим стиховима, први и једини пут у еповима, помиње коришћење сазвежђа за оријентацију на мору. Калипсо саветује Одисеју да, како би задржао прави курс, мора увек

да држи са леве стране Медведа (Ursa Major). Свакако, то значи да ако му је са лева северно сазвежђе, плови ка истоку. Тако је Хомер поставио Калипсино острво Огигију западно од целе Грчке, пошто је и сама Итака, за коју је био везан, била на западу ове земље.

Будући да је Хомер сматрао да је Земља раван кружни диск, окружен Океаном, био је сигуран да Сунце, Месец и звезде излазе из Океана и залазе у њега; само Ursa Major не залази за старе народе који су живели на северним обалама Медитерана. У грчкој митологији, Зевс се заљубио у нимфу Калисто. Хера, његова жена, претворила је због љубоморе нимфу у медведа. Зевс је касније поставио заједно са сином Ареасом на небо и они чине сазвежђе Ursa Major. Аристотел помиње да је медвед једина животиња која због дебелог крзна може неустрашиво да лута леденим северним поларним областима. Циркумполарни карактер сазвежђа Ursa Major је у наше време само делимичан: док у протоисторијска времена, када је Alpha Draconis (Тубан) била 'поларна звезда', ниједна од седам најсјајнијих звезда у сазвежђу Ursa Major није залазила. Данас, услед прецесије Земљине осе, Алкаид (Eta Ursae Majoris, последња звезда у репу) остаје испод северног хоризонта Атине, Итаке и централне Грчке уопште, приближно три сата. Само у северној Грчкој и на местима са географском ширином већом од $\varphi = 40{,}1°$ су све најсјајније звезде овог сазвежђа циркумполарне. Ален (1963, стр. 419) саопштава о овоме на следећи начин: „Сер Џорџ Корнуол Луис пише – за Хомеров правац Арктоса, јединствене звезде која се никада не купа у таласима океана (услед прецесије тада је била много ближе полу него сада)". Разлика у деклинацији Алкаида (η UMa) у хомерска времена и данас је више од 15 степени, тако да је у антици цео Ursa Major био циркумполаран чак и на најјужнијем крајичку Грчке.

Хомер пак не помиње Великог медведа експлицитно, тако да модерни коментатор може да претпостави да је у ствари мислио на Малог медведа, Ursa Minor, или на комбинацију оба. То је највероватније означавало Великог медведа, пошто има много сјајније звезде, много је веће и импресивније сазвежђе, а Малог медведа је (према традицији) код Грка увео Талес из Милета у 6. веку пре н.е., дакле два века после Хомера. Ursa Minor је још увек, како се види из Грчке, потпуно циркумполарно сазвежђе.

Последње сазвежђе поменуто у пасажу из *Одисеје* је Орион, Ловац. Његова појава на ноћном небу сваке године се подударала са почетком најкишнијег и најолујнијег дела године, па је Орион називан „олујни" и деструктивни. Хесиод и Аристотел помињу да је излазак Ориона упозорење за морнаре да долазе олује (Hesiod, *Works and Days* 598, 615, 619 и Arist. *Meteor.* 2.5.4).

У Певању XXII *Илијаде*, помињу се Орион и Сиријус. Најсјајнија звезда Сиријус наводи се као Орионов пас; данас је познат као најзначајнија звезда сазвежђа Великог пса (Canis Major), Alpha Canis Majoris. Хомер представља Сиријус као злослутан знак на небу, пошто је сваког лета повезан са такозваним „пасјим врућинама“:

> као звезда која нам долази у јесен, натсијавајући све
> своје другове на јесењем небу – зову је Орионов пас, и,
> премда је најсјајнија од свих звезда, не предсказује добро
> доносећи много грознице нама, јадним смртницима
> [*The Iliad*, trans. by E. V. Rieu, Penguin Books,
> New York 1950 (Ch. 22, v. 25–31)].

„Пасје врућине“ и „пасји дани“

У антици, хелијакални излазак Сиријуса повезан је са изузетно топлим периодом године, *„κυνικά καύματα“* („пасја врелина“). То, у медитеранском крају, одговара касном јулу, августу и раном септембру. Римљани су такође за ове дане знали као за „dies caniculariae“, најтоплије доба целе године, повезано са сазвежђем Великог пса, и Ловчевим (Орионовим) псом, Сиријусом. Стари Грци су претпостављали да вишак топлоте потиче од додавања Сиријусовог зрачења Сунчевом.

У фолклору старе Грчке, народ је летње дане после хелијакалног изласка Сиријуса називао „пасје врућине“ без повезивања са Пасјом звездом или сазвежђем, већ са псима уопште, мислећи да су само пси толико луди да иду напоље када је толико топло. Ово веровање је истрајало кроз векове и може се наћи у модерном грчком фолклору у веровању да су за време врелих јулских и августовских дана, нарочито између 24. јула и 6. августа, псећи уједи посебно заразни (Theodossiou, Danezis 1991, стр. 115).

Према старом миту, становници острва Кеа умирали су од глади услед суше коју је око 1600. пре н.е. донела пасја врућина. Тада је бог Аполон дао пророчанство да се позове Птија Аристеј, божји син, да им помогне. Пошто је дошао на Кеу, Аристеј је извео ритуале очишћења и жртвовања Зевсу Икмејском, господару киша и неба, и Аполону. Оба бога су слушали њихове молбе и послали су Етезијске ветрове, северне ветрове који четрдесет дана дувају преко целог Егејског мора средином лета, тако да људи могу да преживе неподношљиву врелину. После тога, народ Кее, подстакнут Аристејем, принео је жртве сазвежђу Canis Major и Сиријусу; да би памтили његово доброчинство, славили су Аристеја као „Ари-

стеја Аполона“ и стављали његову главу на једну страну новца, а на другу Сиријуса са круном са зрацима.

Бивши професор и академик са Националног техничког универзитета у Атини Перикле С. Теохарес пише: „Овај мит алудира на однос Сиријуса са Земљом. Жртве су приношене Зевсу Мејлихију, богу времена, сунца и кише, и Сиријусу, који ствара пасје врућине на Земљи; сматрали су да за велику летњу топлоту није одговорно само Сунце, него такође и Сиријус када дође после Сунца. То је вероватно било веровање градитеља арголидских пирамида, који су оријентисали њихове улазне ходнике према азимуту Сиријуса“ (Theochares, 1995).

У старој поезији Сиријус се помиње као звезда са посебно негативним утицајем, што је очигледно из Хомерових стихова „не предсказује добро... нама јадним смртницима“ (*Илијада*, XXII 25–31). Пошто су запазили да људи постају троми током пасјих дана, учврстили су веровање да Сиријус има успоравајуће деловање на људске активности. Зато чак и Хипократ саопштава о лошем утицају ове звезде на људе. Хипократ је у делима *Epidemics* и *Aphorisms* писао доста о утицају моћи ове звезде на време и последичне физичке ефекте на људе (Allen 1963, стр. 126).

Планета Венера

Венера се помиње и у *Илијади* и у *Одисеји*. У Певању XXII (стих 317) *Илијаде*, Хомер помиње Хесперос, Вечерњу звезду, а у XXIII (стих 226) Еосфорос (Lucifer на латинском), Јутарњу звезду, која доноси светлост зоре. У оба случаја у ствари се помиње Венера, мада их Хомер вероватно сматра за две посебне звезде: „И као што међу звездама излази сјајна вечерња звезда, најлепша међу звездама на небу, тако је сијало копље, бачено његовом десном руком према божанском Хектору са злобном намером, гледајући да нађе непокривени део његовог меког тела“ (*Илијада*, XXII 317–321). Слично у другом пасажу: „Када Луцифер најављује светлост и златни Еос (Зора) излази из морских дубина, огањ бледи и пламенови се заустављају“ (*Илијада*, XXIII 226–228).

Пасаж у Хомеровој *Одисеји* опет нас доводи мору: „Како је изронила блистава звезда, која долази да прва најави светло Зоре рођене из ноћи, брод се пенећи од среће приближавао острву“ (*Од.* xiii 98–100). Значи да је Одисеј досегао Итаку пре зоре, у време када се појављује Венера, најсјајнија звезда која „долази“ пре зоре.

Солстиције

У *Одисеји* се такође јасно помињу солстиције као „окретања Сунца“: „Они једно острво зову Сирија – ако сте икада чули за њега – где је Сунце више него у Ортигији, када се окреће“ (*Од.* xv 403–404).

Други стари аутори о звездама, сазвежђима и Сиријусу

Хомерови епови су несумњиво утицали на друге старогрчке песнике и ауторе у помињању звезда и сазвежђа на небу. Највише је присутна најсјајнија звезда, Сиријус.

Захваљујући сјајној привидној величини (-1.46), Сиријус је имао посебно место у митологији, легендама и традицији већине народа на Земљи. Само његово име на грчком значи „блештави“, „пламени“ или „горећи“, успламтео; ово име је веома старо, пошто је присутно у орфичкој традицији: „када је три дана за редом изгубила светлост пламена звезда“ (*Argonautics*, 121–122, Petrides, 2005), као и код Хомера (*Илијада*, XXII 25–32 и *Od.* 4).

У приближно истом времену са Хомером, или мало касније, Хесиод у свом делу *Послови и дани* помиње неколико сазвежђа која су сељацима потребна да би пазили на свој свакодневни рад, а три пута наводи и солстиције. На пример, Хесиод сугерише да жетва треба да почне када Плејаде изађу (хелијакални излазак), а сетва када су при заласку. Хесиод говори о свим звездама и сазвежђима које помиње Хомер, са посебним нагласком на Сиријусу. Заиста, Сиријус помиње у три различита пасажа. У првом даје савете брату Персу о берби грожђа: „А када Орион и Сиријус досегну средину неба и рујнопрстаста зора гледа Арктура, тада, Персе, обери све грожђе и донеси га кући“ (*Послови и дани* 609), док у друга два говори о пасјој врућини: „Тада звезда Сиријус напредује сваког дана мало више изнад глава смртника и узима већи део ноћи“ (ibid., 417). „Јер Сиријус суши главу и колена и тело је суво од топлоте“ (ibid., 587).

Друго Хесиодово дело *Хераклов ш̄ш̄ит̄*, у извесном степену је имитација *Ахилејевог ш̄ш̄ит̄а*, како је описан у *Илијади* (XVIII 468–817). У овом делу, такође, Хесиод два пута помиње сјајну звезду Сиријус: „Њихове душе силазе у Хад да би биле прекривене земљом, док су њихове кости, када је кожу око њих истопио пламени Сиријус, иструнуле у црној земљи“ (*Shield of Hercules*, 151). И: „Када бучни, плавокрили цврчак, седећи лети на зеленој грани, почне да пева људима, а његова храна и пиће је мека роса, и током целог дана,

почевши у зору, пушта свој глас по најстрашнијој топлоти, када Сиријус сагорева тело, почињу да се јављају младице на просу посејаном у лето“ (ibid., 391).

Песник трагичар Есхил (525–456. ВС) у трагедији *Агамемнон* такође помиње пса Сиријуса (стих 967).

Аполоније са Родоса (3. век пре н.е.) пише у делу *Аргонаутика*, великом епу који преобликује у поетску форму митску експедицију Аргонаута из Тесалије у Колхиду на Црном мору. Аполоније такође помиње Сиријус у вези са неподношљивом летњом врућином: „Када минојско острво са неба загреје Сиријус и за дуго време његови становници не могу наћи никакав спас од тога...“ (*Argonautics*, Песма III, стих 517). И касније: „Опет се појавио као Сиријус, који се уздиже на висине са руба Океана“ (Песма III, стих 956).

Теогнис (570–480. пре н.е.), значајни песник елегичар из Мегаре, написао је неколко гозбених песама, изузетних по достојанству и поштовању богова. Чак даје правила за пијење вина, додајући обавештења за период око изласка Сиријуса: „Неразумни су они људи, и глупи, који не пију вина ни када Пасја звезда почиње...“ (Wender, 1984, *Theognis*, 1039–1040).

Ератостен (276–194. пре н.е.) користи реч ’сириос’ као придев, пишући на пример: „Такве звезде астрономи зову сириос због треперавог кретања њихове светлости“.

Грчки епски песник из 5. века Ноно, из египатског града Панополиса, пише у својој *Дионисијака* о пасјим врелинама Сиријуса: „Послао је супротни удар ветра да пресече врелу Сиријусову грозницу“ (*Dionysiaka*, 275).

У византијском периоду, принцеза Ана Комнина у својој *Алексијади Алексијасу* пише: „премда је било лето и Сунце је прошло кроз Рака и било је пред уласком у Лава – сезона у којој, како кажу, излази звезда Пас“ (*Алексијада* I, Књига 3, XII.4).

ОПИС ПОТПУНОГ ПОМРАЧЕЊА СУНЦА У *ОДИСЕЈИ*

У Певању XX *Одисеје* налази се следећи пасаж: „Улаз и цело двориште испуњени су сенима мртвих, које се крећу у мраку. Сунце је нестало са неба и свугде је била слаба видљивост“ (XX 356–357).

Овај пасаж вероватно описује астрономску појаву, и можда је најстарији опис потпуног помрачења Сунца на Западу. Како је то релативно ретка астрономска појава за дато место, и јавља се у просеку једном у 360 година, ако је област ограничена, може се одредити вероватан датум овог помрачења (Varvoglis, 2009).

Мада се помрачења Сунца и Месеца не помињу директно у хомерским текстовима, претходни стихови су мотивисали два астронома, Константина Бајкузиса (Constantino Baikouzis) из Лабораторије за математичку физику на Рокфелеровом универзитету у Њујорку, и Марчела Мањаска (Marcelo Magnasco) са Proyecto Observatorio, Secretaría de Extensión, Observatorio Astronómico de La Plata, да покушају да тачно одреде датум када се Одисеј вратио на Итаку. Претпоставили су (2008) да Хомер у *Одисеји* XX 356–357 говори о потпуном помрачењу Сунца које се догодило на дан истребљења Пенелопиних просаца.

Наговештај предвидљивој природи оваквог догађаја је дат: Пророчанство Теоклимена је упозорило просце да ће: „Сунце бити избрисано са неба, и несрећна тама ће испунити свет када се домаћин врати и крв ће бити нађена у њиховим тањирима“ (*Од.* XX 350–355).

Ово навођење Бајкузис и Мањаско су упоређивали са другим помињањима древних помрачења Сунца у старим текстовима и нашли су извесне сличности. У хомерским текстовима, постоје још четири астрономске ознаке у вези са Одисејевим повратком на Итаку.

Прва је Месечева фаза; Хомер помиње више пута да је било време младог месеца, тако да је први услов за потпуно помрачење Сунца, према Бајкузису и Мањаску (2008) задовољен.

Друга се односи на Венеру, која је шест дана пре покоља просаца била видљива високо на небу: „Како је изронила блистава звезда, која долази да прва најави светло Зоре рођене из ноћи, брод се пенећи од среће приближавао острву“ (*Од.* xiii 98–100).

Трећа ознака је о звездама и сазвежђима, које је Одисеј видео када је напустио Калипсино острво, 29 дана пре разматраног догађаја: после заласка Сунца виделе су се Плејаде и сазвежђе Boötes.

Четврта се односи на бога Хермеса (Меркур) који је „стигао“ на острво Огигију 34 дана пре помрачења. Према Бајкузису и Мањаску (2008) то се односи на планету Меркур, која је била у западној елонгацији када се види на истоку пре свитања а „стигла“ је у тренутку свог хелијактичког изласка, односно када је први пут постала видљива, што се догодило 13. марта 1178. године пре н.е. Када је у западној елонгацији, Меркур се види ниско на небу пре изласка Сунца и има ретроградно кретање близу источног руба своје привидне путање, што се дешава једном сваких 116 дана.

Харис Варвоглис (2009), професор астрономије на Универзитету у Солуну, примећује да, ако претпоставимо да се последњи пасаж односи на планету Меркур, то се заједно са три остале астрономске ознаке поклапа једном у 2000 година. Пошто је, на основу археолошких ископавања Троје, познато да је разорена око 1190.

пре н.е., јасно је да, ако се у деценијама пре или после ове године догодила таква астрономска коинциденција, то би била независна потврда године разарања Троје (Varvoglis 2009, стр. 3).

Бајкузис и Мањаско, знајући вероватну годину разарања Троје и комбинујући поменуте астрономске информације које даје Хомер, размотрили су 1684 млада месеца између 1250. и 1125. пре н.е. и, користећи планетаријумски софтвер, истражили су астрономску прошлост области Јонског мора. Открили су да се потпуно помрачење догодило 1178. пре н.е. и да је било видљиво са Итаке. После прецизнијих прорачуна добили су да би по Јулијанском календару дан истребљена просаца био 16. април 1178. пре н.е. Ако је то тачно, и ако су Одисејева лутања трајала заиста десет година, како саопштава Хомер, освајање и разарање Троје догодило се 1188. пре н.е.

Бајкузис и Мањаско кажу да њихово истраживање не може без сваке сумње потврдити време Одисејевог повратка на Итаку, али свакако показује да је Хомер знао за извесне астрономске појаве које су се догодиле вековима пре његовог доба. Ако су у праву и ако је Хомер стварно „везао“ овај датум за астрономски догађај који се може проверити, онда то може помоћи историчарима да са великом прецизношћу одреде време пада Троје.

Могући контрааргумент овом ставу је да би Хомеру, који је живео у 8. веку пре н.е., било тешко да опише астрономску појаву која се догодила пре више од четири столећа. Такође, мада изгледа да речи Теоклимена описују помрачење Сунца, песник вероватно жели да дâ општу слику, везујући га за мрачну судбину Пенелопиних просаца. Или је можда Хомер спевао овај пасаж на основу помрачења које је сам доживео, и повезао то са општом ситуацијом у вези са масовним убиством. Ц. Р. Минкел пише у часопису *Scientific American*: „Истраживачи кажу да се позивањем на планете и сазвежђа у *Одисеји*, описује помрачење Сунца које се догодило 1178. пре н.е., скоро три века пре него што се сматра да је Хомер саздао причу. Ако је то тачно, налаз би указивао да је древни песник изненађујуће детаљно познавао астрономију... Грчки учени људи Плутарх и Хераклит истичу идеју да је Теоклименов говор поетски опис помрачења. Они наводе помињања у причи да је дан пророчанства био млад месец, што би било тачно за једно помрачење. У двадесетим, истраживачи су спекулисали да је Хомер могао имати на уму стварно помрачење, после прорачуна да је потпуно помрачење (када Месец потпуно заклања Сунце) било видљиво 16. априла 1178. пре н.е. изнад Јонских острва, где се догађаји из Хомерове поеме смештају. Ипак, идеја није заживела, пошто су се први грчки астрономски записи појавили вековима после тога“ (Minkel 2008).

Напомињемо да се неодређено помињање „неких истраживача“ из двадесетих година у горњем пасажу у ствари односи на Шоха (Schoch, 1926a, b, c), који је први одредио 16. април 1178. пре н.е. као датум потпуног помрачења Сунца, повезаног са Теоклименовим речима, као и на Нојгебауера (Neugebauer, 1929).

ЗАКЉУЧЦИ

Хомеров козмолошки модел, који бележи погледе његовог времена, или можда чак и старије, преживео је у Јонији вековима после његове смрти.

Стварајући највероватније у 8. веку пре н.е., Хомер представља Земљу као диск са свих страна окружен воденим Океаном. Звездано небо је чврста купола која се мора придржавати да не би пала, док испод Земље постоји подземни свет Хад, који је исто толико далеко од Земље као и небо.

У Хомеровим еповима не помињу се све планете познате у антици, али постоји убедљива чињеница да су њихове особине и повезаност са променом изгледа неба са проласком времена биле широко познате после великог броја емпиријских посматрања.

Може се рећи, као закључак, да хомерски извори показују да су поједина сазвежђа и небеске појаве били познати старим Грцима тога времена. Известан број звезда је био именован и биле су тако познате да су коришћене за поређења у односу на богове и људе. Занимљива је чињеница да постоје звезде и сазвежђа које Хомер помиње под потпуно истим именима као што су данашња.

У *Илијади*, први пут се нека звезда помиње у Певању 5 (5), где је Сиријус представљен као јесења звезда; изгледа природно да је прва поменута звезда најсјајнија на ноћном небу. Богатији астрономски садржај је у опису Ахилејевог штита (XVIII 478–488). Хомер каже да су на њему били насликани Орион, Хијаде, Плејаде и Медвед или Кола, „која се окрећу увек на истом месту, гледајући на Орион“ и никада не додирујући Океан. То је изгледа јасна назнака да је ово сазвежђе циркумполарно и увек видљиво са географских ширина где се епска прича одиграва. То Медведа чини погодном, лако видљивом помоћи за оријентацију, тако да би његово укључивање у популарну поему било практично и корисно за заједницу. Када идемо према крају *Илијаде*, Хомер опет помиње Сиријус, називајући га Орионов пас (XXII 29).

У *Одисеји* се помињу циркумполарне звезде и уобичајена сазвежђа (V 279–287); овога пута, додато је и Βοώτης.

Тако Хомер помиње укупно три сазвежђа (циркумполарно Ursa Major, Орион и Boötes), два отворена звездана јата тада позната као сазвежђа (Плејаде и Хијаде), индиректно и најсјајнију звезду Сиријус (као јесењу звезду, Орионовог пса и „лошу звезду“ која људима доноси пасје врућине) и планету Венеру као звезду са старим грчким именима за Вечерњу и Јутарњу звезду.

Математичар Константин Мавроматис (Konstantinos Mavrommatis, 2000) претпоставља да је „звезда“ која се без имена помиње у *Одисеји* („Јер му је казала да увек ту звезду држи са леве стране док плови“, (*Од.*, 276) вероватно поларна звезда тога доба. Астроном Харитон Томбулидис (Chariton Tomboulidis, 2008) помиње да се у *Илијади* IV богиња Атина пореди са „блештавом“ звездом: „Са врхова Олимпа она је јурнула као звезда коју су Хроновићи бацили људима као знак... ...сјајна звезда и безбројни блескови што су бачени“ (IV 75–78).

Вероватно Хомер овде алудира на падајућу звезду или метеор; такве „звезде“ требало би много чешће да се виде на веома тамном небу старе Грчке.

У *Одисеји* такође се веома јасно помињу солстицији (xv 403–404) и један вероватни опис треперења звезда (xii 318).

Коначно, мада помрачења Сунца и Месеца нису експлицитно помињана у хомерским еповима, било је сугерисано (Baikouzis и Magnasco, 2008) да у *Одисеји* (XX 356–357) Хомер алудира на потпуно помрачење Сунца, одакле се чак може извући датум Одисејевог повратка на Итаку. Ту треба бити опрезан да се не би помешале поетичке метафоре са стварним астрономским догађајем, пошто је Хомер живео четири века после помрачења 16. априла 1178. пре н.е.

Чињеница је да постоји само један случај да се користе звезде или сазвежђа за оријентацију у хомерским текстовима (*Одисеја*, 271–277). Задатак да се астрономија доведе до практичних примена предузео је Хесиод, пола столећа касније, својим делом *Послови и дани*, које је пружило грчком народу први календар земљорадничких послова, водич за сезонске активности заснован на хелијактичком изласку или заласку различитих звезда, сазвежђа или јата Плејада.

Хомерску астрономску књижевну традицију следило је неколико старих грчких аутора, као што је Хесиод са својим делима *Послови и дани* и *Хераклов ш̄ш̄ит̄*, песник трагичар Есхил у трагедији *Аг̄амемнон*, Аполоније са Родоса у *Арг̄онаут̄ици*, Ератостен из Кирене, Ноно и чак византијска принцеза Ана Комнина у *Алексијади*.

Сва ова навођења указују да бар од древне Грчке, почевши са *Орфичким химнама* и Хомеровим еповима па до наших дана, неке звезде и сазвежђа носе потпуно иста имена.

ЛИТЕРАТУРА

Aeschylus, 2000, *Agamemnon*. Daedalus-Zacharopoulos Publications, Athens [in Greek].

Allen, R. H., 1963, *Star Names – Their Lore and Meaning*, Constable & Co., London.

Apollonius of Rhodes, 1988, *Argonautics*. Kardamitsa Publications, Athens [in Greek].

Aristotle, 1952. *Meteorologica*. Heinemann, London (The Loeb Classical Library; English Translation by H. D. P. Lee).

Baikouzis, C. and Magnasco, M. O., July 1, 2008, "Is an eclipse described in the Odyssey?", *Proceedings of the National Academy of Sciences*, 105: 8823.

Bible: *The New International version Bible*, 1984, Zondervan Bible Publishers, Grand Rapids, Michigan, U.S.A.

Comnene, Anna, 2005, *Alexias*, Books I to XV. Agra Publications, Athens [in Greek].

Cotsakis, D., 1976, *The Pioneers of Science and the Creation of the World*. Zoe Publications, Athens [in Greek].

Dicks, D. R., 1970, *Early Greek Astronomy to Aristotle*. Thames & Hudson, United Kingdom.

Flanders, T., 2007, "Did the Greeks, in Homer's time, name a constellation or asterism after Achilles?", *Sky and Telescope*, Vol. 114, No. 8, p. 82.

Gendler, J. R., 1984, "Jupiter-Saturn Conjunctions in Homer's Odyssey and Iliad", *Bull. American Astron. Soc.*, Vol. 16, p. 49.

Genuth, S. S., 1992, "Astronomical imagery in a passage of Homer", *J. Hist. Astron.*, Vol. 23, p. 293.

Eratosthenes, 1997, *Catasterismoi*. Trans. By Theony Contos in *Star Myths of the Greeks and Romans: A Sourcebook*. Phanes Press, Grand Rapids.

Hesiod, 1914, *The Homeric Hymns and Homerica (Theogony)*. Heinemann, London (The Loeb Classical Library; English translation by Hugh G. Evelyn-White, reprinted 1954).

Hesiod and Apollonius of Rhodes, 2005, *Theogony, Works and Days, Shield of Hercules, Argonautics*. Zetros Publications, Thessaloniki [in Greek].

Homer, 1924, *The Iliad*. Heinemann, London (The Loeb Classical Library; English translation by A. T. Murray, 1954).

Homer, 1919, *The Odyssey*. Heinemann, London (The Loeb Classical Library; English translation by A. T. Murray, revised by G. E. Dimock, reprinted 1995).

Kirk, G. S., Raven, J. E., and Schofield, M., 1995, *The Presocratic Philosophers*. A critical History with a selection of Texts, Cambridge University Press (First printed 1883)

Konstantopoulos, P., 1998, *Homeric Greeks*, 2 vols. Metron Publications. Athens [in Greek].
Lorimer, H. L., 1951, "Stars and Constellations in Homer and Hesiod", *The Annual of the British School in Athens*, vol. 46, pp. 86–101.
Lovi, G., 1989, "Stargazing with Homer", *Sky and Telescope*, Vol. 77, No. 1, January, p. 57.
Mavrommatis, K., April 2000, *Ouranos* No. 35, Volos, p. 114 [in Greek].
Minkel J. R., June 23, 2008, "Homer's Odyssey Said to Document 3,200 Year-Old Eclipse – Clues in the text hint that the poet knew his astronomy". *Scientific American* (http://www.scientificamerican.com/article.cfm?id=homers-odyssey-may-document-eclipse).
Mireaux, E., 1959, *Daily Life in the Time of Homer*. Transl. Iris Sells, The Macmillan Company, New York.
Nonnus, *Dionysiaca*, (s.d.), Transl. E. Darviri, Ancient Authors Series, Georgiades-Elliniki Agoge Publications, Athens, [in Greek].
Neugebauer, P. V., 1929, *Astronomische Chronologie*, Verlag W. de Gruyter, Berlin.
Orphic Hymns, 2006, Ideotheatro Publications, Athens [in Greek].
Petrides, S., 2002, *The Orphic Hymns – Astronomy in the Age of Ice*, (author's publ.), Athens.
Petrides, S., 2005, *Orpheus' Argonautica – A dissertation on seafaring of the late Pleistocene*, (author's publ.), Athens.
Schoch, C., 1926a, "The eclipse of Odysseus", *The Observatory*, 49, p. 19.
Schoch, C., 1926b, *Die Sterne*, 6, p. 88.
Schoch, C., 1926c, Die sechs griechischen Dichter-Finsternisse, Steglitz, Selbstverlag, Berlin.
The Iliad, 1950, Trans. by E. V. Rieu, Penguin Books, New York.
Theochares, P., 12–13 May, 1995, *The pyramids of Argolis and their dating*, 11th Panhellenic Conference, Nafplio [in Greek].
Theodossiou, E., Danezis, E., 1991, *The Stars and their Myths – Introduction to Uranography*, Diavlos Publications, Athens [in Greek].
Theognis, 1997, *Lyrical poems III*. Epikairotita Publications, Athens [in Greek].
Tomboulidis, C., April 2008, *Ouranos* No. 67, Volos, p. 132 [in Greek].
Trypanis, K. A., 1975, *The Homeric epics*. Prometheus-Hestia Publ., Athens [in Greek].
Varvoglis, H., Sunday September 6, 2009, "Pharmacology and Astronomy in Odyssey". *BemaScience*, History, p. 3 [in Greek].
Walker, G. J., 1872, "Astronomical allusions in Homer, Dante, Shakespeare and Milton", *The Astronomical Register,* No. 118, 229.
Wender, D., 1984, *Hesiod and Theognis*, Penguin Books, New York.
Wood, F. & Wood, K., 1999, *Homer's Secret Iliad: The Epic of the Night Skies Decoded*. London: John Murray, Albemarle Street, p. 199.

Efstratios Th. Theodossiou, Vassilios N. Manimanis,
Petros Mantarakis, Milan S. Dimitrijević

ASTRONOMY AND CONSTELLATIONS IN HOMERIC *ILIAD* AND *ODYSSEY*

Summary

The *Iliad* and the *Odyssey*, in addition to their supreme status as cornerstones of world literature, they are a rich source of information about the scientific and technological knowledge of ancient Greeks in both pre-Homeric and Homeric times. The two Homeric epic poems, dated in the 8th century BC, include, *inter alia*, a wealth of astronomical elements, informing about the Earth, the Sky, the stars and constellations such as Ursa Major, Boötes, Orion, Sirius, the Pleiades and the Hyades. They also offer a more erudite image of Homer, which reflects the cosmological views of his period. The model of the Universe that is presented is continuous and has three levels: the lower level corresponds to the underworld, the middle one to the Earth and the upper one to the sky. The cosmological model and astronomical elements presented in *Iliad* and *Odissey* are considered in this work.

Key words: History of Astronomy, Homer, Antique cosmology

ЗБОРНИК

МАТИЦЕ СРПСКЕ
ЗА КЛАСИЧНЕ СТУДИЈЕ

JOURNAL OF CLASSICAL STUDIES
MATICA SRPSKA

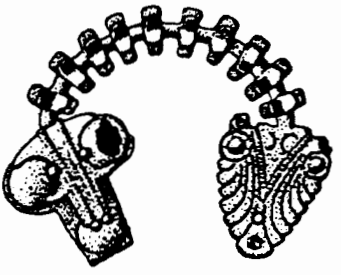

10

НОВИ САД
2008

UDC 1(38):113

Ефстратиос Теодосију, Петрос Мандаракис,
Милан С. Димитријевић, Василиос Н. Маниманис,
Емануел Данезис

ОД АНАКСИМАНДРОВОГ „БЕСКОНАЧНО" (APEIRON) У СТАРОЈ ГРЧКОЈ ДО ТЕОРИЈЕ О БЕСКОНАЧНОСТИ УНИВЕРЗУМА У МОДЕРНОЈ КОЗМОЛОГИЈИ

АПСТРАКТ: Предузето је истраживање старих грчких текстова да би се показало како је Анаксимандар увео ἄπειρον (безгранично) као почетак свега (први принцип). Према његовој теорији, ἄπειρον је недефинисан и увек покретан. Он рађа супротности „топло" и „хладно", као и „влажно" и „суво" и њихову вечну борбу. Резултат овог бесконачног процеса је мноштво постојећих ствари и бесконачан број универзума.

Козмолошки аспект Анаксимандрове теорије има необичну лепоту; небројени светови се рађају из *апеирона* и нестају у њему. Дакле, *апеирон* је повезан са вечним козмолошким процесом — током времена.

Козмолошки проблем огромности Универзума или њихов бесконачан број је елементарни филозофски проблем, док је теорија Великог праска, са концептом простор-времена, полазна тачка за описивање наше Васионе.

КЉУЧНЕ РЕЧИ: Пресократовска филозофија, Анаксимандар, апеирон, бесконачност, козмологија

1. УВОД

Пресократовска филозофија настала је у грчким градовима Јоније крајем 7. века пре наше ере. У то време, ту су се филозофски погледи брзо развијали, као нигде на другом месту у Грчкој. Веровање да богови контролишу свет, уплићући се по-

времено у животе људи, није могло више да да задовољавајуће одговоре.

Милетска школа (Талес, Анаксимандар, Анаксимен) спојила је античку митологију са рационалним мишљењем, тражећи које силе делују у природи. Пресократовски философи истраживали су главни узрок настанка Космоса и силе на којима је заснован Универзум.

При томе, они су се усредсредили углавном на природни свет, проучавајући реалност која их окружује. Јонски философи, који су живели и размишљали у Малој Азији, пажљиво су посматрали природне појаве и њихова улога у истраживању истинитости митова била им је пресудна. Трудили су се да изведу све могуће закључке на основу посматрања природе, користећи основну логику. Проблем првобитне супстанце (ἀρχή) био је један од главних за разматрање питања структуре нашег света и његовог настанка. Ови философи вероватно су покушавали, на основу неке теорије, да објасне „зашто" у некој појави више него „како".

У сваком случају, у то време је учињен преокрет, и прилично неочекивани помак, од мистицизма и религиозности на разматрање узрочности. То је била промена која је показивала узвишеност античке грчке философије и имала огроман утицај на цео свет.

Свакако, нећемо занемарити чињеницу да су већина грчких пресократовских философа били уствари природњаци, пошто су покушавали да дефинишу ἀρχή, првобитну супстанцу од које је све постало.

Талес из Милета (624—546. пре н. е.), отац античке грчке философије, веровао је да је вода основа свега и примарни принцип Универзума. Њен значај у животу и природи био је вероватно главни разлог који је Талеса навео на овакав закључак. Према Диогену Лаертију: „*Његово учење било је да је вода универзална првобитна супстанца и да је свет продуховљен и пун божанстава*" (Diog. Laert. 1, 27). Анаксимандар (610—540. пре н. е.), Талесов ученик, доделио је ову особину појму ἄπειρον (бесконачност): „*Поставио је као свој принцип, један елемент који је неограничен без одређености*" (Diog. Laert II, 1, 1). Разматрајући античке грчке философске погледе, који материју сматрају једнаком води, ваздуху или ватри, наводимо да је Анаксимандров израз ἄπειον изведен од грчког α- и именице πέρας (тачније πεῖρασ, граница, крај), са значењем да нешто нема почетка ни краја у времену ни границе у простору.

Овај појам је пресудан у образлагању како су се основе космологије и јонске физике одвојиле од митологије, нешто што сматрамо првом револуцијом у науци. У то време су грчки филозофи покушавали да одговоре на два основна питања о којима су дубоко размишљали: како је настао Космос и каквог је облика. Овај напор их је учинио оцима филозофског мишљења и оснивачима науке. Пресократовци су спојили античку грчку митологију са рационалним мишљењем и тражили силе које чине природу, као и главни узрок стварања света.

Уз то, идеја о мноштву светова, изведена из напора да се схвати Универзум, доноси нама, као астрономима, више питања за даља истраживања, пошто Физика и Астрономија нису и не треба да буду далеко од Филозофије.

Питања постављена у антици, као што је оно о постојању мноштва Светова, о коначности или бесконачности Универзума, као и теорија Великог праска, између осталог, још једном покрећу разматрање основних егзистенцијалних филозофских проблема. То су питања на која још немамо потпуни одговор, пошто је коначна судбина Универзума неизвесна.

2. АНАКСИМАНДРОВ Ἄπειρον

Анаксимандар (610—540. пре н. е.) је живео када и Талес. Био му је ученик, а после учитељеве смрти преузео је његову школу. Многи учени људи сматрали су да му је раван, и да је први са Емпедоклеом из Акраганта (500—428. или 483—430. пре н. е.), увео експериментално истраживање физичких појава. У ствари био је први који је дао научни поглед на свет, ослобођен митологије (Themist. Or. 36, стр. 317 или Vorsokratiker 2, 7, Diels Hermann, 1996). Увео је појам о Универзуму, бесконачном у времену и простору.

Анаксимандар је веровао у постојање природног закона, неку врсту космичке правде, која четири основна елемента држи у равнотежи. Ови елементи су у бесконачној борби због различите природе и неједнаке густине. За Анаксимандра природна равнотежа треба вечно да се одржава, спречавајући да један елемент надвлада друге. Ово је водило одбацивању Талесовог учења о води као првобитном принципу Космоса, пошто то противречи идеји природне правде и равнотеже. Ако би један елемент превладао и одбацио друге, Свет не само да би био друкчији него би се кретао ка уништењу.

Важан аргумент Анаксимандрове теорије је филозофска идеја о вечној и непроменљивој космичкој основи из које све настаје и у коју се све враћа. Она постоји изван четири примарна елемента и идентична је са бесконачним (ἄπειρον). У његовој раној космологији то је самоодређујућа, непроменљива, бесмртна супстанца, нешто без облика и особина, без граница у времену и простору и без одређених својстава. ''Απειρον је бескрајно и неуништиво и то је разлог зашто светови настају из њега и ту се враћају.

Анаксимандар је, пак, веровао, да се ἄπειρον претвара у четири елемента који, делујући између себе, воде настанку света. Они се пак распадају и враћају назад у њега. Заснивао је своје филозофске погледе на дефиницији речи ἀρχή, која има двоструко значење: почетак, али и владавина (од грчког глагола ἄρχω).

Он такође помиње ἀρχή (почетак) који није сличан било ком другом ἀρχή или неком елементу Космоса, то јест ἀρχή „који обухвата све и управља свиме". Према Аристотелу:

> *„Тако се 'безграничнo' не може извести из било ког другог принципа, него се само сматра као принцип свега другог, обухватајући и управљајући свиме. Ово 'безграничнo' би онда било само божанство, 'бесмртно и неуништиво', како Анаксимандар и већина природњака изјављују да јесте"* (Arist. *Phys.*, III. iv. 203b 11).

Анаксимандар и његов учитељ Талес потпуно су одбацили антропоморфни чин сексуалне репродукције међу божанским бићима, који је био у основи свих митолошких космогонија тога времена. Анаксимандар је претпостављао да је „материца Космоса", у основи ἄπειρον, способна да подари живот. У ствари, живот почиње уз помоћ плодоносног семена постављеног унутар космолошког јајета. Семе оплођује своју супротност, одвојену од **апеирона**, која расте у огњеној сфери која садржи хладну масу. У почетној фази стварања, две супротности, *топло* које укључује *суво*, и *хладно* које укључује *влажно*, одвојене су. Услед деловања *топлог*, *суво* и *влажно* се раздвајају и стварају копно и море. Последица деловања топлог на хладно је влага која доноси живот. Према Аетију (Aetius), Анаксимандар је сматрао да је море оно што је остало од примарне влаге [Aet. III, 16, I (D, 381)].

Изгледа да је Анаксимандар користио **апеирон** са још апстрактнијим значењем, као математички појам за бесконачно. Могуће је да је сматрао да је то огромна материјална маса или примарна маглина. Могао га је такође користити за природну

силу или енергију, неограничену у времену и вероватно без унутрашње структуре. Многи се слажу да „безгранично" долази од *топлог* и *хладног*, који су касније раздвојени, при чему прво образује спољашњу огњену сферу, односно πῦρ (ватра), а затим ваздух, воду и земљу унутар Космоса. Ови елементи се спајају и потом раздвајају стварајући море и копно, док су цепањем огњене сфере и захватањем πῦρ-а у прстенове, настали Сунце, Месец и звезде. На крају, деловањем Сунчеве топлоте и путем струјања изазваних кретањима небеских тела, вода испарава стварајући ваздух.

Према Псеудо-Плутарху:

> *„Анаксимандар је рекао да је једино 'Бесконачно' одговорно за настанак и нестанак Универзума. Анаксимандар изјављује да су различита небеса излучена из овог Бесконачног, као што су уопште и сви светови којих је бесконачно. Рекао је да се нестанак и (много раније) стварање догађа тако што се циклус понавља из бесконачне прошлости"* (*Stromata*, fr. 172. 2).

Што се тиче Анаксимандровог **апеирона**, Диоген Лаертије бележи:

> *„Анаксимандар, син Праксијадов, био је пореклом из Милета. Установио је, као принцип, елемент који је безграничан, не одређујући га као ваздух или воду или нешто друго. Сматрао је да делови трпе промену, али је целина непроменљива"* (D. L. II, 1, 1).

Универзум је, према Анаксимандру, бесконачан, а Светови безбројни. Од бесмртног и неуништивог **апеирона** његовим вечним кретањем настају „супротности" које бивају ношене у њему. То значи да је Анаксимандар сматрао да супротни елементи, ватра и вода, не могу да буду у хармонији него су у вечној борби.

Нажалост, протекле векове је преживео само мали одломак Анаксимандрове чувене књиге *О природи*. Симпликије (у Аристотеловој књизи *Physic*. 23—24, 1882) од Теофраста преноси само уопштено тумачење појма ἄπειρον, са парафразом о стварању и пропасти Светова и тачном изјавом, која описује однос између козмолошких фактора под окриљем осветничке правде:

> *„Анаксимандар је рекао да је ἄπειρον почетак свих ствари; сва небеса и светови долазе из њега; рођење долази из њега и ту се све враћа, када је једном уништено. На тај начин дата је правда и освета за неправду, коју једни другима наносе током времена"* [Simplic. *Phys*. 24, 13 (Z. 3—8 Theophrastus *Phys. Opin*. Fr. 2 Dox. 476)].

G. S. Kirk, J. E. Raven и M. Schofield (1995) су мишљења да је Анаксимандар веровао у низ појединачних светова, који се стварају из Бесконачности и враћају у њу. То води закључку да је вероватно имао слику *периодичног* Универзума.

Аристотел (384—322. пре н. е.), расправљајући о бесконачном и начину на који је Анаксимандар користио овај појам каже:

> *„Све ствари су почетак или имају почетак, односно порекло; ако је то тако, онда ће такође бити и крај; бесмртно је неуништиво, како Анаксимандар и многи други философи кажу"* (Arist. *Phys.* III. iv. 203b 6).

У своме делу *Физика* (*Physikes Acroaseos*), Аристотел разматра Анаксимандрово „бесконачно". Веома је заинтересован за апсолутни почетак, који има двојну мисију, да буде узрок материје и кретања (W. Jaeger, 1964). Напор да се споји *божанско* са кретањем водили су Анаксимандровом **апеирону** и *бесмртном*, како је написано у његовим фрагментима (Arist. *Phys.* III. iv. 203b 10—15).

Како су рекли Аетије [*De Plac.* I 3, 3 (D. 227)] и Симпликије (*Phys.* 24, 13), Анаксимандар је био мишљења да је **апеирон** извор многих светова.

Закључујемо да је Анаксимандар сматрао да су све ствари настале из **апеирона** и, као што су писали Аетије и Симпликије, хиљаде светова је настало и нестало, као што ће и наш једнога дана. Анаксимандар је, као и Демокрит, претпостављао да у Универзуму постоји бесконачан број козмолошких система, поглед који је упадљиво близак схватањима модерне астрофизике. Могао је да има различите дефиниције за појмове „Козмос" и „Универзум" у свом козмолошком прилазу. Земљу је стављао у центар нашег Света, али није био мишљења да је она у центру Универзума, који садржи милионе различитих Светова.

Према другим студијама, Анаксимандар је стављао Земљу у центар сферичног Универзума, док су остале планете обилазиле око ње. *„Земља, која је сферичног облика, лежи у средини, заузимајући место центра"* (D. L. II 1, 131).

Такође, према другим студијама, каснији погледи Анаксимандрови одражавају јасно његову веру у геоцентрично уређење Козмоса, унутар сферичног Универзума који описује. То објашњава зашто Земља стоји у ваздуху, у центру огромне сфере. Земља је у равнотежи у средини Универзума, због тога што је подједнако удаљена од крајева сфере на чијој су унутрашњој страни учвршћене звезде.

3. ДРУГИ ФИЛОСОФИ О БЕСКОНАЧНОСТИ

Према философском и космолошком приступу, бесконачност се односи на Универзум и природу у целини, а још одређеније, на материју и њено кретање. *Бесконачно* схватамо као супротност *коначног*. Ова два философска појма су дијалектички повезана и изражавају супротна својства материје, као философског објекта који постоји у простору и времену и бесконачно се креће. Материју схватамо као нешто коначно, зато што су њени различити облици (специфични објекти, функције и квалитети) такође коначни у простору и времену. Са друге стране, сматрамо да материја има особину бесконачности, услед непрекидног кретања, неисцрпивог, вечног процеса трансформације у бескрајну, квалитативну и квантитативну разноликост објеката, облика и својстава. То је, са једне стране, видљиви Универзум који нас окружује, а, са друге стране, несазнајни облици „тамне" материје од којих су неки можда унутар анти-паралелног Универзума.

Погледе сличне Анаксимандровим о бесконачном космичком *бићу* или о бесконачном броју универзума имали су и други пресократовски философи као Хераклит, Мелис, оци атомистичке теорије Леукип и Демокрит, Питагорејци, затим Платон, Аристотел, Неоплатоничари и други.

Изгледа да је идеја **апеирона** један од најстаријих и најкоришћенијих појмова пресократовске философије.

Према Питагори, свет је без граница. Демокрит је слично користио реч **апеирон** за празнину простора и *не-биће*.

Епикурејци су такође прихватали бесконачност броја светова, а Елеаћани су сматрали да је основни садржај Универзума бесконачан, поглед који је прихватио и Платон. Стоичари су, напротив, веровали да је само простор бесконачан, а да је наш Свет коначан. Неоплатоничари су сматрали да је једино Бог бесконачан, а да је Свет — креација бесконачног Бога, коначан у времену.

Осим тога, Анаксимандар је веома утицао на космолошке системе Анаксимена из Милета (585—525. пре н. е.) и Диогена из Аполоније (510—400. пре н. е.). Наиме, први је био Анаксимандров ученик, који је наставио његов рад и, мада је као основни принцип узео ваздух ἀήρ, ставио је ἄπειρον као супротност одређеним стварима које су од њега настале.

> *„Анаксимен каже да је порекло свих ствари ваздух; и да су оне настале неком врстом кондензације, супротном од разређивања. Промена је, пак, одувек постојала"* (Псеудо-Плутарх, *Stromata*. fr. 179. 3).

Додатно, према Симпликију:

> *„Анаксимен из Милета, син Еуристратов, који је био садруг Анаксимандров, говорио је, попут њега, да је супстанца која се налази у основици једна и бесконачна. Ипак, није говорио да је она неодређена, него одређена и то, како је рекао, ваздух. Он се разликује у разним супстанцама сходно његовом разређивању или кондензовању"* (*Phys.* стр. 24, 26).

Како је напоменуо Диоген Лаертије:

> *„Диоген из Аполоније, син Аполотемидов, био је философ природњак и веома славан човек. Антистен га назива Анаксименовим учеником; али је живео у време Анаксагоре... Диогеново учење било је следеће. Ваздух је универзални елемент. Постоје светови чији је број неограничен и безграничан празан простор"* (D. L. IX 9, 57).

Диоген је сматрао да је Универзум бесконачан и да садржи безбројне светове. Они су коначни, а крећу се унутар овог бесконачног простора. Веровао је да је наш свет најбољи од свих могућих, зато што су појаве, које доноси, уређене на посебан начин. Да би се одржао овај поредак, треба да је присутна духовна сила, наиме Νόησις (разумевање, садржајност); она доводи ствари у ред и надгледа очување савршенства. Ово основно веровање важило је за *ваздух*, а истовремено је називано *божанство*, које представља Анаксимандров и Анаксагорин духовни *Ум*, Νοῦς, који је створио свет.

Питагорејци и Платон сматрали су да је *бесконачно*, простран и безобличан почетак, који, заједно са својом супротношћу, *коначним* (πέρας), представља основни део *онога што јесте* (τὸ ὄν); то је пасивни почетак света који даје материју, потребну за свако стварање. На крају, *бесконачно* је фундаментални део питагорејског мишљења (*бесконачно* и *коначно* у њиховој познатој листи супротности) и управља бројем као почетком времена. Питагорејци су сматрали да је свет спој супротности и да је створен из нечег бесконачног, супротности појму коначног, а сматрали су да у Универзуму постоји и музичка хармонија.

Они су третирали Један као једнако јединици, савршен и примаран број, који је суштина целокупног стварања и истовремено стваралац материјалне јединице ствари, свакако јединствени принцип свих других бића (Arist. *Metaphys.* I, 5). Један је јединствен, све, и вечан. Ипак, Један, идентичан са *коначним*, појам је супротстављен *бесконачном*. Са гледишта Један-Све, то води контрадикцији између суштине и појаве. Према Аристотелу, Питагорејци су сматрали да добро настаје из

коначног, а зло из *бесконачног*: „*Јер 'зло' је облик неограниченог, као у старој питагорејској уобразиљи, а 'добро', ограниченог*" (*Никомахова Етика*, II. vi. 14).

Платон (427—347. пре н. е.) је класификовао *биће* унутар структуре Света, на следећи начин: а) *бесконачно*, б) *коначно*, с) мешавина *бесконачног* и *коначног* и в) *узрок* ове мешавине. Он сматра *бесконачно* за нешто без украса и одређености.

Учења Плотина су реакција на Аристотелова и стоичка учења о материји. Као извор узима Платоновог *Филеба* „*Како је бесконачан број ствари које улазе у биће ове јединице*" (15b), „*Они стављају бесконачно одмах после јединице*" (17a,) и (23c—25b) где помиње *бесконачно*.

Демокрит (460—370. пре н. е.), изгледа, има конкретнији, више материјалистички, поглед, што се тиче *бесконачног*, зато што говори о бесконачном броју атома и према томе бића и појава. Постоји ипак аргумент да Демокрит сматра празнину за *бесконачно*:

> „*Његова мишљења су ова. Први принципи универзума су атоми и празан простор... Светови су неограничени; настају и пропадају. Ништа не може да настане из онога што није нити да нестане у оно што није. Надаље, атоми су неограничени у величини и броју, те настају широм целог Универзума у вртлогу, и стварају све сложене ствари — ватра, вода, ваздух, земља; чак и они су конгломерати атома*" (D. L. IX 7, 44).

Што се тиче Леукипових ставова, Диоген Лаертије каже:

> „*Он изјављује да је Све безграничнo, као што је већ рекао; али део Свега је пун, а део празан; (под 'пуним' се подразумева материја, атоми: под 'празним', простор); и те он назива елементима. Од њих настају светови, чији је број неограничен и у њих се распадају*" (D. L. IX 6, 30).

Према Симпликију: „*Леукип и Демокрит кажу да има бесконачно много Светова у бесконачној празнини, који су начињени од бесконачног броја атома*" (Simplic. *De Caelo* 202, 16). Један, од тих безбројних Светова је наш.

Леукип и Демокрит се сматрају оснивачима Атомистичке теорије, теоријског козмолошког система са материјалном јединичном основом, што спада међу највеће научне продоре античке грчке мисли.

Демокрит, желећи да дода свој сопствени поглед на структуру Света, покушао је да у Атомистичку теорију укључи схватања Парменида и Хераклита, односно мишљење да постоји граница, испод које се атоми више не могу делити и остају као непроменљиви ентитети. То је блиско Парменидовом погледу

о стабилности, изван променљивог Света; постојаности, којој се може приближити само наша мисао. Осим тога, Демокрит помиње разноликост комбинација атома. Ове комбинације настају током вечног кретања, усвајајући Хераклитове ставове о свету где се све непрестано креће.

Према Атомистичкој теорији, атоми стварају бесконачан број облика, и због њиховог спиралног кретања спајају се формирајући ватру, ваздух, воду и земљу, односно четири основна елемента. Заиста, два философа су била мишљења да је степен густине објекта сразмеран броју атома који се налазе заједно; ове ствари се вечно крећу у *празнини*. Њихово кретање ствара непрекидно вртложење, које је одговорно за нова спајања атома, од којих је настао Свет и све ствари.

Леукип и Демокрит су сматрали да је Универзум бесконачан и састављен од атома; његови безбројни светови, пуни живота, последица су спајања атома. Вртложним кретањем ових акумулација настају Светови; неки изгледају као наш, а неки су потпуно друкчији.

Хиполит (*Refut.*) I, 13, 2—4, (D. 565, W. 16) пише:

> *„Светова је бесконачан број, а разликују се по облику. На некима од њих нема ни Сунца ни Месеца, код неких је оно веће а други имају више Сунаца и Месеца. Растојања између светова су неједнака, те у овом делу празнине може их бити више, а у другом мање. И једни светови се још развијају, други су достигли свој максимум, а трећи се разграђују, једни се рађају, а други нестају. Светови се разарају када се сударе. Постоје светови без биљака, животиња и воде."*

Према Аристотелу, *бесконачно* постоји само као нешто што је *могуће да буде* (ἐν δυνάμει) а не као нешто што *стварно постоји*. То показује да је он прихватио бесконачно кретање и време, али је одбацио идеју о просторно бесконачном Универзуму.

Платонски појам Бога повезан је са погледом о *бесконачном*, одбацивши негативно значење, а задржавајући само позитивно. Изузетак је Парменидова теорија (рани 5. век пре н. е.), која узима *бесконачно* као почетак свих ствари. Неоплатоничари су такође сматрали да је *бесконачно* везано за Бога. Платонистичко и касније Неоплатонистичко схватање о злу, отпаднутом од Бога, прихватили су хришћански мислиоци. Овакав поглед је коришћен и снажно пројектован у идеалистичку теолошку философију, која дефинише *бесконачно* као производ свести. Материјалистички философски поглед, напротив, посматра *бесконачно* као својство времена и простора, са матема-

тичког и козмолошког гледишта. Такође, дијалектичко-материјалистички концепт *бесконачног* и *коначног* произлази из позитивне стране Хегелове идеје о овом питању. Он је био први који је поменуо дијалектички однос између *коначног* и *бесконачног* (Niarchos, C., 1997, стр. 216).

4. БЕСКОНАЧАН БРОЈ СВЕТОВА У АНТИЧКОЈ ГРЧКОЈ МИСЛИ

Ксенофан из Колофона (565—488. пре н. е.) је сматрао да је Универзум вечан, а да није у почетку створен. Сматрао је само да су поједини светови подвргнути непрестаним променама. Према Диогену, Ксенофан је веровао у постојање бесконачног низа светова:

> *„Ксенофан, пореклом из Колофона, син Дексијев, сматрао је да су четири елемента у основи постојећих ствари, неограничен број светова, који се не преклапају [у времену]"* (D. L. IX 2, 19).

Мелис са Самоса (5. век пре н. е.), Парменидов ученик, мислио је да је Универзум нешто јединствено, бесконачно, испуњено, непокретно и хомогено. Према Диогену Лаертију:

> *„Мелис, син Итагенов, био је родом са Самоса и Парменидов ученик. Сходно његовим погледима, Универзум је безграничан, непроменљив и непокретан, јединствен је, хомоген и испуњен материјом. Не постоји стварно него само привидно кретање"* (D. L. IX 4, 24).

Симпликије (*Phys.* 35, 3) напомиње да је Анаксагора (500—428. пре н. е.) сматрао да постоји бесконачан број светова, мишљење које су такође делили, као што је раније поменуто, Леукип и Демокрит.

Диоген Лаертије је такође представио две Епикурове (341—270. пре н. е.) посланице Херодоту и Питоклу, које сведоче о погледима овог филозофа о мноштву светова. Прва је упућена Херодоту и односи се на филозофију природе:

> *„Опет, збир ствари је бесконачан... Штавише, сума објеката је неограничена, како због мноштва атома тако и због размера празнине. Осим тога, постоји бесконачан број светова, неки као овај, а други различити. Атоми чији је број бесконачан, као што је управо доказано, ношени су све даље у своме кретању. Атоми, од којих свет може да се створи, или да се од њих састоји, нису потрошени на један, или на коначан број светова, сличних или различитих од овог. Сходно томе, ништа не може да спречи бесконачност броја светова".* (D. L. X 44—46).

Друга посланица је намењена Питоклу и односи се на астрономију и метеорологију:

„Свет је заокружени део Универзума, који садржи звезде и Земљу и све друге видљиве објекте, исечак из бесконачног и ограничен [међом која може бити дебела или танка, чије ће растурање донети разарање свему унутар њеј" (D. L. X 88).

Поврх тога, Метродор са Хиоса, Епикуров учитељ, напомиње, према Аетију, да је:

„... апсурдно да један једини клас расте у пољу и само један свет буде у бесконачности. Чињеница да их је бесконачно мноштво, следи из тога да постоји бесконачан број узрока. Да је свет коначан, а узрока његовог стварања бесконачно, такође би било бесконачно много светова, јер где је бесконачан број узрока, бесконачно је и резултата. А узроци су атоми или елементи." (Aet. 15, 4d 292).

Говорећи уопштено, можемо рећи да се појам бесконачног не може осетити, него је производ интелектуалног размишљања комбинованог са имагинацијом.

Постоје два начина како представа бесконачности може да се образује у човековој свести:

а) Емпиријски: сходно томе, потпуно разумевање појма коначности, води настанку појма бесконачности. На тај начин, нема бесконачности као такве, већ је то динамички процес стварања преко непрекидног пораста (бесконачно велико) или смањивања коначности (бесконачно мало).

б) Идеалистички: постојање Бесконачног претходи сваком Стварању и то је појам који се мора схватити као примаран и потпун, а не изведен из других коначних реалности (стварно постојећих).

У модерној филозофији има више предлога у односу на бесконачно. Простор, време и материју, многи филозофи и научници сматрају бесконачним. Често постоји забуна између апсолутне и релативне бесконачности. Прва по дефиницији негира увођење било каквих ограничења у свој садржај, будући основни и потпуни појам и недељива јединица (идеалистичка бесконачност), док је друга представљена само без одређених граница (емпиријска бесконачност). Релативна бесконачност представља могућност преиначења коначности, док се апсолутна бесконачност разматра као потпуно и целовито својство. С апсолутном бесконачношћу стављамо се изван било каквог схватања величине. Дакле, између релативне и апсолутне бес-

коначности постоји пре квалитативна него квантитативна филозофска дистинкција.

5. БЕСКОНАЧНОСТ У МОДЕРНОЈ КОЗМОЛОГИЈИ

Као астрофизичари, сматрамо да је бесконачност Универзума филозофско исходиште. При свему томе, модерна Космологија је такође заснована на филозофским принципима.

Модерни приступ овом онтолошком проблему засновао је Алберт Ајнштајн (1879—1955), који је, развијајући Општу теорију релативности, покушао да да научни одговор на проблем бесконачности или ограничености простора. За овај напор битна је била не-Еуклидска геометрија, коју је развио немачки математичар Г. Риман (1826—1866). Он је увео идеју закривљености простора, наговестивши сферичност Универзума (са позитивном закривљеношћу), што је са једне стране коначно, а са друге бесконачно.

Један од већих проблема модерне космологије је питање да ли је Универзум бесконачан. Да ли је његова бескрајност илузија, настала можда и вишеструким кривљењем путање светлости коначног космоса, тако да уместо једног, видимо више ликова неке галаксије, као да се налазимо између два огледала?

Сагласно Теорији релативности, простор је динамички медијум који, у зависности од масе у њему, може бити закривљен на три различита начина, који се описују геометријама Римана, Еуклида и Лобачевског.

Ајнштајн је у своје једначине увео космолошку константу да би добио стационаран Универзум, који је, мада коначан, неограничен.

Чувени руски математичар А. Фридман (1888—1925) вратио се на изворне Ајнштајнове једначине и предложио 1922. године модел нестационарног Универзума, који се шири и скупља услед гравитационе силе, у коме су време и простор коначни, али просторно неограничени.

Едвин Хабл (1889—1953), чувени амерички астроном, пружио је 1929. године доказе да се Универзум шири, посматрајући међусобно удаљавање галаксија.

Тако су неки погледи пресократовских филозофа нашли своје место међу идејама модерне Астрофизике.

Хуго Еверет III, студент професора Џона Арчибалда Вилера са Универзитета у Принстону, био је један од првих који је,

1950. године, применио законе Квантне механике на Космологију. Претпоставио је универзалну таласну функцију и проучавао ефекте међусобног уплива различитих области Универзума. Био је изненађен открићем да овај ефекат може да објасни процес стварања његових копија. Оне су резултат групе могућих последица овог утицаја. Та теорија је позната као „Објашњење многих светова мултиверзума или разгранати Универзум" (1957). Према њој, посматрач није умешан у процедуру квантног мерења, што се подразумева у пробабилистичком објашњењу копенхашке Ψ таласне функције. Теоријска анализа разгранатог Универзума може да да толико независних копија колико је могућих резултата. М. Гел-Ман и Џ. Б. Хертл проучавали су прилаз Џ. Еверета III и предложили измењену верзију његове теорије „Несагласне историје" (Decoherent Histories), према којој Универзум може да еволуира на много начина, од којих сваки има специфичну могућност. Ова теорија указује да је за наш Универзум већ изабрана једна од њих. Према другим теоријама, постоји могућност да он еволуира у много праваца, од којих ми спознајемо само један.

Х. Еверет III је дао философско мишљење:

> *„... Универзум се непрекидно дели у импозантан број паралелних реалности. У таквом Космосу, не само да постоји неограничени број светова, него коегзистирају и сва могућа исходишта било ког догађаја."* Такође је предложио *„Васиону која се непрестано дели у огроман број огранака (светова), који произлазе из деловања много чинилаца. Поврх тога, унутар таквог Универзума, свака квантна промена у било којој звезди, галаксији или најдаљој забити, дели га на 'зилионе' копија самог себе."*

Осим наведених теорија, ту је и поглед познатог индијског астрофизичара Џајанта Нарликара (1993), који већина астрономске јавности прихвата. Према њему, Универзум који сазнајемо је само један, од бесконачног броја других, који сви заједно чине Хипер-универзум или Мултиверзум.

Узевши ово у обзир, можемо цео процес стварања да посматрамо слично течности која се пени, а сваки мехурић у њој представља један од безброј независних Универзума. Као што описује руски физичар Андреј Линде (1989, 1990, 1994), који од 1990. предаје Физику и Космологију на Универзитету у Стенфорду: ако представимо Универзум као хомогени мехур, сваки поремећај у њему створиће нови мехур. То је представа самостварајућег, Универзума који се шири и развија на начин који математичари зову „фрактални". Фрактална копија има особи-

ну само-сличности, тако да је сваки њен део идентична копија целог обрасца.

Пространствени мехури су примарно омеђени неодређеним границама; оне се шире и развијају брзином повезаном са светлосном. Теорија Великог праска, при том, опис је само једног мехура, а не фракталног Хипер-универзума „козмичке пене". Сваки мехур може да има своје сопствене физичке законе и, сходно томе, различите математичке структуре. Како астроном Мартин Клатон Брок (Martin Clatton Brock) каже:

> *„По дефиницији, реч Универзум укључује све. Према томе погодније је говорити о бројним световима, а да је Универзум подељен на безброј њих. Ми сазнајемо само један. Постоје отворени и затворени светови. Има их са делимичном структуром и хаотичних. У некима, неће никада настати живот. У другима живот постоји, али само у елементарном облику. На крају, само у веома мало њих постоји обиље живота (Talbot 1981)."*

6. ЗАКЉУЧЦИ

Проблем огромности Универзума је у основи филозофске природе. „**Апеирон**" (безгранично) Анаксимандра, заједно са „Хаосом" Хесиода односно с „бесконачним световима" Епикура и филозофа атомиста помогли су нам да га боље сагледамо.

Козмолошка идеја простор-времена, како је представљена у Општој теорији релативности, повезана је са Теоријом Великог праска, која је такође полазна тачка три Фридманова модела, са позитивном, нултом и негативном закривљеношћу.

Према овој теорији, Универзум је настао пре око 15 милијарди година (најновији резултати су 13,7 милијарди), великом експлозијом из неке врсте „космичког јајета" (теоријски) бесконачне густине и температуре, која је стварала (теоријски) бесконачну закривљеност простор-времена. Да би превазишли недореченост закона физике услед којих се добијају решења која садрже бесконачне величине — сингуларитете, астрофизичари се окрећу формулисању Квантне теорије гравитације, која би, како се очекује, могла да превазиђе ове тешкоће.

Да ли ће успети да превазиђе и неувидљивост појма „бесконачно"?*

---

* **Захвалница**: Овај рад је урађен у оквиру пројекта „Астрономија, историја и филозофија", потписаног између Астрономске опсерваторије у Београду и Катедре за Астрономију, Астрофизику и Механику, Школе за Физику, Универзитета у Атини. Такође је део пројекта 146022 *Историја и еписте-*

ЛИТЕРАТУРА

Aetii, *Ton areskonton synagoge* (*Xynagoge*); *De Placitorum Compositione (De Vetustis Placitis)* in: Diels Hermann: *Doxographi Graeci 45*. Berolini. Apud Walter De Gruyter et Socios. Editio Quarta, 1965.

Aristotle, *The Metaphysics*. Vol. I—IX, The Loeb Classical Library, Book XVII with an English Translation by H. Rackham. London: William Heinemann Ltd. Cambridge, Massachusetts: Harvard University Press, 1956.

Aristotle, *The Physics*. The Loeb Classical Library, Vol. I, Book III, with an English Translation by Philip H. Wicksteed. London: William Heinemann Ltd. Cambridge, Massachusetts: Harvard University Press, 1957.

Aristotle, *The Nicomachean Ethics*, The Loeb Classical Library, with an English Translation by Hugh Tredenick. London: William Heinemann Ltd. Cambridge, Massachusetts: Harvard University Press, 1968.

Diels Hermann, *Die Fragmente der Vorsokratiker*, herausgegeben von Walther Kranz, Erster und Zweiter Band, Weidmann, Zurich, 1996 (reprint 6. izdanja iz 1951/52).

Diogenes Laertius, *Lives of Eminent Philosophers*. The Loeb Classical Library, Vol. I, with an English Translation by R. D. Hicks. London: William Heinemann Ltd. Cambridge, Massachusetts: Harvard University Press, 1958.

Diogenes Laertius, *Lives of Eminent Philosophers*. The Loeb Classical Library, Vol. I—II, with an English Translation by R. D. Hicks, M. A. London. William Heinemann Ltd. Cambridge, Massachusetts, Harvard University Press, 1958—1959.

Everett III H., *On the Foundation of Quantum Mechanics*. Thesis, Princeton University, March 1, 1957.

Hippolytus, *Kata pason haireseon eleghos or A Refutation of All Heresies: Refutationis Omnium Haeresium (Philosophumena)*. Patrologia Graeca (P. G.) 16, In: Origenes, Liber VII, 404—405, 339. Typographi Brepols Editores Pontificii, Parisiis 1857—1866.

Jaeger W., *The Theology of the Early Greek Philosophers*, Transl. E. S. Robinson, Oxford, Clarenton Press, pp. 25—28, 1964.

Kirk G. S., Raven J. E. and Schofield M., *The Presocratic Philosophers. A critical History with a selection of Texts*, Cambridge University Press, First printed 1983, 2nd edition 1995.

Linde, A., *Particle Physics and Inflationary Cosmology*, Gordon and Breach, 1989.

Linde, A., *Inflation and Quantum Cosmology*, Academic Press, 1990.

мологија ūриродних наука, код Министарства за науку Републике Србије. Будући да је рад израђен у међународној сарадњи, српски преводи наведених аутора нису коришћени. Хронолошки подаци су дати према публикацији: Encyclopaedia Papyros — Larousse — Britannica. Издање To Vima, Атина, 1998.

Linde, A., *The self-Reproducing inflationary Cosmology*, Scientific American, p. 32, November 1994.
Narlikar, J. V., *Introduction to Cosmology*. Cambridge University Press, 1993.
Niarchos, C., *Problems of the European Philosophy*, Publications of the Athens University, Athens 1997. (in Greek).
Plato, *Philebus*. The Loeb Classical Library, with an English Translation by H. N. Fowler, Ph. D., William Heinemann Ltd. Cambridge, Massachusetts, Harvard University Press, 1962.
(Pseudo)-Plutarch, *Moralia*, Vol. XV: *Fragments: Stromata (A Patchwork)*, with an English Translation by F. H. Sandbach, William Heinemann Ltd. Cambridge, Massachusetts, Harvard University Press, 1969.
Simplicius, *On Aristotle's Physics (In Aristotelis Physicorum Libras IV)* 24, 13 (Z. 3—8 aus Theophrastus *Phys. Opin.* Fr. 2 Dox. 476), *Priores Commentaria*, Edidit Hermannus Diels, Berolini, Typis et Impensis G. Reimeri, 1882.
Simplicius, *Peri Ouranou (De Caelo)* 202, 16, Priores Commentaria, Edidit Hermannus Diels, Berolini, Typis et Impensis G. Reimeri, 1882.
Talbot, M., *Mysticism and Modern Science*, Bantam Books, New York, 1981.

Efstratios Theodossiou, Petros Mantarakis,
Milan S. Dimitrijević, Vassilios N. Manimanis,
Emmanuel Danezis

FROM THE *INFINITY* (APEIRON) OF ANAXIMANDER IN ANCIENT GREECE TO THE THEORY OF INFINITE UNIVERSES IN MODERN COSMOLOGY

Summary

An investigation of ancient Greek writings is undertaken to demonstrate that Anaximander introduced the **apeiron** (the boundless) as the beginning of everything (the first principle). According to his theory, the **apeiron** is undefined and ever moving. It gives birth to the oposite terms of warm and cold, and of moist and dry, and their perpetual strife. Man is able to comprehend the result of this eternal process from the vast plurality of things and the infinite number of Universes.

The cosmological aspect in Anaximander's theory is beautiful; innumerable worlds are born from the **apeiron** and absorbed by it, once they are destroyed. Thus, the **apeiron** is related to the eternal, throughout time, cosmological procedure.

The cosmological problem of the vastness of the Universe or of the innumerability of Universes is an elementary philosophical problem, while the Theory of Big Bang bounded with the notion of time-space, is a starting point for understanding the models that describe our Universe.

J. Phys. D: Appl. Phys. 27 (1994) 247–252. Printed in the UK

Stark broadening of Al III and Cu IV lines for diagnostic of the rail gun arc plasma

M S Dimitrijević†, Z Djurić‡ and A A Mihajlov‡†

† Astronomical Observatory, Volgina 7, 11050 Beograd, Yugoslavia
‡ Institute of Physics, PO Box 57, 11001 Beograd, Yugoslavia

Received 23 November 1992

Abstract. Stark broadening parameters of Al III lines of interest in the diagnostics of an electrodynamic macroparticle accelerator (rail gun) arc plasma created by evaporation of an Al foil have been calculated using the semi-classical perturbation formalism. Stark widths of Cu IV lines of interest for an arc plasma created by Cu foil evaporation have also been calculated by using the modified semi-empirical method.

1. Introduction

The electrodynamic acceleration of macroparticles enables the creation of dense plasmas at relatively low temperatures. An example (based on the conductor acceleration in the circuit's magnetic field) consists of an electrical power source and two parallel metal rails with a macroparticle moving between them (Rasheigh and Marshall 1978, Powell and Batteh 1983). The circuit is closed by the electrical arc created between the rails. The arc plasma (formed by the evaporated metal foil through which the discharge is initiated) is accelerated by the magnetic field, and its hydrodynamic pressure accelerates the macroparticle (projectile). For arcs with real geometry, a method has recently been developed for the calculation of corresponding plasma parameters (Rolader and Batteh 1989). This method has been applied to the case of arc plasmas created by Cu foil and Al foil evaporation (which are usually used in experimental work) (Rasheigh and Marshall 1978, Rolader and Batteh 1989, Sedghinasab *et al* 1989, Lehmann *et al* 1989), and the corresponding axial profiles of temperature T and electron density N_e have been determined.

Experimental verification of the corresponding parameter profiles is closely connected to the plasma diagnostic problem. Besides the theoretical point of view this is important for the further development of experiments connected with rail guns. The electrodynamic macroparticle accelerator arc plasma is quite a difficult object for spectroscopic investigations. In this context each possibility for diagnostic study is of particular interest. In some recent papers (Sedghinasab *et al* 1989, Lehmann *et al* 1989), spectroscopic diagnostics have been carried out. This problem still remains open, especially as up to now there have been no links between certain model methods (Powell and Batteh 1983) for the complete calculation of plasma parameters with certain diagnostic techniques. One possibility for the diagnostics of such plasma makes use of corresponding Stark broadening parameters (see, e.g. the work of Griem (1964)). The aim of this paper is to give the necessary elements for the diagnostics of plasmas based on the values of plasma parameters calculated by the model of Djurić and Mihajlov (1989).

In this article we present axial profiles of T and N_e for Cu and Al plasmas for typical experimental conditions and the corresponding Stark broadening parameters for Al III and Cu IV lines of interest for the diagnostics of such plasmas. Using the semi-classical perturbation model (Sahal-Bréchot 1969a, b), Stark broadening parameters for the most intense Al III lines have been calculated. The corresponding Cu IV line widths have been calculated using the modified semi-empirical method (Dimitrijević and Konjević 1980). The results presented here may be used for the diagnostics and modelling of an electrodynamic macroparticle accelerator arc plasma created by the evaporation of Al and Cu foils.

2. Basic characteristics of a rail gun arc plasma created by Al and Cu foil evaporation

The rail gun arc plasma considered is characterized by T and N_e profiles calculated here using the method developed by Djurić and Mihajlov (1989). These parameters are presented in table 1 for Al and Cu as functions of the axial normalized coordinate $x_{norm} = x/l$, where x is the distance from the front of the arc and l is its length. Table 1 illustrates the relatively wide T and N_e range, existing for the rail gun plasma case. One can see that T varies from $1–2\times10^4$ K up to around 5×10^4 K for the Cu case and up to around $9–10\times10^4$ K for the Al case. Regarding the comparison of calculated T values

0022-3727/94/020247+06$07.50

Table 1. Electron density N_e and temperature T for Cu and Al operated rail guns as functions of axial normalized coordinate $x_{norm} = x/l$, where x is the distance from the front of the arc and l is its length.

	Cu		Al	
x_{norm}	$T(\times 10^3$ K)	$N_e(\times 10^{17}$ cm^{-3})	$T(\times 10^3$ K)	$N_e(\times 10^{17}$ cm^{-3})
0.05	46.71	1214.0	79.24	1536.0
0.10	50.74	1122.0	90.56	1336.0
0.20	54.07	1006.0	100.10	1145.0
0.30	54.00	917.0	100.60	1020.0
0.40	51.81	824.4	95.23	902.3
0.50	47.99	715.0	84.63	781.1
0.60	43.22	591.7	70.19	668.7
0.70	37.28	446.8	53.31	554.1
0.80	30.02	282.3	38.75	395.1
0.90	20.82	115.1	27.12	182.5
0.92	17.96	82.5	24.17	132.3
0.94	15.17	56.3	21.21	92.6
0.96	12.21	29.1	17.58	57.3
0.98	10.11	9.53	13.69	25.8
0.99	10.10	1.21	12.71	2.68

in the case of Cu we can give the following results. The average calculated T value in the work of Powell and Batteh (1983) is 37 000 K, with the input data from the same experiment (Rasheigh and Marshall 1978); Rolader and Batteh (1989) give typical T values of such a plasma between 10 000 and 50 000 K; the maximum temperature given by Sedghinasab *et al* (1989) is around 57 000 K. These data demonstrate good agreement between our results and the literature. The electron density ranges from $\sim 10^{18}$ cm^{-3} up to ~ 2–4×10^{20} cm^{-3}. Table 1 also demonstrates that a relatively wide range exists where we might expect to find spectral lines in the optical range, suitable for diagnostics by using Stark broadening parameters.

In order to gain an idea of arc plasma composition, we also present calculated characteristic density values for Al III and Cu IV ions. In the case of Al III, the calculated ion density values are $> 6 \times 10^{18}$ cm^{-3} at the front of the arc ($x_{norm} = 0$) and decrease to 5.2×10^{18} cm^{-3} at $x_{norm} = 0.9$; the density shows a step decrease to $\sim 3.1 \times 10^{15}$ cm^{-3} at $x_{norm} = 0.98$. Cu IV density values increase from $\sim 4 \times 10^{11}$ cm^{-3} to $\sim 6.4 \times 10^{15}$ cm^{-3} for $0 \leqslant x_{norm} \leqslant 0.25$ and then decrease to $\sim 6 \times 10^{11}$ cm^{-3} for $0.25 \leqslant x_{norm} < 1$.

3. Stark broadening of Al III

In the case of the plasma created by Al foil evaporation the most intense lines of Al III have been chosen due to the suitability of the Al III spectrum (in comparison with the Al IV spectrum). In the case considered, Al III ions are the most abundant but Al IV ions are also present. However, in the Ne-like Al IV spectrum there are no convenient lines in the visible part of the spectrum. On the other hand, in the case of Al III, such lines do exist and, moreover, there are sufficient atomic data available for reliable semi-classical calculations. Within the semi-classical perturbation formalism (Sahal-Bréchot 1969a, b), applied here to the Al III line, full halfwidth (W) and shift (d) of an electron-impact broadened isolated spectral line can be expressed as:

$$W = N_e \int_0^\infty v f(v)\, dv \Big(\sum_{i' \neq i} \sigma_{ii'}(v) + \sum_{f' \neq f} \sigma_{ff'}(v) + \sigma_{el}(v) \Big) + W_R \qquad (1)$$

$$d = N_e \int_0^\infty v f(v)\, dv \int_{R_3}^{R_D} 2\pi\rho \sin(2\phi_p)\, d\rho \qquad (2)$$

where $f(v)$ is the Maxwellian velocity distribution function for electrons, ρ denotes the impact parameter of the incoming electron, i and f the initial and final atomic energy levels, i' and f' their corresponding perturbing levels and W_R gives the contribution of Feshbach resonances (Fleurier *et al* 1977). The inelastic cross section $\sigma_{jj'}(v)$, where $j = i, f$, can be expressed by an integral over the impact parameter of the transition probability $P_{jj'}(\rho, v)$ as

$$\sum_{j \neq j'} \sigma_{jj'}(v) = \tfrac{1}{2}\pi R_1^2 + \int_{R_1}^{R_D} 2\pi\rho \sum_{j \neq j'} P_{jj'}(\rho, v)\, d\rho \qquad (3)$$

and the elastic cross section is given by

$$\sigma_{el}(v) = 2\pi R_2^2 + \int_{R_2}^{R_D} 8\pi\rho \sin^2\delta\, d\rho$$

$$\delta = (\phi_p^2 + \phi_q^2)^{1/2}. \qquad (4)$$

The phase shifts ϕ_p and ϕ_q due to the polarization potential (r^{-4}) and to the quadrupolar potential (r^{-3}) respectively, are given in section 3 of chapter 2 of the work of Sahal-Bréchot (1969a). Here, R_d is the Debye radius and the cut-offs R_1, R_2 and R_3 are described in section 1 of chapter 3 of Sahal-Bréchot (1969b), and by Dimitrijević *et al* (1991). We present here Stark broadening parameters due to electron

Table 2. Electron-impact broadening parameters for Al III multiplets, for perturber densities of 10^{17}–10^{20} cm^{-3} and temperatures from 10 000 to 100 000 K. Transitions and averaged wavelengths for the multiplet (in Å) are also given. By using c (see equation (5) of Dimitrijević and Sahal-Bréchot (1984)), we obtain an estimate for the maximum perturber density for which the line may be treated as isolated and tabulated data may be used. The asterisk denotes cases for which the collision volume multiplied by the perturber density (the condition for the validity of the impact approximation) lies between 0.1 and 0.5.

Transition	$T(\times 10^3$ K)	W(Å)	d(Å)
Perturber density = 10^{17} cm^{-3}			
3S–3P	10	0.519×10^{-1}	0.903×10^{-5}
$\lambda = 1857.4$ Å	15	0.427×10^{-1}	-0.139×10^{-3}
$c = 1.9 \times 10^{20}$	20	0.371×10^{-1}	-0.322×10^{-3}
	50	0.240×10^{-1}	-0.349×10^{-3}
	100	0.179×10^{-1}	-0.400×10^{-3}
3S–4P	10	0.164×10^{-1}	0.110×10^{-3}
$\lambda = 696.0$ Å	15	0.138×10^{-1}	0.192×10^{-3}
$c = 8.5 \times 10^{18}$	20	0.122×10^{-1}	0.320×10^{-3}
	50	0.898×10^{-2}	0.258×10^{-3}
	100	0.757×10^{-2}	0.366×10^{-3}
3P–3D	10	0.451×10^{-1}	-0.105×10^{-3}
$\lambda = 1609.8$ Å	15	0.375×10^{-1}	0.261×10^{-3}
$c = 7.2 \times 10^{19}$	20	0.328×10^{-1}	0.574×10^{-3}
	50	0.216×10^{-1}	0.545×10^{-3}
	100	0.165×10^{-1}	0.702×10^{-3}
3P–4D	10	0.491×10^{-1}	0.330×10^{-2}
$\lambda = 893.3$ Å	15	0.425×10^{-1}	0.384×10^{-2}
$c = 1.5 \times 10^{18}$	20	0.386×10^{-1}	0.401×10^{-2}
	50	0.297×10^{-1}	0.386×10^{-2}
	100	0.251×10^{-1}	0.362×10^{-2}
3P–4S	10	0.582×10^{-1}	0.115×10^{-1}
$\lambda = 1382.6$ Å	15	0.474×10^{-1}	0.791×10^{-2}
$c = 3.3 \times 10^{19}$	20	0.415×10^{-1}	0.750×10^{-2}
	50	0.286×10^{-1}	0.573×10^{-2}
	100	0.232×10^{-1}	0.494×10^{-2}
3D–4F	10	0.192	-0.552×10^{-2}
$\lambda = 1935.9$ Å	15	0.164	-0.603×10^{-2}
$c = 6.8 \times 10^{18}$	20	0.147	-0.563×10^{-2}
	50	0.108	-0.583×10^{-2}
	100	0.890×10^{-1}	-0.408×10^{-2}
3D–4P	10	0.434	0.244×10^{-2}
$\lambda = 3606.2$ Å	15	0.367	0.368×10^{-2}
$c = 2.3 \times 10^{20}$	20	0.327	0.660×10^{-2}
	50	0.242	0.536×10^{-2}
	100	0.205	0.777×10^{-2}
4S–4P	10	1.43	-0.470×10^{-1}
$\lambda = 5706.9$ Å	15	1.19	-0.520×10^{-1}
$c = 5.7 \times 10^{20}$	20	1.07	-0.487×10^{-1}
	50	0.814	-0.503×10^{-1}
	100	0.707	-0.482×10^{-1}
4P–4D	10	1.41	0.683×10^{-1}
$\lambda = 4524.9$ Å	15	1.22	0.833×10^{-1}
$c = 3.7 \times 10^{19}$	20	1.12	0.828×10^{-1}
	50	0.879	0.842×10^{-1}
	100	0.761	0.741×10^{-1}
Perturber density = 10^{18} cm^{-3}			
3S–3P	10	0.519	-0.919×10^{-4}
$\lambda = 1857.4$ Å	15	0.427	-0.160×10^{-2}
$c = 1.9 \times 10^{21}$	20	0.371	-0.331×10^{-2}
	50	0.240	-0.364×10^{-2}
	100	0.179	-0.396×10^{-2}

Table 2. Continued.

Transition	$T(\times 10^3$ K)	W(Å)	d(Å)
3S–4P	10	0.164	0.921×10^{-3}
$\lambda = 696.0$ Å	15	0.138	0.196×10^{-2}
$c = 8.5 \times 10^{19}$	20	0.122	0.295×10^{-2}
	50	0.898×10^{-1}	0.246×10^{-2}
	100	0.757×10^{-1}	0.358×10^{-2}
3P–3D	10	0.452	-0.107×10^{-2}
$\lambda = 1609.8$ Å	15	0.374	0.296×10^{-2}
$c = 7.2 \times 10^{20}$	20	0.328	0.560×10^{-2}
	50	0.216	0.550×10^{-2}
	100	0.165	0.697×10^{-2}
3P–4D	10	0.491	0.210×10^{-1}
$\lambda = 893.3$ Å	15	0.424	0.291×10^{-1}
$c = 1.5 \times 10^{19}$	20	0.386	0.313×10^{-1}
	50	0.297	0.330×10^{-1}
	100	0.251	0.340×10^{-1}
3P–4S	10	0.582	0.111
$\lambda = 1382.6$ Å	15	0.474	0.769×10^{-1}
$c = 3.3 \times 10^{20}$	20	0.415	0.721×10^{-1}
	50	0.286	0.556×10^{-1}
	100	0.232	0.486×10^{-1}
3D–4F	10	1.92	-0.210×10^{-1}
$\lambda = 1935.9$ Å	15	1.64	-0.317×10^{-1}
$c = 6.8 \times 10^{19}$	20	1.47	-0.331×10^{-1}
	50	1.07	-0.431×10^{-1}
	100	0.889	-0.353×10^{-1}
3D–4P	10	4.34	0.204×10^{-1}
$\lambda = 3606.2$ Å	15	3.67	0.375×10^{-1}
$c = 2.3 \times 10^{21}$	20	3.27	0.603×10^{-1}
	50	2.42	0.505×10^{-1}
	100	2.05	0.755×10^{-1}
4S–4P	10	14.3	−0.423
$\lambda = 5706.9$ Å	15	11.9	−0.488
$c = 5.7 \times 10^{21}$	20	10.7	−0.454
	50	8.14	−0.478
	100	7.07	−0.477
4P–4D	10	14.1	0.379
$\lambda = 4524.9$ Å	15	12.2	0.594
$c = 3.7 \times 10^{20}$	20	11.2	0.613
	50	8.79	0.703
	100	7.60	0.690
Perturber density $= 10^{19}$ cm^{-3}			
3S–3P	10	5.19	0.726×10^{-2}
$\lambda = 1857.4$ Å	15	4.27	-0.136×10^{-1}
$c = 1.9 \times 10^{22}$	20	3.71	-0.272×10^{-1}
	50	2.40	-0.338×10^{-1}
	100	1.79	-0.373×10^{-1}
3S–4P	10	*1.64	$*0.133 \times 10^{-2}$
$\lambda = 696.0$ Å	15	1.38	0.142×10^{-1}
$c = 8.5 \times 10^{20}$	20	1.22	0.245×10^{-1}
	50	0.898	0.219×10^{-1}
	100	0.757	0.337×10^{-1}
3P–3D	10	4.52	-0.271×10^{-1}
$\lambda = 1609.8$ Å	15	3.74	0.235×10^{-1}
$c = 7.2 \times 10^{21}$	20	3.27	0.449×10^{-1}
	50	2.16	0.494×10^{-1}
	100	1.65	0.648×10^{-1}

Table 2. Continued.

Transition	$T(\times 10^3$ K)	W(Å)	d(Å)
3P–4D	10	*4.52	*−0.218
$\lambda = 893.3$ Å	15	4.01	-0.340×10^{-1}
$c = 1.5 \times 10^{20}$	20	3.68	0.446×10^{-1}
	50	2.88	0.164
	100	2.44	0.230
3P–4S	10	5.82	0.982
$\lambda = 1382.6$ Å	15	4.74	0.677
$c = 3.3 \times 10^{21}$	20	4.16	0.646
	50	2.86	0.510
	100	2.32	0.453
3D–4F	10	17.8	0.994
$\lambda = 1935.9$ Å	15	15.5	0.613
$c = 6.8 \times 10^{20}$	20	14.0	0.431
	50	10.4	0.451×10^{-1}
	100	8.68	-0.413×10^{-1}
Perturber density $= 10^{20}$ cm^{-3}			
3S–4P			
$\lambda = 696.0$ Å	20	*12.1	$*0.668 \times 10^{-1}$
$c = 8.5 \times 10^{-21}$	50	*8.96	*0.129
	100	7.56	0.275

impacts while eventual corrections for the ion-impact broadening contribution may be calculated by using simple expressions within the quasistatic approximation (Griem 1974, Sahal-Bréchot 1991).

Energy levels for Al III lines have been taken from Bashkin and Stoner (1975). Oscillator strengths have been calculated using the method of Bates and Damgaard (1949) and tables in Oertel and Shomo (1968). For higher levels, the method described by Van Regemorter *et al* (1979) has been used. Our results are shown in table 1 for $N_e = 10^{17}$–10^{20} cm^{-3} and $T = 10\,000$–$100\,000$ K. We also specify a parameter (Dimitrijević and Sahal-Bréchot 1984) denoted by c which, when it is divided by the corresponding electron impact full width at half maximum (FWHM), gives an estimate for the maximum perturber density for which the line may be treated as isolated. For each value given in table 1, the collision volume V multiplied by the perturber density N_e is much less than unity, and the impact approximation is valid (Sahal-Bréchot 1969a, b). Values for $0.1 < N_e V \leqslant 0.5$ are denoted by an asterisk. When $N_e V > 0.5$ the impact approximation is not valid and corresponding values are not given in table 1. Results are presented as a function of density since at high densities Stark broadening parameters are no longer linear functions of density due to Debye screening. This effect is more important for the shift than for the width.

Our results are in satisfactory agreement with Stark widths calculated by Davis and Morin (1971) for the Al III $3p^2P^0$–$4d^2D$ multiplet.

4. Stark broadening of Cu IV lines

In the rail gun arc plasma created by Cu foil evaporation, Cu III ions are the most abundant, but Cu IV ions are also present in significant quantities. From the theoretical point of view, the spectrum of Cu IV is less complex and therefore more convenient for Stark broadening calculations than that of Cu III. Consequently, one can obtain more reliable data. However, for the Cu IV spectrum there are no sufficient, reliable atomic data in order to perform a semi-classical calculation as in the case of Al III. In this case, the modified semi-empirical approach (Dimitrijević and Konjević 1980) provides a possible way to obtain the corresponding Stark widths.

Within the modified semi-empirical approach, electron impact full halfwidth W_{MSE} can be calculated from the following expression (Dimitrijević and Konjević 1980):

$$W_{MSE} = 2(2\pi\hbar/3m)^2(6m/\pi kT)^{1/2}N_e \times \left\{ \sum_{j,j'=i,i'f,f'} [R^2_{l_j,l_{j+1}}\tilde{g}(E/\Delta E_{l_j,l_{j+1}}) + R^2_{l_j,l_{j-1}}\tilde{g}(E/\Delta E_{l_j,l_{j-1}}) + \sum_{j'=0i',\Delta f} (R^2_{j,j'})_{\Delta n\neq 0} g(3kTn_j^3/4Z^2E_H)] \right\} \quad (5)$$

$$\tilde{g}(x) = 0.7 - 1.1/Z + g(x) \quad (6)$$

$$R^2_{l,l'} = (3n/2Z)^2[\max(l,l')/(2l+1)][n^2 - \max^2(l,l')]\phi^2 \quad (7)$$

$$\sum_{j'}(R^2_{j,j'})_{\Delta n\neq 0} = (3n_j/2Z)^2(n_j^2 + 3l_j^2 + 3l_j + 11)/9. \quad (8)$$

Here, n is the effective principal quantum number, $Z-1$ is the ionic charge, ϕ the Bates and Damgaard (1949) factor and $E = 3kT/2$. Atomic energy level data are taken from Schröder and van Kleef (1970).

Electron impact full halfwidths for six Cu IV multiplets are presented in table 2 at $N_e = 10^{17}$ cm^{-3} (for arc plasma tail conditions) for $T = 10\,000$–$150\,000$ K.

Table 3. Electron-impact full halfwidths W_{MSE} calculated using the modified semi-empirical approach (Dimitrijević and Konjević 1980) for six Cu IV multiplets, for a perturber density of 10^{17} cm^{-3} and temperatures from 10 000 to 150 000 K. Transitions and averaged wavelengths for the multiplet (in Å) are also given.

Transition	$T(\times 10^3$ K)	W_{MSE}(Å)
$3d^7(^4F)4s^3F-$	10	1.44×10^{-2}
$3d^7(^4F)4p^3D$	20	1.02×10^{-2}
$\lambda = 1381.6$ Å	30	8.34×10^{-3}
	50	6.46×10^{-3}
	100	4.57×10^{-3}
	150	3.75×10^{-3}
$3d^7(^4F)4s^3F-$	10	1.57×10^{-2}
$3d^7(^4F)4p^3F$	20	1.11×10^{-2}
$\lambda = 1435.6$ Å	30	9.08×10^{-3}
	50	7.03×10^{-3}
	100	4.97×10^{-3}
	150	4.10×10^{-3}
$3d^7(^4F)4s^3F-$	10	1.60×10^{-2}
$3d^7(^4F)4p^3G$	20	1.13×10^{-2}
$\lambda = 1445.8$ Å	30	9.22×10^{-3}
	50	7.14×10^{-3}
	100	5.05×10^{-3}
	150	4.17×10^{-3}
$3d^7(^4F)4s^5F-$	10	1.33×10^{-2}
$3d^7(^4F)4p^5G$	20	9.41×10^{-3}
$\lambda = 1359.5$ Å	30	7.68×10^{-3}
	50	5.95×10^{-3}
	100	4.21×10^{-3}
	150	3.45×10^{-3}
$3d^7(^4F)4s^5F-$	10	1.37×10^{-2}
$3d^7(^4F)4p^5D$	20	9.70×10^{-3}
$\lambda = 1378.4$ Å	30	7.92×10^{-3}
	50	6.14×10^{-3}
	100	4.34×10^{-3}
	150	3.56×10^{-3}
$3d^7(^4F)4s^5F-$	10	1.47×10^{-2}
$3d^7(^4F)4p^5F$	20	1.04×10^{-2}
$\lambda = 1422.5$ Å	30	8.49×10^{-3}
	50	6.58×10^{-3}
	100	4.65×10^{-3}
	150	3.83×10^{-3}

5. Conclusion

Results presented here may be used for diagnostics and modelling of rail gun arc plasmas on the basis of ion line profiles. Results are given for a larger T range than needed for rail gun arc plasma analysis, since they are also of interest for other laboratory and astrophysical plasmas. For all needed purposes the data density in the tables enables a good interpolation. Semi-classical data for Al III are of better accuracy than semi-empirical data for Cu IV. Since within the semi-classical theory we take into account Debye screening, results for Al III are not linear with electron density (especially the shift), like semi-empirical Cu IV data. Consequently, Al III results are presented as a function of electron density. Since the importance of the Stark shift usually decreases with increasing ionization, and Cu IV shifts are not of importance for rail gun plasma diagnostics, they are not presented here.

Besides Cu and Al ionic lines, H and Li are also of importance for rail gun plasma research (Rolader and Batteh, 1989). Corresponding Stark broadening parameter tables may be found in Griem (1974) for H I and Li II. Present often as impurities, Ca, Si, C and Fe ions may be also of interest for diagnostic purposes. Stark widths for the most intense Si III and C IV lines may be found in the works of Dimitrijević (1988) and Stark broadening parameter tables for Si IV and C IV in Dimitrijević *et al* (1991a–d).

We hope that the presented results will be helpful for diagnostics, modelling and other investigations of rail gun arc plasmas.

Acknowledgment

We are indebted to Dr Sylvie Sahal-Bréchot for providing us with the computer code for the semi-classical perturbation calculations of Stark broadening parameters.

References

Bashkin S and Stoner J O Jr 1975 *Atomic Energy Levels and Grotrian Diagrams* vol I (Amsterdam: North Holland)
Bates D R and Damgaard A 1949 *Trans. R. Soc. Ser.* A **242** 101
Davis J and Morin S 1971 *J. Quant. Spectrosc. Radiat. Transf.* A **11** 495
Dimitrijević M S 1988 *Astron. Astrophys. Suppl. Series* **76** 53
Dimitrijević M S and Konjević N 1980 *J. Quant. Spectrosc. Radiat. Transf.* **24** 451
Dimitrijević M S and Sahal-Bréchot S 1984 *J. Quant. Spectrosc. Radiat. Transf.* **31** 301
Dimitrijević M S Sahal-Bréchot S and Bommier V 1991a *Astron. Astrophys. Suppl. Series* **89** 581
—— 1991b *Bull. Obs. Astron. Belgrade* **144** 81
—— 1991c *Astron. Astrophys. Suppl. Series* **89** 591
—— 1991d *Bull. Obs. Astron. Belgrade* **144** 65
Djurić Z and Mihajlov A A 1989 *Contrib. Plasma Phys.* **29** 627
Fleurier C, Sahal-Bréchot S and Chapelle J 1977 *J. Quant. Spectrosc. Radiat. Transf.* **17** 595
Griem H R 1964 *Plasma Spectroscopy* (New York: McGraw-Hill)
—— 1974 *Spectral Line Broadening by Plasmas* (New York: Academic)
Lehmann P, Wey J, Mach H, Eichhorn A and Darée K 1989 *IEEE Trans. Plasma Sci.* **17** 371
Oertel G K and Shomo L P 1968 *Astrophys. J. Suppl. Series* **16** 175
Powell J D and Batteh J H 1983 *J. Appl. Phys.* **54** 2242
Rasheigh S C and Marshall R A 1978 *J. Appl. Phys.* **49** 2540
Rolader G E and Batteh J H 1989 *IEEE Trans. Plasma Sci.* **17** 439
Sahal-Bréchot S 1969a *Astron. Astrophys.* **1** 91
—— 1969b *Astron. Astrophys.* **2** 322
—— 1991 *Astron. Astrophys.* **245** 322
Schröder J F and van Kleef Th A M 1970 *Physica* **49** 388
Sedghinasab A, Keefer D R and Crowder H L 1989 *IEEE Trans. Plasma Sci.* **17** 360
Van Regemorter H, Hoang Binh Dy and Prud'homme M 1979 *J. Phys. B: At. Mol. Phys.* **12** 1073

Journal of Physics: Conference Series **207** (2010) 012024 doi:10.1088/1742-6596/207/1/012024

Similarities in Calculated Stark Broadening Parameters of Argon Spectral Lines

M Christova[1], M S Dimitrijević[2], A Kovačević[2]

[1]Department of Applied Physics, Technical University-Sofia, BG-1000 Sofia, Bulgaria
[2]Astronomical Observatory, Volgina 7, 11060 Belgrade 38, Serbia

E-mail: mchristo@tu-sofia.bg, mdimitrijevic@aob.bg.ac.yu, andjelka@matf.bg.ac.yu

Abstract. The similarities of the calculated Stark broadening parameters of four argon spectral lines within a spectral series $3p^5nd \rightarrow 3p^54p$ have been analyzed. The Stark broadening parameters have been calculated using Sahal-Bréchot theory within the semi-classical perturbation formalism. The dependeces of the Stark width and shift versus the effective quantum number have been presented.

1. Introduction

The broadening of spectral lines of heavy elements in plasmas is principally determined by two factors, the plasma environment and the atomic structure of the emitting atom or ion. Since atomic structures exhibit many great regularities and similarities, one must expect the same for the width and shift parameters of plasma broadened lines. A comprehensive study and analysis of regularities and similarities of the existing experimental data for the Stark broadening parameters have been presented in [1], based on the *L-S* coupling scheme.

One of the most useful gases for laboratory plasmas, argon, is also interesting in astrophysics since with the development of space-borne spectroscopy, the importance of atomic data, including line broadening parameters for trace elements like argon [2], is increasing. For example argon is found in CVn binary σ^2 Coronae Borealis [3], and "Chandra's" X-ray spectra of young supernovas 1998S and 2003bg revealed an argon over-abundance [4]. Recently, argon lines are observed in the optical spectrum of the Be star Hen 2-90 [5], as well as in planetary nebulae and H II regions in the two dwarf irregular galaxies Sextans A and B [6]. Also argon abundance has been determined from spectral lines, e.g. for LSE 78, an extreme helium star [7], for the similar star BD-9º4395 [8], for DY Cen [9] and γ Peg [10], as well as for the Sun [11]. Consequently, Stark line broadening parameters for neutral and ionized argon are of interest for the modeling and investigation of astrophysical plasmas. Often, the modeling of astrophysical objects needs atomic data for thousands and sometimes millions transitions. It is difficult and cumbersome to calculate the Stark broadening parameters for all these lines, so that methods enabling interpolation and extrapolation of the calculated results on the basis of similarities and systematic trends are of interest. For example we can obtain new Stark broadening parameters from regularities within spectral series.

In this work, the systematic trend of Stark broadening parameters of Ar I 522.1, 549.6, 603.2 and 737.2 nm spectral lines within the same spectral series with the corresponding transitions $3p^57d - 3p^54p$, $3p^56d - 3p^54p$, $3p^55d - 3p^54p$ and $3p^54d - 3p^54p$ has been investigated. The behavior of these parameters with the increase of the effective quantum number of the initial energy levels of the

corresponding transition within the spectral series has been obtained. The results for Ar I 522.1, 549.6 and 603.2 are given in [12] where the calculations are oriented to laboratory plasmas. The examined perturbers are electrons, argon ions and protons. The presented calculations in this work are oriented for astrophysical purposes and the studied perturbers are electrons, protons and helium ions.

2. Theory

The Stark broadening parameters have been calculated using Sahal-Bréchot theory within the semi-classical perturbation formalism [13, 14], where the full width (W) at half maximum and the shift (d) of an isolated line originating from the transition between the initial level i and the final level f is expressed as:

$$W = 2n_e \int_0^\infty v f(v) dv \left[\sum_{i' \neq i} \sigma_{ii'}(v) + \sum_{f' \neq f} \sigma_{ff'}(v) + \sigma_{el} \right] \tag{1}$$

$$d = \int_0^\infty v f(v) dv \int_{R_3}^{R_d} 2\pi\rho d\rho \sin 2\varphi_p \,, \tag{2}$$

where i' and f' are perturbing levels, n_e and v are the electron density and the velocity of perturbers, respectively, and $f(v)$ is the Maxwellian distribution of the electron velocities.

The inelastic cross sections $\sigma_{ii'}$ (v) (respectively $\sigma_{ff'}$ (v)) can be expressed by an integration of the transition probability $P_{ii'}$ over the impact parameter ρ:

$$\sum_{i' \neq i} \sigma_{ii'}(v) = \frac{1}{2}\pi R_1^2 + \int_{R_1}^{R_d} 2\pi\rho d\rho \sum_{i' \neq i} P_{ii'}(\rho, v) \,. \tag{3}$$

The elastic collision contribution to the width is given by:

$$\sigma_{el} = 2\pi R_2^2 + \int_{R_2}^{R_d} 8\pi\rho d\rho \sin^2 \delta \tag{4}$$

$$\delta = \left(\varphi_p^2 + \varphi_q^2 \right)^{1/2} . \tag{5}$$

The phase shifts φ_p and φ_q are due to the polarization and to the quadrupole potential, respectively. The cut-off parameters R_1, R_2, R_3, the Debye cut-off R_d, and the symmetrization procedure are described in [13, 14].

The impact approximation is valid when the duration of collisions is much shorter than the separation time between strong collisions (collisions whose resulting phase shift is bigger than 1 rad): $n_e \pi \rho_{typ}^3 << 1$, where ρ_{typ} is the typical impact parameter for strong collisions.

The resulting profiles are Lorentzian. This condition is well verified for electron collisions for a large range of densities. For ion collisions the impact approximation might fail, especially for high densities or low temperatures. Within the impact approximation the ion broadening contribution has a Lorentzian shape and the total full width or shift is simply the sum of the corresponding full widths or shifts for electron and ion broadening. If the impact approximation is not applicable to ion broadening, it is possible to apply the quasistatic approximation given by Griem in [15]. Then the ion broadening parameters obtained within the quasistatic approximation, denoted here with the index iq, are:

$$W_{iq} = 1{,}75.10^{-4} n_e^{1/4} A [1 - 0{,}068 n_e^{1/6} T^{-1/2}] W_e \tag{6}$$

$$d_{iq} = 10^{-4} n_e^{1/4} A [1 - 0{,}068 n_e^{1/6} T^{-1/2}] W_e \,, \tag{7}$$

where W_e is the impact contribution of electrons to the total width, T is in Kelvin, and n_e in cm^{-3}. A is the quasistatic parameter, defined in [15] as follows:

$$A = \left(\frac{eF_0^2}{\hbar W_e} \left| \alpha_i - \alpha_f \right| \right)^{3/4} , \tag{8}$$

where $F_0 = 2\pi(4/15)^{2/3} e n_e^{2/3}$ is the normal field strength. The polarizability of the initial level α_i (resp. α_f is the polarizability of the final level) is expressed as:

$$\alpha_i = 4a_0^3 \sum_{i' \neq i} f_{ii'} \left(\frac{I_H}{\Delta E_{ii'}} \right)^2 , \quad (9)$$

where a_0 is the Bohr radius, $f_{ii'}$ is the oscillator strength, and I_H is the ionization energy of hydrogen.

3. Results

The calculations were performed for particular lines within multiplets (spin-orbital interaction is included). The most appropriate *j-L* coupling scheme for argon atoms has been used. The values of the energy levels have been taken from the NIST catalogue [16]. The oscillator strengths (*j-L* coupling) have been calculated within the Bates & Damgaard approximation. The calculations have been made for a set of temperatures $(2.5 – 5.0)\times10^4$ K at a perturber (electrons, protons and helium ions) density of 10^{16} cm^{-3}.

In this work we present the calculated Stark broadening parameters for the Ar I 737.2 nm spectral line. In table 1 the wavelengths of the studied argon lines, the corresponding transitions in *j-L* coupling, the perturbing levels *i'* and *f'*, the energy values, and the effective quantum number of the initial level are presented.

Table 1. Basic data on the considered Ar I spectral lines. Here λ denotes the wavelength, *i* and *f* are the initial and final level of the transition (within the frame of *j-L* coupling), *i*' and *f*' are the corresponding perturbing levels, E_i and E_f are the energy values, and *n** is the effective quantum number of the initial level.

λ (nm)	Transition (*i* – *f*)	*i*' levels	*f*' levels	E_i (cm^{-1})	E_f (cm^{-1})	*n**
522.1	$3p^5 7d - 3p^5 4p$ $^2[7/2]^\circ_4 - {}^2[5/2]_3$	5f, 6f, 7f, 8f, 9f, 5p, 6p, 7p, 8p, 9p	4s, 5s, 6s, 3d, 4d, 5d, 6d	124610	105463	6.62
549.6	$3p^5 6d - 3p^5 4p$ $^2[7/2]^\circ_3 - {}^2[5/2]_3$	4f, 5f, 6f, 7f, 4p, 5p, 6p, 7p	4s, 5s, 6s, 3d, 4d, 5d, 6d	123653	105463	5.63
603.2	$3p^5 5d - 3p^5 4p$ $^2[7/2]^\circ_4 - {}^2[5/2]_3$	4f, 5f, 6f, 7f, 4p, 5p, 6p, 7p	4s, 5s, 6s, 3d, 4d, 5d, 6d	122036	105463	4.65
737.2	$3p^5 5d' - 3p^5 4p$ $^2[7/2]^\circ_4 - {}^2[5/2]_3$	4f, 5f, 6f, 4p, 5p, 6p	4s, 5s, 6s, 3d, 4d, 5d, 6d	119024	105463	3.68

The results are presented in table 2 for the Ar I 737.2 nm argon line. The calculated Stark widths (full width at half intensity maximum) *W* and shifts *d* for collisions with electrons (W_e, d_e), He^+ ions – (W_{He+}, d_{He+}), and protons – (W_p d_p) are given. The ratio *C/W* gives the value of the maximum density for which the line is isolated for the corresponding perturber.

For the atmospheres of the main branch stars the total Stark width *W* and shift *d* are approximatelly:

$$W = W_e + 0.9W_p + 0.1W_{He+} \quad (10)$$

$$d = d_e + 0.9d_p + 0.1d_{He+} . \quad (11)$$

Table 2. Stark broadening parameters for Ar I 737.2 nm for a perturber (electrons, helium ions, and protons) density of 10^{16} cm^{-3} and temperatures from 2500 up to 50000 K.

Perturbers are:		Electrons		Ionized helium		Protons	
Transition	T (10^3 K)	W_e (0.1 nm)	d_e (0.1 nm)	W_{He+} (0.1 nm)	d_{He+} (0.1 nm)	W_p (0.1 nm)	d_p (0.1 nm)
4d $^2[7/2]_4$	2.5	0.572	0.367	-	-	0.171	0.787×10^{-1}
4p $^2[5/2]_3$	5	0.646	0.425	0.168	0.0756	0.182	0.980×10^{-1}
737.2 nm	10	0.739	0.428	0.176	0.0917	0.193	0.117
	20	0.871	0.371	0.185	0.108	0.205	0.136
$C = 0.65\times10^{19}$	30	0.964	0.318	0.19	0.117	0.213	0.148
	50	1.07	0.275	0.198	0.13	0.224	0.163

In figures 1 and 2 the temperature dependences of the electron impact width and shift (electron density 10^{16} cm^{-3}) of Ar I 737.2 nm are illustrated.

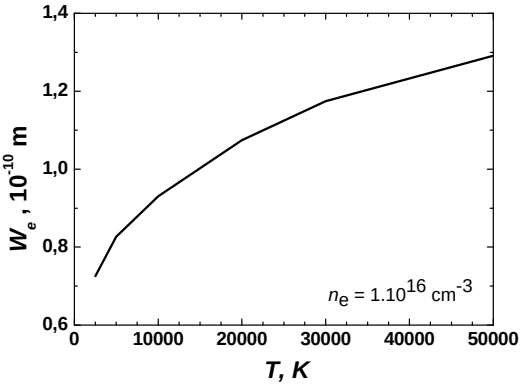

Figure 1. Electron impact width of the Ar I 737.2 nm spectral line versus the temperature for a 10^{16} cm^{-3} electron density.

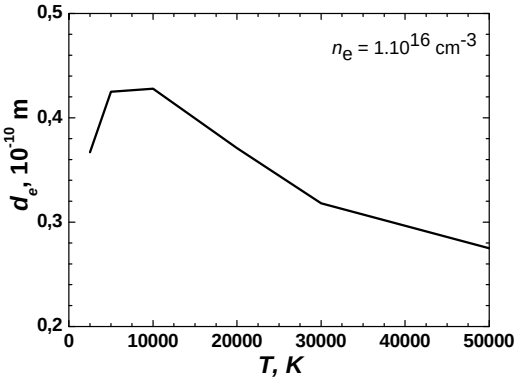

Figure 2. Electron impact shift of the Ar I 737.2 nm spectral line versus the temperature for a 10^{16} cm^{-3} electron density.

The contributions of the different collisions between emitters and perturbers (inelastic and elastic (polarization) collisions) in the Stark width of the examined argon lines from one spectral series show a similar behavior versus the temperature. One example for this behavior is presented in figure 3 for the Ar I 522.1 nm argon line. The broadening coefficient ($\beta = W / n_e$) and their components (β_{in} – contribution of inelastic collisions, β_{el} – contribution of elastic collisions, and β_p – contribution of polarization (the polarization interactions are elastic ones) collisions) have been analyzed. The inelastic component increases with the temperature while the elastic and polarization ones decrease for the argon lines from the studied series. The quadruple component (β_q) depends only by the initial and final states of the emitters and does not depend on the temperature and perturber density, and is not included in the figure.

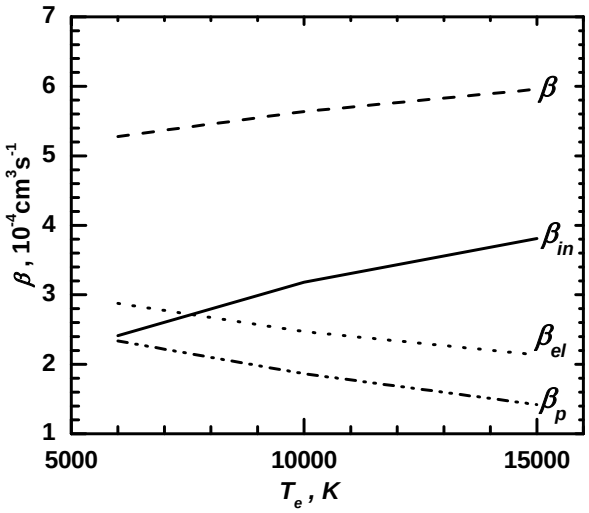

Figure 3. Stark broadening coefficient for Ar I 522.1 nm ($\beta = W / n_e$) and their components: $\beta = \beta_{in} + \beta_{el}$, where β_{in} is the contribution of the inelastic argon emitter-perturber collisions, β_{el} is the contribution of elastic ones, $\beta_{el} = \beta_p + \beta_q$ (β_p gives the contribution of polarisation interactions and β_q – of the quadruple interactions). The quadruple interactions do not depend on the temperature and the perturber density so it is not presented in the figure.

In figures 4 and 5 the electron impact width and shift, respectively, are given. From one side, the argon spectral lines are broadened mainly due to the collisions with electrons, usually. From the other side, it is more correct to study the width and shift trends of the spectral lines for each kind of perturbers separately.

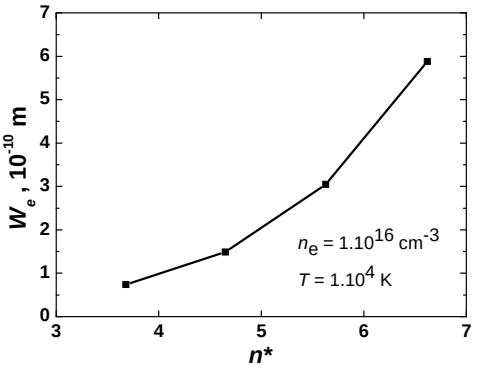

Figure 4. Electron impact widths of Ar I spectral lines within the spectral series versus the effective quantum number of the initial energy level.

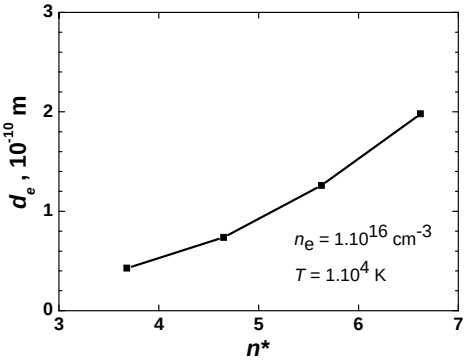

Figure 5. Electron impact shifts of Ar I spectral lines within the spectral series versus the effective quantum number of the initial energy level.

One can see that the behavior of the electron impact widths and shifts within the considered spectral series is so regular, that interpolation and extrapolation of new data is possible. The complete

analysis of the results of this paper and the comparison with other theoretical and experimental data available in the literature will be given in [17].

Acknowledgments
This work was partially financed by the Technical University – Sofia and is a part of the project 146001 supported by the Ministry of Science and Technological Development of Serbia.

References
[1] Konjević N, Lessage A, Fuhr J R and Wiese W L 2002 *J. Phys. Chem. Ref. Data* **31** 819
[2] Werner K, Rauch T and Kruk J W 2007 *Astron. Astrophys.* **466** 317
[3] Suh J A, Audard M, Güdel M and Paerels F B S 2005 *Astrophys. J.* **630** 1074
[4] Lewin W 2005 Chandra Proposal ID #07500185
[5] Kraus M, Borges F M, De Araújo F X and Lamers H J G L M 2005 *Astron. Astrophys.* **441** 289
[6] Kniazev A Yu, Grebel E K, Pustilnik S A, Pramskij A G and Zucker D B 2005 *Astron. J.* **130** 1558
[7] Jeffery C S 1993 *Astron. Astrophys.* **279** 188
[8] Jeffery C S and Heber U 1992 *Astron. Astrophys.* **260** 133
[9] Jeffery C S and Heber U 1993 *Astron. Astrophys.* **270** 167
[10] Peters G J 1976 *Astrophys. J. Suppl. Series* **30** 551
[11] Anders E and Grevesse N 1989 *Geochim. Cosmochim. Acta* **53** 197
[12] Dimitrijević M S, Christova M and Sahal-Bréchot S 2007 *Phys. Scripta* **75** 809
[13] Sahal-Bréchot S 1969 *Astron. Astrophys.* **1** 91
[14] Sahal-Bréchot S 1969 *Astron. Astrophys.* **2** 322
[15] Griem H R 1974 *Spectral line broadening by plasmas* (New York: Academic)
[16] http://physics.nist.gov/
[17] Christova M, Dimitrijević M S and Kovačević A (to be published)

Journal of Physics: Conference Series **207** (2010) 012025 doi:10.1088/1742-6596/207/1/012025

Stark Broadening Parameters of Ne I 837.8 nm Spectral Line

M Christova[1], M S Dimitrijević[2], Z Simić[2] and S Sahal-Bréchot[3]

[1]Department of Applied Physics, Technical University-Sofia, BG-1000 Sofia, Bulgaria
[2]Astronomical Observatory, Volgina 7, 11060 Belgrade 38, Serbia
[3]Observatoire de Paris, 92195 Meudon Cedex, France

mchristo@tu-sofia.bg, mdimitrijevic@aob.bg.ac.yu, zsimic@aob.bg.ac.yu, sylvie.sahal-brechot@obspm.fr

Abstract. The Stark broadening parameters of Ne I 837.8 nm spectral line corresponding to the transition $2p^5 3d\ ^2[7/2]^\circ_4 - 2p^5 3p\ ^2[5/2]_3$ have been calculated using Sahal-Bréchot theory. The temperature dependence of the width and shift has been obtained.

1. Introduction

Stark broadening parameters of neon lines are of importance not only for laboratory plasma diagnostics and for technological plasma investigations and development but also for astrophysics. Neon is the most abundant element in the universe after hydrogen, helium, oxygen, and carbon, and it is, for example, one of the products of hydrogen and helium burning in the orderly evolution of stellar interiors. Consequently, its lines are present in stellar spectra and, for example, neon spectral lines have been used to determine its abundances in late- to mid-B stars [1]. The neon spectral line at 837.8 nm, corresponding to the transition $2p^5 3d\ ^2[7/2]^\circ_4 - 2p^5 3p\ ^2[5/2]_3$, is one of the most useful for plasma diagnostics [2]. It is intensive, well isolated, and in the visible part of the spectrum. The Stark broadening of this line was theoretically investigated, for example, by Griem in [3] and experimentally by Purić et al. [4] and del Val et al. [5]. In this paper, calculations of the Stark broadening parameters of Ne I 837.8 nm for astrophysical purposes are presented.

2. Theory

In this work the semi-classical theory of Sahal-Bréchot [6,7] for Stark broadening calculations, also presented in [8], has been used.

3. Results

3.1. Atomic data

In table 1 the wavelengths of the studied neon line, along with the corresponding transition in *j-L* coupling scheme, the perturber energy levels, the energy values of the initial and final level of the transition, and the effective quantum number of the initial level are included.

Table 1. Basic data for the considered Ne I spectral line. Here λ denotes wavelength, *i* and *f* are initial and final level of the transition (within the frame of *j*-*L* coupling), *i*' and *f*' are the corresponding perturbing levels, E_i and E_f are the energy values, and *n** is the effective quantum number of the initial level.

λ (nm)	Transition ($i - f$)	*i*' levels	*f*' levels	E_i (cm^{-1})	E_f (cm^{-1})	*N**
837.7	$2p^5 3d' - 2p^5 3p$ $^2[7/2]^\circ_4 - {}^2[5/2]_3$	4f, 5f, 3p, 4p, 5p	3s, 4s, 5s, 3d, 4d, 5d	161590.3	149657.0	2.98

3.2. Calculations

The calculations have been oriented for the diagnostic of astrophysical objects where the perturbers are electrons, helium ions, and protons, and have been made for a set of temperatures $(2.5 - 5.0)\times10^4$ K at a perturber density of 10^{16} cm^{-3}. The values of the energy levels have been taken from the NIST catalogue [9]. The oscillator strengths (*j*-*L* coupling) have been calculated within the Bates & Damgaard approximation.

3.3. Temperature dependence

The calculated results for the Stark width and shift of the examined neon spectral line are included in table 2. The contribution of the interactions between: (*i*) emitters and electrons (W_e, d_e); (*ii*) emitters and helium ions (W_{He+}, d_{He+}) and (*iii*) emitters and protons (W_p, d_p) in the Stark width and shift are given. The value of the maximum density for which the line is isolated for the corresponding perturber can be calculated using the ratio *C*/*W*, where *C* is the parameter, included in table 2 and *W* is the total width. For the ordinary stellar plasma the total Stark width *W* and shift *d*, respectively, are approximatelly:

$$W = W_e + 0.9W_p + 0.1W_{He+} \quad (1)$$

$$d = d_e + 0.9d_p + 0.1d_{He+}. \quad (2)$$

Table 2. Stark broadening parameters for Ne I 837.7 nm for a perturber (electrons, helium ions and protons) density of 10^{16} cm^{-3} and temperatures from 2500 up to 50000 K.

Perturbers are:		Electrons		Ionized helium		Protons	
Transition	*T* (10^3 K)	W_e (0.1 nm)	d_e (0.1 nm)	W_{He+} (0.1 nm)	d_{He+} (0.1 nm)	W_p (0.1 nm)	d_p (0.1 nm)
$3d\ ^2[7/2]_4$ $3p\ ^2[5/2]_3$ 837.7 nm	2.5	0.306	0.21	0.0788	0.031	0.918×10^{-1}	0.502×10^{-1}
	5	0.35	0.233	0.0831	0.0386	0.974×10^{-1}	0.601×10^{-1}
	10	0.383	0.239	0.0868	0.046	0.104	0.701×10^{-1}
	20	0.417	0.222	0.0909	0.0535	0.112	0.806×10^{-1}
$C = 0.65\times10^{19}$	30	0.436	0.196	0.0935	0.058	0.117	0.870×10^{-1}
	50	0.465	0.162	0.0973	0.064	0.125	0.956×10^{-1}

3.3.1. *Width*. The values of the three components of the width, corresponding to the different perturbers, and the total Stark width increase with the temperature in the examined interval (perturber density 10^{16} cm^{-3}). The temperature dependence of the electron width is illustrated in figure 1.

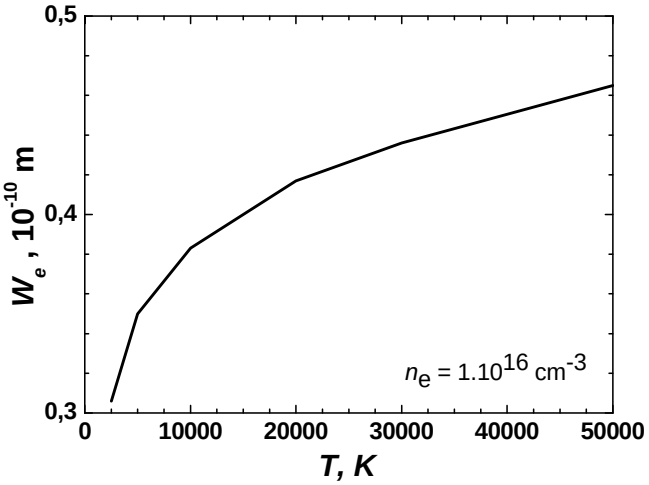

Figure 1. Electron impact width of the Ne I 837.7 nm spectral line versus the temperature for electron density 10^{16} cm^{-3}.

In ordinary stellar plasma for temperatures $(0.25 - 5)\times10^4$ K and at an electron density 10^{16} cm^{-3}, the contribution of the collisions between neon emitters and electrons in the total Stark width is 77 – 79 %, of emitters-helium ions collisions – 1–2 %, and the contribution of the emitters-protons is 19–20 %.

3.3.2. *Shift.* The electronic component of the shift due to the collisions between the emitters and electrons increases with the temperature up to near 10^4 K and after that decreases. This dependency governs the temperature variation of the total Stark shift, as it is shown in figure 2. The values of the shift due to the collisions of the emitters with the helium ions and protons increase with the temperature in the considered temperature interval.

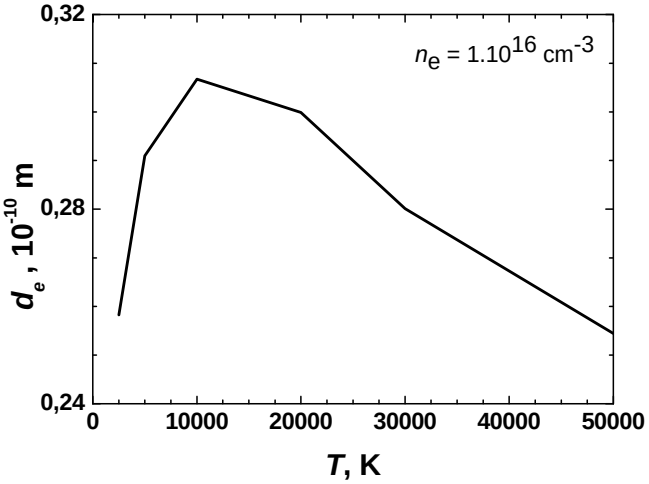

Figure 2. Electron impact shift of Ne I 837.7 nm spectral line versus the temperature for electron density 10^{16} cm^{-3}.

For ordinary stellar plasmas, for example in the temperature interval $(0.25 - 5)\times10^4$ K and at an electron density 10^{16} cm^{-3}, the contribution of the collisions between neon emitters and electrons in the total Stark shift is 64–81 %, this one of the emitters-helium ions collisions – 1–2.5 %, and the contribution of the emitters-protons is 17–33 %.

A complete analysis of the obtained results and a comparison with the theoretical and experimental results available in the literature will be given in [10].

Acknowledgments
This work was partially financed by the Technical University – Sofia and is a part of the project 146001 supported by the Ministry of Science and Technological Development of Serbia.

References
[1] Sigut T A A 1999 *Astrophys. J.* **519** 303
[2] Konjević N, Lessage A, Fuhr J R and Wiese W L 2002 *J. Phys. Chem. Ref. Data* **31** 819
[3] Griem H R 1974 *Spectral line broadening by plasmas* (New York: Academic)
[4] Purić J, Srećković A, Djeniže S, Labat J and Ćirković Lj 1988 *Phys. Lett A* **126** 280
[5] del Val J A, Aparicio J A and Mar S 1999 *Astrophys. J.* **513** 535
[6] Sahal-Bréchot S 1969 *Astron. Astrophys.* **1** 91
[7] Sahal-Bréchot S 1969 *Astron. Astrophys.* **2** 322
[8] Christova M, Dimitrijević M S and Kovačević 2008 Similarities in Calculated Stark broadening Parameters of Argon Spectral Lines *J. Phys.: Conf. Ser.* Third International Workshop and Summer Scool on Plasma Physics 02
[9] http://physics.nist.gov/
[10] Christova M, Dimitrijević M S, Simić Z and Sahal-Bréchot S (to be submitted)

Journal of Physics: Conference Series **133** (2008) 012028 doi:10.1088/1742-6596/133/1/012028

Kinematical parameters in the coronal and post-coronal regions of the Oe stars

A Antoniou[1], E Danezis[1], E Lyratzi[1,2], L Č Popović[3], and M S Dimitrijević[3]

[1]University of Athens, Faculty of Physics, Department of Astrophysics, Astronomy and Mechanics, Panepistimioupoli, Zographou 157 84, Athnes – Greece
[2]Eugenides Foundation, 387 Sygrou Av., 17564, Athens, Greece
[3]Astronomical Observatory, Volgina 7, 11160 Belgrade, Serbia

e-mail: ananton@phys.uoa.gr, edanezis@phys.uoa.gr, elyratzi@phys.uoa.gr, lpopovic@aob.bg.ac.yu, mdimitrijevic@aob.bg.ac.yu

Abstract. In this progress report we present the main results of our research. Using a new model we studied the kinematical parameters such as the random velocities of the ions, which create the spectral lines of C IV, N IV and N V in the spectra of 20 Oe stars, as well as the rotational and radial velocities of the regions, where the above ions are created. We calculated the values of the above parameters and we present the relations between them as well as their variation as function of the spectral subtype. We also present the random velocities of the ions for each one of the C IV, N IV and N V regions as a function of the photospheric rotational velocities. Finally, we propose an explanation for the large widths that we observe in the studied spectral lines, as these widths can not be explained as large rotational or random velocities.

1. Introduction

The spectra of Hot Emission Stars (Oe and Be stars) contain peculiar line profiles. In order to explain this peculiarity, we propose and use the Discrete Absorptions Components (DACs) [1] and Satellite Absorptions Components (SACs) [2] theory.

DACs or SACs arise from spherical density regions surrounding the star or lying far away from it, that having spherical (or apparent spherical) symmetry around the star or its own center [3].

In the case of DACs or SACs phenomenon we need to calculate the line function of the complex line profile. Recently, our group proposed a model in order to explain the complex structure of the density regions of hot emission stars and some Active Galactic Nuclei (AGNs), where the spectral lines which have SACs or DACs are created [2,4].

As we know, in order to find the mechanism responsible for the structure of DACs or SACs density regions we need to calculate the values of a group of parameters, such as the rotational, the random and the radial velocities, the Full Width at Half Maximum (FWHM), the optical depth, the absorbed or emitted energy, the column density, and the Gaussian standard deviation, as well as the relation among them. Directly from the model we can calculate the apparent radial velocities (V_{rad}) of the absorbing or emitting density regions, the Gaussian typical deviation (σ) of the random thermal motions, the apparent rotational velocities (V_{rot}) of the absorbing or emitting density region and the optical depth (ξ) in the center of the spectral line. From the above parameters we can calculate the percentage

contribution (G%) of the random velocities to the broadening of the spectral line, the Full Width at Half Maximum (FWHM), the random velocities of the ions (V_{rand}) that produce the spectral lines, the absorbed or emitted energy (Ea, Ee) and the column density (CD).

We point out that with the proposed model we can study and reproduce specific spectral lines. This means that we can study specific density regions in the plasma surrounding the studied object.

In this paper we present some kinematical parameters of C IV, N IV and N V regions in the spectra of 20 Oe stars. We calculate the values of the rotational, random and radial velocities, the relation among them, as well as the variation of the radial velocities as a function of the spectral subtype. Finally, we give a possible explanation of the measured high values of the rotational velocities.

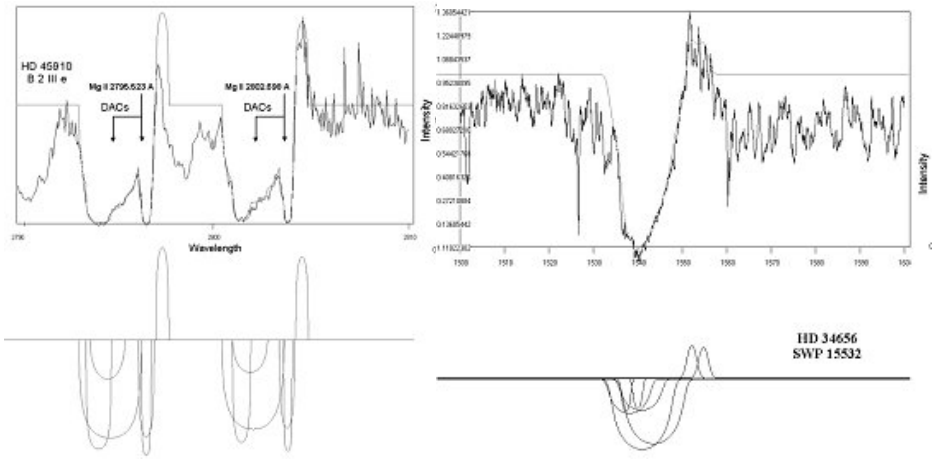

Figure 1. DACs in the spectrum of a Be star (left) and SACs in the spectrum of an Oe star (right). Below the fit one can see the decomposition of the observed profile to its DACs and SACs.

2. Observational Data

For this analysis we used the high resolution spectra (0.1 to 0.3 Å) taken with International Ultraviolet Explorer (IUE) found at the VILSPA database (http://archive.stsci.edu/cgi-bin/iue).

In Figure 1 we present the UV resonance lines of Mg II in the spectrum of HD 45910 and the UV resonance lines of C IV in the spectrum of HD 34656 which have DACs or SACs, respectively. In Table 1 we present the studied stars. As we know it is not possible to find stars between O0 and O3 spectral subtypes.

Table 1 The Studied Stars

The studied stars	Spectral subtype	The studied stars	Spectral subtype
HD24534	O9.5 III	HD57061	O9.0I
HD24912	O7.5 III ((f))	HD60848	O8.0Vpe
HD34656	O7 II (f)	HD91824	O7V((f))
HD36486	O9.5 II	HD93521	O9.5II
HD37022	O6 Vp	HD112244	O8.5Iab
HD47129	O7.5 III	HD149757	O9V(e)
HD47839	O7 III	HD164794	O4V((f))
HD48099	O6.5 V	HD203064	O8V
HD49798	O6p	HD209975	O9.5I
HD57060	O8.5If	HD210839	O6.0I

3. Studying the rotational velocities of the density layers of matter

Using the mentioned model we are able to calculate the values of the apparent rotational velocities of the independent regions which produce the main and the satellite components of the studied spectral lines.

In Figure 2 we present the rotational velocities' mean values of the ions of the C IV (λλ 1548.155, 1550.774 Å) and N V (λλ 1238.821, 1242.804 Å) resonance lines. In the C IV regions we detected two levels of values. The first level has values between 800 and 1800 kms^{-1} and the second level has values between 50 and 200 kms^{-1}. We detected the same phenomenon in the N V region. The first level has values between 1200 and 1800 kms^{-1} and the second level has values between 200 and 400 kms^{-1}.

An important phenomenon that we can detect in the UV spectra of some hot emission stars [5 - 10] are the very broad absorption or emission lines that we can not explain as rotational or random velocities of the density layers that construct these lines.

In order to explain this very large width we propose that around a central density region which produces the main absorption lines (and which may have the form of spiral streams and have accepted values of rotational and random velocities), we can detect micro-turbulent movements, which produce narrow absorption components with different shifts (see Figure 3). These narrow lines create a sequence of lines, on the left and on the right side of the main components. The density of these lines and their widths, which are added, give us the sense of line broadening (SACs phenomenon, see [4, 11]). As a result, what we measure as very broad absorption line, is the composition of the narrow absorption lines that are created by micro-turbulent effects. If this hypothesis is correct, the calculated width gives only the maximum value of the radial velocities of these very narrow components. Their appearance depends on the inclination of the rotational axis of the stellar disk.

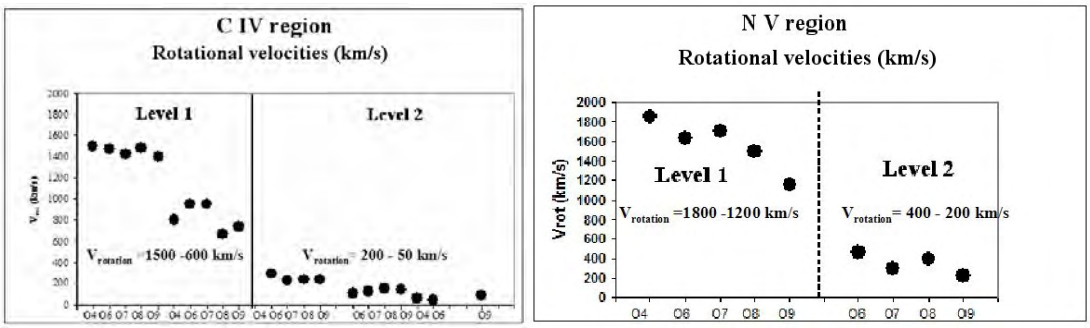

Figure 2. The rotational velocities' mean values of the ions of the C IV (λλ 1548.155, 1550.774 Å) (left) and N V (λλ 1238.821, 1242.804 Å) (right) resonance lines.

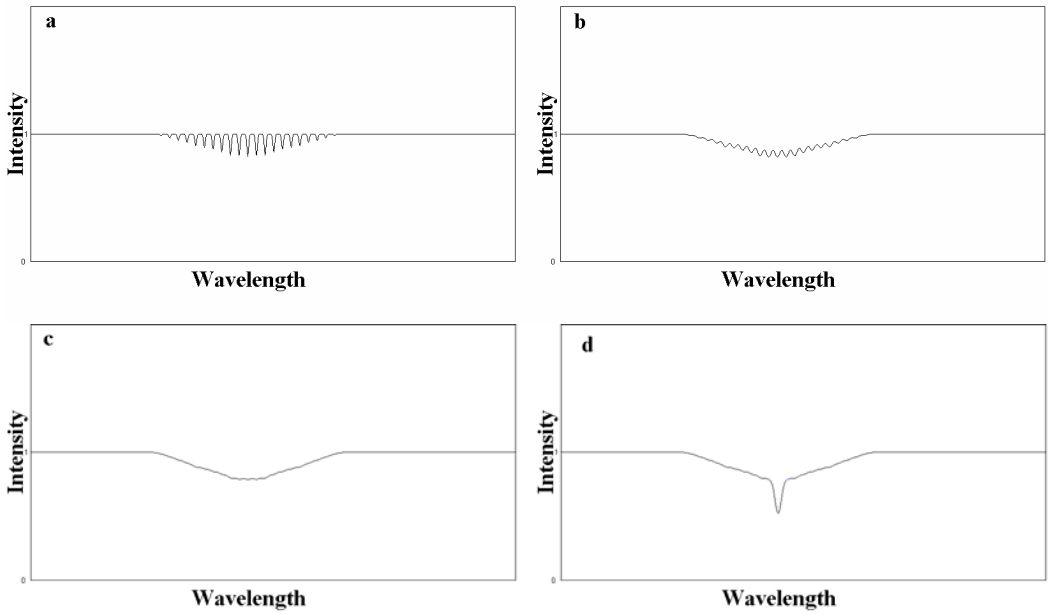

Figure 3. In (a) to (c) one can see how a sequence of lines could produce an apparent very broad absorption spectral line as an effect of SACs phenomenon. This means that when the width of each of the narrow lines is increasing (from a to c), the final observed feature looks like a single very broad absorption spectral line. In (d) one can see a combination of the apparent very broad absorption spectral line with a classical absorption line.

4. Studying the random velocities of the density layers of matter

Using our model we calculated the random velocities of the ions in the layers that produce the C IV, N IV and N V satellite components in the spectra of 20 Oe stars, which have different photospheric rotational velocities. In Figures 4, 5 and 6 we present the random velocities (V_{rand}) of the C IV, N IV and N V ions as a function of the apparent photospherical rotational velocities (V_{phot}), respectively.

In the C IV region the obtained values are about 160 kms^{-1} for the first component, 115 kms^{-1} for the second, 80 kms^{-1} for the third and 90 kms^{-1} for the fourth component. In the N IV region the obtained values are about 267 kms^{-1} for the first component and 133 kms^{-1} for the second one. Finally, in the N V region the measured values are about 190 kms^{-1} for the first component, 160 kms^{-1} for the second and 108 kms^{-1} for the third one. In each region we detected similar average values of the random velocities of the ions for each component for all the studied stars. This happens because the ionization potential of each studied ion, for all the studied stars, is the same, so the respective random velocities should be the same. As the values of the random velocities do not depend on the inclination of the rotational axis, we expect similar average values of the random velocities for each component, for all the studied stars.

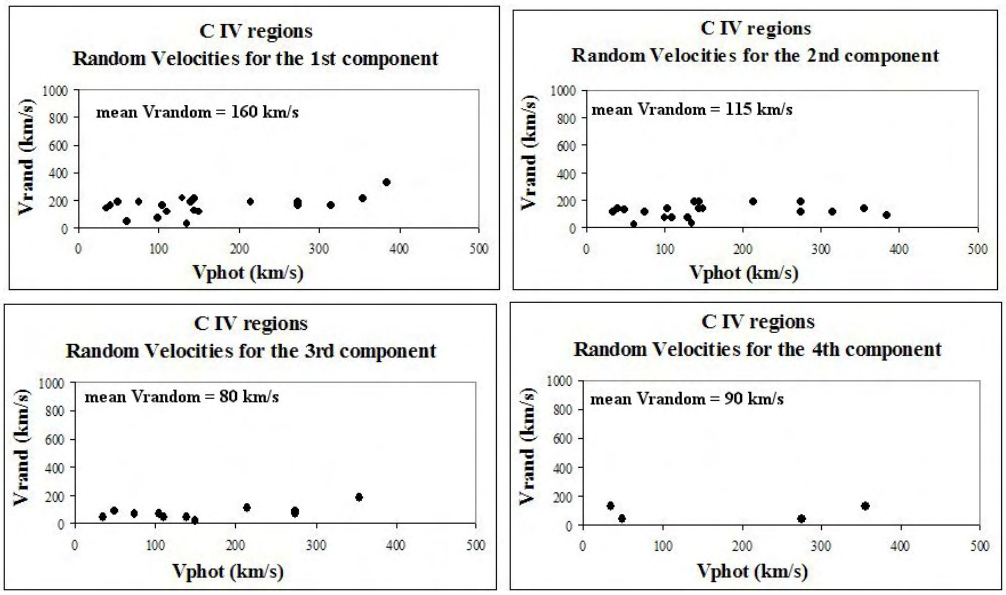

Figure 4. Random velocities (V_{rand}) of the C IV ions as a function of the apparent photospheric rotational velocities (V_{phot}).

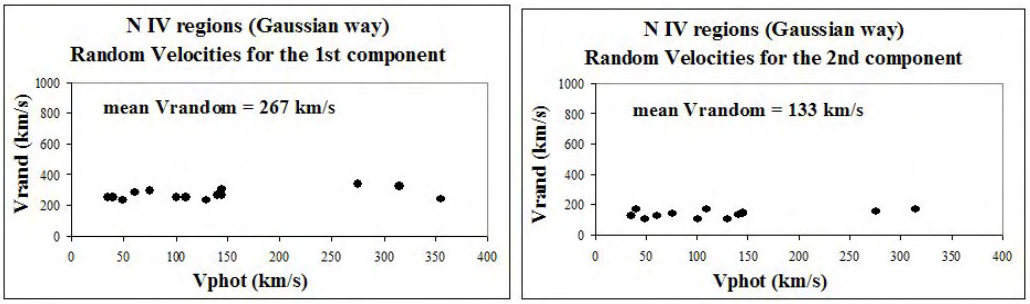

Figure 5. The same as in Figure 4 but for the N IV ions.

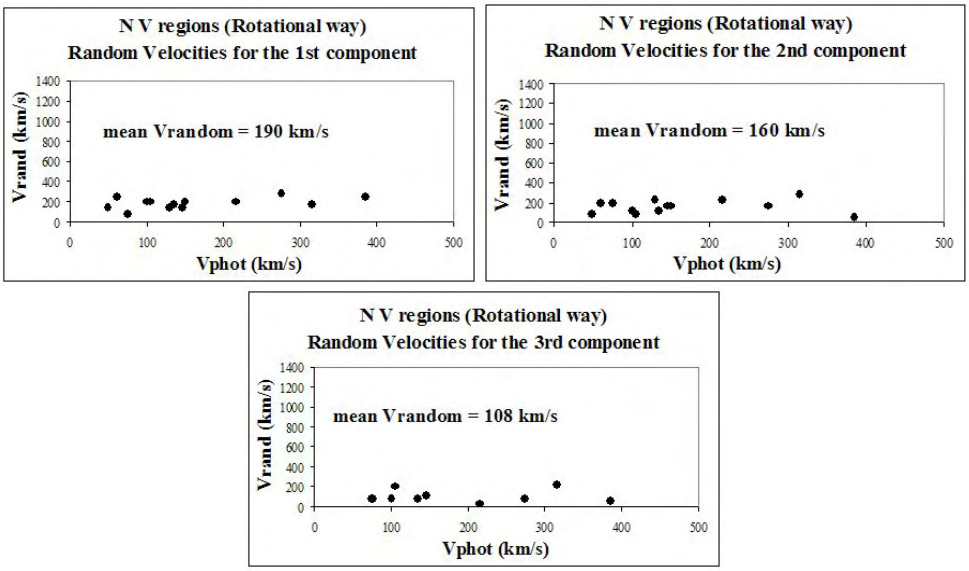

Figure 6. The same as in Figure 4 but for the N V ions.

5. Studying the relations among the kinematical parameters

In Figures 7 and 8 we present the relations among the studied kinematical parameters (V_{rand}, V_{rad}, V_{rot}), for C IV and N V density regions of the studied 20 Oe stars.

In Figure 7 we see the random (left) and the rotational velocities (right) as a function of the radial velocities in the C IV regions of the studied 20 Oe stars and in Figure 8 we present the corresponding results for the N V regions. In most cases we detect that the random and the rotational velocities increase when the absolute radial velocities increase.

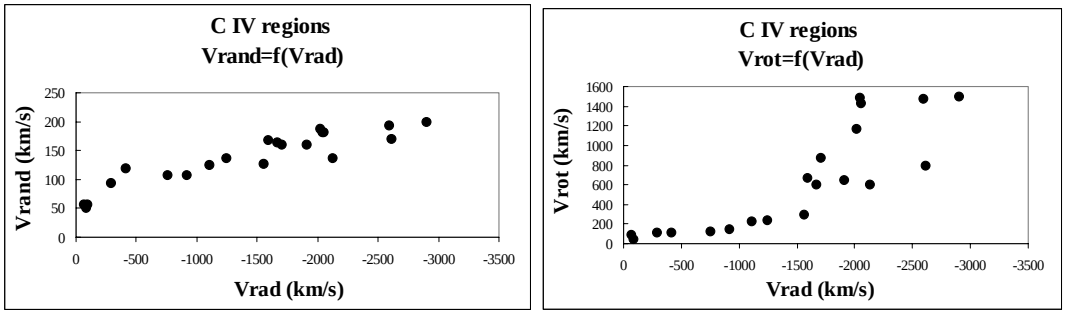

Figure 7: Random velocities (V_{rand}) (left) of the ions and rotational velocities (V_{rot}) (right) in the C IV regions, as a function of the radial velocities (V_{rad}).

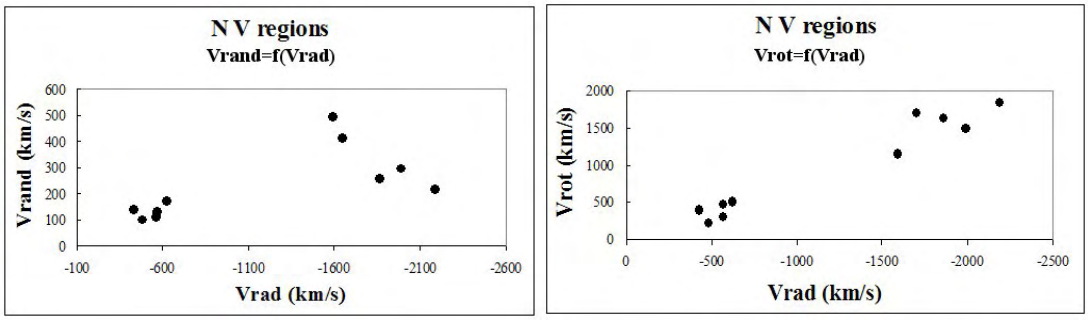

Figure 8. The same as in Figure 7 but for the N V regions.

6. Studying the radial velocities as a function of the spectral subtypes

Using the mentioned model we are able to calculate the values of the apparent radial velocities, of the independent regions which produce the main and the satellite components of the studied spectral lines as a function of spectral subtype.

In Figure 9 we present the radial velocities' mean values of the ions for the C IV (λλ 1548.155, 1550.774 Å) (left) and N V resonance lines (λλ 1238.821, 1242.804 Å) (right) as a function of the spectral subtype. In the C IV region we detected two levels of radial velocities. The first level has values between -3000 and -1500 kms^{-1} and the second one between -500 and -20 kms^{-1}. In the N V region we also detected two levels of values. The first level has values between -2300 and -1500 kms^{-1} and the second one between -500 and -100 kms^{-1}. There are two mechanisms which may create the radial velocities. One of these mechanisms creates high radial velocities and the second one low [2]. From many observations of Be stars, it has become clear over the last decade(s) that the slow part of the wind is equatorially condensed in a disk-like structure. Fore the hottest Be stars this disk co-exists with a fast stellar wind (most likely at higher latitudes). In this fast wind DACs are seen at high velocities (more than 1000km/s towards the observer). The fast winds are radiation driven from relatively slow speeds near the star, to very high speeds far away from the star.

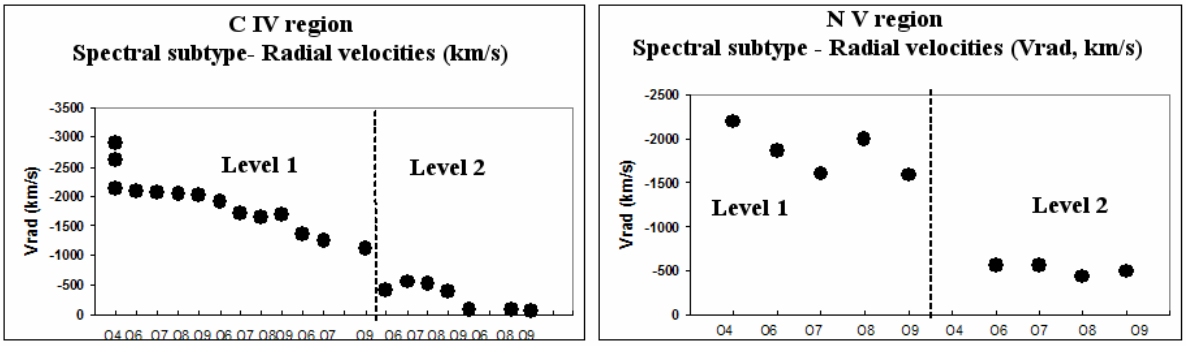

Figure 9. Radial velocities (V_{rad}) in the C IV region (left) and in the N V region (right) as a function of the spectral subtype. We detect two levels of radial velocities in both regions. The first level has high values (between -3000 and -1500 kms^{-1} in the C IV region and between -2300 and -1500 kms^{-1} in the N V region) and the second level has low values (between -500 and -20 kms^{-1} in the C IV region and between -500 and -100 kms^{-1} in the N V region).

7. Conclusions

The results deriving from this study are the following:

1. Using the proposed model, we can calculate the values of some parameters, such as the rotational, the random and the radial velocities, the FWHM, the optical depth, the absorbed or emitted energy, the column density and the Gaussian typical deviation, as well as the relation among them. This means that now we can try to understand the mechanism that is responsible for the DACs or SACs phenomenon.
2. The acceptance of SACs and DACs phenomena as the reason of the spectral line complex structure lead us to accept smaller values of the FWHM, the rotational and random velocities and the column densities and different values for the radial velocities and the optical depths because now the idea is that the complex line profile does not present a single spectral line, but a group of satellite components (DACs or SACs). This idea leads us to a different mechanism for the construction of the density regions that produce the DACs or SACs regions.
3. Finally, we propose an explanation for the large widths that we observe in the studied spectral lines, as these widths can not be explained as large rotational or random velocities. Around a central density region that produces the main absorption lines (that may have the form of spiral streams and which have accepted values of rotational and random velocities), we can detect micro-turbulent movements, which produce narrow absorption components with different shifts. These narrow lines create a sequence of lines, on the left and on the right of the main components. The density of these lines and their widths, which are superposed, give us the sense of line broadening [12]. As a result, what we measure as very broad absorption line, is the composition of the narrow absorption lines that are created by micro-turbulent effects. If this hypothesis is correct, the calculated width gives only the maximum value of the radial velocities of these very narrow components. Their appearance depends on the inclination of the rotational axis of the stellar disk.

Acknowledgments

This research project is progressing at the University of Athens, Department of Astrophysics, Astronomy and Mechanics, under the financial support of the Special Account for Research Grants, which we thank very much. This work also was supported by Ministry of Science Technological Development of Serbia and, through the projects “Influence of collisional processes on astrophysical plasma line shapes” and “Astrophysical spectroscopy of extragalactic objects”.

References

[1] Bates B and Halliwell D R 1986 *Mon. Not. R. Astr. Soc.* **223** 673
[2] Danezis E, Nikolaidis D, Lyratzi E, Antoniou A, Popović L Č and Dimitrijević M S 2005 *Mem. Soc. It. Suppl.* **7** 107
[3] Lyratzi E, Danezis E, Popović L Č, Dimitrijević M S, Nikolaidis D and Antoniou A 2007 *Publ. Astron. Soc. Japan* **59** 357
[4] Danezis E, Nikolaidis D, Lyratzi E, Popović L Č, Dimitrijević M S, Antoniou A and Theodosiou E 2007 *Publ. Astron. Soc. Japan* **59** 827
[5] Andrillat Y and Fehrenbach Ch 1982 *Astron. Astrophys.* **48** 93
[6] Andrillat Y 1983 *Astron. Astrophys*. **53** 319
[7] Marlborough J M 1969 *Astrophys. J*. **156** 135
[8] Poeckert R, Marlborough J M 1979 *Astrophys. J.* **233** 259
[9] Doazan V 1970 *Astron. Astrophys.* **8** 148
[10] Antoniou A, Danezis E, Lyratzi E, Popović L Č, Dimitrijević M S 2008 *Publ. Astron. Soc. Japan* (submitted)
[11] Lyratzi E and Danezis E 2004 *AIP Conf. Proc.***740** 458
[12] Danezis E, Lyratzi E, Popović L Č, Antoniou A and Dimitrijević M S 2008 *Publ. Astron. Obs. Belgrade* **84** 463

Journal of Physics: Conference Series **257** (2010) 012032 doi:10.1088/1742-6596/257/1/012032

European Virtual Atomic Data Centre - VAMDC

Milan S Dimitrijević[1], Sylvie Sahal-Bréchot[2], Andjelka Kovačević[3], Darko Jevremović[1], Luka Č. Popović[1]
[1]Astronomical Observatory, Volgina 7, 11060 Belgrade, Serbia

[2] Paris Observatory, CNRS-UMR8112 and University Pierre et Marie Curie, LERMA, 5 Place Jules Janssen, 92190 Meudon, France

[3]Department of Astronomy, Faculty of Mathematics, Studentski Trg 15, 11000 Belgrade, Serbia

mdimitrijevic@aob.bg.ac.rs, sylvie.sahal-brechot@obspm.fr, andjelka@matf.bg.ac.rs

Abstract.
The Virtual Atomic and Molecular Data Centre (http://www.vamdc.eu, VAMDC) is an European Union funded FP7 project aiming to build a secure, documented, flexible and interoperable e-science environment-based interface to existing atomic and molecular data. It will also provide a forum for training potential users and dissemination of expertise worldwide. This review describes the VAMDC project and its objectives.

1. Introduction

Reliable atomic and molecular data are of critical importance for different applications in astrophysics, atmospheric physics, fusion, environmental sciences, combustion chemistry, and in industrial applications from plasmas and lasers to lighting. Resources of such data are highly fragmented, presented in different, non-standardized ways, available through a variety of highly specialized and often poorly documented interfaces, so that their full exploitation is limited, which make difficulties in many research fields like for example the understanding the chemistry of Solar system and of the wider universe, the study of the terrestrial atmosphere, the development of the fusion rersearch, lasers etc.

The development of powerful computers stimulates the development of atomic data on a large scale. The modelling of stellar atmospheres and of the stellar interiors needs extensive sets of atomic data, including collisional broadening. For example, the PHOENIX computer code [1] developed for stellar modelling includes a database containing more than 10^7 atomic, ionic and molecular spectral lines.

The development of satellite astronomy, providing a huge amount of high quality astronomical spectra produced an information avalanche and leaded to the creation of huge data collections as e. g. IUE and HST archive. For example Sloan Digital Sky Survey SDSS, contains spectra of ~ 230 million objects. The problem is how to analyse such amount of data?

The idea of Virtual Observatory was formulated at the end of 2000, and from 2001 the FP5 project Astrophysical Virtual Observatory – AVO was the basis for creation of European Virtual Observatory - EURO-VO (http://www.euro-vo.org).

Virtual observatories today combine research in different areas of astrophysics (some of which are fairly new): multi-wavelength astrophysics, archival research, survey astronomy, temporal astronomy, theory and simulations (comparisons with observations) and information technology, digital detectors, massive data storage, the Internet, data representation standards.

In order to facilitate the international coordination and collaboration necessary for the development and deployment of the tools, systems and organizational structures necessary to enable the international utilization of astronomical archives as an integrated and interoperating virtual observatory, International Virtual Observatory Alliance (IVOA, http://www.ivoa.net) was formed in June of 2002. So the work of the IVOA mainly focuses on the development of standards.

SerVO - Serbian virtual observatory (http://www.servo.aob.rs/~darko) is a project whose funding was approved through a grant TR13022 from Ministry of Science and Technological Development of Republic of Serbia [2]. The project objectives are: a) Establishing SerVO and join the EuroVO and IVOA; b) Establishing SerVO data Center for digitizing, archiving and publishing in VO format photo-plates [3] and other astronomical data produced at Belgrade Astronomical Observatory; c) Development of tools for visualization of data; d) Publishing, together with Observatoire de Paris, STARK-B - Stark broadening data base containing as the first step Stark broadening parameters obtained within the semiclassical perturbation approach by two of us (MSD-SSB) in VO compatible format; e) Make a mirror site for DSED (Darthmouth Stellar Evolution Database [4,5] in the context of VO.

2. VAMDC – Virtual Atomic and Molecular Data Centre

In order to enable an efficacious and convenient search for available atomic and molecular data and their adequate use, we should try to solve existing problems in A&M data community, preventing productive search and data mining, which leaded to the VAMDC Idea. Main of such problems are: a) Lack of standards and common guidelines; b) Interoperability problem. c) Data exchange problem. Namely data exchange is often informal, via e-mails, ASCII files… without a standardization; d) Overlapping of efforts; e) Need of hiring computer engineers since the majority of developers are Astronomers, Physicists, Chemists; f) Data identification problem - XML schemata keys not only for data exchange but also for data identification; g) Need for a critical evaluation of data.

This means that at present, every time the same A&M database is used for a new application, the output has to be adapted. For example if we want to develop automatic tools for the visualisation of simulations of planetary, stellar or the interstellar medium spectra, this will require automatic access to different A&M databases, cross-matching the retrieved data as well as checking the quality of data. For such a purpose there is no actually a coherent and sufficiently general infrastructure to perform such tasks.

Additionally, if we want to enable an efficacious search for A&M data, we have a need for the:

-Creation of search engines that must look “everywhere” in order to map A&M Universe;

-An accessible and interoperable e-infrastructure for A&M data.

Very useful will be also the creation of a forum of data producers, data users and databases developers, as well as the training of potential users in European Research Area and wider.

All above mentioned problems will address Virtual Atomic and Molecular Data Centre (VAMDC – [6]), a FP7 founded project which started on July 1 2009 with budget of 2.9 MEuros over 42 months. Its aim is to build accessible and interoperable e-infrastructure for atomic and molecular data upgrading and integrating European (and wider) A&M database services and catering for the needs of variety of data users in science, research and development, and industry.

The VAMDC will build a secure, documented, flexible, easily accessible and interoperable e-infrastructure for A&M data that on the one hand can directly extract data from the existing depositories, while on the other hand be sufficiently flexible to be tuned to the needs of a wide variety of users from academic, governmental, industrial communities or by the general public.

The starting points are infrastructure and capabilities developed by EURO-VO (Virtual Observatory) EGEE (**E**nabling **G**rids for **E**-scienc**E**) and Astrogrid and a series of network and service

activities will be organized in order to establish self-sustainable computational and data mining services. It has the specific aim of creating an infrastructure

The VAMDC can be understood as a publisher infrastructure. The VAMDC will deploy yellow pages (registries) in order to find resources, design user applications in order to meet the user needs, build data access layers above databases to provide unified outputs from these databases, care about asynchronous queries with workflows and the storage of large quantity of data with VO space, and connect its infrastructure to the grid.

VAMDC

Virtual Atomic and Molecular Data Centre

Fig. 1 VAMDC logo.

In fulfilling these aims, the VAMDC project will organise a series of Networking Activities specifically aimed at engaging data providers, coordinating activities among existing database providers, ascertaining and responding to the needs of different user communities and providing training and awareness of the VAMDC across the international A&M community and communities of other users.

Project leader is Marie-Lise Dubernet from Observatoire de Paris and core consortium is made of 15 institutions with 24 scientific groups from France, Serbia, Russia, England, Austria, Italia, Germany, Sweden and Venezuela.

Partners in the Consortium of the Project are: 1) The coordinator, Centre National de Recherche Scientifique - CNRS (Université Pierre et Marie Curie, Paris; Observatoire de Paris; Université de Reims; Université Joseph Fourier de Grenoble, Université de Bordeaux 1: Université de Bourgogne, Dijon; Université Toulouse 3); 2) The Chancellor, Masters and Scholars of the University of Cambridge – CMSUC; 3) University College London – UCL; 4) Open University – OU (Milton Keynes, England); 5) Universitaet Wien - UNIVIE; 6) Uppsala Universitet – UU; 7) Universitaet zu Koeln – KOLN; 8) Istituto Nazionale di Astrofisica – INAF (Catania, Cagliari); 9) Queen's University Belfast – QUB; 10) Astronomska Opservatorija - AOB (Belgrade, Serbia); 11) Institute of Spectroscopy RAS – ISRAN (Troitsk, Russia); 12) Russian Federal Nuclear Center - All-Russian Institute of Technical Physics - RFNC-VNIITF (Snezhinsk, Chelyabinsk Region, Russia); 13) Institute of Atmospheric Optics - IAO (Tomsk, Russia); 14) Corporacion Parque tecnologico de Merida – IVIC (Merida, Venezuela); 15) Institute for Astronomy RAS - INASAN (Moscow, Russia).

External VAMDC partner is also NIST – National Institute for Standards and Technology in Washington.

The main users of VAMDC facilities will be Astronomy, Plasma science, Atmospheric Science Radiation science and Fusion community as well as Industries using technological plasmas and Lightning industry

3. Databases

The core of the VAMDC e-infrastructure is the databases upon which it is based. The actual (the number will change) databases are shortly described below.

VALD database [7] of atomic data for analysis of radiation from astrophysical objects, developed and maintained by researchers at 7 European institutes, is created in 1995 in Vienna. The main nodes are in Vienna, Uppsala and Moscow, where are the three mirror sites . VALD contains a vast collection of spectral line parameters (central wavelengths, energy levels, statistical weights, transition probabilities, line broadening parameters) for all chemical elements of astronomical importance (http://vald.astro.univie.ac.at/).

CHIANTI [8] is an atomic database for spectroscopic diagnostics of astrophysical plasmas. Created in 1997, it contains critically evaluated set of up-to-date atomic data for the analysis of optically thin collisionally ionised astrophysical plasmas and is the preferred reference database in solar physics. It lists experimental and calculated wavelengths, radiative data and rates for electron and proton collisions (http://sohowww.nascom.nasa.gov/solarsoft, http:// www.damtp.cam.ac.uk/ user/ astro/chianti/)

EMol Database [9], at the Open University in Milton Keynes, contains a comprehensive listing of critically evaluated and regularly updated measured and calculated cross sections for electron interactions with molecular systems. It is of interest for the plasma industry, and for the disciplines of discharge physics, fusion, aeronomy and radiation chemistry. It also offers a suite of semi-empirical theoretical methods so that cross sections may be evaluated for targets for which there are currently no experimental data.

CDMS - Cologne Database for Molecular Spectroscopy (http://www.ph1.uni-koeln. de/ vorhersagen/) provides recommendations for spectroscopic transition frequencies and intensities for atoms and molecules of astronomical interest and for studying the Earth atmosphere in the frequency range 0-10 THz, i.e. 0-340 cm^{-1}. The CDMS is cross correlated with its US counterpart, the JPL Jet Propulsion Laboratory Submillimeter Catalogue (http://spec.jpl.nasa.gov/) [10].

BASECOL database [11] (http://basecol.obspm.fr) contains excitation rate coefficients for ro-vibrational excitation of molecules by electrons, He and H_2 and it is mainly used for the study of interstellar, circumstellar and cometary atmospheres.

GhoSST (Grenoble astrophysics and planetology Solid Spectroscopy and Thermodynamics, http://ghosst.obs.ujf-grenoble.fr) database service, offers spectroscopic laboratory data on molecular and atomic solids and liquids from the near UV to the far-infrared.

UMIST - University of Manchester Institute of Science and Technology (UMIST) database for astrochemistry [12] (http://www.udfa.net/), created [13] in 1991, provides reaction rate data and related software for chemical kinetic modelling of astronomical regions.

KIDA - KInetic Database for Astrochemistry will contain data on chemical reactions used in the modelling of the chemistry in the interstellar medium and in planetary atmospheres. A preliminary version was released in June 2009 (http://kida.obs.u-bordeaux1.fr).

PAHs (Polycyclic Aromatic Hydrocarbon) and carbon clusters spectral database (http://astrochemisty.ca.astro.it/database/) in Cagliari, is developed by the CESR (Centre d'Etude Spatiale des Rayonnements/CNRS), and provides a number of properties for a sample of presently about 60 species in four charge states: anion, neutral, cation and dication [14]. The properties include general energetic such as electron affinity and ionisation energies, static polarizability, permanent dipole moment, van der Waals coefficients, symmetry, multiplicity, and optimised geometry of the ground electronic state; harmonic vibrational analyses, i. e. normal modes, their frequencies and IR activities; and vertical electronic photoabsorption cross-sections and complex frequency-dependent electronic polarisabilities in the linear regime.

LASP (Laboratorio di Astrofisica Sperimentale) Database (http://web.ct.astro.it/weblab/ dbindex.html#dbindex) at the INAF (Istituto Nazionale di Astrofisica) - Catania Astrophysical Observatory, contains (i) infrared (IR) spectra of molecules in the solid phase for both pure species and their mixtures before and after processing with energetic ions and UV photons [15, 16, 17] (ii) IR

optical constants of molecules in the solid phase and after processing with energetic ions [18, 19]; (iii) band strengths of the IR absorption bands [20, 21]; and (iv) density values of frozen samples [21,22].

Spectr-W^3 [23] atomic database (http://spectr-w3.snz.ru), created in 2002 in collaboration between the Russian Federal Nuclear Centre All-Russian Institute of Technical Physics (RFNC VNIITF - Snezhinsk, Chelyabinsk Region, Russia) and the Institute for High Energy Densities of the Joint Institute for High Temperatures of the Russian Academy of Sciences (IHED JIHT RAS - Moscow). It lists experimental, calculated, and compiled data on ionization potentials, energy levels, wavelengths, radiation transition probabilities and oscillator strengths, and also parameters for analytic approximations for electron-collision cross-sections and rates for atoms and ions.

The V.E. Zuev Institute of Atmospheric Optics (IAO) in Tomsk (http://www.iao.ru/) hosts the following databases:

CDSD - The Carbon Dioxide Spectroscopic Databank [24] (http://cdsd.iao.ru and ftp://ftp.iao.ru/pub/CDSD-2008), containing calculated spectral line parameters for seven isotopologues of carbon dioxide

S&MPO - Spectroscopy & Molecular Properties of Ozone) relational database [25] (http://ozone.iao.ru and http://ozone.univ-reims.fr/), developed in collaboration with the University of Reims, contains spectral line parameters for the ozone molecule, experimental UV cross-sections, information on ozone's molecular properties, updated reference lists classified by type as well as programs and extended facilities for user applications.

"Spectroscopy of Atmospheric Gases" (http://spectra.iao.ru), containing the well-known databases such as HITRAN [25], GEISA [26] and HITEMP [27]. Both "Spectroscopy of Atmospheric Gases" and S&MPO have the programs for simulation of synthetic spectra from microwave to visible wavelengths.

W@DIS - Water Internet @ccessible Distributed Information System (http://wadis.saga.iao.ru) lists experimental water-vapour spectroscopy data from the literature and calculated line lists. W@DIS contains energy levels, transition positions and line intensities, and line profile characteristics.

Databases under the management of Corporacion Parque tecnologico de Merida – IVIC (Instituto Venezoelano de Investigaciones Scientificas) and CeCalCULA (Centro Nacional de Cálculo Científico de la Universidad de Los Andes).

TIPTOPbase [28] located at the Centre de Données astronomiques de Strasbourg, France (http://cdsweb.u-strasbg.fr/topbase/home.html), contains:

TOPbase (http://cdsweb.u-strasbg.fr/topbase/topbase.html), listing atomic data computed in the Opacity Projec, namely LS-coupling energy levels, gf-values and photoionization cross sections for light elements ($Z \leq 26$) of astrophysical interest.

TIPbase (http://cdsweb.u-strasbg.fr/tipbase/home.html). Intermediate-coupling energy levels, A-values and electron impact excitation cross sections and rates for astrophysical applications ($Z \leq 28$), computed by the IRON Project.

OPserver [29], located at the Ohio Supercomputer Center, USA, (http://opacities.osc.edu/), a remote, interactive server for the computation of mean opacities for stellar modelling using the monochromatic opacities computed by the Opacity Project.

Within VAMDC e-infrastructure are also:

XSTAR database [30], used by the XSTAR code (http://heasarc.gsfc.nasa.gov/ docs/software/ xstar/xstar.html) for modelling photoionised plasmas.

HITRAN - HIgh-resolution TRANsmission molecular absorption database [25] (http://www.cfa.harvard.edu/hitran/), used extensively by the atmospheric and planetology research communities. It lists individual line parameters for molecules in the gas phase (microwave through to the UV), photoabsorption cross-sections for many molecules, and refractive indices of several atmospheric aerosols.

GEISA - Gestion et Etude des Informations Spectroscopiques Atmosphériques (Management and Study of Atmospheric Spectroscopic Information) database [26] (http://ara.lmd.polytechnique.fr/index.php?page=geisa-2 or http://ether.ipsl.jussieu.fr/etherTypo/?id=950) is a computer accessible

database system, designed to facilitate accurate and fast forward, calculations of atmospheric radiative transfer.

HITEMP, a high temperature extension to HITRAN [27] (To access the HITEMP data: ftp to cfa-ftp.harvard.edu; user = anonymous; password = e-mail address). So far HITEMP contains data for water, CO_2, CO, NO and OH.

The external partner of VAMDC is NIST - National Institute of Standards and Technology, a major centre for atomic and molecular data compilation, which has developed a number of numerical and bibliographic atomic and molecular databases. Among others it hosts:

Atomic Spectra Database (http://physics.nist.gov/asd3) listing critically evaluated data on about 77,000 energy levels and 144,000 spectral lines from atoms and ions of 99 elements.

The Handbook of Atomic Spectroscopic Data [31] (http://physics.nist.gov/Handbook) listing energy levels and prominent spectral lines for neutral and singly ionised atoms.

The Spectral Data for the Chandra X-Ray Observatory database [32] (http://physics.nist.gov/chandra) presenting critically compiled wavelengths (20 A to 170 A), energy levels, line classifications, and transition probabilities for several astrophysically important elements.

SAHA, The NLTE plasma population kinetic modeling database containing theoretical data [33, 34]. (http://nlte.nist.gov/SAHA).

Three bibliographic databases providing references on atomic energy levels and spectra (http://physics.nist.gov/cgi-bin/ASBib1/ELevBib.cgi), transition probabilities (http://physics.nist.gov/cgi-bin/ASBib1/TransProbBib.cgi) and spectral line shapes and line broadening (http://physics.nist.gov/cgi-bin/ASBib1/LineBroadBib.cgi.).

4.STARK-B database

Our contribution to the VAMDC e-infrastructure is the STARK-B database (http://stark-b.obspm.fr) [35], a collaborative project between Laboratoire d'Etude du Rayonnement et de la matière en Astrophysique of the Observatoire de Paris-Meudon and the Astronomical Observatory of Belgrade. This is a database of the theoretical widths and shifts of isolated lines of atoms and ions due to collisions with charged perurbers, obtained within the impact approximation. For the moment STARK-B contains results obtained using the semiclassical perturbation approach [36,37]. The corresponding computer code has been optimized and updated in Refs. [38, 39, 40] and following papers. For the review and all updates see e.g. Ref. [41].

This database is devoted to modelling and spectroscopic diagnostics of stellar atmospheres and envelopes. In addition, it is also relevant to laboratory plasmas, laser equipment and technological plasmas. The database is currently developed in Paris, and a mirror is planned in Belgrade. It is already on line though not yet complete. It is described in detail in Ref. [35].

The precursor of STARK-B as well as of SerVO was BELDATA and its main content was database on Stark broadening parameters. A history of BELDATA can be traced in Refs [42, 43, 44, 45, 46, 47].

The participants of AOB (Astronomical Observatory – Belgrade) VAMDC Node are: Milan S. Dimitrijević, Luka Č. Popović, Andjelka Kovačević, Darko Jevremović, Zoran Simić, Edi Bon and Nenad Milovanović.

We also have a close collaboration with Sylvie Sahal-Bréchot from Paris Observatory, Nebil Ben Nessib, Walid Mahmoudi, Rafik Hamdi, Haykel Elabidi, Besma Zmerli and Neila Larbi-Terzi from Tunisia, Magdalena Christova from Technical University of Sofia and Tanya Ryabchikova from Institute of Theoretical Astronomy in Moscow.

Initiatives like VAMDC are important for both producers of atomic and molecular data and stellar atmosphere modellers as one of prime users. VAMDC is an example of the global collaborations and innovations in e-science. It is expected to become one of major European cyber-infrastructures with a world wide impact.

Acknowledgments

A part of this work has been supported by VAMDC, funded under the "Combination of Collaborative Projects and Coordination and Support Actions" Funding Scheme of The Seventh Framework Program. Call topic: INFRA-2008-1.2.2 Scientific Data Infrastructure. Grant Agreement number: 239108. The authors are also grateful for the support provided by Ministry of Science and Development of Republic of Serbia through projects TR13022 "Serbian Virtual Observatory", 146001 "Influence of collisional processes on astrophysical plasma spectra" and 146002 "Astrophysical Spectroscopy of Extragalactic Objects".

References

[1] Bildsten S, Chang P and Paerels P 2003 *Astrophys. J*. **591** L2936.
[2] Jevremović D, Dimitrijević MS, Popović LČ, et al. 2009, *New Astron. Rev*. **53** 222.
[3] Tsvetkova K, Tsvetkov M, Protić-Benišek V and Dimitrijević MS 2009 *Publ. Astron. Soc. "Rudjer Bošković"* **9** 255.
[4] Dotter A, Chaboyer B, Ferguson JW, Lee H-C, Worthey G, Jevremović D and Baron E 2007 *Astrophys. J.* **666** 403.
[5] Dotter A, Chaboyer B, Jevremović D, Kostov V, Baron E and Ferguson JW 2008 *Astrophys. J. Suppl*. **178** 89.
[6] Dubernet ML, Boudon V, Culhane JL, et al. 2010 *JQSRT* **111** 2151
[7] Kupka F, Piskunov N, Ryabchikova TA, Stempels HC and Weiss WW 1999 VALD-2: Progress of the Vienna Atomic Line Data Base *Astron. Astrophys. Sup. Ser*. **138** 119.
[8] Dere KP, Landi E, Young PR, Del Zanna G, Landini M and Mason HE 2009 CHIANTI - an atomic database for emission lines IX. Ionization rates, recombination rates, ionization equilibria for the elements hydrogen through zinc and updated atomic data *Astron Astrophys.* **498** 915.
[9] Mason NJ 2007 Electron Induced Processing; Applications and Data Needs, Proceedings of ICAMDATA06, AIP Conference proceedings **901** 74.
[10] Müller HSP, Schlöder F, Stutzki J and Winnewisser G 2005, The Cologne Database for Molecular Spectroscopy, CDMS: a useful tool for astronomers and spectroscopists *J. Mol. Struct*. **742** 215.
[11] Dubernet ML, Grosjean A, Daniel F, Flower D, Roueff E, Daniel F, Moreau N and Debray B 2006 Ro-vibrational Collisional Excitation Database BASECOL, Proceedings Joint Meeting ITC14 and ICAMDATA 2004, Toki, Japan *Journal of Plasma and Fusion Research* **7** 356.
[12] Woodall J, Agundez M, Markwick-Kemper AJ and Millar TJ 2007 The UMIST database for astrochemistry *Astron. Astrophys*. **466** 1197.
[13] Millar TJ, Rawlings JMC, Bennett A, Brown PD and Charnley SB 1991 Gas-phase reactions and rate coefficients for use in astrochemistry – the UMIST ratefile *Astron. Astrophys. Suppl. Ser*. **87** 585.
[14] Malloci G, Joblin C and Mulas G 2007 On-line database of the spectral properties of polycyclic aromatic hydrocarbons *Chem. Phys*. **332** 353.
[15] Strazzulla G, Leto G and Palumbo ME 1993 *Adv. Space Res.* **13** 189.
[16] Palumbo ME, Baratta GA, Fulvio D, Garozzo M, Gomis O, Leto G, Spinella F and Strazzulla G 2008 *J. Phys. Conf. Series* **101** 012002.
[17] Leto G and Baratta GA 2003 *Astron. Astrophys.* **397** 7.
[18] Palumbo ME, Baratta GA, Collings MP and McCoustra MRS 2006 *Physical Chemistry Chemical Physics* **8** 279.
[19] Brunetto R and Roush TL 2008 *Astron. Astrophys*. **481** 879.
[20] Mulas G, Baratta GA, Palumbo ME and Strazzulla G 1998 *Astron. Astrophys*. **333** 1025.
[21] Brunetto R, Caniglia G, Baratta GA and Palumbo ME 2008 *Astrophys. J.* **686** 1480.
[22] Fulvio D, Sivaraman B, Baratta GA, Palumbo ME and Mason NJ 2009 *Spectrochimica Acta Part A* **72** 1007.
[23] Faenov AY, Magunov AI, Pikuz TA, Skobelev IY, Loboda PA. Bakshayev NN, Gagarin SV,

Komosko VV, Kuznetsov KS, Markelenkov SA. Petunin SA and Popova VV 2002 Spectr-W-3 online database on atomic properties of atoms and ions, in "Atomic and Molecular Data and Their Applications", Schultz DR, Krstic PS, Ownby F (Eds.) *AIP Conf. Proc*. **636** 253.

[24] Perevalov VI and Tashkun SA. 2008 CDSD-296 (Carbon Dioxide Spectroscopic Databank): Updated and Enlarged Version for Atmospheric Applications, 10th HITRAN Database Conference, Cambridge, MA, USA.

[25] Rothman LS, Gordon IE, Barbe A, Benner DC, Bernath PF, Birk M, et al. 2009 The *HITRAN* 2008 Molecular Spectroscopic Database *JQSRT* **110** 533.

[26] Jacquinet-Husson N, Scott NA, Chedin A, et al. 2008 The GEISA spectroscopic database: Current and future archive for Earth and planetary atmosphere studies *JQSRT* **109** 1043.

[27] Rothman LS, Gordon IE, Barber RJ, Dothe H, Gamache RR, Goldman A, Perevalov VI, Tashkun SA and Tennyson J 2010 HITEMP, the High-Temperature Molecular Spectroscopic Database *JQSRT* 111 2139.

[28] Cunto W, Mendoza C, Ochsenbein F and Zeippen C 1993 TOPbase at the CDS *Astron. Astrophys.* **275** L5.

[29] Mendoza C, Seaton MJ, Buerger P, Bellorin A, Melendez M, Gonzalez J, Rodriguez LS, Delahaye F, Palacios E, Pradhan AK and Zeippen CJ 2007 OPserver: interactive online computations of opacities and radiative accelerations *Mon. Not. R. Astr. Soc.* **378** 1031.

[30] Bautista MA and Kallman TR 2001 The XSTAR atomic database *Astrophys. J. Suppl.* **134** 139.

[31] Sansonetti JE, Martin WC and Young SL 2005 *Handbook of Basic Atomic Spectroscopic Data* National Institute of Standards and Technology, Gaithersburg, MD.

[32] Podobedova LI, Musgrove A, Kelleher DE, Reader J, Wiese WL, Coursey JS and Olsen K 2003 *Spectral Data for the Chandra X-Ray Observatory*, National Institute of Standards and Technology, Gaithersburg, MD.

[33] Ralchenko Yu 2006 *NIST SAHA Plasma Kinetics Database,* National Institute of Standards and Technology, Gaithersburg, MD.

[34] Rubiano JG, Florido R, Bowen C, Lee RW and Ralchenko Yu 2007, Review of the 4th NLTE Code Comparison Workshop *High Energy Density Physics* 3 225.

[35] Sahal-Bréchot S 2010 Case studies on recent Stark broadening calculations and STARK-B database development in the framework of the European project VAMDC (Virtual Atomic and Molecular Data Centre) *J. Phys. Conf. Series* This issue.

[36] Sahal-Bréchot S 1969 *Astron. Astrophys.* **1** 91.

[37] Sahal-Bréchot S 1969 *Astron. Astrophys.* **2** 322.

[38] Sahal-Bréchot S 1974 *Astron. Astrophys.* **35** 321.

[39] Fleurier C, Sahal-Bréchot S and Chapelle J 1977 *JQSRT* **17** 595.

[40] Dimitrijević MS and Sahal-Bréchot S 1984 *JQSRT* **31** 301.

[41] Dimitrijević MS 1996 *J. Aplied Spectrosc.* **63** 684.

[42] Popović LČ, Dimitrijević MS, Milovanović N and Trajković N 1999 *Publ. Astron. Obs. Belgrade* **65** 225.

[43] Popović LČ, Dimitrijević MS, Milovanović N and Trajković N 1999 *J. Res. Phys*. **28** 307.

[44] Milovanović N, Popović LČ and Dimitrijević MS 2000 *Publ. Astron. Obs. Belgrade* **68** 117.

[45] Milovanović N, Popović LČ and Dimitrijević MS 2000 *Baltic Astron*. **9** 595.

[46] Dimitrijević MS, Popović LČ, Bon E, Bajčeta V, Jovanović P and Milovanović N 2003 *Publ. Astron. Obs. Belgrade* **75** 129.

[47] Dimitrijević MS and Popović LČ 2006, in Virtual Observatory; Plate Content Digitization, Archive Mining, Image Sequence Processing, eds. M. Tsvetkov, V. Golev, F. Murtagh, R. Molina, Heron Press Science Series, Sofia, 115.

Journal of Physics: Conference Series **257** (2010) 012035 doi:10.1088/1742-6596/257/1/012035

Studying the complex BAL profiles in the BALQSOs spectra

E. Lyratzi[1,2], E. Danezis[1], L. Č. Popović[3], A. Antoniou[1], M. S. Dimitrijević[3], and D. Stathopoulos[1]

1 University of Athens, Faculty of Physics, Department of Astrophysics, Astronomy and Mechanics, Panepistimioupoli, Zographou 157 84, Athens, Greece,

2 Eugenides Foundation, Syngrou 387, 175 64 P. Faliro, Greece

3 Astronomical Observatory, Volgina 7, 11060 Belgrade, Serbia

elyratzi@phys.uoa.gr

Abstract. Most of Broad Absorption Lines (BALs) in quasars (QSOs) present very complex profiles. This means that we cannot fit them with a known physical distribution. An idea to explain these profiles is that the dynamical systems of Broad Line Regions (BLRs) are not homogeneous but consist of a number of density regions or ion populations with different physical parameters. Each one of these density regions gives us an independent classical absorption line. If the regions that give rise to such lines rotate with large velocities and move radially with small velocities, the produced lines have large widths and small shifts. As a result they are blended among themselves as well as with the main spectral line and thus they are not discrete. Based on this idea we study the BALs of UV C IV resonance lines in the spectra of a group of Hi ionization Broad Absorption Line Quasars (Hi BALQSOs) using the Gauss-Rotation model (GR model).

1. Introduction

Approximately about 10% of all quasars present broad, blue shifted absorption lines. The outflow velocity can reach up to 0.1 0.2 c. Usually, in their spectra we observe the lines of high ionization species, as C IV λ 1549 Å, Si IV λ 1397 Å, N V λ 1240 Å and Lya. Rarely, some low ionization lines, such as Mg II λ 2798 Å and Al III λ 1857 Å, also exhibit broad absorption lines [see e.g. 1, 2]. Broad Absorption Lines (BALs) can have different shapes. Also different types of these objects may have differences in their continua [3].

One proposed explanation of the Broad Absorption Line (BAL) phenomenon is that BALQSOs (Broad Absorption Line Quasars) and non-BALQSOs are distinct populations of objects [4]. Similarly, some have argued that only low-ionization BALQSOs (LoBALs) are a different class of quasars [5].

Others suggest that BALQSOs and non-BALQSOs are the same type of quasar but viewed from different orientations [6-8] or at different stages in their life cycles [9].

The spectrum of a BALQSO is usually interpreted as a combination of (i) a broadband continuum arising from the central engine, (ii) the broad emission lines coming from the Broad Emission Line Regions (BELR), emerging near the center of the QSO and (iii) the broad absorption lines that are superposed, originating in a separate outlying region, so called Broad Absorption Line Region

(BALR) (see also [10]). However, it is also possible, that emission and absorption occur in the same line-forming region [11].

An important question is: Which are the physical connections between the BLR (Broad Line Region) and BALR? This is also important, since at least a part of the BLR seems to originate from wind of accretion disk [see 12, 13].

Another question is: Where is the BALR placed with respect to the center of a BALQSO and the BLR? To answer this question, one should investigate the kinematical properties of the emission and absorption lines.

Disk wind models [12, 14, 15] explain many properties of BAL quasars, but it is unclear if they can explain the full range of BAL profiles and column densities. BALs are caused by outflowing gas intrinsic to the quasar and are not produced by galaxies along the line of sight (as is the case for most narrow-absorption systems).

Determining whether a quasar is a BALQSO is a complicated task. The standard method is to calculate the "balnicity" index (BI), defined by Weymann et al. in [6]. A BI of zero indicates that broad absorption is absent, while a positive BI indicates not only the presence of one or more broad absorption lines but also the amount of absorption. The BI is essentially a modified equivalent width of the broad absorption line, expressed in velocity units and is defined as follows: (i) absorption should appear between 3000 and 25000 km/s blueward of C IV emission redshift and (ii) at this place and for at least 2000 km/s the absorption must fall at least 10% below the continuum. BIs can range from 0 to 20000 km/s.

We can classify the QSOs using the BI criterion in the following categories [16]:

- HiBALs: BALQSOs that present broad absorption trough just blueward of C IV emission.
- LoBALs: BALQSOs that present broad absorption troughs just blueward of both the C IV and Mg II emission lines.
- Non-BALs: BALQSOs that present no broad absorption troughs just blueward of the C IV and Mg II emission lines.
- FeLoBALs: BALQSOs with excited iron absorption features.

The 25000 km/s limit for the BI is chosen to avoid emission and absorption from Si IV. Absorption lines within 3000 km/s with width smaller than 2000 km/s are excluded to avoid contamination from absorption that might not be due to an outflow. These lines are called "associated absorption lines" [17]. Some of these associated systems are known to be intrinsic outflows, but others may simply be the result of absorption in the host galaxy or a nearby galaxy.

Here, we present some ideas in order to explain the complex structure of BALs in QSOs and especially we study the BALs of UV C IV resonance lines in the spectra of a group of Hi BALQSOs using the Gauss-Rotation model (GR model).

2. The multi-structure of BALs in QSOs

Most of BALs in QSOs present very complex profiles. This means that we cannot fit them with a known physical distribution. An idea is that the dynamical systems of BLRs are not homogeneous but consist of a number of density regions or ion populations with different physical parameters.

Each one of these density regions gives us an independent classical absorption line. If the regions that give rise to such lines rotate with large velocities and move radially with small velocities, the produced lines have large widths and small shifts. As a result they are blended among themselves as well as with the main spectral line and thus they are not discrete. A similar phenomenon can explain the very complex profiles of a great number of very broad lines in the spectra of hot emission stars [10, 18, 19].

Based on this idea we study the BALs of UV C IV resonance lines in the spectra of a group of Hi BALQSOs using the GR model [10, 18, 19].

The proposed model is relatively simple, aiming to describe the regions where the spectral lines are created. We assume that the BALR and BELR are composed of a number of successive independent absorbing/emitting density layers of matter (that originate in a disk wind). The absorbing regions have

three apparent velocities (projected on the line-of-sight of an observer): radial velocity (V_{rad}) of the BALR, random velocity of the ions (V_{rand}) in the BALR and the rotational velocity (V_{rot}) of the BALR.

3. Data

In order to study the C IV resonance lines (λλ 1548.187, 1550.772 Å) we apply the GR model to the spectra of 15 Broad Absorption Line Quasars (BALQSOs) taken from the Sloan Digital Sky Survey's Data Release 7. The SDSS imaging survey uses a wide-field multi-CCD camera [20]. The spectra cover the optical range 3800–9200 Å at a resolution of 1800–2100.

In table 1, column 1 lists the name of the QSOs, using the SDSS format of J2000.0 right ascension (hhmmss.ss) and declination (±ddmmss.s), column 2 lists the modified Julian date-plate-fiber, column 3 lists the redshift and column 4 lists the dates of observations.

Table 1. Studied BALQSOs

Object Name (SDSS)	MJD-Plate-Fiber	Redshift	Date
J015024.44+004432.99	51793-0402-485	2.00596	9/6/2000, 10:06
J015048.83+004126.29	51793-0402-505	3.70225	9/6/2000, 10:06
J021327.25-001446.92	51816-0405-197	2.39948	9/29/2000, 9:57
J023252.80-001351.17	51820-0407-158	2.03289	10/3/2000, 9:41
J023908.99-002121.42	51821-0408-179	3.74	10/4/2000, 9:38
J025331.93+001624.79	51816-0410-391	1.8214	9/24/2000, 11:26
J025747.75-000502.91	51816-0410-117	2.19139	9/24/2000, 11:26
J031828.91-001523.17	51929-0413-170	1.98447	1/20/2001, 4:23
J102517.58+003422.17	51941-0272-501	1.88842	2/1/2001, 9:30
J104109.86+001051.76	51913-0274-482	2.25924	1/4/2001, 11:00
J104152.62-001102.18	51913-0274-159	1.70876	1/4/2001, 11:00
J104841.03+000042.81	51909-0276-310	2.03044	12/31/2000, 11:08
J110041.20+003631.98	51908-0277-437	2.01143	12/30/2000, 11:19
J110736.68+000329.60	51900-0278-271	1.74162	12/22/2000, 12:12
J112602.81+003418.23	51614-0281-432	1.7819	3/11/2000, 6:52

4. Method

The relevant broadening mechanism, in the case of BALs, is the random motion of the absorbing gas, but also a part comes from the rotation caused by the massive black hole. In order to find the limits for the rotational and random velocities, we fitted the observed lines using two approaches:

1. Gauss-Rotation approach (GR approach): We assume that random motion is dominant, i.e. the random velocity is maximal and the rotational component is minimal,
2. Rotation-Gauss approach (RG approach): We assume that the rotational component is dominant.

After that we used F-test to conclude on which approach of the model is more appropriate to explain the complex absorption line profiles.

In figure 1 we give some examples of the fitted spectra. The black line corresponds to the observed spectra and the blue line corresponds to the theoretical line profiles given by the GR model. Below each fitting, the green line represents the residual, which gives the differences between the observed spectrum and the theoretical profile.

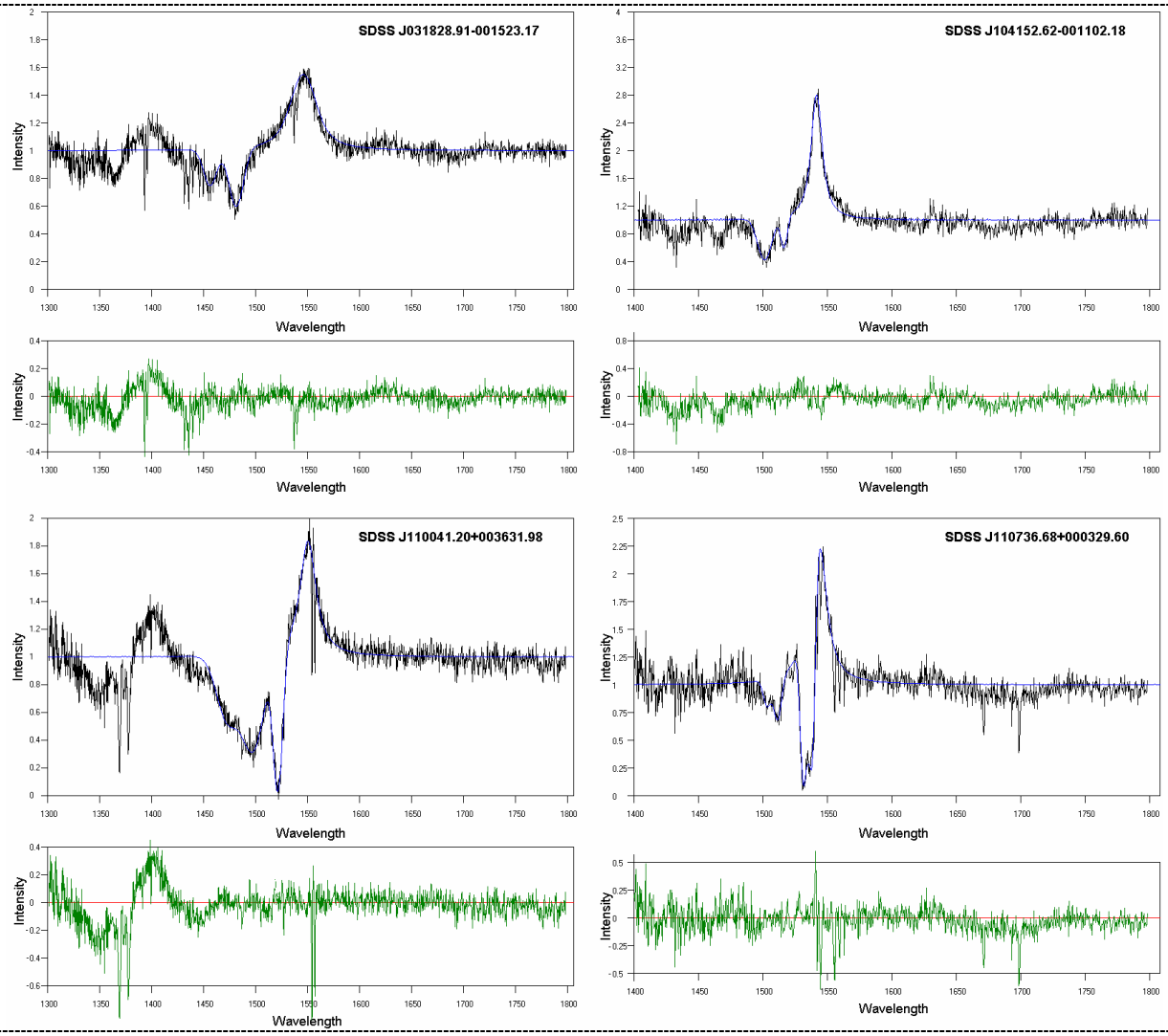

Figure 1. Examples of the fitted spectra. The black line corresponds to the observed spectra and the blue line corresponds to the theoretical line profiles given by the GR model. Below each fitting, the green line represents the residual, which gives the differences between the observed spectrum and the theoretical profile.

5. Results

Using the GR model, we were able to fit the studied C IV spectral lines with 2 up to 4 absorption components and we calculated the values of the kinematical parameters (rotational, radial and random velocities), as well as the column density and the absorbed energy. The calculated values are given in tables 2-5. As one can see in tables 2-5, the radial velocity of the studied BALRs takes values between -2225 km/s and -17994 km/s, the values of the rotational velocity of the BALRs are between 30 km/s and 2400 km/s and the random velocity of the ions take values between 228 km/s and 2280 km/s. In most cases, the best fit of the observed spectral features is given by the GR approach. However, there were 4 cases (indicated with italics in tables 2-5), where the best fit is accomplished with the RG approach.

Table 2. Radial Velocities (km/s)

Object Name (SDSS)	$Vrad_1$	$Vrad_2$	$Vrad_3$	$Vrad_4$
J015024.44+004432.99	-3483	-7546		
J015048.83+004126.29	-3473	-5611		
J021327.25-001446.92	-3096	-5321		
J023252.80-001351.17	-5224	-8649		
J023908.99-002121.42	-8513			
J025331.93+001624.79	-4257	-5611		
J025747.75-000502.91	-7352			
J031828.91-001523.17	-13157	-17994		
J102517.58+003422.17	*-6772*	*-8126*	*-10545*	
J104109.86+001051.76	-2225	-5417	-6675	-9867
J104152.62-001102.18	-6385	-9287		
J104841.03+000042.81	*-5998*	*-8320*	*-11609*	
J110041.20+003631.98	*-5417*	*-10061*	*-14704*	
J110736.68+000329.60	*-2360*	*-3618*	*-7352*	*-8900*
J112602.81+003418.23	-6288	-7642		

Table 3. Rotational and Random Velocities (km/s)

	Rotational Velocities				Random Velocities			
Object Name (SDSS)	$Vrot_1$	$Vrot_2$	$Vrot_3$	$Vrot_4$	$Vrand_1$	$Vrand_2$	$Vrand_3$	$Vrand_4$
J015024.44+004432.99	2200	1500			1140	1368		
J015048.83+004126.29	500	200			456	228		
J021327.25-001446.92	100	100			935	912		
J023252.80-001351.17	100	1800			388	388		
J023908.99-002121.42	30				2280			
J025331.93+001624.79	250	200			570	410		
J025747.75-000502.91	1000				2052			
J031828.91-001523.17	350	150			1482	1368		
J102517.58+003422.17	*800*	*750*	*100*		*228*	*228*	*342*	
J104109.86+001051.76	200	50	50	100	342	342	570	798
J104152.62-001102.18	50	50			456	1140		
J104841.03+000042.81	*1000*	*500*	*500*		*388*	*410*	*456*	
J110041.20+003631.98	*1200*	*2400*	*1500*		*456*	*1482*	*2052*	
J110736.68+000329.60	*900*	*300*	*500*	*600*	*228*	*251*	*342*	*360*
J112602.81+003418.23	50	50			502	502		

Table 4. Column Density ($\times 10^{10}$ cm^{-2})

	λ 1548.187 Å				λ 1550.772 Å			
Object Name (SDSS)	CD_1	CD_2	CD_3	CD_4	CD_1	CD_2	CD_3	CD_4
J015024.44+004432.99	-8.81	-3.51			-8.15	-3.20		
J015048.83+004126.29	-2.29	-0.78			-2.11	-0.71		
J021327.25-001446.92	-4.12	-2.03			-3.80	-1.85		
J023252.80-001351.17	-3.11	-3.67			-2.95	-3.38		
J023908.99-002121.42	-7.67				-7.04			
J025331.93+001624.79	-1.31	-0.87			-1.19	-0.80		
J025747.75-000502.91	-6.43				-5.90			
J031828.91-001523.17	-2.45	-1.39			-2.23	-1.26		
J102517.58+003422.17	*-1.82*	*-2.04*	*-0.51*		*-1.68*	*-1.89*	*-0.46*	
J104109.86+001051.76	-2.12	-1.58	-2.00	-2.81	-1.98	-1.46	-1.84	-2.58
J104152.62-001102.18	-0.94	-2.72			-0.85	-2.48		
J104841.03+000042.81	*-2.56*	*-1.73*	*-0.72*		*-2.36*	*-1.59*	*-0.66*	
J110041.20+003631.98	*-3.80*	*-5.65*	*-4.04*		*-3.51*	*-5.18*	*-3.68*	
J110736.68+000329.60	*-3.46*	*-1.87*	*-0.78*	*-0.53*	*-3.23*	*-1.74*	*-0.71*	*-0.48*
J112602.81+003418.23	-1.52	-2.21			-1.39	-2.04		

Table 5. Absorbed Energy (eV)

	λ 1548.187 Å				λ 1550.772 Å			
Object Name (SDSS)	Ea_1	Ea_2	Ea_3	Ea_4	Ea_1	Ea_2	Ea_3	Ea_4
J015024.44+004432.99	-13.55	-5.40			-12.53	-4.91		
J015048.83+004126.29	-3.52	-1.19			-3.25	-1.09		
J021327.25-001446.92	-6.34	-3.12			-5.85	-2.84		
J023252.80-001351.17	-4.78	-5.65			-4.53	-5.19		
J023908.99-002121.42	-11.81				-10.82			
J025331.93+001624.79	-2.01	-1.34			-1.83	-1.22		
J025747.75-000502.91	-9.90				-9.06			
J031828.91-001523.17	-3.77	-2.14			-3.42	-1.94		
J102517.58+003422.17	*-2.80*	*-3.14*	*-0.78*		*-2.57*	*-2.90*	*-0.70*	
J104109.86+001051.76	-3.27	-2.43	-3.08	-4.32	-3.04	-2.24	-2.83	-3.96
J104152.62-001102.18	-1.44	-4.19			-1.31	-3.81		
J104841.03+000042.81	*-3.94*	*-2.67*	*-1.11*		*-3.62*	*-2.45*	*-1.01*	
J110041.20+003631.98	*-5.84*	*-8.70*	*-6.21*		*-5.40*	*-7.95*	*-5.65*	
J110736.68+000329.60	*-5.32*	*-2.87*	*-1.20*	*-0.81*	*-4.97*	*-2.68*	*-1.09*	*-0.73*
J112602.81+003418.23	-2.33	-3.40			-2.13	-3.14		

6. Final remarks

The main purpose of this study is to answer to the question: Is a multi-structure of BLR regions able to explain the complex profile of Hi BALQSOs spectra?

Additionally, if the answer of the above question is positive, our next step is to test whether the GR model is able to reproduce the complex profiles of Hi BALQSOs and to calculate a group of physical parameters of the corresponding BLRs.

Concluding the results of our study we could remark that:

1. It is possible that the dynamical systems of BLRs are not homogeneous but consist of a number of density regions or ion populations with different physical parameters. Each one of these density regions gives us an independent classical absorption line. If the regions that give rise to such lines rotate with large velocities and move radially with small velocities, the produced lines have large widths and small shifts. As a result they are blended among themselves as well as with the main spectral line and thus they are not discrete.
2. As we can see in tables 2-5, the GR model is able to reproduce accurately the complex profiles of Hi BALQSOs and to calculate a group of physical parameters of the corresponding BALRs.

Acknowledgements

This research project is progressing at the University of Athens, Department of Astrophysics, Astronomy and Mechanics, under the financial support of the Special Account for Research Grants, which we thank very much. This work also was supported by Ministry of Science Technological Development of Serbia and, through the projects “Influence of collisional processes on astrophysical plasma line shapes” and “Astrophysical spectroscopy of extragalactic objects”.

Funding for the SDSS and SDSS-II has been provided by the Alfred P. Sloan Foundation, the Participating Institutions, the National Science Foundation, the U.S. Department of Energy, the National Aeronautics and Space Administration, the Japanese Monbukagakusho, the Max Planck Society, and the Higher Education Funding Council for England. The SDSS Web Site is http://www.sdss.org/.

The SDSS is managed by the Astrophysical Research Consortium for the Participating Institutions. The Participating Institutions are the American Museum of Natural History, Astrophysical Institute Potsdam, University of Basel, University of Cambridge, Case Western Reserve University, University of Chicago, Drexel University, Fermilab, the Institute for Advanced Study, the Japan Participation Group, Johns Hopkins University, the Joint Institute for Nuclear Astrophysics, the Kavli Institute for Particle Astrophysics and Cosmology, the Korean Scientist Group, the Chinese Academy of Sciences (LAMOST), Los Alamos National Laboratory, the Max-Planck-Institute for Astronomy (MPIA), the Max-Planck-Institute for Astrophysics (MPA), New Mexico State University, Ohio State University, University of Pittsburgh, University of Portsmouth, Princeton University, the United States Naval Observatory, and the University of Washington.

References

[1] Hamann F, Korista K T and Morris S L 1993 *ApJ* **415** 541
[2] Crenshaw M D, Kraemer S B and George I M 2003 *ARAA* **41** 117
[3] Reichard T A, Richards G T, Hall P B, Schneider D P, Vanden Berk D E, Fan X, York Donald G, Knapp G R and Brinkmann J 2003 *AJ* **126** 2594
[4] Surdej J and Hutsemekers D 1987 *A&A* **177** 42
[5] Boroson T A and Meyers K A 1992 *ApJ* **397** 442
[6] Weymann R J, Morris S L, Foltz C B and Hewett P C 1991 *ApJ* **373** 23
[7] Ogle P M, Cohen M H, Miller J S, Tran H D, Goodrich R W and Martel A R 1999 *ApJS* **125** 1
[8] Schmidt G D and Hines D C 1999 *ApJ* **512** 125
[9] Becker R H, White R L, Gregg M D, Brotherton M S, Laurent-Muehleisen S A and Arav N 2000 *ApJ* **538** 72
[10] Lyratzi E, Popović L·Č, Danezis E, Dimitrijević M S, Antoniou A 2009 *NewAR* **53** 179

[11] Branch D, Leighly K M, Thomas R C and Baron E 2002 *ApJL* **578** L37
[12] Murray N and Chiang J 1998 *ApJ* **494** 125
[13] Popović L·Č, Mediavilla E, Bon E, Ilić D 2004 *A&A* **423** 909
[14] Proga D, Stone J M and Kallman T R 2000 *ApJ* **543** 686
[15] Williams R J R, Baker A C, Perry J J 1999 *MNRAS* **310** 913
[16] Richards G T et al. 2001 *AJ* **121** 2308
[17] Foltz C B, Weymann R J, Peterson B M, Sun L, Malkan M A and Chaffee F H 1986 *ApJ* **307** 504
[18] Danezis E, Popović L·Č, Lyratzi E and Dimitrijević M S 2006 *AIP Conference Proceedings* **876** 373
[19] Danezis E, Nikolaidis D, Lyratzi E, Popović L·Č, Dimitrijević M S, Antoniou A and Theodosiou E 2007 *PASJ* **59** 827
[20] Gunn J E et al. 1998 *AJ* **116** 3040

Virtual Laboratory Astrophysics: the STARK-B database for spectral line broadening by collisions with charged particles and its link to the European project VAMDC

2012 J. Phys.: Conf. Ser. 397 012019

(http://iopscience.iop.org/1742-6596/397/1/012019)

Journal of Physics: Conference Series **397** (2012) 012019 doi:10.1088/1742-6596/397/1/012019

Virtual Laboratory Astrophysics: the STARK-B database for spectral line broadening by collisions with charged particles and its link to the European project VAMDC

Sylvie Sahal-Bréchot[1 4], Milan S Dimitrijević[2 1 3] and Nicolas Moreau[1]
[1] Laboratoire d'Étude du Rayonnement et de la Matière en Astrophysique (LERMA), Observatoire de Paris, UMR CNRS 8112, UPMC, Bâtiment Evry Schatzman, 5 Place Jules Janssen, F-92195 Meudon Cedex, France
[2] Astronomical Observatory, Volgina 7, 11060 Belgrade 38, Serbia
[3] Institute Isaac Newton of Chile, Yugoslavia Branch, Volgina 7, 11060 Belgrade 38, Serbia

E-mail: sylvie.sahal-brechot@obspm.fr

Abstract. Atomic physics in plasmas has been an essential tool for many years. Accurate spectroscopic diagnostics and modeling require the knowledge of numerous collisional line profiles. **"**Stark broadening" theories and calculations have been extensively developed for about 50 years. Nowadays, the access to such data via an on line database becomes essential. The aim of STARK-B is to reply to this need. It is a collaborative project between the Astronomical Observatory of Belgrade (AOB) and the "Laboratoire d'Étude du Rayonnement et de la matière en Astrophysique" (LERMA) of the Paris Observatory and CNRS. It is a database of widths and shifts of isolated lines of atoms and ions due to electron and ion impacts that we have calculated and published in international refereed journals (more than 150 papers by Dimitrijević & Sahal-Bréchot, and colleagues). It is devoted to modeling and spectroscopic diagnostics of stellar atmospheres and envelopes, laboratory plasmas, magnetic fusion plasmas, laser equipments and technological plasmas. Hence, the domain of temperatures and densities covered by the tables is wide and depends on the ionization degree of the considered ion. The STARK-B database is in free access and is is a part of VAMDC: the Virtual Atomic and Molecular Data Centre is an European Union funded collaboration between groups involved in the generation and use of atomic and molecular data. VAMDC aims to build a secure, documented, flexible and interoperable e-science environment-based interface to existing atomic and molecular data. STARK-B and its VAMDC context are presented in this paper.

1. Introduction

Pressure broadening of spectral lines arises when an atom or a molecule which emits or absorbs light in a gas or in a plasma, is perturbed by its interactions with the other particles of the medium. An atom or a molecule may be neutral as well as charged. The so-called Stark broadening is due to electron and ion colliders. The theory has been extensively developed for about 50 years and is currently used for many spectroscopic diagnostics and modeling. A number of its developments have been stimulated by the advances in Astrophysics, by the needs in laboratory and technological plasmas (tokamaks, laser produced plasmas, inertial fusion plasmas…), and also by the needs in industrial plasmas (discharge lighting). Due to the developments of the accuracy of observations in astrophysics and laboratory physics, many needs of atomic data appear at the end of the 20th century, and the needs are constantly

[4] To whom any correspondence should be addressed.

increasing. Hence, calculations based on a simple but enough accurate and fast methods are necessary for obtaining numerous results. Furthermore, the development of powerful computers also stimulates the development of atomic data on a large scale. Besides, the access to these atomic data via on line databases becomes essential.

In section 2, we will recall the physical conditions where Stark broadening plays a role in different plasmas. Section 3 will be devoted to a brief review of the standard impact Stark broadening theory that is at the basis of the theory, calculations and the database presented in the present paper. In fact, Dimitrijević and Sahal-Bréchot have updated and operated at a large scale the numerical code (SCP) created by Sahal-Bréchot since about thirty years. This code is based on the impact semiclassical-perturbation theory for isolated spectral lines of neutral and ionized atoms broadened and shifted by collisions with electrons and ions, [1] [2] [3] [4]. More than 150 papers are issued from the first update [5]. Then, the new need of creation of an on-line database appeared in the beginning of the 21th century, particularly in correlation with the birth and the growth of virtual Observatories and to the increasing need of exchange of interoperable data. Thus, the database STARK-B (formerly called BELDATA) was initiated in the Astronomical Observatory of Belgrade (AOB), and then a collaborative project between AOB and LERMA was born and led to the present database. STARK B, which is in free access, is currently developed at Paris Observatory and has opened on line since the end of 2008 (http://stark-b.obspm.fr [6]), and now contains the published data of all our papers obtained through the SCP theory and code. It is a part of the atomic and molecular databases of the Paris Observatory, and there is a link to the Serbian Virtual Observatory (SerVO, http://servo.aob.rs/~darko). A mirror site is planned at AOB. More details are given in Section 4, as well as the scheduled developments. STARK-B has been a database of VAMDC (Virtual Atomic and Molecular Data Centre) since the end of 2009. This FP7 European project "Research Infrastructures" was created in summer 2009 for 3.5 years. It is an interoperable e-Infrastructure for exchange of atomic and molecular data. It is an international consortium that has built an e-science interoperable platform [7] [8] (http://www.vamdc.eu, and http://portal.vamdc.eu) permitting an automated exchange of atomic and molecular data. The software infrastructure is based on an ensemble of standards and softwares ((http://www.vamdc.eu/software/). VAMDC addresses data producers and users, and gives a support for introducing new databases in the consortium, and for using standards and softwares. This will be presented in Section 5.

2. Importance of Stark broadening in plasmas

On the one hand, in astrophysics, thanks to the considerable developments of the spectral resolution and sensitivity (high *S/N*) of the recent past years, and of large ground-based telescopes and space-born missions, it becomes possible to observe very faint objects and spectra in all ranges of wavelengths (from XUV to radio) with an unequalled accuracy. For interpreting the spectra, the atomic parameters responsible for their intensities and their profiles must be known. The development of realistic models of interiors and of atmospheres of stars including stratification, and the interpretation of their evolution and the creation of elements through nuclear reactions, requires the knowledge of numerous profiles, especially for trace elements. Abundances of elements are crucial parameters to be determined. This needs an accurate interpretation of the detailed line spectra of stellar objects and thus extensive sets of atomic data, including collisional broadening and especially Stark broadening. Neglecting Stark broadening can lead to 40% error in abundances. Nowadays collisional broadening data are needed, not only for strong lines of abundant elements (H, He, C, N, O, Ne) as in the past, but also for weak lines of abundant elements, for elements of lower abundance (the Iron-peak), and then, that is more recent, for heavy elements of very low abundance which are always very weak. Even some radioactive elements, such as thorium and uranium have been recently discovered in low-metallicity stars (stars of the first or second generation), and are used for chronometric age determination. An extreme domain of temperatures (about 10^6 - 10^7 K) and electron densities (about 10^{24} cm^{-3}) concern interiors of stars. They cannot be observed but are mirrored via asteroseismology, and Stark broadening of abundant ions plays an important role for modeling and for deriving radiative

opacities. In the very dense and hot atmospheres of neutron stars, the physical conditions are typical of those of stellar interiors, and highly-ionized atoms such as H and He-like Fe have been observed in X rays and the measured line strengths of lines indicate that the lines are significantly broadened by Stark effect [9], and this should provide an opportunity to determine both the mass and the radius of these exotic objects. On less extreme conditions of temperatures (10^4 to a few 10^4 K) and densities (10^{13} to 10^{15} cm^{-3}), Stark broadening is efficient for modeling and analyzing spectra of moderately hot (A), hot (B) and very hot (O) types of stars. It is dominant in comparison with thermal Doppler effect in deep layers of stellar atmospheres. In white dwarfs, collisional broadening and especially Stark broadening is dominant in all layers of the atmosphere (temperatures in the region of 10^4 K, electronic densities of the order of 10^{18}-10^{19} cm^{-3}) In stars like sun, and especially in the chromosphere which lays above the photosphere, Stark broadening can be operative for lines arising from high excited levels.

On the other hand, in laboratory and technological plasmas, considerable developments are also in progress and require new and numerous atomic data for spectroscopic diagnostics and modeling. Magnetic confinement fusion plasmas (tokamaks, such as ITER) are moderately hot (electron and ion temperatures about 0.5 to 40 keV in the core and 0.05 to 10 keV at the edge) and dense (10^{14} cm^{-3}), especially in the divertor and edge plasma regions. Expected impurities include a wide range of elements (such as tin), but some important elements are not the same as in astrophysics, with nuclear charge Z, ranging from above 70 (as tungsten) and down to 1. Light elements are also important, such as Helium-like krypton. Inertial confinement fusion plasmas (laser fusion, ion-beam fusion, such as JET, laser LMJ) are hot (several keV) and very dense (up to 10^{24} cm^{-3} for the density) and their thermodynamical conditions look like those of stellar interiors.

In addition, industrial plasmas also require atomic data for optimizing the performances of discharge lamps and lighting sources [10]. The temperatures are various: the discharge can attain 45000K, whereas the emitted white light corresponds to 3000-5000K. The electron density is rather high, so Stark broadening can play an important role in the modeling. The interesting elements are rare earth phosphors (Dy, Ho, Ce) because they are excellent radiation sources in fluorescent lamps. Temperatures of HID (High Intensity Discharge) lamps, such as metal halides, are about 1000K on the wall and 7000K on axis. The buffer gas is usually mercury vapor at high pressure. Ga and Al atomic data are needed.

3. Basis of STARK-B data: the standard theory of Stark impact broadening of isolated lines

The theory and calculation of collisional line broadening in the impact approximation follows the founding work by Baranger [11] [12] [13].

3.1. The impact approximation

First, the impact approximation is the fundamental one: the interactions are separated in time. Consequently the duration of an interaction $\tau = \rho_{typ} / v_{typ}$, where ρ_{typ} is a typical impact parameter and v_{typ} a typical relative velocity, must be much smaller than the mean time interval between two collisions ΔT, which is of the order of the inverse of the collisional line width $N v_{typ} \pi \rho_{typ}^2$, where N is the density of the perturbers. The condition of validity of the impact approximation can be written as $\rho_{typ} / v_{typ} \ll \Delta T$, or, which is equivalent, $N V_{typ} \ll 1$, V_{typ} being the collision volume [11] [12], i.e., $\rho_{typ} \ll N^{-1/3}$.

In other words, the studied radiating atom interacts with one perturber only at a time, and the perturbers are independent and their effects are additive.

3.2. The complete collision approximation

Second, the collision is assumed to be complete. This means that the atom has no time to emit or absorb a photon during the collision process. This is valid if the duration of an interaction is much smaller than the interval between two successive emissions (or absorptions) of photons, which is of the

order of the inverse of the detuning, when larger than the line width. So, if the impact approximation is valid, the complete collision approximation is valid in the line center but can be invalid in the wings. In the very far wings the interactions can become "quasistatic", which means that a photon can be emitted or absorbed before the perturbers had time to move. The data of STARK-B do not apply in this case.
Consequently, within the complete collision approximation, radiative and collision processes are decoupled and the impact broadening theory becomes an application of the theory of collisions between an emitting (or absorbing) neutral (or ionized) atom and interacting particles. These two approximations are at the basis of the STARK-B data.

3.3. The case of "isolated lines"

Third, STARK-B data apply to "isolated lines" only and do not apply to "overlapping lines" [12]. This means that the levels next to the upper or lower level of the studied transition and likely to modify the broadening by introducing optical coherences do not overlap with them. So, hydrogen and hydrogenic ionic lines are excluded from the database, as well as some specific helium lines and some lines arising from Rydberg levels.

3.4. Lorentz profile

Therefore the profile of the *i-f* line emitted or absorbed between the *i* and *f* levels studied is Lorentzian, with a full width at half maximum *W* (in angular frequency units) and a shift *d* [13]. *W* can be expressed in terms of inelastic cross-sections and elastic processes as (cf. [13]):

$$W = N \int v\, f(v) \left(\sum_{i' \neq i} \sigma_{ii'}(v) + \sum_{f' \neq f} \sigma_{ff'}(v) + \sigma_{el}(v) \right),$$

where N is the density of the colliding perturbers, $f(v)$ the Maxwell distribution of the relative atom-perturber velocity v, $\sigma_{ii'}$ and $\sigma_{ff'}$ the inelastic cross-sections between the initial level i (resp. f final level) and the perturbing levels i' (resp. f') of the i-f transition. $\sigma_{el}(v)$ represents the contribution of elastic collisions and includes Feshbach resonances when ion-electron collisions are studied.
The shift is not given in the present paper, and we refer to [13] for its quantum expression.
We notice that the widths and shifts are proportional to the density N in the above expression, and depend on the temperature of the plasma through the distribution of velocities. In fact, since interactions with charged particles are concerned, at high densities, the Debye screening has to be taken into account and reduces the cross-sections. So, the widths and shifts become reduced.
Consequently, for a series of lines of a given neutral or ionized atom, STARK-B displays widths *W* and shifts *d* for a set of temperatures and densities and for various perturbers (electrons and ions). For low densities, which are not on the tables, the data, which are provided at medium densities, can be deduced through a linear extrapolation. At high densities some data are not given because the impact approximation is not valid; an asterisk, which replaces the data, indicates this. Data which are given but preceded by an asterisk mean that the impact approximation reaches its limit of validity, i.e. when $0.2 < N V_{typ} \leq 0.5$.
In addition, when the density increases, the lines, which are isolated at low densities, can overlap; the impact width becomes comparable to the separation $\Delta E(nl, nl \pm 1)$ between the perturbing energy levels and the initial or final level. The isolated line approximation becomes invalid. This is indicated in the database by a parameter *C* defined in [5] and in following papers. *C* is provided in the tables and can be used as follows: for a perturber density *N* lower than the limiting value N_{lim} (cm^{-3}) = *C/W*, the line can be treated as isolated even if a weak forbidden component due to the failure of this approximation remains in the wing.

3.5. Effect of fine structure and hyperfine structure on the widths and shifts

The following remark holds in LS coupling. The atomic electronic spin *S* and the orbital kinetic momentum *L* are decoupled. For electronic collisions and most often by collisions with ions, the

collision time (of the order of ρ_{typ}/v_{typ}) is very much smaller than the fine structure splitting. So the electronic spin has no time to rotate during the collision and can be ignored. Thus all the fine structure components have the same widths and shifts, which are equal to those of the multiplet. This is a fortiori the same for the hyperfine components. So our calculations have most often been performed for multiplets only, and STARK-B data are most often given for multiplets. This remark does not apply for heavy atoms where departures from LS coupling can be important.

3.6. Compared orders of magnitude of electron and ion Stark widths and shifts

For isolated lines, the widths and shifts due to electron collisions are generally ten times higher than the widths and shifts due to ion collisions. This is due to the fact that inelastic collisions with positive ions are generally negligible, owing to the mass effect that decreases the relative velocity, and, in addition, if the radiator is an ion, the Coulomb repulsion acts. This can be not the case when the perturbing levels are very close to the levels of the studied transition. This can also be not the case at very high temperatures, and especially for ion radiators when the Coulomb repulsion becomes weak.

3.7. Calculation of the cross-sections, and then widths and shifts

3.7.1. The Semi-Classical Perturbation (SCP) approach. For the purposes of STARK-B, the semi-classical-perturbation treatment is adapted and gives results with a sufficient accuracy (about 20%). This is especially the case if the perturbing levels are not too far from the levels of the studied line. The basic formalism has been developed and discussed in detail in [1] [2]. Classical straight rectilinear paths for neutral radiators, and hyperbolic paths have been introduced for ion-electron and ion-ion collisions. Then the *S*-matrix has been obtained within the second order perturbation theory. The needed cross-sections are obtained through integration over the impact parameter of the transition probabilities. The needed cut-offs are determined in order to maintain the unitarity of the scattering *S*-matrix, and Debye screening is taken into account. A very fast computer code has been created. This formalism, and the computer code, have been updated and optimized several times: [3] for complex atoms, [4] for the inclusion of Feshbach resonances in the elastic ion-electron cross-sections, [5] and further papers, and [14] for transitions arising from very complex configurations.

3.7.2. The atomic structure. In the semiclassical picture, oscillator strengths and needed energy levels enter the expressions of the inelastic cross-sections. They are input data of the numerical code.

The STARK-B data issued from our oldest papers (eighties and nineties), the Coulomb approximation with quantum defect (Bates & Damgaard approximation, [15]) was used, together with measured or calculated energy levels.

In the more recent papers modern ab initio methods are used (cf. [14]). The different atomic structure computer codes or the data can be downloaded on line. Thus the calculations of widths and shifts can be made from the beginning to the end without any additional external input or experimental adjustment. The chosen atomic structure package enters our computer semi-classical code and that allows, when these methods are applicable, to obtain widths and shifts for one-two hundred of lines:

– TOPbase, the Opacity Project atomic database, contains accurate calculated oscillator strengths and energy levels for abundant neutral atoms and ions of astrophysics. They have been obtained within the close-coupling scattering theory by means of the R-matrix method with innovative asymptotic techniques [17] [18]. L-S coupling is assumed. So, TOPbase data have been especially used to light and low and moderately ionized atoms and ions.
– The Cowan code [19] is an online atomic structure package consisting of a set of computer programs for calculation of energy levels, radiative transition wavelengths and probabilities, electron impact excitation and photoionization cross sections, etc. The Hartree-Fock-Slater multi-configuration expansion method with statistical exchange is the normal option since it is most computationally efficient. The relativistic corrections are treated by perturbations. So this method is especially suited to moderately heavy atoms which are little and moderately ionized.
– SUPERSTRUCTURE (SST) [20] is well suited for computation of large quantities of atomic data for highly charged ions. The wave functions are determined by diagonalization of the nonrelativistic

Hamiltonian using orbitals calculated in a scaled Thomas-Fermi-Dirac-Amaldi potential. Relativistic corrections are introduced according to the Breit-Pauli approach. Atomic data are obtained in intermediate coupling.

Si V and Ne V line widths and shifts data have been calculated with both Bates & Damgaard and SST atomic data [21] [22]. The difference does not exceed 30%. C II widths and shifts data have been calculated with both TOPBase and Bates & Damgaard atomic data [23], and the difference does not exceed a few percent, except when configuration interaction plays an important role by making permitted a forbidden transition. This gives an idea and an order of magnitude of the importance of the chosen atomic structure on the Stark broadening data.

3.7.3. The Modified Semi-Empirical Method (MSE). A number of applications were also achieved with the Modified Semi-Empirical (MSE) method [24] [25] [26] and other papers cited in [27]. It is less accurate, though simpler to use due to the considerably smaller set of atomic data needed in comparison with the SCP theory. It can effectively replace the SCP method when this one cannot be used due to a lack of atomic data. The MSE data have not still been introduced in STARK-B.

4. Organization of the database

Since STARK-B is devoted to modeling and spectroscopic diagnostics in various plasmas, the domain of temperatures and densities covered by the tables is wide and depends on the ionization degree of the considered ion. The temperatures can vary from several thousands for neutral atoms to several millions of Kelvin for highly charged ions. The electron or ion densities can vary from 10^{12} (case of stellar atmospheres) to several 10^{22} cm^{-3} (some white dwarfs, subphotospheric layers and some laboratory and fusion plasmas). The datamodel, especially the definition of configurations, terms and levels follow the VAMDC standards, in order to allow interoperability with other atomic databases.

It is important to notice that the provided wavelengths (Å units) are most often calculated from the energy levels that are used in the calculations. Consequently, these wavelengths can be different from the measured ones, especially if energy levels originate from TOPBase, SST or Cowan code. The lines can be identified through the configurations, terms and levels. In addition, the widths and shifts data are provided in units of wavelengths (Å) and not in angular frequency units. So, if widths and shifts data are needed for measured wavelengths ($\lambda_{measured}$), or for fine structure data whereas the data are only provided for multiplets (cf. section 3.5), one has to multiply the STARK-B data by $(\lambda_{measured}/\lambda_{STARK\text{-}B})^2$.

We refer to section 3.4 for the cases of departures from the impact approximation and from the isolated line approximation at high densities.

Currently, STARK-B contains Stark widths and shifts for spectral lines of the following elements and ionization degrees:

Ag I, Al I, Al III, Al XI, Ar I, Ar II, Ar VIII, Au I, B II, B III, Ba I, Ba II, Be I, Be II, Be III,
Br I, C II, C III, C IV, C V, Ca I, Ca II, Ca V, Ca IX, Ca X, Cd I, Cd II, Cl I, Cl VII, Cr I, Cr II, Cu I, F I, F II, F III, F IV, F V, F VI, F VII, Fe II, Ga I, Ge I, He I, Hg II, I I, In II, In III, K I, K VIII, K IX, Kr I, Kr II, Kr VIII, Li I, Li II, Mg I, Mg II, Mg XI, Mn II, N I, N II, N III, N IV, N V, Na I, Na X,
Ne I, Ne II, Ne III, Ne IV, Ne V, Ne VIII, Ni II, O I, O II, O III (in progress), O IV, O V, O VI, O VII, P IV, P V, Pb IV, Pd I, Rb I, S III, S IV, S V, S VI, Sc III, Sc X, Sc XI, Se I, Si I, Si II, Si IV, Si V, Si VI, Si XI, Si XII, Si XIII, Sr I, Te I, Ti IV, Ti XII, Ti XIII, Tl III, V V, V XIII, Y III, Zn I.

Apart O III data, all the data corresponding to our already published papers have now been implemented.

The homepage (Fig.1) proposes several menus, among which “Introduction”, “Data Description” and “Access to the Data”. “Introduction” briefly recalls the approximations and methods of calculation. “Data Description” describes the data that are in the files. A graphical interface is provided in “Access to the Data” (Fig.2): first, the consumer clicks on the wished element in the Mendeleev periodic table and then on the ionization degree of interest. Yellow cells contain data, while white cells are empty. Next, with a few clicks, the user chooses the colliding perturber(s), the perturber density, the

transition(s) by quantum numbers and the plasma temperature(s). The consumer can also make a query by domain of wavelengths instead by transitions. Then a table displaying the widths and shifts is generated. Bibliographic references are given and linked to the publications via the SAO/NASA ADS Physics Abstract Service [55] and/or within DOI. They can be freely downloaded if the access is not restricted. The widths and shifts data can be downloaded in ASCII and in VOTable format (XML format), adapted to Virtual Observatories.

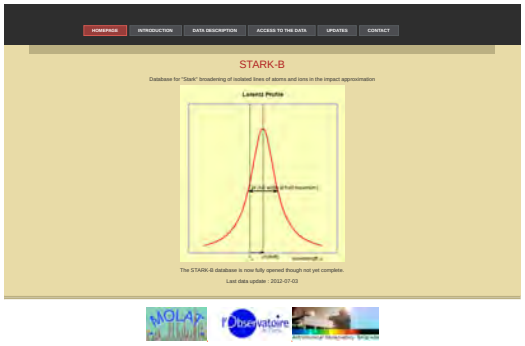

Figure1. The STARK-B home page: http://stark-b.obspm.fr

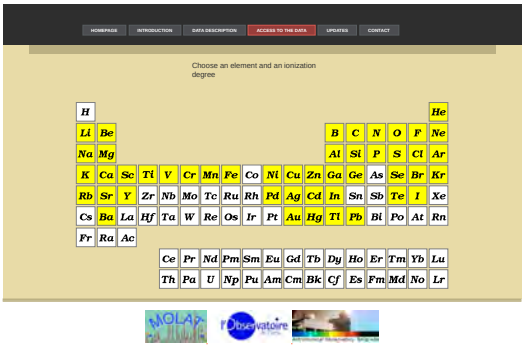

Figure 2. "Access to the data": the graphical interface

The database will be completed when new data will be calculated and published (e.g. C II results of [23]). The implementation of MSE data is planned for a next future. The implementation of our quantum data will be another future step. The further developments also concern insertion of little apps (fitting along temperatures, along principal quantum number for a given multiplet, charge of the ion collider along isoelectronic sequences, of the radiating ion, homologous ions…) by using fittings or systematic trends in order to obtain data that are missing on the database.

5. The STARK-B database and VAMDC (Virtual Atomic and Molecular Data Centre)

Many fields in astronomy, physics, energy production and industry depend on databases for atomic, molecular and particle-surface interaction processes. A reliable exchange of such data has become crucial for decades. Nowadays, many databases do exist, but they are organized and presented in different manners, with heterogeneous standards, rules and selection criteria. This is a barrier for an efficient search for data and their use. The free exchange of atomic and molecular data requires the definition both of standards which model the data structure and of tools that implement these standards and that help to carry out science using these data. Developments in computer technologies offer opportunities for new distributed tools and applications in various fields of physics. The convenient and reliable exchange of data is clearly an important component of such applications. So VAMDC [7] [8] was created in summer 2009 for 3.5 years in the framework of the FP7 "Research Infrastructures - INFRA-2008-1.2.2 - Scientific Data Infrastructures" initiative. It is an European collaboration between groups involved in the generation and use of atomic and molecular data. VAMDC involves 15 administrative partners representing 24 teams from 6 European Union member states, partners in non-EU countries (Serbia, the Russian Federation and Venezuela), and external partners in the US. It includes scientists in atomic and molecular physics with a strong coupling to the users of their data (astrochemistry, atmospheric physics, plasmas) and scientists and engineers from the Information and Communication Technologies community used to deal with interoperable e-infrastructure. The core of the VAMDC-infrastructure is founded on the databases detailed in [7]. VAMDC aims to build a secure, documented, flexible and interoperable e-science environment-based interface to existing atomic and molecular data. The VAMDC portal (http://portal.vamdc.eu/) has been released in the mid-April 2012 for the external users. It can be tested and is frequently updated from the development version that is still in progress. The results of the queries can be downloaded in XSAMS format (XML Schema for Atoms, Molecules and Solids). The XSAMS schema provides a framework for a structured presentation of atomic, molecular, and particle-solid-interaction data in an XML file. XML

(Extensible Markup Language) is the current standard for exchange of such data. It enables an automated exchange of complex contents between heterogeneous information systems through interoperability. STARK-B is one of the databases of VAMDC and participates to this undertaking.

6. Conclusion

Nowadays, numerical databases in Atomic and Molecular Physics are essential for both the modeling and the interpretation of spectra provided by observations and laboratory measurements of various plasmas. The free exchange of atomic and molecular data requires the definition both of standards which model the data structure and of tools that implement these standards and that help to carry out science using these data. The continuation of such developments and services of powerful and constantly updated online databases, like STARK-B, is crucial.

Acknowledgments

A part of this work has been supported by VAMDC. VAMDC is funded under the "Combination of Collaborative Projects and Coordination and Support Actions" Funding Scheme of The Seventh Framework Program. Call topic: INFRA-2008-1.2.2 Scientific Data Infrastructure. Grant Agreement number: 239108

References

[1] Sahal-Bréchot S 1969a *A&A* **1** 91
[2] Sahal-Bréchot S 1969b *A&A* **2** 322
[3] Sahal-Bréchot S 1974 *A&A* **35** 321
[4] Fleurier C, Sahal-Bréchot S and Chapelle J 1977 *JQSRT* **17** 595
[5] Dimitrijević M S and Sahal-Bréchot S 1984 *JQSRT* **31** 301
[6] Sahal-Bréchot S, Dimitrijević M S and Moreau N 2012 *STARK-B database, [online]. Available: http://stark-b.obspm.fr [Jul 8, 2012]. Observatory of Paris, LERMA and Astronomical Observatory of Belgrad*e
[7] Dubernet ML, Boudon V et al. 2010 *JQSRT* **111** 2151, http://www.vamdc.eu/
[8] Rixon G, Dubernet M L, et al. 2011 *7th International Conference on Atomic and Molecular Data and their Applications -ICAMDATA-2010, AIP Conf. Proc.* **1344** 107
[9] Rovenskaya N I 2004 *Astrophys. Space Sci*. **291** 113
[10] Lister G and Curry J J 2011 *7th International Conference on Atomic and Molecular Data and their Applications -ICAMDATA-2010, AIP Conf. Proc.* **1344** 219
[11] Baranger M 1958a *Phys. Rev*. **111** 481
[12] Baranger M 1958b *Phys. Rev*. **111** 494
[13] Baranger M 1958c *Phys. Rev*. **112** 855
[14] Mahmoudi W F, Ben Nessib N and Sahal-Bréchot S 2008 *EPJD* **47** 7
[15] Bates D R Damgaard A 1949 *Trans. Roy. Soc. Lond. Ser. A* **242** 101
[16] Ben Nessib N 2009 *New Astron. Rev.* **53**, 255
[17] Cunto W, Mendoza C, Ochsenbein F and Zeippen CJ 1993 *A&A* **275** L5
[18] http://cdsweb.u-strasbg.fr/topbase/topbase.html
[19] Cowan RD 1981 *The Theory of Atomic Structure and Spectra* (Berkeley, CA: University of California Press)
[20] Eissner W Jones M and Nussbaumer H 1974 *Comput. Phys. Commun.* **8** 270
[21] Ben Nessib N, Dimitrijević M S and Sahal-Bréchot S 2004 *A&A* **423** 397
[22] Hamdi R, Ben Nessib N, Dimitrijević M S and Sahal-Bréchot S 2007 *ApJS* **170** 243
[23] Larbi-Terzi N, Sahal-Bréchot S, Ben Nessib N and Dimitrijević M S 2012 *MNRAS* **423** 766
[24] Dimitrijević M S and Konjević J 1980 *JQSRT* **24** 451
[25] Dimitrijević M.S and Popović L Č 2001 *J. Appl. Spectr*. **68** 893
[26] Dimitrijević M S and Kršljanin V 1986 *A&A* **165** 269
[27] Dimitrijević M S 2003 *A&A Trans.* **22** 389

The quasi-molecular absorption bands in UV region caused by the non-symmetric ion-atom radiative processes in the solar photosphere

2012 J. Phys.: Conf. Ser. 397 012054

(http://iopscience.iop.org/1742-6596/397/1/012054)

Journal of Physics: Conference Series **397** (2012) 012054 doi:10.1088/1742-6596/397/1/012054

The quasi-molecular absorption bands in UV region caused by the non-symmetric ion–atom radiative processes in the solar photosphere

A A Mihajlov[1], V A Srećković, LJ M Ignjatović[1], M S Dimitrijević[2] and A Metropoulos[3]

[1] University of Belgrade, Institute of Physics, P.O.Box 57, Pregrevica 118, Belgrade, Serbia
[2]Astronomical Observatory, Volgina 7, 11060 Belgrade, Serbia
[3]Theoretical and Physical Chemistry Institute, National Hellenic Research Foundation, Athens, Greece

E-mail: mihajlov@ipb.ac.rs

Abstract. The aim of this research is to show that the radiative processes in strongly non- symmetric ion- atom collisions significantly influence on the opacity of the solar photosphere in UV region. Within this work only the $He+H^+$ and $H+A^+$ ion-atom systems, where A is the atom of one of the metal (Mg, Si and Al), are taken in to account. It is caused by the fact that the needed characteristics of the corresponding molecular ions, i.e. molecular potential curves and dipole matrix elements, have been determined by now. Here the non-symmetric radiative processes are considered under the conditions characterizing the non-LTE standard model of the solar atmosphere (Vernazza J, Avrett E and Loser R 1981 *ApJS* **45** 635), which gives the possibility to perform all needed calculations and determined the corresponding spectral absorption coefficients. It is shown that the examined processes generate rather wide quasi-molecular absorption bands in the UV and VUV regions, whose intensity is comparable and sometimes even larger than the intensity of known one's caused by the $H+H^+$ radiative collision processes, which are included now in the solar atmosphere models. Consequently, the presented results suggest that the non-symmetric ion-atom absorption processes have to be also included in standard models of the solar atmosphere.

1. Introduction

The significant influence of some ion-atom radiative collision processes on the optical characteristics of the stellar atmospheres was already established. Here we keep in mind such symmetric radiative processes as photo absorption/emission and radiative charge exchange, which can be described by

$$\varepsilon_\lambda + A_2^+ \leftrightarrow A + A^+ \quad (1)$$

$$\varepsilon_\lambda + A^+ + A \leftrightarrow A + A^+ \quad (2)$$

where A = H(1s) or He($1s^2$), A^+ and A_2^+ are the corresponding positive, single charged atomic and molecular ions in the ground electronic states, and ε_λ - the energy of the photon. It was shown that these processes can influence to the opacity of atmospheres of Sun (see e.g. [2] and [3]). However, the mentioned papers have leaved opened the questions of the significance of the non-symmetric radiative processes.

The main aim of this work is to draw attention to the possible significance of the non-symmetric radiative processes as factors which influence to the opacity of stellar atmosphere in UV and VUV region. Here we will consider the processes of absorption charge exchange and photo-dissociation of the type

$$\varepsilon_\lambda + AB^+ \leftrightarrow A^+ + B \quad (3)$$

$$\varepsilon_\lambda + A + B^+ \leftrightarrow A^+ + B \quad (4)$$

$$\varepsilon_\lambda + A + B^+ \leftrightarrow (AB^+)^* \quad (5)$$

where B is the ground state atom with the ionization potential I_B which is less than the ionization potential I_A of the atom A, AB^+ - the corresponding molecular ion in one of the electronic states which are asymptotically correlated with the state of the system $A + B^+$.

Let us note that the processes (3) and (4) represent the analogues of the processes (1) and (2), while the process (5) has not it's symmetric analog. In this work the non-symmetric radiative processes are considered under the conditions characterizing the models of the solar atmosphere presented in [1].

Namely, all data needed for the calculations of the spectral absorption coefficients are provided in tabular form only for the chosen models. In accordance with this model is possible that $A = He(1s^2)$ and B = H(1s), and A = H(1s) and B = Mg, Si and Al. Let us note that for the ions HeH^+ and $(HeH^+)^*$ the corresponding potential curves and the dipole matrix elements (as the functions of the internuclear distances) are taken from Green et al. [4] and [5], while for all other considered molecular ions the mentioned quantities are calculated within this work.

The corresponding spectral absorption coefficients, as the function of λ, the local temperature T and the relevant particle densities are determined in the region $40nm \leq \lambda \leq 230nm$.

2. Results and discussion

The non-symmetric processes (3) – (5) are schematically shown in figure 1, where: bf-, ff-, and fb denote the bound-free, free-free and free-bound radiative transitions; $\Delta I = I_A - I_B$; $E = E_{imp}$ and E'_{impa} are the impact energies of the corresponding ion-atom systems; $U_{in}(R)$ and $U_{fin}(R)$ - are the adiabatic potential curves of the initial and final molecular electronic states ; v , v' , J, and J' - the quantum numbers of the corresponding bound (ro-vibration) and free states.

The contribution of the considered non-symmetric ion-atom absorption processes (3) - (5) to the opacity of the solar atmosphere is described here by the spectral absorption coefficient $\kappa_{ia;nsim}(\lambda; T)$. The behavior of $\kappa_{ia;nsim}(\lambda; T)$ for several values of λ is illustrated by figure 2, where h is the distance of considered layer from the referent one (h=0) in accordance with Vernazza et al. (1981) [1].

The behavior of the quantity $G = \kappa_{ia;nsim}(\lambda; T)/ \kappa_{ia;tot}(\lambda; T)$, where $\kappa_{ia;tot}(\lambda; T)$ characterize the total contribution of all ion-atom absorption processes, i.e. (1) - (5), is shown in figure 3. Than, in figure 4 is presented the behavior of the quantities $F_{sim} = \kappa_{ia;sim}(\lambda; T)/ \kappa_{ea}(\lambda; T)$ and $F_{tot} = \kappa_{ia;tot}(\lambda; T)/\kappa_{ea}(\lambda; T)$, dash and full lines respectively. Here $\kappa_{ia;sim}(\lambda; T)$ characterize the contribution of the symmetric ion-atom absorption processes (1) and (2), and $\kappa_{ea}(\lambda; T)$ - the contribution of the concurrent electron-atom processes (H^- continuum), which were treated until recently as the absolutely dominant.

Even the results presented in these figures shows that the neglecting of the contribution of the non-symmetric processes (3) - (5) to the opacity of the solar atmosphere, in respect to the contribution of symmetric processes (1) and (2) would caused significant errors.

From the presented material it follows that the considered non-symmetric ion-atom absorption processes can not be treated only as one of the channel among many equal channels of the influence on the opacity of the stellar atmospheres and should be included together with the processes studied in our previous papers [6-10].

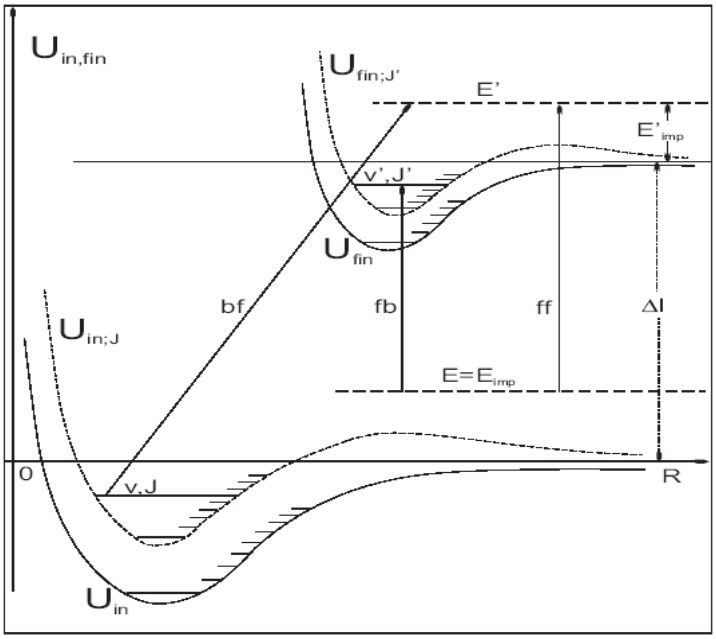

Figure 1. Schematic presentation of the non-symmetric processes (3-5) caused by the bound-free, free-free and free-bound radiative transitions.

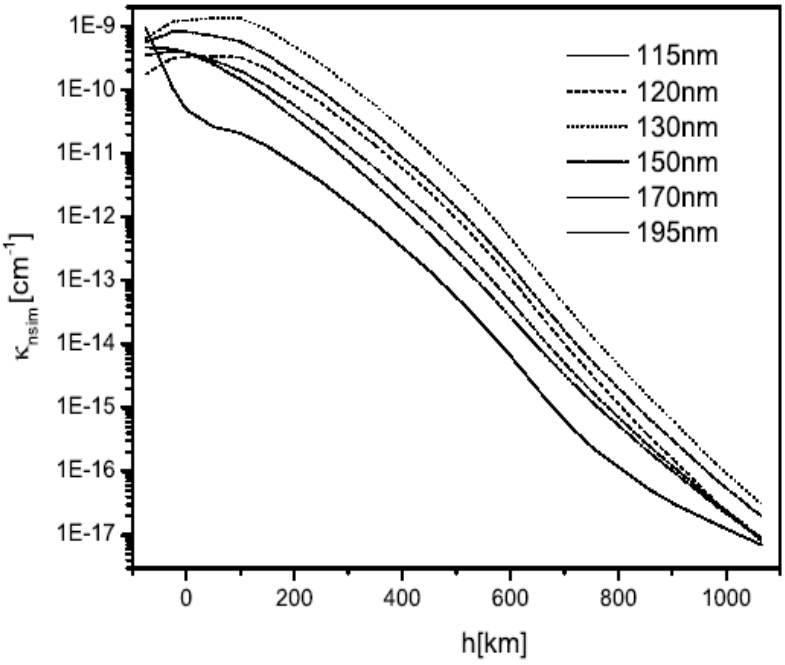

Figure 2. Quiet Sun. Spectral absorption coefficient κia;nsim(λ; T) for the spectral region 115nm < λ < 195nm.

From here it follows that the non-symmetric absorption processes (3)-(5) should be *ab initio* included in the same models.

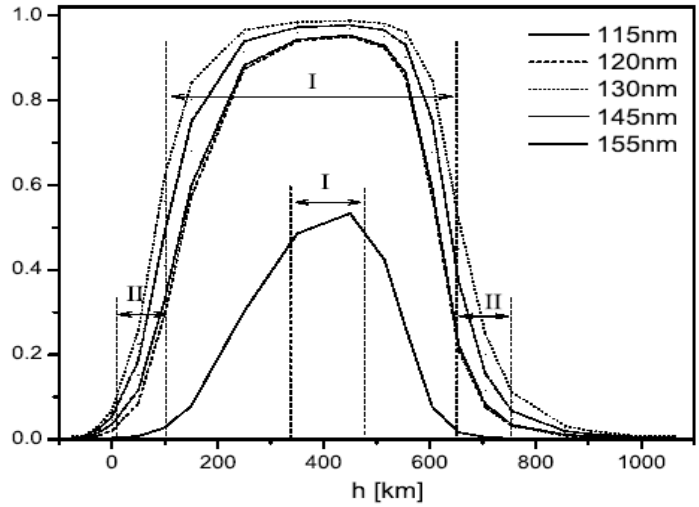

Figure 3. The behaviour of the quantity $G = \kappa_{ia;nsim}(\lambda; T)/ \kappa_{ia;tot}(\lambda; T)$.

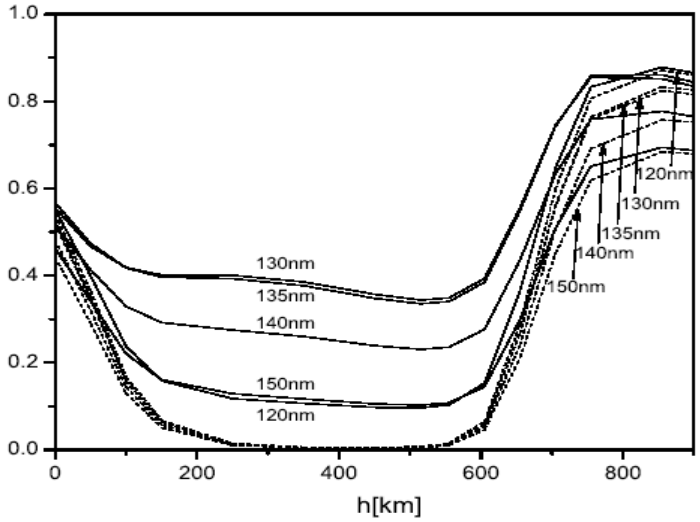

Figure 4. The behaviour of the quantities $F_{sim} = \kappa_{ia;sim}(\lambda; T)/ \kappa_{ea}(\lambda; T)$ and $F_{tot} = \kappa_{ia;tot}(\lambda; T)/\kappa_{ea}(\lambda;T)$.

Acknowledgements
This work was supported by the Ministry of Education and Science of the Republic of Serbia as a part of the projects 176002, III4402.

References
[1] Vernazza J, Avrett E and Loser R 1981 *ApJS* **45** 635
[2] Mihajlov A, Dimitrijevic M and Ignjatovic Lj 1993 *A&A* **276** 187
[3] Mihajlov A, Ignjatović Lj , Sakan N and Dimitrijević M 2007 *A&A* **437** 1023
[4] Green T, Browne J, Michels H and Madsen M 1974 *J. Chem. Phys*. **61** 5198
[5] Green T, Michels H, Browne J and Madsen M 1974 *J. Chem. Phys*. **61** 5186
[6] Mihajlov A A, Sakan N M, Sreckovic V A and Vitel Y 2011 *J. Phys*.A **44** 9
[7] Mihajlov A A, Sreckovic V A, Ignjatovic Lj and Klyucharev A N 2012 *J. Cluster Sci.* **23** 47-75
[8] Mihajlov A A, Ignjatovic Lj, Sreckovic V A and Dimitrijevic M 2011 *Baltic Astronomy* **20** 566
[9] Mihajlov A A, Sakan N M, Sreckovic V A and Vitel Y 2011 *Baltic Astronomy* **20** 604
[10] Mihajlov A A, Ignjatovic Lj M, Sreckovic V A and Dimitrijevic M S 2011 *ApJS* **193**:2 2

Electron-Impact Broadening of C II Spectral Lines

2012 J. Phys.: Conf. Ser. 397 012056

(http://iopscience.iop.org/1742-6596/397/1/012056)

Journal of Physics: Conference Series **397** (2012) 012056 doi:10.1088/1742-6596/397/1/012056

Electron-Impact Broadening of C II Spectral Lines

Neila Larbi-Terzi[1], **Nébil Ben Nessib** [1,2], **Sylvie Sahal-Bréchot** [3], **Milan S. Dimitrijević** [3,4]

[1]Groupe de Recherche en Physique Atomique et Astrophysique, Institut National des Sciences Appliquées et de Technologie, University of Carthage, Centre Urbain Nord B. P. No. 676, 1080 Tunis Cedex, Tunisia
[2]Department of Physics and Astronomy, College of Science, King Saud University. PO Box 2455, Riyadh 11451, Saudi Arabia.
[3]Laboratoire d'Étude du Rayonnement et de la Matière en Astrophysique, Observatoire de Paris, UMR CNRS 8112, UPMC, Bâtiment Evry Schatzman, 5 Place Jules Janssen, F-92195 Meudon Cedex, France
[4]Astronomical Observatory, Volgina 7, 11060 Belgrade 38, Serbia

E-mail: nebilbennessib@planet.tn, sylvie.sahal-brechot@obspm.fr, mdimitrijevic@aob.bg.ac.rs

Abstract. Using semiclassical perturbation approach in the impact approximation, we have obtained Stark broadening parameters for 149 C II multiplets. Energy levels and oscillator strengths are taken from the TOPbase database. Results are obtained as a function of temperature, for a perturber densities of 10^{14}, 10^{17} and 10^{18} cm^{-3}. In addition to electron-impact full half widths and shifts, Stark broadening parameters due to singly ionized carbon-impacts have been calculated, in order to provide Stark broadening data for the important charged perturbers in the atmospheres of carbon white dwarfs. The complete results will be published elsewhere, as well as the comparison to the existing experimental and other theoretical data. As an example of obtained results, we present data for a part of multiplets with wavelengths in the visible part of the spectrum.

1. Introduction

Recently, Dufour et al. [1], [2] discovered a new type of white dwarfs with the surface composition mostly composed of carbon. In order to consider their origin and evolution, it is necessary to develop a new generation of accurate models. Broadening by electron impact and C II ion interactions (Stark broadening) is the dominant line broadening mechanism at the temperatures and pressures of interest (effective temperatures within 19,000-23,000 K, electron density within 10^{15}cm^{-3}-10^{18}cm^{-3}), so that the inclusion of accurate Stark broadening parameters is essential for this type of white dwarf atmosphere modelling.

In order to provide data needed for analysis and investigations of such stars, we have undertaken to calculate a great number of widths and shifts of C II lines colliding with electrons and C II ions for plasma conditions of interest for these carbon white dwarfs. For this work, we have used the impact semi-classical perturbation (SCP) method [3], [4], [5] for electron and ion collisions. We have used the needed atomic data from the TOPbase, (R-matrix with innovative asymptotic techniques), [6] http://cdsweb.u-strasbg.fr/TOPbase/. It is suitable for CII and offers a great number of levels and line strengths for the transitions.

Table 1. Calculated C II full widths at half intensity maximum and shifts for wavelengths 3500 Å- 7500 Åcovering the visible part of the spectrum for the electron density $N_e = 10^{14}$ cm^{-3}. In the first column, we give multiplets, wavelengths of the multiplets in Å and C values which give an estimate for the maximum perturber density for which the line may be treated as isolated if it is divided by the corresponding full width. Non-empty cells preceded by an asterisk mean that the impact approximation reaches its limit of validity ($0.1 < NV \leq 0.5$). Empty cells which are denoted by an asterisk mean that the impact approximation is not valid. The energy levels (terms) and the wavelengths of the multiplets are those of TOPbase.

Multiplet	T [K]	W_e [Å]	d_e [Å]	W_{CII} [Å]	d_{CII} [Å]
$2s^2$ 4s ^{2}S - $2s^2$ 3p ^{2}P^o	5000.	0.106E-02	0.571E-03	0.417E-04	0.454E-04
	10000.	0.758E-03	0.464E-03	0.587E-04	0.556E-04
3935.7 Å	20000.	0.678E-03	0.378E-03	0.730E-04	0.657E-04
C=0.82E+17	30000.	0.657E-03	0.327E-03	0.832E-04	0.739E-04
	50000.	0.643E-03	0.278E-03	0.948E-04	0.799E-04
	80000.	0.643E-03	0.232E-03	0.101E-03	0.835E-04
$2s^2$ 6s ^{2}S - $2s^2$ 4p ^{2}P^o	5000.	0.838E-02	0.461E-02	0.614E-03	0.593E-03
	10000.	0.702E-02	0.431E-02	0.776E-03	0.718E-03
5362.0 Å	20000.	0.664E-02	0.358E-02	0.923E-03	0.803E-03
C=0.51E+17	30000.	0.664E-02	0.330E-02	0.932E-03	0.880E-03
	50000.	0.703E-02	0.280E-02	0.111E-02	0.934E-03
	80000.	0.725E-02	0.238E-02	0.118E-02	0.103E-02
$2s^2$ 7s ^{2}S - $2s^2$ 4p ^{2}P^o	5000.	0.108E-01	0.644E-02	0.103E-02	0.991E-03
	10000.	0.940E-02	0.645E-02	0.125E-02	0.112E-02
4326.7 Å	20000.	0.875E-02	0.543E-02	0.152E-02	0.132E-02
C=0.19E+17	30000.	0.900E-02	0.477E-02	0.153E-02	0.135E-02
	50000.	0.933E-02	0.430E-02	0.164E-02	0.151E-02
	80000.	0.942E-02	0.358E-02	0.187E-02	0.149E-02
$2s^2$ 7s ^{2}S - $2p^3$ ^{2}P^o	5000.	0.236E-01	0.141E-01	0.222E-02	0.215E-02
	10000.	0.205E-01	0.143E-01	0.268E-02	0.246E-02
6368.7 Å	20000.	0.187E-01	0.120E-01	0.332E-02	0.288E-02
C=0.41E+17	30000.	0.191E-01	0.106E-01	0.333E-02	0.294E-02
	50000.	0.196E-01	0.965E-02	0.359E-02	0.327E-02
	80000.	0.196E-01	0.807E-02	0.401E-02	0.325E-02
$2s^2$ 8s ^{2}S - $2s^2$ 4p ^{2}P^o	5000.	0.149E-01	0.945E-02	0.163E-02	0.160E-02
	10000.	0.135E-01	0.961E-02	0.218E-02	0.177E-02
3864.2 Å	20000.	0.128E-01	0.797E-02	0.224E-02	0.197E-02
C=0.98E+16	30000.	0.133E-01	0.709E-02	0.227E-02	0.211E-02
	50000.	0.138E-01	0.628E-02	0.284E-02	0.220E-02
	80000.	0.139E-01	0.519E-02	0.297E-02	0.267E-02
$2s^2$ 8s ^{2}S - $2p^3$ ^{2}P^o	5000.	0.293E-01	0.187E-01	0.321E-02	0.315E-02
	10000.	0.266E-01	0.190E-01	0.429E-02	0.347E-02
5414.9 Å	20000.	0.249E-01	0.159E-01	0.439E-02	0.389E-02
C=0.19E+17	30000.	0.258E-01	0.141E-01	0.448E-02	0.416E-02
	50000.	0.267E-01	0.126E-01	0.552E-02	0.435E-02
	80000.	0.267E-01	0.104E-01	0.587E-02	0.529E-02

Table 1. Continued

Multiplet	T [K]	W_e [Å]	d_e [Å]	W_{CII} [Å]	d_{CII} [Å]
2s2p(^{3}P^o) 3p ^{2}P - 2s^2 4p ^{2}P^o	5000.	0.203E-02	-0.676E-03	0.204E-03	-0.474E-04
	10000.	0.161E-02	-0.520E-03	0.232E-03	-0.601E-04
5089.1 Å	20000.	0.142E-02	-0.420E-03	0.255E-03	-0.729E-04
C=0.20E+17	30000.	0.136E-02	-0.373E-03	0.266E-03	-0.808E-04
	50000.	0.132E-02	-0.315E-03	0.270E-03	-0.913E-04
	80000.	0.130E-02	-0.272E-03	0.281E-03	-0.972E-04
2s^2 3p ^{2}P^o - 2s^2 3s ^{2}S	5000.	0.139E-02	-0.281E-04	0.605E-04	-0.648E-05
	10000.	0.104E-02	-0.334E-04	0.814E-04	-0.105E-04
6741.6 Å	20000.	0.837E-03	-0.287E-04	0.924E-04	-0.146E-04
C=0.63E+18	30000.	0.784E-03	-0.310E-04	0.989E-04	-0.167E-04
	50000.	0.750E-03	-0.348E-04	0.106E-03	-0.191E-04
	80000.	0.730E-03	-0.308E-04	0.109E-03	-0.214E-04
2s^2 3p ^{2}P^o - 2s 2p^2 ^{2}P	5000.	0.589E-03	0.172E-03	0.357E-04	0.744E-05
	10000.	0.459E-03	0.111E-03	0.482E-04	0.110E-04
5165.8 Å	20000.	0.377E-03	0.851E-04	0.549E-04	0.150E-04
C=0.37E+18	30000.	0.350E-03	0.768E-04	0.589E-04	0.167E-04
	50000.	0.329E-03	0.675E-04	0.628E-04	0.191E-04
	80000.	0.315E-03	0.586E-04	0.649E-04	0.214E-04
2s^2 4p ^{2}P^o - 2s^2 3d ^{2}D	5000.	0.251E-02	0.717E-03	0.276E-03	0.555E-04
	10000.	0.199E-02	0.523E-03	0.313E-03	0.718E-04
5921.7 Å	20000.	0.177E-02	0.397E-03	0.344E-03	0.865E-04
C=0.19E+18	30000.	0.174E-02	0.345E-03	0.355E-03	0.956E-04
	50000.	0.174E-02	0.290E-03	0.368E-03	0.107E-03
	80000.	0.174E-02	0.239E-03	0.369E-03	0.118E-03
2p^3 ^{2}P^o - 2s^2 3d ^{2}D	5000.	0.816E-03	-0.281E-04	0.237E-04	-0.124E-04
	10000.	0.644E-03	-0.297E-04	0.328E-04	-0.172E-04
4115.6 Å	20000.	0.541E-03	-0.247E-04	0.384E-04	-0.210E-04
C=0.31E+17	30000.	0.503E-03	-0.177E-04	0.414E-04	-0.232E-04
	50000.	0.471E-03	-0.168E-04	0.457E-04	-0.263E-04
	80000.	0.447E-03	-0.143E-04	0.498E-04	-0.296E-04
2s^2 5p ^{2}P^o - 2s^2 4s ^{2}S	5000.	0.384E-02	0.234E-03	0.661E-03	0.892E-04
	10000.	0.356E-02	0.195E-03	0.731E-03	0.109E-03
5390.0 Å	20000.	0.366E-02	0.132E-03	0.758E-03	0.130E-03
C=0.72E+17	30000.	0.381E-02	0.116E-03	0.784E-03	0.144E-03
	50000.	0.402E-02	0.104E-03	0.788E-03	0.156E-03
	80000.	0.413E-02	0.107E-03	0.794E-03	0.167E-03
2s2p(^{3}P^o) 3s ^{2}P^o- 2s^2 4s ^{2}S	5000.	0.450E-02	-0.135E-02	0.510E-03	-0.519E-03
	10000.	0.383E-02	-0.109E-02	0.643E-03	-0.615E-03
4669.4 Å	20000.	0.343E-02	-0.907E-03	0.759E-03	-0.708E-03
C=0.44E+16	30000.	0.323E-02	-0.788E-03	0.882E-03	-0.778E-03
	50000.	0.302E-02	-0.655E-03	0.864E-03	-0.830E-03
	80000.	0.283E-02	-0.551E-03	0.980E-03	-0.864E-03

Table 1. Continued

Multiplet	T [K]	W_e [Å]	d_e [Å]	W_{CII} [Å]	d_{CII} [Å]
$2s^2$ 6p $^2P^o$ - $2s^2$ 4s ^2S	5000.	0.514E-02	0.253E-02	0.944E-03	0.389E-03
	10000.	0.490E-02	0.215E-02	0.100E-02	0.462E-03
3887.0 Å	20000.	0.497E-02	0.167E-02	0.108E-02	0.535E-03
C=0.11E+17	30000.	0.523E-02	0.144E-02	0.112E-02	0.581E-03
	50000.	0.551E-02	0.120E-02	0.121E-02	0.656E-03
	80000.	0.566E-02	0.990E-03	0.110E-02	0.681E-03
$2s^2$ 6p $^2P^o$ - $2s^2$ 4d ^2D	5000.	0.173E-01	0.740E-02	0.286E-02	0.107E-02
	10000.	0.168E-01	0.639E-02	0.308E-02	0.126E-02
6739.8 Å	20000.	0.170E-01	0.515E-02	0.323E-02	0.145E-02
C=0.35E+17	30000.	0.177E-01	0.447E-02	0.340E-02	0.161E-02
	50000.	0.184E-01	0.376E-02	0.341E-02	0.169E-02
	80000.	0.186E-01	0.312E-02	0.322E-02	0.181E-02
$2s^2$ 7p $^2P^o$ - $2s^2$ 5s ^2S	5000.	0.356E-01	0.168E-01	0.688E-02	0.307E-02
	10000.	0.358E-01	0.140E-01	0.721E-02	0.352E-02
7473.6 Å	20000.	0.386E-01	0.107E-01	0.779E-02	0.396E-02
C=0.35E+17	30000.	0.410E-01	0.928E-02	0.763E-02	0.427E-02
	50000.	0.436E-01	0.762E-02	0.760E-02	0.455E-02
	80000.	0.451E-01	0.608E-02	0.799E-02	0.468E-02
$2s^2$ 7p $^2P^o$ - $2s^2$ 4d ^2D	5000.	0.197E-01	0.968E-02	0.362E-02	0.161E-02
	10000.	0.194E-01	0.849E-02	0.380E-02	0.183E-02
5388.4 Å	20000.	0.204E-01	0.671E-02	0.413E-02	0.206E-02
C=0.18E+17	30000.	0.213E-01	0.596E-02	0.403E-02	0.224E-02
	50000.	0.223E-01	0.489E-02	0.405E-02	0.244E-02
	80000.	0.228E-01	0.401E-02	0.421E-02	0.248E-02
$2s^2$ 8p $^2P^o$ - $2s^2$ 5s ^2S	5000.	0.467E-01	-0.165E-02	0.865E-02	-0.345E-02
	10000.	0.480E-01	-0.104E-02	0.939E-02	-0.402E-02
6335.0 Å	20000.	0.517E-01	-0.331E-03	0.980E-02	-0.447E-02
C=0.63E+16	30000.	0.544E-01	-0.130E-03	0.988E-02	-0.474E-02
	50000.	0.570E-01	0.170E-03	0.108E-01	-0.536E-02
	80000.	0.584E-01	-0.950E-04	0.105E-01	-0.607E-02
$2s^2$ 8p $^2P^o$ - $2s^2$ 4d ^2D	5000.	0.272E-01	0.202E-03	0.494E-02	-0.194E-02
	10000.	0.278E-01	0.448E-03	0.536E-02	-0.227E-02
4770.3 Å	20000.	0.295E-01	0.671E-03	0.554E-02	-0.252E-02
C=0.36E+16	30000.	0.308E-01	0.941E-03	0.560E-02	-0.266E-02
	50000.	0.320E-01	0.842E-03	0.612E-02	-0.296E-02
	80000.	0.326E-01	0.651E-03	0.604E-02	-0.346E-02
$2s^2$ 3d ^2D - $2s^2$ 3p $^2P^o$	5000.	0.173E-02	-0.845E-04	0.120E-03	-0.117E-04
	10000.	0.132E-02	-0.470E-04	0.147E-03	-0.179E-04
7226.4 Å	20000.	0.109E-02	-0.278E-04	0.166E-03	-0.246E-04
C=0.72E+18	30000.	0.102E-02	-0.436E-04	0.177E-03	-0.272E-04
	50000.	0.976E-03	-0.357E-04	0.185E-03	-0.311E-04
	80000.	0.951E-03	-0.307E-04	0.191E-03	-0.349E-04

Table 1. Continued

Multiplet	T [K]	W_e [Å]	d_e [Å]	W_{CII} [Å]	d_{CII} [Å]
$2s^2$ 4d ^{2}D - $2p^3$ ^{2}D^o	5000.	0.348E-02	0.939E-03	0.367E-03	0.279E-03
	10000.	0.323E-02	0.833E-03	0.439E-03	0.334E-03
6022.4 Å	20000.	0.303E-02	0.678E-03	0.528E-03	0.395E-03
C=0.29E+17	30000.	0.293E-02	0.634E-03	0.564E-03	0.425E-03
	50000.	0.281E-02	0.553E-03	0.596E-03	0.466E-03
	80000.	0.270E-02	0.465E-03	0.648E-03	0.513E-03
$2s^2$ 5d ^{2}D - $2s^2$ 4p ^{2}P^o	5000.	0.139E-01	0.368E-02	0.172E-02	0.142E-02
	10000.	0.129E-01	0.306E-02	0.213E-02	0.166E-02
6289.5 Å	20000.	0.123E-01	0.242E-02	0.223E-02	0.184E-02
C=0.79E+16	30000.	0.121E-01	0.215E-02	0.252E-02	0.203E-02
	50000.	0.117E-01	0.177E-02	0.297E-02	0.217E-02
	80000.	0.113E-01	0.144E-02	0.340E-02	0.245E-02
$2s^2$ 5d ^{2}D - $2p^3$ ^{2}D^o	5000.	0.440E-02	0.152E-02	0.583E-03	0.500E-03
	10000.	0.412E-02	0.121E-02	0.736E-03	0.583E-03
3713.2 Å	20000.	0.392E-02	0.103E-02	0.771E-03	0.652E-03
C=0.28E+16	30000.	0.381E-02	0.924E-03	0.868E-03	0.711E-03
	50000.	0.366E-02	0.765E-03	0.102E-02	0.759E-03
	80000.	0.349E-02	0.629E-03	0.116E-02	0.853E-03
$2s^2$ 6d ^{2}D - $2s^2$ 4p ^{2}P^o	5000.	0.128E-01	0.363E-02	0.179E-02	0.137E-02
	10000.	0.127E-01	0.257E-02	0.213E-02	0.161E-02
4658.2 Å	20000.	0.129E-01	0.224E-02	0.223E-02	0.175E-02
C=0.62E+16	30000.	0.129E-01	0.196E-02	0.253E-02	0.204E-02
	50000.	0.128E-01	0.149E-02	0.251E-02	0.229E-02
	80000.	0.125E-01	0.129E-02	0.258E-02	0.224E-02
$2s^2$ 6d ^{2}D - $2p^3$ ^{2}P^o	5000.	0.297E-01	0.900E-02	0.413E-02	0.323E-02
	10000.	0.294E-01	0.677E-02	0.495E-02	0.379E-02
7114.0 Å	20000.	0.296E-01	0.595E-02	0.514E-02	0.411E-02
C=0.14E+17	30000.	0.297E-01	0.508E-02	0.598E-02	0.478E-02
	50000.	0.293E-01	0.397E-02	0.588E-02	0.538E-02
	80000.	0.283E-01	0.341E-02	0.600E-02	0.526E-02
$2s^2$ 7d ^{2}D - $2p^3$ ^{2}P^o	5000.	0.305E-01	0.105E-01	0.475E-02	0.338E-02
	10000.	0.316E-01	0.804E-02	0.575E-02	0.390E-02
5761.9 Å	20000.	0.335E-01	0.692E-02	0.592E-02	0.432E-02
C=0.82E+16	30000.	0.342E-01	0.569E-02	0.594E-02	0.444E-02
	50000.	0.343E-01	0.459E-02	0.712E-02	0.478E-02
	80000.	0.336E-01	0.395E-02	0.751E-02	0.580E-02
$2s^2$ 7d ^{2}D - $2s^2$ 4p ^{2}P^o	5000.	0.150E-01	0.496E-02	0.235E-02	0.165E-02
	10000.	0.156E-01	0.374E-02	0.283E-02	0.192E-02
4037.8 Å	20000.	0.165E-01	0.321E-02	0.293E-02	0.212E-02
C=0.41E+16	30000.	0.169E-01	0.262E-02	0.293E-02	0.217E-02
	50000.	0.171E-01	0.210E-02	0.354E-02	0.236E-02
	80000.	0.167E-01	0.181E-02	0.369E-02	0.285E-02

So, we have modified the SCP code of Sahal-Bréchot by coupling it to the energy level and oscillator strength data for C II data in the TOPbase ([6], http://cdsweb.u-strasbg.fr/TOPbase/), in order to calculate Stark broadening parameters for a large number (149) of C II multiplets.

2. Results and discussion

The Stark broadening parameters (Full Width at Half intensity Maximum - FWHM) have been obtained for 149 C II multiplets and the complete results are available on line in electronic form as Supporting information for Ref. [8], given in tables S1, S2 and S3. There is presented, as well, the comparison with existing experimental and other theoretical results and analysis of determined Stark broadening parameters. The results are presented for temperatures from 5000 up to 80000 K and electron densities 10^{14} (Table S1 in Supporting information for Ref. [8]), 10^{17} (Table S2, see Ref. [8]) and 10^{18} cm^{-3} (Table S3, see Ref. [8]). As an example of obtained results here are selected from the tables in electronic form given as additional information for Ref. [8], Strak broadening parameters for 27 C II multiplets for wavelengths 3500 Å- 7500 Åcovering the visible part of the spectrum, for the electron density $N_e = 10^{14}$ cm^{-3}. They are presented in Table 1. Values of the parameter C, given also in Table 1, divided by the corresponding full widths, give an estimate for the maximum perturber density for which the line may be treated as isolated (see Eq.(5) in Ref. [7]). For each value given in tables, the collision volume V multiplied by the perturber density N is much less than unity and the impact approximation is valid. Values for $NV > 0.5$ are not given but denoted by an asterisk and values for $0.1 < NV \leq 0.5$ are given but preceded by an asterisk.

The results will be also implemented in the STARK-B database, http://stark-b.obsmp.fr [9], [10], the result of a collaborative project between LERMA (Laboratoire d'Étude du Rayonnement et de la Matière en Astrophysique, Observatoire de Paris) and AOB (Astronomical Observatory, Belgrade). The STARK B database is currently developed at Paris Observatory. It is in free access, and is on line since the end of 2008. It is a part of the atomic and molecular databases of the Paris Observatory, and there is a link to the Serbian Virtual Observatory (SerVO, http://servo.aob.rs/ darko). A mirror site is planned at AOB. STARK-B is, as well, one of databases of VAMDC (Virtual Atomic and Molecular Data Centre - http://vamdc.eu and http://portal.vamdc.eu) [11], [12], the FP7 European project created in summer 2009 for 3.5 years. Its aim is to create and maintain an interoperable e-Infrastructure for exchange of atomic and molecular data, to serve as a forum for data producers and users, and to develop standards and softwares for exchange of atomic and molecular data. ore details on VAMDC and STARK-B are given in Ref. [10] in this issue.

References

[1] Dufour P, Liebert J, Fontaine G and Behara N 2007 *Nature Letters* **450** 522
[2] Dufour P, Fontaine G, Liebert J, Schmidt G D and Behara N 2008 *ApJ* **683** 978
[3] Sahal-Bréchot S 1969 *A&A* **1** 91
[4] Sahal-Bréchot S 1969 *A&A* **2** 322
[5] Sahal-Bréchot S 1974 *A&A* **35** 319
[6] Cunto W, Mendoza C, Ochsenbein F and Zeippen C J 1993 *A&A* **275** L5
[7] Dimitrijević M S, Sahal-Bréchot S and Bommier V 1991 *A&A* **89** 581
[8] Larbi-Terzi N, Sahal-Bréchot S, Ben Nessib N and Dimitrijević M S 2012 *MNRAS* **423** 766
[9] Sahal-Bréchot S, Dimitrijević M S and Moreau N 2012 STARK-B database, [online]. Available: http://stark-b.obspm.fr [Jul 15, 2012]. Observatory of Paris, LERMA and Astronomical Observatory of Belgrade
[10] Sahal-Bréchot S, Dimitrijević M S and Moreau N 2012 *J. Phys.: Conf. Series* this issue
[11] Dubernet ML, Boudon V et al. 2010 JQSRT 111 2151, http://www.vamdc.eu/
[12] Rixon G, Dubernet M L, et al. 2011 7th International Conference on Atomic and Molecular Data and their Applications -ICAMDATA-2010, AIP Conf. Proc. 1344 107

J. Quant. Spectrosc. Radiat. Transfer. Vol. 19. pp. 407–416. Pergamon Press 1978. Printed in Great Britain

LONG-RANGE POTENTIALS AND STARK BROADENING OF NEUTRAL LINES†

M. S. DIMITRIJEVIĆ and P. GRUJIĆ
Institute of Physics, 11001 Beograd, P.O. Box 57, Yugoslavia

(*Received* 4 *March* 1977)

Abstract—The influence of the dipole polarization and quadrupole potentials on the Stark broadening of isolated neutral lines in a plasma has been investigated within the semiclassical approximation. It has been shown that both the perturbing electron trajectories and the minimum impact parameter may undergo a noticeable change when reaction of the emitter on the impact electron is taken into account. The effects on the halfwidths of selected lines have been examined within the impact approximation. Calculated results are compared both with available experimental data and other theoretical results. The importance of including long-range effects is also discussed.

1. INTRODUCTION

ALTHOUGH there exist a number of quantum-mechanical theories of the Stark broadening of lines in plasma [e.g. BARANGER,[1] TRAN MINH and VAN REGEMORTER,[2] BASSALO and CATTANI,[3]], the semiclassical theory of GRIEM, BARANGER, KOLB and OERTEL[4] (GBKO) has been most widely used in actual calculations. The essential part of this approximation is that, instead of dealing with cross sections for the electron–atom (ion) scattering [as in BARANGER's[5] and SAHAL-BRECHOT's[6] work], one calculates relevant probabilities for transitions from upper and lower levels of the line to various perturbing levels, caused by the time-dependent perturbations involving impact electrons moving along well defined classical paths. This method is extensively used in the theory of electron–atom (and ion–atom) collisions [SEATON[7]] and it is particularly useful in describing the mechanism of line broadening, where "weak collisions" are usually dominant and can be successfully treated by the perturbation method.

In an early stage of the application of the GBKO theory, several further approximations were made which, though not inherent to the theory, were introduced to simplify numerical calculations. One of these was the neglect of the influence of an emitter on the motion of perturbers. This approximation turned out to be very crude in the case of the ionized emitters, and introduction of hyperbolic paths instead of rectilinear ones resulted in a considerable improvement of calculated halfwidths and shifts of ionized emitter lines. On the other hand, because of the much shorter range of a neutral atom potential which an impact electron sees, the rectilinear-path approximation has been retained in treating the electron–atom perturbing collisions. This approximation was justified by the fact that even those multipole potentials with longest range, like the polarization and quadrupole potentials, are weak enough for large electron–atom separations which are mainly encountered in the process of line broadening (weak collisions).

However, under some conditions, the assumption of the straight-line trajectories may break down for electron–atom collisions within some range of the impact parameter of the impinging electron. These deviations may affect the halfwidth of the emitted line in two ways, via the Stark broadening functions A_2 and by an appearance of a critical impact parameter, which separates "normal" trajectories from those passing through the origin.

In the next section, we present some analytical calculations regarding the electron motion in the presence of the leading terms of the excited atom long-range potential. The critical parameter and new A_2 functions are then calculated. Numerical results for the halfwidths of lines from a multiplet of $N(I)$ are given in the third section. In the last section, the importance of long-range potential effects is discussed as well as applicability of the method used.

†This work was supported by the RZN of SR Serbia.

2. ANALYTICAL CALCULATIONS

(1) *An electron-excited-atom, long-range interaction*

If one disregards contributions of the inner electrons, the interaction potential between the impact electron and an excited atom in the ith state can be expanded into the multipole series

$$V(\mathbf{R}) = \sum_{\lambda} \frac{1}{R^{\lambda+1}} \langle i | r^{\lambda} P_{\lambda}(\cos\theta) | i \rangle, \tag{1}$$

where $\mathbf{R}$ is the position of the impact electron and r, θ are coordinates of the atomic electron (θ being the angle between $\mathbf{R}$ and $\mathbf{r}$). For a nonhydrogenic system, the series starts with the $\lambda = 2$ term. We shall assume that the colliding electron moves so slowly that one may take the line joining the electron with the atom to be the quantization axis. Then the quadrupole ($\lambda = 2$) term in eqn (1) is given by [LANDAU and LIFSHITZ[8]]

$$V_{q_i} = \frac{q_i}{2R^3} \frac{J(J+1) - 3M^2}{J(2J-1)}, \quad q_i = \langle i | r^2 | i \rangle \frac{2J-1}{2J+2}, \tag{2}$$

where q_i is the quadrupole moment of the excited atom in the ith state, J is the total angular momentum quantum number, and $M = -J, -J+1, \ldots, J$.

Distortion of the atom in the presence of the weak external electric field of the impact electron gives rise to the polarization potential, which behaves asymptotically as

$$V_p(r) \sim -\frac{\alpha}{2r^4}, \quad r \to \infty, \tag{3}$$

where α is the atomic polarizability. Excluding virtual transitions to those higher states to which real excitations are energetically possible, we may calculate the so called effective polarizability [e.g. DAMBURG and GELTMAN[9]], viz.

$$\alpha = 2 \sum_{n} \frac{|\langle i | r | n \rangle|^2}{3(E_n - E_i)}, \quad E_n - E_i > \frac{1}{2} k^2, \tag{4}$$

where E_j is the energy of jth state of the atom and k is the impact electron velocity at infinity. As can be seen from eqns (2) and (4), α is an essentially positive quantity whereas V_{q_i} may assume both positive and negative values.

(2) *Electron motion in the long-range atomic potential*

Let an electron be moving in the field of an excited atom. We shall examine this motion under the following conditions: (a) The electron impact parameter is much larger than the mean radius of the excited target: $r_a \simeq (n_i^*)^2$, where n_i^* is the effective quantum number of the ith excited state. (b) the electron velocity is small enough so that, together with (a), conditions for an adiabatic collision are fulfilled.

Under these conditions, we may assume that, first, an asymptotic form of the atomic potential can be used, and secondly the relative change $|\Delta\mathbf{R}|/R$ of the impact electron is slow enough so that the atom can adjust itself adiabatically to this change. In particular, polarization of the atom remains along the quantization axis. Otherwise, dynamical effects must be taken into account [see, e.g. LABAHN and CALLAWAY[10]].

(a) *The Vogt and Wannier theory and electron-excited atom scattering.* In their paper, VOGT and WANNIER[11] analyzed scattering of a charged particle on a neutral atom in a gas, taking into account the polarization potential interaction of the form of eqn (3). They analyzed in detail the motion of the electron and ion in this long-range potential, both classically and quantum mechanically, and in the former case defined a classical capture cross section determined by the critical impact parameter ρ_c, which exists for any value of the particle mass. However, in the limiting, zero energy case, the quantum mechanical treatment revealed a marked difference between electron and ion behaviour for small impact parameters. It was found that, in the case of ion scattering, the origin may be treated as a sink, regardless of the shape of the ion–atom interaction potential near the origin (more precisely, at the distance from the origin comparable with the diameter of the atom). The wave function can be written as [see eqn (22) in their paper]

$$\psi \simeq \exp i(A/r + pz/A), \quad A = \sqrt{\alpha m}, \quad p = km\sqrt{\alpha}, \tag{5}$$

where α is the target polarizability, m the reduced mass and k the impact-particle velocity. For ions, the reduced mass is always large and when p is very small ($k \ll 1$), the first term in the exponent of ψ in eqn (5) describes an infall near the origin ($r \to 0$), whereas the long-distance behaviour of ψ is governed by the second term: pz/A. These conditions are not fulfilled in the case of electron–atom scattering (in any case, not for the ground state) and a small distance, repulsive

potential must be accounted for [CASE[12]]. The crucial quantity is A: if it is sufficiently large, the change of phase of ψ near the atom is very rapid and the outgoing waves add incoherently, which thus differs from to the case of an electron scattering. In the latter case, A is small and the coherently scattered waves may produce effects similar to those observed with Ramsauer–Townsend effect for electron–noble gas elastic scattering.

In the finite energy case ($k \neq 0$), the corresponding capture cross section obtained quantum-mechanically showed small oscillations around the classical values and assumed twice the value at $k = 0$. This result is of importance since it shows that, apart from the zero-energy limit, the classical trajectory method should be applicable in treating ion-atom, low energy collisions. However, in Stark broadening, it is electron–atom scattering which is dominant, and we must examine this process in some detail in view of the Vogt and Wannier theory.

The long-range potentials are important in electron–atom scattering even when the target is in the ground state, particularly for low impact energies. Moreover, if the atom is in an excited state, this interaction is an especially prominent one. All constants determining strengths of various polarization and multipole potential constants become larger as the effective quantum number of the excited target, n^*, increases. Therefore, the electric dipole polarizability, given by eqn (4), behaves as

$$\alpha \sim (n^*)^6,$$

while the quadrupole moment, q, rises proportionally to $\langle r^2 \rangle$ and consequently as $(n^*)^4$. For large n^*, when the valence electron is loosely bound, the slow incoming, perturbing electron and the atomic electron should be treated on an equal footing, i.e. the reaction of the excited target on the electron may be comparable in magnitude with the impact–electron perturbation.

As outlined above, the Vogt and Wannier theory did not seem, at first sight, relevant to the Stark broadening theory. However, two points must be emphasized here.

(1) Unlike the ground states of inert gases, an excited atom has a very unstable configuration, which may be greatly perturbed by close electron collisions. Therefore, though the ray patterns need not necessarily correspond to a "fall in" case, the probability for the collision to be an elastic one for $\rho < \rho_c$ might be negligible compared with the amplitudes of various inelastic processes. A low-energy impact electron can cause only virtual excitations, for a target in the ground state. These transitions effectively cause the polarization potential. In an excited state, the atom may undergo superelastic collisions even with a zero-energy impact electron. Whatever the fate of the infalling electron is, it is bound to produce a large perturbation of the excited atom for $\rho < \rho_c$. Hence, all collisions with $\rho < \rho_c$ may be regarded as strong ones.

(2) Even if we disregard inelastic processes, the condition for a capture to take place may be realized for $\rho < \rho_c$ and, consequently, the elastic cross section is again diminished. To illustrate this, let the target atom be in an excited state with effective quantum number n^*. The mean radius of the atom is of the order $(n^*)^2$ and the constant A from eqn (5) is

$$A \sim (n^*)^3 \sim r_a^{3/2}. \tag{6}$$

The "period" τ of ψ is given, at a distance $r \simeq r_a$, by

$$\tau(r_a) = 2\pi r_a^2/(A - 2\pi r_a). \tag{7}$$

The relative change of the phase of ψ at $r = r_a$ is given by

$$\tau(r_a)/r_a = 1/(br_a^{1/2} - 1) \sim 1/n^*, \quad b \equiv A/2 \tag{8}$$

if $bn^* \gg 1$, which may be realized for highly excited states. In this case, one has again incoherent superposition of outgoing waves and no qualitative difference arises between electron and ion scattering for $\rho < \rho_c$. Hence, we may expect the Vogt and Wannier theory to be applicable also for the electron impact.

We conclude that, for electron-excited-atom collisions, for $\rho < \rho_c$, both classical and quantum mechanical descriptions of the process will lead to strong collisions.

(b) *Electron trajectories.* An electron path in the field with potential $V(R) = V_{q_i} + V_p$ is given by the elliptic integral [e.g. GOLDSTEIN[13]]

$$\phi = k\rho \int_R^\infty \frac{dr}{\sqrt{\xi(r)}}, \quad \xi(r) \equiv k^2 r^4 - k^2 \rho^2 r^2 - Qr + \alpha, \tag{9}$$

where ρ is the impact parameter and

$$Q \equiv q_i \frac{J(J+1)-3M^2}{J(2J-1)} \tag{10}$$

is the projection of the quadrupole moment onto the quantization axis. Unlike the case of the polarization potential, when the simple analytical expression for the critical impact parameter can be derived [VOGT and WANNIER[11]], viz.

$$\rho_c = \sqrt{\frac{2}{k}}\,\alpha^{1/4}, \tag{11}$$

now it is more convenient to calculate ρ_c numerically, as is shown in Appendix I. With $\rho < \rho_c$, the particle moves through the origin, which is the common feature of singular potentials of the form $V(r) = a/r^{\mathcal{H}}, 2 < \mathcal{H} \leq 4, a < 0$.

(c) *The Stark-broadening functions.* In the theory of Stark broadening for neutral emitters, second order perturbation theory is usually used and an electron–atom collision is treated as a time-dependent perturbation of the emitter by the impinging electron moving along a straight line. In the dipole approximation, the interaction-potential matrix is then given by

$$V_{ij}(t) = \left\langle i \left| \frac{1}{R(t)} - \frac{1}{|\mathbf{R}(t)-\mathbf{r}(t)|} \right| j \right\rangle \simeq \frac{\langle i|r|j\rangle}{\rho^2 + k^2 t^2}, \tag{12}$$

where $\mathbf{R}(t)$ and $\mathbf{r}(t)$ are instantaneous positions of the impact and atomic electrons, respectively. However, as we have shown, the electron motion is better represented by curvilinear paths (see Fig. 21) than by straight lines. This deviation from the uniform electron motion modifies the GBKO Stark broadening functions $A_2(z)$ [e.g. GRIEM[14]].

Instead of calculating the A_2 functions via the electron trajectories given by eqn (9), we have simplified the problem by approximating the actual paths by broken lines, as indicated in Fig. 3. Then the new A_2 functions depend on two arguments: $Z_{jj'} = \rho\omega_{jj'}/k$ and θ, where θ is half of the angle between the asymptotic electron velocities $\mathbf{v}(-\infty)$ and $\mathbf{v}(+\infty)$, viz.

$$\theta = \pi - k\rho \int_{r_{\min}}^{\infty} [\xi(r)]^{-1/2}\,\mathrm{d}r. \tag{13}$$

If one denotes roots of $\xi(r)$ by $r_{\min} = a > b > c > d$, eqn (13) can be written as

$$\theta = \pi - \frac{2\rho}{\sqrt{(a-c)(b-d)}} K(\epsilon), \quad \epsilon^2 \equiv \frac{(a-d)(b-c)}{(a-c)(b-d)},$$

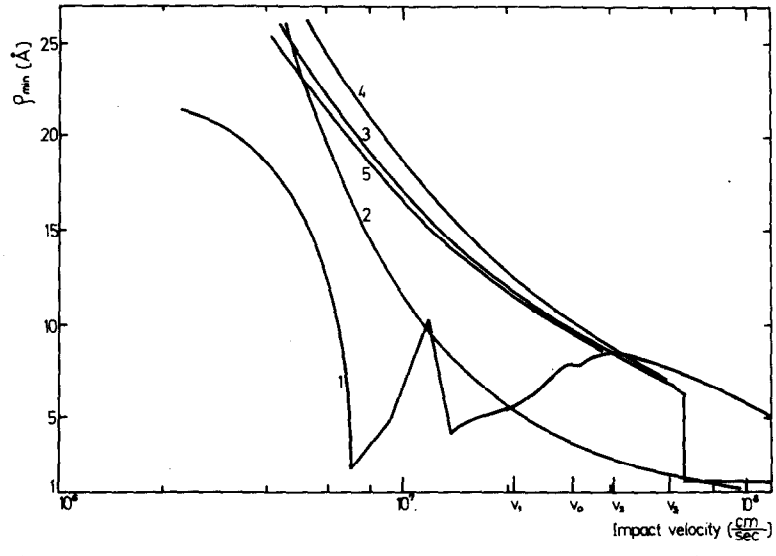

Fig. 1. Minimum impact parameters for the impact electron: (1) semiclassical (no interaction); (2) λ; (3) polarization potential only; (4) polarization plus attractive quadrupole interaction; (5) average critical impact parameter ρ^{LR} (see the text); v_0, the most probable velocity (Maxwellian distribution).

where $K(\epsilon)$ is the complete elliptic integral of the first kind [ABRAMOVITZ and STEGUN[15]]. How the $A_2(Z, \theta)$, $a_2(Z, \theta)$ and $b_2(Z, \theta)$ functions are calculated is shown in Appendix II.

(3) *Electron impact line broadening*

The half-halfwidth and shift of the neutral line can be calculated by a formula derived from the GBKO theory by COOPER and OERTEL,[16] viz.

$$w + id = N_e \int_0^\infty v f(v)\, dv \{\pi(\rho_{\min}^2 - \lambda\!\!\!^{-2}) + \frac{4}{3}\pi\lambda\!\!\!^{-2} \sum_{i'} \mathbf{R}_{ii'}^2 [a_2(|Z_{ii'}^{\min}|, \theta) + ib_2(Z_{ii'}^{\min}, \theta)] + \frac{4}{3}\pi\lambda\!\!\!^{-2} \sum_{f'} \mathbf{R}_{ff'}^2 [a_2(|Z_{ff'}^{\min}|, \theta) - ib_2(Z_{ff'}^{\min}, \theta)]\Big\}. \tag{14}$$

In the GBKO theory, $\rho_{\min}$ is imposed by the unitarity of the scattering matrix S through the equation

$$|\{1 - \langle i|S|i\rangle\langle f|S^{-1}|f\rangle\}| = 1. \tag{15}$$

However, if this value is smaller than $\lambda\!\!\!^{-}$, the latter is taken instead and the first term on the right-hand side of eqn (14) is set equal to zero. On the other hand, as we have seen, all collisions with $\rho < \rho_c$ may be regarded as strong ones and consequently ρ_c should be used instead of $\rho_{\min}$. Hence, for a fixed velocity k, we have calculated $\lambda\!\!\!^{-}$, $\rho_{\min}$ and ρ_c and then employed the largest of these.

3. NUMERICAL CALCULATIONS

We have considered several lines in order to estimate the effect of the polarization and quadrupole (if present) potentials on the Stark broadening. Matrix elements for dipole transitions are taken from WIESE.[17] We have used the computer program developed by OERTEL [from the paper by COOPER and OERTEL[16]]. Although the program provides facilities for calculating quadrupole transition contributions, we have used only optically allowed transitons perturbing levels. As is shown by contributions in Ref. (16), quadrupole transitions are usually negligible. Moreover,[16] if these contributions are large, the perturbation expansion may break down. The upper integration limit for ρ is taken to be at infinity since the shielding effect may be neglected, as discussed by JONES.[18] Calculations have been carried out for the temperature range 5000–40,000 K. Although the lowest temperature is too low for the usual laboratory experimental conditions, we have carried out computations for this temperature, since it is expected that long-range potential effects are most prominent for low impact velocities. The unsymmetrized form of the Z-arguments of the a_2 functions has been used, although the computer program provides facilities both for symmetrized and unsymmetrized versions. We have made this choice because, in our approach, the reaction of the emitter on the perturber is already effectively taken into account, to some extent, by the nonuniform motion of perturbing electrons.

Since the reliability of both theoretical and experimental values for shifts is rather dubious, only halfwidths of neutral spectral lines have been calculated.

$$\mathrm{N(I)},\ 3s^4P - 3p^4D^0, \quad \lambda = 8692\ \text{Å (multiplet 1)}$$

We have chosen this line for the following reasons. The effective polarizability of the upper level of the transition is fairly large and the emitter possesses a non-zero quadrupole moment in the upper level state, so that we can investigate the relative contribution of quadrupole interactions. Furthermore there are experimental results available for the halfwidth.

The structure of multiplet 1 is given in Table 3. Lines 1, 2, 4, 5, 6 and 7 have non-zero quadrupole moment in the initial state, as may be seen from Table 3. According to eqn (10), lines 1 and 5 may have three different projections of the quadrupole moment of the upper state, whereas the 2, 4 and 7 lines possess two projections only; finally line 6 has four different projections. For lines 3 and 8, only the polarization potentials come into play. We shall examine

lines 2, 4 and 7 in greater detail. The quadrupole moment of the upper state $1s^22s^22p^2(^3P)3p(^4D^0)_{3/2}$ can be calculated according to eqn (2) by taking into account the quadrupole moment of the excited $3p$ electron. The factor $\langle i|r^2|i\rangle$ in eqn (2) has been calculated according to a standard formula [e.g. JONES[18]].

We have calculated the minimum impact parameter according to eqn (11) (i.e. without Q) and numerically (see Appendix I). We present numerical values for a temperature $T = 5000$ K in Fig. 1, together with values obtained from eqn (15).

As can be seen from Fig. 1, the influence of the quadrupole interaction on ρ_c is negligible in this particular case. Of course, if the effective polarizability α is small enough, the relative contribution of the quadrupole interaction may be comparable with that of the polarization potential contribution but, in this case, both can be neglected. One peculiar feature of the polarization potential interaction, shown in Fig. 1, are steps in the potential curve due to sudden changes of magnitude of α as a function of the impact-electron velocity [see eqn (4)]. As for the semiclassical ρ_{min} curve, one sees in Fig. 1 that in some low-velocity region, the curve is not smooth because of numerical difficulties in solving eqn (15) as discussed in Appendix I. However, this velocity region does not contribute to the calculated halfwidths, since it is π which counts there if long-range effects are neglected.

Clearly, for velocities smaller than some $v = v_1$ (see Fig. 1), the critical impact parameter ρ_c is larger than semiclassical ρ_{min} and should be used instead.

We shall now investigate numerically the influence of the deviation of perturber paths from rectilinear trajectories. The set of trajectories for a particular case, $\alpha = 568.6$ a.u. (this effective polarizability corresponds to $v < v_0$ in Fig. 1) is given in Fig. 2; for a particular impact parameter, trajectories with additional contributions for $Q = \pm 10.54$ a.u. are also given. As can be seen from Fig. 2, it is only for ρ not much different from ρ_c that the deviation from the straight path is significant. Moreover, in case $\rho \gtrsim \rho_c$ it is the scattering angle which changes rapidly but the curves may be approximated by a broken line, as is indicated in Fig. 3. This is a general feature of all noncoulombic long-range interaction. We have calculated the $A_2(|Z|, \theta)$ function, by using applicable formulae in Appendix II for particular numerical values of the relevant parameters for our lines and along several paths from Fig. 2. The results are given in Table 1, where the functions $A_2(|Z|)$ are also presented for comparison.

As can be seen from Table 1, introduction of the long-range potential gives rise to a change of many orders of magnitude in the numerical values of the A_2 functions. However, the new A_2

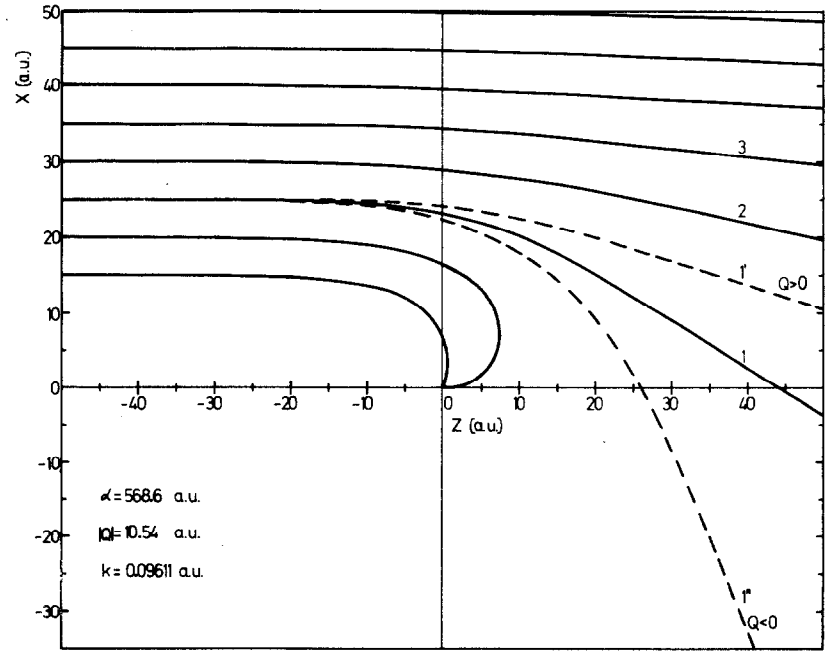

Fig. 2. Electron trajectories for the long-range potential of $N(I)(3p^4D^0)$.

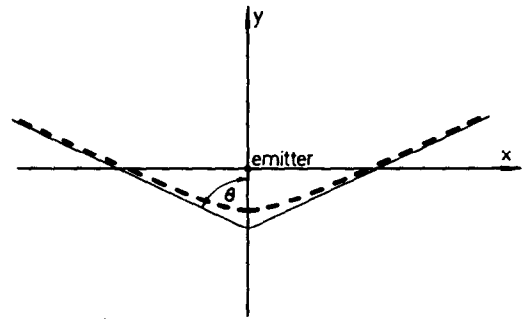

Fig. 3. - - - -, The perturber path in a long-range potential; ——, the approximate perturber path.

Table 1. The A_2 functions for Stark broadening.

α = 568.6 a.u.						
v_1 = 0.09611 a.u. (=2.102.10^7 cm/sec)						v_3 = 0.274 a.u (=6·10^7 cm/sec
ρ(a.u)	35	30	25			15.71
Z	19.084	16.36	13.63			3
A_2(|z|)	1.59·10^{-15}	3.168·10^{-13}	6.206·10^{-11}			0.02537
Q(a.u)	0	0	+10.54	0	-10.54	0
θ(rad)	1.517	1.462	1.422	1.265	0.976	1.363
A_2(|z|,θ)	8.120·10^{-6}	4.474·10^{-5}	1.236·10^{-4}	5.121·10^{-4}	1.771·10^{-3}	0.01942

Table 2. Half-halfwidths of N(I), multiplet 1, ($3s^4P - 3p^4D^0$), λ = 8692 Å, $N_e = 10^{16}$ cm^{-3}.

T(K)	w^{CO}(Å)	w^G(Å)	w^P(Å)	w^{LR}(Å)
5000	0.0339	0.0334	0.0375	0.0371
10000	0.0420	0.0448	0.0437	0.0435
20000	0.0566	0.0613	0.0572	0.0571
30000	0.0721	-	0.0724	0.0724
40000	0.0866	0.0805	0.0869	0.0868

functions are still negligibly small and consequently are not expected to influence noticeably th final results. This is due to the fact that values of the argument Z are too small for th particular choice of the relevant parameters.

In order to investigate the possible effect of the long-range potential influence, we hav picked up a more suitable set of parameters and then calculated the $A_2(|Z|, \theta)$ functions. Th numerical results are also given in Table 1 ($v = v_3$).

As can be seen from Fig. 1, the velocity v_3 is rather far away from the most probabl velocity v_0 and consequently the change in A_2 values (see Table 1) should not cause noticeabl change in the final values of the halfwidth. However, this may not be the case for lines wit large effective polarizabilities α with denser perturbing levels.

We have computed half-halfwidths for five different temperatures. The results are given i Table 2 where w^{CO} are the half-halfwidths computed by using the program of COOPER an OERTEL,[16] the w^G are taken from Griem's book,[14] w^P are our numerical results wit

polarization potential interaction only, and w^{LR} are values with the complete long-range interaction (polarization + quadrupole interaction). These last results have been obtained by setting $\rho_c = \frac{1}{2}[\rho_c(Q^+) + \rho_c(Q^-)]$ instead of using an average over $\rho_c(Q)$. This approximation is of course justified, if the function under the integral does not vary greatly in the lower integration region. The approximation also affects the strong collision term but, according to our estimates, the error thus introduced is only about 2%.

For some lines from multiplet 1 there exist experimental results by MORRIS, KREY and GARRISON[19] obtained at $T = 13{,}000$ K and $N_e = 10^{16}$ cm^{-3}. More recent results (the recommended values) for lines of multiplet 1 (lumped together) by HELBIG, KELLEHER and WIESE,[20] for the temperature range 10,000–16,000 K are also available. We present these in Table 3, together with the theoretical results extrapolated graphically to these temperatures.

As is seen from Table 3, the experimental situation is not clear since MORRIS, KREY and GARRISON[19] obtained different values for different lines within the multiplet whereas HELBIG, KELLEHER and WIESE,[20] whose measurements should be regarded as more reliable, recommend a unique value for the entire multiplet. Since our analysis has shown, in this particular case, that the quadrupole interaction is negligible, it should be used as additional evidence of the negligible variation of w within this multiplet. This conclusion should remain unaltered even if one carried out calculations by making use of proper matrix elements $R^2_{jj'}$ for each particular line within each multiplet, instead of using lumped values as we have done. The theoretical results in Table 3 do not differ greatly from each other and are slightly larger than the value of HELBIG, KELLEHER and WIESE.[20]

4. DISCUSSION

It is clear from the above analysis that the overall effect of the long-range interaction on the halfwidths of spectral lines of neutral emitters will crucially depend on the effective polarizability α of the upper level of transition, and on the magnitude of an (eventual) quadrupole moment of the same state. Obviously the most favourable case would be that when α remains large in a sufficiently large velocity region, particularly if the latter comprises the velocity distribution maximum. This will be achieved if one of dominant terms in eqn (4) is sufficiently far

Table 3. Half-halfwidths for N(I), multiplet 1 at $T = 13{,}000$ K, $N_e = 10^{16}$ cm^{-3}; experimental values: w^M—MORRIS *et al.*;[19] w^H—HELBIG *et al.*;[20] theoretical values: w^G—GRIEM;[14] w^{CO}—COOPER and OERTEL,[16] w^P—present work (using the polarization potential only).

No	J_f	J_i	λ (Å)	w^M (Å)
1	5/2	5/2	8718.8	0.0495
2	3/2	3/2	8711.7	0.0495
3	1/2	1/2	8703.3	0.0515
4	1/2	3/2	8686.2	0.0515
5	3/2	5/2	8683.4	0.0615
6	5/2	7/2	8680.3	0.0590
7	5/2	3/2	8747.4	-
8	3/2	1/2	8728.9	-
multiplet 1 $3s^4P - 3p^4D^o$			8692.	$w^H = 0.0450$ $w^G = 0.0500$ $w^{CO} = 0.0462$ $w^P = 0.0478$

away from the upper level of the transition. However, if there are some close perturbing levels of the upper state and/or of the lower, one, the corresponding semiclassical ρ_{min} may also be large and consequently the long-range interaction effect need not be noticeable. In any case, if α is everywhere small, or if it is large but in the velocity region far away from the distribution function maximum, the effect we have investigated is negligible. As an example of the second case we have investigated He(I) line $\lambda = 4713.2$ Å, where the effective polarizability has its maximum value: $\alpha = 6.92 \cdot 10^4$ a.u. Halfwidths of this line have been computed for the same temperatures as in the case of N(I) line from the previous section, and no significant change from the values computed according to the Cooper and Oertel method has been revealed. The same conclusion is obtained in case of lines Li(I), $\lambda = 5707.8$ and 8126.4 Å and Mg(I), $\lambda = 11828$ Å.

As expected, the most prominent change in calculated halfwidths is obtained in the low temperature region, where the average velocity is small enough. However, if the average velocity is too low, $\rho_{min} = \bar{\lambda}$ dominates both ρ_{min}^{SC} and ρ_c.

According to our results from the previous section, it turns out that the choice of ρ_{min} in the velocity region $v < v_2$ (see Fig. 1) does not affect the calculated halfwidth appreciably. However, one might make use of this negative result and compute ρ_{min} in this region only by ρ_c and $\bar{\lambda}$, what is much simpler and more safe from the numerical point of view and consequently saves some computing time.

We have not taken into account quadrupole polarizabilities of the atoms. One might think that this polarizability could play an important role in the velocity region where α drops to very small values. However, since the distance of the minimum approach is generally much larger than 1 a.u., the contribution from the quadrupole polarization potential, which falls down as r^{-6}, would be negligible compared to the quadrupole potential interaction (if present). If $Q = 0.$ and $\alpha \simeq 0.$, the quadrupole polarization potential could be the dominant one, but its effect would be very small in any case.

We chose N(I), multiplet 1, for our analysis partly because of the availability of the experimental results. However, one might find other lines where long-range interaction effects are more prominent ones, and where the quadrupole interaction could give rise to a noticeable change in halfwidths of different components within a multiplet. This last effect could be the best criterion for an estimate of the importance of the long-range effects for the spectral lines from neutrals.

Acknowledgements—We would like to thank Prof. H. R. GRIEM for the very illuminating discussion and useful suggestions. Thanks are due to Dr N. KONJEVIĆ for supplying us with the computer code of Dr G. K. OERTEL. All computations have been done on the IBM 360/44 at the Institute of Mathematics, Beograd.

REFERENCES

1. M. BARANGER, *Phys. Rev.* **111**, 481 (1958).
2. TRAN MINH and H. VAN REGEMORTER, *J. Phys. B* **5**, 903 (1972).
3. J. M. BASSALO and M. CATTANI, *Can. J. Phys.* **53**, 2285 (1975).
4. H. R. GRIEM, M. BARANGER, A. C. KOLB and G. K. OERTEL, *Phys. Rev.* **125**, 177 (1962).
5. M. BARANGER, *Phys. Rev.* **112**, 855 (1958).
6. S. SAHAL-BRECHOT, *Astron. Astrophys.* **1**, 91 (1969).
7. M. J. SEATON, *Proc. Phys. Soc. (London)* **79**, 1105 (1962).
8. L. D. LANDAU and E. M. LIFSHITZ, *Quantum Mechanics.* Pergamon Press, London (1965).
9. R. DAMBURG and S. GELTMAN, *Phys. Rev. Lett.* **20A**, 485 (1968).
10. R. B. LABAHN and J. CALLAWAY, *Phys. Rev.* **147**, 2870 (1966).
11. E. VOGT and G. H. WANNIER, *Phys. Rev.* **95**, 1190 (1959).
12. K. M. CASE, *Phys. Rev.* **80**, 797 (1950).
13. H. GOLDSTEIN, *Classical Mechanics.* Addison-Wesley, London (1950).
14. H. R. GRIEM, *Spectral Line Broadening by Plasmas*, Academic Press, New York (1974).
15. M. ABRAMOWITZ and I. A. STEGUN, *Handbook of Mathematical Functions* (Edited by M. ABRAMOWITZ and I. A. STEGUN) (NBS, Appl. Math. Ser., Vol. 55, 1964).
16. J. COOPER and G. K. OERTEL, *Phys. Rev.* **180**, 286 (1969).
17. W. L. WIESE, M. W. SMITH and B. M. GLENNON, *Atomic Transition Probabilities*, Vol. I. U.S. Govt. Print. Office, Washington D.C. (1969).
18. W. W. JONES, *Phys. Rev.* **A7**, 1826 (1973).
19. J. C. MORRIS, U. R. KREY and R. L. GARRISON, *Radiation Studies of Arc Heated Nitrogen, Oxygen and Argon Plasmas*, AVCO Corporation, Space Systems Division, Report AVVSSD-0049-68-RR (1968).
20. V. HELBIG, D. E. KELLEHER and W. L. WIESE, *Phys. Rev. A* **14**, 1082 (1976).

APPENDIX I

Electron motion in the joint polarization and quadrupole potential

If the projection of the quadrupole moment of an atom onto the line connecting its nucleus with the incoming electron (quantization axis) is denoted by Q, then the leading terms of the long-range interaction potential are given by

$$V(r) = \frac{Q}{2r^3} - \frac{\alpha}{2r^4}, \tag{I.1}$$

where α is the effective atomic polarizability ($\alpha > 0$). The equation for the electron path is again given by an elliptic integral [GOLDSTEIN[13]]

$$\phi = k\rho \int_R^\infty [\xi(r)]^{-1/2}\, dr, \tag{I.2}$$

where k is the impact velocity and ρ the impact parameter. If $Q = 0$, one has the following formulae for the electron trajectories:

$$\phi = \frac{1}{r_1} F(\Delta/m), \quad \sin\Delta = \frac{r_1}{r}, \quad m = \frac{r_2^2}{r_1^2} < 1, \quad \rho > \rho_c, \tag{I.3}$$

$$\phi = \sqrt{2}\,\mathrm{arccoth}\frac{r\sqrt{2}}{\rho}, \quad \rho = \rho_c = \sqrt{\frac{2}{k}}\alpha^{1/4}, \tag{I.4}$$

$$\phi = \frac{\rho}{\rho_c\sqrt{2}} F(\Delta/m), \quad \cos\Delta = \frac{2r^2 - \rho_c^2}{2r^2 + \rho_c^2}, \quad m = \frac{1}{2}\left[1 + \left(\frac{\rho}{\rho_c}\right)^2\right], \quad \rho < \rho_c \tag{I.5}$$

where $F(\Delta/m)$ are elliptic functions of the first kind [ABRAMOVITZ and STEGUN[15]] and r_1 and r_2 are positive roots of $\xi(r)$. In the general case ($Q \neq 0$) it is more convenient to calculate the integral in eqn (I.2) numerically, as it was done for drawing the electron paths in Fig. 2. As for the impact parameter ρ_c, which separates "normal" trajectories from those passing through the origin, one looks for the roots of the polynomial $\xi(r)$ again. However, since the coefficients of the polynomial contain four parameters, an analytical solution of the equation $\xi(r) = 0$ would be cumbersome. On the other hand, a straightforward numerical search for the roots would be inconvenient too, because, first, we do not need all possible roots, and second, any likely improper construction of the initial conditions causes much computational trouble (as revealed in Fig. 1). We have, therefore, adopted another procedure for finding the largest (positive) root.

One finds, first, analytically, the largest root R_{max} of a polynomial of the third order $\eta(r) = d\xi/dr$, which corresponds to the rightmost minimum of $\xi(r)$ (the other minimum is, in our case, always situated in the negative r region), and then checks the sign of $\xi(R_{max})$. Starting with a sufficiently large value of ρ (for fixed values of k, Q and α), we adopt for the ρ_c that value of ρ at which $\xi(R_{max})$ has just become positive, i.e. for which real positive roots of $\xi(r)$ cease to exist. In other words, for $\rho \leq \rho_c$ the point of closest approach disappears and the particle passes through the centre.

APPENDIX II

Stark broadening functions

From the definition [GBKO,[4] SAHAL-BRECHOT,[6] COOPER and OERTEL,[16] GRIEM[14]] GBKO Stark broadening functions for the straight-line perturber paths are

$$a_2(Z) = \int_Z^\infty dZ' \frac{A_2(Z')}{Z'}, \tag{II.1}$$

$$b_2(Z) = \int_Z^\infty dZ' \frac{B_2(Z')}{Z'}, \tag{II.2}$$

$$B_2(Z) = \frac{2Z}{\pi} P \int_0^\infty dZ' \frac{A_2(Z')}{Z^2 - Z'^2}. \tag{II.3}$$

Here, P indicates Coshy's principal value of the integral.

In calculating A_2 functions we adopt the procedure used by SAHAL-BRESCHOT,[6] with the straight-line path substituted by the broken rectinlinear line [see Fig. 3]. If one denotes the angle between two parts of the trajectory by 2θ, one obtains, after some simple calculations

$$A_2(|Z|, \theta) = (A^2 + B^2)\cos^2\theta + (C^2 + D^2)\sin^2\theta + (BC - AD)\sin 2\theta, \tag{II.4}$$

where $Z = \rho\omega/k$ and

$$A = \int_0^\infty \frac{X\cos ZX}{(1+X^2)^{3/2}} dX \equiv \frac{dB}{dZ} = \frac{\pi}{2}|Z|[L_0(|Z|) - I_0(|Z|)] + 1, \tag{II.5}$$

$$B = \int_0^\infty \frac{\sin ZX}{(1+X^2)^{3/2}} dX = \frac{\pi}{2}|Z|[L_1(|Z|) - I_1(|Z|)] + |Z|, \tag{II.6}$$

$$C = -|Z|K_0(|Z|), \tag{II.7}$$

$$D = |Z|K_1(|Z|), \tag{II.8}$$

where L_ν is the modified Struve function, I_ν is the modified Bessel function of the first kind and K_ν is the modified Bessel function of the second kind [ABRAMOVITZ and STEGUN[15]]. Inserting A_2 into eqns (II.1) and (II.3) and then eqn (II.3) into eqn (II.2) one obtains finally $a_2(|Z|, \theta)$ and $b_2(Z, \theta)$ needed for eqn (14).

J. Quant. Spectrosc. Radiat. Transfer Vol. 20, pp. 223–226

0022-4073/78/0901-0223/$02.00/0

ON THE TEMPERATURE DEPENDENCE OF GAUNT FACTORS

M. DIMITRIJEVIĆ and N. KONJEVIĆ
Institute of Applied Physics, 11001 Beograd, P.O. Box 24, Yugoslavia

(*Received* 31 *October* 1977)

Abstract—The temperature dependence of Gaunt factors has been deduced from experimentally determined Stark widths of Ar(II) and Ca(II) spectral lines at various electron temperatures.

OUTLINE OF THRESHOLD GAUNT FACTOR STUDIES

THE MAGNITUDES of the Stark-broadening parameters for a spectral line in plasmas at low electron temperatures often depend on the presence of a very few perturbing levels. In these cases, the Stark widths can be evaluated from Griem's semiempirical formula[1] if the atomic characteristics of the nearest perturbing level are known. Conversely, it should be possible for these cases to deduce from experimentally determined Stark-broadening parameters the electron-atom scattering cross sections, which are proportional to the free–free Gaunt factors.

Recently, HEY[2,3,5] and HEY and BRYAN[4] have used the indicated procedure to deduce, from experimentally determined Stark widths, new semiempirical Gaunt-factor thresholds for single- and multiple-ionized atoms. In order to obtain reliable values for the Gaunt factors, these authors took into account the complexities of the particular atomic structure (e.g. deviations from LS coupling, configuration mixing, and optically forbidden transitions). In this way, a number of effective Gaunt factors of singly- (N(II), O(II) and F(II)), double- (N(III), O(III), Cl(III) and A(III)) and triply-ionized (A(IV)) atoms were obtained. The Gaunt factors at the threshold were found to be constant and independent of the electron temperature for a single ionization stage of an element.

In the evaluation of effective Gaunt factors, HEY[2,3,5] and HEY and BRYAN[4] used experimentally measured Stark-widths[6–9] obtained in a relatively narrow temperature range (21,000–26,000 K) by assuming that a semiempirical formula describes correctly the Stark-width dependence on temperature. This assumption is, however, questionable in some cases and the resulting effective Gaunt factors should be used with caution in application to other temperature ranges.

RESULTS AND DISCUSSION

In order to illustrate the temperature dependence of effective Gaunt factors deduced from the semiempirical formula, we have analyzed, in as wide a temperature range as possible, the available experimental results for the line widths of several multiplets of A(II) and one multiplet of Ca(II). In choosing these multiplets, two different criteria were applied: (a) there exists a large number of accurate experimental data in a wide temperature range [see, e.g. KONJEVIĆ and WIESE[10]] and (b) the elastic scattering term is dominant in the evaluation of line widths (the closest perturbing level is so far away that all perturbing levels may be lumped together), so that one can use the following approximative formula[1] for the Stark half-halfwidth (in angular frequency units):

$$W = 8\left(\frac{\pi}{3}\right)^{3/2}\frac{\hbar}{ma_0}\left(\frac{E_H}{kT}\right)^{1/2} N_e\left[\langle i|\mathbf{r}^2|i\rangle g_{se}\left(\frac{3kT}{2|\Delta E_i|}\right)+\langle f|\mathbf{r}^2|f\rangle g_{se}\left(\frac{3kT}{2|\Delta E_f|}\right)\right], \tag{1}$$

where

$$\langle i|\mathbf{r}^2|i\rangle = \frac{n_i^2}{2(Z+1)}[5n_i^2+1-3l_i(l_i+1)]a_0^2$$

and

$$n_i^2 = (Z+1)^2 E_H/(I - E_i).$$

In the above formulae, g_{se} is the effective semiempirical Gaunt factor, N_e is the electron concentration, T is the electron temperature, a_0 equals the Bohr radius, l_i represents the orbital quantum number of the bound valence electron, E_H is the ionization energy of the H-atom, E_i and I are empirical excitation and ionization energies of the ion, ΔE_i and ΔE_f are the energy separations of the upper (i) and lower (f) energy levels to the nearest perturbing levels: m is the mass of the electron, k is Boltzmann's constant, and $Z = 1$ stands for singly-charged ions.

From eqn (1) and selected experimental results, it was possible to deduce effective Gaunt factors; the results are given in Figs. 1 and 2. In spite of the large scatter of the experimental

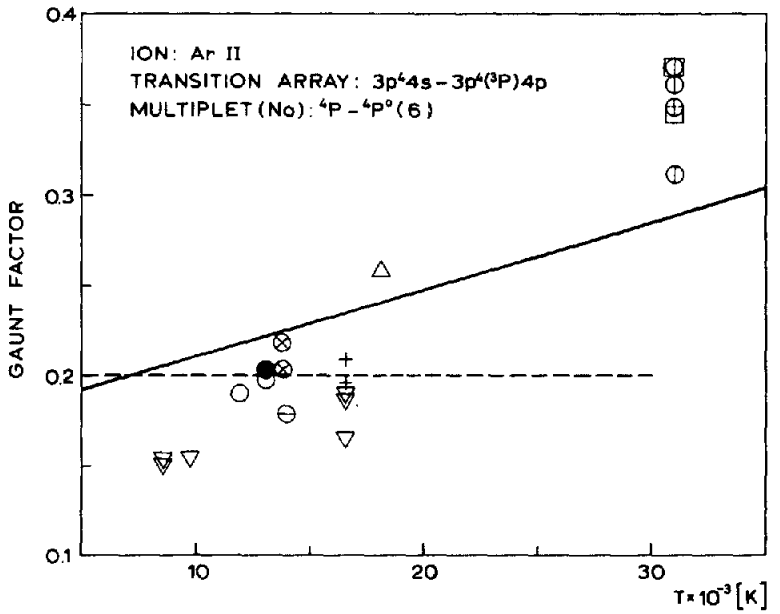

Fig. 1(a).

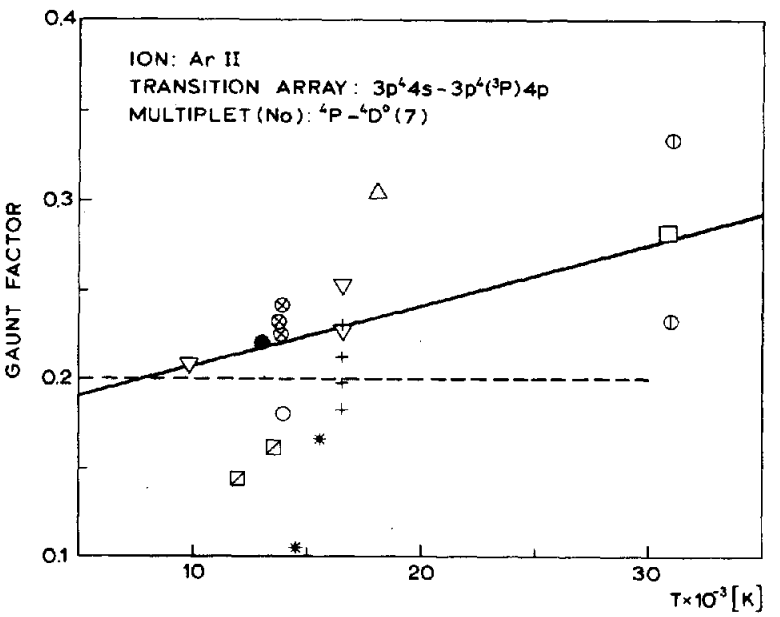

Fig. 1(b).

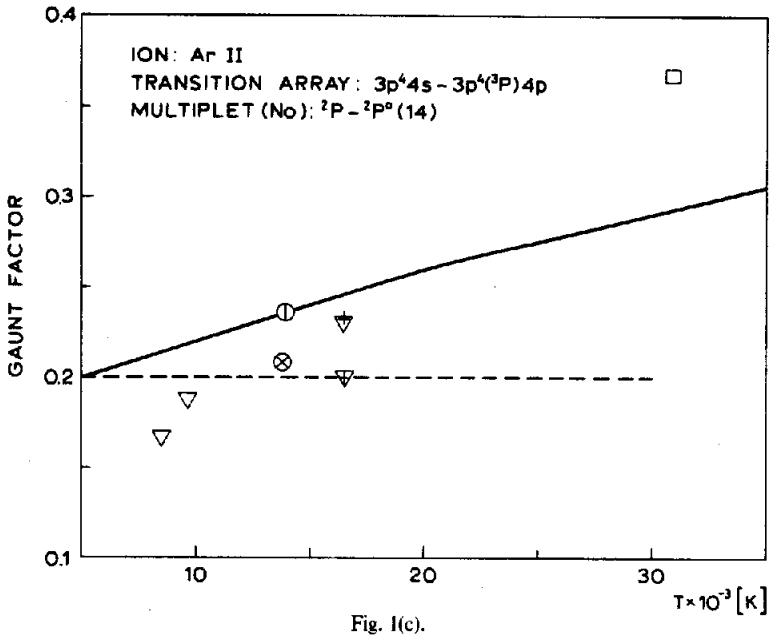

Fig. 1(c).

Fig. 1. Effective Gaunt factors for Ar(II): multiplet No. 6, Fig. 1(a); multiplet No. 7, Fig. 1(b); multiplet No. 14, Fig. 1(c). The solid line is from JONES *et al.*[11] [see also GRIEM[13]]. Experimentally determined Gaunt factors were derived from POPENOE and SHUMAKER (○),[15] JALUFKA *et al.* (△),[16] ROBERTS (□),[17] CHAPELLE *et al.* (⊕),[18] CHAPELLE *et al.* (●),[19] ROBERTS (⊕),[20] POWELL (⊖),[21] KONJEVIĆ *et al.* (▽),[22] LABAT *et al.* (+),[23] MURAKAWA *et al.* (*),[24] and KLEIN (⊠).[25]

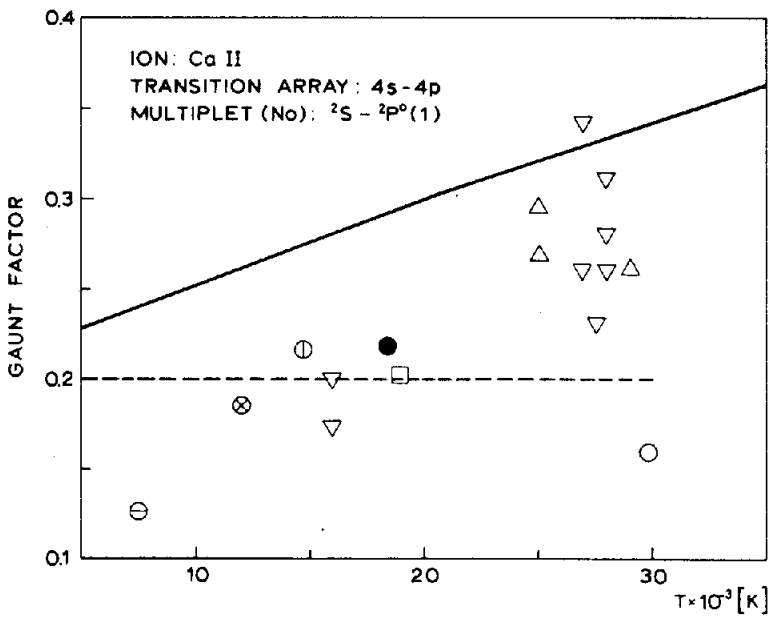

Fig. 2. Effective Gaunt factors for the Ca(II) multiplet No. 1. The solid line is from JONES *et al.*[11] [see also GRIEM[13]]. Experimentally determined Gaunt factors were derived from the results of ROBERTS and ECKERLE (○),[26] SHAPELLE and BRECHOT (⊕),[27] HILDUM and COOPER (●),[28] JONES *et al.* (□),[29] ROBERTS and BARNARD (▽),[30] HADŽIOMERSPAHIĆ *et al.* (△),[31] BAUR and COOPER (⊖),[32] and FLEURIER *et al.* (⊕).[33]

data, we notice that, instead of a constant value for the effective Gaunt factor of 0.2, much better agreement would be obtained with a temperature-variable Gaunt factor.

In Figs. 1 and 2, we also give values of Gaunt factors evaluated by JONES *et al.*[11] on the basis of a comparison between results obtained from the semiempirical formulas and the semiclassical approach, assuming the latter being exact. This assumption was previously proved

in a number of experiments where the semiclassical results and experimental data agreed within ±20% [see, e.g. JONES,[21] GRIEM,[13] KONJEVIĆ and WIESE[10]]. The results for effective Gaunt factors deduced in this manner agree better with the experimental results of Figs. 1 and 2 and they are well within the typical experimental errors of ±20–40%. However, the theoretical Gaunt factors show a different trend with temperature. This result indicates that even the semiclassical theoretical approach (see Fig. 1a) does not describe correctly the dependence of line width on temperature in some cases. Similar discrepancy has been noted at elevated temperatures when comparing experimental and semiclassical results for neutral-atom lines [see, e.g. KONJEVIĆ and ROBERTS[14]]. Comparisons were based on a relatively small number of experimental data (only s–p transitions). However, the results in Figs. 1 and 2 indicate that the effective Gaunt factors deduced from experimental data may be used with confidence only within the same temperature region. Outside of this temperature region, uncertainties will increase.

Finally, we may conclude that, in order to clarify the dependence of semiempirical effective Gaunt factors on the temperature (i.e. possible discrepancies between semiempirical and semiclassical theoretical approaches and the experiments), reliable experimental data over a wide temperature range are urgently needed.

Acknowledgement—The authors are indebted to Dr. J. HEY for making available the results in Ref. (5) prior to publication.

REFERENCES

1. H. R. GRIEM, *Phys. Rev.* **165**, 258 (1968).
2. J. D. HEY, *JQSRT* **16**, 575 (1976).
3. J. D. HEY, *JQSRT* **17**, 729 (1976).
4. J. D. HEY and R. J. BRYAN, *JQSRT* **17**, 221 (1977).
5. J. D. HEY, *JQSRT* **18**, 649 (1977).
6. M. PLATIŠA, M. POPOVIĆ, M. DIMITRIJEVIĆ and N. KONJEVIĆ, *Z. Naturforsch.* **30a**, 212 (1975).
7. M. V. POPOVIĆ, M. PLATIŠA and N. KONJEVIĆ, *Astron. Astrophys.* **41**, 463 (1975).
8. M. PLATIŠA, M. V. POPOVIĆ and N. KONJEVIĆ, *Astron. Astrophys.* **45**, 325 (1975).
9. M. PLATIŠA, M. DIMITRIJEVIĆ, M. POPOVIĆ and N. KONJEVIĆ, *Astron. Astrophys.* **54**, 837 (1977).
10. N. KONJEVIĆ and W. L. WIESE, *J. Phys. Chem. Ref. Data* **5**, 259 (1976).
11. W. W. JONES, S. M. BENETT and H. R. GRIEM, University of Maryland Technical Rep. No. 71-178, College Park, Maryland (1971).
12. W. W. JONES, *Phys. Rev.* **A7**, 1826 (1973).
13. H. R. GRIEM, *Spectral Line Broadening by Plasmas*. Academic Press, New York (1974).
14. N. KONJEVIĆ and J. R. ROBERTS, *J. Phys. Chem. Ref. Data* **5**, 209 (1976).
15. C. H. POPENOE and J. B. SHUMAKER, JR., *J. Res. Nat. Bur. Stand. Sect.* **A69**, 495 (1965).
16. H. W. JALUFKA, G. K. OERTEL and G. S. OFELT, *Phys. Rev. Lett.* **16**, 1073 (1966).
17. D. E. ROBERTS, *Phys. Lett.* **22**, 417 (1966).
18. J. CHAPELLE, A. SY, F. CABANNES and J. BLANDIN, *JQSRT* **8**, 1201 (1968).
19. J. CHAPELLE, A. SY, F. CABANNES and J. BLANDIN, *C.R.H. Acad. Sci. Ser.* **B266**, 1513 (1968).
20. D. E. ROBERTS, *J. Phys. B.* **1**, 53 (1968).
21. W. R. POWELL, dissertation, John Hopkins University, Baltimore, Maryland, unpublished (1966).
22. N. KONJEVIĆ, J. LABAT, LJ. ĆIRKOVIĆ and J. PURIĆ, *Z. Phys.* **235**, 35 (1970).
23. J. LABAT, S. DIENIŽE, LJ. ĆIRKOVIĆ and J. PURIĆ, *J. Phys. B.* **7**, 1174 (1974).
24. K. MURAKAVA, M. YAMAMOTO and S. HASHIMOTO, *Proc. of the 7th Int. Conf. Ioniz. Phen. Gases*, Vol. II, p. 594, Gradjevinska knjiga Publishing House, Belgrade (1965).
25. L. KLEIN, *JQSRT* **13**, 567 (1973).
26. J. R. ROBERTS and K. L. ECKERLE, *Phys. Rev.* **159**, 104 (1967).
27. J. CHAPELLE and S. SAHAL-BRECHOT, *Astron. Astrophys.* **6**, 415 (1970).
28. J. S. HILDUM and J. COOPER, *Phys. Lett.* **A36**, 153 (1971).
29. W. W. JONES, A. SANCHEZ, J. R. GRIEG and H. R. GRIEM, *Phys. Rev.* **A5**, 2318 (1972).
30. D. E. ROBERTS and A. J. BARNARD, *JQSRT* **12**, 1205 (1972).
31. D. HADŽIOMERSPAHIĆ, M. PLATIŠA, N. KONJEVIĆ and M. POPOVIĆ, *Z. Phys.* **262**, 169 (1973).
32. J. F. BAUR and J. COOPER, *JQSRT* **17**, 311 (1977).
33. C. FLEURIER, S. SAHAL-BRECHOT and J. CHAPELLE, *JQSRT* **17**, 595 (1977).

J. Quant. Spectrosc. Radiat. Transfer Vol. 22, pp. 333–335
Pergamon Press Ltd., 1979. Printed in Great Britain

STARK BROADENING OF S(III) AND S(IV) LINES†

M. PLATIŠA and M. POPOVIĆ
Institute of Physics, 11001 Beograd, P.O. Box 57, Yugoslavia

and

M. DIMITRIJEVIĆ and N. KONJEVIĆ
Institute of Applied Physics, 11001 Beograd, P.O. Box 24, Yugoslavia

(*Received* 30 *March* 1979)

Abstract—Measurements of the Stark widths of doubly and triply ionized sulfur lines were made in a low pressure, pulsed arc plasma of electron density 5.1×10^{16} cm^{-3} at an electron temperature of 28,500°K. The experimental S(III) and S(IV) Stark-profile halfwidths were compared with calculated values obtained with Griem's semiempirical and approximate semiclassical approach. The experimental results agree better with the semiclassical results.

INTRODUCTION

THE EXPERIMENTAL study of line broadening of prominent S(III) and S(IV) lines represents an extension of the systematic study of Stark broadening of doubly and triply ionized atoms. This work started in 1975 with the measurements of line widths of A(III) and A(IV)[1] and further continued with the measurements of N(III),[2] O(III),[3] Cl(III),[4] Si(III) and Si(IV).[5]

The intention of this work is to supply Stark-broadening data for some prominent lines of S(III) and S(IV). The experimental results are then compared with the theoretical results calculated from Griem's semiempirical[6] and approximative semiclassical approach.[7]

THEORY

The main problem we have encountered in the theoretical evaluations of linewidths of multiply ionized atom lines is a lack of the data for higher perturbing energy levels. Fortunately, the energy gaps between energy levels of multiply ionized atoms are usually large enough to permit successful use of approximate methods which take into account only one or a few nearest perturbing levels. Therefore, for theoretical calculations of the Stark linewidths of S(III) and S(IV) we have used Griem's semiempirical[6] and approximate semiclassical formula for multiply ionized atoms.[7] All perturbing levels in Griem's semiempirical approach were lumped together.[6]

When using an approximate semiclassical formula for multiply-ionized atoms [Eq. (526) in Ref. 7], lower level broadening is included in the weak collision term together with the Bates and Damgaard factors, as suggested by GRIEM.[7]

Data for atomic energy levels neccessary for these computations were taken from MOORE.[8] The data for an additional level $4d^3P$ of S(III) were taken from the work of DYNEFORS and MARTINSON.[9]

APPARATUS AND PROCEDURE

The apparatus and procedure were described in more detail previously.[1–5,10] The plasma source was a low pressure (0.15 torr) pulsed arc, 20 cm long, with a pyrex discharge tube 24 mm internal diameter. Holes of 1 mm diameter were located at the centres of both electrodes for laser interferometric measurements of N_e and for end-on plasma observations. The discharge was driven by a 150 μF condenser bank charged to 1.4 kV.

The light from the pulsed arc was observed end-on by a photomultiplier-monochromator system (with 1 m focal length and inverse linear dispersion of 4.16 Å mm^{-1}). This instrument has a measured instrumental half-widths of 0.046 Å with 10 μm slit width. Scanning of S(III) and S(IV) lines was accomplished by repeated pulsing of the arc while advancing the monochromator in steps of 0.02 Å. The output of the photomultiplier, together with the discharge-

†This work was partially performed under a grant from the U.S. National Bureau of Standards.

current waveform, were recorded on a dual-beam oscilloscope. All signals were analyzed at the maximum of electron density. In order to obtain optically thin S(III) and S(IV) lines, SF_6 was diluted with nitrogen. The ratio 1:25 was determined after a number of experiments in which SF_6 was gradually diluted while line shapes and line intensities within multiplets were carefully observed (see Ref. 1). A helium–neon laser interferometer at 6328 Å (with a plane external mirror) was used to determine the axial electron density. The peak electron density was $5.1 \times 10^{16}\,cm^{-3}$, with estimated measurement errors not exceeding $\pm 7\%$.

An electron temperature of 28,500 K $\pm$ 12% was determined from the Boltzmann plot of the relative intensities of five S(III) lines (2756.89, 2856.02, 2964.80, 3370.38, 3387.53 Å); the transition probabilities were taken from the book of WIESE *et al.*[11] For these measurements, the spectral response of the photomultiplier-monochromator system was calibrated by using a standard tungsten coiled-coil quartz–iodine lamp. The quoted electron temperature and density were taken at the peak of the electron density.

The experimentally observed line profiles are the result of the superposition of a Stark profile, an instrumental profile, and the profiles induced by other broadening mechanisms. On the basis of well known formulae,[12] we have estimated the contribution of various broadening mechanisms to the widths of the S(III) and S(IV) lines. It was found that only the contribution of Doppler broadening is comparable with electron impact broadening. Therefore, the experimental line profiles consist of two parts: electron impact broadening (Lorentzian) and Doppler and instrumental broadening (Gaussian). To obtain the Stark profile from the measured profile, it was necessary to use a deconvolution procedure for the Lorentzian and Gaussian profiles.[13]

RESULTS AND DISCUSSION

The experimentally determined full halfwidths of S(III) and S(IV) lines (in Å), at an electron concentration of $5.1 \times 10^{16}\,cm^{-3}$ and an electron temperature of 28,500 K, are given in Table 1. The estimated measurement error for these linewidths is $\pm$ 18%. This estimated error does not include the uncertainty in electron-density and temperature measurements. For the same

Table 1. Experimentally determined full halfwidths for S(III) and S(IV) in Å (W_m), compared with semiempirical (W_{SE}) and semiclassical (W_{SC}) theoretical results, $N_e = 5.1 \times 10^{16}\,cm^{-3}$ and $T_e = 28{,}500°K$.

Ion	Transition array	Multiplet (No.)	λ[Å]	W_m[Å]	W_{SE}[Å]	W_{SC}[Å]
SIII	3p3d-3p($^2P^o$)4p	$^3P^o$-^3P	3370.38	0.07_6	0.041	0.075
		(2)	3387.13	0.07_7	0.041	0.075
		$^3D^o$-^3P	3928.62	0.08_8	0.058	0.105
		(8)	3983.77	0.08_6	0.058	0.105
	3p4s-3p($^2P^o$)4p	$^3P^o$-^3D	4332.71	0.12_5	0.084	0.212
		(4)	4361.53	0.12_6	0.084	0.212
		$^3P^o$-^3P	3831.95	0.10_1	0.069	0.176
		(5)	3899.09	0.09_8	0.069	0.176
		$^3P^o$-^3S	3662.01	0.09_3	0.065	0.166
		(6)				
	3p4p-3p($^2P^o$)4d	^3D-$^3F^o$	2856.02	0.10_5	0.057	0.139
		(15 UV)	2863.53	0.10_3	0.057	0.139
			2872.00	0.10_2	0.057	0.139
		^3D-$^3D^o$	2718.88	0.10_3	0.054	0.131
		(16 UV)	2756.89	0.10_5	0.054	0.131
		^3P-$^3D^o$	2950.23	0.10_7	0.064	0.155
		(18 UV)	2964.80	0.10_8	0.064	0.155
SIV	4s-(^1S)4p	^2S-$^2P^o$	3097.46	0.05_9	0.036	0.100
		(1)				

experimental conditions, two sets of theoretical data were calculated and are also given in the table. Results obtained with the semiempirical formula are given under W_{SE}, while the results of approximate semiclassical calculations are listed under W_{SC}.

From the comparison of theoretical and experimental results, we conclude that the semiempirical results are systematically lower than the experimental data. On the other hand, the approximate semiclassical results are systematically higher (with the exception of the S(III) multiplet 2 where the agreement is excellent). However, in general, the semiclassical results agree better with the experiments.

Theoretical results for the S(III) multiplets 4 and 5 have been calculated only up to 20,000°K.[14] Nevertheless, the results under our experimental conditions for an electron temperature of 20,000°K (multiplet 4, $W = 0.144$ Å and multiplet 5, $W = 0.137$ Å) are in better agreement than the results derived from either of the two theoretical approaches used. Since theoretical linewidths decrease with the electron temperature at 28,500°K, the agreement should be even better.

Acknowledgement—The authors gratefully acknowledge the interest of Dr. W. L. WIESE in this work.

REFERENCES

1. M. PLATIŠA, M. POPOVIĆ, and N. KONJEVIĆ, *Z. Naturforsch.* **30a**, 212 (1975).
2. M. V. POPOVIĆ, M. PLATIŠA, and N. KONJEVIĆ, *Astron. Astrophys.* **41**, 463 (1975).
3. M. PLATIŠA, M. V. POPOVIĆ, and N. KINJEVIĆ, *Astron. Astrophys.* **45**, 325 (1975).
4. M. PLATIŠA, M. DIMITRIJEVIĆ, M. POPOVIĆ, and N. KONJEVIĆ, *Astron. Astrophys.* **54**, 837 (1977).
5. M. PLATIŠA, M. DIMITRIJEVIĆ, M. POPOVIĆ, and N. KONJEVIĆ, *J. Phys. B: Atom. Molec. Phys.* **10**, 2997 (1977).
6. H. R. GRIEM, *Phys. Rev.* **165**, 258 (1968).
7. H. R. GRIEM, *Spectral Line Broadening by Plasmas*. Academic Press, New York (1974).
8. C. E. MOORE, *Atomic Energy Levels*, Vol. 1. U.S. Government Printing Office, NSRDS-NBS 35 (1971).
9. B. I. DYNEFORS and I. MARTINSON, *Physica Scripta* **17**, 123 (1978).
10. N. KONJEVIĆ, M. PLATIŠA, and J. PURIĆ, *J. Phys. B: Atom. Molec. Phys.* **4**, 1541 (1971).
11. W. L. WIESE, M. W. SMITH, and B. M. MILES, *Atomic Transition Probabilities*, Vol. 2. Sodium through Calcium. U.S. Government Printing Office, NSRDS-NBS 22 (1968).
12. H. R. GRIEM, *Plasma Spectroscopy*. McGraw-Hill, New York (1964).
13. J. T. DAVIES and J. M. VAUGHAN, *Astrophys. J.* **137**, 1302 (1963).
14. S. SAHAL-BRECHOT, *Astron. Astrophys.* **2**, 322 (1969).

J. Quant. Spectrosc. Radiat. Transfer Vol. 24, pp. 451–459
Pergamon Press Ltd., 1980. Printed in Great Britain

STARK WIDTHS OF DOUBLY- AND TRIPLY-IONIZED ATOM LINES†

M. S. DIMITRIJEVIĆ and N. KONJEVIĆ
Institute of Applied Physics, 11001 Beograd, P.O. Box 24, Yugoslavia

(*Received* 28 *March* 1980)

Abstract—In this paper, we report modifications of well known semiempirical and semiclassical approximation formulas for Stark line-width calculations. Comparisons with experiments for doubly ionized atoms yield, as an average ratio of measured to calculated widths 1.06 ± 0.31 for a modified semiempirical formula and 0.96 ± 0.24 for a modified semiclassical formula. For triply ionized atoms these ratios are 0.91 ± 0.42 and 1.08 ± 0.41, respectively. Comparison with other theoretical calculations have also been made.

1. INTRODUCTION

For evaluation of Stark widths and shifts of non-hydrogenic spectral lines of ionized atoms, various theoretical approaches have been used (see, e.g. Ref. 1). Comprehensive calculations of Stark-broadening parameters of spectral lines emitted by singly ionized atoms from lithium through calcium have been performed by Jones *et al.*;[2] the results are included in Ref. 1. These calculations were based on a generalization of semiclassical methods, as used previously for neutral helium lines.[3] The experimental results for singly ionized atom line widths are generally in fairly good agreement[1,4,5] (on the average, within $\pm 20\%$) with these calculations. Fully quantum-mechanical impact approaches, based on the original formulation by Baranger,[6] have been used also for the calculations of the line widths for Be(II),[7] Mg(II)[8,9], and Ca(II)[9,10] resonance lines. Agreement with the experiments falls within the limits of accuracy of the semiclassical theory.

Both semiclassical and fully quantum-mechanical methods can be used for the evaluation of isolated line widths of multiply charged ions. However, both approaches involve considerable labour, especially the quantum-mechanical method.

Whenever large numbers of theoretical data of the Stark linewidths are required (e.g. for opacity evaluations), tedious calculations can be avoided if one uses simple, approximate formulas. For this purpose simple formulas with good average accuracy are especially convenient.

In 1968, Griem[11] suggested a simple semiempirical impact approximation based on Baranger's[12] original formulation, together with the use of an effective Gaunt-factor approximation proposed by Seaton[13] and Van Regemorter.[14] For singly ionized atoms, this semiempirical formula agrees on the average within $\pm 50\%$ with experiments.[1] For multiply ionized atoms, the agreement becomes worse and few attempts have been made to extend the applicability of this approach to higher ionisation stages.[15–18] This extension was done by adjustments of the effective Gaunt factors and by taking into account also the complexities of particular atomic structures (deviations from LS coupling, configuration mixing and optically forbidden transitions. Some limitations of these attempts[15–18] have been discussed recently by Dimitrijević and Konjević.[19]

An approximate semiclassical approach for the evaluation of the Stark line widths of multiply ionized atoms has been suggested by Griem.[1] This approach yielded results that compared well with the experimental results for C(III) and C(IV)[20] which, at that time, were the only reliable data. In the meantime, a number of experimental results for the Stark widths of the prominent spectral lines of Ar(III) and Ar(IV)[21], N(III)[11], O(III)[23], Si(III)[24,25] and Si(IV)[25], Cl(III)[26] and S(III) and S(IV)[27] have become available and detailed comparison was possible.

†This work was partially performed under a grant from the U.S. National Bureau of Standards, Washington, D.C.

2. THEORY

Within the impact approximation, Baranger[12] derived a quantum-mechanical expression for the width of an isolated ion line:

$$W = N\left\{v\left[\sum_{i'}\sigma_{i'i} + \sum_{f'}\sigma_{f'f}\right]\right\}_{av} + W_{el}, \tag{1}$$

where W is the full half-width (FWHM) in units of angular frequency and N is the electron concentration. The symbols $\sigma_{i'i}$ and $\sigma_{f'f}$ represent the inelastic cross sections for collisional transitions to i', f' from initial (i) and final (f) levels, respectively, of the optical transition. W_{el} is the line width induced by elastic collisions. The averaging in Eq. (1) has to be performed over the electron velocity (v) distribution.

Within the framework of the dipole approximation, one may use Bethe's[28] relation

$$\sigma_{j'j} = \frac{8\pi}{3}\lambda\!\!\!^{-2}\mathbf{R}^2_{j'j}\frac{\pi}{\sqrt{3}}g \tag{2}$$

to evaluate inelastic cross sections. In this expression $\lambda\!\!\!^{-} = \hbar/mv$ is the reduced de Broglie wavelength of an electron and $\mathbf{R}^2_{j'j}$ (in units of the Bohr radius a_0) is the square of the coordinate operator matrix element summed over all components of the operator, the magnetic substates of total angular momentum J', and averaged over the magnetic substates of J.

For higher electron temperatures, Griem[11] assumed that the contribution of elastic collisions to the line width [see Eq. (1)] can be neglected. The same author[11] made an attempt to take elastic collisions into account at the low temperature limit by using the threshold value of the inelastic cross section below the threshold. The Stark line width can then be calculated from the well known semiempirical formula[11]

$$W = N\frac{8\pi}{3}\frac{\hbar^2}{m^2}\left(\frac{2m}{\pi kT}\right)^{1/2}\frac{\pi}{\sqrt{3}}\left[\sum_{i'}\mathbf{R}^2_{j'j}g\left(\frac{E}{\Delta E_{ii}}\right) + \sum_{f'}\mathbf{R}^2_{f'f}g\left(\frac{E}{\Delta E_{f'f}}\right)\right] \tag{3}$$

Here, $E = 3kT/2$ is the energy of the perturbing electron and $\Delta E_{j'j} = |E_{j'} - E_j|$ is the energy difference between levels j and j'; $g(x) = 0.20$ for $x \leq 2$ and $g(x) = 0.24$, 0.33, 0.56, 0.98, and 1.33 for $x = 3$, 5, 10, 30, and 100.

If the nearest perturbing level in Eq. (3) is so far from E_i or E_f that the condition $E/\Delta E_{j'j} \leq 2$ is satisfied, g becomes a constant.[11] Then, the summation in Eq. (3) can be performed straightforwardly leading to considerable simplification of the relation. The line width (FWHM) in Å units then becomes

$$W(\text{Å}) = 0.4430 \cdot 10^{-8}\frac{\lambda\!\!\!^{-2}(\text{cm})N(\text{cm}^{-3})}{T^{1/2}}(\mathbf{R}^2_{ii} + \mathbf{R}^2_{ff}), \tag{4}$$

$$\mathbf{R}^2_{jj} = \sum_{j'}\mathbf{R}^2_{j'j} \simeq \frac{1}{2}\left(\frac{n_j}{Z}\right)^2[5n_j^2 + 1 - 3l_j(l_j+1)], \tag{5}$$

where n_j is the effective principal and l_j the orbital angular momentum quantum number, while $(Z-1)$ is the ionic charge.

As we have pointed out previously, the semiempirical relation[11] agrees on the average within $\pm 50\%$ with experimental data for singly-ionized atoms. Griem[1] suggested that the same expression with an effective Gaunt factor threshold value of 0.2 can be used for multiply-ionized atoms with an error $\pm 100\%$. However, the comparison with the experimental values of the line widths of doubly- and triply-ionized atoms[15-18,20,26,27,29] shows that the theoretical results are systematically lower. This observation is an indication that the threshold value of 0.2 for the Gaunt factor is rather small for higher ionization stages.

For the transitions with the principal quantum number n unchanged, Kobzev[30] suggested an empirical value of $g = 0.9 - 1/Z$ at threshold. We have adopted this suggestion. Therefore, in Eq. (3), the contribution of the collisional transitions with $\Delta n = 0$ is treated separately.

For higher electronic energies, the Gaunt factor is calculated from the following equation:

$$\tilde{g}(x) = 0.7 - 1.1/Z + g(x). \tag{6}$$

If one uses Eq. (3) to calculate Stark line widths, a lack of atomic data causes difficulties in the evaluation of the needed matrix elements. These difficulties are especially serious for multiply-ionized atoms for which data on higher perturbing levels are sometimes completely missing in the literature. To overcome this problem, we have separated the transitions with $\Delta n = 0$. Also, the LS coupling approximation is assumed. In this case, only two matrix elements are calculated: one for the transition array $l \to l+1(\mathbf{R}^2_{l,l+1})$ and the other for $l \to l-1(\mathbf{R}^2_{l,l-1})$. The same technique has been used by Griem[1] for semiclassical calculations of multiply charged ion line widths.

Equation (3) becomes now

$$W = N\frac{8\pi}{3}\frac{\hbar^2}{m^2}\left(\frac{2m}{\pi kT}\right)^{1/2}\frac{\pi}{\sqrt{3}}\left[\mathbf{R}^2_{l_i,l_i+1}\tilde{g}\left(\frac{E}{\Delta E_{l_i,l_i+1}}\right)+\mathbf{R}^2_{l_i,l_i-1}\tilde{g}\left(\frac{E}{\Delta E_{l_i,l_i-1}}\right)+\mathbf{R}^2_{l_f,l_f+1}\tilde{g}\left(\frac{E}{\Delta E_{l_f,l_f+1}}\right)\right.$$
$$\left.+\mathbf{R}^2_{l_f,l_f-1}\tilde{g}\left(\frac{E}{\Delta E_{l_f,l_f-1}}\right)+\sum_{i'}(\mathbf{R}^2_{ii'})_{\Delta n\neq 0}g\left(\frac{3kTn_i^3}{4Z^2E_H}\right)+\sum_{f'}(\mathbf{R}^2_{ff'})_{\Delta n\neq 0}g\left(\frac{3kTn_f^3}{4Z^2E_H}\right)\right], \tag{7}$$

$$\mathbf{R}^2_{l,l'} \simeq \left(\frac{3n}{2Z}\right)^2\frac{\max(l,l')}{2l+1}[n^2-\max^2(l,l')]\phi^2, \tag{8}$$

$$\sum_{j'}(\mathbf{R}^2_{jj'})_{\Delta n\neq 0} \simeq \left(\frac{3n_j}{2Z}\right)^2\frac{1}{9}(n_j^2+3l_j^2+3l_j+11). \tag{9}$$

For the inelastic part in Eq. (7) the nearest perturbing level is estimated from

$$\Delta E_{n,n+1} \approx 2Z^2E_H/n^3.$$

At the high temperatures, say $3kT/2\Delta E > 50$, all Gaunt factors in Eq. (7) are calculated in accordance with the GBKO high temperature limit,[3] viz.

$$\tilde{g}_{j'j} = g_{j'j} = \frac{\sqrt{3}}{\pi}\left[\frac{1}{2}+\ln\left(\frac{2ZkT}{n_j^2\Delta E_{j'j}}\right)\right]. \tag{10}$$

Our semiempirical formula, Eq. (7), is very similar in form to the equation for isolated line widths of multiply-charged ions derived by Griem[1] using the semiclassical approach, i.e.

$$W = N\frac{8\pi}{3}\frac{\hbar^2}{m^2}\int_0^\infty\frac{f(v)}{v}\,dv\left\{\left[\left(\mathbf{R}^2\ln\frac{\epsilon_{\max}}{\epsilon_{\min}}\right)_{l_i,l_i+1}+\left(\mathbf{R}^2\ln\frac{\epsilon_{\max}}{\epsilon_{\min}}\right)_{l_i,l_i-1}+\left(\mathbf{R}^2\ln\frac{\epsilon_{\max}}{\epsilon_{\min}}\right)_{l_f,l_f+1}\right.\right.$$
$$\left.\left.+\left(\mathbf{R}^2\ln\frac{\epsilon_{\max}}{\epsilon_{\min}}\right)_{l_f,l_f-1}\right]_{\Delta n=0}+\sum_{i'}(\mathbf{R}^2_{i'i})_{\Delta n\neq 0}\left(\ln\frac{\epsilon_{\max}}{\epsilon_{\min}}\right)_{n_i,n_i+1}+\sum_{f'}(\mathbf{R}^2_{f'f})_{\Delta n\neq 0}\left(\ln\frac{\epsilon_{\max}}{\epsilon_{\min}}\right)_{n_f,n_f+1}\right\}+W_c. \tag{11}$$

For $\Delta n = 0$,

$$\left(\ln\frac{\epsilon_{\max}}{\epsilon_{\min}}\right)_{l,l'} = \ln\left\{5-\frac{4.5}{\sqrt{Z}}+\xi^{-1}_{l,l'}\left[1+\frac{mv^2n_i^2}{2E_HZ(Z-1)}\right]^{-1}\right\}, \tag{12}$$

$$\xi_{l,l'} = \frac{(Z-1)e^2\omega_c}{mv^3}, \tag{13}$$

$$\omega_c = \max\{|\omega_{l,l'}|, \omega_P, \omega_F, \Delta\omega_i\}. \tag{14}$$

Here, ϵ is the eccentricity of the hyperbolic perturber path, $\omega_{l,l'}$ is the frequency separation between l, l' levels, $\omega_P = (4\pi Ne^2/m)^{1/2}$ is the plasma frequency, ω_F is the fine structure splitting,

and $\Delta\omega_i$ is the ion splitting. For the strong lines of doubly- and triply-ionized atoms, $\omega_c = \max\{|\omega_{l,l'}|, \omega_p\}$ may be used in most cases.

For the transitions with $\Delta n \neq 0$ in Eq. (12), $5 - (4.5/\sqrt{Z})$ (corresponding to $g = 0.9 - 1.1/Z$ near threshold) must be replaced by 1.4, the value of which corresponds to $g = 0.2$ for energies up to about three times the threshold energy.[1,14] Furthermore, since the $n \to n+1$ transitions dominate between all $\Delta n \neq 0$ contributions,[1] one should take $\hbar\omega_c \approx 2Z^2 E_H/n^3$.

In Eq. (11), W_c is the line width induced by strong collisions and higher multipole interactions,[1] i.e.

$$W_c = 2\pi N \left(\frac{2m}{\pi kT}\right)^{1/2} \left(\frac{\hbar}{mZ}\right)^2 n_i^4 \left[1 + \frac{kT}{E_H\left(1 + \frac{kT}{E_H} + \frac{Z^2}{n_i^4}\right)}\right]. \tag{15}$$

Griem[1] has tested Eq. (11) by comparing with one experiment[20] (for C(III) and C(IV) lines at 58,000° K) and with the semiclassical calculations of Sahal-Bréchot and Segre.[31] On the basis of this comparison, he assigns a ±50% error to the results of Eq. (11). In the meantime, a large number of new experimental data[21-27] have become available at electron temperatures in the range 20,000–30,000° K. For most of these lines, the electron energy is lower than or near the threshold for inelastic transitions to the closest perturbing level. For these energies, elastic collisions are dominant and widths from Eq. (11) "may be relatively too large, because the possible cancellation of elastic contributions to the width was ignored".[1] In order to compensate in some way for this effect, we used 1.4 instead of $5 - 4.5/Z$ on the r.h.s. of Eq. (12), on the basis of the following argument: below the inelastic transition threshold, the elastic contribution is taken into account twice via the strong collision correction and via the extrapolated Gaunt factor. At higher temperatures, the difference between these two versions of Eq. (11) is small, well within theoretical uncertainties for this relation.

3. RESULTS AND COMPARISONS WITH EXPERIMENTS

The results of theoretical calculations on electron impact line widths for the prominent, isolated lines of Be(III) through Ar(III) and B(IV) through Ar(IV) will be published elsewhere and only the comparison with experimental and other theoretical results will be given here.

It is not necessary to discuss here uncertainties in all of the approximations involved in our calculations since the criteria for their application are described in detail elsewhere.[1,3,11,32-34] However, it should be noted that the principal shortcomings of the methods applied for the evaluation of line widths lie in the uncertainty in the estimation of strong and elastic contributions. The use of a common Gaunt factor threshold value for all elements is a very crude approximation which, however, introduces great simplification whenever it is necessary to calculate, with modest accuracy, large numbers of line widths.

The sources of errors which are not inherent in the various theoretical approaches are related to the calculation of the matrix elements and to the lack of atomic data.

For evaluation, of the radial integrals, tables of Bates and Damgaard[35,36] have been used. Cases with an initial atomic state with equivalent electrons were avoided. If such a state causes the perturbation corresponding coefficients of fractional parentages[37] are included whenever possible.

Data for atomic energy levels were taken from Refs. 38–44. Some additional information was found for S(III).[45] For S(III), data on the $4f$ and $5p$ levels are unavailable which may affect the results for the multiplets 15–18 UV. Results for the multiplets 2 and 6 of Ar(IV) are probably of lover accuracy since data for the $4d$ level are missing.

In order to compare experimental with theoretical results, a critical evaluation has been made of the available experimental data. The basis for the experimental review was a comprehensive bibliography on atomic line shapes and shifts.[46] The criteria imposed for the selection of experimental line widths are as follows: (a) an independent and accurate determination of plasma electron density must exist, (b) a reasonably accurate determination of the electron temperature should have been performed, and (c) a discussion of other interfering broadening mechanisms and appropriate experimental problems must be described. The importance of these criteria has been discussed in detail previously.[5,47]

Table 1. Comparison of measured and calculated linewidths of doubly-ionized atoms. The values for the experimental widths W_m are normalized for an electron density $N_e = 1 \times 10^{17}\,\mathrm{cm}^{-3}$. The element, transition, multiplet number, averaged wavelength for the multiplet (in Angström units), and the electron temperatures are given. Ratios of measured, W_m, to theoretical results are given in the following order: W_{SEM}, modified semiempirical formula, Eqs. (7)–(10); W_{SE}, semiempirical formula, Eqs. (4) and (5); W_{GM}, modified semiclassical formula, Eqs. (11)–(15) with 1.4 instead of $5-4.5/Z$ on the r.h.s. of Eq. (12); W_G, semiclassical formula, Eqs. (11)–(15).

Ion	Transition (mult. No.)	T[K]	W_m[Å] at $1\times10^{17}\,\mathrm{cm}^{-3}$	$\frac{W_m}{W_{SEM}}$	$\frac{W_m}{W_{SE}}$	$\frac{W_m}{W_{GM}}$	$\frac{W_m}{W_G}$	$\frac{3kT}{2\Delta E}$	Ref.
C III	$3s^3S$-$3p^3P^0$(1)	58000	0.24	0.98	1.39	0.89	0.70	5.88	a
	$3s'^1P^0$-$3p'^1D$(7)	58000	0.52	2.02	2.74	1.95	1.59	6.23	a
	$3p^1P^0$-$3d^1D$(2)	58000	0.48	1.39	1.84	1.07	0.90	5.14	a
	$4p^3P^0$-$5d^3D$(10)	58000	1.55	0.66	0.63	0.71	0.64	47.9	a
	$3p^1P^0$-$4d^1D$	58000	0.11	1.02	0.76	0.80	0.74	40.0	a
	$3d^1D$-$4f^1F^0$	58000	0.12	1.71	0.60	0.70	0.66	40.0	a
	$4f^1F^0$-$5g^1G$(18)	58000	1.02	1.28	0.51	0.66	0.64	40.0	a
N III	$3s^2S$-$3p^2P^0$(1)	24300	0.17	0.82	1.47	0.90	0.62	2.78	b
	$3p^2P^0$-$3d^2D$(2)	24300	0.21	0.76	1.35	0.68	0.52	1.18	b
	$3s^4P^0$-$3p^4D$(5)	24300	0.18	1.18	2.30	1.26	0.88	1.97	b
O III	$3s^3P^0$-$3p^3D$(2)	25900	0.14	1.03	1.94	1.12	0.78	1.65	c
	$3s^3P^0$-$3p^3P$(4)	25900	0.11	1.09	2.06	1.17	0.82	1.67	c
	$3p^3D$-$3d^3F^0$(8)	25900	0.12	1.15	1.99	0.97	0.76	1.12	c
	$3p^3P$-$3d^3D^0$(14)	25900	0.14	0.93	1.59	0.80	0.62	1.18	c
Si III	$4s^3S$-$4p^3P^0$(2)	16400	0.38	0.67	1.11	0.76	0.51	0.78	d
		25600	0.31	0.68	1.14	0.71	0.49	1.22	e
	$4p^3P^0$-$4d^3D$(5)	25600	0.35	0.72	1.04	0.64	0.48	3.36	e
	$4p^3P^0$-$5s^3S$(6)	25600	0.32	0.61	1.02	0.61	0.44	3.03	e
S III	$3d^3P^0$-$4p^3P$(2)	28500	0.15	1.16	1.86	1.00	0.77	1.17	f
	$3d^3D^0$-$4p^3P$(8)	28500	0.17	0.96	1.51	0.83	0.64	1.32	f
	$4s^3P^0$-$4p^3D$(4)	28500	0.25	0.88	1.49	0.90	0.63	1.32	f
	$4s^3P^0$-$4p^3P$(5)	28500	0.20	0.86	1.46	0.88	0.62	1.27	f
	$4s^3P^0$-$4p^3S$(6)	28500	0.18	0.84	1.44	0.86	0.61	1.27	f
	$4p^3D$-$4d^3F^0$(15UV)	28500	0.20	1.56	1.84	1.09	0.89	1.32	f
	$4p^3D$-$4d^3D^0$(16UV)	28500	0.20	1.64	1.91	1.13	0.92	1.32	f
	$4p^3P$-$4d^3D^0$(18UV)	28500	0.21	1.43	1.67	1.00	0.81	1.17	f
Cl III	$3d^4P$-$4p^4P^0$(7)	24200	0.19	1.04	1.72	0.94	0.72	1.18	g
	$4s^4P$-$^4p^4D^0$(1)	24200	0.10	1.00	1.68	1.06	0.74	1.10	g
	$4s^4P$-$^4p^4P^0$(2)	24200	0.17	1.08	1.81	1.13	0.79	1.01	g
	$4s^4P$-$4p^4S^0$(3)	24200	0.17	1.10	1.86	1.16	0.81	0.95	g
	$4s^2P$-$4p^2D^0$(5)	24200	0.19	0.92	1.50	0.96	0.67	1.34	g
	$4s'^2D$-$4p'^2F^0$(10)	24200	0.18	1.05	1.72	1.10	0.77	1.23	g
	$4s'^2D$-$4p'^2D^0$(11)	24200	0.14	0.90	1.49	0.94	0.66	1.33	g
Ar III	$3d''^3P^0$-$^4p''^3P$(6)	21100	0.13	1.18	1.72	0.99	0.78	0.87	h
	$4s^5S^0$-$4p^5P$(1)	21100	0.15	1.02	1.66	1.09	0.75	0.73	h
	$4s'^3D^0$-$4p'^3D$(2)	21100	0.13	0.81	1.34	0.87	0.60	0.77	h
	$4s'^3D^0$-$4p'^3F$(3)	21100	0.14	0.94	1.56	1.02	0.70	0.77	h

References: a-20, b-22, c-23, d-24, e-25, f-27, g-26, h-21.

Table 2. Comparison of measured and calculated linewidths of triply-ionized atoms. The values for the experimental widths W_m are normalized for an electron density $N_e = 1 \times 10^{17}$ cm^{-3}. Theoretical linewidths W_{SEM}, W_{SE}, W_{GM}, and W_G are calculated as described in the caption of Table 1.

Ion	Transition (mult. No)	T K	W_m Å	$\frac{W_m}{W_{SEM}}$	$\frac{W_m}{W_{SE}}$	$\frac{W_m}{W_{GM}}$	$\frac{W_m}{W_G}$	$\frac{3kT}{2E}$	Ref.
C IV	$2s^2S$-$2p^2P^0$(1UV)	58000	0.006	1.09	3.78	2.14	1.52	0.94	a
	$3s^2S$-$3p^2P^0$(1)	58000	[illegible]	[illegible]	[illegible]	[illegible]	[illegible]	[illegible]	a
Si IV	$4s^2S$-$4p^2P^0$(1)	25600	0.22	0.57	1.23	0.78	0.47	1.10	b
	$4p^2P^0$-$4d^2D$(2)	25600	0.24	0.75	1.62	0.90	0.61	6.48	b
S IV	$4s^2S$-$4p^2P^0$(1)	28500	0.12	0.90	1.[illegible]	1.06	0.64	0.99	b
Ar IV	$4s^4P$-$4p^4D^0$(4UV)	20750	0.06	0.74	1.21	0.91	0.58	0.63	c
		22200	0.06	0.74	1.22	0.90	0.58	0.68	c
	$4s^4P$-$4p^4D^0$(5UV)	20750	0.06	0.76	1.23	0.93	0.59	0.63	c
		22200	0.06	0.79	1.29	0.95	0.61	0.68	c

References: a-20, b-25, c-21

Selected experimental data are compared with calculated line widths and the results for doubly- and triply-ionized atoms are given in Tables 1 and 2, respectively. In Table 3, we show a comparison with other theoretical results for doubly- and triply-ionized atoms.

4. DISCUSSION AND CONCLUSIONS

From the results shown in Tables 1 and 2, it appears that, for the specified temperature and electron density regions, agreement of modified semiempirical (ratios given under W_m/W_{SEM}) and semiclassical (ratios W_m/W_{GM}) results with experiments is quite good. The errors seem to be random and are caused by uncertainties in both, calculations and experiments. The average values of the ratios of measured to calculated widths of ionized atoms are as follows: for doubly-charged ions, $R_{SEM} = 1.06 \pm 0.31$, $R_{SE} = 1.53 \pm 0.46$, $R_{GM} = 0.96 \pm 0.24$, $R_G = 0.72 \pm 0.19$; for triply-charged ions, $R_{SEM} = 0.91 \pm 0.42$, $R_{SE} = 1.56 \pm 0.85$, $R_{GM} = 1.08 \pm 0.41$, $R_G = 0.72 \pm 0.32$. Indicated error represents an average quadratic error δ calculated from $\delta = \sqrt{\left[\sum_{i=1}^{m} \Delta_i^2/m(m-1)\right]}$ where Δ_i is difference between ith average ratio for the multiplet and average ratio for all multiplets.

The average ratios of measured to theoretical data for various elements are given in Table 4. The discrepancy with the experiments rarely exceeds 30%.

The principal deficiency in the comparisons with experiments comes from the lack of experimental line widths at elevated electron temperatures.

Comparisons with other theoretical data and, in particular, with the semiclassical calculations of Sahal-Bréchot and Segre[31] indicate reasonably good agreement with both modified approaches. It is difficult to explain large discrepancies in the case of Al(III) (multiplet No. 2) and Si(III) (multiplet No. 6 UV).

At the present time there are not enough experimental data to show which modified approach is the better one, especially at high temperatures. If one draws a conclusion based on a single experiment for C(III) and C(IV) lines,[20] the modified semiclassical approach seems to describe the experiment better. However, it should be emphasized here that there is not much difference between the results derived from the modified and unmodified semiclassical expression at higher electron temperatures.

Table 3. Comparison of the calculated Stark linewidths W_{SEM}, W_{SE}, W_{GM}, and W_G for an electron density of 1×10^{17} cm^{-3} with the results of other theoretical calculations, W. That for W_{SE} are given only when the condition $kT/\Delta E \lesssim 3$ is satisfied.

Ion	Transition (mult.no.) wavelength Å	T[K]	W_{SEM}	W_{SE}	W_{GM}	W_G	W	Ref.
Al III	$4s^2S$-$4p^2P^0$	10000	1.48	0.86	1.20	1.87	0.30	a
	(2)	20000	1.04	0.61	0.95	1.40	0.22	a
	5705.9							
	$4p^2P^0$-$4d^2D$	10000	1.33	-	1.37	1.90	1.08	a
	(3)	20000	0.97	-	1.14	1.47	0.96	a
	4523.2	30000	0.86	-	1.04	1.30	0.92	a
Si III	$3p^3P^0$-$4s^3S$	10000	0.0089	0.0076	0.0148	0.0165	0.0079	b
	(5UV)	20000	0.0063	0.0054	0.0110	0.0122	0.0059	b
	1111.6	40000	0.0045	0.0038	0.0086	0.0094	0.0046	b
	$3p^3P^0$-$4s^3S$	10000	0.0175	0.0109	0.0165	0.0242	0.0090	b
	(6UV)	20000	0.0124	0.0077	0.0129	0.0180	0.0068	b
	996.1	40000	0.0088	0.0063	0.0106	0.0139	0.0095	b
	$4s^3S$-$4p^3P^0$	10000	0.728	0.438	0.604	0.932	0.474	c
	(2)	11600	0.688	0.418	0.578	0.884	0.463	d
	4560.2	20000	0.514	0.310	0.473	0.693	0.397	c
		58000	0.295	-	0.364	0.472	0.275	d
	$4s^1S$-$4p^1P^0$	11600	0.1180	0.0684	0.0960	0.1510	0.839	d
	(4)	58000	0.0527	-	0.0638	0.0840	0.629	d
	5739.7							
S III	$3s^2P^0$-$4p^3D$	10000	0.472	0.277	0.388	0.598	0.384	c
	(4)	20000	0.334	0.196	0.303	0.444	0.298	c
	4287.1							
	$4s^3P^0$-$4p^3P$	10000	0.389	0.229	0.322	0.459	0.344	c
	(5)	20000	0.275	0.162	0.251	0.368	0.266	c
	3840.0							
C IV	$2s^2S$-$2p^2P^0$	10000	0.0073	0.0038	0.0057	0.0087	0.0102	b
	(1UV)	20000	0.0052	0.0027	0.0042	0.0063	0.0064	b
	1549.1	40000	0.0036	0.0019	0.0032	0.0046	0.0051	b
		60000	0.0030	0.0016	0.0028	0.0040	0.0094	e
	$3s^2S$-$3p^2P^0$	60000	0.398	0.295	0.335	0.455	0.516	e
	(1)							
	5801.5							
Si IV	$3s^2S$-$3p^2P^0$	10000	0.0141	0.0073	0.0104	0.0170	0.0145	b
	(1UV)	20000	0.0100	0.0052	0.0076	0.0122	0.0103	b
	1396.7	40000	0.0070	0.0037	0.0059	0.0090	0.0083	b
	$3p^2P^0$-$3d^2D$	10000	0.0109	0.0066	0.0116	0.0156	0.0128	b
	(3UV)	20000	0.0768	0.0047	0.0086	0.0114	0.0101	b
	1126.4	40000	0.0054	0.0033	0.0066	0.0085	0.0074	b

References: a-48, b-31, c-49, d-50, e-51.

Table 4. Average ratios of measured and calculated linewidths for various doubly-ionized atoms.

Ion	$\frac{W_m}{W_{SEM}}$	$\frac{W_m}{W_G}$	$\frac{W_m}{W_{GM}}$	$\frac{W_m}{W_G}$
C III	1.29	1.21	0.97	0.84
N III	0.9[illegible]	1.21	0.95	0.67
O III	1.06	1.90	1.02	0.74
Si III	0.67	1.38	0.68	0.48
S III	1.16	1.45	0.96	0.74
Cl III	1.01	1.49	1.04	0.74
Ar III	0.99	1.37	0.99	0.71

Acknowledgement—The authors gratefully acknowledge the interest of Dr W. L. Wiese in this work.

REFERENCES

1. H. R. Griem, *Spectral Line Broadening by Plasmas*. Academic Press, New York (1974).
2. W. W. Jones, S. M. Benett, and H. R. Griem, "Calculated Electron Impact Broadening Parameters for Isolated Spectral Lines from the Singly Charged Ions: Lithium through Calcium". *Tech. Rep. No.* 71-128, Univ. of Maryland, College Park, Maryland (1971).
3. H. R. Griem, M. Baranger, A. C. Kolb, and G. Oertel, *Phys. Rev.* **125**, 177 (1962).
4. W. W. Jones, *Phys. Rev.* **A7**, 1826 (1973).
5. N. Konjević and W. L. Wiese, *J. Chem. Phys. Ref. Data* **5**, 259 (1976).
6. M. Baranger, In *Atomic and Molecular Processes* (Edited by D. R. Bates), Chap. 13. Academic Press, New York (1962).
7. A. Sanchez, M. Blaha, and W. W. Jones, *Phys. Rev.* **A8**, 774 (1973).
8. O. Belly and H. R. Griem, *Phys. Rev.* **A1**, 97 (1970).
9. K. S. Barnes, *J. Phys.* **B4**, 1377 (1971).
10. K. S. Barnes and G. Peach, *J. Phys.* **B3**, 350 (1970).
11. H. R. Griem, *Phys. Rev.* **165**, 258 (1968).
12. M. Baranger, *Phys. Rev.* **112**, 855 (1958).
13. M. J. Seaton, In *Atomic and Molecular Processes* (Edited by D. R. Bates), Chap. 11. Academic Press, New York (1962).
14. H. Van Regemorter, *Astrophys. J.* **136**, 906 (1962).
15. J. D. Hey, *JQSRT* **16**, 575 (1976).
16. J. D. Hey, *JQSRT* **17**, 729 (1976).
17. J. D. Hey and R. J. Bryan, *JQSRT* **17**, 221 (1977).
18. J. D. Hey, *JQSRT* **18**, 649 (1977).
19. M. Dimitrijević and N. Konjević, *JQSRT* **20**, 223 (1978).
20. P. Bogen, *Z. Naturforsch.* **27A**, 210 (1972).
21. M. Platiša, M. Popović, M. Dimitrijević, and N. Konjević, *Z. Naturforsch.* **30A**, 212 (1975).
22. M. Platiša, M. Popović, and N. Konjević, *Astron. Astrophys.* **41**, 463 (1975).
23. M. Platiša, M. Popović, and N. Konjević, *Astron. Astrophys.* **45**, 325 (1975).
24. J. Purić, S. Djeniže, J. Labat, and Lj. Ćirković, *Z. Phys.* **267**, 71 (1974).
25. M. Platiša, M. Dimitrijević, M. Popović, and N. Konjević, *J. Phys.* **B10**, 2997 (1977).
26. M. Platiša, M. Dimitrijević, M. Popović, and N. Konjević, *Astron. Astrophys.* **54**, 837 (1977).
27. M. Platiša, M. Popović, M. Dimitrijević, and N. Konjević, *JQSRT* **22**, 333 (1979).
28. H. A. Bethe, *Ann. Physik* **5**, 3251 (1930).
29. M. S. Dimitrijević and N. Konjević, *J. Phys. (Paris)* **40**, C7-815 (1979) Suppl. 7.
30. G. A. Kobzev, *Opt. Spectrosc. (USSR)* **30**, 106 (1971).
31. S. Sahal-Bréchot and E. R. H. Segre, *Astron. Astrophys.* **13**, 161 (1971).
32. H. R. Griem, *Plasma Spectroscopy*, Chap. 4. McGraw-Hill, New York (1964).
33. D. E. Roberts, *JQSRT* **8**, 1241 (1968).
34. J. Cooper and G. K. Oertel, *Phys. Rev.* **180**, 281 (1969).
35. D. R. Bates and A. Damgaard, *Phil. Trans. R. Soc. London Ser. A* **242**, 101 (1949).
36. G. K. Oertel and L. P. Shomo, *Astrophys. J. Suppl. Series* **16**, 175 (1968).
37. B. W. Shore and D. H. Menzel, *Astrophys. J. Suppl. Series* **12**, 187 (1965).
38. C. E. Moore, *Atomic Energy Levels*, Circular 467 National Bureau of Standards, Vol. I (1949), reprinted as NSRDS-NBS 35, Vol. I (1971).
39. W. L. Wiese, M. W. Smith, and B. M. Glenon, *Atomic Transition Probabilities*, Vol. I. U.S. Government Printing Office, Washington D.C. (1966).
40. W. L. Wiese, M. W. Smith, and B. M. Miles, *Atomic Transition Probabilities*, Vol. II. U.S. Government Printing Office, Washington D.C. (1969).
41. C. E. Moore, *Selected Tables of Atomic Spectra*. Nat. Stand. Ref. Data Ser. Nat. Bur. Stand. **3**, Sects 1–6 (1967–72).
42. B. Edlén, *Nucl. Instruments Methods* **90**, 1 (1970).
43. V. Kaufman and B. Edlén, *J. Phys. Chem. Ref. Data* **3**, 825 (1974).

44. S. Bashkin and J. O. Stoner Jr., *Atomic Energy Levels and Grotrian Diagrams*, Vols. I–II. North Holland, Amsterdam (1975).
45. B. I. Dynefors and I. Martinson, *Physica Scripta* **17**, 123 (1978).
46. J. R. Fuhr, W. L. Wiese, and L. J. Roszman, *Bibliography on Atomic Line Shapes and Shifts*, Nat. Bur. Stand. (U.S.) Spec. Publ. 366 (1972); J. R. Fuhr, L. J. Roszman, and W. L. Wiese, Nat. Bur. Stand. (U.S.) Spec. Publ. 366, Suppl. 1 (1974); J. R. Fuhr, G. A. Martin,, and B. J. Specht, Nat. Bur. Stand. (U.S.) Spec. Publ. 366, Suppl. 2 (1975); J. R. Fuhr, B. J. Miller, and G. A. Martin, Nat. Bur. Stand. (U.S.) Spec. Publ. 366, Suppl. 3 (1978).
47. N. Konjević and J. R. Roberts, *J. Phys. Chem. Ref. Data* **5**, 209 (1976).
48. J. Davies and S. Morin, *JQSRT* **11**, 495 (1971).
49. S. Sahal-Bréchot, *Astron. Astrophys.* **2**, 322 (1969).
50. E. A. Yukov, *Sov. Astron. AJ* **15**, 867 (1972).
51. G. S. Romanov, K. L. Stepanov, and M. I. Sirkin, *Opt. Spectrosc. (USSR)* **47**, 860 (1979).

J. Quant. Spectrosc. Radiat. Transfer Vol. 25, pp. 387–392, 1981
Printed in Great Britain.

0022-4073/81/040387-06$02.00/0

48/II

NOTE

ON THE STARK BROADENING OF IONIZED NITROGEN LINES

M. S. DIMITRIJEVIĆ and N. KONJEVIĆ
Institute of Applied Physics, 11001 Beograd, P. O. Box 24, Yugoslavia

(*Received* 17 *June* 1980)

Abstract—In this paper, we report an analysis of the experimental procedure and results obtained in a recently published paper on the Stark broadening of singly-, doubly-, and triply-ionized nitrogen lines. The results of this analysis indicate that the influence of self-absorption on the line profiles is not taken into account properly and that therefore the results of Ref. 6 cannot be applied with confidence. Comparisons of experimental results with numerous theoretical calculations have also been performed.

1. INTRODUCTION

A critical review[1] of available experimental data on the Stark widths and shifts of non-hydrogenic lines of singly-ionized atoms indicates that measured widths are generally in fairly good agreement (on the average within ±20%) with the comprehensive semiclassical theory developed by Greim *et al.*[2,3] This conclusion is a confirmation of earlier studies of this subject by Jones[4] and Griem.[2] Experimental results for singly-ionized nitrogen fit well within this picture (see Ref. 1). Until recently, only a single experimental paper has appeared in which measurements were reported of the Stark-broadening parameter for four doubly-ionized nitrogen lines.[5] However, for comparison with these experiments, semiclassical theoretical data were not available and therefore the test of this theory could not be performed.

Recently, a new experimental study has been reported of the Stark broadening of N(II), N(III) and N(IV) ion lines at the high electron density of $1.4 \times 10^{18}\,\mathrm{cm}^{-3}$ and the elevated electron temperature 58,000 K.[6] These experimental results are listed with other experimental and theoretical data in Table 1. Direct comparison with other experimental results[5,7–9] for $3s$–$3p$ and $3p$–$3d$ transitions of N(II) indicates a discrepancy of the order of two. When scaling of the linewidths with temperature is taken in account, the average discrepancy approaches a factor of three. Unfortunately, with the exception of multiplets 20, 39, and 48 of N(II), threre are no semiclassical results to compare with.

Even the result for multiplet No. 20 must be viewed with caution, since there is an indication of incompleteness in the set of the perturbing levels used for line-width calculations (see the value for $\Delta S/S$ in Ref. 3). Results for the transition $3s$–$3p$ (multiplet No. 1) of doubly-ionized nitrogen may be compared with a unique available experimental linewidth. The discrepancy goes up to a factor of three. It is also interesting to note that linewidths within this multiplet differ by more than 30%. A similar situation applies also for the $3p$–$3d$ transition (multiplet No. 9) of N(III) and $3p$–$3d$ transition (multiplet No. 20) of N(II).

In Ref. 6, apart from experimental results, theoretical widths are reported for measured N(II), N(III), and N(IV) lines. These results were calculated from semiclassical formulae [Eq. (526) in Ref. 2]. The authors[6] conclude "that the widths predicted by a simple calculation agree within 20% for $3s$–$3p$ transitions for singly- and doubly-charged nitrogen, while there is strong disagreement for $3p$–$3d$ transitions for doubly- and triply-charged ions". No comment was made regarding other experimental data. Numerical results from Ref. 6 are also given in Table 1 under W_T.

In order to clarify the rather large discrepancy with other experiments and with theory, we have performed an analysis of the experimental procedure and the results reported in Ref. 6. A number of the theoretical linewidths are also evaluated. The results are given in the following sections.

2. ANALYSIS OF THE EXPERIMENTAL PROCEDURE AND RESULTS OF REF. 6

The plasma source used was a theta pinch with a single turn coil driven by a 60 kV capacitor bank. The quartz discharge tube with an inside diameter of 6.4 cm was filled with a gas mixture

Table 1. Experimental N(II), N(III), and N(IV) full half-widths W_m in Å units, compared with the theoretical results of Griem *et al.*[2,3] (W_{SC}) and Källne *et al.*[6] (W_T).

Transition array Ion	Multiplet (No)	Wavelength [Å]	Temperature [K]	W_m[Å] at $N_e = 1 \times 10^{17}$ cm^{-3}	W_{SC}[Å]	W_T[Å]	Ref.
$2p3s-2p(^2P^o)3p$	$^1P^o-^1D$	3995.0	22000	0.34			7
NII	(12)		22800	0.30			8
			16200-18300	0.28-0.30			9
			23150	0.31			5
			58000	0.77		0,80	6
$2p3p-2p(^2P^o)3d$	$^1P-^1D^o$	4447.0	22000	0.45			7
NII	(15)		22800	0.28			8
			23150	0.31			5
			58000	0.58		0.61	6
	$^3D-^3D^o$	4803.3	23150	0.33	0.37		5
	(20)		58000	0.62	0.34*	0.74	6
		4790.4 ?	58000	0.44	0.34*	0.75	6
$2p3d-2p(^2P^o)4f$	$^3F^o-^3G$	4041.3	23150	0.83	1.15*		5
NII	(39)	4040.9	58000	1.89	1.15*	1.16	6
	$^3D^o-^3F$	4239.4	58000	1.54	1.49*	1.35	6
$3s-(^1S)3p$	$^2S-^2P^o$	4097.3	24300	0.17			5
NIII	(1)		58000	0.54		0.41	6
		4103.4	58000	0.41		0.41	6
$2s2p3s-2s2p(^3P^o)3p$	$^4P^o-^4D$	4510.9	58000	0.38			6
NIII	(3)						
	$^2P^o-^2D$	4200.0	58000	0.53		0.53	6
	(6)	4195.7	58000	0.59		0.53	6
$2s2p3p-2s2p(^3P^o)3d$	$^4D-^4F^o$	4858.9	58000	0.61		0.26	6
NIII	(9)	4865.8 ?	58000	0.46		0.26	6
$2s3p-2s(^2S)3d$ NIV	$^1P^o-^1D$ (3)	4057.8	58000	0.53		0.10	6

of 49% He and 51% N_2 to an initial pressure of 3 torr. The plasma was diagnosed by measuring the Stark profile of the He(II) 4686 Å line and by taking shadowgrams of the plasma development. Electron temperatures were measured from the relative intensities of emission lines, as well as from the line-to-continuum ratio. The analysis of the plasma parameters gave an electron density of 1.4×10^{18} cm^{-3} and an electron temperature 5.0 eV. The line profiles were measured with an optical multi-channel analyzer, mounted on the exit slit of a 0.5-m monochromator with a resolution of 0.3 Å. The nitrogen ion lines studied were all much broader than the instrumental resolution and therefore no correction for instrumental broadening was necessary. Although contributions of other broadening mechanisms to the line width were not discussed, it was clear that, at such high electron densities, Stark broadening should be dominant. The influence of self-absorption as a competing effect to the broadening of spectral line was treated theoretically by computing the optical depths for the transitions investigated and self-absorption was found to be negligible.

This last conclusion concerns our main objection to the experimental measurements of the

line profiles. The self-absorption check was only done theoretically. A variety of well established techniques exists to determine the presence of this effect (e.g. Refs. 1 and 10). Particularly straightforward is the method of checking the line intensity ratios within multiplets, which are expected to adhere closely to *LS*-coupling. The well-known ratios for *LS*-coupling line strengths[11,12] should be used for comparison with the observed line-intensity ratios. A reduction in the observed intensity of the stronger line in a multiplet relative to weaker one indicates that self-absorption is present. For this comparison, tables on atomic transition probabilities[13,14] are useful. Since the lines in a multiplet have nearly the same theoretical shape and width, ratios may be found by simply comparing peak heights.

If one compares the intensities of the N(III) 4097.3 and 4103.4 Å lines (multiplet 1) in the spectrum shown in Fig. 6 of Ref. 6, one obtains $I_{4097.3}/I_{4103.4} = 1.6:1$ instead of 1.98:1, as is expected for *LS*-coupling. In Fig. 7 of Ref. 6, the ratio of N(III) 4200.0 and 4195.7 Å (multiplet 6) is $I_{4200.0}/I_{4195.7} = 1.12:1$ instead 1.8:1. Both examples indicate strong self-absorption.

The ratio of the line widths within a multiplet may also be used as an indication of self-absorption. According to the present theories of the Stark broadening,[2] the widths of all lines in a multiplet should be practically identical. They interact with the same set of perturbing levels, the energies of different upper as well as lower levels in a multiplet are nearly the same, and the radial integrals for the interacting states are, for all practical purposes, the same for the entire multiplet. This general prediction of the Stark broadening theory for isolated lines of singly- and multiply-ionized atoms has been confirmed previously.[1] Rare exceptions to this rule may be multiplets with large separation of the energy levels in comparison with the nearest perturbing level (see, e.g. Refs. 15 and 16). Since this exception does not apply for the multiplets of N(II) and N(III) in Ref. 6, one would expect similar line widths (within the limits of experimental uncertainty) within a multiplet. However, for the transition $3s$–$3p$ (multiplet 1) N(III), the width of the 4097.3 Å line at an electron density of 1.4×10^{18} cm^{-3} is 7.6 Å, while for the 4103.3 Å it is 5.8 Å. We suspect that the difference is caused by self-absorption since the stronger 4097.3 Å line, which would be more strongly self-absorbed, is broader than the weaker line in the multiplet. On the other hand, for multiplet 6 of the same transition, the weaker 4195.7 Å line has a larger ($\approx 15\%$) width. In all other cases, large differences between linewidths within multiplet exist: for the N(II) transition $3p$–$3d$, multiplet 20, $W_{4790.4} = 6.2$ Å and $W_{4803.3} = 8.7$ Å; N(III) transition $3p$–$3d$, multiplet 9, $W_{4858.9} = 8.5$ Å and $W_{4865.8} = 6.4$ Å. Unfortunately within these multiplets similar analysis can not be performed since we could not identify transitions at the wavelengths 4790.4 Å and 4865.8 Å. These wavelengths of N(II) and N(III) do not exist in the wavelength tables.[17–19]

3. NUMERICAL RESULTS AND COMPARISONS

In order to compare experimental results for the Stark widths of N(II), N(III), and N(IV) lines in Table 1 with various theoretical approaches we have performed calculations of the line width dependence upon electron temperature using a semiclassical theoretical approach[2,3] and its simplified version (Chap. IV.6 in Ref. 2).

Recently Dimitrijević and Konjević[20] have reported modification of well known semiempirical[21] and the semiclassical formula (Eq. 526 in Ref. 2). Comparison with experiments[21] for doubly ionized atoms yielded, as an average ratio of measured to calculated linewidths, 1.06 ± 0.31 for modified semiempirical (MSE) formula, and 0.96 ± 0.24 for modified semiclassical (MSC) formula. For triply-ionized atoms these ratios were 0.91 ± 0.42 and 1.08 ± 0.41, respectively. The good agreement of these approximate formulae with experiment indicated that they can be used with a reasonable confidence for the comparison with the results for doubly- and triply-ionized atoms. Therefore, results obtained from MSE and MSC formulas for N(II), N(III), and N(IV) lines are also listed in Table 2, together with the semiclassical data published by Griem and coworkers[2,3] for singly-ionized nitrogen (multiplets 20, 39, and 48). Here, the $\Delta S/S$ values given in column 1 of Table 2 should be noted; these represent a measure of the failure to satisfy the sum rules for the squares of the dipole matrix elements.[2] Results for line width with $|\Delta S/S| > 0.4$ are omitted in Ref. 2 but may be found in Ref. 3. Using the same criterion as before our results for singly-ionized nitrogen, multiplet 15, also show poor accuracy.

Some of our theoretical results are shown in Fig. 1 together with available experimental[5–9] and other theoretical data.[6]

Table 2. Calculated N(II), N(III), and N(IV) full half-widths in Å at 10^{17} cm^{-3} vs the electron temperature: W_{SC}, semiclassical theory; W_T, semiclassical formula (Chap. IV.6, Ref. 2); W_{GM}, and W_{SEM}, modified semiclassical and semiempirical formulae, respectively.[20] Results designated by an asterisk are taken from Ref. 3; $kT/\Delta E$ is the ratio of the thermal energy at $T = 10^4$ K to the energy separation from the nearest perturbing level; $\Delta S/S$ is a measure of the failure to satisfy the sum rules for the squares of the dipole matrix elements (S is the sum of the squares of these matrix elements).[2]

Ion-transition (Multiplet no)	Temperature [K]	W_{SC} [Å]	W_T [Å]	W_{GM} [Å]	W_{SEM} [Å]
NII $3s^1P$-$3p^1D$					
(12)	10000	0.414	0.572	0.477	0.364
$\Delta S/S$ = 0.06	20000	0.358	0.451	0.390	0.257
$kT/\Delta E$ = 0.29	30000	0.340	0.401	0.356	0.213
	60000	0.326	0.341	0.314	0.171
NII $3p^1P$-$3d^1D^o$	10000	0.620	0.892	0.798	0.504
(15)	20000	0.520	0.699	0.639	0.356
$\Delta S/S$ = 0.43	30000	0.488	0.620	0.575	0.292
$kT/\Delta E$ = 0.42	60000	0.464	0.524	0.497	0.227
NII $3p^3D$-$3d^3D^o$	10000	0.464*	1.05	0.935	0.596
(20)	20000	0.380*	0.818	0.744	0.421
$\Delta S/S$ = -0.43	30000		0.724	0.668	0.344
$kT/\Delta E$ = 0.44	40000	0.336*			
	60000		0.609	0.576	0.265
NII $3d^3F^o$-$4f^3G$	10000	1.450*	2,47	2.34	1.06
(39)	20000	1.270*	2.02	1.94	0.752
$\Delta S/S$ = -0.12	30000		1.82	1.76	0.692
$kT/\Delta E$ = 4.42	40000	1.152*	1.55	1.52	0.548
	60000				
NII $3d^3D$-$4f^3F$	10000	2.04*	2.83	2.71	1.15
(48)	20000	1.714*	2.34	2.27	0.814
$\Delta S/S$ = -0.06	30000		2.11	2.06	0.679
$kT/\Delta E$ = 8.97	40000	1.488*			
	60000		1.80	1.77	0.597
NIII $3s^2S$-$3p^2P^o$	10000	0.510	0.408	0.261	0.333
(1)	20000	0.384	0.304	0.205	0.236
$\Delta S/S$ = -0.05	30000	0.332	0.260	0.183	0.192
$kT/\Delta E$ = 0.59	60000	0.268	0,208	0,160	0.142
NIII $3s^4P^o$-$3p^4D$	10000	0.558	0.486	0.310	0.399
(3)	20000	0.412	0.249	0.193	0.172
$\Delta S/S$ = -0.33	30000	0.352	0.239	0.189	0.165
$kT/\Delta E$ = 0.55	60000	0.274	0.224	0.183	0.156
NIII $3s^2P^o$-$3p^2D$	10000	0.540	0.513	0.330	0.418
(6)	20000	0.402	0.275	0.220	0.191
$\Delta S/S$ = -0.30	30000	0.344	0.265	0.216	0.185
$kT/\Delta E$ = 0.53	60000	0.272	0.250	0.211	0.178
NIII $3p^4D$-$3d^4F^o$	10000	0.634	0.588	0.430	0.435
(9)	20000	0.470	0.303	0.253	0.186
$\Delta S/S$ = -0.21	30000	0.402	0.291	0.246	0.179
$kT/\Delta E$ = 0.53	60000	0.318	0.274	0.237	0.166
NIV $3p^1P^o$-$3d^1D$	10000	0.500	0.308	0.201	0.247
(3)	20000	0.360	0.226	0.153	0.175
$\Delta S/S$ = -0.12	30000	0.300	0.191	0.135	0.143
$kT/\Delta E$ = 0.83	60000	0.226	0.150	0.114	0.106

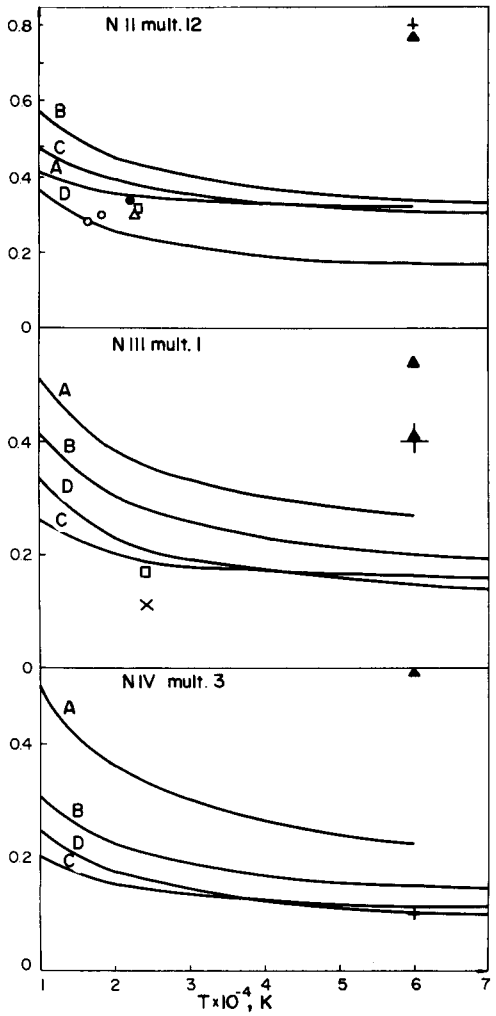

Fig. 1. Measured and calculated full Stark halfwidths for N(II), N(III), and N(IV) multiplets, normalized to an electron density, of 10^{17} cm^{-3}, as a function of electron temperature. Curves: A, W_{SC}; B, W_T; C, W_{GM}; D, W_{SEM}; Experimental points: ▲, Källne *et al.*[6]; ●, Berg *et al.*;[7] △, Jalufka and Craig;[8] ○, Konjević *et al.*;[9] □, Popović *et al.*[5] Theoretical results: +, Källne *et al.*;[6] ×, Hey.[22]

4. DISCUSSION AND CONCLUSIONS

We conclude that self-absorption was considerable in the examples presented in Ref. 6. The line widths of N(II), N(III), and N(IV) are broader than semiclassical and other experimental results. It is interesting to note that the discrepancy with semiclassical theory for N(II) decreases for transitions between higher energy levels (in particular, for the $3p$–$4f$ transition, multiplet 48), which may be another indication of the presence of self-absorption that is more pronounced for transitions between lower lying energy levels. It appears that a new experiment is needed with lower initial partial pressures of N_2 in nitrogen-helium mixtures.

Acknowledgement—The authors have been fortunate in obtaining a computer program for the evaluation of Stark widths of singly-ionized atoms from H. R. Griem, to whom they would like to express their special thanks.

REFERENCES

1. N. Konjević and W. L. Wiese, *J. Phys. Chem. Ref. Data* **5**, 259 (1976).
2. H. R. Griem, *Spectral Line Broadening by Plasmas.* Academic Press, New York (1974).
3. W. W. Jones, S. M. Benett, and H. R. Griem, "Calculated Electron Impact Broadening Parameters for Isolated Spectral Lines from the Singly Charged Ions from Lithium through Calcium", University of Maryland, *Tech. Rep. No.* 71–178, College Park, Maryland (1971).
4. W. W. Jones, *Phys. Rev.* **A7**, 1826 (1973).
5. M. Popović, M. Platiša, and N. Konjević, *Astron. Astrophys.* **41**, 463 (1975).
6. E. Källne, L. A. Jones and A. J. Barnard, *JQSRT* **22**, 589 (1979).

7. H. F. Berg, W. Ervens and B. Furch, *Z. Phys.* **206**, 309 (1967).
8. N. W. Jalufka and J. P. Craig, *Phys. Rev.* **A1**, 221 (1970).
9. N. Konjević, V. Mitrović, Lj. Ćirković, and J. Labat, *Fizika* **2**, 129 (1970).
10. N. Konjević and J. R. Roberts, *J. Phys. Chem. Ref. Data* **5**, 209 (1976).
11. C. W. Allen, *Astrophysical Quantities*, 3rd Edn. Humanities Press, New Jersey (1974).
12. B. W. Shore and D. H. Menzel, *Principles of Atomic Spectra*, Wiley, New York (1968).
13. W. L. Wiese, M. W. Smith and B. M. Glennon, *Atomic Transition Probabilities*, Vol. I, NSRDS-NBS **4**, U.S. Government Printing Office, Washington D.C. (1966).
14. W. L. Wiese, M. W. Smith and B. M. Miles, *Atomic Transition Probabilities*, Vol. II, NSRDS-NBS22. U.S. Government Printing Office, Washington, D.C. (1969).
15. T. Bach, *JQSRT* **19**, 483 (1978).
16. K. Behringer and P. Thoma, *JQSRT* **20**, 615 (1978).
17. A. R. Striganov and N. S. Sventitskiy, *Tables of Spectral lines of Neutral and Ionized Atoms.* Atomizdat, Moskow (1966).
18. C. E. Moore, *A Multiplet Table of Astrophysical Interest* NSRDS-NBS40. U.S. Government Printing Office, Washington D.C. (1972).
19. A. N. Zaydel, V. K. Prokofyev, S. M. Raiskiy, V. A. Slavniy, and E. Yu. Schreider, *Tables of Spectral Lines.* Nauka, Moskow (1977).
20. M. S. Dimitrijević and N. Konjević, *JQSRT*, **24**, 451 (1980).
21. H. R. Griem, *Phys. Rev.* **165**, 258 (1968).
22. J. D. Hey, *JQSRT* **16**, 575 (1976).

J. Quant. Spectrosc. Radiat. Transfer Vol. 28, No. 3, pp. 185–198, 1982
Printed in Great Britain.

0022-4073/82/090185-14$03.00/0
Pergamon Press Ltd.

REGULARITIES AND SIMILARITIES IN PLASMA BROADENED SPECTRAL LINE WIDTHS (STARK WIDTHS)

W. L. WIESE and N. KONJEVIC

National Bureau of Standards, Washington, DC 20234, U.S.A. and Institute of Applied Physics, Belgrade, Yugoslavia

(*Received* 18 *November* 1981)

Abstract—Regularities and similarities in plasma broadened line widths have been studied by a comprehensive analysis of existing experimental data. Regularities are expected on the basis of general atomic structure considerations, and should be evident for spectral series, for corresponding transitions in homologous atoms and in isoelectronic sequences. Furthermore, similarities of line widths are expected for multiplets, supermultiplets and, to a lesser degree, for transition arrays. A comprehensive examination of literature data has been undertaken, which shows generally a close adherence of the measured data to the expected regularities. A few notable exceptions are also given.

INTRODUCTION

The broadening of spectral lines of heavy elements in plasmas is principally determined by two factors, the plasma environment and the atomic structure of the emitting atom or ion. Since atomic structures exhibit a great many regularities and similarities, one must expect that these find their way into the width and shift parameters of plasma broadened lines. However, an interesting question is how clearly and rigorously these show up. Also, it is important to find out if regularities are apparent to such a degree that accurate interpolations and extrapolations of new data as well as meaningful assessments of existing data are possible.

The fundamental formulas for plasma-broadened (or Stark-broadened) lines, in conjunction with atomic structure considerations, provide a general guide as to what types of regularities might be expected for the line shapes. But the existing numerical calculations of line shape parameters involve a considerable number of approximations and consequently may not reveal the full extent of the systematic behavior (nor the irregularities). For example, in theoretical calculations it is usually assumed that all lines within a multiplet exhibit the same width. On the other hand, experiments are now readily capable of assessing the validity of this assumption.

In earlier short reports,[1–3] we have briefly developed the general framework for plasma line-broadening regularities and have presented some examples of regularities and similarities for the widths of plasma-broadened, isolated lines of various elements. Puric *et al.*,[4–6] by appeal to the dependence of Startk widths on atomic oscillator strengths and their regularities, have studied systematic trends of Stark widths of homologous atoms and have reported in detail on the alkalis and alkali-like ions. Miller *et al.*[7] extended similar studies to some other ions. More recently, Puric *et al.*[8] noticed that periodicities in line widths follow periodicities in the ionization potentials, and they attempted to demonstrate a systematic dependence of line width on the "effective" ionization energy.[9,10] A special study by Helbig *et al.*[11] has demonstrated some systematic trends for neutral nitrogen lines. The purpose of this paper is to put some of these earlier ideas and observations on a firmer and more general basis by presenting a comprehensive set of experimental data and to demonstrate the strong dependence of Stark widths on atomic structure. For this we use experimental data exclusively, since, as noted above, plasma line broadening calculations contain at their present level of refinement numerous approximations and may therefore not show the regularities clearly. Thus, the main data sources are comprehensive experiments, which have produced consistent sets of data for large groups of lines and are expected to show especially clearly the variations from line to line. The experimentally established regularities should not only provide guidance for further theoretical work, but should also be useful for extrapolations and interpolations of needed data, and should indicate the limitations of such procedures.

GENERAL CONSIDERATIONS OF ATOMIC STRUCTURE

Regularities and similarities have been observed in atomic data from the beginning of spectroscopy, and have been shown to exist for wavelengths and energy levels, as well as for oscillator strengths, collision cross sections and other quantities. All these regularities are readily understood and expected from general principles of atomic structure. For plasma line broadening, such regularities should follow from regularities in the cross sections for elastic and inelastic collision processes between the free plasma electrons and the radiating atoms (or ions) that experience the broadening. The theoretical result for the width Δw of an isolated line broadened by plasma electrons (ion broadening is usually unimportant) may be expressed quite generally as[12,13]

$$\Delta w = \frac{1}{2} N_e \left\langle v_e \left(Q_{if} + \sum_i Q_{ii'} + \sum_f Q_{ff'} \right) \right\rangle_{av} .$$

In this expression, N_e and v_e denote the electron density and velocity, respectively; and the average extends over the velocity distribution of the perturbing electrons. The atomic quantities entering here are the cross sections $Q_{ii'}$ and Q'_{ff} for inelastic scattering (i.e., electron impact excitation and de-excitation) between either the initial (i) or final (f) state of the line and interacting states i' and f'. Interactions with optically allowed neighboring states are most important. Also, the expression contains an "effective" elastic scattering cross section Q_{if}, involving essentially the difference of scattering amplitudes between initial and final states.

While scattering cross sections as atomic quantities exhibit regular behavior, it is not clear if regularities in Stark broadening parameters are equally evident, since a variety of scattering processes contribute to the line shapes: (a) elastic as well as inelastic collisions are included, and in addition to the usually dominant electron–atom (or electron–ion) collisions also ion–atom (or ion–ion) collisions are sometimes significant; (b) collisions involve both the upper state and, usually to a lesser degree, the lower state of the transition; (c) sums over cross sections, i.e., total cross sections of excited states i and f are involved.

The most pronounced regularities should be expected for such simple atomic systems as the alkalis, alkaline earths, etc. Regularities should become less evident as the degree of complexity of the atomic structure increases. Thus, it should be interesting to investigate the extent of regularities and their changes as one proceeds from simple to complex atomic systems.

In the following, we present a large set of experimental data, ordered in various ways described below, which show the various regularities in plasma line broadening parameters. On the basis of the above discussed general theoretical description of line broadening in terms of scattering processes, especially scattering with optically interacting neighboring states, three types of regularities and similarities are expected:[1–3]

I. Regularities within a given spectrum: (a) for atoms or ions of simple structure, systematic trends along a spectral series; and (b) for complex spectra, similarities within multiplets, supermultiplets and transition arrays.

II. Similarities for analogous transitions in homologous atoms.

III. Systematic trends for given transitions along isoelectronic sequences.

Each of these regularities will be discussed and the numerical data reviewed. The numerical samples have been chosen after an extensive search through all existing experimental material and, in our judgement, represent the best available data. We have used two critical reviews[14,15] of experimental line-broadening data, published in 1976, as main guides for this selection. In addition, we have selected more recent material according to the same criteria as in the above-cited reviews. The new papers are listed either in the most recent NBS bibliography on "Line Shapes and Shifts"[16] or in an up-to-date NBS master list.[17] For a detailed discussion of the selection criteria, see the section "Critical Factors" in the introduction of Ref. 14. When several data sources of comparable quality were available, we have usually used only the most comprehensive one. Comprehensiveness is a very important requirement here, since it is especially the *variations* in the data, on a common relative scale, that matter most. At this point, it should be emphasized that Stark widths are not atomic constants, but parameters that depend on density and temperature. Thus, a large body of data, all consistently measured under the same conditions, even if temperature and density might be somewhat uncertain on an

absolute basis, are very valuable for the detection of regularities and similarities. The demonstration of regularities, based on a combination of results from several independent experiments, is much less satisfactory, unless the experimental conditions are not too different and there are sufficient points of overlap to check for mutual consistency so that one may make adjustments in the data to account, for example, for uncertainties in the absolute scale.

We shall now review the experimental data in the order of the three above-stated types of regularities, combined with a more detailed discussion of the expected regularities.

1. *Similarities and systematic trends within a given spectrum*

(a) *Spectral series trends in simple spectra.* This regularity applies especially to simple atomic systems with one or two electrons outside closed shells, where the spectral series structure is readily apparent. Since the lines of a spectral series occur between a fixed lower state (n, l) [n = principal quantum number, l = orbital angular momentum quantum number] and upper states with increasing $n' = n, n+1, n+2, \ldots$ but with *constant* orbital angular momentum quantum number (either $l+1$ or $l-1$), the set of interacting states remains the same, except for stepwise changes with n'. Expected is a gradual increase in the Stark widths with the principal quantum number n' of the upper state, since the energy differences between the upper level and the principal interacting levels decrease with n' and thus cross sections increase as n' (or the effective principal quantum number $n^{*\prime}$) increases. However, for large n', the increasingly smaller energy differences to perturbing levels become comparable to the line widths. Thus, in the plasma fields, these levels become degenerate and experience a first order Stark effect.[12] The experimental literature contains very little material on spectral series data. An extensive data set exists from the work of Gridneva and Kasalov[18] for the diffuse series of the alkali Cs. For He, Kelleher[19] has recently measured Stark widths for three successive transitions of two singlet and triplet series. The Cs and He data, given in Figs. 1 and 2 respectively, show clearly a smooth dependence of the widths on n'.

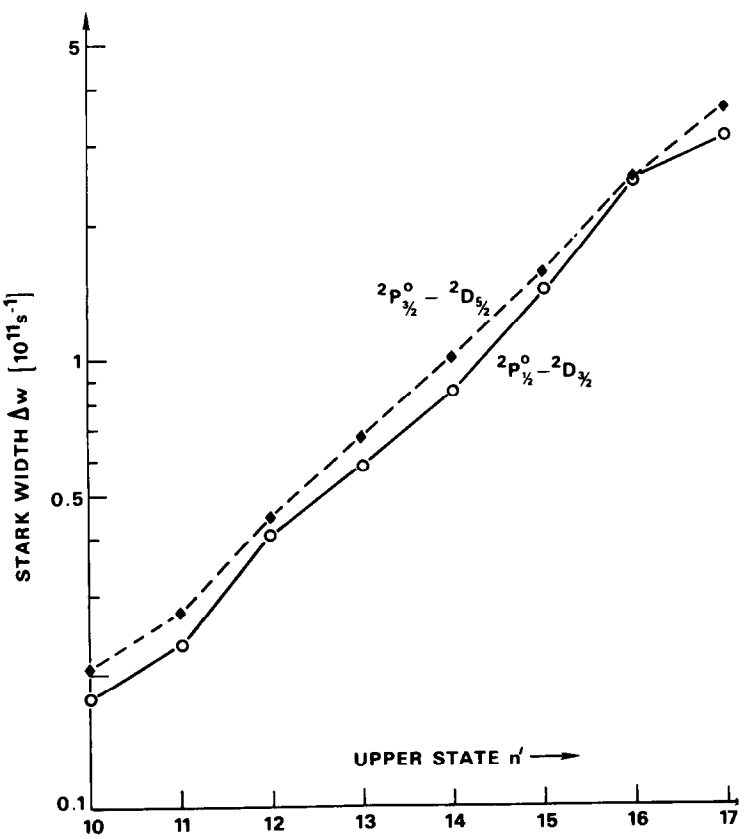

Fig. 1. Stark widths for the $6p$–nd series ($^2P^0_{1/2} \rightarrow {}^2D_{3/2}$ and $^2D^0_{5/2}$ lines) of CsI vs the principal quantum number n' of the upper state.

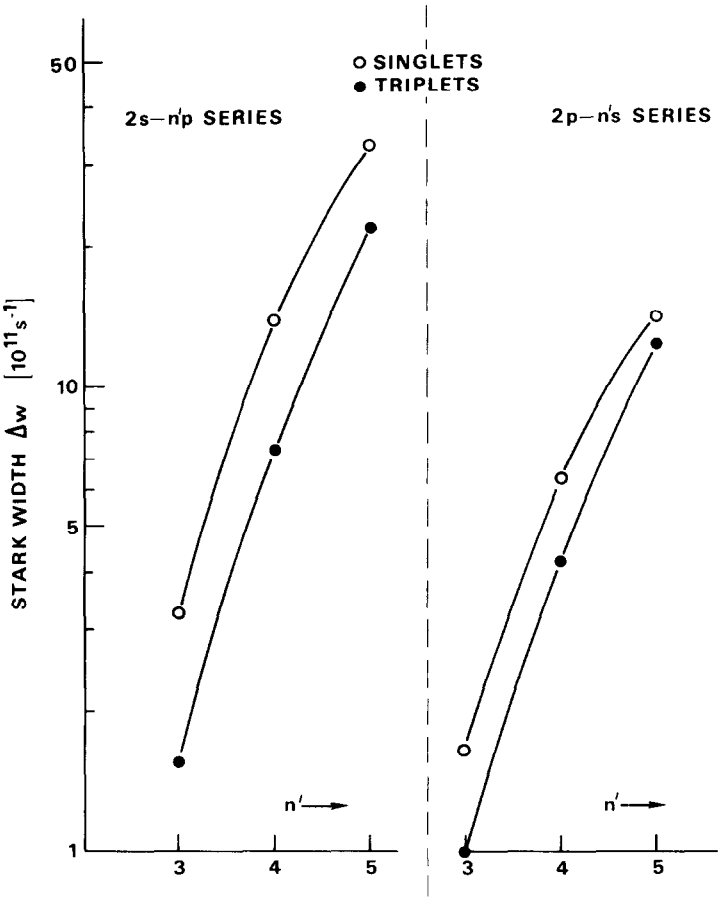

Fig. 2. Stark widths for HeI $2s$–n' p and $2p$–n' s series vs the principal quantum number n' of the upper state.

(b) *Trends for transition arrays in complex spectra.* For complex atoms, the spectral series structure is not apparent; however, a similar analysis may be made for the dependence of the Stark widths on principal and orbital angular momentum quantum numbers n' and l' of the jumping electron. Since these quantum numbers have constant values for an entire transition array (n, $l \rightarrow n'$, l', with $l' = l \pm 1$) which may contain numerous lines, data are actually needed for all these lines (or at least the stronger ones) so that an average width for the array may be established. If these data are available, one may compare different transition arrays. Upper states are of dominant importance, so that it is especially interesting to observe trends for transition arrays of the same (or similar) lower n, l and a succession of n', l' states, where l' stays constant ($l' = l+1$ or $l-1$) and n' runs through successively larger numbers (generalization of a spectral series). However, data for such a comprehensive analysis, which involves line averaging for each of the different transition arrays, are available only for very few cases. The most extensive example is provided by several transition arrays of OI (Table 1). Several experimental investigations had to be combined for this analysis,[20–23] but these were carried out at similar electron densities and temperatures ($4.9 \times 10^{16} < N_e < 10^{17}$ cm^{-3}; $11000 < T < 12800$ K), and the data partially overlap. Clearly, the Stark widths increase in distinct steps with principal quantum number n' for constant l' and also with orbital angular momentum quantum number l' for constant n'. This is to be expected on account of increasing Stark perturbations, since interacting energy levels become more closely spaced with increasing n' and l'. At higher n', the transition from an isolated line to a hydrogen-like line will again take place as discussed under (a).

(c) *Individual transition arrays and supermultiplets.* Transition arrays are groups of lines and multiplets with common upper and lower configurations, usually denoted by the n and l quantum numbers of the valence electrons. Furthermore, for multiplets within supermultiplets,

Table 1. Stark widths for various transition arrays in OI. Plasma conditions: $N_e = 5.7 \times 10^{16}$ cm^{-3}; $T \approx 12\,000$ K. The arrays are ordered in increasing n and l of the upper configurations.

Transition Array†	Full Stark half-width [10^{12} s^{-1}]‡	Multiplets utilized	Ref.
3s' - 3p'	0.16	$^1D^o$ - ^1D	20
3s" - 3p"	0.15	$^3P^o$ - ^3D, $^1P^o$ - ^1S	20
3s - 4p	1.0	$^5S^o$ - ^5P, $^3S^o$ - ^3P	21
4s - 4p	1.0	$^3P^o$ - ^3P, $^5S^o$ - ^5P	22
4p - 4d	6.4	^3P - $^3D^o$, ^5P - $^5D^o$	22
3d - 4f	4.5	$^3D^o$ - ^3F, $^5D^o$ - ^5F	22
3p - 5s	2.9	^3P - $^3S^o$, ^5P - $^5S^o$	21
3p - 5d	27	^5P - $^5D^o$	23
3p - 6s	10	^5P - $^5S^o$, ^3P - $^3S^o$	21,23

†Transition arrays are specified by the n and ℓ values of the jumping electron. Singly and doubly primed arrays denote configurations based on $2p^3\ ^2D^o$ and $2p^3\ ^2P^o$ parent terms for the core electrons.

‡When two multiplets are utilized, the tabulated value represents the arithmetic mean.

the parent term and the spin multiplicity $(2S+1)$ remain the same; here, S is the spin angular momentum quantum number, which is the vector sum of single-electron spin quantum numbers s ($s = 1/2$). For such groups of multiplets, one expects Stark widths of roughly the same size, since the excitation energies of all energy levels having a common electronic configuration usually lie within a relatively narrow range and interactions occur with the same entity of other levels so that the Qs should be similar for all multiplets within a transition array. Nevertheless, appreciable variations in Q may occur for different multiplets within an array, since the relatively small energy differences between the upper (or lower) term of a multiplet and the important neighboring perturbing terms may vary significantly from multiplet to multiplet (multiplets within an array are principally characterized by different resultant orbital and spin angular momentum quantum numbers L and S).

For specific transition arrays and supermultiplets, the number of transitions involved is fairly small, so that numerous experimental Stark widths are available. While there is to our knowledge no case where a complete set of lines within a transition array or supermultiplet is covered, often the measured part is most significant. A large sample of the available data,[24–32] which should represent a good cross section of the recent experimental material, is presented in Table 2, parts 1 and 2. In practically all cases, similarities for the line widths within the various groups are clearly observed. Within transition arrays (examples 1.a–1.e), the variations are about 30–40%, while, for supermultiplets containing smaller groups of lines (examples 1.a–1.e and 2.a–2.b), they are usually in the range from 15 to 30%. However, the CI transition array 3s–4p, for which Nubbemeyer and Wende[27] observe variations up to a factor of 3, provides an exception. The closeness of the high lying $4p\ ^1S$ and $4p\ ^1D$ terms to the $5s\ ^1P^o$ and $4d\ ^1D^o$ perturber terms may offer a partial explanation for this behavior.

(d) *Multiplets.* Descending further down the hierarchy of complex spectra, the smallest distinct grouping of lines occurs as a multiplet. This applies especially to lighter atoms, where LS coupling is well approximated and with which most of the available line-broadening experiments and calculations are concerned. These lines arise between those closely spaced upper and lower levels which have the same n, l, S, L and n', l', S', L' but for which the total

Table 2. Similarities of line half-widths within transition arrays, supermultiplets and multiplets.

Designation	Multiplet	Line Wavelength [Å]	Full half-width Δw [10^{11} s^{-1}]	Ref.
1. Transition arrays (all incomplete):				
(a) Transition array 3s - 3p of O II:				
$2p^2(^3P)3s - 2p^2 3p^+$	$^4P - {}^4S^o$	3712.75	1.45	24
		3727.33	1.35	"
	$^4P - {}^4P^o$	4366.90	1.14	"
		4317.14	1.15	"
	$^4P - {}^4D^o$	4649.14	1.03	"
		4650.84	1.07	"
	$^2P - {}^2P^o$	3973.26	1.41	"
	$^2P - {}^2D^o$	4414.91	1.34	"
$2p^2(^1D)3s - 2p^2 3p$	$^2D - {}^2P^o$	3911.96	1.44	"
	$^2D - {}^2D^o$	4347.43	1.13	"
	$^2D - {}^2F^o$	4590.97	1.18	"
		4596.17	1.14	"
Experimental conditions: $T = 25\,900$ K; $N_e = 5.2 \times 10^{16}$ cm^{-3}				
(b) Transition array 4s - 4p of Cℓ II:				
$3p^3(^4S^o)4s - 3p^3 4p$	$^5S^o - {}^5P$	4810.06	2.12	25
		4819.46	2.19	"
		4794.54	2.38	"
	$^3S^o - {}^3P$	5221.34	2.14	"
$3p^3(^2D^o)4s - 3p^3 4p$	$^3D^o - {}^3D$	5078.25	2.59	"
	$^3D^o - {}^3F$	4896.77	2.44	"
	$^3D^o - {}^3P$	4291.76	2.66	"
		4304.07	2.65	"
		4336.26	2.41	"
		4343.62	2.60	"
	$^1D^o - {}^1D$	4132.48	3.31	"
$3p^3(^2P^o)4s - 3p^3 4p$	$^3P^o - {}^3D$	4785.44	1.98	"
		4768.68	1.99	"
		4778.93	1.90	"
Experimental conditions: $T = 18\,600$ K; $N_e = 6.8 \times 10^{16}$ cm^{-3}				
(c) Transition array 4s - 4p of Cℓ III:				
$3p^2(^3P)4s - 3p^2 4p$	$^4P - {}^4S^o$	3191.45	1.78	26
	$^4P - {}^4P^o$	3283.41	1.70	"
		3289.80	1.69	"
		3340.42	1.69	"
	$^4P - {}^4D^o$	3602.10	1.54	"
		3612.85	1.49	"
		3656.95	1.45	"
		3705.45	1.36	"
$3p^2(^1D)4s - 3p^2 4p$	$^2D - {}^2D^o$	3392.89	1.39	"
		3393.45	1.33	"
	$^2D - {}^2F^o$	3530.03	1.59	"
Experimental conditions: $T = 24\,200$ K; $N_e = 5.8 \times 10^{16}$ cm^{-3}				

Table 2. (*Contd*).

Designation	Multiplet	Line Wavelength [Å]	Full half-width Δw [10^{11} s^{-1}]	Ref.
(d) Transition array 3s - 4p of C I:				
$2p(^2p^o)3s$ - 2p4p	$^3P^o$ - ^3S	4812.84	9.0	27
		4817.33	9.3	"
		4826.73	9.7	"
	$^3P^o$ - ^3P	4766.62	8.3	"
		4771.72	6.6	"
		4775.87	6.2	"
	$^1P^o$ - ^1S	4932.00	19	"
	$^1P^o$ - ^1P	5380.24	7.2	"
	$^1P^o$ - ^1D	5052.12	15	"
Experimental conditions: T = 11 100 K; $N_e = 5 \times 10^{16}$ cm^{-3}				
(e) Transition array 4s - 4p of Ar II:				
$3p^4(^3P)4s$ - $3p^4$4p	^4P - $^4S^o$	3850.58	4.19	28
		3928.63	4.03	"
	^4P - $^4P^o$	4806.02	3.51	"
		4847.82	3.61	"
	^4P - $^4D^o$	4348.06	3.99	"
		4426.01	3.85	"
		4430.19	3.84	"
	^2P - $^2S^o$	4579.35	3.78	"
	^2P - $^2P^o$	4726.86	4.05	"
	^2P - $^2D^o$	4545.05	4.56	"
		4657.89	4.17	"
Experimental conditions: T = 13 800 K; $N_e = 1.2 \times 10^{17}$ cm^{-3}				
2. Supermultiplets (see also transition array samples):				
(a) 4s - 4p and 4p - 4d triplets of S III:				
$3p(^2p^o)4s$ - 3p4p	$^3P^o$ - ^3D	4337.71	1.26	29
		4361.53	1.25	"
	$^3P^o$ - ^3P	3831.95	1.30	"
		3899.09	1.22	"
	$^3P^o$ - ^3S	3662.01	1.31	"
$3p(^2p^o)4p$ - 3p4d	^3D - $^3F^o$	2856.02	2.43	"
		2863.53	2.37	"
		2872.00	2.33	"
	^3D - $^3D^o$	2718.88	2.63	"
		2756.89	2.60	"
	^3P - $^3D^o$	2950.23	2.32	"
		2964.80	2.32	"
Experimental conditions: T = 28 500 K; $N_e = 5.1 \times 10^{16}$ cm^{-3}				
(b) 3s - 3p quartets of N I:				
$2p^2(^3P)3s$ - $2p^2$3p	^4P - $^4D^o$	8718.84	4.14	30
		8711.71	4.15	"
		8703.26	4.33	"
		8686.16	4.35	"
		8683.40	5.18	"
		8680.27	4.83	"
	^4P - $^4P^o$	8216.32	4.33	"
		8210.71	4.84	"
		8242.37	4.91	"
		8223.12	4.54	"
		8184.85	4.45	"
		8188.01	4.19	"
	^4P - $^4S^o$	7468.31	5.14	"
		7442.30	5.07	"
		7423.64	5.10	"

Table 2. (*Contd.*)

Designation	Multiplet	Line Wavelength [Å]	Full half-width Δw [10^{11} s^{-1}]	Ref.
Experimental conditions: T = 13 000 K; N_e = 1.61 × 10^{17} cm^{-3}				
3. Multiplets (see also earlier samples):				
(a) Si I:				
$3p(^2P^o)4s$ - $3p5p$	$^3P^o$ - ^3P	5645.61	43.8	23
		5665.55	42.9	"
		5690.43	44.8	"
		5701.11	37.7	"
		5708.40	41.1	"
Experimental conditions: T = 11 000 K; N_e = 1.0 × 10^{17} cm^{-3}				
(b) P I:				
$3p^3$ - $3p^2(^3P)4s$	$^2P^o$ - ^2P	2533.99	3.26	31
		2535.61	3.22	"
		2553.25	3.21	"
		2554.90	3.18	"
Experimental conditions: T = 12 700 K; N_e = 9.3 × 10^{16} cm^{-3}				
(c) S II:				
$p^2(^3P)4s$ - $3p^24p$	^4P - $^4D^o$	5453.81	2.47	32
		5432.77	2.68	"
		5428.64	2.49	"
		5509.67	2.61	"
		5473.59	2.83	"
Experimental conditions: T = 11 100 K; N_e = 7.0 × 10^{16} cm^{-3}				

†For the listed transitions, the parent term does not change and is therefore only given once.

angular momentum quantum numbers J vary, thus producing the individual lines. In comprehensive Stark broadening calculations,[12] usually only one width has been determined per multiplet and all line widths are assumed to be the same. This is normally to be expected (for an exception see below) since, aside from differences in J, the interacting levels are the same for all these lines and thus the cross sections should be essentially identical. In all 3 sections of Table 2, many experimental results are listed which bear this out. A few special experimental checks on line widths in multiplets have been made,[28,33] which support the theoretical assumption very nicely. These results are reproduced in Figs. 3 and 4, and indicate that within the experimental precision, which is in the few-percent range, the line widths in multiplets are the same.

However, irregularities occasionally occur when some principal perturbing levels are embedded right in the upper (or lower) levels of the multiplet. This is the case, for example, for the ArII multiplet $4s^2P$–$4p'\ ^2P$ with four lines in the range 2892 to 3034 Å. Two perturbing $3d'\ ^2D_{3/2}$ and $3d'\ ^2D_{5/2}$ levels lie very close to the upper $4p'\ ^2P_{1/2}$ and $^2P_{3/2}$ levels, respectively, but by significantly different amounts, and thus cause significantly different interactions and widths for the individual lines. Variations of 60% in widths have been measured by Behringer and Thoma[34] for the four lines of this multiplet and detailed calculations by Hey[35] resulted in variations of 35%.

2. *Similarities for homologous atoms and ions*

Homologous atoms and ions, i.e. species with the same electronic charge and the same number of valence electrons (e.g., all neutral alkalis, etc.) often exhibit similar atomic structures. Therefore, the cross sections for scattering into interacting levels should exhibit similarities for analogous atomic states which differ only by the addition or subtraction of an electron shell ($n \rightarrow n \pm 1$), and systematic trends such as gradual variations are expected in such cases.

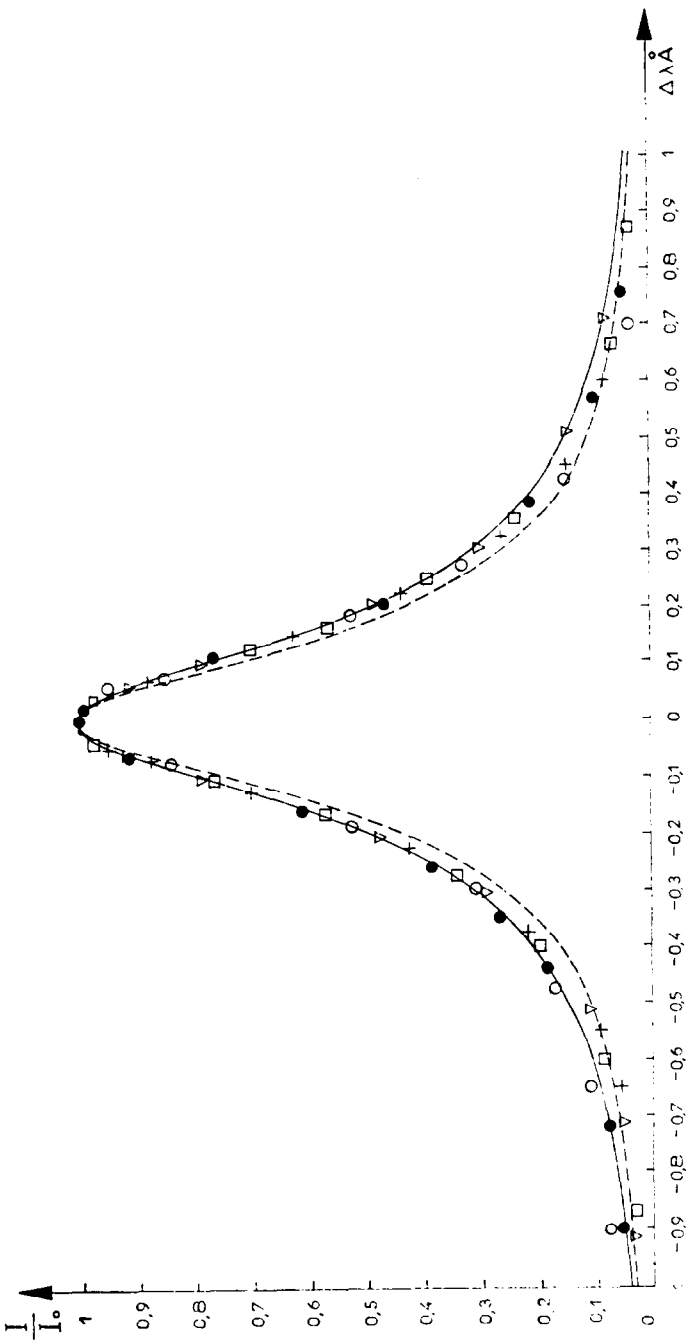

Fig. 3. Stark profiles for 5 lines of the ArII $4s^4P$–$4p\ ^4P^0$ multiplet according to the plasma jet emission measurements by Chapelle *et al.*[28] Within the experimental precision, the line widths are identical.

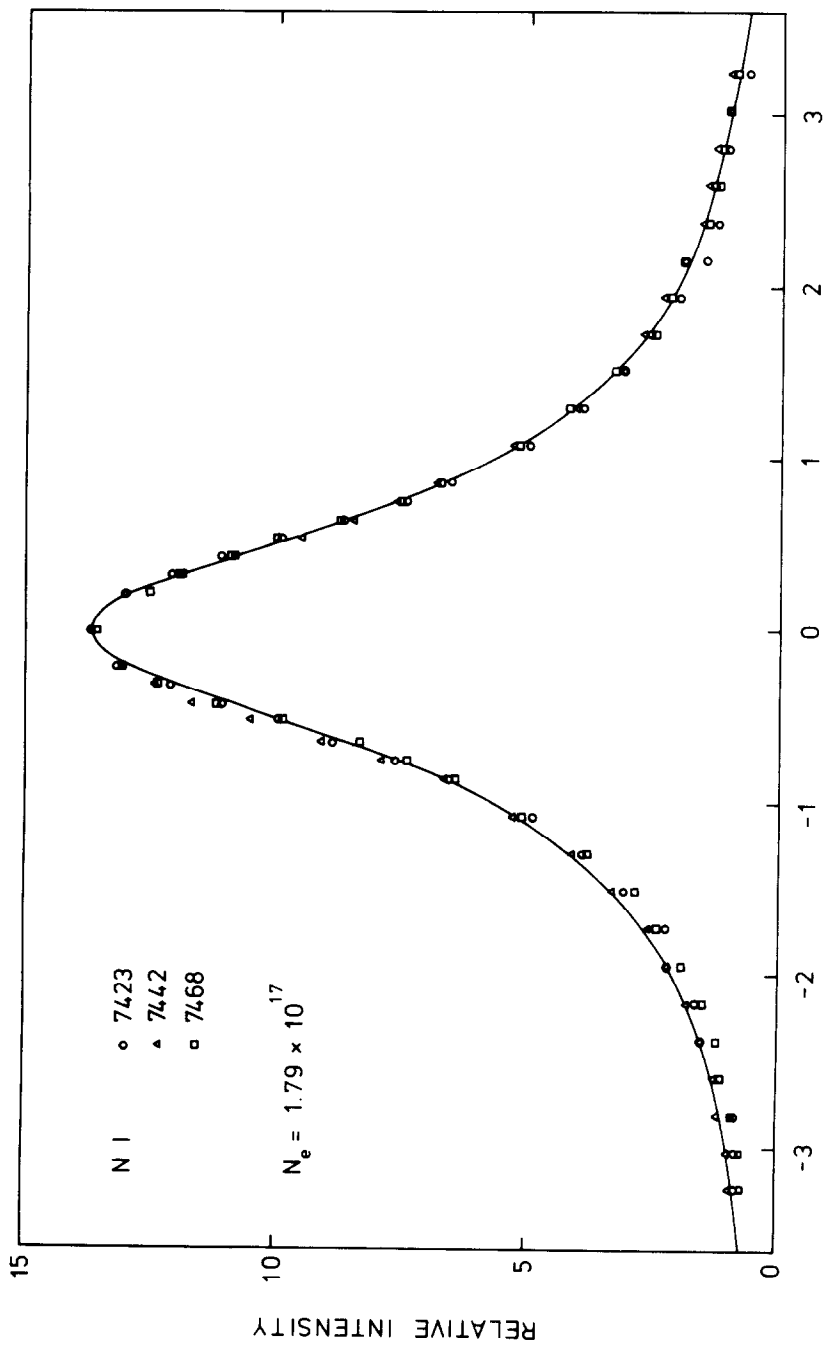

Fig. 4. Stark profiles for the three lines of the *N I* multiplet $3s\ ^4P$–$3p\ ^4S^0$ from stabilized arc emission measurements by Helbig *et al.*[33] The relative intensities are scaled by the inverse *LS*-coupling intensity ratios, i.e. 1:2:3 for 7423:7442:7468 Å. Line shapes and widths are identical within the experimental precision.

Several interesting sets of experimental data illustrate this type of regularity, of which we present two cases in Figs. 5 and 6. Figure 5 shows the situation for the resonance lines, *ns-np*, of the alkalis (n is the principal quantum number of the ground state) according to the data of Puric *et al.*[5] and Lakicevic *et al.*[36] We illustrate the positions of lower and upper energy levels as well as the two nearest perturbing levels *nd* [$(n+1)d$ in the case of Li] and $(n+1)s$. The interaction of the upper level with these levels is both a function of closeness of the perturbing levels as well as the interaction strength. The latter, which is proportional to the optical line

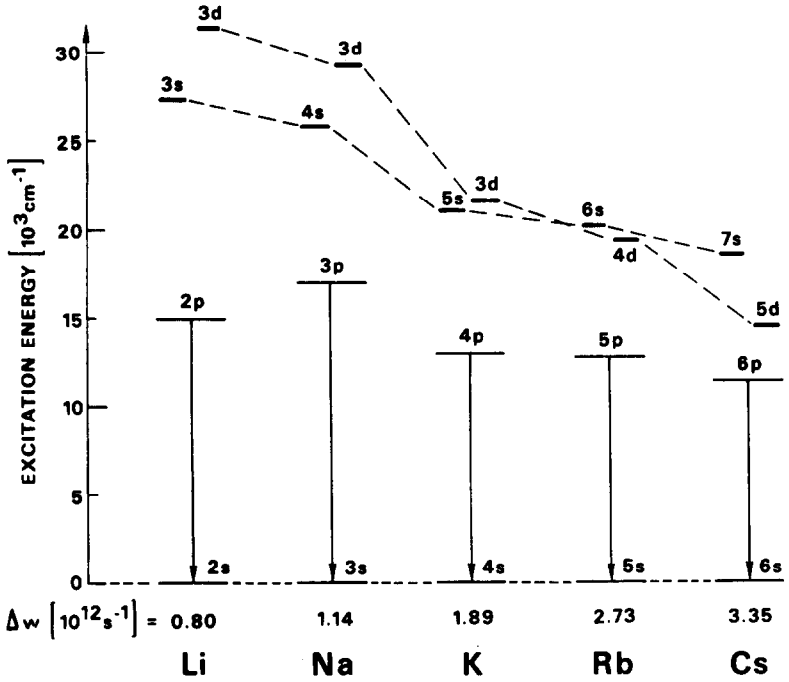

Fig. 5. Energy level positions for the resonance lines of the alkalis, and locations of the nearest perturbing levels. The stronger perturbing level, *nd*, is gradually moving closer to the upper level of the transition, causing the increasingly larger Stark widths.

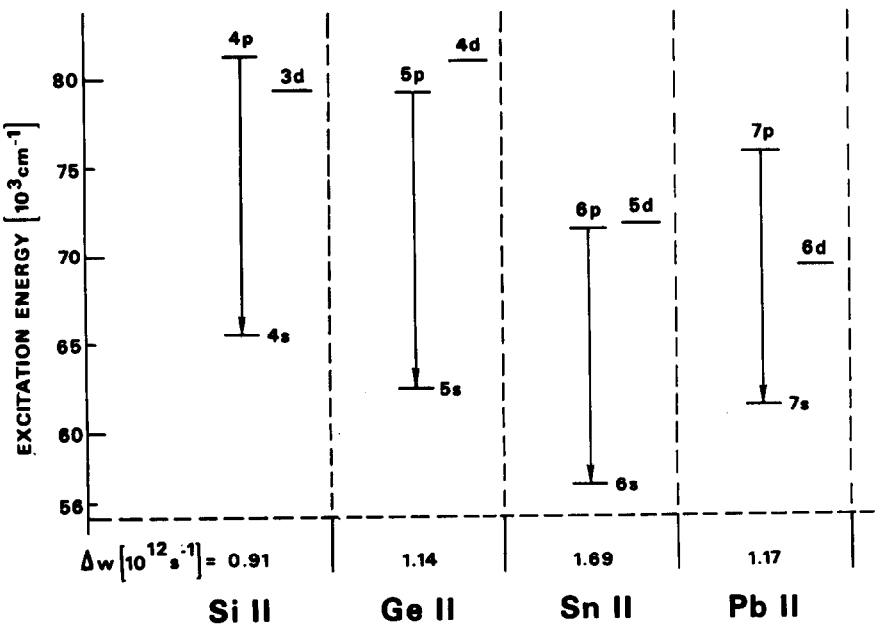

Fig. 6. Energy level positions for the $(n+1)s$–$(n+1)p$ transitions of Group III ions and location of the nearest strong perturbing level *nd*. (n = principal quantum number of the ground state valence electrons.)

strength,[13] is about 4 to 5 times stronger between the *np* and *nd* levels than between the *np* and $(n+1)s$ levels. Thus, the *nd* level should dominate if it is about the same distance (or less) from the upper level as the $(n+1)s$ level. Indeed, as the *nd* level moves gradually closer to the *np* level, the distance $(n+1)s$–*np* remains nearly constant and the line width for the *ns*–*np* transition increases strongly. Detailed studies of this and other transitions of alkalis and alkali-like ions have been carried out by Puric *et al.* since 1973.[4–6]

In Fig. 6, the situation for the $(n+1)s$-$(n+1)p$ transitions of Group III ions (SiII, GeII, SnII, and PbII is illustrated in a similar fashion (n is again the principal quantum number of the ground state). The data are all taken from shock tube emission experiments by Miller *et al.*[7,37–40] For SnII, the closest interacting level, *nd*, almost coincides with $(n+1)p$, and is thus expected to cause a greatly increased line width there in contrast to the other three ions, which is indeed observed by experiment.

Miller *et al.*[7] have also recently studied several corresponding transitions for homologous ions of some other element groups and arrive again at clearly recognizable trends in their experimental data.

3. TRENDS ALONG ISOELECTRONIC SEQUENCES

For the corresponding lines of ions in an isoelectronic sequence, systematic trends with nuclear charge Z are expected since the cross sections scale with nuclear charge. While such trends are expected to show up quite clearly, one may often encounter transitions for which significant changes in the neighboring level structure take place along the sequence. Isoelectronic sequence studies of Stark widths have to be limited to ionic species and cannot include neutral atoms, since the interaction between charged radiators and perturbers is different from that involving neutral radiating atoms.

Some experiments have produced data for several times ionized atoms (however, nowhere near the regime where relativistic atomic structure effects would become important) so that a few transitions in some sequences may be followed through two or three ions. The very scarce data at this time demonstrate clearly that the widths decrease strongly with increasing ionic charge. A sample is shown in Table 3.[26,32,41]

4. OTHER TRENDS

Puric *et al.*[8] have recently demonstrated a systematic dependence of the widths of resonance lines with the periodicity of ionization potentials. They attributed this phenomenon basically to the circumstance that energy level schemes compress or expand as the ionization potential decreases or increases, and that specifically the energy gaps between the closest perturbing levels and the upper level of the resonance are following the periodicity of the ionization potentials.

In a more recent paper, Puric *et al.* (1981)[10] have attempted to demonstrate a general dependence of the line width Δw (for non-resonance transitions) on a "reduced" ionization potential I'. By a best fit of experimental and theoretical data points, they have obtained a power series dependence of Δw on I' and they show some examples of *ns*–*np* and *ns*–$(n+1)p$

Table 3. Scaling of Stark widths with nuclear charge. Sample: PI isoelectronic sequence. Widths are given for $N_e = 10^{17}$ cm^{-3}, by scaling measured densities linearly. Experimental densities are within a factor of 2 of this value.

Ion	Multiplet	Stark half-width [10^{12} s^{-1}]	Ref.
S II	$3p^2(^3P)4s\ ^4P - 3p^2 4p\ ^4D^o$	0.38	32
Cl III	$4s\ ^4P - 4p\ ^4D^o$	0.25	26
	$^4P - \ ^4P^o$	0.28	26
Ar IV	$4s\ ^4P - 4p\ ^4D^o$	0.15	40
	$^4P - \ ^4P^o$	0.15	40

transitions where this dependence appears. However, it is not clear that this dependence should hold up for a larger sample of data, since all other aspects of atomic structure are neglected and the group *I* elements (alkalis) with simple atomic structure are included along with much more complex elements, such as from groups IV and V. In fact, they state earlier[9] that they have averaged data over all selected elements to come up with a single functional dependence of width on ionization potential. They thus effectively smooth out trends and variations.

SUMMARY

General considerations of atomic structure and Stark broadening indicate that many similarities and systematic trends should exist for plasma line broadening parameters. However, since it is uncertain just how rigorously these regularities show up, a large sample of experimental line-broadening data (in large part, accurate data from comprehensive experiments) has been analyzed for the predicted trends. The following conclusions may be drawn:

(1) Line widths in multiplets usually agree within a few per cent, and possibly better than one per cent. Exceptions are cases where some perturbing levels are accidentally extremely close to the upper (or lower) levels of a multiplet.

(2) Line widths in supermultiplets are usually the same within about 30%.

(3) Line widths within transition arrays stay normally within a range of about ±40%.

(4) For complex spectra, line widths show pronounced stepwise increases with increasing n and l of the upper states. However, present experimental material is too sparse to make quantitative statements.

(5) For simple spectra, where the line widths within a spectral series can be observed, the widths show a smooth increase with the n of the upper state, so that interpolations or limited extrapolations along a series should produce additional reliable data.

(6) For most of the transitions studied in homologous atoms, clear systematic trends are discernible for analogous lines (e.g. resonance lines). Therefore, interpolations or extrapolations to other homologous atoms appear feasible.

(7) For ions along isoelectronic sequences, clear trends of stepwise decreases in the widths are seen in the experimental data. However, the available material is very meager and does not extend far enough along the sequences to be considered reliable enough for extrapolations.

REFERENCES

1. W. L. Wiese and N. Konjevic, In *Physics of Ionized Gases* 1976 (*contributions*) p. 416. J. Stefan Institute, Univ. of Ljubljana Publ., Yugoslavia (1976).
2. W. L. Wiese and N. Konjevic, In *The Physics of Ionized Gases*, (Edited by R. K. Janev), p. 257. Institute of Physics, Beograd (1978).
3. N. Konjevic and M. S. Dimitrijevic, In *Spectral Line Shapes* (Edited by B. Wende), p. 241. Walter de Gruyter, Berlin (1981).
4. J. Puric and Lj. Cirkovic, *Proc. 11th Int. Conf. Phen. Ion. Gases* (Prague 1973), p. 398.
5. J. Puric, J. Labat, Lj. Cirkovic, I. Lakicevic, and S. Djenize, *J. Phys.* B **10**, 2375 (1977).
6. J. Puric, M. S. Dimitrijevic, and I. S. Lakicevic, *Phys. Lett.* **67A**, 189 (1978).
7. M. H. Miller, A. Lesage, and J. Puric, *Astrophys. J.* **239**, 410 (1980).
8. J. Puric, I. Lakicevic, and V. Glavonjic, *J. Phys.* (*Paris*), *Colloq. C7*, *Suppl.* 7, **40**, 795 and 835 (1979).
9. J. Puric, I. Lakicevic, and V. Glavonjic, *Phys. Lett.* A **76**, 128 (1980).
10. J. Puric, O. Labat, and I. Lakicevic, In *Spectral Line Shapes* (Edited by B. Wende), p. 249. Walter de Gruyter, Berlin (1981).
11. V. Helbig, D. E. Kelleher, and W. L. Wiese, In *Physics of Ionized Gases* 1976 (*contributions*), p. 412. J. Stefan Institute, Univ. of Ljubljana Publ., Yugoslavia (1976).
12. H. R. Griem, In *Adv. At. Molec. Phys.* **11**, 331, Academic Press, New York, 1975; H. R. Griem, *Spectral Line Broadening by Plasmas*, Academic Press, New York (1974).
13. M. Baranger, In *Atomic and Molecular Processes* (Edited by D. R. Bates) Academic Press, New York (1962).
14. N. Konjevic and W. L. Wiese, *J. Phys. Chem. Ref. Data* **5**, 259 (1976).
15. N. Konjevic and J. R. Roberts, *J. Phys. Chem. Ref. Data* **5**, 209 (1976).
16. J. R. Fuhr, B. J. Miller, and G. A. Martin, *Bibliography on Atomic Line Shapes and Shifts* (June 1975 through June 1978), NBS Spec. Publ. 366, Suppl. 3, Washington, D.C. (1978).
17. J. R. Fuhr and B. J. Miller (private communication).
18. S. M. Gridneva and G. A. Kasalov, *Proc.* VIIth *Int. Conf. Phenom. Ioniz. Gases*, Vol. II, p. 581. Gradevinska Knjiga Publ. House, Belgrade, 1966.
19. D. E. Kelleher, *JQSRT* **25**, 191 (1981).
20. M. Jung, *Z. Astrophys.* **58**, 93 (1963).
21. W. L. Wiese and P. W. Murphy, *Phys. Rev.* **131**, 2108 (1963).
22. R. Assous, *JQSRT* **10**, 975 (1970).

23. M. H. Miller and R. D. Bengtson, *Phys. Rev.* **A1**, 983 (1970).
24. M. Platisa, M. V. Popovic, and N. Konjevic, *Astron. Astrophys.* **45**, 325 (1975).
25. N. Konjevic, M. Platisa, and J. Puric, *J. Phys.* **B 4**, 1541 (1971).
26. M. Platisa, M. Dimitrijevic, M. Popovic, and N. Konjevic, *Astron. Astrophys.* **54**, 837 (1977).
27. H. Nubbemeyer and B. Wende, *Z. Phys.* **225**, 69 (1969).
28. J. Chapelle, A. Sy, F. Cabannes, and J. Blandin, *JQSRT* **8**, 1201 (1968).
29. M. Platisa, M. Popovic, M. Dimitrijevic, and N. Konjevic, *JQSRT* **22**, 333 (1979).
30. J. C. Morris, R. V. Krey, and R. L. Garrison, "Radiation Studies of Arc Heated Nitrogen Oxygen and Argon Plasmas", AVCO Corp. Space Syst. Div., Wilmington, Mass *Rep. AVSSD-0049-68-RR* (1968).
31. P. A. Voigt and J. R. Roberts, *Phys. Rev.* **A15**, 1006 (1977).
32. J. M. Bridges and W. L. Wiese, *Phys. Rev.* **159**, 31 (1967).
33. V. Helbig, D. E. Kelleher, and W. L. Wiese, *Phy. Rev. A* **14**, 1082 (1976).
34. K. Behringer and P. Thoma, *JQSRT* **20**, 615 (1978).
35. J. D. Hey (unpublished, data cited in Ref. 35).
36. I. Lakicevic, J. Puric, and J. Labat, *Proc. 13th Int. Conf. Phen. Ion. Gases*, p. 123. East Berlin (1977).
37. A. Lesage, S. Sahal-Brechot, and M. H. Miller, *Phys. Rev. A* **16**, 1617 (1977).
38. W. W. Jones and M. H. Miller, *Phys. Rev. A* **10**, 1803 (1974).
39. M. H. Miller and R. D. Bengtson, *Phys. Rev.* A **20**, 499 (1979).
40. M. H. Miller, R. D. Bengston, and J. M. Lindsay, *Phys. Rev.* A **20**, 1997 (1979).
41. M. Platisa, M. Popovic, M. Dimitrijevic, and N. Konjevic, *Z. Naturforsch.* **30a**, 212 (1975).

J. Quant. Spectrosc. Radiat. Transfer Vol. 30, No. 1, pp. 45–54, 1983
Printed in Great Britain.

0022-4073/83/070045-10$03.00/0
Pergamon Press Ltd.

STARK BROADENING OF ISOLATED SPECTRAL LINES OF HEAVY ELEMENTS IN PLASMAS†

M. S. DIMITRIJEVIĆ and N. KONJEVIĆ
Institute of Applied Physics, 11071 Beograd, P. O. Box 58, Yugoslavia

(*Received* 31 *March* 1982)

Abstract—In this paper, we present results of semiclassical calculations of Stark broadening parameters for some lines of heavy neutral atoms. Comparisons with experiment show large discrepancies previously undetected for lighter elements. Critical evaluation of experimental data indicate that in most cases the experiment must be blamed for these discrepancies.

1. INTRODUCTION

Stark broadening of spectral lines by plasmas has been used as an important plasma diagnostic tool for a number of years. In the early 1960s, a considerable effort was made to improve existing theories of Stark broadening of spectral lines in plasmas. Most of this work was concerned with the Stark broadening of hydrogen lines. Because of the large linear Stark effect, these studies were useful for plasma diagnostic purposes. However, it is not always convenient to seed a plasma with hydrogen, and sometimes it is not possible to do so. Further, because of the large Stark effect, hydrogen lines may not be useful for diagnostic purposes, since they become so broad at high electron densities that it is difficult to determine a line shape because of interference with neighboring lines. Therefore, there has been interest in the Stark broadening of non-hydrogenic lines of neutrals and ions. Because of the quadratic Stark effect, these can be used for diagnostic purposes at high electron densities, especially where seeding a plasma with hydrogen is not possible.

The first calculations of Stark-broadening parameters of prominent lines of non-hydrogenic atom were published in 1962[1] (see also Ref. 2). Since then, numerous experiments were performed (for a review of experimental data which were available as of 1976, see Refs. 3 and 4) in order to provide new Stark-broadening parameters and to check theoretical predictions. At the same time, further sophistications of the theory were made (see, e.g., Refs. 3 and 5). New, comprehensive theoretical calculations of Stark-broadening parametrers for lines of non-hydrogenic neutral atoms (He through Ca, as well as Cs) were published in 1971[6] and in 1974.[3] For these elements, the comparison with experiments showed average agreement within $\pm 20\%$.[3,4] Although some experimental data for heavier elements were available at that time, there were no theoretical data with which these could be compared.

In this paper, we present the results of semiclassical calculations of Stark-broadening parameters for spectral lines of elements heavier than Ca. These results represent an extension of the data tabulated by Griem.[3] The calculations were made for elements for which experimental results were available, so that comparison with experiment became feasible; the results of this comparison are presented in this paper.

2. THEORY AND RESULTS

The basis for the calculation of Stark-broadening parameters was the computer code developed by Jones *et al.*[7] for the lines of singly-charged ions. We made it suitable for neutral atoms in accordance with the Benett and Griem version of the semiclassical theory.[6] The computer solves the following set of equations:

$$w + id = N_e \int vf(v)\, \mathrm{d}v(w_d + w_q + id_d),$$

†This work was partially performed under a grant from the U.S. National Bureau of Standards, Washington, D.C.

where the index d denotes the dipole contribution $w_d + id_d$,

$$w_d + id_d = \frac{4\pi}{3}\left(\frac{\hbar}{mv}\right)^2 \left\{\frac{3}{4}\left(\frac{mv\rho_{\min}}{\hbar}\right)^2 + \sum_{i' \neq f} \mathbf{R}^2_{ii'}[a_{ii'}(z^{\min}_{ii'}) - i\epsilon_{ii'}b_{ii'}(\tilde{z}^{\min}_{ii'})]\right.$$

$$\left. + \sum_{f' \neq i} \mathbf{R}^2_{ff'}[a_{ff'}(z^{\min}_{ff'}) + i\epsilon_{ff'}b_{ff'}(\tilde{z}^{\min}_{ff'})] + \frac{3Ry\bar{f}}{|E_i - E_f|}\left(1 + \frac{2l_f+1}{2l_i+1}\right)[a_{if}(z^{\min}_{if}) - ib_{if}(\tilde{z}^{\min}_{if})]\right\},$$

and the index q denotes the quadrupole contribution w_q,

$$w_q = \frac{\pi}{45}\left(\frac{\hbar a_0}{mv\rho_{\min}}\right)^2 (2l_i+1)\begin{pmatrix} l_i & 2 & l_i \\ 0 & 0 & 0 \end{pmatrix}^2 R^4_{ii} + (2l_f+1)$$

$$\times \begin{pmatrix} l_f & 2 & l_f \\ 0 & 0 & 0 \end{pmatrix}^2 R^4_{ff} + 2(2l_i+1)(2l_f+1)\begin{pmatrix} l_i & 2 & l_i \\ 0 & 0 & 0 \end{pmatrix}\begin{pmatrix} l_f & 2 & l_f \\ 0 & 0 & 0 \end{pmatrix}\begin{Bmatrix} l_i & 2 & l_i \\ l_f & 1 & l_f \end{Bmatrix} R^2_{ii}R^2_{ff}.$$

Here, w is the half halfwidth (HWHM), d is the shift, N_e is the electron density, $f(v)$ is the Maxwellian distribution of the electron velocity (v) and Ry is the Rydberg constant; i, f denote the initial and final states of the isolated line, respectively; i', f' are the corresponding perturbing states within the dipole approximation. The quantity $\epsilon_{jj'}$ determines the signs of individual contributions to the shift, viz.,

$$\epsilon_{jj'} = (E_j - E_{j'})/|E_j - E_{j'}|,$$

where E_j and $E_{j'}$ are the energies of the corresponding states. In the above expressions, $\mathbf{R}^2_{jj'}$ is the square of the coordinate-operator matrix element in units of a_0^2 (a_0 is the Bohr radius), R^2_{jj} is the sum of the matrix elements of the radius-vector squares, $\bar{f}$ is the absorption oscillator strength for the transition $i \rightarrow f$ summed over upper states in which the outer electron has constant quantum numbers n and l and the atom has constant total spin quantum number S. The minimum impact parameter $\rho_{\min}$ allowed by the unitarity condtion[3] is given by

$$\rho^2_{\min} = \left(\frac{4}{3}\right)^{3/2}\left(\frac{\hbar}{mv}\right)^2\left[\sum_{i' \neq f} \mathbf{R}^2_{ii'}[A_{ii'}(z_{ii'}) - i\epsilon_{ii'}B_{ii'}(\tilde{z}_{ii'})] + \sum_{f' \neq i} \mathbf{R}^2_{ff'}[A_{ff'}(z_{ff'}) + i\epsilon_{ff'}B_{ff'}(\tilde{z}_{ff'})]\right.$$

$$\left. + \frac{3Ry\bar{f}}{|E_i - E_f|}\left(1 + \frac{2l_f+1}{2l_i+1}\right)[A_{if}(z_{if}) - iB_{if}(\tilde{z}_{if})]\right],$$

where $a_{jj'}$, $b_{jj'}$, $A_{jj'}$ and $B_{jj'}$ are the GBKO[3,8] Stark-broadening functions of the arguments $z_{jj'}$ and $\tilde{z}_{jj'}$,

$$z_{jj'} = \rho(E_j - E_{j'})/\hbar v, \qquad \tilde{z}_{jj'} = 0.75\, z_{jj'},$$

and ρ is the impact parameter; in the expression for $z^{\min}_{jj'}$, $\rho_{\min}$ is used instead of ρ.

The necessary coordinate-operator matrix elements have been calculated by using the Coulomb approximation.[9,10] For atomic states with equivalent electrons, the corresponding coefficients of fractional parentage[11] are included. Data for atomic energy levels were taken from Moore[12] and Kaufman and Edlén.[13] The completeness of a particular set of perturbing energy levels with respect to the sums of dipole matrix elements $\mathbf{R}^2_{jj'}$ is tested by means of the parameter $\Delta S/S$ as defined by Jones *et al.*:[7]

$$\frac{\Delta S}{S} = \left[\sum_{i' \neq f} \mathbf{R}^2_{ii'} + \sum_{f' \neq i} \mathbf{R}^2_{ff'} + \frac{3Ry\bar{f}}{|E - E_f|}\left(1 + \frac{2l_f+1}{2l_i+1}\right) - R^2_{ii} - R^2_{ff}\right] \Big/ (R^2_{ii} + R^2_{ff}),$$

where

$$R_{jj}^2 = \frac{n_j^{*2}}{2}[5n_j^{*2} + 1 - 3l_j(l_j + 1)]$$

and n_j^* is the corresponding effective principal quantum number. For a complete set of perturbers, $\Delta S/S = 0$.

Calculated Stark broadening parameters for elements heavier than calcium are given in Table 1 for 4 electron temperatures and for an electron density of $10^{17}\,\mathrm{cm}^{-3}$. It should be noted that theoretical calculations were performed only for the lines to which LS-coupling approximation could be applied.

3. ANALYSIS OF EXPERIMENTAL DATA AND COMPARISONS

The starting point for the search for experimental papers available as of 1976 was Ref. 4. For the period 1976–78, Ref. 14 was used. For the same period, and from 1978 through the end of 1981, the authors of this article made a thorough search of the literature for additional experimental work on the Stark broadening of neutral-atom lines. Not all experiments are included in the final results. The criteria imposed were as follows: (a) an

Table 1. Calculated Stark-broadening parameters in Å at $10^{17}\,\mathrm{cm}^{-3}$ vs electron temperature. The letter W denotes full halfwidths, and d denotes the shift. The parameter W_S/W is the ratio of the strong collision term to the total width; the ion-broadening parameter α, which scales[3] as $N_e^{1/4}$, is a measure of the quasistatic broadening by ions. Also shown is the Gaunt factor g which, when used in the averaged version of the semi-empirical method,[1] would result in the width; $kT/\Delta E$ is the ratio of the thermal energy at $T = 10^4$K to the energy separation from the nearest perturbing level, and $\Delta S/S$ is a measure of the failure to satisfy the sum rules for the squares of the dipole matrix elements (S is the sum of the squares of these elements).

Element	Transition	T(k)	W(Å)	d(Å)	α	W_S/W	g
Br I	$5s^4P$-$6p^4D^o$	5000	1.102	0.453	0.100	0.79	0.05
	λ = 4677 Å	10000	1.192	0.492	0.094	0.66	0.08
	ΔS/S = -0.63	20000	1.372	0.497	0.085	0.54	0.12
	kT/ΔE= 2.61	40000	1.558	0.451	0.077	0.45	0.20
Cd I	$5p^3P^o$-$6s^3S$	5000	0.514	0.233	0.077	0.96	0.08
	λ = 4941 Å	10000	0.534	0.271	0.075	0.85	0.12
	ΔS/S = -0.14	20000	0.616	0.302	0.067	0.71	0.20
	kT/ΔE = 0.98	40000	0.724	0.304	0.060	0.59	0.33
Cd I	$5p^3P^o$-$5d^3D$	5000	0.796	-0.222	0.12	0.56	0.17
	λ = 3539 Å	10000	0.838	-0.161	0.11	0.47	0.26
	ΔS/S = -0.12	20000	0.892	-0.0915	0.11	0.41	0.39
	kT/ΔE = 7.28	40000	0.926	-0.0350	0.11	0.37	0.57
Ge I	$4p^1S$-$5s^1P^o$	5000	0.388	0.178	0.077	0.94	0.11
	λ = 4228 Å	10000	0.408	0.205	0.074	0.81	0.16
	ΔS/S = -0.06	20000	0.468	0.222	0.067	0.66	0.26
	kT/ΔE = 1.16	40000	0.540	0.216	0.060	0.54	0.43
Hg I	$6p^3P^o$-$7s^3S$	5000	0.402	-0.192	0.072	0.96	0.07
	λ = 4864 Å	10000	0.420	-0.224	0.069	0.87	0.11
	ΔS/S = -0.25	20000	0.486	-0.251	0.062	0.73	0.17
	kT/ΔE = 0.34	40000	0.574	-0.258	0.055	0.61	0.29
Pb I	$6p^2\ ^3P$-$7s^3P^o$	5000	0.218	0.101	0.074	0.96	0.09
	λ = 3748 Å	10000	0.230	0.117	0.071	0.85	0.13
	ΔS/S = -0.05	20000	0.270	0.129	0.063	0.71	0.21
	kT/ΔE = 0.86	40000	0.320	0.128	0.056	0.59	0.35

Table 1. (*Contd*).

Element	Transition	T(k)	W(Å)	d(Å)	α	W_S/W	g
Rb I	$5s^2S$-$5p^2P^o$	5000	0.906	0.374	0.11	0.88	0.06
	λ = 7852 Å	10000	1.110	0.393	0.092	0.77	0.10
	ΔS/S = -0.02	20000	1.438	0.388	0.076	0.65	0.18
	kT/ΔE = 1.05	40000	1.816	0.343	0.064	0.56	0.32
Sn I	$5p^2\ ^1S$-$6s\ ^1P^o$	5000	0.382	0.184	0.086	0.96	0.07
	λ = 4526 Å	10000	0.412	0.210	0.081	0.85	0.10
	ΔS/S = -0.08	20000	0.492	0.230	0.071	0.72	0.17
	kT/ΔE = 0.95	40000	0.594	0.228	0.062	0.60	0.30
Zn I	$4p^3P^o$-$5s^3S$	5000	0.408	0.195	0.076	0.96	0.08
	λ = 4767 Å	10000	0.432	0.226	0.073	0.85	0.12
	ΔS/S = -0.14	20000	0.502	0.251	0.065	0.72	0.19
	kT/ΔE = 0.91	40000	0.596	0.253	0.057	0.59	0.32
Zn I	$4p^3P^o$-$4d^3D$	5000	0.520	-0.137	0.12	0.63	0.13
	λ = 3325 Å	10000	0.582	-0.0999	0.11	0.53	0.20
	ΔS/S = -0.12	20000	0.662	-0.0548	0.097	0.45	0.33
	kT/ΔE = 4.72	40000	0.726	-0.0163	0.091	0.40	0.51
Zn I	$4p^3P^o$-$6s^3S$	5000	0.812	0.367	0.16	0.91	0.09
	λ = 3055 Å	10000	0.920	0.404	0.15	0.76	0.15
	ΔS/S = -0.04	20000	1.122	0.420	0.13	0.62	0.26
	kT/ΔE = 2.61	40000	1.338	0.396	0.11	0.51	0.44
Zn I	$4p^3P^o$-$5d^3D$	5000	3.96	0.364	0.24	0.47	0.35
	λ = 2787 Å	10000	4.04	0.288	0.24	0.38	0.51
	ΔS/S = -0.08	20000	4.08	0.230	0.24	0.32	0.73
	kT/ΔE = 27.46	40000	3.96	0.191	0.24	0.29	0.99

independent and accurate determination of plasma electron density; (b) a reasonably accurate determination of the plasma temperature; (c) a discussion of other, interfering broadening mechanisms and appropriate experimental problems. Detailed discussions on these selection criteria are given elsewhere.[4,15]

Selected experimental results for the Stark width w_m and shift d_m are given in Table 2, where they are also compared with theoretical results (w_m/w_{th} and d_m/d_{th}). Table 2 also shows the experimental conditions (electron density and temperature). In the first three columns, the transitions are spectroscopically identified by quantum numbers and multiplet designations and by their wavelengths.

Even a brief survey of results given in Table 2 reveals very poor agreement between the semiclassical theory and experiments. Rubidium resonance lines are the only exception. This result is in contradiction to the findings for lighter elements.[3,4]

In order to explain for this discrepancy, we have critically evaluated the experimental data. For this purpose, the most comprehensive results (see Table 2) for Cd(I) and Zn(I) have been used and are given in Table 3 in angular-frequency units. In addition, Table 3 shows line strengths S (in atomic units) of multiplet components.

The comparisons of Cd(I) and Zn(I) Stark linewidths within multiplets indicate that, for the same experimental conditions, there were large width variations. These may be caused by improper treatment of self-absorption,[4,15] especially for stronger lines (see, the S-values in Table 3). The weaker lines, which are least affected by this effect, exhibit smaller widths. According to the present theories on Stark broadening, widths of lines within a multiplet should be practically identical. They interact with the same set of perturbing levels; the energies of different upper (or, alternatively, of different lower) levels are nearly the same. Also the radial integrals for the interacting states are, for all practical

purposes, the same for the entire multiplet. These general assumptions of Stark-broadening theory in relation to isolated lines of neutral, singly- and multiply-ionized atoms have been confirmed previously.[4,15] Rare exceptions to this rule may be multiplets with large energy-level separations in comparison to the nearest perturbing level.[25] Since this exception does not apply to the particular Cd(I) and Zn(I) multiplets tabulated here, one would expect similar linewidths within these multiplets.

The analysis of experimental data in Table 3 can be performed from the point of view of similarities and systematic trends of spectral linewidths.[25,26] This subject has recently been investigated in detail.[26] General considerations of atomic energy structure showed that, for lines belonging to spectral series, one should expect a gradual increase in the Stark widths with increasing principal quantum number of the upper state, since the density of levels and thus the number of significant perturbers increases with principal quantum number. This result was convincingly proved experimentally for Cs(I) and He(I) lines.[26] Such behavior of the linewidths should also be expected for the first two members of the $4p$–ns and $4p$–nd series in Zn(I). This fact is also illustrated in Fig. 1 by means of an energy-level scheme. It is obvious that, in both cases ($4p$–ns and $4p$–nd series), the nearest perturbing levels are closer to the upper energy level of the higher-lying, as compared to that of the lower-lying, of the two lowest members of the series. Therefore, the linewidth should increase. This behavior is consistent with the theoretical results, while the experiments[23] on the $4p$–ns series gives linewidths which are almost identical for the two lowest series members. The results for $4p$–nd increase for a higher member, but the difference is smaller than expected.

For Cd(I), an energy-level diagram (Fig. 2) can be used to illustrate that the linewidth of the $^3P^0$–^3D multiplet should be greater than that of $^3P^0$–^3S (see Table 3). The position of the nearest perturbing level is so much closer to the upper level of the former transition that one must expect larger linewidths for the $^3P^0$–^3D multiplet. This result has not been found experimentally (see Table 3), which means that the experiments should be repeated and the linewidths measured under optically thin conditions and with a homogeneous plasma source.

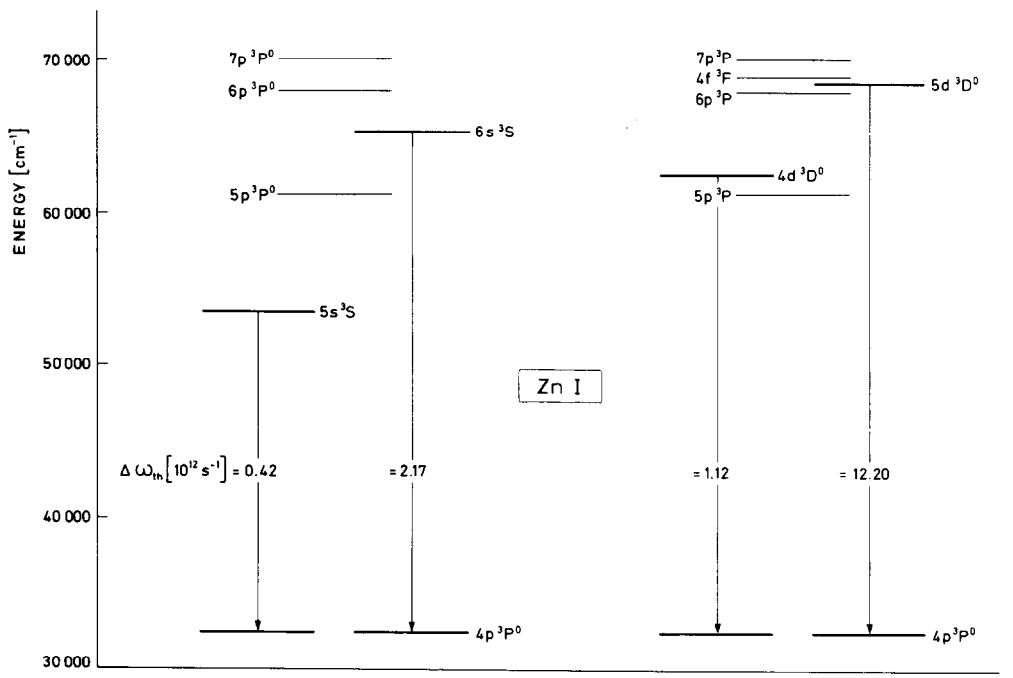

Fig. 1. Energy-level positions for two consecutive members of the $4p$–ns and $4p$–nd series of Zn(I). Theoretical results, expressed in frequency units, are also given.

Table 2. Comparison of measured and calculated linewidths and shifts of neutral-atom lines. Experimental results for the Stark widths and shifts are designated by w_m and d_m, respectively, while the ratios of measured-to-theoretical widths and shifts are given under w_m/w_{th} and d_m/d_{th}.

Element	Transition array	Multiplet (No.)	Wavelength (Å)	Temperature (K)	Electron density (cm^{-3})	w_m(Å)	w_m/w_{th}	d_m(Å)	d_m/d_{th}	Ref.
Br I	$4p^4 5s$-$4p^4(^3P_2)6p$	^4P-$^4D^o$	4525.59	11000	1.0×10^{17}	9.9	7.51			a
			4441.74	11000	1.0×10^{17}	10.4	7.89			a
Cd I	$4d^{10}5s5p$-$4d^{10}5s(^2S)6s$	$^3P^o$-^3S (2)	5085.82	11100	1.0×10^{17}	3.67	6.34			b
			4799.91	11100	1.0×10^{17}	3.84	6.63			b
			4678.15	11100	1.0×10^{17}	1.74	3.00			b
	$4d^{10}5s5p$-$4d^{10}5s(^2S)5d$	$^3P^o$-^3D	3610.51	11100	1.0×10^{17}	1.84	1.97			b
			3466.20	11100	1.0×10^{17}	1.63	1.74			b
			3403.65	11100	1.0×10^{17}	0.94	1.01			b
Ge I	$4s^2 4p^2$-$4s^2 4p(^2P^o)5s$	^1S-$^1P^o$	4226.56	11100	1.0×10^{17}	3.18	7.20			c
Hg I	$5d^{10}6s6p$-$5d^{10}6s(^2S)7s$	$^3P^o$-^3S	5460.74	6000	1.0×10^{16}	0.303	5.68			d
Pb I	$6s^2 6p^2$-$6s^2 6p(^2P^o)7s$	^3P-$^3P^o$ (1)	4057.81	11600	1.0×10^{17}	0.62	2.07			e
Rb I	5s-5p	^2S-$^2P^o$ (1)	7947.60	15000-26000	1.0×10^{17}	1.82-2.20	1.28-1.28	0.55-0.45	1.20-0.99	f
			7800.27	15000-26000	1.0×10^{17}	1.66-1.92	1.18-1.12	0.52-0.51	1.14-1.12	f
Sn I	$5s^2 5p^2$-$5s^2 5p(^2P)6s$	^1S-$^1P^o$	4524.74	11600	1.0×10^{17}	1.3	2.94			g

Zn I	$3d^{10}4s4p$- $3d^{10}4s(^2S)5s$	$^3P^o$-^3S (2)	4810.53	11000	1.0×10^{17}	1.65	3.25			h
				11000	4.5×10^{17}	0.92	0.40			i
			4722.16	11000	1.0×10^{17}	1.57	3.09			h
				11000	4.5×10^{17}	1.20	0.52			i
			4680.14	11000	1.0×10^{17}	0.84	1.66			h
				11000	4.5×10^{17}	1.29	0.56			i
	$3d^{10}4s4p$- $3d^{10}4s(^2S)4d$	$^3P^o$-^3D (4)	3345.02	11000	1.0×10^{17}	1.74	2.66			h
			3302.58	11000	1.0×10^{17}	1.40	2.14			h
			3282.33	11000	1.0×10^{17}	0.91	1.39			h
	$3d^{10}4s4p$- $3d^{10}4s(^2S)6s$	$^3P^o$-^3S (5)	3072.06	11000	1.0×10^{17}	0.70	0.65			h
			3035.78	11000	1.0×10^{17}	0.61	0.57			h
			3018.36	11000	1.0×10^{17}	0.56	0.52			h
	$3d^{10}4s4p$- $3d^{10}4s(^2S)5d$	$^3P^o$-^3D (5UV)	2800.9*	11000	1.0×10^{17}	1.96	0.39			h
			2770.9*	11000	1.0×10^{17}	2.49	0.50			h
			2756.45	11000	1.0×10^{17}	1.27	0.25			h

*Blended within multiplet

References: a-16, b-17, c-18, d-19, e-20, f-21, g-22, h-23 and i-24

Table 3. Comparison of measured and theoretical linewidths, in angular-frequency units. The line strengths S (in atomic units) were derived from transition probabilities: Cd(I), from Ref. 27, Zn(I), from Ref. 28.

Element	Multiplet (No)	Wavelength (Å)	Temperature (K)	Electron density cm^{-3}	ω_m ($10^{12}s^{-1}$)	ω_{th} ($10^{12}s^{-1}$)	S (at.u)	Ref.
Cd I	$^3P^o$-^3S (2)	5085.8	11100	1.0×10^{17}	2.67	0.45	10.9	b
		4799.9	11100	1.0×10^{17}	3.14	0.45	6.7	b
		4678.2	11100	1.0×10^{17}	1.49	0.45	2.0	b
	$^3P^o$-^3D	3610.5	11100	1.0×10^{17}	2.66	1.41	21.1	b
		3466.2	11100	1.0×10^{17}	2.56	1.41	12.3	b
		3403.6	11100	1.0×10^{17}	1.52	1.41	4.5	b
Zn I	$^3P^o$-^3S (2)	4810.5	11000	1.0×10^{17}	1.34	0.42	8.9	h
		4722.2	11000	1.0×10^{17}	1.33	0.42	5.1	h
		4680.1	11000	1.0×10^{17}	0.72	0.42	1.7	h
		4810.5	11000	4.5×10^{17}	0.75	1.90	8.9	i
		4722.2	11000	4.5×10^{17}	1.01	1.90	5.1	i
		4680.1	11000	4.5×10^{17}	1.11	1.90	1.7	i
	$^3P^o$-^3D (4)	3345.0	11000	1.0×10^{17}	2.93	1.12	18.9	h
		3302.6	11000	1.0×10^{17}	2.42	1.12	9.9	h
		3282.3	11000	1.0×10^{17}	1.59	1.12	4.3	h
	$^3P^o$-^3S (5)	3072.2	11000	1.0×10^{17}	1.40	2.17		h
		3035.8	11000	1.0×10^{17}	1.25	2.17		h
		3018.4	11000	1.0×10^{17}	1.16	2.17		h
	$^3P^o$-^3D (5UV)	2800.9	11000	1.0×10^{17}	4.71	12.20	4.6	h
		2770.9	11000	1.0×10^{17}	6.11	12.20	2.4	h
		2756.5	11000	1.0×10^{17}	3.15	12.20	1.1	h

References: b-17, h-23 and i-24

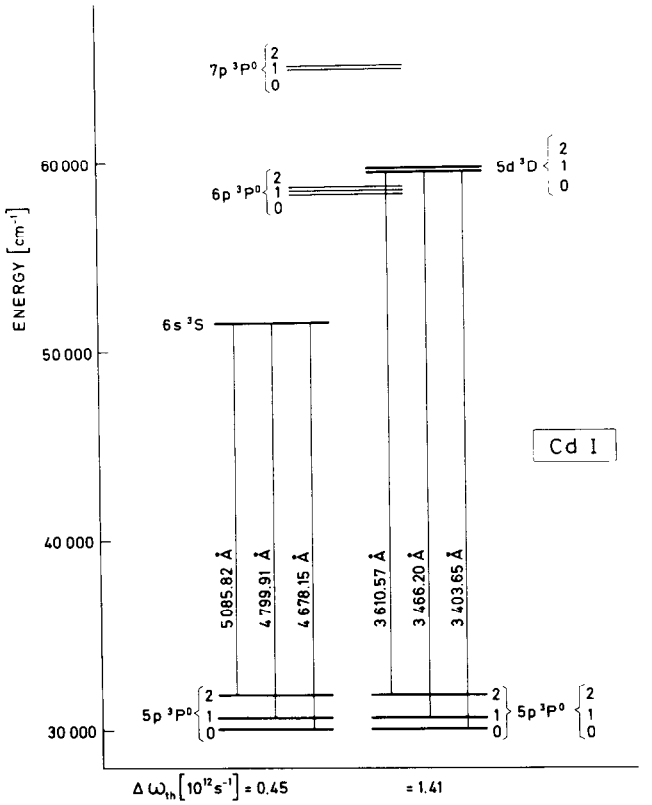

Fig. 2. Energy-level positions of two Cd(I) multiplets. Theoretical results, expressed in frequency units, are also given.

Unfortunately, a similar analysis of experimental results for Br(I), Ge(I), Hg(I), Pb(I) and Sn(I) could not be performed since only a few lines were measured (see Table 1). It is characteristic of most of these data (Br(I), Ge(I), Pb(I), and Sn(I)) that the estimated accuracies are low, usually around $\pm$ 50% or even lower.[4,16,18,20,22] Apart from the Cd(I) multiplet $^3P^0$–^3S, for Br(I), Ge(I), and Hg(I) there are exceptionally large deviations from the theory (see Table 2). For Br(I), a number of perturbing energy levels necessary for Stark-width calculations are missing from the available data tables (see the factor $\Delta S/S$ in Table 1). However, the incompleteness of perturbing levels can be used to explain only a part of the large discrepancies between theory and experiment. In the Hg(I) experiment,[19] the light source was a cylindrical quartz lamp filled with mercury. Since the 5460.7 Å line was optically thick under these experimental conditions, the Stark-broadening constant C_4 was determined by fitting the experimental profiles and comparing their absolute intensities with theoretical values. From the best fits, the authors determined the transition probability and the value of C_4. Since in this paper there was not attempted to estimate the accuracy of the reported data, and since the contributions of van der Waals broadening were considerable (these are claimed to be 20% of the Stark-broadening contribution) and were difficult to estimate because of uncertainty in the value of C_6, the results for the Hg(I) 5460.7 Å line is of low accuracy.

Acknowledgement—The authors gratefully acknowledge the interest of Dr. W. L. Wiese in this work.

REFERENCES

1. H. R. Griem, *Phys. Rev.* **128**, 515 (1962).
2. H. R. Griem, *Palsma Spectroscopy*. McGraw-Hill, New York (1964).
3. H. R. Griem, *Spectral Line Broadening by Plasmas*. Academic Press, New York (1974).
4. N. Konjević and J. R. Roberts, *J. Phys. Chem. Ref. Data* **5**, 209 (1976).
5. S. Sahal-Bréchot, *Astron. Astrophys.* **1**, 91 (1969) and **2**, 322 (1969).

6. S. M. Benett and H. R. Griem, "Calculated Stark Broadening Parameters for Isolated Spectral Lines from the Atoms Helium through Calcium and Cesium", University of Maryland Report No. 71–097, College Park, Maryland (1971).
7. W. W. Jones, S. M. Benett, and H. R. Griem, "Calculated Electron Impact Broadening Parameters for Isolated Spectral Lines from the Singly Charged Ions Lithium through Calcium", University of Maryland Report No. 71–178, College Park, Maryland (1971).
8. H. R. Griem, M. Baranger, A. C. Kolb, and G. K. Oertel, *Phys. Rev.* **125**, 177 (1962).
9. D. R. Bates and A. Damgaard, *Phil. Trans. Roy. Soc. London, Ser. A* **242**, 101 (1949).
10. G. K. Oertel and L. P. Shomo, *Astrophys. J. Suppl. Ser.* **16**, 175 (1968).
11. B. W. Shore and D. H. Menzel, *Astrophys. J. Suppl. Ser.* **12**, 187 (1965)
12. C. E. Moore, *Atomic Energy Levels*, Circular 467, Nat. Bur. Stand., Vols. I–III. U.S. Government Printing Office, Washington, D.C. (1971).
13. V. Kaufman and B. Edlén, *J. Phys. Chem. Ref. Data* **3**, 825 (1974).
14. J. R. Fuhr, B. J. Miller, and G. A. Martin, *Bibliography on Atomic Line Shapes and Shifts* (*June* 1975–*June* 1978), Nat. Bur. Stand. (U.S.), Spec. Publ. 366, Suppl. 3. U.S. Government Printing Office, Washington, D.C. (1978).
15. N. Konjević and W. L. Wiese, *J. Phys. Chem. Ref. Data* **5**, 259 (1976).
16. R. D. Bengtson, University of Maryland Technical Note BN-559. College Park, Maryland (1968).
17. H. J. Kusch and E. Oberschelp, *Z. Astrophys.* **67**, 85 (1967).
18. W. W. Jones and M. H. Miller, *Phys. Rev. A* **10**, 1803 (1974).
19. J. J. Damelincourt, D. Karabourniotis, L. Scoarnec, and P. Herbert, *Proc. 13th Int. Conf. Phen. Ionized Gases*, Part I, p. 127. Phys. Soc. of GDR, Berlin (1977).
20. M. H. Miller, R. D. Bengtson, and J. M. Lindsay, *Phys. Rev. A* **20**, 1997 (1979).
21. J. Purić, J. Labat, Lj. Ćirković, I. Lakićević, and S. Djeniže, *J. Phys. B* **10**, 2375 (1977).
22. M. H. Miller, R. A. Roig, and R. D. Bengtson, *Phys. Rev. A* **20**, 499 (1979).
23. H. J. Kusch and E. Oberschelp, *Z. Astrophys.* **67**, 77 (1967).
24. I. S. Fishman, P. S. Semin, and G. A. Desyatnik, *Opt. Spectrosc.* **47**, 245 (1979).
25. N. Konjević and M. S. Dimitrijević, In *Spectral Line Shapes* (Edited by B. Wende), p. 241. W. de Gruyter, Berlin (1981).
26. W. L. Wiese and N. Konjević, *JQSRT* **28**, 185 (1982).
27. J. Reader, C. H. Corliss, W. L. Wiese, and G. A. Martin, *Wavelengths and Transition Probabilities for Atoms and Atomic Ions*, NSRDS-NBS 68. U.S. Government Printing Office, Washington, D.C. (1980).
28. A. A. Antena and V. S. Zilitis, *Opt. Spectrosc.* **26**, 79 (1969).

J. Quant. Spectrosc. Radiat. Transfer Vol. 31, No. 4, pp. 301–313, 1984
Printed in Great Britain.

0022–4073/84 $3.00 + .00

STARK BROADENING OF NEUTRAL HELIUM LINES

M. S. DIMITRIJEVIĆ† and S. SAHAL-BRÉCHOT
Observatoire de Paris, 92190 Meudon, France

(*Received* 25 *March* 1983)

Abstract—Using a semiclassical approach for the Stark broadening of atomic lines, we have calculated electron and proton impact line widths and shifts of 56 neutral He lines in the ultraviolet, visible and i.r. region of the spectrum. The comprehensive set of results obtained is used for investigation of Stark-broadening parameter regularities within the spectral series.

1. INTRODUCTION

Reliable Stark-broadening data for He lines (the most abundant element after H in the universe) are of particular interest for a large number of problems in the spectroscopy of laboratory as well as astrophysical plasmas. Since He is a simple atomic system and since many experimental Stark-broadening data are available for He lines,[1,2] these data provide an opportunity to test approximations included in the semiclassical-perturbation formalism. Using this formalism,[3,4] we have calculated electron and proton impact line widths and shifts of 56 neutral He lines in the ultraviolet, visible and i.r. regions of the spectrum. In addition to the proton-impact broadening data (which are useful in investigations of astrophysical plasmas), we have also used a semiclassical approach,[3,4] which differs in several respects from the other large scale calculations of neutral He lines.[5,6] The semiclassical–perturbation formalism with convenient approximations to determine the effects of strong collisions,[7] has been developed by Griem and collaborators[7] and has been adopted by many authors.[8] This first paper on the subject[7] contains numerical results for 24 He(I) lines which are not greatly different from more recent calculations.[8]

The results have also been used to investigate Stark-broadening regularities within spectral series. From general considerations of atomic energy structure, it has been shown[9] that, for lines belonging to a spectral series, one should expect a gradual increase in the Stark widths with increasing principal quantum number of the upper state. This result has been convincingly proved experimentally for some Cs(I) and He(I) lines.[9] On the basis of our comprehensive results, we have attempted to find out if systematic trends among Stark-broadening parameters within a spectral series are apparent. If this is the case, accurate interpolations and critical evaluations of experimental results became feasible.

2. THEORY

The basis for calculations is the computer code which evaluates electron and ion impact-broadening parameters of isolated spectral lines, using the semiclassical perturbation approach.[3] The formulae which lead to the full halfwidth ($2W$) and the shift (d) are

$$2W = N\int_0^\infty vf(v)\,\mathrm{d}v\left(\sum_{j\neq i}\sigma_{ij}(v) + \sum_{j'\neq f}\sigma_{jj'}(v) + \sigma_{\mathrm{el}}\right), \tag{1}$$

$$d = \int_0^\infty vf(v)\,\mathrm{d}v\int_{R_3}^{R_d} 2\pi\rho\,\mathrm{d}\rho\,\sin 2\phi_p. \tag{2}$$

The inelastic cross section $\sigma_{ij}(v)$ can be expressed by an integration over the impact parameter of the transition probability P_{ij} as

$$\sum_{j\neq i}\sigma_{ij}(v) = \frac{1}{2}\pi R_1^2 + \int_{R_1}^{R_d} 2\pi\rho\,\mathrm{d}\rho\sum_{j\neq i}P_{ij}(\rho, v); \tag{3}$$

†Present address: Institute of Physics, P.O. Box 57, 11001 Beograd, Yugoslavia.

the elastic cross section is

$$\sigma_{el} = 2\pi R_2^2 + \int_{R_2}^{R_d} 8\pi\rho \, d\rho \, \sin^2 \delta, \tag{4}$$

$$\delta = (\phi_p^2 + \phi_q^2)^{1/2}, \tag{5}$$

$$\phi_p = \sum_{j \neq i} \phi_{ij} - \sum_{j' \neq f} \phi_{ff'}.$$

Here, i and f denote, respectively, the initial and final levels and j, j' the corresponding perturbing levels. The phase shifts ϕ_p and ϕ_q, due respectively to the polarisation ($\sim r^{-4}$) and to the quadrupole potential ($\sim r^{-3}$), are given in Ref. 3 (Section 3, Chap. 2).

All of the cut-offs (R_1, R_2, R_3), as well as the symetrization procedures in the inelastic cross sections, are described in Ref. 4 (Section 1, Chap. 3). We recall here that we allow for Debye shielding by introducing the Debye cut-off R_d as an upper cut-off in the integration procedure.

It is not necessary to discuss uncertainties arising from all of the approximations involved in our calculations, since the criteria for their application are given in detail elsewhere.[3] We recall however, the conditions of validity for the isolated line approximation. A line is isolated if nondegenerate energy levels broadened by collisions do not overlap. Denoting by $2W_i$ and $2W_f$ the corresponding level widths, we can express the specified conditions by

$$2W_i \leq \omega_{ii'}, \qquad 2W_f \leq \omega_{ff'}, \tag{6}$$

where $\omega_{jj'}(j = i, f)$ is the distance to the corresponding nearest perturbing level. If $W \leq \omega_{jj'}$, where W is the halfwidth of the line and $\omega_{jj'}$ is the energy distance to the nearest perturbing level [$\omega_{jj'} = \min(\omega_{ii'}, \omega_{ff'})$], then the line is isolated. It is easy to show from Eq. (6) that $2W(\mathring{A}) \lesssim C/10^{16}$,

$$C = 10^8 \lambda^2(\mathring{A})[(E_j - E_f)(\text{cm}^{-1})], \tag{7}$$

if we want to make certain that the line is isolated. If halfwidths are available for the electron concentration $N = 10^{16}\,\text{cm}^{-3}$,

$$N_l(\text{cm}^{-3}) = C/2W(\text{in Å at } N = 10^{16}\,\text{cm}^{-3}). \tag{8}$$

For an electron concentration lower than N_l, the line can be treated as isolated in the core, even if weak forbidden components due to the failure of this approximation still appear in the wings.

Estimations of the validity conditions[3] show that the impact approximation may be applied for protons in stellar atmospheres ($N \lesssim 10^{15}\,\text{cm}^{-3}$). In most laboratory experiments, protons are not the dominant ion perturbers. In that cases, or when the impact approximation is not valid, the ion broadening contribution may be estimated by using the quasistatic ion-broadening parameter[8] introduced by Griem *et al.*[7]

3. RESULTS

Data for needed energy levels were taken from Ref. 10. The calculated values are divided in three parts. Our results for electron (W_e) and proton (W_p) impact full halfwidths and shifts (d_e and d_p respectively) for He(I) resonance lines (which lie in the far ultraviolet) are shown in Table 1 for $N_e = 10^{16}\,\text{cm}^{-3}$ and T = 10,000, 20,000, 40,000, 100,000, 150,000, and 200,000 K. Because of the impact approximation and the isolated-line approximation, the impact widths and shifts show linear behavior in N_e if Debye shielding effects are negligible. An interpolation is necessary to obtain values for temperatures not listed in the table.

The results for lines between 2500 and 7000 Å are shown in Table 2 for a number of

Table 1. This table lists Stark-broadening parameters for He(I) resonance lines at an electron density of 10^{16} cm^{-3} and temperatures from 10,000 K to 200,000 K. Transitions and averaged wavelengths for the multiplet (in Å) are also given. Under $2W_e$ and $2W_p$ are given electron and proton impact full halfwidths, while d_e and d_p denote corresponding shifts. If we devide C by $2W_e$, we obtain an estimate for the maximum electron density for which the line may be treated as isolated and the tabulated values may be used. Asteriks denote cases when the frequency distance between the upper level and the nearest perturbing level is smaller than or equal to the electron plasma frequency. For these lines the behaviour of N_e deviates from linear (especially for the shift); for another electron density, the influence of Debye shielding must be taken into account (see, e.g., Ref. 8, Appendix IVa)

Transition	T[K]	$2W_e$[Å]	d_e[Å]	$2W_p$[Å]	d_p[Å]
$1s^2{}^1S$-$2p{}^1P^o$	10000	0.326-3	0.113-4	0.966-4	-0.204-4
584.334Å	20000	0.353-3	0.482-4	0.970-4	-0.232-4
C = 1.7+17	40000	0.373-3	0.808-4	0.974-4	-0.263-4
	100000	0.399-3	0.933-4	0.962-4	-0.301-4
	150000	0.408-3	0.799-4	0.939-4	-0.311-4
	200000	0.409-3	0.721-4	0.914-4	-0.316-4
$1s^2{}^1S$-$3p{}^1P^o$	10000	0.668-2	-0.181-2	0.239-2	-0.168-2
537.030 Å	20000	0.629-2	-0.125-2	0.270-2	-0.225-2
C = 3.0+15	40000	0.577-2	-0.830-3	0.308-2	-0.263-2
	100000	0.501-2	-0.475-3	0.367-2	-0.323-2
	150000	0.465-2	-0.372-3	0.388-2	-0.356-2
	200000	0.438-2	-0.310-3	0.395-2	-0.381-2
$1s^2{}^1S$-$4p{}^1P^o$	10000	0.256-1	-0.585-2	0.101-1	-0.637-2
522.213 Å	20000	0.241-1	-0.421-2	0.115-1	-0.846-2
C = 1.3+15	40000	0.220-1	-0.293-2	0.132-1	-0.104-1
	100000	0.189-1	-0.179-2	0.157-1	-0.134-1
	150000	0.174-1	-0.143-2	0.165-1	-0.149-1
	200000	0.163-1	-0.122-2	0.167-1	-0.160-1
$1s^2{}^1S$-$5p{}^1P^o$ *	10000	0.632-1	-0.117-1	0.286-1	-0.119-1
516.617 Å	20000	0.610-1	-0.881-2	0.336-1	-0.200-1
C = 6.5+14	40000	0.563-1	-0.611-2	0.388-1	-0.273-1
	100000	0.487-1	-0.374-2	0.458-1	-0.373-1
	150000	0.449-1	-0.300-2	0.475-1	-0.423-1
	200000	0.420-1	-0.258-2	0.476-1	-0.457-1
$1s^2{}^1S$-$6p{}^1P^o$ *	10000	0.124	-0.139-1	0.589-1	-0.944-2
512.098 Å	20000	0.124	-0.747-2	0.782-1	-0.326-1
C = 3.7+14	40000	0.118	-0.247-2	0.928-1	-0.548-1
	100000	0.104	0.537-3	0.109	-0.835-1
	150000	0.974-1	0.914-3	0.111	-0.966-1
	200000	0.924-1	0.108-2	0.109	-0.105
$1s^2{}^1S$-$7p{}^1P^o$ *	10000	0.496	0.194	0.713-1	-0.413-2
509.998 Å	20000	0.577	0.259	0.106	-0.344-1
C = 2.3+14	40000	0.661	0.328	0.130	-0.694-1
	100000	0.777	0.432	0.129	-0.113
	150000	0.814	0.479	0.123	-0.111
	200000	0.830	0.506	0.125	-0.109

temperatures, while the results for lines with $\lambda > 7000$ Å are presented in Table 3 for $T = 2500$, 5000, 10,000, 20,000, 40,000, and 80,000 K. In Tables 1–3, we also give a parameter denoted by C [see Eq. (7)], which can be used to determine if a line is isolated for the needed electron density. For the He(I) 5016 Å line, we compare our results with different experimental determinations of the Stark widths.[2,11–20] This comparison is presented in Table 4. We see that the averaged disagreement between our results and experimental values is 30% (12% if Refs. 17 and 19 are disregarded).

In Figs. 1–3, our results for the $\lambda = 10830$ Å and $\lambda = 7281$ Å *He(I)* lines are compared with available theoretical[5,6,21] and experimental[2] data. From these results, it appears that agreement between our calculations and experimental data is quite good. However various sets of theoretical assumptions will, in the semiclassical method, result in slightly different temperature trends. High-precision measurements for the high and low temperature limits are needed in order to clarify applicability of various procedures within the semiclassical approach.

We also note that, in several cases, the inclusion of Debye shielding affects the shift calculations significantly. For example, for the 10996.6 Å line, we obtain $d = 0.303$ Å at

Table 2. Same as in Table 1 but for the He(I) lines in the range $2500 \leq \lambda, \text{Å} \leq 7000$ and for temperatures from 5000 to 80,000 K

Transition	T[K]	$2w_e$[Å]	d_e[Å]	$2w_p$[Å]	d_p[Å]
$2s^1S-3p^1P^o$	5000	0.627	-0.236	0.187	-0.131
5015.68 Å	10000	0.597	-0.179	0.210	-0.164
C = 2.6+17	20000	0.568	-0.132	0.237	-0.197
	30000	0.549	-0.110	0.255	-0.216
	40000	0.532	-0.950-1	0.270	-0.231
	80000	0.487	-0.666-1	0.310	-0.269
$2s^1S-4p^1P^o$	5000	1.54	-0.459	0.507	-0.232
3964.73 Å	10000	1.48	-0.345	0.585	-0.367
C = 7.3+16	20000	1.40	-0.249	0.665	-0.488
	30000	1.34	-0.208	0.719	-0.555
	40000	1.29	-0.179	0.762	-0.602
	80000	1.16	-0.126	0.872	-0.727
$2s^1S-5p^1P^o$ *	5000	3.07	-0.757	1.05	-0.161
3613.64 Å	10000	3.10	-0.574	1.40	-0.583
C = 3.2+16	20000	3.00	-0.432	1.64	-0.978
	30000	2.87	-0.354	1.79	-1.19
	40000	2.77	-0.306	1.90	-1.33
	80000	2.50	-0.211	2.17	-1.70
$2s^1S-6p^1P^o$ *	5000	5.09	-0.881	1.66	-0.140-3
3447.59 Å	10000	5.63	-0.627	2.67	-0.428
C = 1.7+16	20000	5.64	-0.335	3.54	-1.48
	30000	5.49	-0.189	3.94	-2.07
	40000	5.34	-0.109	4.21	-2.48
	80000	4.89	0.708-2	4.79	-3.46
$2s^1S-7p^1P^o$ *	5000	28.8	7.32	1.20	0.402-3
3354.55 Å	10000	35.7	14.6	2.80	0.295
C = 1.0+16	20000	41.5	21.2	3.75	1.52
	30000	45.4	24.9	4.07	2.18
	40000	48.5	27.6	4.29	2.58
	80000	57.5	34.3	5.09	3.37
$2p^1P^o-4s^1S$	5000	1.05	0.730	0.231	0.158
5047.74 Å	10000	1.09	0.745	0.260	0.203
C = 1.4+18	20000	1.11	0.668	0.291	0.246
	30000	1.13	0.584	0.312	0.270
	40000	1.14	0.528	0.327	0.288
	80000	1.12	0.417	0.368	0.332
$2p^1P^o-6s^1S$	5000	5.83	3.12	1.10	0.280
4168.97 Å	10000	6.37	3.43	1.37	0.676
C = 2.8+17	20000	6.82	3.49	1.56	1.03
	30000	6.97	3.50	1.68	1.21
	40000	6.99	3.50	1.76	1.34
	80000	6.77	3.39	1.98	1.64
$2p^1P^o-7s^1S$	5000	7.98	0.534	0.167	0.112
4023.97 Å	10000	11.4	0.590	0.188	0.145
C = 1.6+17	20000	15.0	0.569	0.211	0.176
	30000	17.6	0.524	0.225	0.194
	40000	20.1	0.480	0.236	0.207
	80000	29.8	0.380	0.266	0.240
$2p^1P^o-8s^1S$	5000	1.25	0.882	0.283	0.164
3935.91 Å	10000	26.3	0.949	0.320	0.228
C = 1.0+17	20000	101.	0.884	0.360	0.287
	30000	146.	0.794	0.385	0.321
	40000	178.	0.721	0.404	0.345
	80000	256.	0.571	0.454	0.402
$2p^1P^o-3d^1D$	5000	0.714	0.249	0.231	0.171
6678.15 Å	10000	0.666	0.222	0.260	0.211
C = 4.7+17	20000	0.602	0.180	0.295	0.250
	30000	0.565	0.162	0.320	0.274
	40000	0.538	0.144	0.339	0.292
	80000	0.485	0.106	0.386	0.342
$2p^1P^o-4d^1D$ *	5000	2.60	0.436	2.04	0.261
4921.93 Å	10000	2.48	0.368	2.74	1.14
C = 1.3+16	20000	2.24	0.298	2.95	2.01
	30000	2.08	0.252	2.87	2.42
	40000	1.96	0.221	2.74	2.65
	80000	1.69	0.162	2.29	2.97

Table 2. (*Contd*)

Transition	T[K]	$2W_e$[Å]	d_e[Å]	$2W_p$[Å]	d_p[Å]
$2p^1P^o$-$5d^1D$ *	5000	4.97	0.665	1.86	0.807-4
4387.93 Å	10000	5.10	0.558	5.32	0.359
C = 5.4+15	20000	4.81	0.450	7.07	2.77
	30000	4.53	0.382	7.31	4.25
	40000	4.31	0.336	7.15	5.14
	80000	3.75	0.250	6.11	6.56
$2p^1P^o$-$6d^1D$ *	5000	7.83	0.924	1.33	0.142-7
4143.76 Å	10000	8.75	0.856	6.80	0.284-1
C = 2.8+15	20000	8.69	0.775	12.9	1.54
	30000	8.36	0.707	14.4	4.35
	40000	8.04	0.656	14.3	6.75
	80000	7.14	0.528	12.6	11.2
$2p^1P^o$-$7d^1D$ *	5000	41.6	10.4	0.930	0.0
4009.27 Å	10000	50.5	20.7	1.71	0.726-9
C = 1.7+15	20000	57.4	29.7	13.6	0.886-1
	30000	62.0	34.6	25.6	1.67
	40000	65.8	38.0	27.2	4.63
	80000	77.4	46.7	32.9	16.5
$2s^3S$-$3p^3P^o$	5000	0.142	0.752-1	0.396-1	0.279-1
3888.65 Å	10000	0.166	0.609-1	0.434-1	0.332-1
C = 8.1+17	20000	0.182	0.485-1	0.476-1	0.386-1
	30000	0.187	0.400-1	0.504-1	0.418-1
	40000	0.190	0.347-1	0.526-1	0.442-1
	80000	0.190	0.251-1	0.585-1	0.503-1
$2s^3S$-$4p^3P^o$	5000	0.439	0.207	0.115	0.710-1
3187.74 Å	10000	0.500	0.170	0.128	0.922-1
C = 2.3+17	20000	0.527	0.140	0.142	0.112
	30000	0.533	0.116	0.152	0.124
	40000	0.534	0.101	0.159	0.132
	80000	0.519	0.721-1	0.178	0.153
$2s^3S$-$5p^3P^o$	5000	1.13	0.412	0.283	0.127
2945.10 Å	10000	1.27	0.367	0.325	0.199
C = 1.0+17	20000	1.31	0.283	0.364	0.263
	30000	1.31	0.234	0.389	0.299
	40000	1.31	0.203	0.408	0.324
	80000	1.25	0.146	0.461	0.384
$2s^3S$-$6p^3P^o$	5000	3.32	1.35	0.638	0.103
2829.07 Å	10000	3.74	1.48	0.842	0.355
C = 5.4+16	20000	4.05	1.60	0.978	0.588
	30000	4.18	1.68	1.05	0.712
	40000	4.25	1.75	1.10	0.796
	80000	4.28	1.91	1.25	0.989
$2p^3P^o$-$4s^3S$	5000	0.588	0.409	0.128	0.942-1
4713.20 Å	10000	0.620	0.456	0.143	0.117
C = 2.0+18	20000	0.641	0.439	0.161	0.139
	30000	0.645	0.387	0.172	0.152
	40000	0.659	0.349	0.181	0.161
	80000	0.685	0.280	0.203	0.185
$2p^3P^o$-$5s^3S$	5000	1.32	0.890	0.288	0.170
4120.80 Å	10000	1.35	0.931	0.325	0.234
C = 7.7+17	20000	1.38	0.851	0.365	0.294
	30000	1.42	0.737	0.391	0.327
	40000	1.46	0.677	0.410	0.351
	80000	1.48	0.540	0.461	0.410
$2p^3P^o$-$6s^3S$	5000	2.95	1.80	0.607	0.243
3867.50 Å	10000	3.13	1.93	0.710	0.422
C = 3.8+17	20000	3.23	1.81	0.802	0.579
	30000	3.28	1.67	0.859	0.666
	40000	3.30	1.57	0.901	0.725
	80000	3.22	1.29	1.01	0.867
$2p^3P^o$-$8s^3S$	5000	81.8	0.262	1.42	0.0
3652.00 Å	10000	122.	22.8	3.28	0.0
C = 7.2+15	20000	161.	59.5	10.6	0.816-8
	30000	179.	78.7	27.6	0.672-1
	40000	192.	91.2	29.8	1.72
	80000	221.	118.	42.8	14.4

Table 2 (*Contd*)

Transition	T[K]	$2w_e$[Å]	d_e[Å]	$2w_p$[Å]	d_p[Å]
$2p^3P^o$-$3d^3D$	5000	0.277	-0.725-1	0.591-1	-0.445-1
5875.70 Å	10000	0.298	-0.397-1	0.650-1	-0.523-1
C = 1.8+18	20000	0.296	-0.123-1	0.719-1	-0.604-1
	30000	0.295	-0.388-3	0.764-1	-0.653-1
	40000	0.293	0.457-2	0.799-1	-0.690-1
	80000	0.286	0.706-2	0.898-1	-0.784-1
$2p^3P^o$-$4d^3D$ *	5000	1.63	-0.187	1.34	0.316
4471.50 Å	10000	1.61	-0.131	1.69	0.815
C = 1.5+16	20000	1.49	-0.837-1	1.82	1.31
	30000	1.41	-0.556-1	1.74	1.56
	40000	1.35	-0.456-1	1.63	1.74
	80000	1.20	-0.279-1	1.17	1.79
$2p^3P^o$-$5d^3D$ *	5000	3.49	-0.425	2.18	0.180-2
4026.20 Å	10000	3.63	-0.315	3.76	0.544
C = 6.4+15	20000	3.47	-0.209	4.79	2.20
	30000	3.31	-0.161	4.79	3.17
	40000	3.19	-0.136	4.56	3.68
	80000	2.84	-0.878-1	3.37	4.34
$2p^3P^o$-$6d^3D$ *	5000	5.99	-0.698	1.52	0.583-4
3819.60 Å	10000	6.65	-0.558	4.54	0.550-1
C = 3.4+15	20000	6.61	-0.354	9.14	1.79
	30000	6.41	-0.260	9.73	4.04
	40000	6.21	-0.216	10.2	6.10
	80000	5.59	-0.136	8.61	8.21
$2p^3P^o$-$7d^3D$ *	5000	14.0	3.49	1.31	0.136-7
3705.00 Å	10000	17.2	4.87	3.76	0.571-2
C = 2.1+15	20000	19.5	6.41	9.76	0.711
	30000	20.5	7.40	15.7	2.97
	40000	21.1	8.17	16.5	5.37
	80000	22.1	10.1	13.8	11.5

Table 3. The same as in Table 1 but for i.r. He(I) lines with $\lambda > 7000$ Å and for temperatures from 2500 to 80,000 K

Transition	T[K]	$2w_e$[Å]	d_e[Å]	$2w_p$[Å]	d_p[Å]
$2s^1S$-$2p^1P^o$	2500	0.717	-0.392	0.158	-0.101
20581.3 Å	5000	0.749	-0.477	0.169	-0.117
C = 2.1+20	10000	0.793	-0.453	0.181	-0.134
	20000	0.862	-0.439	0.196	-0.152
	40000	0.974	-0.304	0.213	-0.173
	80000	1.09	-0.236	0.231	-0.196
$2p^1P^o$-$3s^1S$	2500	0.491	0.359	0.107	0.789-1
7281.4 Å	5000	0.558	0.401	0.120	0.978-1
C = 7.1+18	10000	0.594	0.426	0.135	0.116
	20000	0.619	0.402	0.151	0.135
	40000	0.638	0.317	0.170	0.155
	80000	0.656	0.247	0.191	0.176
$3s^1S$-$3p^1P^o$	2500	180.	-81.0	39.9	-22.0
74351.0 Å	5000	185.	-83.5	45.2	-31.2
C = 5.8+19	10000	182.	-74.7	50.8	-39.6
	20000	175.	-63.8	57.3	-47.6
	40000	170.	-48.2	65.2	-55.8
	80000	161.	-38.0	74.5	-65.0
$3s^1S$-$4p^1P^o$	2500	23.5	-8.28	5.82	-1.19
15083.7 Å	5000	23.9	-7.84	7.42	-3.38
C = 1.1+18	10000	23.2	-6.66	8.56	-5.36
	20000	22.2	-5.02	9.73	-7.13
	40000	20.8	-3.77	11.1	-8.81
	80000	18.9	-2.78	12.8	-10.6
$3s^1S$-$5p^1P^o$ *	2500	26.9	-7.85	5.67	-.487-3
11013.1 Å	5000	29.2	-7.85	9.78	-1.49
C = 2.9+17	10000	29.5	-6.17	13.0	-5.42
	20000	28.7	-4.81	15.3	-9.10
	40000	26.8	-3.53	17.7	-12.4
	80000	24.3	-2.49	20.2	-15.8

Table 3. (*Contd*)

Transition	T[K]	$2W_e$[Å]	d_e[Å]	$2W_p$[Å]	d_p[Å]
$3s^1S-6p^1P^o$ *	2500	33.1	-7.92	1.38	0.0
9603.4 Å	5000	39.7	-7.17	12.8	-.107-2
C = 1.3+17	10000	43.9	-5.05	20.7	-3.32
	20000	44.2	-3.08	27.5	-11.5
	40000	42.0	-1.38	32.7	-19.3
	80000	38.7	-.462	37.2	-26.9
$3p^1P^o-4s^1S$	2500	27.1	13.7	5.04	2.32
21132.0 Å	5000	28.7	15.6	5.80	3.67
C = 2.5+19	10000	28.8	15.4	6.53	4.87
	20000	28.4	13.1	7.35	6.00
	40000	28.3	10.2	8.28	7.11
	80000	27.2	8.07	9.40	8.27
$3p^1P^o-5s^1S$	2500	23.9	12.3	4.07	1.02
13411.8 Å	5000	25.3	14.4	5.08	2.49
C = 5.0+18	10000	25.6	14.6	5.81	3.80
	20000	25.8	12.4	6.54	4.98
	40000	25.8	9.96	7.35	6.09
	80000	24.6	7.61	8.28	7.19
$3p^1P^o-6s^1S$	2500	40.4	17.8	5.78	0.427-1
11225.9 Å	5000	45.2	23.0	8.09	2.02
C = 2.0+18	10000	49.0	25.3	10.1	4.95
	20000	52.0	25.7	11.6	7.56
	40000	53.0	25.7	13.0	9.91
	80000	51.1	24.8	14.7	12.1
$3d^1D-5p^1P^o$ *	2500	30.8	0.103	1.87	0.284-1
12755.7 Å	5000	36.9	0.120	2.07	0.328-1
C = 3.9+17	10000	38.9	0.141	2.14	0.374-1
	20000	38.1	0.153	2.16	0.425-1
	40000	35.6	0.148	2.17	0.482-1
	80000	32.1	0.127	2.17	0.547-1
$2s^3S-2p^3P^o$	2500	0.106	-0.503-1	0.301-1	-0.135-1
10830.0 Å	5000	0.107	-0.620-1	0.309-1	-0.154-1
C = 1.1+20	10000	0.113	-0.631-1	0.320-1	-0.176-1
	20000	0.129	-0.606-1	0.333-1	-0.199-1
	40000	0.150	-0.466-1	0.348-1	-0.226-1
	80000	0.178	-0.401-1	0.362-1	-0.256-1
$2p^3P^o-3s^3S$	2500	0.271	0.191	0.613-1	0.475-1
7065.3 Å	5000	0.317	0.231	0.686-1	0.574-1
C = 1.2+19	10000	0.349	0.262	0.768-1	0.673-1
	20000	0.366	0.251	0.861-1	0.775-1
	40000	0.380	0.220	0.965-1	0.884-1
	80000	0.406	0.170	0.108	0.100
$2s^3S-4p^3P^o$	2500	6.22	3.28	1.53	0.722
12528.0 Å	5000	7.03	2.37	1.73	1.07
C = 3.6+18	10000	8.19	1.84	1.93	1.39
	20000	8.75	1.29	2.14	1.69
	40000	9.07	0.880	2.38	1.98
	80000	8.96	0.567	2.67	2.29
$3s^3S-5p^3P^o$	2500	10.4	4.77	2.28	0.483
9463.6 Å	5000	11.7	3.83	2.90	1.30
C = 1.0+18	10000	13.3	3.26	3.34	2.04
	20000	13.8	2.38	3.74	2.71
	40000	13.9	1.68	4.19	3.33
	80000	13.4	1.18	4.73	3.94
$3s^3S-6p^3P^o$	2500	19.1	7.65	3.56	0.770-2
8361.8 Å	5000	22.3	7.34	4.98	1.06
C = 4.7+17	10000	25.3	7.23	6.32	2.88
	20000	26.3	6.91	7.27	4.53
	40000	26.2	6.27	8.20	6.00
	80000	25.1	5.43	9.29	7.38
$3p^3P^o-4s^3S$	2500	11.0	5.76	1.94	1.21
21120.0 Å	5000	13.6	7.27	2.17	1.59
C = 4.1+19	10000	15.4	7.57	2.42	1.95
	20000	16.8	7.26	2.70	2.30
	40000	17.8	5.65	3.02	2.67
	80000	18.5	4.62	3.38	3.05
$3p^3P^o-5s^3S$	2500	11.9	7.21	2.32	0.941
12846.0 Å	5000	13.5	8.38	2.71	1.62
C = 7.5+18	10000	14.3	8.59	3.06	2.21
	20000	14.8	7.72	3.43	2.77
	40000	15.9	6.09	3.85	3.30
	80000	16.1	4.85	4.33	3.85

Table 3 (*Contd*)

Transition	T[K]	$2w_e$[Å]	d_e[Å]	$2w_p$[Å]	d_p[Å]
$3p^3P^o$-$6s^3S$	2500	20.5	10.8	3.36	0.432
10667.6 Å	5000	23.0	13.6	4.58	1.84
C = 2.9+18	10000	24.5	14.5	5.35	3.19
	20000	25.5	13.6	6.05	4.38
	40000	26.2	11.7	6.80	5.48
	80000	25.6	9.59	7.65	6.54
$3p^3P^o$-$7s^3S$	2500	49.4	18.8	3.33	0.378-8
9702.7 Å	5000	59.3	28.8	9.15	0.578
C = 1.5+18	10000	68.3	36.4	13.1	4.49
	20000	76.3	42.2	15.7	8.70
	40000	81.9	46.8	17.8	12.4
	80000	83.0	48.7	20.0	15.8
$3d^3D$-$4p^3P^o$	2500	12.7	0.595	1.68	0.160
19543.0 Å	5000	16.4	0.699	1.74	0.188
C = 8.7+18	10000	19.4	0.819	1.76	0.216
	20000	21.3	0.897	1.77	0.247
	40000	21.9	0.871	1.77	0.280
	80000	21.3	0.749	1.77	0.318
$3d^3D$-$5p^3P^o$	2500	15.9	0.137	1.83	0.379-1
12985.0 Å	5000	20.4	0.160	2.01	0.439-1
C = 2.0+18	10000	23.9	0.188	2.07	0.502-1
	20000	25.8	0.210	2.09	0.570-1
	40000	26.1	0.209	2.10	0.647-1
	80000	25.1	0.184	2.10	0.734-1
$3d^3D$-$6p^3P^o$	2500	24.7	0.256	2.43	0.673-1
10996.6 Å	5000	32.8	0.303	2.95	0.796-1
C = 8.1+17	10000	38.7	0.351	3.16	0.922-1
	20000	41.8	0.370	3.24	0.105
	40000	42.6	0.344	3.26	0.120
	80000	41.7	0.283	3.27	0.136

Table 4. Various experimental results for the He(I) 5016 Å line are compared with the present calculations

Author	Year	$N_e(10^{16}cm^{-3})$	W_{meas}/W_T	N_e determination
Wulff[11]	1958	3.2	0.85	Inglis-Teller
Berg et al.[12]	1962	16.5	1.01	H, He lines
Bötticher et al.[13]	1963	1.0-2.0	1.33-1.11	LTE
Lincke[14]	1964	9.3	1.01	H_6, 3889
Greig et al.[15]	1968	1-10	1.35	H_β
Greig and Jones[16]	1970	2.7-17	1.42-1.38	H_β
Kusch[17]	1971	0.8-4.6	1.96-2.19	H_β
Diatta et al.[18]	1974	3.0	1.06	H_β
Einfeld and Sauerbrey[19]	1976	2.0-3.5	2.01	He Continuum
Chiang et al.[20]	1977	10	1.12	Interferometry
Kelleher[2]	1981	0.3-1.3	1.09	H_β

$T = 5000$ K while the result of Benett and Griem[5] (without the correction for Debye shielding suggested in the same paper) is $d = 16.3$ Å for the same conditions. These lines may be used as experimental checks to see if the impact-parameter cut-off treatment of Debye shielding is satisfactory or not.

4. DISCUSSION OF REGULARITIES AND CONCLUSION

It was shown earlier,[9,22] on the basis of existing experimental data, that, for lines belonging to a spectral series, one should expect a gradual increase in the Stark width with increasing principal quantum number of the upper state. In the present paper, we use our

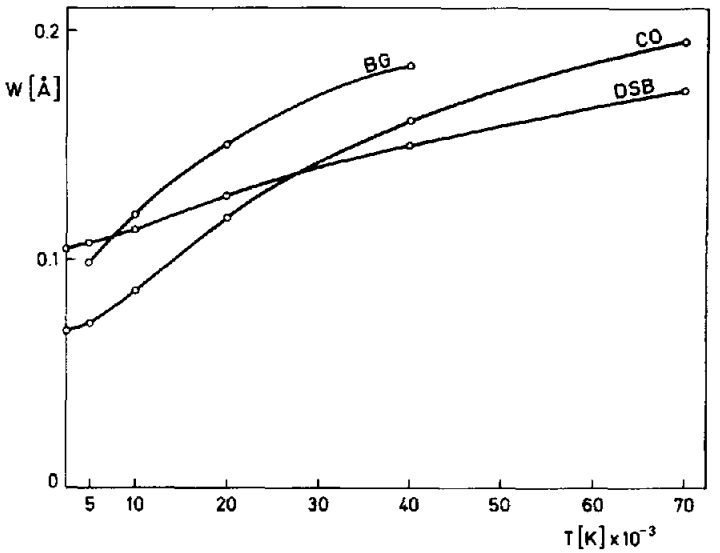

Fig. 1. Full halfwidths for He(I) $2s^3S$–$2p^3P^0$ multiplet ($\lambda = 10{,}830$ Å), as a function of electron temperature; $N_e = 10^{16}$ cm^{-3}. Calculations: BG, Benett and Griem;[5] Co, Cooper and Oertel;[22] DSB, present calculations.

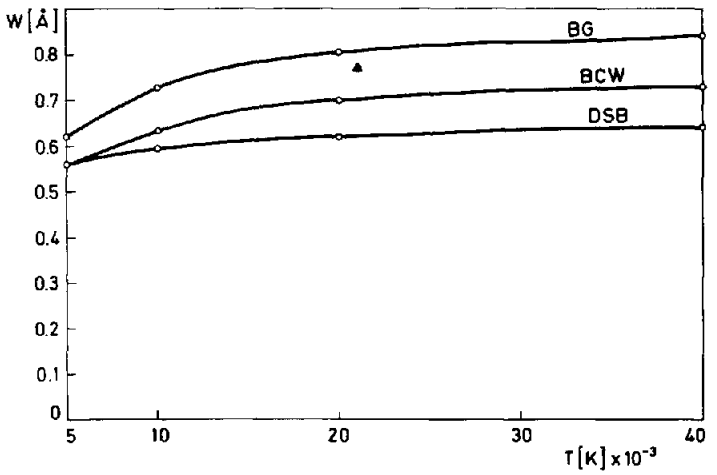

Fig. 2. Full halfwidths for He(I) $2p^1P^0$–$3s^1S$ multiplet ($\lambda = 7281.4$ Å) as a function of electron temperature; $N_e = 10^{16}$ cm^{-3}. Experimental point: ▲, Kelleher.[2] Calculations: BCW, Bassalo *et al.*[6] Otherwise, the same notation applies as in Fig. 1.

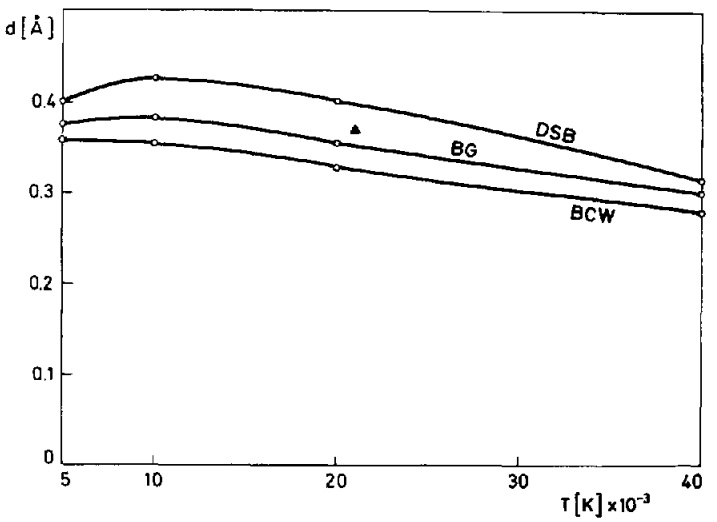

Fig. 3. The same title as in Fig. 2 applies but for the shift.

comprehensive set of results of Stark-broadening data to investigate such width regularities within a spectral series and to see if regular behavior appears also for the shifts (see also Refs. 22 and 23 and cited references).

The full halfwidth (in angular frequency units) and the ratio d/W for the $2s^1S$–np^1P^0 series as a function of the principal quantum number of the upper level (n_i) are shown in Figs. 4 and 5. We see that the values for $n_i = 2$ and 7 deviate considerably from the regular behavior, especially for the d/W ratio.

By inspecting energy separations between the upper level and the principal perturbing levels (Fig. 6), we find that this value decreases gradually within a spectral series. Thus, we expect a gradual change of the Stark-broadening parameters.

The values for $n_i = 2$ deviate from the others because the $2d$ level does not exist. There is no simple explanation for the deviation of the values for $n_i = 7$. The shift is very sensitive to oscillator strengths and may indicate the beginning of the failure of the model for oscillator-strength calculations for highly excited levels. The results also show that systematic behavior depends strongly on plasma conditions, especially in the case of the shift.

As may be seen from Figs. 7–9, a regular increase of widths and shifts also occurs within the $2s^3S$–np^3P^0 and $3p^3P^0$–ns^3S series.

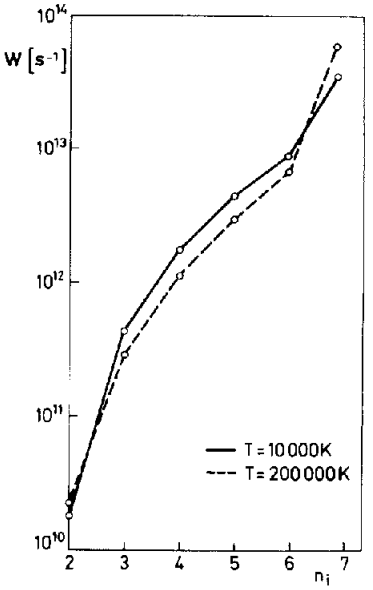

Fig. 4. The Stark halfwidth for He(I) resonance lines as a function of n_i for $T = 10^4$ and 2×10^5 K, $N_e = 10^{16}$ cm^{-3}.

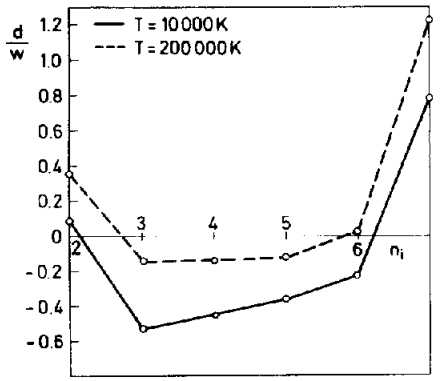

Fig. 5. The ratio d/W for He(I) resonance lines as a function of n_i for $T = 10^4$ and 2×10^5 K, $N_e = 10^{16}$ cm^{-3}.

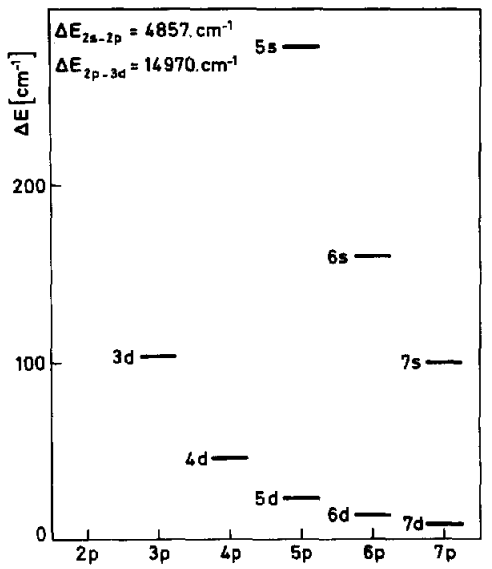

Fig. 6. Energy separations between the upper level and the principal perturbing levels for He(I) resonance lines.

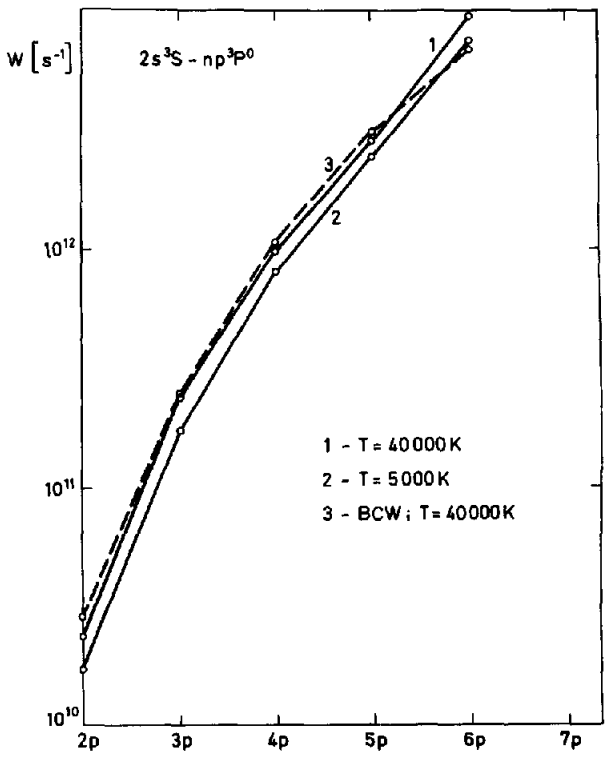

Fig. 7. The Stark halfwidth for He(I) $2s^3S$–np^3P^0 lines as a function of n_i for $T = 5000$ and 40,000 K, BCW denotes the result of Bassalo *et al.*[6]

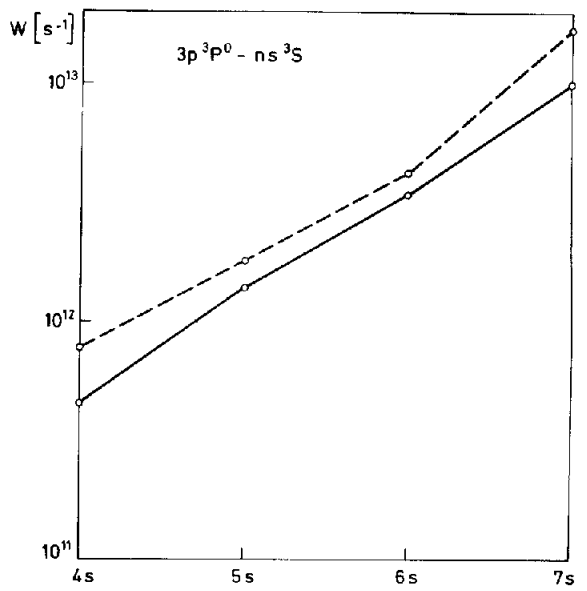

Fig. 8. Full halfwidths for He(I) $3p^3P^0$–ns^3S lines as a function of n for $N_e = 10^{16}\,\mathrm{cm}^{-3}$ (——$T = 2{,}500$ K; - - -T = 80,000 K).

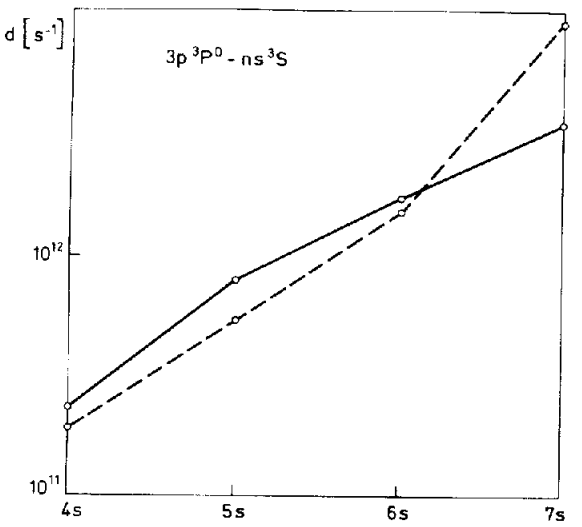

Fig. 9. The same notation applies as in Fig. 8 but for the shift.

REFERENCES

1. N. Konjević and J. R. Roberts, *J. Phys. Chem. Ref.* Data **5**, 209 (1976).
2. D. E. Kelleher, *JQSRT* **25**, 191 (1981).
3. S. Sahal-Bréchot, *Astron. Astrophys.* **1**, 91 (1969).
4. S. Sahal-Bréchot, *Astron. Astrophys.* **2**, 322 (1969).
5. S. M. Benett and H. R. Griem, University of Maryland Technical Report No. 71-097, College Park, Maryland (1971).
6. J. M. Bassalo, M. Cattani, and V. S. Walder, *JQSRT* **28**, 75 (1982).
7. H. R. Griem, M. Baranger, A. C. Kolb, and G. Oertel, *Phys. Rev.* **125**, 177 (1962).
8. H. R. Griem, *Spectral Line Broadening by Plasmas.* Academic Press, New York (1974).
9. W. L. Wiese and N. Konjević, *JQSRT* **28**, 185 (1982).
10. W. C. Martin, *J. Phys. Chem. Ref. Data* **2**, 257 (1973).
11. H. Z. Wulff, *Z. Phys.* **150**, 614 (1958).
12. H. F. Berg, A. W. Ali, R. Lincke, and H. R. Griem, *Phys. Rev.* **125**, 199 (1962).
13. W. Bötticher, O. Roder, and K. H. Wobig, *Z. Phys.* **175**, 480 (1963).
14. R. Lincke, Thesis, University of Maryland, College Park, Maryland (1964).
15. J. R. Greig, C. P. Lim, G. A. Moo-Young, G. Palumbo, and H. R. Griem, *Phys. Rev.* **182**, 148 (1968).

16. J. R. Greig and L. A. Jones, *Phys. Rev.* **A1**, 1261 (1970).
17. H. J. Kusch, *Z. Naturforsch.* **26a**, 1970 (1971).
18. C. S. Diatta, C. Fleurier, J. Chapelle, and S. Sahal, *Phys. Lett.* **49**a, 450 (1974).
19. D. Einfeld and G. Sauerbrey, *Z. Naturforsch.* **31a**, 310 (1976).
20. W. I. Chiang, D. P. Murphy, Y. G. Chen, and H. R. Griem, *Z. Naturforsch.* **32a**, 818 (1977).
21. J. Cooper and G. K. Oertel, *Phys. Rev.* **180**, 286 (1969).
22. N. Konjević and M. S. Dimitrijević, In *Spectral Line Shapes* Edited by B. Wende) p. 241 W. de Gruyter, Berlin (1981).
23. M. S. Dimitrijević, *Astron. Astrophys.* **112**, 251 (1982).

J. Quant. Spectrosc. Radiat. Transfer Vol. 34, No. 2, pp. 149–161, 1985
Printed in Great Britain.

0022-4073/85 $3.00 + .00

STARK BROADENING OF NEUTRAL SODIUM LINES

M. S. DIMITRIJEVIĆ
Astronomical Observatory, Volgina 7, 11050 Beograd and Institute of Physics, P.O. Box 57, 11001 Beograd, Yugoslavia

and

S. SAHAL-BRÉCHOT
Observatoire de Paris-Meudon, 92190 Meudon, France

(*Received* 26 *November* 1984)

Abstract—A semiclassical approach has been used to evaluate Stark broadening of atomic lines and also electron- and proton-impact line widths and shifts of 30 neutral sodium lines. The results are used to investigate Stark broadening-parameter regularities within the spectral series.

1. INTRODUCTION

Reliable Stark-broadening parameters for sodium lines are useful for a number of problems in plasma diagnostics,[1] astrophysics,[2,3] technology of high-pressure discharge lamps,[4,5] etc. Using the semiclassical-perturbation formalism,[6,7] we have calculated electron- and proton-impact line widths and shifts of 30 neutral Na lines. Our results are compared with available theoretical[1,8,9] and reliable experimental[10,11] data. The results have been used to extend our investigation of Stark-broadening regularities within spectral series.[12,13] Using our comprehensive results, we have searched for systematic trends among Stark-broadening parameters within the Na(I) spectral series. If these exist, accurate interpolations and critical evaluations of experimental results become feasible.

2. THEORY

The basis for calculation is a computer code for evaluation of electron- and ion-impact broadening parameters of isolated spectral lines, using the semiclassical-perturbation approach.[6] The formulae which lead to the full halfwidth ($2W$) and the shift (d) are

$$2W = N_e \int_0^\infty vf(v)\,\mathrm{d}v\Big[\sum_{i'\neq i} \sigma_{ii'}(v) + \sum_{f'\neq f} \sigma_{ff'}(v) + \sigma_{\mathrm{el}}(v)\Big] \tag{1}$$

$$d = \int_0^\infty vf(v)\,\mathrm{d}v \int_{R_3}^{R_d} 2\pi\rho\,\mathrm{d}\rho \sin 2\phi_p. \tag{2}$$

Here i and f denote, respectively, the initial and final levels and i', f' the corresponding perturbing levels, N_e is the electron density, $f(v)$ the velocity distribution function for electrons and ρ the impact parameter. Details concerning the calculation of inelastic ($\sigma_{jj'}$; $j = i, f$) and elastic (σ_{el}) cross sections, the phase shift (ϕ_p) and cut-offs are described in Ref. 6 (Sec. 1, Chap. 3). We recall here that we allow for Debye shielding by introducing the Debye cut-off R_d as an upper cut-off in the integration procedure.

It is not necessary to discuss uncertainties arising from all of the approximations involved in our calculations, since the criteria for their application are given in detail elsewhere.[6] If we want to make certain that a line is isolated, we can use the parameter C defined in Ref. 12 and given in Table 1. If halfwidths are available for the electron concentration $N = 10^{16}$ cm^{-3},

$$N_l\,(\mathrm{cm}^{-3}) = C/2W\,(\text{in Å at } N = 10^{16}\ \mathrm{cm}^{-3}). \tag{3}$$

For an electron concentration lower than N_l, the line can be treated as isolated in the

Table 1. This table lists electron- and proton-impact broadening parameters for Na(I) lines at an electron density of 10^{16} cm^{-3} and temperatures from 2500 to 80,000 K. Transitions and averaged wavelengths for the multiplet (in Å) are also given. Under $2W_e$ and $2W_p$ are given electron- and proton-impact full halfwidths, while d_e and d_p denote corresponding shifts. Asterisk denote cases when the frequency distance between the upper and nearest perturbing levels is smaller than or equal to the electron-plasma frequency. For these lines, the behaviour of N_e deviates from linear (especially for the shift); for another electron density, the influence of Debye shielding must be taken into account (see, e.g., Ref. 1, Appendix IVa).

Transition	T/K/	$2W_e$/Å/	d_e/Å/	$2W_p$/Å/	d_p/Å/
$3s^2S$-$3p^2P^o$	2500	0.191(-1)	0.130(-1)	0.126(-1)	0.352(-2)
5891.8 Å	5000	0.212(-1)	0.154(-1)	0.127(-1)	0.404(-2)
	10000	0.249(-1)	0.178(-1)	0.129(-1)	0.459(-2)
	20000	0.316(-1)	0.181(-1)	0.130(-1)	0.521(-2)
C=3.0+19	30000	0.368(-1)	0.178(-1)	0.132(-1)	0.561(-2)
	80000	0.513(-1)	0.130(-1)	0.135(-1)	0.670(-2)
$3s^2S$-$4p^2P^o$	2500	0.649(-1)	-0.231(-1)	0.219(-1)	-0.686(-2)
3302.6 Å	5000	0.725(-1)	-0.141(-1)	0.225(-1)	-0.818(-2)
	10000	0.864(-1)	-0.338(-2)	0.230(-1)	-0.951(-2)
C=1.2+18	20000	0.100	0.281(-2)	0.235(-1)	-0.109(-1)
	30000	0.108	0.558(-2)	0.239(-1)	-0.118(-1)
	80000	0.124	0.733(-2)	0.251(-1)	-0.141(-1)
$3s^2S$-$5p^2P^o$	2500	0.202	-0.102	0.560(-1)	-0.227(-1)
2852.8 Å	5000	0.221	-0.928(-1)	0.611(-1)	-0.303(-1)
	10000	0.254	-0.630(-1)	0.651(-1)	-0.375(-1)
C=4.0+17	20000	0.295	-0.460(-1)	0.693(-1)	-0.445(-1)
	30000	0.313	-0.364(-1)	0.720(-1)	-0.487(-1)
	80000	0.346	-0.207(-1)	0.798(-1)	-0.596(-1)
$3p^2P^o$-$4s^2S$	2500	0.377	0.258	0.869(-1)	0.635(-1)
11397.0 Å	5000	0.433	0.305	0.953(-1)	0.751(-1)
	10000	0.481	0.323	0.105	0.869(-1)
C=5.9+19	20000	0.525	0.379	0.116	0.994(-1)
	30000	0.564	0.355	0.123	0.107
	80000	0.687	0.249	0.143	0.128
$3p^2P^o$-$5s^2S$	2500	0.407	0.275	0.867(-1)	0.617(-1)
6158.6 Å	5000	0.472	0.373	0.973(-1)	0.775(-1)
	10000	0.514	0.379	0.109	0.928(-1)
C=7.0+18	20000	0.564	0.382	0.122	0.108
	30000	0.590	0.340	0.131	0.118
	80000	0.727	0.245	0.154	0.142

(Cont'd)

core, even if weak forbidden components due to the failure of this approximation still appear in the wings.

3. RESULTS

Data for needed energy levels were taken from Ref. 14. For evaluation of the oscillator strengths, tables of Bates and Damgaard[15] and Oertel and Shomo[16] have been used. For low-lying levels, the oscillator strengths where taken from Ref. 17. When tables of Oertel and Shomo[16] are not applicable for higher levels, the method described in Ref. 18 was used.

Table 1. (*Contd*)

$3p^2P^o$–$6s^2S$	2500	0.781	0.512	0.160	0.921(-1)
5151.9 Å	5000	0.894	0.611	0.182	0.129
	10000	0.977	0.673	0.204	0.163
C=2.5+18	20000	1.10	0.624	0.229	0.195
	30000	1.19	0.542	0.245	0.214
	80000	1.46	0.389	0.289	0.262
$3p^2P^o$–$7s^2S$	2500	1.68	0.989	0.324	0.121
4750.6 Å	5000	2.01	1.21	0.382	0.220
	10000	2.35	1.36	0.432	0.307
C=1.2+18	20000	2.69	1.37	0.486	0.388
	30000	2.89	1.32	0.520	0.433
	80000	3.25	1.08	0.613	0.544
$3p^2P^o$–$8s^2S$	2500	11.4	4.41	0.374	0.
4544.2 Å	5000	13.8	7.36	2.44	0.185(-1)
	10000	16.5	9.99	3.42	0.854
C=6.8+17	20000	20.0	12.5	4.27	2.09
	30000	22.4	14.0	4.64	2.76
	80000	28.4	18.2	5.50	4.19
$4p^2P^o$–$9s^2S$*	2500	158.	0	3.96	0
10745.0 Å	5000	583.	0	5.42	0
	10000	0.136(+4)	0.112(-8)	27.0	0
C=2.5+18	20000	0.380(+4)	188.	103.	0
	30000	0.493(+4)	988.	48.2	0
	80000	0.698(+4)	0.335(+4)	823.	0.108(-1)
$4p^2P^o$–$10s^2S$*	2500	270.	0	3.18	0
10294.0 Å	5000	536.	0	6.59	0
	10000	0.151(+4)	0	40.9	0
C=1.6+18	20000	0.385(+4)	0	76.4	0
	30000	0.576(+4)	0	170.	0
	80000	0.254(+5)	0	738.	0

(*Cont'd*)

Our results for electron($2W_e$)- and proton($2W_p$)-impact full halfwidths and shifts (d_e and d_p, respectively) for neutral sodium lines are shown in Table 1 for $N_e = 10^{16}$ cm^{-3} and T = 2500, 5000, 10,000, 20,000, 30,000 and 80,000 K. In Table 1 we also give a parameter denoted by C [see Eq. (3) and Ref. 12], which can be used to determine if a line is isolated for the needed electron density.

In Figs. 1 and 2, our results for the Na(I) $3s^2S$–$3p^2P^0$ multiplet (λ = 5891.8 Å) are compared with available theoretical[1,8,9] and experimental[10,11] data. In both experiments[10,11] the perturbing ion was singly ionized argon.

In some cases, a controversy exists in the literature concerning the impact or quasistatic character of the ionic contribution to the line profile. For the Li(I) $2s$–$2p$ transition perturbed by Ar^+, the impact character of ionic profiles was pointed out by Brissaud *et al.*,[19] which is in contradiction to the GBKO[20] validity criteria for the impact approximation that are not satisfied in the present case. For the Na(I) $3s$–$3p$ multiplet perturbed by Ar^+,

Table 1. (*Contd*)

$4p^2P^o$-$4d^2D$	2500	40.3	14.2	10.5	2.90
23370.0 Å	5000	40.1	13.9	13.0	6.59
	10000	38.5	12.2	14.9	9.83
C=2.2+18	20000	36.6	9.63	17.0	12.8
	30000	35.4	8.16	18.4	14.4
	80000	32.2	5.48	22.1	18.9
$4p^2P^o$-$5d^2D^*$	2500	33.0	0.818	1.82	0.197
14776.0 Å	5000	38.8	0.974	1.96	0.239
	10000	40.9	1.11	2.01	0.280
C=4.5+17	20000	40.4	1.12	2.03	0.323
	30000	39.3	1.07	2.03	0.350
	80000	35.1	0.806	2.04	0.419
$4p^2P^o$-$6d^2D^*$	2500	39.1	0.317	2.48	0.804(-1)
12318.0 Å	5000	52.0	0.375	2.96	0.953(-1)
	10000	58.8	0.434	3.14	0.110
C=1.9+17	20000	60.0	0.458	3.21	0.126
	30000	58.9	0.446	3.22	0.136
	80000	53.0	0.352	3.24	0.163
$4s^2S$-$4p^2P^o$	2500	3.56	- 1.80	1.03	-0.421
22070.0 Å	5000	3.86	- 1.83	1.07	-0.508
	10000	4.40	- 1.62	1.12	-0.595
C=5.4+19	20000	5.29	- 1.21	1.16	-0.686
	30000	5.87	- 1.03	1.20	-0.742
	80000	7.13	- 0.644	1.30	-0.888
$4s^2S$-$5p^2P^o$	2500	2.98	- 1.55	0.803	-0.329
10747.0 Å	5000	3.25	- 1.52	0.878	-0.442
	10000	3.72	- 1.19	0.938	-0.548
C=5.7+18	20000	4.38	- 0.994	1.00	-0.651
	30000	4.70	-0.833	1.04	-0.713
	80000	5.29	-0.515	1.16	-0.868
$4s^2S$-$6p^2P^o$	2500	5.55	-2.97	1.25	-0.397
8650.3 Å	5000	6.04	-2.74	1.51	-0.700
	10000	6.87	-2.06	1.68	-0.968
C=1.9+18	20000	7.92	-1.73	1.83	-1.22
	30000	8.34	-1.46	1.92	-1.36
	80000	9.02	-0.868	2.18	-1.70

(*Cont'd*)

Table 1. (*Contd*)

$4s^2S$-$7p^2P^o$	2500	16.5	6.23	2.15	0.715(-1)
7810.0 Å	5000	21.5	8.65	3.19	0.937
	10000	27.0	11.4	3.95	1.95
C=9.3+17	20000	33.1	14.7	4.47	2.84
	30000	36.8	16.9	4.76	3.32
	80000	44.6	23.3	5.51	4.42
$4s^2S$-$8p^2P^o$*	2500	12.8	0.116	1.66	0.298(-1)
7373.2 Å	5000	17.5	0.136	2.44	0.354(-1)
	10000	23.1	0.161	2.91	0.410(-1)
C=5.3+17	20000	31.1	0.179	3.08	0.470(-1)
	30000	37.8	0.181	3.13	0.507(-1)
	80000	63.9	0.157	3.17	0.606(-1)
$4p^2P^o$-$6s^2S$	2500	8.89	5.37	1.72	0.949
16384.0 Å	5000	10.3	6.30	1.94	1.33
	10000	11.4	6.61	2.17	1.69
C=2.5+19	20000	12.9	6.15	2.43	2.03
	30000	14.2	5.25	2.59	2.23
	80000	17.4	3.85	3.04	2.73
$4p^2P^o$-$7s^2S$	2500	13.0	7.35	2.42	0.897
12915.0 Å	5000	15.6	9.04	2.86	1.64
	10000	18.2	10.1	3.23	2.29
C=8.8+18	20000	20.9	10.2	3.63	2.89
	30000	22.4	9.84	3.88	3.22
	80000	25.4	7.93	4.57	4.05
$4p^2P^o$-$8s^2S^o$	2500	73.2	28.2	2.40	0
11495.0 Å	5000	88.9	47.1	15.6	0.118
C=4.4+18	10000	107.	63.9	21.9	5.47
	20000	129.	80.0	27.3	13.4
	30000	145.	89.7	29.7	17.6
	80000	183.	117.	35.2	26.8

(*Cont'd*)

the validity condition for the impact approximation given in Refs. 6 and 7 is not fulfilled. On the other hand, if we use the collective Kubo number,[21] for estimation of the character of the ionic profile, the ionic profile is the purely impact type[9] for the experimental conditions used in Refs. 10 and 11.

We see from Fig. 1 that data of Baur and Cooper[10] are in excellent agreement with our calculations for static ions. On the other hand, the line widths of Purić *et al.*[11] agree better with numerical results if the ionic contribution is treated within the impact approximation. Results of Purić *et al.*[11] for the shift are in agreement with calculations of Benett and Griem[1,8] and Mazure and Nollez.[9] Impact widths and shifts due to collisions with Ar^+ are presented in Table 2 for the multiplet considered.

4. DISCUSSION OF REGULARITIES AND CONCLUSION

It was shown earlier[22] that, for lines belonging to a spectral series, one should expect a gradual increase in the electron-impact width with increasing principal quantum number

Table 1. (*Contd*)

$3p^2P^o$–$8d^2D$*	2500	12.7	0.695(-1)	0.657	0.169(-1)
4392.3 Å	5000	15.3	0.828(-1)	1.05	0.205(-1)
	10000	20.3	0.952(-1)	1.28	0.240(-1)
C=9.6+15	20000	24.4	0.986(-1)	1.38	0.277(-1)
	30000	26.8	0.948(-1)	1.40	0.299(-1)
	80000	35.6	0.728(-1)	1.43	0.358(-1)
$3p^2P^o$–$9d^2D$*	2500	29.5	0.569(-1)	0.883	0.141(-1)
4323.5 Å	5000	34.1	0.677(1)	1.36	0.169(-1)
	10000	48.2	0.782(-1)	1.87	0.197(-1)
C=4.9+15	20000	91.9	0.818(-1)	2.12	0.227(-1)
	30000	126.	0.792(-1)	2.18	0.245(-1)
	80000	266.	0.617(-1)	2.24	0.293(-1)
$3d^2D$–$4p^2P^o$	2500	71.5	-39.3	16.4	-8.72
91050.0 Å	5000	79.3	-40.4	17.5	-10.6
	10000	87.7	-32.1	18.7	-12.5
C=9.1+20	20000	102.	-24.2	20.1	-14.5
	30000	111.	-21.9	21.0	-15.7
	80000	126.	-13.3	23.6	-18.8
$3d^2D$–$4f^2F^o$	2500	16.3	-2.25	5.12	-1.84
18465.3 Å	5000	15.8	-1.04	6.09	-3.43
	10000	14.7	-0.256	6.95	-4.82
C=1.4+18	20000	13.3	0.206(-1)	7.95	-6.09
	30000	12.7	0.349(-1)	8.64	-6.88
	80000	11.3	0.130	10.2	-9.05

(*Cont'd*)

of the upper state. Recently, on the basis of comprehensive numerical results for Stark broadening of He(I) lines, it was shown,[12,13] for lines belonging to a spectral series, that electron- and proton-impact widths increase gradually with increasing principal quantum number of the upper state. The electron- and proton-impact shift changes gradually within a spectral series if $R_d > R_3$ [R_3 is the lower cut-off for the shift. See Eq. (2) and Ref. 6]. For $R_d < R_3$, the shift is zero.[13] If the shift is negative (blue) for lower numbers of a series due to larger polarization of the lower transition level, it becomes positive (red) for higher members of the series owing to the gradual increase of the upper level contribution.[13] We continue here this investigation using the present results for Na(I) lines.

By inspecting energy separations between the upper level and the principal perturbing levels for the $3p^3P^0$–ns^3S and $4s^3S$–np^3P^0 series (see Grotrian diagrams in Ref. 14), we find that this value decrease gradually within a spectral series. Thus we expect a gradual change of the Stark-broadening parameters. We see that the situation within the $3p^3P^0$–ns^3S series is rather simple. We have one dominant perturbing level, the energy separation changes regularly and we expect very regular behaviour of Stark-broadening parameters within this spectral series. The electron- and proton-impact broadening parameters (in angular frequency units), are shown in Figs. 3–6 as a function of the principal quantum number of the upper level (n_i). In practically all cases we find a gradual increase of the Stark-broadening parameters with an increase of n_i. The unique exception is the proton-

Table 1. (*Contd*)

$3p^2P^0$–$3d^2D$	2500	0.312	0.220	0.813(-1)	0.525(-1)
8191.1 Å	5000	0.356	0.243	0.881(-1)	0.631(-1)
	10000	0.386	0.249	0.959(-1)	0.737(-1)
C=7.3+18	20000	0.411	0.232	0.105	0.848(-1)
	30000	0.423	0.205	0.111	0.916(-1)
	80000	0.455	0.139	0.127	0.110
$3p^2P^0$–$4d^2D^*$	2500	2.25	0.809	0.617	0.172
5686.4 Å	5000	2.21	0.773	0.768	0.389
	10000	2.11	0.672	0.879	0.579
C=1.3+17	20000	1.97	0.552	1.00	0.751
	30000	1.88	0.470	1.08	0.850
	80000	1.64	0.309	1.30	1.11
$3p^2P^0$–$5d^2D^*$	2500	4.62	1.43	1.14	0.216(-3)
4981.4 Å	5000	4.86	1.46	1.76	0.302
	10000	4.81	1.24	2.30	0.991
C=5.2+16	20000	4.59	0.998	2.70	1.63
	30000	4.39	0.851	2.94	1.97
	80000	3.82	0.563	3.54	2.82
$3p^2P^0$–$6d^2D^*$	2500	5.57	0.728(-1)	0.368	0.181(-1)
4667.5 Å	5000	7.40	0.857(-1)	0.442	0.219(-1)
	10000	8.35	0.101	0.470	0.256(-1)
C=2.8+16	20000	8.50	0.113	0.480	0.295(-1)
	30000	8.33	0.115	0.483	0.319(-1)
	80000	7.45	0.990(-1)	0.485	0.381(-1)
$3p^2P^0$–$7d^2D^*$	2500	8.15	0.976(-1)	0.520	0.230(-1)
4496.6 Å	5000	11.0	0.117	0.715	0.282(-1)
	10000	13.6	0.133	0.810	0.333(-1)
C=1.7+16	20000	14.9	0.135	0.844	0.386(-1)
	30000	15.5	0.128	0.853	0.418(-1)
	80000	18.1	0.965(-1)	0.861	0.502(-1)

impact shift for $3p^2P^0$–$8s^2S$ line at 2500 K, which is equal to zero due to the influence of Debye shielding (see Ref. 13). The case of the $4s^2S$–np^2P^0 series is more complicated. There is not a dominant perturbing level. Moreover, the nearest perturbing level is not the most important one. If $f_{jj'}$ is the oscillator strength and $\Delta E_{jj'}$ the energy difference between the perturbing (j') and the np^2P^0 level (j), then the influence of a perturbing level may be estimated as $f_{jj'}/|\Delta E_{jj'}|$. For example, for the $4p^2P^0$ level, the relative influence of the principal perturbing levels is $4d$:$3d$:$4s$ = 2.1:1.8:1. The behaviour of Stark-broadening parameters is now more complicated than in the previous case. For the electron- and proton-impact widths presented in Figs. 7 and 8, we find a regular increase with an increase of n_i, except for the last member of the series. For the $4s^2S$–$8p^2P^0$ electron- and proton-impact line widths, we have a small decrease relative to the $4s^2S$–$7p^2P^0$ line widths, which is probably caused by the influence of Debye shielding and the fact that it is more difficult to obtain a relatively complete set of perturbing levels for higher members of a series.

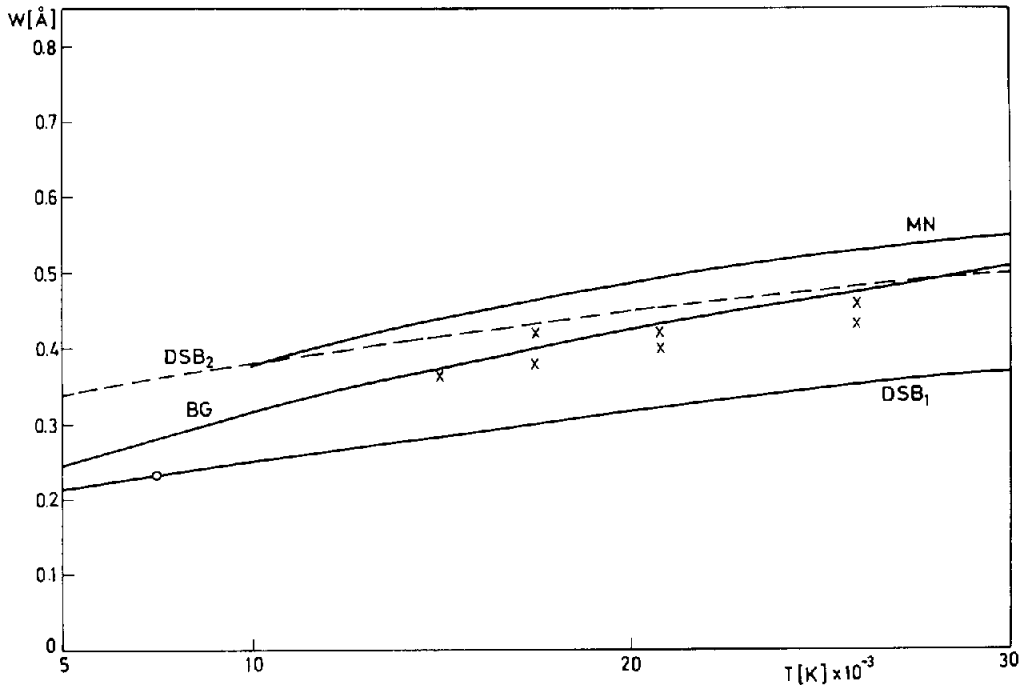

Fig. 1. Full halfwidths for the Na(I) $3s^2S$–$3p^2P^0$ multiplet (λ = 5891.8 Å), as a function of electron temperature; $N_e = 10^{17}$ cm^{-3}. Experimental points: O, Baur and Cooper (Ref. 10); ×, Purić *et al.* (Ref. 11). Calculations: BG, Benett and Griem (Ref. 8); MN, Mazure and Nollez (Ref. 9); DSB_1, present calculations (quasistatic ion-broadening); DSB_2, present calculations (ion-broadening within the impact approximation).

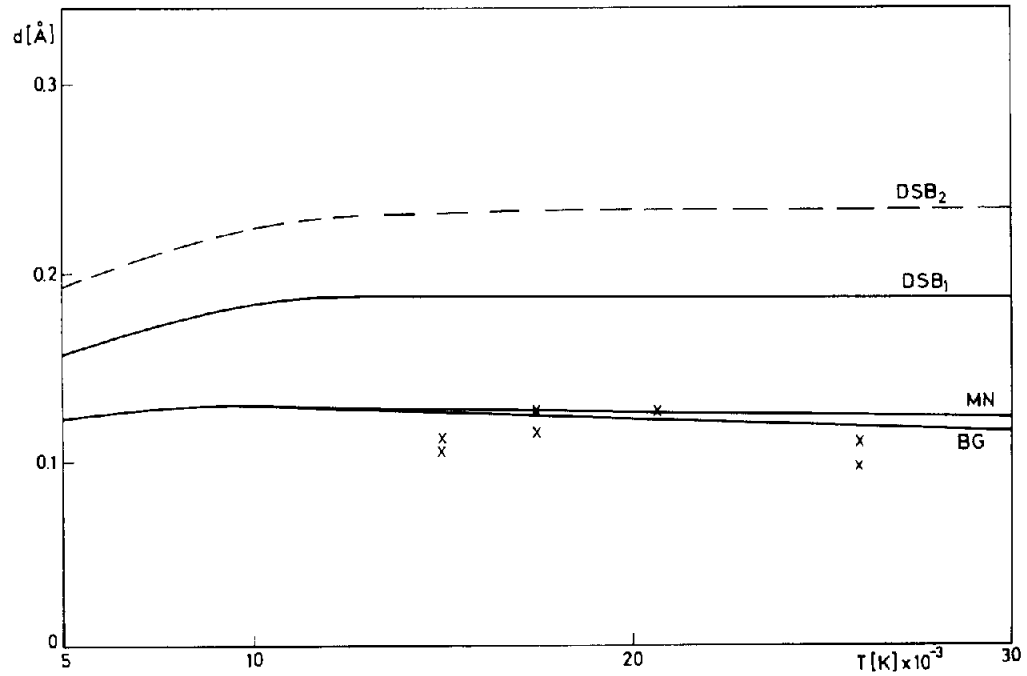

Fig. 2. As in Fig. 1 but for the line shift.

Table 2. Ar^+ impact-broadening parameters at an electron density of 10^{16} cm^{-3}.

Transition	T [K]	$2w_i$ [Å]	d_i [Å]
$3s^2S$-$3p^2P^o$	2500	0.123(-1)	0.217(-2)
5891.8 Å	5000	0.124(-1)	0.252(-2)
	10000	0.125(-1)	0.289(-2)
	20000	0.126(-1)	0.328(-2)
	30000	0.126(-1)	0.353(-2)
	80000	0.128(-1)	0.423(-2)

Electron- and proton-impact shifts for the $4s^2S$–np^2P^0 series are presented in Table 3. For lower members of the series, the shift is negative (blue) due to the larger polarization of the lower level of the transition. The shift is a function of R_3, $f_{jj'}/|\Delta E_{jj'}|$ and $b_2(\rho|\Delta E_{jj'}|/v)$, where b_2 is the GBKO function.[20] R_3 and $f_{jj'}/|\Delta E_{jj'}|$ increase within this series. On the other hand, b_2 is a decreasing function of $Z_{jj'} = \rho|\Delta E_{jj'}|/v$ and the decrease is especially fast for lower values of $Z_{jj'}$. For the most important perturbing levels, the $Z_{jj'}$ values are lower for the upper than for the lower transition level, and the b_2 functions are more strongly influenced by an increase of R_3, which excludes the lowest ρ values and, consequently, the largest b_2 values. Therefore, if the increase of $f_{jj'}/|\Delta E_{jj'}|$ cannot compensate for the decrease of b_2, the shift may even decrease for lower members of a series, as in the present case. The influence of the upper level for lower n_i then decrease with an increase of n_i, while the contribution of the lower level is not so sensitive to a change of R_3. Moreover, for the higher members of the series, the shift becomes positive owing to an increase of the upper level contribution, which is caused by the dominant influence

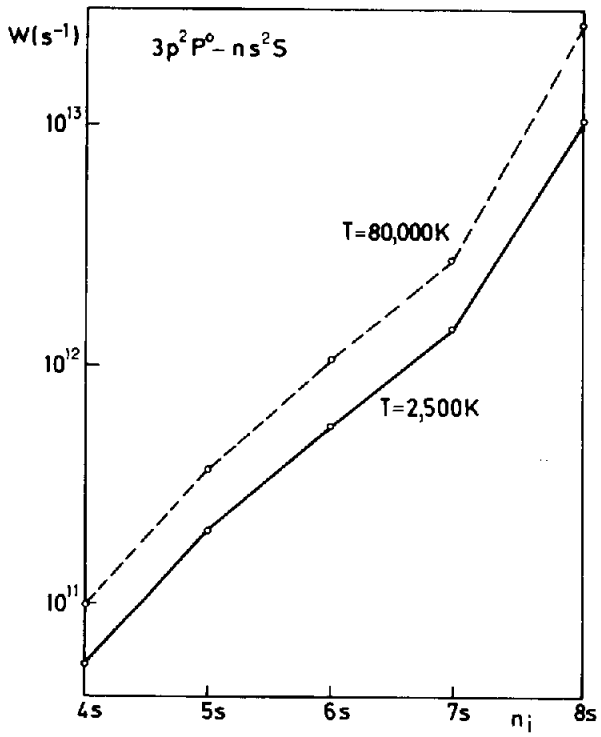

Fig. 3. Electron-impact full halfwidths for Na(I) $3p^2P^0$–ns^2S lines as a function of n_i for T = 2500 and 80,000 K at $N_e = 10^{16}$ cm^{-3}.

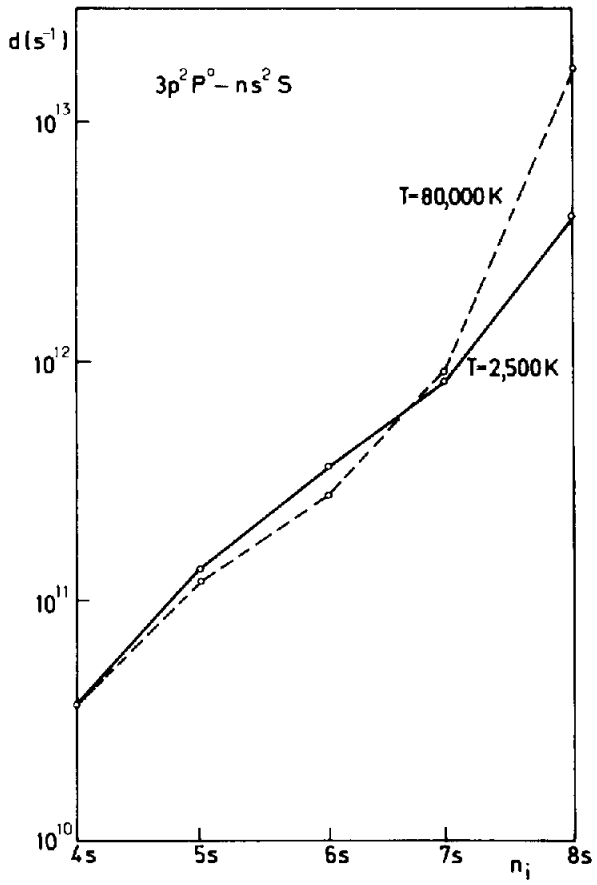

Fig. 4. As in Fig. 3 but for the electron-impact shift.

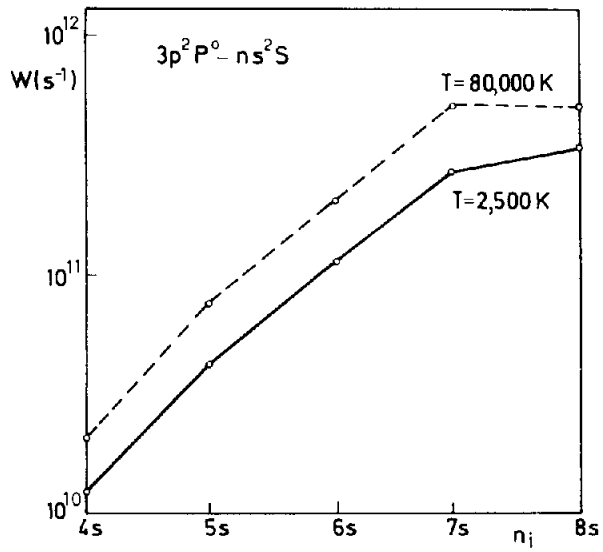

Fig. 5. As in Fig. 3 but for the proton-impact full halfwidth.

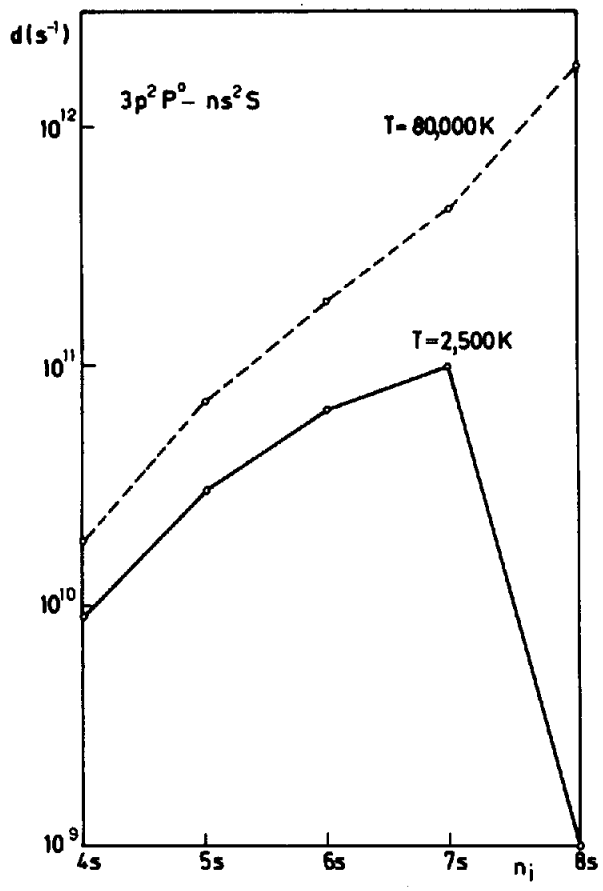

Fig. 6. As in Fig. 3 but for the proton-impact shift.

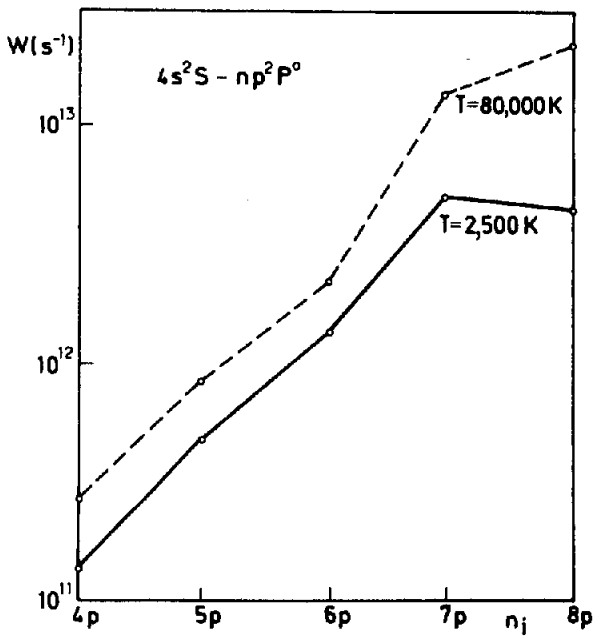

Fig. 7. Electron-impact full halfwidths for Na(I) $4s^2S$–np^2P^0 lines as a function of n_i for T = 2500 and 80,000 K at $N_e = 10^{16}$ cm^{-3}.

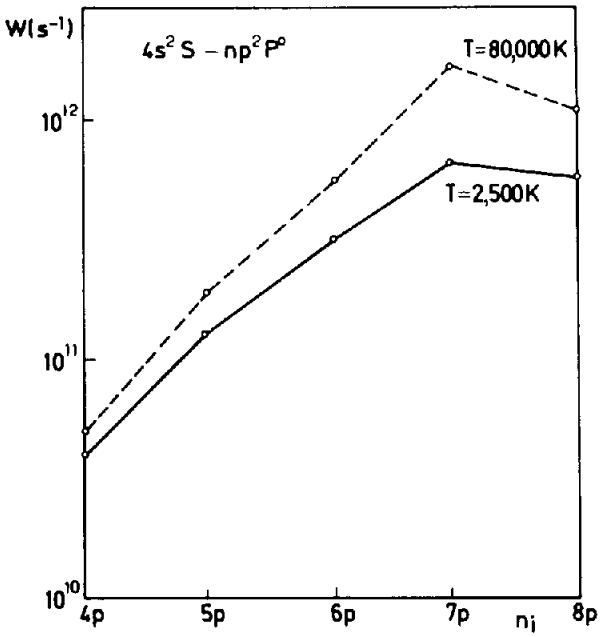

Fig. 8. As in Fig. 7 but for the proton-impact full halfwidth.

Table 3. The electron- and proton-impact shifts for Na(I) $4s^2S$–np^2P^0 lines as a function of n_i for T = 2500 and T = 80,000 K at an electron density of 10^{16} cm^{-3}.

Transition	Electrons		Protons	
	d(s^{-1}) at 2,500 K	d(s^{-1})at 80,000 K	d(s^{-1})at 2,500 K	d(s^{-1})at 80,000 K
4s^{2}S-4p^{2}P^o	-6.96(+10)	-2.49(+10)	-1.63(+10)	-3.43(+10)
4s^{2}S-5p^{2}P^o	-2.53(+11)	-8.40(+10)	-5.36(+10)	-1.42(+11)
4s^{2}S-6p^{2}P^o	-7.47(+11)	-2.18(+11)	-9.99(+10)	-4.28(+11)
4s^{2}S-7p^{2}P^o	+1.92(+12)	+7.19(+12)	+2.21(+10)	+1.36(+12)
4s^{2}S-8p^{2}P^o	+4.02(+10)	+5.44(+10)	+1.03(+10)	+2.10(+10)

of an increase in $f_{jj'}/|\Delta E_{jj'}|$. These situations occur, because for higher members of the series, the atom is larger, the lowest impact parameters are excluded by cut-off, and for larger values of $Z_{jj'}$, the b_2 function is not so sensitive to changes of R_3.

REFERENCES

1. H. R. Griem, *Spectral Line Broadening by Plasmas*. Academic, New York (1974).
2. B. Caccin, M. T. Gomez and G. Roberti, *Astron. Astrophys.* **92,** 63 (1980).
3. I. Vince, M. S. Dimitrijević and V. Kršljanin, in *Spectral Line Shapes*. (Edited by F. Rostas), Vol. 3. Gruyter, Berlin (1985).
4. H. P. Stormberg, *J. Appl. Phys.* **51,** 1963 (1980).
5. D. O. Wharmby, *IEEE Proc.* **127,** 165 (1980).
6. S. Sahal-Bréchot, *Astron. Astrophys.* **1,** 91 (1969).
7. S. Sahal-Bréchot, *Astron. Astrophys.* **2,** 322 (1960).
8. S. M. Benett and H. R. Griem, University of Maryland, Technical Report no 71-097, College Park, Maryland (1971); see also Ref. 1.
9. A. Mazure and G. Nollez, *Z. Naturforsch.* **31a,** 1575 (1978).
10. J. F. Baur and J. Cooper, *JQSRT* **17,** 311 (1977).
11. J. Purić, J. Labat, S. Djeniže, Lj. Cirković and I. Lakicević, *Phys. Lett.* **56A,** 83 (1976).
12. M. S. Dimitrijević and S. Sahal-Bréchot, *JQSRT* **31,** 301 (1984).
13. M. S. Dimitrijević and S. Sahal-Bréchot, *Astron. Astrophys.* **136,** 289 (1984).

14. S. Bashkin and J. O. Stoner Jr., *Atomic Energy Levels and Grotrian Diagrams.* Vol. 1. North Holland, Amsterdam (1975).
15. D. R. Bates and A. Damgaard, *Philos. Trans. R. Soc. London Ser. A* **242,** 101 (1949).
16. G. K. Oertel and L. P. Shomo, *Astrophys. J. Suppl. Series* **16,** 175 (1968).
17. W. L. Wiese, M. W. Smith and B. M. Miles, "Atomic Transition Probabilities," Vol. II, U.S. Government Printing Office, Washington D.C. (1969).
18. H. Van Regemorter, Hoang Binh Dy and M. Prud'homme, *J. Phys. B* **12,** 1073 (1979).
19. A. Brissaud, C. Goldbach, J. Léorat, A. Mazure and G. Nollez, *J. Phys. B* **9,** 1147 (1976).
20. H. R. Griem, M. Baranger, A. C. Kolb and G. K. Oertel, *Phys. Rev.* **125,** 177 (1962).
21. A. Brissaud and U. Frisch, *JQSRT* **11,** 1767 (1971).
22. W. L. Wiese and N. Konjević, *JQSRT* **28,** 185 (1982).

J. Quant. Spectrosc. Radiat. Transfer Vol. 38, No. 1, pp. 37–45, 1987
Printed in Great Britain.

0022-4073/87 $3.00 + 0.00

STARK BROADENING OF NEUTRAL POTASSIUM LINES

M. S. DIMITRIJEVIĆ[1] and S. SAHAL-BRÉCHOT[2]

[1]Astronomical Observatory, Volgina 7, 11050 Beograd, Yugoslavia and [2]Laboratoire de Physique Atomique et Moléculaire et d'Instrumentation en Astrophysique, Unité Associée au C.N.R.S. No. 812, Observatoire de Paris-Meudon, 92190 Meudon, France

(*Received* 10 *November* 1986)

Abstract—Using a semiclassical approach, we have calculated electron–proton and Ar II impact line widths and shifts of 50 neutral potassium lines. The comprehensive set of results obtained is used for investigation of Stark-broadening-parameter regularities within the spectral series.

INTRODUCTION

Stark-broadening parameters for potassium lines are useful for a number of problems in plasma diagnostics, astrophysics, technology of high-pressure discharge lamps, etc. Pulsed lamps, at medium and high pressures, containing potassium vapors are important for neodymium laser optical pumping, since potassium lines coincide with absorption bands of laser material. Using the semiclassical-perturbation formalism,[1,2] we have calculated electron-, proton-, and Ar II-impact line widths and shifts of 50 neutral K lines. Our results are compared with available theoretical[3–5] and reliable experimental[6–8] data. The results obtained have also been used to continue our investigation of systematic trends among Stark-broadening parameters within spectral series.[9–11]

THEORY

The calculation procedure is well described elsewhere.[1,2,9] The final formulae for the full halfwidth ($2W$) and the shift (d) are, respectively,

$$2W = N_e \int_0^\infty v f(v)\,\mathrm{d}v \left[\sum_{i' \neq i} \sigma_{ii'}(v) + \sum_{f' \neq f} \sigma_{ff'}(v) + \sigma_{el}(v) \right], \tag{1}$$

$$d = N_e \int_0^\infty v f(v)\,\mathrm{d}v \int_{R_3}^{R_d} 2\pi\rho\,\mathrm{d}\rho\,\sin 2\phi_p. \tag{2}$$

Here, i and f denote, respectively, the initial and final levels and i', f' the corresponding perturbing levels, N_e is the electron density, $f(v)$ the velocity distribution function for electrons and ρ the impact parameter. Details concerning the calculations of inelastic (σ_{if}; $i = i, f$) and elastic (σ_{el}) cross sections, the phase shift (ϕ_p) and cutoffs are described in Ref. [1] (Section 1, Chap. 3). If we want to make certain that a line is isolated, we can use the parameter C defined in Ref. [9] and given in Table 1. If halfwidths are available for the electron concentration $N = 10^{15}\,\mathrm{cm}^{-3}$,

$$N_l(\mathrm{cm}^{-3}) = C/2\,W(\text{in Å at } N = 10^{15}\,\mathrm{cm}^{-3}). \tag{3}$$

For an electron concentration lower than N_l, the line can be treated as isolated in the core, even if weak forbidden components due to the failure of this approximation still appear in the wing.

RESULTS AND DISCUSSION

Energy levels used in our calculations were taken from Ref. [12]. Oscillator strengths have been calculated using the method of Bates and Damgaard[13] and tables of Oertel and Shomo.[14] For low-lying levels, the oscillator strengths were taken from Ref. [15]. For higher levels, the method described in Ref. [16] was used.

Table 1. This table lists electron-, proton- and Ar II-impact broadening parameters for K(I) lines at an electron density of $10^{15}\,cm^{-3}$ and temperatures from 2000 to 30,000 K. Transitions and averaged wavelengths for the multiplet (in Å) are also given. Under $2W_e$, $2W_p$ and $2W_A$ are given electron-, proton- and Ar II-impact full halfwidths, while d_e, d_p and d_A denote corresponding shifts

Perturbers are:		Electrons		Protons		Ionized argon	
Transition	T (K)	$2W_e$ (Å)	d_e (Å)	$2W_i$ (Å)	d_i (Å)	$2W_A$ (Å)	d_A (Å)
3 *d*–5 *p*	2000	0.551	0.311	0.209	0.805 E − 01	0.198	0.470 E − 01
31453 Å	5000	0.655	0.402	0.214	0.964 E − 01	0.202	0.574 E − 01
$C = 0.27$ E − 20	10,000	0.765	0.373	0.220	0.110	0.204	0.657 E − 01
	20,000	0.926	0.359	0.227	0.124	0.206	0.747 E − 01
	30,000	1.04	0.309	0.232	0.134	0.208	0.803 E − 01
3 *d*–6 *p*	2000	0.335	0.209	0.130	0.522 E − 01	0.118	0.291 E − 01
13384 Å	5000	0.410	0.270	0.135	0.643 E − 01	0.124	0.374 E − 01
$C = 0.21$ E + 19	10,000	0.480	0.262	0.139	0.740 E − 01	0.126	0.438 E − 01
	20,000	0.569	0.241	0.145	0.843 E − 01	0.128	0.504 E − 01
	30,000	0.632	0.207	0.149	0.907 E − 01	0.130	0.544 E − 01
3 *d*–7 *p*	2000	0.531	0.338	0.194	0.768 E − 01	0.165	0.400 E − 01
10482 Å	5000	0.655	0.415	0.205	0.986 E − 01	0.184	0.557 E − 01
$C = 0.68$ E + 18	10,000	0.772	0.420	0.213	0.115	0.190	0.670 E − 01
	20,000	0.924	0.348	0.223	0.133	0.194	0.784 E − 01
	30,000	1.03	0.299	0.229	0.143	0.197	0.852 E − 01
3 *d*–8 *p*	2000	0.923	0.564	0.312	0.118	0.235	0.549 E − 01
9348.6 Å	5000	1.14	0.676	0.338	0.161	0.292	0.869 E − 01
$C = 0.32$ E + 18	10,000	1.36	0.646	0.354	0.192	0.309	0.109
	20,000	1.64	0.534	0.371	0.223	0.319	0.130
	30,000	1.83	0.467	0.383	0.242	0.324	0.143
3 *d*–9 *p*	2000	1.58	0.942	0.484	0.171	0.312	0.647 E − 01
8764.8 Å	5000	1.96	1.07	0.546	0.253	0.447	0.129
$C = 0.18$ E + 18	10,000	2.36	1.03	0.577	0.311	0.491	0.171
	20,000	2.88	0.827	0.609	0.368	0.515	0.211
	30,000	3.18	0.703	0.629	0.402	0.525	0.234
4 *s*–4 *p*	2000	0.430 E − 02	0.324 E − 02	0.276 E − 02	0.887 E − 03	0.270 E − 02	0.530 E − 03
7676.2 Å	5000	0.486 E − 02	0.408 E − 02	0.280 E − 02	0.105 E − 02	0.271 E − 02	0.630 E − 03
$C = 0.47$ E + 19	10,000	0.572 E − 02	0.492 E − 02	0.284 E − 02	0.119 E − 02	0.273 E − 02	0.714 E − 03
	20,000	0.729 E − 02	0.595 E − 02	0.288 E − 02	0.135 E − 02	0.274 E − 02	0.810 E − 03
	30,000	0.861 E − 02	0.518 E − 02	0.288 E − 02	0.144 E − 02	0.275 E − 02	0.873 E − 03
4 *s*–5 *p*	2000	0.926 E − 02	0.567 E − 02	0.403 E − 02	0.150 E − 02	0.384 E − 02	0.874 E − 03
4045.2 Å	5000	0.110 E − 01	0.727 E − 02	0.413 E − 02	0.180 E − 02	0.391 E − 02	0.107 E − 02
$C = 0.44$ E + 18	10000	0.125 E − 01	0.780 E − 02	0.424 E − 02	0.205 E − 02	0.395 E − 02	0.123 E − 02
	20,000	0.145 E − 01	0.757 E − 02	0.436 E − 02	0.232 E − 02	0.399 E − 02	0.140 E − 02
	30,000	0.158 E − 01	0.688 E − 02	0.445 E − 02	0.250 E − 02	0.402 E − 02	0.150 E − 02
4 *s*–6 *p*	2000	0.221 E − 01	0.140 E − 01	0.904 E − 02	0.352 E − 02	0.828 E − 02	0.196 E − 02
3446.7 Å	5000	0.271 E − 01	0.174 E − 01	0.939 E − 02	0.434 E − 02	0.869 E − 02	0.253 E − 02
$C = 0.14$ E + 18	10,000	0.315 E − 01	0.183 E − 01	0.968 E − 02	0.500 E − 02	0.884 E − 02	0.296 E − 02
	20,000	0.371 E − 01	0.172 E − 01	0.100 E − 01	0.569 E − 02	0.898 E − 02	0.340 E − 02
	30,000	0.409 E − 01	0.150 E − 01	0.103 E − 01	0.613 E − 02	0.907 E − 02	0.368 E − 02
4 *s*–7 *p*	2000	0.498 E − 01	0.313 E − 01	0.187 E − 01	0.727 E − 02	0.159 E − 01	0.378 E − 02
3217.3 Å	5000	0.615 E − 01	0.409 E − 01	0.197 E − 01	0.933 E − 02	0.178 E − 01	0.527 E − 02
$C = 0.64$ E + 17	10,000	0.723 E − 01	0.383 E − 01	0.205 E − 01	0.109 E − 01	0.183 E − 01	0.634 E − 02
	20,000	0.863 E − 01	0.339 E − 01	0.214 E − 01	0.125 E − 01	0.187 E − 01	0.742 E − 02
	30,000	0.958 E − 01	0.293 E − 01	0.219 E − 01	0.135 E − 01	0.190 E − 01	0.806 E − 02
4 *s*–8 *p*	2000	0.101	0.621 E − 01	0.346 E − 01	0.130 E − 01	0.262 E − 01	0.604 E − 02
3101.9 Å	5000	0.125	0.748 E − 01	0.375 E − 01	0.177 E − 01	0.325 E − 01	0.957 E − 02
$C = 0.36$ E + 17	10,000	0.149	0.740 E − 01	0.393 E − 01	0.211 E − 01	0.344 E − 01	0.120 E − 01
	20,000	0.180	0.598 E − 01	0.412 E − 01	0.246 E − 01	0.355 E − 01	0.143 E − 01
	30,000	0.200	0.518 E − 01	0.424 E − 01	0.267 E − 01	0.361 E − 01	0.157 E − 01
4 *s*–9 *p*	2000	0.189	0.113	0.583 E − 01	0.205 E − 01	0.375 E − 01	0.776 E − 02
3034.8 Å	5000	0.235	0.129	0.657 E − 01	0.304 E − 01	0.539 E − 01	0.154 E − 01
$C = 0.22$ E + 17	10,000	0.282	0.124	0.695 E − 01	0.373 E − 01	0.593 E − 01	0.205 E − 01
	20,000	0.344	0.976 E − 01	0.733 E − 01	0.441 E − 01	0.620 E − 01	0.253 E − 01
	30,000	0.380	0.852 E − 01	0.757 E − 01	0.482 E − 01	0.633 E − 01	0.280 E − 01
3 *d*–4 *f*	2000	0.252	−0.110	0.584 E − 01	−0.337 E − 01	0.504 E − 01	−0.193 E − 01
15165 Å	5000	0.294	−0.684 E − 01	0.627 E − 01	−0.407 E − 01	0.525 E − 01	−0.240 E − 01
$C = 0.17$ E + 19	10,000	0.354	−0.355 E − 01	0.666 E − 01	−0.465 E − 01	0.541 E − 01	−0.277 E − 01
	20,000	0.404	−0.147 E − 01	0.713 E − 01	−0.527 E − 01	0.561 E − 01	−0.317 E − 01
	30,000	0.431	−0.736 E − 02	0.745 E − 01	−0.567 E − 01	0.575 E − 01	−0.341 E − 01
3 *d*–5 *f*	2000	2.15	0.123	0.789	0.385	0.426	0.969 E − 01
11022.3 Å	5000	1.99	0.277 E − 01	0.946	0.647	0.564	0.301
$C = 0.14$ E + 17	10,000	1.85	0.147 E − 01	1.08	0.825	0.640	0.435
	20,000	1.71	−0.258 E − 02	1.25	1.01	0.719	0.558
	30,000	1.62	−0.368 E − 02	1.34	1.15	0.770	0.627
4 *p*–5 *s*	2000	0.556 E − 01	0.386 E − 01	0.132 E − 01	0.104 E − 01	0.955 E − 02	0.611 E − 02
12492 Å	5000	0.673 E − 01	0.515 E − 01	0.149 E − 01	0.125 E − 01	0.104 E − 01	0.743 E − 02
$C = 0.58$ E + 19	10,000	0.752 E − 01	0.581 E − 01	0.165 E − 01	0.141 E − 01	0.112 E − 01	0.849 E − 02
	20,000	0.831 E − 01	0.536 E − 01	0.182 E − 01	0.160 E − 01	0.122 E − 01	0.964 E − 02
	30,000	0.912 E − 01	0.522 E − 01	0.192 E − 01	0.173 E − 01	0.128 E − 01	0.104 E − 01

continued opposite

Table 1—*continued*

Perturbers are:		*Electrons*		*Protons*		*Ionized argon*	
Transition	T (K)	$2W_e$ (Å)	d_e (Å)	$2W_i$ (Å)	d_i (Å)	$2W_A$ (Å)	d_A (Å)
$4p$–$6s$	2000	0.627 E − 01	0.451 E − 01	0.138 E − 01	0.116 E − 01	0.852 E − 02	0.654 E − 02
6929.5 Å	5000	0.764 E − 01	0.566 E − 01	0.160 E − 01	0.142 E − 01	0.986 E − 02	0.833 E − 02
C = 0.75 E + 18	10,000	0.817 E − 01	0.625 E − 01	0.180 E − 01	0.163 E − 01	0.110 E − 01	0.969 E − 02
	20,000	0.907 E − 01	0.612 E − 01	0.202 E − 01	0.186 E − 01	0.123 E − 01	0.111 E − 01
	30,000	0.941 E − 01	0.538 E − 01	0.216 E − 01	0.200 E − 01	0.132 E − 01	0.120 E − 01
$4p$–$7s$	2000	0.119	0.841 E − 01	0.255 E − 01	0.201 E − 01	0.155 E − 01	0.106 E − 01
5795.3 Å	5000	0.151	0.109	0.297 E − 01	0.255 E − 01	0.181 E − 01	0.145 E − 01
C = 0.27 E + 18	10,000	0.154	0.109	0.333 E − 01	0.297 E − 01	0.203 E − 01	0.173 E − 01
	20,000	0.169	0.963 E − 01	0.374 E − 01	0.341 E − 01	0.227 E − 01	0.202 E − 01
	30,000	0.184	0.878 E − 01	0.400 E − 01	0.368 E − 01	0.243 E − 01	0.220 E − 01
$4p$–$8s$	2000	0.223	0.151	0.450 E − 01	0.324 E − 01	0.272 E − 01	0.156 E − 01
5334.3 Å	5000	0.260	0.187	0.525 E − 01	0.432 E − 01	0.319 E − 01	0.237 E − 01
C = 0.13 E + 18	10,000	0.299	0.189	0.590 E − 01	0.512 E − 01	0.358 E − 01	0.293 E − 01
	20,000	0.323	0.158	0.662 E − 01	0.594 E − 01	0.402 E − 01	0.348 E − 01
	30,000	0.359	0.136	0.708 E − 01	0.644 E − 01	0.430 E − 01	0.381 E − 01
$4p$–$9s$	2000	0.412	0.272	0.834 E − 01	0.520 E − 01	0.490 E − 01	0.209 E − 01
5094.3 Å	5000	0.475	0.338	0.976 E − 01	0.752 E − 01	0.591 E − 01	0.389 E − 01
C = 0.76 E + 17	10,000	0.537	0.316	0.110	0.916 E − 01	0.666 E − 01	0.508 E − 01
	20,000	0.623	0.260	0.123	0.108	0.747 E − 01	0.621 E − 01
	30,000	0.695	0.227	0.132	0.118	0.800 E − 01	0.687 E − 01
$4p$–$10s$	2000	0.702	0.450	0.139	0.721 E − 01	0.758 E − 01	0.206 E − 01
4951.4 Å	5000	0.807	0.517	0.164	0.117	0.987 E − 01	0.556 E − 01
C = 0.48 E + 17	10,000	0.924	0.497	0.184	0.147	0.112	0.786 E − 01
	20,000	1.11	0.395	0.207	0.176	0.126	0.996 E − 01
	30,000	1.23	0.341	0.221	0.194	0.134	0.111
$4p$–$11s$	2000	1.12	0.680	0.212	0.869 E − 01	0.103	0.117 E − 01
4859 Å	5000	1.31	0.763	0.258	0.167	0.153	0.707 E − 01
C = 0.33 E + 17	10,000	1.52	0.702	0.290	0.220	0.176	0.112
	20,000	1.87	0.550	0.326	0.270	0.198	0.148
	30,000	2.06	0.498	0.349	0.298	0.212	0.169
$4p$–$12s$	2000	1.71	0.987	0.291	0.883 E − 01	0.135	0.241 E − 02
4795.7 Å	5000	2.06	1.08	0.372	0.217	0.214	0.781 E − 01
C = 0.24 E + 17	10,000	2.38	0.904	0.420	0.301	0.253	0.144
	20,000	2.98	0.715	0.472	0.378	0.286	0.203
	30,000	3.27	0.648	0.506	0.422	0.307	0.234
$4p$–$3d$	2000	0.246 E − 01	0.125 E − 01	0.867 E − 02	0.322 E − 02	0.837 E − 02	0.192 E − 02
11745 Å	5000	0.268 E − 01	0.139 E − 01	0.886 E − 02	0.381 E − 02	0.844 E − 02	0.229 E − 02
C = 0.44 E + 19	10,000	0.302 E − 01	0.137 E − 01	0.906 E − 02	0.432 E − 02	0.850 E − 02	0.260 E − 02
	20,000	0.373 E − 01	0.108 E − 01	0.928 E − 02	0.491 E − 02	0.858 E − 02	0.294 E − 02
	30,000	0.435 E − 01	0.912 E − 02	0.936 E − 02	0.527 E − 02	0.864 E − 02	0.317 E − 02
$4p$–$4d$	2000	0.734 E − 01	0.530 E − 01	0.194 E − 01	0.128 E − 01	0.154 E − 01	0.715 E − 02
6955.2 Å	5000	0.837 E − 01	0.597 E − 01	0.214 E − 01	0.157 E − 01	0.164 E − 01	0.914 E − 02
C = 0.35 E + 18	10,000	0.909 E − 01	0.576 E − 01	0.232 E − 01	0.180 E − 01	0.173 E − 01	0.107 E − 01
	20,000	0.998 E − 01	0.450 E − 01	0.253 E − 01	0.205 E − 01	0.183 E − 01	0.123 E − 01
	30,000	0.107	0.386 E − 01	0.267 E − 01	0.220 E − 01	0.190 E − 01	0.132 E − 01
$4p$–$5d$	2000	0.159	0.112	0.408 E − 01	0.251 E − 01	0.309 E − 01	0.130 E − 01
5825.3 Å	5000	0.181	0.126	0.454 E − 01	0.323 E − 01	0.341 E − 01	0.182 E − 01
C = 0.14 E + 18	10,000	0.197	0.126	0.494 E − 01	0.378 E − 01	0.362 E − 01	0.219 E − 01
	20,000	0.220	0.950 E − 01	0.540 E − 01	0.435 E − 01	0.385 E − 01	0.257 E − 01
	30,000	0.235	0.821 E − 01	0.570 E − 01	0.470 E − 01	0.401 E − 01	0.280 E − 01
$4p$–$6d$	2000	0.322	0.224	0.795 E − 01	0.439 E − 01	0.555 E − 01	0.197 E − 01
5354.1 Å	5000	0.364	0.247	0.896 E − 01	0.607 E − 01	0.656 E − 01	0.324 E − 01
C = 0.74 E + 17	10,000	0.398	0.226	0.978 E − 01	0.729 E − 01	0.706 E − 01	0.411 E − 01
	20,000	0.452	0.176	0.107	0.851 E − 01	0.756 E − 01	0.495 E − 01
	30,000	0.482	0.156	0.113	0.925 E − 01	0.788 E − 01	0.544 E − 01
$4p$–$7d$	2000	0.604	0.392	0.142	0.677 E − 01	0.883 E − 01	0.226 E − 01
5107.2 Å	5000	0.682	0.424	0.165	0.104	0.116	0.515 E − 01
C = 0.43 E + 17	10,000	0.752	0.383	0.181	0.130	0.128	0.704 E − 01
	20,000	0.863	0.299	0.198	0.155	0.138	0.880 E − 01
	30,000	0.916	0.270	0.210	0.169	0.145	0.980 E − 01
$4p$–$8d$	2000	1.06	0.687	0.233	0.883 E − 01	0.120	0.145 E − 01
4960.2 Å	5000	1.20	0.737	0.283	0.164	0.188	0.710 E − 01
C = 0.28 E + 17	10,000	1.34	0.611	0.313	0.214	0.216	0.110
	20,000	1.54	0.481	0.345	0.261	0.237	0.145
	30,000	1.62	0.435	0.365	0.289	0.249	0.164
$4p$–$9d$	2000	1.75	1.06	0.348	0.896 E − 01	0.174	0.170 E − 02
4865.2 Å	5000	1.99	1.12	0.455	0.233	0.277	0.809 E − 01
C = 0.19 E + 17	10,000	2.24	0.907	0.510	0.327	0.342	0.155
	20,000	2.58	0.741	0.565	0.413	0.383	0.220
	30,000	2.70	0.649	0.599	0.462	0.404	0.255

continued overleaf

Table 1—*continued*

Perturbers are:		*Electrons*		*Protons*		*Ionized argon*	
Transition	T (K)	$2W_e$ (Å)	d_e (Å)	$2W_i$ (Å)	d_i (Å)	$2W_A$ (Å)	d_A (Å)
$4d$–$6p$	2000	6.08	1.51	2.29	0.359	2.20	0.209
62191 Å	5000	9.35	2.20	2.31	0.430	2.28	0.256
$C = 0.28$ E + 20	10,000	12.7	2.38	2.32	0.489	2.30	0.293
	20,000	16.5	2.03	2.33	0.555	2.30	0.333
	30,000	18.8	1.76	2.33	0.597	2.31	0.359
$4d$–$7p$	2000	3.46	1.99	1.20	0.453	1.04	0.239
27199 Å	5000	4.51	2.30	1.26	0.578	1.15	0.328
$C = 0.46$ E + 19	10,000	5.61	2.27	1.30	0.673	1.18	0.392
	20,000	7.01	1.71	1.36	0.772	1.20	0.458
	30,000	7.87	1.54	1.39	0.834	1.22	0.497
$4d$–$8p$	2000	4.50	2.75	1.47	0.558	1.12	0.261
20691 Å	5000	5.69	3.12	1.59	0.756	1.38	0.410
$C = 0.16$ E + 19	10,000	6.90	2.94	1.66	0.901	1.46	0.512
	20,000	8.52	2.32	1.74	1.05	1.50	0.612
	30,000	9.50	1.99	1.80	1.14	1.53	0.671
$4d$–$4f$	2000	42.1	−26.2	7.76	−6.02	5.22	−3.34
136900 Å	5000	48.4	−27.6	8.88	−7.45	5.86	−4.33
$C = 0.14$ E + 21	10,000	52.4	−22.7	9.87	−8.58	6.42	−5.07
	20,000	61.4	−17.3	11.0	−9.78	7.05	−5.84
	30,000	66.6	−14.9	11.7	−10.5	7.46	−6.32
$4d$–$5f$	2000	18.0	0.424	6.26	3.07	3.38	0.778
31162 Å	5000	17.1	−0.648	7.51	5.14	4.46	2.39
$C = 0.11$ E + 18	10,000	15.9	−0.862	8.60	6.56	5.07	3.46
	20,000	15.0	−0.748	9.90	8.03	5.70	4.43
	30,000	14.5	−0.794	10.6	9.00	6.10	4.98
$5s$–$5p$	2000	0.339	0.131	0.174	0.335 E − 01	0.171	0.197 E − 01
27114 Å	5000	0.416	0.119	0.175	0.398 E − 01	0.173	0.238 E − 01
$C = 0.20$ E + 20	10,000	0.544	0.743 E − 01	0.176	0.451 E − 01	0.174	0.271 E − 01
	20,000	0.746	0.414 E − 01	0.177	0.512 E − 01	0.174	0.307 E − 01
	30,000	0.882	0.305 E − 01	0.177	0.552 E − 01	0.174	0.331 E − 01
$5s$–$6p$	2000	0.287	0.179	0.118	0.434 E − 01	0.109	0.243 E − 01
12531 Å	5000	0.352	0.213	0.122	0.535 E − 01	0.114	0.311 E − 01
$C = 0.19$ E + 19	10,000	0.420	0.219	0.126	0.614 E − 01	0.116	0.364 E − 01
	20,000	0.510	0.177	0.130	0.699 E − 01	0.118	0.418 E − 01
	30,000	0.577	0.141	0.132	0.753 E − 01	0.119	0.452 E − 01
$5s$–$7p$	2000	0.476	0.302	0.178	0.685 E − 01	0.152	0.357 E − 01
9951.3 Å	5000	0.588	0.360	0.188	0.878 E − 01	0.170	0.496 E − 01
$C = 0.62$ E + 18	10,000	0.699	0.364	0.195	0.103	0.175	0.597 E − 01
	20,000	0.843	0.287	0.203	0.118	0.179	0.698 E − 01
	30,000	0.943	0.246	0.208	0.127	0.181	0.759 E − 01
$5s$–$8p$	2000	0.840	0.519	0.286	0.107	0.216	0.498 E − 01
8924.4 Å	5000	1.04	0.604	0.310	0.146	0.269	0.788 E − 01
$C = 0.29$ E + 18	10,000	1.24	0.580	0.324	0.174	0.284	0.988 E − 01
	20,000	1.51	0.465	0.340	0.202	0.293	0.118
	30,000	1.68	0.402	0.350	0.220	0.298	0.130
$5s$–$9p$	2000	1.45	0.884	0.445	0.157	0.286	0.593 E − 01
8390.7 Å	5000	1.80	1.00	0.502	0.232	0.412	0.118
$C = 0.17$ E + 18	10,000	2.16	0.927	0.531	0.284	0.453	0.157
	20,000	2.65	0.722	0.560	0.336	0.474	0.193
	30,000	2.92	0.639	0.578	0.367	0.484	0.214
$5p$–$6s$	2000	1.70	1.12	0.431	0.279	0.348	0.158
36529 Å	5000	2.09	1.42	0.473	0.340	0.369	0.200
$C = 0.21$ E + 20	10,000	2.46	1.50	0.510	0.390	0.387	0.232
	20,000	2.95	1.27	0.554	0.443	0.408	0.266
	30,000	3.38	1.05	0.583	0.477	0.422	0.286
$5p$–$7s$	2000	1.15	0.761	0.246	0.188	0.158	0.995 E − 01
17979 Å	5000	1.39	1.12	0.284	0.238	0.180	0.136
$C = 0.26$ E + 19	10,000	1.54	0.967	0.317	0.277	0.200	0.162
	20,000	1.74	0.862	0.354	0.318	0.222	0.189
	30,000	1.96	0.781	0.378	0.343	0.236	0.205
$5p$–$8s$	2000	1.61	1.11	0.332	0.236	0.202	0.113
14178 Å	5000	1.88	1.34	0.387	0.316	0.237	0.173
$C = 0.93$ E + 18	10,000	2.17	1.36	0.434	0.375	0.266	0.214
	20,000	2.41	1.09	0.487	0.435	0.297	0.255
	30,000	2.71	0.942	0.521	0.471	0.318	0.279
$5p$–$9s$	2000	2.53	1.70	0.509	0.317	0.300	0.128
12600 Å	5000	2.90	2.02	0.596	0.458	0.362	0.237
$C = 0.46$ E + 18	10,000	3.32	1.95	0.669	0.558	0.407	0.310
	20,000	3.89	1.53	0.751	0.658	0.457	0.379
	30,000	4.36	1.33	0.803	0.717	0.488	0.419

continued opposite

Table 1—*continued*

Perturbers are:		*Electrons*		*Protons*		*Ionized argon*	
Transition	T (K)	$2W_e$ (Å)	d_e (Å)	$2W_i$ (Å)	d_i (Å)	$2W_A$ (Å)	d_A (Å)
$5p$–$10s$	2000	3.96	2.53	0.781	0.407	0.428	0.116
11761 Å	5000	4.56	2.89	0.924	0.657	0.557	0.314
$C = 0.27\,E + 18$	10,000	5.23	2.76	1.04	0.829	0.630	0.443
	20,000	6.34	2.19	1.17	0.994	0.708	0.561
	30,000	7.06	1.88	1.25	1.09	0.758	0.628
$5p$–$11s$	2000	6.00	3.64	1.14	0.466	0.552	0.629 E − 01
11253 Å	5000	7.02	4.06	1.38	0.894	0.819	0.379
$C = 0.18\,E + 18$	10,000	8.17	3.72	1.56	1.18	0.941	0.599
	20,000	10.1	2.91	1.75	1.44	1.06	0.795
	30,000	11.2	2.56	1.87	1.60	1.14	0.904
$5p$–$4d$	2000	1.97	1.36	0.493	0.323	0.393	0.182
37255 Å	5000	2.32	1.34	0.542	0.395	0.419	0.231
$C = 0.10\,E + 20$	10,000	2.69	0.996	0.587	0.453	0.440	0.269
	20,000	3.38	0.750	0.639	0.515	0.465	0.308
	30,000	3.74	0.647	0.673	0.554	0.482	0.333
$5p$–$5d$	2000	1.55	1.11	0.380	0.242	0.282	0.125
18272 Å	5000	1.76	1.20	0.425	0.311	0.312	0.175
$C = 0.14\,E + 19$	10,000	1.95	1.05	0.464	0.363	0.333	0.211
	20,000	2.26	0.801	0.509	0.418	0.356	0.247
	30,000	2.46	0.723	0.539	0.452	0.372	0.269
$5p$–$6d$	2000	2.30	1.54	0.556	0.313	0.386	0.140
14319 Å	5000	2.60	1.66	0.628	0.432	0.454	0.231
$C = 0.53\,E + 18$	10,000	2.86	1.52	0.687	0.518	0.490	0.292
	20,000	3.29	1.17	0.754	0.605	0.527	0.352
	30,000	3.54	1.02	0.797	0.657	0.550	0.386
$5p$–$7d$	2000	3.73	2.41	0.870	0.417	0.538	0.139
12679 Å	5000	4.22	2.58	1.01	0.643	0.705	0.317
$C = 0.27\,E + 18$	10,000	4.66	2.31	1.11	0.799	0.778	0.433
	20,000	5.37	1.80	1.22	0.952	0.842	0.541
	30,000	5.72	1.58	1.29	1.04	0.881	0.603
$5p$–$8d$	2000	6.02	3.89	1.32	0.501	0.675	0.821 E − 01
11811 Å	5000	6.81	4.15	1.60	0.928	1.06	0.403
$C = 0.16\,E + 18$	10,000	7.60	3.39	1.77	1.21	1.22	0.622
	20,000	8.76	2.68	1.95	1.48	1.34	0.819
	30,000	9.25	2.43	2.07	1.64	1.40	0.929
$5p$–$9d$	2000	9.41	5.68	1.87	0.482	0.936	0.916 E − 02
11286 Å	5000	10.7	6.02	2.44	1.25	1.49	0.436
$C = 0.10\,E + 18$	10,000	12.1	4.84	2.74	1.76	1.83	0.834
	20,000	13.9	3.95	3.03	2.22	2.05	1.18
	30,000	14.6	3.45	3.22	2.48	2.17	1.37

Besides electron-impact full halfwidths ($2W_e$) and shifts (d_e), Stark-broadening parameters due to proton-impacts (for astrophysical purposes) and Ar II-impacts (for laboratory plasma diagnostics) have been calculated. Results obtained are shown in Table 1 for $N_e = 10^{15}\,\mathrm{cm}^{-3}$ and $T = 2000$, 5000, 10,000, 20,000, and 30,000 K. In Table 1, we also give a parameter denoted by C (see equation (3) and Ref. [9]), which can be used to determine if a line is isolated for the needed electron density.

In Fig. 1, our results for the K(I) $4s^2S$–$4p^2P^0$ multiplet ($\lambda = 7676.2$ Å) are compared with other calculations and with experimental values of Purić *et al.*,[6] where the perturbing ions were singly-ionized argon. In some cases, a controversy exists in the literature concerning the impact or quasistatic character of the ionic contribution to the line profile. For the Li(I) $2s$–$2p$ transition perturbed by Ar^+, the impact character of ionic profiles was pointed out by Brissaud *et al.*,[17] which is in contradiction to the GBKO[8] validity criteria for the impact approximation that are not satisfied in the present case. For the K(I) $4s$–$4p$ multiplet perturbed by Ar^+, the validity condition for the impact approximation given in Refs [1] and [2] is not fulfilled. On the other hand, if we use the collective Kubo number[19] for estimation of the character of the ionic profile, the ionic profile is of the purely impact type[5] for experimental conditions used in Refs [6] and [7]. Consequently, this contribution is added in both ways in order to show the difference.

In Table 2, our calculations are compared with experiments of Hohimer.[7,8] We conclude that our results, as well as calculations of Benett and Griem[3,4] when available and simple semiclassical estimates by Konjević,[20] are within the experimental error bars.

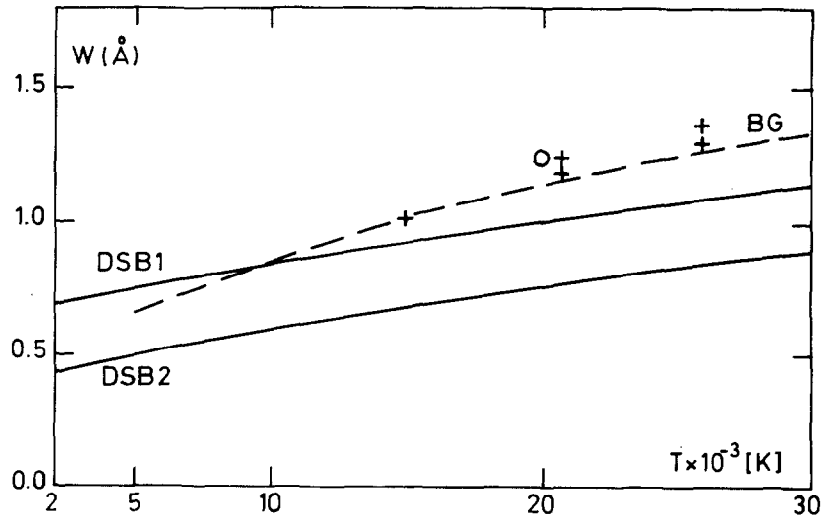

Fig. 1. Full halfwidths for the K(I) $4s\ ^2S$–$4p\ ^2P^0$ multiplet ($\lambda = 7676.2$ Å) as a function of electron temperature; $N_e = 10^{17}\,\mathrm{cm}^{-3}$. Experimental points: +, Puric *et al.* (Ref. [6]). Calculations: BG, Benett and Griem (Ref. [4]); O, Mazure and Nollez (Ref. [5]); DSB_1, present calculations (with impact ion-broadening); DSB_2, present calculations (quasistatic ion broadening).

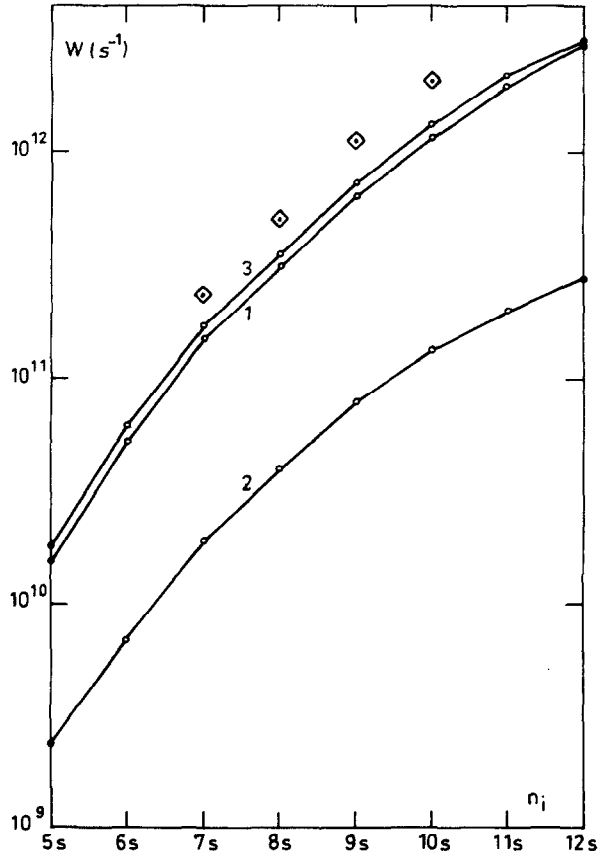

Fig. 2. Electron- (1), proton-impact (2) and total (3) full half-widths for K(I) $4p\ ^2P^0$–$ns\ ^2S$ lines as a function of n for the initial level (n_i) for $T = 2950$ K and $N_e = 2 \times 10^{15}\,\mathrm{cm}^{-3}$. ◇, experimental values of Hohimer.[7,8,20]

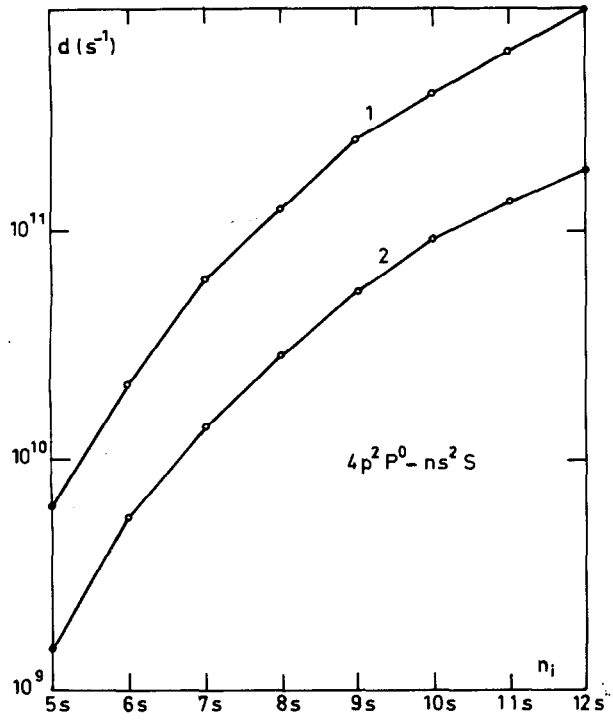

Fig. 3. Electron- and proton-impact (2) shifts for K(I) $4p\ ^2P^0$–$ns\ ^2S$ lines as a function of n_i for $T = 5000$ K and $N_e = 10^{15}$ cm^{-3}.

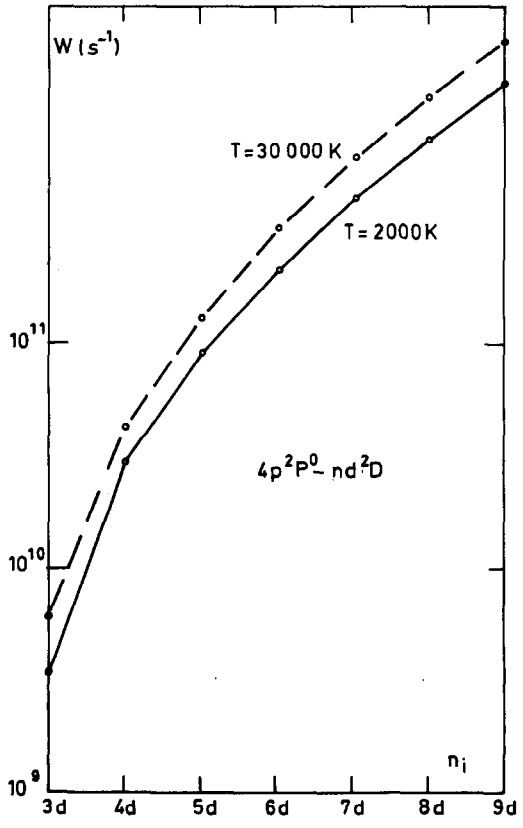

Fig. 4. As in Fig. 2 but for K(I) $4p\ ^2P^0$–$nd\ ^2D$ lines.

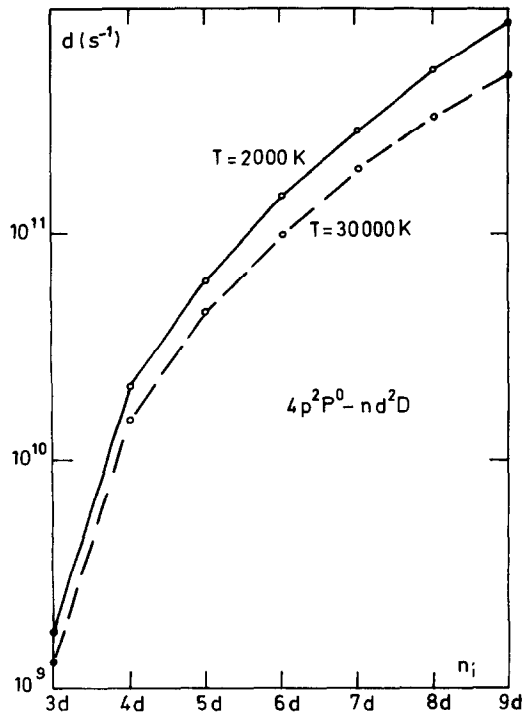

Fig. 5. Electron-impact shift for K(I) $4p\ ^2P^0$–$nd\ ^2D$ lines as a function of n_i for $T = 2000$ K and 30,000 K at $N_e = 10^{15}\,\mathrm{cm}^{-3}$.

Table 2. Experimental Stark widths FWHM[7,8,20] (W_M) compared with theory. The W_I are present calculations of total line widths with impact ion broadening and W_{II} with quasistatic ion-broadening contributions calculated by using the ion-broadening parameter (from Ref. [20]). The results refer to $T = 2950$ K and $N_e = 2 \times 10^{15}\,\mathrm{cm}^{-3}$. W_{BG} are the results of Benett and Griem at $T = 5000$ K and W_K are semiclassical estimates by Konjević[20]

Transition	λ(Å)	W_M(Å)	W_I(Å)	W_{II}(Å)	W_{BG}(Å)	W_K(Å)
$4p\ ^2P^0_{1/2}$–$7s\ ^2S_{1/2}$	5795	0.42 ± 0.20	0.30	0.28	0.35	0.31
$4p\ ^2P^0_{1/2}$–$8s\ ^2S_{1/2}$	5334	0.77 ± 0.36	0.53	0.51	0.70	0.63
$4p\ ^2P^0_{1/2}$–$9s\ ^2S_{1/2}$	5094	1.51 ± 0.66	0.99	0.97	—	1.29
$4p\ ^2P^0_{1/2}$–$10s\ ^2S_{1/2}$	4951	2.60 ± 1.10	1.67	1.66	—	2.39
$4p\ ^2P^0_{3/2}$–$5d\ ^2D_{5/2}$	5825	0.55 ± 0.25	0.40	0.35	—	0.47
$4p\ ^2P^0_{3/2}$–$6d\ ^2D_{5/2}$	5354	0.97 ± 0.44	0.80	0.72	1.10	1.00
$4p\ ^2P^0_{3/2}$–$7d\ ^2D_{5/2}$	5107	1.85 ± 0.80	1.48	1.35	1.98	1.96
$4p\ ^2P^0_{3/2}$–$8d\ ^2D_{5/2}$	4960	3.61 ± 1.50	2.53	2.37	—	3.59

In Figs 2–5, the electron and proton full halfwidths and shifts within the $4p^2P^0$–ns^2S and $4p^2P^0$–nd^2D series are illustrated. We see variation of the results for different types of transitions (s–p and d–p), for different plasma temperatures (2000 and 30,000 K), and different perturber type (electrons and protons). The experimental results of Hohimer[7,8] are also plotted in Figs 2 and 3. By inspecting energy separations between the upper level and the principal perturbing levels (see the Grotrian diagrams in Ref. [12]), we find that this value decrease gradually within a spectral series. Thus, we obtain a gradual change of the Stark-broadening parameters as expected.

Acknowledgements—One of us (M.D.) has been supported by the Observatory of Paris during his stay. The calculations were performed at the Centre Régional de Calcul Electronique (CIRCE) of the Centre National de la Recherche Scientifique (CNRS, Orsay, France) and have been supported by the CNRS.

REFERENCES

1. S. Sahal-Bréchot, *Astron. Astrophys.* **1**, 91 (1969).
2. S. Sahal-Bréchot, *Astron. Astrophys.* **2**, 322 (1969).

3. H. R. Griem, *Spectral Line Broadening by Plasmas*. Academic Press, New York (1974).
4. S. M. Benett and H. R. Griem, University of Maryland, Technical Report No. 71-097, College Park, Md (1971); see also Ref. [3].
5. A. Mazure and G. Nollez, *Z. Naturf.* **31a,** 1575 (1978).
6. J. Purić, J. Labat, S. Djeniže, Lj. Ćirković and I. Lakićević, *Phys. Lett.* **56A,** 83 (1976).
7. J. P. Hohimer, *Phys. Rev.* **A30,** 1449 (1984).
8. J. P. Hohimer, *Phys. Rev.* **A32,** 676 (1985).
9. M. S. Dimitrijević and S. Sahal-Bréchot, *JQSRT* **31,** 301 (1984).
10. M. S. Dimitrijević and S. Sahal-Bréchot, *Astron. Astrophys.* **136,** 289 (1984).
11. M. S. Dimitrijević and S. Sahal-Bréchot, *JQSRT* **34,** 149 (1985).
12. S. Bashkin and J. O. Stoner Jr, *Atomic Energy Levels and Grotrian Diagrams*, Vol. 1. North Holland, Amsterdam (1975).
13. D. R. Bates and A. Damgaard, *Phil. Trans. R. Soc. Lond., Ser. A* **242,** 101 (1949).
14. G. K. Oertel and L. P. Shomo, *Astrophys. J. Suppl. Series* **16,** 175 (1968).
15. W. L. Wiese, M. W. Smith and B. M. Miles, *Atomic Transition Probabilities*, Vol. II. U.S. Government Printing Office, Washington D.C. (1969).
16. H. Van Regemorter, Hoang Binh Dy and M. Prud'homme, *J. Phys. B* **12,** 1073 (1979).
17. A. Brissaud, C. Goldbach, J. Léorat, A. Mazure and G. Nollez, *J. Phys. B* **9,** 1147 (1976).
18. H. R. Griem, M. Baranger, A. C. Kolb and G. K. Oertel, *Phys. Rev.* **125,** 177 (1962).
19. A. Brissaud and U. Frisch, *JQSRT* **11,** 1767 (1977).
20. N. Konjević, *Phys. Rev. A* **32,** 673 (1985).

J. Quant. Spectrosc. Radiat. Transfer Vol. 44, No. 4, pp. 421–431, 1990
Printed in Great Britain.

0022-4073/90 $3.00 + 0.00

STARK BROADENING OF Na(I) LINES WITH THE PRINCIPAL QUANTUM NUMBER OF THE UPPER STATE BETWEEN 6 AND 10

M. S. DIMITRIJEVIĆ† and S. SAHAL-BRÉCHOT‡

†Astronomical Observatory, Volgina 7, 11050 Beograd, Yugoslavia and
‡Département "Atomes et Molécules en Astrophysique", Unité Associée au CNRS No. 812, Observatoire de Paris, 92195 Meudon Cedex, France

(*Received* 29 *September* 1989; *received for publication* 24 *April* 1990)

Abstract—A semiclassical approach has been used to evaluate electron-, proton- and ionized helium-impact line widths and shifts for 46 neutral sodium multiplets with the principal quantum number of the upper state between 6 and 10. Calculations have been performed as a function of temperature and at a perturber density of 10^{13} cm^{-3}. The results have been used to investigate Stark-broadening-parameter regularities within spectral series.

INTRODUCTION

Stark-broadening parameters for neutral sodium lines are needed in plasma spectroscopy,[1] the technology of high-pressure discharge lamps[2,3] and astrophysics.[4,5] In solar spectroscopy, the influence of Stark broadening increases with an increase in the principal quantum number (n) of the initial energy level[5] because the bond between the optical electron and the core becomes weaker and the influence of external electric microfields increases. Using a semiclassical-perturbation formalism[6,7] and a Stark-broadening computer code derived from this method, we have calculated electron-, proton- and ionized helium-impact line widths and shifts for 46 neutral sodium multiplets for the conditions specified in the Abstract.

The present data extend and complete our previous calculations.[8] We also correct a number of the previously published data,[8] which are erroneous for high quantum numbers ($n \geqslant 7$). The Stark-broadening computer code of Sahal-Bréchot requires inputs of the energies of the upper, lower and perturbing levels, associated mean radii, and oscillator strengths. For the oscillator strengths, we had used the computer code of Hoang Binh Dy, which is based on the work of Van Regemorter et al;[9] in 1984, this code yielded erroneous data for high values of n. We have now used an improved code and have used the new oscillator strengths to modify some of our previously obtained Stark-broadening and shift data.

We have also improved the integration procedure for the impact parameter in the Stark-broadening and shift code that is used at elevated temperatures, where line-shift values remain uncertain because of the growing importance of the Debye cutoff. The Debye cutoff, which has physical meaning but is implemented by using *ad hoc* procedures, also leads to a departure from the linear density law. While this result is expected, it constitutes another source of uncertainty. For most astrophysical cases, this departure is small and well within the accuracy of the method. When one wants to investigate regularities within spectral series or make precise comparisons with measurements obtained at different densities, computed data are needed at a number of different densities (N). We have therefore calculated an extensive, self-consistent set of data ($N = 10^{13} - 10^{19}$ cm^{-3}) as a basis for these investigations. Data for densities other than those specified in this paper will be published elsewhere.[10]

THEORY

The semiclassical perturbational formalism is described in Refs. 6 and 7. For this reason, only a few details are given here. For the impact approximation, the full halfwidth ($2w$) and shift (d)

of an electron-impact broadened line may be expressed as[6,7]

$$2w = N_e \int_0^\infty vf(v)\,dv\left[\sum_{i'\neq i}\sigma_{ii'}(v) + \sum_{f'\neq f}\sigma_{ff'}(v) + \sigma_{el}(v)\right],$$

$$d = N_e \int_0^\infty vf(v)\,dv \int_{R_3}^{R_D} 2\pi\rho\,d\rho\,\sin^2\phi_p. \tag{1}$$

Here, N_e is the electron density and $f(v)$ the Maxwellian velocity distribution function for electrons, ρ denotes the impact parameter of the incoming electron, i and f denote, respectively, the initial and final atomic energy levels, and i′, f′ are their perturbing levels. The inelastic cross section $\sigma_{ii'}(v)$ may be obtained from an integration over the impact parameter of the transition probability $P_{ii'}(\rho, v)$, viz.

$$\sum_{i'\neq i}\sigma_{ii'}(v) = \tfrac{1}{2}\pi R_1^2 + \int_{R_1}^{R_D} 2\pi\rho\,d\rho \sum_{i'\neq i} P_{ii'}(\rho, v). \tag{2}$$

The elastic cross section is given by

$$\sigma_{el} = 2\pi R_2^2 + \int_{R_2}^{R_D} 8\pi\rho\,d\rho\,\sin^2\delta, \quad \delta = [\phi_p^2 + \phi_q^2]^{1/2}. \tag{3}$$

The phase shifts ϕ_p and ϕ_q are due, respectively, to the polarization potential (r^{-4}) and to the quadrupolar potential (r^{-3}) parts; they are given in Chap. 3, Sec. 3, Ref. 6. All of the cutoffs R_1, R_2, R_3, R_D are described in Chap. 1, Sec. 3, Ref. 7.

If we want to make certain that a line is isolated, we can use the parameter c defined in Ref. 11 and given in Table 1. For an electron concentration lower than

$$N_1(\text{cm}^{-3}) = [c/2w(\text{Å})][N(\text{cm}^{-3})/10^{16}], \tag{4}$$

the line may be treated as isolated in the core, even if a weak forbidden component due to failure of this approximation remains in the wing.

The formulae for the proton-impact (or He^+-impact) widths and shifts are analogous, but inelastic collisions are negligible.

RESULTS AND DISCUSSION

Energy-level data were taken from Ref. 12. The mean atomic radius and mean-square radius were calculated in the hydrogenic approximation. Oscillator strengths were obtained from the computer code available at the Observatory of Meudon and derived from the work of Van Regemorter et al.[9]

Our results for electron-, proton-, and ionized helium-impact full halfwidths ($2w$) and shift (d), for Na I lines are shown in Table 1 for a perturber density 10^{13} cm^{-3} and temperatures of $T = 2500$, 5000, 10,000, 20,000, 40,000, and 80,000 K. We also specify a parameter c [see Eq. (4)], which gives an estimate for the maximum perturber density for which the line may be treated as isolated when it is divided by $2w$.

For each value given in the Table 1, the collision volume (V) multiplied by the perturber density (N) is much less than one and the impact approximation is valid.[6,7] Values for $NV > 0.5$ are not given in Table 1; values for $0.1 < NV \leqslant 0.5$ are denoted by an asterisk. When the impact approximation is not valid, the ion-broadening contribution may be estimated by using the quasistatic ion-broadening parameter[1] introduced by Griem et al.[13]

Electron-impact broadening parameters at an electron density of 10^{16} cm^{-3} are given in Table 2. These data extend and correct our previously published data,[8] and have also been used to extend and continue our investigations of systematic trends of Stark-broadening parameters within spectral series.

Inspection of energy separations between the upper level and the principal perturbing levels for the $3p^2P^0$–ns^2S series (see the Grotrian diagrams in Ref. 12) shows that this value decreases gradually within a spectral series, i.e., we expect a gradual change of the Stark-broadening

Table 1. This table shows electron-, proton- and ionized helium-impact broadening parameters for Na (I) lines with the principal quantum number of the upper state between 6 and 10, for a perturber density of 10^{13} cm^{-3} and temperatures from 2500 to 80,000 K. Transitions and averaged wavelengths for the multiplet (in Å) are also given. By using c [see Eq. (4)], we obtain an estimate for the maximum perturber density for which the line may be treated as isolated and the tabulated data may be used. The asterisk identifies cases for which the collision volume multiplied by the perturber density (the condition for validity of the impact approximation) lies between 0.1 and 0.5.†

PERTURBER DENSITY 10(+13)cm(-3)							
		ELECTRONS		PROTONS		IONIZED HELIUM	
TRANSITION	T(K)	WIDTH(A)	SHIFT(A)	WIDTH(A)	SHIFT(A)	WIDTH(A)	SHIFT(A)
3S - 6P	2500.	0.528E-03	-0.341E-03	0.144E-03	-0.950E-04	0.131E-03	-0.766E-04
2680.4A	5000.	0.573E-03	-0.286E-03	0.152E-03	-0.108E-03	0.137E-03	-0.869E-04
c= 0.19E+18	10000.	0.653E-03	-0.206E-03	0.163E-03	-0.121E-03	0.145E-03	-0.980E-04
	20000.	0.749E-03	-0.145E-03	0.176E-03	-0.136E-03	0.154E-03	-0.110E-03
	30000.	0.785E-03	-0.110E-03	0.184E-03	-0.146E-03	0.160E-03	-0.118E-03
	80000.	0.843E-03	-0.366E-04	0.208E-03	-0.172E-03	0.178E-03	-0.140E-03
3S - 7P	2500.	0.118E-02	-0.747E-03	0.305E-03	-0.217E-03	0.273E-03	-0.174E-03
2593.9A	5000.	0.127E-02	-0.669E-03	0.327E-03	-0.246E-03	0.289E-03	-0.199E-03
c= 0.10E+18	10000.	0.145E-02	-0.473E-03	0.354E-03	-0.279E-03	0.309E-03	-0.225E-03
	20000.	0.164E-02	-0.334E-03	0.385E-03	-0.314E-03	0.332E-03	-0.254E-03
	30000.	0.170E-02	-0.247E-03	0.405E-03	-0.337E-03	0.347E-03	-0.272E-03
	80000.	0.178E-02	-0.749E-04	0.464E-03	-0.397E-03	0.391E-03	-0.322E-03
3S - 8P	2500.	0.235E-02	-0.157E-02	0.590E-03	-0.437E-03	0.519E-03	-0.350E-03
2543.8A	5000.	0.252E-02	-0.126E-02	0.639E-03	-0.499E-03	0.556E-03	-0.401E-03
c= 0.63E+17	10000.	0.288E-02	-0.922E-03	0.696E-03	-0.566E-03	0.598E-03	-0.456E-03
	20000.	0.321E-02	-0.676E-03	0.762E-03	-0.640E-03	0.649E-03	-0.517E-03
	30000.	0.331E-02	-0.455E-03	0.805E-03	-0.686E-03	0.682E-03	-0.555E-03
	80000.	0.340E-02	-0.126E-03	0.929E-03	-0.811E-03	0.775E-03	-0.656E-03
3S - 9P	2500.	0.431E-02	-0.273E-02	0.106E-02	-0.800E-03	0.920E-03*	-0.638E-03*
2512.1A	5000.	0.461E-02	-0.234E-02	0.115E-02	-0.919E-03	0.992E-03*	-0.738E-03*
c= 0.42E+17	10000.	0.526E-02	-0.145E-02	0.126E-02	-0.105E-02	0.108E-02	-0.843E-03
	20000.	0.578E-02	-0.105E-02	0.139E-02	-0.119E-02	0.117E-02	-0.958E-03
	30000.	0.593E-02	-0.746E-03	0.147E-02	-0.128E-02	0.124E-02	-0.103E-02
	80000.	0.600E-02	-0.234E-03	0.171E-02	-0.151E-02	0.141E-02	-0.122E-02
3S -10P	2500.	0.739E-02	-0.462E-02	0.179E-02*	-0.136E-02*	0.154E-02*	-0.108E-02*
2490.7A	5000.	0.789E-02	-0.387E-02	0.196E-02*	-0.158E-02*	0.167E-02*	-0.126E-02*
c= 0.29E+17	10000.	0.898E-02	-0.263E-02	0.215E-02	-0.180E-02	0.182E-02*	-0.145E-02*
	20000.	0.974E-02	-0.162E-02	0.238E-02	-0.205E-02	0.199E-02*	-0.165E-02*
	30000.	0.994E-02	-0.113E-02	0.252E-02	-0.221E-02	0.211E-02*	-0.178E-02*
	80000.	0.990E-02	-0.270E-03	0.294E-02	-0.262E-02	0.242E-02	-0.212E-02
3P - 6S	2500.	0.780E-03	0.574E-03	0.162E-03	0.152E-03	0.131E-03	0.122E-03
5151.9A	5000.	0.892E-03	0.651E-03	0.182E-03	0.171E-03	0.147E-03	0.138E-03
c= 0.25E+19	10000.	0.974E-03	0.677E-03	0.204E-03	0.192E-03	0.165E-03	0.155E-03
	20000.	0.110E-02	0.640E-03	0.229E-03	0.216E-03	0.186E-03	0.175E-03
	30000.	0.119E-02	0.546E-03	0.245E-03	0.231E-03	0.199E-03	0.187E-03
	80000.	0.146E-02	0.375E-03	0.289E-03	0.272E-03	0.234E-03	0.221E-03
3P - 7S	2500.	0.152E-02	0.108E-02	0.303E-03	0.281E-03	0.245E-03	0.227E-03
4750.6A	5000.	0.173E-02	0.123E-02	0.340E-03	0.318E-03	0.275E-03	0.257E-03
c= 0.12E+19	10000.	0.190E-02	0.118E-02	0.381E-03	0.358E-03	0.309E-03	0.290E-03
	20000.	0.219E-02	0.101E-02	0.428E-03	0.403E-03	0.347E-03	0.326E-03
	30000.	0.245E-02	0.845E-03	0.458E-03	0.432E-03	0.371E-03	0.350E-03
	80000.	0.293E-02	0.528E-03	0.540E-03	0.509E-03	0.437E-03	0.413E-03

continued overleaf

Table 1—*continued*

PERTURBER DENSITY 10(+13)cm(-3)							
		ELECTRONS		PROTONS		IONIZED HELIUM	
TRANSITION	T(K)	WIDTH(A)	SHIFT(A)	WIDTH(A)	SHIFT(A)	WIDTH(A)	SHIFT(A)
3P - 8S	2500.	0.271E-02	0.191E-02	0.533E-03	0.492E-03	0.432E-03	0.396E-03
4544.2A	5000.	0.307E-02	0.207E-02	0.599E-03	0.558E-03	0.485E-03	0.450E-03
c= 0.68E+18	10000.	0.361E-02	0.199E-02	0.672E-03	0.631E-03	0.545E-03	0.510E-03
	20000.	0.423E-02	0.151E-02	0.755E-03	0.710E-03	0.611E-03	0.574E-03
	30000.	0.475E-02	0.126E-02	0.808E-03	0.761E-03	0.654E-03	0.616E-03
	80000.	0.555E-02	0.692E-03	0.952E-03	0.898E-03	0.771E-03	0.727E-03
3P - 9S	2500.	0.460E-02	0.316E-02	0.886E-03	0.810E-03	0.718E-03	0.651E-03
4423.5A	5000.	0.526E-02	0.327E-02	0.995E-03	0.922E-03	0.806E-03	0.743E-03
c= 0.43E+18	10000.	0.627E-02	0.299E-02	0.112E-02	0.104E-02	0.905E-03	0.843E-03
	20000.	0.770E-02	0.218E-02	0.125E-02	0.118E-02	0.102E-02	0.953E-03
	30000.	0.861E-02	0.178E-02	0.134E-02	0.126E-02	0.109E-02	0.102E-02
	80000.	0.986E-02	0.694E-03	0.158E-02	0.149E-02	0.128E-02	0.121E-02
3P - 6D	2500.	0.145E-01	0.654E-02	0.414E-02*	0.362E-02*	0.336E-02*	0.289E-02*
4667.5A	5000.	0.135E-01	0.495E-02	0.466E-02	0.418E-02	0.377E-02*	0.335E-02*
c= 0.28E+17	10000.	0.125E-01	0.319E-02	0.525E-02	0.477E-02	0.423E-02	0.384E-02
	20000.	0.113E-01	0.216E-02	0.598E-02	0.542E-02	0.476E-02	0.437E-02
	30000.	0.106E-01	0.167E-02	0.649E-02	0.585E-02	0.510E-02	0.470E-02
	80000.	0.876E-02	0.630E-03	0.776E-02	0.714E-02	0.613E-02	0.559E-02
3P - 7D	2500.	0.278E-01	0.109E-01	0.819E-02*	0.692E-02*		
4496.6A	5000.	0.260E-01	0.880E-02	0.921E-02*	0.810E-02*	0.745E-02*	0.646E-02*
c= 0.17E+17	10000.	0.239E-01	0.455E-02	0.104E-01*	0.932E-02*	0.836E-02*	0.748E-02*
	20000.	0.216E-01	0.355E-02	0.119E-01*	0.106E-01*	0.941E-02*	0.856E-02*
	30000.	0.201E-01	0.270E-02	0.129E-01*	0.115E-01*	0.101E-01*	0.923E-02*
	80000.	0.165E-01	0.851E-03	0.153E-01	0.142E-01	0.121E-01*	0.110E-01*
3P - 8D	2500.	0.512E-01	0.203E-01				
4392.3A	5000.	0.473E-01	0.144E-01				
c= 0.96E+16	10000.	0.432E-01	0.821E-02	0.203E-01*	0.178E-01*		
	20000.	0.386E-01	0.428E-02	0.233E-01*	0.205E-01*		
	30000.	0.358E-01	0.408E-02	0.252E-01*	0.223E-01*		
	80000.	0.290E-01	0.108E-02	0.294E-01*	0.278E-01*	0.239E-01*	0.214E-01*
3P - 9D	2500.	0.840E-01	0.290E-01				
4323.5A	5000.	0.776E-01	0.186E-01				
c= 0.67E+16	10000.	0.708E-01	0.124E-01				
	20000.	0.631E-01	0.651E-02				
	30000.	0.584E-01	0.454E-02				
	80000.	0.472E-01	0.138E-02	0.493E-01*	0.469E-01*		
3D - 6P	2500.	0.114E-01	-0.702E-02	0.299E-02	-0.203E-02	0.272E-02	-0.164E-02
12309.2A	5000.	0.125E-01	-0.640E-02	0.318E-02	-0.230E-02	0.286E-02	-0.185E-02
c= 0.39E+19	10000.	0.142E-01	-0.448E-02	0.342E-02	-0.259E-02	0.302E-02	-0.209E-02
	20000.	0.163E-01	-0.309E-02	0.369E-02	-0.291E-02	0.322E-02	-0.236E-02
	30000.	0.171E-01	-0.229E-02	0.387E-02	-0.312E-02	0.336E-02	-0.252E-02
	80000.	0.184E-01	-0.564E-03	0.439E-02	-0.368E-02	0.374E-02	-0.298E-02

continued opposite

Table 1—*continued*

PERTURBER DENSITY 10(+13)cm(-3)							
		ELECTRONS		PROTONS		IONIZED HELIUM	
TRANSITION	T(K)	WIDTH(A)	SHIFT(A)	WIDTH(A)	SHIFT(A)	WIDTH(A)	SHIFT(A)
3D - 7P	2500.	0.201E-01	-0.127E-01	0.514E-02	-0.368E-02	0.459E-02	-0.296E-02
10674.6A	5000.	0.218E-01	-0.113E-01	0.552E-02	-0.419E-02	0.487E-02	-0.338E-02
c= 0.18E+19	10000.	0.248E-01	-0.754E-02	0.598E-02	-0.474E-02	0.520E-02	-0.383E-02
	20000.	0.281E-01	-0.471E-02	0.651E-02	-0.534E-02	0.560E-02	-0.432E-02
	30000.	0.292E-01	-0.359E-02	0.686E-02	-0.572E-02	0.586E-02	-0.463E-02
	80000.	0.307E-01	-0.537E-03	0.786E-02	-0.673E-02	0.661E-02	-0.547E-02
3D - 8P	2500.	0.356E-01	-0.238E-01	0.887E-02	-0.659E-02	0.780E-02	-0.528E-02
9875.6A	5000.	0.383E-01	-0.195E-01	0.961E-02	-0.752E-02	0.835E-02	-0.606E-02
c= 0.96E+18	10000.	0.436E-01	-0.128E-01	0.105E-01	-0.854E-02	0.900E-02	-0.689E-02
	20000.	0.487E-01	-0.764E-02	0.115E-01	-0.965E-02	0.976E-02	-0.781E-02
	30000.	0.503E-01	-0.593E-02	0.121E-01	-0.103E-01	0.103E-01	-0.838E-02
	80000.	0.517E-01	-0.881E-03	0.140E-01	-0.122E-01	0.117E-01	-0.990E-02
3D - 9P	2500.	0.607E-01	-0.373E-01	0.148E-01	-0.112E-01	0.129E-01*	-0.896E-02*
9414.4A	5000.	0.649E-01	-0.331E-01	0.162E-01	-0.129E-01	0.139E-01*	-0.104E-01*
c= 0.58E+18	10000.	0.741E-01	-0.221E-01	0.177E-01	-0.147E-01	0.151E-01	-0.118E-01
	20000.	0.815E-01	-0.125E-01	0.195E-01	-0.167E-01	0.164E-01	-0.135E-01
	30000.	0.836E-01	-0.979E-02	0.207E-01	-0.179E-01	0.173E-01	-0.145E-01
	80000.	0.846E-01	-0.175E-02	0.240E-01	-0.212E-01	0.198E-01	-0.171E-01
3D -10P	2500.	0.993E-01	-0.656E-01	0.240E-01*	-0.182E-01*	0.206E-01*	-0.145E-01*
9120.8A	5000.	0.106	-0.483E-01	0.262E-01*	-0.211E-01*	0.224E-01*	-0.169E-01*
c= 0.39E+18	10000.	0.121	-0.363E-01	0.289E-01	-0.242E-01	0.244E-01*	-0.195E-01*
	20000.	0.131	-0.202E-01	0.319E-01	-0.275E-01	0.267E-01*	-0.222E-01*
	30000.	0.134	-0.156E-01	0.338E-01	-0.296E-01	0.282E-01	-0.239E-01
	80000.	0.133	-0.332E-02	0.394E-01	-0.351E-01	0.325E-01	-0.284E-01
4S - 6P	2500.	0.556E-02	-0.356E-02	0.150E-02	-0.995E-03	0.137E-02	-0.802E-03
8650.3A	5000.	0.604E-02	-0.311E-02	0.159E-02	-0.113E-02	0.144E-02	-0.910E-03
c= 0.19E+19	10000.	0.687E-02	-0.218E-02	0.170E-02	-0.127E-02	0.151E-02	-0.103E-02
	20000.	0.793E-02	-0.156E-02	0.183E-02	-0.143E-02	0.161E-02	-0.116E-02
	30000.	0.834E-02	-0.116E-02	0.192E-02	-0.153E-02	0.167E-02	-0.124E-02
	80000.	0.902E-02	-0.292E-03	0.218E-02	-0.180E-02	0.186E-02	-0.146E-02
4S - 7P	2500.	0.107E-01	-0.676E-02	0.277E-02	-0.197E-02	0.248E-02	-0.158E-02
7810.0A	5000.	0.116E-01	-0.603E-02	0.297E-02	-0.224E-02	0.262E-02	-0.180E-02
c= 0.94E+18	10000.	0.132E-01	-0.424E-02	0.321E-02	-0.253E-02	0.280E-02	-0.205E-02
	20000.	0.150E-01	-0.301E-02	0.349E-02	-0.285E-02	0.301E-02	-0.231E-02
	30000.	0.156E-01	-0.197E-02	0.368E-02	-0.306E-02	0.315E-02	-0.247E-02
	80000.	0.164E-01	-0.312E-03	0.421E-02	-0.361E-02	0.355E-02	-0.292E-02
4S - 8P	2500.	0.198E-01	-0.131E-01	0.496E-02	-0.367E-02	0.437E-02	-0.294E-02
7373.3A	5000.	0.213E-01	-0.112E-01	0.537E-02	-0.419E-02	0.467E-02	-0.337E-02
c= 0.53E+18	10000.	0.242E-01	-0.789E-02	0.585E-02	-0.476E-02	0.503E-02	-0.384E-02
	20000.	0.271E-01	-0.524E-02	0.640E-02	-0.538E-02	0.545E-02	-0.435E-02
	30000.	0.280E-01	-0.341E-02	0.677E-02	-0.576E-02	0.573E-02	-0.467E-02
	80000.	0.288E-01	-0.523E-03	0.781E-02	-0.682E-02	0.651E-02	-0.552E-02

continued overleaf

Table 1—*continued*

PERTURBER DENSITY 10(+13)cm(-3)							
		ELECTRONS		PROTONS		IONIZED HELIUM	
TRANSITION	T(K)	WIDTH(A)	SHIFT(A)	WIDTH(A)	SHIFT(A)	WIDTH(A)	SHIFT(A)
4S - 9P	2500.	0.346E-01	-0.217E-01	0.849E-02	-0.641E-02	0.738E-02*	-0.512E-02*
7113.0A	5000.	0.370E-01	-0.178E-01	0.925E-02	-0.737E-02	0.795E-02*	-0.592E-02*
c= 0.33E+18	10000.	0.422E-01	-0.134E-01	0.101E-01	-0.839E-02	0.862E-02	-0.676E-02
	20000.	0.465E-01	-0.856E-02	0.111E-01	-0.952E-02	0.940E-02	-0.768E-02
	30000.	0.477E-01	-0.548E-02	0.118E-01	-0.102E-01	0.991E-02	-0.826E-02
	80000.	0.483E-01	-0.103E-02	0.137E-01	-0.121E-01	0.113E-01	-0.979E-02
4S -10P	2500.	0.575E-01	-0.381E-01	0.139E-01*	-0.106E-01*	0.120E-01*	-0.839E-02*
6944.0A	5000.	0.614E-01	-0.297E-01	0.152E-01*	-0.122E-01*	0.130E-01*	-0.980E-02*
c= 0.22E+18	10000.	0.698E-01	-0.204E-01	0.167E-01	-0.140E-01	0.141E-01*	-0.113E-01*
	20000.	0.758E-01	-0.130E-01	0.185E-01	-0.159E-01	0.155E-01*	-0.129E-01*
	30000.	0.774E-01	-0.924E-02	0.196E-01	-0.172E-01	0.164E-01*	-0.138E-01*
	80000.	0.771E-01	-0.197E-02	0.229E-01	-0.203E-01	0.188E-01	-0.165E-01
4P - 6S	2500.	0.890E-02	0.586E-02	0.175E-02	0.158E-02	0.145E-02	0.128E-02
16384.0A	5000.	0.103E-01	0.675E-02	0.195E-02	0.178E-02	0.161E-02	0.144E-02
c= 0.25E+20	10000.	0.114E-01	0.692E-02	0.218E-02	0.200E-02	0.179E-02	0.162E-02
	20000.	0.129E-01	0.634E-02	0.243E-02	0.225E-02	0.199E-02	0.182E-02
	30000.	0.142E-01	0.544E-02	0.260E-02	0.241E-02	0.212E-02	0.195E-02
	80000.	0.174E-01	0.382E-02	0.305E-02	0.284E-02	0.248E-02	0.230E-02
4P - 7S	2500.	0.117E-01	0.808E-02	0.228E-02	0.210E-02	0.185E-02	0.169E-02
12915.0A	5000.	0.134E-01	0.936E-02	0.255E-02	0.238E-02	0.207E-02	0.192E-02
c= 0.88E+19	10000.	0.151E-01	0.879E-02	0.286E-02	0.267E-02	0.232E-02	0.216E-02
	20000.	0.174E-01	0.752E-02	0.321E-02	0.301E-02	0.260E-02	0.243E-02
	30000.	0.195E-01	0.629E-02	0.343E-02	0.322E-02	0.278E-02	0.261E-02
	80000.	0.233E-01	0.394E-02	0.404E-02	0.380E-02	0.327E-02	0.308E-02
4P - 8S	2500.	0.178E-01	0.123E-01	0.343E-02	0.316E-02	0.278E-02	0.254E-02
11495.0A	5000.	0.203E-01	0.134E-01	0.385E-02	0.358E-02	0.312E-02	0.289E-02
c= 0.44E+19	10000.	0.235E-01	0.129E-01	0.432E-02	0.405E-02	0.351E-02	0.327E-02
	20000.	0.281E-01	0.100E-01	0.485E-02	0.456E-02	0.393E-02	0.369E-02
	30000.	0.315E-01	0.826E-02	0.519E-02	0.488E-02	0.421E-02	0.395E-02
	80000.	0.368E-01	0.465E-02	0.612E-02	0.577E-02	0.495E-02	0.467E-02
4P - 9S	2500.	0.277E-01	0.189E-01	0.528E-02	0.483E-02	0.428E-02	0.388E-02
10745.0A	5000.	0.317E-01	0.197E-01	0.593E-02	0.549E-02	0.481E-02	0.443E-02
c= 0.25E+19	10000.	0.379E-01	0.182E-01	0.666E-02	0.622E-02	0.540E-02	0.502E-02
	20000.	0.464E-01	0.136E-01	0.747E-02	0.701E-02	0.606E-02	0.568E-02
	30000.	0.519E-01	0.112E-01	0.800E-02	0.752E-02	0.648E-02	0.608E-02
	80000.	0.594E-01	0.572E-02	0.944E-02	0.888E-02	0.763E-02	0.719E-02
4P - 6D	2500.	0.100	0.459E-01	0.284E-01*	0.249E-01*	0.231E-01*	0.198E-01*
12318.0A	5000.	0.943E-01	0.356E-01	0.319E-01	0.287E-01	0.259E-01*	0.230E-01*
c= 0.20E+18	10000.	0.871E-01	0.239E-01	0.360E-01	0.328E-01	0.290E-01	0.264E-01
	20000.	0.793E-01	0.144E-01	0.410E-01	0.372E-01	0.326E-01	0.300E-01
	30000.	0.743E-01	0.112E-01	0.445E-01	0.402E-01	0.350E-01	0.323E-01
	80000.	0.619E-01	0.414E-02	0.533E-01	0.489E-01	0.420E-01	0.384E-01

continued opposite

Table 1—*continued*

PERTURBER DENSITY 10(+13)cm(-3)							
		ELECTRONS		PROTONS		IONIZED HELIUM	
TRANSITION	T(K)	WIDTH(A)	SHIFT(A)	WIDTH(A)	SHIFT(A)	WIDTH(A)	SHIFT(A)
4P - 7D	2500.	0.173	0.754E-01	0.508E-01*	0.429E-01*		
11195.0A	5000.	0.161	0.564E-01	0.571E-01*	0.502E-01*	0.462E-01*	0.400E-01*
c= 0.10E+18	10000.	0.149	0.356E-01	0.644E-01*	0.577E-01*	0.518E-01*	0.464E-01*
	20000.	0.134	0.224E-01	0.735E-01*	0.659E-01*	0.583E-01*	0.530E-01*
	30000.	0.125	0.161E-01	0.798E-01*	0.712E-01*	0.626E-01*	0.572E-01*
	80000.	0.103	0.493E-02	0.948E-01	0.878E-01	0.753E-01*	0.684E-01*
4P - 8D	2500.	0.297	0.110				
10570.0A	5000.	0.274	0.855E-01				
c= 0.56E+17	10000.	0.251	0.437E-01	0.118*	0.103*		
	20000.	0.224	0.315E-01	0.135*	0.119*		
	30000.	0.208	0.185E-01	0.146*	0.129*		
	80000.	0.169	0.587E-02	0.170*	0.161*	0.138*	0.124*
4D - 6P	2500.	0.195	-0.101	0.410E-01	-0.349E-01	0.345E-01	-0.281E-01
36390.1A	5000.	0.199	-0.923E-01	0.454E-01	-0.396E-01	0.379E-01	-0.319E-01
c= 0.52E+19	10000.	0.203	-0.673E-01	0.504E-01	-0.447E-01	0.418E-01	-0.362E-01
	20000.	0.214	-0.444E-01	0.564E-01	-0.503E-01	0.462E-01	-0.407E-01
	30000.	0.217	-0.347E-01	0.604E-01	-0.540E-01	0.492E-01	-0.437E-01
	80000.	0.215	-0.129E-01	0.718E-01	-0.645E-01	0.575E-01	-0.516E-01
4D - 7P	2500.	0.155	-0.876E-01	0.330E-01	-0.261E-01	0.285E-01	-0.210E-01
25050.1A	5000.	0.162	-0.764E-01	0.361E-01	-0.297E-01	0.309E-01	-0.239E-01
c= 0.25E+19	10000.	0.174	-0.508E-01	0.396E-01	-0.337E-01	0.336E-01	-0.272E-01
	20000.	0.188	-0.288E-01	0.438E-01	-0.379E-01	0.367E-01	-0.307E-01
	30000.	0.193	-0.217E-01	0.465E-01	-0.407E-01	0.388E-01	-0.329E-01
	80000.	0.195	-0.626E-02	0.544E-01	-0.482E-01	0.446E-01	-0.389E-01
4D - 8P	2500.	0.193	-0.108	0.426E-01	-0.328E-01	0.370E-01	-0.263E-01
21052.6A	5000.	0.203	-0.867E-01	0.465E-01	-0.375E-01	0.399E-01	-0.302E-01
c= 0.18E+19	10000.	0.224	-0.473E-01	0.509E-01	-0.426E-01	0.433E-01	-0.344E-01
	20000.	0.245	-0.294E-01	0.561E-01	-0.482E-01	0.472E-01	-0.390E-01
	30000.	0.251	-0.207E-01	0.594E-01	-0.516E-01	0.498E-01	-0.418E-01
	80000.	0.253	-0.297E-02	0.691E-01	-0.611E-01	0.571E-01	-0.494E-01
4D - 9P	2500.	0.274	-0.153	0.623E-01	-0.477E-01	0.538E-01*	-0.381E-01*
19062.1A	5000.	0.290	-0.127	0.680E-01	-0.549E-01	0.582E-01*	-0.441E-01*
c= 0.14E+19	10000.	0.325	-0.697E-01	0.747E-01	-0.626E-01	0.633E-01	-0.504E-01
	20000.	0.354	-0.323E-01	0.823E-01	-0.710E-01	0.692E-01	-0.572E-01
	30000.	0.361	-0.204E-01	0.873E-01	-0.763E-01	0.730E-01	-0.616E-01
	80000.	0.362	-0.853E-03	0.102	-0.902E-01	0.838E-01	-0.730E-01
4D -10P	2500.	0.404	-0.255	0.932E-01*	-0.713E-01*	0.799E-01*	-0.566E-01*
17895.5A	5000.	0.429	-0.189	0.102*	-0.827E-01*	0.868E-01*	-0.661E-01*
c= 0.13E+19	10000.	0.483	-0.990E-01	0.112	-0.946E-01	0.948E-01*	-0.761E-01*
	20000.	0.521	-0.380E-01	0.124	-0.108	0.104*	-0.867E-01*
	30000.	0.530	-0.283E-01	0.132	-0.116	0.110*	-0.934E-01*
	80000.	0.525	-0.136E-01	0.154	-0.137	0.127	-0.111

continued overleaf

Table 1—*continued*

PERTURBER DENSITY 10(+13)cm(-3)							
		ELECTRONS		PROTONS		IONIZED HELIUM	
TRANSITION	T(K)	WIDTH(A)	SHIFT(A)	WIDTH(A)	SHIFT(A)	WIDTH(A)	SHIFT(A)
5S - 6P	2500.	0.470E-01	-0.303E-01	0.122E-01	-0.821E-02	0.111E-01	-0.662E-02
24414.1A	5000.	0.515E-01	-0.291E-01	0.129E-01	-0.930E-02	0.116E-01	-0.751E-02
c= 0.15E+20	10000.	0.584E-01	-0.223E-01	0.139E-01	-0.105E-01	0.123E-01	-0.847E-02
	20000.	0.680E-01	-0.162E-01	0.150E-01	-0.118E-01	0.131E-01	-0.954E-02
	30000.	0.725E-01	-0.128E-01	0.157E-01	-0.126E-01	0.136E-01	-0.102E-01
	80000.	0.796E-01	-0.560E-02	0.178E-01	-0.149E-01	0.152E-01	-0.121E-01
5S - 7P	2500.	0.628E-01	-0.410E-01	0.160E-01	-0.114E-01	0.143E-01	-0.919E-02
18726.6A	5000.	0.681E-01	-0.350E-01	0.172E-01	-0.130E-01	0.152E-01	-0.105E-01
c= 0.54E+19	10000.	0.775E-01	-0.228E-01	0.186E-01	-0.147E-01	0.162E-01	-0.119E-01
	20000.	0.887E-01	-0.158E-01	0.202E-01	-0.165E-01	0.174E-01	-0.134E-01
	30000.	0.929E-01	-0.102E-01	0.213E-01	-0.177E-01	0.182E-01	-0.143E-01
	80000.	0.986E-01	-0.329E-02	0.244E-01	-0.209E-01	0.206E-01	-0.170E-01
5S - 8P	2500.	0.987E-01	-0.651E-01	0.246E-01	-0.182E-01	0.216E-01	-0.146E-01
16398.8A	5000.	0.106	-0.541E-01	0.266E-01	-0.208E-01	0.231E-01	-0.167E-01
c= 0.26E+19	10000.	0.121	-0.348E-01	0.290E-01	-0.236E-01	0.249E-01	-0.190E-01
	20000.	0.136	-0.220E-01	0.317E-01	-0.267E-01	0.270E-01	-0.216E-01
	30000.	0.141	-0.102E-01	0.336E-01	-0.286E-01	0.284E-01	-0.232E-01
	80000.	0.146	-0.369E-02	0.387E-01	-0.338E-01	0.323E-01	-0.274E-01
5S - 9P	2500.	0.158	-0.979E-01	0.386E-01	-0.292E-01	0.336E-01*	-0.233E-01*
15165.3A	5000.	0.169	-0.825E-01	0.421E-01	-0.335E-01	0.362E-01*	-0.269E-01*
c= 0.15E+19	10000.	0.193	-0.549E-01	0.461E-01	-0.382E-01	0.392E-01	-0.308E-01
	20000.	0.213	-0.337E-01	0.507E-01	-0.433E-01	0.428E-01	-0.350E-01
	30000.	0.219	-0.124E-01	0.537E-01	-0.466E-01	0.451E-01	-0.376E-01
	80000.	0.222	-0.587E-02	0.623E-01	-0.550E-01	0.516E-01	-0.445E-01
5S -10P	2500.	0.248	-0.165	0.600E-01*	-0.456E-01*	0.516E-01*	-0.362E-01*
14417.5A	5000.	0.265	-0.129	0.657E-01*	-0.528E-01*	0.559E-01*	-0.423E-01*
c= 0.97E+18	10000.	0.302	-0.856E-01	0.722E-01	-0.605E-01	0.610E-01*	-0.486E-01*
	20000.	0.328	-0.515E-01	0.797E-01	-0.687E-01	0.668E-01*	-0.554E-01*
	30000.	0.336	-0.351E-01	0.846E-01	-0.740E-01	0.706E-01*	-0.597E-01*
	80000.	0.335	-0.986E-02	0.986E-01	-0.877E-01	0.812E-01	-0.710E-01
5P - 6S	2500.	0.280	0.174	0.574E-01	0.445E-01	0.503E-01	0.359E-01
75075.1A	5000.	0.324	0.195	0.623E-01	0.502E-01	0.539E-01	0.407E-01
c= 0.28E+21	10000.	0.367	0.196	0.680E-01	0.566E-01	0.582E-01	0.458E-01
	20000.	0.417	0.167	0.745E-01	0.636E-01	0.632E-01	0.515E-01
	30000.	0.458	0.142	0.788E-01	0.681E-01	0.665E-01	0.552E-01
	80000.	0.538	0.986E-01	0.908E-01	0.803E-01	0.758E-01	0.651E-01
5P - 7S	2500.	0.969E-01	0.611E-01	0.182E-01	0.159E-01	0.152E-01	0.128E-01
33658.7A	5000.	0.113	0.697E-01	0.202E-01	0.180E-01	0.168E-01	0.145E-01
c= 0.56E+20	10000.	0.129	0.702E-01	0.224E-01	0.202E-01	0.186E-01	0.164E-01
	20000.	0.148	0.569E-01	0.250E-01	0.228E-01	0.206E-01	0.184E-01
	30000.	0.164	0.467E-01	0.266E-01	0.244E-01	0.219E-01	0.197E-01
	80000.	0.193	0.288E-01	0.311E-01	0.288E-01	0.255E-01	0.233E-01

continued opposite

Table 1—*continued*

PERTURBER DENSITY 10(+13)cm(-3)							
	ELECTRONS			PROTONS		IONIZED HELIUM	
TRANSITION	T(K)	WIDTH(A)	SHIFT(A)	WIDTH(A)	SHIFT(A)	WIDTH(A)	SHIFT(A)
5D - 7P	2500.	1.25	-0.512	0.345	-0.298	0.286	-0.239
66489.4A	5000.	1.21	-0.426	0.385	-0.340	0.317	-0.273
c= 0.91E+19	10000.	1.14	-0.337	0.431	-0.385	0.352	-0.311
	20000.	1.04	-0.247	0.488	-0.436	0.393	-0.352
	30000.	0.982	-0.199	0.527	-0.468	0.419	-0.378
	80000.	0.828	-0.106	0.629	-0.571	0.499	-0.447
5D - 8P	2500.	1.22	-0.601	0.251	-0.209	0.210*	-0.167*
44208.7A	5000.	1.25	-0.443	0.278	-0.240	0.231	-0.192
c= 0.40E+19	10000.	1.30	-0.224	0.309	-0.272	0.256	-0.220
	20000.	1.36	-0.164	0.345	-0.309	0.283	-0.249
	30000.	1.37	-0.101	0.370	-0.332	0.301	-0.268
	80000.	1.32	-0.113E-01	0.439	-0.395	0.352	-0.317
5D - 9P	2500.	1.24	-0.673	0.257*	-0.206*	0.218*	-0.164*
36258.2A	5000.	1.28	-0.448	0.284	-0.237	0.239*	-0.190*
c= 0.27E+19	10000.	1.38	-0.233	0.314	-0.271	0.262*	-0.218*
	20000.	1.47	-0.121	0.348	-0.307	0.289	-0.248
	30000.	1.48	-0.918E-01	0.371	-0.331	0.306	-0.267
	80000.	1.45	-0.299E-02	0.437	-0.392	0.355	-0.316
5D -10P	2500.	1.51	-0.822	0.322*	-0.251*	0.274*	-0.199*
32258.1A	5000.	1.58	-0.545	0.355*	-0.292*	0.299*	-0.233*
c= 0.21E+19	10000.	1.73	-0.322	0.392*	-0.335*	0.328*	-0.269*
	20000.	1.84	-0.123	0.435	-0.381	0.361*	-0.307*
	30000.	1.86	-0.914E-01	0.463	-0.409	0.383*	-0.330*
	80000.	1.82	-0.355E-01	0.542	-0.486	0.443	-0.393

†The present table represents only a sample of the results. Additional data may be obtained from the authors on request, by electronic mail or on a floppy disk.

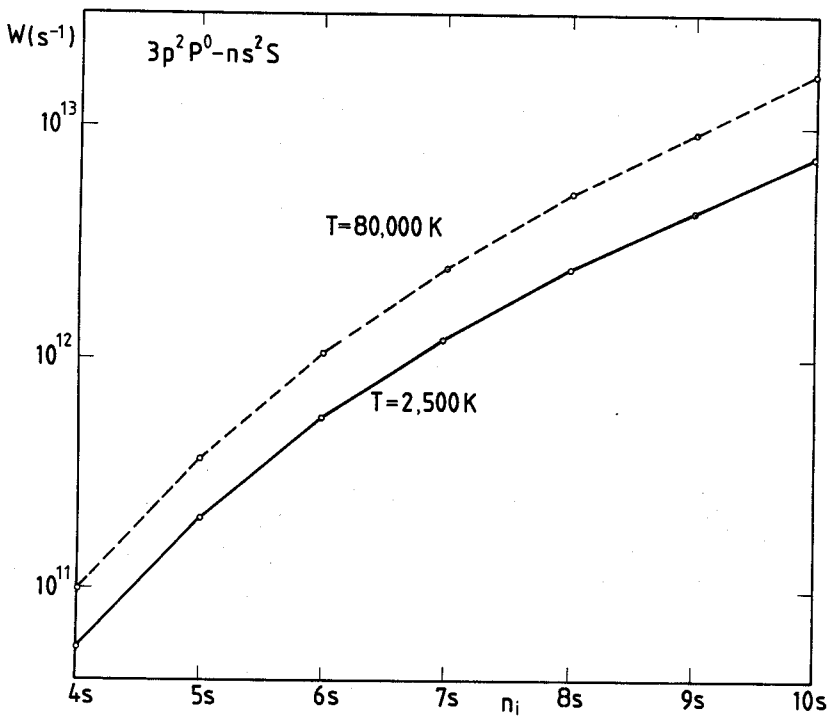

Fig. 1. Electron-impact full halfwidths for Na(I) $3p^2P^0$–ns^2S lines as a function of n_i for $T = 2500$ and 80,000 K at $N_e = 10^{16}$ cm^{-3}.

Table 2. As in Table 1 but for electron-impact broadening parameters for an electron density of 10^{16} cm^{-3}.

PERTURBER DENSITY 10(+16)cm(-3)			
	ELECTRONS		
TRANSITION	T(K)	WIDTH(A)	SHIFT(A)
3S - 6P	2500.	0.527	-0.283
2680.4A	5000.	0.573	-0.257
c= 0.19E+18	10000.	0.653	-0.186
	20000.	0.749	-0.143
	30000.	0.785	-0.108
	80000.	0.842	-0.356E-01
3S - 7P	2500.	1.16*	-0.529*
2593.9A	5000.	1.26	-0.524
c= 0.10E+18	10000.	1.44	-0.393
	20000.	1.63	-0.325
	30000.	1.70	-0.240
	80000.	1.78	-0.749E-01
3S - 8P	2500.	2.19*	-0.920*
2543.8A	5000.	2.42*	-0.863*
c= 0.63E+17	10000.	2.81	-0.670
	20000.	3.16	-0.571
	30000.	3.27	-0.433
	80000.	3.38	-0.126
3S - 9P	2500.		
2512.1A	5000.	4.08*	-1.19*
c= 0.42E+17	10000.	4.90*	-0.956*
	20000.	5.53	-0.827
	30000.	5.73	-0.639
	80000.	5.87	-0.203
3S -10P	2500.		
2490.7A	5000.	5.99*	-1.39*
c= 0.29E+17	10000.	7.71	-1.21
	20000.	8.85	-1.12
	30000.	9.22	-0.874
	80000.	9.46	-0.270
3P - 7S	2500.	1.52	0.920
4750.6A	5000.	1.73	1.12
c= 0.12E+19	10000.	1.90	1.12
	20000.	2.19	0.986
	30000.	2.45	0.832
	80000.	2.93	0.528
3P - 8S	2500.	2.71*	1.51*
4544.2A	5000.	3.07	1.81
c= 0.68E+18	10000.	3.61	1.85
	20000.	4.23	1.45
	30000.	4.75	1.23
	80000.	5.55	0.692

NE= 0.1E+17			
	ELECTRONS		
TRANSITION	T(K)	2WE(A)	DE(A)
3P - 9S	2500.	4.57*	2.26*
4423.5A	5000.	5.24	2.69
c= 0.43E+18	10000.	6.26	2.67
	20000.	7.69	2.07
	30000.	8.61	1.71
	80000.	9.85	0.694
3P - 6D	2500.	7.05*	2.13*
4667.5A	5000.	8.36	2.29
c= 0.28E+17	10000.	8.83	2.02
	20000.	8.74	1.55
	30000.	8.47	1.28
	80000.	7.47	0.630
3P - 7D	2500.	9.20*	2.85*
4496.6A	5000.	12.4*	3.25*
c= 0.17E+17	10000.	14.3	2.94
	20000.	14.8	2.25
	30000.	14.5	1.84
	80000.	13.1	0.818
3D - 5P	2500.	7.85	-4.29
17038.7A	5000.	8.74	-4.29
c= 0.14E+20	10000.	9.86	-3.25
	20000.	11.5	-2.58
	30000.	12.3	-2.26
	80000.	13.6	-1.04
3D - 6P	2500.	11.4	-5.81
12309.2A	5000.	12.5	-5.67
c= 0.39E+19	10000.	14.2	-4.25
	20000.	16.3	-3.01
	30000.	17.1	-2.25
	80000.	18.4	-0.564
4S - 7P	2500.	10.6*	-4.80*
7810.0A	5000.	11.5	-4.76
c= 0.94E+18	10000.	13.1	-3.61
	20000.	14.9	-2.77
	30000.	15.5	-1.85
	80000.	16.4	-0.305

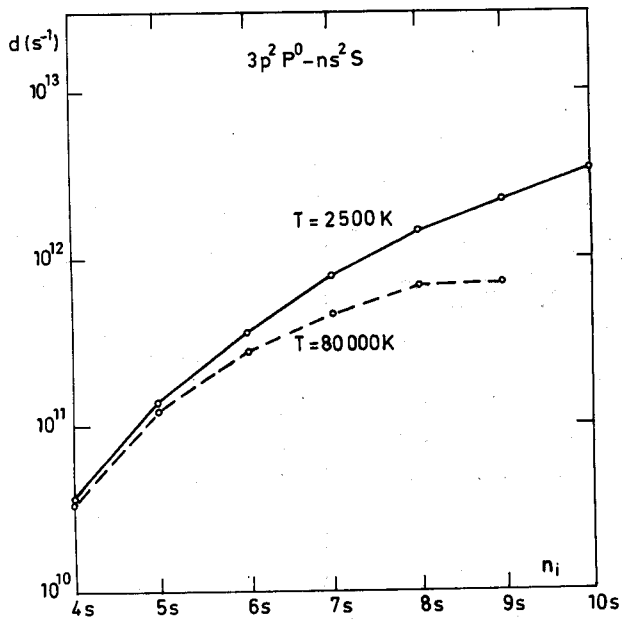

Fig. 2. As in Fig. 1 but for the electron-impact shift.

parameters. This result was proved and analyzed in detail in Ref. 8. However, data for the $8s^2S$–$3p^2P^0$ line in Figs. 3 and 4 of Ref. 8 deviate from the expected trend. Our new data have been extended up to $n = 10$ and are presented in Figs. 1 and 2. We now find that the expected trend continues for series members up to $n = 10$.

Acknowledgements—One of us (M.D.) was supported by the Observatory of Paris-Meudon. This work was supported by C.N.R.S. and is a part of French–Yugoslav collaboration through the project "L'éllargissement Stark des raies spectrales des plasmas astrophysique et de laboratoire". This study was supported in part by SKNTI under the project "Atomic, Molecular and Plasma Spectroscopy". Calculations were performed on the VAX 8600 of the Observatory of Paris-Meudon and on the IBM computers of CIRCE (Orsay).

REFERENCES

1. H. R. Griem, *Spectral Line Broadening by Plasmas*, Academic Press, New York, NY (1974).
2. H. P. Stormberg, *J. Appl. Phys.* **51,** 1963 (1980).
3. D. O. Wharmby, *IEEE Proc.* **127,** 165 (1980).
4. B. Caccin, M. T. Gomez, and G. Roberti, *Astron. Astrophys.* **92,** 63 (1980).
5. I. Vince, M. S. Dimitrijević, and V. Kršljanin, in *Spectral Line Shapes*, Vol. 3, p. 650, F. Rostas ed., de Gruyter, Berlin (1985).
6. S. Sahal-Bréchot, *Astron. Astrophys.* **1,** 91 (1969).
7. S. Sahal-Bréchot, *Astron. Astrophys.* **2,** 322 (1969).
8. M. S. Dimitrijević and S. Sahal-Bréchot, *JQSRT* **34,** 149 (1985).
9. H. Van Regemorter, Hoang Binh Dy, and M. Prud'homme, *J. Phys. B* **12,** 1073 (1979).
10. M. S. Dimitrijević and S. Sahal-Bréchot, *Bull. Obs. Astron. Belgrade* **142** (1990).
11. M. S. Dimitrijević and S. Sahal-Bréchot, *JQSRT* **31,** 301 (1984).
12. S. Bashkin and J. J. Stoner, Jr., *Atomic Energy Levels and Grotrian Diagrams*, Vol. 1, North Holland, Amsterdam (1975).
13. H. R. Griem, M. Baranger, A. C. Kolb, and G. Oertel, *Phys. Rev.* **125,** 177 (1962).

J. Quant. Spectrosc. Radiat. Transfer Vol. 45, No. 3, pp. 181–188, 1991
Printed in Great Britain.

0022-4073/91 $3.00 + 0.00

EFFECT OF BACK REACTION ON BROADENING OF ATOMIC SPECTRAL LINES IN THE IMPACT APPROXIMATION

B. GRABOWSKI and A. CZAIŃSKI
Institute of Physics, Pedagogical University, Oleska 48, PL-45-052 Opole, Poland
M. S. DIMITRIJEVIĆ
Astronomical Observatory, Volgina 7, YU-11050 Belgrade, Yugolsavia

(Received 18 July 1988; received for publication 29 August 1990)

Abstract—The phase shift (PS) due to a particle–perturber collision in a plasma has been investigated without using the classical straight-line path approximation. The curvilinear trajectory of the perturber is taken into account through the back reaction. The electrostatic potential interactions $V \sim \Sigma_l C_l r^{-l}$ and the corresponding shifts of the energy levels $\Delta E \sim \Sigma_n C_n r^{-n}$ are considered by using for V the leading terms only when both, one or none of the interacting particles are charged or have a permanent electric dipole moment. Thus, the PS is parameterized by at least two indices, n and l. In general, $l \neq n$. Analytic specification for $\eta_{n,l}$ are given for (n, l)-combinations corresponding to resonance and van der Waals type perturbations, and also to the linear and quadratic Stark effects in a perturbed system. Our approach should be especially useful at relatively high plasma densities and at the adiabatic limit.

1. INTRODUCTION

In a number of calculations of atomic collision processes and of spectral line shapes, the frequency phase shift (PS) is often used[1,2] for the classical path approximation (CPA). When both colliding particles are electrically charged, the hyperbolic CPA-trajectory is often a good approximation.[3,4] When the perturbed system is electrically neutral (in a macroscopic sense), its effect on a particle passing is usually neglected and a rectilinear path is assumed for the perturber. However, this assumption may become crude in some cases (e.g., Refs. 5–7). Consequently, a number of attempts have been made to take account of the back reaction of the perturbed atom on the motion of the perturber and on the resulting line broadening (see, e.g., Dimitrijević[4,7] and references therein and also Burgess[6]).

As a result of interaction, the perturbed system shows induced electric moments, especially at low temperatures, which have an effect on the perturber trajectory and on the final phase shift during the collision. Since it is not easy to obtain an analytical solution for each case of interest, the approximation of using an average mean perturbation (i.e., an effective rectilinear trajectory)[8] has been introduced in order to improve the CPA, thereby retaining analytic solutions for the rectilinear case. Unfortunately, this approximation is often not suitable, especially in cases of potentials of low degree in r (Ref. 9) or of close approach.[7] We may also perform numerical calculations, but each numerical calculation refers to a special case that is parameterized by the assumed physical conditions.

In this paper, we present phase-shift calculations by the curvilinear-path model, with proper account of a variety of long-range potentials, and we also present, as an improvement over our earlier papers,[4,7,9,10] some exact algebraic results that are of spectroscopic interest.

2. BASIC ASSUMPTIONS

We consider the phase shift in the spectral line during an atom–perturber collision in a plasma assuming that: (i) the trajectory of the perturber is specified by the CPA-model; the collisions are (ii) binary and (iii) adiabatic; (iv) the closest approach distance is much larger than the size of a

target (i.e., than the diameter of an excited atom); (v) the shift of the atomic energy or line frequency follows a power law. In (i), we do not use the rectilinear-trajectory hypothesis; instead, we allow for effects of curvilinearity of the perturber trajectory resulting from back reaction in the field of the electric multipole that is induced in the perturbed (macroscopically neutral) particle.

The classical path approximation may be applied when the de Broglie wavelength $\lambda\!\!\!^{-}$ of the perturber is much smaller than the distance of closest approach to the atom in the rest frame. This assumption is equivalent to large values for the orbital angular momentum quantum number l of the perturber. For a typical perturber, l^3 is of the order of the statistical factor $\Gamma = 2(2\pi mkT)^{3/2}/N_e h^3$,[5] which in a typical cool plasma ($T \approx 1$ eV, $N_e \approx 10^{15}$ cm^{-3}) is indeed a large number of the order of 10^6 for electrons. This condition corresponds approximately to the criterion $T^{(n/2)-1} C_n \gg \hbar^{n-1} k^{(2-n)/2}/m^{n/2}\psi_n$, $C_n = C_n^i - C_n^f$, where the superscripts i and f indicate the initial and final states of the quantum transition in a spectral line (cf. Ref. 1), which is usually fulfilled for a typical perturber in a cool plasma. Furthermore, following Baranger,[5] one can show that the contributions to broadening from these typical (distant) perturbers dominate over very close perturbers because of the long-range nature of the interaction. Additional arguments for the suitability of the classical path assumption in line-shape investigations have also been discussed in Ref. 11 on the basis of results from Ref. 12. For example, most of the Stark-broadening calculations have been performed by using the CPA model (e.g., Ref. 3).

3. FORMALISM

We have explicit expressions for the electrostatic potential interactions V and for the corresponding shifts ΔE of the atomic energy states, i.e.

$$V(R) = \sum_l \hbar C_l R^{-l}, \quad \Delta E(R) = \sum_n C_n R^{-n}. \tag{1}$$

Calculations of C_l are discussed in Refs. 13 and 14. Following the assumptions made in Sec. 2, the phase shift due to collision with the perturber is given by[4,15,16]

$$\eta_{n_1,n_2,\ldots;l_1,l_2,\ldots}(\rho) = \frac{2}{v} \sum_n C_n \int_{R_{\max}(l)}^{\infty} \frac{dR}{R^{n-1}\sqrt{R^2(1 - \Sigma_l \hbar C_l R^{-l}/E_0) - \rho^2}}, \tag{2}$$

where $n \geqslant 2$ and $R_{\max}(l)$ is the largest of the positive roots of the denominator. In Refs. 4, 9, 10, the physical assumptions are specified and adequate albegraic descriptions of the PS are given for special cases of the physically interesting (n, l) pairs, i.e., of leading terms of the power expansions for ΔE and V, respectively. The simplest PS calculation in the rectilinear CPA, $\eta_n^0 = \psi_n C_n/v\rho^{n-1}$ (e.g., Ref. 17), corresponds to complete neglect of the back reaction ($C_{l_i} = 0, i = 1, 2, \ldots$).

For pairs of relatively high (n, l) numbers our earlier calculation procedure leads to very cumbersome results (cf. $\eta_{6,3}$ in Ref. 10). In this paper we present the results of $\eta_{n,l}$ calculations obtained by independent technique, following to our preliminary works.[15,16] We consider cases when both, one, or none of the interacting particles are charged macroscopically or have permanent electric moments.

4. LONG-RANGE POTENTIALS AND CORRESPONDING SHIFTS ΔE

The role of the various long-range potentials in the consideration of back reaction effects on spectral line shapes and phase shifts has been discussed in details elsewhere.[4,9,11] Here, we only enumerate some binary interactions of interest.

4.1. van der Waals attraction[18]

The interaction between two neutral atoms is often approximated by the van der Waals potential (r^{-6}), sometimes with the additional Lenard–Jones (R^{-12}) correction term.

(i) *The orientation effect*; two particles with permanent dipole moments $\mathbf{p}_1, \mathbf{p}_2$

Low-temperature limit ($kT \ll |V|$): the particles tend to align their axes, and

$$V^{or} = -2p_1 p_2/R^3. \tag{3}$$

High-temperatures limit ($kT \gg |V|$): averaging over all orientations of $\mathbf{p}_1$ and $\mathbf{p}_2$ yields

$$V^{\text{or}} = -(2/3)(p_1^2 p_2^2)/R^6)(1/kT). \tag{3'}$$

First-order energy perturbation corresponding to both Eqs. (3) and (3'):

$$\Delta E_n' = V_{nn}^{\text{or}} \sim R^{-6}. \tag{4}$$

(ii) *The induction (polarization) effect*; the particles as in (i)
In this case,

$$V^{\text{ind}} = -2(\alpha_2 p_1^2 + \alpha_1 p_2^2)/R^6, \tag{5}$$

and

$$V^{\text{ind}} = -(\alpha_2 p_1^2 + \alpha_1 p_2^2)/R^6, \tag{5'}$$

for the low- and high-temperature limits, respectively; α_1, α_2 = the polarizabilities of the particles. Corresponding shift $\Delta E_n'$ as in Eq. (4).

(iii) *The dispersion effect*

The attraction potential between two particles 1 and 2 with polarizabilities α and instantaneous dipole moments $\mathbf{p}^{\text{inst}}$, averaged over time, is

$$V^{\text{disp}} \approx -4\langle \alpha_2 (p_1^{\text{inst}})^2/R^6 \rangle_{\text{av}}. \tag{6}$$

This potential acts on the movement of the first particle and, correspondingly,

$$\Delta E_2^{\text{disp}} = -(KR^{-6} + LR^{-9} + MR^{-12} + \cdots), \tag{7}$$

where $K, L, M > 0$.

In real situations, with the influence of many particles superimposed according to orientation and induction interactions from different sides, it is the dispersion effect which makes the dominant contribution to the R^{-6} law.

4.2. *The resonance effect*

For particles of the same type but in different excitation states,[19]

$$V^{\text{res}} \sim R^{-3}, \quad \Delta E' \sim R^{-3}. \tag{8}$$

4.3. *Interactions of a neutral particle with a point-charge perturber*

We now have a number of different possibilities:[4] r^{-2} (linear Stark effect), r^{-4} (polarization potential, quadratic Stark effect), r^{-5}, 2nd order quadrupole potential, etc. Some interesting combinations of numbers are presented in Table 1.

5. RESULTS

We present for $\eta_{n,l}$ results that include all of the important cases for $n = 2, 3, 4, 6, 9$, and 12 (the linear and quadratic Stark effects and resonance and van der Waals broadening) at $l = 3$ or

Table 1. Combinations of (n, l) numbers of physical interest for weak interactions. Abbreviations: d = dipole, q = quadrupole, pc = point charge, res = resonance, vdW = van der Waals.

n, l	interaction $V_l(R)$	Refs. of $\eta_{n,l}$
2, 2	d–pc	7
2, 3	q–pc	9, 10, 15
2, 4	d–pc	9, 10
3, 3	res, d–d	7, 15
4, 3	q–pc	15
4, 4	d–pc	7, 21, 22
5, 5	vdW, d–d	—
6, 3	vdW, d–d	15
6, 6	vdW, d–d	16
9, 6	vdW, d–d	16
12, 6	vdW, d–d	16

6. These refer to ordinary rectilinear-path model calculations, η_n^0. We maintain the previous designations in order to complete our earlier results for the (2, 3), (2, 4)[9,10] and (3, 3)[4,7] combinations. Thus,

$$\eta_{2,3}(\rho)=\frac{2C_2}{v}\int_{x_1}^{\infty}\frac{x\,\mathrm{d}x}{\sqrt{(x-x_1)(x-x_2)(x-x_3)x}}=\eta_2^0\frac{4\rho}{\pi}\frac{F(\varphi,k)}{\sqrt{x_1(x_3-x_2)}}, \tag{9}$$

where

$$k^2=\frac{x_3}{x_1}\frac{x_1-x_2}{x_3-x_2},\ \sin^2\varphi=\frac{x_2-x_3}{x_2-x_1},\quad C_3<0; \tag{10}$$

$$\eta_{2,3}(\rho)=\eta_2^0\frac{4\rho}{\pi}\frac{F(\varphi,k)}{\sqrt{x_2(x_3-x_1)}}, \tag{11}$$

where

$$k^2=\frac{x_3}{x_1}\frac{x_1-x_2}{x_1-x_3},\ \sin^2\varphi=\frac{x_2}{x_2-x_1},\quad C_3>0. \tag{12}$$

For $\eta_{3,3}$, we have the same values of k^2 and $\sin^2\varphi$ [Eq. (10) or Eq. (12) for $C_3<0$ or $C_3>0$, respectively], and

$$\eta_{3,3}(\rho)=\eta_3^0\frac{2\rho^2}{x_3\sqrt{x_1(x_3-x_2)}}\left\{F(\varphi,k)+\left(\frac{x_3}{x_1}-1\right)\Pi(\varphi,-k^2,k)\right\}, \tag{13}$$

or

$$\eta_{3,3}(\rho)=\eta_3^0\frac{2\rho^2}{x_3\sqrt{x_2(x_3-x_1)}}\left\{F(\varphi,k)+\left(\frac{x_3}{x_1}-1\right)E(\varphi,k)\right\}. \tag{14}$$

The preceding results correspond to

$$x_i'=2\cos(\xi+(i-1)2\pi/3),\quad x_i'=x_i/(\rho/\sqrt{3}),\quad i=1,2,3, \tag{15}$$

$$\cos 3\xi=\delta,\quad \delta=\hbar C_3/(2E_0\rho'^3)\leqslant 1,\quad \rho'=\rho/\sqrt{3}, \tag{16}$$

with δ being a perturbation parameter equal to half of the ratio of the potential energy of the perturber at the distance ρ' to its kinetic energy E_0 at infinity. F, E, and Π are elliptic integrals of the first, second, and third kind, respectively.

When $\delta\geqslant 1$, the following relations apply:

$$\eta_{3,3}(\rho)=\eta_3^0\frac{3\Delta}{\Gamma}\left(-\frac{c}{a}-F(\varphi,k)-\Delta\frac{I_1}{ab}\right), \tag{13'}$$

$$k^2=\frac{1}{1+k_1^2},\quad \cos\varphi=-\frac{d}{c},$$

$$k_1=A-\sqrt{A^2+1},\quad A=\frac{\gamma^2-(\alpha-\beta)\beta}{\gamma\alpha},$$

$$\alpha=B+C,\quad \beta=-\alpha/2,\quad \gamma=(C-B)\frac{\sqrt{3}}{2},$$

$$B=(\delta-\sqrt{\delta^2-1})^{1/3},\quad C=(\delta+\sqrt{\delta^2-1})^{1/3},$$

$$a=\frac{\alpha}{2}(c+d),\quad b=a,\quad c=\alpha-\beta-\frac{\gamma}{k_1},$$

$$d=\beta-\alpha-\gamma k_1,\quad \Delta=ad-bc,$$

$$\Gamma=[(\alpha-\beta)^2+\gamma]\sqrt{(c^2-d^2)(\beta^2-\gamma^2)},$$

$$I_1=[(1-\cos\varphi)/\sin\varphi]\sqrt{1-k^2\sin^2\varphi}. \tag{12'}$$

For $(n, l) = (2, 4)$, the phase shift is given by

$$\eta_{2,4}(\rho) = \eta_2^0 \frac{2\rho}{\pi} \frac{K(k)}{\sqrt{x_2}}, \quad k^2 = x_1/x_2, \quad C_4 < 0; \tag{17}$$

$$\eta_{2,4}(\rho) = \eta_2^0 \frac{2\rho}{\pi} \frac{K(k)}{\sqrt{x_2 - x_1}}, \quad k^2 = x_1/(x_2 - x_1), \quad C_4 > 0, \tag{18}$$

where

$$x_{1,2} = \rho'^2(1 \mp \sqrt{1+\delta}), \quad \delta = \hbar C_4/(E_0 \rho'^4), \tag{19}$$

with $\rho' = \rho/\sqrt{2}$. $K(k)$ it the complete elliptic integral of the first kind. We always have $\eta_{n,l} \to \eta_n^0$ at the limit $\delta \to 0$.

For more complicated cases, routine calculations lead to results that have been formulated previously but not clearly (see, e.g., $\eta_{6,3}$ in Ref. 10). We now calculate the phase shift for the entire physically important series of $(n, l = 3)$ combinations, viz.,

$$\eta_{n,3} = \frac{2C_n}{v} \int_{x_1}^{\infty} \frac{dx}{x^{n-2} y}, \quad y = \sqrt{x(x-x_1)(x-x_2)(x-x_3)}, \tag{20}$$

using the technique of canonical Legendre transformations of elliptic integrals[23,24] and auxiliary integrals of the form $J_n(x) = \int (x^n/y)\, dx$. For the entire series, the values of k, φ, and x_i are the same as those given in Eqs. (10), (12) and (15), (16), respectively. We obtain

$$J_0 = gF(\varphi, k), \tag{21}$$

irrespective of the sign of C_3, and

$$J_{-1} = \frac{g\rho^2}{3x_3} \left\{ F(\varphi, k) + \left(\frac{x_3}{x_1} - 1 \right) \Pi(\varphi, -k^2, k) \right\}, \tag{22}$$

$$\Pi(\varphi, -k^2, k) = [E(\varphi, k) - gx_3/2]/k'^2, \tag{23}$$

$$g = 2/\sqrt{x_1(x_3 - x_2)} \tag{24}$$

for $C_3 < 0$, or

$$J_{-1} = \frac{g\rho^2}{3x_3} \left\{ F(\varphi, k) + \left(\frac{x_3}{x_1} - 1 \right) E(\varphi, k) \right\}, \tag{25}$$

$$g = 2/\sqrt{x_2(x_3 - x_1)} \tag{26}$$

for $C_3 > 0$. Next,

$$J_m = -[1 + 3(m+1)J_{m+1} - (m+2)J_{m+3}]/(2m+1)\delta, \tag{27}$$

for $-m = 2$, 3, and 4, irrespective of the sign of C_3.
Finally,

$$\eta_{n,3}/\eta_n^0 = 2\sqrt{3^{n-1}} J_{2-n}/\psi_n, \quad n = 2, \ldots, 6. \tag{28}$$

In the region $\delta < 0$ (attractive forces), $\eta_{n,3}/\eta_n^0 > 1$; in the region $\delta > 0$ (repulsive forces), $\eta_{n,3}/\eta_n^0 < 1$. The deviation from unity is the stronger the greater n.

The indicated iterative procedure for calculations of $n_{n,3}$ is convenient for numerical applications. However, when $|\delta| \to 0$, $\eta_{n,3}$ in Eq. (28) becomes an indeterminate expression of the type 0/0 [cf. Eq. (27)]. Specifications of $\eta_{n,3}$ that are adequate for this region, i.e., Eq. (28) expanded in a series of positive powers of the small perturbation parameter δ, are as follows:

$$\eta_{2,3} = \eta_2^0[1 - 3^{1/2}(4/9\pi)\delta - (5/36)\delta^2 - \cdots], \tag{29}$$

$$\eta_{3,3} = \eta_3^0[1 - 3^{1/2}(\pi/12)\delta + (8/27)\delta^2 - \cdots], \tag{30}$$

$$\eta_{4,3} = \eta_4^0[1 - 3^{1/2}(32/81\pi)\delta + (35/72)\delta^2 - \cdots], \tag{31}$$

$$\eta_{6,3} = \eta_6^0[1 - 3^{5/2}(256/1215)\delta - (35/36)\delta^2 - \cdots]. \tag{32}$$

For $|\delta| \lesssim 0.01$, these specifications are reliable at least up to six decimal points, except for $\eta_{3,3}$ for which the description is less exact by approximately one order of magnitude.

In Fig. 1, we present values of the ratio $\eta_{n,3}/\eta_n^0$ for $n = 2, 3, 4$, and 6 vs the perturbation parameter δ. In the region $\delta < 0$, we encounter attractive forces; in the region $\delta > 0$, the forces are repulsive. Deviation from the horizontal axis is a measure of the effect of curvilinearity of the perturber trajectory on the phase shift during collision.

Using the procedure involving Legendre's canonical transformations of the elliptical integrals, we have calculated $\eta_{n,6}$ for $n = 6$, 9, and 12. We note that $J_n = \int (x^2/y)\,dx$, where $y = \sqrt{(x-x_1)(x-x_2)(x-x_3)}$ for $n = 9$, and $y = \sqrt{(x-x_1)(x-x_2)(x-x_3)x}$ for $n = 6$ and 12.

In order to adapt this approach to iterative evaluations, we denote J_n by XJ_n for $n = 6$ and 12 and by YJ_n for $n = 9$. For $\eta_{n,6}$, we obtain

$$x_i' = 2\cos(\xi + (i-1)2\pi/3) + 1, \quad x_i' = x_i/\rho'^2, \tag{33}$$

where $i = 1, 2, 3$, and

$$\rho' = \rho/\sqrt{3}, \quad \cos 3\xi = 1 + \delta, \quad \delta = \hbar C_6/(2E_0\rho'^6). \tag{34}$$

The perturbation parameter δ equals one-half of the ratio of the potential energy at the interparticle distance ρ' to the kinetic energy E_0 of the perturber at infinity.

In the particular case $\eta_{9,6}$,

$$YJ_0 = g'F(\varphi, k), \tag{35}$$

$$YJ_{-1} = \frac{g'}{x_3'}\left[F(\varphi, k) + \left(\frac{x_3}{x_1} - 1\right)\Pi(\varphi, -k^2, k)\right], \tag{36}$$

$$\Pi(\varphi, -k^2, k) = [E(\varphi, k) - \tfrac{1}{2}g'x_3']/k'^2,$$

$$YJ_{-3} = (2YJ_0 - 9YJ_{-1})/(10\delta), \tag{37}$$

where

$$k^2 = \frac{x_3}{x_1}\frac{x_1 - x_2}{x_3 - x_2}, \quad \sin^2\varphi = \frac{x_3 - x_2}{x_1 - x_2}, \quad g' = \frac{2}{\sqrt{x_1'(x_3' - x_2')}}. \tag{38}$$

For $\eta_{n,6}$, $n = 6$ and 12, we obtain

$$XJ_0 = g'K(k), \tag{39}$$

$$XJ'_{+1} = g'x_1\left[K(k) + \left(\frac{x_2}{x_1} - 1\right)E(k)\right], \tag{40}$$

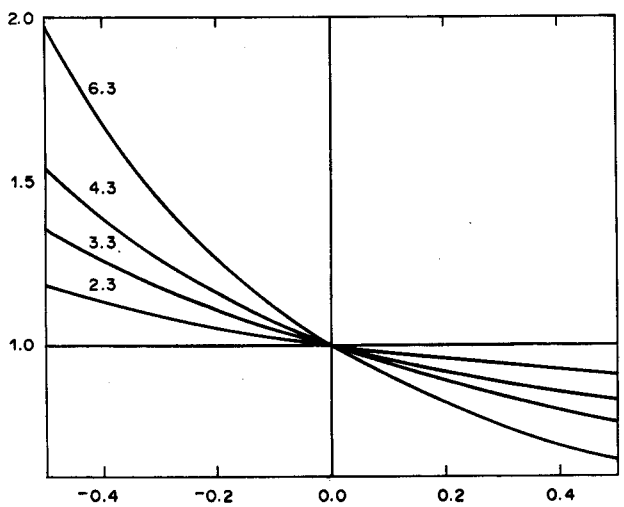

Fig. 1. Values of the $\eta_{n,3}/\eta_n^0$ ratios for $n = 2$, 3, 4, and 6 as functions of the perturbation parameter δ. The curves are parameterized in terms of the (n, l) numbers. The ratio $\eta_{n,3}/\eta_n^0$ tends toward 1 when $\delta \to 0$ and has a singularity at $\delta = -1$.

$$XJ_{-1} = \frac{g'}{x_3'}\left[K(k) + \left(\frac{x_3}{x_1} - 1\right)\Pi(\pi/2, -x_3/x_1, k)\right], \tag{41}$$

$$\Pi(\pi/2, -x_3/x_1, k) = K(k) + (\tan\vartheta)/\sqrt{1 - k^2\sin^2\vartheta}\,[E(\vartheta, k')K(k) - F(\vartheta, k')E(k)];$$

recursively,

$$XJ_m = [(2m+5)XJ_{m+3} - 3(2m+4)XJ_{m+2}]/4(m+1)\delta, \tag{42}$$

for $-m = 2, \ldots, 5$,

$$k^2 = (x_3 - x_2)/(x_1 - x_2), \quad \sin^2\vartheta = x_3/x_1k^2, \quad g' = 2/\sqrt{x_1' - x_2'}. \tag{43}$$

F (or K), E, and Π are again the elliptic integrals of first, second, and third kind, respectively. Finally, compact descriptions of the phase shifts are

$$\eta_{n,6}/\eta_n^0 = \sqrt{3^{n-1}}XJ_{(2-n)/2}/\psi_n, \quad n = 6, 12, \tag{44}$$

$$\eta_{9,6}/\eta_9^0 = \sqrt{3^8}YJ_{-3}/\psi_9, \tag{45}$$

where η_n^0—the ordinary phase shift calculated in the rectilinear CPA approach, $\eta_n^0 = \psi_n C_n/v\rho^{n-1}$, $\psi_n = 3\pi/8, 32/35, 63\pi/256$ for $n = 6$, 9, and 12, respectively.

From Eqs. (37) to (42), we see that the $\eta_{n,6}$ given by Eqs. (44) and (45) become indeterminate (0/0) when $\delta \to 0$. For this region of extremely weak perturbations, useful power expansions of Eqs. (44) and (45) in terms of the small perturbation parameters δ are as follows:

$$\eta_{6,6} = \eta_6^0[1 - (35/144)\delta + (5005/62208)\delta^2 + \cdots], \tag{44'}$$

$$\eta_{9,6} = \eta_9^0[1 - (320/891)\delta + \cdots], \tag{45'}$$

$$\eta_{12,6} = \eta_{12}^0[1 - (715/1512)\delta + (230945/1119744)\delta^2 + \cdots]. \tag{44''}$$

For $|\delta| < 0.01$, these expansions yield results that are valid at least up to seven decimal points, except for $\eta_{9,6}$ for which the accuracy is reduced by about three orders of magnitude.

Equations (44) and (45) hold only for attractive forces, i.e., for $\delta < 0$. The ratio $\eta_{n,6}/\eta_n^0$ tends toward 1 when $\delta \to 0$ and has a logarithmic singularity at $\delta = -2$; $\eta_{n,6}/\eta_{m,6} > 1$ when $n > m$.

In Fig. 2, we show values of the phase-shift ratio $\eta_{n,l}/\eta_n^0$ as a function of the perturbation (attraction) parameter δ. The curves are labelled in pairs of $(n, l = 6)$ numbers. Deviations from the horizontal axis measure the importance of the back reaction.

We will now calculate some numerical values of the line parameters as a quantitative illustration of the importance of the back reaction for the van der Waals interaction. We have calculated the

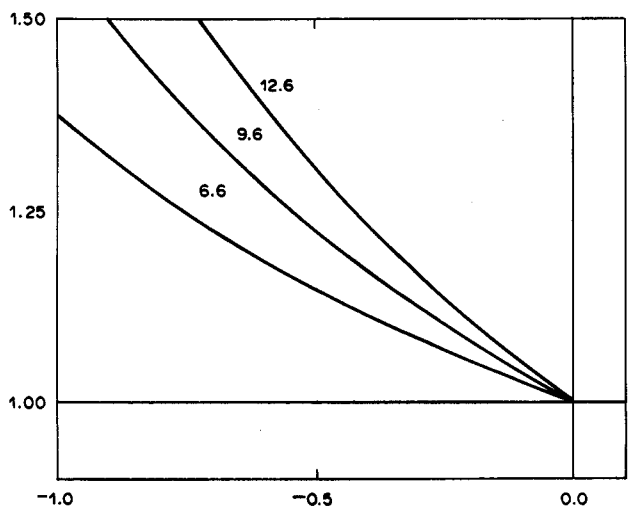

Fig. 2. As in Fig. 1, for $\eta_{n,6}/\eta_n^0$ at $n = 6$, 9 and 12. This quantity tends toward 1 when $\delta \to 0$ and has a singularity at $\delta = -2$.

Table 2

C_6	-10^{-30}	-10^{-26}
w	0.618	0.791
d	0.980	0.997

semi-half width $w_{6,6}$ and the shift $d_{6,6}$ by taking account of the back reaction to the quasi-classical, adiabatic approximation, as given by the relation[1]

$$w + id = N_e \int vf(v)\,dv \int 2\pi\rho\,d\rho[1 - \exp(-i\eta)]. \tag{46}$$

The quantities w and d, presented in Table 2, are calculated at $T = 5000$ K (the back effect does not depend on N_e). These quantities are expressed in the units of w_6^0 and d_6^0 calculated by using the standard straight-line path approximation.

These quantities are calculated by averaging η over the range $\rho_{min} < \rho < \infty$, where ρ_{min} is (in the case of attractive forces) the minimum impact parameter which separates normal perturber trajectories from those with $\rho < \rho_{min}$ (these last-named paths formally pass through the radiator and are designated as PTR, e.g., Ref. 4).

Estimation of the contributions made by perturbers arriving on the PTR trajectories is a problem because, for $\rho < \rho_{min}$, the phase-shift method and the simple multipole form of potentials break down. To describe such passages, a complete quantum treatment should be used, taking into account the entire radiator–perturber system. We know *a priori*, however, that we may show that the importance of PTR collisions (relatively rare) in problems on line-parameter calculations is not crucial. A closely-interacting atomic quantum system finds itself in an energetic state different from that before collision and the probability of making a contribution to the radiation at the original frequency ω_0 is small. The shift d is considerably less dependent than width w on the effects of non-uniform motion of the perturber, even at low temperatures.

These results presented here should improve the description of interparticle collisions and, consequently, the calculations of widths and shifts of spectral lines formed in the laboratory and in astrophysical plasmas.

Acknowledgements—This work was performed under partial sponsorship of the Polish Academy of Sciences, Programme CPBP.02.02 and RZN of Serbia.

REFERENCES

1. I. I. Sobelman, L. A. Vainstein, and E. A. Yukov, *Excitation of Atoms and Broadening of Spectral Lines*, Springer, New York, NY (1981).
2. G. Peach, *Adv. in Phys.* **30,** 367 (1981).
3. H. R. Griem, *Spectral Line Broadening by Plasmas*, Academic Press, New York, NY (1974).
4. M. S. Dimitrijević, in *Classical Dynamics in Atomic and Molecular Physics*, p. 403, T. Grozdanov, P. Grujić, and P. Krstić eds., World Scientific, Singapore (1989).
5. M. Baranger, in *Atomic and Molecular Processes*, p. 439, D. R. Bates ed., Academic Press, New York, NY (1962).
6. D. D. Burgess, *Phys. Rev. A* **176,** 150 (1968).
7. M. S. Dimitrijević, *J. Phys. B: Atom. Molec. Phys.* **17,** L283 (1984).
8. O. Vallee, P. Ranson, and J. Chapelle, *J. Phys. B: Atom. Molec. Phys.* **9,** L289 (1976).
9. B. Grabowski, *J. Phys.-WSP Opole* (in Polish) **23,** 77 (1989).
10. B. Grabowski and M. S. Dimitrijević, XIII SPIG'86, Sibenik 1-5.09.1986, Contrib. Papers, p. 299 (1986).
11. M. S. Dimitrijević and P. Grujić, *JQRST* **19,** 407 (1978).
12. E. Vogt and G. H. Wannier, *Phys. Rev.* **95,** 1190 (1959).
13. J. Szudy and W. B. Baylis, *Can. J. Phys.* **54,** 2287 (1976).
14. J. L. Le Gouet and P. R. Berman, *Phys. Rev.* **A24,** 1831 (1981).
15. B. Grabowski and A. Czaiński, *Proc. 9th Int. Conf. on Spectral Lines*, 25–29 July 1988, p. D23, Nicholas Copernicus Univ. Press, Toruń (1988).
16. B. Grabowski and A. Czaiński, *ibid.* p. D24.
17. K. R. Lang, *Astrophysical Formulae*, Springer, Berlin (1974).
18. D. Langbein, *Theory of van der Waals Attraction*, Springer, Berlin (1974).
19. S. Flügge, *Practical Quantum Mechanics*, Springer, New York (1974).
20. L. D. Landau and E. M. Lifshitz, *Quantum Mechanics* (in Russian), Moscow (1948).
21. M. S. Dimitrijević, Ph.D. Thesis, Belgrade (1978).
22. M. S. Dimitrijević and P. Grujić, *Z. Naturf.* **34a,** 1362 (1979).
23. G. A. Korn and T. M. Korn, *Mathematical Handbook*, 2nd edn, Chap. 21.6-5, McGraw-Hill, New York, NY (1968).
24. W. Grobner und N. Hofreiter, *Integraltafel*, Springer, Wien (1957).

J. Quant. Spectrosc. Radiat. Transfer Vol. 46, No. 1, pp. 41–53, 1991
Printed in Great Britain.

0022-4073/91 $3.00 + 0.00

STARK BROADENING OF Li(I) LINES

M. S. DIMITRIJEVIĆ† and S. SAHAL-BRÉCHOT‡

†Astronomical Observatory, Volgina 7, 11050 Beograd, Yugoslavia and ‡Département Atomes et Molécules en Astrophysique, Unité associée au CNRS No. 812, Observatoire de Paris, 92195 Meudon Cedex, France

(Received 1 June 1990; received for publication 13 November 1990)

Abstract—A semiclassical approach has been used to evaluate electron-, proton- and ionized helium-impact line widths and shifts for 61 neutral lithium multiplets. Calculations have been performed as a function of temperature and at a perturber density of $10^{13}\,cm^{-3}$. The results have been used to investigate Stark-broadening-parameter regularities within spectral series.

1. INTRODUCTION

Stark-broadening parameters for neutral lithium are of interest in plasma spectroscopy[1] and may be employed in deducing the electron concentration of a high-density plasma.[2] Profiles of neutral lithium lines are also of interest to astrophysicists since the surface content (abundance) of Li involves problems correlated with nucleogenesis and with mixing between the atmosphere and the interior.[3] They should also be of interest in connection with the study of extremely strong Li(I) features observed in a number of C and S stars,[3] as well as in investigations connected with the evidence of deep Li depletions in the mid-F stars, which were first observed in the Hyades.[4] Even for the study of stars in the late stages of evolution, Stark broadening is of interest since its influence increases with an increase in the principal quantum number (n) of the initial energy level[5] because the bond between the optical electron and the core becomes weaker and the influence of external electric microfields increases. Using a semiclassical perturbation formalism[6,7] and a Stark-broadening computer code derived from this method, we have calculated electron-, proton- and ionized helium-impact line widths and shifts for 61 neutral lithium multiplets for the conditions specified in the Abstract.

The extensive and self-consistent set of data obtained by us has been used also for the continuation of our research of regularities within spectral series (see, e.g., Ref. 8).

2. THEORY

The semi-classical-perturbational formalism is described in Refs. 6 and 7. For this reason, only a few details are given here. For the impact approximation, the full halfwidth ($2w$) and shift (d) of an electron-impact broadened line may be expressed as[6,7]

$$2w = N_e \int_0^\infty v f(v)\,dv \left[\sum_{i' \neq i} \sigma_{ii'}(v) + \sum_{f' \neq f} \sigma_{ff'}(v) + \sigma_{el}(v) \right]$$

$$d = N_e \int_0^\infty v f(v)\,dv \int_{R_3}^{R_D} 2\pi\rho\,d\rho\,\sin 2\phi_p. \tag{1}$$

Here, N_e is the electron density and $f(v)$ the Maxwellian velocity distribution function for electrons, ρ denotes the impact parameter for the incoming electron, i and f denote, respectively, the initial and final atomic energy levels, and i′, f′ are the corresponding perturbing levels. The inelastic cross section $\sigma_{ii'}(v)$ may be obtained from integration over the impact parameter of the transition probability $P_{ii'}(\rho, v)$, viz.

$$\sum_{i' \neq i} \sigma_{ii'}(v) = \tfrac{1}{2}\pi R_1^2 + \int_{R_1}^{R_D} 2\pi\rho\,d\rho \sum_{i' \neq i} P_{ii'}(\rho, v). \tag{2}$$

The elastic cross section is given by

$$\sigma_{el} = 2\pi R_2^2 + \int_{R_2}^{R_D} 8\pi\rho \, d\rho \, \sin^2 \delta, \quad \delta = [\phi_p^2 + \phi_q^2]^{1/2}. \tag{3}$$

The phase shifts ϕ_p and ϕ_q are due, respectively, to the polarization potential (r^{-4}) and to the quadrupolar potential (r^{-3}) parts; they are given in Chap. 3, Sec. 3, Ref. 6. All of the cutoffs R_1, R_2, R_3, R_D are described in Chap. 1, Sec. 3, Ref. 7.

If we want to make certain that a line is isolated, we can use the parameter c defined in Ref. 9 which is given in Table 1. For an electron concentration lower than

$$N_l(\text{cm}^{-3}) = [c/2W(\text{Å})][N(\text{cm}^{-3})/10^{16}], \tag{4}$$

the line may be treated as isolated in the core, even if a weak forbidden component due to failure of this approximation remains in the wing.

The formulae for the proton-impact or He^+-impact widths and shifts are analogous to the relations given in Eq. (3), but inelastic collisions are negligible.

3. RESULTS AND DISCUSSION

Energy-level data were taken from Ref. 10. The mean atomic radius and mean-square radius were calculated in the hydrogenic approximation, and the oscillator strengths in the Coulomb approximation.[11–13]

In order to provide all relevant Stark-broadening data needed in astrophysical problems,[3] we calculated broadening parameters due to collisions with the principal constituents of stellar atmospheres. Our results for electron-, proton-, and ionized helium-impact full halfwidths ($2w$) and shifts (d) for Li(I) lines are shown in Table 1 for a perturber density of 10^{13} cm^{-3} and temperatures $T = 2500$, 5000, 10,000, 20,000, 30,000, and 40,000 K. This temperature range was selected since experimental data exist for temperatures up to 26,000 K[14] and values at 10,000, 20,000, 30,000 and 40,000 K are needed for good nonlinear interpolation and extrapolation. Moreover, at 40,000 K, there exist theoretical results for 18 multiplets,[1,15] so that the possibility arises for different types of comparisons. We also specify in Table 1 a parameter c [see Eq. (4)] which when it is divided by $2w$, gives an estimate for the maximum perturber density for which the line may be treated as isolated.

For each value given in Table 1, the collision volume V multiplied by the perturber density N is much less than unity and the impact approximation is valid.[6,7] Values for $NV > 0.5$ are not given in Table 1; values for $0.1 < NV \leqslant 0.5$ are denoted by an asterisk. When the impact approximation is not valid, the ion-broadening contribution may be estimated by using the quasistatic ion-broadening parameter[1] introduced by Griem et al.[16] One must take into account also, that the "collision volume" criterion for the validity of the impact approximation is often not sufficient for ions, since electrons naturally dominate the time variations of the perturbing fields.[1] The time variations of the ion-produced fields can be ignored as long as they occur over time scales longer than $1/\omega$, where ω is the angular frequency halfwidth caused by electron impacts.[1] Consequently, in order to check the validity of the impact approximation for ions, Eq. (82) from Ref. 1 might be used. It is interesting also that in some cases, a controversy exists in the literature concerning the impact or quasistatic character of the ionic contribution to the line profile. For the Li(I) $2s$–$2p$ transition perturbed by Ar^+, the impact character of ionic profiles was pointed out by Brissaud et al,[17] which is in contradiction to the GBKO[15] validity criteria for the impact approximation that are not satisfied for the same plasma conditions.

For Li(I), 12 papers with experimental data were reviewed in Ref. 18 and 1 in Ref. 19. Of these, only four papers provide sufficient information to ascertain that acceptable data have been produced[2,14,20,21] but with relatively low, critically estimated accuracies.[18,19] In addition to the semiclassical calculations for the 18 Li(I) multiplets,[1,15] there exist for the resonance $2s$–$2p$ multiplet quantum-mechanical strong-coupling[22] and model microfield[23] calculations. These are compared with the present results in Tables 2 and 3. We see that, as expected the agreement with quantum-mechnical calculations becomes relatively better at higher temperatures. For the shift, we obtain larger values than in Refs. 20 and 14. One must take into account the fact that the shift

Table 1. This table shows electron-, proton- and ionized-helium-impact broadening parameters for Li(I) lines, for a perturber density of 10^{13} cm^{-3} and temperatures from 2500 to 40,000 K. Transitions and averaged wavelengths for the multiplet (in Å) are also given. By using c [see Eq. (4)] we obtain an estimate for the maximum perturber density for which the line may be treated as isolated and the tabulated data may be used. The asterisk identifies cases for which the collision volume multiplied by the perturber density (the condition for validity of the impact approximation) lies between 0.1 and 0.5. The present table represents only a sample of the results, additional data may be obtained from the authors on request, by electronic mail or on a floppy disk.

PERTURBER DENSITY= 0.1D+14							
	ELECTRONS			PROTONS		IONIZED HELIUM	
TRANSITION	T(K)	WIDTH(A)	SHIFT(A)	WIDTH(A)	SHIFT(A)	WIDTH(A)	SHIFT(A)
2S - 2P	2500.	0.230E-04	-0.588E-05	0.113E-04	-0.165E-05	0.113E-04	-0.138E-05
6709.6 A	5000.	0.234E-04	-0.691E-05	0.113E-04	-0.185E-05	0.113E-04	-0.155E-05
C= 0.55D+20	10000.	0.254E-04	-0.755E-05	0.113E-04	-0.208E-05	0.113E-04	-0.174E-05
	20000.	0.319E-04	-0.745E-05	0.113E-04	-0.233E-05	0.113E-04	-0.195E-05
	30000.	0.378E-04	-0.646E-05	0.113E-04	-0.249E-05	0.113E-04	-0.209E-05
	40000.	0.428E-04	-0.581E-05	0.113E-04	-0.262E-05	0.113E-04	-0.219E-05
2S - 3P	2500.	0.122E-03	0.859E-04	0.323E-04	0.272E-04	0.283E-04	0.228E-04
3233.6 A	5000.	0.130E-03	0.741E-04	0.355E-04	0.306E-04	0.308E-04	0.256E-04
C= 0.37D+18	10000.	0.140E-03	0.586E-04	0.392E-04	0.344E-04	0.338E-04	0.288E-04
	20000.	0.142E-03	0.449E-04	0.435E-04	0.387E-04	0.372E-04	0.324E-04
	30000.	0.142E-03	0.360E-04	0.463E-04	0.414E-04	0.395E-04	0.347E-04
	40000.	0.141E-03	0.299E-04	0.484E-04	0.434E-04	0.412E-04	0.364E-04
2S - 4P	2500.	0.399E-03	0.268E-03	0.101E-03	0.885E-04	0.870E-04	0.739E-04
2742.0 A	5000.	0.420E-03	0.218E-03	0.112E-03	0.100E-03	0.960E-04	0.837E-04
C= 0.12D+18	10000.	0.444E-03	0.171E-03	0.125E-03	0.113E-03	0.106E-03	0.943E-04
	20000.	0.441E-03	0.122E-03	0.139E-03	0.127E-03	0.118E-03	0.106E-03
	30000.	0.435E-03	0.937E-04	0.149E-03	0.136E-03	0.126E-03	0.114E-03
	40000.	0.429E-03	0.747E-04	0.156E-03	0.143E-03	0.131E-03	0.119E-03
2S - 5P	2500.	0.103E-02	0.661E-03	0.263E-03	0.230E-03	0.224E-03	0.192E-03
2563.1 A	5000.	0.109E-02	0.499E-03	0.292E-03	0.262E-03	0.248E-03	0.219E-03
C= 0.52D+17	10000.	0.114E-02	0.399E-03	0.326E-03	0.296E-03	0.276E-03	0.248E-03
	20000.	0.111E-02	0.252E-03	0.365E-03	0.334E-03	0.308E-03	0.279E-03
	30000.	0.109E-02	0.184E-03	0.390E-03	0.358E-03	0.328E-03	0.299E-03
	40000.	0.107E-02	0.139E-03	0.409E-03	0.376E-03	0.343E-03	0.315E-03
2S - 6P	2500.	0.225E-02	0.122E-02	0.583E-03	0.508E-03	0.495E-03	0.421E-03
2475.8 A	5000.	0.242E-02	0.984E-03	0.650E-03	0.580E-03	0.551E-03	0.483E-03
C= 0.28D+17	10000.	0.248E-02	0.686E-03	0.727E-03	0.659E-03	0.614E-03	0.550E-03
	20000.	0.240E-02	0.431E-03	0.814E-03	0.746E-03	0.685E-03	0.624E-03
	30000.	0.235E-02	0.309E-03	0.871E-03	0.799E-03	0.731E-03	0.669E-03
	40000.	0.229E-02	0.238E-03	0.917E-03	0.840E-03	0.766E-03	0.703E-03
2S - 7P	2500.	0.447E-02	0.249E-02	*0.117E-02	*0.100E-02	*0.989E-03	*0.826E-03
2426.2 A	5000.	0.479E-02	0.189E-02	0.130E-02	0.115E-02	*0.110E-02	*0.958E-03
C= 0.17D+17	10000.	0.482E-02	0.130E-02	0.146E-02	0.132E-02	0.123E-02	0.110E-02
	20000.	0.467E-02	0.657E-03	0.164E-02	0.149E-02	0.137E-02	0.125E-02
	30000.	0.454E-02	0.464E-03	0.175E-02	0.161E-02	0.147E-02	0.134E-02
	40000.	0.441E-02	0.280E-03	0.185E-02	0.169E-02	0.154E-02	0.141E-02
2P - 3S	2500.	0.222E-03	0.165E-03	0.521E-04	0.471E-04	0.444E-04	0.395E-04
8128.7 A	5000.	0.261E-03	0.197E-03	0.580E-04	0.530E-04	0.492E-04	0.444E-04
C= 0.25D+20	10000.	0.293E-03	0.220E-03	0.646E-04	0.595E-04	0.548E-04	0.499E-04
	20000.	0.312E-03	0.224E-03	0.722E-04	0.668E-04	0.610E-04	0.560E-04
	30000.	0.329E-03	0.225E-03	0.770E-04	0.715E-04	0.650E-04	0.599E-04
	40000.	0.334E-03	0.206E-03	0.807E-04	0.750E-04	0.681E-04	0.629E-04
2P - 4S	2500.	0.355E-03	0.270E-03	0.803E-04	0.752E-04	0.674E-04	0.630E-04
4973.1 A	5000.	0.418E-03	0.318E-03	0.901E-04	0.847E-04	0.756E-04	0.709E-04
C= 0.36D+19	10000.	0.455E-03	0.356E-03	0.101E-03	0.952E-04	0.848E-04	0.798E-04
	20000.	0.475E-03	0.351E-03	0.113E-03	0.107E-03	0.951E-04	0.897E-04
	30000.	0.482E-03	0.323E-03	0.121E-03	0.115E-03	0.102E-03	0.960E-04
	40000.	0.493E-03	0.299E-03	0.127E-03	0.120E-03	0.107E-03	0.101E-03

continued overleaf

Table 1—*continued*

PERTURBER DENSITY= 0.1D+14							
		ELECTRONS		PROTONS		IONIZED HELIUM	
TRANSITION	T(K)	WIDTH(A)	SHIFT(A)	WIDTH(A)	SHIFT(A)	WIDTH(A)	SHIFT(A)
2P - 5S	2500.	0.796E-03	0.594E-03	0.174E-03	0.162E-03	0.146E-03	0.135E-03
4274.3 A	5000.	0.905E-03	0.687E-03	0.195E-03	0.183E-03	0.164E-03	0.153E-03
C= 0.13D+19	10000.	0.947E-03	0.719E-03	0.219E-03	0.206E-03	0.184E-03	0.173E-03
	20000.	0.992E-03	0.683E-03	0.246E-03	0.232E-03	0.206E-03	0.194E-03
	30000.	0.102E-02	0.582E-03	0.263E-03	0.248E-03	0.220E-03	0.208E-03
	40000.	0.107E-02	0.540E-03	0.276E-03	0.261E-03	0.231E-03	0.218E-03
2P - 6S	2500.	0.172E-02	0.127E-02	0.362E-03	0.334E-03	0.303E-03	0.279E-03
3986.7 A	5000.	0.191E-02	0.146E-02	0.406E-03	0.379E-03	0.340E-03	0.317E-03
C= 0.64D+18	10000.	0.209E-02	0.146E-02	0.456E-03	0.428E-03	0.382E-03	0.358E-03
	20000.	0.202E-02	0.121E-02	0.512E-03	0.481E-03	0.429E-03	0.403E-03
	30000.	0.215E-02	0.100E-02	0.547E-03	0.516E-03	0.459E-03	0.432E-03
	40000.	0.225E-02	0.848E-03	0.574E-03	0.542E-03	0.481E-03	0.454E-03
2P - 7S	2500.	0.328E-02	0.244E-02	0.694E-03	0.635E-03	0.582E-03	0.529E-03
3836.7 A	5000.	0.351E-02	0.270E-02	0.780E-03	0.723E-03	0.653E-03	0.603E-03
C= 0.37D+18	10000.	0.379E-02	0.265E-02	0.875E-03	0.819E-03	0.734E-03	0.684E-03
	20000.	0.395E-02	0.199E-02	0.983E-03	0.923E-03	0.823E-03	0.773E-03
	30000.	0.418E-02	0.162E-02	0.105E-02	0.989E-03	0.881E-03	0.828E-03
	40000.	0.437E-02	0.127E-02	0.110E-02	0.104E-02	0.924E-03	0.870E-03
2P - 8S	2500.	0.633E-02	0.447E-02	0.125E-02	0.113E-02	0.104E-02	0.934E-03
3747.7 A	5000.	0.654E-02	0.467E-02	0.140E-02	0.129E-02	0.117E-02	0.107E-02
C= 0.23D+18	10000.	0.652E-02	0.438E-02	0.157E-02	0.146E-02	0.132E-02	0.122E-02
	20000.	0.707E-02	0.308E-02	0.176E-02	0.165E-02	0.148E-02	0.138E-02
	30000.	0.778E-02	0.248E-02	0.189E-02	0.177E-02	0.158E-02	0.148E-02
	40000.	0.798E-02	0.198E-02	0.198E-02	0.186E-02	0.166E-02	0.156E-02
2P - 3D	2500.	0.339E-03	-0.149E-03	0.741E-04	-0.645E-04	0.640E-04	-0.540E-04
6105.3 A	5000.	0.368E-03	-0.989E-04	0.819E-04	-0.725E-04	0.703E-04	-0.607E-04
C= 0.13D+19	10000.	0.375E-03	-0.552E-04	0.909E-04	-0.815E-04	0.776E-04	-0.683E-04
	20000.	0.365E-03	-0.163E-04	0.101E-03	-0.916E-04	0.860E-04	-0.768E-04
	30000.	0.359E-03	0.118E-05	0.108E-03	-0.980E-04	0.914E-04	-0.821E-04
	40000.	0.354E-03	0.673E-05	0.113E-03	-0.103E-03	0.956E-04	-0.862E-04
2P - 4D	2500.	0.304E-02	0.941E-04	0.138E-02	0.123E-02	0.114E-02	0.102E-02
4604.2 A	5000.	0.276E-02	0.264E-04	0.159E-02	0.141E-02	0.129E-02	0.117E-02
C= 0.14D+17	10000.	0.245E-02	-0.360E-04	0.182E-02	0.164E-02	0.148E-02	0.133E-02
	20000.	0.212E-02	-0.447E-04	0.197E-02	0.196E-02	0.170E-02	0.152E-02
	30000.	0.194E-02	-0.227E-04	0.185E-02	0.209E-02	0.183E-02	0.166E-02
	40000.	0.182E-02	-0.117E-04	0.178E-02	0.226E-02	0.191E-02	0.178E-02
2P - 5D	2500.	0.630E-02	0.585E-03	0.198E-02	0.176E-02	0.166E-02	0.146E-02
4133.8 A	5000.	0.605E-02	0.312E-03	0.224E-02	0.202E-02	0.186E-02	0.168E-02
C= 0.16D+17	10000.	0.556E-02	0.102E-03	0.257E-02	0.230E-02	0.210E-02	0.191E-02
	20000.	0.493E-02	-0.133E-04	0.296E-02	0.264E-02	0.239E-02	0.217E-02
	30000.	0.455E-02	-0.726E-04	0.317E-02	0.290E-02	0.259E-02	0.234E-02
	40000.	0.428E-02	0.556E-04	0.354E-02	0.320E-02	0.275E-02	0.248E-02
2P - 6D	2500.	0.195E-01	0.241E-03				
3916.5 A	5000.	0.173E-01	-0.180E-04				
C= 0.24D+16	10000.	0.149E-01	-0.248E-03	*0.150E-01	*0.134E-01		
	20000.	0.126E-01	-0.151E-03	*0.146E-01	*0.160E-01	*0.143E-01	*0.125E-01
	30000.	0.114E-01	-0.782E-04	*0.133E-01	*0.170E-01	*0.150E-01	*0.139E-01
	40000.	0.106E-01	-0.219E-04	*0.126E-01	*0.179E-01	*0.152E-01	*0.149E-01

Table 1—*continued*

PERTURBER DENSITY= 0.1D+14							
	ELECTRONS			PROTONS		IONIZED HELIUM	
TRANSITION	T(K)	WIDTH(A)	SHIFT(A)	WIDTH(A)	SHIFT(A)	WIDTH(A)	SHIFT(A)
2P - 7D	2500.	0.354E-01	-0.812E-04				
3796.1 A	5000.	0.316E-01	-0.343E-03				
C= 0.17D+16	10000.	0.274E-01	-0.468E-03				
	20000.	0.233E-01	-0.189E-03				
	30000.	0.210E-01	-0.108E-03	*0.256E-01	*0.291E-01		
	40000.	0.195E-01	-0.167E-03	*0.216E-01	*0.317E-01		
3S - 3P	2500.	0.811E-02	0.423E-02	0.207E-02	0.170E-02	0.182E-02	0.142E-02
26887.1 A	5000.	0.981E-02	0.273E-02	0.226E-02	0.191E-02	0.197E-02	0.160E-02
C= 0.26D+20	10000.	0.112E-01	0.137E-02	0.249E-02	0.215E-02	0.215E-02	0.180E-02
	20000.	0.119E-01	0.320E-03	0.275E-02	0.242E-02	0.236E-02	0.203E-02
	30000.	0.122E-01	-0.751E-04	0.292E-02	0.259E-02	0.250E-02	0.217E-02
	40000.	0.123E-01	-0.200E-03	0.306E-02	0.271E-02	0.261E-02	0.227E-02
3S - 4P	2500.	0.614E-02	0.401E-02	0.156E-02	0.136E-02	0.134E-02	0.113E-02
10795.1 A	5000.	0.654E-02	0.298E-02	0.173E-02	0.154E-02	0.148E-02	0.129E-02
C= 0.18D+19	10000.	0.704E-02	0.197E-02	0.192E-02	0.173E-02	0.163E-02	0.145E-02
	20000.	0.708E-02	0.133E-02	0.214E-02	0.195E-02	0.181E-02	0.163E-02
	30000.	0.706E-02	0.725E-03	0.228E-02	0.208E-02	0.193E-02	0.175E-02
	40000.	0.701E-02	0.533E-03	0.240E-02	0.219E-02	0.202E-02	0.183E-02
3S - 5P	2500.	0.112E-01	0.709E-02	0.286E-02	0.251E-02	0.244E-02	0.209E-02
8467.8 A	5000.	0.119E-01	0.538E-02	0.319E-02	0.285E-02	0.271E-02	0.238E-02
C= 0.57D+18	10000.	0.125E-01	0.360E-02	0.355E-02	0.323E-02	0.301E-02	0.270E-02
	20000.	0.123E-01	0.224E-02	0.397E-02	0.364E-02	0.335E-02	0.304E-02
	30000.	0.121E-01	0.956E-03	0.425E-02	0.390E-02	0.357E-02	0.326E-02
	40000.	0.119E-01	0.830E-03	0.446E-02	0.409E-02	0.374E-02	0.343E-02
3S - 6P	2500.	0.211E-01	0.125E-01	0.547E-02	0.476E-02	0.465E-02	0.395E-02
7584.5 A	5000.	0.227E-01	0.964E-02	0.610E-02	0.544E-02	0.517E-02	0.454E-02
C= 0.27D+18	10000.	0.233E-01	0.698E-02	0.682E-02	0.618E-02	0.576E-02	0.516E-02
	20000.	0.227E-01	0.384E-02	0.763E-02	0.700E-02	0.643E-02	0.585E-02
	30000.	0.222E-01	0.280E-02	0.817E-02	0.752E-02	0.686E-02	0.628E-02
	40000.	0.217E-01	0.124E-02	0.860E-02	0.788E-02	0.719E-02	0.659E-02
3S - 7P	2500.	0.387E-01	0.211E-01	*0.101E-01	*0.865E-02	*0.856E-02	*0.715E-02
7137.1 A	5000.	0.415E-01	0.165E-01	0.113E-01	0.998E-02	*0.953E-02	*0.829E-02
C= 0.15D+18	10000.	0.418E-01	0.110E-01	0.126E-01	0.114E-01	0.106E-01	0.950E-02
	20000.	0.405E-01	0.623E-02	0.142E-01	0.129E-01	0.119E-01	0.108E-01
	30000.	0.394E-01	0.435E-02	0.152E-01	0.139E-01	0.127E-01	0.116E-01
	40000.	0.384E-01	0.262E-02	0.160E-01	0.146E-01	0.133E-01	0.122E-01
3P - 4S	2500.	0.109E-01	0.299E-02	0.109E-02	0.642E-03	0.104E-02	0.538E-03
24469.7 A	5000.	0.143E-01	0.449E-02	0.114E-02	0.722E-03	0.107E-02	0.605E-03
C= 0.21D+20	10000.	0.166E-01	0.585E-02	0.120E-02	0.812E-03	0.111E-02	0.680E-03
	20000.	0.181E-01	0.640E-02	0.126E-02	0.912E-03	0.117E-02	0.764E-03
	30000.	0.186E-01	0.599E-02	0.130E-02	0.982E-03	0.120E-02	0.817E-03
	40000.	0.190E-01	0.555E-02	0.131E-02	0.103E-02	0.123E-02	0.858E-03
3P - 5S	2500.	0.872E-02	0.541E-02	0.158E-02	0.146E-02	0.133E-02	0.122E-02
13560.9 A	5000.	0.103E-01	0.646E-02	0.177E-02	0.164E-02	0.149E-02	0.138E-02
C= 0.66D+19	10000.	0.112E-01	0.656E-02	0.198E-02	0.185E-02	0.167E-02	0.155E-02
	20000.	0.120E-01	0.623E-02	0.222E-02	0.208E-02	0.187E-02	0.174E-02
	30000.	0.124E-01	0.550E-02	0.238E-02	0.223E-02	0.200E-02	0.187E-02
	40000.	0.129E-01	0.490E-02	0.249E-02	0.234E-02	0.209E-02	0.196E-02

continued overleaf

Table 1—*continued*

PERTURBER DENSITY= 0.1D+14							
		ELECTRONS		PROTONS		IONIZED HELIUM	
TRANSITION	T(K)	WIDTH(A)	SHIFT(A)	WIDTH(A)	SHIFT(A)	WIDTH(A)	SHIFT(A)
3P - 6S	2500.	0.135E-01	0.951E-02	0.270E-02	0.249E-02	0.226E-02	0.208E-02
11034.8 A	5000.	0.151E-01	0.109E-01	0.303E-02	0.282E-02	0.254E-02	0.236E-02
C= 0.44D+19	10000.	0.160E-01	0.104E-01	0.340E-02	0.318E-02	0.285E-02	0.266E-02
	20000.	0.168E-01	0.887E-02	0.381E-02	0.358E-02	0.319E-02	0.300E-02
	30000.	0.178E-01	0.732E-02	0.408E-02	0.384E-02	0.342E-02	0.322E-02
	40000.	0.187E-01	0.629E-02	0.428E-02	0.403E-02	0.359E-02	0.338E-02
3P - 7S	2500.	0.225E-01	0.163E-01	0.464E-02	0.424E-02	0.389E-02	0.353E-02
9957.7 A	5000.	0.242E-01	0.180E-01	0.520E-02	0.482E-02	0.436E-02	0.402E-02
C= 0.25D+19	10000.	0.263E-01	0.172E-01	0.584E-02	0.546E-02	0.490E-02	0.456E-02
	20000.	0.273E-01	0.121E-01	0.656E-02	0.616E-02	0.550E-02	0.516E-02
	30000.	0.293E-01	0.979E-02	0.702E-02	0.660E-02	0.588E-02	0.552E-02
	40000.	0.306E-01	0.866E-02	0.736E-02	0.693E-02	0.617E-02	0.580E-02
3P - 8S	2500.	0.372E-01	0.281E-01	0.778E-02	0.702E-02	0.652E-02	0.583E-02
9379.3 A	5000.	0.392E-01	0.291E-01	0.873E-02	0.802E-02	0.732E-02	0.669E-02
C= 0.14D+19	10000.	0.415E-01	0.261E-01	0.981E-02	0.911E-02	0.822E-02	0.761E-02
	20000.	0.453E-01	0.166E-01	0.110E-01	0.103E-01	0.922E-02	0.862E-02
	30000.	0.487E-01	0.137E-01	0.118E-01	0.111E-01	0.987E-02	0.925E-02
	40000.	0.509E-01	0.123E-01	0.124E-01	0.116E-01	0.104E-01	0.972E-02
3P - 3D	2500.	1.56	-0.898	0.302	-0.271	0.257	-0.227
279548.3A	5000.	1.61	-0.709	0.336	-0.305	0.285	-0.256
C= 0.28D+22	10000.	1.70	-0.508	0.374	-0.343	0.317	-0.288
	20000.	1.69	-0.370	0.418	-0.386	0.353	-0.323
	30000.	1.66	-0.264	0.447	-0.413	0.377	-0.346
	40000.	1.64	-0.213	0.469	-0.433	0.394	-0.363
3P - 4D	2500.	0.475E-01	-0.108E-02	0.200E-01	0.178E-01	0.165E-01	0.148E-01
17550.0 A	5000.	0.432E-01	-0.201E-02	0.230E-01	0.204E-01	0.187E-01	0.169E-01
C= 0.21D+18	10000.	0.391E-01	-0.253E-02	0.263E-01	0.235E-01	0.213E-01	0.192E-01
	20000.	0.343E-01	-0.154E-02	0.282E-01	0.284E-01	0.246E-01	0.220E-01
	30000.	0.316E-01	-0.104E-02	0.266E-01	0.302E-01	0.266E-01	0.241E-01
	40000.	0.298E-01	-0.729E-03	0.252E-01	0.325E-01	0.275E-01	0.257E-01
3P - 5D	2500.	0.566E-01	0.415E-02	0.173E-01	0.154E-01	0.145E-01	0.128E-01
12240.6 A	5000.	0.544E-01	0.871E-03	0.196E-01	0.176E-01	0.163E-01	0.147E-01
C= 0.14D+18	10000.	0.504E-01	0.388E-03	0.225E-01	0.198E-01	0.183E-01	0.167E-01
	20000.	0.448E-01	-0.464E-03	0.259E-01	0.231E-01	0.209E-01	0.190E-01
	30000.	0.415E-01	-0.166E-04	0.277E-01	0.254E-01	0.227E-01	0.205E-01
	40000.	0.391E-01	0.198E-03	0.309E-01	0.280E-01	0.241E-01	0.217E-01
3P - 6D	2500.	0.141	0.126E-02				
10513.1 A	5000.	0.125	-0.718E-03				
C= 0.17D+17	10000.	0.108	-0.321E-02	*0.108	*0.968E-01		
	20000.	0.920E-01	-0.132E-02	*0.105	*0.115	*0.103	*0.902E-01
	30000.	0.832E-01	-0.570E-03	*0.957E-01	*0.122	*0.108	*0.999E-01
	40000.	0.772E-01	-0.837E-03	*0.905E-01	*0.129	*0.109	*0.107
3P - 7D	2500.	0.231	-0.887E-03				
9688.9 A	5000.	0.207	-0.275E-02				
C= 0.11D+17	10000.	0.179	-0.364E-02				
	20000.	0.152	-0.159E-02				
	30000.	0.138	-0.777E-03	*0.167	*0.207		
	40000.	0.128	-0.515E-03	*0.141	*0.207		

Table 1—*continued*

PERTURBER DENSITY= 0.1D+14							
		ELECTRONS		PROTONS		IONIZED HELIUM	
TRANSITION	T(K)	WIDTH(A)	SHIFT(A)	WIDTH(A)	SHIFT(A)	WIDTH(A)	SHIFT(A)
3D - 4P	2500.	0.228E-01	0.139E-01	0.512E-02	0.453E-02	0.437E-02	0.379E-02
19281.0 A	5000.	0.237E-01	0.116E-01	0.569E-02	0.513E-02	0.484E-02	0.429E-02
C= 0.57D+19	10000.	0.249E-01	0.864E-02	0.634E-02	0.577E-02	0.538E-02	0.483E-02
	20000.	0.247E-01	0.571E-02	0.708E-02	0.650E-02	0.599E-02	0.544E-02
	30000.	0.242E-01	0.438E-02	0.757E-02	0.696E-02	0.638E-02	0.583E-02
	40000.	0.238E-01	0.278E-02	0.794E-02	0.731E-02	0.668E-02	0.612E-02
3D - 5P	2500.	0.276E-01	0.173E-01	0.670E-02	0.591E-02	0.571E-02	0.492E-02
12932.5 A	5000.	0.291E-01	0.132E-01	0.747E-02	0.671E-02	0.634E-02	0.560E-02
C= 0.13D+19	10000.	0.303E-01	0.979E-02	0.834E-02	0.760E-02	0.705E-02	0.635E-02
	20000.	0.296E-01	0.589E-02	0.933E-02	0.856E-02	0.786E-02	0.716E-02
	30000.	0.290E-01	0.449E-02	0.998E-02	0.917E-02	0.839E-02	0.768E-02
	40000.	0.284E-01	0.331E-02	0.105E-01	0.963E-02	0.879E-02	0.806E-02
3D - 6P	2500.	0.452E-01	0.271E-01	0.115E-01	0.100E-01	0.974E-02	0.830E-02
10979.7 A	5000.	0.484E-01	0.199E-01	0.128E-01	0.114E-01	0.108E-01	0.953E-02
C= 0.56D+18	10000.	0.496E-01	0.152E-01	0.143E-01	0.130E-01	0.121E-01	0.108E-01
	20000.	0.482E-01	0.840E-02	0.160E-01	0.147E-01	0.135E-01	0.123E-01
	30000.	0.470E-01	0.625E-02	0.172E-01	0.158E-01	0.144E-01	0.132E-01
	40000.	0.459E-01	0.487E-02	0.180E-01	0.166E-01	0.151E-01	0.139E-01
3D - 7P	2500.	0.776E-01	0.429E-01	*0.201E-01	*0.172E-01	*0.170E-01	*0.142E-01
10066.2 A	5000.	0.832E-01	0.327E-01	0.224E-01	0.199E-01	*0.190E-01	*0.165E-01
C= 0.30D+18	10000.	0.837E-01	0.227E-01	0.251E-01	0.227E-01	0.212E-01	0.189E-01
	20000.	0.811E-01	0.123E-01	0.282E-01	0.257E-01	0.237E-01	0.215E-01
	30000.	0.788E-01	0.929E-02	0.302E-01	0.277E-01	0.253E-01	0.231E-01
	40000.	0.767E-01	0.686E-02	0.318E-01	0.291E-01	0.265E-01	0.244E-01
4S - 4P	2500.	0.251	0.117	0.585E-01	0.506E-01	0.505E-01	0.422E-01
68611.1 A	5000.	0.300	0.648E-01	0.648E-01	0.571E-01	0.556E-01	0.478E-01
C= 0.72D+20	10000.	0.330	0.363E-01	0.719E-01	0.643E-01	0.614E-01	0.539E-01
	20000.	0.344	-0.238E-02	0.801E-01	0.724E-01	0.680E-01	0.606E-01
	30000.	0.348	-0.119E-01	0.855E-01	0.775E-01	0.723E-01	0.649E-01
	40000.	0.350	-0.192E-01	0.896E-01	0.814E-01	0.756E-01	0.682E-01
4S - 5P	2500.	0.974E-01	0.536E-01	0.246E-01	0.215E-01	0.210E-01	0.179E-01
24978.1 A	5000.	0.107	0.371E-01	0.273E-01	0.245E-01	0.232E-01	0.204E-01
C= 0.50D+19	10000.	0.114	0.258E-01	0.305E-01	0.277E-01	0.258E-01	0.231E-01
	20000.	0.114	0.100E-01	0.341E-01	0.312E-01	0.288E-01	0.261E-01
	30000.	0.113	0.448E-02	0.365E-01	0.334E-01	0.307E-01	0.280E-01
	40000.	0.112	0.159E-02	0.383E-01	0.351E-01	0.321E-01	0.294E-01
4S - 6P	2500.	0.127	0.693E-01	0.327E-01	0.285E-01	0.278E-01	0.237E-01
18591.6 A	5000.	0.138	0.327E-01	0.365E-01	0.326E-01	0.309E-01	0.271E-01
C= 0.16D+19	10000.	0.142	0.314E-01	0.408E-01	0.370E-01	0.345E-01	0.309E-01
	20000.	0.140	0.978E-02	0.457E-01	0.419E-01	0.385E-01	0.350E-01
	30000.	0.137	0.679E-02	0.489E-01	0.449E-01	0.411E-01	0.376E-01
	40000.	0.135	0.465E-02	0.515E-01	0.472E-01	0.430E-01	0.395E-01
4S - 7P	2500.	0.197	0.106	*0.514E-01	*0.441E-01	*0.436E-01	*0.364E-01
16115.3 A	5000.	0.213	0.758E-01	0.574E-01	0.508E-01	*0.485E-01	*0.422E-01
C= 0.76D+18	10000.	0.214	0.455E-01	0.642E-01	0.580E-01	0.541E-01	0.483E-01
	20000.	0.209	0.134E-01	0.721E-01	0.658E-01	0.605E-01	0.550E-01
	30000.	0.204	0.104E-01	0.773E-01	0.708E-01	0.647E-01	0.591E-01
	40000.	0.199	0.854E-02	0.814E-01	0.744E-01	0.678E-01	0.623E-01

continued overleaf

Table 1—*continued*

PERTURBER DENSITY= 0.1D+14							
	ELECTRONS			PROTONS		IONIZED HELIUM	
TRANSITION	T(K)	WIDTH(A)	SHIFT(A)	WIDTH(A)	SHIFT(A)	WIDTH(A)	SHIFT(A)
4P - 5S	2500.	0.212	0.705E-02	0.234E-01	-0.175E-01	0.211E-01	-0.146E-01
54645.4 A	5000.	0.262	0.389E-01	0.253E-01	-0.197E-01	0.226E-01	-0.165E-01
C= 0.46D+20	10000.	0.297	0.583E-01	0.275E-01	-0.222E-01	0.242E-01	-0.186E-01
	20000.	0.319	0.724E-01	0.302E-01	-0.249E-01	0.263E-01	-0.209E-01
	30000.	0.328	0.653E-01	0.322E-01	-0.267E-01	0.276E-01	-0.224E-01
	40000.	0.336	0.596E-01	0.339E-01	-0.280E-01	0.287E-01	-0.235E-01
4P - 6S	2500.	0.103	0.474E-01	0.134E-01	0.120E-01	0.114E-01	0.998E-02
28424.5 A	5000.	0.123	0.588E-01	0.149E-01	0.135E-01	0.127E-01	0.113E-01
C= 0.12D+20	10000.	0.136	0.572E-01	0.166E-01	0.152E-01	0.141E-01	0.128E-01
	20000.	0.145	0.510E-01	0.186E-01	0.172E-01	0.157E-01	0.144E-01
	30000.	0.152	0.422E-01	0.198E-01	0.184E-01	0.167E-01	0.154E-01
	40000.	0.157	0.375E-01	0.207E-01	0.193E-01	0.175E-01	0.162E-01
4P - 7S	2500.	0.121	0.754E-01	0.212E-01	0.193E-01	0.178E-01	0.161E-01
22230.4 A	5000.	0.135	0.825E-01	0.238E-01	0.220E-01	0.200E-01	0.183E-01
C= 0.76D+19	10000.	0.146	0.798E-01	0.267E-01	0.249E-01	0.224E-01	0.208E-01
	20000.	0.156	0.574E-01	0.300E-01	0.281E-01	0.251E-01	0.235E-01
	30000.	0.167	0.431E-01	0.320E-01	0.301E-01	0.269E-01	0.252E-01
	40000.	0.173	0.373E-01	0.336E-01	0.316E-01	0.282E-01	0.264E-01
4P - 8S	2500.	0.168	0.114	0.327E-01	0.295E-01	0.274E-01	0.245E-01
19540.6 A	5000.	0.180	0.120	0.367E-01	0.337E-01	0.308E-01	0.281E-01
C= 0.59D+19	10000.	0.193	0.110	0.412E-01	0.383E-01	0.345E-01	0.320E-01
	20000.	0.212	0.714E-01	0.463E-01	0.433E-01	0.388E-01	0.362E-01
	30000.	0.227	0.453E-01	0.495E-01	0.464E-01	0.415E-01	0.389E-01
	40000.	0.234	0.401E-01	0.519E-01	0.488E-01	0.435E-01	0.408E-01
4P - 5D	2500.	0.608	0.400E-02	0.164	0.146	0.137	0.121
38089.6 A	5000.	0.584	-0.161E-01	0.186	0.167	0.154	0.139
C= 0.14D+19	10000.	0.549	-0.266E-01	0.213	0.190	0.174	0.159
	20000.	0.494	-0.133E-01	0.246	0.219	0.198	0.180
	30000.	0.459	-0.557E-02	0.262	0.241	0.216	0.194
	40000.	0.435	-0.875E-02	0.270	0.257	0.228	0.205
4P - 6D	2500.	0.838	-0.793E-02				
25203.1 A	5000.	0.744	-0.135E-01				
C= 0.98D+17	10000.	0.650	-0.218E-01	*0.619	*0.555		
	20000.	0.554	-0.164E-01	*0.604	*0.662	*0.590	*0.518
	30000.	0.503	-0.208E-02	*0.549	*0.701	*0.621	*0.573
	40000.	0.468	-0.144E-02	*0.517	*0.737	*0.627	*0.616
4P - 7D	2500.	1.09	-0.141E-01				
20933.9 A	5000.	0.980	-0.166E-01				
C= 0.50D+17	10000.	0.855	-0.226E-01				
	20000.	0.729	-0.777E-02				
	30000.	0.660	-0.352E-02	*0.776	*0.966		
	40000.	0.614	-0.472E-03	*0.656	*0.963		
4D - 6P	2500.	0.358	0.149	0.384E-01	0.331E-01	0.342E-01	0.275E-01
26543.2 A	5000.	0.364	0.110	0.408E-01	0.371E-01	0.370E-01	0.314E-01
C= 0.48D+18	10000.	0.362	0.720E-01	0.443E-01	0.405E-01	0.395E-01	0.356E-01
	20000.	0.343	0.293E-01	0.521E-01	0.436E-01	0.421E-01	0.391E-01
	30000.	0.330	0.222E-01	0.598E-01	0.463E-01	0.446E-01	0.408E-01
	40000.	0.319	0.183E-01	0.669E-01	0.491E-01	0.473E-01	0.421E-01

Table 1—*continued*

PERTURBER DENSITY= 0.1D+14							
		ELECTRONS		PROTONS		IONIZED HELIUM	
TRANSITION	T(K)	WIDTH(A)	SHIFT(A)	WIDTH(A)	SHIFT(A)	WIDTH(A)	SHIFT(A)
4D - 7P	2500.	0.424	0.195	0.819E-01	0.702E-01	*0.697E-01	*0.581E-01
21767.8 A	5000.	0.443	0.145	0.911E-01	0.809E-01	*0.774E-01	*0.672E-01
C= 0.32D+18	10000.	0.440	0.874E-01	0.101	0.921E-01	0.861E-01	0.769E-01
	20000.	0.420	0.577E-01	0.113	0.104	0.958E-01	0.873E-01
	30000.	0.405	0.241E-01	0.122	0.111	0.102	0.939E-01
	40000.	0.393	0.205E-01	0.129	0.117	0.107	0.986E-01
5S - 5P	2500.	3.24	1.23	0.720	0.627	0.616	0.523
139659.0A	5000.	3.81	0.740	0.800	0.712	0.682	0.595
C= 0.15D+21	10000.	4.06	0.303	0.891	0.806	0.756	0.674
	20000.	4.19	-0.876E-01	0.996	0.907	0.841	0.759
	30000.	4.23	-0.133	1.07	0.973	0.897	0.814
	40000.	4.24	-0.182	1.12	1.02	0.939	0.855
5S - 6P	2500.	0.860	0.427	0.213	0.185	0.181	0.154
47816.9 A	5000.	0.960	0.283	0.237	0.212	0.201	0.176
C= 0.11D+20	10000.	0.996	0.162	0.265	0.240	0.224	0.201
	20000.	0.996	0.602E-01	0.297	0.272	0.250	0.228
	30000.	0.989	0.275E-01	0.318	0.292	0.267	0.244
	40000.	0.978	-0.158E-01	0.335	0.306	0.280	0.256
5S - 7P	2500.	0.902	0.446	*0.231	*0.198	*0.196	*0.164
34272.2 A	5000.	0.982	0.294	0.258	0.229	*0.218	*0.190
C= 0.34D+19	10000.	0.996	0.160	0.289	0.261	0.244	0.217
	20000.	0.981	0.541E-01	0.324	0.296	0.272	0.247
	30000.	0.962	0.324E-01	0.348	0.318	0.291	0.266
	40000.	0.943	0.186E-01	0.366	0.334	0.305	0.280
5P - 6S	2500.	2.18	-0.109	0.296	-0.248	0.257	-0.207
102872.2A	5000.	2.60	0.181	0.326	-0.281	0.282	-0.235
C= 0.84D+20	10000.	2.87	0.407	0.361	-0.318	0.310	-0.266
	20000.	3.03	0.454	0.403	-0.357	0.342	-0.299
	30000.	3.12	0.381	0.431	-0.383	0.364	-0.321
	40000.	3.17	0.415	0.454	-0.402	0.380	-0.337
5P - 7S	2500.	0.786	0.251	0.604E-01	0.480E-01	0.535E-01	0.401E-01
51220.6 A	5000.	0.931	0.325	0.658E-01	0.544E-01	0.578E-01	0.455E-01
C= 0.21D+20	10000.	1.04	0.333	0.719E-01	0.614E-01	0.629E-01	0.514E-01
	20000.	1.11	0.249	0.783E-01	0.691E-01	0.686E-01	0.578E-01
	30000.	1.16	0.205	0.818E-01	0.743E-01	0.722E-01	0.620E-01
	40000.	1.19	0.170	0.839E-01	0.779E-01	0.749E-01	0.651E-01
5P - 8S	2500.	0.745	0.393	0.109	0.976E-01	0.918E-01	0.811E-01
38887.2 A	5000.	0.835	0.416	0.122	0.111	0.103	0.928E-01
C= 0.12D+20	10000.	0.915	0.386	0.137	0.126	0.115	0.105
	20000.	0.997	0.248	0.153	0.143	0.129	0.119
	30000.	1.06	0.165	0.164	0.153	0.138	0.128
	40000.	1.08	0.144	0.172	0.161	0.144	0.135
5P - 6D	2500.	7.06	-0.413				
70335.4 A	5000.	6.31	-0.452				
C= 0.76D+18	10000.	5.60	-0.315	*4.79	*4.31		
	20000.	4.83	-0.152	*4.64	*5.11	*4.57	*4.01
	30000.	4.41	-0.125	*4.69	*5.70	*4.80	*4.45
	40000.	4.12	-0.553E-01	3.61	5.53	*4.84	*4.77

continued overleaf

Table 1—*continued*

PERTURBER DENSITY= 0.1D+14							
	ELECTRONS			PROTONS		IONIZED HELIUM	
TRANSITION	T(K)	WIDTH(A)	SHIFT(A)	WIDTH(A)	SHIFT(A)	WIDTH(A)	SHIFT(A)
5P - 7D	2500.	5.23	-0.224				
44824.2 A	5000.	4.70	-0.269				
C= 0.23D+18	10000.	4.14	-0.165				
	20000.	3.55	-0.798E-01				
	30000.	3.22	-0.733E-01	*3.52	*4.41		
	40000.	3.00	-0.278E-01	*2.98	*4.39		
5D - 6P	2500.	4.34	1.08	0.333	-0.271	0.280	-0.226
77166.4 A	5000.	4.35	0.820	0.387	-0.310	0.312	-0.258
C= 0.57D+19	10000.	4.27	0.525	0.459	-0.375	0.357	-0.293
	20000.	3.97	0.189	0.516	-0.427	0.421	-0.336
	30000.	3.77	0.137	0.512	-0.467	0.464	-0.368
	40000.	3.62	0.112	0.522	-0.465	0.498	-0.405
5D - 7P	2500.	2.46	0.862	0.297	0.253	*0.255	*0.210
47116.2 A	5000.	2.54	0.631	0.328	0.291	0.282	0.242
C= 0.21D+19	10000.	2.51	0.387	0.360	0.331	0.312	0.276
	20000.	2.37	0.249	0.394	0.370	0.344	0.313
	30000.	2.26	0.101	0.423	0.392	0.362	0.336
	40000.	2.18	0.862E-01	0.448	0.406	0.375	0.352
6S - 7P	2500.	5.29	2.26	*1.28	*1.09	*1.08	*0.904
81320.0 A	5000.	5.87	1.53	1.43	1.26	*1.21	*1.05
C= 0.19D+20	10000.	5.99	0.551	1.60	1.44	1.35	1.20
	20000.	5.99	0.260	1.79	1.63	1.50	1.36
	30000.	5.93	-0.538E-01	1.92	1.76	1.61	1.47
	40000.	5.85	-0.908E-01	2.02	1.85	1.68	1.55
6P - 8S	2500.	4.41	0.974	0.206	-0.811E-01	0.201	-0.676E-01
83593.9 A	5000.	5.15	1.24	0.211	-0.921E-01	0.204	-0.767E-01
C= 0.32D+20	10000.	5.71	1.32	0.221	-0.104	0.208	-0.864E-01
	20000.	6.12	0.903	0.244	-0.120	0.215	-0.983E-01
	30000.	6.37	0.686	0.271	-0.140	0.222	-0.105
	40000.	6.46	0.580	0.294	-0.146	0.231	-0.113

Table 2. Li(I) $2s^2S$–$2p^2P^0$ at $\lambda = 6707.8$ Å: full halfwidths are given in Å for $N = 10^{16}$ cm^{-3} as a function of the temperature. The experiments of Purić et al[14] yield $W = 0.038$ Å, $d = 0.0042$ Å and $W = 0.046$ Å, $d = 0.0039$ Å at 17,5000 and 26,500 K, respectively, for the same density.

T (K)	2,500	5,000	10,000	20,000
Present results	0.023	0.023	0.025	0.032
Quantum-mechanical[21]	0.044	0.034	0.028	0.030
Semi-classical[1,20]	....	0.020	0.028	0.040
Model microfield[22]	0.017	0.024	0.030	0.042

Table 3. As in Table 2, but for the shift; a positive shift is red.

T (K)	2,500	5,000	10,000	20,000
Present results	-0.0058	-0.0069	-0.0076	-0.0074
Semi-classical[1,20]	----	-0.0043	-0.0044	-0.0042
Model microfield[22]	-0.0044	-0.0044	-0.0043	-0.0041

values are smaller and that the accuracy of the shift calculations is not as good as in the case for the width, especially at elevated temperatures because the shift is very sensitive to the number of perturbing levels, and to the choice of the lower and upper cut-offs. Therefore, the integration over the impact parameter converges slowly, as is shown in Ref. 24.

It is interesting to note, for the resonance transition $2s$–$2p$, that the widths due to proton and He^+ collisions do not depend on the temperature. This result is caused by the fact that the quadrupolar interaction is predominant and leads to a width that is constant with T, as is shown in Ref. 24. As a matter of fact, the polarization interaction is weaker than the quadrupolar interaction because the perturbing levels are widely spaced. As a consequence of this result, it follows for the calculation of the quasistatic width which is relevant at high densities and/or low temperatures, that the quadrupolar interaction should be used in place of the polarization interaction. It has been used consistently, for instance, in the tables of Ref. 1.

Since the energy separations between the upper level and the principal perturbing levels for the $2p^2P^0$–ns^2S series (see the Grotrian diagrams in Ref. 10) decrease gradually, we expect a gradual and regular change of the Stark-broadening parameters.[8] We see in Figs. 1–4 that this type of change occurs for electron- and proton-impact widths and shifts within the $2p^2P^0$–ns^2S series.

It is interesting also to analyze how the emission-line widths change with a change of the principal quantum number of the final state. We see in Fig. 5 for the ns^2S–$7p^2P^0$ lines that the line width in angular frequency units is practically the same for all members. The largest difference occurs for the $6s$–$7p$ transition for which the line widths are $1.51 \times 10^{10}\,\mathrm{sec}^{-1}$ for $T = 2500$ K and $1.67 \times 10^{10}\,\mathrm{sec}^{-1}$ for $T = 40{,}000$ K (as compared with 1.43 and $1.41 \times 10^{10}\,\mathrm{sec}^{-1}$ for the $2s$–$7p$ line). These observations are a consequence of the much smaller relative importance of lower-level broadening contributions.

Our findings should be of interest in astrophysics and for making quick estimates. In these cases, the only difference is attributed to the difference in the wavelengths and we can scale from one available result to other series members.

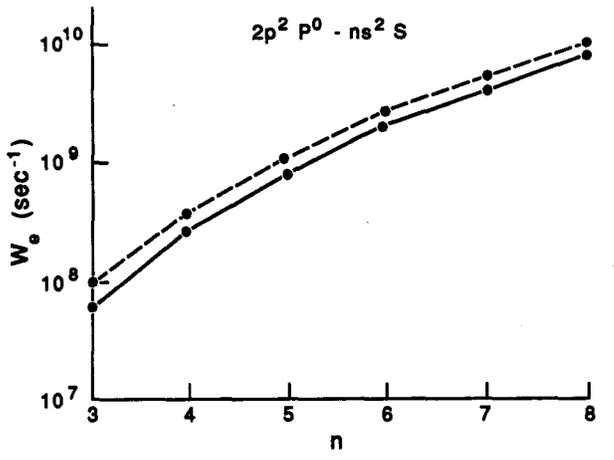

Fig. 1. Electron full halfwidths (in angular frequency units) for the Li(I) $2p^2P^0$–ns^2S lines as a function of n_i for $T = 2500$ K (——) and 40,000 K (– – –) at $N_e = 10^{13}\,\mathrm{cm}^{-3}$

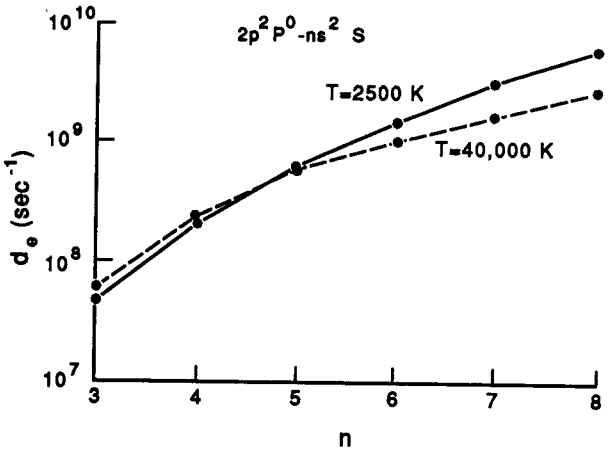

Fig. 2. As in Fig. 1 but for the electron-impact shift.

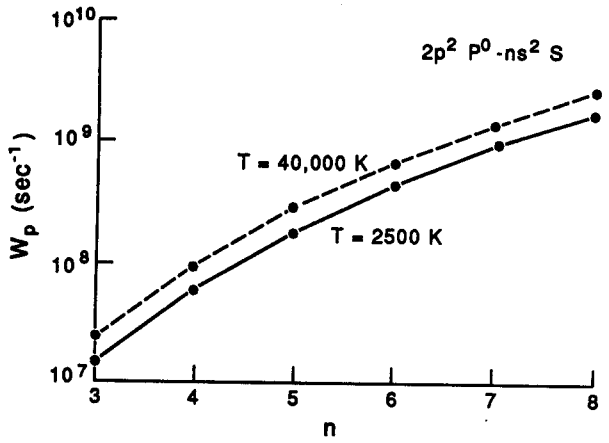

Fig. 3. As in Fig. 1 but for the proton-impact full halfwidth.

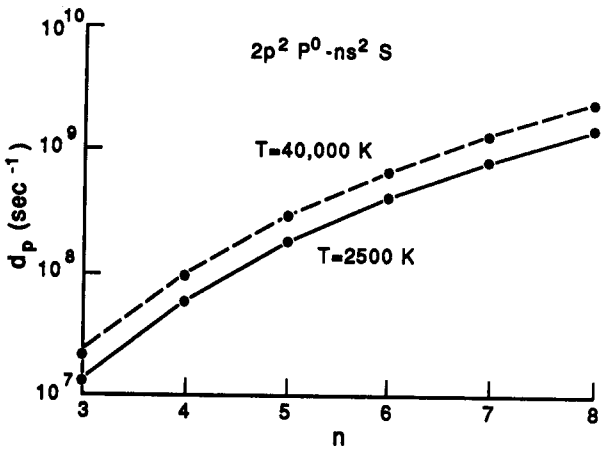

Fig. 4. As in Fig. 1 but for the proton-impact shift.

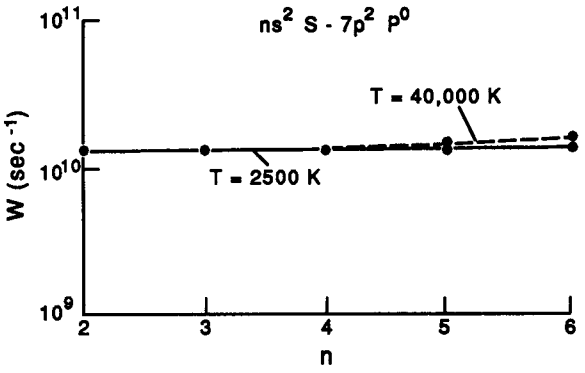

Fig. 5. As in Fig. 1 but for electron-impact full halfwidths for Li(I) ns^2S–$7p^2P^0$ lines.

Acknowledgements—One of us (M.S.D.) was supported by the Observatory of Paris-Meudon. This work was supported by C.N.R.S. and is a part of French–Yugoslav collaboration through the project "L'élargissement Stark des raies spectrales des plasmas astrophysique et de laboratoire". This study was supported, in part, by SKNTI under the project "Atomic, Molecular and Plasma Spectroscopy". Calculations were performed on the Vax 8600 of the Observatory of Paris-Meudon and on the IBM computers of CIRCE (Orsay).

REFERENCES

1. H. R. Griem, *Spectral Line Broadening by Plasmas*, Academic Press, New York, NY (1974).
2. B. Ya'akobi, *Phys. Rev.* **176,** 227 (1968).
3. A. M. Boesgaard, *Vistas in Astronomy* **31,** 167 (1988).
4. A. M. Boesgaard and M. J. Trippico, *Astrophys. J.* **302,** L49 (1986).
5. I. Vince, M. S. Dimitrijević, and V. Kršljanin, in *Spectral Line Shapes*, Vol. 3, p. 650, F. Rostas ed., de Gruyter, Berlin (1985).
6. S. Sahal-Bréchot, *Astron. Astrophys.* **1,** 91 (1969).
7. S. Sahal-Bréchot, *Astron. Astrophys.* **2,** 322 (1969).
8. M. S. Dimitrijević and S. Sahal-Bréchot, *JQSRT* **44,** 421 (1990).
9. M. S. Dimitrijević and S. Sahal-Bréchot, *JQSRT* **31,** 301 (1984).
10. S. Bashkin and J. J. Stoner, Jr., *Atomic Energy Levels and Grotrian Diagrams*, Vol. 1, North Holland, Amsterdam (1975).
11. D. R. Bates and A. Damgaard, *Phil. Trans. R. Soc. Lond.* **242A,** 101 (1949).
12. G. K. Oertel and L. P. Shomo, *Astrophys. J. Suppl. Ser.* **16,** 175 (1968).
13. H. van Regemorter, H. B. Dy, and M. Prud'homme, *J. Phys. B* **12,** 1073 (1979).
14. J. Purić, J. Labat, Lj. Ćirković, I. Lakićević, and S. Djeniže, *J. Phys. B* **10,** 2375 (1977).
15. S. M. Benett and H. R. Griem, Technical Report No. 71-097, University of Maryland, College Park, MD (1971).
16. H. R. Griem, M. Baranger, A. C. Kolb, and G. Oertel, *Phys. Rev.* **125,** 177 (1962).
17. A. Brissaud, C. Goldbach, J. Léorat, A. Mazure, and G. Nollez, *J. Phys. B* **9,** 1147 (1976).
18. N. Konjević and J. R. Roberts, *J. Phys. Chem. Ref. Data* **5,** 209 (1976).
19. N. Konjević, M. S. Dimitrijević, and W. L. Wiese, *J.Phys. Chem. Ref. Data* **13,** 619 (1984).
20. R. von der Heyde and H. J. Kusch, *Z. Astrophys.* **68,** 1 (1968).
21. V. A. Zhirnov and Yu. A. Tetyukhlin, *Zh. Prikl. Spektrosk.* **18,** 596 (1973).
22. M. S. Dimitrijević, N. Feautrier, and S. Sahal-Bréchot, *J. Phys. B* **14,** 2559 (1981).
23. A. Mazure and G. Nollez, *Z. Naturf.* **339,** 15 (1978).
24. S. Sahal-Bréchot and H. van Regemorter, *Ann. d'Astrophys.* **27,** 432 (1964).

J. Quant. Spectrosc. Radiat. Transfer Vol. 47, No. 5, pp. 315–318, 1992
Printed in Great Britain.

0022-4073/92 $5.00 + 0.00

STARK-BROADENING PARAMETERS OF IONIZED MERCURY SPECTRAL LINES OF ASTROPHYSICAL INTEREST

MILAN S. DIMITRIJEVIĆ
Astronomical Observatory, Volgina 7, 11050 Beograd, Yugoslavia

(Received 13 September 1991)

Abstract—Using a semiclassical approach, we have calculated electron-, proton-, and ionized-helium-impact line widths and shifts for seven ionized mercury lines observed in the spectra of Mn and magnetic stars, as well as in laboratory plasmas.

INTRODUCTION

Stark-broadening data for some Hg II lines are of importance for investigation of stellar spectra. For example, the $6s^2{}^2D_{5/2}$–$6p^2P^0_{3/2}$ 3983.9 Å Hg II line is a strong and characteristic feature in the spectrum of HgMn Bp stars, most of the Mn stars, and in some magnetic Ap stars.[1–4] This line is used, e.g., for Hg abundance determination in the atmosphere of ϕ Her.[5] The significance of the resonance $6s^2S$–$6p^2P^0$ 1942 Å Hg II line for Hg stellar-abundance determination has been pointed out in Ref. 1. The mentioned Hg II multiplets, as well as the $6p^2P^0$–$6d^2D$ and $6p^2P^0$–$7s^2S$ transitions, have been observed in the α And spectrum.[6,7]

By using the semiclassical perturbation formalism,[8,9] we have calculated electron-, proton-, and ionized-helium-impact line widths and shifts for seven Hg II lines. A summary of the formalism is given in Ref. 10. Here, we present and discuss the results for ionized mercury lines and a comparison with the experimental data.[11,12]

RESULTS AND DISCUSSION

Energy levels for Hg II lines have been taken from Ref. 13, and oscillator strengths have been calculated by using the method of Bates and Damgaard.[14,15] For higher levels, the method described in Ref. 16 has been applied. For the most critical transitions, the values for $\log gf$ (3984 Å) $= -1.85$, $\log gf$ (1649.9 Å) $= -0.06$ and $\log gf$ (1942.3 Å) $= -0.31$, derived in Ref. 1 from published laboratory and theoretical data, have been used. If we use the Coulomb approximation, we obtain $\log gf$ (3984 Å) $= -0.25$ and $\log gf$ (1649.9 Å) $= +0.12$. For our case, these differences are very important since, if we use Coulomb-approximation $\log gf$ values, the differences in line-width results may be as great as 50%.

In addition to the electron-impact full halfwidths and shifts, Stark-broadening parameters due to proton-, and ionized-helium impacts have been calculated. Thus, we have provided Stark-broadening data for all of the important charged perturbers in stellar atmospheres. Our results are shown in Table 1 for a perturber density of 10^{17} cm^{-3} and temperatures T from 3000 to 50,000 K. For perturber densities lower than 10^{17} cm^{-3}, all of the corresponding data are practically linear with density, because the effect of Debye screening is negligible. We also specify a parameter c,[17] which gives an estimate for the maximum perturber density for which the line may be treated as isolated when it is divided by $2W$.

For each value given in Table 1, the collision volume (V) multiplied by the perturber density (N) is much less than one and the impact approximation is valid.[8,9] When the impact approximation is not valid, the ion-broadening contribution may be estimated by using quasistatic estimations.[18,19] One should note the fact that the accuracy of the results obtained decreases when broadening by ion interactions is important.

Table 1. This table shows electron-, proton-, and ionized-helium-impact broadening parameters for ionized mercury lines, at perturber density of $10^{17}\,cm^{-3}$ and temperatures from 3000 to 50,000 K. Transitions and wavelengths (in Å) are also given. By using c [see Eq. (5) of Ref. 10], we obtain an estimate for the maximum perturber density for which the line may be treated as isolated and tabulated data may be used. Data for densities N lower than $10^{17}\,cm^{-3}$ can be obtained by multiplying the results given at $10^{17}\,cm^{-3}$ by $N/10^{17}$. Data for the 3983.9 Å line have lower accuracy than the data for other lines

PERTURBER DENSITY = 0.1D+18							
		ELECTRONS		PROTONS		IONIZED HELIUM	
TRANSITION	T(K)	WIDTH(A)	SHIFT(A)	WIDTH(A)	SHIFT(A)	WIDTH(A)	SHIFT(A)
HgII 6S-6P	3000.	0.687E-01	0.551E-04	0.345E-03	0.648E-05	0.618E-03	0.648E-05
1942.3 A	5000.	0.548E-01	-0.410E-04	0.692E-03	0.133E-04	0.110E-02	0.133E-04
C= 0.17E+21	10000.	0.401E-01	0.342E-04	0.137E-02	0.297E-04	0.182E-02	0.296E-04
	20000.	0.290E-01	0.107E-03	0.206E-02	0.611E-04	0.251E-02	0.593E-04
	30000.	0.240E-01	0.114E-03	0.247E-02	0.876E-04	0.272E-02	0.817E-04
	50000.	0.193E-01	0.117E-03	0.275E-02	0.128E-03	0.299E-02	0.114E-03
HgII 6S-6P	3000.	0.583E-01	0.343E-03	0.377E-03	0.512E-04	0.654E-03	0.511E-04
1649.9 A	5000.	0.459E-01	0.898E-03	0.733E-03	0.104E-03	0.112E-02	0.103E-03
C= 0.96E+20	10000.	0.331E-01	0.111E-02	0.138E-02	0.223E-03	0.176E-02	0.211E-03
	20000.	0.238E-01	0.119E-02	0.201E-02	0.394E-03	0.234E-02	0.347E-03
	30000.	0.198E-01	0.105E-02	0.233E-02	0.485E-03	0.253E-02	0.423E-03
	50000.	0.160E-01	0.104E-02	0.257E-02	0.624E-03	0.275E-02	0.519E-03
HgII 6P-7S	3000.	0.246	0.973E-01	0.921E-03	0.185E-02	0.139E-02	0.171E-02
2261.0 A	5000.	0.191	0.782E-01	0.208E-02	0.332E-02	0.269E-02	0.298E-02
C= 0.64E+20	10000.	0.136	0.608E-01	0.439E-02	0.542E-02	0.460E-02	0.463E-02
	20000.	0.953E-01	0.464E-01	0.756E-02	0.775E-02	0.682E-02	0.628E-02
	30000.	0.838E-01	0.402E-01	0.894E-02	0.868E-02	0.785E-02	0.706E-02
	50000.	0.737E-01	0.351E-01	0.107E-01	0.100E-01	0.924E-02	0.812E-02
HgII 6P-7S	3000.	0.392	0.144	0.174E-02	0.282E-02	0.266E-02	0.262E-02
2848.5 A	5000.	0.304	0.114	0.370E-02	0.507E-02	0.489E-02	0.456E-02
C= 0.10E+21	10000.	0.216	0.883E-01	0.741E-02	0.830E-02	0.802E-02	0.709E-02
	20000.	0.153	0.665E-01	0.124E-01	0.119E-01	0.113E-01	0.966E-02
	30000.	0.135	0.572E-01	0.144E-01	0.134E-01	0.129E-01	0.108E-01
	50000.	0.119	0.499E-01	0.171E-01	0.155E-01	0.152E-01	0.126E-01
HgII 6S-6P	3000.	0.305	0.684E-01	0.221E-02	0.511E-03	0.382E-02	0.509E-03
3985.0 A	5000.	0.229	0.612E-01	0.430E-02	0.104E-02	0.656E-02	0.102E-02
C= 0.40E+21	10000.	0.164	0.436E-01	0.811E-02	0.214E-02	0.103E-01	0.197E-02
	20000.	0.118	0.338E-01	0.119E-01	0.358E-02	0.137E-01	0.306E-02
	30000.	0.974E-01	0.292E-01	0.138E-01	0.436E-02	0.149E-01	0.375E-02
	50000.	0.778E-01	0.238E-01	0.153E-01	0.542E-02	0.162E-01	0.439E-02
HgII 6P-6D	3000.	0.169	0.959E-02	0.235E-02	0.165E-02	0.332E-02	0.149E-02
1869.2 A	5000.	0.135	0.637E-02	0.412E-02	0.293E-02	0.498E-02	0.255E-02
C= 0.12E+20	10000.	0.102	0.449E-02	0.659E-02	0.471E-02	0.734E-02	0.396E-02
	20000.	0.806E-01	0.405E-02	0.884E-02	0.646E-02	0.875E-02	0.529E-02
	30000.	0.712E-01	0.359E-02	0.101E-01	0.729E-02	0.952E-02	0.589E-02
	50000.	0.611E-01	0.333E-02	0.114E-01	0.845E-02	0.108E-01	0.689E-02
HgII 6P-6D	3000.	0.289	0.548E-01	0.422E-02	0.411E-02	0.564E-02	0.362E-02
2225.4 A	5000.	0.231	0.453E-01	0.766E-02	0.704E-02	0.839E-02	0.575E-02
C= 0.14E+20	10000.	0.177	0.332E-01	0.125E-01	0.110E-01	0.127E-01	0.892E-02
	20000.	0.146	0.256E-01	0.170E-01	0.146E-01	0.156E-01	0.117E-01
	30000.	0.132	0.219E-01	0.193E-01	0.163E-01	0.176E-01	0.132E-01
	50000.	0.118	0.174E-01	0.222E-01	0.189E-01	0.200E-01	0.154E-01

Table 2. Comparison of the experimentally determined Stark full half widths of Hg II lines (W_M) with the present results (W_{SC}) and with calculations performed in Ref. 12 by using the simple semiempirical method[20] (W_{SE}). The experimental data were obtained by Murakawa (1966)[11] and Djeniže et al (1990)[12]

Transition in Hg II	λ(Å)	T(K)	N/10^{16} (cm^{-3})	W_M (Å)	W_{SC} (Å)	W_{SE} (Å)	d_M (Å)	d_{SC} (Å)	Ref.
$6s^2{}^2D_{5/2}$–$6p^2P^0_{3/2}$	3983.9	6500	1	0.0238	0.0201	0.036	0.002	0.006	11
		37,000	4.2	0.066	0.037	0.064			12
$6p^2P^0$–$7s^2S$	2847.7	37,000	4.2	0.061	0.054	0.080			12

In Table 2, we compare our results with experimental data[11,12] and with calculations performed in Ref. 10 by using the simple semiempirical method.[20] We must take into account the fact that for a heavy emitter with a complex spectrum, the accuracy of the semiclassical method is lower than it is for lighter atoms. However, the agreement with experimental data is very satisfactory for the 2847.3 Å line. In the case of the astrophysically important 3983.9 Å line, our results underestimate the real Stark width since, for broadening of the lower levels, only the most important transition $6s^2\ {}^2D_{5/2}$–$6p^2P^0_{3/2}$ has been taken into account. For this particular line, the accuracy may be improved by multiplying the semiclassical line widths by an averaged ratio of measured to calculated values. In this manner, we have a semiclassical temperature dependence, and the influence of neglected perturbing transitions is partly compensated for. The good agreement between experimental data and values obtained by using the simple semiempirical approach for the 3983.9 Å line indicates that various approximate methods (see, e.g. Ref. 20 and references therein) may be of interest for the analysis of the heavier atom spectra, especially in view of the lack of reliable atomic data needed for more sophisticated calculations.

Acknowledgements—I am indebted to S. Sahal-Bréchot for providing me with the semiclassical computer code. I am also indebted to M. Dworetsky who drew my attention to the astrophysical importance of Stark broadening of the observed Hg II lines.

REFERENCES

1. M. Dworetsky, *Astron. Astrophys.* **84,** 350 (1980).
2. C. R. Cowley and G. C. L. Aikman, *Publ. Astron. Soc. Pacific* **87,** 513 (1975).
3. R. E. White, A. H. Vaughan, Jr., G. W. Preston, and J. P. Swings, *Astrophys. J.* **204,** 131 (1976).
4. S. C. Wolf, *The A Stars: Problems and Perspectives*, NASA SP-463, Washington, DC (1983).
5. T. A. Ryabchikova and N. E. Piskunov, In *Magnetic Stars (Proc. Intl. Meeting on Physics and Evolution of Stars)*, p. 124, Yu. V. Glagolevsky and I. M. Kopylov eds., Nizhny Arkhyz (1988).
6. C. Aydin and M. Hack, *Astron. Astrophys. Suppl. Ser.* **33,** 27 (1978).
7. R. Stalio, *Astron. Astrophys.* **36,** 279 (1974).
8. S. Sahal-Bréchot, *Astron. Astrophys.* **1,** 91 (1969).
9. S. Sahal-Bréchot, *Astron. Astrophys.* **2,** 322 (1969).
10. M. S. Dimitrijević, S. Sahal-Bréchot, and V. Bommier, *Astron. Astrophys. Suppl. Ser.* **89,** 581 (1991).
11. K. Murakava, *Phys. Rev.* **146,** 135 (1966).
12. S. Djeniže, A. Srećković, M. Platiša, J. Labat, R. Konjević, and J. Purić, *JQSRT* **44,** 405 (1990).
13. C. E. Moore, "Atomic Energy Levels III", *NSRDS-NBS 35*, Washington, DC (1971).
14. D. R. Bates and A. Damgaard, *Trans. R. Soc. Lond. Ser. A* **242,** 101 (1949).
15. G. K. Oertel and L. P. Shomo, *Astrophys. J. Suppl. Ser.* **16,** 175 (1968).
16. H. Van Regemorter, Hoang Binh Dy, and M. Prud'homme, *J. Phys. B* **12,** 1073 (1979).
17. M. S. Dimitrijević and S. Sahal-Bréchot, *JQSRT* **31,** 301 (1984).
18. S. Sahal-Bréchot, *Astron. Astrophys.* **245,** 322.

19. H. R. Griem, *Spectral Line Broadening by Plasmas*, Academic Press, New York, NY (1974).
20. H. R. Griem, *Phys. Rev.* **165,** 258 (1968).
21. M. S. Dimitrijević and N. Konjević, *JQSRT* **24,** 451 (1980).

J. Quant. Spectrosc. Radiat. Transfer Vol. 48, No. 3, pp. 349–351, 1992
Printed in Great Britain.

0022-4073/92 $5.00 + 0.00

NOTE

ASYMPTOTIC BEHAVIOUR OF THE *A* AND *a* FUNCTIONS FOR IONIZED EMITTERS IN SEMICLASSICAL STARK-BROADENING THEORY

M. S. DIMITRIJEVIĆ†‡ and S. SAHAL-BRÉCHOT§

†Astronomical Observatory, Volgina 7, 11050 Beograd, Yugoslavia and §Laboratoire "Astrophysique, Atomes et Molécules" Unité associée au C.N.R.S. No 812, Département Atomes et Molécules en Astrophysique, Observatoire de Paris-Meudon, 92195 Meudon Cedex, France

(Received 27 September 1991; received for publication 17 April 1992)

Abstract—The asymptotic behaviour of the characteristic *A* and *a* functions has been studied in semiclassical Stark-broadening theory for ionized emitters (attractive hyperbolic paths). The approximate expressions for $\xi \gg 1$ and $\delta = \xi(\epsilon - 1) = \mathcal{O}(\xi\epsilon)^{1/3}$ are presented.

ANALYSIS

For the impact and semiclassical perturbation approximations,[1–3] Stark-broadening theory requires second-order expansions of the radiator–perturber collision operator (the so-called scattering *S*-matrix). This development is contained in the characteristic functions[1–3] *A*, *a*, *B*, and *b*. For ionic emitters, the incident electron moves in a classical hyperbolic path (attractive interaction). Hence, for calculation of the linewidth, we need the function

$$A(\xi, \epsilon) = (\xi\epsilon)^2 \exp(\pi\xi)\{|K_{i\xi}(\xi\epsilon)|^2 + [(\epsilon^2 - 1)/\epsilon^2]|K'_{i\xi}(\xi\epsilon)|^2\}, \tag{1}$$

where $K_{i\xi}(x)$ and $K'_{i\xi}(x)$ are a modified Bessel function of imaginary order and its derivative, ϵ is the perturber-path eccentricity,

$$\xi = (e^2/\hbar v)(\hbar\omega_{ii'}/mv^2) \tag{2}$$

for the case of i and i' energy levels of a singly-ionized radiator, and

$$a(\xi\epsilon) = \exp(\pi\xi)\xi\epsilon K_{i\xi}(\xi\epsilon)|K'_{i\xi}(\xi\epsilon)|. \tag{3}$$

When $\xi > 10$, the following assymptotic relations have been proposed by Klarsfeld[4] for $A(\xi, \epsilon)$ and $a(\xi, \epsilon)$:

$$A(\xi, \epsilon) = \pi^{1/2}\epsilon^{3/2}\{2\exp(-i\pi/3)\xi^{2/3}G_1(\zeta) - [(0.125\epsilon^{-1} - 0.525)G_0(\zeta) - 1.1\zeta G_1(\zeta) - 0.3\zeta^2 G_2(\zeta)]\}, \tag{4}$$

where

$$G_n \equiv \int_0^\infty t^{n+1/2}\exp(\zeta t - t^3/3)\,dt,$$

$$\zeta \equiv 2\exp(2\pi i/3)(\epsilon - 1)\zeta^{2/3},$$

and

$$a(\xi, \epsilon) = \pi^{1/2}\epsilon^{3/2}\{G_0(\zeta) + 0.5\exp(i\pi/3)\xi^{-2/3} \times [(0.45 - 0.75\epsilon^{-1})\zeta G_0(\zeta) + 0.3\zeta^2 G_1(\zeta) + (0.05 - 0.75\epsilon^{-1})G_2(\zeta)]\}, \tag{5}$$

‡To whom all correspondence should be addressed.

Table 1. Characteristic $A(\xi, \delta)$ and $a(\xi, \delta)$ functions.

ξ	δ	A[Eq.(6)]	A[Eq.(4)]	a[Eq.(6)]	a[Eq.(5)]
15.0	0.000E+00	10.9	0.000E+00	1.88	0.299
15.0	0.100E-01	11.0	13.5	1.87	1.87
15.0	0.200E-01	11.1	11.0	1.86	1.80
15.0	0.300E-01	11.2	11.1	1.86	1.82
15.0	0.400E-01	11.2	11.2	1.85	1.83
15.0	0.500E-01	11.3	11.3	1.84	1.83
15.0	0.600E-01	11.4	11.4	1.83	1.82
15.0	0.700E-01	11.5	11.5	1.83	1.82
15.0	0.800E-01	11.6	11.6	1.82	1.81
15.0	0.900E-01	11.7	11.7	1.81	1.80
15.0	0.100	11.7	11.7	1.80	1.80
15.0	0.200	12.4	12.4	1.72	1.72
0.100E+04	0.000E+00	167.	0.000E+00	1.82	0.182E-01
0.100E+04	0.100E-01	168.	0.595E-10	1.82	0.132E-12
0.100E+04	0.200E-01	168.	31.9	1.81	0.137
0.100E+04	0.300E-01	168.	208.	1.81	1.34
0.100E+04	0.400E-01	169.	213.	1.81	1.79
0.100E+04	0.500E-01	169.	186.	1.81	1.79
0.100E+04	0.600E-01	170.	170.	1.81	1.74
0.100E+04	0.700E-01	170.	168.	1.81	1.73
0.100E+04	0.800E-01	170.	170.	1.80	1.74
0.100E+04	0.900E-01	171.	171.	1.80	1.75
0.100E+04	0.100	171.	172.	1.80	1.76
0.100E+04	0.200	175.	175.	1.78	1.77
0.100E+04	0.300	178.	178.	1.77	1.76
0.100E+04	0.400	181.	181.	1.75	1.74
0.100E+04	0.500	184.	184.	1.73	1.73
0.100E+04	0.600	187.	187.	1.71	1.71
0.100E+04	0.700	190.	190.	1.69	1.69
0.100E+04	0.800	192.	192.	1.67	1.67
0.100E+04	0.900	194.	194.	1.65	1.65
0.100E+04	1.00	197.	197.	1.63	1.63
0.100E+04	2.00	208.	208.	1.43	1.43
0.100E+04	3.00	205.	205.	1.22	1.22
0.100E+04	4.00	193.	193.	1.03	1.02
0.100E+04	5.00	175.	174.	0.845	0.842
0.100E+04	6.00	155.	153.	0.686	0.679
0.400E+04	0.000E+00	421.	0.000E+00	1.82	0.722E-02
0.400E+04	0.100E-01	421.	0.767E-52	1.81	0.427E-55
0.400E+04	0.200E-01	422.	0.114E-02	1.81	0.123E-05
0.400E+04	0.300E-01	422.	43.3	1.81	0.696E-01
0.400E+04	0.400E-01	423.	351.	1.81	0.751
0.400E+04	0.500E-01	424.	548.	1.81	1.46
0.400E+04	0.600E-01	424.	552.	1.81	1.75
0.400E+04	0.700E-01	425.	506.	1.81	1.80
0.400E+04	0.800E-01	425.	466.	1.81	1.79
0.400E+04	0.900E-01	426.	437.	1.81	1.76
0.400E+04	0.100	427.	424.	1.80	1.73
0.400E+04	0.200	433.	433.	1.79	1.76
0.400E+04	0.300	438.	439.	1.78	1.77
0.400E+04	0.400	444.	444.	1.77	1.76
0.400E+04	0.500	449.	449.	1.76	1.75
0.400E+04	0.600	454.	454.	1.75	1.74
0.400E+04	0.700	459.	459.	1.74	1.73
0.400E+04	0.800	464.	464.	1.73	1.72
0.400E+04	0.900	468.	468.	1.72	1.71
0.400E+04	1.00	473.	473.	1.70	1.70
0.400E+04	2.00	505.	505.	1.58	1.58
0.400E+04	3.00	521.	521.	1.45	1.45

We have tested these expressions for a large range of ξ and ϵ values and found that when ϵ is close to 1 [$\delta = \xi(\epsilon - 1)$ is small], the proposed relations are not good. We have improved the asymptotic expressions by developing $K_{i\xi}(\xi\epsilon)$ and $|K'_{i\xi}(\xi\epsilon)|$ in series.[5] For $\xi \gg 1$ and $\delta = \xi(\epsilon - 1) = \mathcal{O}(\xi\epsilon)^{1/3}$, one obtains

$$K_{i\xi}(\xi\epsilon) = (3^{1/2}/6)\exp(-\pi\xi/2)\{\Gamma(1/3)(6/\xi\epsilon)^{1/3} - \Gamma(2/3)(6/\xi\epsilon)^{2/3}\delta + \Gamma(4/3)(6/\xi\epsilon)^{4/3}(\delta/3) \times (0.5\delta^2 + 0.2) - [\Gamma(5/3)/8](6/\xi\epsilon)^{5/3}[(\delta^4 + \delta^2)/3 + 1/35]\}$$

$$|K'_{i\xi}(\xi\epsilon)| = (3^{1/2}/2)\exp(-\pi\xi/2)(6/\xi\epsilon)^{2/3}\{2\Gamma(2/3) + (6/\xi\epsilon)^{2/3}[-\Gamma(4/3)(\delta^2 + 2/15) + (1/9)\Gamma(1/3)] + (6/\xi\epsilon)[\Gamma(5/3)(\delta/6)(1 + 2\delta^2) - (2/9)\delta\Gamma(2/3)]\}. \quad (6)$$

The A and a functions calculated by using the proposed asymptotic relations are compared in Table 1 with our calculations using Klarsfeld's expressions. One can see that for small δ, the proposed relations give good results unlike Eqs. (4) and (5). These new asymptotic expansions are necessary for good calculations of Stark line broadening in highly-ionized atoms.

REFERENCES

1. H. R. Griem, M. Baranger, A. C. Kolb, and G. K. Oertel, *Phys. Rev.* **125,** 177 (1962).
2. S. Sahal-Bréchot, *Astron. Astrophys.* **1,** 91 (1969).
3. S. Sahal-Bréchot, *Astron. Astrophys.* **2,** 322 (1969).
4. S. Klarsfeld, cited as a private communication in W. W. Jones, S. M. Benett, and H. R. Griem, Techn. Rep. No 71-178, College Park, MD (1971).
5. H. Bateman, *Higher Transcendental Functions*, A. Erdelyi ed., McGraw–Hill, New York, NY (1953).

J. Quant. Spectrosc. Radiat. Transfer Vol. 48, No. 4, pp. 397–403, 1992
Printed in Great Britain.

0022-4073/92 $5.00 + 0.00

STARK BROADENING OF Be II SPECTRAL LINES

M. S. DIMITRIJEVIĆ†‡ and S. SAHAL-BRÉCHOT§

†Astronomical Observatory, Volgina 7, 11050 Beograd, Yugoslavia and
§Laboratoire "Astrophysique, Atomes et Molécules", Unité associée au C.N.R.S. No 812,
Département Atomes et Molécules en Astrophysique, Observatoire de Paris-Meudon,
92190 Meudon, France

(Received 24 March 1992)

Abstract—Using a semiclassical approach, we have calculated electron-, proton-, and ionized helium-impact line widths and shifts for 30 Be II multiplets. The resulting data have been compared with existing experimental and theoretical values.

INTRODUCTION

Besides the interest for plasma spectroscopy,[1–4] the Be II Stark-broadening parameters are important to astrophysicists since the surface content (abundance) of light elements, especially Li and Be, involves problems correlated with nucleogenesis, mixing between the atmosphere and the interior, and stellar structure and evolution.[5] Moreover, Be II profiles are of importance for opacity calculations as well.[6]

By using the semiclassical-perturbation formalism,[7,8] we have calculated electron-, proton-, and ionized helium-impact line widths and shifts for 30 Be II multiplets. A summary of the formalism is given in Ref. 9. Here, we present and discuss the results for Be II, along with a comparison with experimental data[1–3] and other theoretical results.[4,6,10–13]

RESULTS AND DISCUSSION

Energy levels for Be II lines have been taken from Ref. 14. Oscillator strengths have been calculated by using the method of Bates and Damgaard.[15,16] For higher levels, the method described in Ref. 17 has been used. In the case of the $2s$–$2p$ transition, the contribution of resonances has been neglected. The method for estimation of resonance contributions described in Ref. 18 assumes the existence of a series of resonances below the corresponding excitation threshold. This condition is especially well satisfied for multicharged ions and for higher transitions. For $2s$–$2p$ Be II transitions, conditions for the utilisation of the proposed method are not satisfied, and the resonance contribution is overestimated.

In addition to electron-impact full halfwidths and shifts, Stark-broadening parameters due to proton- and ionized-helium impacts have been calculated. Thus, we have provided Stark-broadening data for all of the important charged perturbers in stellar atmospheres. Our results are shown in Table 1 for a perturber density of $10^{15}\,\mathrm{cm}^{-3}$ and temperatures $T = 2500$–$50{,}000$ K. For perturber densities lower than $10^{15}\,\mathrm{cm}^{-3}$, all of the data are practically linear functions of the density because the effect of Debye screening is negligible. We also specify a parameter[6] c which, when it is divided by the corresponding electron-impact full width at half maximum, gives an estimate for the maximum perturber density for which the line may be treated as isolated.

For each value given in Table 1, the collision volume (V) multiplied by the perturber density (N) is much less than one and the impact approximation is valid.[7,8] Values for $0.1 < NV \leqslant 0.5$ are denoted by an asterisk. When the impact approximation is not valid, the ion-broadening contribution may be estimated by using quasistatic estimations.[11,19] The accuracy of the results obtained decreases when broadening by ion interactions becomes important. At high densities, the results are no longer linear with density due to Debye screening. This effect is more important for the shift than for the width. Stark-broadening parameter tables for high densities will be published elsewhere.[20]

‡To whom all correspondence should be addressed.

Table 1. This table shows electron-, proton-, and He II-impact broadening parameters for Be II lines, for perturber densities of $10^{15}\,cm^{-3}$ and temperatures from 2500 to 50,000 K. Transitions and averaged wavelengths for the multiplet (in Å) are also given. By using c [see Eq. (5) of Ref. 9], we obtain an estimate for the maximum perturber density for which the line may be treated as isolated and tabulated data may be used. The asterisk identifies cases for which the collision volume multiplied by the perturber density (the condition for validity of the impact approximation) lies between 0.1 and 0.5.

PERTURBER DENSITY = 0.1D+16(cm-3)							
PERTURBERS ARE		ELECTRONS		PROTONS		IONIZED HELIUM	
TRANSITION	T(K)	WIDTH(A)	SHIFT(A)	WIDTH(A)	SHIFT(A)	WIDTH(A)	SHIFT(A)
Be II 2S-2P	2500.	0.126E-02	-0.109E-03	0.374E-05	-0.348E-05	0.637E-05	-0.348E-05
3131.5 A	5000.	0.802E-03	-0.106E-03	0.998E-05	-0.713E-05	0.154E-04	-0.705E-05
C= 0.31E+19	10000.	0.576E-03	-0.472E-04	0.219E-04	-0.134E-04	0.293E-04	-0.127E-04
	20000.	0.444E-03	-0.499E-04	0.366E-04	-0.216E-04	0.433E-04	-0.191E-04
	30000.	0.405E-03	-0.402E-04	0.460E-04	-0.261E-04	0.508E-04	-0.232E-04
	50000.	0.384E-03	-0.477E-04	0.552E-04	-0.326E-04	0.571E-04	-0.275E-04
Be II 2S-3P	2500.	0.655E-03	0.536E-04	0.163E-04	0.206E-04	0.212E-04	0.193E-04
1036.3 A	5000.	0.555E-03	0.359E-04	0.304E-04	0.317E-04	0.340E-04	0.285E-04
C= 0.17E+17	10000.	0.478E-03	0.478E-04	0.484E-04	0.436E-04	0.463E-04	0.366E-04
	20000.	0.420E-03	0.435E-04	0.611E-04	0.524E-04	0.574E-04	0.445E-04
	30000.	0.392E-03	0.399E-04	0.684E-04	0.577E-04	0.637E-04	0.493E-04
	50000.	0.362E-03	0.403E-04	0.795E-04	0.646E-04	0.719E-04	0.557E-04
Be II 2S-4P	2500.	0.126E-02	0.241E-03	0.871E-04	0.894E-04	0.923E-04	0.782E-04
842.0 A	5000.	0.111E-02	0.231E-03	0.130E-03	0.119E-03	0.122E-03	0.101E-03
C= 0.47E+16	10000.	0.101E-02	0.206E-03	0.166E-03	0.146E-03	0.151E-03	0.123E-03
	20000.	0.948E-03	0.169E-03	0.202E-03	0.172E-03	0.180E-03	0.146E-03
	30000.	0.915E-03	0.163E-03	0.221E-03	0.192E-03	0.195E-03	0.154E-03
	50000.	0.873E-03	0.139E-03	0.247E-03	0.196E-03	0.222E-03	0.175E-03
Be II 2S-5P	2500.	0.253E-02	0.784E-03	0.292E-03	0.250E-03	0.272E-03	0.209E-03
775.4 A	5000.	0.231E-02	0.690E-03	0.368E-03	0.326E-03	0.338E-03	0.273E-03
C= 0.20E+16	10000.	0.221E-02	0.540E-03	0.472E-03	0.399E-03	0.401E-03	0.338E-03
	20000.	0.214E-02	0.469E-03	0.526E-03	0.448E-03	0.493E-03	0.368E-03
	30000.	0.209E-02	0.416E-03	0.552E-03	0.507E-03	0.473E-03	0.404E-03
	50000.	0.202E-02	0.332E-03	0.618E-03	0.523E-03	0.577E-03	0.453E-03
Be II 2P-3S	2500.	0.187E-02	0.836E-03	0.681E-05	0.265E-04	0.927E-05	0.253E-04
1776.2 A	5000.	0.133E-02	0.631E-03	0.229E-04	0.454E-04	0.254E-04	0.404E-04
C= 0.26E+18	10000.	0.941E-03	0.486E-03	0.452E-04	0.639E-04	0.449E-04	0.563E-04
	20000.	0.722E-03	0.373E-03	0.730E-04	0.802E-04	0.651E-04	0.678E-04
	30000.	0.661E-03	0.334E-03	0.874E-04	0.888E-04	0.759E-04	0.755E-04
	50000.	0.605E-03	0.278E-03	0.105E-03	0.102E-03	0.903E-04	0.844E-04
Be II 2P-4S	2500.	0.223E-02	0.101E-02	0.450E-04	0.779E-04	0.444E-04	0.677E-04
1197.2 A	5000.	0.157E-02	0.922E-03	0.833E-04	0.111E-03	0.814E-04	0.958E-04
C= 0.47E+17	10000.	0.118E-02	0.749E-03	0.129E-03	0.138E-03	0.113E-03	0.117E-03
	20000.	0.100E-02	0.658E-03	0.162E-03	0.165E-03	0.143E-03	0.140E-03
	30000.	0.950E-03	0.585E-03	0.194E-03	0.183E-03	0.157E-03	0.155E-03
	50000.	0.900E-03	0.490E-03	0.220E-03	0.198E-03	0.181E-03	0.166E-03
Be II 2P-5S	2500.	0.341E-02	0.177E-02	0.162E-03	0.209E-03	0.159E-03	0.179E-03
1048.2 A	5000.	0.272E-02	0.166E-02	0.256E-03	0.270E-03	0.222E-03	0.228E-03
C= 0.18E+17	10000.	0.220E-02	0.152E-02	0.332E-03	0.329E-03	0.285E-03	0.277E-03
	20000.	0.200E-02	0.129E-02	0.419E-03	0.395E-03	0.358E-03	0.325E-03
	30000.	0.190E-02	0.120E-02	0.471E-03	0.415E-03	0.396E-03	0.359E-03
	50000.	0.190E-02	0.102E-02	0.531E-03	0.471E-03	0.432E-03	0.384E-03

Table 1—*continued*

PERTURBER DENSITY = 0.1D+16(cm-3)							
PERYRBERS ARE		ELECTRONS		PROTONS		IONIZED HELIUM	
TRANSITION	T(K)	WIDTH(A)	SHIFT(A)	WIDTH(A)	SHIFT(A)	WIDTH(A)	SHIFT(A)
Be II 2P-3D	2500.	0.167E-02	0.899E-04	0.149E-04	-0.274E-04	0.194E-04	-0.256E-04
1512.4 A	5000.	0.124E-02	0.697E-04	0.348E-04	-0.448E-04	0.366E-04	-0.393E-04
C= 0.36E+17	10000.	0.927E-03	0.298E-04	0.580E-04	-0.625E-04	0.587E-04	-0.539E-04
	20000.	0.709E-03	0.142E-04	0.810E-04	-0.763E-04	0.742E-04	-0.646E-04
	30000.	0.612E-03	0.737E-05	0.909E-04	-0.844E-04	0.833E-04	-0.715E-04
	50000.	0.531E-03	0.272E-05	0.108E-03	-0.969E-04	0.962E-04	-0.801E-04
Be II 2P-4D	2500.	0.526E-02	0.117E-03	*0.116E-02	*0.103E-02	*0.100E-02	*0.858E-03
1143.0 A	5000.	0.433E-02	0.210E-03	0.143E-02	0.136E-02	*0.120E-02	*0.114E-02
C= 0.33E+15	10000.	0.360E-02	0.228E-03	0.178E-02	0.166E-02	*0.152E-02	*0.141E-02
	20000.	0.300E-02	0.187E-03	0.198E-02	0.195E-02	0.171E-02	0.154E-02
	30000.	0.271E-02	0.147E-03	0.227E-02	0.205E-02	0.191E-02	0.180E-02
	50000.	0.237E-02	0.101E-03	0.237E-02	0.213E-02	0.187E-02	0.201E-02
Be II 2P-5D	2500.	0.121E-01	-0.113E-03				
1026.9 A	5000.	0.103E-01	0.375E-03				
C= 0.14E+15	10000.	0.877E-02	0.591E-03				
	20000.	0.747E-02	0.422E-03	*0.667E-02	*0.561E-02		
	30000.	0.678E-02	0.336E-03	*0.637E-02	*0.638E-02		
	50000.	0.598E-02	0.234E-03	*0.638E-02	*0.670E-02	*0.631E-02	*0.550E-02
Be II 3S-3P	2500.	0.137	-0.212E-01	0.191E-02	0.184E-02	0.254E-02	0.172E-02
12099.6 A	5000.	0.110	-0.159E-01	0.352E-02	0.300E-02	0.402E-02	0.262E-02
C= 0.23E+19	10000.	0.879E-01	-0.106E-01	0.535E-02	0.416E-02	0.540E-02	0.358E-02
	20000.	0.756E-01	-0.746E-02	0.667E-02	0.507E-02	0.647E-02	0.428E-02
	30000.	0.715E-01	-0.700E-02	0.753E-02	0.569E-02	0.714E-02	0.477E-02
	50000.	0.671E-01	-0.541E-02	0.854E-02	0.640E-02	0.790E-02	0.535E-02
Be II 3S-4P	2500.	0.220E-01	0.299E-02	0.129E-02	0.131E-02	0.137E-02	0.115E-02
3275.6 A	5000.	0.190E-01	0.278E-02	0.193E-02	0.175E-02	0.183E-02	0.149E-02
C= 0.71E+17	10000.	0.169E-01	0.226E-02	0.246E-02	0.217E-02	0.224E-02	0.181E-02
	20000.	0.157E-01	0.173E-02	0.304E-02	0.253E-02	0.267E-02	0.218E-02
	30000.	0.151E-01	0.166E-02	0.318E-02	0.278E-02	0.298E-02	0.232E-02
	50000.	0.145E-01	0.139E-02	0.384E-02	0.293E-02	0.326E-02	0.261E-02
Be II 3S-5P	2500.	0.265E-01	0.703E-02	0.291E-02	0.249E-02	0.271E-02	0.208E-02
2454.6 A	5000.	0.240E-01	0.621E-02	0.365E-02	0.325E-02	0.337E-02	0.272E-02
C= 0.20E+17	10000.	0.228E-01	0.508E-02	0.469E-02	0.399E-02	0.399E-02	0.337E-02
	20000.	0.220E-01	0.416E-02	0.528E-02	0.446E-02	0.497E-02	0.371E-02
	30000.	0.216E-01	0.363E-02	0.552E-02	0.505E-02	0.473E-02	0.401E-02
	50000.	0.209E-01	0.289E-02	0.618E-02	0.521E-02	0.572E-02	0.451E-02
Be II 3P-4S	2500.	0.470E-01	0.165E-01	0.751E-03	0.114E-02	0.836E-03	0.101E-02
5272.1 A	5000.	0.360E-01	0.155E-01	0.134E-02	0.164E-02	0.139E-02	0.144E-02
C= 0.43E+18	10000.	0.292E-01	0.125E-01	0.206E-02	0.208E-02	0.187E-02	0.177E-02
	20000.	0.268E-01	0.110E-01	0.261E-02	0.252E-02	0.235E-02	0.209E-02
	30000.	0.254E-01	0.979E-02	0.306E-02	0.275E-02	0.264E-02	0.231E-02
	50000.	0.244E-01	0.813E-02	0.336E-02	0.304E-02	0.289E-02	0.256E-02

continued overleaf

Table 1—*continued*

PERTURBER DENSITY = 0.1D+16(cm-3)							
PERTURBERS ARE		ELECTRONS		PROTONS		IONIZED HELIUM	
TRANSITION	T(K)	WIDTH(A)	SHIFT(A)	WIDTH(A)	SHIFT(A)	WIDTH(A)	SHIFT(A)
Be II 3P-5S	2500.	0.336E-01	0.164E-01	0.148E-02	0.191E-02	0.147E-02	0.164E-02
3242.7 A	5000.	0.265E-01	0.163E-01	0.236E-02	0.249E-02	0.205E-02	0.209E-02
C= 0.16E+18	10000.	0.230E-01	0.139E-01	0.303E-02	0.303E-02	0.264E-02	0.256E-02
	20000.	0.214E-01	0.118E-01	0.366E-02	0.362E-02	0.326E-02	0.303E-02
	30000.	0.206E-01	0.109E-01	0.425E-02	0.391E-02	0.356E-02	0.328E-02
	50000.	0.206E-01	0.924E-02	0.484E-02	0.438E-02	0.391E-02	0.352E-02
Be II 3P-3D	2500.	4.20	-0.423	0.702E-01	-0.120	0.855E-01	-0.109
64174.1 A	5000.	3.36	-0.290	0.139	-0.178	0.145	-0.158
C= 0.64E+20	10000.	2.76	-0.279	0.227	-0.231	0.209	-0.198
	20000.	2.34	-0.245	0.288	-0.278	0.259	-0.235
	30000.	2.15	-0.223	0.330	-0.306	0.285	-0.257
	50000.	1.95	-0.208	0.370	-0.345	0.333	-0.295
Be II 3P-4D	2500.	0.811E-01	-0.128E-02	*0.168E-01	*0.150E-01	*0.144E-01	*0.124E-01
4362.1 A	5000.	0.677E-01	0.796E-03	0.208E-01	0.197E-01	*0.175E-01	*0.164E-01
C= 0.48E+16	10000.	0.570E-01	0.154E-02	0.258E-01	0.240E-01	*0.220E-01	*0.204E-01
	20000.	0.481E-01	0.109E-02	0.286E-01	0.282E-01	0.249E-01	0.222E-01
	30000.	0.437E-01	0.910E-03	0.329E-01	0.298E-01	0.275E-01	0.261E-01
	50000.	0.387E-01	0.465E-03	0.346E-01	0.306E-01	0.268E-01	0.290E-01
Be II 3P-5D	2500.	0.108	-0.992E-03				
3047.5 A	5000.	0.925E-01	0.227E-02				
C= 0.13E+16	10000.	0.793E-01	0.422E-02				
	20000.	0.678E-01	0.300E-02	*0.586E-01	*0.494E-01		
	30000.	0.617E-01	0.251E-02	*0.561E-01	*0.561E-01		
	50000.	0.546E-01	0.155E-02	*0.561E-01	*0.590E-01	*0.555E-01	*0.485E-01
Be II 3D-4P	2500.	0.487E-01	0.825E-02	0.282E-02	0.307E-02	0.295E-02	0.268E-02
4829.6 A	5000.	0.421E-01	0.772E-02	0.425E-02	0.405E-02	0.399E-02	0.346E-02
C= 0.15E+18	10000.	0.378E-01	0.705E-02	0.548E-02	0.499E-02	0.483E-02	0.420E-02
	20000.	0.348E-01	0.591E-02	0.673E-02	0.591E-02	0.608E-02	0.500E-02
	30000.	0.333E-01	0.560E-02	0.757E-02	0.645E-02	0.645E-02	0.528E-02
	50000.	0.316E-01	0.478E-02	0.795E-02	0.679E-02	0.737E-02	0.594E-02
Be II 3D-5P	2500.	0.467E-01	0.143E-01	0.506E-02	0.437E-02	0.470E-02	0.366E-02
3234.5 A	5000.	0.424E-01	0.125E-01	0.644E-02	0.573E-02	0.588E-02	0.479E-02
C= 0.35E+17	10000.	0.403E-01	0.966E-02	0.823E-02	0.695E-02	0.699E-02	0.592E-02
	20000.	0.387E-01	0.826E-02	0.917E-02	0.790E-02	0.848E-02	0.641E-02
	30000.	0.378E-01	0.733E-02	0.969E-02	0.894E-02	0.832E-02	0.710E-02
	50000.	0.364E-01	0.589E-02	0.106E-01	0.913E-02	0.995E-02	0.792E-02
Be II 3D-4F	2500.	0.595E-01	0.258E-02	0.155E-01	-0.143E-01	*0.133E-01	*-0.117E-01
4674.7 A	5000.	0.483E-01	0.239E-03	0.193E-01	-0.184E-01	*0.165E-01	*-0.157E-01
C= 0.56E+16	10000.	0.394E-01	-0.554E-03	0.251E-01	-0.230E-01	0.210E-01	-0.188E-01
	20000.	0.322E-01	-0.740E-03	0.279E-01	-0.251E-01	0.254E-01	-0.220E-01
	30000.	0.288E-01	-0.551E-03	0.309E-01	-0.282E-01	0.265E-01	-0.228E-01
	50000.	0.252E-01	-0.166E-03	0.380E-01	-0.302E-01	0.272E-01	-0.249E-01

Table 1—*continued*

PERTURBER DENSITY = 0.1D+16(cm-3)							
PERTURBERS ARE		ELECTRONS		PROTONS		IONIZED HELIUM	
TRANSITION	T(K)	WIDTH(A)	SHIFT(A)	WIDTH(A)	SHIFT(A)	WIDTH(A)	SHIFT(A)
Be II 3D-5F	2500.	0.130	-0.687E-03				
3198.1 A	5000.	0.110	-0.223E-03				
C= 0.16E+15	10000.	0.912E-01	-0.496E-04				
	20000.	0.749E-01	-0.108E-02				
	30000.	0.665E-01	-0.557E-03				
	50000.	0.570E-01	-0.628E-03				
Be II 4S-4P	2500.	2.40	-0.361E-01	0.905E-01	0.833E-01	0.101	0.741E-01
30339.8 A	5000.	2.07	-0.707E-01	0.138	0.117	0.133	0.976E-01
C= 0.61E+19	10000.	1.83	-0.117	0.172	0.142	0.161	0.120
	20000.	1.73	-0.122	0.212	0.169	0.189	0.142
	30000.	1.68	-0.114	0.233	0.187	0.205	0.153
	50000.	1.63	-0.113	0.247	0.205	0.215	0.167
Be II 4S-5P	2500.	0.264	0.649E-01	0.255E-01	0.217E-01	0.238E-01	0.181E-01
7403.3 A	5000.	0.243	0.468E-01	0.322E-01	0.280E-01	0.292E-01	0.235E-01
C= 0.19E+18	10000.	0.230	0.301E-01	0.402E-01	0.349E-01	0.339E-01	0.286E-01
	20000.	0.222	0.237E-01	0.470E-01	0.393E-01	0.430E-01	0.334E-01
	30000.	0.219	0.200E-01	0.473E-01	0.430E-01	0.430E-01	0.339E-01
	50000.	0.213	0.131E-01	0.562E-01	0.460E-01	0.503E-01	0.401E-01
Be II 4P-5S	2500.	0.517	0.143	0.139E-01	0.131E-01	0.153E-01	0.116E-01
11662.1 A	5000.	0.449	0.144	0.211E-01	0.181E-01	0.203E-01	0.152E-01
C= 0.90E+18	10000.	0.409	0.140	0.264E-01	0.222E-01	0.242E-01	0.186E-01
	20000.	0.392	0.120	0.319E-01	0.261E-01	0.293E-01	0.221E-01
	30000.	0.387	0.109	0.367E-01	0.286E-01	0.316E-01	0.239E-01
	50000.	0.385	0.967E-01	0.388E-01	0.317E-01	0.325E-01	0.259E-01
Be II 4P-5D	2500.	1.14	-0.503E-01				
9478.9 A	5000.	0.978	-0.535E-02				
C= 0.12E+17	10000.	0.843	0.157E-01				
	20000.	0.728	0.164E-01	*0.558	*0.473		
	30000.	0.667	0.632E-02	*0.543	*0.539		
	50000.	0.596	0.741E-03	*0.532	*0.567	*0.537	*0.467
Be II 4D-5P	2500.	0.823	0.152	0.705E-01	-0.641E-01	*0.636E-01	-0.530E-01
10470.5 A	5000.	0.726	0.118	0.903E-01	-0.830E-01	*0.810E-01	-0.706E-01
C= 0.28E+17	10000.	0.660	0.880E-01	0.108	-0.101	0.954E-01	-0.865E-01
	20000.	0.606	0.734E-01	0.141	-0.118	0.111	-0.102
	30000.	0.577	0.661E-01	0.141	-0.120	0.125	-0.106
	50000.	0.540	0.551E-01	0.168	-0.141	0.129	-0.113
Be II 4D-5F	2500.	1.58	-0.154E-01				
10098.4 A	5000.	1.34	-0.188E-01				
C= 0.16E+16	10000.	1.12	-0.200E-01				
	20000.	0.925	-0.255E-01				
	30000.	0.825	-0.185E-01				
	50000.	0.712	-0.145E-01				

continued overleaf

Table 1—*continued*

PERTURBER DENSITY = 0.1D+16(cm-3)							
PERTURBERS ARE		ELECTRONS		PROTONS		IONIZED HELIUM	
TRANSITION	T(K)	WIDTH(A)	SHIFT(A)	WIDTH(A)	SHIFT(A)	WIDTH(A)	SHIFT(A)
Be II 4F-5D	2500.	1.36	0.209E-01				
10138.4 A	5000.	1.15	0.605E-01				
C= 0.14E+17	10000.	0.978	0.699E-01				
	20000.	0.832	0.496E-01	*0.711	*0.569		
	30000.	0.755	0.391E-01	*0.727	*0.670		
	50000.	0.665	0.248E-01	*0.722	*0.710	*0.662	*0.581

In Tables 2 and 3, the present results are compared with experimental data,[1,3,4] with other semiclassical,[10,11] with quantum-mechanical strong-coupling,[4,6] and with semiempirical calculations.[12,13] We see that for the shifts large disagreements exist. It should be noted that the shift values are of lesser accuracy for semiclassical calculations than the widths.[21–23] They are also smaller, and different contributions to the shift have different signs which is an additional theoretical difficulty.

Acknowledgements—One of us (M.D.) has been supported by the Observatory of Paris-Meudon. This work has also been supported by the French C.N.R.S. and is a part of French–Yugoslav collaboration through the project "L'élargissement Stark des raies spéctrales des plasmas astrophysiques et de laboratoire". It is also a part of the project "Physics and Dynamics of Celestial Bodies", supported by RFN of Serbia.

Table 2. Comparison between the experimental Stark full half-halfwidths of Be II lines (*Wm*) in the $2s^2S$–$2p^2P^0$ multiplet, with different calculations. Semiclassical calculations: WDSB—present results; WJBG—Jones, Benett, and Griem (1971);[10,11] quantum-mechanical calculations: WS—Seaton (1988);[6] WSBJ—Sanchez, Blaha, and Jones;[4] semiempirical calculations: WMSE—Dimitrijević and Konjević (1981);[12] WDK—Dimitrijević and Konjević (1981).[13] The electron density N is equal to 10^{17} cm^{-3}.

λ(A)	T(K)	Wm(A)	Wm/WDSB	Wm/WJBG	Wm/WS	Wm/WSBJ	Wm/ WMSE	Wm/WDK	Ref.
3130.4	19000	0.070	0.80	0.82	2.43	1.69	1.43	1.51	4
	34800	0.04	0.60	0.57	1.49	1.09	1.10	1.01	3
3131.1	19000	0.070	0.80	0.82	2.43	1.69	1.43	1.51	4
	34800	0.06	0.91	0.86	2.23	1.64	1.66	1.51	3

Table 3. As in Table 2 but for the shift (*d*).

λ(A)	T(K)	dm(A)	dm/dDSB	dm/dJBG	dm/dS	Ref.
3130.4	16800	-0.03	6.1	0.80	2.32	1
	34800	-0.04	10.0	1.41	4.09	3
3131.1	16800	-0.03	6.1	0.80	2.32	1
	34800	-0.03	7.5	1.03	3.07	3

REFERENCES

1. J. Purić and N. Konjević, *Z. Phys.* **249,** 440 (1972).
2. M. Platiša, J. Purić, N. Konjević, and J. Labat, *Astron. Astrophys.* **15,** 325 (1971).
3. D. Hadžiomerspahić, M. Platiša, N. Konjević, and M. Popović, *Z. Phys.* **262,** 169 (1973).
4. A. Sanchez, M. Blaha, and W. W. Jones, *Phys. Rev. A* **8,** 774 (1973).
5. A. M. Boesgaard, *Vistas Astron.* **31,** 167 (1988).
6. M. J. Seaton, *J. Phys. B* **21,** 3033 (1983).
7. S. Sahal-Bréchot, *Astron. Astrophys.* **1,** 91 (1969).
8. S. Sahal-Bréchot, *Astron. Astrophys.* **2,** 322 (1969).
9. M. S. Dimitrijević and S. Sahal-Bréchot, *JQSRT* **31,** 301 (1984).
10. W. W. Jones, S. M. Benett, and H. R. Griem, "Calculated Electron Impact Broadening Parameters for Isolated Spectral Lines from Singly Charged Ions Lithium through Calcium", Univ. Maryland, Tech. Rep. No. 71-128, College Park, Maryland (1971).
11. H. R. Griem, *Spectral Line Broadening by Plasmas*, Academic Press, New York, NY (1974).
12. M. S. Dimitrijević and N. Konjević, in *Spectral Line Shapes*, p. 211, B. Wende ed., De Gruyter, New York, NY (1981).
13. M. S. Dimitrijević and N. Konjević, *Astron. Astrophys.* **102,** 93 (1981).
14. S. Bashkin and J. J. Stoner Jr., *Atomic Energy Levels and Grotrian Diagrams*, Vol. 1, North Holland, Amsterdam (1975).
15. D. R. Bates and A. Damgaard, *Trans. R. Soc. Lond. Ser. A* **242,** 101 (1949).
16. G. K. Oertel and L. P. Shomo, *Astrophys. J. Suppl. Series* **16,** 175 (1968).
17. H. Van Regemorter, Hoang Binh Dy, and M. Prud'homme, *J. Phys. B* **12,** 1073 (1979).
18. C. Fleurier, S. Sahal-Bréchot, and J. Chapelle, *JQSRT* **17,** 595 (1977).
19. S. Sahal-Bréchot, *Astron. Astrophys.* **245,** 322 (1991).
20. M. S. Dimitrijević and S. Sahal-Bréchot, *Bull. Astron. Belgrade* **145,** 65 (1991).
21. H. R. Griem and C. S. Shen, *Phys. Rev.* **125,** 196 (1962).
22. D. E. Roberts, *J. Phys. B* **1,** 53 (1968).
23. M. S. Dimitrijević, N. Featurier, and S. Sahal-Bréchot, *J. Phys. B* **14,** 2559 (1981).

J. Quant. Spectrosc. Radiat. Transfer Vol. 49, No. 2, pp. 157–164, 1993
Printed in Great Britain.

0022-4073/93 $6.00 + 0.00

STARK BROADENING OF Ca II SPECTRAL LINES

M. S. DIMITRIJEVIĆ†‡ and S. SAHAL-BRÉCHOT§

†Astronomical Observatory, Volgina 7, 11050 Beograd, Yugoslavia and §Laboratoire "Astrophysique, Atomes et Molécules", Unité associée au C.N.R.S. No 812, Département Atomes et Molécules en Astrophysique, Observatoire de Paris-Meudon, 92190 Meudon, France

(Received 17 December 1991; received for publication 21 March 1992)

Abstract—Using a semiclassical approach, we have calculated electron-, proton-, and ionized-helium-impact line widths and shifts for 28 Ca II multiplets. The resulting data have been compared with existing experimental values.

INTRODUCTION

Calcium is among the most abundant elements in stellar plasmas after hydrogen and helium. Particularly important for stellar spectral analysis are the well known resonance lines of Ca II, which are present in all spectra starting with B-type stars and reaching maximal intensity in stars of the K0 spectral type. Consequently, knowledge of reliable Ca II Stark-broadening parameters is of great importance for detailed investigation of stellar atmospheres, as well as for opacity research. Furthermore, Ca II lines are of particular interest for investigations of laboratory plasmas, since calcium is often present as an impurity. By using the semiclassical-perturbation formalism,[1,2] we have calculated electron-, proton-, and ionized-helium-impact line widths and shifts for 28 Ca II multiplets. A summary of the formalism is given in Ref. 3. Here, we present and discuss the results for Ca II, along with a comparison with experimental data[4–15] and other theoretical results.[13,16–19]

RESULTS AND DISCUSSION

Energy levels for Ca II lines have been taken from Ref. 20. Oscillator strengths have been calculated by using the method of Bates and Damgaard.[21,22] For higher levels, the method described in Ref. 23 has been used. In the case of the $3d$-$4p$ and $4s$-$4p$ transitions, the contribution of resonances has been neglected. The method for estimation of resonance contributions described in Ref. 4 assumes the existence of a series of resonances below the corresponding excitation threshold. This condition is especially well satisfied for multicharged ions and for higher transitions. For $3d$-$4p$ and $4s$-$4p$ Ca II transitions, conditions for the utilization of the proposed method are not satisfied, and the resonance contribution is overestimated.

In addition to electron-impact full halfwidths and shifts, Stark-broadening parameters due to proton- and ionized-helium-impacts have been calculated. In this manner, we have provided Stark-broadening data for all of the important charged perturbers in stellar atmospheres. Our results are shown in Table 1 for a perturber density of $10^{15}\,\mathrm{cm}^{-3}$ and temperatures $T = 5000$–$50{,}000$ K. For perturber densities lower than $10^{15}\,\mathrm{cm}^{-3}$, all of the data are practically linear functions of the density because the effect of Debye screening is negligible. We also specify a parameter[24] c which, when it is divided by the corresponding electron-impact full width at half maximum, gives an estimate for the maximum perturber density for which the line may be treated as isolated.

For each value given in Table 1, the collision volume (V) multiplied by the perturber density (N) is much less than one and the impact approximation is valid.[1,2] Values for $0.1 < NV \leq 0.5$ are denoted by an asterisk. When the impact approximation is not valid, the ion-broadening contribution may be estimated by using quasistatic estimates.[19,25] The accuracy of the results

‡To whom all correspondence should be addressed.

Table 1. This table shows electron-, proton-, and ionized-helium-impact broadening parameters for Ca II lines and for perturber densities of 10^{15} cm^{-3} and temperatures from 5000 to 50,000 K. Transitions and averaged wavelengths for the multiplet (in Å) are also given. By using c [see Eq. (5) of Ref. 24], we obtain an estimate for the maximum perturber density for which the line may be treated as isolated and tabulated data may be used. The asterisk identifies cases for which the collision volume multiplied by the perturber density (the condition for validity of the impact approximation) lies between 0.1 and 0.5.

PERTURBER DENSITY = 0.1D+16(cm-3)							
PERTURBERS ARE		ELECTRONS		PROTONS		IONIZED HELIUM	
TRANSITION	T(K)	WIDTH(A)	SHIFT(A)	WIDTH(A)	SHIFT(A)	WIDTH(A)	SHIFT(A)
CA II 3D-4P	5000.	0.134E-01	0.818E-03	0.404E-03	-0.758E-04	0.576E-03	-0.741E-04
8581.1 A	10000.	0.105E-01	0.304E-03	0.669E-03	-0.138E-03	0.834E-03	-0.128E-03
C= 0.86E+19	20000.	0.856E-02	0.229E-03	0.928E-03	-0.212E-03	0.101E-02	-0.185E-03
	30000.	0.776E-02	0.881E-04	0.101E-02	-0.258E-03	0.109E-02	-0.222E-03
	50000.	0.707E-02	0.748E-04	0.112E-02	-0.310E-03	0.118E-02	-0.255E-03
CA II 3D-5P	5000.	0.303E-02	-0.382E-03	0.249E-03	-0.936E-04	0.290E-03	-0.808E-04
2132.3 A	10000.	0.241E-02	-0.235E-03	0.312E-03	-0.130E-03	0.332E-03	-0.108E-03
C= 0.17D+18	20000.	0.207E-02	-0.233E-03	0.360E-03	-0.157E-03	0.373E-03	-0.130E-03
	30000.	0.196E-02	-0.185E-03	0.390E-03	-0.175E-03	0.390E-03	-0.144E-03
	50000.	0.189E-02	-0.147E-03	0.410E-03	-0.199E-03	0.402E-03	-0.162E-03
CA II 3D-6P	5000.	0.413E-02	-0.140E-02	0.558E-03	-0.279E-03	0.586E-03	-0.226E-03
1644.1 A	10000.	0.358E-02	-0.106E-02	0.652E-03	-0.339E-03	0.667E-03	-0.279E-03
C= 0.48D+17	20000.	0.333E-02	-0.812E-03	0.732E-03	-0.404E-03	0.723E-03	-0.328E-03
	30000.	0.328E-02	-0.654E-03	0.757E-03	-0.439E-03	0.747E-03	-0.365E-03
	50000.	0.332E-02	-0.556E-03	0.806E-03	-0.481E-03	0.746E-03	-0.375E-03
CA II 3D-7P	5000.	0.721E-02	-0.315E-02	0.120E-02	-0.659E-03	0.121E-02	-0.539E-03
1474.4 A	10000.	0.645E-02	-0.266E-02	0.137E-02	-0.802E-03	0.135E-02	-0.667E-03
C= 0.21D+17	20000.	0.619E-02	-0.202E-02	0.149E-02	-0.935E-03	0.141E-02	-0.753E-03
	30000.	0.631E-02	-0.169E-02	0.161E-02	-0.103E-02	0.143E-02	-0.816E-03
	50000.	0.649E-02	-0.143E-02	0.161E-02	-0.106E-02	0.153E-02	-0.881E-03
CA II 3D-4F	5000.	0.174E-02	0.716E-03	0.133E-03	0.588E-04	0.160E-03	0.505E-04
1839.2 A	10000.	0.137E-02	0.549E-03	0.178E-03	0.824E-04	0.188E-03	0.694E-04
C= 0.16D+18	20000.	0.116E-02	0.429E-03	0.206E-03	0.101E-03	0.213E-03	0.831E-04
	30000.	0.112E-02	0.384E-03	0.223E-03	0.112E-03	0.225E-03	0.920E-04
	50000.	0.109E-02	0.323E-03	0.242E-03	0.127E-03	0.239E-03	0.103E-03
CA II 3D-5F	5000.	0.784E-02	0.225E-02	0.145E-02	0.136E-02	0.124E-02	0.112E-02
1554.1 A	10000.	0.673E-02	0.197E-02	0.181E-02	0.166E-02	0.157E-02	0.131E-02
C= 0.31D+16	20000.	0.591E-02	0.158E-02	0.210E-02	0.192E-02	0.171E-02	0.153E-02
	30000.	0.552E-02	0.137E-02	0.242E-02	0.213E-02	0.190E-02	0.166E-02
	50000.	0.512E-02	0.115E-02	0.238E-02	0.224E-02	0.228E-02	0.173E-02
CA II 3D-6F	5000.	0.170E-01	0.550E-02	*0.409E-02	*0.348E-02	*0.345E-02	*0.282E-02
1433.3 A	10000.	0.154E-01	0.485E-02	*0.466E-02	*0.415E-02	*0.379E-02	*0.323E-02
C= 0.17D+16	20000.	0.139E-01	0.378E-02	*0.551E-02	*0.481E-02	*0.415E-02	*0.384E-02
	30000.	0.131E-01	0.329E-02	*0.625E-02	*0.532E-02	*0.475E-02	*0.412E-02
	50000.	0.122E-01	0.278E-02	0.692E-02	0.618E-02	*0.543E-02	*0.414E-02
CA II 4S-4P	5000.	0.296E-02	-0.526E-03	0.108E-03	-0.372E-04	0.150E-03	-0.355E-04
3946.3 A	10000.	0.228E-02	-0.425E-03	0.174E-03	-0.633E-04	0.214E-03	-0.564E-04
C= 0.18E+19	20000.	0.188E-02	-0.327E-03	0.238E-03	-0.901E-04	0.255E-03	-0.776E-04
	30000.	0.177E-02	-0.278E-03	0.259E-03	-0.106E-03	0.275E-03	-0.871E-04
	50000.	0.171E-02	-0.257E-03	0.287E-03	-0.122E-03	0.301E-03	-0.999E-04

continued opposite

Table 1—*continued*

PERTURBER DENSITY = 0.1D+16(cm-3)							
PERTURBERS ARE		ELECTRONS		PROTONS		IONIZED HELIUM	
TRANSITION	T(K)	WIDTH(A)	SHIFT(A)	WIDTH(A)	SHIFT(A)	WIDTH(A)	SHIFT(A)
CA II 4S-5P	5000.	0.191E-02	-0.175E-03	0.157E-03	-0.582E-04	0.181E-03	-0.504E-04
1650.6 A	10000.	0.151E-02	-0.157E-03	0.195E-03	-0.810E-04	0.207E-03	-0.671E-04
C= 0.10D+18	20000.	0.129E-02	-0.166E-03	0.225E-03	-0.975E-04	0.232E-03	-0.809E-04
	30000.	0.122E-02	-0.144E-03	0.241E-03	-0.108E-03	0.242E-03	-0.900E-04
	50000.	0.118E-02	-0.129E-03	0.255E-03	-0.122E-03	0.253E-03	-0.985E-04
CA II 4S-6P	5000.	0.283E-02	-0.899E-03	0.377E-03	-0.186E-03	0.395E-03	-0.151E-03
1342.1 A	10000.	0.244E-02	-0.644E-03	0.439E-03	-0.227E-03	0.449E-03	-0.186E-03
C= 0.32D+17	20000.	0.226E-02	-0.541E-03	0.494E-03	-0.271E-03	0.486E-03	-0.220E-03
	30000.	0.222E-02	-0.458E-03	0.510E-03	-0.293E-03	0.502E-03	-0.244E-03
	50000.	0.225E-02	-0.398E-03	0.543E-03	-0.322E-03	0.501E-03	-0.251E-03
CA II 4S-7P	5000.	0.505E-02	-0.218E-02	0.833E-03	-0.457E-03	0.841E-03	-0.373E-03
1226.8 A	10000.	0.451E-02	-0.184E-02	0.950E-03	-0.556E-03	0.937E-03	-0.462E-03
C= 0.15D+17	20000.	0.432E-02	-0.142E-02	0.104E-02	-0.648E-03	0.979E-03	-0.522E-03
	30000.	0.440E-02	-0.119E-02	0.112E-02	-0.715E-03	0.998E-03	-0.566E-03
	50000.	0.452E-02	-0.101E-02	0.112E-02	-0.737E-03	0.106E-02	-0.610E-03
CA II 4P-5S	5000.	0.935E-02	0.385E-02	0.216E-03	0.294E-03	0.222E-03	0.255E-03
3727.6 A	10000.	0.671E-02	0.308E-02	0.364E-03	0.410E-03	0.356E-03	0.340E-03
C= 0.12D+19	20000.	0.510E-02	0.246E-02	0.506E-03	0.493E-03	0.456E-03	0.410E-03
	30000.	0.456E-02	0.229E-02	0.585E-03	0.549E-03	0.511E-03	0.455E-03
	50000.	0.421E-02	0.194E-02	0.700E-03	0.620E-03	0.600E-03	0.502E-03
CA II 4P-4D	5000.	0.605E-02	0.275E-02	0.237E-03	0.228E-03	0.273E-03	0.198E-03
3173.5 A	10000.	0.457E-02	0.208E-02	0.370E-03	0.317E-03	0.363E-03	0.260E-03
C= 0.38D+18	20000.	0.368E-02	0.161E-02	0.468E-03	0.383E-03	0.440E-03	0.313E-03
	30000.	0.343E-02	0.143E-02	0.526E-03	0.422E-03	0.490E-03	0.348E-03
	50000.	0.320E-02	0.121E-02	0.594E-03	0.474E-03	0.539E-03	0.390E-03
CA II 4P-5D	5000.	0.588E-02	0.333E-02	0.581E-03	0.417E-03	0.581E-03	0.340E-03
2110.3 A	10000.	0.485E-02	0.272E-02	0.707E-03	0.508E-03	0.678E-03	0.416E-03
C= 0.79D+17	20000.	0.438E-02	0.220E-02	0.833E-03	0.609E-03	0.793E-03	0.503E-03
	30000.	0.423E-02	0.194E-02	0.920E-03	0.665E-03	0.821E-03	0.538E-03
	50000.	0.418E-02	0.164E-02	0.102E-02	0.743E-03	0.935E-03	0.599E-03
CA II 4D-5P	5000.	0.645	-0.251	0.362E-01	-0.263E-01	0.407E-01	-0.229E-01
26778.0 A	10000.	0.504	-0.191	0.484E-01	-0.349E-01	0.485E-01	-0.288E-01
C= 0.27D+20	20000.	0.441	-0.154	0.586E-01	-0.418E-01	0.566E-01	-0.344E-01
	30000.	0.422	-0.132	0.656E-01	-0.467E-01	0.600E-01	-0.376E-01
	50000.	0.411	-0.111	0.709E-01	-0.515E-01	0.650E-01	-0.422E-01
CA II 4D-6P	5000.	0.551E-01	-0.217E-01	0.625E-02	-0.362E-02	0.645E-02	-0.294E-02
5662.9 A	10000.	0.471E-01	-0.174E-01	0.736E-02	-0.440E-02	0.732E-02	-0.360E-02
C= 0.57D+18	20000.	0.437E-01	-0.138E-01	0.857E-02	-0.529E-02	0.819E-02	-0.426E-02
	30000.	0.433E-01	-0.119E-01	0.912E-02	-0.585E-02	0.850E-02	-0.458E-02
	50000.	0.440E-01	-0.101E-01	0.946E-02	-0.626E-02	0.871E-02	-0.502E-02

continued overleaf

Table 1—*continued*

PERTURBER DENSITY = 0.1D+16(cm-3)							
PERTURBERS ARE		ELECTRONS		PROTONS		IONIZED HELIUM	
TRANSITION	T(K)	WIDTH(A)	SHIFT(A)	WIDTH(A)	SHIFT(A)	WIDTH(A)	SHIFT(A)
CA II 4D-7P	5000.	0.572E-01	-0.251E-01	0.882E-02	-0.508E-02	0.886E-02	-0.414E-02
4055.2 A	10000.	0.513E-01	-0.217E-01	0.102E-01	-0.620E-02	0.994E-02	-0.517E-02
C= 0.16D+18	20000.	0.489E-01	-0.169E-01	0.111E-01	-0.720E-02	0.104E-01	-0.580E-02
	30000.	0.498E-01	-0.145E-01	0.120E-01	-0.791E-02	0.105E-01	-0.631E-02
	50000.	0.514E-01	-0.124E-01	0.122E-01	-0.833E-02	0.113E-01	-0.685E-02
CA II 4D-4F	5000.	0.407E-01	-0.134E-02	0.164E-02	-0.576E-03	0.203E-02	-0.532E-03
8923.7 A	10000.	0.350E-01	-0.122E-02	0.233E-02	-0.859E-03	0.257E-02	-0.754E-03
C= 0.30D+19	20000.	0.334E-01	-0.116E-02	0.278E-02	-0.116E-02	0.293E-02	-0.948E-03
	30000.	0.339E-01	-0.131E-02	0.301E-02	-0.129E-02	0.313E-02	-0.106E-02
	50000.	0.352E-01	-0.127E-02	0.330E-02	-0.146E-02	0.331E-02	-0.121E-02
CA II 4D-5F	5000.	0.744E-01	0.158E-01	0.131E-01	0.124E-01	0.111E-01	0.102E-01
4720.6 A	10000.	0.640E-01	0.135E-01	0.165E-01	0.152E-01	0.143E-01	0.120E-01
C= 0.29D+17	20000.	0.566E-01	0.110E-01	0.190E-01	0.175E-01	0.154E-01	0.140E-01
	30000.	0.534E-01	0.958E-02	0.217E-01	0.195E-01	0.171E-01	0.151E-01
	50000.	0.500E-01	0.784E-02	0.219E-01	0.205E-01	0.209E-01	0.159E-01
CA II 4D-6F	5000.	0.118	0.362E-01	*0.279E-01	*0.239E-01	*0.235E-01	*0.194E-01
3758.4 A	10000.	0.107	0.314E-01	*0.319E-01	*0.284E-01	*0.260E-01	*0.222E-01
C= 0.12D+17	20000.	0.969E-01	0.241E-01	*0.376E-01	*0.330E-01	*0.285E-01	*0.263E-01
	30000.	0.916E-01	0.208E-01	*0.428E-01	*0.366E-01	*0.325E-01	*0.284E-01
	50000.	0.855E-01	0.175E-01	0.473E-01	0.425E-01	*0.373E-01	*0.285E-01
CA II 5S-5P	5000.	0.141	-0.544E-01	0.871E-02	-0.499E-02	0.978E-02	-0.435E-02
11878.9 A	10000.	0.107	-0.426E-01	0.111E-01	-0.665E-02	0.113E-01	-0.547E-02
C= 0.53D+19	20000.	0.903E-01	-0.339E-01	0.131E-01	-0.803E-02	0.130E-01	-0.661E-02
	30000.	0.857E-01	-0.296E-01	0.144E-01	-0.892E-02	0.136E-01	-0.716E-02
	50000.	0.834E-01	-0.250E-01	0.152E-01	-0.984E-02	0.144E-01	-0.800E-02
CA II 5S-6P	5000.	0.349E-01	-0.139E-01	0.425E-02	-0.224E-02	0.444E-02	-0.182E-02
4475.8 A	10000.	0.297E-01	-0.115E-01	0.496E-02	-0.273E-02	0.500E-02	-0.224E-02
C= 0.36D+18	20000.	0.274E-01	-0.904E-02	0.573E-02	-0.329E-02	0.551E-02	-0.264E-02
	30000.	0.272E-01	-0.793E-02	0.607E-02	-0.361E-02	0.569E-02	-0.285E-02
	50000.	0.277E-01	-0.675E-02	0.624E-02	-0.391E-02	0.581E-02	-0.309E-02
CA II 5S-7P	5000.	0.405E-01	-0.176E-01	0.645E-02	-0.358E-02	0.654E-02	-0.292E-02
3407.9 A	10000.	0.362E-01	-0.151E-01	0.743E-02	-0.437E-02	0.726E-02	-0.365E-02
C= 0.11D+18	20000.	0.345E-01	-0.121E-01	0.807E-02	-0.508E-02	0.762E-02	-0.408E-02
	30000.	0.352E-01	-0.104E-01	0.866E-02	-0.559E-02	0.769E-02	-0.444E-02
	50000.	0.364E-01	-0.884E-02	0.877E-02	-0.587E-02	0.817E-02	-0.483E-02
CA II 5P-5D	5000.	0.110	0.508E-01	0.848E-02	0.697E-02	0.822E-02	0.565E-02
8235.7 A	10000.	0.897E-01	0.439E-01	0.105E-01	0.848E-02	0.996E-02	0.698E-02
C= 0.12D+19	20000.	0.813E-01	0.377E-01	0.127E-01	0.101E-01	0.115E-01	0.819E-02
	30000.	0.787E-01	0.330E-01	0.140E-01	0.110E-01	0.127E-01	0.914E-02
	50000.	0.779E-01	0.278E-01	0.154E-01	0.120E-01	0.132E-01	0.936E-02

continued opposite

Table 1—*continued*

PERTURBER DENSITY = 0.1D+16(cm-3)							
PERTURBERS ARE		ELECTRONS		PROTONS		IONIZED HELIUM	
TRANSITION	T(K)	WIDTH(A)	SHIFT(A)	WIDTH(A)	SHIFT(A)	WIDTH(A)	SHIFT(A)
CA II 5D-6P	5000.	7.36	-3.46	0.654	-0.498	0.640	-0.412
56116.1 A	10000.	6.31	-2.85	0.808	-0.617	0.750	-0.503
C= 0.56D+20	20000.	5.89	-2.40	0.955	-0.718	0.885	-0.593
	30000.	5.77	-2.15	1.02	-0.799	0.894	-0.627
	50000.	5.87	-1.81	1.14	-0.822	1.02	-0.709
CA II 5D-7P	5000.	0.506	-0.244	0.671E-01	-0.443E-01	0.664E-01	-0.362E-01
11385.3 A	10000.	0.457	-0.208	0.794E-01	-0.541E-01	0.737E-01	-0.437E-01
C= 0.13D+19	20000.	0.442	-0.176	0.906E-01	-0.633E-01	0.804E-01	-0.507E-01
	30000.	0.449	-0.153	0.974E-01	-0.691E-01	0.895E-01	-0.574E-01
	50000.	0.465	-0.130	0.102	-0.749E-01	0.859E-01	-0.592E-01
CA II 5D-5F	5000.	1.30	0.735E-01	0.198	0.191	0.163	0.154
18843.3 A	10000.	1.12	0.809E-01	0.248	0.229	0.213	0.189
C= 0.46D+18	20000.	1.02	0.646E-01	0.287	0.265	0.232	0.208
	30000.	0.983	0.552E-01	0.315	0.300	0.264	0.234
	50000.	0.942	0.436E-01	0.341	0.313	0.314	0.249
CA II 5D-6F	5000.	0.748	0.186	*0.167	*0.146	*0.141	*0.118
9319.1 A	10000.	0.679	0.158	*0.196	*0.173	*0.160	*0.134
C= 0.71D+17	20000.	0.622	0.121	*0.230	*0.202	*0.174	*0.160
	30000.	0.593	0.105	*0.261	*0.225	*0.192	*0.172
	50000.	0.559	0.863E-01	0.282	0.258	*0.227	*0.175

obtained decreases when broadening by ion interactions becomes important. At high densities, the results are no longer linear with density due to Debye screening. This effect is more important for the shift than for the width. Stark-broadening parameter tables for high densities will be published elsewhere.[26]

Since the carrier gas was argon in most experiments and since the impact approximation may often be used for $3d$-$4p$ and $4s$-$4p$ Ca II multiplets with Ar^+-impact broadening of the Ca II

Table 2. As in Table 1 but for Ar^+-impact-broadening parameters for Ca II lines at an Ar^+ density of $10^{17}\,cm^{-3}$.

PERTURBER DENSITY = 0.1D+18(cm-3)
PERTURBER IS IONIZED ARGON

TRANSITION	T(K)	WIDTH(A)	SHIFT(A)
CA II 3D-4P	5000.	0.744E-01	-0.586E-02
8581.1 A	10000.	0.971E-01	-0.103E-01
C= 0.86E+21	20000.	0.111	-0.151E-01
	30000.	0.119	-0.170E-01
	50000.	0.125	-0.199E-01
CA II 4S-4P	5000.	0.190E-01	-0.263E-02
3946.3 A	10000.	0.241E-01	-0.425E-02
C= 0.18E+21	20000.	0.277E-01	-0.593E-02
	30000.	0.295E-01	-0.666E-02
	50000.	0.311E-01	-0.780E-02

Table 3. Comparison between the experimental Stark full half-halfwidths of Ca II lines (Wm) with different calculations. Semi-classical calculations: WDSB—present results; WJBG—Jones, Benett, and Griem (1971);[18,19] WHC—Hildum and Cooper (1971);[13] quantum-mechanical calculations: WQ—Barnes (1971)[16] and Barnes and Peach (1970);[17] N = electron density.

Transition	λ(A)	T(K)	N/10+17(cm-3)	Wm(A)	Wm/WDSB	Wm/WJBG	Wm/WHC	Wm/WQM	Ref.
3d-4p	8542.09	13000	1.08	0.95	0.91	0.64		1.10	4
	8662.14	13000	1.08	0.95	0.91	0.64		1.10	4
4s-4p	3933.66	11400	0.40	0.039	0.45	0.33	0.41	0.42	6
		11600	0.64	0.079	0.57	0.43	0.52	0.54	6
		12240	0.80	0.0914	0.53	0.41	0.49	0.51	7
		13000	1.08	0.235	1.04	0.78	0.95	0.99	4
		13350	1.32	0.180	0.65	0.50	0.60	0.63	7
		16000	1.00	0.16	0.81	0.62	0.75	0.78	8
		17500	10.0	10.0	5.15	3.95	4.81	5.05	9
		19000	1.00	0.172	0.91	0.69	0.51	0.45	10
		25100	1.00	0.22	1.22	0.92	1.15	1.25	11
		28000	1.00	0.25	1.40	1.07	1.32	1.44	8
		29200	1.00	0.18	1.01	0.78	0.95	1.05	11
		30000	2.35	0.24	0.58	0.47	0.53	0.63	9
	3968.47	7450	1.00	0.210	0.82	0.67	----	----	5
		12240	0.80	0.0846	0.49	0.38	0.46	0.47	7
		13000	1.08	0.235	1.04	0.78	0.95	0.99	4
		13350	1.32	0.161	0.59	0.44	0.54	0.56	7
		16000	1.00	0.16	0.81	0.62	0.75	0.78	8
		17500	10.0	10.3	5.31	4.07	4.95	5.20	9
		18560	1.00	0.188	0.98	0.75	0.93	1.04	13
		25100	1.00	0.20	1.11	0.84	1.04	1.14	11
		28000	1.00	0.25	1.40	1.07	1.32	44	8
4p-5s	3736.20	7500	10.0	18.2	2.37	2.98			9
		10000	1.00	0.69	1.03	1.00			14
		13000	1.12	0.79	1.21	0.94			4
		25100	1.00	0.30	0.63	0.53			11
	3706.03	10000	1.00	0.70	1.04	1.01			14
		13000	1.12	0.79	1.21	0.94			4
		17500	10.0	13.7	2.68	2.24			9
4p-4d	3179.33	13000	1.13	0.66	1.40	1.03			4
	3158.87	13000	1.13	0.66	1.40	1.03			4
		25100	1.00	0.32	0.90	0.74			11
		29200	1.00	0.30	0.87	0.71			11
	3181.28	13000	1.13	0.66	1.40	1.03			4

Table 4. As in Table 3 but for the shift (d).

Transition	λ(A)	T(K)	N/10+17(cm-3)	dm(A)	dm/dDSB	dm/dJBG	dm/dQM	Ref.
4s-4p	3933.66	11400	0.40	-0.0046	0.30	0.09	0.11	6
		11600	0.64	-0.0155	0.64	0.19	0.24	6
		13000	1.08	-0.048	1.18	0.38	0.45	4
		14200	1.00	-0.09	2.49	0.71	0.94	15
		16000	1.00	-0.01	0.29	0.09	0.11	8
		25100	1.00	-0.06	2.11	0.60	0.72	11
		28000	1.00	-0.04	1.40	0.35	0.48	8
		29200	1.00	-0.05	1.79	0.52	0.60	11
	3968.47	13000	1.08	-0.048	1.18	0.38	0.45	4
		14200	1.00	-0.09	2.49	0.71	0.94	15
		16000	1.00	-0.01	0.29	0.09	0.11	8
		25100	1.00	-0.06	2.11	0.60	0.72	11
		28000	1.00	-0.04	1.40	0.35	0.48	8
		29200	1.00	-0.06	2.15	0.62	0.72	11
4p-5s	3736.20	7500	10.0	4.16	1.33	1.13		9
		10000	1.00	0.186	0.61	0.51		14
		13000	1.12	0.390	1.22	1.03		4
		14200	1.00	0.18	0.64	0.53		15
		25100	1.00	0.16	0.66	0.53		11
	3706.03	10000	1.00	0.238	0.79	0.65		14
		13000	1.12	0.390	1.22	1.03		4
		14200	1.00	0.17	0.60	0.50		15
		17500	10.0	3.3	1.30	1.03		9
		25100	1.00	0.17	0.71	0.57		11
4p-4d	3179.33	13000	1.13	0.295	1.40	1.05		4
	3158.87	13000	1.13	0.295	1.40	1.05		4
		14200	1.00	0.18	1.00	0.73		15
		25100	1.00	0.15	1.00	0.70		11
		29200	1.00	0.15	1.05	0.72		11
	3181.28	13000	1.13	0.295	1.40	1.05		4

multiplets (see Refs. 1,2 and the discussion in Ref. 27), the corresponding Stark-broadening parameters are provided in Table 2. In Tables 3 and 4, the present results are compared with experimental data[4–15] and with other semiclassical[13,18,19] and quantum mechanical strong coupling calculations.[16,17] For the Ca II $4s$-$4p$ and $4p$-$5s$ multiplets, semiempirical calculations also exist.[28] We see that the widths fall within the error bars of both methods. However, for the shifts, larger disagreements exist. It should be noted that the shifts are of lesser accuracy for semiclassical calculations than are the widths.[29–31] Additional reliable experimental data for the shifts would be very helpful from the theoretical point of view. This is also the case for the $4s$-$4p$ Ca II widths, for which new experimental data, especially at lower temperatures, will be of great interest.

Acknowledgements—One of us (M.D.) has been supported by the Observatory of Paris-Meudon. This work has also been supported by the French C.N.R.S. and is a part of French–Yugoslav collaboration through the project "L'élargissement Stark des raies spéctrales des plasmas astrophysiques et de laboratoire". It is also a part of the project "Physics and Dynamics of Celestial Bodies" supported by RFN of Serbia.

REFERENCES

1. S. Sahal-Bréchot, *Astron. Astrophys.* **1,** 91 (1969).
2. S. Sahal-Bréchot, *Astron. Astrophys.* **2,** 322 (1969).
3. M. S. Dimitrijević, S. Sahal-Bréchot, and V. Bommier, *Astron. Astrophys. Suppl. Series* **89,** 581 (1991).
4. C. Fleurier, S. Sahal-Bréchot, and J. Chapelle, *JQSRT* **17,** 595 (1977).
5. J. F. Baur and J. Cooper, *JQSRT* **17,** 311 (1977).
6. M. Yamamoto, *Phys. Rev.* **146,** 137 (1966).
7. C. Goldbach, G. Nollez, P. Plomdeur, and J. P. Zimmermann, *Phys. Rev.* **28,** 234 (1983).
8. D. E. Roberts and A. J. Barnard, *JQSRT* **12,** 1205 (1972).
9. H. J. Kusch and H. P. Pritschow, *Astron. Astrophys.* **4,** 31 (1970).
10. W. W. Jones, A. Sanchez, J. R. Grieg, and H. R. Griem, *Phys. Rev. A* **5,** 2318 (1972).
11. D. Hadžiomerspahić, M. Platiša, N. Konjević, and M. Popović, *Z. Phys.* **262,** 169 (1973).
12. J. R. Roberts and K. L. Eckerle, *Phys. Rev.* **159,** 104 (1967).
13. J. S. Hildum and J. Cooper, *Phys. Lett. A* **36,** 153 (1971).
14. R. Hühn and H. J. Kusch, *Astron. Astrophys.* **28,** 159 (1973).
15. J. Purić and N. Konjević, *Z. Phys.* **249,** 440 (1972).
16. K. S. Barnes, *J. Phys. B* **4,** 1377 (1971).
17. K. S. Barnes and G. Peach, *J. Phys. B* **3,** 350 (1970).
18. W. W. Jones, S. M. Benett, and H. R. Griem, "Calculated Stark Broadenining Parameters for Isolated Spectral Lines from the Atom Helium through Calcium and Cesium", Univ. Maryland, Tech. Rep. No 71-097, College Park, MD (1971).
19. H. R. Griem, *Spectral Line Broadening by Plasmas*, Academic Press, New York, NY (1974).
20. S. Bashkin and J. J. Stoner Jr., *Atomic Energy Levels and Grotrian Diagrams*, Vol. 1, North Holland, Amsterdam (1975).
21. D. R. Bates and A. Damgaard, *Trans. R. Soc. London, Ser. A* **242,** 101 (1949).
22. G. K. Oertel and L. P. Shomo, *Astrophys. J. Suppl. Series*, **16,** 175 (1968).
23. H. Van Regemorter, Hoang Binh Dy, and M. Prud'homme, *J. Phys. B* **12,** 1073 (1979).
24. M. S. Dimitrijević and S. Sahal-Bréchot, *JQSRT* **31,** 301 (1984).
25. S. Sahal-Bréchot, *Astron. Astrophys.* **245,** 322 (1991).
26. M. S. Dimitrijević and S. Sahal-Bréchot, *Bull. Obs. Astron. Belgrade* **145,** 83 (1992).
27. A. Mazure and G. Nollez, *Z. Naturf.* **339,** 15 (1978).
28. M. S. Dimitrijević and N. Konjević, *Astron. Astrophys.* **102,** 93 (1981).
29. H. R. Griem and C. S. Shen, *Phys. Rev.* **125,** 196 (1962).
30. D. E. Roberts, *J. Phys. B* **1,** 53 (1968).
31. M. S. Dimitrijević, N. Feautrier, and S. Sahal-Bréchot, *J. Phys. B* **14,** 2559 (1981).

J. Quant. Spectrosc. Radiat. Transfer Vol. 50, No. 2, pp. 227–232, 1993
Printed in Great Britain.

0022-4073/93 $6.00 + 0.00

CONTINUOUS EMISSION FROM A LOW-TEMPERATURE HELIUM PLASMA DUE TO RADIATIVE CHARGE EXCHANGE AND RADIATIVE ION–ATOM RECOMBINATION

A. A. MIHAJLOV,†‡ A. M. ERMOLAEV,§¶ and M. S. DIMITRIEVIC‡

†Institute of Physics, P.O. Box 57, 11001 Belgrade, Yugoslavia, ‡Astronomical Observatory, Volgina 7, 11050 Belgrade, Yugoslavia, and §Department of Physics, University of Durham, Science Laboratories Site, South Road, Durham DH1 3LE, U.K.

(Received 23 July 1992; received for publication 20 April 1993)

Abstract—Radiative recombination and radiative charge exchange in symmetrical $He^+ + He$ collisions are considered using a semiclassical adiabatic model of collisions in low-temperature plasmas. The reaction channels are assumed to be uncoupled and the corresponding total and partial spectral coefficients for the spontaneous continuous electromagnetic emission are calculated for helium-plasma temperatures below 3×10^4 K. The results are compared with the similar spectral densities for electron–ion and electron–atom scattering. It is found that in a wide range of physical conditions radiative processes involving ion–atom collisions should be taken into account in the analysis of the continuum radiation from helium plasmas.

INTRODUCTION

The influence of ion–atom radiative collisional processes on the opacity of partially ionized gas plasmas is usually ignored assuming that its contribution is negligible. In the present paper we shall obtain an estimate of this contribution using a semiclassical adiabatic model of collision for the case where partially ionized helium plasma is at relatively low temperatures. This type of plasma is realized in laboratory conditions as well as in stellar atmospheres of some stars. It will be shown that within a certain range of physical conditions the ion–atom radiative collisions may contribute significantly to the continuous radiation from gaseous plasmas.

ION–ATOM RADIATIVE PROCESSES

We shall consider the processes of photoassociation and photodissociation,

$$He^+(1s) + He(1s^2) \leftrightarrow \epsilon_\lambda + He_2^+ \tag{1a}$$

as well as radiative charge exchange

$$He^+(1s) + He(1s^2) \rightarrow \begin{cases} \epsilon_\lambda + He^+ + He \\ \epsilon_\lambda + He + He^+ \end{cases} \tag{1b}$$

In these reactions, $\epsilon_\lambda = 2\pi\hbar c/\lambda$ denotes the energy of a photon with the wavelength λ and the molecular helium ion He_2^+ is assumed to be in the electronic ground state Σ_u^+. We shall consider the contribution of processes (1a) and (1b) to the optical continuum (infrared, visible and near ultraviolet) in the range $400 \leqslant \lambda \leqslant 800$ nm. The present discussion will be limited by considering spontaneous emission for plasma temperatures T not exceeding 3×10^4 K.

We introduce partial spectral densities of the continuum electromagnetic radiation emitted from a unit volume of the plasma into a solid angle of 4π, $I^{(a)}(\lambda, T)$ and $I^{(b)}(\lambda, T)$ for reactions (1a) and (1b), and the corresponding total spectral density $I^{(ab)}(\lambda, T)$. We shall also introduce the spectral densities per unit atomic and ionic concentrations, $S^{(a)}(\lambda, T)$, $S^{(b)}(\lambda, T)$, and $S^{(ab)}(\lambda, T)$. Then

$$I^{(ab)} = I^{(a)} + I^{(b)},$$

¶To whom all correspondence should be addressed.

where

$$I^{(a,b)} = S^{(a,b)} N_{He} N_{He^+},$$
$$S^{(ab)} = S^{(a)} + S^{(b)}. \tag{2}$$

N_{He} and N_{He^+} are the atomic and ionic concentrations in question. Partial spectral coefficients $S^{(a)}$ and $S^{(b)}$ will be used in the form:

$$S^{(a,b)}(\lambda, T) = S^{(ab)}(\lambda, T) X^{(a,b)}(\lambda, T) \tag{3}$$
$$X^{(a)}(\lambda, T) + X^{(b)}(\lambda, T) = 1. \tag{4}$$

The total spectral coefficient $S^{(ab)}(\lambda, T)$ has been given earlier in an analytical form in Ref. 1 and coefficients $X^{(a,b)}(\lambda, T)$ in Ref. 2. Functions $X^{(a)}$ and $X^{(b)}$ give the yield of channels (1a) and (1b) to the total spontaneous emission of electromagnetic radiation due to the $He + He^+$ collisions. These quantities have also been defined explicitly in Ref. 2.

The method used for calculating spectral coefficients, $S^{(a)}$, $S^{(b)}$ and $S^{(ab)}$, does not take into account the influence of the ambient medium on the $He + He^+$ collision. Consequently, the reported results are applicable only to weakly non-ideal plasmas where the absolute value of the mean potential energy of ion–atom interaction is much less than the mean kinetic energy of atomic particles. We treat here the weakly-ionized helium plasmas of ionization degree 10^{-3} or less. Therefore the condition of weak nonideality is satisfied within a wide range of the helium densities (for $T \approx 10^4$ K, the densities up to 10^{19} cm^{-3} can be treated by the present theory).

THE RADIATIVE PROCESSES USED FOR COMPARISON

In the course of the present work we shall be able to investigate the relative importance of the radiative process (1a, b) comparing with other processes occurring in the plasma, chiefly those involving electron scattering on helium atoms and ions, that is

$$\bar{e} + He^+ \rightarrow \begin{cases} \epsilon_\lambda + He^* \\ \epsilon_\lambda + \bar{e}' + He^+ \end{cases} \tag{5}$$

and

$$\bar{e} + He \rightarrow \epsilon_\lambda + \bar{e}' + He^* \tag{6}$$

where $\bar{e}$ and $\bar{e}'$ denote the scattered electron in the initial and final (free) states and He* is the helium atom in the final (bound) state. Equation (5) corresponds to free–bound and free–free electron transitions in electronic collisions with He^+. Equation (6) corresponds to free–free electron transitions in electronic collisions with He, with the subsequent excitation of the target atom. These reactions are generally known to be an important source of continuum radiation emitted from plasmas. We shall see that Eq. (6), in particular, may give significant contribution if helium plasma has a low degree of ionization as in the present case.

For the emission reaction in Eq. (5), i.e. for electron–ion bremsstrahlung and electron–ion photorecombination, the corresponding total spectral density $I^{(ei)}(\lambda, T) = S^{(ei)}(\lambda, T) N_e N_{He^+}$, where $S^{(ei)}$ is total spectral coefficient and N_e is the free–electron density. The ratio $F^{ab}_{ei}(\lambda, T)$,

$$F^{ab}_{ei}(\lambda, T) = I^{(ab)}(\lambda, T)/I^{(ei)}(\lambda, T) = S^{(ab)}(\lambda, T)(N_{He}/N_e) S^{(ei)}(\lambda, T) \tag{7}$$

gives the relative magnitude of the ion–atom and electron–ion contributions to electromagnetic emission from the plasma.

Similarly, we shall also consider the emission channel in Eq. (6). The corresponding spectral density is $I^{(ea)} = S^{(ea)} N_{He} N_e$ where $S^{(ae)}$ is the spectral coefficient for electron–atom bremsstrahlung, and the ratio F^{ab}_{ea} is:

$$F^{ab}_{ea}(\lambda, T) = I^{(ab)}(\lambda, T)/I^{(ea)}(\lambda, T) = S^{(ab)}(\lambda, T)(N_{He^+}/N_e)/S^{(ea)}(\lambda, T). \tag{8}$$

The ratio (8) gives the contribution of radiative ion–atom collisions relative to the electron–atom bremsstrahlung.

For the LTE conditions prevailing in the plasmas under discussion, the ratio (8) can be replaced by the ratio $\kappa^{(ab)}/\kappa^{(ea)}$, where $\kappa^{(ab)}$ is the absorption coefficient for reactions (1a, b) calculated in

Ref. 3 and $\kappa^{(ea)}$ is the absorption coefficient due to electron–atom collisions, both coefficients being functions of the plasma temperature T and wavelength λ.

BASIC RELATIONS

In the regime of *termal* velocities v for the relative motion of He and He^+, it is sufficient to take into account only two electronic states of the molecular ion He_2^+ that is the ground state Σ_g^+ and the first excited state Σ_u^+ adiabatically correlated at large separations R with the electronic state of the $He^+ + He$ system. Their adiabatic energies $U_1(R)$ and $U_2(R)$ have been taken from Ref. 4. The zero energy is chosen in such a way that $U_{1,2}(R) \to 0$ as $R \to \infty$. We shall also introduce quantities $E(R)$ and R_λ, where the term splitting is

$$E(R) = U_2(R) - U_1(R). \tag{9}$$

The resonant separation R_λ is defined as a root of the transcendental equation:

$$E(R) = \epsilon_\lambda \tag{10}$$

and has been tabulated for the molecular ion He_2^+ in Ref. 3.

The spectral coefficient of spontaneous emission $S^{(ab)}(\lambda, T)$ may be expressed as follows:[1]

$$S^{(ab)}(\lambda, T) = 4.777 \times 10^{-34} \frac{(R_\lambda/a_0)^4}{(R_\lambda)} (\epsilon_\lambda/2\ \mathrm{Ry})^5 \exp[-U_2(R_\lambda)/kT] \tag{11}$$

where a_0 is the Bohr radius and $\gamma(R_\lambda)$ will be defined below. Equation (11) is obtained on the assumption that the electron-dipole matrix element between the Σ_u^+ and Σ_g^+ states of the He_2^+ molecular ion is taken to be $eR_\lambda/2$ for $R > R_\lambda$. This approximation is known to be accurate for such compact systems as H(1s) and He_2^+ if $R_\lambda > 2a_0$.[5] For the molecular ion He_2^+, this condition is satisfied even to a better extent so that we use in the present calculations the same approximation to the dipole moment.

The quantity γ in Eq. (9) is defined as

$$\gamma(R_\lambda) = |d \log[\epsilon(R)/2\ \mathrm{Ry}]/d(R/a_0)|_{R=R_\lambda} \tag{12}$$

According to Ref. 2, Eq. (12) may be approximated sufficiently accurately by putting $\gamma \approx \gamma_{He}(1 - O(\delta/\gamma_{He}R))$; $\gamma_{He}^2/2 = I_{He}(\mathrm{a.u.})$; $\delta = (2/\gamma_{He}) - 1$; where I_{He} is the ionization potential of the ground state of the helium atom. For $R_\lambda > R_{min}$ where R_{min} corresponds to the position of the minimum of the molecular potential $U_1(R)$, $\gamma \approx \gamma_{He} = 1.345$.

With the numerical coefficients given in Eq. (11), the spectral coefficient $S^{(ab)}$ is expressed in units of [J cm^3 sec^{-1} nm^{-1}].

The relative contribution of radiative channels (1a) and (1b) to the EM emission as well as to the absorption, may be expressed via the yield parameters $X^{(a)}$ and $X^{(b)}$ related to each other by Eq. (4). Therefore it is sufficient to determine only one of these parameters. For this purpose, we use $X^{(b)}(\lambda, T)$ related to radiative charge exchange.[2] In the latter case

$$X^{(b)}(Z) = 1 - \Phi(\sqrt{Z}) + (2/\sqrt{2})\sqrt{Z} \exp(-Z), \tag{13}$$

$$Z = |U_1(R_\lambda)|/kT \tag{14}$$

where Φ is the error function tabulated for instance in Ref. 6.

RESULTS AND DISCUSSION

The computed total and partial spectral coefficients for the EM emission due to ion–atom recombination and radiative charge exchange in the helium plasma are presented in Tables 1 and 2. In Table 2 we give numerical values of the total spectral coefficient $S^{(ab)}$ for the sum of the direct reactions (1a) and (1b) for $4000 \leqslant T \leqslant 30{,}000$ K and for a selected set of wavelengths in the interval between 365 and 820 nm. The yield function $X^{(b)}$ is presented in Table 2 in the same range of T and λ. Table 2 shows that the contribution from radiative capture (1b) increases as T and λ increase, within the ranges considered.

Figure 1 presents the ratio F_{ei}^{ab}, Eq. (7), at four selected wavelengths. The ratio was obtained for $N_{He}/N_e = 5 \times 10^3$ and within the same range of T. The spectral coefficient $S^{(ab)}$ is calculated using

Table 1. Total spectral coefficient $S^{(ab)}(\lambda, T)$ [in 10^{-36} J cm^3 sec^{-1} nm^{-1}] as a function of plasma temperature T and the wavelength λ of continuous EM emission.

λ \ T	4000	6000	8000	10,000	15,000	20,000	25,000	30,000
4000	0.308 (−2)	0.186 (−1)	0.456 (−1)	0.782 (−1)	0.160 (+0)	0.230 (+0)	0.285 (+0)	0.329 (+0)
5000	0.377 (−2)	0.149 (−1)	0.295 (−1)	0.445 (−1)	0.769 (−1)	0.101 (+0)	0.119 (+0)	0.133 (+0)
6000	0.390 (−2)	0.115 (−1)	0.199 (−1)	0.276 (−1)	0.426 (−1)	0.529 (−1)	0.603 (−1)	0.657 (−1)
7000	0.379 (−2)	0.925 (−2)	0.144 (−1)	0.189 (−1)	0.269 (−1)	0.322 (−1)	0.358 (−1)	0.385 (−1)
8000	0.351 (−2)	0.746 (−2)	0.109 (−1)	0.136 (−1)	0.184 (−1)	0.214 (−1)	0.235 (−1)	0.249 (−1)

Table 2. Relative contribution of radiative charge exchange, reaction (1b), that is $X^{(b)}(\lambda, T) = S^{(b)}(\lambda, T)/S^{(ab)}(\lambda, T)$ as a function of plasma temperature T and the wavelength λ of continuous EM emission.

λ \ T	4000	6000	8000	10,000	15,000	20,000	25,000	30,000
4000	0.066	0.187	0.308	0.411	0.589	0.696	0.765	0.811
5000	0.103	0.249	0.378	0.481	0.649	0.745	0.804	0.844
6000	0.141	0.303	0.435	0.535	0.692	0.779	0.832	0.866
7000	0.177	0.350	0.482	0.579	0.726	0.805	0.852	0.883
8000	0.215	0.395	0.525	0.618	0.755	0.827	0.870	0.897

Eqs. (11) and (12), with the corresponding values of R_λ taken from Ref. 3. The spectral coefficient $S^{(ei)}$ has been determined in Kramer's approximation (see, for instance, momographs[7,8]). The value of N_{He}/N_e used in the present calculations is typical for low-temperature gas plasmas in the temperature range $\approx 10^4$ K. For laboratory plasmas, such values of this ratio are also typical for non-equilibrium plasmas where the electronic temperature is $\approx 10^4$ K and the atomic temperature is significantly lower.[9] Figure 1 shows that the reactions (1a) and (1b) dominate the electron–ion source of continuous EM radiation in a wide range of plasma conditions. Apart from laboratory plasmas, similar conditions take place also in some astrophysical plasmas, chiefly in the helium enriched DB white dwarfs where hydrogen had been partially or completely burnt up in the course of the star evolution.[10] The models of the atmospheres of such stars had been described by Koester[11] who suggested the existence of layers of the helium plasma in these stars with the temperatures and densities corresponding to the conditions studied in the present work.

The processes (1a, b) may compete not only with the electron–ion reactions (5) but also with the electron–atom reaction (6). A crude estimate of the ratio $F_{ea}^{ab} = I^{(ab)}/I^{(ea)}$ for scattering on He may be obtained from[12] where the spectral coefficient of continuous emission had been expressed in terms of the effective transport cross sections at collisional energy $E \to 0$. The estimate is good only

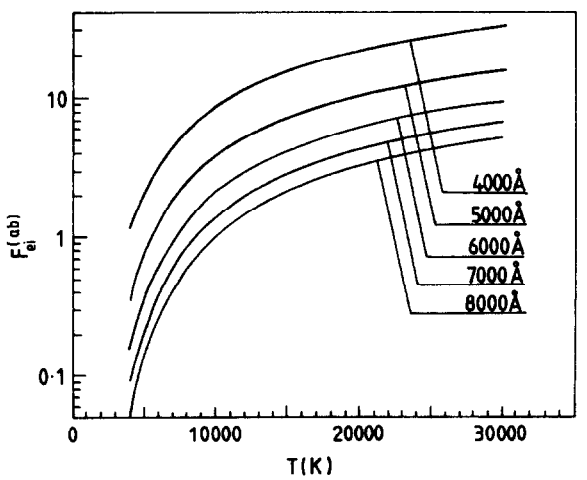

Fig. 1. The ratio F_{ei}^{ab} of the total spectral density $I^{(ab)}(\lambda, T)$ due to ion–atom collisions, to the spectral density $I^{(ei)}(\lambda, T)$ due to electron–ion scattering in helium plasma [see Eq. (7)], as a function of temperature T and wavelength λ. $N_{He}/N_e = 5 \times 10^3$.

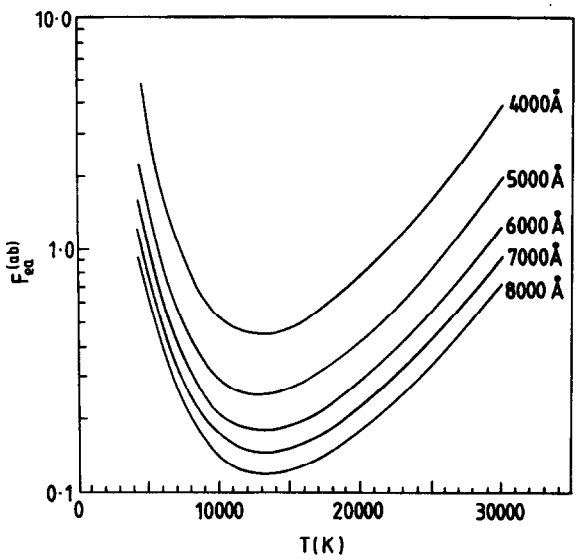

Fig. 2. The ratio F_{ca}^{ab} of the total spectral density $I^{(ab)}(\lambda, T)$ due to ion–atom collisions, to the radiation spectral density $I^{(ca)}(\lambda, T)$ due to electron–atom scattering in helium plasma [see Eq. (8)], as a function of temperature T and wavelength λ.

if the cross sections are a slow-varying function of E. This however is not the case for e + He collisions, and for the absorption channel in Eq. (6) we have used the quantal results of Bell et al.[13] F_{ca}^{ab} computed using data from Refs. 3 and 13 are presented in Fig. 2 for selected wavelengths in the interval between 400 and 800 nm, and for $N_{He^+}/N_e = 1$. Figure 2 shows that the contribution of ion–atom processes (1a, b) is more important than that of (6) for all temperatures in the range if $\lambda \leqslant 500$ nm. For longer wavelengths, $500 \leqslant \lambda \leqslant 800$ nm, this is true only if $T \leqslant 10{,}000$ K or $T \geqslant 20{,}000$ K. Nevertheless, even in the region of the minimum of F_{ca}^{ab} the ion–atom radiative scattering should not be entirely neglected. For low-temperature helium plasmas, the contribution from (1a) and (1b) should, in fact, be always taken into account in the analysis of the continuous radiation in the optical range of the spectrum.

CONCLUSIONS

In a wide range of physical conditions, the character of spontaneous electromagnetic emission from helium low-temperature plasmas is practically fully determined by the ion–atom processes (1a) and (1b) considered together with the electron–ion and electron–atom processes (5) and (6). This result is similar to that established earlier for hydrogen plasmas. We note however that due to the absence of stable negative ions He^- the total picture of the processes in helium-like atmospheres looks simpler than that in hydrogen-rich atmospheres. In the latter case, there is an additional important role played by stable negative ions H^- (see, for instance Ref. 14). It has been shown in the present work that for low ionization of the helium plasma, the role of the ion–atom collisions as a source of continuous emission, is much more prominent than it had been suggested earlier, for instance, in the original work.[12] This is particularly true for the cases such as Ref. 9 where conditions of the helium plasma are close to those of the LTE. We expect that the theory developed here will find applications in diagnostics of laboratory plasmas and in the analysis of radiation from helium-rich stars such, for instance, as the DB white dwarfs.

Acknowledgements—This work was supported in part by a SERC grant and by a travel grant from the British Council in Belgrade. We thank Mr Lj. Ignjatovic for his help in compiling the numerical material.

REFERENCES

1. A. A. Mihajlov and M. M. Popovic, *Phys. Rev.* **A23**, 1679 (1981).
2. A. A. Mihajlov and M. S. Dimitrijevic, *Astron. Astrophys.* **155**, 319 (1986).
3. A. A. Mihajlov and M. S. Dimitrievic, *Astron. Astrophys.* **256**, 305 (1992).
4. B. K. Gupta and F. A. Matsen, *J. Chem. Phys.* **47**, 4860 (1967).

5. D. Ramaker and J. Peek, *J. Phys. B* **5,** 2175 (1972).
6. M. Abramovitz and I. Stegun, *Handbook of Mathematical Functions*, p. 295, Dover, New York, NY (1972).
7. D. H. Menzel, *Selected Papers on Physical Processes in Ionized Plasmas*, Dover, New York, NY (1973).
8. I. I. Sobelman, *Introduction to the Theory of Atomic Spectra*, Pergamon, New York, NY (1973).
9. V. Y. Aleksandrov, D. B. Gurevich, and I. V. Podmeshenskii, *Opt. Spectrosc.* **26,** 18 (1969).
10. D. Mihalas, *Stellar Atmospheres*, Chap. 4.4, Freeman, San Francisco, CA (1978).
11. D. Koester, *Astron. Astrophys. Suppl. Ser.* **39,** 401 (1980).
12. O. B. Firsov and M. I. Chibisov, *ZhETF* **39,** 1770 (1967).
13. K. L. Bell, K. A. Berrington, and J. P. Croskery, *J. Phys. B* **15,** 977 (1982).
14. H. S. W. Massey, *Negative Ions*, 3rd edn., Chap. 15, Cambridge Univ. Press (1976).

Pergamon

PII: S0022-4073(98)00002-8

J. Quant. Spectrosc. Radiat. Transfer Vol. 61, No. 3, pp. 361–375, 1999

Printed in Great Britain
0022–4073/98 $19.00 + 0.00

STARK BROADENING PARAMETERS OF ANALOGOUS SPECTRAL LINES ALONG THE LITHIUM AND BERYLLIUM ISOELECTRONIC SEQUENCES

B. BLAGOJEVIĆ,*† M. V. POPOVIĆ,* N. KONJEVIĆ* and M. S. DIMITRIJEVIĆ‡

*Institute of Physics, 11081 Belgrade, P.O. Box 68, Yugoslavia and ‡Astronomical Observatory, 11050 Belgrade, Volgina 7, Yugoslavia

(Received 30 October 1997)

Abstract—We report the results of theoretical and experimental study of the Stark broadening and shifting of analogous spectral lines along the lithium ($3s^2S$–$3p^2P^\circ$) and beryllium ($3s^3S$–$3p^3P^\circ$) isoelectronic sequences. For the evaluation of Stark broadening parameters the impact semiclassical method is used. The Stark widths and shifts along both sequences are measured in the plasma of a low-pressure pulsed arc. Plasma electron densities were determined from the width of the He II P_α line while electron temperatures were measured from the relative line intensities. Both experiments agree within estimated uncertainties with our semiclassical results. Although the overall agreement between theory and experiments is found, gradual change of the discrepancy for the widths along the sequence is detected. The comparison of experimental Stark shifts with the theories shows that the magnitude and direction of line shifts along the Li-sequence may not always be predicted by theory. The comparison of experimental Stark widths along the Be-sequence for B II, C III, N IV and O V with semiclassical theory shows a similar tendency. The discrepancy with theory is large for the B II and it is improved for higher members of the sequence. The only measured Stark shifts for N IV and O V are of a different sign (red for N IV and blue for O V), and this change of sign along the sequence cannot be explained by the theory.

1. INTRODUCTION

The study of plasma broadening and shifting of analogous spectral lines along isoelectronic sequences offer good opportunity for testing theory under the conditions of gradual change of energy levels structure of the emitter with gradual increase of ionic charge. These studies also enable determination of the Stark width and/or shift dependence upon spectroscopic charge number Z (Z is equal to 2 for singly charged ions) of the emitter. This is also of importance for the estimation of broadening parameters of ions with no available data. The greatest difficulty in this type of study is the necessity to compare the results measured at different electron temperatures. Namely, experimental data for low charge ions usually determined at relatively low temperatures have to be compared with the results for higher charge ions measured at much higher temperatures. Since Stark broadening parameters depend upon both, electron density N_e (linear dependence; here we exclude from discussion many particle effects beyond Debye approximation) and electron temperature T_e, one has to perform temperature scaling whenever comparison of results measured at different T_e is performed. Since width $w(T_e)$ and shift $d(T_e)$ dependencies are not yet firmly established one has to be cautious and try to determine these dependencies. Experimentally, this is a very difficult task well illustrated by the fact that we are still lacking good tests of theories in a wider temperature range. Thus, for the comparisons along isoelectronic sequences theoretical predictions of $w(T_e)$ and $d(T_e)$ are usually used and therefore the theory employed for temperature scaling should be clearly stated.

According to the first systematic studies of experimental Stark widths[1] and later shifts[2] both quantities gradually decrease with an increase of Z along the isoelectronic sequence. This

†To whom all correspondence should be addressed.

conclusion[1,2] is drawn on the basis of a relatively small number of experimental data. Since then, several systematic experimental studies along Li and B sequence are published.[3–6] all of them indicating some difficulties in comparison between some theoretical approaches and experiment.

Studies of the largest number of ions are performed along Li- isoelectronic sequence for $3s^2S$–$3p^2P^\circ$ transitions of C IV, N V, O VI, F VII and Ne VIII.[3] For Be II, B III, C IV, N V, O VI, F VII, Ne VIII, Na IX, Al XI and Si XII theoretical results within semiclassical perturbation approach exists as well (see Refs. 7–9 and references therein). Moreover, close coupling results exist for 42 transitions for Be II, B III, C IV, O VI and Ne VII.[10] Besides the comparisons with the semiclassical perturbation and quantum mechanical results the experimental results are compared with simplified semiclassical formula (SSC), Eq. 526 in Ref. 11, modified semiempirical formula (MSE)[12] and electron impact broadening method with the semiclassical Gaunt factor approximation (Hey private communication in Ref. 3). All three simplified theoretical calculations gave systematically smaller values. Furthermore, none of them could explain the deviation from linear scaling of experimental widths which appeared for Ne VIII Stark widths. These experimental results further initiated theoretical studies, see e.g. Ref. 13 and references therein. Although the agreement with experiment is considerably improved[13] the discrepancy for Ne VIII Stark width still remains.

In another systematic study experimental Stark widths of $3s^2S$–$3p^2P^\circ$, $3p^2P^\circ$–$3d^2D$ and $2s2p3s^4P^\circ$–$2s2p3p^4D$ transitions of N III, O IV, F V and Ne VI along B-sequence were reported.[4] For comparison, the theoretical results of SSC[11], MSE[12] and classical-path approximation (CPA) [14] are used. Again none of the theoretical results fully predicted the trend of Stark widths along the B-isoelectronic sequence; the discrepancy of experimental widths (always larger than the theoretical predictions) increases with the spectroscopic charge number Z. The results of SSC[11] agree best with experiment. An attempt is made to explain the increased width of the Ne VI $2s2p3s^4P^\circ$–$2s2p3p^4D$ transition at high temperatures by the contribution of proton collisions.

Two recent papers[5,6] report the experimental and theoretical study of the same $3s$–$3p$ and $3p$–$3d$ doublet transitions of N III, O IV and F V along the B-sequence. In addition, Stark shifts of N III and O IV are also studied. For evaluation of Stark broadening parameters the semiclassical perturbation formalism is used (for details see theoretical part of this paper).

This paper represents a continuation of systematic theoretical and experimental studies of analogous transitions within isoelectronic sequences. Along the Li-sequence, Stark widths and shifts for $3s^2S$–$3p^2P^\circ$ transition of C IV, N V and O VI are remeasured at different electron temperatures and widths are compared with Ref. 3. The results along this sequence are extended here to B III. For the Be-isoelectronic sequence, Stark widths and shifts of $3s^3S$–$3p^3P^\circ$ transition of B II, C III, N IV and O V are measured. To test the theory, Stark broadening parameters for both sequences are calculated using semiclassical perturbation formalism. For comparison with the experiment results evaluated from SSC[11] and MSE[12] are also used.

2. THEORY

By using the semiclassical-perturbation formalism[15,16] we have investigated Stark broadening parameters for Li-like B III, C IV, N V and O VI $3s^2S$–$3p^2P^\circ$ multiplet. We note here that the Z scaling within this isoelectronic sequence was investigated theoretically recently in Ref. 17 and references therein, and the corresponding Stark widths were evaluated. Here, we have calculated Stark broadening parameters for Be-like B II, C III, N IV and O V $3s^3S$–$3p^3P^\circ$ multiplet. Besides electron-impact line widths and shifts, Stark broadening parameters due to all relevant ion perturbers were calculated as well. Electron-, proton-, and ionized helium-impact full widths-at-half-maximum (FWHM) and shifts have been published previously for Li-like B III,[18,19] C IV,[20,21], N V[22] and O VI[23] and they will not be repeated here. The data for electron-, proton-, and He III - impact broadening parameters for Be-like O V were also published.[24] So electron-, proton-, He II-, and He III-impact parameters have been calculated for all emitters whenever they are not available in the literature. Therefore, the corresponding data for B II when the perturbers are Cl II–Cl IV and B II–B V, for B III when the perturbers are Cl II–Cl IV and B II–B V, for C III and C IV when the perturbers are C II–C VI, for N IV when the perturbers are N II–N VI, for N V when the perturbers are N II–N VII, for O V when the perturbers are O III–O VII, and for O VI when the perturbers are

Table 1. Stark broadening parameters (full-widths-at-half-maximum and shifts) for $3s^3S$–$3p^3P^\circ$ Be-like B II, C III, N IV and O V multiplets for a perturber density of 10^{17} cm^{-3} and temperatures from 20 000 up to 300 000 K. Transitions and averaged wavelengths (in Å) for the multiplet are also given. If one divides the C value with the Stark width value, one obtains an estimate for the maximum perturber density (in cm^{-3}) for which the line can be treated as isolated and tabulated data may be used. The asterisk identifies cases for which the collision volume multiplied by the perturber density (the condition for validity of the impact approximation) lies between 0.1 and 0.5

Perturber density = 10^{17} cm^{-3} Transition	T(K)	Width (Å)	Shift(Å)	Width (Å)	Shift (Å)
Perturbers are:			Electrons	He III	
B II 3s–3p	20 000	1.32	−0.113	0.223	0.432 [−01]
7033.0 Å	50 000	1.17	−0.934 [−01]	0.260	0.643 [−01]
$C = 0.33E + 21$	100 000	1.10	−0.714 [−01]	0.289	0.773 [−01]
	150 000	1.05	−0.569 [−01]	0.296	0.862 [−01]
	200 000	1.02	−0.570 [−01]	0.302	0.923 [−01]
	300 000	0.957	−0.548 [−01]	0.311	0.983 [−01]
			Electrons	He III	
C III 3s–3p	20 000	0.524	−0.117 [−01]	0.243 [−01]	−0.437 [−03]
4650.1 Å	50 000	0.369	−0.747 [−02]	0.414 [−01]	−0.114 [−02]
$C = 0.22E + 21$	100 000	0.298	−0.129 [−01]	0.496 [−01]	−0.197 [−02]
	150 000	0.266	−0.108 [−01]	0.534 [−01]	−0.251 [−02]
	200 000	0.247	−0.108 [−01]	0.560 [−01]	−0.287 [−02]
	300 000	0.222	−0.103 [−01]	0.594 [−01]	−0.346 [−02]
			Electrons	He III	
N IV 3s–3p	20 000	0.236	−0.172 [−02]	0.332 [−02]	−0.577 [−03]
3481.8 Å	50 000	0.155	−0.306 [−02]	0.849 [−02]	−0.154 [−02]
$C = 0.17E + 21$	100 000	0.117	−0.310 [−02]	0.127 [−01]	−0.268 [−02]
	150 000	0.101	−0.421 [−02]	0.152 [−01]	−0.338 [−02]
	200 000	0.916 [−01]	−0.375 [−02]	0.162 [−01]	−0.389 [−02]
	300 000	0.807 [−01]	−0.360 [−02]	0.176 [−01]	−0.465 [−02]

O IV–O VIII are calculated. The formalism used here, was updated several times[20,25,26] and its summary is presented in Refs. 20 and 26.

Energy levels needed for calculations were taken from Ref. 27; for O V and from Ref. 28 for all other emitters. Electron-impact and proton-impact broadening data for Be-like isoelectronic sequence are shown in Table 1 for the perturber density 10^{17} cm^{-3} and temperatures $T = 20\,000$–$300\,000$ K or B II, C III and N IV, and $T = 50\,000$–$300\,000$ K for O V. We also specify a parameter C[20] which, when divided by the corresponding electron-impact full-width-at-half-maximum, gives an estimate for the maximum perturber density for which the line may be treated as isolated.

The resonance contribution to the electron-impact width may be added in two ways.[25] The increase of the collision strength at the excitation energy threshold due to resonances, may be calculated by using the semiclassical limit of Gailitis formula.[29] Then in the first method, this increase of the collision strength at the threshold is kept constant below the threshold. Such extrapolation is good when the emitter has numerous doubly excited states below the considered threshold, with the energy greater than the ionization energy of the lower ionization stage, like for multiply charged ions or highly excited states. In the second method, it is assumed that the corresponding increase at the threshold, of the cross-section and not of the collision strength is constant below the threshold. Such extrapolation is more accurate where there are few resonances and gives a smaller value of the electron-impact width. The analysis in Ref. 25 shows that for low-lying transitions of Mg II, Ca II, Sr II and Ba II, the agreement with experimental values is better if we take the second method, i.e. to keep constant below threshold, the corresponding increase of the cross-section. Moreover, this analysis shows that the difference between values obtained without the resonance correction, and values obtained with the resonance correction according to the second method is only a few percent. Consequently, in Table 1, electron-impact widths without the resonance correction are presented as well.

In order to test the influence of the differences in oscillator strength values, the oscillator strengths from the TOP base (the complete package of the opacity project (OP) data with the database management system is usually referred to as TOP base[30–31]) have been taken for the Be-like isoelectronic sequence, where the expected differences are larger than for the Li-like isoelectronic

sequence. These oscillator strengths were calculated in Ref. 32. In order to study the influence of the transitions with different parent terms, calculations with and without the inclusion of such transitions are performed. Such transitions are $2s3s^3S$–$2p3s^3P^\circ$ for B II, $2s3s^3S$–$2p3s^3P^\circ$, $2s3s^3S$–$2p3d^3P^\circ$, $2s3p^3P^\circ$–$2p3p^3D^\circ$, $2s3p^3P^\circ$–$2p3p^3S^\circ$, $2s3p^3P^\circ$–$2p3p^3P^\circ$ for C III, and $2s3s^3S$–$2p3s^3P^\circ$, $2s3s^3S$–$2p3d^3P^\circ$, $2s3p^3P^\circ$–$2p3p^3D^\circ$, $2s3p^3P^\circ$–$2p3p^3S^\circ$, $2s3p^3P^\circ$–$2p3p^3P^\circ$ for N IV. The differences between widths calculated with the TOP base oscillator strengths and with those calculated within the Coulomb approximation are small, while for shifts the differences are larger. The other relevant calculated data for impact widths and shifts may be obtained from the authors upon request.

3. EXPERIMENT

The experimental apparatus and procedure are described in Ref. 5, so minimum details will be given here.

The discharge was driven by a 15.2 μF low inductance capacitor charged between 3.0 and 3.8 kV and switched by ignitron. The stepper motor and the oscilloscope are controlled by a personal computer which was also used for data acquisition. Recordings of spectral line shapes were performed shot by shot. At each wavelength position of the monochromator time evolution and the decay of plasma radiation were recorded by the oscilloscope. Eight such signals were averaged at each wavelength. To construct the line profiles the averaged signals at different wavelengths and at various times of the plasma existence were used. All line profiles were recorded with 15 μm entrance and exit slits of the monochromator. With these slits, the measured instrumental half widths were 0.168 or 0.086 Å when operating the monochromator in the first or second order of the diffraction grating, respectively, and the instrumental line shape was very close to Gaussian. To determine the Stark width from the measured profiles, the standard deconvolution procedure[33] was used. For the line-shift measurements we used line profiles at different times of the plasma existence.[34]

Special care was taken to avoid possible self-absorption of studied spectral lines (see e.g. Ref. 35) so the investigated gases are diluted by helium until the ratio of line intensities within a multiplet are within a few percent from LS coupling theoretical predictions (see e.g. Refs. 36 and 37). In this way, the total gas pressure, p, the ratio in the gas mixtures and the capacitor voltage, V_c, are determined as follows:

B II and B III lines: $p = 3$ Torr, 96% He + 4% BCl_3, $V_c = 3.0$ kV, C III and C IV lines: $p = 3$ Torr, 95.2% He + 4.8% C_2H_2, $V_c = 3.0$ kV, N IV and N V lines: $p = 3$ Torr, 98% He + 2% N_2, $V_c = 3.0$ kV, and for O V and O VI lines: $p = 1.4$ Torr, 99.4% He + 0.6% O_2, $V_c = 3.8$ kV.

For electron density measurements the width of the He II P_α 4686 Å line was used.[38] Our main concern in electron density measurements is a possible presence of self-absorption of the 4686 Å line which may distort the line profile.[5–6] In order to determine the optical thickness of the 4686 Å line, an additional movable electrode has been introduced in the discharge[39] and self-absorbtion correction is performed in accordance with Ref. 40.

The axial electron temperatures for the He–O_2 mixture were determined from the Boltzman plot of the O IV 3063.43, 3071.60, 3403.60 and 3411.76 Å line intensities. For the He–N_2 mixture, axial electron temperatures were determined from the Boltzman plot of the N III 4097.33, 4103.43, 4634.16, and 4640.64 Å line intesities. Since it was not possible to detect suitable spectral lines for T_e measurements in the He–C_2H_2 and He–BCl_3 mixtures, the axial electron temperature are taken as for the He–N_2 mixture. This may be justified by (a) the same discharge conditions and (b) the main gas in the discharge for all three is almost pure helium with a small admixture of the investigated gas ($< 5\%$).

The spectral response of a photomultiplier-monochromator system was calibrated against a standard coiled-coil quartz iodine lamp.

4. RESULTS AND DISCUSSION

4.1. Li-isoelectronic sequence

The experimental results for Stark widths (FWHM) and shifts are given in Tables 2 and 3, respectively. These results are presented together with plasma parameters and estimated errors for

Table 2. Experimental Stark widths w_m (FWHM) of investigated Li-like B III, C IV, N V and O VI lines from the $3s^2S$–$3p^2P^\circ$ multiplets are compared in this table with theoretical widths: w^e_{DSB}, semiclassical electron impact; w^{ei}_{DSB}, electron + ion impact; w_G, simplified semiclassical approach after Griem,, Eq.(526) of Ref. 11; w_{DK}, modified semiempirical formula after Dimitrijević and Konjević[12]; w_S, quantum mechanical calculation after Seaton[10]

Ion	Transition	λ (Å)	N_e (10^{17} cm^{-3})	T_e(K)	w_m(Å)	w_m/w^e_{DSB}	w_m/w^{ei}_{DSB}	w_m/w_G	w_m/w_{DK}	w_m/w_S
B III	$3s^2S_{1/2}$–$3p^2P^\circ_{3/2}$	7835.25	0.28 ± 17%	65 000 ± 15%	0.334 ± 7%	0.82	0.74	0.65	0.95	1.15
			0.58 ± 17%	72 400 ± 15%	0.602 ± 7%	0.74	0.67	0.58	0.84	1.03
	$3s^2S_{1/2}$–$3p^2P^\circ_{1/2}$	7841.41	0.28 ± 17%	65 000 ± 15%	0.311 ± 7%	0.76	0.69	0.60	0.88	1.07
			0.58 ± 17%	72 400 ± 15%	0.626 ± 7%	0.76	0.70	0.60	0.87	1.07
C IV	$3s^2S_{1/2}$–$3p^2P^\circ_{3/2}$	5801.33	0.58 ± 15%	72 400 ± 15%	0.244 ± 7%	0.84	0.80	0.80	1.06	1.22
			0.76 ± 15%	78 300 ± 15%	0.313 ± 7%	0.84	0.80	0.80	1.05	1.23
			0.80 ± 15%	80 100 ± 15%	0.329 ± 7%	0.85	0.81	0.80	1.06	1.24
	$3s^2S_{1/2}$–$3p^2P^\circ_{1/2}$	5811.98	0.58 ± 15%	72 400 ± 15%	0.229 ± 7%	0.79	0.75	0.75	0.99	1.14
			0.76 ± 15%	78 300 ± 15%	0.304 ± 7%	0.82	0.78	0.77	1.02	1.19
N V	$3s^2S_{1/2}$–$3p^2P^\circ_{3/2}$	4603.73	0.86 ± 15%	72 400 ± 15%	0.186 ± 7%	0.90	0.84	1.05	1.32	
			0.99 ± 15%	78 300 ± 15%	0.210 ± 7%	0.91	0.84	1.05	1.32	
			1.13 ± 15%	80 100 ± 15%	0.234 ± 6%	0.90	0.82	1.03	1.30	
			1.21 ± 15%	80 700 ± 15%	0.243 ± 6%	0.88	0.80	1.00	1.26	
			1.33 ± 15%	82300 ± 15%	0.282 ± 6%	0.94	0.86	1.06	1.34	
	$3s^2S_{1/2}$–$3p^2P^\circ_{1/2}$	4619.98	0.86 ± 15%	72 400 ± 15%	0.186 ± 7%	0.90	0.84	1.05	1.32	
			0.99 ± 15%	78 300 ± 15%	0.204 ± 7%	0.89	0.82	1.02	1.29	
			1.13 ± 15%	80 100 ± 15%	0.231 ± 6%	0.89	0.81	1.02	1.28	
			1.21 ± 15%	80 700 ± 15%	0.249 ± 6%	0.90	0.82	1.03	1.29	
			1.33 ± 15%	82 300 ± 15%	0.282 ± 6%	0.94	0.86	1.06	1.34	
O VI	$3s^2S_{1/2}$–$3p^2P^\circ_{3/2}$	3811.35	1.09 ± 15%	65 500 ± 24%	0.136 ± 7%	1.00	0.96	1.25	1.53	†
			1.38 ± 15%	61 900 ± 21%	0.178 ± 6%	1.01	0.97	1.27	1.55	†
			1.42 ± 15%	79 700 ± 20%	0.171 ± 6%	1.05	1.02	1.28	1.56	†
	$3s^2S_{1/2}$–$3p^2P^\circ_{1/2}$	3834.24	1.09 ± 15%	65 500 ± 24%	0.132 ± 7%	0.97	0.94	1.21	1.48	†
			1.38 ± 15%	61 900 ± 21%	0.176 ± 6%	1.00	0.96	1.26	1.53	†
			1.42 ± 15%	79 700 ± 20%	0.178 ± 6%	1.09	1.05	1.33	1.64	†

†The theoretical calculations are given for a higher temperature range (T_e(K) > 125 000 K)

Table 3. Experimental Stark shifts Δd_m of investigated Li-like B III, C IV, N V and O VI lines from the $3s^2S$–$3p^2P^\circ$ multiplets, determined as a wavelength shift between two line profiles, compared with corresponding theoretical shifts: Δd^e_{DSB}, electron impact; Δd^{ei}_{DSB}, electron + ion impact; Δd^e_{DKr}, modified semiempirical formula after Dimitrijević and Kršljanin[41]

Ion	Transition	λ(Å)	$N_{e1}(10^{17}\,\mathrm{cm}^{-3})$	T_{e1}(K)	$N_{e2}(10^{17}\,\mathrm{cm}^{-3})$	T_{e2}(K)	Δd_m (Å)	$\Delta d_m/\Delta d^e_{DSB}$	$\Delta d_m/\Delta d^{ei}_{DSB}$	$\Delta d_m/\Delta d_{DKr}$
B III	$3s^2S_{1/2}$–$3p^2P^\circ_{3/2}$	7835.25	0.28	65 000	0.58	72 400	−0.03	1.77	a	0.175
	$3s^2S_{1/2}$–$3p^2P^\circ_{1/2}$	7841.41	0.28	65 000	0.58	72 400	−0.03	1.77	a	0.175
C IV	$3s^2S_{1/2}$–$3p^2P^\circ_{3/2}$	5801.33	0.58	72 400	0.80	80 100	0.03	a	a	a
	$3s^2S_{1/2}$–$3p^2P^\circ_{1/2}$	5811.98	0.58	72 400	0.80	80 100	0.03	a	a	a
N V	$3s^2S_{1/2}$–$3p^2P^\circ_{3/2}$	4603.73	0.86	72 400	1.21	80 700	0.04	a	a	a
	$3s^2S_{1/2}$–$3p^2P^\circ_{1/2}$	4619.98	0.86	72 400	1.21	80 700	0.03	a	a	a
O VI	$3s^2S_{1/2}$–$3p^2P^\circ_{3/2}$	3811.35	1.09	65 500	1.42	79 700	−0.03	52.8	64.0	2.78
	$3s^2S_{1/2}$–$3p^2P^\circ_{1/2}$	3834.24	1.09	65 500	1.42	79 700	−0.03	52.8	64.0	2.78

[a] The theory predicts opposite sign of shift

various measured quantities. Since shift measurements require the knowledge of plasma parameters at two different times of plasma existence (see Sec. 3), in Table 3 for the shifts two values of electron densities and temperature are given. Both Tables 2 and 3 also contain spectroscopic data and wavelengths of investigated lines as well as the comparison with the theoretical results (see Sec. 2): w_{DSB} and d^{e}_{DSB} are electron impact widths and shifts, respectively, w^{ei}_{DSB} and d^{ei}_{DSB} are electron + ion impact widths and shifts and w_G and w_{DK} are SSC and MSE half-widths calculated after Refs. 11 and 12, respectively, and d_{DKr} are shifts calculated after Ref. 41. In order to evaluate the contribution of ion impact widths and shifts it was necessary to compute plasma composition data for the plasma conditions of the width and shift measurements (electron density and temperature). Here to simplify calculations we assumed LTE for our plasma conditions ($N_e > 10^{17}$ cm^{-3}) and the plasma composition data were evaluated as described for plasmas in LTE conditions.[42] The assumption of the LTE conditions is very crude but its use may be justified by the fact that (a) the expected contribution of all ions in the plasma to the linewidth or shift may not exceed 7% of the electron width, see Tables 2 and 3, and (b) the difference in the contribution of various ions to the linewidths and shifts is so small (see Table 1) that differences in the computed concentrations of various ions is of negligible importance for the final result.

To facilitate comparison between various experiments and theories all available results for Stark widths studied along Li-sequence are given in graphical form in Figs. 1–4.

Figure 1 shows B III experimental results which are in very good agreement with fully quantum mechanical calculation[10] and MSE formula[12] but they are systematically below newly calculated semiclassical results (see Table 2). The inclusion of ion broadening increases the discrepancy with experiment. The SSC results (after Ref. 11) are systematically larger than the experimental result but they are still in agreement within the estimated uncertainty ($\pm$ 50%) of the theory.[11]

With the exception of the experimental result[43] there is a good mutual agreement between experimental data for C IV;[3,44–46] see Fig. 2. All theoretical results agree within 30% and they are in good agreement with the experiments.

If one takes into account $w(T_e)$ dependence, our experimental results for N V are in good agreement with Glenzer et al[3]; see Fig. 3. The result of Purić et al[47] is lower and agrees well with MSE formula[12]. Our experiment and Ref. 3 agree with both the semiclassical results calculated here (see Table 1) and the SSC[11].

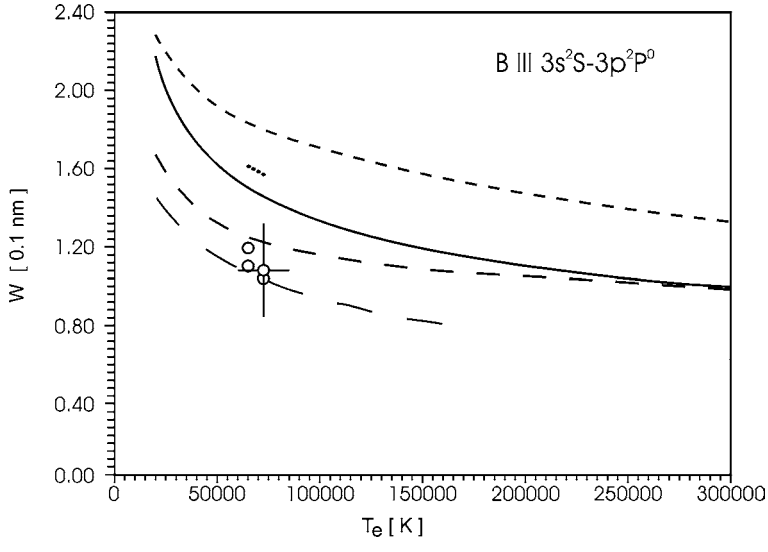

Fig. 1. Full Stark widths (normalized to an electron density of 10^{17} cm^{-3}) for the B III $3s^2S$–$3p^2P^\circ$ multiplet vs electron temperature. Theory: —, semiclassical, electron impact widths (see Table 1.); (· · · ·) semiclassical, electron + ion impact widths (see Table 1) evaluated only for the experimental conditions of this experiment; (- - -) simplified semiclassical approximation (after Griem, Eq. (526) of Ref. 11.) and; (– – –) modified semiempirical formula (after Dimitrijević and Konjević[12]); (— — — —) close coupling calculation (after Seaton[10]). Experiment: ○, this work.

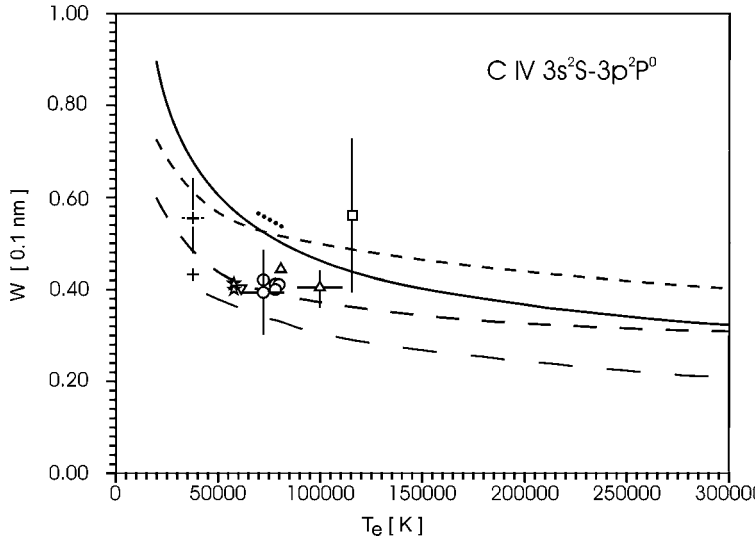

Fig. 2. Same as in Fig. 1 but for the C IV $3s^2S$–$3p^2P^\circ$ multiplet. Experiment: (○), this work; (△), Glenzer et al[3]; (▽), Bogen[44]; ★, El Farra et al[45]; (+), Djeniže et al[46]; (□), Ackermann et al.[43]

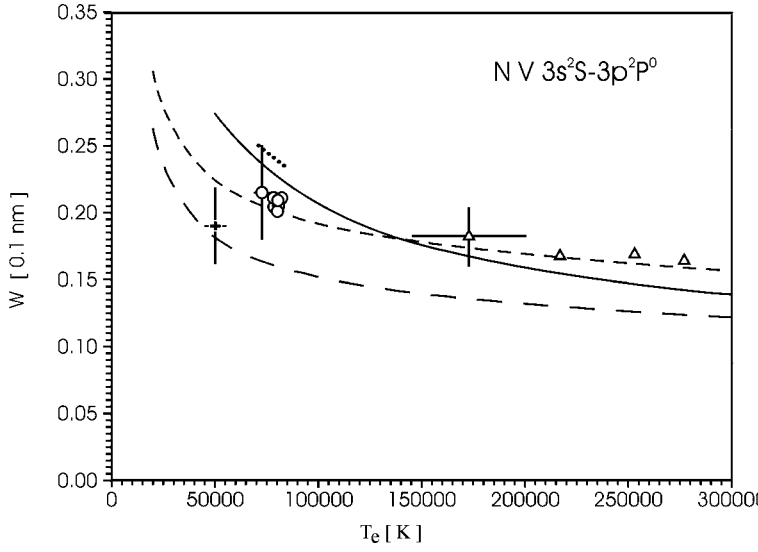

Fig. 3. Same as in Fig. 1 but for the N V $3s^2S$–$3p^2P^\circ$ multiplet. Experiment: (○), this work; (△), Glenzer et al[3]; (+), Purić et al.[47]

Our O VI experimental data, see Fig. 4, are again in good agreement with Ref. 3 and both experiments agree best with our semiclassical results. The SSC theory[11] is closer to the experiments, while quantum mechanical results[10] are significantly below the experimental data of Glenzer et al.[3]

Unfortunately, technical limitations of our plasma source did not allow us to study F VII and Ne VIII lines, so in Fig. 5, within the comparison of all experimental data along Li-isoelectronic sequence, our contribution for these ions is missing. In this figure all experimental results are normalized to the electron temperature of 7.5 eV using electron impact $w(T_e)$ dependence from Table 1. From the comparison between theories and experiments in Fig. 5 one can draw the following conclusions: (i) discrepancy with all sets of theoretical results gradually changes, (ii) with the exception of the highest and lowest Z (Ne VIII and B III), results from Table 1 agree best with experiments and (iii) the inclusion of ion broadening does not influence the agreement between theory and experiment to a large extent. The results of fully quantum mechanical calculations[10] for Li-like ions (B III, C IV and O VI) are in good agreement with B III while for the other two ions they

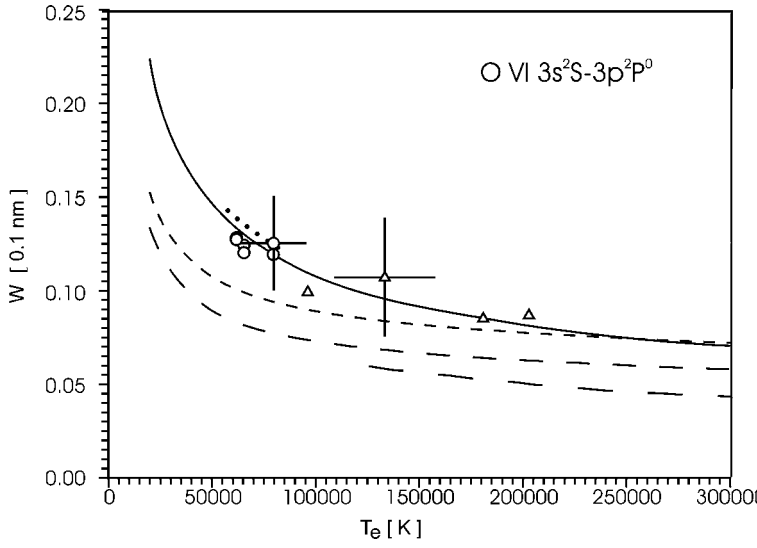

Fig. 4. Same as in Fig. 1 but for the O VI $3s^2S$–$3p^2P^\circ$ multiplet. Experiment: (○), this work; (△), Glenzer et al.[3]

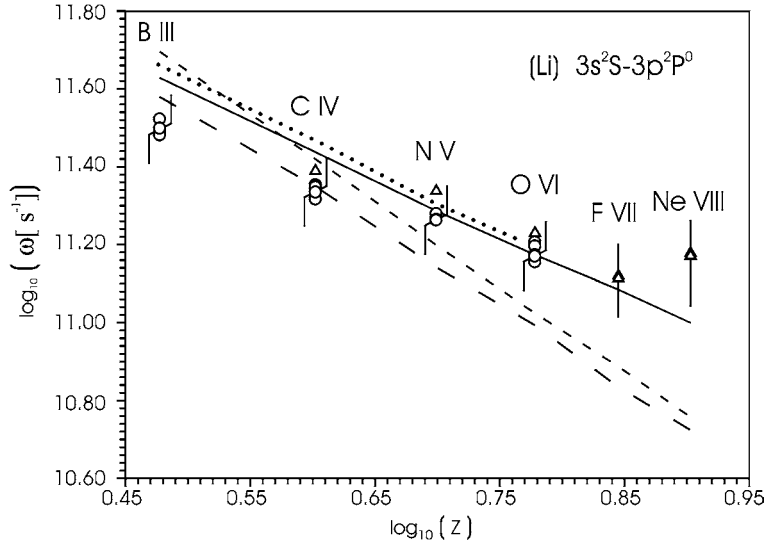

Fig. 5. Stark widths of the Li-like spectral lines (in angular frequency units) as a function of log Z. Experimental data are scaled according to the temperature dependence obtained with a semiclassical perturbation approach to a value of the electron density of 10^{17} cm^{-3} and to a value of the electron temperature 87000 K (7.5 eV); theoretical data are calculated for these values. Error flags are calculated uncertainties including the error in the determination of the full-width at half-maximum and of the electron density measurements. Theory: (——), semiclassical, electron impact widths (see Table 1.); (· · · ·), semiclassical, electron + ion impact widths (see Table 1.) evaluated only for the experimental conditions of this experiment; (- - -), simplified semiclassical approximation (after Griem, Eq.(526) of Ref. 11.); and (– – –) modified semiempirical formula (after Dimitrijević and Konjević[12]). Experiment: (○), this work; (△), Glenzer et al.[3]

are systematicaly lower (see Figs. 1, 2 and 4). Unfortunately, data for other ions are missing so one cannot draw a more comprehensive conclusion. It seems however that for both semiclassical and quantum mechanical calculations some other effects related to the spectroscopic charge number Z of ions are more important for further improvement of the theory.

Table 3 shows a comparison between the experimental and theoretical Stark shifts. The results of another experiment[46] which is in very good agreement with our data are also given in Fig. 6. None of the theoretical calculations was successful in predicting $d(Z)$ dependence along the Li-isoelectronic

Table 4. Same as in Table 2 but for $3s^3S$–$3p^3P^\circ$ Be-like B II, C III, N IV and O V multiplets. Theoretical widths w^e_{DSB} are calculated from the data in Table 1

Ion	Transition	λ(Å)	$N_e(10^{17}$ cm$^{-3})$	T_e(K)	w_m(Å)	w_m/w^e_{DSB}	w_m/w^{ei}_{DSB}	w_m/w_G	w_m/w_{DK}
B II	$3s^3S_1$–$3p^3P^\circ_2$	7030.20	0.21 ± 17%	65 000 ± 15%	0.149 ± 5%	0.63	0.56		1.18
	$3s^3S_1$–$3p^3P^\circ_1$	7031.90	0.21 ± 17%	65 000 ± 15%	0.149 ± 5%	0.63	0.56		1.18
	$3s^3S_1$–$3p^3P^\circ_0$	7032.54	0.21 ± 17%	65 000 ± 15%	0.149 ± 5%	0.63	0.56		1.18
C III	$3s^3S_1$–$3p^3P^\circ_2$	4647.42	0.28 ± 15%	65 000 ± 15%	0.083 ± 7%	0.90	0.87	0.75	1.20
			0.58 ± 15%	72 400 ± 15%	0.161 ± 6%	0.88	0.85	0.72	1.15
			0.76 ± 15%	78 300 ± 15%	0.219 ± 5%	0.93	0.90	0.76	1.22
	$3s^3S_1$–$3p^3P^\circ_1$	4650.25	0.28 ± 15%	65 000 ± 15%	0.083 ± 7%	0.90	0.87	0.75	1.20
			0.58 ± 15%	72 400 ± 15%	0.170 ± 6%	0.93	0.90	0.76	1.22
			0.63 ± 15%	78 300 ± 15%	0.219 ± 5%	0.93	0.90	0.76	1.22
	$3s^3S_1$–$3p^3P^\circ_0$	4651.47	0.28 ± 15%	65 000 ± 15%	0.083 ± 7%	0.90	0.87	0.75	1.20
			0.76 ± 15%	72 400 ± 15%	0.163 ± 6%	0.89	0.86	0.73	1.17
N IV	$3s^3S_1$–$3p^3P^\circ_2$	3478.71	0.86 ± 15%	72 400 ± 5%	0.122 ± 5%	1.12	1.04	1.10	1.57
			0.99 ± 15%	78 300 ± 5%	0.136 ± 5%	1.11	1.03	1.09	1.56
			1.13 ± 15%	80 100 ± 5%	0.148 ± 5%	1.07	1.00	1.04	1.49
			1.21 ± 15%	80 700 ± 5%	0.153 ± 5%	1.03	0.96	1.01	1.44
			1.33 ± 15%	82 300 ± 5%	0.172 ± 5%	1.06	0.99	1.04	1.48
	$3s^3S_1$–$3p^3P^\circ_1$	3482.99	0.86 ± 15%	72 400 ± 5%	0.122 ± 5%	1.12	1.04	1.10	1.57
			0.99 ± 15%	78 300 ± 5%	0.136 ± 5%	1.11	1.03	1.09	1.56
			1.13 ± 15%	80 100 ± 5%	0.150 ± 5%	1.08	1.01	1.06	1.51
			1.21 ± 15%	80 700 ± 5%	0.150 ± 5%	1.01	0.94	0.99	1.41
			1.33 ± 15%	82 300 ± 5%	0.174 ± 5%	1.08	1.00	1.05	1.50
	$3s^3S_1$–$3p^3P^\circ_0$	3484.96	0.86 ± 15%	72 400 ± 5%	0.122 ± 5%	1.12	1.04	1.10	1.57
			0.99 ± 15%	78 300 ± 5%	0.146 ± 5%	1.19	1.11	1.17	1.67
			1.13 ± 15%	80 100 ± 1%	0.146 ± 5%	1.05	0.98	1.03	1.47

O V	$3s^3S_1$–$3p^3P_1^\circ$	2786.99	$0.95 \pm 15\%$	$54\,600 \pm 27\%$	$0.077 \pm 7\%$	1.12	1.07	1.35	1.71
			$1.09 \pm 15\%$	$65\,500 \pm 24\%$	$0.073 \pm 7\%$	1.03	0.98	1.18	1.52
			$1.38 \pm 15\%$	$61\,900 \pm 21\%$	$0.102 \pm 7\%$	1.10	1.05	1.28	1.64
			$1.41 \pm 15\%$	$79\,700 \pm 20\%$	$0.100 \pm 7\%$	1.18	1.13	1.32	1.74
			$1.57 \pm 15\%$	$88\,700 \pm 19\%$	$0.105 \pm 7\%$	1.15	1.10	1.29	1.71
			$1.68 \pm 15\%$	$91\,600 \pm 18\%$	$0.102 \pm 7\%$	1.05	1.00	1.18	1.57
			$1.54 \pm 15\%$	$93\,300 \pm 18\%$	$0.105 \pm 7\%$	1.18	1.13	1.33	1.78
	$3s^3S_1$–$3p^3P_0^\circ$	2789.85	$1.38 \pm 15\%$	$61\,900 \pm 21\%$	$0.098 \pm 7\%$	1.06	1.01	1.23	1.58
			$1.42 \pm 15\%$	$79\,700 \pm 20\%$	$0.098 \pm 7\%$	1.15	1.10	1.30	1.71
			$1.57 \pm 15\%$	$88\,700 \pm 19\%$	$0.105 \pm 7\%$	1.15	1.10	1.29	1.71
			$1.68 \pm 15\%$	$91\,600 \pm 18\%$	$0.108 \pm 7\%$	1.11	1.06	1.18	1.66

Table 5. Same as in Table 3 but for $3s^3S$–$3p^3P^\circ$ Be-like N IV and O V multiplets

Ion	Transition	λ (Å)	N_{e1} (10^{17} cm^{-3})	T_{e1}(K)	N_{e2}(10^{17} cm^{-3})	T_{e2} (K)	Δd_m (Å)	$\Delta d_m/\Delta d^e_{DSB}$	$\Delta d_m/\Delta d^{ei}_{DSB}$	$\Delta d_m/\Delta d_{DKr}$
N IV	$3s^3S_1$–$3p^3P_2^\circ$	3478.71	0.86	72 400	1.33	82 300	0.04	a	a	a
	$3s^3S_1$–$3p^3P_1^\circ$	3482.99	0.86	72 400	1.33	82 300	0.03	a	a	a
O V	$3s^3S_1$–$3p^3P_1^\circ$	2786.99	1.38	61 900	1.54	93 300	−0.020	b	b	7.35
	$3s^3S_1$–$3p^3P_0^\circ$	2789.85	1.38	61 900	1.54	93 300	−0.015	b	b	5.52

[a] Theory predicts opposite sign of shift
[b] $\Delta d^{ei}_{DSB} \simeq 0$

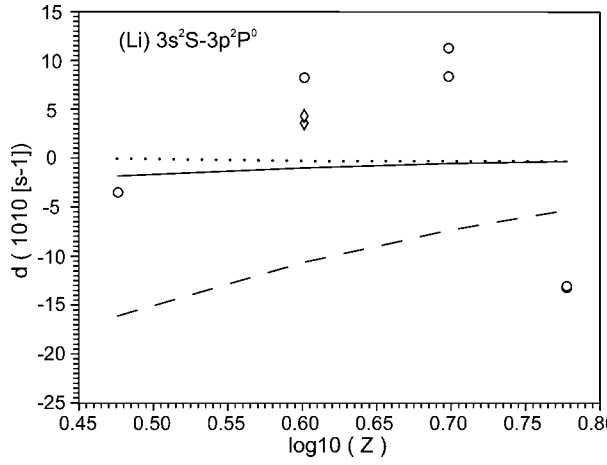

Fig. 6. Stark shifts of the Li-like spectral lines (in angular frequency units) as a function of log Z. Experimental data are scaled according to the temperature dependence obtained with a semiclassical perturbation approach to a value of the electron density of 10^{17} cm^{-3} and to a value of the electron temperature 87000 K (7.5 eV); theoretical data are calculated for these values. Theory: (——), semiclassical, electron impact shifts (see Table 1); (· · ·) semiclassical, electron + ion impact shifts (see Table 1) evaluated only for the experimental conditions of this experiment and (– – –) modified semiempirical formula.[41] Experiment: (○) this work; (◇) Djeniže et al.[46]

sequence. The inculsion of ion impact shifts did not improve the agreement between semiclassical theory and experiment. The calculated MSE (after Ref. 41) are always blue (towards shorter wavelengths) and they have a similar trend and the same direction as semiclassical electron impact shifts. Here, when comparing shifts, one should bear in mind large uncertainty of both, theory and experiment whenever one is dealing with exceedingly small shifts. On the other hand, it should be emphasised that the change of the sign of shift from red for N V to blue for O VI cannot be explained within an experimental error. Namely, the experimental technique used here for shift measurements may introduce a relatively large error in absolute value measurements but determination of the shift direction is quite certain.

4.2. Be-isoelectronic sequence

The experimental results and comparison with theoretical predictions for $3s^3S–3p^3P^\circ$ multiplets are presented as for the Li-isoelectronic sequence and the results are given in Tables 4 and 5.

Table 4 shows good agreement of B II experimental results with MSE formula[12] and a large discrepancy with our semiclassical results. The inclusion of ion broadening worsens the comparison. For C III, our experimental results agree better with semiclassical results and the inclusion of ion broadening does not improve the agreement. The earlier experiment by Bogen[44] agrees better with the MSE formula.[12] The newly measured Stark widths for N IV agree with Ref. 48 and with both experiments with semiclassical results and SSC[11]. The inclusion of ion broadening contribution improves the agreement between semiclassical results and our experiment. The experiment by Purić et al,[47] however, agrees better with MSE.[12] Although our experimental data for O V lines are systematically larger than all other theoretical calculations, the best agreement is with electron impact half-widths enlarged for ion broadening. The general picture in Fig. 7 shows, as for the Li-isoelectronic sequence, a similar trend of results of the comparison between the theory and the experiment: a large discrepancy for the lowest Z member of the sequence, and a good agreement for the next two members with already visible tendency of gradual change of the ratio experiment/theory which is proven with the result for O V. Unfortunately the data for high Z members of the sequence to confirm this conclusion fully are missing.

Stark shifts are measured only for N IV and O V lines. The agreement with another experiment[48] for N IV lines is very good. Again, theoretical shifts are very small and change the sign of shift from red for N IV to blue for O V which is experimentally detected and not predicted by theories, see Table 5.

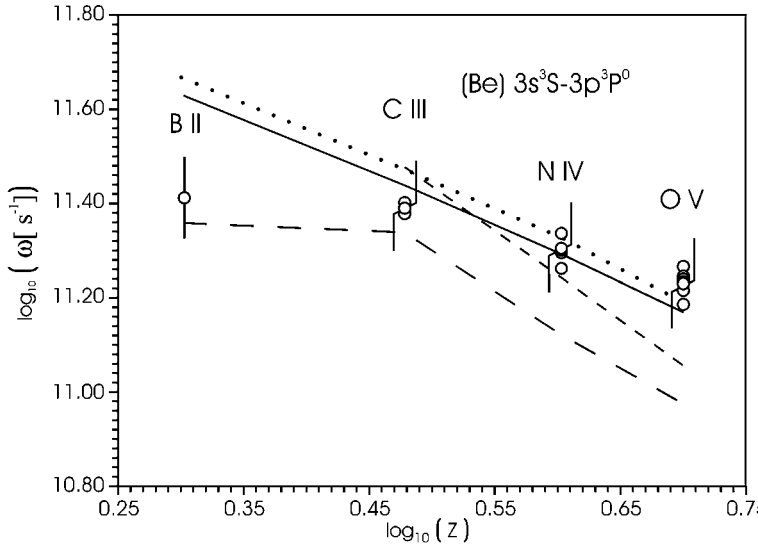

Fig. 7. Same as in Fig. 5 but for the Be-like spectral lines (in angular frequency units) as a function of log Z.

5. CONCLUSIONS

The results of semiclassical theoretical calculations of the Stark widths and shifts for some ions along the Li- ($3s^2S$–$3p^2P^\circ$) and Be- ($3s^3S$–$3p^3P^\circ$) isoelectronic sequences were reported; see Table 1. In addition to the electron impact widths and shifts, ion widths and shifts induced by the collisions with ions of interest are calculated as well. Furthermore, for B II, C III and N IV lines in addition to the electron impact Stark broadening parameters evaluated using oscillator strengths calculated with the help of the Coulomb approximation, another set of data with TOP base oscillator strengths and with the inclusion of transitions with different parent terms were generated. The influence of transitions with different parent terms is not significant for widths but is larger for shifts.

The plasma source in this experiment is a low-pressure pulsed arc. Plasma electron density is determined from the width of He II P_α line while the electron temperatures are determined from the Boltzmann plots of the relative intensities of ionic spectral lines. Assuming plasma LTE conditions, plasma composition data are evaluated and in conjunction with the results for the theoretical Stark broadening data, electron and ion impact widths and shifts are calculated. The experimental Stark widths and shifts of B III, C IV, N V and O VI (Li-sequence) are determined and the widths were found to be in good agreement with another systematic experimental study along this sequence,[3] see Fig. 5. The only exception are Stark widths for B III which are reported in this experiment. In the same plasma source Stark widths and shifts along the Be-sequence (B II, C III, N IV and O V) were also measured. Stark shifts along this sequence have been determined only for N IV and O V lines.

The comparison of experimental and our semiclassical theoretical Stark widths along both the sequences show a similar trend. For the lowest Z members of both the sequences theoretical results are systematically larger than the experiment. Further, with an increase of spectroscopic charge number Z the agreement is improving while for highest Z experimental results become larger than theory, see Figs. 5 and 7. The inclusion of ion broadening does not change this conclusion essentially. Although the measured and theoretical Stark shifts along the Li-sequence are small (see Fig. 6), and their uncertainties are very large, the change of the shift sign from red for N V to blue for O VI which is only experimentally detected is rather puzzling. Similar experimental Stark shift behavior can be noted for N IV and O V lines in the Be-sequence. In all these comparisons, one always should bear in mind that the temperature dependence of Stark parameters are not satisfactorily established and this may influence the comparison of widths and shifts along Z-sequences.

The final conclusion of the comparison between the experimental Stark widths and shifts for both studied sequences is as follows.

(i) Our semiclassical calculations describe reasonably well the experimental Stark widths although certain improvements are still required in particular for lowest and highest Z ions. The existence

of an ion broadening contribution cannot be confirmed with certainty. On the other hand, the additional precision experimental data for the lines of high and low Z ions are required.

(ii) Although it is well known that the evaluation of small Stark shifts is a great challenge, some of the changes of the shift sign experimentally determined in both sequences should be possible to predict. Experimental Stark shifts for higher Z ions are almost completely missing in literature so the new data are urgently needed.

(iii) It is very difficult to form a conclusion on comparing the experiment and quantum mechanical calculations[10] since only data for three ions of the Li-sequence are available. Nevertheless, the discrepancy along the sequence changes gradually with Z. Both approximate formulaes SSC[11] and MSE[12] for Stark widths and shifts[41] should be further improved to describe a better width and shift dependence upon the spectroscopic ion number.

Acknowledgements—This research is supported by the Ministry for Science and Technology of the Republic of Serbia.

REFERENCES

1. Wiese, W. L. and Konjević, N., *JQSRT*, 1982, **28,** 185.
2. Wiese, W. L. and Konjević, N., *JQSRT*, 1992, **47,** 185.
3. Glenzer, S., Uzelac, N. I., and Kunze, H.-J., *Phys. Rev. A*, 1992, **45,** 8795 and In *Spectral Line Shapes*, Vol. 7, eds, R. Stamm and B. Talin. Nova, New York, 1993.
4. Glenzer, S., Hey, J. D. and Kunze, H.-J., *J. Phys. B*, 1994, **27,** 413.
5. Blagojević, B., Popović, M. V., Konjević, N. and Dimitrijević, M. S., *Phys. Rev. E*, 1996, **54,** 743.
6. Blagojević, B., Popović, M. V., Konjević, N. and Dimitrijević, M. S., *Phys. Rev. E*, 1994, **50,** 2986.
7. Dimitrijević, M. S. and Sahal-Bréchot, S., *JQSRT*, 1992, **48,** 397.
8. Dimitrijević, M. S. and Sahal-Bréchot, S., *Astron. Astrophys. Suppl. Series*, 1996, **119,** 369.
9. Dimitrijević, M. S. and Sahal-Bréchot, S., *Astron. Astrophys. Suppl. Series*, 1992, **105,** 245.
10. Seaton, M. J., *J. Phys. B*, 1988, **21,** 3033.
11. Griem, H. R., *Spectral Line Broadening by Plasmas*, Academic Press, New York, 1974.
12. Dimitrijević, M. S. and Konjević, N., *JQSRT*, 1980, **24,** 451.
13. Alexiou, S. and Ralchenko, Yu, *Phys. Rev. A* 1994, **49,** 106.
14. Hey, J. D. and Breger, P., *JQSRT*, 1980, **24,** 349; ibid 1980, **24,** 427; *S. Afr. J. Phys*, 1982, **5,** 111.
15. Sahal-Bréchot, S., *Astron. Astrophys*, 1969, **1,** 91.
16. Sahal-Bréchot, S., *Astron. Astrophys*, 1969, **2,** 322.
17. Dimitrijević, M. S. and Sahal-Bréchot, S., *Astron. Astrophys. Suppl. Ser.*, 1994, **107,** 349.
18. Dimitrijević, M. S. and Sahal-Bréchot, S., *Astron. Astrophys. Suppl. Ser.*, 1996, **119,** 369.
19. Dimitrijević, M. S. and Sahal-Bréchot, S., *Bull. Astron. Belgrade*, 1996, **153,** 101.
20. Dimitrijević, M. S., Sahal-Bréchot, S. and Bommier, V., *Astron. Astrophys. Suppl. Ser.*, 1991, **89,** 581.
21. Dimitrijević, M. S., Sahal-Bréchot, S., Bommier, V., *Bull. Obs. Astron. Belgrade*, 1996, **144,** 65.
22. Dimitrijević, M. S. and Sahal-Bréchot, S., *Astron. Astrophys. Suppl. Ser.*, 1992, **95,** 109.
23. Dimitrijević, M. S. and Sahal-Bréchot, S., *Astron. Astrophys. Suppl. Ser.*, 1992, **93,** 359.
24. Dimitrijević, M. S. and Sahal-Bréchot, S., *Astron. Astrophys. Suppl. Ser.*, 1995, **109,** 551.
25. Fleurier, C., Sahal-Bréchot, S. and Chapelle, J., *JQSRT*, 1977, **17,** 595.
26. Dimitrijević, M. S. and Sahal-Bréchot, S., *Physica Scripta*, 1995, **52,** 41.
27. Moore, C. E., *Selected Tables of Atomic Spectra, Atomic Energy Levels and Multiplet Tables*, O V, NSRDS-NBS 3, Section 9, U.S. Dept. of Commerce, Washington
28. Bashkin, S. and Stoner, Jr., J. J., *Atomic Energy Levels and Grotrian Diagrams*, Vol. **1,** North-Holland, Amsterdam, 1975.
29. Gailitis, M., *Sov. Phys. JETP*, 1963, **17,** 1328.
30. Butler, K., Mendoza, C. and Zeippen, C. J., *J. Phys. B*, 1993, **26,** 4409.
31. Cunto, W., Mendoza, C., Ochsenbein, F. and Zeippen, C. J., *Astron. Astrophys.*, 1993, **275,** L5.
32. Tully, J. A., Seaton, M. J. and Berrington, K. A., *J. Phys. B*, 1990, **23,** 3811.
33. Davies, J. T. and Vaughan, J. M., *Astrophys. J.*, 1963, **137,** 1302.
34. Purić, J. and Konjević, N., *Z. Phys.*, 1972, **249,** 440.
35. Konjević, N. and Wiese, W. L., *J. Phys. Chem. Ref. Data*, 1976, **5,** 259.
36. Wiese, W. L., Smith, M. W. and Glennon, B. M., *Atomic Transition Probabilities*, Vol. I, NSRDS-NBS 4, U.S. Govt. Printing Office, Washington, D.C. 1966.
37. Wiese, W. L., Fuhr, J. R., and Deters, T. M., Atomic Transition Probabilities of Carbon, Nitrogen and Oxygen — A Critical Compilation, *J. Phys. Chem. Ref. Data Monograph No.* 7, 1996.
38. Büscher, S., Glenzer, S., Wrubel, Th. and Kunze, H.-J., *J. Phys. B*, 1996, **29,** 4107.
39. Kobilarov, R., Konjević, N. and Popović, M. V., *Phys. Rev. A*, 1981, **40,** 3871.
40. Wiese, W. L., In *Plasma Diagnostic Techniques*, eds. R. H. Huddleston and S. L. Leonard. Academic Press, New York, 1965.
41. Dimitrijević, M. S. and Kršljanin, V., *Astron. Astrophys.* 1986, **165,** 269.

42. Griem, H. R., *Plasma Spectroscopy*, McGraw-Hill, New York, 1964.
43. Ackerman, U., Finken, K. H. and Musielok, J., *Phys. Rev. A*, 1985, **31,** 2597.
44. Bogen, P. and Naturforsch, Z., *Tail A*, 1972, **27,** 210.
45. El Farra, M. A. and Hughes, T. P., *JQSRT*, 1983, **30,** 335.
46. Djeniže, S., Srećković, A., Milosavljević, M., Labat, O., Platiša, M. and Purić, J., *Z. Phys*., 1988, **D9,** 129.
47. Purić, J., Srećković, A., Djeniže, S. and Platiša, M., *Phys. Rev.A*, 1987, **36,** 3957.
48. Milosavljević, V., Djeniže, S. and Labat, J., 18th SPIG Kotor, Yugoslavia, Book of Contributed Papers, 1996, 263.

Journal of Research in Physics Vol.28, No. 3, 221-221 (1999)

Abstract of Invited lecture

QUASIMOLECULAR BANDS IN OPTICAL SPECTRA OF WEAKLY IONIZED PLASMAS

Lj. M. IGNjATOVIĆ[1], A. A. MIHAJLOV[1,2] AND M. S. DIMITRIJEVIĆ[1]
1) Institute of Physics, Pregrevica 118, 11080 Beograd, Yugoslavia
2) Astronomical Observatory, Volgina 7, 11050 Beograd, Yugoslavia

Even though the ion-atom radiative charge exchange and photoassociative processes has known for a long time, their investigation, as a sources of continuous electromagnetic spectra of low temperature plasmas, has been begun recently The aim of this work is that underlines necessity of taking into account above mentioned radiative processes during the analysis of molecular bands or atomic spectral lines.

The significant progress in this area has been reached by very detailed investigations of the influence of the slow symmetrical radiative collisions

$$A^+ + A \leftrightarrow \hbar\omega + A + A^+, \tag{1.a}$$
$$A^+ + A \leftrightarrow \hbar\omega + A_2^+, \tag{1.b}$$

at the radiative characteristics of weakly ionized plasmas. Their importance were shown convincingly in the cases $A=H$, *He*, *Li* and *Na* for different types of both astrophysical and laboratorical plasmas, which could be treated as a chemically homogenous plasmas (Mihajlov et al 1993, Mihajlov et al 1994, Ermolaev et al 1995). However, in the chemically inhomogenous, weakly ionized plasmas, we have to take into account the non-symmetrical ion-atom processes. The following processes will be considered:

$$A^+ + B \leftrightarrow \hbar\omega + A + B^+, \tag{2.a}$$
$$A^+ + B \leftrightarrow \hbar\omega + AB^+, \tag{2.b}$$
$$(AB^+)^* \leftrightarrow \hbar\omega + A + B^+. \tag{2.c}$$

In dependence on varying of ionization potentials I_A and I_B, the character of the considered ion-atom systems changes in the wide borders: from the almost symmetrical systems, which are composed of the atom and ion of different isotopes of the same element, to the quite non-symmetrical systems. Accordingly to that, the features of ion-atom systems are change very strong, as well as the spectra of photons emmited/absorbed in the course of reactions (2). Because of that, in the frame of this work we shall consider two characteristical cases:

- the collisional system is weakly non-symmetrical; representative for this case will be the system with $A=Li$ and $B=Na$,
- the collisional system is extremely non-symmetrical; representative for this case will be the system with $A=H$ and $B=Li$.

References

Ermolaev A.M., Mihajlov A.A., Ignjatović Lj.M. and Dimitrijević M.S.: 1995, *J. Phys. D: Appl. Phys.*, **28**, 1047

Mihajlov A.A., Dimitrijević M.S. and Ignjatović Lj.M.:1993, *Astronomy and Astrophys.*, **276**, 187

Mihajlov A.A., Dimitrijević M.S. and Ignjatović Lj.M.:1994, *Astronomy and Astrophys.*, **287**, 1026

Journal of Research in Physics Vol. 28, No. 3, 287-290 (1999)

ON THE STARK BROADENING OF AR VIII SPECTRAL LINES

MILAN S. DIMITRIJEVIĆ[1] AND SYLVIE SAHAL-BRECHOT[2]

[1] *Astronomical Observatory, Volgina 7, 11000 Belgrade, Yugoslavia*
E-mail mdimitrijevic@aob.bg.ac.yu

[2] *Observatoire de Paris, 92195 Meudon Cedex, France*
E-mail sahal@obspm.fr

Abstract. Within the semiclassical perturbation approach, we have considered electron-, proton-, and He III-impact line widths and shifts for 9 Ar VIII transitions, for perturber densities 10^{18} - 10^{22} cm^{-3} and temperatures T = 200,000 − 3,000,000 K.

1. INTRODUCTION

Stark broadening data for argon in different ionization stages are of interest for a number of problems in research of astrophysical, laboratory, laser produced and fusion plasmas, like *e.g.* plasma diagnostic and modelling. Stark broadening of Ar VIII spectral lines has been considered experimentaly (Hegazy *et al.* 1997) and theoreticaly (Purić *et al.* 1988, Hegazy *et al.* 1997, Djeniže and Srećković 1998, Konjević and Konjević 1998). In Hegazy *et al.* (1997) Stark broadening of 5f-6g and 5g-6h Ar VIII line profiles has been experimentaly investigated in gas-liner pinch. Obtained experimental results have been compared with the theoretical calculations performed in the same paper. These results has been discussed in Konjević and Konjević (1998). In Purić *et al.* (1988) and Djeniže *et al.* (1998), regularities and systematic trends have been used to estimate Ar VIII Stark broadening parameters. Moreover, Stark width for Ar VIII $4s^2S$-$4p^2P^o$ multiplet has been calculated in Djeniže *et al.* (1998) by using the symplified modified semiempirical approach (Dimitrijević and Konjević 1986).

As a continuation of our project (Dimitrijević 1996) to provide an as much as possible large set of reliable Stark broadening data for laboratory, laser produced, fusion and astrophysical plasma research, we have calculated within the semiclassical-perturbation formalism (sahal-Bréchot 1969ab, electron-, proton-, and ionized helium-impact line widths and shifts for 9 Ar VIII transitions.

2. RESULTS AND DISCUSSION

All relevant details concerning the obtained results and the calculation procedure will be published in Dimitrijević and Sahal–Bréchot (1999a). Here, we present only tables of Stark broadening parameters. Atomic energy levels needed for calculations have been taken from Bashkin and Stoner (1975). Our results for electron-, proton-, and He III-impact line widths and shifts for 9 Ar VIII transitions for perturber densities 10^{18}cm^{-3} – 10^{22}cm^{-3}, and the temperature range T = 200,000 – 3,000,000 K, will be published in Dimitrijević and Sahal-Bréchot (1999ab).

Table 1

Table 1. This table shows electron-, proton-, and He III-impact broadening parameters for Ar VIII for perturber density of 10^{18} cm^{-3} and temperatures from 200,000 up to 3,000,000 K. Transitions and corresponding wavelengths (in Å) are also given in the table. By dividing C by the corresponding full width at half maximum (Dimitrijević *et al.*, 1991), we obtain an estimate for the maximum perturber density for which the line may be treated as isolated and tabulated data may be used.

PERTURBER DENSITY = 1.E+18cm-3

PERTURBERS ARE :		ELECTRONS		PROTONS	
TRANSITION	T(K)	WIDTH(Å)	SHIFT(Å)	WIDTH(Å)	SHIFT(Å)
Ar VIII3S 3P	200000.	0.930E-02	-0.137E-03	0.150E-03	-0.973E-04
714.0 Å	500000.	0.614E-02	-0.156E-03	0.374E-03	-0.208E-03
C=0.71E+21	1000000.	0.464E-02	-0.149E-03	0.557E-03	-0.304E-03
	1500000.	0.400E-02	-0.149E-03	0.656E-03	-0.368E-03
	2000000.	0.362E-02	-0.145E-03	0.701E-03	-0.403E-03
	3000000.	0.317E-02	-0.141E-03	0.780E-03	-0.448E-03
Ar VIII3S 3P	200000.	0.899E-02	-0.130E-03	0.146E-03	-0.918E-04
700.4 Å	500000.	0.593E-02	-0.148E-03	0.362E-03	-0.197E-03
C=0.69E+21	1000000.	0.448E-02	-0.142E-03	0.538E-03	-0.288E-03
	1500000.	0.386E-02	-0.142E-03	0.633E-03	-0.349E-03
	2000000.	0.350E-02	-0.138E-03	0.675E-03	-0.382E-03
	3000000.	0.307E-02	-0.134E-03	0.750E-03	-0.425E-03
Ar VIII3S 4P	200000.	0.119E-02	0.977E-05	0.702E-04	0.100E-04
159.0 Å	500000.	0.815E-03	0.147E-04	0.112E-03	0.199E-04
C=0.13E+20	1000000.	0.638E-03	0.125E-04	0.131E-03	0.276E-04
	1500000.	0.562E-03	0.119E-04	0.140E-03	0.316E-04
	2000000.	0.516E-03	0.119E-04	0.148E-03	0.342E-04
	3000000.	0.462E-03	0.113E-04	0.158E-03	0.380E-04

Table 1 continued

PERTURBER DENSITY = 1.E+18cm-3

PERTURBERS ARE :		ELECTRONS		PROTONS	
TRANSITION	T(K)	WIDTH(Å)	SHIFT(Å)	WIDTH(Å)	SHIFT(Å)
Ar VIII4S 4P	200000.	0.210	-0.497E-02	0.106E-01	-0.586E-02
1887.0 Å	500000.	0.147	-0.561E-02	0.174E-01	-0.960E-02
C=0.19E+22	1000000.	0.117	-0.547E-02	0.209E-01	-0.120E-01
	1500000.	0.103	-0.527E-02	0.230E-01	-0.134E-01
	2000000.	0.952E-01	-0.512E-02	0.248E-01	-0.145E-01
	3000000.	0.852E-01	-0.447E-02	0.276E-01	-0.161E-01
Ar VIII3P 4S	200000.	0.161E-02	0.108E-03	0.535E-04	0.110E-03
229.4 Å	500000.	0.112E-02	0.130E-03	0.136E-03	0.176E-03
C=0.28E+20	1000000.	0.880E-03	0.122E-03	0.208E-03	0.216E-03
	1500000.	0.773E-03	0.118E-03	0.243E-03	0.239E-03
	2000000.	0.708E-03	0.115E-03	0.269E-03	0.257E-03
	3000000.	0.628E-03	0.104E-03	0.314E-03	0.282E-03
Ar VIII3P 4S	200000.	0.164E-02	0.110E-03	0.542E-04	0.111E-03
230.9 Å	500000.	0.114E-02	0.131E-03	0.137E-03	0.178E-03
C=0.28E+20	1000000.	0.893E-03	0.124E-03	0.211E-03	0.219E-03
	1500000.	0.784E-03	0.119E-03	0.245E-03	0.242E-03
	2000000.	0.718E-03	0.117E-03	0.272E-03	0.260E-03
	3000000.	0.637E-03	0.105E-03	0.318E-03	0.285E-03
Ar VIII3P 3D	200000.	0.573E-02	-0.637E-04	0.148E-03	-0.359E-04
519.2 Å	500000.	0.379E-02	-0.616E-04	0.314E-03	-0.798E-04
C=0.38E+21	1000000.	0.287E-02	-0.816E-04	0.438E-03	-0.120E-03
	2000000.	0.225E-02	-0.711E-04	0.513E-03	-0.165E-03
	3000000.	0.198E-02	-0.682E-04	0.551E-03	-0.183E-03
Ar VIII3P 3D	200000.	0.591E-02	-0.665E-04	0.153E-03	-0.379E-04
526.6 Å	500000.	0.391E-02	-0.648E-04	0.324E-03	-0.841E-04
C=0.40E+21	1000000.	0.296E-02	-0.849E-04	0.453E-03	-0.127E-03
	1500000.	0.255E-02	-0.727E-04	0.498E-03	-0.154E-03
	2000000.	0.232E-02	-0.741E-04	0.530E-03	-0.173E-03
	3000000.	0.204E-02	-0.711E-04	0.569E-03	-0.192E-03
Ar VIII3D 4P	200000.	0.547E-02	0.102E-03	0.346E-03	0.785E-04
337.6 Å	500000.	0.376E-02	0.127E-03	0.547E-03	0.141E-03
C=0.60E+20	1000000.	0.295E-02	0.124E-03	0.636E-03	0.194E-03
	1500000.	0.260E-02	0.116E-03	0.683E-03	0.215E-03
	2000000.	0.239E-02	0.116E-03	0.721E-03	0.233E-03
	3000000.	0.214E-02	0.111E-03	0.770E-03	0.258E-03

As a sample of our results, the Stark broadening parameters for Ar VIII spectral lines broadened by electron and proton impacts, for a perturber density of 10^{18} cm^{-3},

are shown in Table 1. We also specify a parameter C (Dimitrijević and Sahal–Bréchot 1984), which gives an estimate for the maximum perturber density for which the line may be treated as isolated when it is divided by the corresponding full width at half maximum. For each value given in Table 1, the collision volume (V) multiplied by the perturber density (N) is much less than one and the impact approximation is valid (Sahal–Bréchot, 1969ab).

There is not an enough complete set of reliable atomic data to perform an adequate semiclassical perturbation calculation of the Stark broadening of Ar VIII 5f-6g and 5g-6h line profiles, experimentaly and theoreticaly investigated in Hegazy *et al.* (1997). This is similar for Ar VIII 4p-4d and 4p-5s Stark widths estimated on the basis of regularities and systematic trends in Djeniže *et al.* (1998). In Purić *et al.* (1988), full Stark width at half maximum (W) for $4s^2S$-$4p^2P^o$ multiplet has been estimated on the basis of the regular dependence on the upper level ionization potential to be 0.0244 Å at the temperature T=80,000 K and for an electron density of $10^{17}cm^{-3}$. For the same multiplet and electron density, W=0.018Å has been obtained in Djeniže *et al.* (1998) on the basis of established regularities along the argon isonuclear sequence, for T=150,000 K. Our result for T=200,000 K is 0.0210Å which is a good agreement.

The new experimental data will be very useful for further development and rafinement of the theory of multicharged ion lines and for the investigation of regularities and systematic trends.

References

Bashkin, S., Stoner, J. O. Jr. : 1978, Atomic Energy Levels and Grotrian Diagrams, Vol. 2, North Holland, Amsterdam.

Dimitrijević, M. S., Konjević, N. : 1986, *Astron. Astrophys.*, **163**, 297 .

Dimitrijević, M.S., and Sahal-Bréchot, S. : 1984, *JQSRT* **31**, 301.

Dimitrijević M.S. and Sahal-Bréchot, S. : 1999a, *Zh. Prikl. Spektrosk.* submitted.

Dimitrijević, M. S., and Sahal–Bréchot, S. : 1999b, *Serb. Astron. J.*, **159**, in press.

Djeniže, S., Srećković, A. : 1998, *Serb. Astron. J.*, **157**, 25.

Griem, H. R. : 1974, Spectral Line Broadening by Plasmas, Academic Press, New York.

Hegazy, H., Büscher, S., Kunze, H. J., Wrubel, Th. : 1997, *J. Quant. Spectrosc. Radiat. Transfer*, **58**, 627.

Konjević, R., Konjević, N. : 1998, 19^{th} SPIG, Zlatibor 1998, Contributed papers, Faculty of Physics, Belgrade, p. 373.

Purić, J., Djeniže, S., Srećković, A., Ćuk, M., Labat, J., Platiša, M. : 1988, *Z. Phys. D*, **8**, 343.

Sahal-Bréchot, S. : 1969a, *Astron. Astrophys.* **1**, 91.

Sahal-Bréchot, S. : 1969b, *Astron. Astrophys.* **2**, 322.

Journal of Research in Physics Vol. 28, No. 3, 291-294 (1999)

ON THE STARK BROADENING OF NEUTRAL SILVER SPECTRAL LINES

MILAN S. DIMITRIJEVIĆ[1] AND SYLVIE SAHAL-BRECHOT[2]

[1] *Astronomical Observatory, Volgina 7, 11050 Belgrade, Yugoslavia*
E-mail mdimitrijevic@aob.aob.bg.ac.yu

[2] *Observatoire de Paris, 92195 Meudon Cedex, France*
E-mail sahal@obspm.fr

Abstract. Within the semiclassical perturbation approach, we have calculated electron-, proton-, and ionized helium-impact line widths and shifts for 48 Ag I lines, for perturber densities $10^{12} - 10^{19}$ cm^{-3} and temperatures T = 2,500 − 50,000 K.

1. INTRODUCTION

Stark broadening contribution to neutral silver spectral line shapes has been considered experimentaly (Holtsmark and Trumpy 1925, Kitaeva 1956) and theoreticaly (Kitaeva 1956, Pichler 1972). In Pichler (1972) quadratic Stark broadening constants of neutral silver spectral lines, calculated in the Coulomb approximation, have been determined. Our objective here, is to continue efforts to provide to plasma physicists and astrophysicists Stark broadening parameters needed for investigation and modelling of various plasmas (see Dimitrijević and Sahal - Bréchot 1984, Dimitrijević 1996, and references therein). In this contribution, a part of our results for electron-, proton-, and ionized helium-impact line widths and shifts for 48 Ag I spectral lines is presented.

2. RESULTS AND DISCUSSION

A summary of the formalism is given e. g. in Dimitrijević and Sahal-Bréchot 1984. Energy levels have been taken from Moore (1971).

Our results for 48 neutral silver spectral lines as a function of the perturber density and temperature will be published in Dimitrijević and Sahal-Bréchot (1999).

As a sample of our results, the Stark broadening parameters for Ag I spectral lines broadened by electron and proton impacts, for a perturber density of 10^{16} cm^{-3}, are shown in Table 1.

The existing experimental data (Holtsmark and Trumpy 1925, Kitaeva 1956) are not included in the review of critically selected experimental Stark broadening data

(Konjević and Roberts 1976). In order to make a comparison of theory with reliable experimental data, the results of corresponding experiments to determine the Stark broadening of Ag I lines will be of interest for further development and rafinement of the theory.

Table 1

This table shows electron- and proton-impact broadening full half-widths (FWHM) and shifts for Ag I for a perturber density of 10^{16} cm^{-3} and temperatures from 2,500 up to 50,000 K. By deviding C with the full linewidth, we obtain an estimate for the maximum perturber density for which the line may be treated as isolated and tabulated data may be used (Dimitrijević and Sahal-Bréchot 1984). For each value given in Table 1, the collision volume (V) multiplied by the perturber density (N) is much less than one and the impact approximation is valid (Sahal–Bréchot, 1969ab). Values for NV > 0.5 are not given and values for 0.1 < NV ≤ 0.5 are denoted by an asterisk.

PERTURBER DENSITY = 1.E+16cm-3

PERTURBERS ARE :		ELECTRONS		PROTONS	
TRANSITION	T(K)	WIDTH(Å)	SHIFT(Å)	WIDTH(Å)	SHIFT(Å)
AgI 5S - 5P	2500.	0.375E-02	0.179E-02	0.227E-02	0.482E-03
0.5 0.5	5000.	0.422E-02	0.208E-02	0.228E-02	0.548E-03
3383.9 Å	10000.	0.443E-02	0.225E-02	0.229E-02	0.622E-03
C= 0.15E+20	20000.	0.500E-02	0.218E-02	0.231E-02	0.700E-03
	30000.	0.567E-02	0.183E-02	0.232E-02	0.751E-03
	50000.	0.691E-02	0.142E-02	0.234E-02	0.819E-03
AgI 5S - 5P	2500.	0.385E-02	0.199E-02	0.230E-02	0.555E-03
1.5 0.5	5000.	0.437E-02	0.243E-02	0.232E-02	0.632E-03
3281.6 Å	10000.	0.465E-02	0.275E-02	0.233E-02	0.717E-03
C= 0.13E+20	20000.	0.523E-02	0.275E-02	0.235E-02	0.809E-03
	30000.	0.589E-02	0.240E-02	0.237E-02	0.867E-03
	50000.	0.707E-02	0.191E-02	0.239E-02	0.946E-03
AgI 5S - 6P	2500.	0.459E-01	0.312E-01	*0.116E-01	*0.723E-02
0.5 0.5	5000.	0.493E-01	0.303E-01	*0.128E-01	*0.912E-02
2070.5 Å	10000.	0.521E-01	0.268E-01	0.141E-01	0.110E-01
C= 0.19E+18	20000.	0.529E-01	0.221E-01	0.157E-01	0.128E-01
	30000.	0.525E-01	0.190E-01	0.168E-01	0.139E-01
	50000.	0.518E-01	0.149E-01	0.183E-01	0.154E-01
AgI 6S - 6P	2500.	3.07	1.94	*0.787	*0.490
0.5 0.5	5000.	3.34	1.67	*0.867	*0.616
17417.9 Å	10000.	3.73	1.23	0.957	0.738
C= 0.14E+20	20000.	4.02	0.900	1.06	0.861
	30000.	4.12	0.690	1.13	0.936
	50000.	4.23	0.453	1.24	1.03

Table 1 continued

PERTURBER DENSITY = 1.E+16cm-3

PERTURBERS ARE :		ELECTRONS		PROTONS	
TRANSITION	T(K)	WIDTH(Å)	SHIFT(Å)	WIDTH(Å)	SHIFT(Å)
AgI 6S - 6P	2500.	3.90	2.22	*0.992	*0.617
1.5 0.5	5000.	4.21	1.75	*1.11	*0.799
16821.9 Å	10000.	4.44	1.32	*1.24	*0.973
C= 0.69E+19	20000.	4.49	0.877	1.40	1.15
	30000.	4.50	0.630	1.50	1.25
	50000.	4.50	0.384	1.67	1.38
AgI 5P - 6S	2500.	0.113	0.796E-01	0.265E-01	0.207E-01
0.5 0.5	5000.	0.132	0.954E-01	0.292E-01	0.242E-01
7689.9 Å	10000.	0.148	0.115	0.324E-01	0.279E-01
C= 0.34E+20	20000.	0.159	0.120	0.360E-01	0.318E-01
	30000.	0.170	0.121	0.383E-01	0.343E-01
	50000.	0.181	0.106	0.415E-01	0.376E-01
AgI 5P - 6S	2500.	0.129	0.914E-01	0.308E-01	0.237E-01
0.5 1.5	5000.	0.151	0.112	0.339E-01	0.278E-01
8275.8 Å	10000.	0.169	0.132	0.375E-01	0.320E-01
C= 0.39E+20	20000.	0.183	0.137	0.416E-01	0.365E-01
	30000.	0.197	0.138	0.443E-01	0.393E-01
	50000.	0.211	0.119	0.479E-01	0.431E-01
AgI 5P - 7S	2500.	0.163	0.113	0.348E-01	0.258E-01
0.5 0.5	5000.	0.190	0.137	0.391E-01	0.319E-01
4477.3 Å	10000.	0.209	0.162	0.439E-01	0.379E-01
C= 0.43E+19	20000.	0.226	0.152	0.492E-01	0.440E-01
	30000.	0.239	0.147	0.526E-01	0.477E-01
	50000.	0.262	0.125	0.573E-01	0.526E-01
AgI 5P - 7S	2500.	0.177	0.121	0.379E-01	0.281E-01
0.5 1.5	5000.	0.206	0.148	0.425E-01	0.347E-01
4669.8 Å	10000.	0.230	0.172	0.477E-01	0.412E-01
C= 0.47E+19	20000.	0.246	0.164	0.535E-01	0.478E-01
	30000.	0.260	0.159	0.572E-01	0.518E-01
	50000.	0.285	0.134	0.623E-01	0.571E-01
AgI 5P - 8S	2500.	0.346	0.226	*0.709E-01	*0.434E-01
0.5 0.5	5000.	0.398	0.274	*0.800E-01	*0.587E-01
3841.8 Å	10000.	0.438	0.298	*0.899E-01	*0.730E-01
C= 0.15E+19	20000.	0.497	0.287	*0.101	*0.870E-01
	30000.	0.533	0.252	*0.108	*0.952E-01
	50000.	0.603	0.215	0.118	0.106

Table 1 continued

PERTURBER DENSITY = 1.E+16cm-3

PERTURBERS ARE :		ELECTRONS		PROTONS	
TRANSITION	T(K)	WIDTH(Å)	SHIFT(Å)	WIDTH(Å)	SHIFT(Å)
AgI 5P - 8S	2500.	0.372	0.243	*0.762E-01	*0.466E-01
0.5 1.5	5000.	0.428	0.302	*0.860E-01	*0.631E-01
3982.7 Å	10000.	0.470	0.319	*0.966E-01	*0.784E-01
C= 0.16E+19	20000.	0.531	0.308	*0.108	*0.934E-01
	30000.	0.573	0.270	*0.116	*0.102
	50000.	0.649	0.231	0.126	0.114
AgI 6P - 7S	2500.	8.95	-0.462	*1.41	-0.745
0.5 0.5	5000.	11.8	0.868	1.50	-0.905
27858.3 Å	10000.	14.0	2.09	1.61	-1.06
C= 0.35E+20	20000.	16.0	2.84	1.75	-1.23
	30000.	17.0	2.68	1.86	-1.33
	50000.	18.3	2.39	2.02	-1.46
AgI 6P - 7S	2500.	14.2	-1.73	*2.44	-1.52
0.5 1.5	5000.	17.1	0.652E-01	*2.71	-1.92
29531.5 Å	10000.	19.0	1.96	3.01	-2.31
C= 0.21E+20	20000.	20.5	3.08	3.38	-2.70
	30000.	21.3	3.00	3.65	-2.93
	50000.	22.4	2.92	4.08	-3.24

References

Dimitrijević, M. S. : 1996, *Zh. Prikl. Spektrosk.* **63**, 810.
Dimitrijević, M.S., and Sahal-Bréchot, S. : 1984, *JQSRT* **31**, 301.
Dimitrijević M.S. and Sahal-Bréchot, S. : 1999, *Atomic Data and Nuclear Data Tables* submitted.
Holtsmark, J., Trumpy, B. : 1925, *Z. Phys.* **31**, 803.
Kitaeva, V. F. : 1956, *Tr. Fiz. Inst. Acad. Nauk SSSR* **11**, 3.
Konjević, N., Roberts, J. R. : 1976, *J. Phys. Chem. Ref. Data* **5**, 209.
Moore, C. E. : 1971, *Atomic Energy Levels III*, NSRDS-NBS 35, Washington.
Pichler, G. : 1972, *Fizika* **4**, 235.
Sahal-Bréchot, S. : 1969a, *Astron.Astrophys.* **1**, 91.
Sahal-Bréchot, S. : 1969b, *Astron.Astrophys.* **2**, 322.

Journal of Research in Physics Vol. 28, No. 3, 295-298 (1999)

ON THE STARK BROADENING OF NEUTRAL CALCIUM LINES

MILAN S. DIMITRIJEVIĆ[1] AND SYLVIE SAHAL-BRECHOT[2]

[1] *Astronomical Observatory, Volgina 7, 11050 Belgrade, Yugoslavia*
E-mail mdimitrijevic@aob.aob.bg.ac.yu

[2] *Observatoire de Paris, 92195 Meudon Cedex, France*
E-mail sahal@obspm.fr

Abstract. Using a semiclassical approach, we have calculated electron-, proton-, He II-, Mg II-, Si II-, and Fe II-impact line widths and shifts for 189 neutral calcium lines, as a function of temperature and perturber density. Perturbers selected here, are the main perturbers in solar and stellar atmospheres.

1. INTRODUCTION

Neutral calcium lines are very important for stellar spectra synthesis and stellar plasma analysis due to cosmical abundance of this element. Stark broadening parameters of Ca I are important as well for laboratory plasma diagnostics, modelling and investigation. In order to complete as much as possible Stark broadening data needed for astrophysical and laboratory plasma research and stellar opacities calculations, we have published in a series of papers, results of large scale calculations of Stark broadening parameters for a number of spectral lines of various emitters (Dimitrijević, 1996, 1997 and references therein). Our calculations have been performed within the semiclassical - perturbation formalism (Sahal-Bréchot, 1969ab), for transitions when a sufficiently complete set of reliable atomic data exist and the good accuracy of obtained results is expected.

Up to now, Stark broadening parameters for 79 He I, 62 Na, 51 K, 61 Li, 25 Al, 24 Rb, 3 Pd, 19 Be, 270 Mg, 31 Se, 33 Sr, 14 Ba, 28 Ca II, 30 Be II, 29 Li II, 66 Mg II, 64 Ba II, 19 Si II, 3 Fe II, 2 Ni II, 12 B III, 23 Al III, 10 Sc III, 27 Be III, 32 Y III, 20 In III, 2 Tl III, 10 Ti IV, 39 Si IV, 90 C IV, 5 O IV, 114 P IV, 2 Pb IV, 19 O V, 30 N V, 25 C V, 51 P V, 34 S V, 26 V V, 30 O VI, 21 S VI, 2 F VI, 14 O VII, 10 FVII, 10 Cl VII, 20 Ne VIII, 4 K VIII, 6 Kr VIII, 4 Ca IX, 30 K IX, 8 Na IX, 57 Na X, 48 Ca X, 4 Sc X, 7 Al XI, 4 Si XI, 18 Mg XI, 4 Ti XI, 10 Sc XI, 9 Si XII, 27 Ti XII, 61 Si XIII and 33 V XIII multiplets become available.

Data for particular lines of F I, B II, C III, N IV, Ar II, Ga II, Ga III, Cl I, Br I, I I, Cu I, Hg II, N III, F V and S IV also exist.

In order to continue our project to provide to physicists and astrophysicists an as much as possible complete set of needed reliable Stark broadening data, we have

calculated within the semiclassical-perturbation formalism, electron-, proton-, He II-, Mg II-. Si II-, and Fe II - impact line widths and shifts for 189 neutral calcium lines, as a function of temperature and perturber density. Perturbers selected here, are the main perturbers in solar and stellar atmospheres.

2. RESULTS AND DISCUSSION

A summary of the formalism has been published several times (see e. g. Dimitrijević and Sahal-Bréchot 1984). Energy levels have been taken from Sugar and Corliss (1979). .

Our results for 189 Ca I multiplets as a function of the perturber density and temperature and the comparison with available experimental and theoretical data will be published in Dimitrijević and Sahal-Bréchot (1999a,b).

Table 1

This table shows electron- and proton-impact broadening full half-widths (FWHM) and shifts for Ca I for a perturber density of 10^{16} cm^{-3} and temperatures from 2,500 up to 50,000 K. By deviding C with the full linewidth, we obtain an estimate for the maximum perturber density for which the line may be treated as isolated and tabulated data may be used (Dimitrijević and Sahal-Bréchot 1984). For each value given in Table 1, the collision volume (V) multiplied by the perturber density (N) is much less than one and the impact approximation is valid (Sahal–Bréchot, 1969ab). Values for NV $>$ 0.5 are not given and values for 0.1 $<$ NV $\leq$ 0.5 are denoted by an asterisk.

PERTURBER DENSITY = 1.E+16cm-3

PERTURBERS ARE :		ELECTRONS		PROTONS	
TRANSITION	T(K)	WIDTH(Å)	SHIFT(Å)	WIDTH(Å)	SHIFT(Å)
4S - 4P	2500.	0.103E-01	0.578E-02	0.581E-02	0.155E-02
4227.9 Å	5000.	0.115E-01	0.665E-02	0.587E-02	0.178E-02
C= 0.17E+20	10000.	0.124E-01	0.795E-02	0.592E-02	0.202E-02
Singlet	20000.	0.143E-01	0.807E-02	0.600E-02	0.229E-02
	30000.	0.162E-01	0.724E-02	0.605E-02	0.245E-02
	50000.	0.193E-01	0.585E-02	0.613E-02	0.268E-02
4S - 5P	2500.	0.672E-01	0.474E-01	*0.180E-01	*0.110E-01
2722.5 Å	5000.	0.726E-01	0.456E-01	*0.197E-01	*0.137E-01
C= 0.42E+18	10000.	0.798E-01	0.364E-01	0.216E-01	0.163E-01
Singlet	20000.	0.864E-01	0.289E-01	0.238E-01	0.190E-01
	30000.	0.878E-01	0.245E-01	0.254E-01	0.206E-01
	50000.	0.887E-01	0.185E-01	0.276E-01	0.228E-01

Table 1 continued

PERTURBER DENSITY = 1.E+16cm-3

PERTURBERS ARE :		ELECTRONS		PROTONS	
TRANSITION	T(K)	WIDTH(Å)	SHIFT(Å)	WIDTH(Å)	SHIFT(Å)
5S - 5P	2500.	7.36	3.52	* 1.85	* 1.07
29288.1 Å	5000.	9.21	2.15	2.00	1.32
C= 0.49E+20	10000.	11.4	0.952	2.17	1.57
Singlet	20000.	12.7	0.146	2.38	1.82
	30000.	13.4	-0.315	2.52	1.97
	50000.	14.0	-0.477	2.73	2.17
5S - 6P	2500.	1.82	0.810	*0.616	*0.172
11959.2 Å	5000.	2.24	0.884	*0.644	*0.212
C= 0.14E+20	10000.	2.83	0.902	*0.661	*0.251
Singlet	20000.	3.54	0.705	0.676	0.291
	30000.	3.99	0.624	0.686	0.315
	50000.	4.49	0.565	0.700	0.347
4P - 5S	2500.	0.363	0.219	0.826E-01	0.581E-01
12678.8 Å	5000.	0.407	0.275	0.897E-01	0.680E-01
C= 0.83E+20	10000.	0.441	0.325	0.979E-01	0.784E-01
Singlet	20000.	0.496	0.321	0.107	0.894E-01
	30000.	0.535	0.290	0.113	0.963E-01
	50000.	0.618	0.241	0.122	0.106
4P - 4D	2500.	0.394	-0.172	0.873E-01	-0.537E-01
7328.2 Å	5000.	0.428	-0.111	0.948E-01	-0.654E-01
C= 0.30E+19	10000.	0.466	-0.625E-01	0.103	-0.770E-01
Singlet	20000.	0.475	-0.263E-01	0.114	-0.889E-01
	30000.	0.481	-0.437E-02	0.121	-0.962E-01
	50000.	0.488	0.320E-02	0.132	-0.106
4P - 5D	2500.	0.460	-0.241	*0.134	*-0.540E-01
5190.3 Å	5000.	0.511	-0.225	*0.143	*-0.693E-01
C= 0.16E+19	10000.	0.581	-0.164	*0.151	*-0.838E-01
Singlet	20000.	0.697	-0.119	*0.160	*-0.984E-01
	30000.	0.758	-0.105	0.166	-0.107
	50000.	0.825	-0.808E-01	0.175	-0.119
5S - 5P	2500.	2.24	1.53	0.704	0.360
19897.4 Å	5000.	2.64	1.49	0.746	0.436
C= 0.47E+20	10000.	3.13	1.05	0.791	0.511
Triplet	20000.	3.93	0.687	0.844	0.590
	30000.	4.34	0.593	0.879	0.638
	50000.	4.72	0.388	0.929	0.702

4P - 5S	2500.	0.820E-01	0.652E-01	0.208E-01	0.168E-01
6143.9 Å	5000.	0.983E-01	0.777E-01	0.232E-01	0.198E-01
C= 0.19E+20	10000.	0.114	0.925E-01	0.259E-01	0.229E-01
Triplet	20000.	0.124	0.993E-01	0.290E-01	0.262E-01
	30000.	0.130	0.100	0.309E-01	0.282E-01
	50000.	0.136	0.912E-01	0.336E-01	0.309E-01
4P - 6S	2500.	0.146	0.104	*0.326E-01	*0.237E-01
3966.5 Å	5000.	0.172	0.127	0.367E-01	0.296E-01
C= 0.32E+19	10000.	0.190	0.149	0.411E-01	0.353E-01
Triplet	20000.	0.202	0.150	0.462E-01	0.411E-01
	30000.	0.211	0.143	0.494E-01	0.447E-01
	50000.	0.222	0.121	0.538E-01	0.493E-01
4P - 4D	2500.	0.943E-01	-0.316E-01	0.244E-01	-0.998E-02
4446.3 Å	5000.	0.106	-0.174E-01	0.252E-01	-0.118E-01
C= 0.23E+19	10000.	0.126	-0.237E-02	0.261E-01	-0.137E-01
Triplet	20000.	0.141	0.108E-01	0.273E-01	-0.157E-01
	30000.	0.149	0.137E-01	0.281E-01	-0.169E-01
	50000.	0.157	0.164E-01	0.294E-01	-0.185E-01

As a sample of our results, the Stark broadening parameters for Ca I spectral lines broadened by electron and proton impacts, for a perturber density of 10^{16} cm^{-3}, are shown in Table 1.

References

Dimitrijević, M. S. : 1996, *Zh. Prikl. Spektrosk.* **63**, 810.
Dimitrijević, M. S. : 1997, *Astrophys. Space Sci.* **252**, 415.
Dimitrijević, M.S., and Sahal-Bréchot, S. : 1984, *JQSRT* **31**, 301.
Dimitrijević M.S. and Sahal-Bréchot, S. : 1999a, *Astron. Astrophys. Suppl. Series* submitted.
Dimitrijević M.S. and Sahal-Bréchot, S. : 1999b, *Serb. Astron. J.* **160**, in press.
Sahal-Bréchot, S. : 1969a, *Astron.Astrophys.* **1**, 91.
Sahal-Bréchot, S. : 1969b, *Astron.Astrophys.* **2**, 322.
Sugar, J. and Corlis, C. : 1979, *J. Phys. Chem. Ref. Data* **8**, 865.

Journal of Research in Physics Vol. 28, No. 3, 299-302 (1999)

THE ELECTRON-IMPACT BROADENING PARAMETERS FOR ASTROPHYSICALLY IMPORTANT LINES IN Co II SPECTRA

D. TANKOSIĆ, L. Č. POPOVIĆ, M. S. DIMITRIJEVIĆ
Astronomical Observatory, Volgina 7, 11000 Belgrade, Yugoslavia

1. INTRODUCTION

The spectral lines for singly ionized cobalt are present in stellar spectra, as e.g. in Hg-Mn star spectra (Bolcal and Didelon, 1987). The abundance of cobalt is derived by fitting-synthesis analysis of co-added high-resolution *International Ultraviolet Explorer (IUE) spectra*. The investigation of cobalt abundance in Hg-Mn stars shows that the most of the Hg-Mn stars are evidently largely cobalt-deficient ([Co/H]≤ -2dex), but exceptions for mildly cobalt-rich stars, νCnc and φHer, and cobalt-normal stars 87 Psc and 36 Lyn are notable (Smith and Dworetsky, 1993). Also, in hot star atmospheres Stark broadening mechanism is the main pressure broadening mechanism (Dimitrijević, 1989). Consequently, in order to investigate and modeling the Hg-Mn star and other type of hot star atmospheres, the Stark broadening parameters for Co II spectral lines are needed.

There is not measured Stark broadening parameters for Co II lines. However for the resonant $3d^8\ ^3F\text{-}3d^7 4p\ ^3G^o$ (λ=2058.9Å) Co II line the Stark broadening data have been estimated based on regularities and systematic trends by Lakićević (1983).

In order to provide to astrophysicist the needed data, we have calculated Stark broadening parameters for 12 Co II spectral lines, from the $a^5F\text{-}z^5G^0$ multiplet. Calculations were performed by using the modified semiempirical approach (Dimitrijević and Konjević, 1980; Dimitrijević and Konjević, 1981; Popović and Dimitrijević, 1996). Also, considering that Co II (λ=2307.85Å) line has been used for cobalt abundance determination (see e.g. Smith and Dworetsky, 1993) in HgMn stars, we have tested the influence of Stark mechanism on width of this line in layers of A type stars, as well as DA and DB white dwarfs. This has been done with the help of Kurucz's model atmospheres (Kurucz, 1979) of an A type star (T_{eff}=10000K, log*g*=4), and with Wickramasinghe's models of DA (T_{eff}=10000K, log*g*=6) and DB (T_{eff}=15000K, log*g*=7) white dwarf atmospheres (Wickramasinghe, 1972).

2. RESULTS AND DISCUSSION

As an example of our results, we present here the electron-impact broadening parameters for $a^5F_4 - z^5G^0_5$ Co II line as a function of temperature, calculated by using the modified semiempirical approach. The energy levels were taken from Pickering et al (1998). Oscillator strength data have been calculated by using the Bates-Damgaard method (Bates and Damgaard, 1949).

In Table 1, Stark widths and shifts for $a^5F_4 - z^5G^0_5$ Co II spectral line, for an electron density of $10^{23}m^{-3}$ and temperature range 5000-50000K, are shown. The configuration mixing has been taken into account in calculation.

It is no possible to compare our data with other, since experimental data do not exist and we have not calculated Stark broadening data for the line treated by Lakićević (1983).

We have considered the influence of the Stark broadening mechanism on Co II (λ=2307.85 Å) line in stellar plasma, by using the Kurucz's model atmospheres of an A type star (T_{eff}=10000K, log g=4), and with Wickramasinghe's models of DA (T_{eff}=10000K, log g=6) and DB (T_{eff}=15000K, log g=7) white dwarf atmospheres. The results of our investigation are presented in Table 2 and Figs. 1 and 2.

Thermal Doppler and Stark widths as functions of optical depth, for the considered Co II line, are compared in Figs.1. and 2. for an A type star and DA and DB white dwarf, respectively. As one can see from Fig. 1, in photospheric layers of hot A type stars the Stark line width is one order of magnitude larger than thermal Doppler one. In higher layers of stellar atmospheres (τ≈-4) however, the thermal Doppler mechanism is more important. In Fig. 2 one can see, that in the case of DA and DB white dwarf atmospheres Stark broadening mechanism is important in all atmospheric layers, especially in deeper layers, where the Stark width is two or three orders of magnitude larger than the thermal Doppler width.

Table 1. Stark (full) widths and shifts for the Co II λ=2307.85Å spectral line. The electron density is $10^{23}m^{-3}$.

Transition	T(K)	Stark FWHM (Å)	d(Å)
$a^5F_4 - z^5G^0_5$ λ=2307.85 Å	5000	0.751E-01	-0.182E-01
	10000	0.524E-01	-0.130E-01
	20000	0.363E-01	-0.928E-02
	30000	0.293E-01	-0.768E-02
	40000	0.253E-01	-0.675E-02
	50000	0.227E-01	-0.608E-02

Table 2. Thermal Doppler and Stark full widths for the Co II λ=2307.85Å line as a function of optical depth for a DA white dwarf model (T_{eff}=10000K, log g=6).

τ	T(K)	log(p_e)	Stark FWHM (Å)	Thermal Doppler FWHM (Å)
0.00	7009	1.068	0.762E-04	0.342E-03
0.05	8034	2.599	0.210E-02	0.366E-03
1.25	11501	4.211	0.498E-01	0.438E-03
2.00	12474	4.413	0.701E-01	0.457E-03
6.00	14914	4.657	0.935E-01	0.499E-03
10.00	16102	4.716	0.953E-01	0.519E-03

Table 3. Thermal Doppler and Stark full widths for the Co II λ=2307.85Å line as a function of optical depth for a DB white dwarf model (T_{eff}=15000K, log g=7).

τ	T(K)	log(p_e)	Stark FWHM (Å)	Thermal Doppler FWHM (Å)
0.00	8998	2.465	0.130E-02	0.388E-03
0.05	9158	3.815	0.253E-01	0.406E-03
1.25	13859	4.877	0.173	0.481E-03
2.00	14847	5.062	0.239	0.498E-03
6.00	18222	5.699	0.758	0.552E-03
10.00	19934	6.000	1.320	0.577E-03

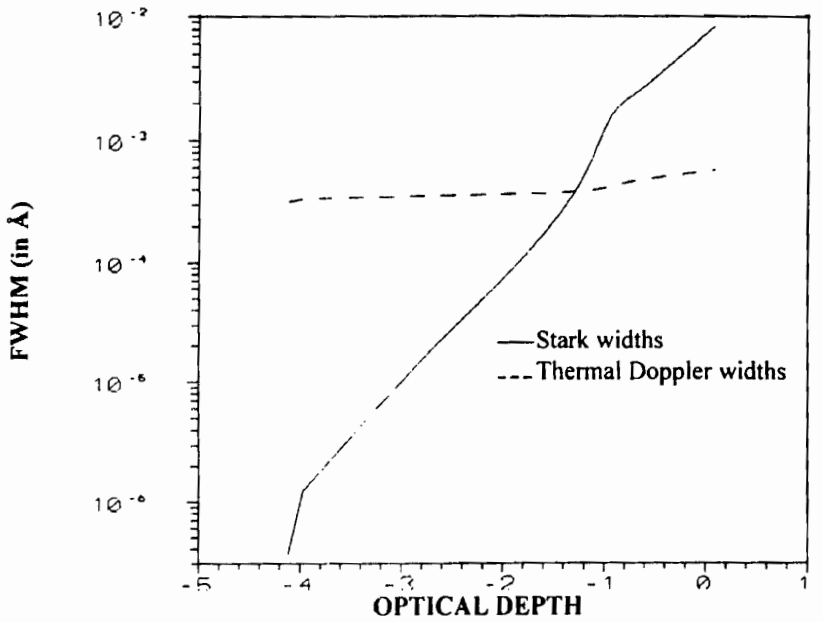

Fig. 1. Thermal Doppler and Stark full widths for the Co II λ=2307.85 Å line as functions of optical depth for an A type star (T_{eff}=10000K, log g=4).

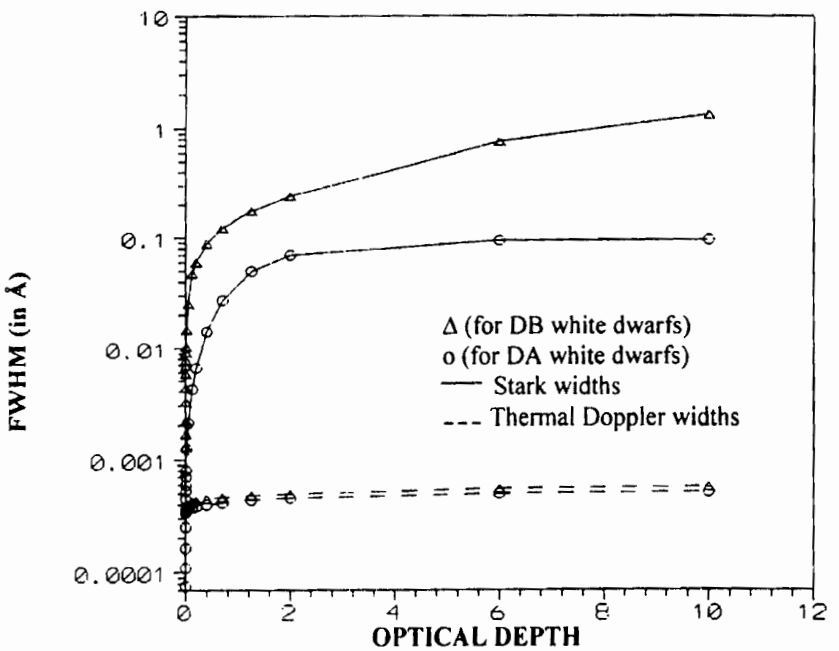

Fig. 2. Thermal Doppler and Stark full widths for the Co II λ=2307.85 Å line as functions of optical depth for DA (T_{eff}=10000K, log g=6) and DB (T_{eff}=15000K, log g=7) models.

ACKNOWLEDGEMENT

This work is a part of the project "**Astrometrical, Astrodynamical and Astrophysical Investigations**".

References

Bates, D. R. and Damgaard, A: 1949, Trans. Roy. Soc. London, Ser. A **242**, 101.
Bolcal, C. and Didelon P.: 1987, *Elemental Abundance Analyses*, Istitut d'Astronomie de l'Université de Lausane, Chavannes-des-Bois, Switzerland, p.152
Dimitrijević, M. S.: 1989, *Bull. Obs. Astron. Belgrade* **140**, 111.
Dimitrijević, M. S. and Konjević, N.: 1980, JQSRT, **24**, 454.
Dimitrijević, M. S. and Konjević, N.: 1981, *Spectral Line Shapes*, Berlin, New York.
Kurucz, R. L.: 1979, Astrophys. J. Suppl. Series, **120**, 373.
Lakićević, I. S., Astron. Astrophys.: 1983, **127**, 37.
Pickering, J. C, Raassen, A. J. J., Uylings, P. H. M. and Johansson, S.: 1998, Astrophys. J. Suppl. Series, **117**, 261.
Popović, L. Č. and Dimitrijević, M. S.: 1996, Phys. Scr., **53**, 325.
Smith, K. I. and Dworetsky, M. M.: 1993, Astron. Astrophys., **274**, 335.
Wickramasinghe, D. T.: 1972, Mem. R. Astron. Soc., **76**, 129.

Journal of Research in Physics Vol. 28, No. 3, 303-305 (1999)

THE ELECTRON-IMPACT EFFECT IN Hg-Mn STARS: ASTROPHYSICAL IMPORTANT Zr III LINES

Luka Č. Popović and Milan S. Dimitrijević
Astronomical observatory, Volgina 7, Yu-11000 Belgrade, Serbia

1. INTRODUCTION

As it is very well known the Hg-Mn stars are non-magnetic late B type stars. In their spectra unusually strong lines of many heavy ions are present (see e.g. Preston 1971, Heacox 1979, Dworetsky 1980, Adelman 1987, Lecrone et al. 1993, Wahlgren et al. 1995). In A and B type stars the electron-impact broadening is the main pressure broadening mechanism (e.g. Dimitrijević 1989). Considering that the resonant lines of ionized heavy elements (z>30) are located in the ultraviolet spectral region, the abundance analysis of these elements has become possible due to satellite observations by high resolution spectrograph as e.g. International Ultraviolet Explorer (IUE) satellite or Goddard High Resolution Spectrograph (GHSR) installed at Hubble Space Telescope. The number of heavy ion lines observations with the higher photometric quality and spectral resolution is growing up. Consequently, experimental and theoretical spectroscopic data for modeling of these lines are required.

In order to investigate the Hg-Mn star atmospheres as well as other types of hot stars, the Stark broadening parameters for heavy ion lines are needed. Zr III lines are presented in spectra of Hg-Mn stars. E.g. in spectra of Chi Lupi, a B-type star, well-resolved lines of Zr III λ = 1937.22 Å, 1940.24 Å and 1941.06 Å have been observed. Here we present the electron-impact broadening parameters for these four astrophysical important Zr III lines as a function of temperature, calculated by using the modified semi-empirical approach (Dimitrijević and Konjević 1980, Popović and Dimitrijević 1996).

2. RESULTS AND DISCUSSION

The atomic energy levels needed for the calculations were taken from Reader and Acquista (1997). Oscillator strengths have been calculated by using the method

of Bates and Damgaard (1949) and the tables of Oertel and Shomo (1968). For calculation of Stark broadening widths the modified semi-empirical apporach has been used (Dimitrijević and Konjević 1980, Popović and Dimitrijević 1996)

Results obtained using the MSE approach for electron – impact line widths and shifts for three Zr III lines as a function of temperature are presented in Tables 1. The calculations have been performed for a perturber density of $10^{23}\mathrm{m}^{-3}$, since within the MSE formalism, the results for the electron-impact broadening parameters are linear with electron density.

Table 1. Stark widths (FWHM) of Zr III spectral lines at an electron density of $10^{23}\mathrm{m}^{-3}$ as a function of temperature.

Transition	T (K)	W (nm)
$a^3P_1 - z^3P_1^0$	5000	.452E-02
	10000	.317E-02
	20000	.220E-02
λ=194.662 nm	30000	.178E-02
	40000	.153E-02
	50000	.137E-02
$a^3P_0 - z^3P_1^0$	5000	.447E-02
	10000	.314E-02
	20000	.218E-02
λ=193.665 nm	30000	.176E-02
	40000	.152E-02
	50000	.136E-02
$a^3P_2 - z^3P_2^0$	5000	.474E-02
	10000	.332E-02
	20000	.231E-02
	30000	.187E-02
λ=194.106 nm	40000	.161E-02
	50000	.144E-02
$a^1G_4 - z^1F_3^0$	5000	.459E-02
	10000	.321E-02
	20000	.224E-02
	30000	.181E-02
λ=194.020 nm	40000	.156E-02
	50000	.140E-02

There is no experimental data for the Stark broadening parameters of Zr III spectral lines, and such data will be of importance for the refinement of the Stark broadening theory for spectral lines from complex spectra.

References

Adelman S. J.: 1987, Mon. Not. R. Astron. Soc. **228**, 573.

Bates D.R. and Damgaard A.: 1949, Trans. Roy. Soc. London, Ser. A **242**, 101.

Dimitrijević M. S.: 1989, Bull. Obs. Astron. Belgrade **140**, 111.

Dimitrijević M. S. and Konjević N.: 1980, J. Quant. Spectrosc. Radiat. Transf. **24**, 454.

Dworetsky M. M.: 1980, Astron. Astrophys. **84**, 350.

Heacox W. D.: 1979, Astrophys. J. Supl. Series **41**, 675.

Leckrone D. S., Wahlgren G. M., Johansson S. G., Adelman S. J.: 1993, ASP Conference Series **44**, 42

Oertel G.K. and Shomo L.P.: 1968, Astrophys. J. Supl. Series **16**, 175.

Preston G. W.: 1971, Publ. Astron. Soc. Pac. **83**, 571.

Popović L. Č. and Dimitrijević M. S.: 1996, Phys. Scr. **53**, 325.

Reader J. and Acquista N.: 1997, Phys. Scr. **55**, 310.

Wahlgren G. M., Leckrone D. S., Johansson S. G., Rosberg M. and Brage T.: 1995, Astrophys. J. **444**, 438.

Journal of Research in Physics Vol. 28, No. 3, 307-309 (1999)

BELDATA - THE ASTRONOMICAL DATABASE OF ASTRONOMICAL OBSERVATORY: STARK BROADENING DATA INVESTIGATIONS

L. Č. POPOVIĆ, M. S. DIMITRIJEVIĆ, N. D. MILOVANOVIĆ and N. TRAJKOVIĆ
Astronomical Observatory, Volgina 7, YU-11000 Belgrade, Serbia
lpopovic@aob.bg.ac.yu

1. INTRODUCTION

In early-type stars like B and A stars and white dwarfs, Stark broadening is the main pressure broadening mechanism, and the corresponding Stark broadening parameters are of interest for a number of investigations related to stellar plasma. One may mention as examples calculation of stellar opacities, stellar atmospheres modeling and investigations, abundance determinations, interpretation and modeling of stellar spectra and investigation and modeling of subphotospheric layers.

The interest for a very extensive list of line broadening data is additionally stimulated by the development of space astronomy where an extensive amount of spectroscopic information over large spectral regions of all kind of celestial objects has been and will be collected, stimulating the spectral-line-shape research. Consequently, the interest not only for abundant, but also for trace elements data increases. Not only in astrophysics, but also in physics and plasma technology, a number of problems depend on very extensive list of elements and line transitions with their atomic and line broadening parameters. One may mention as examples laboratory plasma diagnostic, research and modeling, radiative transfer calculations and investigation of laser produced plasmas (not only in laboratory but as well in industry during the laser welding, melting and evaporation of different targets), and plasma created in fusion research (particularly inertial confinement and pellet compression fusion), development and modeling of lasers, as well as of light sources.

In a series of papers, large scale calculations of Stark broadening parameters for a number of spectral lines of various emitters (Dimitrijević, 1996, 1997 and references therein) performed on Belgrade Observatory have been published. In order to complete as much as possible Stark broadening data needed for astrophysical and laboratory plasma research and stellar opacities calculations we are making a continuous effort to provide Stark broadening data for a large set of atoms and ions. Our calculations have been performed within the semiclassical - perturbation formalism (Sahal-Bréchot, 1969ab), for transitions when a sufficiently complete set of reliable atomic data exist and the good accuracy of obtained results is expected. From a large set of data for Stark broadening parameters we are going to make a database.

2. CONTENTS OF THE DATABASE

Extensive calculations have been performed, up to now (Dimitrijević, 1996, 1997 and references therein) for a number of radiators, and consequently, Stark broadening parameters for 79 He I, 62 Na, 51 K, 61 Li, 25 Al, 24 Rb, 3 Pd, 19 Be, 270 Mg, 31 Se, 33 Sr, 14 Ba, 189 Ca, 28 Ca II, 30 Be II, 29 Li II, 66 Mg II, 64 Ba II, 19 Si II, 3 Fe II, 2 Ni II, 12 B III, 23 Al III, 10 Sc III, 27 Be III, 32 Y III, 20 In III, 2 Tl III, 10 Ti IV, 39 Si IV, 90 C IV, 5 O IV, 114 P IV, 2 Pb IV, 19 O V, 30 N V, 25 C V, 51 P V, 34 S V, 26 V V, 30 O VI,

21 S VI, 2 F VI, 14 O VII, 10 F VII, 10 Cl VII, 20 Ne VIII, 4 K VIII, 4 Ca IX, 30 K IX, 8 Na IX, 57 Na X, 48 Ca X, 4 Sc X, 7 Al XI, 4 Si XI, 18 Mg XI, 4 Ti XI, 10 Sc XI, 9 Si XII, 27 Ti XII, 61 Si XIII and 33 V XIII multiplets become available.

Data for particular lines of F I, B II, C III, N IV, Ar II, Ga II, Ga III, Cl I, Br I, I I, Cu I, Hg II, N III, F V and S IV also exist.

In order to complete as much as possible the needed Stark broadening data, Belgrade group (Milan S. Dimitrijević, Luka Č. Popović, Vladimir Kršljanin, Dragana Tankosić, Nenad D. Milovanović) used the modified semiempirical approach developed by Dimitrijević and Konjević 1980 for radiators where there is not a sufficiently complete atomic data set for reliable semiclassical calculations. The width and in some cases the shift data for the most intensive lines for the following atom and ion species were calculated by them: Ar II, Ti II, Mn II, Fe II, Pt II, Bi II, Zn II, Cd II, As II, Br II, Sb II, I II, Xe II, La II, Y II, Zr II, Sc II, Be III, B III, Mn III, Ga III, Ge III, S III, As III, Se III, Zn III, Mg III, Ca III, La III, C III, N III, O III, F III, Ne III, Na III, Al III, Si III, P III, S III, Cl III, Ar III, B IV, Cu IV, Ge IV, C IV, N IV, O IV, Ne IV, Mg IV, Si IV, P IV, S IV, Cl IV, Ar IV, C V, O V, F V, Ne V, Al V, Si V, N VI, F VI, Ne VI, Si VI, P VI, and Cl VI lines.

3. THE STRUCTURE OF THE DATABASE

Astronomical Database System has as a goal to provide the fast and easy data exchange between Internet users and database. Astronomical Database will be placed on server of the Astronomical Observatory in Belgrade. Access will be managed through Internet with 24 hour online support on address http://www.aob.bg.ac.yu/BELDATA. Astronomical Observatory already has Internet presentation on http://www.aob.bg.ac.yu but Astronomical Database is not in function yet.

The atomic data, part of BELDATA system, will be based on the following components (Fig. 1.):

1. Database is the Stark broadening data set.
2. HTTPD (Hyper Text Transfer Protocol Daemon) or www server that has role to provide mutual HTML document communication between Internet and local server.
3. MI (Manager Interface) will transform HTML format document from HTTPD in appropriate form for DataBase Manager System.
4. DBMS (DataBase Manager System) is capable for manipulating with the database. After data processing DBMS will retrieve the data.

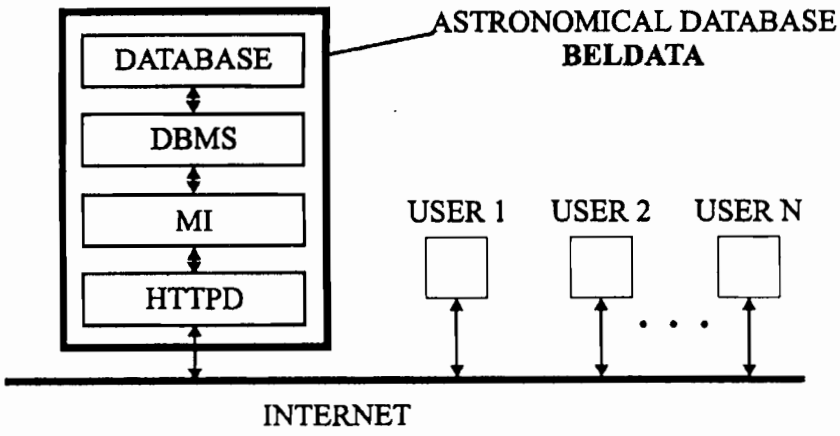

Fig. 1. Scheme of the Astronomical Database

The data will be taken by MI, transformed to HTML format document and proceeded by HTTPD over Internet to user.

Query form, which will be fulfilled by an Internet user, have two return option: data needed for laboratory plasma modeling and data needed for stellar plasma modeling. In future, BELDATA will be extended with spectra of active galactic nuclei and solar spectra. New Stark broadening parameter data will be added to the database when calculated.

Whole system needs constant maintenance effort. Moreover, we have planned to expand capabilities of DBMS. Presently, it is one executable program which may take the needed data from the database but in the future it will be a complex system with numerous functions. These functions will include various database multiple search options fully configurable within one HTML form controlled by user.

References

Dimitrijević, M. S.: 1996, *Zh. Prikl. Spektrosk.*, **63**, 810.
Dimitrijević, M. S.: 1997, *Astrophys. Space Sci.*, **252**, 415.
Dimitrijević, M.S., and Konjević, N.: 1980, *JQSRT*, **24**, 451.
Sahal-Bréchot, S.: 1969a, *Astron.Astrophys.*, **1**, 91.
Sahal-Bréchot, S.: 1969b, *Astron.Astrophys.*, **2**, 322.

Journal of Research in Physics Vol. 28, No. 3, 315-318 (1999)

BELGRADE MERIDIAN CIRCLE OBSERVATIONS OF STARS OF INTEREST FOR THE INVESTIGATIONS OF THE STARK BROADENING INFLUENCE ON STELLAR SPECTRAL LINES

MILAN S. DIMITRIJEVIĆ, ZORICA CVETKOVIĆ AND MIODRAG DAČIĆ
Astronomical Observatory, Volgina 7, 11000 Belgrade, Yugoslavia
E-mail mdimitrijevic@aob.bg.ac.yu
E-mail mdacic@aob.bg.ac.yu
E-mail zcvetkovic@aob.bg.ac.yu

Abstract. Belgrade meridian circle observations of stars of B6-A9 spectral type, which are of interest for the investigations of the Stark broadening influence on stellar spectra has been reviewed. In spectra of such stars the Stark broadening is the dominant pressure broadening mechanisme and data on their positions (right ascension and declination) are needed e.g. for the formulation of projects for space telescopes.

1. INTRODUCTION

Stark broadening data are of interest for a number of astrophysical problems as diagnostics and modeling of stellar plasma, abundance research, stellar spectra interpretation and modeling, radiative transfer etc. Among different pressure broadening mechanisms, Stark broadening is the dominant one for stars with the effective temperature larger or of the order of magnitude of 10000 K. Such stars are A, B and O type stars and white dwarfs. However, for O stars and early B type stars, electron density is so small that the pressure broadening is negligible in comparison with Doppler broadening, except for transitions involving high principal quantum numbers. The most interesting stars for the investigation of Stark broadening influence on stellar spectral lines are white dwarfs, A type and late B type stars.

With the placement of telescopes on the orbit around the Earth, and with the development of satellite observations, it becomes possible to investigate spectral lines of even trace elements and their ions. Now exist possibilities to formulate and submit various observational projects with the use of telescopes and various devices on orbit. One can see from instructions for project applications for observations with the help of Hubble Space telescope (Madau, 1994), that basic data needed, are the name of target and its precise position (right ascension and declination), total apparent magnitude, instrumental configuration and operation mode, as well as spectral elements and wavelength range. For application is needed also the number of the telescope orbits needed for observation and additional comments and requests if exist.

As one can see, the object position is one of very important basic data needed for the project application. The aim of this paper is to review observational data for the B6-A9 spectral type stars obtained with the Belgrade Meridian circle. For such stars The Stark broadening mechanism is the dominant pressure broadening mechanism, so that such data may be used for the formulation of eventual projects for stellar spectral lines investigations with the help of the Hubble telescope and similar devices on satellites.

2. B6-A9 SPECTRAL TYPE STAR OBSERVATIONS WITH THE BELGRADE MERIDIAN CIRCLE

Seven observational catalogues have been done from 1968 to 1995 on the Belgrade meridian circle, an instrument typical for astrometrical observations. During this period of almost three decads, positions of a large number of stars were determined, among them B6-A9 spectral type star positions, of interest for Stark broadening investigations. So we will review observational programs realized on the Belgrade meridian circle and will show the number of B6-A9 spectral type stars included.

The first observational program was the Belgrade Catalogue of Latitude Stars with 3957 stars included, which declinations have been determined with the relative method (Sadžakov and Šaletić, 1972). After this, follows the catalogue of right ascensions and declinations of Northern chemisphere zenith telescopes (NPZT) program stars. This catalogue (Sadžakov et al., 1981) contains the positions of 1638 stars, with more than 300 fundamental stars within the FK4 system.

From 1981 to 1987, the double star positions were determined (Sadžakov i Dačić, 1990), for stars whose components were not separable photographically or photoelectrically at that time. Among these stars, which number in our program is 1576, we found 483 stars with the spectral type within the B6-A9 range. We can obtain their positions for J2000.0 epoch and choose most interesting for spectral line investigations with the help of the Hubble telescope.

The Catalogue of stars in the vicinity of radio sources (Sadžakov et al., 1991) was done from 1982 up to 1987. With this catalogue, Belgrade observatory gave its contribution to the efforts to conect optical and radio interferometrical observations, i.e. to make transfer from the dynamical to the kinematical reference system. This program contains around 300 stars and we identified 48 B6-A9 spectral type stars.

Moreover, several smaller observational stellar catalogues have been made with the Belgrade meridian circle. The program of Ondrejov photograph zenith telescope contained 223 stars observed within 1985-1990 periode (Sadžakov et al., 1992). Among them 71 stars are of interest for this article.

Within the period when Hipparcos was collecting the data, high luminosity stars (HLS) and radio stars have been observed with the Belgrade meridian circle (Sadžakov et al., 1996). In the same time stars from an enlarged list of stars in the vicinity of radio sources have been observed (Sadžakov et al., 1997). In the list of FK5 fundamental stars observed for this programs, 138 B6-A9 spectral type stars have been identified..

We show here as example, a page from a catalogue of stellar positions. One can see that besides the position (right ascension and declination), some additional

Table 1. One page of the observational catalogue

No	BD	m_v	S_p	α	E_p	δ	E_p
1	41.04933	6.1	A2	0 02 02.099	1984.31	41 48 50.61	1984.31
2	36.00004	8.8	A5	0 06 16.094	1984.30	36 56 14.48	1984.30
3	45.00016	8.1	A3	0 07 26.710	1983.61	46 06 44.22	1983.61
4	53.00025	8.3	A0	0 11 56.656	1983.61	53 32 59.22	1983.61
5	42.00041	6.1	A0	0 13 43.563	1984.30	43 19 02.62	1984.30
6	53.00031	7.8	A3	0 14 01.491	1983.61	54 22 57.10	1983.62
7	35.00035	7.1	A0	0 14 06.000	1984.33	36 21 09.10	1984.30
8	25.00029	7.6	A2	0 15 54.438	1984.30	25 51 48.08	1984.30
9	53.00054	8.8	A5	0 20 09.390	1984.30	54 03 08.22	1984.30
10	-4.00040	7.8	A0	0 21 26.482	1983.87	-3 45 07.12	1983.87
11	70.00039	8.0	A0	0 39 31.085	1983.61	71 05 32.49	1984.11
12	32.00124	8.1	A3	0 41 40.970	1985.08	33 20 40.35	1984.98
13	50.00143	7.2	A0	0 45 08.322	1985.08	51 10 20.64	1985.08
14	68.00057	8.0	A2	0 49 33.628	1983.61	68 35 41.36	1983.61
15	51.00179	6.3	A0	0 50 53.942	1983.62	52 25 06.37	1983.61
16	-19.00147	7.2	A0	0 55 09.602	1984.39	-19 16 07.80	1984.39
17	43.00193	6.0	B9	0 57 13.070	1985.08	44 26 39.05	1985.08
18	46.00241	8.0	A0	0 59 53.927	1983.62	47 25 49.76	1983.61
19	-20.00191	8.7	A2	1 02 46.099	1984.39	-20 07 21.62	1984.24
20	46.00285	9.0	A0	1 09 09.629	1985.08	46 44 07.43	1985.08
21	50.00236	8.9	A0	1 09 19.693	1984.06	51 15 35.44	1984.31
22	48.00392	7.1	A0	1 14 49.088	1985.08	48 44 43.70	1985.08
23	53.00271	8.2	A2	1 14 57.706	1985.08	53 39 14.55	1985.08
24	65.00151	8.3	A0	1 15 34.065	1984.31	65 53 42.70	1984.31
25	36.00220	6.4	A3	1 15 56.394	1985.08	37 07 24.94	1985.08
26	72.00069	7.3	A0	1 20 18.976	1984.31	72 35 11.89	1984.31
27	-25.00555	6.8	A5	1 21 11.773	1985.09	-24 36 49.62	1985.09
28	-6.00270	6.8	A0	1 22 29.358	1985.08	-6 12 22.44	1985.08
29	2.00211	6.6	B8	1 24 18.352	1985.08	3 16 35.60	1985.08
30	35.00296	8.3	A2	1 31 18.652	1984.31	35 56 03.84	1984.31

characteristics enabling better identification of the star and the epoch of observation are included. The columns of the shown example represent :

The first column - the ordinal number (for the program or for the given list);

The second column - the number according to the Bon list (Bonner Durchmusterung) which contains more than 300000 northern sky stars up to 9.5 apparent magnitude;

The third column - visual apparent stellar magnitude;

The fourth column - spectral type;

The fifth column - right ascension (hour, minute and second of time);

The sixth column - epoch of the right ascension observation (determination);

The seventh column - declination (degree, minute and second of arc);

The eighth column - epoch of the declination observation (determination);

We hope that this review of Belgrade meridian circle observation and corresponding observational data will be of help to our colleagues wishing to prepare projects for satellite telescopes.

References

Madau, P. (ed.) : 1994, "Hubble Space Telescope, Cycle 5, Phase I Proposal Instructions, Space Telescope Science Institute, (Version 4.0, June 1994), 9.

Sadžakov, S., Šaletić, D. : 1972, "Catalogue of declinations of the latitude programme stars (KŠZ)", *Publ. Obs. Astron. Belgrade*, **17**.

Sadžakov, S., Šaletić, D., Dačić, M. : 1981,"Catalogue of NPZT programme stars", *Publ. Obs. Astron. Belgrade*, **30**.

Sadžakov, S., Dačić, M. : 1990, "Belgrade catalogue of double stars" *Publ. Obs. Astron. Belgrade*, **38**.

Sadžakov, S., Dačić, M., Cvetković, Z. : 1991, *Astron. Journal*, **101**, 713.

Sadžakov, S., Dačić, M., Cvetković, Z. : 1992, *Bull. Astron. Belgrade*, **146**, 1.

Sadžakov, S., Dačić, M., Cvetković, Z. : 1996, *Bull. Astron. Belgrade*, **153**, 1.

Sadžakov, S., Dačić, M., Cvetković, Z. : 1997, *Bull. Astron. Belgrade*, **155**, 3.

Mem. S.A.It. Suppl. Vol. 15, 126

Memorie della
Supplementi

Stark broadening of spectral lines of inert gases

Magdalena Christova[1] and Milan S. Dimitrijević[2,3]

[1] Technical University of Sofia, Department of Applied Physics, Sofia, Bulgaria
e-mail: mchristo@tu-sofia.bg
[2] Astronomical Observatory, Volgina 7, 11060 Belgrade, Serbia
[3] Laboratoire d'Étude du Rayonnement et de la Matière en Astrophysique, UMR CNRS 8112, Observatoire de Paris-Meudon, 92195 Meudon, France
e-mail: mdimitrijevic@aob.bg.ac.yu

Abstract. We summarize our previous results for Stark broadening parameters (width and shift) with application for astrophysical purposes, especially for diagnostics of hot stars and their atmospheres. The calculated results for Stark broadening parameters of several Ar I and Ne I lines in the wide temperature range have been analyzed. The comparison of results for analogous transitions has been presented.

Key words. Atomic processes: Stark broadening, Line broadening, Plasma diagnostics

1. Introduction

Stark broadening parameters are of interest for a number of problems in astrophysics, physics and laboratory plasma. They are needed in order to solve various problems, for example, diagnostics and modeling of stellar and laboratory plasma, investigation of its physical properties and for abundance determination. These investigations provide information useful for the modeling of stellar evolution, for the processes occurring within the stellar interiors, and radiative transfer in stellar atmospheres.

Stark broadening parameters of spectral lines of inert gases can play an important role in astrophysics. From one side, helium is the most abundant element after hydrogen in the universe and reliable Stark broadening data for He lines are of particular interest in the spectroscopic study of astrophysical plasma (Dimitrijević and Sahal-Bréchot 1984). From the other side, with the development of space-born spectroscopy, the importance of atomic data, including the Stark broadening parameters, for trace elements like neon and argon, increases. Argon lines are observed in the optical spectrum of Be star Hen 2-90 (Kraus et al. 2005), as well as in planetary nebulae and H II regions in the two dwarf irregular galaxies Sextans A and B (Kniazev et al. 2005). For the first time, the discovery of photospheric neon and argon lines in very hot central stars of planetary nebulae and white dwarfs is reported in (Werner et al. 2007a,b). In the new NLTE model atmospheres the Stark broadening of argon lines is included (Werner et al. 2007b). Therefore, there is a need for Stark broadening results for spectral lines of inert gases. Factors governing the broadening of spectral lines in plasmas are plasma environment and atomic structure of emitting atom. Observed regularities in atomic data (wavelengths and energy levels, oscillator strengths, collision cross sec-

Send offprint requests to: M. Christova

tions and other quantities) and similarities, result in the regularities and similarities of the width and shift parameters of plasma broadened lines.

In this paper we show the similarities and regularities of Stark broadening parameters (Dimitrijević et al. 2007; Christova et al. 2009a,b) within one spectral series at high temperatures, of interest for the study of hot stars and their atmospheres. Additionally, we give a comparison of calculated Stark broadening parameters of Ne I 837.7 nm and Ar I 737.2 nm which have analogous transitions $2p^5 3d$ - $2p^5 3p$ and $3p^5 4d$ - $3p^5 4p$, respectively.

2. Theory

Within the semi-classical perturbation formalism (Sahal-Bréchot 1969a,b), the full half width (W) and the shift (d) of an isolated line originating from the transition between the initial level i and the final level f is expressed as:

$$W = 2n_e \int_0^\infty v f(v) dv \left[\sum_{i' \neq i} \sigma_{ii'}(v) + \right. \\ \left. + \sum_{f' \neq f} \sigma_{ff'}(v) + \sigma_{el} \right] \quad (1)$$

$$d = \int_0^\infty v f(v) dv \int_{R_3}^{R_d} 2\pi \rho d\rho \sin 2\varphi_p \quad (2)$$

where i' and f' are perturbing levels, n_e and v are the electron density and the velocity of perturbers respectively, and $f(v)$ is the Maxwellian distribution of electron velocities.

The inelastic cross sections $\sigma_{ii'}(v)$ (respectively $\sigma_{ff'}(v)$) can be expressed by an integration of the transition probability $P_{ii'}$ over the impact parameter ρ:

$$\sum_{i' \neq i} \sigma_{ii'}(v) = \frac{1}{2}\pi R_1^2 + \\ + \int_{R_1}^{R_d} 2\pi \rho d\rho \sum_{i' \neq i} P_{ii'}(\rho, v) \quad (3)$$

The elastic collision contribution to the width is given by:

$$\sigma_{el} = 2\pi R_2^2 + \int_{R_2}^{R_d} 8\pi \rho d\rho \sin^2 \delta \quad (4)$$

$$\delta = \left(\varphi_p^2 + \varphi_q^2 \right)^{1/2} \quad (5)$$

The phase shifts ϕ_p and ϕ_q are due to the polarization and quadrupole potential respectively. The cut-offs parameters R_1, R_2, R_3, the Debye cut-off R_d and the symmetrization procedure are described in (Sahal-Bréchot 1969a,b).

The impact approximation is valid when strong collisions are separated in time, or when the duration of collisions is much shorter than the separation time between strong collisions: $C_1 = n_e \pi \rho_{typ}^3 << 1$, where ρ_{typ} is typical impact parameter for strong collisions. C_1 is the impact approximation validity criterion.

The resulting profiles are Lorentzian. This condition is well verified for electron collisions for a large range of densities. For ion collisions the impact approximation might fail, especially for high densities or low temperatures.

3. Discussion

3.1. Argon

Theoretical results for spectral lines from one spectral series

We present results for the Stark broadening coefficient of argon lines from spectral series $3p^5 nd$ - $3p^5 4p$ for n = 4 – 7: 522.1, 549.6, 603.2 and 737.2 nm. The corresponding atomic data from NIST catalogue are given in Table 1. The analysis of the contribution of particular atomic processes to the Stark broadening parameters shows a similar behavior within the spectral series.

For the considered spectral lines, we obtain the similar behavior with temperature of the total broadening coefficient ($\beta = W / n_e$) and its components. In Figure 1 we illustrate this behavior with an example for Ar I 522.1 nm spectral line. The resulting broadening coefficient is: $\beta = \beta_{in} + \beta_{el}$, where β_{in} is the contribution

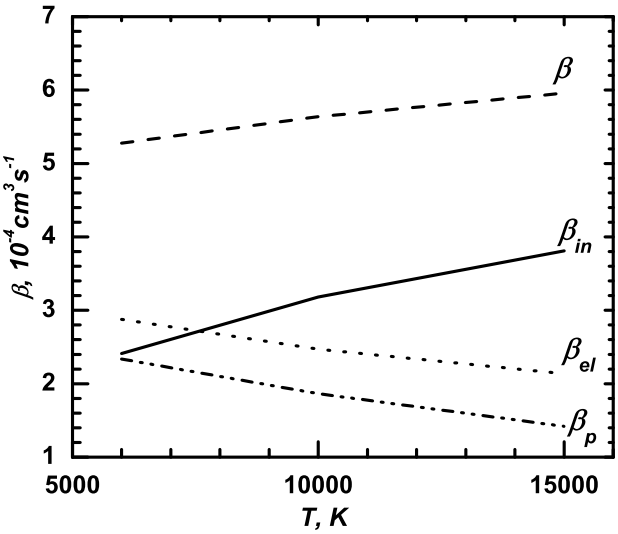

Fig. 1. Stark broadening coefficient ($\beta = W / n_e$) and its components (β_{in}, β_{el}, β_p and β_q) versus the temperature for Ar I 522.1 nm.

Table 1. Basic data on the considered Ar I spectral lines. Here λ denotes wavelength, i and f are initial and final level of the transition (within the frame of $j - L$ coupling), i' and f' are the corresponding perturbing levels, E_i and E_f are the energy values and n* is the effective quantum number of the initial level.

λ nm	Transition (i - f)	i' levels	f' levels	E_i cm^{-1}	E_f cm^{-1}	n*
522.1	$3p^5 7d - 3p^5 4p$ $^2[7/2]^o_4$-$^2[5/2]_3$	5f, 6f, 7f, 8f, 9f, 5p, 6p, 7p, 8p, 9p	4s, 5s, 6s, 3d, 4d, 5d, 6d	124610	105463	6.62
549.6	$3p^5 6d - 3p^5 4p$ $^2[7/2]^o_3$-$^2[5/2]_3$	4f, 5f, 6f, 7f, 4p, 5p, 6p, 7p	4s, 5s, 6s, 3d, 4d, 5d, 6d	123653	105463	5.63
603.2	$3p^5 5d - 3p^5 4p$ $^2[7/2]^o_4$-$^2[5/2]_3$	4f, 5f, 6f, 7f, 4p, 5p, 6p, 7p	4s, 5s, 6s, 3d, 4d, 5d, 6d	122036	105463	4.65
737.2	$3p^5 5d' - 3p^5 4p$ $^2[7/2]^o_4$-$^2[5/2]_3$	4f, 5f, 6f, 4p, 5p, 6p	4s, 5s, 6s, 3d, 4d, 5d, 6d	119024	105463	3.68

of the inelastic collisions, β_{el} is the contribution of elastic ones, $\beta_{el} = \beta_p + \beta_q$ (β_p gives the contribution of polarisation interactions and β_q – of the quadrupole interactions).

The quadrupole component (β_q) depends only on the initial and final states of the emitter and does not depend on the temperature and perturber density. It is not included in the figure, since from the behavior of β_{el} and β_p it is easy to conclude on its behavior too.

For all these lines the total coefficient and the component due to inelastic interac-

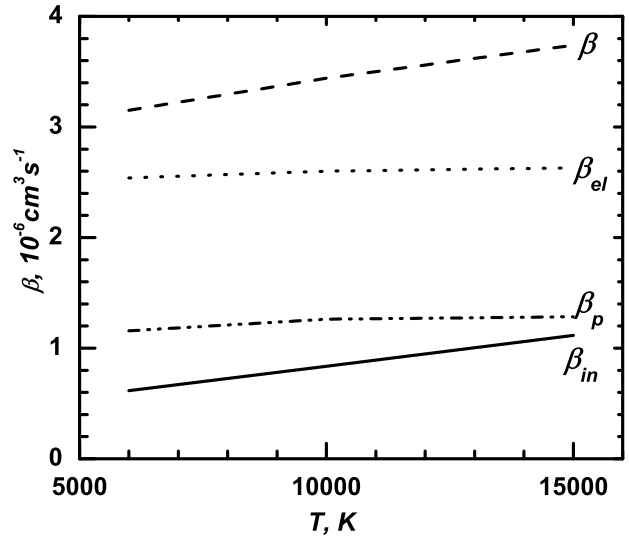

Fig. 2. Stark broadening coefficient ($\beta = W / n_e$) and its components (β_{in}, β_{el}, β_p and β_q) versus the temperature for Ar I 696.5 nm.

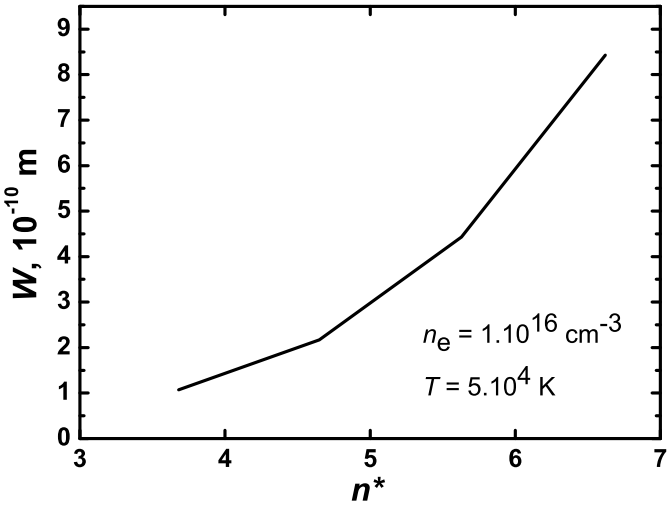

Fig. 3. Electron impact widths of Ar I spectral lines within the spectral series versus effective quantum number of the initial energy level for electron density of 10^{16} cm^{-3} and temperature of 5.10^4 K.

tions increase with the temperature, while β_p and β_{el}, respectively decrease with T. It means that the principal contribution to the broadening of these lines comes from inelastic collisions between emitters and surrounding particles. This contribution gives the trend of the total broadening coefficient in whole temperature interval.

The contribution of elastic collisions is dominated by the polarization interactions

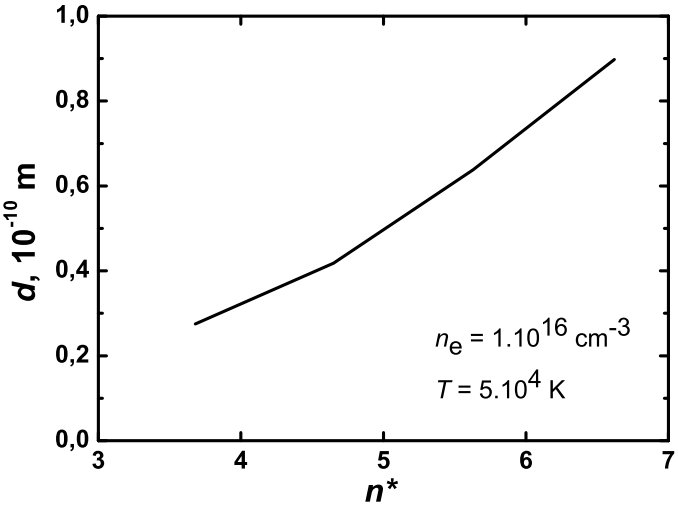

Fig. 4. Electron impact shifts of Ar I spectral lines within the spectral series versus effective quantum number of the initial energy level for electron density of 10^{16} cm^{-3} and temperature of 5.10^4 K.

($\beta_{el} >> \beta_q$). We note that: (i) the contribution of polarization interactions increases with effective quantum number; (ii) the principal contribution to the Stark broadening – 85% is due to the collisions with electrons.

For comparison, in the Figure 2 is shown the behavior of broadening coefficients for Ar I 696.5 nm line, which does not belong to the considered spectral series. The interactions which most contribute to the broadening of this line are the elastic ones. Their contribution practically does not vary with temperature. Namely the increase with T is very small. In this case, we found that the polarization and quadrupole components have the same values.

This means that the quadrupole contribution is larger for spectral lines emitted from lower energy levels. The smallest component in the total broadening for Ar I 696.5 nm is due to inelastic collisions between emitters and perturbers, four times lower than β_{el}. The conclusion is that the average free-electron energy is not so high for enough inelastic transitions to produce larger inelastic collision contribution to the line profile at the examined temperature interval. For this argon line, with low laying upper energy level, the contribution of collisions with ions is up to 30%. Therefore, for the considered transition involving lower energy levels, the quadrupole interactions and ion collisions play an important role in the total broadening, while the contribution of inelastic collisions is smallest. However, since the increase of β_{in} with temperature is largest, it gives the temperature trend to the β.

Often, the modeling of astrophysical objects needs atomic data for thousands and sometimes millions transitions. It is difficult and cumbersome to calculate the Stark broadening parameters for all these lines, so that methods enabling interpolation and extrapolation of the calculated results on the basis of similarities and systematic trends are of interest.

For example we can obtain new Stark broadening parameters from regularities within spectral series. In the next two figures we present the electron impact Stark width (Fig. 3) and shift (Fig. 4) for the argon lines (see Table 1) from the considered spectral series. Since, one of aims of this work is the applicability of Stark broadening results in the case of hot stars, we give our data for the temperature of 50 000 K, which is typical for DO white dwarfs where Stark broadening is important.

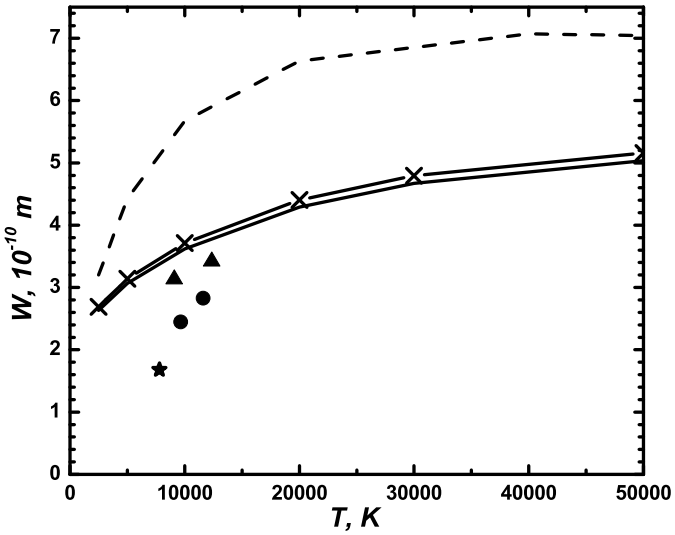

Fig. 5. Stark width of Ar I 549.6 nm versus temperature for electron density of 10^{16} cm^{-3}. (Theoretical results: dashed line - Griem (1964); solid line - Dimitrijević et al. (2007) for impact-electrons and impact-ions; solid line and cross symbols - Dimitrijević et al. (2007) for impact-electrons and quasistatic-ions; single symbols: experimental results from critical reviews (Lesage (2009) and references therein)

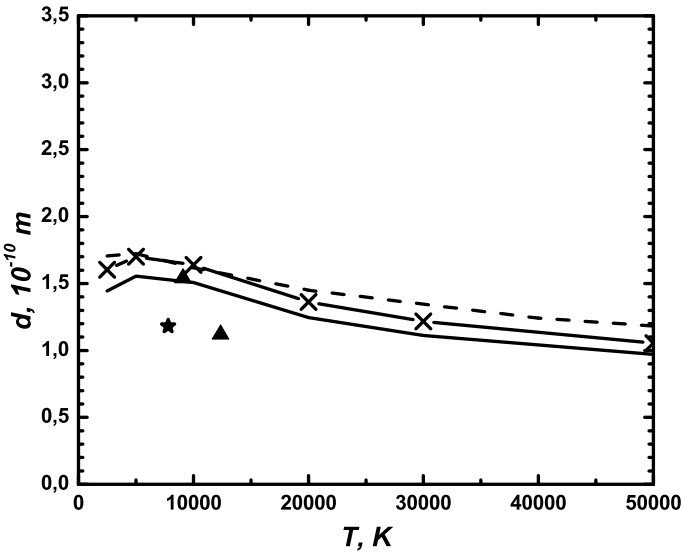

Fig. 6. Stark shift of Ar I 549.6 nm versus temperature for electron density of 10^{16} cm^{-3}. (Theoretical results: dashed line - Griem (1964); solid line - Dimitrijević et al. (2007) for impact-electrons and impact-ions; solid line and cross symbols - Dimitrijević et al. (2007) for impact-electrons and quasistatic-ions; single symbols: experimental results from critical reviews (Lesage (2009) and references therein)

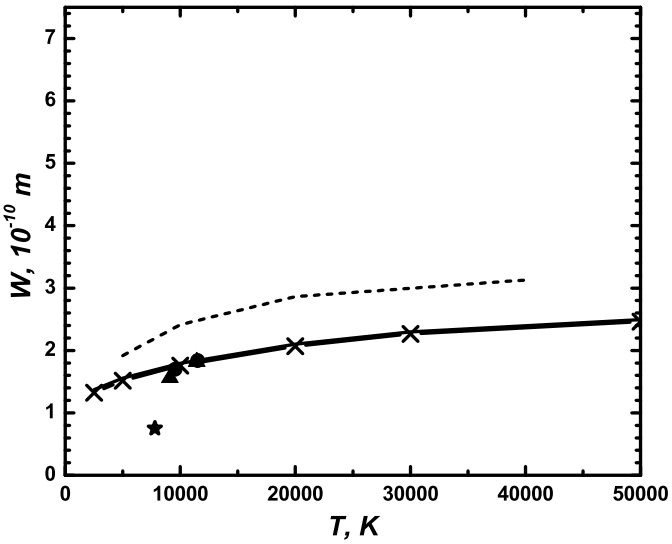

Fig. 7. Stark width of Ar I 603.2 nm versus temperature for electron density of 10^{16} cm^{-3}. (Theoretical results: dashed line - Griem (1974); solid line - Dimitrijević et al. (2007) for impact-electrons and impact-ions; solid line and cross symbols - Dimitrijević et al. (2007) for impact-electrons and quasistatic-ions; single symbols: experimental results from critical reviews (Lesage (2009) and references therein)

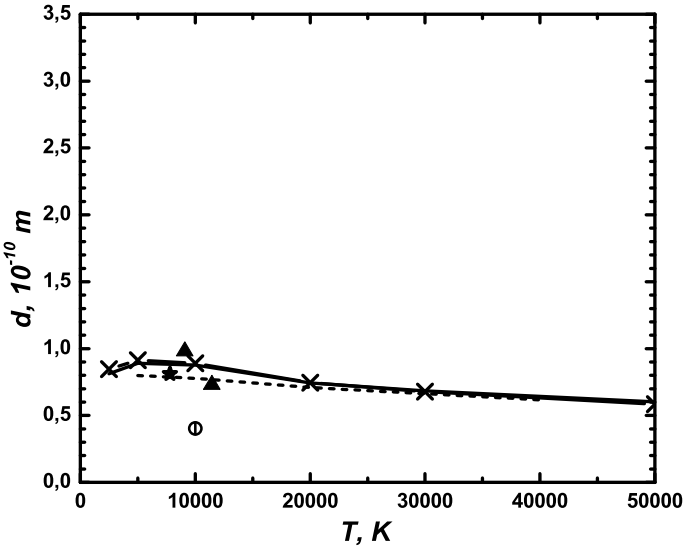

Fig. 8. Stark shift of Ar I 603.2 nm versus temperature for electron density of 10^{16} cm^{-3}. (Theoretical results: dashed line - Griem (1974); solid line - Dimitrijević et al. (2007) for impact-electrons and impact-ions; solid line and cross symbols - Dimitrijević et al. (2007) for impact-electrons and quasistatic-ions; single symbols: experimental results from critical reviews (Lesage (2009) and references therein))

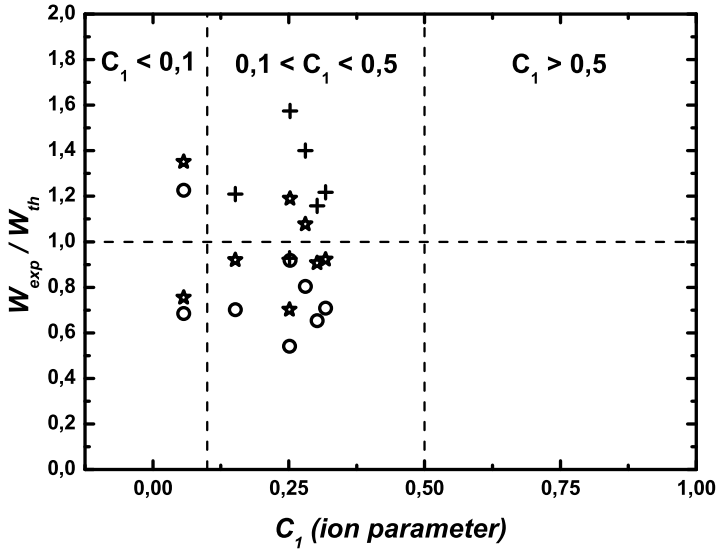

Fig. 9. Ratio of experimental and theoretical (◯ according to Griem's theory, ⋆ Sahal-Bréchot theory with impact ions, + according to Sahal-Bréchot theory with quasistatic ions) Stark widths for Ar I 696.5 nm versus the validity criterion of the impact approximation for ions (the impact approximation for ions is valid if the parameter C_1 is small compared to unity).

Also for example, temperatures around 50 000 K are typical for Be star Hen 2-90.

One can see that the behavior of the electron impact widths and shifts within the considered spectral series is so regular, therefore interpolation and extrapolation of new data is possible.

Comparison with other theoretical and experimental results

In Figures 5-8 the calculations of Dimitrijević et al. (2007) for the Stark broadening parameters of studied spectral lines in pure argon gas are compared with those published by Griem (1974, 1964) and with the experimental widths and shifts, with estimated accuracy A or B, from published critical reviews (see Lesage (2009) and references therein). For lines, where there are no results in Griem (1974), corresponding data from Griem (1964, 1962) were used.

For the Ar I 549.6 and 603.2 nm spectral lines the impact approximation is not valid for ions under all experimental conditions (Dimitrijević et al. 2007) in the relevant papers (Lesage (2009) and references therein on critical reviews for earlier period).

In Figures 5-8, the electron-impact width from Dimitrijević et al. (2007) is presented once with impact ion contribution, and once with quasistatic, so that two curves may be compared. The theoretical results for Stark broadening obtained in Dimitrijević et al. (2007) are closer to the experimental points for these lines.

The difference between curves with total Stark broadening parameters with impact and quasistatic ion broadening is small. For 549.6 nm, one obtains smaller widths and shifts with impact ions (Figures 5, 6). The shift values for 549.6 nm from Griem (1964) are in very good agreement with impact-electrons + quasistatic-ions values in Dimitrijević et al. (2007), and coincide for temperatures up to 20000 K. In fact, for 603.2 nm the broadening and shift values in the cases of impact and quasistatic ions obtained in Dimitrijević et al. (2007) are the same (see Figures 7, 8). Shift values from Sahal-Bréchot theory are a little bit

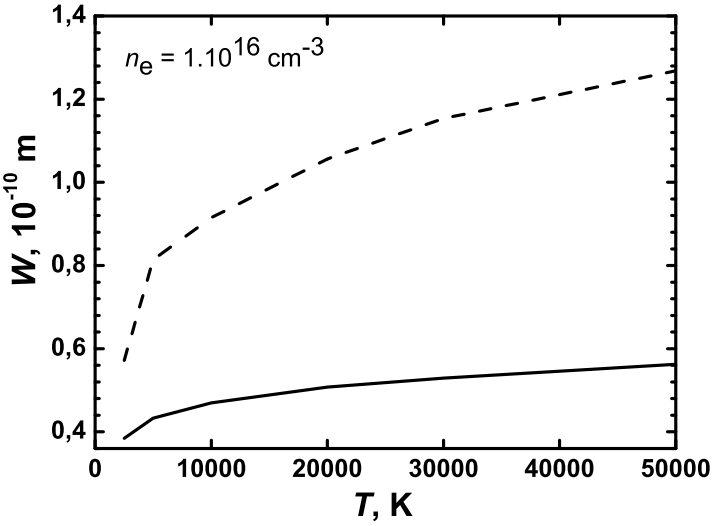

Fig. 10. Electron impact width of: Ne I 837.7 nm (solid line) and Ar I 737.2 nm (dashed line) spectral lines versus the temperature for electron density of 10^{16} cm^{-3}.

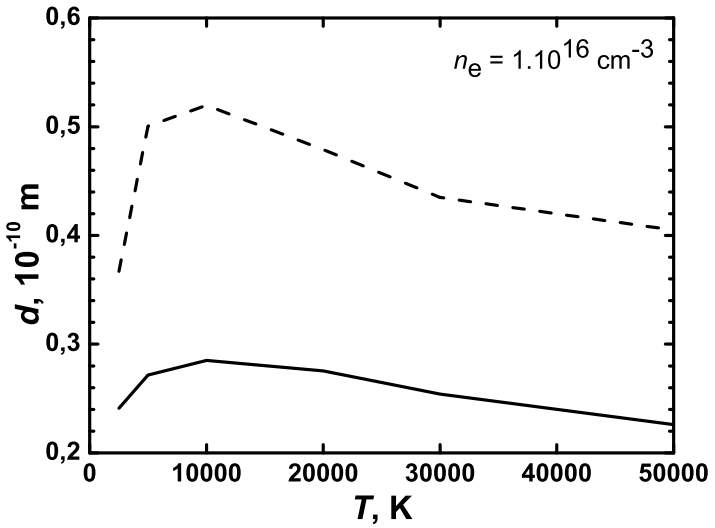

Fig. 11. Electron impact shift of: Ne I 837.7 nm (solid line) and Ar I 737.2 nm (dashed line) spectral line versus the temperature for the electron density of 10^{16} cm^{-3}.

larger, then Griem's calculated ones, for temperatures up to 20000 K and practically equal for higher temperatures.

The Ar I 696.5 nm spectral line is one of the most used argon lines for the diagnostic purposes. It is well isolated, visible and intense. This explains the great interest for it. This line is usually applied to measure the electron densities over 1.10^{16} cm^{-3}. In Figure 9 the ratios of measured widths for this line and

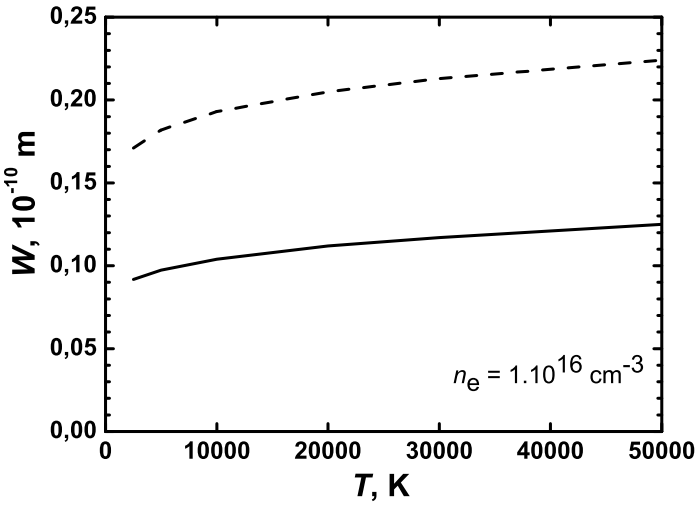

Fig. 12. Impact width due to protons collisions of: Ne I 837.7 nm (solid line) and Ar I 737.2 nm (dashed line) spectral lines versus the temperature for electron density of 10^{16} cm^{-3}.

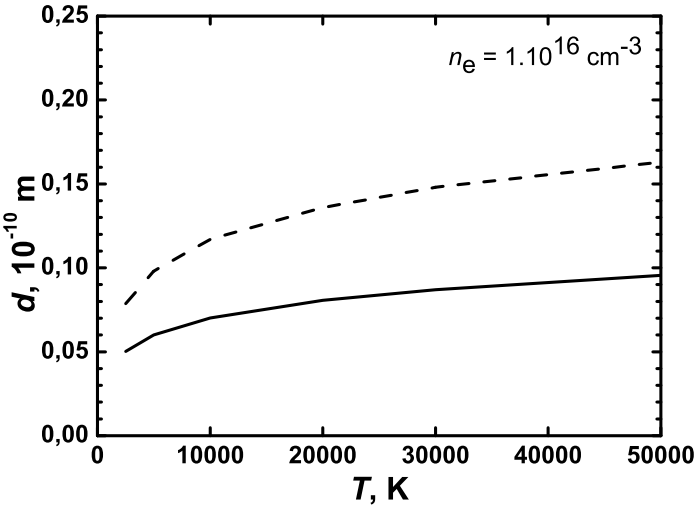

Fig. 13. Impact shift due to proton collisions of: Ne I 837.7 nm (solid line) and Ar I 737.2 nm (dashed line) spectral line versus the temperature for the electron density of 10^{16} cm^{-3}.

calculated ones (according to Griem's (Griem 1964) and Sahal-Bréchot theory with impact and quasistatic ion contribution) versus the parameter C_1 for ion perturbers are presented. C_1 is the impact approximation validity criterion (C_1 should be much less than one. We use here less or equal to 0.1). The values of C_1 correspond to the experimental n_e and T conditions, according to (Konjević et al 2002). The majority (six) of experimental widths fall within the transitional range (from impact to quasistatic regime for ion perturbers, $0.5 > C_1 > 0.1$),

Table 2. Basic data for the considered Ne I spectral line. Here λ denotes wavelength, i and f are initial and final level of the transition (within the frame of $j - L$ coupling), i' and f' are the corresponding perturbing levels, E_i and E_f are the energy values and n* is the effective quantum number of the initial level.

λ nm	Transition (i - f)	i' levels	f' levels	E_i cm^{-1}	E_f cm^{-1}	n*
837.7	$2p^5 3d' - 2p^5 3p$ $^2[7/2]^o{}_4 - ^2[5/2]_3$	4f, 5f, 3p, 4p, 5p	3s, 4s, 5s, 3d, 4d, 5d	161590.3	149657.0	2.98

two – in the impact regime ($C_1 < 0.1$) and there are no data for $C_1 > 0.5$, when only the quasistatic approximation is applicable. The both theories predict similar values in the impact regime. One can see that in average the Griem's theory overestimates the experimental Stark widths in the transitional range. The Sahal-Bréchot theory gives better results in this region. The ratio values for impact ions (Dimitrijević et al. 2007) are near to unity in the second region, while those for quasistatic ions (Dimitrijević et al. 2007) are underestimated.

A comprehensive study of the experimental Stark broadening of Ar I 696.5 nm, published over the period of 30 years was reported in Pellerin et al. (1996) yielding $W = 0.0814$ nm ± 5.0%, normalized to $n_e = 10^{17}$ $cm^{-3}$and $T = 13\,000$ K. There is a good agreement between this value and our calculated Stark width using Sahal-Bréchot theory which is 0.0857-0.0884 nm ± 30%.

The good agreement between available experimental results in the literature and our calculated Stark broadening parameters shows that the Stark theoretical data can be applied for modeling of stellar atmospheres of hot stars and for the analysis and synthesis of their spectra. One advantage of the results in Dimitrijević et al. (2007) is that the results for Stark broadening parameters for ions and protons are given in impact approximation which is often more appropriate in the case of hot stars.

A comparison of analogous neon and argon transitions

We will consider now Stark broadening for analogous transitions on the example of spectral lines: Ne I 837.7 nm $2p^5 3d$ - $2p^5 3p$ and Ar I 737.2 nm $3p^5 4d$ - $3p^5 4p$. The corresponding atomic data for neon transition are given in Table 2.

In the next four figures we give a comparison of their calculated Stark broadening parameters in order to study the variation of the width and shift of spectral line from analogues transitions. In Figures 10 and 11 the electron impact width and shift are presented as a function of temperature.

The Stark width due to collisions with electrons of the argon line is larger from 1.5 to 2.3 times than the neon one, while the corresponding Stark shift ratio vary from 1.5 to 1.8 in the whole temperature range. In Figures 12 and 13 the proton-impact widths and shifts are given.

The contribution of proton collisions in the Stark width for argon line is around 1.9 greater than those for neon line. The corresponding ratio for the Stark shift due to proton collisions slowly increases from 1.6 to 1.7. It is obvious that the difference of electron impact parameters for considered analogous transitions is larger than that of the protons.

4. Conclusion

The good agreement between available experimental results in the literature and our calculated Stark broadening parameters shows that the Stark theoretical data can be applied for the modeling of stellar atmospheres of hot stars and their spectra.

The observed similarities and regularities of Stark broadening parameters of spectral line within a spectral series can be used to obtain new data.

The study of Stark widths and shifts of spectral lines belonging to analogous transitions needs further efforts.

Acknowledgements. This work is a part of the project 146 001 "Influence of collisional processes on astrophysical plasma lineshapes" supported by the Ministry of Science and Technological development of Serbia. Partial support by the Technical University – Sofia was also given.

References

Christova, M., Dimitrijević, M. S., Kovačević, A. 2009a, J. Phys.: Conf. Series – in press

Christova, M., Dimitrijević, M. S., Simić, Z., Sahal-Bréchot, S. 2009b, J. Phys.: Conf. Series – in press

Dimitrijević M. S., Christova, M. and Sahal-Bréchot, S. 2007, Phys. Scripta, 75, 809

Dimitrijević, M. S. and Sahal-Bréchot, S. 1984, JQSRT, 31, 301

Griem, H. R. 1962, Phys. Rev., 128, No 2, 515—23

Griem, H. R. 1964, Plasma Spectroscopy (New York, McGraw Hill)

Griem, H. R. 1974, Spectral line broadening by plasmas (New York, Academic)

Kniazev, A. Yu., Grebel, E. K., Pustilnik, S. A., Pramskij, A. G., Zucker, D. B. 2005, Astron. J., 130, 1558

Konjević, N., Lesage, A., Fuhr, J. R. and Wiese, W. L. 2002, J. Phys. Chem. Ref. Data, Vol. 31 No. 3, 820-927

Kraus, M., Borges, F. M., De Araújo, F. X., Lamers, H. J. G. L. M. 2005, Astron. Astrophys., 441, 289

Lesage, A. 2009, New Astron. Rev., 52, 471

Pellerin, S., Musiol, K., Pokrzywka, B. and Chappelle, J. 1996, J. Phys. B: At. Mol. Opt. Phys., 29, 3911

Sahal-Bréchot, S. 1969a, Astron. Astrophys., 1, 91

Sahal-Bréchot, S. 1969b, Astron. Astrophys., 2, 322

Werner, K., Rauch, T., Kruk, J. W. 2007a, Astronomy and Astrophysics, Volume 474, Issue 2, November I 2007, pp. 591

Werner, K., Rauch, T. and Kruk, J. W. 2007b, A&A, 466, 317

Mem. S.A.It. Suppl. Vol. 15, 13

Memorie della
Supplementi

Studying the complex spectral line profiles in the spectra of hot emission stars and quasars

E. Danezis[1], E. Lyratzi[1,2], A. Antoniou[1], L. Č. Popović[3], and M. S. Dimitrijević[3,4]

[1] University of Athens, Faculty of Physics Department of Astrophysics, Astronomy and Mechanics, Panepistimioupoli, Zographou 157 84, Athens, Greece;
e-mail: edanezis@phys.uoa.gr
[2] Eugenides Foundation, 387 Sygrou Av., 17564, Athens, Greece
[3] Astronomical Observatory of Belgrade, Volgina 7, 11160 Belgrade, Serbia
[4] Laboratoire d'Étude du Rayonnement et de la Matiére en Astrophysique, Observatoire de Paris-Meudon, UMR CNRS 8112, Bâtiment 18, 5 Place Jules Janssen, F-92195 Meudon Cedex, France

Abstract. Some Hot Emission Stars and AGNs present peculiar spectral line profiles which are due to DACs and SACs phenomena. The origin and the mechanisms which are responsible for the creation of DACs/SACs is an important problem that has been studied by many researchers. This paper is a review of our efforts to study the origin and the mechanisms of these phenomena. At first we present a theoretic ad hoc picture for the structure of the plasma that surrounds the specific category of hot emission stars that present DACs or SACs. Then we present the mathematical model that we constructed, which is based on the properties of the above ad hoc theoretical structure. Finally, we present some results from our statistical studies that prove the consistency of our model with the classical physical theory.

Key words. Hot Emission Stars: spectral lines; Quasars: spectral lines

1. Introduction

One of the main characteristics of hot emission stars, which also distinguish them from the classical hot stars, is the presence of strong PCygni profiles in their Balmer series (Curtiss 1916). When the UV spectral region of these stars was studied, some emission lines were observed in that spectral region too (Underhill & Doazan 1982).

Additionally, in the UV spectral region, some hot emission stars (Oe and Be stars) present some absorption components that should not appear in their spectra, according to the classical physical theory (Fig.1). We call these absorption spectral lines, which do not correspond to any known absorption line of the same spectral type stars, Discrete Absorption Components (DACs) (Bates & Halliwell 1986).

The mechanisms which are responsible for the creation of DACs is an important problem that has been studied by many researchers. Some of them have suggested mechanisms that allow the

Send offprint requests to: E. Danezis

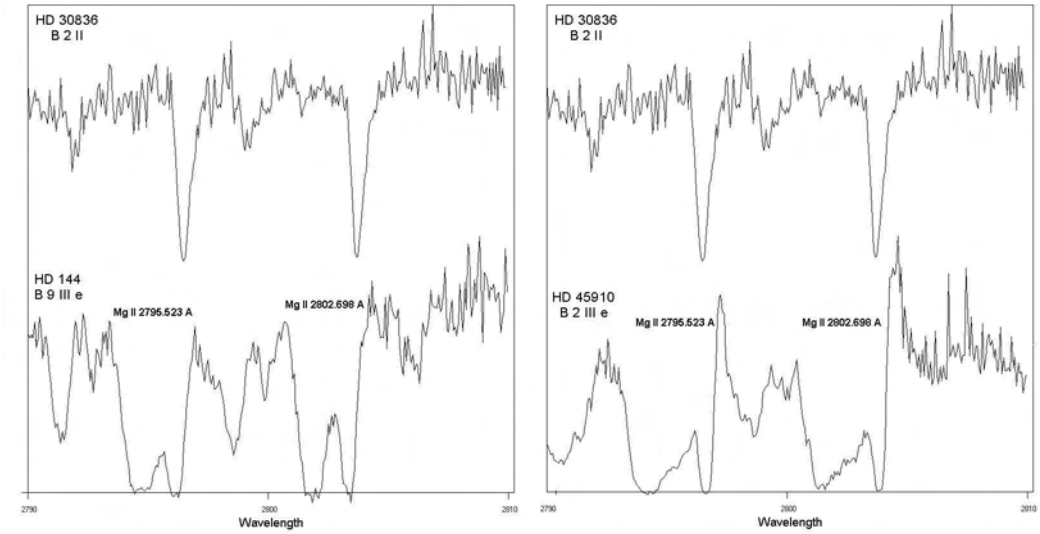

Fig. 1. Comparison of the Mg II resonance lines between the spectrum of a normal B star and the spectra of two active Be stars that present complex and peculiar spectral lines. As we can observe the Be stars present some absorption components that do not appear in the spectrum of the classical B star.

existence of structures which cover all or a significant part of the stellar disk, such as shells, blobs or puffs (Underhill 1975; Henrichs 1984; Underhill & Fahey 1984; Bates & Halliwell 1986; Grady et al. 1987; Lamers et al. 1988; Waldron et al. 1992, 1994; Cranmer & Owocki 1996; Rivinius et al. 1997; Kaper et al. 1996, 1997, 1999; Markova 2000), interaction of fast and slow wind components, co-rotation Interaction Regions (CIRs), structures due to magnetic fields or spiral streams as a result of the stellar rotation (Cranmer & Owocki 1996; Kaper et al. 1996, 1997, 1999; Mulan 1984a,b, 1986; Prinja & Howarth 1988; Fullerton et al. 1997; Cranmer et al. 2000). According to these ideas, DACs result from independent high density regions in the stellar environment, which have different rotational and radial velocities.

However, DACs are not unknown absorption spectral lines, but spectral lines of the same ion and the same wavelength as a main spectral line, shifted at different $\Delta\lambda$, as they are created in different density regions which rotate and move radially with different velocities (Danezis 1983, 1987; Danezis et al. 1991, 2003; Lyratzi & Danezis 2004).

Another problem of the hot emission stars that present DACs is the presence of very complex profile of the main or the discrete components of the spectral lines that we can't reproduce theoretically. This means that we can't fit these line profiles with a known distribution, such as Gaussian, Voight, or Lorenzian. As a result we could not know the physical conditions that exist in the high density regions that construct these spectral lines. In order to explain this complex line profiles Danezis et al. (2003, 2007a); Lyratzi & Danezis (2004); Lyratzi et al. (2007a) proposed the phenomenon of SACs (Satellite Absorption Components). If the regions that construct the DACs rotate with large velocities and move radially with small velocities, the produced lines have large widths and small shifts. As a result, they are blended among themselves as well as with the main spectral line and thus they are not discrete. In such a case the name Discrete Absorption Components is inappropriate and we use the name: Satellite Absorption Components (SACs) (Danezis 1983, 1987; Sahade et al. 1984; Sahade & Brandi 1985; Danezis et al. 2003, 2006, 2007a; Lyratzi & Danezis 2004). The existence of SACs results to the formation of the complex structure of the observed spectral features.

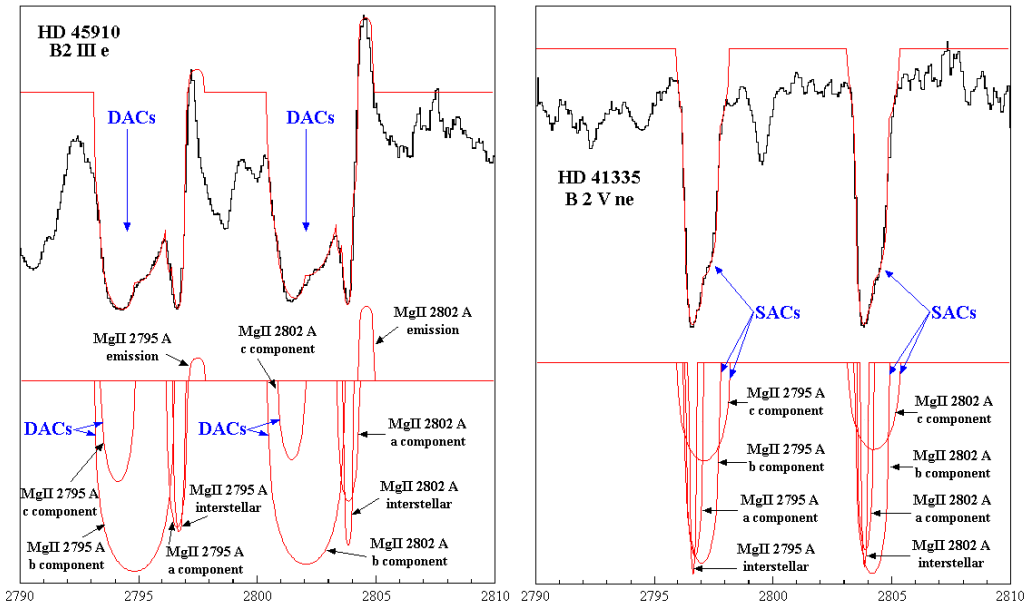

Fig. 2. DACs of the Mg II UV resonance line profiles of the Be star AX Mon (HD 45910) and SACs of the Be star HD 41335 are produced in the same way. The black line presents the observed spectral line's profile and the red one the model's fit. All the components which contribute to the observed features are shown separately.

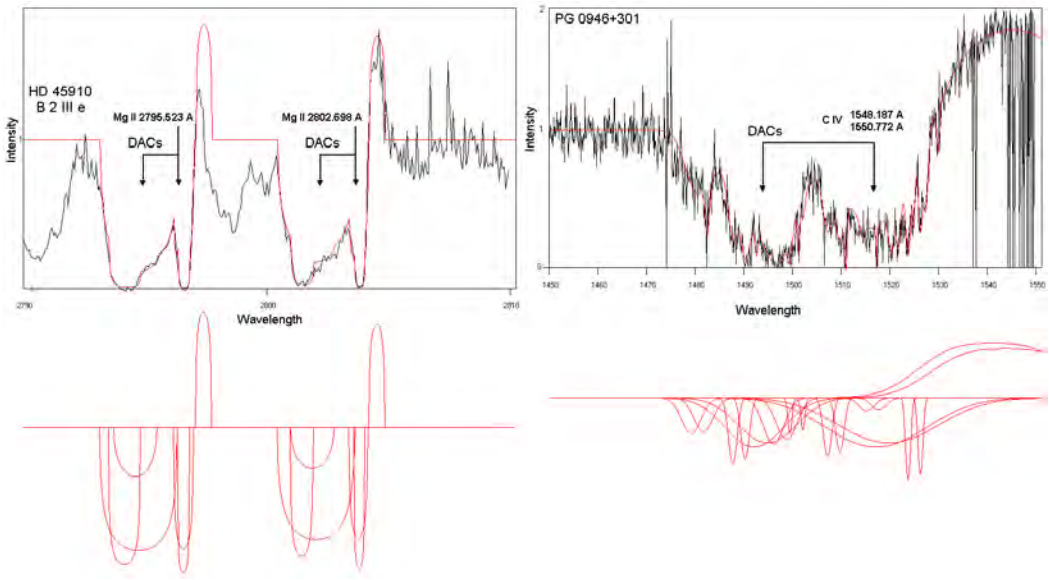

Fig. 3. DACs phenomena in AGNs spectra: Similarity of DACs phenomenon in Be star's HD 45910 spectrum (Mg II UV resonance lines) with AGNs' PG 0946+301spectrum (C IV doublet). In the case of the C IV doublet, the two discrete features do not correspond to the two resonance lines, as the two members of the doublet have small difference in wavelength (1548.187Å and 1550.772 Å) and they both lie at the right feature.

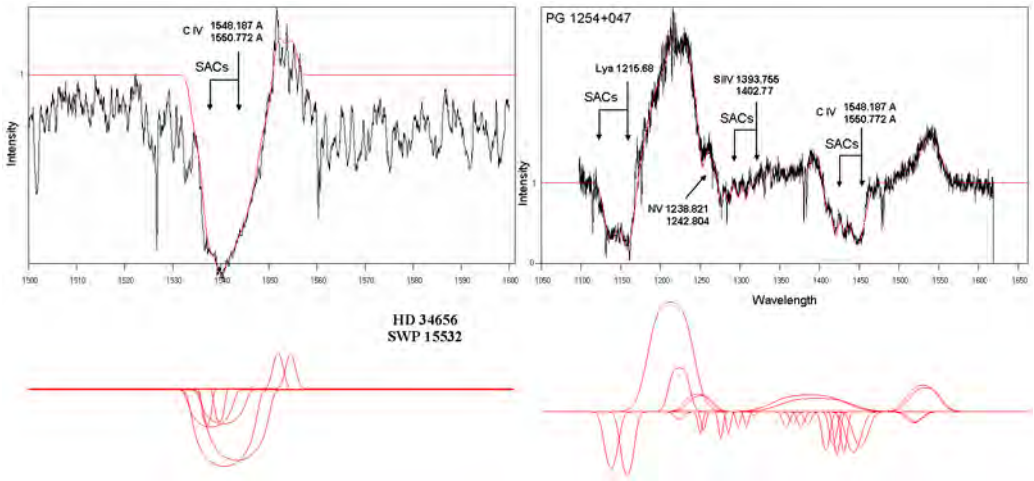

Fig. 4. SACs phenomena in AGNs spectra: Similarity of SACs phenomenon in Oe star's HD 34656 spectrum (C IV doublet) with AGNs PG 1254+047 spectrum (Lya and Si IV and C IV doublets).

As we can deduce from the above, the DACs and SACs are two aspects of the same phenomenon. In Fig. 2 it is clear that the Mg II line profiles of the star AX Mon (HD 45910), which presents DACs and the star HD 41335, which presents SACs are produced in the same way. The only difference between them is that the components of HD 41335 are much less shifted and thus they are blended among themselves.

It is very important to point out that we can detect the same phenomenon in the spectra of some Active Galactic Nuclei (AGN) (Danezis et al. 2006). In Fig. 3 (right) we can see the CIV UV doublet of an AGN (PG 0946+301). The values of radial displacements and the ratio of the line intensities indicate that the two observed C IV shapes present DACs phenomenon similar with the DACs phenomenon that we detect in the spectra of hot emission stars (e.g. HD 45910). Since the DACs phenomenon is present in some AGNs spectra, we also expect the presence of SACs phenomenon, which is able to explain the observed absorption lines complex profiles (Fig. 4). In the case of AGNs, accretion, wind (jets, ejection of matter etc.), BLR (Broad Line Regions) and NLR (Narrow Line Regions) are the density regions that construct peculiar profiles of the spectral lines (Fig. 5) (Danezis et al. 2006).

- Based on the above mentioned observational facts, our first step was the composition of a theoretic ad hoc picture for the structure of the plasma that surrounds the hot emission stars, which present DACs or SACs. This theoretic ad hoc picture should cover all the regions (and thus all ionization potentials) around hot emission stars, from the photosphere to the outer atmospherical regions (e.g. the Fe II, Mg II regions). Our second step was the construction of a mathematical model which, based on the properties of the described theoretical structure, should be able to:

- Reproduce the complex (due to DACs and SACs) profiles of the spectral lines and calculate a series of physical parameters of the regions where the spectral lines are created.

Be consistent with the physical theory. This means that statistically, the calculated values should lead to common physical properties of the studied atmospherical regions for all the studied stars that produce similar spectral lines.

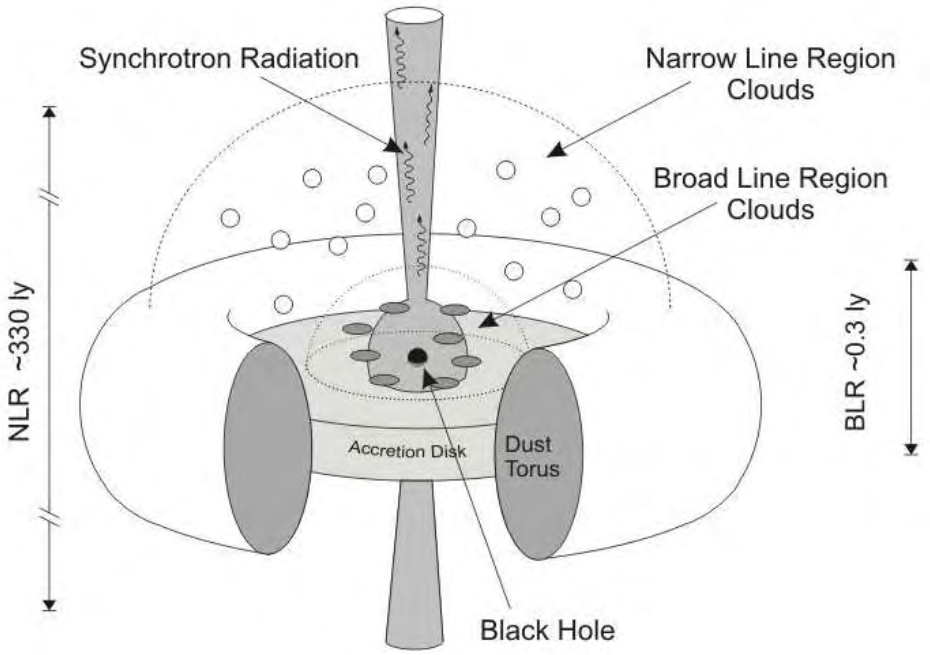

Fig. 5. The origin of DACs/SACs phenomenon in AGNs.

2. The theoretical model

According to Hubert - Delplace (1981), the existence of emission lines can be a repeated phenomenon for a star and we should consider as a fact that the ability of a B star to become Be is a function of the spectral subtype. However, we should always have in mind that there is no definite spectral classification in UV, as the spectral classification is based on the optical spectral range (Henize et al. 1981; Prinja 1990). As a result, the mechanisms of mass ejection from Be stars depend on the factors which classify the star to a specific spectral type. First, Struve (1931a,b) proposed that the Be stars are rapid rotators with velocities up to some hundreds km/s. According to Struve's model, these rapid rotators eject mass, forming a nebulous ring, when the rotational velocity takes the critical value at which the centrifugal force becomes equal to the gravitational force at the equator. However, Collins & Harrington (1966); Slettebak (1976, 1979); Friedjung (1968); Stoeckley (1968); Hardorp & Strittmater (1968) were opposed to this assumption of critical rotational velocity. They proposed that according to observations, Be stars rotate with velocities near, but not equal, to the critical one. Marlborough & Snow (1976), studying UV spectra of B stars, found a relation between the projected rotational velocity of B0-B4 stars and the results of mass loss and they proposed that the mass loss from Be stars could lead to the existence of stellar winds of large velocity, only if the rotation is able to diminish the apparent gravity near the equator. Our proposition is that in the case of Be stars that present DACs or SACs phenomena the rotational velocity could increase to greater values than the critical one, in such a way that Struve's model can be applied. This means that the Be stars of this kind may

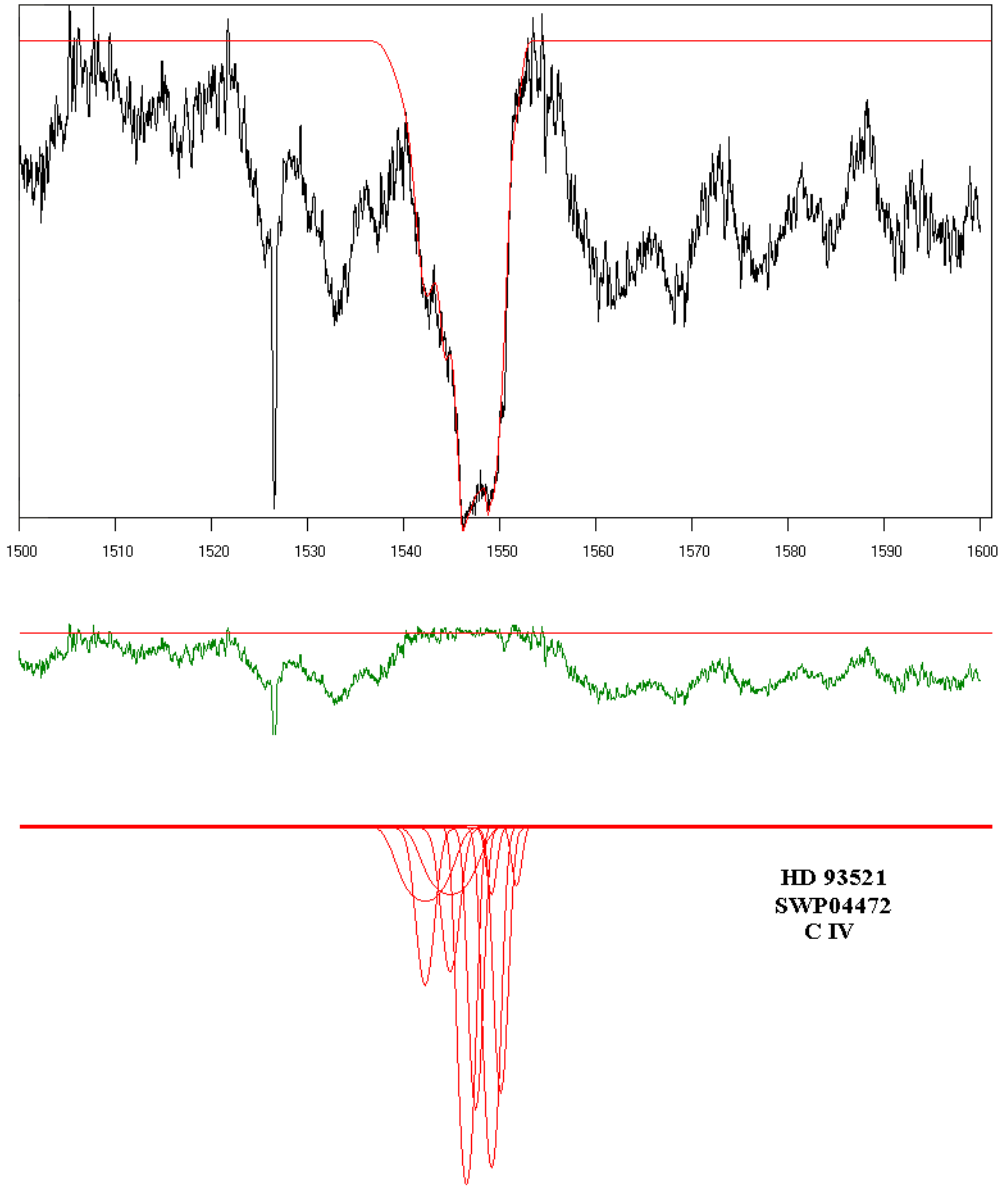

Fig. 6. Fitting of the C IV resonance lines ($\lambda\lambda$ 1548.187, 1550.772 Å) of the Oe star HD 93521, with the proposed model. The SACs phenomenon is able to explain the observed shape. Below the fitting one can see the difference graph (green), which indicates the differences between the observed and the theoretical line profile, as well as the analysis of the observed profile in its SACs (red).

eject mass from the regions around the equator, through a physical instability of the star, which disappears right after the mass ejection (Huang 1977).

The plasma which is ejected from the equatorial active regions in small but different angles, constructs a dense and expanding spherical envelope around the active star. According to the

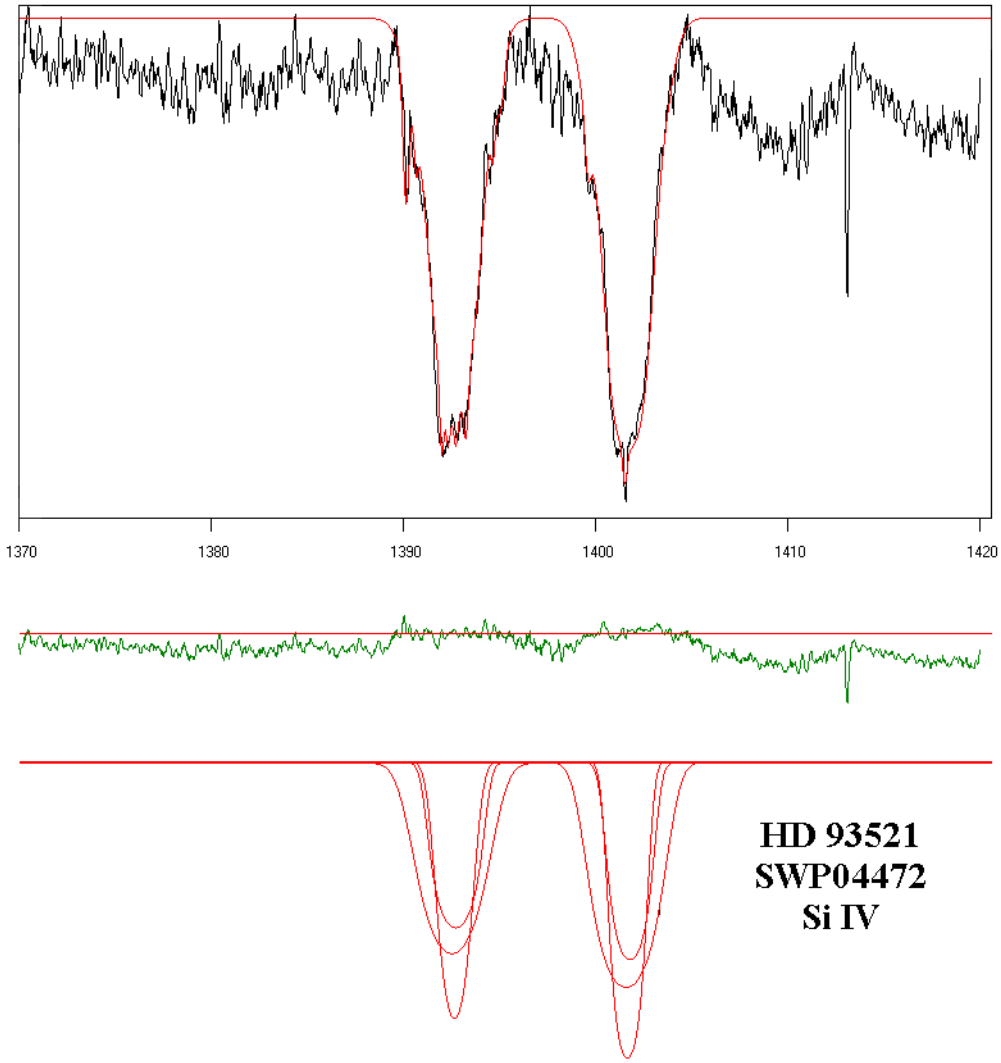

Fig. 7. Fitting of the Si IV resonance lines ($\lambda\lambda$ 1393.755, 1402.77 Å) of the Oe star HD 93521, with the proposed model. The SACs phenomenon is able to explain the observed shape. Below the fitting one can see the difference graph (green), which indicates the differences between the observed and the theoretical line profile, as well as the analysis of the observed profile in its SACs (red).

statistical study of Hubert - Delplace (1981), the e (emission) phenomenon can be repeated in the case of B stars. According to Huang (1977), sometime after the first mass ejection, the star may become unstable again and thus it may eject mass again from the equatorial regions, as its rotational velocity's value may become larger than the critical value. According to that, when we construct the mathematical model, we should also consider that the star ejects mass from the equatorial zone not once, but successively and repeatedly. In such a case, independent and successive spherical density plasma regions would surround the star (Danezis 1983). These inde-

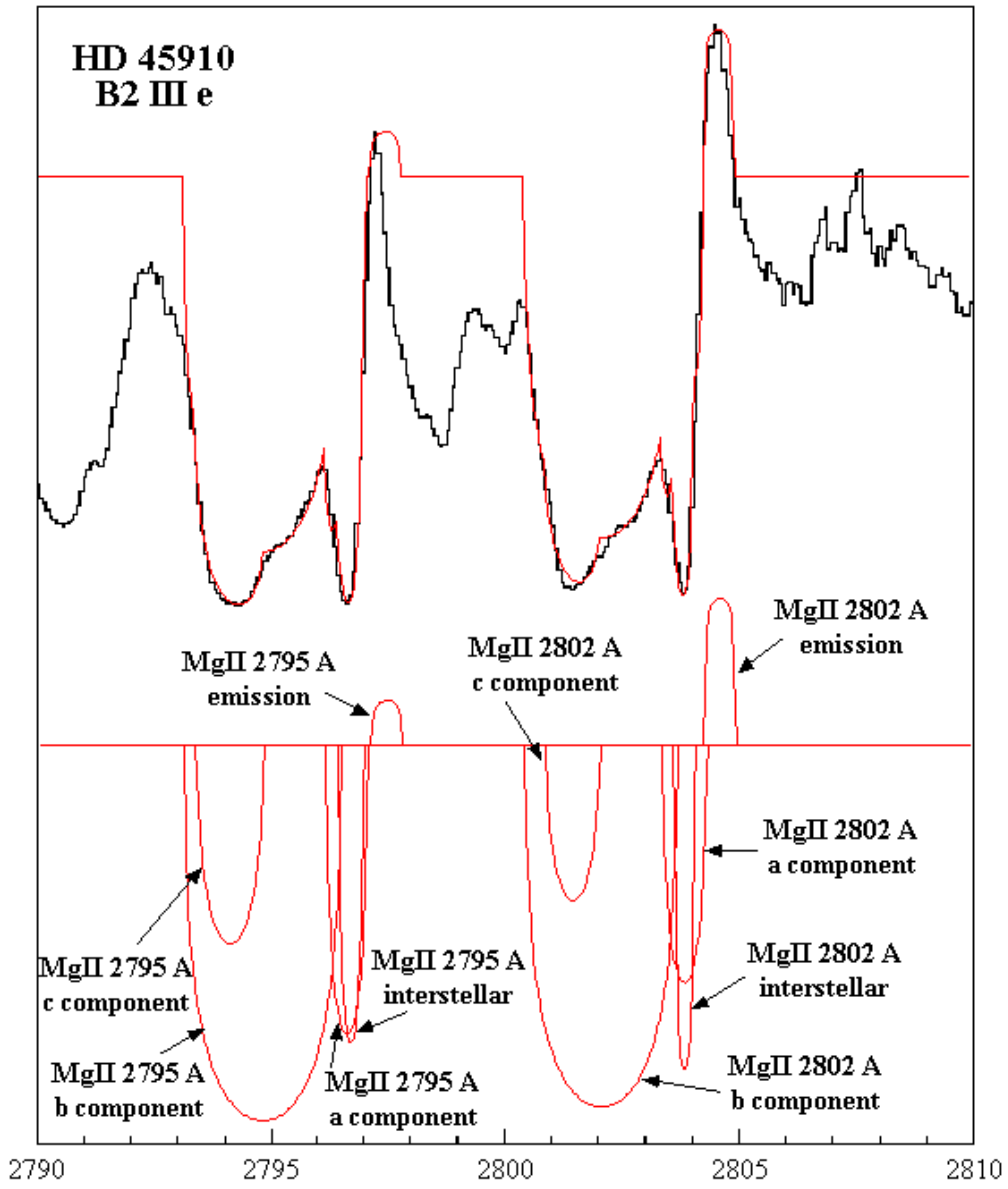

Fig. 8. Fitting of the Mg II resonance lines ($\lambda\lambda$ 1393.755, 1402.77 Å) of the Be star HD 45910, with the proposed model. The DACs and SACs phenomena is able to explain the observed shape. Below the fitting one can see the analysis of the observed profile in its DACs and SACs.

pendent density regions which move and rotate with different velocities create discrete absorption or emission components of the same spectral line in the stellar spectra. A similar phenomenon is also observed in the spectra of super novae.

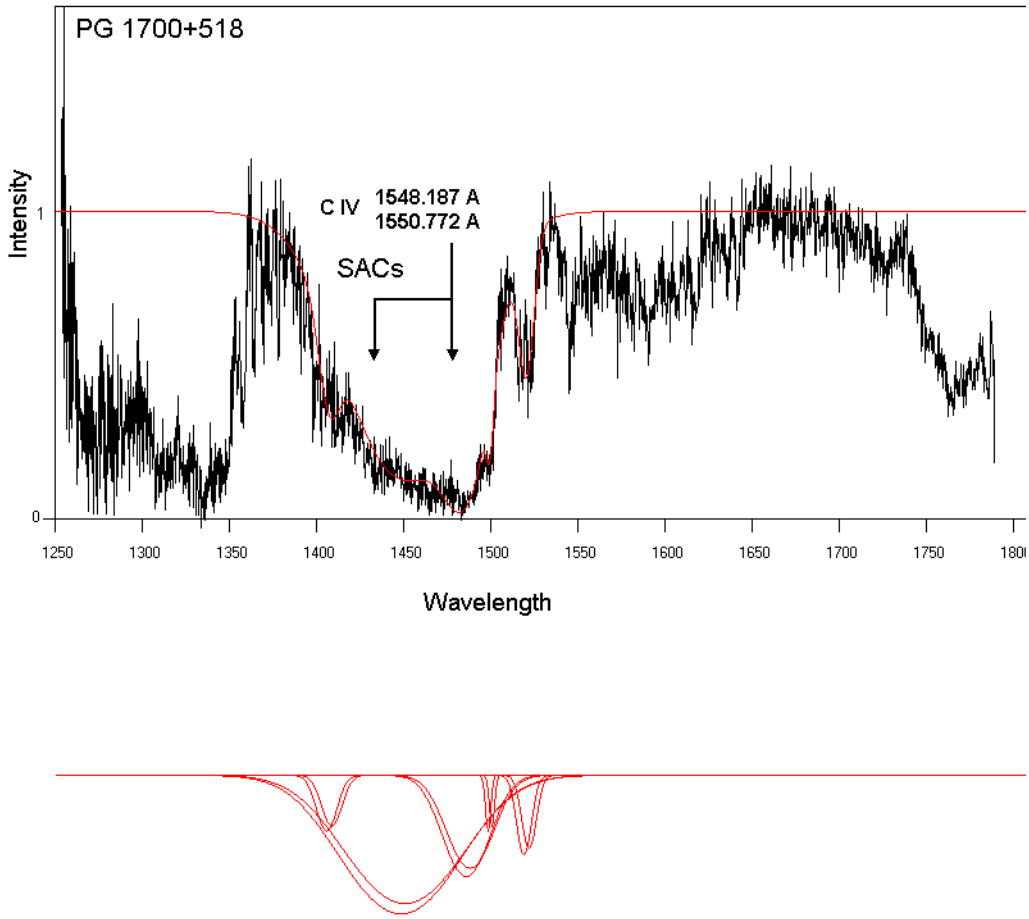

Fig. 9. Fitting of the C IV resonance lines ($\lambda\lambda$ 1548.187, 1550.772 Å) of the AGN PG 1700+518, that present SACs, with the proposed model. The SACs phenomenon is able to explain the observed shape.

As Struve's model considers, the spherical density regions that may exist around the star, evolve to an equatorial disk (Struve 1931a,b, 1942).

The plasma jets which are ejected from the equatorial active regions form blobs or structures due to magnetic fields or spiral streams resulting from the stellar rotation, which evolve in the regions where DACs and SACs are created (Cranmer & Owocki 1996; Kaper et al. 1996, 1997, 1999; Mulan 1984a,b, 1986; Prinja & Howarth 1988; Fullerton et al. 1997; Cranmer et al. 2000), These structures are local regions of high density, which have spherical symmetry around their own center and not around the star. These density regions result to the existence of absorption or emission spectral lines in the stellar spectra.

Near the hot emission stars we can detect density regions that have the characteristics of chromosphere, corona and post-coronal regions (Franco et al. 1983; Franco & Stalio 1983; Underhill & Doazan 1982, Part II, chapter 13). The corona of hot emission stars is detected in X-rays and the post-coronal regions (Si IV, C IV, N IV, N V lines e.t.c.) in UV. All the

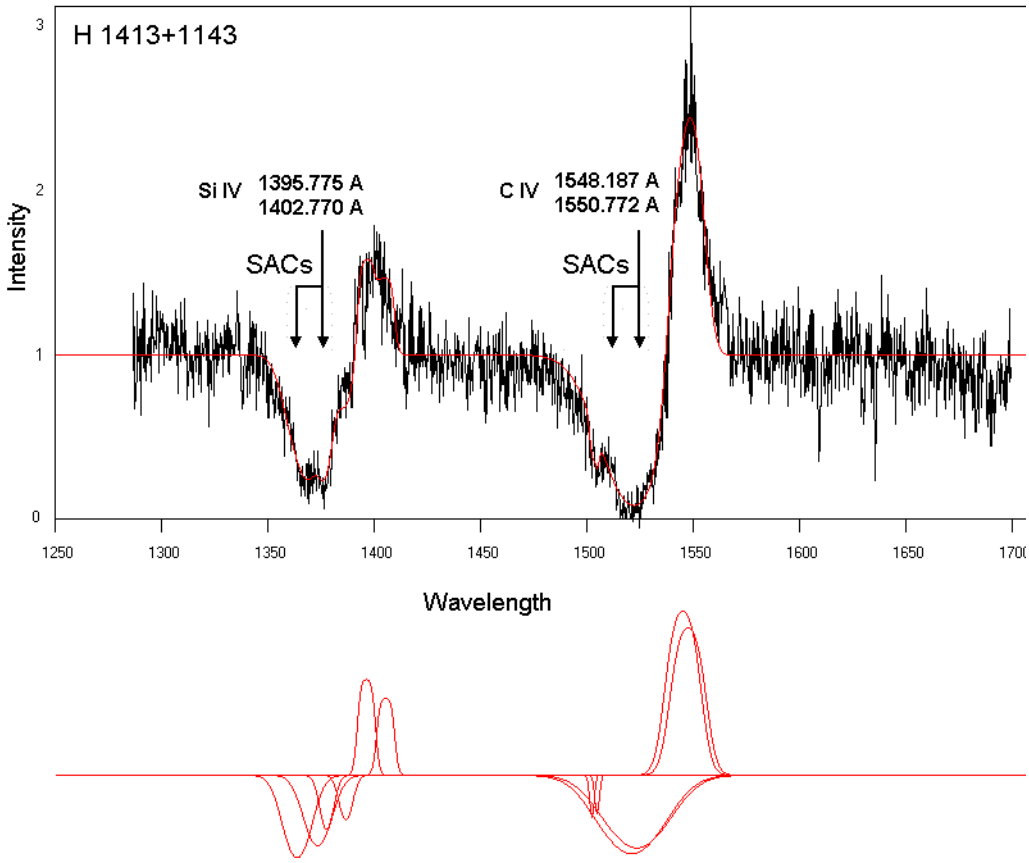

Fig. 10. Fitting of the Si IV ($\lambda\lambda$ 1393.755, 1402.77 Å) and C IV resonance lines ($\lambda\lambda$ 1548.187, 1550.772 Å) of the AGN H 1413+1143, that present SACs with the proposed model. The SACs phenomenon is able to explain the observed shape.

above lead us to the connection of Struve's model with the corona model of Thomas-Doazan (Underhill & Doazan 1982), which suggests the existence of coronal and post coronal regions.

Many ad hoc models have been proposed that do not accept the existence of chromosphere and corona. These models were constructed to represent only the observations made in the optical and infrared regions and point out that they all produce good agreement between the observed and computed spectra. We should also remind that all the models that have been proposed are ad hoc; as such, they cannot and do not pretend to be physically self-consistent. In this respect, one must keep in mind the arbitrary nature of certain hypotheses on which their construction is based, and one must not expect this picture of reality to closely describe a real star (Underhill & Doazan 1982).

All the above lead us to the conclusion that in the inner regions of the stellar atmosphere (from the photosphere to the first regions of the disk) of the stars that present DACs or SACs, the plasma is violently deranged and it does not have the form of calm stellar wind, for as long

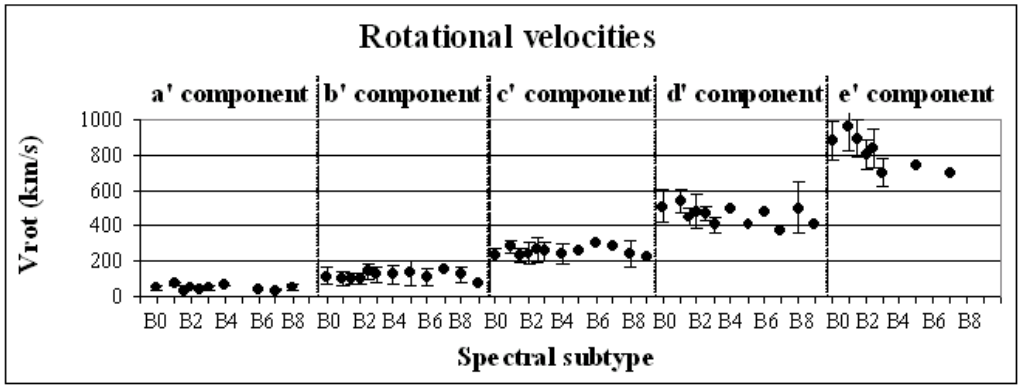

Fig. 11. Mean rotational velocities of the independent density regions of matter which create the SACs of the Si IV resonance lines ($\lambda\lambda$ 1393.755, 1402.77 Å) as a function of the spectral subtype, in a sample of 68 Be stars (Lyratzi et al. 2007b).

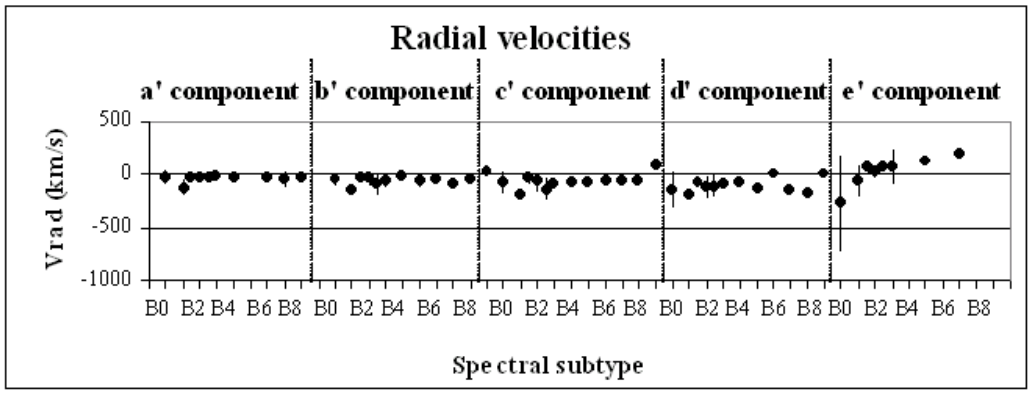

Fig. 12. Mean radial velocities of the independent density regions of matter which create the SACs of the Si IV resonance lines ($\lambda\lambda$ 1393.755, 1402.77 Å) as a function of the spectral subtype, in a sample of 68 Be stars (Lyratzi et al. 2007b).

as the e phenomenon lasts. During the e phenomenon, in the regions where the DACs or SACs are created, the majority of plasma is distributed in the density regions of spherical symmetry around the star or around their own centers. These density regions were created as a result of the violent mass ejection during the period of e phenomenon. The ejected matter takes the form of stellar wind as it goes away from the disturbed area of the inner atmospherical layers of the hot emission stars. Among the density regions, the rest of the matter has the form of stellar wind, but its density is very low compared with the matter of the density regions and thus we considered it negligible when we constructed the mathematical model.

3. The mathematical model – The line function

As we have already mentioned, in order to accept, even theoretically, all the above, we should construct a mathematical model which should include all the above ideas. This means that by solving the radiation transfer equations through a complex structure as the one described, we

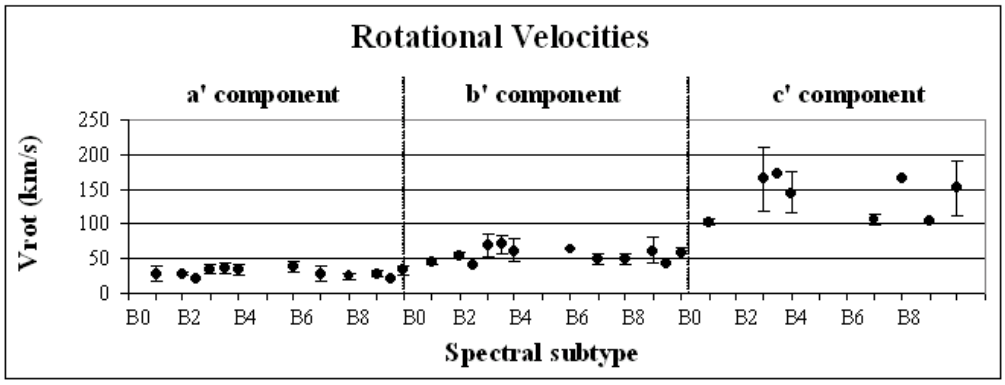

Fig. 13. Mean rotational velocities of the independent density regions of matter which create the SACs of the Mg II resonance lines ($\lambda\lambda$ 2795.523, 2802.698 Å) as a function of the spectral subtype, in a sample of 64 Be stars (Lyratzi et al. 2007b).

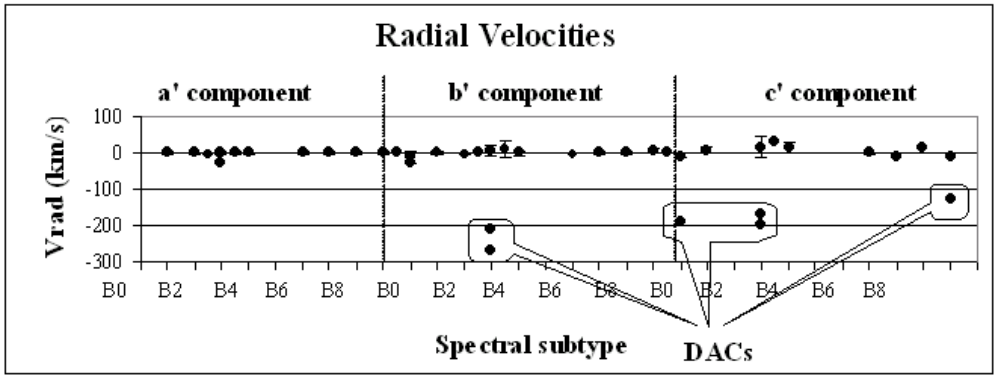

Fig. 14. Mean radial velocities of the independent density regions of matter which create the SACs of the Mg II resonance lines ($\lambda\lambda$ 2795.523, 2802.698 Å) as a function of the spectral subtype. The existence of DACs is clearly indicated, in a sample of 64 Be stars (Lyratzi et al. 2007b).

should calculate a line function, able to reproduce theoretically the observed spectral line profiles. The term line function corresponds to the function that relates the intensity with the wavelength. This function includes as parameters many physical conditions that construct the line profile. By giving values to these parameters we try to find the right ones in order to have the best theoretical fit of the observed line profile. If we accomplish the best fit, we accept that the theoretical values of the physical parameters are the actual ones that describe the physical conditions in the region that produces the specific spectral line. However, the calculation of a line function is not simple and includes many problems, such as the following. A line function able to reproduce theoretically any spectral line of any ion should include all the atomic parameters. As a result the line function would be very complex. Also, if we wanted a time dependent line function, we should include as parameter the time. The existence of many parameters makes the solution of the radiation transfer equations problematic. Another problem is to choose the correct values of so many parameters.

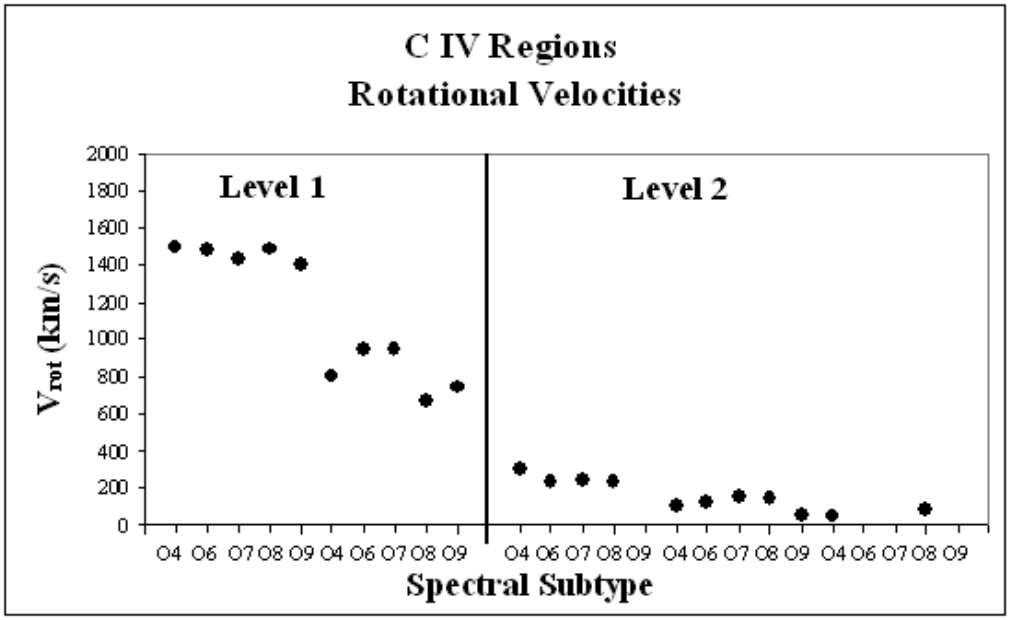

Fig. 15. Rotational velocities (V_{rot}) in the C IV region as a function of the spectral subtype, in a sample of 20 Oe stars. We detect two levels of rotational velocities (Antoniou et al. 2007a).

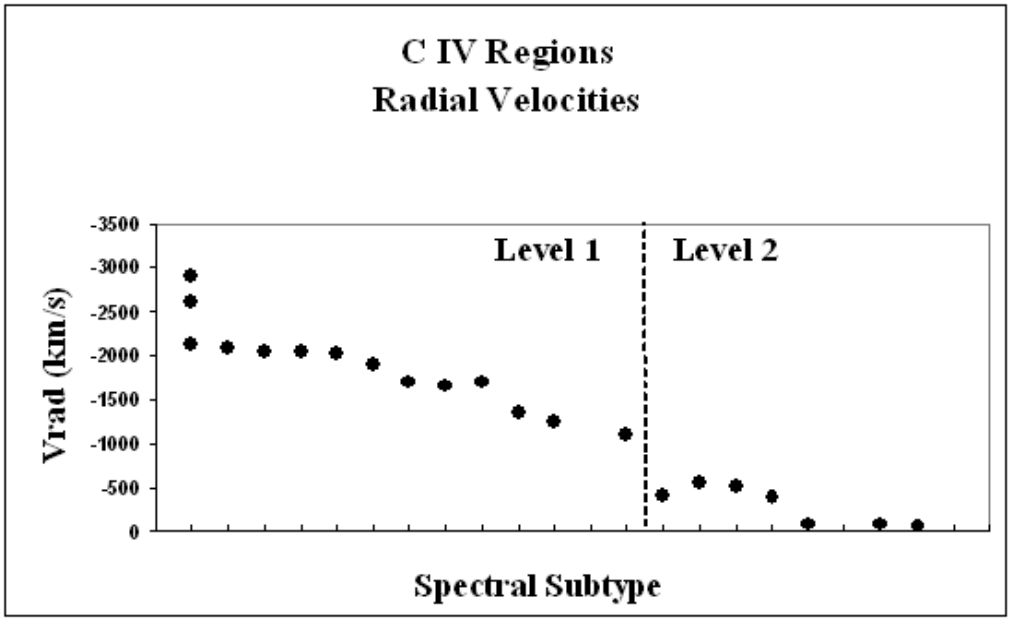

Fig. 16. Radial velocities (V_{rad}) in the C IV region as a function of the spectral subtype, in a sample of 20 Oe stars. We detect two levels of radial velocities (Antoniou et al. 2007a).

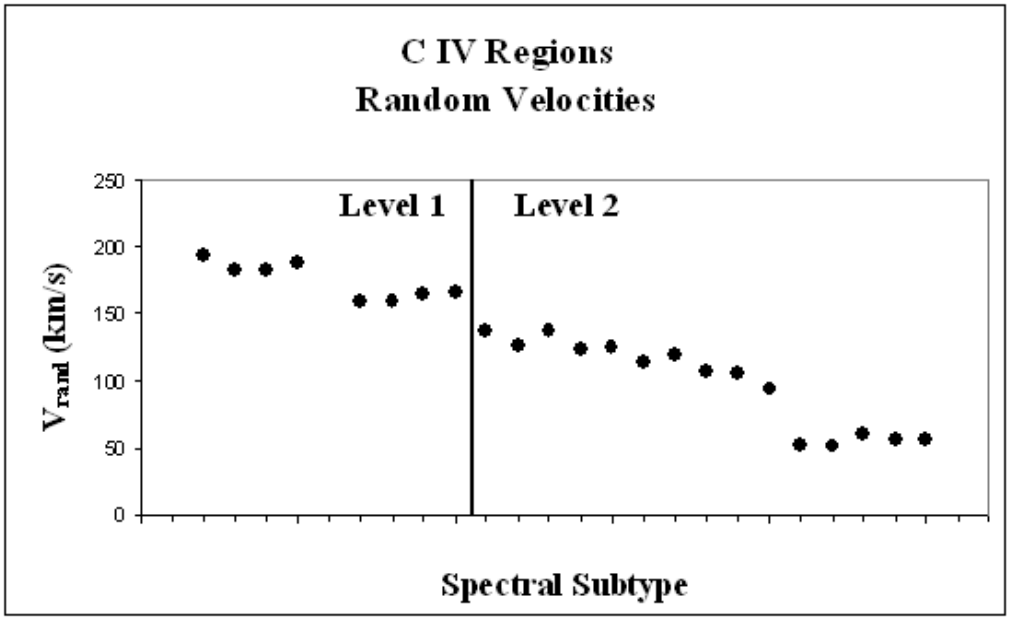

Fig. 17. Random velocities (V_{rand}) in the C IV region as a function of the spectral subtype, in a sample of 20 Oe stars. We detect two levels of random velocities (Antoniou et al. 2007a).

In order to eliminate some of these problems we considered that in the calculation of a line function we should not include variation with time, as our purpose was to describe the structure of the regions where the DACs/SACs are created at the specific moment when a spectrum is taken. In order to study the time-variation of the calculated physical parameters, we should study many spectra of the same star, taken at different moments. Additionally, we needed a line function with which we could study a specific spectral line of a specific ion. This means that we did not need to include the atomic parameters, as in such a case the atomic parameters remain constant. In this way, we were able to solve the radiation transfer equations and to find the correct group of parameters that give the best fit of the observed spectral line.

We considered that in the stellar atmosphere the radiation passes through a number of successive independent absorbing and/or emitting density regions of matter until it arrives at the observer. By solving the radiation transfer equations through such a complex structure we obtain a line function (Eq. 1) for the line profile, able to give the best fit for the main spectral line and its DACs/SACs at the same time (see Danezis et al. 2003, 2007a).

$$I_\lambda = \prod_g \exp\left\{-L_g \xi_g\right\}\left[I_{\lambda 0}\prod_i \exp\left\{-L_i \xi_i\right\} + \sum_j S_{\lambda ej}\left(1 - \exp\left\{-L_{ej}\xi_{ej}\right\}\right)\right] \quad (1)$$

where:

$I_{\lambda 0}$: is the initial radiation intensity,

L_i, L_{ej}, L_g: are the distribution functions of the absorption coefficients $k_{\lambda i}$, $k_{\lambda ej}$, $k_{\lambda g}$,

ξ: is the optical depth in the center of the spectral line,

$S_{\lambda ej}$: is the source function that is constant during one observation. The geometry and many physical conditions of the region that produces the spectral line are included in the factors L_i,

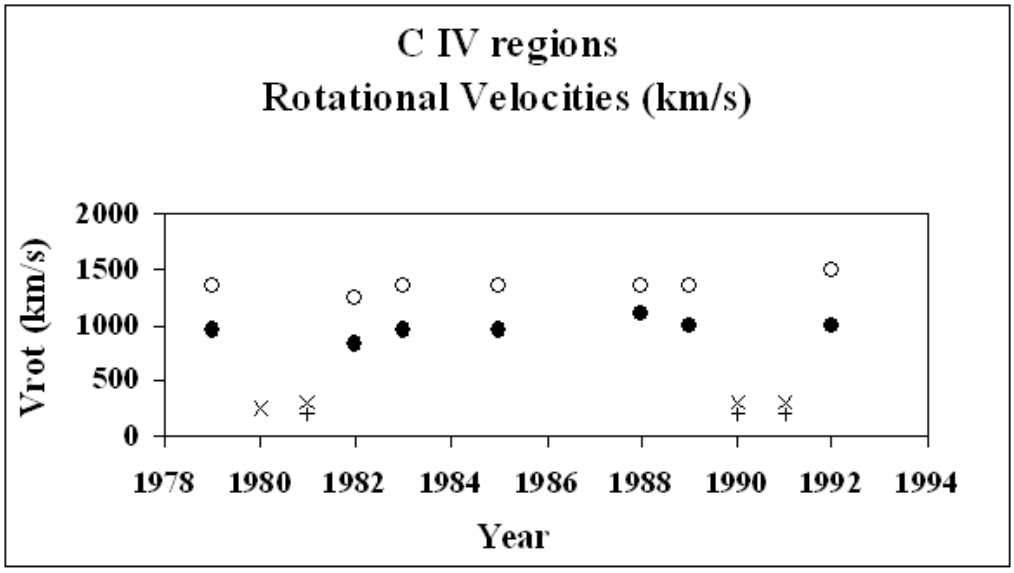

Fig. 18. Variation of the rotational velocities of the C IV density regions of the Oe star HD 149757, as a function of time (Antoniou et al. 2007c).

L_{ej} and L_g and not in the calculation of I_λ. So, the decision on the geometry and the physical conditions is essential for the calculation of the distribution function that we use for each component. Specifically, the physical conditions indicate the exact distribution that we must use.This means that for a different geometry and different physical conditions we have a different analytical form of L_i, L_{ej}, L_g and thus a different shape for the spectral line profile of each SAC. In our model we considered the spherical geometry. In order to decide on the appropriate geometry we took into consideration that the spectral line profile is reproduced in the best way when we consider spherical symmetry for the independent density regions. Such symmetry has been proposed by many researchers (Waldron et al. 1992; Rivinius et al. 1997; Markova 2000; Lamers et al. 1982; Bates & Gilheany 1990; Gilheany et al. 1990; Cidale 1998). Besides, we had to consider the fact that hot emission stars are rapid rotators and present violent mass ejection, producing density regions that create the observed DACs or SACs and which also rotate quickly around their own center. According to this, we should accept that the rapid rotation of the density regions is one of the main broadening factors of the spectral lines originating from them. This means that the rotation of the density regions should be included in the calculations of our model, in order to be able to reproduce the observed spectral lines. As a first step, our scientific group constructed a distribution function L that considers as the only reason of the line broadening the rotation of the regions that produce the spectral lines. We called it Rotation distribution (see Danezis et al. 2003; Lyratzi et al. 2007a). However, it is known that in a gaseous region we always detect random motions, which must be taken into consideration as a second reason of line broadening (Doppler broadening). The distribution function that expresses these random motions is the Gaussian. This means that in order to have a spectral line that has as broadening factors the rotation of the regions and the random motions of the ions, we should construct a new distribution function L that would include both of these reasons (rotation and random motions). Our scientific group constructed this distribution function L (Eq. 2) and named it Gauss-Rotation distribution (GR distribution) (Danezis et al. 2007a).

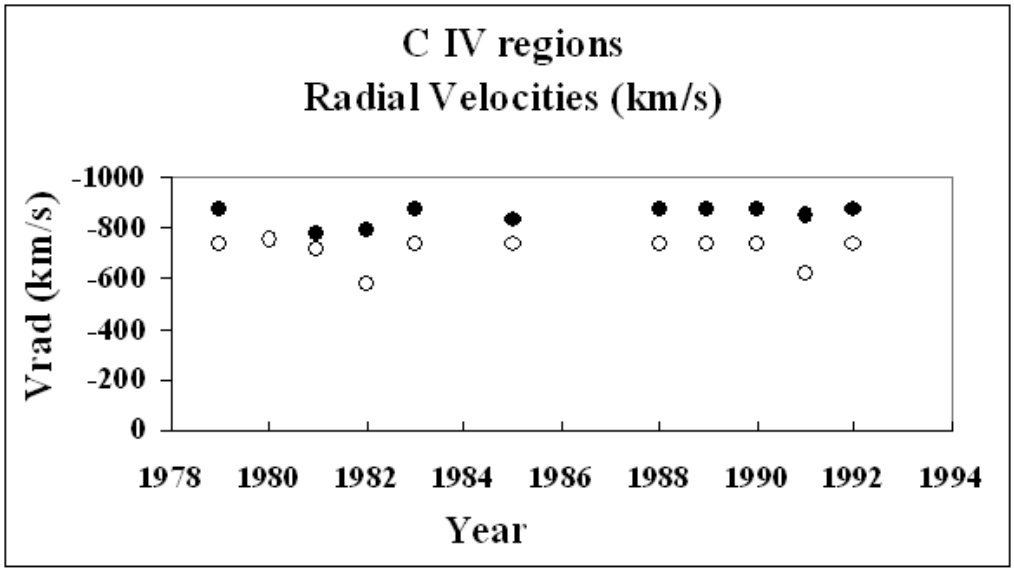

Fig. 19. Variation of the radial velocities of the C IV density regions of the Oe star HD 149757, as a function of time (Antoniou et al. 2007c).

$$L_{final}(\lambda) = \frac{\sqrt{\pi}}{2\lambda_0 z}\int_{-\frac{\pi}{2}}^{\frac{\pi}{2}}\left[erf\left(\frac{\lambda-\lambda_0}{\sigma\sqrt{2}}+\frac{\lambda_0 z}{\sigma\sqrt{2}}\cos\theta\right)--erf\left(\frac{\lambda-\lambda_0}{\sigma\sqrt{2}}-\frac{\lambda_0 z}{\sigma\sqrt{2}}\cos\theta\right)\right]\cos\theta d\theta \quad (2)$$

where

λ is the wavelength of each point of the spectral line profile,

$\lambda_0 = \lambda_{lab} \pm \Delta\lambda_{rad}$, where λ_0 is the wavelength of the center of the observed spectral line which is shifted from the laboratory wavelength λ_{lab} of the spectral line at $\Delta\lambda_{rad}$, from which we calculate the radial velocity V_{rad} of the density region,

$z = \frac{V_{rot}}{c}$, from which we calculate the rotational velocity V_{rot} of the density region,

σ is the Gaussian typical deviation from which we calculate the random velocity V_{rand} of the ions as $V_{rand} = \frac{\sigma c\sqrt{2\ln 2}}{\lambda_0}$ and

$erf(x) = \frac{2}{\pi}\int_0^x e^{-u^2}du$, the known error function (see also Danezis et al. 2007a).

The analytical form and the calculations of the GR distribution function can be found in Danezis et al. (2007a).

Using the GR model, we can calculate some important parameters of the density region that construct the DACs/SACs. Directly, we can calculate the apparent rotational velocities of absorbing or emitting density layers (V_{rot}), the apparent radial velocities of absorbing or emitting density layers (V_{rad}), the Gaussian typical deviation of the ion random motions (σ) and the optical depth in the center of the absorption or emission components (ξ). Indirectly, we calculate the random velocities of the ions (V_{rand}), the Full Width at Half Maximum (FWHM), the absorbed or emitted energy (Ea, Ee) and the column density (CD) (see also Danezis et al. 2005).

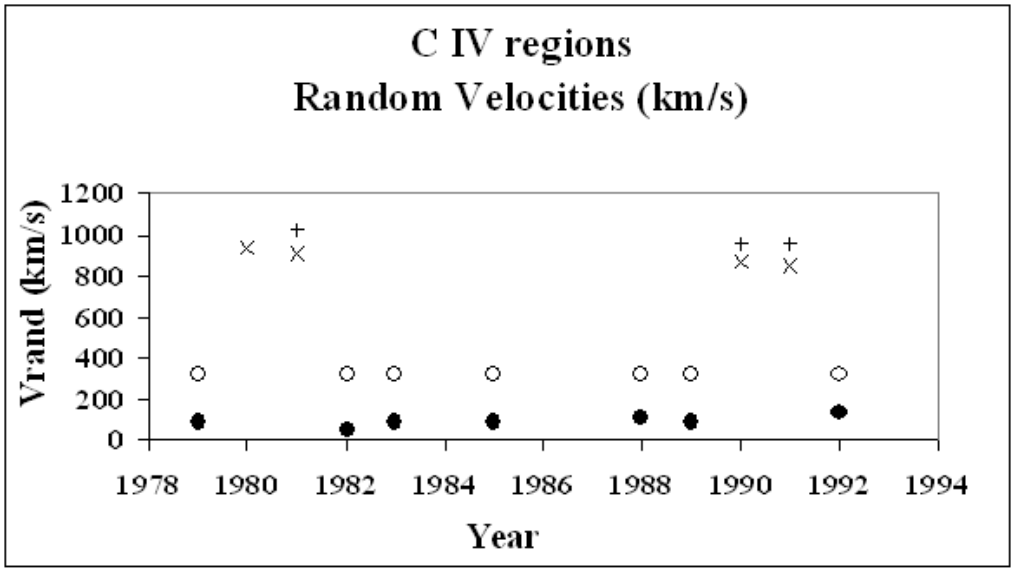

Fig. 20. Variation of the random velocities of the C IV density regions of the Oe star HD 149757, as a function of time.

4. Applications

As we have already mentioned, the validity of GR model should be judged by its application and the model should be consistent with the following two points:

- The GR model must be able to reproduce the complex (due to DACs and SACs) profiles of the spectral lines and calculate a series of physical parameters of the regions where the spectral lines are created.

- The results of GR model must be consistent with the physical theory. This means that statistically, the calculated values should lead to common physical properties of the studied atmospherical regions for all the studied stars that produce similar spectral lines.

A series of papers have been published, where the GR model is applied on a great number of stellar and galactic spectra, calculating the physical parameters of the regions where the spectral lines are created and giving consistent results with the classical physical theory (Danezis et al. 2007b, 2009; Lyratzi et al. 2007a,b, 2009; Antoniou et al. 2007a,b,c, 2008). Some of these results are presented in the following figures. In Figs. 6-10 we present the fittings of some peculiar profiles of spectral lines, observed in the spectra of hot emission stars and AGNs. In Figs. 11-17 we present the variation of kinematical parameters of the regions that create DACs or SACs, as a function of the spectral subtype, in samples of Be and Oe stars. In Figs. 18-20, we present the variation of the kinematical parameters of the C IV regions of the Oe star HD 149757, as a function of time.

5. Conclusions

In brief, the results of our study are as follows:

– We proposed a theoretic ad hoc picture for the structure of the plasma that surrounds hot emission stars, which is able to explain the origin of DACs phenomenon and we proposed

the SACs phenomenon in order to explain the complex structure of the observed profiles of many spectral lines that are created in the environment of hot emission stars.
- We observed the same phenomenon in the spectra of quasars and we proposed that its origin is similar as in the case of hot emission stars.
- Based on the properties of the theoretic ad hoc picture for the structure of the plasma that surrounds hot emission stars, we constructed a new mathematical model (GR model), able to reproduce theoretically the observed complex spectral line profiles. In order to do so, we calculated for the first time a line function through the solution of the radiation transfer equation.
- We calculated two new distribution functions (Rotation distribution and Gauss-Rotation distribution).
- We constructed a first version of software, in order to reproduce the observed spectral lines and to calculate some physical parameters.
- We applied successfully the GR model in a great number of spectral lines of hot emission stars and quasars. The results of GR model are consistent with the physical theory. This means that statistically, the calculated values lead to common physical properties of the studied atmospherical regions for all the studied stars or quasars that produce similar spectral lines.

Acknowledgements. This research project is progressing at the University of Athens, Department of Astrophysics, Astronomy and Mechanics, under the financial support of the Special Account for Research Grants, which we thank very much. This work also was supported by Ministry of Science Technological Development of Serbia and, through the projects 'Influence of collisional processes on astrophysical plasma line shapes' and 'Astrophysical spectroscopy of extragalactic objects'.

References

Antoniou, A. et al. 2007a, UVAstronomyJD04, 113
Antoniou, A. et al. 2007b, AIPC, 938, 194
Antoniou, A. et al. 2007c, AIPC, 938, 198
Antoniou et al. 2008, JPhCS, 133a, 2028
Bates, B. & Halliwell, D. R. 1986, MNRAS, 223, 673
Bates, B. & Gilheany, S. 1990, MNRAS, 243, 320
Cidale, L. S. 1998, ApJ, 502, 824
Cranmer, S. R. & Owocki, S. P. 1996, ApJ, 462, 469
Cranmer, S. R. et al. 2000, ApJ, 537, 433
Collins, G. W. & Harrington, J. P. 1966, ApJ, 146, 152
Curtiss, R. H. 1916, Publ. Obs. Univ. Michigan, 2, 1
Danezis, E. 1983, The nature of Be stars, PhD Thesis (University of Athens)
Danezis, E. 1987, IAU, Colloq. No 92, Physics of Be Stars (Cambridge University Press)
Danezis, E. et al. 1991, Ap&SS179, 111
Danezis, E. et al. 2003, Ap&SS, 284, 1119
Danezis, E. et al. 2005, MemSAIS, 7, 107
Danezis, E. et al. 2006, AIPC, 876, 373
Danezis, E. et al. 2007a, PASJ, 59, 827
Danezis, E. et al. 2007b, AIPC, 938, 119
Danezis, E. et al. 2009, NewAR, 53, 214
Franco, M. L. et al. 1983, A&A, 122, 9
Franco, M. L. & Stalio, R. 1983, MemSAI, 54, 537
Friedjung, M. 1968, ApJ, 151,779
Fullerton, A. W. et al. 1997, A&A, 327, 699
Gilheany, S. et al. 1990, Ap&SS, 169, 85

Grady, C. A. et al. 1987, ApJS, 65, 673.
Hardorp, J. & Strittmater, P. A. 1968, ApJ, 153, 465
Henize et al. 1981, AJ, 86, 1658
Henrichs, H. F. 1984, Proc. 4th European IUE Conf., ESA SSSP-218, p.43, eds Rolfe, E. & Battrick, B., Rome
Hubert - Delplace, A.M. 1981 in Proc. IAU Symp. 98, Be stars, eds. M. Jaschek and H. G. Groth (Dordrecht: Reidel), p. 125
Huang, S. S. 1977, ApJ, 212, 121
Kaper, L. et al. 1996, A&AS, 116, 257
Kaper, L. et al. 1997, A&A, 327, 281
Kaper, L. et al. 1999, A&A, 344, 231
Lamers et al. 1982, ApJ, 258, 186
Lamers et al. 1988, ApJ, 325, 342
Lyratzi, E. & Danezis, E. 2004, AIPC, 740, 458
Lyratzi, E. et al. 2007a, PASJ, 59, 357
Lyratzi, E. et al. 2007b, AIPC, 938, 176
Lyratzi, E. et al. 2009, NewAR, 53, 179
Markova, N. 2000, A&AS, 144, 391
Marlborough, J. M. & Snow, T. P. 1976, in Proc. IAU Symp. 70, Be and Shell Stars, ed. A. Slettebak (Dordrecht: Reidel), p. 179
Mulan, D. J. 1984a, ApJ, 283, 303
Mulan, D. J. 1984b, ApJ, 284, 769
Mulan, D. J.: 1986, A&A, 165, 157
Prinja, R. K. & Howarth, I. D. 1988, MNRAS, 233, 123
Prinja, R. K. 1990, MNRAS, 246, 392
Rivinius, Th. et al. 1997, A&A, 318, 819
Sahade, J. et al. 1984, A&AS, 56, 17
Sahade, J. & Brandi, E. 1985, Rev. Mex. Astron. Astrofis. 10, 229
Slettebak, A. 1976, in Proc. IAU Symp. 70, Be and Shell Stars, ed. A. Slettebak (Dordrecht: Reidel), p. 123
Slettebak, A. 1979, SSRv, 23, 541
Stoeckley, T. R. 1968, MNRAS, 140, 141
Struve, O. 1931a, ApJ, 73, 94
Struve, O. 1931b, ApJ, 74, 225
Struve, O. 1942, ApJ, 95, 134
Tuthill, P. et al. 1999, Nature, 398, 487
Underhill, A. B. 1975, ApJ, 199, 693
Underhill, A. B. & Doazan, V. 1982, B Stars with and without emission lines, NASA SP–456, Part II, chapter 10
Underhill, A. B. & Fahey, R. P. 1984, ApJ, 280, 712
Waldron, W. L. et al. 1992, nvos.work, 181
Waldron, W. L. et al. 1994, ApJ, 426, 725

Mem. S.A.It. Suppl. Vol. 15, 138

Memorie della
Supplementi

Studying the location of SACs and DACs regions in the environment of hot emission stars

A. Antoniou[1], E. Danezis[1], E. Lyratzi[1,2], L.Č. Popović[3], M.S. Dimitrijević[3,4], and E. Theodossiou[1]

[1] University of Athens, Faculty of Physics Department of Astrophysics, Astronomy and Mechanics, Panepistimioupoli, Zographou 157 84, Athens, Greece
e-mail: ananton@phys.uoa.gr
[2] Eugenides Foundation, 387 Sygrou Av., 17564, Athens, Greece
[3] Astronomical Observatory of Belgrade, Volgina 7, 11160 Belgrade, Serbia
[4] Laboratoire d'Étude du Rayonnement et de la Matiére en Astrophysique, Observatoire de Paris-Meudon, UMR CNRS 8112, Bâtiment 18, 5 Place Jules Janssen, F-92195 Meudon Cedex, France

Abstract. Hot emission stars (Oe and Be stars) present complex spectral line profiles, which are formed by a number of DACs and/or SACs. In order to explain and reproduce theoretically these complex line profiles we use the GR model (Gauss-Rotation model). This model presupposes that the regions, where the spectral lines are created, consist of a number of independent and successive absorbing or emitting density regions of matter. Here we are testing a new approach of the GR model, which supposes that the independent density regions are not successive. We use this new approach in the spectral lines of some Oe and Be stars and we compare the results of this method with the results deriving from the classical GR model that supposes successive regions.

Key words. Stars: hot emission stars– Stars: spectral lines – Stars: DACs, SACs

1. Introduction

In the spectra of Hot Emission Stars (Oe and Be stars) we observe peculiar line profiles. In order to explain this peculiarity, we propose and use the Discrete Absorption Components (DACs) (Bates & Halliwell 1986) and Satellite Absorption Components (SACs) theory (Danezis et al. 2005). DACs or SACs arise from density regions surrounding the star or lying far away from it. These density regions present spherical (or apparent spherical) symmetry around the star or their own center (Lyratzi et al. 2007). This model presupposes that the regions, where the spectral lines are created, consist of a number of independent and successive absorbing or emitting density regions of matter. In this study we are testing a new approach of GR model, which supposes that the density regions are independent but not successive. We use this new approach in order to study the density regions that produce the C IV ($\lambda\lambda$ 1548.155, 1550.774 Å) and the N V ($\lambda\lambda$ 1238.821, 1242.804 Å) resonance lines

Send offprint requests to: A. Antoniou

of a number of Oe stars as well as the Mg II ($\lambda\lambda$ 2795.523, 2802.698 Å) resonance lines and the Fe II (λ 2585.876 Å) spectral lines of a number of Be stars. Comparing the results of this method with the results deriving from the classical GR model that supposes successive regions, we try to conclude to the best method for the case of hot emission stars.

2. Method of analysis

In order to reproduce the peculiar line profiles, which are due to the presence of DACs or SACs, we have to calculate the line function. Recently, Danezis et al. (2005, 2007) proposed a model (the so called Gaussian-Rotational model, GR model), in order to explain the complex structure of the density regions which create the spectral lines with SACs or DACs and which lie in the environment of hot emission stars and some Active Galactic Nuclei (AGNs). As we have already mentioned, this model presupposes that the regions, where the spectral lines are created, consist of a number of independent and successive absorbing or emitting density regions of matter, as the area that contains these spherical density regions is near the star and thus is limited. The GR line function (Danezis et al. 2007) has the following form:

$$I_\lambda = [I_{\lambda 0} \prod_i e^{-L_i \xi_i} + \sum_j S_{\lambda ej}(1 - e^{-L_{ej}\xi_{ej}}] \prod_g e^{-L_g \xi_g} \quad (1)$$

where:
$I_{\lambda 0}$: is the initial radiation intensity,
L_i, L_{ej}, L_g : are the distribution functions of the absorption coefficients k_i, k_{ej}, k_g,
ξ: is the optical depth in the centre of the spectral line,
S_{ej}: is the source function that is constant during one observation.

The $e^{-L_i \xi_i}$ and $e^{-L_g \xi_g}$ are the distribution functions of each absorption satellite component and $S_{\lambda ej}(1 - e^{-L_{ej}\xi_{ej}})$ is the distribution function of each satellite emission component. In the GR line function, in the case of a number of independent but successive absorbing or emitting density layers of matter the final profile that is produced by a group of absorption lines is given by the product of the line functions of each component. On the other hand, the final profile that is produced by a group of emission lines is given by the addition of the line functions of each SAC. The addition of a group of functions is completely different from the multiplication of functions. The spectral line profile that results from the addition of a group of functions is exactly the same with the profile that results from a composition of the same functions. A new idea of our scientific group is to examine the form of the GR line function in the case that the density regions of matter which produce the satellite absorption or emission components are independent but not successive. In this case the above line function takes the following form:

$$I_\lambda = I_{\lambda 0} \sum_i e^{-L_i \xi_i} + \sum_j S_{\lambda ej}(1 - e^{-L_{ej}\xi_{ej}}) \quad (2)$$

The new idea of this study is to measure the new values of the parameters that we calculate in the case that the independent density regions of matter that produce the absorption or emission satellite components are successive or not.

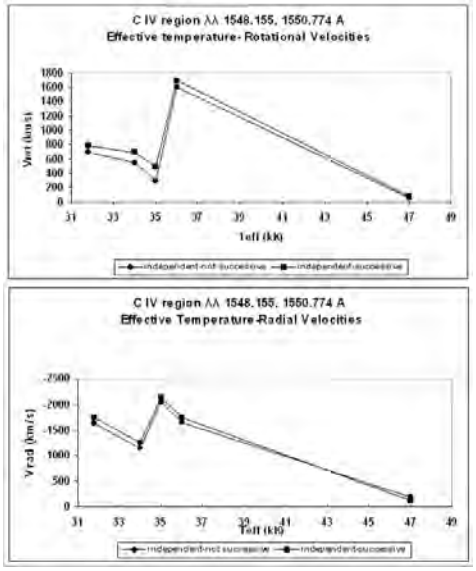

Fig. 1. Variation of the values of the rotational (up) and radial (down) velocities of the C IV ($\lambda\lambda$ 1548.155, 1550.774 Å) density regions, as a function of the effective temperature of the studied Oe stars.

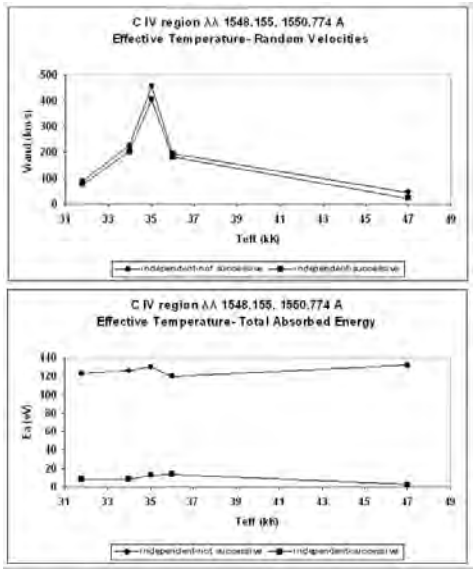

Fig. 2. Variation of the values of the random velocities (up) and the total absorbed energy (down) of the ions of the C IV ($\lambda\lambda$ 1548.155, 1550.774 Å) density regions, as a function of the effective temperature of the studied Oe stars.

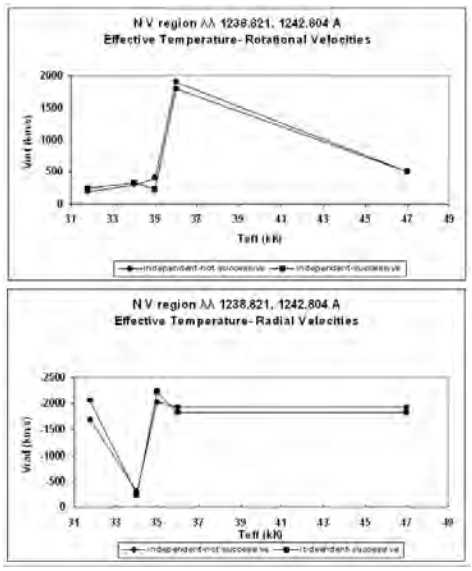

Fig. 3. Variation of the values of the rotational (up) and radial (down) velocities of the N V ($\lambda\lambda$ 1238.821, 1242.804 Å) density regions, as a function of the effective temperature of the studied Oe stars.

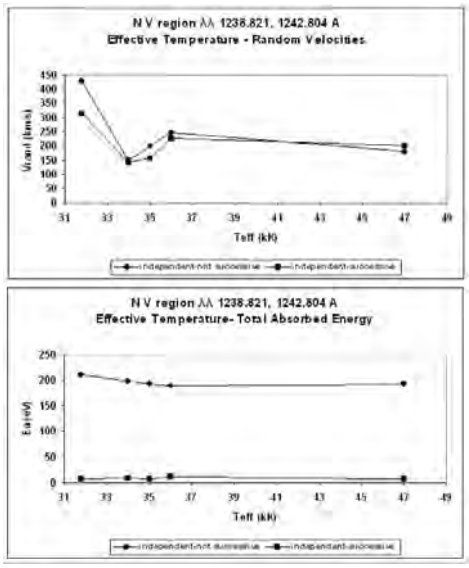

Fig. 4. Variation of the random velocities (up) and the total absorbed energy (down) of the N V ($\lambda\lambda$ 1238.821, 1242.804 Å) density regions, as a function of the effective temperature of the studied Oe stars.

3. The results of our study

We study the density regions that produce the C IV ($\lambda\lambda$ 1548.155, 1550.774 Å) and the N V ($\lambda\lambda$ 1238.821, 1242.804 Å) resonance lines in the HD 57061, HD 93521, HD 47129, HD 24911 and HD 49798 Oe stars, as well as the Mg II ($\lambda\lambda$ 2795.523, 2802.698 Å) resonance lines and the Fe II (λ 2585.876 Å) spectral line in the HD 30386, HD 42335, HD 53367, HD 45910 and HD 200120 Be stars.

3.1. The Oe stars

In figures 1 and 2 we present the variation of the values of the rotational, the radial and the random velocities as well as the total absorbed energy of the density layers of matter which corresponds to the highest value of the radial velocity in the C IV ($\lambda\lambda$ 1548.155, 1550.774 Å) regions, as a function of the effective temperature of the studied Oe stars.

In figures 3 and 4 we present the variation of the same parameters in the N V ($\lambda\lambda$

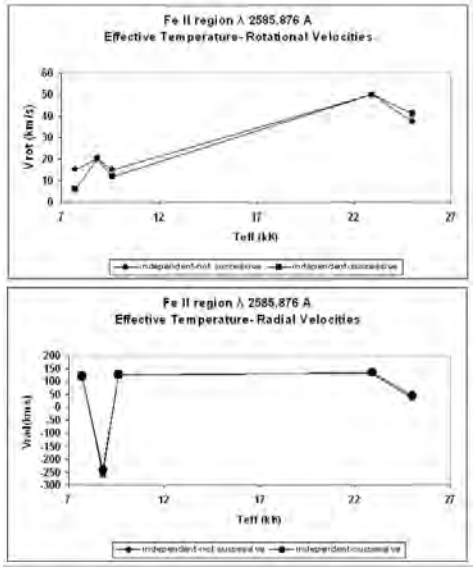

Fig. 5. Variation of the values of the rotational (up) and radial (down) velocities of the Fe II (λ 2585.876 Å) density regions, as a function of the effective temperature of the studied Be stars.

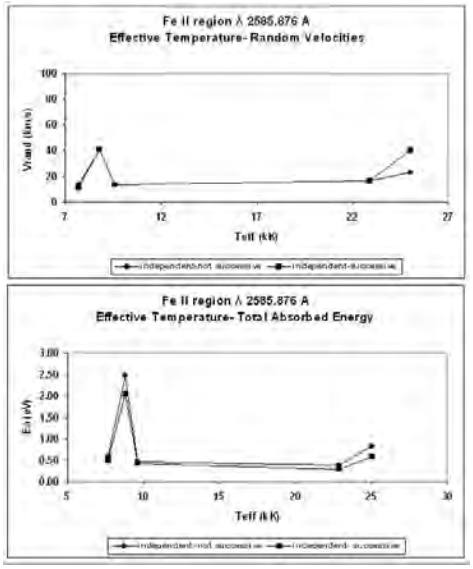

Fig. 6. Variation of the values of the random velocities (up) and the total absorbed energy (down) of the Fe II (λ 2585.876 Å) density regions, as a function of the effective temperature of the studied Be stars.

1238.821, 1242.804 Å) regions, as a function of the effective temperature of the studied Oe stars. In each case the points indicated with a circle correspond to the case of independent but not successive layers of matter, while the points indicated with a square correspond to the case of the independent and successive layers of matter.

3.2. The Be stars

In figures 5 and 6 we present the variation of the values of the rotational, the radial and the random velocities, as well as the total absorbed energy of the density layer of matter, which corresponds to the highest value of the radial velocity in the Fe II (λ 2585.876 Å) region, as a function of the effective temperature of the studied Be stars.

In figures 7 and 8 we present the variation of the same parameters in the Mg II ($\lambda\lambda$ 2795.523, 2802.698 Å) regions as a function of the effective temperature of the studied Be stars. The points indicated with a circle correspond to the case of independent but not suc-

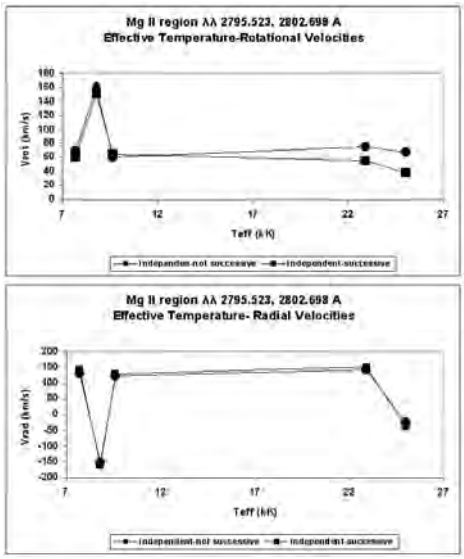

Fig. 7. Variation of the values of the rotational(up) and radial (down) velocities of the Mg II ($\lambda\lambda$ 2795.523, 2802.698 Å) density regions, as a function of the effective temperature of the studied Be stars.

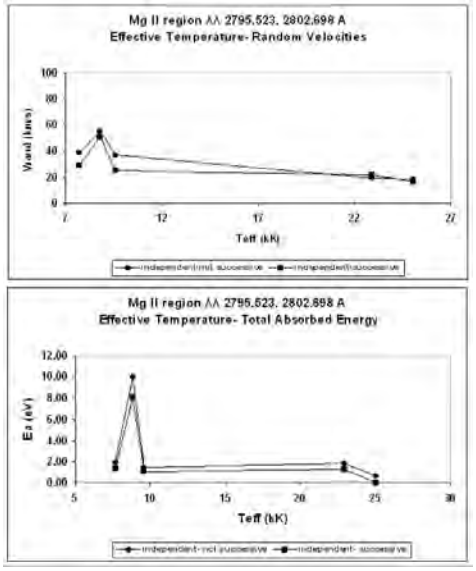

Fig. 8. Variation of the values of the random velocities (up) and the total absorbed energy (down) of the Mg II ($\lambda\lambda$ 2795.523, 2802.698 Å) density regions, as a function of the effective temperature of the studied Be stars.

cessive layers of matter, while the points indicated with a square correspond to the case of the independent and successive layers of matter.

4. Conclusions

In all cases, comparing the results, we observe that the mean values of all the kinematic parameters do not change depending on the applied method. However, in the case of Oe stars, studying the absorbed energy of C IV and N V spectral lines, the method of the independent but not successive layers of matter gives higher values than the method of the independent and successive layers of matter. This is what we theoretically expected. On the contrary, in the case of Be stars, studying the absorbed energy of the Fe II and Mg II spectral lines both methods give the same results. Theoretically, in all cases (of Oe and Be stars), we expected to find higher values for the total absorbed energy when we supposed not successive layers of matter, than when we supposed successive layers of matter. As we said, this is what we found in the case of Oe stars, studying the C IV and N V spectral lines, which lie in the post-coronal regions, which are hotter regions, in small distance from the star (Underhill & Doazan 1982). However, in the case of Be stars, studying the Fe II and Mg II spectral lines, which lie in the cool envelope (i.e. cooler regions, in greater distance from the star (Underhill & Doazan 1982)), both methods (of successive and not successive layers of matter) gave the same values for the total absorbed energy. This difference is a quite interesting phenomenon and our future work includes a study of a great number of Oe and Be stars, in order to make a statistical study on this different behavior. Probably, it depends on the extent of the area in which the density regions of matter evolve, as well as on the optical depth of the lines that are created in these regions.

Acknowledgements. This research project is progressing at the University of Athens, Department of Astrophysics, Astronomy and Mechanics, under the financial support of the Special Account for Research Grants, which we thank very much. This work also was supported by Ministry of Science Technological Development of Serbia and, through the projects 'Influence of collisional processes on astrophysical plasma line shapes' and 'Astrophysical spectroscopy of extragalactic objects'.

References

Bates, B. & Halliwell, D. R. 1986, MNRAS, 493, 206
Danezis, E. et al. 2005, MemSAIS, 7, 107
Danezis, E. et al. 2007, PASJ, 59, 827
Lyratzi, E. et al. 2007, PASJ, 59, 357
Underhill, A. B. & Doazan, V. 1982, B Stars with and without emission lines, NASA SP-456

Mem. S.A.It. Suppl. Vol. 15, 143

Memorie della
Supplementi

On the Stark broadening in hot stars

Zoran Simić[1], Milan S. Dimitrijević[1,2], and Andjelka Kovačević[2]

[1] Astronomical Observatory, Volgina 7, 11160 Belgrade, Serbia
e-mail: zsimic@aob.bg.ac.rs
[2] Observatoire de Paris-Meudon, 92195 Meudon, France
[3] Department for Astronomy, Faculty for Mathematics, Studentski Trg 16, 11000 Belgrade, Serbia

Abstract. In hot star atmospheres exist conditions where Stark widths are comparable and even larger than the thermal Doppler widths, so that the corresponding line broadening parameters are of importance for the hot star plasma investigation. Here, we investigated theoretically the influence of collisions with charged particles on heavy element spectral line profiles for Te I, Cr II and Sn III in spectra of A stars and white dwarfs. We applied semiclassical perturbation theory. When it can not be applied in an adequate way, due to the lack of reliable atomic data, we used modified semiempirical theory.

Key words. Stark broadening – line profiles – atomic data – stellar atmospheres

1. Introduction

With the development of new space techniques, the quality and quantity of spectroscopic data for trace elements has increased. For example, Yuschenko & Gopka (1996), identified one line of tellurium in the Procyon photosphere spectrum. Chayer et al. (2005) observed tellurium spectral lines in ultraviolet spectra of the cool DO white dwarf HD199499. They report as well presence of tellurium lines in the cool DO dwarf HZ21.

Chromium lines are interesting due to their presence in stellar atmospheres, so that they give possibility to determine chromium abundance and investigate chromium stratification in stelar atmospheres (Dimitrijević et al. 2005, 2007) and to be used for the diagnostics of stellar plasma and for more rafined synthesis of stellar spectra. They have been identified in A-type star spectra, as e.g. o Peg (Adelman 1994), 7 Sex (Adelman & Philip 1996), ϕ Aqu (Caliskan & Adelman 1997) which are all and chemically peculiar stars.

Spectral lines of neutral tin are present in the spectra of A type stars, for example γ Equ (Adelman et al. 1979). Also, a Sn II spectral line is observed in Przybylski's star by Cowley et al. (2000).

Here we use the semiclassical perturbation method (Sahal-Bréchot 1969a,b) to calculate the Stark broadening parameters. When it can not be applied in an adequate way, due to the lack of reliable atomic data, we used modified semiempirical theory (Dimitrijević & Konjević 1980).

2. Results and discussions

For Te I, Cr II and Sn III spectral line Stark broadening parameters, the full

Send offprint requests to: Z. Simić

semiclassical perturbation approach (Sahal-Bréchot 1969a,b) has been applied. A summary of the formalism for ionized emitters is given in Dimitrijević et al. (1991) and Dimitrijević & Sahal-Bréchot (1996). Also, for Sn III spectral line Stark width, modified semiempirical approach (Dimitrijević & Konjević 1980) has been applied. The needed energy levels have been taken from Moore (1971) and Wiese & Musgrove (1989). The oscillator strengths have been calculated by using the method of Bates & Damgaard (1949), and the tables of Oertel & Shomo (1968). For higher levels, the method of van Regemorter et al. (1979) has been used.

There are no experimental and other theoretical data for the 2 Te I and 4 Cr II multiplets. For the considered Sn III 6s $^1S_0 - 6p\ ^1P^o_1$ spectral line, Kieft et al. (2004) measured Stark width and they also, obtained the first theoretical result by using semiempirical (Griem 1968) approach.

For example, we investigated the influence of Stark broadening on Te I spectral lines in DB white dwarf atmospheres for 6s $^5S^o$ - 7p ^5P (5125.2 Å) and the 6s $^5S^o$ - 6p ^5P (9903.9 Å) multiplet by using the corresponding model with T_{eff} = 15000 K and $\log g$ = 7 (Wickramasinghe 1972). For the model atmosphere of the DB white dwarfs the prechosen optical depth points at the standard wavelength λ_s=5150 Å(τ_{5150}) are used in Wickramasinghe (1972). As one can see in Fig. 1, for the plasma conditions in the DB white dwarf atmospheres, thermal Doppler broadening is much less important compared to Stark broadening.

Stark broadening parameters, line widths and shifts for 4 Cr II $3d^5$ - $3d^4$4p multiplets are shown in Table 1. This table shows electron-, and proton-impact broadening parameters for Cr II, for a perturber density of 10^{17} cm^{-3} and temperatures from 5000 up to 100000 K. The quantity C (given in Å cm^{-3}), when divided by the corresponding full width at half maximum, gives an estimate for the maximum perturber density for which tabulated data may be used.

We synthesized Cr II 4588.2 Å line profile using SYNTH code Piskunov (1992) (Fig. 3) and, DIPSO program package, for the corresponding equivalent width, for a model atmosphere with T_{eff} = 8 750 K and $\log g$ =4.0 as a function of chromium abundance. One can see in Fig. 3 that the influence of Stark broadening increases in line wings and with chromium abundance as expected. From Figs. 3 and 4. one can see that in A type CP stars exist atmospheric layers where Doppler and Stark widths are comparable, so that the influence of Stark broadening is important.

One can see from Table 2, a good agreement with experimental value of both our results for Stark width for Sn III 6s $^1S_0 - 6p\ ^1P^o_1$ obtained by using semiclassical and modified semiempirical approach. Obviously, this ratio is better for our values than for

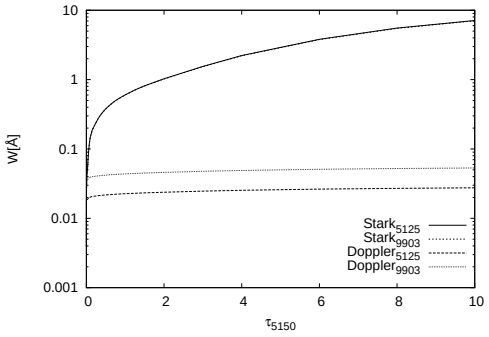

Fig. 1. Thermal Doppler and Stark widths for Te I 5125.2 and 9903.9 Åspectral lines for a DB white dwarf atmosphere model: T_{eff} = 15000 K, $\log g$ = 7 (Wickramasinghe 1972), as a function of optical depth τ_{5150}.

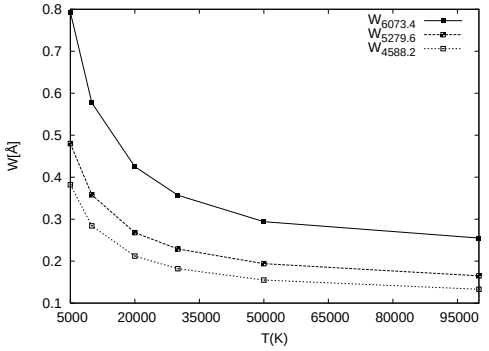

Fig. 2. Stark widths for resonant Cr II spectral lines as a function of temperature.

Table 1. Stark broadening parameters for Cr II, $3d^5$ - $3d^4 4p$ spectral lines.With *W* is denoted Full width at half maximum (FWHM) (e - electrons,p - protons) and with d shift.

TRANSITION	T(K)	W_e(Å)	d_e(Å)	W_p(Å)	d_p(Å)
	5000	0.514E-01	-0.334E-03	0.148E-02	-0.542E-04
CrII	10000	0.382E-01	-0.379E-03	0.268E-02	-0.120E-03
^{6}S-^{6}P^o	20000	0.282E-01	-0.438E-03	0.382E-02	-0.232E-03
2060.4 Å	30000	0.238E-01	-0.425E-03	0.431E-02	-0.311E-03
C=0.15E+21	50000	0.196E-01	-0.460E-03	0.473E-02	-0.405E-03
	100000	0.157E-01	-0.515E-03	0.528E-02	-0.547E-03
	5000	0.382	0.718E-01	0.102E-01	0.117E-02
CrII	10000	0.284	0.491E-01	0.175E-01	0.244E-02
^{4}F-^{4}D^o	20000	0.212	0.378E-01	0.244E-01	0.416E-02
4588.2 Å	30000	0.182	0.319E-01	0.268E-01	0.505E-02
C=0.40E+21	50000	0.155	0.265E-01	0.295E-01	0.639E-02
	100000	0.133	0.219E-01	0.329E-01	0.770E-02
	5000	0.480	0.743E-01	0.120E-01	0.874E-03
CrII	10000	0.358	0.514E-01	0.209E-01	0.188E-02
^{4}F-^{4}F^o	20000	0.268	0.399E-01	0.293E-01	0.337E-02
5279.6 Å	30000	0.229	0.338E-01	0.325E-01	0.425E-02
C=0.53E+21	50000	0.194	0.274E-01	0.357E-01	0.546E-02
	100000	0.165	0.229E-01	0.398E-01	0.679E-02
	5000	0.793	0.264	0.144E-01	0.411E-02
CrII	10000	0.577	0.197	0.258E-01	0.806E-02
^{4}F-^{4}P^o	20000	0.425	0.155	0.368E-01	0.127E-01
6073.4 Å	30000	0.357	0.134	0.414E-01	0.156E-01
C=0.70E+21	50000	0.294	0.110	0.459E-01	0.184E-01
	100000	0.255	0.920E-01	0.521E-01	0.221E-01

Table 2. Comparison between W_m-experimental Stark width with theoretical: W_{se}-semiempirical, W_{sc}-semiclassical and W_{mse}-modified semiempirical.

Transition	W_m(Å)	Rel. error	$\frac{W_m}{W_{se}}$	$\frac{W_m}{W_{sc}}$	$\frac{W_m}{W_{mse}}$
Sn III					
$6s\ ^1S_0 - 6p\ ^1P^o_1$	1.22	50%	1.70	0.92	1.15
5226.2 Å					

semiempirical one obtained by Kieft et al. (2004) using Griem (1968) method, not applicable for multiply charged ions, see Dimitrijević & Konjević (1980).

In order to see the influence of Stark broadening mechanism for Sn III spectral line in stellar plasma conditions, we have calculated Stark widths for a Kurucz (1979) A type star (T_{eff} = 10000 K, $\log g$ = 4.5) atmosphere model and compared them with Doppler ones. Obtained results in function of the Rosseland optical depth are presented in Fig. 5. One can see, that exist photospheric layers where Doppler and Stark widths are comparable and

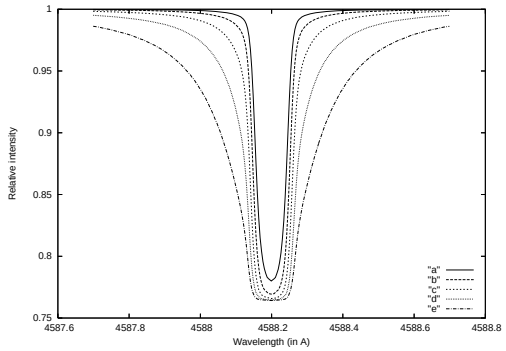

Fig. 3. Comparison of the Cr II 4588.2 Åline profile ("a") without Stark broadening contribution and with this contribution for different Cr abundances log Cr/H: ("b") Solar one, ("c") -3.75, ("d") -3.25 , ("e") -2.75. The atmosphere model: T_{eff} = 8750 K, log g= 4 (Piskunov 1992).

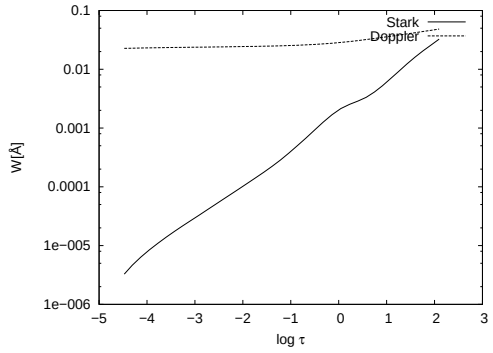

Fig. 4. Thermal Doppler and Stark widths for Cr II 4588.2 Åfor a model: T_{eff} = 10000 K, log g = 4.5 (Kurucz 1979) of an A type star, as a function of the Rosseland optical depth.

even where the Stark width is dominant and must be taken into account. Also, in Fig. 5, for the same atmosphere model, we presented Stark widths and contributions of different collision processes to the total Stark width in comparison with Doppler one. In this case, elastic and strong collisions and inelastic collision from upper levels have a similar contribution to the full Stark width as well as the similar behaviour with temperature.

We note that in all cases considered here Stark broadening influences on line shapes of

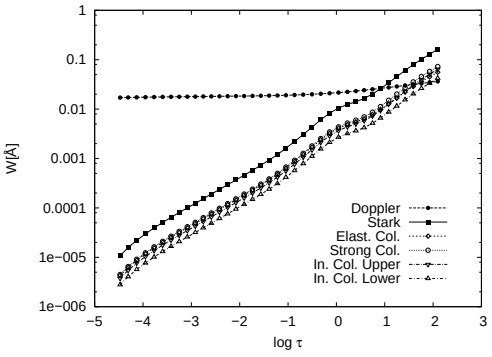

Fig. 5. Thermal Doppler, Stark and contributions of different collision processes to the total Stark width of Sn III 5226.2 Åline as functions of optical depth for an A type star (Kurucz 1979) model: T_{eff} = 10000 K and log g = 4.5.

considered stellar types and should be taken into account.

Acknowledgements. This work is a part of the project 146 001 "Influence of collisional processes on astrophysical plasma lineshapes", supported by the Ministry of Science and Technological Development of Serbia.

References

Adelman, S.J. 1994, MNRAS, 271, 355
Adelman, J., & Philip, A.G. 1996, Mon. Not. R. Astron. Soc., 282, 1181
Adelman, J., Bidelman, P., Pyper, M. 1979, ApJ SS, 40, 371
Bates, D. R., & Damgaard, A. 1949, Trans.Roy.Soc. London, Ser. A, 242, 101
Caliskan, H., & Adelman, J. 1997, Mon. Not. R. Astron. Soc., 288, 501
Chayer, P., Vennes, S., Dupuis, J., & Kruk, J.W. 2005, ApJ, 630, L169
Cowley, C.R., Ryabchikova, T., Kupka, F., Bord, D.J., Mathys, G., Bidelman, W.P.: 2000, MNRAS, 317, 299
Dimitrijević, M.S., & Konjević N. 1980, JQSRT, 24, 451
Dimitrijević, M.S., & Sahal-Bréchot, S. 1996, Physica Scripta, 54, 50
Dimitrijević, M.S., Sahal-Bréchot, S., & Bommier, V. 1991, A&A S 89, 581

Dimitrijević, M. S., Ryabchikova, T., Popović, L. Č., Shylyak, D., & Khan, S. 2005, A&A, 435, 1191

Dimitrijević, M.S., Ryabchikova, T., Simić, Z., Popović, L. Č., & Dačić, M. 2007, A&A, 469, 681

Griem, H. R. 1968, Phys. Rev. 165, 258

Kieft, E.R., van der Mullen, J.J.A.M., Kroesen, G.M.W., Banine, V. Koshelec, K.N. 2004, Physical Review, E 70, 066402

Kurucz, R.L. 1979, Astrophys. J. Suppl. Series, 40, 1

Moore, C.E. 1971, Atomic Energy Levels, Vol.II, U.S. Department of Commerce, NBS, Government Printing Office, Washington D.C.

Oertel, G. K. & Shomo. L. P. 1968, ApJS, 16, 175

Piskunov N. 1992, In: Stellar Magnetism, Eds. Yu.Glagolevskij, I.Romanyuk, 92

Sahal-Bréchot, S. 1969a, A&A, 1, 91

Sahal-Bréchot, S. 1969b, A&A, 2, 322

van Regemorter, H., Hoang Binh Dy, & Prud'homme, M. 1979, J. Phys. B, 12, 1073

Wickramasinghe, D.T. 1972, Mem. R. Astron. Soc., 76, 129

Wiese, W.L., & Musgrove, A. 1989, Atomic Data for Fusion Vol. 6, Spectroscopic Data for Titanium, Chromium and Nickel, Vol.2, Chromium, Controled Fusion Atomic Data Center, Oak Ridge National Laboratory, Oak Ridge

Yuschenko, A. V., & Gopka, V. F. 1996, Astron. Astrophys. Transactions, 10, 307

Mem. S.A.It. Suppl. Vol. 15, 148

Memorie della
Supplementi

Ab initio calculations of Ca V Stark broadening parameters

Rafik Hamdi[1], Nébil Ben Nessib[1],
Milan S. Dimitrijević[2,3], and Sylvie Sahal-Bréchot[3]

[1] Groupe de Recherche en Physique Atomique et Astrophysique, Institut National des Sciences Appliquées et de Technologie, Centre Urbain Nord B. P. No. 676, 1080 Tunis Cedex, Tunisia.
[2] Astronomical Observatory, Volgina 7, 11060 Belgrade 74, Serbia.
[3] Laboratoire d'Étude du Rayonnement et de la Matière en Astrophysique, UMR CNRS 8112, Observatoire de Paris-Meudon, 92195 Meudon, France.
e-mail: mdimitrijevic@aob.bg.ac.rs

Abstract. We have determined Stark broadening parameters for 8 Ca V multiplets by using the semiclassical perturbation approach. The calculations have been performed ab initio, since energy levels and oscillator strengths are calculated using SUPERSTRUCTURE code. The obtained results are presented as a function of temperature, for perturber density of 10^{17} cm^{-3}. In order to provide Stark broadening data for the most important charged perturbers in stellar atmospheres, electron-, proton-, and ionized helium-impact full halfwidths and shifts have been calculated. There is no other theoretical or experimental Stark broadening data for Ca V for comparison and new Stark broadening parameters calculations and measurements will be of interest for comparison with our calculations.

Key words. atomic processes – line: profiles – atomic data

1. Introduction

Stark broadening mechanism is important for the investigation, analysis, and modelling of B-type, and particularly A-type stellar atmospheres as well as for white dwarf atmospheres. In Popović et al. (2001), the influence of Stark broadening on Nd II lines in A-type stellar atmospheres was investigated. It was demonstrated that neglecting this mechanism introduces an error between 10% and 45% in the equivalent width determination and influences on abundance values. Hamdi et al. (2008) investigated the influence of Stark broadening on Si VI lines in DO white dwarf spectra. It was found that this mechanism is dominant in broad regions of the atmospheres considered.

Spectral analysis by means of NLTE model atmospheres has presently arrived at a high level of sophistication, which is now hampered largely by the lack of reliable atomic data and accurate line-broadening tables. Strong efforts should be made to improve upon this situation (Rauch et al. 2007).

Ca V belongs to the sulfure-like sequence, its ground state configuration is [Ne]$3s^2 3p^4$

Send offprint requests to: M.S. Dimitrijević

with the term ^{3}P. The cosmic abundance of calcium is 2×10^{-6} by number relative to hydrogen (Allen 1973), and lines emitted by neutral and ionized calcium are visible in astrophysical spectra. In particular, Calcium lines are detected in the atmospheres of white dwarfs (see Zuckerman et al. (2003), for example). Recently, calcium in higher ionization stage (Ca X) is observed in photosphere of the hot white dwarf KPD 0005+5106 (Werner, Rauch, & Kruk 2008). Ca V lines are introduced in atmospheric model used by Rauch et al. (2007) to study the white dwarf central star of Sh 2-216 planetary nebula.

The aim of this work is to provide ab initio calculations of Stark broadening parameters of Ca V lines. In addition to electron-impact full halfwidths and shifts, Stark broadening parameters due to proton- and ionized helium-impacts have been calculated. Thus, we have provided Stark broadening data for all the important charged perturbers in stellar atmospheres. In previous papers (Ben Nessib, Dimitrijević, & Sahal-Bréchot 2004; Hamdi et al. 2007), we have calculated Stark broadening parameters of Si V and Ne V using SUPERSTRUCTURE and Bates & Damgaard (1949) method for oscillator strengths. It was found that the difference is tolerable.

2. The method

The energy levels and oscillator strengths were carried out with the general purpose atomic structure program SUPERSTRUCTURE (Eissner, Jones, & Nussbaumer 1974), as modified by Nussbaumer & Storey (1978). The adopted atomic model for Ca V includes 12 configurations $3s^23p^4$, $3s3p^5$, $3s^23p^33d$, $3s^23p^34\ell$, $3s^23p^35\ell$ ($\ell \leq n-1$). The wave functions are of configuration mixing type, and each configuration is expanded in terms of Slater States. The radial functions are calculated in scaled Thomas-Fermi statistical model potential, which depends on parameters λ_{nl} determined variationally by optimizing the weighted sum of energy terms. Scaling parameters used in this work are λ_{1s}=1.4368, λ_{2s}=1.1125, λ_{2p}=1.0540, λ_{3s}=1.1460, λ_{3p}=1.1346, λ_{3d}=1.1080, λ_{4s}=1.1491, λ_{4p}=1.1144, λ_{4d}=1.1249, λ_{4f}=1.2739, λ_{5s}=1.1581, λ_{5p}=1.1285, λ_{4d}=1.14699, λ_{4f}=1.9600, λ_{5g}=1.800. Relativistic corrections are introduced by means of Breit-Pauli approximation in intermediate coupling.

We have calculated mean radii and mean square radii within the hydrogenic approximation with a quantum defect, using the effective quantum numbers n_i^* obtained from the Ritz formula.

Stark broadening parameter calculations have been performed within the semiclassical perturbation method (Sahal-Bréchot 1969a,b). This formalism has been reviewed briefly .e.g. in (Hamdi et al. 2008).

3. Results and discussion

By combining the SUPERSTRUCTURE code for calculating energy levels and oscillator strengths and the code for the Stark broadening calculations, we calculated ab initio Stark broadening parameters. Calculated Stark broadening widths [full width at half-maximum (FWHM)] and shifts for a perturber density of 10^{17}cm^{-3} and temperature from 50 000 K to 500 000 K are shown in Table 1 for electron-, proton-and singly ionized helium-impact broadening. Such temperatures are of interest for modelling of some hot star atmospheres. Higher temperatures are of interest for fusion plasma as well as for stellar interiors. We also specify a parameter C (Dimitrijević & Sahal-Bréchot 1984), which gives an estimate for the maximal perturber density for which the line may be treated as isolated, when it is divided by the corresponding full width at half maximum. For each value given in Table 1 the collision volume V multiplied by the perturber density N is much less than one and the impact approximation is valid (Sahal-Bréchot 1969a,b). When the impact approximation is not valid, the ion broadening contribution may be estimated by using the quasi-static approach (Sahal-Bréchot 1991). In the region where neither approximation is valid, a unified-type theory should be used. For example, in Barnard, Cooper, & Smith (1974)

Table 1. This table gives electron-, proton and singly-charged helium-impact broadening parameters for Ca V lines calculated using SUPERSTRUCTURE oscillator strength, for a perturber density of 10^{17} cm^{-3} and temperatures from 50000 to 500000 K. Transitions, averaged wavelength for the multiplet (in Å) and parameter C are also given. This parameter when divided with the corresponding Stark width gives an estimate for the maximal pertuber density for which the line may be treated as isolated. w_e: electron-impact full Stark width at half maximum, d_e: electron-impact Stark shift, w_{H^+}: proton-impact full Stark width at half maximum, d_{H^+}: proton-impact Stark shift, w_{He^+}: singly charged helium-impact full Stark width at half maximum, d_{He^+}: singly charged helium-impact Stark shift.

Transition	T(kK)	w_e	d_e	w_{H^+}	d_{H^+}	w_{He^+}	d_{He^+}
$3p^4\ ^3P$-$3s3p^5\ ^3P^\circ$	50.	0.19E-2	-0.28E-3	0.76E-5	-0.95E-5	0.14E-4	-0.94E-5
694.6 Å	100.	0.14E-2	-0.17E-3	0.20E-4	-0.18E-4	0.30E-4	-0.18E-4
C= 0.69E+20	150.	0.11E-2	-0.14E-3	0.30E-4	-0.26E-4	0.42E-4	-0.24E-4
	200.	0.95E-3	-0.14E-3	0.40E-4	-0.31E-4	0.49E-4	-0.28E-4
	300.	0.78E-3	-0.12E-3	0.51E-4	-0.39E-4	0.61E-4	-0.34E-4
	500.	0.62E-3	-0.11E-3	0.70E-4	-0.50E-4	0.72E-4	-0.42E-4
$3p^4\ ^1D$-$3s3p^5\ ^1P^\circ$	50.	0.12E-2	-0.82E-4	0.70E-5	-0.51E-5	0.13E-4	-0.51E-5
591.6 Å	100.	0.87E-3	-0.52E-4	0.17E-4	-0.10E-4	0.26E-4	-0.97E-5
C= 0.48E+20	150.	0.71E-3	-0.47E-4	0.25E-4	-0.14E-4	0.35E-4	-0.13E-4
	200.	0.62E-3	-0.49E-4	0.33E-4	-0.17E-4	0.41E-4	-0.16E-4
	300.	0.51E-3	-0.47E-4	0.41E-4	-0.23E-4	0.50E-4	-0.19E-4
	500.	0.41E-3	-0.46E-4	0.54E-4	-0.29E-4	0.57E-4	-0.25E-4
$3p^4\ ^1D$-$3p^3(^2D)3d\ ^1D^\circ$	50.	0.63E-3	-0.30E-4	0.16E-5	-0.19E-5	0.29E-5	-0.19E-5
433.7 Å	100.	0.43E-3	-0.18E-4	0.42E-5	-0.38E-5	0.67E-5	-0.37E-5
C= 0.30E+20	150.	0.35E-3	-0.16E-4	0.68E-5	-0.55E-5	0.98E-5	-0.52E-5
	200.	0.30E-3	-0.18E-4	0.90E-5	-0.69E-5	0.12E-4	-0.64E-5
	300.	0.25E-3	-0.18E-4	0.13E-4	-0.91E-5	0.15E-4	-0.79E-5
	500.	0.20E-3	-0.18E-4	0.17E-4	-0.12E-4	0.19E-4	-0.10E-4
$3p^4\ ^3P$-$3p^3(^2P)3d\ ^3D^\circ$	50.	0.59E-3	-0.39E-4	0.12E-5	-0.21E-5	0.23E-5	-0.21E-5
376.5 Å	100.	0.39E-3	-0.24E-4	0.34E-5	-0.40E-5	0.54E-5	-0.39E-5
C= 0.20E+20	150.	0.32E-3	-0.22E-4	0.56E-5	-0.57E-5	0.79E-5	-0.53E-5
	200.	0.27E-3	-0.22E-4	0.74E-5	-0.70E-5	0.97E-5	-0.65E-5
	300.	0.22E-3	-0.21E-4	0.10E-4	-0.91E-5	0.12E-4	-0.78E-5
	500.	0.18E-3	-0.20E-4	0.14E-4	-0.12E-4	0.16E-4	-0.99E-5
$3p^4\ ^3P$-$3p^3(^2P)3d\ ^3P^\circ$	50.	0.58E-3	-0.37E-4	0.12E-5	-0.20E-5	0.23E-5	-0.20E-5
375.6 Å	100.	0.39E-3	-0.23E-4	0.38E-5	-0.40E-5	0.54E-5	-0.38E-5
C= 0.20E+20	150.	0.32E-3	-0.21E-4	0.56E-5	-0.56E-5	0.78E-5	-0.52E-5
	200.	0.27E-3	-0.21E-4	0.74E-5	-0.69E-5	0.97E-5	-0.64E-5
	300.	0.22E-3	-0.20E-4	0.10E-4	-0.90E-5	0.12E-4	-0.77E-5
	500.	0.18E-3	-0.20E-4	0.14E-4	-0.11E-4	0.15E-4	-0.98E-5
$3p^4\ ^3P$-$3p^3(^2D)3d\ ^3S^\circ$	50.	0.53E-3	-0.56E-4	0.12E-5	-0.18E-5	0.23E-5	-0.18E-5
343.6 Å	100.	0.38E-3	-0.33E-4	0.33E-5	-0.35E-5	0.52E-5	-0.33E-5
C= 0.12E+20	150.	0.31E-3	-0.28E-4	0.53E-5	-0.49E-5	0.75E-5	-0.45E-5
	200.	0.27E-3	-0.28E-4	0.70E-5	-0.60E-5	0.91E-5	-0.55E-5
	300.	0.22E-3	-0.25E-4	0.96E-5	-0.78E-5	0.11E-4	-0.67E-5
	500.	0.18E-3	-0.22E-4	0.13E-4	-0.98E-5	0.14E-4	-0.85E-5

Table 1. continued

Transition	T(kK)	w_e	d_e	w_{H^+}	d_{H^+}	w_{He^+}	d_{He^+}
$3p^4\ ^3P$-$3p^3(^2D)3d\ ^3P^\circ$	50.	0.48E-3	-0.84E-4	0.13E-5	-0.19E-5	0.24E-5	-0.19E-5
322.1 A	100.	0.35E-3	-0.47E-4	0.34E-5	-0.37E-5	0.53E-5	-0.35E-5
C= 0.11E+20	150.	0.29E-3	-0.40E-4	0.54E-5	-0.51E-5	0.75E-5	-0.47E-5
	200.	0.25E-3	-0.38E-4	0.72E-5	-0.63E-5	0.90E-5	-0.57E-5
	300.	0.21E-3	-0.34E-4	0.96E-5	-0.79E-5	0.11E-4	-0.69E-5
	500.	0.17E-3	-0.28E-4	0.13E-4	-0.10E-4	0.14E-4	-0.86E-5
$3p^4\ ^3P$-$3p^3(^4S)3d\ ^3D^\circ$	50.	0.47E-3	-0.70E-4	0.13E-5	-0.15E-5	0.24E-5	-0.15E-5
316.2 A	100.	0.34E-3	-0.38E-4	0.33E-5	-0.30E-5	0.52E-5	-0.29E-5
C= 0.75E+19	150.	0.28E-3	-0.33E-4	0.53E-5	-0.42E-5	0.74E-5	-0.39E-5
	200.	0.24E-3	-0.32E-4	0.69E-5	-0.52E-5	0.87E-5	-0.48E-5
	300.	0.20E-3	-0.28E-4	0.91E-5	-0.67E-5	0.11E-4	-0.58E-5
	500.	0.16E-3	-0.24E-4	0.12E-4	-0.85E-5	0.13E-4	-0.73E-5

a simple analytical formula for such a case is given.

We see that using the SUPERSTRUCTURE code one obtains a set of energy levels and oscillator strengths, enabling an ab initio calculation of Stark broadening parameters. This is suitable especially for multicharged ions when other theoretical and experimental atomic data are scare. The Stark broadening parameters obtained here, contribute to the creation of a set of such data for as large as possible number of spectral lines, of significance for a number of problems in astrophysics. As for example, spectral analysis by means of NLTE model atmospheres, that need a large set of atomic data and accurate line-broadening tables.

There is no other theoretical or experimental Stark broadening data for Ca V for comparison and new Stark broadening parameters calculations and measurements will be of interest for comparison with our calculations.

Acknowledgements. This work is a part of the Project 146 001 Influence of collisional processes on astrophysical plasma lineshapes, supported by the Ministry of Science and Technological Development of Serbia.

References

Allen, C. W. 1973, Astrophysical Quantities, Athlone, London

Barnard, A. J., Cooper, J., & Smith, E. W. 1974, J. Quant. Spectrosc. Radiat. Transfer, 14, 1025

Bates, D. R. & Damgaard, A. 1949, Philos. Trans. R. Soc. London A, 242, 101

Ben Nessib, N., Dimitrijević, M. S., & Sahal-bréchot, S. 2004, A&A, 423, 397

Dimitrijević, M. S. & Sahal-Bréchot, S. 1984, J. Quant. Spectrosc. Radiat. Transfer, 31, 301

Eissner, W., Jones, M., & Nussbaumer, H. 1974, Comput. Phys. Commun., 8, 270

Hamdi, R., Ben Nessib, N., Dimitrijević, M. S., & Sahal-Bréchot, S. 2007, ApJS, 170, 243

Hamdi, R., Ben Nessib, N., Milovanović, N., Popović, L. Č., Dimitrijević, M. S., & Sahal-Bréchot, S. 2008, MNRAS, 387, 871

Nussbaumer, H. & Storey, P. J. 1978, A&A, 64, 139

Popović, L. Č., Simić, S., Milovanović, N., & Dimitrijević, M. S. 2001, ApJS, 135, 109

Rauch, T., Ziegler, M., Werner, K., et al. 2007, A&A, 470, 317

Sahal-Bréchot, S. 1969a, A&A, 1, 91

Sahal-Bréchot, S. 1969b, A&A, 2, 322

Sahal-Bréchot, S. 1991, A&A, 245, 322

Werner, K., Rauch, T., & Kruk, J. W. 2008, A&A, 492, L43

Zuckerman, B. Koester, D., Reid, I. N., & Hünsch, M. 2003, ApJ, 596, 477

Mem. S.A.It. Suppl. Vol. 15, 152

Memorie della
Supplementi

On the Stark broadening of CuI spectral lines

Besma Zmerli[1], Nébil Ben Nessib[1], Milan S. Dimitrijević[2,3] and Sylvie Sahal-Bréchot[3]

[1] Groupe de Recherche en Physique Atomique et Astrophysique, Institut National des Sciences Appliquées et de Technologie, University of 7 November at Carthage, Centre Urbain Nord B. P. No. 676, 1080 Tunis Cedex, Tunisia
[2] Astronomical Observatory, Volgina 7, 11060 Belgrade 38, Serbia
[3] Laboratoire d'Étude du Rayonnement et de la Matière en Astrophysique, Observatoire de Paris-Meudon, UMR CNRS 8112, Bâtiment 18, 5 Place Jules Janssen, F-92195 Meudon Cedex, France e-mail: mdimitrijevic@aob.bg.ac.yu

Abstract. Using the semiclassical perturbation theory of Sahal-Bréchot Stark widths and shifts for CuI 324.75, 327.39, 510.55, 570.02 and 578.21 nm spectral lines have been calculated. Obtained results are compared with different available data. Also, they are used to study the dependence of Stark broadening parameters with temperature.

Key words. line: profiles – atomic data

1. Introduction

We investigate here the Stark broadening parameters of neutral cooper spectral lines. This metal is often used in electrical industry as electrode materials, so that the data on its spectral lines are important not only for plasma research but also for diagnostic techniques in industrial laboratories.

Recently, the temperature dependence of Stark widths for neutral atom spectral lines is investigated (Zmerli et al., 2008), in order to find a method for scaling of Stark broadening parameters with temperature, better than the dependence $T^{-1/2}$, used often in astrophysics. In Zmerli et al., (2008), Stark width dependence on T is analyzed using the lines of neutral helium, and it was found that for considered lines Stark width increases with T, contrary to the $T^{-1/2}$ dependence. It was found also that after a critical temperature, Stark width starts to decrease, and a simple method for interpolation with temperature is proposed.

In the present work, we calculate the Stark width and shift of CuI spectral lines due to collisions with electrons using the semiclassical perturbation formalism Sahal-Bréchot, (1969a,b). The obtained results are used here to confirm the conclusions of Zmerli et al., (2008) on the Stark width behaviour with temperature, using the more sophisticated theory and the spectrum of another neutral emitter.

2. Theory

For the transition between the levels i and f, the total width at half intensity FWHM ($W = 2w$) and the shift d can be put under the form (Sahal-Bréchot, 1969a,b, 1974):

Send offprint requests to: M. S. Dimitrijević

$$W = 2w = N \int_0^\infty v f(v)\, dv \times \left(\sum_{i' \neq i} \sigma_{ii'}(v) + \sum_{f' \neq f} \sigma_{ff'}(v) + \sigma_{el} \right), \quad (1)$$

$$d = \int_0^\infty v f(v)\, dv \int_{R_3}^{R_D} 2\pi\rho d\rho \sin 2\phi_p. \quad (2)$$

Here, i' and f' are the perturbing levels, N is the density of perturbers, v is the relative velocity and $f(v)$ is the Maxwellian distribution of velocities.

The inelastic cross section $\sigma_{ii'}(v)$ (resp. $\sigma_{ff'}(v)$) are given by an integration over the impact parameter ρ of the transition probability $P_{ii'}(v,\rho)$ (resp. $P_{ff'}(v,\rho)$) as:

$$\sum_{i' \neq i} \sigma_{ii'}(v) = \frac{1}{2}\pi R_1^2 + \int_{R_1}^{R_D} 2\pi\rho d\rho \sum_{i' \neq i} P_{ii'}(\rho, v)\,. \quad (3)$$

The elastic contribution to the width or elastic cross section is given by

$$\sigma_{el} = 2\pi R_2^2 + \int_{R_2}^{R_D} 8\pi\rho d\rho \sin^2 \delta, \quad (4)$$

with

$$\delta = (\phi_p^2 + \phi_q^2)^{1/2}. \quad (5)$$

The phase shifts ϕ_p and ϕ_q are respectively due to the quadratic and quadrupolar interactions, described in Sahal-Bréchot, (1969a); Sahal-Bréchot and Van Regemorter, (1964) for one-electron atoms, and in Sahal-Bréchot, (1974) for complex atoms.

All the cutoffs (R_1, R_2, R_3), as well as the symmetrization procedures in the inelastic cross sections, are described in Sahal-Bréchot, (1969b). R_D is the upper cutoff allowing for Debye shielding. A description of the semiclassical perturbation formalism used here is given in Sahal-Bréchot, (1969a,b); Dimitrijević and Sahal-Bréchot, (1985).

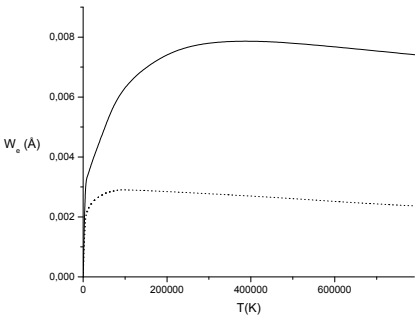

Fig. 1. Electron Stark width for the $4s\ ^2S_{1/2} - 4p\ ^2P^o_{3/2}$ transition of copper resonance spectral line (3247.54 Å) as a function of temperature T. (dot line)- electron width for the 3-level model and (solid line)- electron width for the multi-level model.

Table 1. Critical temperature T_c for CuI spectral lines.

λ (Å)	Transition	T_c (kK)
5105.54	$4s^2\ ^2D_{5/2} - 4p\ ^2P^o_{3/2}$	292
5700.24	$4s^2\ ^2D_{3/2} - 4p\ ^2P^o_{3/2}$	370
5782.13	$4s^2\ ^2D_{3/2} - 4p\ ^2P^o_{1/2}$	301
3273.96	$4s\ ^2S_{1/2} - 4p\ ^2P^o_{1/2}$	398
3247.54	$4s\ ^2S_{1/2} - 4p\ ^2P^o_{3/2}$	361

3. Results and discussion

In our calculations, energy levels and oscillator strengths have been taken from Fu et al., (1995), a compilation of CuI data including transition probabilities, oscillator strengths and lifetimes. The best values from this compilation are included in Corliss, (1970).

The widths W_{line} in Table 2 and the shifts d_{line} in Table 3 for a particular line within a multiplet are obtained by scaling the multiplet values W and d respectively using (Popović et al., 2001; Griem, 1964):

$$W_{line} = \left(\frac{\lambda}{\langle\lambda\rangle} \right)^2 W,\ d_{line} = \left(\frac{\lambda}{\langle\lambda\rangle} \right)^2 d, \quad (6)$$

Table 2. Electron widths: W_{eK} - results of Konjević and Konjević, (1986) using the approximate method of Dimitrijević and Konjević, (1986), W_{eG} - results of Grishina et al., (1998a,b) (without the accounting for the "back reaction" and the λ cutoff), W_{eGb} - results of Grishina et al., (1999) (with the accounting for the "back reaction"), W_{eB} - results of Babina et al., (2003), W_e - our calculations according to the semiclassical formalism of Sahal-Bréchot, (1969a), for CuI lines as a function of temperature T, for electron density of $N_e = 10^{16}$ cm^{-3}.

λ (Å)	T (K)	W_{eK} (Å)	W_{eG} (Å)	W_{eGb} (Å)	W_{eB} (Å)	W_e (Å)
5105.54	$4s^2\ ^2D_{5/2} - 4p\ ^2P^o_{3/2}$					
	5000	0.0149	0.0103	0.0117	0.0085	0.0093
	10000	0.0193	0.0126	0.0122	0.0099	0.0102
	20000	0.0238	0.0156	0.0139	0.0123	0.0105
	30000	0.0262	0.0177	0.0161	0.0142	0.0111
5700.24	$4s^2\ ^2D_{3/2} - 4p\ ^2P^o_{3/2}$					
	5000	0.0186	0.0128	0.0146	0.0106	0.0114
	10000	0.0240	0.0157	0.0152	0.0123	0.0136
	20000	0.0297	0.0194	0.0173	0.0153	0.0127
	30000	0.0327	0.0221	0.0201	0.0177	0.0143
5782.13	$4s^2\ ^2D_{3/2} - 4p\ ^2P^o_{1/2}$					
	5000	0.0191	0.0132	0.0150	0.0109	0.0117
	10000	0.0247	0.0162	0.0156	0.0127	0.0129
	20000	0.0306	0.0200	0.0178	0.0158	0.0134
	30000	0.0336	0.0227	0.0206	0.0182	0.0133
3273.96	$4s\ ^2S_{1/2} - 4p\ ^2P^o_{1/2}$					
	5000	-	0.00332	0.00403	0.00267	0.00300
	10000	-	0.00433	0.00400	0.00304	0.00321
	20000	-	0.00581	0.00475	0.00408	0.00330
	30000	-	0.00687	0.00563	0.00508	0.00391
3247.54	$4s\ ^2S_{1/2} - 4p\ ^2P^o_{3/2}$					
	5000	-	0.00327	0.00397	0.00263	0.00320
	10000	-	0.00426	0.00394	0.00299	0.00332
	17000	-	0.00567	0.00473	0.00401	0.00385
	20000	-	0.00572	0.00467	0.00401	0.00380
	30000	-	0.00676	0.00554	0.00500	0.00398

where, W, d and $\langle\lambda\rangle$ are values for the multiplet, and W_{line}, d_{line} and λ refer to the line within the multiplet.

We can see in Table 1 that Stark widths increase with temperature as the helium lines in Zmerli et al., (2008), contrary to the $T^{-1/2}$ dependence. However, if we calculate the temperature dependence far beyond the physical temperature range for neutral copper, we can see in Fig. 1, that after some critical temperature, Stark width values will start to decrease.

In Table 1 are given the critical temperature from which the width start to decrease for the different transitions of Cu I.

One can see that they are at very high temperatures where neutral copper lines do not exist, so that for the lower temperatures, of interest for Stark broadening of Cu I, Stark widths of considered lines always increase with temperature, and the using of $T^{-1/2}$ dependence for interpolation with temperature is incorrect.

4. Conclusion

We have calculated electron Stark widths and shifts for five lines of neutral copper, using the semiclassical perturbation formalism. These data can be used for laboratory and stellar plasmas diagnostics, investigation and modelling.

Table 3. Electron shifts: d_{eK} - results of Konjević and Konjević, (1986) using the approximate method of Dimitrijević and Konjević, (1986), d_{eG} - results of Grishina et al., (1998a,b) (without the accounting for the "back reaction" and the λ cutoff), d_{eGb} - results of Grishina et al., (1999) (with the accounting for the "back reaction"), d_{eB} - results of Babina et al., (2003), d_e - our calculations according to the semiclassical formalism Sahal-Bréchot, (1969a), for CuI lines as a function of temperature T, for electron density of $N_e = 10^{16}$ cm^{-3}.

λ (Å)	T (K)	d_{eK} (Å)	d_{eG} (Å)	d_{eGb} (Å)	d_{eB} (Å)	d_e (Å)
5105.54	$4s^2\ ^2D_{5/2} - 4p\ ^2P^o_{3/2}$					
	5000	-0.00027	0.00799	0.00783	0.00783	0.00683
	10000	-0.00082	0.00883	0.00889	0.00886	0.00802
	20000	-0.00118	0.00929	0.00947	0.00947	0.00882
	30000	-0.00136	0.00925	0.00945	0.00944	0.00853
5700.24	$4s^2\ ^2D_{3/2} - 4p\ ^2P^o_{3/2}$					
	5000	-0.00034	0.00996	0.00976	0.00976	0.00838
	10000	-0.00102	0.01101	0.01108	0.01104	0.01020
	20000	-0.00147	0.01158	0.01180	0.01180	0.01060
	30000	-0.00170	0.01153	0.01178	0.01177	0.01090
5782.13	$4s^2\ ^2D_{3/2} - 4p\ ^2P^o_{1/2}$					
	5000	-0.00035	0.01025	0.01004	0.01004	0.00816
	10000	-0.00105	0.01133	0.01140	0.01136	0.00977
	20000	-0.00152	0.01192	0.01215	0.01215	0.00995
	30000	-0.00175	0.01186	0.01212	0.01211	0.01000
3273.96	$4s\ ^2S_{1/2} - 4p\ ^2P^o_{1/2}$					
	5000	-	0.00237	0.00230	0.00228	0.00210
	10000	-	0.00251	0.00254	0.00254	0.00210
	20000	-	0.00243	0.00250	0.00251	0.00184
	30000	-	0.00227	0.00234	0.00234	0.00144
3247.54	$4s\ ^2S_{1/2} - 4p\ ^2P^o_{3/2}$					
	5000	-	0.00231	0.00226	0.00224	0.00241
	10000	-	0.00247	0.00250	0.00250	0.00273
	20000	-	0.00239	0.00246	0.00247	0.00272
	30000	-	0.00223	0.00230	0.00230	0.00237

Our results demonstrate that the considered Stark widths increase with temperature for all T values of interest and that the critical temperature when they start to decrease is beyond the temperature range of interest. The temperature trend of Stark widths is not in accordance with $T^{-1/2}$ dependence.

References

Babina, E. M., Il'in, G. G., Konovalova, O. A., Salakhov, M. Kh. and Sarandaev, E. V., 2003 Publ. Astron. Obs. Belgrade No 76 163

Corliss, C. H., 1970 J. Res. Nat. Bur. Stand **74 A** 781

Dimitrijević, M. S. and Konjević, N., 1986 Astron. Astrophys. **163** 297

Dimitrijević, M. S. and Sahal-Bréchot, S., 1985 Phys. Rev. A **31** 316

Fu, K., Jogwich, M., Knebel, M. and Wiesemann, K., 1995 Atomic Data and Nuclear Data Tables **61** 1

Griem, H. R., 1964 PlasmaSpectroscopy, Mc Graw-Hill, NewYork

Grishina, N. A., Il'in, G. G., Salakhov, M. Kh. and Sarandaev, E. V., 1998a 19th *SPIG Contributed papers*, 361

Grishina, N. A., Il'in, G. G., Salakhov, M. Kh. and Sarandaev, E. V., 1998b *Coherent Optics and Optical Spectroscopy*, Kazan, Russia 43

Grishina, N. A., Il'in, G. G., Salakhov, M. Kh. and Sarandaev, E. V., 1999 *Coherent Optics and Optical Spectroscopy*, Kazan, Russia 23
Konjević, R. and Konjević, N., 1986 Fizika. **18** 327
Popović, L .Č., Milovanović, N. and Dimitrijević, M. S., 2001 Astron. Astrophys. **365** 656
Sahal-Bréchot, S. and Van Regemorter, H., 1964 Ann. d'Astron. **27** 432
Sahal-Bréchot, S., 1969a Astron. Astrophys. **1** 91
Sahal-Bréchot, S., 1969b Astron. Astrophys. **2** 322
Sahal-Bréchot, S., 1974 Astron. Astrophys. **35** 321
Zmerli, B., Ben Nessib N & Dimitrijević M S 2008, Eur. J. Phys. D **48** 389

Mem. S.A.It. Suppl. Vol. 15, 157

Memorie della
Supplementi

Van der Waals broadening in atmospheric pressure surface wave discharges sustained in rare gases

Jose Muñoz[1], Cristina Yubero[1], Milan S. Dimitrijević[2,3], and Maria Dolores Calzada[1]

[1] Grupo de Espectroscopía de Plasmas, Edificio C-2. Campus Rabanales. Universidad de Córdoba E-14071 Córdoba (Spain)
[2] Astronomical Observatory, Volgina 7, 11060, Belgrade, Serbia
[3] Laboratoire d'Étude du Rayonnement et de la Matière en Astrophysique, Observatoire de Paris-Meudon, UMR CNRS 8112, Bâtiment 18, 5 Place Jules Janssen, F-92195 Meudon Cedex, France e-mail: mdimitrijevic@aob.bg.ac.rs

Abstract. The profiles of several He, Ne and Ar gas atomic lines arising from an atmospheric pressure microwave (2.45 GHz) surface wave discharge have been studied in order to determine the most suitable lines for measuring gas temperatures. Gas temperature results obtained from van der Waals Broadening of rare gas lines are in good agreement with results obtained from the rovibrational spectra of molecular species and those previously reported in the literature for the same kind of discharges.

Key words. van der Waals broadening, surface wave discharges, gas temperature, noble gases

1. Introduction

Research on van der Waals broadening has become one of the most important issues in recent spectroscopy studies since the values of this parameter can be easily related by means of the Lindholm–Foley theory to that of the gas temperature, being the knowledge of the later determining on the heavy particles kinetics.

In the present study, the profiles of several rare gas atomic lines arising from an atmospheric pressure microwave (2.45 GHz) surface wave discharge have been studied in order to determine the most suitable lines for measuring gas temperatures.

Send offprint requests to: Jose Muñoz

2. Line broadening of atomic lines

From the Lindholm–Foley theory (see Yubero et al. (2007) and references therein) it is possible to obtain the following expression relating the gas temperature (T_{gas}) and the van der Waals broadening (w_W) of a given spectral line

$$w_W = 8.18 \times 10^{-26} \lambda^2 (\alpha < \bar{R}^2 >)^{2/5} \left(\frac{T_{gas}}{\mu} \right)^{3/10} N \quad (1)$$

being λ the wavelength of the spectral line in nm, α the pertuber polarizability in cm^{-3} $< \bar{R}^2 >$ the difference of the square radius of the emitting atom in the upper and lower levels of the considered transition, μ the reduced emitter-perturber mass in a.m.u. and N the density of pertubing atoms in cm^{-3}. The previous

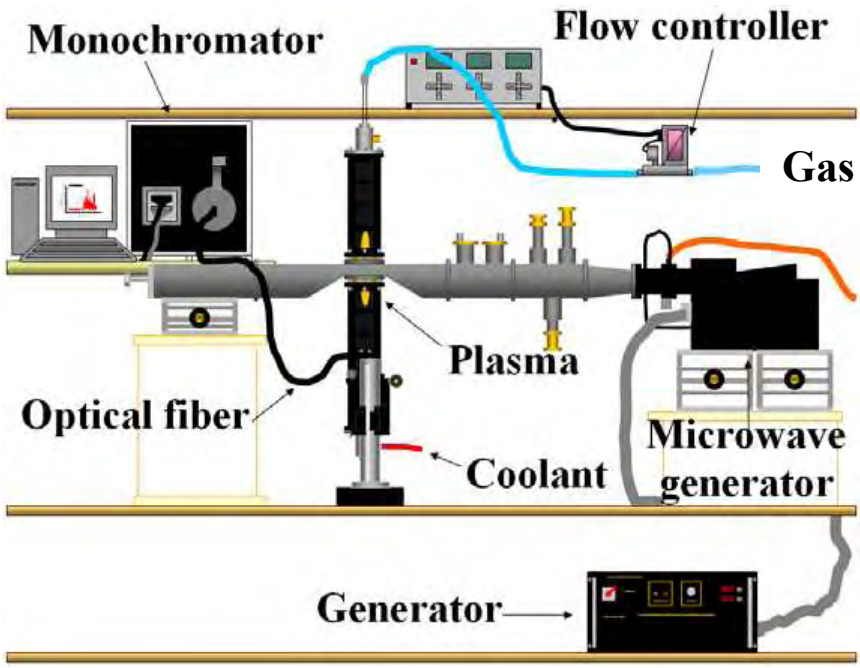

Fig. 1. Experimental Setup

equation can be simplified using the appropriate atomic parameters and the ideal gas law to obtain the following expression,

$$w_W(\mathrm{nm}) = \frac{C_W}{T_{gas}^{0.7}} \tag{2}$$

being C_W a coefficient that depends on the transition and the nature of the interacting atoms considered.

However, not every spectral line can be used for the calculation of gas temperature. Recent experimental research (Yubero et al. 2007; Munoz et al. 2009) has demonstrated that only a few lines can be used for this purpose as a consequence of the limitations arising from the theory not describing equally well the van der Waals broadening for each spectral line and each kind of perturbers, and the need of a deconvolution process to separate the van der Waals broadening. Moreover, the contribution of the Stark broadening must also be considered since its contribution to the total Lorentz width can become non negligible (Yubero et al. 2007).

3. Experimental setup

Microwave power was provided to the plasma by a SAIREM 12 kT/t microwave (2.45 GHz) generator of 2000 W maximum power in continuous mode. The power was coupled to the plasma by a surfaguide device.

High purity (99.999%) He, Ne and Ar were used as plasma gases with different flows ranging from 0.5 to 2 slm (standard litre per minute). The discharge was contained in quartz

Table 1. Experimental broadenings of the lines measured in this work. Stark broadening was calculated from the electron density.

System	λ (nm)	$w_G(\cdot 10^{-2}\text{nm})$	$w_L(\cdot 10^{-2}\text{nm})$	$n_e(\cdot 10^{14}\text{cm}^{-3})$	$w_S(\cdot 10^{-2}\text{nm})$
He I	396.47	1.91 ± 0.06	0.72 ± 0.06	0.50 ± 0.05	0.088 ± 0.009
He I	492.19	2.01 ± 0.05	1.06 ± 0.05	0.50 ± 0.05	0.163 ± 0.017
Ne I	724.51	1.34 ± 0.02	0.65 ±0.02	1.04 ± 0.07	0.045 ± 0.005
Ar I	425.93	1.93 ± 0.03	0.98 ± 0.04	1.37 ± 0.09	0.030 ± 0.003
Ar I	603.21	1.33 ± 0.02	3.07 ± 0.20	1.37 ± 0.09	0.22 ± 0.03

Table 2. Coefficients for Tgas determination from the van der Waals broadening and atomic data employed in its calculation.

System	λ (nm)	$\alpha\ (\cdot 10^{-25}\text{cm}^{-3})$	$< \bar{R}^2 >$	μ	C_W(nm)
He I	396.47	2.049	575.73	2	1.298
He I	492.19	2.049	471.82	2	1.847
Ne I	724.51	3.956	14.25	10	0.792
Ar I	425.93	16.411	378.12	20	1.479
Ar I	603.21	16.411	932.83	20	4.217

Table 3. Gas temperature calculated from the different rovibrational bands and the van der Waals broadening neglecting (T^L_{gas}) and considering (T^W_{gas}) the Stark broadening.

System	λ (nm)	T^{OH}_{gas}(K)	T^{N2+}_{gas}(K)	T^L_{gas}(K)	T^W_{gas}(K)
He I	396.47	–	2000 ± 200	1700 ± 200	2000 ± 350
He I	492.19	–	2000 ± 200	1600 ± 100	2000 ± 300
Ne I	724.51	1200 ± 120	–	1000 ± 50	1100 ± 150
Ar I	425.93	1400 ± 140	–	1300 ± 100	1400 ± 150
Ar I	603.21	1400 ± 140	–	1100 ± 100	1300 ± 150

tubes of several radii ranging from 2 to 5 mm (inner radii) and from 3 to 6 mm (outer radii).

Light emited by the discharge was analyzed with a 1m Czerny-Turner monochromator (Jobin-Ybon Horiba 1000 M) previously calibrated and equipped with a 2400 grooves/mm holographic grating.

Together with He, Ne and Ar atomic lines, the H_β (486.13 nm) line from the Balmer series and the rovibrational spectra from OH (306–312 nm) and N_2^+ (389 –392 nm) molecular species were registered for electron density measurement (Griem 1964) and gas temperature calculation respectively. A Hamamatsu R928P photomultiplier was used as detector for the atomic (He, Ne, Ar and H) lines and a Symphony CCD was the detector used for OH and N_2^+ radical spectra.

4. Experimental results

The first step to analyse the profiles is to separate the Gaussian (Doppler and Instrumental) and Loretzian (Stark and van der Waals) contributions using a commercial process of deconvolution based on the Levenberg-Marquardt non-linear algorithm for minimum squares (Table I).

Electron density was measured using Stark broadening of the H_β hydrogen line (Griem 1964) and this value was used to calculate the Stark broadening of the atomic lines used for T_{gas} calculation and evaluate its influence.

On the other hand, substituting the atomic data available in expression (1), C_W coefficients appearing in (2) were calculated for the lines used in this work. Results and data used in this calculation are shown in Table II.

Using these coefficients, gas temperature values were calculated considering and neglecting the influence of the Stark effect. Results obtained with rovibrational bands in agreement with previous experimental results (Yubero et al. 2007; Kabouzi et al. 2002; Sainz et al. 2008) are provided for comparison.

5. Conclusions

Gas temperature results obtained from van der Waals Broadening of rare gas lines are in good agreement with results obtained from the rovibrational spectra of molecular species and those previously reported in the literature for the same kind of discharges.

Even though the Stark broadening is small, its influence must be taken into account for gas temperature calculation purposes, especially in the case of He.

Further theoretical and experimental research on the description of the van der Waals broadening is needed.

Acknowledgements. This work was supported by the Ministry of Science and Technology (Spain) within the framework of the project no. ENE2005-00314, and by the Ministry of Science of Serbia through the project 146001.

References

Griem, H. R. 1964, Plasma spectroscopy, McGraw-Hill (New York)

Kabouzi Y. et al. 2002, Journal of Applied Physics, 91, 1008 – 1019

Muñoz, J. et al. 2009, Spectrochimica Acta B, 64, 167 – 172

Sainz A. et al. 2008, Spectrochimica Acta B, 63, 948 – 956

Yubero, C. et al. 2007, Spectrochimica Acta B, 62, 69 – 176

Mem. S.A.It. Suppl. Vol. 15, 161

Memorie della
Supplementi

Kinematic properties of the Broad Absorption Line Regions in the spectra of quasars

E. Lyratzi[1,2], E. Danezis[1], L.Č. Popović[3], M.S. Dimitrijević[3,4], A. Antoniou[1], and D. Stathopoulos[1]

[1] University of Athens, Faculty of Physics Department of Astrophysics, Astronomy and Mechanics, Panepistimioupoli, Zographou 157 84, Athens, Greece
e-mail: elyratzi@phys.uoa.gr
[2] Eugenides Foundation, 387 Sygrou Av., 17564, Athens, Greece
[3] Astronomical Observatory of Belgrade, Volgina 7, 11160 Belgrade, Serbia
[4] Laboratoire d'Étude du Rayonnement et de la Matiére en Astrophysique, Observatoire de Paris-Meudon, UMR CNRS 8112, Bâtiment 18, 5 Place Jules Janssen, F-92195 Meudon Cedex, France

Abstract. We use the GR model in order to fit broad spectral lines (absorption and emission) of several BAL QSOs. According to this motdel, we assume that the Broad Line Regions (BLR), which originate in a disk wind, are composed of a number of successive independent absorbing density layers, which may have different random, rotational and radial velocities. The GR model is easily used in order to fit the observed absorption lines, providing us with basic parameters of BLRs, such as random, rotational and radial velocities, as well as column density and total absorbed or emitted energy. This model supposes that the density regions of matter that construct the BLRs are independent and successive. Here we present a new form of this model, supposing that the density regions of matter are independent but not successive. We apply the two forms of the GR model on the UV spectral lines of several BAL QSOs observed with the HST and we compare the results of the two methods. Finally, we present some first concluding remarks about this comparison.

Key words. Quasars: spectral lines

1. Introduction

Assuming that the Broad Line Regions - BLR (originated in a disk wind) are composed of a number of successive independent absorbing density layers, which may have different random, rotational and radial velocities, we used the GR model (Danezis et al. 2007) in order to fit broad spectral lines. The model can be easily used in fitting the observed absorption lines, providing us with basic parameters of BLRs (random, rotational and radial velocities and column density). This model supposes that the density regions of matter that construct the BLRs are independent and successive. In this paper we present a new form of this model, supposing that the density regions of matter are independent but not successive. We apply the two forms of the GR model on

Send offprint requests to: E. Lyratzi

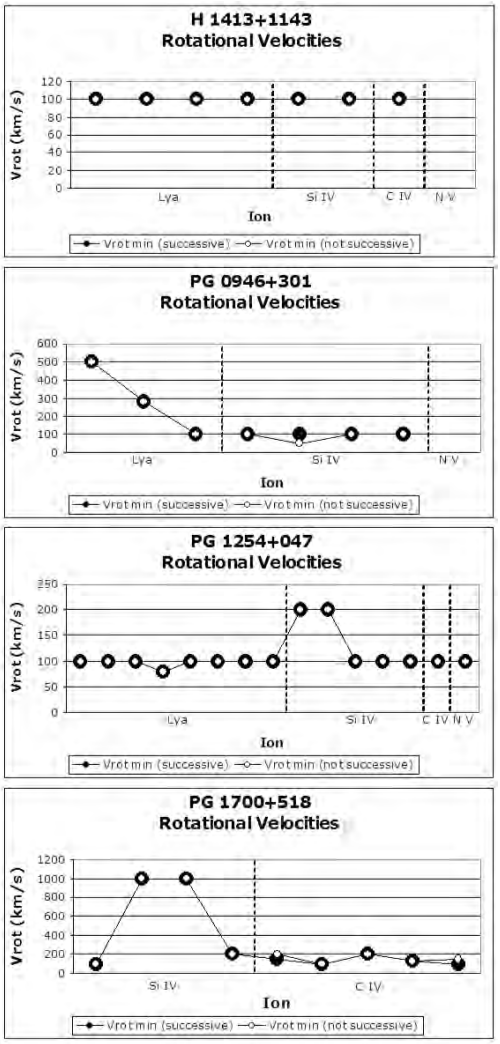

Fig. 1. Rotational Velocities taken from the analysis of the Lya, Si IV, C IV and N V spectral lines in the case of successive (black circles) or not successive (white circles) density regions. One can see that there is almost no difference between the two cases.

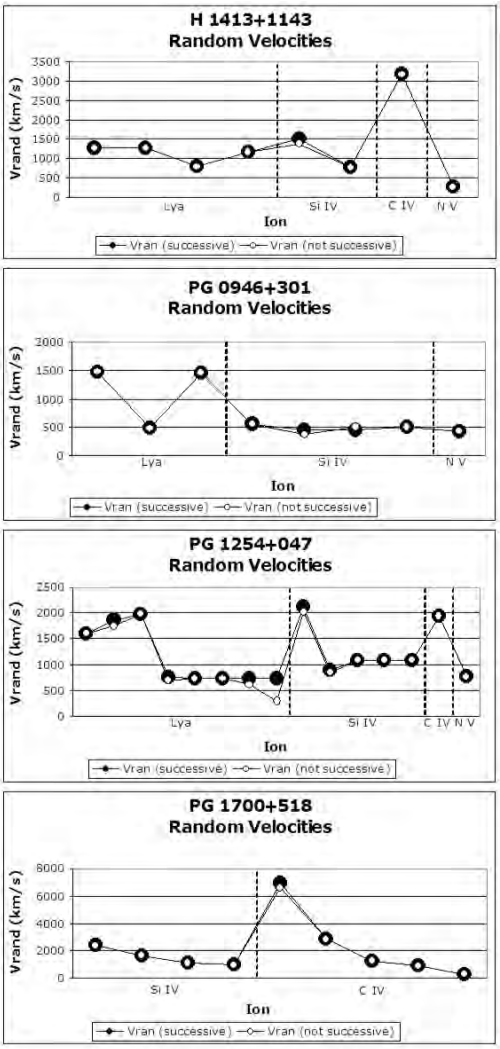

Fig. 2. Random Velocities taken from the analysis of the Lya, Si IV, C IV and N V spectral lines in the case of successive (black circles) or not successive (white circles) density regions. One can see that there is almost no difference between the two cases.

the UV C IV ($\lambda\lambda$ 1548.187, 1550.772 Å), Si IV ($\lambda\lambda$ 1393.755, 1402.77 Å), N V ($\lambda\lambda$ 1238.821, 1242.804 Å) as well as the Lya (λ 1215.68 Å) spectral lines of H 1413+1143, PG 0946+301, PG 1254+047 and PG 1700+518 BAL QSOs observed with the HST. We calculate the kinematical parameters (rotational, radial and random velocities) as well as the total absorbed energy per ion and compare the results of the two methods. We also compare our results with the respective study concerning some hot emission stars (Antoniou et al. 2010). Finally, we present some first concluding remarks about these comparisons.

2. The model

In order to study the BALs and the BELs we use the GR model (Danezis et al. 2007), which can be used successfully, for both hot emission stars and AGNs (Danezis et al. 2005). By solving the radiation transfer equations through a complex structure, as the one described, we conclude to a function for the line profile, able to give the best fit for the main spectral line and its Satellite Components at the same time.

$$I_\lambda = [I_{\lambda 0} \prod_i e^{-L_i \xi_i} + \sum_j S_{\lambda ej}(1 - e^{-L_{ej}\xi_{ej}}] \prod_g e^{-L_g \xi_g} \quad (1)$$

where: $I_{\lambda 0}$: is the initial radiation intensity,
L_i, L_{ej}, L_g : are the distribution functions of the absorption coefficients k_i, k_{ej}, k_g,
ξ: is the optical depth in the centre of the spectral line,
S_{ej}: is the source function that is constant during one observation.

2.1. The case of many absorption or emission components

In the GR line function, in the case of a number of independent and successive absorbing or emitting density layers of matter, the final profile that is produced by a group of absorption lines is given by the product of the line functions of each component. On the other hand, the final profile that is produced by a group of emission lines is given by the addition of the line functions of each component. The addition of a group of functions is completely different from the multiplication of functions. The spectral line profile that results from the addition of a group of functions is exactly the same with the profile that results from a composition of the same functions. On the contrary, the product of a group of functions is completely different from the composition of the same functions. As a result, we can use the composition of functions for the emission lines, but not for a group of absorption components. This means that in such a case we can not refer to the law of reversion of the spectral lines.

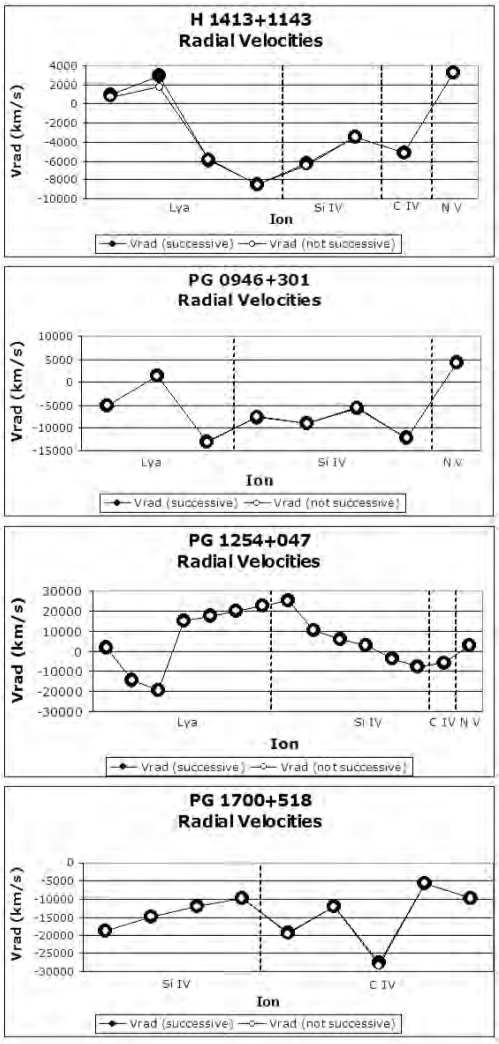

Fig. 3. Radial Velocities taken from the analysis of the Lya, Si IV, C IV and N V spectral lines in the case of successive (black circles) or not successive (white circles) density regions. One can see that there is almost no difference between the two cases.

2.2. The case of independent but not successive regions of matter

An idea of our scientific group is to examine the form of GR line function if the density regions of matter that produce the satellite absorption or emission components are

Independent but Not Successive. In this case the GR line function has the following form:

$$I_\lambda = I_{\lambda 0} \sum_i e^{-L_i \xi_i} + \sum_j S_{\lambda ej}(1 - e^{-L_{ej}\xi_{ej}}) \qquad (2)$$

We expect considerable changes in the absorbed energy. When the density regions are not successive, the initial energy flux is the same for all of them. On the other hand, when the density regions are successive, the initial energy flux for the second region is smaller than for the first, as the first density region has already absorbed an amount of the initial energy. In the same way, the initial energy flux for the third region is smaller than for the second and so on. The new idea of this study is to measure the values of the parameters that we calculate in the case that the independent density regions of matter producing the absorption or emission satellite components are not successive. Then, we compare the values extracted from both cases (successive and not successive density regions).

3. Spectral analysis

In Table 1 we present the quasars and the spectral lines that we have studied in each one of them.

3.1. Kinematical parameters

In figures 1, 2 and 3 we give a comparison of the kinematical parameters (rotational, random and radial velocities) of the regions which create the Lya, Si IV, C IV and N V spectral lines, calculated in the cases when the independent density regions of matter producing the absorption or emission satellite components are successive (black circles) or not (white circles). As one can see, the values of the kinematical parameters remain the same in both cases of successive or not successive density regions.

3.2. Total absorbed energy

In figure 4, we present the values of the total absorbed energy of the regions which create the Lya, Si IV, C IV and N V spectral lines, calculated in the cases when the independent density regions of matter producing the absorption or emission satellite components are successive (black circles) or not (white circles). As one can see there is no considerable change in

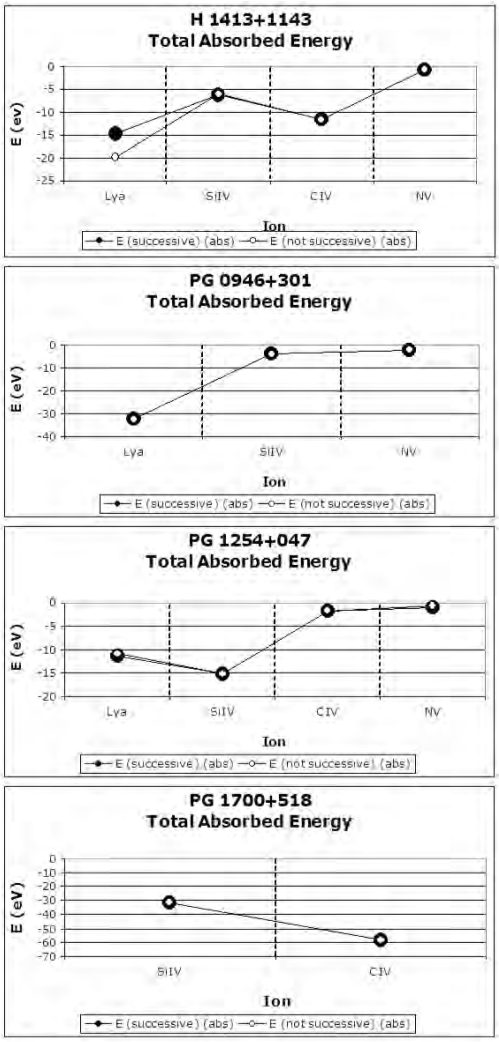

Fig. 4. Total absorbed energy, taken from the analysis of the Lya, Si IV, C IV and N V spectral lines in the case of successive (black circles) or not successive (white circles) density regions. One can see that there is almost no difference between the two cases. These results are opposed to what we theoretically expected, i.e. differentiation in the absorbed energy.

Table 1. The list of selected BAL QSOs with basic observational data

Name	z	Obs.Date	Ins./grat	Lines
H 1413+1143	2.551	Jun 23, 1993, Dec 23,1994	FOS/G400H,G570H	Lya, Si IV, C IV
PG 0946+301	1.216	Feb 16,1992	FOS/G400,G570	Lya, Si IV, C IV
PG 1254+047	1.024	Feb 17, 1993	FOS/G160L,G270H	Lya, Si IV, C IV, N V
PG 1700+518	0.212	Sep 12, 2000	STIS/G430L,G750L	Si IV, C IV

the values of the total absorbed energy depending on the two methods of calculation.

4. Concluding remarks

As we have already explained, we expected that the values of the total absorbed energy should present considerable differences supposing successive and not successive density regions. However, this is not the case in the spectral lines of the studied quasars. As one of our purposes is to compare the origin of DACs and SACs in hot emission stars and quasars, we made a similar study on hot emission stars (see Antoniou et al. 2010). In the case of Be stars presenting DACs and SACs, we found the same results as in the case of quasars, i.e. no considerable change in the values of the total absorbed energy depending on the two methods of calculation. On the contrary, in the case of Oe stars, when we considered that the density regions of matter that produce the observed DACs and SACs are not successive, we calculated larger values for the total absorbed energy, as we expected theoretically. As we have checked the validity of GR model and as we know that these differences are not due to mistakes of the mathematical model, in the near future we intend to study a great number of quasars of the same type, in order to make a statistical study on this phenomenon and its origin. A first aspect is that it depends on the extent of the area in which the density regions of matter evolve, as well as on the optical depth of the lines that are created in these regions (see also Antoniou et al. 2010).

Acknowledgements. This research project is progressing at the University of Athens, Department of Astrophysics, Astronomy and Mechanics, under the financial support of the Special Account for Research Grants, which we thank very much. This work also was supported by Ministry of Science Technological Development of Serbia and, through the projects 'Influence of collisional processes on astrophysical plasma line shapes' and 'Astrophysical spectroscopy of extragalactic objects'.

References

Antoniou, A. et al. 2010, MemSAIS, this issue
Danezis, E. et al. 2005, MemSAIS, 7, 107
Danezis, E. et al. 2007, PASJ, 59, 827

Mem. S.A.It. Suppl. Vol. 15, 176

Memorie della
Supplementi

The optical Fe II emission lines in Active Galactic Nuclei

Jelena Kovačević[1], Luka Č. Popović[1], and Milan S. Dimitrijević[1,2]

[1] Astronomical Observatory, Volgina 7, 11060 Belgrade, Serbia
e-mail: jkovacevic@aob.bg.ac.rs
[2] Laboratoire d'Étude du Rayonnement et de la Matière en Astrophysique, UMR CNRS 8112, Observatoire de Paris-Meudon, 92195 Meudon, France

Abstract. In order to investigate the origin of iron lines and to analyse their correlations with other lines and spectral properties, we constructed the Fe II template in $\lambda\lambda$ 4400-5500 Å range. We selected the 50 Fe II lines identified as the strongest in this wavelength band. The 35 of them are separated in the three line groups according to their lower level of transition, and their relative intensities within the group are calculated. The relative intensities of the rest of 15 lines are obtained from I Zw 1 object. Here we present the description of constructed template and its comparison with some other empirical and theoretical Fe II templates. We found that template can satisfactorily fit the Fe II lines. In spectra where the Fe II emission lines have different relative intensities than in I Zw 1, this template fits better than the templates based on I Zw 1.

Key words. Active galactic nuclei: spectral lines

1. Introduction

Optical Fe II ($\lambda\lambda$ 4400-5500 Å) lines are one of the most interesting features in AGN spectra. They arise in numerous transitions of the complex Fe II ion, and they can be seen only in spectra of AGN type 1 and NLSy 1 galaxies. There are many open questions about iron lines which make them very attractive for investigation. Their origin, i.e. geometrical place of their emission region in AGN, is still not clear, as well as the processes of excitation which produce Fe II emission. Also, there are many correlations of the Fe II lines and other AGN spectra properties which need a physical explanation. It is established that the Fe II emission depends on the radio, X and IR parts of the continuum and also some correlations with other lines in spectra are observed. One of the most interesting is the relation between optical Fe II and [O III] lines, which physical background is still not explained (Boroson, & Green 1992).

For investigation of the origin of iron lines and for analysis of their correlations with other lines, it is necessary to apply a good template which will fit well iron lines within $\lambda\lambda$ 4400-5500 Å range. But, the construction of iron template is very difficult since the iron lines form the features of a complex shape. In this paper, we present our model of iron template, based on the physical properties of iron region, and we compare it with other models.

Send offprint requests to: J. Kovačević

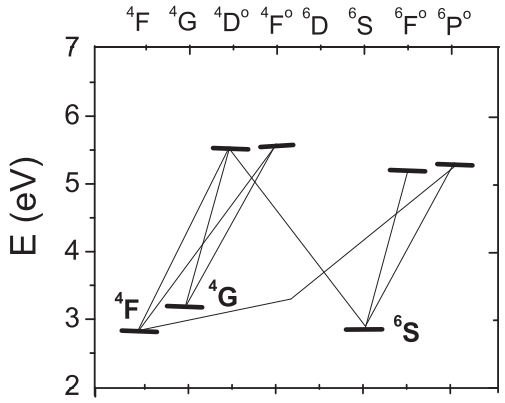

Fig. 1. Grotrian diagram shows the strongest Fe II transitions within $\lambda\lambda$ 4400-5500 Å range: lines are separated in three groups according to the lower levels of transition (^4F, ^6S and ^4G).

2. The Fe II template

We calculated the Fe II template, using the 50 Fe II emission lines, identified as the strongest within the $\lambda\lambda$ 4400-5500 Å range. The 35 of them are separated in the three line groups according to their lower level of transition: $3d^6(\,^3F2)4s\,^4F$, $3d^54s^2\,^6S$ and $3d^6(\,^3G)4s\,^4G$ (in further text ^4F, ^6S and ^4G group of lines). A simplified scheme of those transitions is shown in Fig 1. The ^4F group is consisted of 19 lines and they dominate in the blue bump of iron lines ($\lambda\lambda$ 4400-4700 Å). The lines from ^6S group (5 lines) describe the Fe II emission under the [O III] and Hβ lines, and partly from the red Fe II bump ($\lambda\lambda$ 5150-5400 Å), and ^4G lines (11 lines) dominate in the red bump.

The lines from three line groups describe about 75% of Fe II emission in observed range ($\lambda\lambda$ 4400-5500 Å), but about 25% of Fe II emission can not be explained with permitted lines which excitation energies are close to these of lines from the three line groups. The missing parts are around ~4450 Å, ~4630 Å, ~5130 Å and ~5370 Å.

There are some indications that the process of fluorescence (self-fluorescences, continuum-fluorescences or Lyα and Lyβ pumping) may have a role in appearing of some Fe II lines (Verner et al. 1999; Hartmann, & Johanson 2000). They could supply enough energy for exciting the Fe II lines with high energy of excitation, which could be one of the explanation for emission in these wavelengths.

Table 1. The list of the lines taken from Kurucz (http://kurucz.harvard.edu/linelists.html). In the first column are wavelengths, in the second oscillator strengths and in the third relative intensities measured in I Zw 1.

Wavelength	gf	Relative intensity
4414	2.65E-03	3.00
4449	2.52E-02	1.50
4471	6.40E-03	1.20
4493	3.74E-02	1.60
4611	4.13E-03	0.70
4625	8.51E-03	0.70
4628	1.83E-02	1.20
4631	1.34E-02	0.60
4660	1.15E-03	1.00
4668	3.13E-03	0.90
4734	1.28E-03	0.50
5134	2.48E-03	1.10
5366	5.37E-01	1.45
5401	1.43E-01	0.40
5427	2.17E-02	1.40

In order to complete the template for missing 25%, we selected 15 lines which probably arise with some of these mechanisms, from Kurutcz database[1]. The selected lines have wavelengths on missing parts, strong oscillator strengh and their energy of excitation goes up to ~11 eV. Relative intensities of these 15 lines are obtained from I Zw 1 spectrum by making the best fit together with Fe II lines from three line groups. The selected lines and their relative intensities are shown in Table 1.

We have assumed that each of lines can be represented with a Gaussian, described by width (W), shift (d) and intensity (I). Since all FeII lines from the template probably originate in the same region, with the same kinematical properties, values of d and W are the same for all Fe II lines in the case of one AGN, but intensities are assumed to be different. We suppose that relative intensities between the lines

[1] http://kurucz.harvard.edu/linelists.html

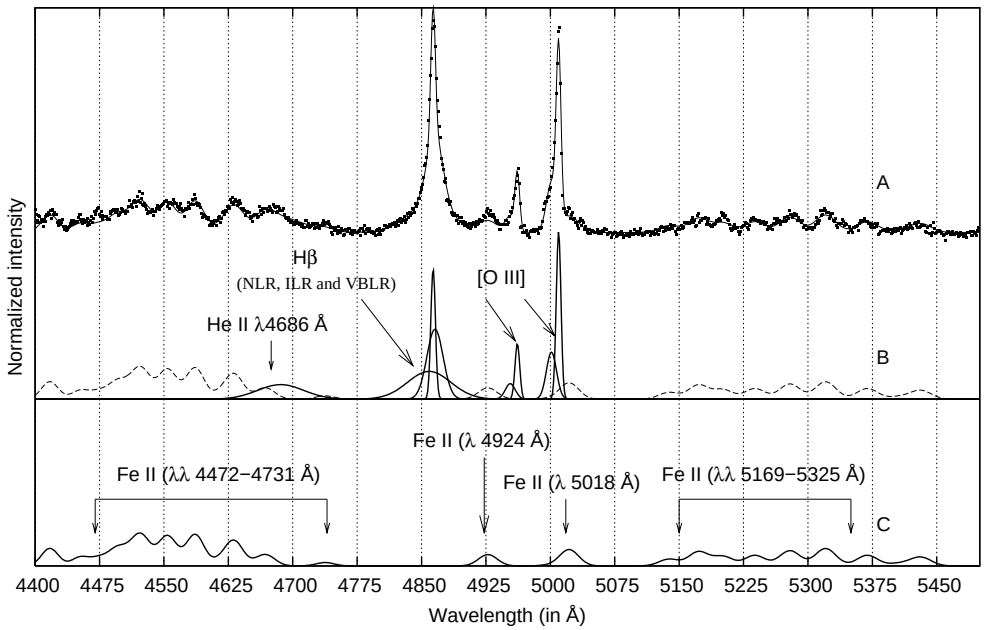

Fig. 2. Spectrum of SDSS J141755.54+431155.8 in the $\lambda\lambda$ 4400-5500 Å range: A) observed spectra (dots) and the best fit (solid line). B) decomposition of lines on Gauss functions. Template of Fe II is denoted with dashed line, and represented separately in panel C (below).

within one line group (^4F, ^6S or ^4G) can be obtained as:

$$\frac{I_1}{I_2} = \left(\frac{\lambda_2}{\lambda_1}\right)^3 \frac{f_1}{f_2} \cdot \frac{g_1}{g_2} \cdot e^{-(E_1-E_2)/kT} \quad (1)$$

where I_1 and I_2 are intensities of the lines with the same lower level of transition, λ_1 and λ_2 are transition wavelengths, g_1 and g_2 are statistical weights for the upper energy level of the corresponding transition, and f_1 and f_2 are oscillator strengths, E_1 and E_2 are energies of the upper level of transitions, k is the Boltzman constant and T is the excitation temperature.

According to that, the template of Fe II is described by 7 free parameters in fit: width, shift, four parameters of intensity - for ^4F, ^6S and ^4G line groups and for lines with relative intensities obtained from I Zw 1. The 7th parameter is excitation temperature included in calculating relative intensities whithin ^4F, ^6S and ^4G line groups.

The fit of the Fe II template is shown in Fig 2. We apply this template on large sample of AGNs (305) from SDSS database, and we found that the template fits well Fe II emission. In cases when Fe II emission of object has different properties than the one in I Zw 1, small disagreement is noticed in lines which relative intensities are obtained from I Zw 1 (see Fig 4, top). The list of 35 selected lines from three line groups, their oscillator strengths and calculated relative intensities for different excitation temperatures are shown in Table 2.

2.1. Comparison with other templates

We applied empirical template from Dong et al. (2008) and Veron-Cetty et al. (2004) and theoretical one calculated by Bruhweiler, & Verner (2008) in order to compare them with our template. Veron-Cetty et al. (2004) constructed the Fe II template by identifying a system of broad and a system of narrow Fe II lines in I Zw 1 spectrum, and measuring their relative intensities in that object.

Table 2. The list of the 35 strongest Fe II lines within the $\lambda\lambda$ 4400-5500 Å range used to calculate the Fe II template. In the first column are wavelengths, in the second terms of transitions, in the third are gf values used for the template calculation, in the fourth are the references for the source of oscillator strengths, and in the 5th-7th columns are relative intensities, calculated for T=5000 K, 10000 K and 15000 K. Intensities of lines from ^4F, ^6S and ^4G groups are normalized on intensities of λ 4549.474 Å, λ 5018.44 Å and λ 5316.6 Å lines (respectively). References for oscillator strengths are: 1 – Fuhr et al. (1981), 2 – Giridhar, & Ferro (1995), 3 – NIST Atomic Spectra Database (http://physics.nist.gov/PhysRefData/ASD/), 4 – Kurucz (1990) and 5 – http://kurucz.harvard.edu/linelists.html.

Wavelength	Terms	gf	ref.	Relative intensity		
				T=5000 K	T=10000 K	T=15000 K
4472.929	b $^4F_{5/2}$ - z $^4F^o_{3/2}$	4.02E-04	1	0.033	0.036	0.037
4489.183	b $^4F_{7/2}$ - z $^4F^o_{5/2}$	1.20E-03	1	0.105	0.110	0.111
4491.405	b $^4F_{3/2}$ - z $^4F^o_{3/2}$	2.76E-03	1	0.226	0.243	0.249
4508.288	b $^4F_{3/2}$ - z $^4D^o_{1/2}$	4.16E-03	2	0.345	0.367	0.375
4515.339	b $^4F_{5/2}$ - z $^4F^o_{5/2}$	3.89E-03	2	0.333	0.348	0.353
4520.224	b $^4F_{9/2}$ - z $^4F^o_{7/2}$	2.50E-03	3	0.235	0.233	0.233
4522.634	b $^4F_{5/2}$ - z $^4D^o_{3/2}$	9.60E-03	3	0.827	0.859	0.870
4534.168	b $^4F_{3/2}$ - z $^4F^o_{5/2}$	3.32E-04	3	0.028	0.029	0.030
4541.524	b $^4F_{3/2}$ - z $^4D^o_{3/2}$	8.80E-04	3	0.075	0.078	0.079
4549.474	b $^4F_{7/2}$ - z $^4D^o_{5/2}$	1.10E-02	4	1.000	1.000	1.000
4555.893	b $^4F_{7/2}$ - z $^4F^o_{7/2}$	5.20E-03	3	0.477	0.474	0.474
4576.340	b $^4F_{5/2}$ - z $^4D^o_{5/2}$	1.51E-03	4	0.136	0.136	0.136
4582.835	b $^4F_{5/2}$ - z $^4F^o_{7/2}$	7.80E-04	3	0.070	0.070	0.070
4583.837	b $^4F_{9/2}$ - z $^4D^o_{7/2}$	1.44E-02	2	1.420	1.353	1.331
4620.521	b $^4F_{7/2}$ - z $^4D^o_{7/2}$	8.32E-04	4	0.080	0.076	0.075
4629.339	b $^4F_{9/2}$ - z $^4F^o_{9/2}$	4.90E-03	4	0.497	0.459	0.447
4666.758	b $^4F_{7/2}$ - z $^4F^o_{9/2}$	6.02E-04	4	0.060	0.055	0.054
4993.358	b $^4F_{9/2}$ - z $^6P^o_{7/2}$	3.26E-04	4	0.041	0.030	0.027
5146.127	b $^4F_{7/2}$ - z $^6F^o_{7/2}$	1.22E-04	5	0.016	0.011	0.010
4731.453	a $^6S_{5/2}$ - z $^4D^o_{7/2}$	1.20E-03	2	0.025	0.030	0.032
4923.927	a $^6S_{5/2}$ - z $^6P^o_{3/2}$	2.75E-02	4	0.656	0.693	0.706
5018.440	a $^6S_{5/2}$ - z $^6P^o_{5/2}$	3.98E-02	4	1.000	1.000	1.000
5169.033	a $^6S_{5/2}$ - z $^6P^o_{7/2}$	3.42E-02	1	0.929	0.854	0.831
5284.109	a $^6S_{5/2}$ - z $^6F^o_{7/2}$	7.56E-04	2	0.022	0.019	0.018
5197.577	a $^4G_{5/2}$ - z $^4F^o_{3/2}$	7.92E-03	5	0.532	0.620	0.652
5234.625	a $^4G_{7/2}$ - z $^4F^o_{5/2}$	8.80E-03	3	0.615	0.695	0.723
5264.812	a $^4G_{5/2}$ - z $^4D^o_{3/2}$	1.08E-03	1	0.075	0.084	0.087
5276.002	a $^4G_{9/2}$ - z $^4F^o_{7/2}$	1.148e-02	2	0.861	0.928	0.951
5316.615	a $^4G_{11/2}$ - z $^4F^o_{9/2}$	1.17E-02	4	1.000	1.000	1.000
5325.553	a $^4G_{7/2}$ - z $^4F^o_{7/2}$	6.02E-04	4	0.044	0.047	0.048
5316.784	a $^4G_{7/2}$ - z $^4D^o_{5/2}$	1.23E-03	5	0.089	0.097	0.099
5337.732	a $^4G_{5/2}$ - z $^4D^o_{5/2}$	1.28E-04	5	0.009	0.010	0.010
5362.869	a $^4G_{9/2}$ - z $^4D^o_{7/2}$	1.82E-03	5	0.142	0.146	0.148
5414.073	a $^4G_{7/2}$ - z $^4D^o_{7/2}$	1.60E-04	5	0.012	0.012	0.013
5425.257	a $^4G_{9/2}$ - z $^4F^o_{9/2}$	4.36E-04	5	0.035	0.035	0.035

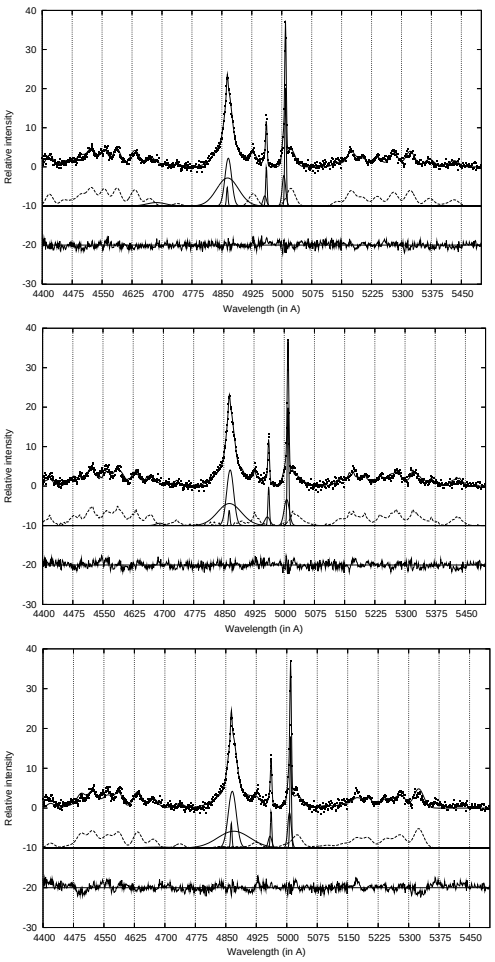

Fig. 3. Examples of fit of SDSS J020039.15-084554.9 object: with our template (top), with empirical template of Dong et al. (2008) (middle) and with theoretical template of Bruhweiler, & Verner (2008) (bottom). Since object have iron emission equally strong in blue and red iron bump (as I Zw 1), all three models fit well observed lines.

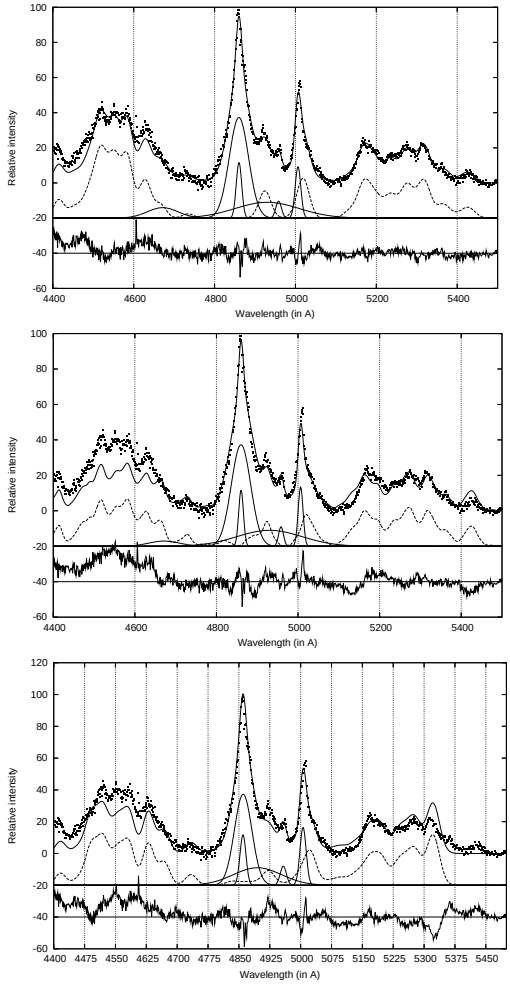

Fig. 4. Examples of fit of SDSS J111603.13 + 020852.2 object: with our template (top), with empirical template of Dong et al. (2008) (middle) and with theoretical template of Bruhweiler, & Verner (2008) (bottom). In this object iron emission is much stronger in the blue then in the red bump. Our template show disagreement in lines which relative intensity is taken from I Zw 1, but other three wavelength regions based on three line groups fit well observed Fe II. Other two models can not fit well this kind of Fe II emission.

In $\lambda\lambda$ 4400-5500 Å range they identified 46 broad and 95 narrow lines. Dong et al. (2008) improved that template by fitting with two parameters of intensity - one for broad, one for narrow Fe II lines.

Bruhweiler, & Verner (2008) calculated Fe II template using CLOUDY and an 830 level model atom, taking into account the processes of continuum and line pumping. In calculation, they apply solar abundances for a range of physical conditions as flux of ionizing photons [Φ_H], hydrogen density [n_H] and microturbulence [ξ]. We found that model with $\log[n_H/(cm^{-3})]=11$, $[\xi]/(1\ km\ s^{-1})=20$ and $\log[\Phi_H/(cm^{-2}\ s^{-1})]=21$ corresponds better than others to Fe II lines in observed spectra. In Fig 3 is shown the spectrum of SDSS J020039.15-084554.9 (NLSy1), fitted with our template (top), with template based on line intensities from I Zw 1 (Dong et al. 2008) (middle) and with template calculated by CLOUDY (Bruhweiler, & Verner 2008) (bottom). Since this object has the Fe II emission similar as I Zw 1, all three templates fit well iron lines. But, in the case of object SDSS J111603.13 + 020852.2 (Fig 4), the iron lines in the blue bump are stronger comparing to those in the red, which is significantly different from I Zw 1 object. In this case our model shows disagreement only in lines which relative intensity is taken from I Zw 1 (Fig 4, top), but other two models show larger disagreement in fit of this kind of Fe II emission (Fig 4, middle and bottom).

3. Conclusions

We found that template can satisfactorily fit the Fe II lines, which enable more precise investigation of the Fe II lines. In the spectra which Fe II emission lines have different relative intensities than in I Zw 1, this template fits better than templates based on I Zw 1 object.

Acknowledgements. This work is a part of the projects (146002): "Astrophysical Spectroscopy of Extragalactic Objects" and (146001): "Influence of collisions with charged particles on astrophysical spectra", supported by Serbian Ministry of Science and Technological Development.

Data for the present study have been entirely collected at the SDSS database.

References

Boroson, T. A., & Green, R. F. 1992, ApJS, 80, 109

Bruhweiler, F., & Verner, E. 2008, ApJ, 675, 83

Dong, X., Wang, T., Wang, J., Yuan, W., Zhou, H., Dai, H., & Zhang, K. 2008, MNRAS, 383, 581

Fuhr, J. R., Martin, G. A., Wiese, W. L., & Younger, S. M. 1981, J. Phys. Chem. Ref. Data, 10, 305

Giridhar, S. & Ferro, A. A. 1995, RMxAA, 31, 23

Hartmann, H., & Johanson, S. 2000, A&A, 359, 627

Kurucz, R.L. 1990, Trans. I. A. U. XXB, ed. M. McNally (Dordrecht: Kluwer), 168

Veron-Cetty, M.-P., Joly, M., Veron, P., 2004, A&A, 417, 515

Verner, E. M., Verner, D. A., Korista, K. T. et al. 1999, ApJS, 120, 101

Mem. S.A.It. Suppl. Vol. 15, 192

Memorie della
Supplementi

Wide-field plate archives in Rozhen and Belgrade observatories

Katya Tsvetkova[1], Milcho Tsvetkov[1], Milan S. Dimitrijević[2,3], Vojislava Protić-Benišek[2], Vladimir Benišek[2], and Darko Jevremović[2]

[1] Institute of Astronomy, Bulgarian Academy of Sciences, 72 Tsarigradsko shosse Blvd, Sofia-1784, Bulgaria e-mail: katya@skyarchive.org
[2] Astronomical Observatory, Volgina 7, 11060 Belgrade, Serbia
[3] Laboratoire d'Étude du Rayonnement et de la Matière en Astrophysique, Observatoire de Paris-Meudon, UMR CNRS 8112, Bâtiment 18, 5 Place Jules Janssen, F-92195 Meudon Cedex, France

Abstract. The wide-field plate archives at disposal in Rozhen Observatory (9332 plates obtained in the period 1979 – 1994) and Belgrade Observatory (14500 plates obtained in the period 1936 - 1996) are presented. The plate archives, made in the frames of different observing programmes, reflect the tendencies in the development of astronomy in these countries. The results from the joint collaboration concerning the plate cataloguing and digitization with EPSON flatbed scanners providing good speed of scanning and good astrometric and photometric accuracy while generating digital data, as well as the inclusion of the images of the scanned plates in WFPDB and BELDATA and their online access in the frames of the Virtual Observatory, are presented too.

Key words. Astronomical Databases: miscellaneous – Catalogs – History and philosophy of astronomy

1. Introduction

In 1872 B. Gould began the first systematic astronomical observations of stellar clusters using photographic plates. The advantages of the photographic observations with plates (or films) as detectors and information storage in comparison with the visual observations soon prepared the coming of photographic era in astronomy which lasted about 130 years and was replaced by the CCD one. Today the plates are on one hand - unique source of information for the past of the different astronomical objects, and on the other hand - scientific heritage representing the previous stage of the present astronomical knowledge. A compiled list of astronomical tasks based on the present exploitation of the archival plates can be found in Tsvetkova (2009).

Since 1991 thanks to the development of information and communication technologies we undertook large-scale work on expanding the use of the stored astronomical plate collections with establishment and development of a database for wide-field ($> 1^0$) plates - Wide-Field Plate Database (WFPDB, http://www.skyarchive.org, (Tsvetkov 1991).

Send offprint requests to: K. Tsvekova

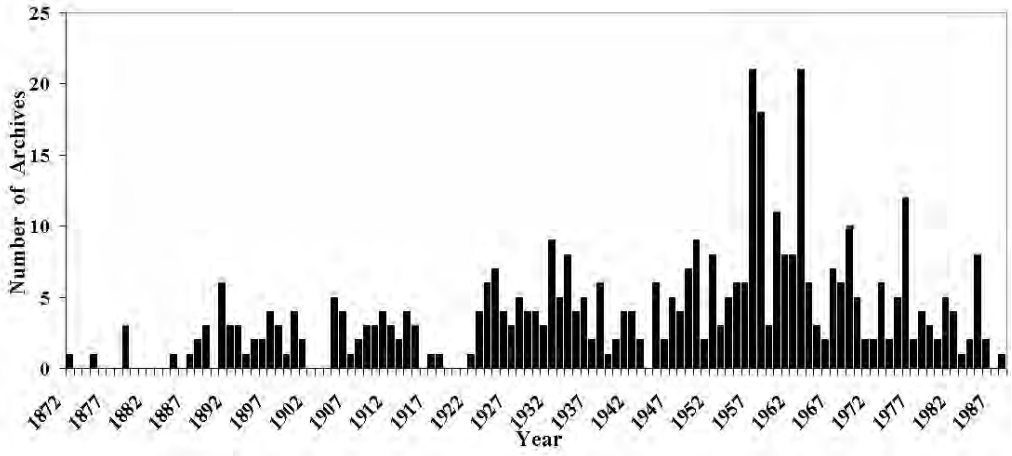

Fig. 1. Time distribution of the number of worldwide plate archives.

Today the WFPDB comprises the information for 442 plate archives containing about 2200000 plates (in the Catalogue of Wide-Field Plate Archives, (Tsvetkova and Tsvetkov 2008) and the descriptive information for 546000 plates (in the Catalogue of Plate Indexes). Combining the information from the both catalogues one can be completely informed about the archives and its contents.

As "plate archive" we denote a collection of plates obtained with a definite telescope at a definite observational site and stored at a definite place. This means that one telescope may have more than one archive, if the telescope was moved or if its plates are stored at different observatories or institutions. The most of the wide-field plate archives are established with small apertures telescopes up to 50-60 cm, mostly refractors, astrographs and cameras. The number of plates in the individual archives ranges between several tenths to more than 100000. Only a small number of archives have more than 10000 plates. The establishment of the plate archives in the different observatories is shown in Fig. 1 using the data from the Catalogue of the Wide-Field Plate Archives (Tsvetkova and Tsvetkov 2006, 2008).

This distribution reveals the history and tendency of development of astronomy. For instance, one can notice a peak around 1892 when the photographic observations in astronomy began to be widely used, and quickly increased number since 1960, when was the "Golden Age" of wide-field photography, as well as the both depressions because of the two world wars. The maximum in the appearance of new archives is after 1955 up to the beginning of 1970, when the plate observations comprised in more than 130 archives started. It is interesting fact that while in the observatories in Bulgaria, Romania and Serbia there are plate collections with total number of plates respectively 9332, 16403 and 14500, in the observatories of the both neighbouring countries Greece and Turkey no any plate observations were conducted, due obviously to the specific development of astronomy in these countries. Analysing the content of the plate archives, namely the number of plates and its time distribution, the observing programmes in the frames of which the plates were obtained, observed object type, used method of observation, exposure multiplicity and duration, emulsions and filters for realization of given photometric system, one can have a look to history and development of astronomy in the respective country. Very often the time distribution of the plates reveals a coincidence between the maximums of the observational activity and the periods of some observational campaigns executed in the respective observatory: sky sur-

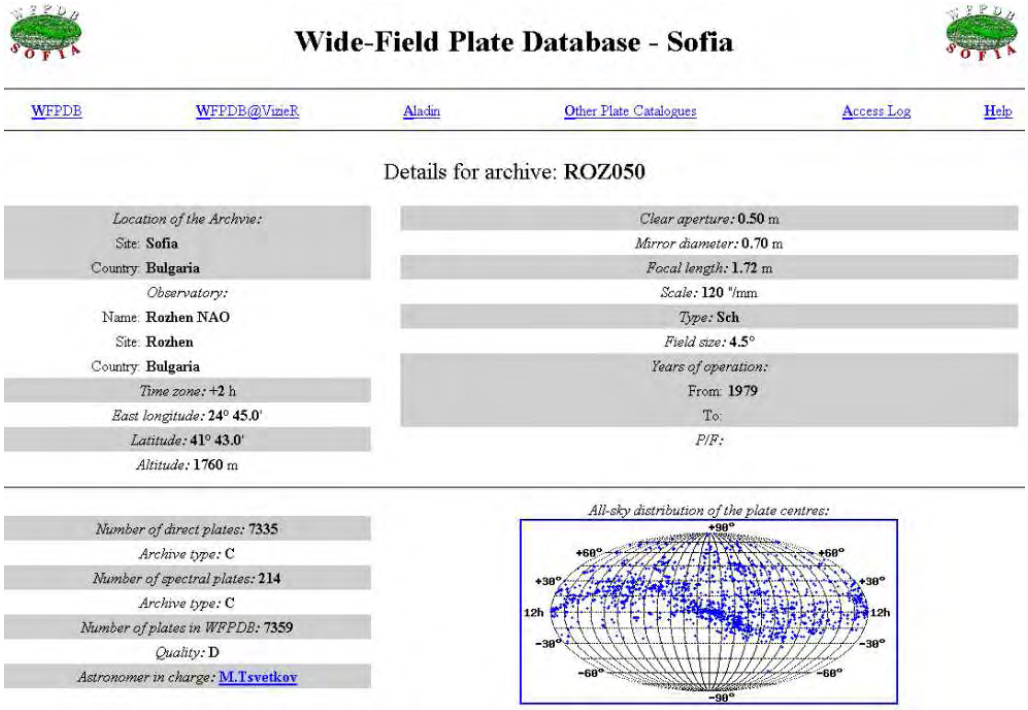

Fig. 2. WFPDB search result with instrument identifier ROZ050.

vey, supernova search, investigations of flare stars in stellar associations and clusters.

2. Rozhen Observatory wide-field plate archives

The plate observations in Rozhen Observatory began immediately after the installation and test observations of the both wide-field telescopes - 2m Ritchey-Chretien-Coude (RCC, in 1980) and Schmidt (in 1979) telescopes, and when in 1981 the observatory was officially opened, already there were a lot of plates obtained. In Tables 1 and 2 the essencial information for the Rozhen telescopes and plate archives respectively, as an excerpt of the Catalogue of Wide-Field Plate Archives (version 5.2 August 2009) is present.

Using the data retrieval from the WFPDB with instrument identifier ROZ200 and ROZ050 respectively, a statistics concerning the all-sky distribution of the plate centres, the distribution of the number of plates according to the type of the observed objects (asteroids, planets, comets, variable stars, open or globular clusters, galaxies, etc.), the exposure duration influencing the plate limit, as well as the exposure multiplicity as a method of observation required by different programmes (for asteroids, search for flare stars, etc.), the used emulsions, the plate size when it concerns the plate digitization, is presented here. In the Wide-Field Plate Database - Sofia Search Page (http://draco.skyarchive.org/search/) can be obtained details for the both archives of the Rozhen Observatory (see Fig. 2 for the details of the archive of the 50/70 cm Schmidt telescope under the WFPDB identifier ROZ050), as well as the all-sky distribution of the plate centres. The distribution of the number of the obtained 1984 plates with the 2m RCC telescope within the period 1980 – 1992 (Fig. 3) is influenced not only by the astroclimatic conditions, but also by such facts in the history of the observatory as the realuminization of the primary mirror of the telescope in 1987.

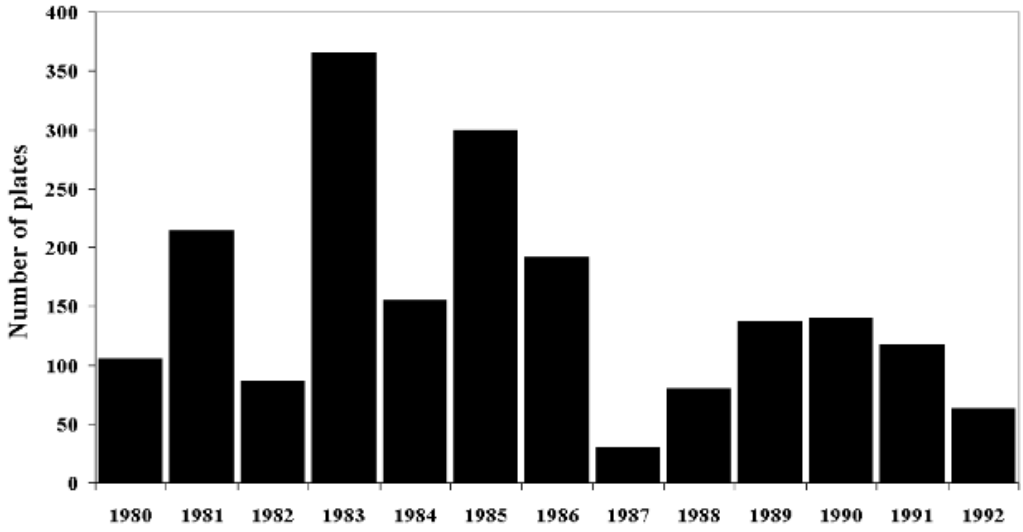

Fig. 3. Time distribution of the number of plates of the Rozhen 2m RCC telescope.

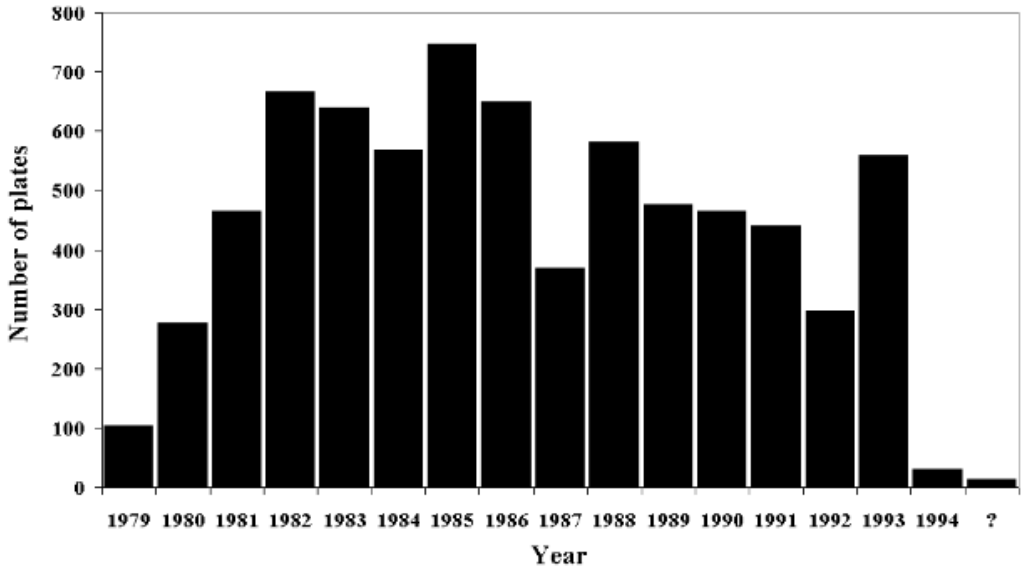

Fig. 4. Time distribution of the number of plates of the Rozhen 50/70 cm Schmidt telescope.

The time distribution of all 7348 plates (170 of them with objective prism) obtained with the Rozhen Schmidt telescope in the period 1979 – 1994 is shown in Fig. 4. The distribution of the number of the ROZ200 and ROZ050 plates by month reflects the better conditions for observations in July, August, September and October in Rozhen Observatory.

The plate observations were performed in the Johnson wide band photographic system – UBVRI, or in pg, for the ROZ200 plates with about 57% of all obtained in B colour,

Table 1. Rozhen Observatory wide-field telescopes

WFPDB identifier	Aperture (m)	Focal length (m)	Scale "/mm	Tel. type	Field size (deg)
ROZ050	0.50/0.70	1.72	120	Schmidt	4.5
ROZ200	2.00	16	13	Ritchey-Chretien	1.0

Table 2. Rozhen Observatory wide-field plate archives

WFPDB instr. identifier	Years of operation	Number of plates	Size of plates (cm)	Archive type	Astronomer in duty
ROZ050	1979-1994	7348	13x13, 16x16	C	M. Tsvetkov
ROZ200	1980-1992	1984	30x30	C	N. Petrov

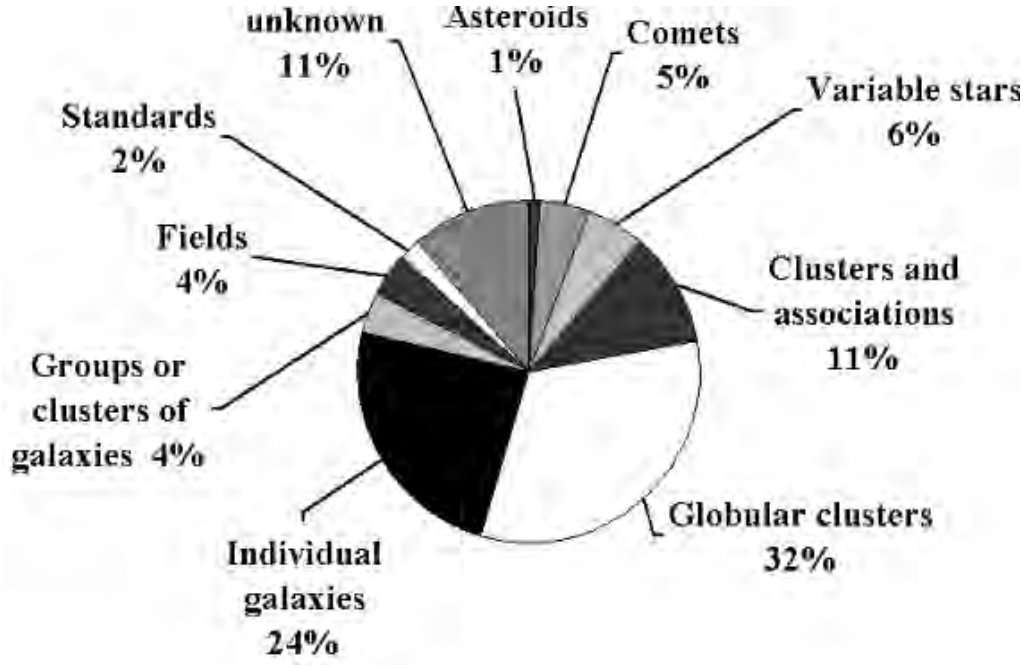

Fig. 5. Observing programmes carried out with the Rozhen 2m RCC telescope.

while for ROZ050 plates 52% are pg plates. From the distribution of the duration of exposures used for observations carried out with the 2m RCC telescope it is seen that 44% of all plates were obtained with exposure duration less and equal of 30 min. In the distribution the very short exposures less than 5 min constitute about one third - 28% of them, present by an observed maximum. The plates with exposure duration equal of 30 min are another third – 29%. Half of the plates with exposure duration bigger than 30 min and less than 100 min were obtained with exposure equal of 60 min which give another maximum in this distribution. The plates with exposure duration bigger than 100 min up to the maximum exposure

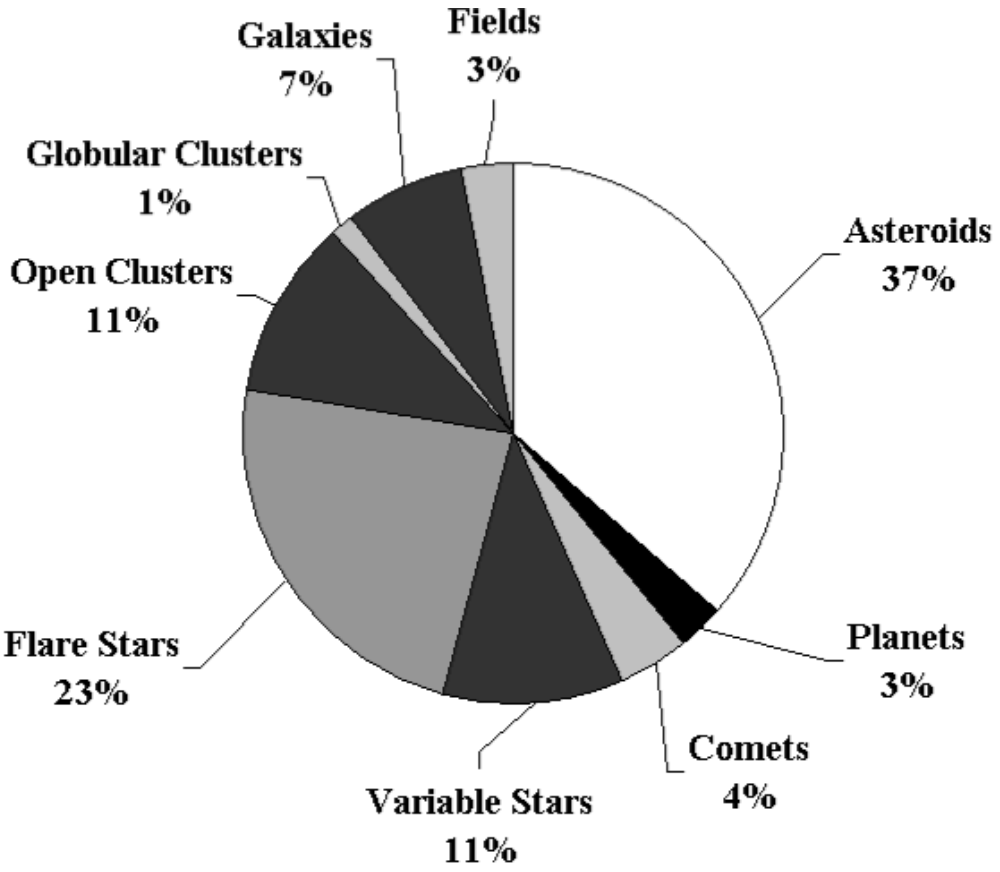

Fig. 6. Observing programmes carried out with the Rozhen 50/70 cm Schmidt telescope.

used (300 min) constitute about 16% of all 2m RCC plates. Predominantly such long exposure plates were used for observations of M31 and other galaxies. 93% of all ROZ050 plates are with exposures less than 40 min. The predominant exposures are 20 min (29%) and 30 min (18%).

The observing programmes of the Rozhen 2m RCC telescope include the observations of globular clusters (639 plates), active galaxies (Starburst, Seyfert, quasars, Markarian's, Arakelian's), and interacting galaxies (475 plates), stellar clusters and associations (217 plates), variable stars (112 plates), comets (90 plates), as well as groups or clusters of galaxies, different fields, asteroids, standards, etc. The used emulsions were Kodak (103aO, 103a D, 103aF, IIaO, IIaD, IIaF, IIIaF, IIIaJ, etc.) and ORWO (ZU 21, ZP3, RP1, etc).

In the observing programmes of the Rozhen 50/70 cm Schmidt telescope the most observed objects were the asteroids (2450 plates), followed by the search for flare-ups of flare stars in stellar clusters and associations as the Pleiades, Gamma Cygni region, M42/43 in Orion, Praesepe, Alpha Per, Tauri Dark Clouds, the open cluster NGC 2264, the emission nebula NGC 7000 (with totally 1564 plates). Another observed objects were open stellar clusters - among them IC 4665 with 263 plates available, IC 5146 with 80 plates available; different type variable stars (e.g. for the unusual nova-like star KR Aur there are 177 plates); different type galaxies; comets: Halley, Shoemaker-Levy 9 (1993e),

Giacobini-Zinner (21P), Tempel 1, Tempel 2, Schaumasse, Panther, Metcalf-Brewington (1991a), Tanaka-Machholz (1992d), Austin, Bradfield (C/2004 F4), Encke, Helin (1977e), Kopff, Levy (1990 XX), Machholz (C/2004 Q2); different fields; major planets; globular clusters, etc.

3. Belgrade Observatory wide-field plate archives

At the time of the establishment in 1887 the Belgrade Observatory was located in the center of the city of Belgrade. The photographic plate observations began after moving the observatory in 1932 on the Veliki Vračar Hill (today Zvezdara) with better conditions with the supplied wide-field telescopes 16 cm Zeiss Astrograph, Zeiss Refractor with 16 cm photographic camera and Askania Equatorial Refractor with 12.5 cm photographic camera. The systematic observations started in 1936 with the Zeiss astrograph when with exposure duration of 3 hours the most productive observer M. Protić reached 14-15th stellar magnitude while observed minor planets. The observing programmes executed with the Belgrade wide-field telescopes include search for new minor planets (33 new discovered) and investigations of known minor planets, observations of comets, Sun, major planets, stellar regions, stars and stellar clusters, zone observations, nebulae, etc. (Protić-Benišek 2006). Details for the inventory of the Belgrade plate collection, cataloguing and plate digitization can be found in (Tsvetkova et al. 2009).

In Tables 3 and 4 the main characteristics of the Belgrade Observatory wide-field telescopes (with respective WFPDB identifiers and the names under which the telescopes are known in the observatory), as well as the characteristics of their plate archives are respectively given as an excerpt of the Catalogue of Wide-Field Plate Archives (version 5.2 August 2009). In Fig. 7 the time distribution of 3000 scanned Belgrade plates is given. Fig. 8 presents the observing programmes carried out with the Belgrade wide-field telescopes.

The preparation of the computer-readable versions of the Belgrade Observatory wide-field plate archives from the stored logbooks is running simultaneously with the plate scanning. The used emulsions were Kodak 103aO, IIaO, 103aJ, 103aF, etc., Ferrania Panchro anti-halo, Agfa Astro, Perutz, Gevaert Super Chromosa, ORWO ZU2, ZU21, Ilford.

4. Plate digitization

The main requirements to the scanners, suitable for plate digitization, are good astrometric and photometric accuracies while generating archival quality digital data with fast scanning speeds. The available PDS1010plus microdensitometer in Sofia Sky Archive Data Center (SSADC), giving possibility for high precision, is too slow for systematic plate scanning. The improved flatbed scanners fulfill the requirements and facilitate large-scale digitization making it more cost-effective. In Table 5 the flatbed scanners EPSON at disposal in Rozhen Observatory, SSADC and Belgrade Observatory, and their scanning platforms as far as they are dependent on the plate size, are present.

In Table 6 the main parameters of the available flatbed scanners are present: Optical density (Dmax), Color depth (bit internal/bit external), Grayscale depth (bit internal/bit external), Maximum hardware resolution.

The used software for scanning is the standard one for making preview images - Adobe Photoshop, and the programme Scanfits developed by S. Mottola (Barbieri et al. 2003) for the real scans in FITS format.

The plate scanning was done with whole density range (0 – 255) and Gamma = 1.00. The chosen resolution is a compromise between the outcome file size and the astronomical task. The chosen color depth is dependent also from the task: for preview images in order to save the observer's marks on the plate, the image type is 8-bit 24 bit Color, for the real scans – 16-bit Grayscale.

Concerning the easier web accessibility and to store the information from the observer's marks on the plate a system for quick plate visualization – plate previews, was developed. The preview images are done with 600 (or 1200) dpi in TIFF format and compressed

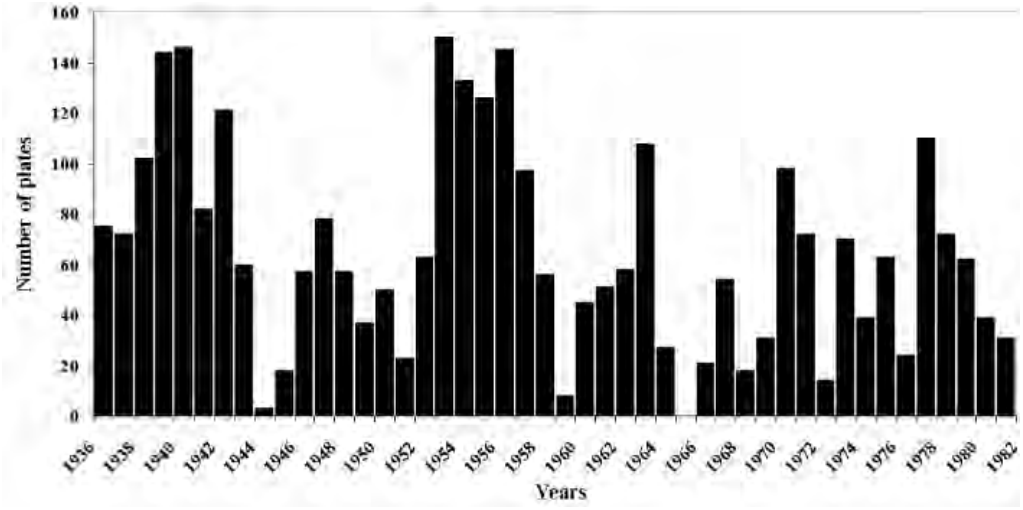

Fig. 7. Time distribution of 3000 scanned Belgrade plates.

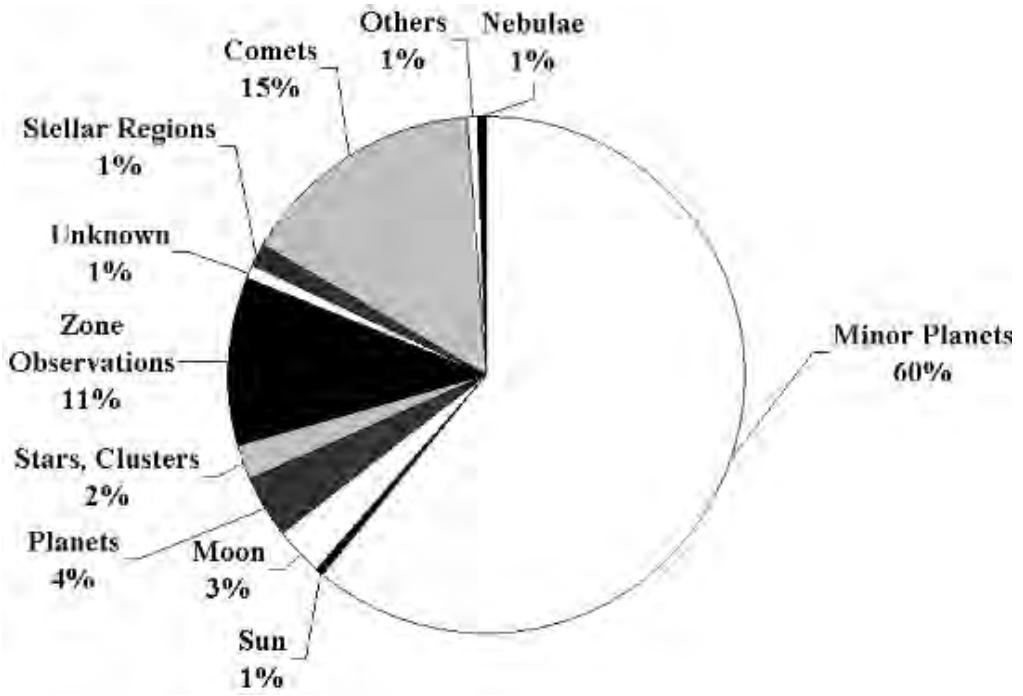

Fig. 8. Observing programmes carried out with the Belgrade Observatory wide-field telescopes.

Table 3. Belgrade Observatory wide-field telescopes

WFPDB identifier	Aperture (m)	Focal length (m)	Scale "/mm	Tel. type	Field size (deg)
BEL012	0.12	1.00	206	Askania Rfr	7.0
BEL016A	0.16	0.80	258	Zeiss Ast	11.5
BEL016B	0.16	0.80	258	Zeiss Rfr	11.5

Table 4. Belgrade Observatory wide-field plate archives

WFPDB instr. identifier	Years of operation	Number of plates	Size of plates (cm)	Archive type	Astronomer in duty
BEL012	1970-1996	4000	9x12, 13x18	TC	V. Protić-Benišek
BEL016A	1936-1985	10000	9x12, 13x18	TC	V. Protić-Benišek
BEL016B	1936-1941	500	6x9	T	V. Protić-Benišek

Table 5. Flatbed scanners at disposal

Institution	EPSON flatbed scanner type	Transparency scanning area (mm)
Rozhen Obs.	EXPRESSION 10000XL	310x419
SSADC	EXPRESSION 1640XL	290x419
	PERFECTION V700 PHOTO	203x254
Belgrade Obs.	PERFECTION V700 PHOTO	203x254

2000x2000 pxl JPEG format. The real scans for photometric or astrometric tasks are done with optimal big resolution 1600 (or 2400) dpi. In order to have adequate web archiving among the variety of file formats we keep within FITS format for digitized plate images as requirements of Virtual Observatory.

The standards and metadata for digitized photographic plates in order to provide indexing, accessing, preserving, and searching for plate images are similar to the developed ones in AIP for the Potsdam CdC plates included in the German Astrophysical Virtual Observatory (GAVO, http://vo.aip.de/plates/, (Tsvetkov et al. 2009). The search interface for the scanned plates give information for the plate identifier, coordinates, date, file type (compressed JPEG, TIFF, FITS format), header of the FITS file, file size, and the scan.

What concerns the preservation of digital content, stored on the servers of WFPDB and Serbian VO (Jevremović et al. 2009), using the advanced information technologies we are in process of application of wavelet based approaches to more effective compression of the huge volume of scanned plate data.

A preview image of the ROZ050 000382 plate in M42/M43 in the Orion region with the marks of the observer is shown in Fig. 9. In Fig. 10 a part of scanned BEL016A480007 plate with image of comet 1948a (Mrkos), and with the marks of Milorad Protić is shown. The history of the discovery of this comet is that on 1947 Dec 20, A. Mrkos discovered the comet on his plate obtained in the Skalnate Pleso Observatory, but because bad weather next days he could not confirm it. Again he observed on 1948 Jan 18 and anounced the

Table 6. Main parameters of the available flatbed scanners

Scanner	Dmax	Color depth	Grayscale depth	Resolution (dpi)
1640XL	3.6	42/42	14/14	1600
10000XL	3.8	42/42	16/16	2400x4800
V700 PHOTO	4	42/42	16/16	4800x9600

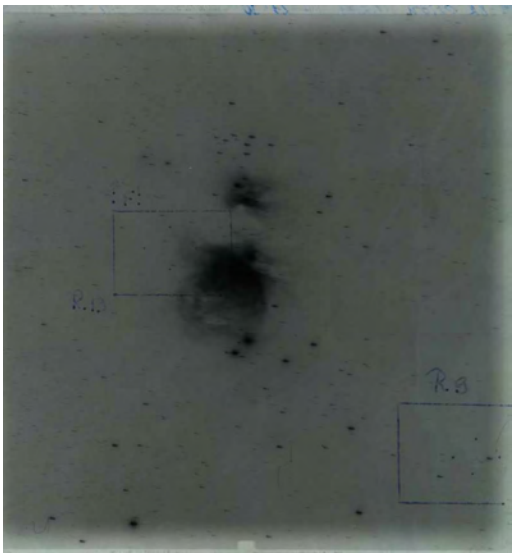

Fig. 9. The scanned ROZ050 000382 plate in the Orion region.

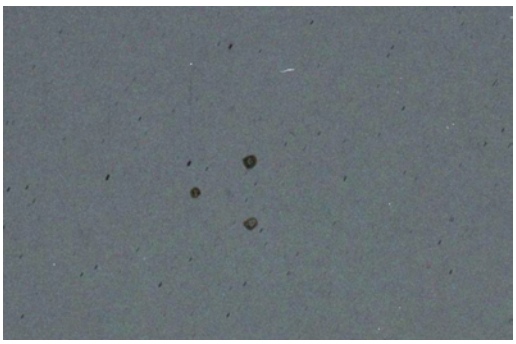

Fig. 10. A part of scanned BEL016A480007 plate with image of 1948a comet.

discovery of a new comet named 1948a. In Belgrade Milorad Protic observed the same comet on 1948 Jan 10, i.e. before the announced discovery. Thus this plate was used for improving the comet coordinates.

5. Collaboration results

The collaboration in the wide-field plate archiving was in the frames of joint bilateral projects between the Astronomical Observatory of Belgrade and Space Research Institute, Bulgarian Academy of Sciences (2004-2006) and the Astronomical Observatory of Belgrade and Institute of Astronomy, Bulgarian Academy of Sciences (2007-2009). The topics were Cataloguing the wide-field photographic observations, Digitization of selected plates, Plate processing (with the routines supplied by IRAF software packages and IDL astronomy users library), Application of archived observations, Exchange of experience in development and application of astronomical databases (WFPDB and BELDATA) and organization of mirror sites of the databases.

The working programme included: Preparation of plate catalogues for the wide-field photographic observations at Belgrade Observatory in the WFPDB format; Digitization of Belgrade plates; Inclusion of the plate catalogues in the WFPDB and in BELDATA; Estimation of the quality of the digitization data; Inclusion of the images of the scanned plates in WFPDB and BELDATA and online access; Organization of mirror sites.

As results the information for the Belgrade plate archives is already included in the WFPDB, there is an online access to this information for all the astronomical community through the WFPDB updated version in SSADC. The plate archiving is included

as a topic in the project Serbian Virtual Observatory (Jevremović et al. 2009), running since February 2008. The Belgrade plates in the region of the Pleiades have been scanned and added to the Pleiades Plate Database (PPDB) aiming to reveal the long-term behaviour of some Pleiades stars. Already there is a systematic plate scanning and as a result up to August 2009 about 3000 plates have been scanned.

6. Future plans

The further work aims an acceleration of the plate cataloguing in Belgrade Observatory in the WFPDB format. The next step will be analysis of the Belgrade plate catalogues based on the data retrieval from the WFPDB. The pipeline of the systematic scanning of Belgrade Observatory includes procreation of archives of digitized Belgrade plates with low resolution for quick plate visualisation and their online access as a main priority, making the preview images in TIFF and JPEG file format and linkage of the preview images to the WFPDB, preparation for including the plate scans data into Virtual Observatory - putting the data on the local servers in Belgrade Observatory. As priority tasks are scanning selected Belgrade plates containing images of minor planets and comets, and scanning plate envelopes (with flatbed scanner or even with digital camera), for saving the information written on them, not put in the catalogue format.

The last step before the systematic astronomical research is an organization of the plate scans in an image database and the development of a software system for object plate identifications and for searching in an image database with many data storage variants as current tasks. The preparation of digital plate archives according to the main observing programmes is already running process in Rozhen Observatory. The aims are to assemble and explore massive data sets in order to reveal a new knowledge existing in the data, but still not recognized in any individual data set. Some of the representative plates obtained with the Schmidt telescope of Rozhen Observatory during the observation campaign for search and investigations of the flare stars in stellar clusters and associations in 1970 – 1990 are already scanned. Besides the primary aim to serve for investigations of the flare stars another result is the realization of an interlinking the electronic Information Bulletin on Variable Stars (IBVS) where the discovered flare stars are published with the Wide-Field Plate Database (WFPDB) where one can find the scanned plates containing the images of the respective flare stars.

Acknowledgements. K.T., M.T. and M.S.D. thank Dr. E. Lyratzi and Prof. E. Danezis for the invitation and excellent organization of the workshop. The work on the archives is supported by the bilateral project between Bulgarian Academy of Sciences and Serbian Academy of Sciences and Art and partially supported by the BG NSF DO-02-273 grant. It is also supported by Ministry of Science and Technological Development of Republic of Serbia through projects TR13022 Serbian Virtual Observatory, and 146001 Influence of collisional processes on astrophysical plasma spectra.

References

Barbieri, C., Blanco, C., Bucciarelli, B., Coluzzi, R., di Paola, A., Lanteri, L., Luca Li Causi, G., Marilli, E., Massimino, P., Mezzalira, V., et al. 2003, Experimental Astronomy, 15, 29-43.

Jevremović, D., Dimitrijević, M. S., Popović, L. Č., Dačić, M., Protić Benišek, V., Bon, E., Gavrilović, N., Kovačević, J., Benišek, V., Kovačević, A., Ilić, D., Sahal-Bréchot, S., Tsvetkova, K., Malović, M. 2009, New Astronomy Review, in press.

Protić-Benišek, V., 2006, Publ. Astron. Obs. Belgrade 80, 355 – 360.

Tsvetkov, M.K.: 1991, IAU Commission 9, Working Group on Wide-Field Imaging, Newsletter No. 1, 17.

Tsvetkov, M., Tsvetkova, K., Boehm, P., Enke, H., Nickelt, I., Steinmetz, M., Demleitner, M. 2009, in preparation.

Tsvetkova, K., Tsvetkov, M. 2006, in Virtual Observatory, Plate Content Digitization, Archive Mining, Image Sequence Processing, Eds. M. Tsvetkov, V. Golev, F. Murtagh, R. Molina, Heron Press Science Series, Sofia, 45-53.

Tsvetkova, K. and Tsvetkov, M. 2008, Catalogue of the Wide-Field Plate Archive, VizieR On-line Data Catalog: VI/126, 10/2008.

Tsvetkova, K. 2009, Proc. VI Serbian-Bulgarian Astronomical Conference, 07 – 11 May 2008, Belgrade, Eds. M. S. Dimitrijević et al., Publ. Astron. Soc. "Rudjer Boskovic", 9, 245-254.

Tsvetkova, K., Tsvetkov, M., Protić-Benišek, V., Dimitrijević, M. S. 2009, Proc. VI Serbian-Bulgarian Astronomical Conference, 07 – 11 May 2008, Belgrade, Eds. M.S.Dimitrijevic et al., Publ. Astron. Soc. "Rudjer Boskovic", 9, 255-260.

Mem. S.A.It. Suppl. Vol. 15, 32

Memorie della
Supplementi

Astronomical spectra and collisions with charged particles

Milan S. Dimitrijević[1,2]

[1] Astronomical Observatory, Volgina 7, 11060 Belgrade 38, Serbia
[2] Laboratoire d'Étude du Rayonnement et de la Matiére en Astrophysique, Observatoire de Paris-Meudon, UMR CNRS 8112, Bâtiment 18, 5 Place Jules Janssen, F-92195 Meudon Cedex, France e-mail: mdimitrijevic@aob.bg.ac.yu

Abstract. We analyze here the significance of Stark broadening for analyzis, interpretation and synthesis of stellar spectra, and analyzis, diagnostics and modeling of stellar plasma. It was considered for which types of stars and for which investigations Stark broadening is significant and methods for theoretical determination of Stark broadening parameters are discussed. Such investigations on Belgrade Astronomical Observatory are reviewed as well.

Key words. Stark broadening, line profiles, stellar atmospheres, white dwarfs, radio recombination lines, neutron stars, atomic data, data bases

1. Introduction

By analysis of stellar spectral lines, we can determine their temperatures, the temperature in particular atmospheric layers, the chemical composition of stellar plasma, surface gravity. We can understand better nuclear processes in stellar interiors, and determine the spectral type and effective temperature by comparing the considered stellar spectrum with the standard spectra for particular types.

In comparison with laboratory plasma sources, plasma conditions in astrophysical plasmas are exceptionally various. So that line broadening due to interaction between absorber/emitter and charged particles (Stark broadening) is of interest in astrophysics in plasmas of such extreme conditions like in the interstellar molecular clouds or neutron star atmospheres.

Send offprint requests to: M. S. Dimitrijević

In interstellar molecular clouds, typical electron temperatures are around 30 K or smaller, and typical electron densities are 2-15 cm^{-3}. In such conditions, free electrons may be captured (recombination) by an ion in very distant orbit with principal quantum number (n) values of several hundreds and deexcite in cascade to energy levels n-1, n-2,... radiating in radio domain. Such distant electrons are weakly bounded with the core and may be influenced by very weak electric microfield, so that Stark broadening may be important.

In interstellar ionized hydrogen clouds, electron temperatures are around 10 000 K and electron density is of the order of $10^4 cm^{-3}$. Corresponding series of adjacent radio recombination lines originating from energy levels with high (several hundreds, even more than thousand) n values are influenced by Stark broadening.

For temperatures larger than around 10 000 K, hydrogen, the main constituent of stellar atmospheres is mainly ionized, and among collisional broadening mechanisms for spectral lines, the dominant is the Stark effect. This is the case for white dwarfs and hot stars in particular of A and late B types, since due to high temperature, stars of O and early B types have smaller surface gravity so that the electron density is smaller. Even in cooler star atmospheres as e.g. Solar one, Stark broadening may be important, since the influence of Stark broadening within a spectral series increases with the increase of the principal quantum number of the upper level, and also in subphotospheric layers electron density and temperature increase and Stark broadening becomes dominant.

The density and temperature range of interest for the radiative envelopes of A and F stars is $10^{14}\mathrm{m}^{-3} \leq \mathrm{N}_e \leq 10^{16}\mathrm{m}^{-3}$; $10^4 \leq \mathrm{T} \leq 4\ 10^5$ (Stehleé 1994).

White dwarfs of DA and DB type have effective temperatures between around 10 000 K and 30 000 K so that Stark broadening is of interest for their spectra investigation and plasma research, analysis and modeling. Spectra of DA white dwarfs are characterized by broad hydrogen lines, while those of DB white dwarfs are dominated by the lines of neutral helium. White dwarfs of DO type have effective temperatures from approximately 45000 up to around 120 000 (Dreizler and Werner 1996) and Stark broadening may be very important for the investigation of their spectra (Hamdi et al. 2008).

For applications of results of Stark broadening investigations, very interesting are PG1159 stars, hot hydrogen deficient prewhite dwarfs, with effective temperatures ranging from T_{eff} = 100 000 K to 140 000 K, where of course Stark broadening is very important (Werner et al. 1991). These stars have high surface gravity (log g= 7), and their photospheres are dominated by helium and carbon with a significant amount of oxygen present (C/He = 0.5 and O/He = 0.13) (Werner et al. 1991). Their spectra, strongly influenced by Stark broadening, are dominated by He II, C IV, O VI and N V lines.

The densities of matter and electron concentrations and temperatures in atmospheres of neutron stars are orders of magnitude larger than in atmospheres of white dwarfs, and are typical for stellar interiors. Surface temperatures for the photospheric emission are of the order of 10^6 - 10^7 K, and electron densities of the order of 10^{24} cm^{-3} (Paerels 1997).

In this work we will consider the significance of Stark broadening for investigations of astrophysical plasma and some results obtained in the Group for Astrophysical Spectroscopy on Belgrade Astronomical Observatory.

2. Stellar plasma research

Line shapes enter in the modelisation of stellar atmospheric layers by the determination estimation of the quantities such as absorption coefficient κ_ν, Rosseland optical depth τ_{Ross} and the total opacity cross-section per atom σ_ν.

Let we take the direction of gravity as z-direction, dealing with a stellar atmosphere. If the atmosphere is in macroscopic mechanical equilibrium and with *rho* is denoted gas density, the optical depth is

$$\tau_\nu = \int_z^\infty \kappa_\nu \rho dz, \tag{1}$$

$$\kappa_\nu = N(A,i)\phi_\nu \frac{\pi e^2}{mc} f_{ij}, \tag{2}$$

where κ_ν is the absorption coefficient at a frequency ν, $N(A,i)$ is the volumic density of radiators in the state i, f_{ij} is the absorption oscillator strength, m is the electron mass and ϕ_ν spectral line profile. The total opacity cross-section per atom is

$$\sigma_\nu(op) = M\kappa_\nu, \tag{3}$$

where M is the mean atom mass, and the opacity per unit length is

$$\rho\kappa_\nu = N\sigma_\nu(op), \tag{4}$$

Let us introduce an independent variable, a mean optical depth

$$\tau_{Ross} = \int_z^\infty \kappa_{Ross}\rho dz. \tag{5}$$

For the Rosseland mean optical depth τ_{Ross}, κ_{Ross} is defined as

$$\frac{1}{\kappa_{\rm Ross}}\int_0^\infty \frac{dB_\nu}{dT}d\nu = \int_0^\infty \frac{1}{\kappa_\nu}\frac{dB_\nu}{dT}d\nu, \quad (6)$$

where

$$B_\nu(T) = \frac{2h\nu^3}{c^2}(e^{h\nu/kT}-1)^{-1}. \quad (7)$$

Now the Rosseland-mean opacity cross-section is

$$\sigma_{Ross} = M\kappa_{Ross}. \quad (8)$$

Stark broadening parameters are needed as well for the determination of the chemical composition of stellar atmospheres i.e. for stellar elemental abundances determination. The method which uses synthetic and observed spectra and adjustment of atmospheric model parameters to obtain the best agreement is well developed and applied to many stars. It has been found that exist chemically peculiar stars especially within the spectral class interval F0-B2 (see e.g. (Khokhlova 1994)) with abundances for particular elements for several order of magnitude different from solar ones. It has been found as well that the CP stars surface is chemically inhomogeneous so that local chemical composition depending on coordinates on the stellar surface has been introduced. Such anomalies are explained mainly by diffusion mechanism occurring in stellar envelopes and (or) atmospheres and differences in radiative acceleration of particular elements (LeBlanc and Michaud 1995). The radiative acceleration g_r at ν, in the frequency interval $d\nu$, acting on the element A (with density $N(A)$ and mass m_A) is (Stehlé 1995)

$$m_A g_r = \frac{\kappa_\nu(A)}{N(A)}\Phi_\nu\frac{d\nu}{c}, \quad (9)$$

where $\kappa_\nu(A)$ is the contribution of A to the monochromatic absorption coefficient, and Φ_ν the radiative flux. In the opaque envelope of the radius r, the radiative flux is approximately equal to (Stehlé 1995)

$$\Phi_\nu = \frac{4\pi}{3}\frac{1}{\rho\kappa_\nu}\frac{\partial B_\nu}{\partial T}(\frac{-\partial T}{\partial r}), \quad (10)$$

$$\kappa_\nu = \kappa_\nu(A) + \kappa_{rest}, \quad (11)$$

where κ_{rest} are other contributions to the total absorption coefficient apart $\kappa_\nu(A)$. The majority of CP stars are A and B type stars where Stark broadening is the main pressure broadening mechanism.

With the improved sensitivity of space born X-ray instruments, spectral lines originating from neutron star atmospheres are of increasing interest. Since the characteristic density in the atmosphere is directly proportional to the acceleration of gravity at the stellar surface, measurement of the pressure broadening of absorption lines will yield a direct measurement of M/R^2, where M and R are the stellar mass and radius. When this is coupled with a measurement of the gravitational redshift (proportional to M/R) in the same, or any other, line or set of lines, the mass and radius can be determined separately. These mass and radius measurements do not involve the distance to star, which is usually poorly determined, or the size of the emitting area (Paerels 1997).

The Stark width for a hydrogen - dominated plasma ($z = 1, N_{pert} = N_e, \mu = 1/2$), assuming that electron and proton broadening are comparable in the static approximation (Griem et al. 1979) is (Paerels 1997)

$$W_{Stark}[eV] = 163\cdot Z^{-1}M_{1.4}^{2/3}R_6^{-4/3}T_6^{-2/3}\text{eV}. \quad (12)$$

Here, Z is the ionic nuclear charge, $M_{1.4}$ the stellar mass in units of 1.4 solar masses, R_6 the radius in units of 10^6 cm, and T_6 the atmospheric temperature in units of 10^6 K.

In Paerels (1997) a typical Stark width of 20 eV has been found for H-like oxygen Lyα, and a Stark width of 60 eV has been predicted for oxygen Lyβ.

3. Application of the semiclassical method for Stark broadening investigation on Belgrade Astronomical Observatory

In spite of the fact that the most sophisticated theoretical method for the calculation of a Stark broadened line profile is

the quantum mechanical strong coupling approach, due to its complexity and numerical difficulties, only a small number of such calculations exist (see e. g. references in Dimitrijević and Sahal-Bréchot (1996)). An example of the contribution of the Group for Astrophysical Spectroscopy on Belgrade Astronomical Observatory is the first calculation of Stark broadening parameters within the quantum mechanical strong coupling method for a nonhydrogen neutral emitter for Li I 2s ^{2}S - 2p ^{2}P^o transition (Dimitrijević et al. 1981).

In a lot of cases such as e.g. complex spectra, heavy elements or transitions between highly excited energy levels, the more sophysticated quantum mechanical approach is very difficult or even practically impossible to use and, in such cases, the semiclassical approach remains the most efficient method for Stark broadening calculations.

In order to complete as much as possible Stark broadening data needed for astrophysical and laboratory plasma research and stellar opacities determinations, we have performed in a series of papers large scale calculations of Stark broadening parameters for a number of spectral lines of various emitters (see e.g. (Dimitrijević and Sahal-Bréchot 1996) references therein and (Jevremović et al. 2009)), within the semiclassical perturbation formalism (Sahal-Bréchot 1969a,b) optimized and updated several times ((Fleurier et al. 1977; Dimitrijević and Sahal-Bréchot 1984, 1996) and references therein), for transitions when a sufficiently complete set of reliable atomic data exists and a good accuracy of obtained results is expected.

Up to now are published Stark broadening parameters for 79 He, 62 Na, 51 K, 61 Li, 25 Al, 24 Rb, 3 Pd, 19 Be, 270 Mg, 31 Se, 33 Sr, 14 Ba, 189 Ca, 32 Zn, 6 Au, 48 Ag, 18 Ga, 70 Cd I, 9 Cr I, 4 Te I, 25 Ne I, 28 Ca II, 30 Be II, 29 Li II, 66 Mg II, 64 Ba II, 19 Si II, 3 Fe II, 2 Ni II, 22 Ne II, 5 F II, 1 Cd II, 1 Kr II, 2 Ar II, 7 Cr II, 12 B III, 23 Al III, 10 Sc III, 27 Be III, 5 Ne III, 32 Y III, 20 In III, 2 Tl III, 5 F III, 2 Ne IV, 10 Ti IV, 39 Si IV, 90 C IV, 5 O IV, 114 P IV, 2 Pb IV, 19 O V, 30 N V, 25 C V, 51 P V, 34 S V, 16 Si V, 26 V V, 26 Ne V, 30 O VI, 21 S VI, 2 F VI, 15 Si VI, 14 O VII, 10 F VII, 10 Cl VII, 20 Ne VIII, 4 K VIII, 9 Ar VIII, 6 Kr VIII, 4 Ca IX, 30 K IX, 8 Na IX, 57 Na X, 48 Ca X, 4 Sc X, 7 Al XI, 4 Si XI, 18 Mg XI, 4 Ti XI, 10 Sc XI, 9 Si XII, 27 Ti XII, 61 Si XIII and 33 V XIII particular spectral lines and multiplets.

The obtained semiclassical result have been compared with critically selected experimental data for 13 He I multiplets (Dimitrijević and Sahal-Bréchot 1985). The agreement between experimental and semiclassical calculations is within the limits of ± 20%, that is the predicted accuracy of the semiclassical method (Griem 1974).

4. Application of semiclassical Stark broadening parameters for the consideration of its influence on stellar spectral lines

In a number of papers, the influence of Stark broadening on Au II (Popović et al. 1999a), Co III (Tankosić et al. 2003), Ge I (Dimitrijević et al. 2003a), Ga I (Dimitrijević et al. 2004), Cd I (Simić et al. 2005) and Te I (Simić et al. 2009) on spectral lines in chemically peculiar A type stellar atmospheres was investigated and for each investigated spectrum are found atmospheric layers where the contribution of this broadening mechanism is dominant or could not be neglected. In mentioned papers as the model for a chemically peculiar star atmosphere of A type star was used model with plasma conditions close to χ Lupi HgMn star of Ap type. Such investigations were also performed for DA, DB and DO white dwarf atmospheres (Popović et al. 1999a; Tankosić et al. 2003; Hamdi et al. 2008) and it was found that for such stars Stark broadening is dominant compared to Doppler in practically all relevant atmospheric layers.

As an example of the influence of Stark broadening in atmospheres of hot stars in Fig. 1 is given Stark widths for Te I 6s ^{5}S^o - 6p ^{5}P (9903.9 Å) multiplet (Simić et al. 2009) compared with Doppler widths for a model (T_{eff}=10000 K, log g= 4.5) of A type star atmosphere (Kurucz 1979). Namely Doppler broadening is in hot atmospheres an important concurrent broadening mechanism and by comparison of Stark and Doppler widths one

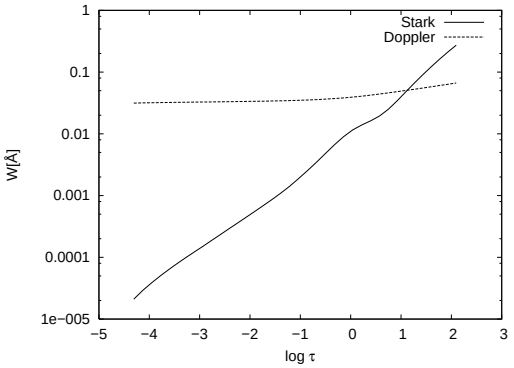

Fig. 1. Thermal Doppler and Stark widths for Te I 6s $^5S^o$ - 6p ^5P (9903.9 Å) multiplet as functions of optical depth for an A type star (T_{eff} = 10000 K, log g = 4.5).

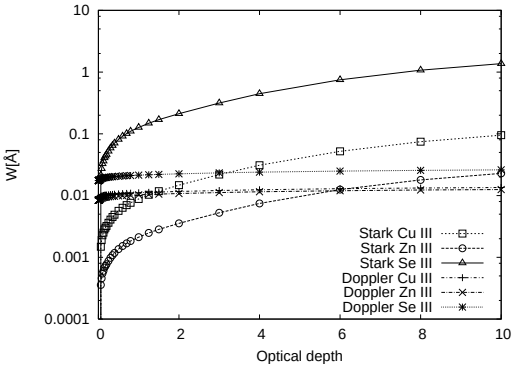

Fig. 2. Thermal Doppler and Stark widths for Cu III 4s ^2F - 4p $^2G^o$ (λ=1774.4 Å), Zn III 4s ^3D - 4p $^3P^o$ (λ=1667.9 Å) and Se III 4p5s $^3P^o$ - 5p ^3D (λ=3815.5 Å) spectral lines for a DB white dwarf atmosphere model with T_{eff} = 15,000 K and *log* g = 7, as a function of optical depth τ_{5150}.

can conclude on the importance of this mechanism. One should take into account however, that due to differences in Gauss distribution function for Doppler profile and Lorentz distribution for Stark, even if the Stark width is smaller, this broadening mechanism may influence line wings. Our results are presented in Fig. 1 as a function of Rosseland optical depth - log τ. One can see that the Stark broadening mechanism is absolutely dominant in comparison with the thermal Doppler mechanism in deeper layers of stellar atmosphere.

The influence of the Stark broadening on Cu III, Zn III and Se III spectral lines in DB white dwarf atmospheres was investigated also in Simić et al. (2006) for 4s ^2F - 4p $^2G^o$ (λ=1774.4 Å), 4s ^3D - 4p $^3P^o$ (λ=1667.9 Å) and 4p5s $^3P^o$ - 5p ^3D (λ=3815.5 Å) by using the corresponding model with T_{eff} = 15000 K and $\log g$ = 7 (Wickramasinghe 1972). For the considered model atmosphere of the DB white dwarfs the prechosen optical depth points at the standard wavelength λ_s=5150 Å(τ_{5150}) are used in Wickramasinghe (1972) and in Simić et al. (2006). As one can see in Fig. 2 for the DB white dwarf atmosphere plasma conditions, thermal Doppler broadening has much less importance in comparison with the Stark broadening mechanism. For example Stark width of the considered Se III 3815.5 Å line is larger than Doppler one up

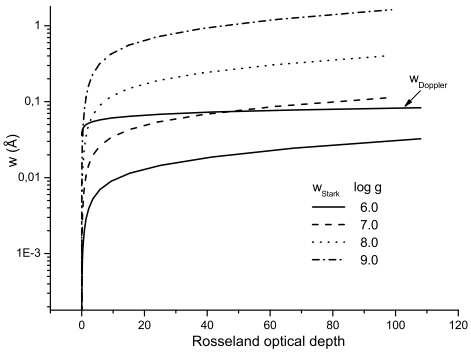

Fig. 3. Stark and Doppler width for Si VI $2p^4(^3P)3s$ ^2P-$2p^4(^3P)3p$ $^2D^o$(λ = 1226, 7Å) spectral line as a function of Rosseland optical depth. Stark and Doppler width are given for four models of DO white dwarfs with log g = 6–9 i T_{eff} = 80 000 K.

to two orders of magnitude within the considered range of optical depths. Much larger Stark widths in DB white dwarf atmospheres in comparison with A type stars are the consequence of larger electron densities due to much larger $\log g$ and larger T_{eff}, so that electron-impact (Stark) broadening mechanism is more effective.

Hamdi et al. (2008) investigated the influence of Stark broadening on Si VI lines in

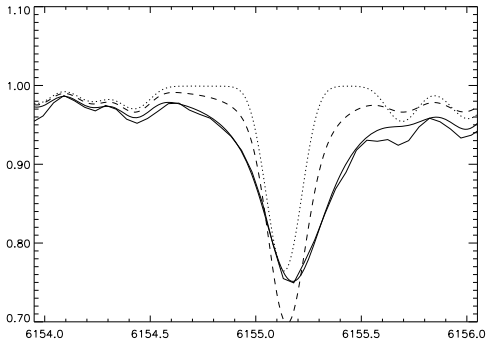

Fig. 4. A comparison between the observed Si I, 6155 Å line profile in the spectrum of Ap star 10 Aql (thick line) and synthetic spectra calculated with Stark widths and shifts from Table 1 in Dimitrijević et al. (2003b) and Si abundance stratification (thin line), with the same Stark parameters but for homogeneous Si distribution (dashed line), and with Stark width calculated by approximation formulae for the same stratification (dotted line).

DO white dwarf spectra for 50000 K $\leq T_{eff}$ $\leq$ 100000 K and 6 $\leq$ log $g \leq$ 9. It was found that the influence increases with log g and that is dominant in broad regions of the cosidered atmospheres (Fig. 3).

An example of the application of Stark broadening data in astrophysics may be found in Dimitrijević et al. (2003b) where the influence of Stark broadening and stratification on neutral silicon lines in spectra of normal late type A star HD 32115, and Ap stars HD 122970 and 10 Aql was investigated. They found that synthetic line profile of λ = 6155.13 Å Si I line fit much better to the observed one when it was calculated with Stark width and shift. Also authors reproduced the asymmetric and shifted profile of this line in HD 122970 reasonably well using the uniform distribution of neutral silicon and their results for Stark broadening parameters. Authors stressed that with their theoretical Stark broadening parameters the sensitivity of Si I λ 6155.13 Å asymmetry to Si abundance changes in the 10 Aql atmosphere, can be successfully used in empirical studies of abundance stratification. They found also that for considered Si I lines the contribution of electron impacts is dominant but, impacts with protons and He II ions should be taken into account as well.

Dimitrijević et al. (2007) have investigated Cr II lines in the spectrum of the Ap star HD 133792, for which careful abundance and stratification analysis has been performed (Kochukhov et al. 2006). HD133792 has an effective temperature of T_{eff}=9400 K, a surface gravity of log g = 3.7, and a mean Cr overabundance +2.6 dex relative to the solar Cr abundance (Kochukhov et al. 2006). All calculations were carried out with the improved version SYNTH3 of the code SYNTH for synthetic spectrum calculations. Stark broadening parameters were introduced in the spectrum synthesis code. The stratified Cr distribution in the atmosphere of HD133972 derived in Kochukhov et al. (2006) was used. Figure 5 shows a comparison between the observed line profiles of Cr II lines 3403.30 Å and synthetic calculations with the Stark damping constants from Kurucz (Kurucz 1993) line lists and with the data by Dimitrijević et al. (2007). Good agreement between observations and calculations for a set of weak Cr II lines proves the use of the stratified Cr distribution, while all four strong Cr II lines demonstrate a good accuracy for obtained theoretical Stark broadening parameters (Dimitrijević et al. 2007).

This opens a new possibility, to check the theoretical and experimental Stark broadening results additionally with the help of stellar spectra, which will be particularly interesting with the development of space born spectroscopy, building of giant telescopes of the new generation and increase of accuracy of computer codes for modellisation of stellar atmospheres. The Cr II lines analyzed in Dimitrijević et al. (2007) are particularly suitable for such purpose since they have clean wings where the influence of Stark broadening is the most important.

5. Modified semiempirical method for Stark broadening and astrophysical applications

The modified semiempirical (MSE) approach (Dimitrijević and Konjević 1980; Dimitrijević

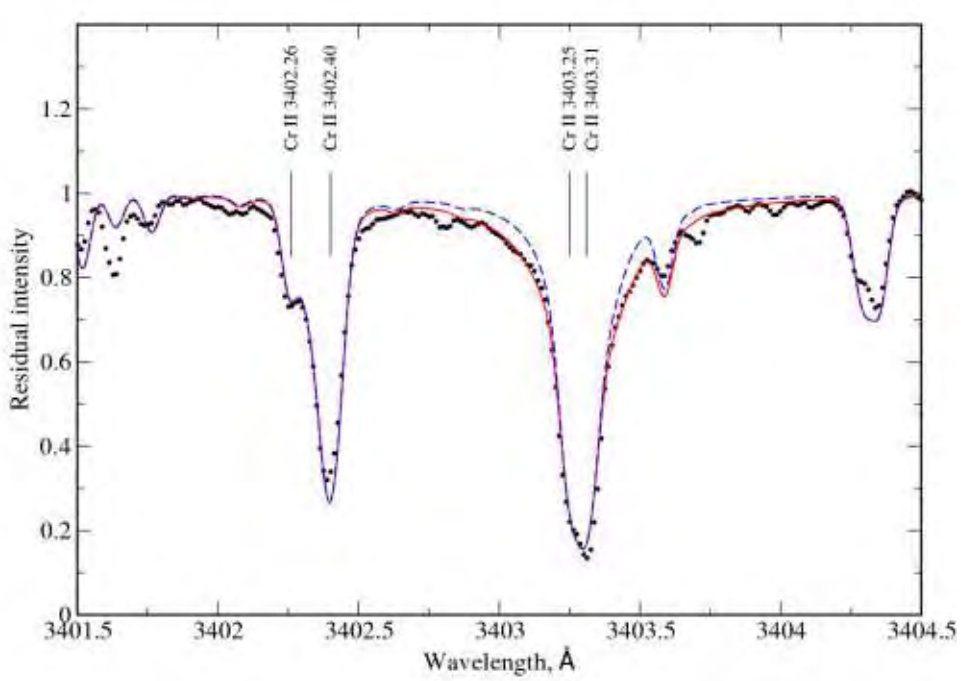

Fig. 5. Comparison between the observed Cr II 3403.30 line profile (dots) and synthetic calculations with the Stark parameters from paper by Dimitrijević et al. (2007) (full line) and those from Kurucz (1993) (dashed line).

and Kršljanin 1986; Dimitrijević and Konjević 1987; Dimitrijević and Popović 1993, 2001; Popović and Dimitrijević 1996a) for the calculation of Stark broadening parameters for non-hydrogenic ion spectral lines, has been applied successfully many times for different problems in astrophysics and physics.

In comparison with the full semiclassical approach (Sahal-Bréchot 1969a,b; Griem 1974) and the Griem's semiempirical approach (Griem 1968) who needs practically the same set of atomic data as the more sophysticated semiclassical one, the modified semiempirical approach needs a considerably smaller number of such data. In fact, if there are no perturbing levels strongly violating the assumed approximation, for e.g. the line width calculations, we need only the energy levels with the difference of the principal quantum numbers n for the upper and lower level of transition forming the considered spectral line, $\Delta n = 0$, since all perturbing levels with $\Delta n \neq 0$, needed for a full semiclasical investigation or an investigation within the Griem's semiempirical approach (Griem 1968), are lumped together and approximately estimated.

Due to the considerably smaller set of needed atomic data in comparison with semiclassical and semiempirical methods (Sahal-Bréchot 1969a,b; Griem 1974, 1968), the MSE method is particularly useful for stellar spectroscopy depending on very extensive list of elements and line transitions with their atomic and line broadening parameters where it is not possible to use sophisticated theoretical approaches in all cases of interest.

The MSE method is also very useful whenever line broadening data for a large number of lines are required, and the high precision of every particular result is not so important like e.g. for opacity calculations or plasma modeling. Moreover, in the case of more complex

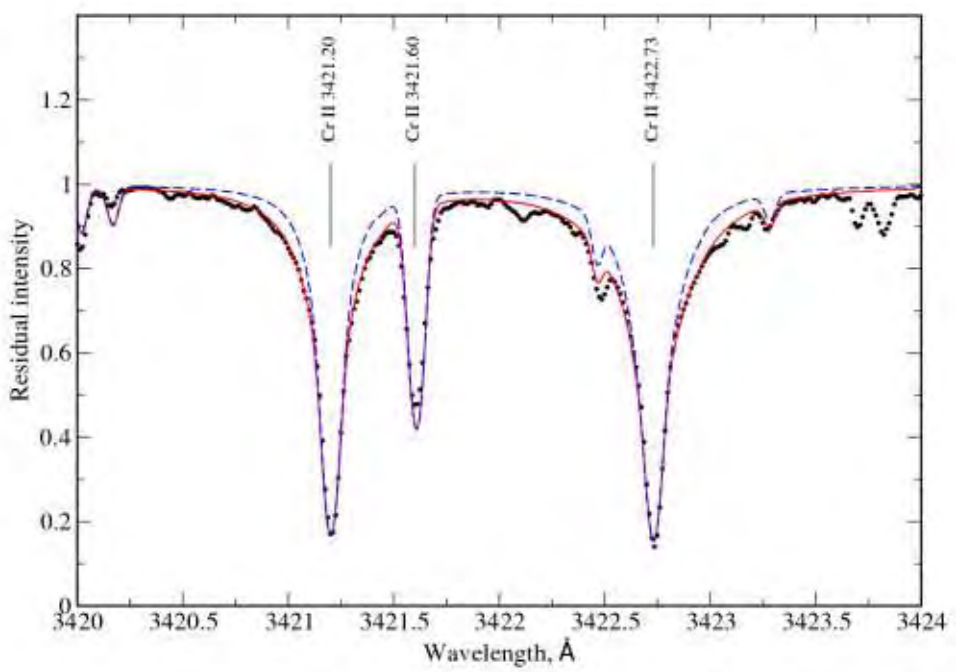

Fig. 6. The same as in Fig.5 but for the Cr II 3421.20, 3422.73 Å lines.

atoms or multiply charged ions the lack of the accurate atomic data needed for more sophysticated calculations, makes that the reliability of the semiclassical results decreases. In such cases the MSE method might be very interesting as well.

The modified semiempirical approach has been tested several times on numerous examples (Dimitrijević and Popović 2001). In order to test this method, selected experimental data for 36 multiplets (7 different ion species) of triply-charged ions were compared with theoretical line widths. The averaged values of the ratios of measured to calculated widths are as follows (Dimitrijević and Konjević 1980): for doubly charged ions 1.06 ± 0.32 and for triply-charged ions 0.91 ± 0.42. The assumed accuracy of the MSE method is about ±50%, but it has been shown in Popović and Dimitrijević (1996b), Popović and Dimitrijević (1998) and Popović et al. (2001a) that the MSE approach, even in the case of the emitters with very complex spectra (e.g. Xe II and Kr II), gives very good agreement with experimental measurements (in the interval ± 30%.). For example for Xe II, 6s-6p transitions, the averaged ratio between experimental and theoretical widths is 1.15 ± 0.5 (Popović and Dimitrijević 1996b).

Stark widths, and in some cases also and shifts are determined for spectral lines of the following emitters/absorbers: Ar II, Fe II, Pt II, Bi II, Zn II, Cd II, As II, Br II, Sb II, I II, Xe II, Mn II, La II, Au II, Eu II, V II, Ti II, Kr II, Na II, Y II, Zr II, Sc II, Nd II, Be III, B III, S III, C III, N III, O III, F III, Ne III, Na III, Al III, Si III, P III, S III, Cl III, Ar III, Mn III, Ga III, Ge III, As III, Se III, Zn III, Mg III, La III, V III, Ti III, Bi III, Sr III, Cu III, Co III, Cd III, B IV, Cu IV, Ge IV, C IV, N IV, O IV, Ne IV, Mg IV, Si IV, P IV, S IV, Cl IV, Ar IV, V IV, Ge IV, C V, O V, F V, Ne V, Al V, Si V, N VI, F VI, Ne VI, Si VI, P VI and Cl VI.

An example of the application of the MSE method is the consideration of so called "zirconium conflict" in χ Lupi star atmosphere (Popović et al. 2001a). Namely, the zirco-

nium abundance determination from weak Zr II optical lines and strong Zr III lines (detected in UV) is quite different (see e. g. Sikström (1999)) in HgMn star χ Lupi. Sikström (1999) supposed that this difference is probably due to non adequate use of stellar models, e.g. if the influence of non-LTE effects or if diffusion is not taken into account.

In Popović et al. (2001a), the electron-impact broadening parameters calculation of two astrophysically important Zr II and 34 Zr III lines has been performed, in order to test the influence of this broadening mechanism on determination of equivalent widths and to discuss its possible influence on zirconium abundance determination. Obtained results have been used to see how much the electron-impact broadening can take part in so called "zirconium conflict" in the HgMn star χ Lupi.

Popović et al. (2001a) have calculated the equivalent widths with the electron-impact broadening effect and without it for different abundances of zirconium. The obtained results for ZrIII[194.0nm] and ZrII[193.8nm] lines show that the electron-broadening effect is more important in the case of higher abundance of zirconium. The equivalent width increases with abundance for both lines, but the equivalent width for ZrIII[194.0nm] line is more sensitive than for ZrII[193.8nm] line. It may cause error in abundance determination in the case when the electron-impact broadening effect is not taken into account. In any case synthesizing of these two lines in order to measure the zirconium abundance without taking into account the electron-impact widths will give that with the ZrIII[194.0nm] the abundance of zirconium is higher than with the ZrII[193.8nm] line. However, this effect cannot cause the difference of one order of magnitude in abundance. Although the "zirconium conflict" in HgMn star χ Lupi cannot be explained only by this effects, one should take into account that this effect may cause errors in abundance determination.

Another example of the applicability of MSE method in astrophysics is the investigation of rare earth element (REE) spectral lines in the spectra of CP stars. In Popović et al. (1999b), the Stark widths and shifts for six Eu II lines and widths for three La II and six La III multiplets have been calculated by using the MSE method. The influence of the electron-impact mechanism on line shapes and equivalent widths in hot star atmospheres has been considered. It has been shown that Stark broadening is significant in hot stars, and it should be taken into account in the analysis of stellar spectral lines for the $T_{eff} > 7000$ K, in particular if europium is overabundant.

In Popović et al. (2001b) Stark widths for 284 Nd II lines have been determined within the symplified MSE approach. The lines of Nd II are observed in spectra of CP stars as well as in spectra of other stars (see e.g. Cowley et al. (2000); Guthrie (1985); Adelman (1987), etc.). Due to conditions in stellar atmospheres, the Nd II lines are dominant in comparison with Nd I and Nd III lines, e.g. in spectra of HD101065, a roAp star, Cowley et al. (2000) found 71 lines of Nd II and only 6 and 7 lines of Nd I and Nd III, respectively.

It is the reason why for determination of Neodymium abundance in spectra of CP and other stars the Nd II lines are usually used. On the other side, due to complexity of Nd II spectrum, it is very difficult to obtain atomic data (oscillator strengths, Stark widths, etc.) needed for astrophysical purposes.

Popović et al. (2001b) used for Stark width calculation the simplified MSE approach of Dimitrijević and Konjević (1987). This formula gives better results than older approximate formula of Cowley (1971) often used for Stark width estimations when more sophisticated methods are not applicable.

In order to test the importance of the electron-impact broadening effect in stellar atmospheres, Popović et al. (2001b) have synthesized the line profiles of 38 Nd II lines using SYNTH code (Popović et al. 1999c) and the Kurucz's ATLAS9 code for stellar atmosphere models (Kurucz 1993) in the temperature range of $6000 \leq T_{eff} \leq 16000$ K, and $3.0 \leq \log g \leq 5.0$.

They have synthesized the line profiles with and without taking the electron-impact broadening mechanism for different types of stellar atmospheres. First, they have synthesized all considered line profiles for

Neodymium abundance of A = log[Nd/H]=-7.0, and two values of log g=4.0 and 4.5 for different effective temperatures (T_{eff}= 6000 – 16000). All considered lines have similar dependence on effective temperature.

In order to point out the type of stars where the electron-impact broadening effect is the most important, Popović et al. (2001b) summarized this influence in different types of stellar atmospheres, considering the minimal and maximal influence for all studied lines. They found that the most important influence of Stark broadening mechanism is in the A-type stellar atmospheres. Taking into account that Stark width depends on electron density, the effect is dominant in hot star atmospheres where electron density is higher, since hydrogen becomes ionized. However for stars of O and early B type the surface gravity is smaller and electron density decreases in spite of higher temperatures. Starting from the fact that ionization potential of Nd II is 10.73 eV and consequently the layers where Nd II ion density is maximal have electron temperature between 7000 K and 9000 K, Popović et al. (2001b) have calculated the averaged electron density in these layers of stellar atmosphere for different stellar types for log g=4.0 and they found that the averaged electron density decreases with effective temperature. This is the reason why the maximal influence of Stark broadening effect in the case of Nd II is in A-type stellar atmospheres.

6. Serbian Virtual Observatory, STARK-B Database and VAMDC FP7 project

Serbian virtual observatory (SerVO) is a new project whose objectives are to publish in VO compatible format data obtained by Serbian astronomers in order to make them accessible to scientific community, as well as to provide astronomers in Serbia with VO tools for their research. The project objectives are:

- establishing SerVO and join the EuroVO and IVOA;
- establishing SerVO data Center for digitizing and archiving astronomical data obtained at Belgrade Astronomical Observatory;
- development of tools for visualization of data.

One of the aims of this project, is to publish together with Observatoire de Paris, in collaboration with Sylvie Sahal-Bréchot, Marie Lise Dubernet and Nicolas Moreau, STARK-B - Stark broadening data base containing as the first step Stark broadening parameters obtained within the semiclassical perturbation approach by Sylvie Sahal-Bréchot and myself in VO compatible format, and make two mirror sites - in Paris and Belgrade.

In this database which is also included in the database MOLAT of Paris Observatory and in the European Virtual Atomic and Molecular Data centre (VAMDC) FP7 project, enter just Stark broadening data on which was written in this paper. We will note that the precursor of SerVO was BELDATA and its principal content was database on Stark broadening parameters. The history of BELDATA may be followed in Popović et al. (1999c,d); Milovanović et al. (2000); Dimitrijević et al. (2003c) and Dimitrijević and Popović (2006). After intensification of collaboration with French colleagues around MOLAT database of Paris observatory BELDATA became STARK-B. (see http://stark-b.obspm.fr/elements.php).

This database is dedicated for modellisation of stellar atmospheres, stellar spectra analysis and synthesis, as well as for laboratory plasma research, inertial fusion plasma, laser development and plasmas in technology investigations.

The simple graphical interface to the data is provided. User first chooses the element of interest from the periodic system of elements. After that the ionization stage, perturber (s), perturber density, transition and plasma temperature can be set and page with description of data and table with shifts and widths is generated.

This database enters also in european FP7 project Virtual Atomic and Molecular Data Centre - VAMDC. In Consortium are 15 institutions from 9 countries. Its objective is to build accessible and interoperable e-

infrastructure for atomic and molecular data upgrading and integrating extensive portfolio of database services and catering for the needs of variety of data users from academia and industry.

7. Conclusions

One can conclude that the multidisciplinary research field of Stark broadening of Spectral lines, gives many possibilities for scientific research. Such investigations in astronomy have and its conference in Serbia. I-III Yugoslav conference on spectral line shapes were organized 1995, 1997 and 1999, in Krivaja at Bačka Topola, Bela Crkva and Brankovac on Fruška Gora, IV Serbian conference on spectral line shapes in Arandjelovac 2003, and V-VII Serbian conference on spectral line shapes in astrophysics 2005, 2007 and 2009, in Vršac, Sremski Karlovci and Zrenjanin.

Acknowledgements. This work is a part of the project (146001): "Influence of collisions with charged particles on astrophysical spectra", supported by Serbian Ministry of Science and Technological Development.

References

Adelman, S. J. 1987, in: Elemental Abundance Analyses, Proc. of the IAU working group on Ap stars Workshop, eds. S. J. Adelman and T. Lanz, Institut d'Astronomie de l'Université de Lausanne, p. 58.

Cowley, C. R. 1971, The Observatory, 91, 139.

Cowley, C. R., Ryabchikova, T., Kupka, F., Bord, D. J., Mathys, G. and Bidelman, W. P. 2000, Mon. Not. Roy. Astron. Soc., 317, 299.

Dimitrijević, M. S., Dačić, M., Cvetković, Z. and Simić, Z. 2004, Astron. Astrophys., 425, 1147.

Dimitrijević, M. S., Feautrier, N. and Sahal-Bréchot, S. 1981, J. Phys. B, 14, 2559.

Dimitrijević, M. S., Jovanović, P. and Simić, Z. 2003a, Astron. Astrophys., 410, 735.

Dimitrijević, M. S. and Konjević, N. 1980, J. Quant. Spectrosc. Radiat. Transfer, 24, 451.

Dimitrijević, M. S. and Konjević, N. 1987, Astron. Astrophys., 172, 345.

Dimitrijević, M. S. and Kršljanin, V. 1986, Astron. Astrophys., 165, 269.

Dimitrijević, M. S. and Popović, L. Č. 1993, Astron. Astrophys. Suppl. Series, 101, 583.

Dimitrijević, M. S. and Popović, L. Č. 2001, Zh. Prikl. Spektrosk., 68, 685.

Dimitrijević, M. S., and Popović, L. Č. 2006, in Virtual Observatory; Plate Content Digitization, Archive Mining, Image Sequence Processing, eds. M. Tsvetkov, V. Golev, F. Murtagh, R. Molina, Sofia: Heron Press Science Series, p. 115.

Dimitrijević, M. S., Popović, L. Č., Bon, E., Bajčeta, V., Jovanović, P. and Milovanović, N. 2003b, Publ. Astron. Obs. Belgrade, 75, 129.

Dimitrijević, M. S., Ryabchikova, T., Popović, L. Č., Shulyak, D. and Tsymbal, V. 2003c, Astron. Astrophys., 404, 1099.

Dimitrijević, M. S., Ryabchikova, T., Simić, Z., Popović, L. Č. and Dačić, M. 2007, Astron. Astrophys., 469, 681.

Dimitrijević, M. S. and Sahal-Bréchot, S. 1984, J. Quant. Spectrosc. Radiat. Transfer, 31, 301.

Dimitrijević, M. S. and Sahal-Bréchot, S. 1985, Phys. Rev., A, 31, 316.

Dimitrijević, M. S. and Sahal-Bréchot, S. 1996, Physica Scripta, 54, 50.

Dreizler, S. and Werner, K. 1996, Astron. Astrophys., 314, 217.

Fleurier, C., Sahal-Bréchot, S. and Chapelle, J. 1977, J. Quant. Spectrosc. Radiat. Transfer, 17, 595.

Griem, H. R. 1968, Phys. Rev., 165, 258.

Griem, H. R. 1974, Spectral Line Broadening by Plasmas, New York and London: Academic Press.

Griem, H. R., Blaha, M., Kepple, P. C. 1979, Phys. Rev. A, 19, 2421.

Guthrie, B. N. G. 1985, Mon. Not. Roy. Astron. Soc., 216, 15.

Hamdi, R., Ben Nessib, N., Milovanović, N., Popović, L. Č., Dimitrijević, M. and Sahal-Bréchot, S. 2008, MNRAS, 387, 871.

Jevremović, D., Dimitrijević, M. S., Popović, L. Č., Dačić, M., Protić-Benišek, V., Bon, E., Gavrilović, N., Kovačević, J., Benišek, V., Kovačević, A., Ilić, D., Sahal-Bréchot,

S., Tsvetkova, K. Malović, M. 2009, New Astron. Rev In press.
Khokhlova, V. L. 1994, Pis'ma v Astron. Zh., 20, 110.
Kochukhov, O., Tsymbal, V., Ryabchikova, T., Makaganyk, V. and Bagnulo, S. 2006, Astron. Astrophys., 460, 831.
Kurucz, R.L. 1979, Astrophys. J. Suppl. Series, 40, 1.
Kurucz, R. L. 1993, CDROMs 13, 22, 23, SAO, Cambridge.
LeBlanc, F. and Michaud, G. 1995, Astron. Astrophys., 303, 166.
Milovanović, N., Popović, L. Č. and Dimitrijević, M. S. 2000, Publ. Astron. Obs. Belgrade, 68, 117.
Paerels, F. 1997, Astrophys., 476, L47.
Popović, L. Č., Dimitrijević, M. S. 1996a, Phys. Scripta, 53, 325.
Popović, L. Č. and Dimitrijević, M. S. 1996b, Astron. Astrophys. Suppl. Series, 116, 359.
Popović, L. Č. and Dimitrijević, M. S. 1998, Astron. Astrophys. Suppl., Series, 127, 259.
Popović, L. Č., Dimitrijević, M. S. and Tankosić, D. 1999a, Astron. Astrophys., 139, 617.
Popović, L. Č., Dimitrijević, M. S., Milovanović, N. and Trajković, N. 1999b, Publ. Astron. Obs. Belgrade, 65, 225.
Popović, L. Č., Dimitrijević, M. S., Milovanović, N. and Trajković, N. 1999c, J. Res. Phys., 28, 307.
Popović, L. Č., Dimitrijević, M. S. and Ryabchikova, T. 1999d, Astron. Astrophys., 350, 719.
Popović, L. Č., Milovanović, N. and Dimitrijević, M. S. 2001a, Astron. Astrophys., 365, 656.
Popović, L. Č., Simić, S., Milovanović, N. and Dimitrijević, M. S. 2001b, Astrophys. J. Suppl. Series, 135, 109.
Sahal-Bréchot, S. 1969a, Astron. Astrophys., 1, 91.
Sahal-Bréchot, S. 1969b, Astron. Astrophys., 2, 322.
Sikström, C. M., Lundberg, H., Wahlgren, G. M., Li, Z. S., Lyngå, C., Johansson, S. and Leckrone, D. S. 1999, Astron. Astrophys., 343, 297.
Simić, Z., Dimitrijević, M. S., Kovačević, A. 2009, New Astronomy Review, in press.
Simić, Z., Dimitrijević, M. S., Popović, L. Č. and Dačić, M. 2006, New Astronomy, 12, 187.
Simić, Z., Dimitrijević, M. S., Milovanović, N., Sahal-Bréchot, S. 2005, Astron. Astrophys., 441, 391.
Stehlé, C. 1994, Astron. Astrophys. Suppl. Series, 104, 509.
Stehlé C. 1995, , in Spectral Line Shapes, Vol. 8, eds. A. David May, J. R. Drummond, E. Oks, AIP Conf. Proc. 328, AIP Press, New York, 36.
Tankosić, D., Popović, L. Č. and Dimitrijević, M. S. 2003, Astron. Astrophys., 399, 795.
Werner, K., Heber, U. and Hunger, R. 1991, Astron. Astrophys., 244, 437.
Wickramasinghe, D.T. 1972, Mem. R. Astron. Soc., 76, 129.

Mon. Not. R. Astron. Soc. **387,** 871–882 (2008) doi:10.1111/j.1365-2966.2008.13284.x

Atomic data and electron-impact broadening effect in DO white dwarf atmospheres: Si VI

R. Hamdi,[1] N. Ben Nessib,[1] N. Milovanović,[2] L. Č. Popović,[2] M. S. Dimitrijević[2]★ and S. Sahal-Bréchot[3]

[1]*Groupe de Recherche en Physique Atomique et Astrophysique, Institut National des Sciences Appliquées et de Technologie, Centre Urbain Nord B. P. No. 676, 1080 Tunis Cedex, Tunisia*
[2]*Astronomical observatory, Volgina 7, 11160 Belgrade 74, Serbia*
[3]*Laboratoire d'Étude du Rayonnement et de la Matière en Astrophysique, UMR CNRS 8112, Observatoire de Paris-Meudon, 92195 Meudon, France*

Accepted 2008 April 3. Received 2008 March 28; in original form 2008 January 28

ABSTRACT

Energy levels, electric dipole transition probabilities and oscillator strengths in five times ionized silicon have been calculated in intermediate coupling. The present calculations were carried out with the general purpose atomic structure program SUPERSTRUCTURE. The relativistic corrections to the non-relativistic Hamiltonian are taken into account through the Breit–Pauli approximation. We have also introduced a semi-empirical correction [term energy corrections (TEC)] for the calculation of the energy levels. These atomic data are used to provide semiclassical electron-, proton- and ionized helium-impact linewidths and shifts for 15 Si VI multiplet. Calculated results have been used to consider the influence of Stark broadening for DO white dwarf atmospheric conditions.

Key words: atomic data – atomic processes – line: formation – stars: atmospheres – white dwarfs.

1 INTRODUCTION

Atomic data such as transition probabilities (*A*) play an important role in the diagnostics and modelling of laboratory plasmas (Griem 1974). Various kinetic processes appearing in plasma modelling need reliable knowledge of *A* values. Further, knowledge of *A* values gives a possibility for determination of coefficients (*B*) which characterize the absorption and stimulated emission. These processes are also important in laser physics. The classification of transitions and determination of energy levels are essential parts of the study of a laboratory spectrum. The lack of available atomic data limits our ability to infer reliably the properties of many cosmic plasmas and, hence, address many of the fundamental issues in astrophysics (Savin 2001).

Accurate Stark broadening parameters are important to obtain a reliable modelization of stellar interiors. The Stark broadening mechanism is also important for the investigation, analysis and modelling of *B*-type, and particularly *A*-type, stellar atmospheres, as well as for white dwarf atmospheres (see e.g. Popović et al. 2001; Dimitrijević et al. 2007).

Silicon, in various ionization stages, is detected in the atmospheres of DO white dwarfs (Werner, Dreizler & Wolff 1995). Si VI lines have been observed as well for example in coronal line regions of planetary nebulae NGC 6302 and 6537 (Casassus, Roche & Barlow 2000).

Uzelac and collaborators (Uzelac et al. 1993) studied plasma broadening of Ne II–Ne VI and F IV–F V experimentally and theoretically, they found that the results of simplified semiclassical (Griem 1974, equation 526) calculations show better agreement at higher ionization stages, while the modified semi-empirical formula (Dimitrijević & Konjević 1980) seems to be better for the low-ionization stages. Unfortunately, due to the lack of atomic data, most of the reported sophisticated semiclassical Stark broadening parameters relate to spectral lines of neutral- and low-ionization stages. In previous papers (Ben Nessib, Dimitrijević & Sahal-Bréchot 2004; Hamdi et al. 2007), we calculated Stark broadening parameters of quadruply ionized silicon and neon using SUPERSTRUCTURE and Bates & Damgaard (1949) method for oscillator strengths and we found that the difference is tolerable.

Si VI ion belongs to the fluorine-like sequence, its ground state configuration is $1s^2 2s^2 2p^5$ with the term $^2P^\circ$. In this work we present fine-structure energy levels, transition probabilities and oscillator strengths for Si VI ion. The atomic structure code SUPERSTRUCTURE was used, which allows for configuration interaction (CI), relativistic effects and semi-empirical term energy corrections (TEC). Calculated energies and oscillator strengths are used to provide Stark broadening parameters due to electron-, proton- and ionized helium impact of Si VI lines. The obtained Stark broadening parameters are used to investigate the influence of Stark broadening mechanism

★E-mail: mdimitrijevic@aob.bg.ac.yu

in hot, high gravity star atmospheres, as for example DO white dwarfs.

2 THE METHOD

In this work, the calculations were carried out with the general purpose atomic structure program SUPERSTRUCTURE (Eissner, Jones & Nussbaumer 1974), as modified by Nussbaumer & Storey (1978). The atomic model used to calculate energies of terms or levels and transition probabilities include 26 configurations: $2s^22p^5$, $2s2p^6$, $2s^22p^43\ell$, $2s^22p^44\ell$, $2s^22p^45\ell$, $2s^22p^46\ell$, $2s2p^53\ell$ and $2p^63\ell$ ($\ell \leqslant n - 1$). CI effects were fully taken into account. The wave functions are of the type

$$\Psi = \sum_i \Phi_i C_i, \tag{1}$$

where the basis functions Φ_i are constructed using one-electron orbitals. The latter are calculated with a scaled Thomas–Fermi statistical model potential or obtained from the Coulomb potential. For each radial orbital $P_{nl}(r)$, the potential can be adjusted using a parameter called λ. In the present case, those *n*- and *l*-dependent scaling parameters λ_{nl} were determined variationally by optimizing the weighted sum of the term energies. The P_{nl} are orthogonalized to each other such that the function P_{n_1l} is orthogonalized to the function P_{n_2l} when $n_2 < n_1$. The values adopted for the λ_{nl} parameters are presented in Table 1. In this approach the Hamiltonian is taken to be in the form

$$H = H_{\rm nr} + H_{\rm BP}, \tag{2}$$

relativistic corrections are included in Breit–Pauli Hamiltonian ($H_{\rm BP}$) as perturbation to the non-relativistic Hamiltonian ($H_{\rm nr}$). $H_{\rm BP}$ contains the one-electron operators for the mass correction, the Darwin contact term, the spin–orbit interaction in the field of the nucleus and the two-electron operators for spin–orbit, spin–other orbit and spin–spin interactions. We also use the so-called TEC introduced by Zeippen, Seaton & Morton (1977), in which the Hamiltonian matrix is empirically adjusted to give the best agreement between experimental energies and the final calculated term energies including the relativistic effects. In practice, the TEC for a given term is simply the difference between the calculated and measured energy of the lowest level in the multiplet.

Stark broadening parameter calculations have been performed within the semiclassical perturbation method (Sahal-Bréchot 1969a,b). A detailed description of this formalism with all the innovations is given in Sahal-Bréchot (1969a,b, 1974, 1991), Fleurier, Sahal-Bréchot & Chapelle (1977), Dimitrijević, Sahal-Bréchot & Bommier (1991) and Dimitrijević & Sahal-Bréchot (1996). The full half-width (w) and shift (d) of an electron-impact broadened spectral line can be expressed as

$$W = N \int v f(v)\,{\rm d}v \left[\sum_{i'\neq i} \sigma_{ii'}(v) + \sum_{f'\neq f} \sigma_{ff'}(v) + \sigma_{\rm el}\right] + W_{\rm R},$$
$$d = N \int v f(v)\,{\rm d}v \int_{R_3}^{R_{\rm D}} 2\pi\rho\,{\rm d}\rho \sin(2\varphi_{\rm p}), \tag{3}$$

where N is the electron density, $f(\upsilon)$ the Maxwellian velocity distribution function for electrons, ρ denotes the impact parameter of the incoming electron, i and f denote the initial and the final atomic energy levels and i' and f' their corresponding perturbing levels, while $W_{\rm R}$ gives the contribution of the Feshbach resonances (Fleurier et al. 1977). The inelastic cross-section $\sigma_{ii'}(\upsilon)$ can be expressed by an integral over the impact parameter of the transition probability $P_{jj'}(\rho, \upsilon)$ as

$$\sum_{j\neq j'} \sigma_{ii'}(\upsilon) = \frac{1}{2}\pi R_1^2 + \int_{R_1}^{R_{\rm D}} 2\pi\rho\,{\rm d}\rho \sum_{j\neq j'} P_{jj'}(\rho, \upsilon),\ j = i,\ f, \tag{4}$$

and the elastic cross-section is given by

$$\sigma_{\rm el} = 2\pi R_2^2 + \int_{R_2}^{R_{\rm D}} 2\pi\rho\,{\rm d}\rho \sin^2\delta,$$
$$\delta = \left(\varphi_{\rm p}^2 + \varphi_{\rm q}^2\right)^{1/2}. \tag{5}$$

The phase shifts $\varphi_{\rm p}$ and $\varphi_{\rm q}$ due, respectively, to the polarization potential (r^{-4}) and to the quadrupolar potential (r^{-3}) are given in section 3 of chapter 2 in Sahal-Bréchot (1969a), and $R_{\rm D}$ is the Debye radius. All the cut-offs R_1, R_2, R_3 are described in section 1 of chapter 3 in Sahal-Bréchot (1969b).

For electrons, hyperbolic paths due to the attractive Coulomb force were used, while for perturbing ions the hyperbolic paths are different since the force is repulsive. The formulae for the ion-impact widths and shifts are analogous to equations (3)–(5), without the resonance contribution to the width.

Table 1. Optimized parameters λ_{nl} adopted for the 26-configuration model calculation. Positive values for Thomas–Fermi–Dirac potential and negative values for Coulomb potential.

n, l	λ_{nl}	*n, l*	λ_{nl}	*n, l*	λ_{nl}	*n, l*	λ_{nl}
1s	1.4653	4s	1.1091	5d	1.1015	6f	−0.6629
2s	1.1844	4p	1.0960	5f	1.1135	6g	−1.0777
2p	1.1389	4d	1.1103	5g	1.0776	6h	−1.3002
3s	1.1078	4f	1.0478	6s	4.8162		
3p	1.0762	5s	1.1580	6p	6.2669		
3d	1.1808	5p	1.0902	6d	5.3865		

3 RESULTS AND DISCUSSION

The calculated *ab initio* energies for Si VI are listed in Table 2 along with experimentally determined energies for a number of levels taken from a National Institute of Standards and Technology (NIST) compilation. The configurations for which we present results are $2s^22p^5$, $2s2p^6$, $2s^22p^43\ell$, $2s^22p^44\ell'$; ℓ = s, p, d and ℓ' = s, p, d. We use the LS coupling scheme to designate excited energy.

Two different models are used for the determination of energy levels, the first contains the nine configurations of the model given in Section 2 and the second contains the totality of the 26 configurations. Both nine-configuration model and more elaborated 26-configuration one give energy levels in good agreement with the NIST values, indeed, our energies are lower than the NIST ones by less than 1 per cent except for the two first excited levels, i.e. $2p^5\ {}^2P^\circ_{1/2}$ and $2s2p^6\ {}^2S_{1/2}$. However, the results obtained by the second model are always more accurate that proves the importance of the CI. Besides, if a term is simply shifted relatively to the ground state, then the difference with observed energy should be essentially constant. In some terms the levels are not always in correct order. For example, the observed order of the levels of $2p^4(^3P)3d^4F$ is (9/2, 7/2, 5/2, 3/2) and the present order is (9/2, 3/2, 5/2, 7/2).

We use the calculated energies and the wavefunctions to calculate oscillator strengths and transition probabilities. With the aim of improving the quality of our wavefunctions, the $2s2p^6\ {}^2S_{1/2}$ level is corrected using TEC procedure (see Section 2). This method cannot

Table 2. Energy levels for Si VI in cm^{-1}. Key: a number assigned to each level; LS: LS term and parity (superscript $^\circ$ designate an odd level); *J*: *J* value of the level; E_{9-conf}: *ab initio* energy levels, calculated with nine-configuration model; $E_{26-conf}$: *ab initio* energy levels, calculated with 26-configuration model; E_{NIST}: NIST values.

Key	Configuration	LS	*J*	E_{9-conf}	$E_{26-conf}$	E_{NIST}
1	$2p^5$	$^2P^\circ$	3/2	0	0	0
2			1/2	2 796	2 839	5 090
3	$2s2p^6$	^2S	1/2	435 632	426 462	406 497
4	$2p^4(^3P)3s$	^4P	5/2	971 851	982 366	990 516
5			1/2	975 520	986 496	995 470
6			3/2	975 969	987 021	993 640
7	$2p^4(^3P)3s$	^2P	3/2	987 370	999 127	1 005 430
8			1/2	987 692	999 494	1 009 118
9	$2p^4(^1D)3s$	^2D	5/2	1 024 374	1 036 129	1 041 416
10			3/2	1 024 884	1 036 533	1 041 472
11	$2p^4(^3P)3p$	$^4P^\circ$	3/2	1 052 168	1 061 210	1 069 854
12			5/2	1 052 404	1 061 401	1 068 813
13			1/2	1 053 583	1 062 874	1 071 129
14	$2p^4(^3P)3p$	$^4D^\circ$	7/2	1 059 089	1 070 621	1 078 935
15			1/2	1 061 265	1 073 242	1 083 003
16			3/2	1 062 447	1 074 609	1 082 215
17			5/2	1 062 788	1 074 942	1 080 700
18	$2p^4(^3P)3p$	$^2D^\circ$	5/2	1 068 139	1 080 203	1 086 796
19			3/2	1 068 477	1 080 547	1 089 547
20	$2p^4$ $(^3P)3p$	$^2P^\circ$	1/2	1 077 264	1 080 958	
21			3/2	1 075 947	1 084 287	1 092 171
22	$2p^4(^1S)3s$	^2S	1/2	1 071 075	1 084 295	1 094 449
23	$2p^4(^3P)3p$	$^4S^\circ$	3/2	1 074 673	1 087 671	1 093 752
24	$2p^4(^3P)3p$	$^2S^\circ$	1/2	1 094 162	1 088 558	
25	$2p^4(^1D)3p$	$^2F^\circ$	5/2	1 106 342	1 118 373	1 123 540
26			7/2	1 106 472	1 118 689	1 124 219
27	$2p^4(^1D)3p$	$^2D^\circ$	3/2	1 116 033	1 128 816	1 134 081
28			5/2	1 116 641	1 129 460	1 134 496
29	$2p^4(^1D)3p$	$^2P^\circ$	3/2	1 140 823	1 145 932	1 147 901
30			1/2	1 140 921	1 145 980	1 150 282
31	$2p^4(^1S)3p$	$^2P^\circ$	3/2	1 182 143	1 171 561	
32			1/2	1 182 942	1 172 417	
33	$2p^4(^3P)3d$	^4D	7/2	1 161 013	1 172 209	1 181 167
34			5/2	1 162 025	1 173 271	1 181 649
35			3/2	1 162 165	1 173 376	1 182 311
36			1/2	1 162 754	1 173 979	1 182 894
37	$2p^4(^3P)3d$	^4F	9/2	1 169 569	1 182 612	1 189 844
38			3/2	1 171 689	1 184 525	1 194 327
39			5/2	1 172 030	1 184 838	1 193 223
40			7/2	1 172 047	1 184 946	1 191 541
41	$2p^4(^3P)3d$	^4P	1/2	1 176 385	1 188 594	1 194 899
42			3/2	1 177 207	1 189 543	1 195 984
43			5/2	1 178 908	1 191 510	1 197 727
44	$2p^4(^3P)3d$	^2F	7/2	1 177 148	1 189 950	1 194 987
45			5/2	1 178 364	1 190 848	1 197 151
46	$2p^4(^3P)3d$	^2P	1/2	1 182 736	1 194 144	1 200 710
47			3/2	1 185 454	1 196 939	1 204 740
48	$2p^4(^3P)3d$	^2D	3/2	1 185 167	1 195 061	1 201 100
49			5/2	1 185 973	1 196 247	1 202 960
50	$2p^4(^1D)3d$	^2G	7/2	1 214 568	1 227 449	
51			9/2	1 214 715	1 227 538	1 232 671
52	$2p^4(^1D)3d$	^2S	1/2	1 223 636	1 234 097	1 239 190
53	$2p^4(^1$ $D)3d$	^2P	3/2	1 224 780	1 234 806	1 241 050
54			1/2	1 225 778	1 235 883	1 242 390
55	$2p^4(^1D)3d$	^2F	7/2	1 223 872	1 236 910	1 242 649
56			5/2	1 223 946	1 236 950	1 242 186
57	$2p^4(^1D)3d$	^2D	5/2	1 226 710	1 237 621	1 243 020
58			3/2	1 227 611	1 238 313	1 243 860
59	$2p^4(^1S)3d$	^2D	3/2	1 290 487	1 280 925	1 291 790
60			5/2	1 291 154	1 281 640	1 291 510
61	$2p^4(^3P)4s$	^4P	5/2	1 302 866	1 314 745	
62			1/2	1 305 283	1 317 544	
63			3/2	1 306 890	1 319 305	
64	$2p^4(^3P)4s$	^2P	3/2	1 308 844	1 321 429	1 329 900
65			1/2	1 310 323	1 323 045	
66	$2p^4(^3P)4p$	$^4P^\circ$	5/2	1 333 771	1 340 871	
67			3/2	1 333 474	1 340 979	
68			1/2	1 334 815	1 342 729	
69	$2p^4(^3P)4p$	$^4D^\circ$	7/2	1 335 203	1 347 589	
70			1/2	1 337 989	1 350 092	
71			3/2	1 338 555	1 351 294	
72			5/2	1 338 545	1 352 144	
73	$2p^4(^3P)4p$	$^2D^\circ$	5/2	1 339 973	1 351 228	
74			3/2	1 339 638	1 352 195	
75	$2p^4(^3P)4p$	$^2S^\circ$	1/2	1 340 521	1 352 722	
76	$2p^4(^3P)4p$	$^4S^\circ$	3/2	1 342 995	1 355 616	
77	$2p^4(^3P)4p$	$^2P^\circ$	3/2	1 349 411	1 359 114	
78			1/2	1 349 310	1 359 465	
79	$2p^4(^1D)4s$	^2D	5/2	1 352 262	1 365 126	1 371 820
80			3/2	1 352 767	1 365 515	
81	$2p^4(^3P)4d$	^4D	7/2	1 371 226	1 382 797	
82			5/2	1 372 174	1 384 161	
83			3/2	1 372 430	1 384 614	
84			1/2	1 373 107	1 385 519	
85	$2p^4(^3P)4d$	^4F	9/2	1 374 444	1 387 108	
86			7/2	1 376 125	1 388 760	
87			5/2	1 376 654	1 389 343	
88			3/2	1 376 461	1 389 348	
89	$2p^4(^3P)4d$	^4P	1/2	1 377 931	1 390 631	
90			3/2	1 379 041	1 391 893	
91			5/2	1 380 830	1 393 884	
92	$2p^4(^3P)4d$	^2F	5/2	1 380 128	1 392 885	
93			7/2	1 380 477	1 393 669	
94	$2p^4(^3P)4d$	^2P	1/2	1 381 851	1 393 521	1 402 490
95			3/2	1 384 583	1 396 287	1 403 050
96	$2p^4(^3P)4d$	^2D	3/2	1 385 040	1 395 603	
97			5/2	1 385 544	1 396 797	1 404 870
98	$2p^4(^3P)4p$	$^2F^\circ$	7/2	1 382 852	1 395 696	
99			5/2	1 382 929	1 395 739	
100	$2p^4(^1D)4p$	$^2D^\circ$	3/2	1 386 127	1 399 126	
101			5/2	1 386 673	1 399 653	
102	$2p^4(^1D)4p$	$^2P^\circ$	1/2	1 392 385	1 405 752	
103			3/2	1 392 362	1 405 797	
104	$2p^4(^1D)4s$	^2S	1/2	1 419 675	1 432 175	
105	$2p^4(^1D)4d$	^2G	7/2	1 421 515	1 434 310	
106			9/2	1 421 617	1 434 434	
107	$2p^4(^1D)4d$	^2P	3/2	1 424 977	1 436 510	
108			1/2	1 425 973	1 437 711	
109	$2p^4(^1D)4d$	^2F	7/2	1 424 368	1 437 280	
110			5/2	1 424 453	1 437 401	
111	$2p^4(^1D)4d$	^2D	5/2	1 425 961	1 438 109	1 444 340
112			3/2	1 426 992	1 438 858	1 445 010
113	$2p^4(^1D)4d$	^2S	1/2	1 427 833	1 440 235	
114	$2p^4(^1S)4p$	$^2P^\circ$	1/2	1 453 543	1 466 060	
115			3/2	1 453 658	1 466 257	
116	$2p^4(^1S)4d$	^2D	3/2	1 493 396	1 506 902	
117			5/2	1 494 092	1 507 702	

Table 2 – *continued*

be applied for $2p^5\ ^2P^\circ_{1/2}$ level. Electric dipole transition probabilities and weighted oscillator strengths are presented in Table 3 for transition with lower level from one to 10 and upper level from three to 95. The majority of wavelengths are in extreme ultraviolet (XUV) region. F-like ions are of fundamental importance for current

Table 3. Transition probabilities (A_{ki}), calculated wavelengths (λ) and weighted oscillator strengths (gf) for Si VI spectrum. Present: this work; FF: Froese Fischer & Tachiev (2004); CT: Coutinho & Trigueiros (1999). The numbers in brackets denote powers of 10.

Transition	λ (Å)	$A_{ki}(s^{-1})$			gf			
		present	FF	NIST	present	FF	NIST	CT
1–3	246.004	1.805(10)	1.777(10)	1.77(10)	3.275(−01)	3.210(−01)	3.206(−01)	4.04(−01)
2–3	247.734	8.840(09)	8.517(09)	8.46(09)	1.627(−01)	1.576(−01)	1.573(−01)	2.00(−01)
1–4	101.795	8.982(07)	7.405(07)	7.51(07)	8.372(−04)	6.784(−04)	6.886(−04)	8.00(−04)
1–5	101.369	1.340(09)	8.423(06)	8.55(06)	4.128(−03)	2.547(−05)	2.588(−05)	
2–5	101.661	2.010(09)	2.624(08)	2.64(08)	6.229(−03)	8.016(−04)	8.072(−04)	9.00(−04)
1–6	101.315	1.019(08)	1.167(09)	1.18(09)	6.270(−04)	7.088(−03)	7.161(−03)	7.50(−03)
2–6	101.607	9.716(06)	1.010(08)	1.08(08)	6.016(−05)	6.194(−04)	6.266(−04)	6.00(−04)
1–7	100.087	6.667(10)	6.753(10)	6.74(10)	4.005(−01)	4.004(−01)	3.999(−01)	4.88(−01)
2–7	100.373	1.292(10)	1.098(10)	1.09(10)	7.803(−02)	6.574(−02)	6.561(−02)	7.90(−02)
1–8	100.051	2.509(10)	2.823(10)	2.82(10)	7.530(−02)	8.304(−02)	8.317(−02)	1.02(−01)
2–8	100.336	4.987(10)	5.156(10)	5.15(10)	1.505(−01)	1.532(−01)	1.531(−01)	1.86(−01)
1–9	96.513	3.189(10)	3.087(10)	3.08(10)	2.672(−01)	2.556(−01)	2.558(−01)	
1–10	96.475	4.625(09)	3.056(09)	3.03(09)	2.582(−02)	1.687(−02)	1.674(−02)	2.03(−02)
2–10	96.740	2.674(10)	2.796(10)	2.79(10)	1.501(−01)	1.558(−01)	1.559(−01)	1.94(−01)
3–11	152.739	1.064(05)	7.895(05)		1.488(−06)	1.077(−05)		
4–11	1268.336	3.944(08)	4.159(08)	4.11(08)	3.805(−01)	3.935(−01)	3.908(−01)	
5–11	1338.445	1.569(08)	1.624(08)	1.62(08)	1.685(−01)	1.746(−01)	1.749(−01)	1.89(−01)
6–11	1347.907	8.664(07)	9.855(07)	9.73(07)	9.440(−02)	1.010(−01)	1.004(−01)	1.07(−01)
7–11	1610.745	4.125(05)	5.789(04)	5.56(04)	6.418(−04)	8.312(−05)	8.035(−05)	
8–11	1620.320	1.353(07)	3.677(03)	3.79(03)	2.130(−02)	5.938(−06)	6.165(−06)	
9–11	3987.165	6.968(04)	1.627(04)	1.62(04)	6.643(−04)	1.218(−04)	1.199(−04)	
10–11	4052.352	7.466(03)	5.228(03)	5.44(03)	7.353(−05)	3.929(−05)	4.036(−05)	
4–12	1265.271	5.940(08)	5.712(08)	5.64(08)	8.554(−01)	8.322(−01)	8.279(−01)	8.72(−01)
6–12	1344.446	9.628(07)	1.104(08)	1.10(08)	1.565(−01)	1.744(−01)	1.753(−01)	1.91(−01)
7–12	1605.805	1.630(06)	2.988(05)	3.09(05)	3.781(−03)	6.648(−04)	6.918(−04)	
9–12	246.004	1.458(05)	2.110(03)	2.37(03)	2.054(−03)	2.554(−05)	2.837(−05)	
10–12	247.734	3.719(01)	2.179(02)	2.40(02)	5.410(−07)	2.646(−06)	2.890(−06)	
3–13	101.795	2.939(05)	4.160(05)		2.046(−06)	2.628(−06)		
5–13	1309.272	3.686(07)	7.502(07)	7.46(07)	1.894(−02)	3.900(−02)	3.899(−02)	
6–13	1318.325	5.969(08)	5.915(08)	5.85(08)	3.111(−01)	2.933(−01)	2.917(−01)	3.10(−01)
7–13	1568.682	1.079(06)	8.921(05)	9.49(05)	7.964(−04)	6.160(−04)	6.606(−04)	
8–13	1577.761	1.707(06)	4.217(05)	4.38(05)	1.274(−03)	3.268(−04)	3.419(−04)	
10–13	3796.252	1.573(04)	1.490(04)	1.49(04)	6.798(−05)	5.128(−05)	5.018(−05)	
4–14	1133.080	1.056(09)	1.033(09)	1.03(09)	1.626(+00)	1.581(+00)	1.577(+00)	1.71(+00)
9–14	2899.222	6.193(03)	3.205(03)	3.54(03)	6.244(−05)	2.776(−05)	3.019(−05)	
3–15	149.982	5.880(04)	1.367(06)	1.40(06)	3.966(−07)	8.972(−06)	9.141(−06)	9.00(−05)
5–15	1152.795	9.112(08)	8.776(08)	8.74(08)	3.631(−01)	3.426(−01)	3.419(−01)	3.70(−01)
6–15	1159.808	6.171(07)	1.290(08)	1.29(08)	2.489(−02)	4.836(−02)	4.841(−02)	
7–15	1349.252	9.550(05)	2.566(05)	2.58(05)	5.213(−04)	1.278(−04)	1.228(−04)	
8–15	1355.964	1.964(07)	7.280(05)	7.09(05)	1.083(−02)	3.998(−04)	3.899(−04)	
10–15	2724.120	6.668(04)	8.238(03)		1.484(−04)	1.454(−05)		
3–16	149.675	3.954(05)	5.543(05)	5.73(05)	5.312(−06)	7.292(−06)	7.516(−06)	
4–16	1084.091	2.953(07)	2.000(07)	2.03(07)	2.081(−02)	1.423(−02)	1.452(−02)	
5–16	1134.903	4.668(08)	4.842(08)	4.82(08)	3.606(−01)	3.850(−01)	3.837(−01)	4.13(−01)
6–16	1141.699	5.093(08)	4.957(08)	4.95(08)	3.981(−01)	3.781(−01)	3.768(−01)	4.11(−01)
7–16	1324.806	1.466(06)	1.213(03)	1.88(03)	1.543(−03)	1.232(−06)	1.909(−06)	
8–16	1331.276	2.832(07)	4.541(06)	4.53(06)	3.010(−02)	5.094(−03)	5.081(−03)	
9–16	2598.741	7.183(04)	8.858(03)	9.91(03)	2.909(−04)	3.241(−05)	3.572(−05)	
10–16	2626.277	1.035(02)	1.337(04)	1.45(04)	4.281(−07)	4.908(−05)	5.236(−05)	
4–17	1080.192	2.103(08)	1.903(08)	1.91(08)	2.207(−01)	2.100(−01)	2.113(−01)	2.38(−01)
6–17	1137.375	8.616(08)	7.873(08)	7.83(08)	1.003(+00)	9.320(−01)	9.289(−01)	9.98(−01)
7–17	1318.987	7.133(06)	1.864(07)	1.86(07)	1.116(−02)	2.957(−02)	2.958(−02)	
9–17	2576.446	2.564(03)	8.978(03)	9.31(03)	1.531(−05)	5.316(−05)	5.432(−05)	
4–18	1022.110	5.562(05)	1.307(07)	1.33(07)	5.227(−04)	1.265(−02)	1.285(−02)	
6–18	1073.164	1.749(07)	2.238(07)	2.22(07)	1.811(−02)	2.313(−02)	2.301(−02)	
7–18	1233.405	8.506(08)	8.032(08)	8.02(08)	1.164(+00)	1.090(−01)	1.088(+00)	
9–18	2268.921	7.863(04)	2.465(05)	2.49(05)	3.641(−04)	1.090(−03)	1.086(−03)	
10–18	2289.882	1.355(02)	6.522(03)	6.85(03)	6.391(−07)	2.892(−05)	2.999(−05)	
3–19	148.357	2.047(06)	1.279(07)		2.702(−05)	1.645(−04)		
4–19	1018.526	8.703(06)	2.181(06)	2.75(06)	5.415(−03)	1.326(−03)	1.336(−03)	
5–19	1063.250	9.488(07)	2.892(06)		6.433(−02)	1.952(−03)	1.862(−03)	
6–19	1063.250	1.100(05)	1.283(06)	1.22(06)	7.545(−05)	8.336(−04)	7.961(−04)	

Table 3 – *continued*

Transition	λ (Å)	$A_{ki}(s^{-1})$			gf			
		present	FF	NIST	present	FF	NIST	CT
7–19	1228.189	9.754(07)	4.377(08)	4.54(08)	8.824(−02)	3.701(−01)	3.845(−01)	3.66(−01)
8–19	1233.748	6.973(08)	3.698(08)	3.48(08)	6.365(−01)	3.420(−01)	3.221(−01)	
9–19	2251.333	3.457(05)	6.305(06)	7.30(06)	1.051(−03)	1.648(−02)	1.887(−02)	
10–19	2271.969	4.466(04)	2.421(06)	2.63(06)	1.382(−04)	6.344(−03)	6.807(−03)	
3–20	148.267	1.378(08)	8.949(07)		9.085(−04)	5.760(−04)		
5–20	1058.626	6.333(05)	1.717(05)		2.128(−04)	5.804(−05)		
6–20	1064.537	6.918(06)	1.331(06)		2.351(−03)	4.332(−04)		
7–20	1222.023	5.861(08)	6.643(08)		2.624(−01)	2.813(−01)		
8–20	1227.526	6.666(07)	5.304(07)		3.012(−02)	2.458(−02)		
10–20	2250.959	2.878(07)	2.829(07)		4.373(−02)	3.719(−02)		
3–21	147.538	1.880(08)	1.114(08)	1.10(08)	2.454(−03)	1.422(−03)	1.339(−03)	
4–21	981.153	1.120(07)	7.761(06)	5.01(06)	6.464(−03)	4.476(−03)	2.904(−03)	
5–21	1022.589	4.986(06)	1.343(07)	1.08(07)	3.127(−03)	8.554(−03)	6.902(−03)	
6–21	1028.103	1.619(07)	2.197(06)		1.026(−02)	1.348(−03)		
7–21	1174.254	5.806(08)	2.535(08)	2.33(08)	4.801(−01)	2.008(−01)	1.853(−01)	2.24(−01)
8–21	1179.334	4.876(07)	4.094(08)	4.31(08)	4.067(−02)	3.538(−01)	3.741(−01)	3.42(−01)
9–21	2076.504	4.517(07)	4.361(07)	4.31(07)	1.168(−01)	1.018(−01)	1.002(−01)	
10–21	2094.047	5.294(06)	3.415(06)	3.31(06)	1.392(−02)	7.996(−03)	7.726(−03)	
1–22	92.226	2.083(10)	1.964(10)	1.96(10)	5.314(−02)	4.908(−02)	4.920(−02)	6.70(−02)
2–22	92.468	1.110(10)	1.232(10)	1.23(10)	2.845(−02)	3.108(−02)	3.097(−02)	4.26(−02)
3–23	146.805	5.237(06)	1.548(05)		6.769(−05)	1.968(−06)		
4–23	949.626	7.718(08)	6.774(08)	6.81(08)	4.174(−01)	3.808(−01)	3.837(−01)	3.48(−01)
5–23	988.389	3.575(08)	3.063(08)	3.08(08)	2.095(−01)	1.899(−01)	1.909(−01)	1.89(−01)
6–23	993.539	5.751(08)	5.521(08)	5.52(08)	3.405(−01)	3.301(−01)	3.303(−01)	3.30(−01)
7–23	1129.379	4.435(06)	4.529(05)	5.45(04)	3.393(−03)	3.484(−04)	4.197(−05)	
8–23	1134.078	3.772(06)	7.482(06)	5.32(06)	2.909(−03)	6.270(−03)	4.456(−03)	
9–23	1940.178	1.976(06)	1.302(06)		4.461(−03)	2.892(−03)		
10–23	1955.485	2.723(04)	9.887(04)		6.245(−05)	2.200(−04)		
3–24	146.615	4.880(07)	2.590(07)		3.145(−04)	1.644(−04)		
5–24	979.803	4.553(07)	2.065(06)		1.311(−02)	6.328(−04)		
6–24	984.864	1.963(03)	3.411(06)		5.710(−07)	1.008(−03)		
7–24	1118.182	2.447(08)	1.833(08)		9.173(−02)	6.964(−02)		
8–24	1122.788	7.678(08)	6.707(08)		2.902(−01)	2.772(−01)		
10–24	1922.160	1.678(07)	2.055(07)		1.859(−02)	2.237(−02)		
5–25	735.260	4.657(06)			2.265(−03)			
6–25	761.314	5.428(05)	1.357(04)	1.51(04)	2.830(−04)	7.164(−06)	8.035(−06)	
7–25	838.603	7.411(04)	7.983(04)		4.688(−05)	5.100(−05)		
9–25	1215.905	8.749(07)	7.805(07)	7.65(07)	1.163(−01)	1.035(−01)	1.020(−01)	1.09(−01)
10–25	1221.899	7.763(08)	7.612(08)	7.56(08)	1.043(+00)	1.011(+00)	1.006(+00)	1.11(+00)
4–26	733.553	8.310(05)	1.120(05)	1.20(05)	5.363(−04)	7.446(−05)	8.035(−05)	
9–26	1211.242	8.876(08)	8.628(08)	8.56(08)	1.562(+00)	1.501(+00)	1.499(+00)	1.64(+00)
3–27	138.443	1.456(03)	4.078(06)	4.89(06)	1.674(−08)	4.622(−05)		
4–27	682.827	3.924(05)	6.054(04)	6.24(04)	1.097(−04)	1.749(−05)	1.811(−05)	
5–27	702.641	1.011(06)	5.116(-1)	1.89(00)	2.994(−04)	1.584(−10)	5.902(−10)	
6–27	705.240	1.533(06)	1.283(06)	4.40(05)	4.573(−04)	1.294(−04)	1.339(−04)	
7–27	771.072	1.238(06)	1.967(07)	2.00(07)	4.413(−04)	7.076(−03)	7.244(−03)	
8–27	773.259	5.680(06)	5.306(06)	5.19(06)	2.037(−03)	2.024(−03)	1.995(−03)	
9–27	1078.900	1.254(08)	7.247(07)	7.17(07)	8.756(−02)	5.049(−02)	5.023(−02)	
10–27	1083.616	1.118(09)	1.117(09)	1.11(09)	7.875(−01)	7.792(−01)	7.798(−01)	8.03(−01)
4–28	679.840	2.305(07)	4.734(05)	4.88(05)	9.584(−03)	2.040(−04)	2.118(−04)	
6–28	702.055	4.910(06)	5.481(03)	4.62(03)	2.177(−03)	2.467(−06)	2.094(−06)	
7–28	767.266	6.267(06)	1.070(07)	1.05(07)	3.319(−03)	5.740(−03)	5.675(−03)	
9–28	1071.462	1.150(09)	1.100(09)	1.10(09)	1.187(+00)	1.140(+00)	1.140(+00)	1.17(+00)
10–28	1076.114	1.288(08)	1.137(08)	1.13(08)	1.342(−01)	1.179(−01)	1.174(−01)	1.18(−01)
3–29	135.238	5.172(08)	7.112(08)	7.11(08)	5.673(−03)	7.758(−03)	7.762(−03)	
4–29	611.374	2.805(07)	5.525(05)	5.48(05)	6.287(−03)	1.326(−04)	1.327(−04)	
5–29	627.211	2.072(07)	1.148(05)	1.09(05)	4.888(−03)	2.936(−05)	2.818(−05)	
6–29	629.281	2.656(05)	1.930(07)	1.92(07)	6.306(−05)	4.820(−03)	4.841(−03)	
7–29	681.173	1.678(09)	1.402(09)	1.38(09)	4.670(−01)	4.104(−01)	4.083(−01)	4.32(−01)
8–29	682.880	3.009(08)	2.957(08)	2.92(08)	8.415(−02)	9.122(−02)	9.078(−02)	9.61(−02)
9–29	910.722	1.294(09)	1.235(09)	1.23(09)	6.436(−01)	6.498(−01)	6.486(−01)	
10–29	914.081	1.412(08)	5.801(07)	5.69(07)	7.075(−02)	3.054(−02)	3.013(−02)	
3–30	135.230	5.478(08)	8.058(08)	8.06(08)	3.004(−03)	4.368(−03)	4.355(−03)	

Table 3 – *continued*

Transition	λ (Å)	$A_{ki}(s^{-1})$ present	FF	NIST	gf present	FF	NIST	CT
5–30	627.022	7.195(07)	3.778(06)	3.77(06)	8.482(−03)	4.686(−04)	4.720(−04)	
6–30	629.090	1.571(05)	4.630(06)	4.61(06)	1.864(−05)	5.608(−04)	5.636(−04)	
7–30	680.950	6.378(08)	4.582(08)	4.52(08)	8.868(−02)	6.496(−02)	6.411(−02)	6.83(−02)
8–30	682.655	1.200(09)	1.070(09)	1.06(09)	1.677(−01)	1.596(−01)	1.588(−01)	1.68(−01)
10–30	913.679	1.459(09)	1.448(09)	1.44(09)	3.653(−01)	3.649(−01)	3.647(−01)	3.73(−01)
3–31	130.708	8.779(08)	6.247(08)		8.995(−03)	6.224(−03)		
4–31	528.555	4.887(06)	1.410(05)		8.188(−04)	2.283(−05)		
5–31	540.350	3.953(06)	1.024(04)		6.922(−04)	1.745(−06)		
6–31	541.886	6.974(06)	2.069(06)		1.228(−03)	3.461(−04)		
7–31	579.929	2.418(08)	1.207(08)		4.877(−02)	2.297(−02)		
8–31	581.166	6.960(07)	2.686(07)		1.410(−02)	5.334(−03)		
9–31	738.377	1.559(05)	2.646(06)		5.098(−05)	7.962(−04)		
10–31	740.583	2.238(04)	1.572(06)		7.363(−06)	4.732(−04)		
3–32	130.562	8.400(08)	5.510(08)		4.293(−03)	2.744(−03)		
5–32	537.865	8.805(06)	6.903(05)		7.638(−04)	5.880(−05)		
6–32	539.386	1.317(03)	7.534(05)		1.149(−07)	6.296(−05)		
7–32	577.068	8.320(07)	7.216(07)		8.308(−03)	6.860(−03)		
8–32	578.292	1.931(08)	1.451(08)		1.937(−02)	1.438(−02)		
10–32	735.923	5.602(06)	1.894(06)		9.097(−04)	2.847(−04)		
1–34	85.232	8.382(06)	2.275(07)	2.30(07)	5.477(−05)	1.464(−04)	1.482(−04)	
1–35	85.224	9.086(05)	1.456(08)	1.45(08)	3.958(−06)	6.244(−04)	6.237(−04)	
2–35	85.431	6.482(07)	3.464(07)	3.50(07)	2.837(−04)	1.498(−04)	1.517(−04)	
1–36	85.181	8.300(07)	8.691(07)	8.61(07)	1.806(−04)	1.861(−04)	1.845(−04)	
2–36	85.387	1.621(08)	2.003(08)	1.99(08)	3.545(−04)	4.328(−04)	4.295(−04)	
1–38	84.422	8.666(07)	1.172(09)	1.18(09)	3.704(−04)	4.921(−03)	4.954(−03)	1.03(−01)
2–38	84.625	4.078(08)	2.408(09)	2.44(09)	1.751(−03)	1.020(−02)	1.035(−02)	1.96(−02)
1–41	84.133	8.295(08)	1.409(09)		1.761(−03)	2.958(−03)		
2–41	84.334	5.368(08)	1.743(07)		1.145(−03)	3.690(−05)		
1–42	84.066	4.006(08)	2.740(09)		1.698(−03)	1.148(−02)		
2–42	84.267	3.639(07)	5.164(08)		1.550(−04)	2.182(−03)		3.00(−04)
1–43	83.927	1.359(08)	3.789(08)		8.612(−04)	2.374(−03)		1.46(−02)
1–45	83.974	1.817(10)	2.211(10)		1.153(−01)	1.386(−01)		
1–46	83.742	3.143(10)	2.980(10)	2.99(10)	6.608(−02)	6.196(−02)	6.194(−02)	5.95(−02)
2–46	83.942	5.476(10)	4.368(10)	4.36(10)	1.157(−01)	9.156(−02)	9.141(−02)	8.40(−02)
1–47	83.546	6.063(10)	1.686(10)	1.77(10)	2.538(−01)	6.960(−02)	7.227(-02)	3.09(−01)
2–47	83.745	2.522(10)	9.938(10)	9.74(10)	1.061(−01)	4.138(−01)	4.064(−01)	4.00(−04)
1–48	83.678	4.790(10)	9.699(10)	9.60(10)	2.012(−01)	4.028(−01)	3.990(−01)	7.03(−02)
2–48	83.877	1.934(11)	9.296(10)	9.47(10)	8.162(−01)	3.894(−01)	3.981(−01)	8.26(−01)
1–49	83.595	2.281(11)	2.341(11)	2.34(11)	1.434(+00)	1.545(+00)	1.452(+00)	1.27(+00)
1–52	81.031	3.016(11)	2.850(11)	2.76(11)	5.939(−01)	5.556(−01)	5.395(−01)	6.00(−01)
2–52	81.218	7.742(10)	7.643(10)	8.45(10)	1.531(−01)	1.502(−01)	1.663(−01)	2.13(−01)
1–53	80.984	3.209(11)	2.749(11)	2.74(11)	1.262(+00)	1.068(+00)	1.069(+00)	1.33(+00)
2–53	81.171	3.233(10)	5.658(10)	5.67(10)	1.278(−01)	2.218(−01)	2.218(−01)	2.91(−01)
1–54	80.914	6.868(10)	6.732(10)	6.85(10)	1.348(−01)	1.306(−01)	1.333(−01)	2.11(−01)
2–54	81.100	2.860(11)	2.804(11)	2.78(11)	5.640(−01)	5.484(−01)	5.457(−01)	6.27(−01)
1–56	80.844	3.445(10)	6.766(10)		2.025(−01)	3.939(−01)		7.83(−02)
1–57	80.800	1.848(11)	1.335(11)	1.31(11)	1.085(+00)	7.764(−01)	7.603(−01)	1.59(+00)
1–58	80.755	1.352(10)	3.492(10)	3.50(10)	5.289(−02)	1.351(−01)	1.355(−01)	1.97(−01)
2–58	80.941	1.969(11)	1.891(11)	1.89(11)	7.735(−01)	7.380(−01)	7.362(−01)	1.01(+00)
1–59	78.069	8.919(09)	7.731(09)	7.74(09)	3.260(−02)	2.776(−02)	2.779(−02)	
2–59	78.242	4.642(10)	5.577(10)	5.57(10)	1.704(−01)	2.018(−01)	2.018(−01)	2.72(−01)
1–60	78.025	4.737(10)	5.054(10)	5.05(10)	2.594(−01)	2.723(−01)	2.722(−01)	3.75(−01)
1–61	76.060	2.957(07)			1.539(−04)			
1–62	75.899	3.236(09)			5.589(−03)			
2–62	76.063	6.405(09)			1.111(−02)			
1–63	75.797	1.243(09)			4.281(−03)			1.14(−02)
2–63	75.961	2.661(08)			9.209(−04)			
1–64	75.676	2.243(10)		1.24(10)	7.702(−02)		4.197(−02)	4.21(−02)
2–64	75.839	4.741(09)		2.11(09)	1.635(−02)		7.194(−03)	7.20(−03)
1–65	75.583	5.689(09)			9.746(−03)			
2–65	75.746	1.202(10)			2.069(−02)			
4–66	278.937	1.029(10)			7.204(−01)			
6–66	282.606	2.931(09)			2.106(−01)			

Table 3 – *continued*

Transition	λ (Å)	$A_{ki}(s^{-1})$			gf			
		present	FF	NIST	present	FF	NIST	CT
7–66	292.617	2.511(07)			1.934(−03)			
9–66	328.147	5.179(07)			5.016(−03)			
10–66	328.582	6.473(03)			6.287(−07)			
3–67	107.011	3.996(06)			2.744(−05)			
4–67	278.853	6.399(09)			2.984(−01)			
5–67	282.101	3.730(09)			1.780(−01)			
6–67	282.519	1.629(09)			7.796(−02)			
7–67	292.524	1.005(07)			5.159(−04)			
8–67	292.839	4.215(08)			2.168(−02)			
9–67	328.031	2.309(07)			1.490(−03)			
10–67	328.466	2.775(06)			1.796(−04)			
3–68	106.811	3.368(06)			1.152(−05)			
5–68	280.715	1.075(09)			2.539(−02)			
6–68	281.129	1.059(10)			2.511(−01)			
7–68	291.034	3.005(07)			7.632(−04)			
8–68	291.345	6.976(07)			1.776(−03)			
10–68	326.587	8.116(06)			2.596(−04)			
4–69	273.806	3.264(09)			2.935(−01)			
9–69	321.069	7.827(06)			9.678(−04)			
3–70	105.978	6.730(03)			2.266(−08)			
5–70	275.031	3.121(09)			7.079(−02)			
6–70	275.428	3.863(02)			8.788(−09)			
7–70	284.929	8.093(04)			1.970(−06)			
8–70	285.227	1.165(08)			2.841(−03)			
10–70	318.919	1.142(04)			3.482(−07)			
3–71	105.843	1.511(06)			1.011(−05)			
4–71	271.056	9.192(06)			4.050(−04)			
5–71	274.125	1.417(09)			6.385(−02)			
6–71	274.519	1.151(09)			5.201(−02)			
7–71	283.956	3.861(04)			1.867(−06)			
8–71	284.252	2.438(08)			1.181(−02)			
9–71	317.295	4.312(06)			2.603(−04)			
10–71	317.701	6.615(04)			4.004(−06)			
4–72	270.433	5.068(07)			3.334(−03)			
6–72	273.880	1.299(09)			8.765(−02)			
7–72	283.272	2.124(09)			1.533(−01)			
9–72	316.441	3.720(04)			3.351(−06)			
10–72	316.845	3.494(05)			3.155(−05)			
4–73	271.104	2.072(08)			1.370(−02)			
6–73	274.569	1.876(09)			1.272(−01)			
7–73	284.009	8.893(08)			6.453(−02)			
9–73	317.361	2.303(06)			2.086(−04)			
10–73	317.768	6.699(06)			6.085(−04)			
3–74	105.742	2.059(05)			1.381(−06)			
4–74	270.396	1.558(08)			6.832(−03)			
5–74	273.449	5.931(08)			2.660(−02)			
6–74	273.842	6.104(05)			2.745(−05)			
7–74	283.232	3.949(08)			1.900(−02)			
8–74	283.526	2.129(09)			1.026(−01)			
9–74	316.390	1.947(06)			1.169(−04)			
10–74	316.795	1.613(06)			9.709(−05)			
3–75	105.683	1.462(07)			4.896(−05)			
5–75	273.056	1.449(06)			3.239(−05)			
6–75	273.447	1.060(07)			2.376(−04)			
7–75	282.809	2.598(09)			6.230(−02)			
8–75	283.103	5.264(07)			1.265(−03)			
10–75	316.266	4.386(08)			1.315(−02)			
3–76	105.361	2.021(06)			1.345(−05)			
4–76	267.917	3.085(08)			1.328(−02)			
5–76	270.915	1.073(09)			4.722(−02)			
6–76	271.300	1.127(09)			4.973(−02)			
7–76	280.513	1.603(07)			7.565(−04)			
8–76	280.802	3.923(07)			1.855(−03)			

Table 3 – *continued*

Transition	λ (Å)	$A_{ki}(s^{-1})$ present	FF	NIST	gf present	FF	NIST	CT
9–76	313.002	1.264(06)			7.425(−05)			
10–76	313.398	1.091(06)			6.425(−05)			
3–77	104.974	4.741(07)			3.133(−04)			
4–77	265.429	3.542(06)			1.497(−04)			
5–77	268.371	6.593(07)			2.848(−03)			
6–77	268.750	7.602(06)			3.293(−04)			
7–77	277.787	1.359(09)			6.288(−02)			
8–77	278.07	1.709(08)			7.925(−03)			
9–77	309.612	1.217(09)			6.997(−02)			
10–77	309.999	1.274(08)			7.344(−03)			
3–78	104.935	3.845(07)			1.270(−04)			
5–78	268.119	1.251(08)			2.696(−03)			
6–78	268.497	1.917(07)			4.144(−04)			
7–78	277.517	1.251(06)			2.888(−05)			
8–78	277.800	1.619(09)			3.747(−02)			
10–78	309.663	8.910(08)			2.562(−02)			
1–79	73.253	9.110(09)		8.24(09)	4.398(−02)		3.935(−02)	3.94(−02)
1–80	73.232	1.305(09)			4.198(−03)			
2–80	73.385	7.299(09)			2.357(−02)			
1–82	72.246	2.920(08)			1.371(−03)			
1–83	72.222	1.216(02)			3.802(−10)			
2–83	72.371	2.423(08)			7.611(−04)			
1–84	72.175	5.005(08)			7.818(−04)			
2–84	72.323	9.647(08)			1.513(−03)			
1–87	71.976	2.262(10)			1.054(−01)			1.89(−01)
1–88	71.976	1.382(08)			4.293(−04)			
2–88	72.124	6.586(08)			2.055(−03)			1.03(−01)
1–89	71.910	2.267(09)			3.515(−03)			
2–89	72.057	3.055(09)			4.756(−03)			
1–90	71.845	1.208(09)			3.740(−03)			2.35(−02)
2–90	71.991	2.033(07)			6.318(−05)			2.00(−04)
1–91	71.742	1.462(09)			6.769(−03)			1.96(−02)
1–92	71.793	1.906(10)			8.839(−02)			
1–94	71.761	2.760(10)		2.19(10)	4.261(−02)		3.341(−02)	3.34(−02)
2–94	71.907	5.142(10)		3.56(10)	7.972(−02)		5.457(−02)	5.47(−02)
1–95	71.761	2.760(10)		7.20(10)	4.261(−02)			
2–95	71.907	5.142(10)		3.26(07)	7.972(−02)		1.000(−04)	1.00(−04)

X-ray laser research. Our transition probabilities are compared with NIST values and multiconfiguration Hartree–Fock (MCHF) results of Froese Fischer & Tachiev (2004), who use the observed energies for the calculation of transition probabilities. The agreement is by less than 30 per cent for 70 per cent of strong transitions ($A > 10^8$ s^{-1}) of NIST compilation. The agreement is much less for weak ones. For weighted oscillator strengths, comparison is made also with Coutinho & Trigueiros (1999) results obtained using multiconfiguration Hartree–Fock relativistic (HFR) approach. In their work the adjusted energy levels were used to optimize the electrostatic parameters, these optimized parameters were used again to calculate the gf values. In general, our oscillator strengths are in good agreement with the other works except for a few transitions as for example 2–5, 1–6, 2–6, 2–38 for which we observe large disagreement. For the transitions 1–47, 2–48, 2–42 our oscillator strengths agree better with Coutinho & Trigueiros results. On the other hand, for the transitions 2–47, 1–48, 1–56 the agreement with Froese-Fischer & Tachiev values is better. For the transitions 3–15, 1–38 all three methods give different results. The inclusion of a larger number of configurations has an important effect on wavefunctions and *A* values. TEC of the $2s2p^6\ ^2S_{1/2}$ level improve slightly our results. For example for the 2–3 transition our *A* value was 1.022E+10 s^{-1} and became 8.840E+09 s^{-1}, NIST one is 8.46E+09 s^{-1}. The correction of quartet terms do not improve the results.

By combining the SUPERSTRUCTURE code for calculating energy levels and oscillator strengths and the code for the Stark broadening calculations, we calculated Stark broadening parameters. Calculated Stark broadening widths [full width at half-maximum (FWHM)] and shifts for a perturber densities of 10^{17} cm^{-3} and temperatures from 50 000 up to 800 000 K are shown in Table 4 for electron-, proton- and singly ionized helium-impact broadening. Such temperatures are of interest for the modelling and analysis of X-ray spectra, such as the spectra obtained by *Chandra*, modelling of some hot star atmospheres (e.g. DO white dwarf and PG 1195), subphotospheric layers, soft X-ray lasers and laser produced plasmas. Higher temperatures are of interest for fusion plasma as well as for stellar interiors.

We also specify a parameter *C* (Dimitrijević & Sahal-Bréchot 1984), which gives an estimate for the maximal perturber density for which the line may be treated as isolated, when it is divided by the corresponding FWHM. For each value given in Table 4 the collision volume *V* multiplied by the perturber density *N* is much less than one and the impact approximation is valid (Sahal-Bréchot 1969a,b).

Table 4. This table gives electron-, proton- and singly charged helium-impact broadening parameters for Si VI lines calculated using SUPERSTRUCTURE oscillator strength, for a perturber density of 10^{17} cm^{-3} and temperature of 50 000 to 800 000 K. Transitions, averaged wavelength for the multiplet (in Å) and parameter C are also given. This parameter when divided with the corresponding Stark width gives an estimate for the maximal perturber density for which the line may be treated as isolated. w_e: electron-impact full Stark width at half-maximum; d_e: electron-impact Stark shift; $w_H{}^+$: proton-impact full Stark width at half-maximum; $d_H{}^+$: proton-impact Stark shift; $w_{He}{}^+$: singly charged helium-impact full Stark width at half-maximum; $d_{He}{}^+$: singly charged helium-impact Stark shift; w_{MSE}: electron-impact full Stark width at half-maximum calculated by Dimitrijević (1993) using modified semi-empirical formula (Dimitrijević & Konjević 1980).

Transition	T (K)	w_e	d_e	w_H^+	d_H^+	w_{He}^+	d_{He}^+	w_{MSE}
Si VI 3S-3P	50000	0.750E-02	−0.577E-04	0.360E-04	−0.260E-04	0.687E-04	−0.500E-04	0.415E-02
1226.7 Å	100000	0.532E-02	−0.739E-04	0.897E-04	−0.516E-04	0.173E-03	−0.103E-03	0.294E-02
$C = 0.11$E+21	200000	0.387E-02	−0.784E-04	0.177E-03	−0.920E-04	0.344E-03	−0.185E-03	0.212E-02
	400000	0.291E-02	−0.100E-03	0.269E-03	−0.139E-03	0.529E-03	−0.280E-03	0.169E-02
	800000	0.227E-02	−0.888E-04	0.347E-03	−0.189E-03	0.693E-03	−0.384E-03	0.147E-02
Si VI 3S-3P	50000	0.681E-02	−0.660E-04	0.346E-04	−0.294E-04	0.660E-04	−0.566E-04	0.375E-02
1187.2 Å	100000	0.486E-02	−0.841E-04	0.866E-04	−0.582E-04	0.167E-03	−0.116E-03	0.265E-02
$C = 0.67$E+20	200000	0.354E-02	−0.890E-04	0.171E-03	−0.102E-03	0.335E-03	−0.205E-03	0.191E-02
	400000	0.267E-02	−0.109E-03	0.262E-03	−0.150E-03	0.517E-03	−0.304E-03	0.152E-02
	800000	0.208E-02	−0.993E-04	0.340E-03	−0.203E-03	0.678E-03	−0.412E-03	0.132E-02
Si VI 3S′-3P′	50000	0.716E-02	−0.644E-04	0.471E-04	−0.212E-04	0.899E-04	−0.409E-04	0.389E-02
1228.8 Å	100000	0.509E-02	−0.599E-04	0.113E-03	−0.424E-04	0.219E-03	−0.842E-04	0.275E-02
$C = 0.72$E+20	200000	0.370E-02	−0.615E-04	0.213E-03	−0.771E-04	0.416E-03	−0.155E-03	0.198E-02
	400000	0.278E-02	−0.770E-04	0.314E-03	−0.119E-03	0.618E-03	−0.241E-03	0.158E-02
	800000	0.216E-02	−0.691E-04	0.389E-03	−0.164E-03	0.774E-03	−0.331E-03	0.137E-02
Si VI 3S′-3P′	50000	0.572E-02	−0.376E-04	0.399E-04	−0.131E-04	0.762E-04	−0.252E-04	0.312E-02
1087.4 Å	100000	0.408E-02	−0.358E-04	0.948E-04	−0.263E-04	0.183E-03	−0.521E-04	0.220E-02
$C = 0.56$E+20	200000	0.297E-02	−0.371E-04	0.176E-03	−0.487E-04	0.344E-03	−0.978E-04	0.158E-02
	400000	0.223E-02	−0.460E-04	0.256E-03	−0.774E-04	0.505E-03	−0.156E-03	0.126E-02
	800000	0.174E-02	−0.413E-04	0.313E-03	−0.107E-03	0.623E-03	−0.216E-03	0.109E-02
Si VI 3S-3P	50000	0.842E-02	−0.107E-03	0.361E-04	−0.374E-04	0.690E-04	−0.721E-04	0.436E-02
1314.8 Å	100000	0.598E-02	−0.118E-03	0.927E-04	−0.740E-04	0.179E-03	−0.147E-03	0.309E-02
$C = 0.13$E+21	200000	0.434E-02	−0.116E-03	0.189E-03	−0.129E-03	0.368E-03	−0.260E-03	0.224E-02
	400000	0.326E-02	−0.148E-03	0.295E-03	−0.190E-03	0.582E-03	−0.384E-03	0.180E-02
	800000	0.254E-02	−0.134E-03	0.392E-03	−0.256E-03	0.784E-03	−0.519E-03	0.155E-02
Si VI 3S-3P	50000	0.656E-02	−0.682E-04	0.295E-04	−0.254E-04	0.563E-04	−0.488E-04	0.343E-02
1145.4 Å	100000	0.466E-02	−0.797E-04	0.745E-04	−0.503E-04	0.144E-03	−0.999E-04	0.242E-02
$C = 0.10$E+21	200000	0.338E-02	−0.787E-04	0.149E-03	−0.887E-04	0.290E-03	−0.178E-03	0.175E-02
	400000	0.254E-02	−0.102E-03	0.229E-03	−0.132E-03	0.452E-03	−0.267E-03	0.141E-02
	800000	0.198E-02	−0.909E-04	0.300E-03	−0.179E-03	0.599E-03	−0.364E-03	0.122E-02
Si VI 2P-3S	50000	0.209E-04	−0.851E-06	0.885E-08	0.227E-06	0.169E-07	0.438E-06	0.154E-04
100.2 Å	100000	0.138E-04	0.531E-06	0.665E-07	0.449E-06	0.128E-06	0.891E-06	0.109E-04
$C = 0.73$E+18	200000	0.976E-05	0.815E-06	0.288E-06	0.780E-06	0.571E-06	0.157E-05	0.791E-05
	400000	0.740E-05	0.981E-06	0.709E-06	0.114E-05	0.143E-05	0.231E-05	0.628E-05
	800000	0.577E-05	0.918E-06	0.131E-05	0.153E-05	0.262E-05	0.311E-05	0.541E-05
Si VI 2P-3D	50000	0.267E-04	−0.113E-05	0.147E-06	−0.328E-07	0.280E-06	−0.631E-07	0.194E-04
83.8 Å	100000	0.179E-04	−0.289E-06	0.365E-06	−0.663E-07	0.703E-06	−0.131E-06	0.137E-04
$C = 0.77$E+18	200000	0.130E-04	−0.490E-07	0.715E-06	−0.128E-06	0.139E-05	−0.257E-06	0.969E-05
	400000	0.967E-05	−0.134E-06	0.108E-05	−0.221E-06	0.212E-05	−0.444E-06	0.747E-05
	800000	0.741E-05	−0.802E-07	0.139E-05	−0.321E-06	0.277E-05	−0.647E-06	0.631E-05
Si VI 2P-3D	50000	0.266E-04	−0.116E-05	0.147E-06	−0.165E-07	0.280E-06	−0.318E-07	0.193E-04
83.8 Å	100000	0.174E-04	−0.200E-06	0.364E-06	−0.335E-07	0.701E-06	−0.664E-07	0.137E-04
$C = 0.35$E+18	200000	0.125E-04	0.533E-07	0.712E-06	−0.662E-07	0.139E-05	−0.132E-06	0.967E-05
	400000	0.929E-05	−0.605E-08	0.107E-05	−0.121E-06	0.211E-05	−0.243E-06	0.748E-05
	800000	0.709E-05	0.492E-07	0.139E-05	−0.188E-06	0.275E-05	−0.380E-06	0.631E-05
Si VI 2P-3S′	50000	0.202E-04	−0.613E-06	0.106E-07	0.247E-06	0.202E-07	0.475E-06	0.139E-04
96.7 Å	100000	0.135E-04	0.635E-06	0.787E-07	0.484E-06	0.152E-06	0.961E-06	0.984E-05
$C = 0.45$E+18	200000	0.958E-05	0.879E-06	0.317E-06	0.831E-06	0.629E-06	0.167E-05	0.712E-05
	400000	0.728E-05	0.105E-05	0.752E-06	0.121E-05	0.151E-05	0.244E-05	0.564E-05
	800000	0.570E-05	0.993E-06	0.139E-05	0.158E-05	0.278E-05	0.321E-05	0.486E-05

Table 4 – *continued*

Transition	T (K)	w_e	d_e	w_H^+	d_H^+	w_{He}^+	d_{He}^+	w_{MSE}
Si VI 2P-3D′	50000	0.277E-04	−0.116E-05	0.212E-06	−0.144E-07	0.405E-06	−0.277E-07	0.178E-04
81.2 Å	100000	0.176E-04	−0.202E-06	0.504E-06	−0.291E-07	0.972E-06	−0.578E-07	0.126E-04
$C = 0.58$E+18	200000	0.127E-04	0.363E-07	0.935E-06	−0.577E-07	0.183E-05	−0.115E-06	0.902E-05
	400000	0.937E-05	−0.255E-07	0.136E-05	−0.106E-06	0.268E-05	−0.213E-06	0.710E-05
	800000	0.716E-05	0.289E-07	0.166E-05	−0.166E-06	0.330E-05	−0.336E-06	0.612E-05
Si VI 2P-3D′	50000	0.273E-04	−0.119E-05	0.214E-06	−0.231E-07	0.408E-06	−0.445E-07	0.179E-04
81.2 Å	100000	0.174E-04	−0.260E-06	0.508E-06	−0.468E-07	0.981E-06	−0.928E-07	0.126E-04
$C = 0.59$E+18	200000	0.125E-04	−0.196E-07	0.942E-06	−0.916E-07	0.184E-05	−0.183E-06	0.904E-05
	400000	0.923E-05	−0.845E-07	0.137E-05	−0.161E-06	0.270E-05	−0.324E-06	0.710E-05
	800000	0.704E-05	−0.422E-07	0.167E-05	−0.239E-06	0.332E-05	−0.483E-06	0.610E-05
Si VI 2P-3D′	50000	0.270E-04	−0.107E-05	0.219E-06	−0.148E-07	0.419E-06	−0.285E-07	0.179E-04
81.0 Å	100000	0.175E-04	−0.202E-06	0.520E-06	−0.299E-07	0.100E-05	−0.594E-07	0.127E-04
$C = 0.60$E+18	200000	0.126E-04	0.317E-07	0.960E-06	−0.592E-07	0.187E-05	−0.118E-06	0.905E-05
	400000	0.935E-05	−0.301E-07	0.139E-05	−0.109E-06	0.274E-05	−0.218E-06	0.711E-05
	800000	0.714E-05	0.195E-07	0.169E-05	−0.170E-06	0.336E-05	−0.343E-06	0.609E-05
Si VI 3S′-3P′	50000	0.439E-02	−0.460E-04	0.328E-04	−0.168E-04	0.626E-04	−0.324E-04	0.241E-02
918.8 Å	100000	0.314E-02	−0.597E-04	0.773E-04	−0.333E-04	0.149E-03	−0.662E-04	0.171E-02
$C = 0.40$E+20	200000	0.229E-02	−0.606E-04	0.142E-03	−0.586E-04	0.278E-03	−0.118E-03	0.123E-02
	400000	0.173E-02	−0.737E-04	0.206E-03	−0.869E-04	0.407E-03	−0.176E-03	0.976E-03
	800000	0.135E-02	−0.698E-04	0.252E-03	−0.118E-03	0.500E-03	−0.239E-03	0.845E-03
Si VI 3S-3P	50000	0.510E-02	−0.414E-04	0.244E-04	−0.159E-04	0.465E-04	−0.306E-04	0.263E-02
995.6 Å	100000	0.362E-02	−0.514E-04	0.604E-04	−0.317E-04	0.116E-03	−0.630E-04	0.186E-02
$C = 0.75$E+20	200000	0.263E-02	−0.509E-04	0.118E-03	−0.569E-04	0.230E-03	−0.114E-03	0.134E-02
	400000	0.198E-02	−0.655E-04	0.179E-03	−0.864E-04	0.352E-03	−0.175E-03	0.107E-02
	800000	0.155E-02	−0.589E-04	0.230E-03	−0.118E-03	0.458E-03	−0.240E-03	0.923E-03

When the impact approximation is not valid, the ion broadening contribution may be estimated by using the quasi-static approach (Griem 1974; Sahal-Bréchot 1991; Ben Nessib, Ben Lakhdar & Sahal-Bréchot 1996).

Unfortunately, no experimental data are yet available for the Stark broadening parameters so that the comparison is made only with Dimitrijević's (1993) results obtained using the modified semi-empirical formula (Dimitrijević & Konjević 1980). All our values are greater than Dimitrijević's ones. The ratio w_e/w_{MSE} shows in average an agreement within 56 per cent. Low disagreements are usually found for resonance lines, for example for the spectral line $2p^5\ ^2P^\circ$-$2p^4(^3P)3s\ ^2P$ ($\lambda = 100$, 2 Å) the ratio w_e/w_{MSE} is only 1.06 for $T = 800\,000$ K.

4 STARK BROADENING EFFECT IN WHITE DWARF ATMOSPHERES

White dwarfs are separated in two distinct spectroscopic sequences, the DA and non-DA white dwarfs. The former ones display a pure hydrogen (optical) spectrum. The second, helium-rich sequence comprise DO ($T_{eff} > 45\,000$ K), DB ($11\,000 < T_{eff} < 30\,000$ K) and DC ($T_{eff} < 11\,000$ K) white dwarfs. At the highest effective temperatures the DOs are connected to the helium, carbon and oxygen-rich PG 1159.

Silicon, in various ionization stages, is present in the DO white dwarf atmospheres (Werner et al. 1995). We used our results for Stark widths to examine the importance of electron-impact broadening in atmospheres of DO white dwarfs for a trace element like Si VI. Model atmospheres were taken from Wesemael (1981).

In hot star atmospheres, besides electron-impact broadening (Stark broadening), the important broadening mechanism is a Doppler (thermal) one as well as the broadening due to the turbulence and stellar rotation. Other types of spectral line broadening, such as van der Waals, resonance and natural broadening, are usually negligible. For a Doppler-broadened spectral lines, the intensity distribution is not Lorentzian as for electron-impact broadening but Gaussian, whose full half-width of the spectral lines may be determined by the equation (see e.g. Konjević 1999)

$$w_D\,[\text{Å}] = 7.16 \times 10^{-7} \lambda\,[\text{Å}] \sqrt{\frac{T\,[\text{K}]}{M_{Si}}}, \quad (6)$$

where atomic weight for silicon is $M_{Si} = 28.1$ au.

The importance of Stark broadening in stellar atmospheres is illustrated in Figs 1–4. In Fig. 1 Stark (FWHM) and Doppler widths for Si VI $2p^4(^3P)3s\ ^2P$-$2p^4(^3P)3p\ ^2D^\circ$ ($\lambda = 1226$, 7 Å) spectral line as a function of atmospheric layer temperatures are shown. Stark widths are shown for six atmospheric models with effective temperature $T_{eff} = 50\,000$–$100\,000$ K and logarithm of surface gravity $\log g = 8$. We can see in Fig. 1 that Stark broadening is more important than Doppler broadening for deeper atmospheric layers for all effective temperatures. For white dwarf with effective temperature $T_{eff} = 50\,000$ K, Stark and Doppler widths are equal for temperature layer $T \approx 70\,000$ K, and for white dwarf with effective temperature $T_{eff} = 100\,000$ K, Stark and Doppler are equal for temperature layer $T \approx 125\,000$ K. One should take into account, however, that even when the Doppler width is larger than Stark width, due to different behaviour of Gaussian and Lorentzian distributions, Stark broadening may be important in line wings. In Fig. 2 we present Stark (FWHM) and Doppler widths for Si VI ($\lambda = 1226$, 7 Å) spectral line

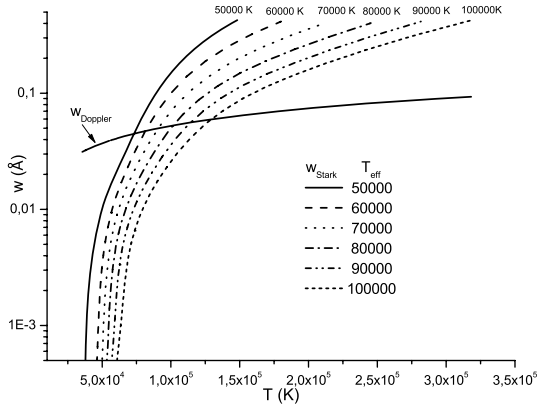

Figure 1. Stark and Doppler widths for Si VI $2p^4(^3P)3s\ ^2P\text{-}2p^4(^3P)3p\ ^2D^\circ$ ($\lambda = 1226,7$ Å) spectral line as a function of atmospheric layer temperatures. Stark widths are shown for six atmospheric models with effective temperature $T_{\rm eff} = 50\,000$–$100\,000$ K and $\log g = 8$.

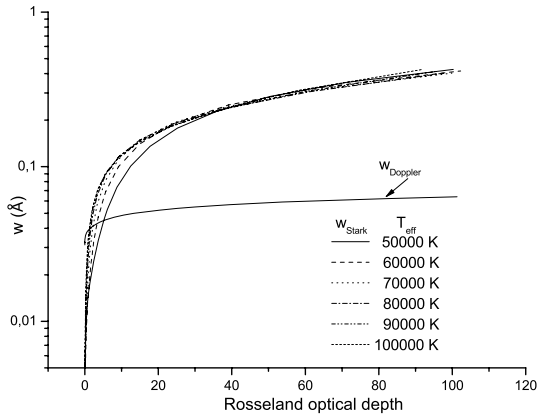

Figure 2. Stark and Doppler widths for Si VI $2p^4(^3P)3s\ ^2P\text{-}2p^4(^3P)3p\ ^2D^\circ$ ($\lambda = 1226,7$ Å) spectral line as a function of Rosseland optical depth. Stark widths are shown for six atmospheric models with effective temperature $T_{\rm eff} = 50\,000$–$100\,000$ K and $\log g = 8$.

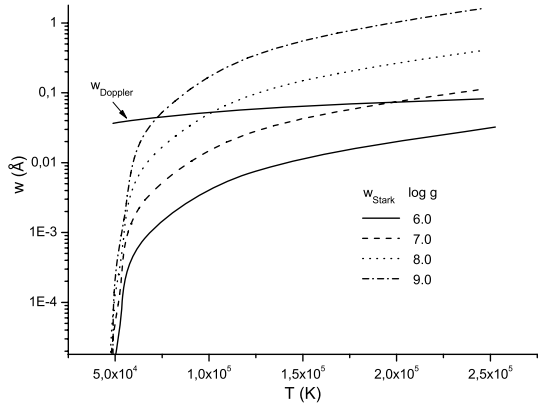

Figure 3. Stark and Doppler widths for Si VI $2p^4(^3P)3s\ ^2P\text{-}2p^4(^3P)3p\ ^2D^\circ$ ($\lambda = 1226,7$ Å) spectral line as a function of atmospheric layer temperatures. Stark widths are shown for four values of model gravity $\log g = 6$–9, $T_{\rm eff} = 80\,000$ K.

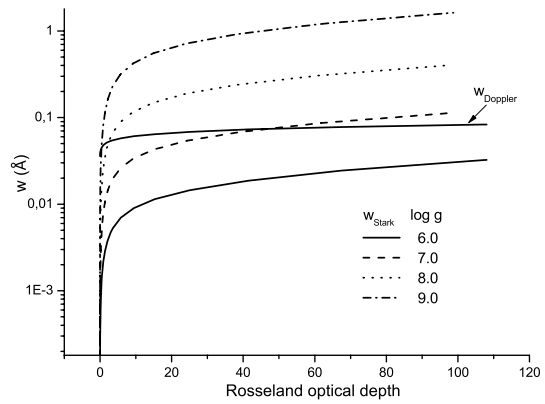

Figure 4. Stark and Doppler widths for Si VI $2p^4(^3P)3s\ ^2P\text{-}2p^4(^3P)3p\ ^2D^\circ$ ($\lambda = 1226,7$ Å) spectral line as a function of Rosseland optical depth. Stark widths are shown for four values of model gravity $\log g = 6$–9, $T_{\rm eff} = 80\,000$ K.

as a function of Rosseland optical depth for the same atmospheric models as in Fig. 1.

The dependence of Stark and Doppler broadening in atmospheric layer temperature for four values of surface gravity is shown in Fig. 3. Atmospheric models used here have effective temperature $T_{\rm eff} = 80\,000$ K. For stellar atmosphere with higher values of surface gravity ($\log g = 8$–9), Stark broadening is significantly larger than Doppler one. For stellar atmosphere with surface gravity $\log g = 7$, Stark widths are comparable to Doppler widths only for deeper hot atmospheric layer. For stellar atmospheres with $\log g = 6$, Doppler broadening is dominant for all atmospheric layers.

5 CONCLUSIONS

In present work we have calculated *ab initio* energy levels for the eight lowest configurations of Si VI. We have also calculated transition probabilities and oscillator strengths for 288 transitions. These data are useful for interpretation of laboratory and astrophysical spectra, since the reliability of the predicted emergent spectra and the derived spectral diagnoses is directly influenced by the quality of radiative data. The method used here is semirelativistic one, the relativistic corrections are included by using the Breit–Pauli Hamiltonian as perturbation to the non-relativistic Hamiltonian. To make fully relativistic calculation, the GRASP code (Dyall et al. 1989) can be used. One should note also that Martin & Wiese (1976) investigated the influence of relativistic effects on the oscillator strength values for the lithium isoelectronic sequences and found that the influence is not important on investigated *f* values for the ionization degrees investigated in our work. We have reported results of Stark broadening parameter calculations for 15 spectral lines of Si VI. For the simple spectrum, the Stark broadening parameters of different lines are nearly the same within a multiplet (Wiese & Konjević 1992). Consequently, we have used the averaged atomic data for a multiplet as a whole and calculate the corresponding Stark widths and shifts. We see that using the SUPERSTRUCTURE code one obtains a set of energy levels and oscillator strengths, enabling a calculation of Stark broadening parameters when other theoretical and experimental data do not exist. The Stark broadening parameters obtained here, contribute to the creation of a set of such data for as large as possible number of spectral lines, of significance for a number of problems in astrophysical, laboratory and technological plasma research. Our analysis of the influence of Stark broadening on Si VI

($\lambda = 1226,7$ Å) spectral line for stellar plasma conditions demonstrates the importance of this broadening mechanism for hot, high gravity star atmospheres, as for example DO white dwarfs.

ACKNOWLEDGMENTS

We would like to thank C. J. Zeippen for providing his version of SUPERSTRUCTURE code. This work is a part of the projects 146001 'Influence of Collisional Processes on Astrophysical Plasma Line Shapes' and 146002 'Astrophysical Spectroscopy of Extragalactic Objects' supported by the Ministry of Science of Serbia.

REFERENCES

Bates D. R., Damgaard A., 1949, Philos. Trans. R. Soc. Lond. A, 242, 101
Ben Nessib N., Ben Lakhdar Z., Sahal-Bréchot S., 1996, Phys. Scr., 54, 608
Ben Nessib N., Dimitrijević M. S., Sahal-Bréchot S., 2004, A&A, 423, 397
Casassus S., Roche P. F., Barlow M. J., 2000, MNRAS, 314, 657
Coutinho L. H., Trigueiros A. G., 1999, ApJS, 121, 591
Dimitrijević M. S., 1993, A&AS, 100, 237
Dimitrijević M. S., Konjević N., 1980, J. Quant. Spectrosc. Radiat. Transfer, 24, 451
Dimitrijević M. S., Sahal-Bréchot S., 1984, J. Quant. Spectrosc. Radiat. Transfer, 31, 301
Dimitrijević M. S., Sahal-Bréchot S., 1996, Phys. Scr., 54, 50
Dimitrijević M. S., Sahal-Bréchot S., Bommier V., 1991, A&AS, 89, 581
Dimitrijević M. S., Ryabchikova T., Simić Z., Popović L.Č., Dačić M., 2007, A&A, 469, 681
Dyall K. G., Grant I. P., Johnson C. T., Parpia F. A., Plummer E. P., 1989, Comput. Phys. Commun., 55, 424
Eissner W., Jones M., Nussbaumer H., 1974, Comput. Phys. Commun., 8, 270
Fleurier C., Sahal-Bréchot S., Chapelle J., 1977, J. Quant. Spectrosc. Radiat. Transfer, 17, 595
Froese Fischer C., Tachiev G., 2004, At. Data Nucl. Data Tables, 87, 1
Griem H. R., 1974, Spectral Line Broadening by Plasmas. McGraw-Hill, New York
Hamdi R., Ben Nessib N., Dimitrijević M. S., Sahal-Bréchot S., 2007, ApJS, 170, 243
Konjević N., 1999, Phys. Rep., 316, 339
Martin G. A., Wiese W. L., 1976, J. Phys. Chem. Ref. Data, 5, 537
Nussbaumer H., Storey J. P., 1978, A&A, 64, 139
Popović L.Č., Simić S., Milovanović N., Dimitrijević M. S., 2001, ApJS, 135, 109
Sahal-Bréchot S., 1969a, A&A, 1, 91
Sahal-Bréchot S., 1969b, A&A, 2, 322
Sahal-Bréchot S., 1974, A&A, 35, 319
Sahal-Bréchot S., 1991, A&A, 245, 322
Savin D. W., 2001, in Ferland G., Savin D. W., eds, ASP Conf. Ser. Vol. 247, Spectroscopic Challenges of Photoionized Plasmas. Astron. Soc. Pac., San Francisco, p. 167
Uzelac N. I., Glenzer S., Konjević N., Hey J. D., Kunze H. J., 1993, Phys. Rev. E, 47, 3623
Werner K., Dreizler S., Wolff B., 1995, A&A, 298, 567
Wesemael F., 1981, ApJS, 45, 177
Wiese W. L., Konjević N., 1992, J. Quant. Spectrosc. Radiat. Transfer, 47, 185
Zeippen C. J., Seaton M. J., Morton D. C., 1977, MNRAS, 181, 527

This paper has been typeset from a TEX/LATEX file prepared by the author.

Mon. Not. R. Astron. Soc. **387,** 871–882 (2008) doi:10.1111/j.1365-2966.2008.13284.x

Atomic data and electron-impact broadening effect in DO white dwarf atmospheres: Si VI

R. Hamdi,[1] N. Ben Nessib,[1] N. Milovanović,[2] L. Č. Popović,[2] M. S. Dimitrijević[2]★ and S. Sahal-Bréchot[3]

[1]*Groupe de Recherche en Physique Atomique et Astrophysique, Institut National des Sciences Appliquées et de Technologie, Centre Urbain Nord B. P. No. 676, 1080 Tunis Cedex, Tunisia*
[2]*Astronomical observatory, Volgina 7, 11160 Belgrade 74, Serbia*
[3]*Laboratoire d'Étude du Rayonnement et de la Matière en Astrophysique, UMR CNRS 8112, Observatoire de Paris-Meudon, 92195 Meudon, France*

Accepted 2008 April 3. Received 2008 March 28; in original form 2008 January 28

ABSTRACT

Energy levels, electric dipole transition probabilities and oscillator strengths in five times ionized silicon have been calculated in intermediate coupling. The present calculations were carried out with the general purpose atomic structure program SUPERSTRUCTURE. The relativistic corrections to the non-relativistic Hamiltonian are taken into account through the Breit–Pauli approximation. We have also introduced a semi-empirical correction [term energy corrections (TEC)] for the calculation of the energy levels. These atomic data are used to provide semiclassical electron-, proton- and ionized helium-impact linewidths and shifts for 15 Si VI multiplet. Calculated results have been used to consider the influence of Stark broadening for DO white dwarf atmospheric conditions.

Key words: atomic data – atomic processes – line: formation – stars: atmospheres – white dwarfs.

1 INTRODUCTION

Atomic data such as transition probabilities (*A*) play an important role in the diagnostics and modelling of laboratory plasmas (Griem 1974). Various kinetic processes appearing in plasma modelling need reliable knowledge of *A* values. Further, knowledge of *A* values gives a possibility for determination of coefficients (*B*) which characterize the absorption and stimulated emission. These processes are also important in laser physics. The classification of transitions and determination of energy levels are essential parts of the study of a laboratory spectrum. The lack of available atomic data limits our ability to infer reliably the properties of many cosmic plasmas and, hence, address many of the fundamental issues in astrophysics (Savin 2001).

Accurate Stark broadening parameters are important to obtain a reliable modelization of stellar interiors. The Stark broadening mechanism is also important for the investigation, analysis and modelling of *B*-type, and particularly *A*-type, stellar atmospheres, as well as for white dwarf atmospheres (see e.g. Popović et al. 2001; Dimitrijević et al. 2007).

Silicon, in various ionization stages, is detected in the atmospheres of DO white dwarfs (Werner, Dreizler & Wolff 1995). Si VI lines have been observed as well for example in coronal line regions of planetary nebulae NGC 6302 and 6537 (Casassus, Roche & Barlow 2000).

Uzelac and collaborators (Uzelac et al. 1993) studied plasma broadening of Ne II–Ne VI and F IV–F V experimentally and theoretically, they found that the results of simplified semiclassical (Griem 1974, equation 526) calculations show better agreement at higher ionization stages, while the modified semi-empirical formula (Dimitrijević & Konjević 1980) seems to be better for the low-ionization stages. Unfortunately, due to the lack of atomic data, most of the reported sophisticated semiclassical Stark broadening parameters relate to spectral lines of neutral- and low-ionization stages. In previous papers (Ben Nessib, Dimitrijević & Sahal-Bréchot 2004; Hamdi et al. 2007), we calculated Stark broadening parameters of quadruply ionized silicon and neon using SUPERSTRUCTURE and Bates & Damgaard (1949) method for oscillator strengths and we found that the difference is tolerable.

Si VI ion belongs to the fluorine-like sequence, its ground state configuration is $1s^2 2s^2 2p^5$ with the term $^2P^\circ$. In this work we present fine-structure energy levels, transition probabilities and oscillator strengths for Si VI ion. The atomic structure code SUPERSTRUCTURE was used, which allows for configuration interaction (CI), relativistic effects and semi-empirical term energy corrections (TEC). Calculated energies and oscillator strengths are used to provide Stark broadening parameters due to electron-, proton- and ionized helium impact of Si VI lines. The obtained Stark broadening parameters are used to investigate the influence of Stark broadening mechanism

★E-mail: mdimitrijevic@aob.bg.ac.yu

in hot, high gravity star atmospheres, as for example DO white dwarfs.

2 THE METHOD

In this work, the calculations were carried out with the general purpose atomic structure program SUPERSTRUCTURE (Eissner, Jones & Nussbaumer 1974), as modified by Nussbaumer & Storey (1978). The atomic model used to calculate energies of terms or levels and transition probabilities include 26 configurations: $2s^22p^5$, $2s2p^6$, $2s^22p^43\ell$, $2s^22p^44\ell$, $2s^22p^45\ell$, $2s^22p^46\ell$, $2s2p^53\ell$ and $2p^63\ell$ ($\ell \leqslant n - 1$). CI effects were fully taken into account. The wave functions are of the type

$$\Psi = \sum_i \Phi_i C_i, \tag{1}$$

where the basis functions Φ_i are constructed using one-electron orbitals. The latter are calculated with a scaled Thomas–Fermi statistical model potential or obtained from the Coulomb potential. For each radial orbital $P_{nl}(r)$, the potential can be adjusted using a parameter called λ. In the present case, those *n*- and *l*-dependent scaling parameters λ_{nl} were determined variationally by optimizing the weighted sum of the term energies. The P_{nl} are orthogonalized to each other such that the function P_{n_1l} is orthogonalized to the function P_{n_2l} when $n_2 < n_1$. The values adopted for the λ_{nl} parameters are presented in Table 1. In this approach the Hamiltonian is taken to be in the form

$$H = H_{\rm nr} + H_{\rm BP}, \tag{2}$$

relativistic corrections are included in Breit–Pauli Hamiltonian ($H_{\rm BP}$) as perturbation to the non-relativistic Hamiltonian ($H_{\rm nr}$). $H_{\rm BP}$ contains the one-electron operators for the mass correction, the Darwin contact term, the spin–orbit interaction in the field of the nucleus and the two-electron operators for spin–orbit, spin–other orbit and spin–spin interactions. We also use the so-called TEC introduced by Zeippen, Seaton & Morton (1977), in which the Hamiltonian matrix is empirically adjusted to give the best agreement between experimental energies and the final calculated term energies including the relativistic effects. In practice, the TEC for a given term is simply the difference between the calculated and measured energy of the lowest level in the multiplet.

Stark broadening parameter calculations have been performed within the semiclassical perturbation method (Sahal-Bréchot 1969a,b). A detailed description of this formalism with all the innovations is given in Sahal-Bréchot (1969a,b, 1974, 1991), Fleurier, Sahal-Bréchot & Chapelle (1977), Dimitrijević, Sahal-Bréchot & Bommier (1991) and Dimitrijević & Sahal-Bréchot (1996). The full half-width (w) and shift (d) of an electron-impact broadened spectral line can be expressed as

$$W = N \int v f(v)\,{\rm d}v \left[\sum_{i'\neq i} \sigma_{ii'}(v) + \sum_{f'\neq f} \sigma_{ff'}(v) + \sigma_{\rm el}\right] + W_{\rm R},$$
$$d = N \int v f(v)\,{\rm d}v \int_{R_3}^{R_{\rm D}} 2\pi\rho\,{\rm d}\rho \sin(2\varphi_{\rm p}), \tag{3}$$

where N is the electron density, $f(\upsilon)$ the Maxwellian velocity distribution function for electrons, ρ denotes the impact parameter of the incoming electron, i and f denote the initial and the final atomic energy levels and i' and f' their corresponding perturbing levels, while $W_{\rm R}$ gives the contribution of the Feshbach resonances (Fleurier et al. 1977). The inelastic cross-section $\sigma_{ii'}(\upsilon)$ can be expressed by an integral over the impact parameter of the transition probability $P_{jj'}(\rho, \upsilon)$ as

$$\sum_{j\neq j'} \sigma_{ii'}(\upsilon) = \frac{1}{2}\pi R_1^2 + \int_{R_1}^{R_{\rm D}} 2\pi\rho\,{\rm d}\rho \sum_{j\neq j'} P_{jj'}(\rho, \upsilon),\ j = i,\ f, \tag{4}$$

and the elastic cross-section is given by

$$\sigma_{\rm el} = 2\pi R_2^2 + \int_{R_2}^{R_{\rm D}} 2\pi\rho\,{\rm d}\rho \sin^2\delta,$$
$$\delta = \left(\varphi_{\rm p}^2 + \varphi_{\rm q}^2\right)^{1/2}. \tag{5}$$

The phase shifts $\varphi_{\rm p}$ and $\varphi_{\rm q}$ due, respectively, to the polarization potential (r^{-4}) and to the quadrupolar potential (r^{-3}) are given in section 3 of chapter 2 in Sahal-Bréchot (1969a), and $R_{\rm D}$ is the Debye radius. All the cut-offs R_1, R_2, R_3 are described in section 1 of chapter 3 in Sahal-Bréchot (1969b).

For electrons, hyperbolic paths due to the attractive Coulomb force were used, while for perturbing ions the hyperbolic paths are different since the force is repulsive. The formulae for the ion-impact widths and shifts are analogous to equations (3)–(5), without the resonance contribution to the width.

Table 1. Optimized parameters λ_{nl} adopted for the 26-configuration model calculation. Positive values for Thomas–Fermi–Dirac potential and negative values for Coulomb potential.

n, l	λ_{nl}	*n, l*	λ_{nl}	*n, l*	λ_{nl}	*n, l*	λ_{nl}
1s	1.4653	4s	1.1091	5d	1.1015	6f	−0.6629
2s	1.1844	4p	1.0960	5f	1.1135	6g	−1.0777
2p	1.1389	4d	1.1103	5g	1.0776	6h	−1.3002
3s	1.1078	4f	1.0478	6s	4.8162		
3p	1.0762	5s	1.1580	6p	6.2669		
3d	1.1808	5p	1.0902	6d	5.3865		

3 RESULTS AND DISCUSSION

The calculated *ab initio* energies for Si VI are listed in Table 2 along with experimentally determined energies for a number of levels taken from a National Institute of Standards and Technology (NIST) compilation. The configurations for which we present results are $2s^22p^5$, $2s2p^6$, $2s^22p^43\ell$, $2s^22p^44\ell'$; ℓ = s, p, d and ℓ' = s, p, d. We use the LS coupling scheme to designate excited energy.

Two different models are used for the determination of energy levels, the first contains the nine configurations of the model given in Section 2 and the second contains the totality of the 26 configurations. Both nine-configuration model and more elaborated 26-configuration one give energy levels in good agreement with the NIST values, indeed, our energies are lower than the NIST ones by less than 1 per cent except for the two first excited levels, i.e. $2p^5\ {}^2P^\circ_{1/2}$ and $2s2p^6\ {}^2S_{1/2}$. However, the results obtained by the second model are always more accurate that proves the importance of the CI. Besides, if a term is simply shifted relatively to the ground state, then the difference with observed energy should be essentially constant. In some terms the levels are not always in correct order. For example, the observed order of the levels of $2p^4(^3P)3d^4F$ is (9/2, 7/2, 5/2, 3/2) and the present order is (9/2, 3/2, 5/2, 7/2).

We use the calculated energies and the wavefunctions to calculate oscillator strengths and transition probabilities. With the aim of improving the quality of our wavefunctions, the $2s2p^6\ {}^2S_{1/2}$ level is corrected using TEC procedure (see Section 2). This method cannot

Table 2. Energy levels for Si VI in cm^{-1}. Key: a number assigned to each level; LS: LS term and parity (superscript $^\circ$ designate an odd level); *J*: *J* value of the level; E_{9-conf}: *ab initio* energy levels, calculated with nine-configuration model; $E_{26-conf}$: *ab initio* energy levels, calculated with 26-configuration model; E_{NIST}: NIST values.

Key	Configuration	LS	*J*	E_{9-conf}	$E_{26-conf}$	E_{NIST}
1	$2p^5$	$^2P^\circ$	3/2	0	0	0
2			1/2	2 796	2 839	5 090
3	$2s2p^6$	^2S	1/2	435 632	426 462	406 497
4	$2p^4(^3P)3s$	^4P	5/2	971 851	982 366	990 516
5			1/2	975 520	986 496	995 470
6			3/2	975 969	987 021	993 640
7	$2p^4(^3P)3s$	^2P	3/2	987 370	999 127	1 005 430
8			1/2	987 692	999 494	1 009 118
9	$2p^4(^1D)3s$	^2D	5/2	1 024 374	1 036 129	1 041 416
10			3/2	1 024 884	1 036 533	1 041 472
11	$2p^4(^3P)3p$	$^4P^\circ$	3/2	1 052 168	1 061 210	1 069 854
12			5/2	1 052 404	1 061 401	1 068 813
13			1/2	1 053 583	1 062 874	1 071 129
14	$2p^4(^3P)3p$	$^4D^\circ$	7/2	1 059 089	1 070 621	1 078 935
15			1/2	1 061 265	1 073 242	1 083 003
16			3/2	1 062 447	1 074 609	1 082 215
17			5/2	1 062 788	1 074 942	1 080 700
18	$2p^4(^3P)3p$	$^2D^\circ$	5/2	1 068 139	1 080 203	1 086 796
19			3/2	1 068 477	1 080 547	1 089 547
20	$2p^4$ $(^3P)3p$	$^2P^\circ$	1/2	1 077 264	1 080 958	
21			3/2	1 075 947	1 084 287	1 092 171
22	$2p^4(^1S)3s$	^2S	1/2	1 071 075	1 084 295	1 094 449
23	$2p^4(^3P)3p$	$^4S^\circ$	3/2	1 074 673	1 087 671	1 093 752
24	$2p^4(^3P)3p$	$^2S^\circ$	1/2	1 094 162	1 088 558	
25	$2p^4(^1D)3p$	$^2F^\circ$	5/2	1 106 342	1 118 373	1 123 540
26			7/2	1 106 472	1 118 689	1 124 219
27	$2p^4(^1D)3p$	$^2D^\circ$	3/2	1 116 033	1 128 816	1 134 081
28			5/2	1 116 641	1 129 460	1 134 496
29	$2p^4(^1D)3p$	$^2P^\circ$	3/2	1 140 823	1 145 932	1 147 901
30			1/2	1 140 921	1 145 980	1 150 282
31	$2p^4(^1S)3p$	$^2P^\circ$	3/2	1 182 143	1 171 561	
32			1/2	1 182 942	1 172 417	
33	$2p^4(^3P)3d$	^4D	7/2	1 161 013	1 172 209	1 181 167
34			5/2	1 162 025	1 173 271	1 181 649
35			3/2	1 162 165	1 173 376	1 182 311
36			1/2	1 162 754	1 173 979	1 182 894
37	$2p^4(^3P)3d$	^4F	9/2	1 169 569	1 182 612	1 189 844
38			3/2	1 171 689	1 184 525	1 194 327
39			5/2	1 172 030	1 184 838	1 193 223
40			7/2	1 172 047	1 184 946	1 191 541
41	$2p^4(^3P)3d$	^4P	1/2	1 176 385	1 188 594	1 194 899
42			3/2	1 177 207	1 189 543	1 195 984
43			5/2	1 178 908	1 191 510	1 197 727
44	$2p^4(^3P)3d$	^2F	7/2	1 177 148	1 189 950	1 194 987
45			5/2	1 178 364	1 190 848	1 197 151
46	$2p^4(^3P)3d$	^2P	1/2	1 182 736	1 194 144	1 200 710
47			3/2	1 185 454	1 196 939	1 204 740
48	$2p^4(^3P)3d$	^2D	3/2	1 185 167	1 195 061	1 201 100
49			5/2	1 185 973	1 196 247	1 202 960
50	$2p^4(^1D)3d$	^2G	7/2	1 214 568	1 227 449	
51			9/2	1 214 715	1 227 538	1 232 671
52	$2p^4(^1D)3d$	^2S	1/2	1 223 636	1 234 097	1 239 190
53	$2p^4(^1$ $D)3d$	^2P	3/2	1 224 780	1 234 806	1 241 050
54			1/2	1 225 778	1 235 883	1 242 390
55	$2p^4(^1D)3d$	^2F	7/2	1 223 872	1 236 910	1 242 649
56			5/2	1 223 946	1 236 950	1 242 186
57	$2p^4(^1D)3d$	^2D	5/2	1 226 710	1 237 621	1 243 020
58			3/2	1 227 611	1 238 313	1 243 860
59	$2p^4(^1S)3d$	^2D	3/2	1 290 487	1 280 925	1 291 790
60			5/2	1 291 154	1 281 640	1 291 510
61	$2p^4(^3P)4s$	^4P	5/2	1 302 866	1 314 745	
62			1/2	1 305 283	1 317 544	
63			3/2	1 306 890	1 319 305	
64	$2p^4(^3P)4s$	^2P	3/2	1 308 844	1 321 429	1 329 900
65			1/2	1 310 323	1 323 045	
66	$2p^4(^3P)4p$	$^4P^\circ$	5/2	1 333 771	1 340 871	
67			3/2	1 333 474	1 340 979	
68			1/2	1 334 815	1 342 729	
69	$2p^4(^3P)4p$	$^4D^\circ$	7/2	1 335 203	1 347 589	
70			1/2	1 337 989	1 350 092	
71			3/2	1 338 555	1 351 294	
72			5/2	1 338 545	1 352 144	
73	$2p^4(^3P)4p$	$^2D^\circ$	5/2	1 339 973	1 351 228	
74			3/2	1 339 638	1 352 195	
75	$2p^4(^3P)4p$	$^2S^\circ$	1/2	1 340 521	1 352 722	
76	$2p^4(^3P)4p$	$^4S^\circ$	3/2	1 342 995	1 355 616	
77	$2p^4(^3P)4p$	$^2P^\circ$	3/2	1 349 411	1 359 114	
78			1/2	1 349 310	1 359 465	
79	$2p^4(^1D)4s$	^2D	5/2	1 352 262	1 365 126	1 371 820
80			3/2	1 352 767	1 365 515	
81	$2p^4(^3P)4d$	^4D	7/2	1 371 226	1 382 797	
82			5/2	1 372 174	1 384 161	
83			3/2	1 372 430	1 384 614	
84			1/2	1 373 107	1 385 519	
85	$2p^4(^3P)4d$	^4F	9/2	1 374 444	1 387 108	
86			7/2	1 376 125	1 388 760	
87			5/2	1 376 654	1 389 343	
88			3/2	1 376 461	1 389 348	
89	$2p^4(^3P)4d$	^4P	1/2	1 377 931	1 390 631	
90			3/2	1 379 041	1 391 893	
91			5/2	1 380 830	1 393 884	
92	$2p^4(^3P)4d$	^2F	5/2	1 380 128	1 392 885	
93			7/2	1 380 477	1 393 669	
94	$2p^4(^3P)4d$	^2P	1/2	1 381 851	1 393 521	1 402 490
95			3/2	1 384 583	1 396 287	1 403 050
96	$2p^4(^3P)4d$	^2D	3/2	1 385 040	1 395 603	
97			5/2	1 385 544	1 396 797	1 404 870
98	$2p^4(^3P)4p$	$^2F^\circ$	7/2	1 382 852	1 395 696	
99			5/2	1 382 929	1 395 739	
100	$2p^4(^1D)4p$	$^2D^\circ$	3/2	1 386 127	1 399 126	
101			5/2	1 386 673	1 399 653	
102	$2p^4(^1D)4p$	$^2P^\circ$	1/2	1 392 385	1 405 752	
103			3/2	1 392 362	1 405 797	
104	$2p^4(^1D)4s$	^2S	1/2	1 419 675	1 432 175	
105	$2p^4(^1D)4d$	^2G	7/2	1 421 515	1 434 310	
106			9/2	1 421 617	1 434 434	
107	$2p^4(^1D)4d$	^2P	3/2	1 424 977	1 436 510	
108			1/2	1 425 973	1 437 711	
109	$2p^4(^1D)4d$	^2F	7/2	1 424 368	1 437 280	
110			5/2	1 424 453	1 437 401	
111	$2p^4(^1D)4d$	^2D	5/2	1 425 961	1 438 109	1 444 340
112			3/2	1 426 992	1 438 858	1 445 010
113	$2p^4(^1D)4d$	^2S	1/2	1 427 833	1 440 235	
114	$2p^4(^1S)4p$	$^2P^\circ$	1/2	1 453 543	1 466 060	
115			3/2	1 453 658	1 466 257	
116	$2p^4(^1S)4d$	^2D	3/2	1 493 396	1 506 902	
117			5/2	1 494 092	1 507 702	

Table 2 – *continued*

be applied for $2p^5\ ^2P^\circ_{1/2}$ level. Electric dipole transition probabilities and weighted oscillator strengths are presented in Table 3 for transition with lower level from one to 10 and upper level from three to 95. The majority of wavelengths are in extreme ultraviolet (XUV) region. F-like ions are of fundamental importance for current

Table 3. Transition probabilities (A_{ki}), calculated wavelengths (λ) and weighted oscillator strengths (gf) for Si VI spectrum. Present: this work; FF: Froese Fischer & Tachiev (2004); CT: Coutinho & Trigueiros (1999). The numbers in brackets denote powers of 10.

Transition	λ (Å)	$A_{ki}(s^{-1})$			gf			
		present	FF	NIST	present	FF	NIST	CT
1–3	246.004	1.805(10)	1.777(10)	1.77(10)	3.275(−01)	3.210(−01)	3.206(−01)	4.04(−01)
2–3	247.734	8.840(09)	8.517(09)	8.46(09)	1.627(−01)	1.576(−01)	1.573(−01)	2.00(−01)
1–4	101.795	8.982(07)	7.405(07)	7.51(07)	8.372(−04)	6.784(−04)	6.886(−04)	8.00(−04)
1–5	101.369	1.340(09)	8.423(06)	8.55(06)	4.128(−03)	2.547(−05)	2.588(−05)	
2–5	101.661	2.010(09)	2.624(08)	2.64(08)	6.229(−03)	8.016(−04)	8.072(−04)	9.00(−04)
1–6	101.315	1.019(08)	1.167(09)	1.18(09)	6.270(−04)	7.088(−03)	7.161(−03)	7.50(−03)
2–6	101.607	9.716(06)	1.010(08)	1.08(08)	6.016(−05)	6.194(−04)	6.266(−04)	6.00(−04)
1–7	100.087	6.667(10)	6.753(10)	6.74(10)	4.005(−01)	4.004(−01)	3.999(−01)	4.88(−01)
2–7	100.373	1.292(10)	1.098(10)	1.09(10)	7.803(−02)	6.574(−02)	6.561(−02)	7.90(−02)
1–8	100.051	2.509(10)	2.823(10)	2.82(10)	7.530(−02)	8.304(−02)	8.317(−02)	1.02(−01)
2–8	100.336	4.987(10)	5.156(10)	5.15(10)	1.505(−01)	1.532(−01)	1.531(−01)	1.86(−01)
1–9	96.513	3.189(10)	3.087(10)	3.08(10)	2.672(−01)	2.556(−01)	2.558(−01)	
1–10	96.475	4.625(09)	3.056(09)	3.03(09)	2.582(−02)	1.687(−02)	1.674(−02)	2.03(−02)
2–10	96.740	2.674(10)	2.796(10)	2.79(10)	1.501(−01)	1.558(−01)	1.559(−01)	1.94(−01)
3–11	152.739	1.064(05)	7.895(05)		1.488(−06)	1.077(−05)		
4–11	1268.336	3.944(08)	4.159(08)	4.11(08)	3.805(−01)	3.935(−01)	3.908(−01)	
5–11	1338.445	1.569(08)	1.624(08)	1.62(08)	1.685(−01)	1.746(−01)	1.749(−01)	1.89(−01)
6–11	1347.907	8.664(07)	9.855(07)	9.73(07)	9.440(−02)	1.010(−01)	1.004(−01)	1.07(−01)
7–11	1610.745	4.125(05)	5.789(04)	5.56(04)	6.418(−04)	8.312(−05)	8.035(−05)	
8–11	1620.320	1.353(07)	3.677(03)	3.79(03)	2.130(−02)	5.938(−06)	6.165(−06)	
9–11	3987.165	6.968(04)	1.627(04)	1.62(04)	6.643(−04)	1.218(−04)	1.199(−04)	
10–11	4052.352	7.466(03)	5.228(03)	5.44(03)	7.353(−05)	3.929(−05)	4.036(−05)	
4–12	1265.271	5.940(08)	5.712(08)	5.64(08)	8.554(−01)	8.322(−01)	8.279(−01)	8.72(−01)
6–12	1344.446	9.628(07)	1.104(08)	1.10(08)	1.565(−01)	1.744(−01)	1.753(−01)	1.91(−01)
7–12	1605.805	1.630(06)	2.988(05)	3.09(05)	3.781(−03)	6.648(−04)	6.918(−04)	
9–12	246.004	1.458(05)	2.110(03)	2.37(03)	2.054(−03)	2.554(−05)	2.837(−05)	
10–12	247.734	3.719(01)	2.179(02)	2.40(02)	5.410(−07)	2.646(−06)	2.890(−06)	
3–13	101.795	2.939(05)	4.160(05)		2.046(−06)	2.628(−06)		
5–13	1309.272	3.686(07)	7.502(07)	7.46(07)	1.894(−02)	3.900(−02)	3.899(−02)	
6–13	1318.325	5.969(08)	5.915(08)	5.85(08)	3.111(−01)	2.933(−01)	2.917(−01)	3.10(−01)
7–13	1568.682	1.079(06)	8.921(05)	9.49(05)	7.964(−04)	6.160(−04)	6.606(−04)	
8–13	1577.761	1.707(06)	4.217(05)	4.38(05)	1.274(−03)	3.268(−04)	3.419(−04)	
10–13	3796.252	1.573(04)	1.490(04)	1.49(04)	6.798(−05)	5.128(−05)	5.018(−05)	
4–14	1133.080	1.056(09)	1.033(09)	1.03(09)	1.626(+00)	1.581(+00)	1.577(+00)	1.71(+00)
9–14	2899.222	6.193(03)	3.205(03)	3.54(03)	6.244(−05)	2.776(−05)	3.019(−05)	
3–15	149.982	5.880(04)	1.367(06)	1.40(06)	3.966(−07)	8.972(−06)	9.141(−06)	9.00(−05)
5–15	1152.795	9.112(08)	8.776(08)	8.74(08)	3.631(−01)	3.426(−01)	3.419(−01)	3.70(−01)
6–15	1159.808	6.171(07)	1.290(08)	1.29(08)	2.489(−02)	4.836(−02)	4.841(−02)	
7–15	1349.252	9.550(05)	2.566(05)	2.58(05)	5.213(−04)	1.278(−04)	1.228(−04)	
8–15	1355.964	1.964(07)	7.280(05)	7.09(05)	1.083(−02)	3.998(−04)	3.899(−04)	
10–15	2724.120	6.668(04)	8.238(03)		1.484(−04)	1.454(−05)		
3–16	149.675	3.954(05)	5.543(05)	5.73(05)	5.312(−06)	7.292(−06)	7.516(−06)	
4–16	1084.091	2.953(07)	2.000(07)	2.03(07)	2.081(−02)	1.423(−02)	1.452(−02)	
5–16	1134.903	4.668(08)	4.842(08)	4.82(08)	3.606(−01)	3.850(−01)	3.837(−01)	4.13(−01)
6–16	1141.699	5.093(08)	4.957(08)	4.95(08)	3.981(−01)	3.781(−01)	3.768(−01)	4.11(−01)
7–16	1324.806	1.466(06)	1.213(03)	1.88(03)	1.543(−03)	1.232(−06)	1.909(−06)	
8–16	1331.276	2.832(07)	4.541(06)	4.53(06)	3.010(−02)	5.094(−03)	5.081(−03)	
9–16	2598.741	7.183(04)	8.858(03)	9.91(03)	2.909(−04)	3.241(−05)	3.572(−05)	
10–16	2626.277	1.035(02)	1.337(04)	1.45(04)	4.281(−07)	4.908(−05)	5.236(−05)	
4–17	1080.192	2.103(08)	1.903(08)	1.91(08)	2.207(−01)	2.100(−01)	2.113(−01)	2.38(−01)
6–17	1137.375	8.616(08)	7.873(08)	7.83(08)	1.003(+00)	9.320(−01)	9.289(−01)	9.98(−01)
7–17	1318.987	7.133(06)	1.864(07)	1.86(07)	1.116(−02)	2.957(−02)	2.958(−02)	
9–17	2576.446	2.564(03)	8.978(03)	9.31(03)	1.531(−05)	5.316(−05)	5.432(−05)	
4–18	1022.110	5.562(05)	1.307(07)	1.33(07)	5.227(−04)	1.265(−02)	1.285(−02)	
6–18	1073.164	1.749(07)	2.238(07)	2.22(07)	1.811(−02)	2.313(−02)	2.301(−02)	
7–18	1233.405	8.506(08)	8.032(08)	8.02(08)	1.164(+00)	1.090(−01)	1.088(+00)	
9–18	2268.921	7.863(04)	2.465(05)	2.49(05)	3.641(−04)	1.090(−03)	1.086(−03)	
10–18	2289.882	1.355(02)	6.522(03)	6.85(03)	6.391(−07)	2.892(−05)	2.999(−05)	
3–19	148.357	2.047(06)	1.279(07)		2.702(−05)	1.645(−04)		
4–19	1018.526	8.703(06)	2.181(06)	2.75(06)	5.415(−03)	1.326(−03)	1.336(−03)	
5–19	1063.250	9.488(07)	2.892(06)		6.433(−02)	1.952(−03)	1.862(−03)	
6–19	1063.250	1.100(05)	1.283(06)	1.22(06)	7.545(−05)	8.336(−04)	7.961(−04)	

Table 3 – *continued*

Transition	λ (Å)	$A_{ki}(s^{-1})$			gf			
		present	FF	NIST	present	FF	NIST	CT
7–19	1228.189	9.754(07)	4.377(08)	4.54(08)	8.824(−02)	3.701(−01)	3.845(−01)	3.66(−01)
8–19	1233.748	6.973(08)	3.698(08)	3.48(08)	6.365(−01)	3.420(−01)	3.221(−01)	
9–19	2251.333	3.457(05)	6.305(06)	7.30(06)	1.051(−03)	1.648(−02)	1.887(−02)	
10–19	2271.969	4.466(04)	2.421(06)	2.63(06)	1.382(−04)	6.344(−03)	6.807(−03)	
3–20	148.267	1.378(08)	8.949(07)		9.085(−04)	5.760(−04)		
5–20	1058.626	6.333(05)	1.717(05)		2.128(−04)	5.804(−05)		
6–20	1064.537	6.918(06)	1.331(06)		2.351(−03)	4.332(−04)		
7–20	1222.023	5.861(08)	6.643(08)		2.624(−01)	2.813(−01)		
8–20	1227.526	6.666(07)	5.304(07)		3.012(−02)	2.458(−02)		
10–20	2250.959	2.878(07)	2.829(07)		4.373(−02)	3.719(−02)		
3–21	147.538	1.880(08)	1.114(08)	1.10(08)	2.454(−03)	1.422(−03)	1.339(−03)	
4–21	981.153	1.120(07)	7.761(06)	5.01(06)	6.464(−03)	4.476(−03)	2.904(−03)	
5–21	1022.589	4.986(06)	1.343(07)	1.08(07)	3.127(−03)	8.554(−03)	6.902(−03)	
6–21	1028.103	1.619(07)	2.197(06)		1.026(−02)	1.348(−03)		
7–21	1174.254	5.806(08)	2.535(08)	2.33(08)	4.801(−01)	2.008(−01)	1.853(−01)	2.24(−01)
8–21	1179.334	4.876(07)	4.094(08)	4.31(08)	4.067(−02)	3.538(−01)	3.741(−01)	3.42(−01)
9–21	2076.504	4.517(07)	4.361(07)	4.31(07)	1.168(−01)	1.018(−01)	1.002(−01)	
10–21	2094.047	5.294(06)	3.415(06)	3.31(06)	1.392(−02)	7.996(−03)	7.726(−03)	
1–22	92.226	2.083(10)	1.964(10)	1.96(10)	5.314(−02)	4.908(−02)	4.920(−02)	6.70(−02)
2–22	92.468	1.110(10)	1.232(10)	1.23(10)	2.845(−02)	3.108(−02)	3.097(−02)	4.26(−02)
3–23	146.805	5.237(06)	1.548(05)		6.769(−05)	1.968(−06)		
4–23	949.626	7.718(08)	6.774(08)	6.81(08)	4.174(−01)	3.808(−01)	3.837(−01)	3.48(−01)
5–23	988.389	3.575(08)	3.063(08)	3.08(08)	2.095(−01)	1.899(−01)	1.909(−01)	1.89(−01)
6–23	993.539	5.751(08)	5.521(08)	5.52(08)	3.405(−01)	3.301(−01)	3.303(−01)	3.30(−01)
7–23	1129.379	4.435(06)	4.529(05)	5.45(04)	3.393(−03)	3.484(−04)	4.197(−05)	
8–23	1134.078	3.772(06)	7.482(06)	5.32(06)	2.909(−03)	6.270(−03)	4.456(−03)	
9–23	1940.178	1.976(06)	1.302(06)		4.461(−03)	2.892(−03)		
10–23	1955.485	2.723(04)	9.887(04)		6.245(−05)	2.200(−04)		
3–24	146.615	4.880(07)	2.590(07)		3.145(−04)	1.644(−04)		
5–24	979.803	4.553(07)	2.065(06)		1.311(−02)	6.328(−04)		
6–24	984.864	1.963(03)	3.411(06)		5.710(−07)	1.008(−03)		
7–24	1118.182	2.447(08)	1.833(08)		9.173(−02)	6.964(−02)		
8–24	1122.788	7.678(08)	6.707(08)		2.902(−01)	2.772(−01)		
10–24	1922.160	1.678(07)	2.055(07)		1.859(−02)	2.237(−02)		
5–25	735.260	4.657(06)			2.265(−03)			
6–25	761.314	5.428(05)	1.357(04)	1.51(04)	2.830(−04)	7.164(−06)	8.035(−06)	
7–25	838.603	7.411(04)	7.983(04)		4.688(−05)	5.100(−05)		
9–25	1215.905	8.749(07)	7.805(07)	7.65(07)	1.163(−01)	1.035(−01)	1.020(−01)	1.09(−01)
10–25	1221.899	7.763(08)	7.612(08)	7.56(08)	1.043(+00)	1.011(+00)	1.006(+00)	1.11(+00)
4–26	733.553	8.310(05)	1.120(05)	1.20(05)	5.363(−04)	7.446(−05)	8.035(−05)	
9–26	1211.242	8.876(08)	8.628(08)	8.56(08)	1.562(+00)	1.501(+00)	1.499(+00)	1.64(+00)
3–27	138.443	1.456(03)	4.078(06)	4.89(06)	1.674(−08)	4.622(−05)		
4–27	682.827	3.924(05)	6.054(04)	6.24(04)	1.097(−04)	1.749(−05)	1.811(−05)	
5–27	702.641	1.011(06)	5.116(-1)	1.89(00)	2.994(−04)	1.584(−10)	5.902(−10)	
6–27	705.240	1.533(06)	1.283(06)	4.40(05)	4.573(−04)	1.294(−04)	1.339(−04)	
7–27	771.072	1.238(06)	1.967(07)	2.00(07)	4.413(−04)	7.076(−03)	7.244(−03)	
8–27	773.259	5.680(06)	5.306(06)	5.19(06)	2.037(−03)	2.024(−03)	1.995(−03)	
9–27	1078.900	1.254(08)	7.247(07)	7.17(07)	8.756(−02)	5.049(−02)	5.023(−02)	
10–27	1083.616	1.118(09)	1.117(09)	1.11(09)	7.875(−01)	7.792(−01)	7.798(−01)	8.03(−01)
4–28	679.840	2.305(07)	4.734(05)	4.88(05)	9.584(−03)	2.040(−04)	2.118(−04)	
6–28	702.055	4.910(06)	5.481(03)	4.62(03)	2.177(−03)	2.467(−06)	2.094(−06)	
7–28	767.266	6.267(06)	1.070(07)	1.05(07)	3.319(−03)	5.740(−03)	5.675(−03)	
9–28	1071.462	1.150(09)	1.100(09)	1.10(09)	1.187(+00)	1.140(+00)	1.140(+00)	1.17(+00)
10–28	1076.114	1.288(08)	1.137(08)	1.13(08)	1.342(−01)	1.179(−01)	1.174(−01)	1.18(−01)
3–29	135.238	5.172(08)	7.112(08)	7.11(08)	5.673(−03)	7.758(−03)	7.762(−03)	
4–29	611.374	2.805(07)	5.525(05)	5.48(05)	6.287(−03)	1.326(−04)	1.327(−04)	
5–29	627.211	2.072(07)	1.148(05)	1.09(05)	4.888(−03)	2.936(−05)	2.818(−05)	
6–29	629.281	2.656(05)	1.930(07)	1.92(07)	6.306(−05)	4.820(−03)	4.841(−03)	
7–29	681.173	1.678(09)	1.402(09)	1.38(09)	4.670(−01)	4.104(−01)	4.083(−01)	4.32(−01)
8–29	682.880	3.009(08)	2.957(08)	2.92(08)	8.415(−02)	9.122(−02)	9.078(−02)	9.61(−02)
9–29	910.722	1.294(09)	1.235(09)	1.23(09)	6.436(−01)	6.498(−01)	6.486(−01)	
10–29	914.081	1.412(08)	5.801(07)	5.69(07)	7.075(−02)	3.054(−02)	3.013(−02)	
3–30	135.230	5.478(08)	8.058(08)	8.06(08)	3.004(−03)	4.368(−03)	4.355(−03)	

Table 3 – *continued*

Transition	λ (Å)	$A_{ki}(s^{-1})$ present	FF	NIST	gf present	FF	NIST	CT
5–30	627.022	7.195(07)	3.778(06)	3.77(06)	8.482(−03)	4.686(−04)	4.720(−04)	
6–30	629.090	1.571(05)	4.630(06)	4.61(06)	1.864(−05)	5.608(−04)	5.636(−04)	
7–30	680.950	6.378(08)	4.582(08)	4.52(08)	8.868(−02)	6.496(−02)	6.411(−02)	6.83(−02)
8–30	682.655	1.200(09)	1.070(09)	1.06(09)	1.677(−01)	1.596(−01)	1.588(−01)	1.68(−01)
10–30	913.679	1.459(09)	1.448(09)	1.44(09)	3.653(−01)	3.649(−01)	3.647(−01)	3.73(−01)
3–31	130.708	8.779(08)	6.247(08)		8.995(−03)	6.224(−03)		
4–31	528.555	4.887(06)	1.410(05)		8.188(−04)	2.283(−05)		
5–31	540.350	3.953(06)	1.024(04)		6.922(−04)	1.745(−06)		
6–31	541.886	6.974(06)	2.069(06)		1.228(−03)	3.461(−04)		
7–31	579.929	2.418(08)	1.207(08)		4.877(−02)	2.297(−02)		
8–31	581.166	6.960(07)	2.686(07)		1.410(−02)	5.334(−03)		
9–31	738.377	1.559(05)	2.646(06)		5.098(−05)	7.962(−04)		
10–31	740.583	2.238(04)	1.572(06)		7.363(−06)	4.732(−04)		
3–32	130.562	8.400(08)	5.510(08)		4.293(−03)	2.744(−03)		
5–32	537.865	8.805(06)	6.903(05)		7.638(−04)	5.880(−05)		
6–32	539.386	1.317(03)	7.534(05)		1.149(−07)	6.296(−05)		
7–32	577.068	8.320(07)	7.216(07)		8.308(−03)	6.860(−03)		
8–32	578.292	1.931(08)	1.451(08)		1.937(−02)	1.438(−02)		
10–32	735.923	5.602(06)	1.894(06)		9.097(−04)	2.847(−04)		
1–34	85.232	8.382(06)	2.275(07)	2.30(07)	5.477(−05)	1.464(−04)	1.482(−04)	
1–35	85.224	9.086(05)	1.456(08)	1.45(08)	3.958(−06)	6.244(−04)	6.237(−04)	
2–35	85.431	6.482(07)	3.464(07)	3.50(07)	2.837(−04)	1.498(−04)	1.517(−04)	
1–36	85.181	8.300(07)	8.691(07)	8.61(07)	1.806(−04)	1.861(−04)	1.845(−04)	
2–36	85.387	1.621(08)	2.003(08)	1.99(08)	3.545(−04)	4.328(−04)	4.295(−04)	
1–38	84.422	8.666(07)	1.172(09)	1.18(09)	3.704(−04)	4.921(−03)	4.954(−03)	1.03(−01)
2–38	84.625	4.078(08)	2.408(09)	2.44(09)	1.751(−03)	1.020(−02)	1.035(−02)	1.96(−02)
1–41	84.133	8.295(08)	1.409(09)		1.761(−03)	2.958(−03)		
2–41	84.334	5.368(08)	1.743(07)		1.145(−03)	3.690(−05)		
1–42	84.066	4.006(08)	2.740(09)		1.698(−03)	1.148(−02)		
2–42	84.267	3.639(07)	5.164(08)		1.550(−04)	2.182(−03)		3.00(−04)
1–43	83.927	1.359(08)	3.789(08)		8.612(−04)	2.374(−03)		1.46(−02)
1–45	83.974	1.817(10)	2.211(10)		1.153(−01)	1.386(−01)		
1–46	83.742	3.143(10)	2.980(10)	2.99(10)	6.608(−02)	6.196(−02)	6.194(−02)	5.95(−02)
2–46	83.942	5.476(10)	4.368(10)	4.36(10)	1.157(−01)	9.156(−02)	9.141(−02)	8.40(−02)
1–47	83.546	6.063(10)	1.686(10)	1.77(10)	2.538(−01)	6.960(−02)	7.227(-02)	3.09(−01)
2–47	83.745	2.522(10)	9.938(10)	9.74(10)	1.061(−01)	4.138(−01)	4.064(−01)	4.00(−04)
1–48	83.678	4.790(10)	9.699(10)	9.60(10)	2.012(−01)	4.028(−01)	3.990(−01)	7.03(−02)
2–48	83.877	1.934(11)	9.296(10)	9.47(10)	8.162(−01)	3.894(−01)	3.981(−01)	8.26(−01)
1–49	83.595	2.281(11)	2.341(11)	2.34(11)	1.434(+00)	1.545(+00)	1.452(+00)	1.27(+00)
1–52	81.031	3.016(11)	2.850(11)	2.76(11)	5.939(−01)	5.556(−01)	5.395(−01)	6.00(−01)
2–52	81.218	7.742(10)	7.643(10)	8.45(10)	1.531(−01)	1.502(−01)	1.663(−01)	2.13(−01)
1–53	80.984	3.209(11)	2.749(11)	2.74(11)	1.262(+00)	1.068(+00)	1.069(+00)	1.33(+00)
2–53	81.171	3.233(10)	5.658(10)	5.67(10)	1.278(−01)	2.218(−01)	2.218(−01)	2.91(−01)
1–54	80.914	6.868(10)	6.732(10)	6.85(10)	1.348(−01)	1.306(−01)	1.333(−01)	2.11(−01)
2–54	81.100	2.860(11)	2.804(11)	2.78(11)	5.640(−01)	5.484(−01)	5.457(−01)	6.27(−01)
1–56	80.844	3.445(10)	6.766(10)		2.025(−01)	3.939(−01)		7.83(−02)
1–57	80.800	1.848(11)	1.335(11)	1.31(11)	1.085(+00)	7.764(−01)	7.603(−01)	1.59(+00)
1–58	80.755	1.352(10)	3.492(10)	3.50(10)	5.289(−02)	1.351(−01)	1.355(−01)	1.97(−01)
2–58	80.941	1.969(11)	1.891(11)	1.89(11)	7.735(−01)	7.380(−01)	7.362(−01)	1.01(+00)
1–59	78.069	8.919(09)	7.731(09)	7.74(09)	3.260(−02)	2.776(−02)	2.779(−02)	
2–59	78.242	4.642(10)	5.577(10)	5.57(10)	1.704(−01)	2.018(−01)	2.018(−01)	2.72(−01)
1–60	78.025	4.737(10)	5.054(10)	5.05(10)	2.594(−01)	2.723(−01)	2.722(−01)	3.75(−01)
1–61	76.060	2.957(07)			1.539(−04)			
1–62	75.899	3.236(09)			5.589(−03)			
2–62	76.063	6.405(09)			1.111(−02)			
1–63	75.797	1.243(09)			4.281(−03)			1.14(−02)
2–63	75.961	2.661(08)			9.209(−04)			
1–64	75.676	2.243(10)		1.24(10)	7.702(−02)		4.197(−02)	4.21(−02)
2–64	75.839	4.741(09)		2.11(09)	1.635(−02)		7.194(−03)	7.20(−03)
1–65	75.583	5.689(09)			9.746(−03)			
2–65	75.746	1.202(10)			2.069(−02)			
4–66	278.937	1.029(10)			7.204(−01)			
6–66	282.606	2.931(09)			2.106(−01)			

Table 3 – *continued*

Transition	λ (Å)	$A_{ki}(s^{-1})$			gf			
		present	FF	NIST	present	FF	NIST	CT
7–66	292.617	2.511(07)			1.934(−03)			
9–66	328.147	5.179(07)			5.016(−03)			
10–66	328.582	6.473(03)			6.287(−07)			
3–67	107.011	3.996(06)			2.744(−05)			
4–67	278.853	6.399(09)			2.984(−01)			
5–67	282.101	3.730(09)			1.780(−01)			
6–67	282.519	1.629(09)			7.796(−02)			
7–67	292.524	1.005(07)			5.159(−04)			
8–67	292.839	4.215(08)			2.168(−02)			
9–67	328.031	2.309(07)			1.490(−03)			
10–67	328.466	2.775(06)			1.796(−04)			
3–68	106.811	3.368(06)			1.152(−05)			
5–68	280.715	1.075(09)			2.539(−02)			
6–68	281.129	1.059(10)			2.511(−01)			
7–68	291.034	3.005(07)			7.632(−04)			
8–68	291.345	6.976(07)			1.776(−03)			
10–68	326.587	8.116(06)			2.596(−04)			
4–69	273.806	3.264(09)			2.935(−01)			
9–69	321.069	7.827(06)			9.678(−04)			
3–70	105.978	6.730(03)			2.266(−08)			
5–70	275.031	3.121(09)			7.079(−02)			
6–70	275.428	3.863(02)			8.788(−09)			
7–70	284.929	8.093(04)			1.970(−06)			
8–70	285.227	1.165(08)			2.841(−03)			
10–70	318.919	1.142(04)			3.482(−07)			
3–71	105.843	1.511(06)			1.011(−05)			
4–71	271.056	9.192(06)			4.050(−04)			
5–71	274.125	1.417(09)			6.385(−02)			
6–71	274.519	1.151(09)			5.201(−02)			
7–71	283.956	3.861(04)			1.867(−06)			
8–71	284.252	2.438(08)			1.181(−02)			
9–71	317.295	4.312(06)			2.603(−04)			
10–71	317.701	6.615(04)			4.004(−06)			
4–72	270.433	5.068(07)			3.334(−03)			
6–72	273.880	1.299(09)			8.765(−02)			
7–72	283.272	2.124(09)			1.533(−01)			
9–72	316.441	3.720(04)			3.351(−06)			
10–72	316.845	3.494(05)			3.155(−05)			
4–73	271.104	2.072(08)			1.370(−02)			
6–73	274.569	1.876(09)			1.272(−01)			
7–73	284.009	8.893(08)			6.453(−02)			
9–73	317.361	2.303(06)			2.086(−04)			
10–73	317.768	6.699(06)			6.085(−04)			
3–74	105.742	2.059(05)			1.381(−06)			
4–74	270.396	1.558(08)			6.832(−03)			
5–74	273.449	5.931(08)			2.660(−02)			
6–74	273.842	6.104(05)			2.745(−05)			
7–74	283.232	3.949(08)			1.900(−02)			
8–74	283.526	2.129(09)			1.026(−01)			
9–74	316.390	1.947(06)			1.169(−04)			
10–74	316.795	1.613(06)			9.709(−05)			
3–75	105.683	1.462(07)			4.896(−05)			
5–75	273.056	1.449(06)			3.239(−05)			
6–75	273.447	1.060(07)			2.376(−04)			
7–75	282.809	2.598(09)			6.230(−02)			
8–75	283.103	5.264(07)			1.265(−03)			
10–75	316.266	4.386(08)			1.315(−02)			
3–76	105.361	2.021(06)			1.345(−05)			
4–76	267.917	3.085(08)			1.328(−02)			
5–76	270.915	1.073(09)			4.722(−02)			
6–76	271.300	1.127(09)			4.973(−02)			
7–76	280.513	1.603(07)			7.565(−04)			
8–76	280.802	3.923(07)			1.855(−03)			

Table 3 – *continued*

Transition	λ (Å)	$A_{ki}(s^{-1})$ present	FF	NIST	gf present	FF	NIST	CT
9–76	313.002	1.264(06)			7.425(−05)			
10–76	313.398	1.091(06)			6.425(−05)			
3–77	104.974	4.741(07)			3.133(−04)			
4–77	265.429	3.542(06)			1.497(−04)			
5–77	268.371	6.593(07)			2.848(−03)			
6–77	268.750	7.602(06)			3.293(−04)			
7–77	277.787	1.359(09)			6.288(−02)			
8–77	278.07	1.709(08)			7.925(−03)			
9–77	309.612	1.217(09)			6.997(−02)			
10–77	309.999	1.274(08)			7.344(−03)			
3–78	104.935	3.845(07)			1.270(−04)			
5–78	268.119	1.251(08)			2.696(−03)			
6–78	268.497	1.917(07)			4.144(−04)			
7–78	277.517	1.251(06)			2.888(−05)			
8–78	277.800	1.619(09)			3.747(−02)			
10–78	309.663	8.910(08)			2.562(−02)			
1–79	73.253	9.110(09)		8.24(09)	4.398(−02)		3.935(−02)	3.94(−02)
1–80	73.232	1.305(09)			4.198(−03)			
2–80	73.385	7.299(09)			2.357(−02)			
1–82	72.246	2.920(08)			1.371(−03)			
1–83	72.222	1.216(02)			3.802(−10)			
2–83	72.371	2.423(08)			7.611(−04)			
1–84	72.175	5.005(08)			7.818(−04)			
2–84	72.323	9.647(08)			1.513(−03)			
1–87	71.976	2.262(10)			1.054(−01)			1.89(−01)
1–88	71.976	1.382(08)			4.293(−04)			
2–88	72.124	6.586(08)			2.055(−03)			1.03(−01)
1–89	71.910	2.267(09)			3.515(−03)			
2–89	72.057	3.055(09)			4.756(−03)			
1–90	71.845	1.208(09)			3.740(−03)			2.35(−02)
2–90	71.991	2.033(07)			6.318(−05)			2.00(−04)
1–91	71.742	1.462(09)			6.769(−03)			1.96(−02)
1–92	71.793	1.906(10)			8.839(−02)			
1–94	71.761	2.760(10)		2.19(10)	4.261(−02)		3.341(−02)	3.34(−02)
2–94	71.907	5.142(10)		3.56(10)	7.972(−02)		5.457(−02)	5.47(−02)
1–95	71.761	2.760(10)		7.20(10)	4.261(−02)			
2–95	71.907	5.142(10)		3.26(07)	7.972(−02)		1.000(−04)	1.00(−04)

X-ray laser research. Our transition probabilities are compared with NIST values and multiconfiguration Hartree–Fock (MCHF) results of Froese Fischer & Tachiev (2004), who use the observed energies for the calculation of transition probabilities. The agreement is by less than 30 per cent for 70 per cent of strong transitions ($A > 10^8$ s^{-1}) of NIST compilation. The agreement is much less for weak ones. For weighted oscillator strengths, comparison is made also with Coutinho & Trigueiros (1999) results obtained using multiconfiguration Hartree–Fock relativistic (HFR) approach. In their work the adjusted energy levels were used to optimize the electrostatic parameters, these optimized parameters were used again to calculate the gf values. In general, our oscillator strengths are in good agreement with the other works except for a few transitions as for example 2–5, 1–6, 2–6, 2–38 for which we observe large disagreement. For the transitions 1–47, 2–48, 2–42 our oscillator strengths agree better with Coutinho & Trigueiros results. On the other hand, for the transitions 2–47, 1–48, 1–56 the agreement with Froese-Fischer & Tachiev values is better. For the transitions 3–15, 1–38 all three methods give different results. The inclusion of a larger number of configurations has an important effect on wavefunctions and *A* values. TEC of the $2s2p^6\ ^2S_{1/2}$ level improve slightly our results. For example for the 2–3 transition our *A* value was 1.022E+10 s^{-1} and became 8.840E+09 s^{-1}, NIST one is 8.46E+09 s^{-1}. The correction of quartet terms do not improve the results.

By combining the SUPERSTRUCTURE code for calculating energy levels and oscillator strengths and the code for the Stark broadening calculations, we calculated Stark broadening parameters. Calculated Stark broadening widths [full width at half-maximum (FWHM)] and shifts for a perturber densities of 10^{17} cm^{-3} and temperatures from 50 000 up to 800 000 K are shown in Table 4 for electron-, proton- and singly ionized helium-impact broadening. Such temperatures are of interest for the modelling and analysis of X-ray spectra, such as the spectra obtained by *Chandra*, modelling of some hot star atmospheres (e.g. DO white dwarf and PG 1195), subphotospheric layers, soft X-ray lasers and laser produced plasmas. Higher temperatures are of interest for fusion plasma as well as for stellar interiors.

We also specify a parameter *C* (Dimitrijević & Sahal-Bréchot 1984), which gives an estimate for the maximal perturber density for which the line may be treated as isolated, when it is divided by the corresponding FWHM. For each value given in Table 4 the collision volume *V* multiplied by the perturber density *N* is much less than one and the impact approximation is valid (Sahal-Bréchot 1969a,b).

Table 4. This table gives electron-, proton- and singly charged helium-impact broadening parameters for Si VI lines calculated using SUPERSTRUCTURE oscillator strength, for a perturber density of 10^{17} cm^{-3} and temperature of 50 000 to 800 000 K. Transitions, averaged wavelength for the multiplet (in Å) and parameter C are also given. This parameter when divided with the corresponding Stark width gives an estimate for the maximal perturber density for which the line may be treated as isolated. w_e: electron-impact full Stark width at half-maximum; d_e: electron-impact Stark shift; $w_H{}^+$: proton-impact full Stark width at half-maximum; $d_H{}^+$: proton-impact Stark shift; $w_{He}{}^+$: singly charged helium-impact full Stark width at half-maximum; $d_{He}{}^+$: singly charged helium-impact Stark shift; w_{MSE}: electron-impact full Stark width at half-maximum calculated by Dimitrijević (1993) using modified semi-empirical formula (Dimitrijević & Konjević 1980).

Transition	T (K)	w_e	d_e	w_H^+	d_H^+	w_{He}^+	d_{He}^+	w_{MSE}
Si VI 3S-3P	50000	0.750E-02	−0.577E-04	0.360E-04	−0.260E-04	0.687E-04	−0.500E-04	0.415E-02
1226.7 Å	100000	0.532E-02	−0.739E-04	0.897E-04	−0.516E-04	0.173E-03	−0.103E-03	0.294E-02
$C = 0.11$E+21	200000	0.387E-02	−0.784E-04	0.177E-03	−0.920E-04	0.344E-03	−0.185E-03	0.212E-02
	400000	0.291E-02	−0.100E-03	0.269E-03	−0.139E-03	0.529E-03	−0.280E-03	0.169E-02
	800000	0.227E-02	−0.888E-04	0.347E-03	−0.189E-03	0.693E-03	−0.384E-03	0.147E-02
Si VI 3S-3P	50000	0.681E-02	−0.660E-04	0.346E-04	−0.294E-04	0.660E-04	−0.566E-04	0.375E-02
1187.2 Å	100000	0.486E-02	−0.841E-04	0.866E-04	−0.582E-04	0.167E-03	−0.116E-03	0.265E-02
$C = 0.67$E+20	200000	0.354E-02	−0.890E-04	0.171E-03	−0.102E-03	0.335E-03	−0.205E-03	0.191E-02
	400000	0.267E-02	−0.109E-03	0.262E-03	−0.150E-03	0.517E-03	−0.304E-03	0.152E-02
	800000	0.208E-02	−0.993E-04	0.340E-03	−0.203E-03	0.678E-03	−0.412E-03	0.132E-02
Si VI 3S′-3P′	50000	0.716E-02	−0.644E-04	0.471E-04	−0.212E-04	0.899E-04	−0.409E-04	0.389E-02
1228.8 Å	100000	0.509E-02	−0.599E-04	0.113E-03	−0.424E-04	0.219E-03	−0.842E-04	0.275E-02
$C = 0.72$E+20	200000	0.370E-02	−0.615E-04	0.213E-03	−0.771E-04	0.416E-03	−0.155E-03	0.198E-02
	400000	0.278E-02	−0.770E-04	0.314E-03	−0.119E-03	0.618E-03	−0.241E-03	0.158E-02
	800000	0.216E-02	−0.691E-04	0.389E-03	−0.164E-03	0.774E-03	−0.331E-03	0.137E-02
Si VI 3S′-3P′	50000	0.572E-02	−0.376E-04	0.399E-04	−0.131E-04	0.762E-04	−0.252E-04	0.312E-02
1087.4 Å	100000	0.408E-02	−0.358E-04	0.948E-04	−0.263E-04	0.183E-03	−0.521E-04	0.220E-02
$C = 0.56$E+20	200000	0.297E-02	−0.371E-04	0.176E-03	−0.487E-04	0.344E-03	−0.978E-04	0.158E-02
	400000	0.223E-02	−0.460E-04	0.256E-03	−0.774E-04	0.505E-03	−0.156E-03	0.126E-02
	800000	0.174E-02	−0.413E-04	0.313E-03	−0.107E-03	0.623E-03	−0.216E-03	0.109E-02
Si VI 3S-3P	50000	0.842E-02	−0.107E-03	0.361E-04	−0.374E-04	0.690E-04	−0.721E-04	0.436E-02
1314.8 Å	100000	0.598E-02	−0.118E-03	0.927E-04	−0.740E-04	0.179E-03	−0.147E-03	0.309E-02
$C = 0.13$E+21	200000	0.434E-02	−0.116E-03	0.189E-03	−0.129E-03	0.368E-03	−0.260E-03	0.224E-02
	400000	0.326E-02	−0.148E-03	0.295E-03	−0.190E-03	0.582E-03	−0.384E-03	0.180E-02
	800000	0.254E-02	−0.134E-03	0.392E-03	−0.256E-03	0.784E-03	−0.519E-03	0.155E-02
Si VI 3S-3P	50000	0.656E-02	−0.682E-04	0.295E-04	−0.254E-04	0.563E-04	−0.488E-04	0.343E-02
1145.4 Å	100000	0.466E-02	−0.797E-04	0.745E-04	−0.503E-04	0.144E-03	−0.999E-04	0.242E-02
$C = 0.10$E+21	200000	0.338E-02	−0.787E-04	0.149E-03	−0.887E-04	0.290E-03	−0.178E-03	0.175E-02
	400000	0.254E-02	−0.102E-03	0.229E-03	−0.132E-03	0.452E-03	−0.267E-03	0.141E-02
	800000	0.198E-02	−0.909E-04	0.300E-03	−0.179E-03	0.599E-03	−0.364E-03	0.122E-02
Si VI 2P-3S	50000	0.209E-04	−0.851E-06	0.885E-08	0.227E-06	0.169E-07	0.438E-06	0.154E-04
100.2 Å	100000	0.138E-04	0.531E-06	0.665E-07	0.449E-06	0.128E-06	0.891E-06	0.109E-04
$C = 0.73$E+18	200000	0.976E-05	0.815E-06	0.288E-06	0.780E-06	0.571E-06	0.157E-05	0.791E-05
	400000	0.740E-05	0.981E-06	0.709E-06	0.114E-05	0.143E-05	0.231E-05	0.628E-05
	800000	0.577E-05	0.918E-06	0.131E-05	0.153E-05	0.262E-05	0.311E-05	0.541E-05
Si VI 2P-3D	50000	0.267E-04	−0.113E-05	0.147E-06	−0.328E-07	0.280E-06	−0.631E-07	0.194E-04
83.8 Å	100000	0.179E-04	−0.289E-06	0.365E-06	−0.663E-07	0.703E-06	−0.131E-06	0.137E-04
$C = 0.77$E+18	200000	0.130E-04	−0.490E-07	0.715E-06	−0.128E-06	0.139E-05	−0.257E-06	0.969E-05
	400000	0.967E-05	−0.134E-06	0.108E-05	−0.221E-06	0.212E-05	−0.444E-06	0.747E-05
	800000	0.741E-05	−0.802E-07	0.139E-05	−0.321E-06	0.277E-05	−0.647E-06	0.631E-05
Si VI 2P-3D	50000	0.266E-04	−0.116E-05	0.147E-06	−0.165E-07	0.280E-06	−0.318E-07	0.193E-04
83.8 Å	100000	0.174E-04	−0.200E-06	0.364E-06	−0.335E-07	0.701E-06	−0.664E-07	0.137E-04
$C = 0.35$E+18	200000	0.125E-04	0.533E-07	0.712E-06	−0.662E-07	0.139E-05	−0.132E-06	0.967E-05
	400000	0.929E-05	−0.605E-08	0.107E-05	−0.121E-06	0.211E-05	−0.243E-06	0.748E-05
	800000	0.709E-05	0.492E-07	0.139E-05	−0.188E-06	0.275E-05	−0.380E-06	0.631E-05
Si VI 2P-3S′	50000	0.202E-04	−0.613E-06	0.106E-07	0.247E-06	0.202E-07	0.475E-06	0.139E-04
96.7 Å	100000	0.135E-04	0.635E-06	0.787E-07	0.484E-06	0.152E-06	0.961E-06	0.984E-05
$C = 0.45$E+18	200000	0.958E-05	0.879E-06	0.317E-06	0.831E-06	0.629E-06	0.167E-05	0.712E-05
	400000	0.728E-05	0.105E-05	0.752E-06	0.121E-05	0.151E-05	0.244E-05	0.564E-05
	800000	0.570E-05	0.993E-06	0.139E-05	0.158E-05	0.278E-05	0.321E-05	0.486E-05

Table 4 – *continued*

Transition	T (K)	w_e	d_e	w_H^+	d_H^+	w_{He}^+	d_{He}^+	w_{MSE}
Si VI 2P-3D′	50000	0.277E-04	−0.116E-05	0.212E-06	−0.144E-07	0.405E-06	−0.277E-07	0.178E-04
81.2 Å	100000	0.176E-04	−0.202E-06	0.504E-06	−0.291E-07	0.972E-06	−0.578E-07	0.126E-04
$C = 0.58$E+18	200000	0.127E-04	0.363E-07	0.935E-06	−0.577E-07	0.183E-05	−0.115E-06	0.902E-05
	400000	0.937E-05	−0.255E-07	0.136E-05	−0.106E-06	0.268E-05	−0.213E-06	0.710E-05
	800000	0.716E-05	0.289E-07	0.166E-05	−0.166E-06	0.330E-05	−0.336E-06	0.612E-05
Si VI 2P-3D′	50000	0.273E-04	−0.119E-05	0.214E-06	−0.231E-07	0.408E-06	−0.445E-07	0.179E-04
81.2 Å	100000	0.174E-04	−0.260E-06	0.508E-06	−0.468E-07	0.981E-06	−0.928E-07	0.126E-04
$C = 0.59$E+18	200000	0.125E-04	−0.196E-07	0.942E-06	−0.916E-07	0.184E-05	−0.183E-06	0.904E-05
	400000	0.923E-05	−0.845E-07	0.137E-05	−0.161E-06	0.270E-05	−0.324E-06	0.710E-05
	800000	0.704E-05	−0.422E-07	0.167E-05	−0.239E-06	0.332E-05	−0.483E-06	0.610E-05
Si VI 2P-3D′	50000	0.270E-04	−0.107E-05	0.219E-06	−0.148E-07	0.419E-06	−0.285E-07	0.179E-04
81.0 Å	100000	0.175E-04	−0.202E-06	0.520E-06	−0.299E-07	0.100E-05	−0.594E-07	0.127E-04
$C = 0.60$E+18	200000	0.126E-04	0.317E-07	0.960E-06	−0.592E-07	0.187E-05	−0.118E-06	0.905E-05
	400000	0.935E-05	−0.301E-07	0.139E-05	−0.109E-06	0.274E-05	−0.218E-06	0.711E-05
	800000	0.714E-05	0.195E-07	0.169E-05	−0.170E-06	0.336E-05	−0.343E-06	0.609E-05
Si VI 3S′-3P′	50000	0.439E-02	−0.460E-04	0.328E-04	−0.168E-04	0.626E-04	−0.324E-04	0.241E-02
918.8 Å	100000	0.314E-02	−0.597E-04	0.773E-04	−0.333E-04	0.149E-03	−0.662E-04	0.171E-02
$C = 0.40$E+20	200000	0.229E-02	−0.606E-04	0.142E-03	−0.586E-04	0.278E-03	−0.118E-03	0.123E-02
	400000	0.173E-02	−0.737E-04	0.206E-03	−0.869E-04	0.407E-03	−0.176E-03	0.976E-03
	800000	0.135E-02	−0.698E-04	0.252E-03	−0.118E-03	0.500E-03	−0.239E-03	0.845E-03
Si VI 3S-3P	50000	0.510E-02	−0.414E-04	0.244E-04	−0.159E-04	0.465E-04	−0.306E-04	0.263E-02
995.6 Å	100000	0.362E-02	−0.514E-04	0.604E-04	−0.317E-04	0.116E-03	−0.630E-04	0.186E-02
$C = 0.75$E+20	200000	0.263E-02	−0.509E-04	0.118E-03	−0.569E-04	0.230E-03	−0.114E-03	0.134E-02
	400000	0.198E-02	−0.655E-04	0.179E-03	−0.864E-04	0.352E-03	−0.175E-03	0.107E-02
	800000	0.155E-02	−0.589E-04	0.230E-03	−0.118E-03	0.458E-03	−0.240E-03	0.923E-03

When the impact approximation is not valid, the ion broadening contribution may be estimated by using the quasi-static approach (Griem 1974; Sahal-Bréchot 1991; Ben Nessib, Ben Lakhdar & Sahal-Bréchot 1996).

Unfortunately, no experimental data are yet available for the Stark broadening parameters so that the comparison is made only with Dimitrijević's (1993) results obtained using the modified semi-empirical formula (Dimitrijević & Konjević 1980). All our values are greater than Dimitrijević's ones. The ratio w_e/w_{MSE} shows in average an agreement within 56 per cent. Low disagreements are usually found for resonance lines, for example for the spectral line $2p^5\ ^2P^\circ$-$2p^4(^3P)3s\ ^2P$ ($\lambda = 100$, 2 Å) the ratio w_e/w_{MSE} is only 1.06 for $T = 800\,000$ K.

4 STARK BROADENING EFFECT IN WHITE DWARF ATMOSPHERES

White dwarfs are separated in two distinct spectroscopic sequences, the DA and non-DA white dwarfs. The former ones display a pure hydrogen (optical) spectrum. The second, helium-rich sequence comprise DO ($T_{eff} > 45\,000$ K), DB ($11\,000 < T_{eff} < 30\,000$ K) and DC ($T_{eff} < 11\,000$ K) white dwarfs. At the highest effective temperatures the DOs are connected to the helium, carbon and oxygen-rich PG 1159.

Silicon, in various ionization stages, is present in the DO white dwarf atmospheres (Werner et al. 1995). We used our results for Stark widths to examine the importance of electron-impact broadening in atmospheres of DO white dwarfs for a trace element like Si VI. Model atmospheres were taken from Wesemael (1981).

In hot star atmospheres, besides electron-impact broadening (Stark broadening), the important broadening mechanism is a Doppler (thermal) one as well as the broadening due to the turbulence and stellar rotation. Other types of spectral line broadening, such as van der Waals, resonance and natural broadening, are usually negligible. For a Doppler-broadened spectral lines, the intensity distribution is not Lorentzian as for electron-impact broadening but Gaussian, whose full half-width of the spectral lines may be determined by the equation (see e.g. Konjević 1999)

$$w_D\,[\text{Å}] = 7.16 \times 10^{-7} \lambda\,[\text{Å}] \sqrt{\frac{T\,[\text{K}]}{M_{Si}}}, \quad (6)$$

where atomic weight for silicon is $M_{Si} = 28.1$ au.

The importance of Stark broadening in stellar atmospheres is illustrated in Figs 1–4. In Fig. 1 Stark (FWHM) and Doppler widths for Si VI $2p^4(^3P)3s\ ^2P$-$2p^4(^3P)3p\ ^2D^\circ$ ($\lambda = 1226$, 7 Å) spectral line as a function of atmospheric layer temperatures are shown. Stark widths are shown for six atmospheric models with effective temperature $T_{eff} = 50\,000$–$100\,000$ K and logarithm of surface gravity $\log g = 8$. We can see in Fig. 1 that Stark broadening is more important than Doppler broadening for deeper atmospheric layers for all effective temperatures. For white dwarf with effective temperature $T_{eff} = 50\,000$ K, Stark and Doppler widths are equal for temperature layer $T \approx 70\,000$ K, and for white dwarf with effective temperature $T_{eff} = 100\,000$ K, Stark and Doppler are equal for temperature layer $T \approx 125\,000$ K. One should take into account, however, that even when the Doppler width is larger than Stark width, due to different behaviour of Gaussian and Lorentzian distributions, Stark broadening may be important in line wings. In Fig. 2 we present Stark (FWHM) and Doppler widths for Si VI ($\lambda = 1226$, 7 Å) spectral line

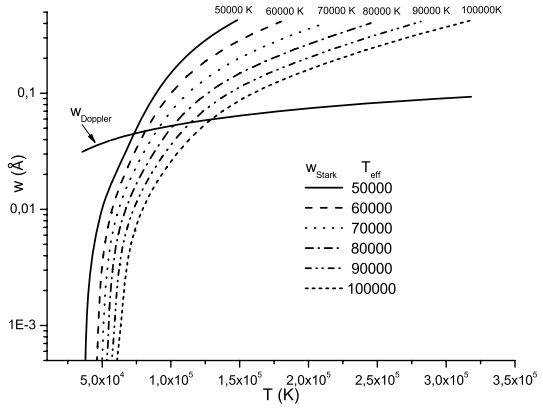

Figure 1. Stark and Doppler widths for Si VI $2p^4(^3P)3s\ ^2P\text{-}2p^4(^3P)3p\ ^2D^\circ$ ($\lambda = 1226,7$ Å) spectral line as a function of atmospheric layer temperatures. Stark widths are shown for six atmospheric models with effective temperature $T_{\rm eff} = 50\,000$–$100\,000$ K and $\log g = 8$.

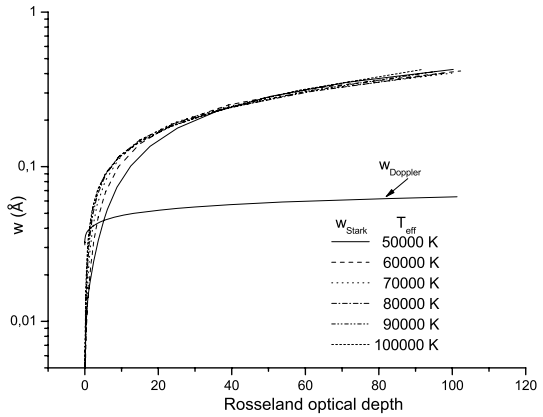

Figure 2. Stark and Doppler widths for Si VI $2p^4(^3P)3s\ ^2P\text{-}2p^4(^3P)3p\ ^2D^\circ$ ($\lambda = 1226,7$ Å) spectral line as a function of Rosseland optical depth. Stark widths are shown for six atmospheric models with effective temperature $T_{\rm eff} = 50\,000$–$100\,000$ K and $\log g = 8$.

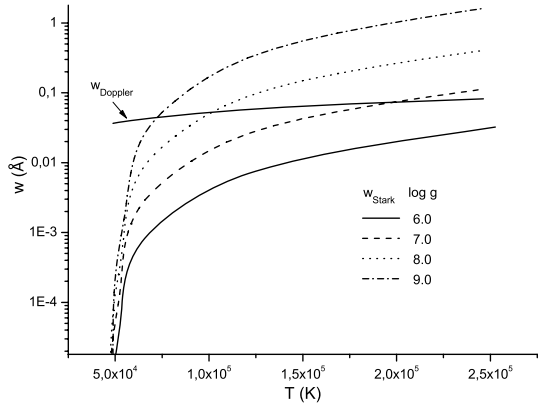

Figure 3. Stark and Doppler widths for Si VI $2p^4(^3P)3s\ ^2P\text{-}2p^4(^3P)3p\ ^2D^\circ$ ($\lambda = 1226,7$ Å) spectral line as a function of atmospheric layer temperatures. Stark widths are shown for four values of model gravity $\log g = 6$–9, $T_{\rm eff} = 80\,000$ K.

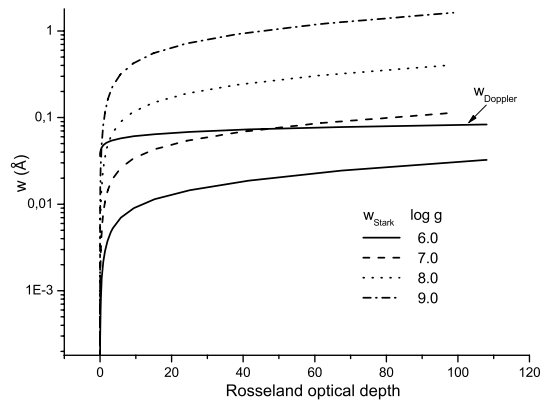

Figure 4. Stark and Doppler widths for Si VI $2p^4(^3P)3s\ ^2P\text{-}2p^4(^3P)3p\ ^2D^\circ$ ($\lambda = 1226,7$ Å) spectral line as a function of Rosseland optical depth. Stark widths are shown for four values of model gravity $\log g = 6$–9, $T_{\rm eff} = 80\,000$ K.

as a function of Rosseland optical depth for the same atmospheric models as in Fig. 1.

The dependence of Stark and Doppler broadening in atmospheric layer temperature for four values of surface gravity is shown in Fig. 3. Atmospheric models used here have effective temperature $T_{\rm eff} = 80\,000$ K. For stellar atmosphere with higher values of surface gravity ($\log g = 8$–9), Stark broadening is significantly larger than Doppler one. For stellar atmosphere with surface gravity $\log g = 7$, Stark widths are comparable to Doppler widths only for deeper hot atmospheric layer. For stellar atmospheres with $\log g = 6$, Doppler broadening is dominant for all atmospheric layers.

5 CONCLUSIONS

In present work we have calculated *ab initio* energy levels for the eight lowest configurations of Si VI. We have also calculated transition probabilities and oscillator strengths for 288 transitions. These data are useful for interpretation of laboratory and astrophysical spectra, since the reliability of the predicted emergent spectra and the derived spectral diagnoses is directly influenced by the quality of radiative data. The method used here is semirelativistic one, the relativistic corrections are included by using the Breit–Pauli Hamiltonian as perturbation to the non-relativistic Hamiltonian. To make fully relativistic calculation, the GRASP code (Dyall et al. 1989) can be used. One should note also that Martin & Wiese (1976) investigated the influence of relativistic effects on the oscillator strength values for the lithium isoelectronic sequences and found that the influence is not important on investigated *f* values for the ionization degrees investigated in our work. We have reported results of Stark broadening parameter calculations for 15 spectral lines of Si VI. For the simple spectrum, the Stark broadening parameters of different lines are nearly the same within a multiplet (Wiese & Konjević 1992). Consequently, we have used the averaged atomic data for a multiplet as a whole and calculate the corresponding Stark widths and shifts. We see that using the SUPERSTRUCTURE code one obtains a set of energy levels and oscillator strengths, enabling a calculation of Stark broadening parameters when other theoretical and experimental data do not exist. The Stark broadening parameters obtained here, contribute to the creation of a set of such data for as large as possible number of spectral lines, of significance for a number of problems in astrophysical, laboratory and technological plasma research. Our analysis of the influence of Stark broadening on Si VI

($\lambda = 1226,7$ Å) spectral line for stellar plasma conditions demonstrates the importance of this broadening mechanism for hot, high gravity star atmospheres, as for example DO white dwarfs.

ACKNOWLEDGMENTS

We would like to thank C. J. Zeippen for providing his version of SUPERSTRUCTURE code. This work is a part of the projects 146001 'Influence of Collisional Processes on Astrophysical Plasma Line Shapes' and 146002 'Astrophysical Spectroscopy of Extragalactic Objects' supported by the Ministry of Science of Serbia.

REFERENCES

Bates D. R., Damgaard A., 1949, Philos. Trans. R. Soc. Lond. A, 242, 101
Ben Nessib N., Ben Lakhdar Z., Sahal-Bréchot S., 1996, Phys. Scr., 54, 608
Ben Nessib N., Dimitrijević M. S., Sahal-Bréchot S., 2004, A&A, 423, 397
Casassus S., Roche P. F., Barlow M. J., 2000, MNRAS, 314, 657
Coutinho L. H., Trigueiros A. G., 1999, ApJS, 121, 591
Dimitrijević M. S., 1993, A&AS, 100, 237
Dimitrijević M. S., Konjević N., 1980, J. Quant. Spectrosc. Radiat. Transfer, 24, 451
Dimitrijević M. S., Sahal-Bréchot S., 1984, J. Quant. Spectrosc. Radiat. Transfer, 31, 301
Dimitrijević M. S., Sahal-Bréchot S., 1996, Phys. Scr., 54, 50
Dimitrijević M. S., Sahal-Bréchot S., Bommier V., 1991, A&AS, 89, 581
Dimitrijević M. S., Ryabchikova T., Simić Z., Popović L.Č., Dačić M., 2007, A&A, 469, 681
Dyall K. G., Grant I. P., Johnson C. T., Parpia F. A., Plummer E. P., 1989, Comput. Phys. Commun., 55, 424
Eissner W., Jones M., Nussbaumer H., 1974, Comput. Phys. Commun., 8, 270
Fleurier C., Sahal-Bréchot S., Chapelle J., 1977, J. Quant. Spectrosc. Radiat. Transfer, 17, 595
Froese Fischer C., Tachiev G., 2004, At. Data Nucl. Data Tables, 87, 1
Griem H. R., 1974, Spectral Line Broadening by Plasmas. McGraw-Hill, New York
Hamdi R., Ben Nessib N., Dimitrijević M. S., Sahal-Bréchot S., 2007, ApJS, 170, 243
Konjević N., 1999, Phys. Rep., 316, 339
Martin G. A., Wiese W. L., 1976, J. Phys. Chem. Ref. Data, 5, 537
Nussbaumer H., Storey J. P., 1978, A&A, 64, 139
Popović L.Č., Simić S., Milovanović N., Dimitrijević M. S., 2001, ApJS, 135, 109
Sahal-Bréchot S., 1969a, A&A, 1, 91
Sahal-Bréchot S., 1969b, A&A, 2, 322
Sahal-Bréchot S., 1974, A&A, 35, 319
Sahal-Bréchot S., 1991, A&A, 245, 322
Savin D. W., 2001, in Ferland G., Savin D. W., eds, ASP Conf. Ser. Vol. 247, Spectroscopic Challenges of Photoionized Plasmas. Astron. Soc. Pac., San Francisco, p. 167
Uzelac N. I., Glenzer S., Konjević N., Hey J. D., Kunze H. J., 1993, Phys. Rev. E, 47, 3623
Werner K., Dreizler S., Wolff B., 1995, A&A, 298, 567
Wesemael F., 1981, ApJS, 45, 177
Wiese W. L., Konjević N., 1992, J. Quant. Spectrosc. Radiat. Transfer, 47, 185
Zeippen C. J., Seaton M. J., Morton D. C., 1977, MNRAS, 181, 527

This paper has been typeset from a TEX/LATEX file prepared by the author.

Mon. Not. R. Astron. Soc. **396,** 2201–2210 (2009) doi:10.1111/j.1365-2966.2009.14870.x

The total and relative contribution of the relevant absorption processes to the opacity of DB white dwarf atmospheres in the UV and VUV regions

Lj. M. Ignjatović,[1,2⋆] A. A. Mihajlov,[1,2] N. M. Sakan,[1] M. S. Dimitrijević[2,3] and A. Metropoulos[4]

[1]*Institute of Physics, PO Box 57, 11001 Belgrade, Serbia*
[2]*Isaac Newton Institute of Chile, Yugoslavia Branch, Volgina 7, 11160 Belgrade 74, Serbia*
[3]*Astronomical Observatory, Volgina 7, 11160 Belgrade 74, Serbia*
[4]*Theoretical and Physical Chemistry Institute, National Hellenic Research Foundation, Athens, Greece*

Accepted 2009 April 3. Received 2009 February 3; in original form 2008 November 12

ABSTRACT

The main aim of this work is to estimate the total contribution of the processes of He_2^+ molecular ion photodissociation and $He + He^+$ collisional absorption charge exchange to the opacity of DB white dwarf atmospheres, and compare this with the contribution of He^- and other relevant radiative absorption processes included in standard models.

The method for the calculations of the molecular ion He_2^+ photodissociation cross-sections is based on the dipole approximation and quantum-mechanical treatment of the internuclear motion, while the quasi-classical method for describing absorption processes in $He + He^+$ collisions is based on the quasi-static approximation.

Absorption coefficients are calculated in the region $50\,\mathrm{nm} \leq \lambda \leq 850\,\mathrm{nm}$ and compared with the corresponding coefficients of other relevant absorption processes; the calculations of the optical depth of the atmosphere layers considered are performed in the far-UV and VUV regions; the contribution of the relevant absorption processes to the opacity of DB white dwarf atmospheres is examined.

We examined the spectral ranges in which the total He_2^+ and He^- absorption processes dominate in particular layers of DB white dwarf atmospheres. In addition, we show that in the region of $\lambda \lesssim 70\,\mathrm{nm}$ the process of H(1s) atom photoionization is also important, in spite of the fact that the ratio of hydrogen and helium abundances in the DB white dwarf atmosphere considered is $1{:}10^5$.

Key words: atomic processes – molecular processes – radiation mechanisms: general – radiative transfer – stars: atmospheres.

1 INTRODUCTION

The main aim of this work is to obtain a realistic estimation of the total and relative contribution of relevant radiative processes to the opacity, caused by continuous absorption in the far-UV and VUV regions, of particular layers within some DB white dwarf atmospheres, models for which are given in Koester (1980). Namely, such an estimation could be useful for the interpretation of real continual stellar spectra.

Calamida et al. (2008) specified the most important processes contributing to white dwarf absorption coefficients, and the processes involving helium quoted by him, relevant for helium-rich DB white dwarfs, are bound–free absorption of neutral helium and free–free absorption of He^-, considered e.g. by John (1994). Previously, and even now, for the DB white dwarf atmosphere conditions considered here ($T_{\rm eff} = 12\,000$–$14\,000\,\mathrm{K}, \log g = 7$–$8$), the more important of these two processes as a source of continuous absorption is the free–free absorption of He^-, hereinafter named the He^- absorption process. Previously, for the DB white dwarf atmospheres considered ($T_{\rm eff} = 12\,000$–$14\,000\,\mathrm{K}, \log g = 7$–$8$) as the main source of the continuous absorption, the He^- absorption process was treated as follows:

$$\epsilon_\lambda + \mathrm{He} + \mathrm{e} \Longrightarrow \mathrm{He} + \mathrm{e}', \tag{1}$$

where ϵ_λ is the energy of a photon with wavelength λ, and e and e′ denote the free electron before and after collision with the He atom. Besides the He^- absorption process, the bound–free absorption processes are usually included, as mentioned by Calamida et al.

⋆E-mail: ljuba@phy.bg.ac.yu

(2008), including the other relevant reaction channel:

$$\epsilon_\lambda + \begin{cases} \mathrm{He}^*(n, L, S) \\ \mathrm{He}^+ + \mathrm{e} \end{cases} \Longrightarrow \mathrm{He}^+ + \mathrm{e}', \tag{2}$$

where $\mathrm{He}^*(n, L, S)$ is the helium atom in the excited state, n the corresponding principal quantum number, and L and S the quantum numbers of orbital momentum and spin. Continuous absorption opacity due to the processes of He_2^+ molecular ion photodissociation can be written as

$$\epsilon_\lambda + \mathrm{He}_2^+ \Longrightarrow \mathrm{He} + \mathrm{He}^+, \tag{3}$$

and $\mathrm{He} + \mathrm{He}^+$ collisional absorption charge exchange as

$$\epsilon_\lambda + \mathrm{He} + \mathrm{He}^+ \Longrightarrow \begin{cases} \mathrm{He}^+ + \mathrm{He} \\ \mathrm{He} + \mathrm{He}^+ \end{cases}, \tag{4}$$

where $\mathrm{He} \equiv \mathrm{He}(1s^2)$, $\mathrm{He}^+ \equiv \mathrm{He}^+(1s)$ and $\mathrm{He}_2^+ \equiv \mathrm{He}_2^+(X^2\Sigma_u^+)$ were neglected in DB white dwarf atmosphere modelling up to the beginning of the 1990s. However, Mihajlov & Dimitrijević (1992) and Mihajlov, Dimitrijević & Ignjatović (1994a), using the DB white dwarf atmosphere models of Koester (1980), demonstrated that at least for $T_{\mathrm{eff}} < 16\,000$ K these processes should contribute to the opacity in the optical region. In these papers the absorption coefficients for both processes (3) and (4) have been determined within the semiclassical (quasi-static) method developed by Bates (1952).

Processes (3) and (4) were considered later in Stancil (1994) but, in contrast to Mihajlov & Dimitrijević (1992) and Mihajlov et al. (1994a), the photodissociation channel (3) was treated completely quantum-mechanically. A significant result of this paper was the inclusion of the absorption coefficients for processes (3) and (4) obtained by Stancil (1994) in modern DB white dwarf atmosphere modelling codes (Bergeron, Wesemael & Beauchamp 1995; Beauchamp et al. 1996; Beauchamp, Wesemael & Bergeron 1997). This inclusion was probably accelerated by the fact that Stancil (1994) suggest the absolute domination of processes (3) and (4), at least in the region shown ($\lambda \leq 500$ nm), in comparison with the He^- absorption processes (1). In connection with this, one should emphasize that such a suggestion is based only on fig. 7 of Stancil (1994), in relation to the model with $\log g = 8, T_{\mathrm{eff}} = 12\,000$ K from Koester (1980). Moreover, this figure shows the behaviour with λ of the He^- and He_2^+ total absorption coefficients determined for only one value of the Rosseland optical depth ($\tau = 1$). However, one can see in this figure that the He^+ density is 10 times larger than the electron density, so that the curve of the He_2^+ total absorption coefficient is obtained with He^+ ion densities (needed for the calculation) ten times larger than in local thermodynamic equilibrium (LTE), which is assumed in the basic model used (Koester 1980). According to this, the real curve should lie much lower and cross the curve of the He^- absorption coefficient. Consequently, the question of the relative importance of particular absorption processes in DB white dwarf atmospheres remains open. This justifies the fact that in some modern investigations of DB white dwarf atmospheres these processes are neglected.

The results from Mihajlov et al. (1994a), obtained for one Koester model ($\log g = 8$ and $T_{\mathrm{eff}} = 12\,000$ K), have already provided a more realistic picture of the relative importance of He^- and He_2^+ total absorption processes, at least in the region $\lambda \geq 300$ nm. From these results follows the above-mentioned crossing of the curves for He^- and He_2^+ absorption coefficients. In a following paper (Mihajlov et al. 1995), the relative importance of He_2^+ and other relevant absorption processes in the region $\lambda \geq 200$ nm was examined for several of Koester's (1980) models ($T_{\mathrm{eff}} = 12\,000, 14\,000, 16\,000$ K, $\log g = 7, 8$). It was shown that, in all cases considered, the contribution to opacity of the processes of He_2^+ molecular ion photodissociation and $\mathrm{He} + \mathrm{He}^+$ collisional absorption charge exchange combined is close to or at least comparable with the contribution of the He^- absorption processes (1) and atomic absorption processes (2).

The continuation of our investigations of processes (3) and (4) was inspired by the results obtained in connection with the processes of H_2^+ molecular ion photodissociation and $\mathrm{H} + \mathrm{H}^+$ collisional absorption charge exchange in the solar atmosphere. Here, we recall that in Mihajlov & Dimitrijević (1986), Mihajlov, Dimitrijević & Ignjatović (1993) and Mihajlov et al. (1994b) the relative importance of the absorption processes was investigated:

$$\epsilon_\lambda + \mathrm{H}_2^+ \Longrightarrow \mathrm{H} + \mathrm{H}^+, \tag{5a}$$

$$\epsilon_\lambda + \mathrm{H} + \mathrm{H}^+ \Longrightarrow \begin{cases} \mathrm{H}^+ + \mathrm{H} \\ \mathrm{H} + \mathrm{H}^+ \end{cases}, \tag{5b}$$

where $\mathrm{H} \equiv \mathrm{H}(1s)$ and $\mathrm{H}_2^+ \equiv \mathrm{H}_2^+(X^2\Sigma_g^+)$, in the optical region of λ in the solar photosphere and lower chromosphere. The efficiency of these processes was compared with the efficiency of the known absorption processes that have already been treated in the literature (Mihalas 1978), namely

$$\epsilon_\lambda + \mathrm{H}^- \Longrightarrow \mathrm{H} + \mathrm{e}', \tag{6a}$$

$$\epsilon_\lambda + \mathrm{H} + \mathrm{e} \Longrightarrow \mathrm{H} + \mathrm{e}', \tag{6b}$$

$$\epsilon_\lambda + \begin{cases} \mathrm{H}^*(n) \\ \mathrm{H}^+ + \mathrm{e} \end{cases} \Longrightarrow \mathrm{H}^+ + \mathrm{e}', \tag{6c}$$

where H^- is the negative hydrogen ion in the ground state, and $\mathrm{H}^*(n)$ is the hydrogen atom in the excited state, with the principal quantum number $n \geq 2$. It was shown that the relative contribution of processes (5) to the opacity of the layers of the solar atmosphere considered in the visible and near-UV regions of continual spectra does not exceed 10–12 per cent. Such a relatively small contribution is a consequence of the presence of the highly efficient absorption process (6a) in the solar atmosphere. However, in Mihajlov et al. (2007) it was shown that the relative contribution of processes (5) to the opacity of particular layers of the solar atmosphere in the far-UV and VUV regions reaches almost 90 per cent of the total contribution of all concurrent processes (6a), (6b) and (6c). This result means that processes (5) in the short-wave region become equally as important as process (6a).

It should be noted in this context that in Mihajlov & Dimitrijević (1992) and Mihajlov et al. (1994a, 1995) it was shown that the relative contribution of processes (4) in some DB white dwarfs ($T_{\mathrm{eff}} = 12\,000$ K, $\log g = 8$) is around 50 per cent, i.e. several times larger than the related contribution of processes (5a) and (5b) in the solar atmosphere. This difference in comparison with the solar atmosphere is due to the absence in DB white dwarf atmospheres of a highly efficient absorption process similar to process (6a) in the solar atmosphere. The above-mentioned work suggests that the relative contribution of absorption processes (3) and (4) to the opacity of DB white dwarf atmospheres in the far-UV and VUV regions ($\lambda < 200$ nm) of continual spectra could be considerably larger than the relative contribution of absorption processes (5) to the opacity of the solar atmosphere.

For this reason, we continued our previous investigations (Mihajlov & Dimitrijević 1992; Mihajlov et al. 1994a, 1995) of

processes (3) and (4) in DB white dwarf atmospheres in the far-UV and VUV regions. In accordance with the aims of this paper, the temperature and particle densities in particular layers should be known. In spite of the fact that Koester's DB white dwarf atmospheric models were published in 1980, only recently were the data needed for such estimation presented, so that they are used for example by Marsh, Nelemans & Steeghs (2004).

In order to examine qualitatively the influence of absorption processes (3) and (4) on the opacity of DB white dwarf atmospheres, Koester's (1980) models with $T_{\rm eff} = 12\,000$ K and $\log g = 8$ and 7 and with $T_{\rm eff} = 14\,000$ K and $\log g = 8$ were used in this work. Here the necessary calculations of absorption coefficients characterizing processes (4) were performed. The determination of these coefficients was obtained from the potential curves of molecular ion He_2^+ in the $X^2\Sigma_u^+$ and $A^2\Sigma_g^+$ states, as well as the corresponding dipole matrix elements, which were precisely calculated during this research. These characteristics of He_2^+ are presented here.

In order to determine the relative efficiency of processes (4) in the UV and VUV regions for particular DB white dwarf atmosphere layers, the corresponding absorption coefficients will be compared with the absorption coefficients that characterize the concurrent processes (1) and (2) for 51 nm $\leq \lambda \leq$ 400 nm. The lower boundary of this region was taken as $\lambda = 51$ nm, which is close to the He atom ionization boundary $\lambda_{\rm He} \cong 50.14$ nm, below which the photoionization of the He atom absolutely dominates in comparison with all other absorption processes.

Also, we will consider here the hydrogen photoionization process

$$\epsilon_\lambda + {\rm H} \Longrightarrow {\rm H}^+ + {\rm e}'. \tag{7}$$

Although according to Koester (1980) the ratio of hydrogen and helium abundances in the considered DB white dwarf atmospheres is $1{:}10^5$, our estimations showed that process (7) could play a certain role for $\lambda < \lambda_{\rm H}$, where $\lambda_{\rm H} \cong 91.13$ nm is the H atom ionization boundary.

As a quantitative characteristic of the contribution of processes (4) to the opacity of a DB white dwarf atmosphere, the increase of the optical depth of particular atmosphere layers caused by these processes was taken here. The corresponding calculations were performed for each of the cases mentioned, in the same region of λ. Also, this increase was compared with the optical depth of the layers considered caused by absorption processes (4), (1), (2) and (7) together.

Here we used the models of DB white dwarf atmospheres from Koester (1980) already mentioned, since they provide all the required data on particle densities and temperatures, in particular DB white dwarf atmospheric layers. In all further discussion it was taken into account that these models assumed the existence of local thermodynamical equilibrium (LTE).

2 CHARACTERISTICS OF PHOTODISSOCIATION AND ION–ATOM ABSORPTION PROCESSES

2.1 The photodissociation cross-section

The photodissociation process (3) is characterized here by the corresponding average cross-section $\sigma_{\rm phd}(\lambda, T)$. This cross-section is defined by

$$\sigma_{\rm phd}(\lambda, T) = \frac{\sum_J \sum_v g_{v,J}\,(2J+1){\rm e}^{-E_{v,J}/(kT)}\,\sigma_{v,J}(\lambda)}{\sum_J \sum_v g_{v,J}\,(2J+1){\rm e}^{-E_{v,J}/(kT)}}, \tag{8}$$

where v and J are the vibrational and rotational quantum numbers of the individual rovibrational states (v, J) of the molecular ion $He_2^+(X^2\Sigma_u^+)$, $\sigma_{v,J}(\lambda)$ the partial photodissociation cross-sections of these states, $E_{v,j}$ and $g_{v,j}(2J+1)$ the corresponding energies with respect to the ground rovibrational state and statistical weights, while factor $g_{v,j}$ describes the influence of nuclear spin. Here we consider that this influence is negligible at temperatures much higher than room temperature (see e.g. Patch 1969; Lebedev & Presnyakov 2002). Since for DB white dwarf atmospheres temperatures $T \gtrsim 8000$ K are relevant, for further consideration we assume that $g_{v,j} = 1$.

Within the dipole approximation the partial cross-sections $\sigma_{v,j}(\lambda)$ are given by the expressions

$$\sigma_{v,J}(\lambda) = \frac{8\pi^3}{3\lambda}\left[\frac{J+1}{2J+1}|D_{E,J+1;v,J}|^2 + \frac{J}{2J+1}|D_{E,J-1;v,J}|^2\right], \tag{9}$$

where $D_{E,J+1;v,J}$ and $D_{E,J-1;v,J}$ are the radial matrix elements given by the relations

$$D_{E,J;v,J'} = < \Psi_{2;E,J'}(R)|D_{12}(R)|\Psi_{1;v,J}(R) >, \quad J = J' \pm 1, \tag{10}$$

$$D_{12}(R) = |\boldsymbol{D}_{12}(R)|, \qquad \boldsymbol{D}_{12}(R) = < 1|\boldsymbol{D}(R)|2 >, \tag{11}$$

where R is the internuclear distance, $\boldsymbol{D}(R)$ the operator of electron dipole momentum, and $|1\rangle \equiv X^2\Sigma_u^+$ and $|2\rangle \equiv A^2\Sigma_g^+$ are the ground and first excited electronic states of the molecular ion He_2^+ with the potential curves $U_1(R)$ and $U_2(R)$, respectively. $\Psi_{1;v,j}(R)$ and $\Psi_{2;E,J'}(R)$ denote the adiabatic nuclear radial wavefunctions of the bound state (v, J) in the potential $U_1(R)$ and the continual state (E, J') in the potential $U_2(R)$ respectively, with

$$E = E_{v,J} + \epsilon_\lambda. \tag{12}$$

It is assumed that the wavefunctions $\Psi_{1;v,j}(R)$ and $\Psi_{2;E,J'}(R)$ satisfy the standard orthonormalization conditions.

In the hydrogen case the whole problem was much simpler, because all the required characteristics of molecular ion H_2^+ were already well known for $0 \leq R \leq \infty$. However, in the helium case the situation was quite different: the calculation of $\sigma_{\rm phd}(\lambda, T)$ required the usage of incompatible data from different sources and, consequently, the introduction of additional approximations (e.g. the characteristics of the He_2^+ molecular ion are determined in Stancil, Bab & Dalgarno (1993) on the basis of data from six different articles). This situation has not changed until now.

That is why within this research a special effort was made to determine the potential energies $U_1(R)$ and $U_2(R)$ and the matrix element $D_{12}(R)$ consistently over a wide region of R. The calculations of these quantities were performed under D_{2h} symmetry using the MOLPRO package of programs (Werner et al. 2006). They were performed at the multi-reference configuration interaction (MRCI) level using multi-configuration self-consistent field (MCSCF) orbitals with the cc-pv5z basis set of Dunning (1989) and Kendall, Dunning & Harrison (1992). We started at the self-consistent field (SCF) level with the ground-state electron configuration $a_g^2 b_{1u}^1$. The active space at the MCSCF step contained $3a_g$ and $3b_{1u}$ orbitals without any closed or core orbitals (all three electrons were involved). The potential curves $U_1(R)$ and $U_2(R)$ obtained are presented in Fig. 1, and the dipole matrix element $D_{12}(R)$ in Fig. 2. Unfortunately, it is not possible to compare the potential curves presented in this paper with the potential curves used in Stancil et al. (1993) and Stancil (1994), since they are not given there. We note that in Stancil et al. (1993) and Stancil (1994) the data from earlier

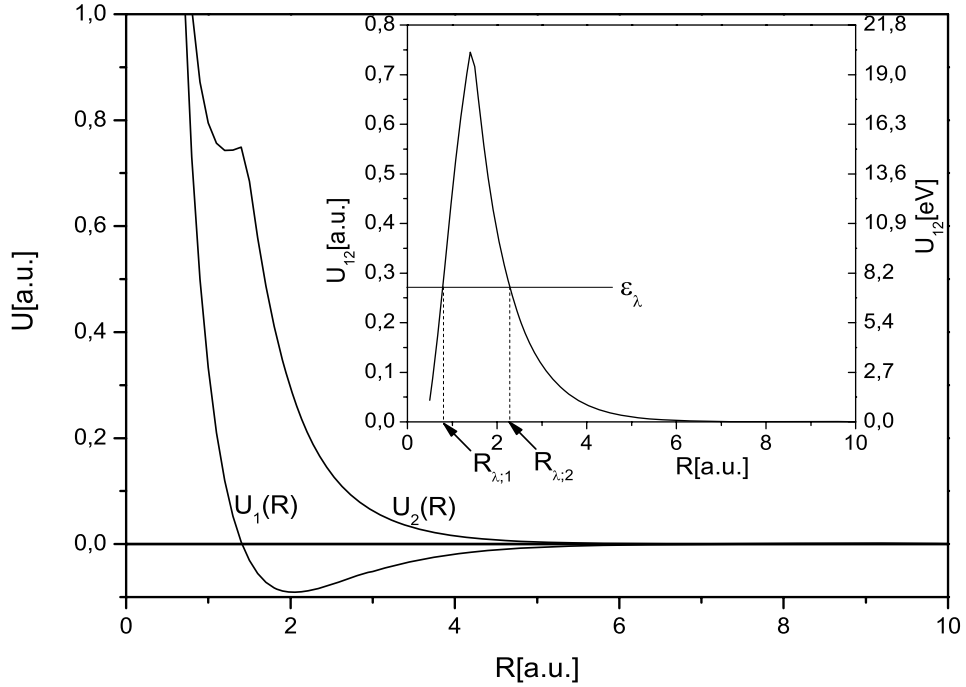

Figure 1. The potential curves of the molecular ion He_2^+: $U_1(R)$ corresponds to the ground electronic state $X^2\Sigma_u^+$, and $U_2(R)$ to the first excited electronic state $A^2\Sigma_g^+$; $U_{12}(R) = U_2(R) - U_1(R)$, 1 au $\approx$ 27.21 eV.

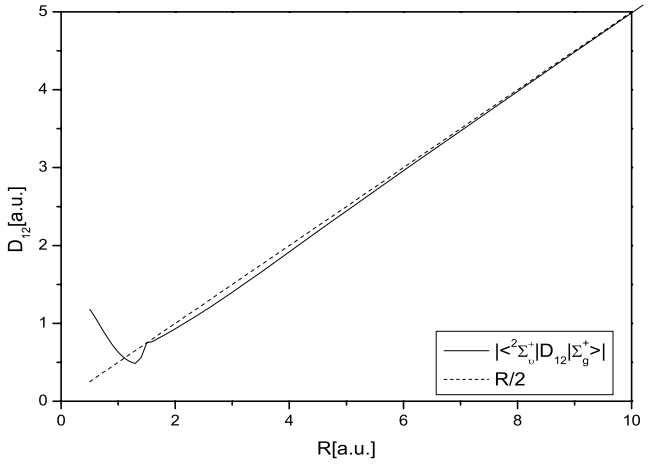

Figure 2. The matrix element $D_{12}(R)$ for the transition between the electronic states $X^2\Sigma_u^+$ and $A^2\Sigma_g^+$ of the ion He_2^+.

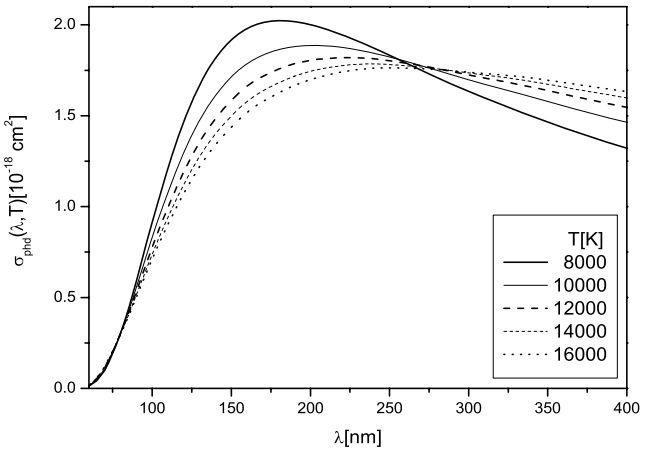

Figure 3. The behaviour of the average cross-section $\sigma_{phd}(\lambda, T)$ for photodissociation of the He_2^+ molecular ion, as a function of λ, for 8000 K $\leq T \leq$ 16 000 K.

papers of Metropoulos and coworkers (Metropoulos, Nicolaides & Buenker 1987; Metropoulos & Nicolaides 1991; Metropoulos et al. 1992) had an especially important role.

With the results obtained here, the required potential curves are self-consistent, since we now have the quantities $U_1(R)$, $U_2(R)$ and $D_{12}(R)$ within a wide region of R, which is enough for determination of the cross-section $\sigma_{phd}(\lambda, T)$ and the corresponding coefficient $K_{ia}^{(a)}(\lambda, T)$ for the photodissociation processes (3). The results obtained are illustrated in Fig. 3, where the behaviour of $\sigma_{phd}(\lambda, T)$ in the UV and VUV regions for T = 8000, 10 000, 12 000, 14 000 and 16 000 K is shown.

From Fig. 3 one can see that the behaviour of $\sigma_{phd}(\lambda, T)$ is similar to the behaviour of photodissociation cross-sections in the hydrogen case obtained in Mihajlov et al. (2007). Because of that in, the helium case one should also expect the increase of absorption caused by ion–atom processes (4) in the short-wave region (λ < 300 nm).

2.2 The partial absorption coefficients

The efficiencies of the photodissociation process (3) and the charge-exchange absorption process (4) are characterized separately by the partial spectral absorption coefficients $\kappa_{ia}^{(a)}(\lambda) \equiv \kappa_{ia}^{(a)}[\lambda; T, N(He_2^+)] = \sigma_{phd}(\lambda, T)N(He_2^+)$ and $\kappa_{ia}^{(b)}(\lambda) \equiv \kappa_{ia}^{(b)}[\lambda; T, N(He), N(He^+)]$ where T, $N(He_2^+)$, $N(He)$ and $N(He^+)$ are the local temperature and the densities of $He_2^+(X^2\Sigma_u^+)$, He and He^+ in the layer of the DB white dwarf atmosphere considered. Following our previous paper (Mihajlov et al. 2007) and assuming the existence of LTE, we will take the photodissociation coefficient $\kappa_{ia}^{(a)}(\lambda)$ in an equivalent form suitable for further consideration,

namely

$$\kappa_{\rm ia}^{\rm (a)}(\lambda) = K_{\rm ia}^{\rm (a)}(\lambda, T) N({\rm He}) {\rm N}({\rm He}^+), \tag{13}$$

$$K_{\rm ia}^{\rm (a)}(\lambda, T) = \sigma_{\rm phd}(\lambda, T)\, \chi_{\rm ia}(T), \tag{14a}$$

$$\chi_{\rm ia}(T) = \frac{N({\rm He}_2^+)}{N({\rm He}) {\rm N}({\rm He}^+)}. \tag{14b}$$

Here the photodissociation cross-section $\sigma_{\rm phd}(\lambda, T)$ is given by equations (8)–(12), and the quantity $\chi_{\rm ia}$, which contains the density $N({\rm He}_2^+)$, is determined from the law of mass action,

$$\chi^{-1}(T) = \left(\frac{\mu k T}{2\pi\hbar^2}\right)^{\frac{3}{2}} \frac{g({\rm He}) g({\rm H}^+)}{\sum\limits_J \sum\limits_v g_{v,J}(2J+1){\rm e}^{-E_{v,J}/(kT)}} \exp\left(-\frac{D}{kT}\right), \tag{15}$$

where μ and D are the reduced mass and the dissociation energy of the molecular ion He_2^+, and $g({\rm He}) = 1$ and $g({\rm He}^+) = 2$ are the statistical weights of the atom He and ion He^+.

The charge-exchange absorption coefficient $\kappa_{\rm ia}^{\rm (b)}(\lambda)$ is defined by

$$\kappa_{\rm ia}^{\rm (b)}(\lambda) = K_{\rm ia}^{\rm (b)}(\lambda, T) N({\rm He}) N({\rm He}^+), \tag{16}$$

where the coefficient $K_{\rm ia}^{\rm (b)}(\lambda, T)$ is determined here by the semiclassical method developed in Bates (1952) on the basis of the quasi-static approximation (see Mihajlov et al. 1994a; Mihajlov et al. 1995, 2007). Within this method, only the λ region where the equation

$$U_{12}(R) \equiv U_2(R) - U_1(R) = \epsilon_\lambda \tag{17}$$

has real roots is considered. Consequently, in the helium case the quasi-static method is applicable in the region $\lambda \gtrsim 62$ nm where this equation has two real roots (see Fig. 1), $R_{\lambda;1}$ and $R_{\lambda;2} > R_{\lambda;1}$. In Mihajlov et al. (1995), where the optical region of λ was treated, only the larger of these roots has been taken into account. However, in the far-UV and VUV regions both roots should be taken into account. Consequently, we will take here $K_{\rm ia}^{\rm (b)}(\lambda, T)$ in the form

$$K_{\rm ia}^{\rm (b)}(\lambda, T) = 0.62 \times 10^{-42} \sum_{i=1}^{2} \frac{\left[\dfrac{2D_{12}(R_{\lambda;i})}{e R_{\lambda;i}}\right]^2}{\gamma(R_{\lambda;i})} \times \left(\frac{R_{\lambda;i}}{a_0}\right)^4 \exp\left[-\frac{U_1(R_{\lambda;i})}{kT}\right] \xi(R_{\lambda;i}), \tag{18}$$

$$\gamma(R_{\lambda;i}) = \left| \frac{{\rm d}\ln\left[\dfrac{U_{12}(R)}{2Ry}\right]}{{\rm d}(R/a_0)} \right|_{R=R_{\lambda;i}}, \tag{19a}$$

$$\xi(R_{\lambda;i}) = \begin{cases} 1, & U_1(R_{\lambda;i}) \geq 0, \\ \dfrac{\Gamma\left(\dfrac{3}{2}; -\dfrac{U_1(R_{\lambda;i})}{kT}\right)}{\Gamma\left(\dfrac{3}{2}\right)}, & U_1(R_{\lambda;i}) < 0, \end{cases} \tag{19b}$$

where e and a_0 are the electron charge and the atomic unit of length, and $K_{\rm ia}^{\rm (b)}(\lambda, T)$ is expressed in $\rm cm^5$.

2.3 The total absorption coefficient

The efficiency of absorption processes (3) and (4) together is characterized by the total spectral absorption coefficient $\kappa_{\rm ia}(\lambda) \equiv \kappa_{\rm ia}[\lambda; T, N({\rm He}), N({\rm He}^+)]$ given by: $\kappa_{\rm ia}(\lambda) = \kappa_{\rm ia}^{\rm (a)}(\lambda) + \kappa_{\rm ia}^{\rm (b)}(\lambda)$. Using equations (13) and (16) for $\kappa_{\rm ia}^{\rm (a)}(\lambda)$ and $\kappa_{\rm ia}^{\rm (b)}(\lambda)$, we will take $\kappa_{\rm ia}(\lambda)$ in the form

$$\kappa_{\rm ia}(\lambda) = K_{\rm ia}(\lambda, T) N({\rm He}) N({\rm He}^+), \tag{20a}$$

$$K_{\rm ia}(\lambda, T) = K_{\rm ia}^{\rm (a)}(\lambda, T) + K_{\rm ia}^{\rm (b)}(\lambda, T), \tag{20b}$$

where $K_{\rm ia}^{\rm (a)}(\lambda, T)$ is given by equations (14) and (8), and $K_{\rm ia}^{\rm (b)}(\lambda, T)$ by equations (18) and (19). For the comparison of the efficiency of processes (4) with the efficiencies of the concurrent processes (1), (2) and (7) only the total absorption coefficients $\kappa_{\rm ia}(\lambda)$ and $K_{\rm ia}(\lambda, T)$ are needed. Table 1 illustrates the behaviour of the coefficient $K_{\rm ia}(\lambda, T)$ for $8000\,{\rm K} \leq T \leq 20\,000\,{\rm K}$ and $50\,{\rm nm} \leq \lambda \leq 850\,{\rm nm}$. Since the values of $K_{\rm ia}(\lambda, T)$ are determined by the new characteristics of the molecular ion $He_2^+(X^2\Sigma_u^+)$, this table covers not only the far-UV and VUV region but also the optical region.

The relative contribution of processes (3) and (4) can be characterized by the branch coefficients

$$X^{\rm (a)}(\lambda, T) = \frac{\kappa_{\rm ia}^{\rm (a)}(\lambda, T)}{\kappa_{\rm ia}(\lambda, T)} = \frac{K_{\rm ia}^{\rm (a)}(\lambda, T)}{K_{\rm ia}(\lambda, T)}, \tag{21a}$$

$$X^{\rm (b)}(\lambda, T) = \frac{\kappa_{\rm ia}^{\rm (b)}(\lambda, T)}{\kappa_{\rm ia}(\lambda, T)} \equiv 1 - X^{\rm (a)}(\lambda, T). \tag{21b}$$

The behaviour of $X^{\rm (a)}(\lambda, T)$ is illustrated by Table 2. This table shows that within the region of λ considered both processes (3) and (4) have to be taken into account together, since neither of them dominates.

The efficiency of processes (4) within a DB white dwarf atmosphere is compared here with the efficiency of the concurrent absorption processes (1) and (2), which are characterized by the spectral absorption coefficients $\kappa_{\rm ea}(\lambda)$ and $\kappa_{\rm ei}(\lambda)$, namely

$$\begin{aligned} \kappa_{\rm ea}(\lambda) &= K_{\rm ea}(\lambda, T) N_{\rm e} N({\rm He}), \\ \kappa_{\rm ei}(\lambda) &= K_{\rm a;ei}(\lambda, T) N_{\rm e} N({\rm He}^+), \end{aligned} \tag{22}$$

$$\begin{aligned} K_{\rm a;ei}(\lambda, T) &= \sum_{n\geq 2, L, S} \sigma_{nLS}(\lambda) \chi_{nLS}(T) + K_{\rm ei}(\lambda, T), \\ \chi_{nLS}(T) &= \frac{N[{\rm He}^*(n, L, S)]}{N_{\rm e} N({\rm He}^+)}. \end{aligned} \tag{23}$$

where $K_{\rm ea}(\lambda, T)$ and $K_{\rm ei}(\lambda, T)$ are the rate coefficients that describe absorption by (e + He) and (e + He^+) collision systems. $N_{\rm e}$ and $N[{\rm He}^*(n, L, S)]$ denote the densities of the free electrons and the excited atoms $He^*(n, L, S)$, and $\sigma_{nLS}(\lambda)$ the corresponding excited atom photoionization cross-section. It was found that in all cases considered the absorption processes (2) play a minor role in comparison with the electron–atom process (1). This is a consequence of the fact that helium plasma in the layers of the DB white dwarf atmosphere considered is weakly ionized. The relative efficiency of processes (4) with respect to processes (1) and (2) together is characterized by the parameter $F_{\rm He}(\lambda)$, defined by

$$\begin{aligned} F_{\rm He}(\lambda) &= \frac{\kappa_{\rm ia}(\lambda)}{\kappa_{\rm ea}(\lambda) + \kappa_{\rm ei}(\lambda)} \\ &= \frac{K_{\rm ia}(\lambda, T)\left[N({\rm He}^+)/N_{\rm e}\right]}{K_{\rm ea}(\lambda, T) + K_{\rm ei}(\lambda, T)\left[N({\rm He}^+)/N({\rm He})\right]}. \end{aligned} \tag{24}$$

In calculations of $F_{\rm He}(\lambda)$, the coefficient $K_{\rm ea}(\lambda, T)$ was determined by means of the data from Somerville (1965), and $K_{\rm a;ei}(\lambda, T)$ by means of expressions from Sobel'man (1979) for the partial

Table 1. The total absorption coefficient $K_{\rm ia}(\lambda, T)$.

λ (nm)	$K_{\rm ia}$(cm^5)						
	8000 K	10 000 K	12 000 K	14 000 K	16 000 K	18 000 K	20 000 K
50	.241E−44	.145E−44	.987E−45	.727E−45	.564E−45	.454E−45	.375E−45
55	.418E−43	.258E−43	.179E−43	.133E−43	.104E−43	.842E−44	.700E−44
60	.195E−41	.118E−41	.811E−42	.600E−42	.467E−42	.377E−42	.312E−42
65	.126E−40	.946E−41	.793E−41	.704E−41	.646E−41	.607E−41	.578E−41
70	.214E−40	.141E−40	.108E−40	.895E−41	.779E−41	.701E−41	.646E−41
80	.576E−40	.332E−40	.230E−40	.177E−40	.146E−40	.125E−40	.111E−40
90	.106E−39	.564E−40	.369E−40	.273E−40	.218E−40	.183E−40	.159E−40
100	.161E−39	.815E−40	.518E−40	.375E−40	.294E−40	.243E−40	.209E−40
125	.275E−39	.135E−39	.838E−40	.597E−40	.462E−40	.379E−40	.323E−40
150	.336E−39	.167E−39	.105E−39	.752E−40	.586E−40	.482E−40	.413E−40
175	.357E−39	.183E−39	.117E−39	.854E−40	.672E−40	.559E−40	.482E−40
200	.360E−39	.191E−39	.126E−39	.931E−40	.743E−40	.624E−40	.542E−40
250	.343E−39	.196E−39	.135E−39	.103E−39	.846E−40	.724E−40	.639E−40
300	.322E−39	.195E−39	.140E−39	.110E−39	.922E−40	.802E−40	.718E−40
350	.302E−39	.192E−39	.143E−39	.115E−39	.980E−40	.865E−40	.783E−40
400	.288E−39	.192E−39	.146E−39	.120E−39	.104E−39	.928E−40	.847E−40
450	.276E−39	.190E−39	.148E−39	.124E−39	.108E−39	.977E−40	.900E−40
500	.267E−39	.189E−39	.151E−39	.128E−39	.113E−39	.103E−39	.953E−40
550	.261E−39	.190E−39	.154E−39	.132E−39	.118E−39	.108E−39	.100E−39
600	.260E−39	.193E−39	.158E−39	.137E−39	.124E−39	.114E−39	.106E−39
650	.258E−39	.195E−39	.162E−39	.142E−39	.128E−39	.118E−39	.111E−39
700	.256E−39	.197E−39	.165E−39	.146E−39	.132E−39	.123E−39	.116E−39
750	.255E−39	.199E−39	.168E−39	.150E−39	.137E−39	.128E−39	.121E−39
800	.251E−39	.199E−39	.170E−39	.152E−39	.140E−39	.131E−39	.124E−39
850	.251E−39	.201E−39	.173E−39	.156E−39	.144E−39	.135E−39	.129E−39

Table 2. The branch coefficient $X^{(a)}(\lambda, T)$.

λ (nm)	$X^{(a)}$						
	8000 K	10 000 K	12 000 K	14 000 K	16 000 K	18 000 K	20 000 K
65	0.560	0.444	0.360	0.298	0.251	0.214	0.186
80	0.861	0.778	0.699	0.628	0.566	0.511	0.464
100	0.922	0.859	0.793	0.728	0.669	0.615	0.566
150	0.927	0.866	0.801	0.738	0.679	0.625	0.576
200	0.904	0.833	0.761	0.694	0.633	0.578	0.530
300	0.825	0.735	0.654	0.583	0.522	0.470	0.425
400	0.745	0.645	0.561	0.492	0.434	0.387	0.347
500	0.673	0.570	0.487	0.421	0.368	0.325	0.289
600	0.602	0.502	0.424	0.363	0.316	0.277	0.246
700	0.546	0.449	0.376	0.320	0.276	0.241	0.213
800	0.501	0.407	0.337	0.285	0.245	0.213	0.187

photoionization cross-section $\sigma_{nLS}(\lambda)$ and the free–free electron–ion absorption coefficient $K_{\rm ei}(\lambda, T)$. The coefficient $K_{\rm ia}(\lambda, T)$ is determined by equations (20), (14) and (18), but all necessary values of $K_{\rm ia}(\lambda, T)$ can be obtained by means of Table 1.

As in Mihajlov et al. (1994a, 1995), the parameter $F_{\rm He}(\lambda)$ is treated as a function of $\log\tau$, where τ is Rosseland optical depth of the atmosphere layer considered (Mihalas 1978). The values of $\log\tau$ are taken from Koester (1980). The behaviour of $F_{\rm He}(\lambda; \log\tau)$ is illustrated in Figs 4, 5 and 6, for atmospheres of DB white dwarfs with $T_{\rm eff} = 12\,000$ K and $\log\tau = 8$, $T_{\rm eff} = 12\,000$ K and $\log\tau = 7$, and $T_{\rm eff} = 14\,000$ K and $\log\tau = 8$, respectively. According to the expectations, the relative efficiency of absorption processes (4) in the far-UV and VUV regions was increased several times with respect to the optical region. The result is that processes (4) in the region $80\,{\rm nm} \lesssim \lambda \lesssim 200\,{\rm nm}$ dominate in comparison with the concurrent processes (1) and (2) in significant parts of DB white dwarf atmospheres (maximal values of $F_{\rm He} \approx 2.5$). From Figs 4 and 6 one can see that the relative efficiency of processes (4) weakly decreases (∼5 per cent) with the decrease of $\log g$ from 8 to 7 for $T_{\rm eff} = 12\,000$ K, while the shape of curves $F_{\rm He}(\lambda; \log\tau)$ stays practically the same. However, Fig. 5 shows that increasing $T_{\rm eff}$ from 12 000 K to 14 000 K for $\log g = 8$ causes significant changes in curves $F_{\rm He}(\lambda; \log\tau)$. The characteristic fluctuations of $F_{\rm He}(\lambda; \log\tau)$ in these figures are caused, exceptionally, by small fluctuations of the temperature and other atmospheric parameters in the corresponding table from Koester (1980), which was examined in detail in Mihajlov et al. (1995). However, the systematic increase of the temperature in the range $\log\tau \lesssim -2$ for about 1500 K causes a significant increase of the parameters $N(\mathrm{He}^+)/N(\mathrm{He})$ and $N(\mathrm{He}_2^+)/N(\mathrm{He}^+)$, and, as a consequence, a significant increase of the absorption coefficients $\kappa_{\rm ia}^{(a)}$ and $\kappa_{\rm ia}^{(b)}$ of both absorption processes (3) and (4). This fact is reflected by the corresponding increase of the quantity $F_{\rm He}$ in Fig. 5 in the case of $T_{\rm eff} = 14\,000$ K with respect to Fig. 4 in the case of $T_{\rm eff} = 12\,000$ K.

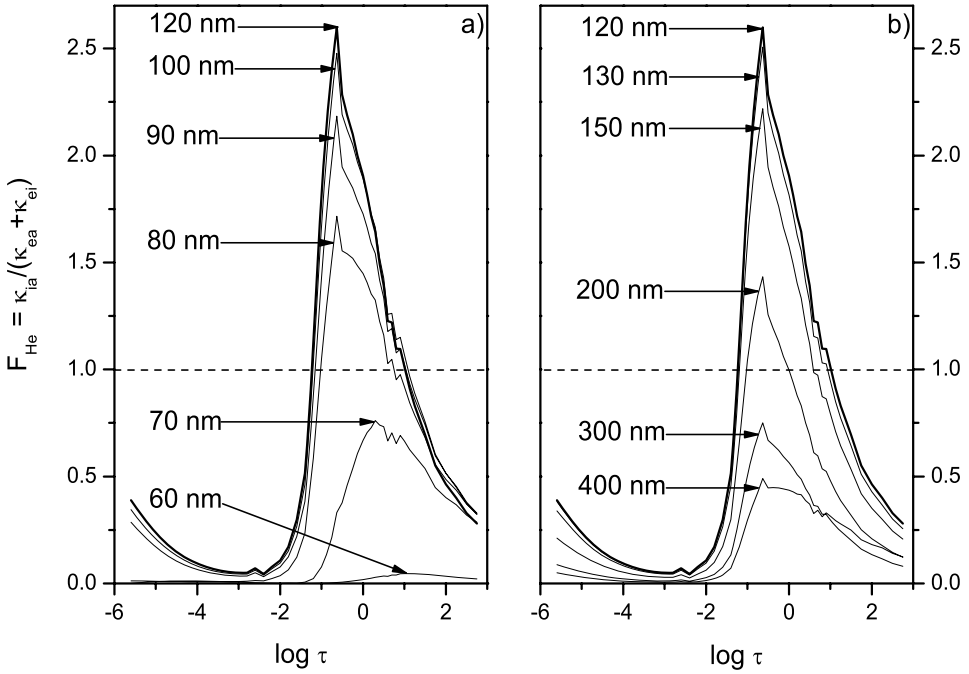

Figure 4. Behaviour of the quantity $F_{\rm He} = \kappa_{\rm ia}/(\kappa_{\rm ea} + \kappa_{\rm ei})$ within the atmosphere of a DB white dwarf in the case $\log g = 8$ and $T_{\rm eff} = 12\,000$ K.

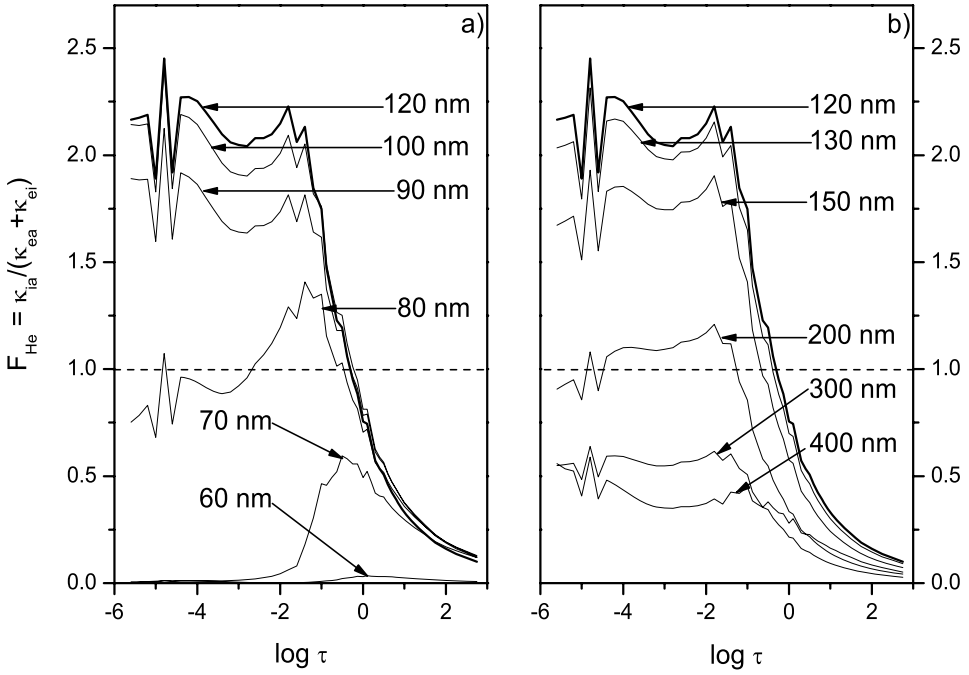

Figure 5. As Fig. 4, but for the case $\log g = 8$ and $T_{\rm eff} = 14000$ K.

Apart from that, the efficiency of the absorption processes (4) in the region $\lambda_{\rm He} < \lambda \leq \lambda_{\rm H}$ is compared with the efficiency of the hydrogen photoionization process (1), which is characterized by the spectral absorption coefficient $\kappa_{\rm H}(\lambda) \equiv \kappa_{\rm H}[\lambda; N({\rm H})]$ defined by

$$\kappa_{\rm H}(\lambda) = \sigma_{\rm phi}(\lambda) N({\rm H}), \tag{25}$$

where N(H) is the local density of atom H, and $\sigma_{\rm phi}(\lambda)$ the corresponding photoionization cross-section. Consequently, the relative efficiency of processes (4) and (7) for $\lambda \leq \lambda_{\rm H}$ can be characterized by the parameter $F_{\rm H}(\lambda)$, defined by

$$F_{\rm H}(\lambda) = \frac{\kappa_{\rm ia}(\lambda)}{\kappa_{\rm H}(\lambda)} = \frac{K_{\rm ia}(\lambda, T) N({\rm He}^+) N({\rm He})}{\sigma_{\rm phi}(\lambda) N({\rm H})}, \tag{26}$$

where the cross-section $\sigma_{\rm phi}(\lambda)$ is taken from Bethe & Salpeter (1957). It was found that the behaviour of $F_{\rm H}(\lambda)$ in all DB white dwarf atmospheres considered is qualitatively similar. Consequently, the behaviour of $F_{\rm H}(\lambda)$ is illustrated in Fig. 7 only for the

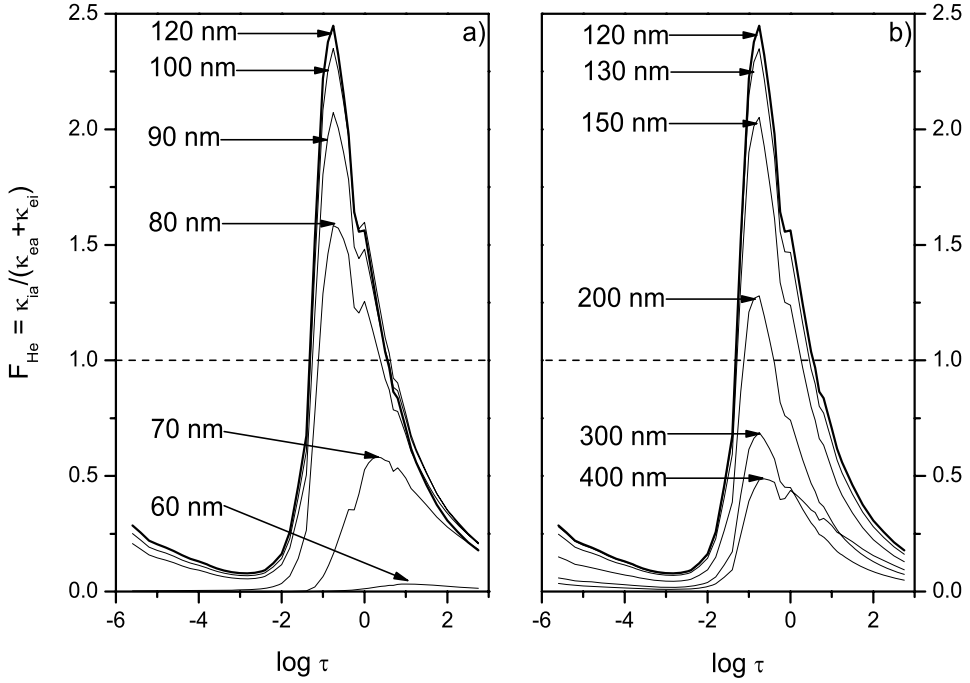

Figure 6. As Fig. 4, but for the case $\log g = 7$ and $T_{\rm eff} = 12\,000$ K.

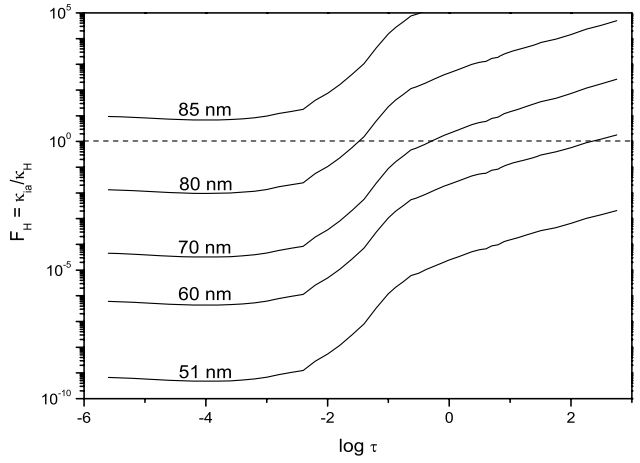

Figure 7. Behaviour of the quantity $F_{\rm H} = \kappa_{\rm ia}/\kappa_{\rm H}$ within the atmosphere of a DB white dwarf in the case $\log g = 8$ and $T_{\rm eff} = 12\,000$ K.

case $T_{\rm eff} = 12\,000$ K and $\log g = 8$. This figure shows that within the region $\lambda_{\rm He} < \lambda \lesssim 80$ nm the hydrogen photoionization process (7) should be treated as an important absorption process. Namely, for each λ from this region there is a significant part of the DB white dwarf atmosphere where process (7) dominates in comparison with the other absorption processes.

On the basis of Figs 4, 5, 6 and 7 one might expect that in the region $\lambda_{\rm He} < \lambda \leq 400$ nm the summary optical depth $\tau_{\rm sum}(\lambda; \log\tau)$ of the atmosphere layers considered, caused by all absorption processes relevant for continual spectra, should be significantly larger with respect to the optical depth caused by processes (1) and (2) only. For $\lambda_{\rm He} < \lambda \lesssim 70$ nm this increase should be caused by process (7), and for $\lambda \gtrsim 70$ nm by processes (4). Since only $\tau_{\rm sum}(\lambda; \log\tau)$ is necessary to describe the radiation transfer in the atmosphere considered, the behaviour of this quantity is examined here, supposing that only processes (4), (1), (2) and (7) cause the continuous absorption.

The contribution of processes (4) to the opacities of the DB white dwarf atmospheres considered is directly characterized by means of the quantity $\Delta\tau_{\rm ia}(\lambda; \log\tau)$, which represents the increase of the optical depth of the atmosphere layer considered that is caused by these processes themselves (see Mihajlov et al. 1995). We will characterize the contribution of the absorption processes considered to the opacity of DB white dwarf atmospheres by $\tau_{\rm sum}(\lambda; \log\tau)$ and the ratio $\Delta\tau_{\rm ia}(\lambda; \log\tau)/\tau_{\rm sum}(\lambda; \log\tau)$.

The behaviour of $\tau_{\rm sum}(\lambda; \log\tau)$ and $\Delta\tau_{\rm ia}(\lambda; \log\tau)/\tau_{\rm sum}(\lambda; \log\tau)$ is illustrated in Figs 8, 9 and 10 for the same cases: $T_{\rm eff} = 12\,000$ K and $\log\tau = 8$, $T_{\rm eff} = 12\,000$ K and $\log\tau = 7$, and $T_{\rm eff} = 14\,000$ K and $\log\tau = 8$. First of all, Figs 8(b)–10(b), which illustrate the behaviour of the ratio $\Delta\tau_{\rm ia}(\lambda; \log\tau)/\tau_{\rm sum}(\lambda; \log\tau)$, show that in the region $70\,{\rm nm} \lesssim \lambda \lesssim 400$ nm processes (4) give the dominant contribution to the opacity of the most important layer $-1 \lesssim \log\tau \lesssim 1$. This holds especially for the region $90\,{\rm nm} \lesssim \lambda \lesssim 150$ nm, where the contribution of processes (4) reaches ∼70 per cent. It means that this layer, according to Figs 8(a)–10(a), would be transparent in the absence of processes (4).

Also, Figs 8(a)–10(a) show that in the region $\lambda_{\rm He} < \lambda \lesssim 70$ nm the hydrogen photoionization process (7) causes the opacity of the layer $-1 \lesssim \log\tau \lesssim 1$. The influence of this process is especially strong in the case $\log g = 7$ and $T_{\rm eff} = 12000$ K, and weaker in the case $\log g = 8$ and $T_{\rm eff} = 14000$ K.

3 CONCLUSIONS

The results obtained allow the possibility of estimating which absorption processes give the main contribution to the opacity in DB white dwarf atmospheres in different spectral regions. Therefore, from our results it follows that the helium absorption processes (3)

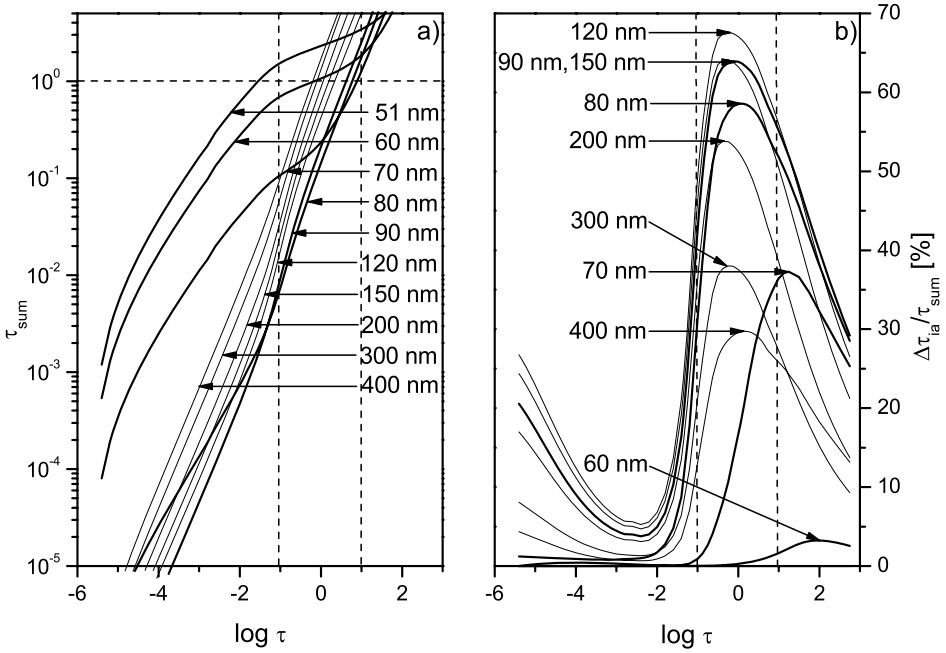

Figure 8. A DB white dwarf atmosphere in the case $\log g = 8$ and $T_{\rm eff} = 12000$ K: (a) the behaviour of the summary optical depth $\tau_{\rm sum}(\lambda; \log\tau)$ caused by the absorption processes (4), (1), (2) and (7); (b) the behaviour of the ratio $\Delta_{\rm ia}(\lambda; \log\tau)/\tau_{\rm sum}(\lambda; \log\tau)$ characterizing the relative contribution of processes (4) to the summary optical depth.

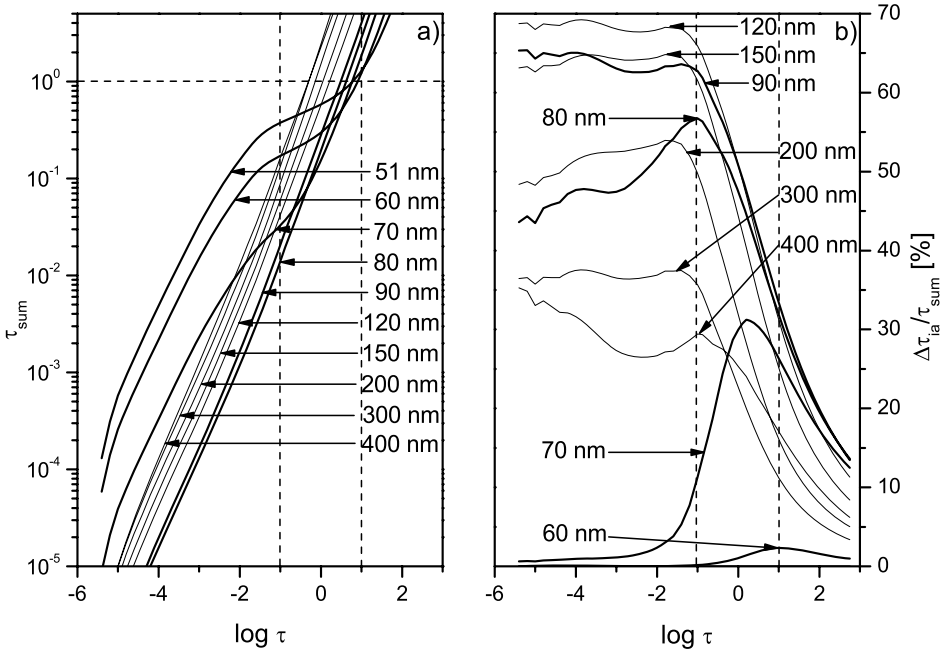

Figure 9. As Fig. 8, but for the case $\log g = 8$ and $T_{\rm eff} = 14\,000$ K.

and (4) are dominant in the region $70\,{\rm nm} \lesssim \lambda \lesssim 200\,{\rm nm}$, while in the region $\lambda > 200$ nm the He^- absorption processes (1) have the principal role, in contrast to the results presented in Stancil (1994). However, absorption processes (3) and (4) deserve to be included not only in the codes developed by e.g. Bergeron et al. (1995) but also in other DB white dwarf research.

Finally, it was shown that in the region $\lambda_{\rm He} < \lambda \lesssim 70\,{\rm nm}$, the hydrogen photoionization processes (7) take the dominant role in spite of the fact that the ratio of hydrogen and helium abundances in the DB white dwarf atmosphere considered is $1{:}10^5$. Consequently, the hydrogen photoionization processes (7) should also be included in DB white dwarf modelling. Moreover, this result opens the question of the eventual influence of metals, the abundance of which in the DB white dwarf considered is 1.5 times larger than that of hydrogen (Koester 1980).

We also note that the results obtained may be useful for the interpretation of observational data for DB white dwarfs. Namely, these results give the possibility of estimating from which atmospheric layers of DB white dwarfs the radiation at a given λ comes. This is important since the temperatures of these layers vary considerably with the Rosseland optical depth (τ), as follows from the models used (Koester 1980).

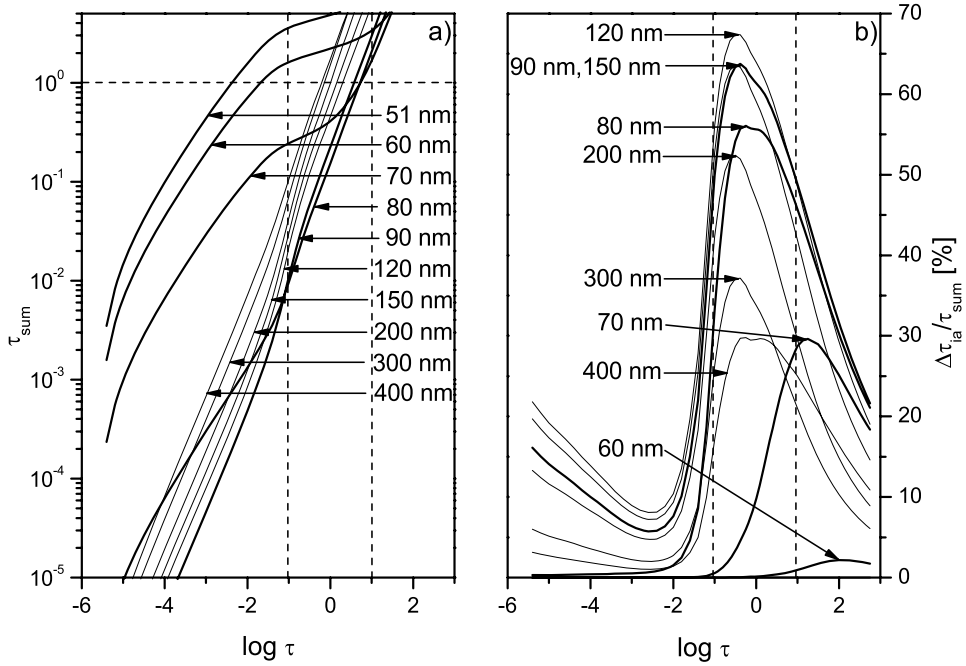

Figure 10. As Fig. 8, but for the case $\log g = 7$ and $T_{\rm eff} = 12\,000$ K.

ACKNOWLEDGMENTS

This work was supported by the Ministry of Science and Technological Development of Serbia as a part of the projects 'Radiation and transport properties of the non-ideal laboratory and ionospheric plasma' (Project number 141033) and 'Influence of collisional processes in astrophysical plasma line shapes' (Project number 146001).

REFERENCES

Bates D. R., 1952, MNRAS, 112, 40
Beauchamp A., Wesemael F., Bergeron P., Lebert J., Saffer R. A., 1996, in Jeffery C. S., Herber U., eds, ASP Conf. Ser. Vol. 96, Hydrogen-Deficient Stars. Astron. Soc. Pac., San Francisco, p. 295
Beauchamp A., Wesemael F., Bergeron P., 1997, ApJS, 108, 559
Bergeron P., Wesemael F., Beauchamp A., 1995, PASP, 107, 1047
Bethe H., Salpeter E., 1957, Quantum mechanics of one and two electron atoms. Springer Verlag, Berlin
Calamida A. et al. 2008, Mem. S. A. It., 79, 347
Dunning T. H., 1989, J. Chem. Phys., 90, 1007
John T. L., 1994, MNRAS, 269, 871
Kendall R. A., Dunning T. H., Harrison R. J., 1992, J. Chem. Phys., 96, 6769
Koester D., 1980, A&AS, 39, 401
Lebedev V. S., Presnyakov L. P., 2002, J. Phys. B: At. Mol. Opt. Phys., 35, 4347
Marsh T. R., Nelemans G., Steeghs D., 2004, MNRAS, 350, 113
Metropoulos A., Nicolaides A., 1991, Chem. Phys. Lett., 187, 487
Metropoulos A., Nicolaides A., Buenker R. J., 1987, Chem. Phys., 114, 1
Metropoulos A., Li Y., Hirsch G., Buenker R. J., 1992, Chem. Phys. Lett., 198, 266
Mihajlov A. A., Dimitrijević M. S., 1986, A&A, 155, 319
Mihajlov A. A., Dimitrijević M. S., 1992, A&A, 256, 305
Mihajlov A. A., Dimitrijević M. S., Ignjatović L. M., 1993, A&A, 276, 187
Mihajlov A., Dimitrijević M., Ignjatović L., 1994a, A&A, 287, 1026
Mihajlov A. A., Dimitrijević M. S., Ignjatović L. M., Djurić Z., 1994b, A&AS, 103, 57
Mihajlov A. A., Dimitrijević M. S., Ignjatović L. M., Djurić Z., 1995, ApJ, 454, 420
Mihajlov A. A., Ignjatović L. M., Sakan N. M., Dimitrijević M. S., 2007, A&A, 437
Mihalas D., 1978, Stellar Atmospheres. W.H. Freeman, San Francisco
Patch R. W., 1969, J. Quant. Spectrosc. Radiative Transfer, 9, 63
Sobel'man I. I., 1979, Atomic Spectra and Radiative Transitions. Springer Verlag, Berlin
Somerville W. B., 1965, ApJ, 141, 811
Stancil P. C., 1994, ApJ, 430, 360
Stancil P. C., Bab J. F., Dalgarno A., 1993, ApJ, 414, 672
Werner H.-J. et al., 2006, MOLPRO, version 2006. 1, a package of ab initio programs, see http://www.molpro.net

This paper has been typeset from a TEX/LATEX file prepared by the author.

Monthly Notices
of the
ROYAL ASTRONOMICAL SOCIETY

Mon. Not. R. Astron. Soc. **406,** 590–596 (2010) doi:10.1111/j.1365-2966.2010.16702.x

Electrical conductivity of plasmas of DB white dwarf atmospheres

V. A. Srećković,[1] Lj. M. Ignjatović,[1,2]★ A. A. Mihajlov[1,2] and M. S. Dimitrijević[2,3,4]

[1]*Institute of Physics, PO Box 57, 11001 Belgrade, Serbia*
[2]*Isaac Newton Institute of Chile, Yugoslavia Branch*
[3]*Astronomical Observatory, Volgina 7, 11160 Belgrade 74, Serbia*
[4]*Observatoire de Paris, 92195 Meudon Cedex, France*

Accepted 2010 March 16. Received 2010 March 16; in original form 2009 December 3

ABSTRACT

The static electrical conductivity of non-ideal, dense, partially ionized helium plasma was calculated over a wide range of plasma parameters: temperatures $1 \times 10^4 \lesssim T \lesssim 1 \times 10^5$ K and mass density $1 \times 10^{-6}\,\mathrm{g\,cm^{-3}} \lesssim \rho \lesssim 2\,\mathrm{g\,cm^{-3}}$. Calculations of electrical conductivity of plasma for the considered range of plasma parameters are of interest for DB white dwarf atmospheres with effective temperatures $1 \times 10^4\,\mathrm{K} \lesssim T_{\mathrm{eff}} \lesssim 3 \times 10^4\,\mathrm{K}$.

Electrical conductivity of plasma was calculated by using the modified random phase approximation and semiclassical method, adapted for the case of dense, partially ionized plasma. The results were compared with the unique existing experimental data, including the results related to the region of dense plasmas. In spite of low accuracy of the experimental data, the existing agreement with them indicates that results obtained in this paper are correct.

Key words: stars: atmospheres – stars: kinematics and dynamics – white dwarfs.

1 INTRODUCTION

DB white dwarf atmospheres belong to the class of astrophysical objects which have been investigated for a long time and from various aspects (Bues 1970; Koester 1980; Stancil, Bab & Dalgarno 1993). Of the previous work, the contribution of the authors of this paper was on the optical properties of DB white dwarf atmospheres within the range of average effective temperatures $1 \times 10^4\,\mathrm{K} \lesssim T_{\mathrm{eff}} \lesssim 2 \times 10^4$ K. Mihajlov & Dimitrijević (1992), Mihajlov, Dimitrijević & Ignjatović (1994) and Mihajlov et al. (1995) worked on the continual absorption in the optical part of electromagnetic spectra, Mihajlov et al. (2003) worked on the chemi-ionization/recombination processes and Ignjatović et al. (2009) investigated the continual absorption in the VUV region of EM spectra.

Recently, the transport properties of helium plasmas, characteristic of some DB white dwarf atmospheres, attracted the authors' attention, first of all the electrical conductivity. Namely, data on the electrical conductivity of plasma of stars with a magnetic field or moving in the magnetic field of the other component in a binary system (see, e.g. Zhang, Wickramasinghe & Ferrario 2009; Rodriguez-Gil, Martinez-Pais & Rodriguez 2009; Potter & Tout 2010) could be of significant interest, since they are useful for the study of the thermal evolution of such objects (cooling, nuclear burning of accreted matter) and the investigation of their magnetic fields. For example, Kopecký (1970) and Kopecký & Kotrč (1973) studied electrical conductivity for stars of various spectral types, in order to investigate the magnetohydrodynamic differences in their atmospheres. Recently, Mazevet, Challacombe & Kowalski (2007) investigated He conductivity in cool white dwarf atmospheres, since the possibility of using these stars for dating stellar populations has generated a renewed interest in modelling their cooling rate (Fontaine, Brassard & Bergeron 2001). Also, the transport processes occurring in the cores of white dwarfs (see, e.g. Baiko & Yakovlev 1995 and numerous references therein) have been considered. Moreover, electrical conductivity was particularly investigated for solar plasma, since it is of interest for consideration of various processes in the observed atmospheric layers, like the relation between magnetic field and convection, the question of magnetic field dissipation and the energy released by such processes (see e.g. Kopecký 1970 and references therein). For example, Feldman (1993) investigated the role of electrical conductivity in the construction of a theoretical model of the upper solar atmosphere, and Kazeminezhad & Goodman (2006) considered the electrical conductivity of solar plasma for magnetohydrodynamic simulations of the solar chromospheric dynamo. Given that electrical conductivity plays an analogous role in other stars as well, it is of interest to investigate its significance, to adapt the methods for research into stellar plasma conditions and to provide the needed data.

An additional interest for data on electrical conductivity in white dwarf atmospheres may be stimulated by the search for extrasolar planets. Namely, Jianke, Ferrario & Wickramasinghe (1998) have shown that a planetary core in orbit around a white dwarf may reveal its presence through its interaction with the magnetosphere of the white dwarf. Such an interaction will generate electrical currents that will directly heat the atmosphere near its magnetic poles. Jianke et al. (1998) emphasize that this heating may be detected within the optical wavelength range as Hα emission. For investigation and modelling of the above-mentioned electrical currents, the data on electrical conductivity in white dwarf atmospheres will be useful.

★E-mail: ljuba@ipb.ac.rs

One of the most frequently used approximations for consideration of transport properties of different plasmas is the approximation of 'fully ionized plasma' (Spitzer 1962; Radke et al. 1976; Adamyan et al. 1980; Kurilenkov 1984; Ropke & Redmer 1989; Djuric et al. 1991; Nurekenov et al. 1997; Zaika, Mulenko & Khomkin 2000; Esser, Redmer & Ropke 2003). It was shown that the electrical conductivity of fully ionized plasmas can be successfully calculated using the modified random-phase approximation (RPA) (Djuric et al. 1991; Adamyan et al. 1994a,b) in the region of strong and moderate non-ideality, while the weakly non-ideal plasmas were successfully treated within the semiclassical approximation (SC) (Mihajlov et al. 1993; Vitel et al. 2001). In practice, even the plasmas with a significant neutral component are treated as fully ionized in order to simplify the considered problems (Ropke & Redmer 1989; Esser & Ropke 1998; Zaika et al. 2000; Esser et al. 2003). However, our preliminary estimates have shown that such an approach is not applicable for the helium plasmas of DB white dwarf atmospheres described in Koester (1980), where the influence of the neutral component cannot be neglected.

Therefore, an adequate method for calculations of electrical conductivity of dense, partially ionized helium plasmas is developed in this paper. This method represents a generalization of methods developed in Djuric et al. (1991) and Mihajlov et al. (1993), namely, modified RPA and SC methods, and gives the possibility of estimating the real contribution of the neutral component to the static electrical conductivity of the considered helium plasmas within a wide range of mass densities (ρ) and temperatures (T).

The calculations were performed for helium plasma in the state of local thermodynamical equilibrium with given ρ and T for $1 \times 10^4\,\mathrm{K} \lesssim T \lesssim 1 \times 10^5\,\mathrm{K}$ and $1 \times 10^{-6}\,\mathrm{g\,cm^{-3}} \lesssim \rho \lesssim 2\,\mathrm{g\,cm^{-3}}$. The obtained results are compared with the corresponding experimental data (Mintsev, Fortov & Gryaznov 1980; Ternovoi et al. 2002; Shilkin et al. 2003). For the calculations of plasma characteristics of DB white dwarf atmospheres, the data from Koester (1980) were used.

2 THEORY

2.1 The plasma electrical conductivity

On the basis of the previous paper of Adamyan et al. (1980), a modified RPA method for calculation of the static conductivity of fully ionized plasma was developed in Djuric et al. (1991) and Adamyan et al. (1994a). The principal role of this method is in the formula for energy-dependent electron–electron (ee) and electron–ion (ei) relaxation times $t_{\mathrm{ee;ei}}(E) = t^{\mathrm{RPA}}_{\mathrm{ee;ei}}$, where E is the energy of a single electron state, determined as a sum over the Matsubara frequencies by using the methods of Green function theory. This method is especially suitable for calculation of the electrical conductivity of dense non-ideal plasmas with electron density (N_e) larger than $10^{17}\,\mathrm{cm^{-3}}$. In the region $N_\mathrm{e} < 10^{17}\,\mathrm{cm^{-3}}$ the static conductivity of fully ionized plasmas can be determined well using the SC method developed in Mihajlov et al. (1993), which is also based on electron relaxation time $t_{\mathrm{ee;ei}}(E) = t^{\mathrm{SC}}_{\mathrm{ee;ei}}$. It is important that the SC method gives practically the same results as the RPA method in a wider region of the electron densities around the value of $N_\mathrm{e} = 10^{17}\,\mathrm{cm^{-3}}$. The SC method was tested from this aspect in Vitel et al. (2001), where it was experimentally verified through comparison with the results from Spitzer (1962) and Kurilenkov (1984), just for the helium plasmas.

However, as was already mentioned, the helium plasma of the considered DB white dwarf atmospheres contains a significant neutral atom component, as follows from Bues (1970) and Koester (1980). Because of that, we will start here from the fact that in both RPA and SC methods effective electron relaxation times $t_{\mathrm{ee;ei}}(E)$ can be expressed as

$$\frac{1}{t_{\mathrm{ee;ei}}(E)} = \nu_{\mathrm{ee;ei}}(E), \tag{1}$$

where E is the electron energy, and $\nu_{\mathrm{ee;ei}}(E)$ – the corresponding total electron–electron and electron–ion collision frequency. This gives the possibility of generalizing the modified RPA and SC methods for the case of partially ionized plasmas, replacing $1/t_{\mathrm{ee;ei}}(E)$ by $\nu_{\mathrm{e;tot}}(E)$

$$\nu_{\mathrm{e;tot}}(E) = \nu_{\mathrm{ee;ei}}(E) + \nu_{\mathrm{ea}}(E) = \frac{1}{t_{\mathrm{ee;ei}}(E)} + \nu_{\mathrm{ea}}(E), \tag{2}$$

where $\nu_{\mathrm{ea}}(E)$ is an effective electron–atom collision frequency. Consequently, the basic RPA and SC expressions for the static electrical conductivity σ_0 transform to the corresponding Frost-like expressions

$$\sigma_0 = \frac{4e}{3m}\int_0^\infty E w(E) \frac{1}{\left[\dfrac{1}{t_{\mathrm{ee;ei}}(E)} + \nu_{\mathrm{ea}}(E)\right]} \frac{\mathrm{d}f_{\mathrm{FD}}(E)}{\mathrm{d}E}\,\mathrm{d}E, \tag{3}$$

where m and e are the mass and the modulus of charge of the electron, $w(E)$ is the density of the single electron states in the energy space, $f_{\mathrm{FD}}(E) \equiv f_{\mathrm{FD}}(E; T, N_\mathrm{e})$ is the Fermi–Dirac distribution function for given N_e and temperature T and $t_{\mathrm{ee;ei}}(E) = t^{\mathrm{RPA}}_{\mathrm{ee;ei}}$ or $t_{\mathrm{ee;ei}}(E) = t^{\mathrm{SC}}_{\mathrm{ee;ei}}$.

On the basis of composition and temperature data of the considered DB white dwarf atmospheres (Bues 1970; Koester 1980), one can note that only four components of these atmospheres are important for determination of σ_0: free electrons, He^+ and He^{2+} ions and helium atoms. In accordance with this, the expression for $1/t^{\mathrm{RPA}}_{\mathrm{ee;ei}}$ from Djuric et al. (1991) can be presented in the form

$$\frac{1}{t^{\mathrm{RPA}}_{\mathrm{ee;ei}}(E)} = \frac{4\pi m N_\mathrm{e} e^4 k_\mathrm{B} T}{(2mE)^{3/2}} \int_0^{\sqrt{8mE}/\hbar} \frac{\mathrm{d}q}{q} \times \sum_n \left\{ \frac{Z_\mathrm{e}^2 \Pi_{\mathrm{e};n}(q)}{N_\mathrm{e}\varepsilon_n^3(q)} + \sum_{j=1,2} \frac{Z_{ij}^2 \Pi_{ij;n}(q)}{N_{ij}\varepsilon_n^3(q)} \right\}, \tag{4}$$

where $\hbar$ and k_B are the Planck and Boltzmann constants, respectively, $Z_\mathrm{e}e$ and $Z_{i1,i2}e$ are the charges of electron and He^+ (1s) and He^{2+} ions ($Z_\mathrm{e} = -1$, $Z_{i1} = 1, Z_{i2} = 2$), N_{i1} and N_{i2} are the corresponding helium ion densities, $\Pi_{\mathrm{e};n}(q)$, $\Pi_{i1;n}(q)$ and $\Pi_{i2;n}(q)$ are the electron and ion polarization operators, $\varepsilon_n(q)$ is the dielectric function, $n = 0, \pm1, \pm2\ldots$ and the summation is extended over all the Matsubara frequencies $\Omega_n = 2\pi n k_\mathrm{B} T/\hbar$. The detailed expressions for polarization operators and dielectric functions are given in Djuric et al. (1991) and Adamyan et al. (1994a).

The SC expression for σ_0 is applied to the outer layers of the considered DB white dwarf atmospheres where $N_\mathrm{e} < 10^{17}\,\mathrm{cm^{-3}}$ and the presence of He^{2+} ions can be neglected. Because of that the expression for $1/t^{\mathrm{SC}}_{\mathrm{ee;ei}}$, in accordance with Mihajlov et al. (1993), can be taken in the form

$$\frac{1}{t^{\mathrm{SC}}_{\mathrm{ee;ei}}(E)} = \left[\frac{1}{\chi_{\mathrm{ee}}} \frac{(2m)^{1/2}E^{3/2}}{2e^4 Z_{i1} N_\mathrm{e}} \frac{1}{\ln\left(1+\Lambda_i^2\right)^{1/2}}\right]^{-1}, \qquad \Lambda_i = \frac{2E}{Z_{i1}e^2} r_{\mathrm{ci}}, \tag{5}$$

where k is the Boltzmann constant and $Z_{i1} = 1$. The correction factor $1/\chi_{\mathrm{ee}} = 1/\chi_{\mathrm{ee}}(Z_{i1}, T)$ is determined within the SC method,

while $r_{ci} \sim (4\pi e^2 N_e/kT)^{-1/2}$ is the corresponding screening length which is an external parameter of the theory. The values of $1/\chi_{ee}$ for $Z_{i1} = 1$ and 10^4 K $\leq T \leq 10^5$ K are taken from Mihajlov et al. (1993). Here, value $r_{ci} = r_{n;i}$ is taken as the screening length, where the ion neutrality radius $r_{n;i}$ is given by the expressions obtained in Mihajlov, Vitel & Ignjatović (2009). Such a choice of the screening length provides overlapping SC and RPA values of σ_0 in a wider region of electron densities around the value of $N_e = 10^{17}$ cm^{-3}.

Finally, the electron–atom collision frequency $\nu_{ea}(E)$ in equation (3) is given here by the known expression

$$\nu_{ea}(E) = N_a v(E) \cdot Q^{tr}_{ea}(E), \tag{6}$$

where N_a is the He($1s^2$) atom density, $v(E) = (2E/m)^{1/2}$ is the relative electron–atom velocity and $Q^{tr}_{ea}(E)$ is the transport cross-section for the elastic e−He($1s^2$) scattering (Mott & Massey 1970).

2.2 The electron–atom transport cross-section

The exact quantum-mechanical calculation of the transport cross-section for elastic electron–atom collisions is a very hard problem in itself. However, in the case of e−He($1s^2$) scattering the problem becomes easier within the considered temperature range where all non-elastic collision processes can be neglected. Namely, in this case it can be treated as scattering of electrons in an adequately chosen model potential $U(r)$, where r is the distance between the electron and the nucleus of the He($1s^2$) atom. Thus, the electron movement is described by a wavefunction $\Psi(r, \theta, \phi) = \frac{\chi_l(r)}{r} Y_{lm}(\theta, \phi)$, where $Y_{lm}(\theta, \phi)$ is a spherical harmonic function of degree l and order m, while the function $\chi_l(r)$ satisfies the radial Schrodinger equation

$$\left[-\frac{1}{2}\frac{d^2}{dr^2} + U(r) + \frac{l(l+1)}{2r^2}\right]\chi(r) = E\chi(r) \tag{7}$$

given in atomic units. Following the previous paper of Ignjatović & Mihajlov (1997), we take the model potential $U(r)$ in the form

$$U(r) = \begin{cases} U_0(r) = -\dfrac{Z}{r} + \dfrac{q}{r + r_0} + \dfrac{Z-q}{r_0}, & 0 < r < r_i \\ U_m(r) = ar^2 + br + c, & r_i < r < r_f \\ U_{as}(r) = -\dfrac{\alpha}{2\left(r^2 + h^2\right)^2} & r_f < r < \infty, \end{cases} \tag{8}$$

where $Z = 2$ is the charge of the nucleus of a helium atom, q and $Z - q$ describe the redistribution of electrons in the 1s shell of the helium atom ($0 < q < 2$), α is the polarizability of the He($1s^2$) atom and r_0 has the meaning of the average radius of an atom. Parameters a, b, c and h are determined from the conditions of continuity and smoothness of the potential $U(r)$ at the points r_i and r_f where $0 < r_i < r_0$ and $r_f > r_0$. The values of the mentioned quantities are given in Table 1.

Equation (7) is solved by the partial wave method described in Ignjatović & Mihajlov (1997). One obtains as the result the phase shifts $\delta_l(E)$ for $l = 0, 1, 2, \ldots$, where each $\delta_l(E)$ corresponds to the partial wave with a given orbital number l. This way of solving equation (7) has advantages since, apart from the transport cross-section

$$Q_{tr}(E) = \frac{2\pi\hbar c}{E}\sum_{l=0}^{\infty}(l+1)\sin^2(\delta_l - \delta_{l+1}), \tag{9}$$

it allows determination of the elastic cross-section, as well as cross-sections of higher order (viscosity cross-section, etc.). As one can see in Fig. 1, there is an excellent agreement between the values of $Q_{tr}(E)$ calculated using the potential (8) and various experimental and theoretical data of other authors.

3 RESULTS AND DISCUSSION

In order to apply our results to the study of DB white dwarf atmosphere plasma properties, helium plasmas with electron (N_e) and atom (N_a) densities and temperatures (T), characteristic of atmosphere models presented in the literature (Koester 1980), are considered here. So, the behaviour of ρ and T for models with the logarithm of surface gravity $\log g = 8$ and effective temperature $T_{eff} = 12\,000$, $20\,000$ and $30\,000$ K is shown in Fig. 2 as a function of Rosseland opacity τ. As one can see, these atmospheres contain layers of dense helium plasma. In order to cover the considered plasma parameter range reliably, we tested our method for calculation of the plasma electrical conductivity within a wider range of mass density 1×10^{-6} g cm$^{-3} \lesssim \rho \lesssim 2$ g cm^{-3} and of temperature 1×10^4 K $\lesssim T \lesssim 1 \times 10^5$ K.

The influence of neutral atoms on the electrical conductivity of helium plasma is shown in Fig. 3. In this figure the electrical conductivities for $T = 15\,000, 20\,000$ and $25\,000$ K are given as functions of mass density ρ. The range between the two vertical dashed lines corresponds to the conditions in the considered DB white dwarf atmospheres. Two groups of curves, calculated using the expression (3), are presented in this figure: (a) the dashed ones, obtained by neglecting the influence of atoms, i.e. with $\nu_{ea} = 0$; (b) the full-line curves calculated with the influence of atoms included, i.e. with ν_{ea} given by equation (6). First, one should note that the behaviour of these two groups of curves is qualitatively different: the first one increases constantly with the increase of ρ, while the other group of curves decreases, reaches a minimum, and then starts to increase with the increase of ρ. One could explain such behaviour of the electrical conductivity by the pressure ionization. This figure also clearly shows when the considered plasma can be treated as 'fully ionized'.

In Fig. 4 we compare our values of the helium plasma conductivity, shown by full curves for $T = 15000$, $20\,000$ and $25\,000$ K within the region 5×10^{-4} g cm$^{-3} < \rho < 2$ g cm^{-3}, with the existing experimental data. Let us note that these experimental results are uniquely available for comparison so that, in spite of their low accuracy, the agreement with them gives the only possible indication that our results are correct.

Within the region $\rho < 0.65$ g cm^{-3}, i.e. to the left of the vertical line in Fig. 4, there are experimental results from Ternovoi et al. (1999) (○) and Shilkin et al. (2003) (▽), where the temperature was determined with an error of less than 20 per cent, which are related to the temperature range 20 000–25 000 K. For $\rho > 0.65$ g cm^{-3}, i.e. right of the vertical line in Fig. 4, are shown several values of the plasma conductivity, obtained by Ternovoi et al. (2002) for the temperature range 15 000–25 000 K. These experimental values are obtained with an experimental error ∼50 per cent and can be treated only as characteristic of this temperature region as a whole. These

Table 1. The parameter values of the model potential $U(r)$ from equation (8) in atomic units.

Z	q	a	b	c	α	h	r_i	r_f	r_0
2	0.7	−0.59597652	2.2545472	−2.19405731	1.384	0.01	0.73	1.75	0.9

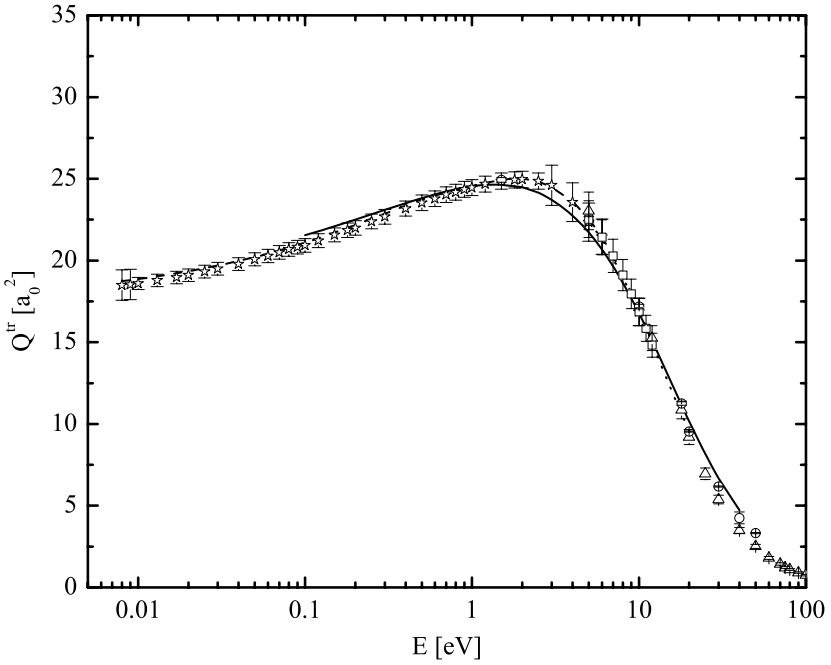

Figure 1. Momentum transfer cross-section Q^{tr} as a function of energy E. Calculated data (full line) for helium together with results of other authors: Nesbet (1979) (dashed line), Fon, Barrington & Hibbert (1981) (dotted line), Register, Trajmer & Strivastava (1980) (△), Crompton, Elford & Robertson (1970) (⋆), Brunger et al. (1992) (○), Milloy & Crompton (1977) (□).

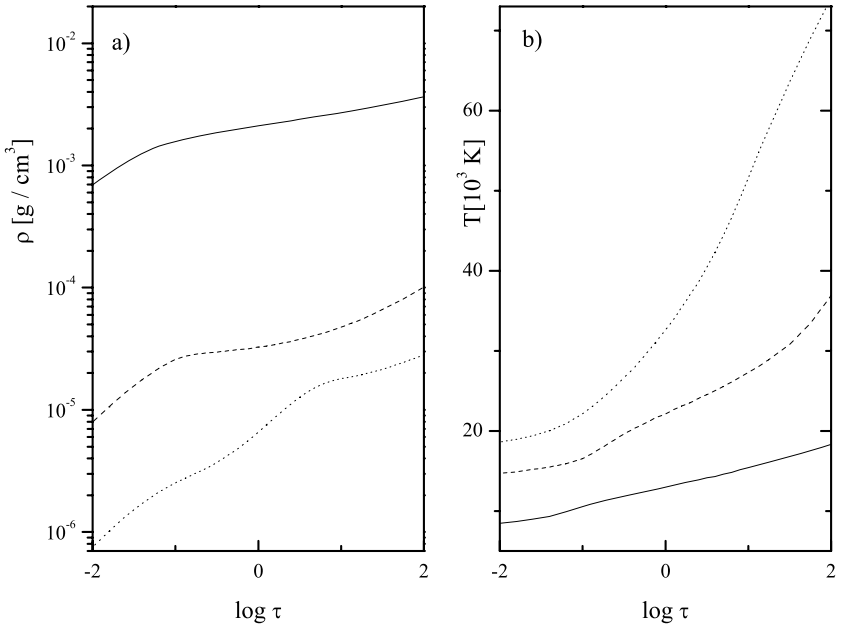

Figure 2. DB white dwarf atmosphere models with $\log g = 8$ and $T_{\rm eff} = 12\,000$ K (full curve), $T_{\rm eff} = 20\,000$ K (dashed curve) and $T_{\rm eff} = 30\,000$ K (dotted curve) from Koester (1980): (a) the mass densities; (b) the temperatures, as functions of Rosseland opacity τ.

data at least indicate that our results for $\rho > 0.65\,{\rm g\,cm^{-3}}$ lie in the correct domain of the electrical conductivity values.

The developed method was then applied to calculation of plasma electrical conductivity for the models of DB white dwarf atmospheres presented in Fig. 2. The results of the calculations are shown in Fig. 5. First, let us note a regular behaviour of the static electrical conductivity which one should expect considering the characteristics of DB white dwarf atmospheres. Further, the electrical conductivity profiles presented in this figure show that, for the considered DB white dwarf models, plasma electrical conductivity changes over the domain of values where our results agree with the experimental ones (see Fig. 4). This indicates that the theoretical apparatus presented here may be adequate to be used for investigation of DB white dwarfs in the magnetic field of their partners in binary systems and magnetic white dwarfs.

In order to provide the possibility for direct applications of our results to different theoretical investigations, the values of static electrical conductivity σ_0 of helium plasma in a wide range of ρ and T

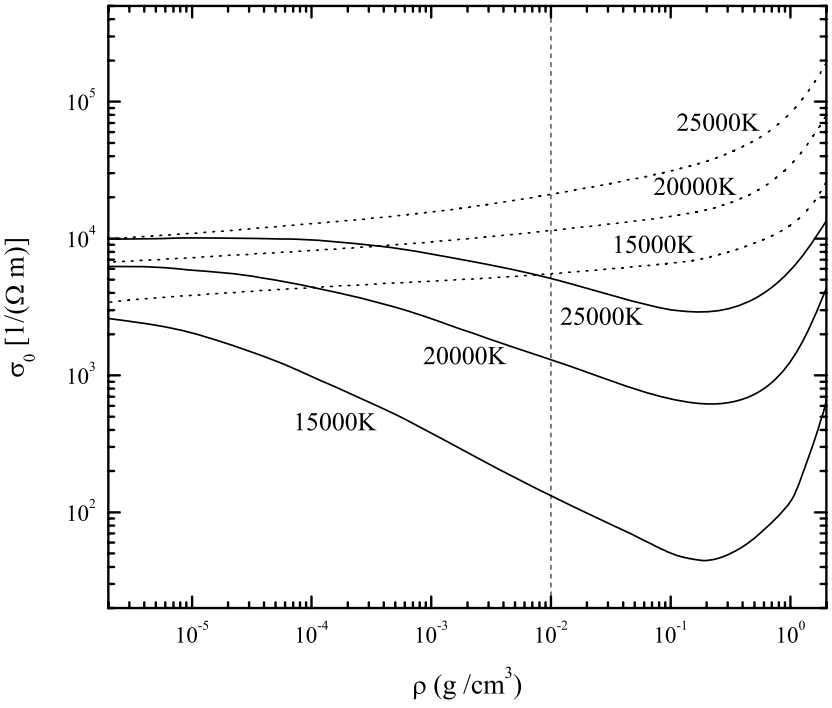

Figure 3. Static electrical conductivity σ_0 of dense He plasmas as a function of mass density ρ (full curves), compared to the Coulomb part of the conductivity (dashed curves). The area left of the vertical dashed line marks the region which is of interest for DB white dwarfs.

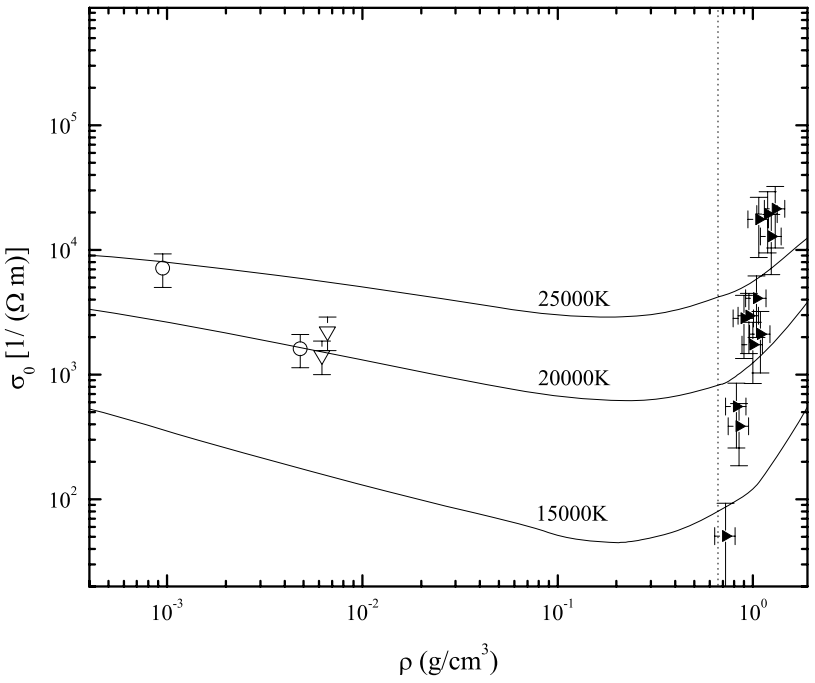

Figure 4. Static electrical conductivity σ_0 of helium plasma for various temperatures as a function of the mass density ρ. The full line represents the calculations based on the expressions (3)–(6); to the right of the vertical dotted line, there is a region of extremely dense plasmas where one should treat the presented calculation as an extrapolation. ▽ – Shilkin et al. (2003), 20 000–23 000 K; ▶ – Ternovoi et al. (2002), 15 000–25 000 K; ◯ – Mintsev et al. (1980), 20 000–25 000 K.

are given in Table 2. This table covers plasma conditions for all models of DB white dwarf atmospheres presented in Koester (1980) and the corresponding values of σ_0 were determined for the helium plasmas in the state of local thermodynamical equilibrium with given ρ and T.

The method developed in this paper also represents a powerful tool for research into white dwarfs with different atmospheric compositions (DA, DC etc.), and for investigation of some other stars (M-type red dwarfs, Sun etc.). Finally, the presented method provides a basis for the development of methods to

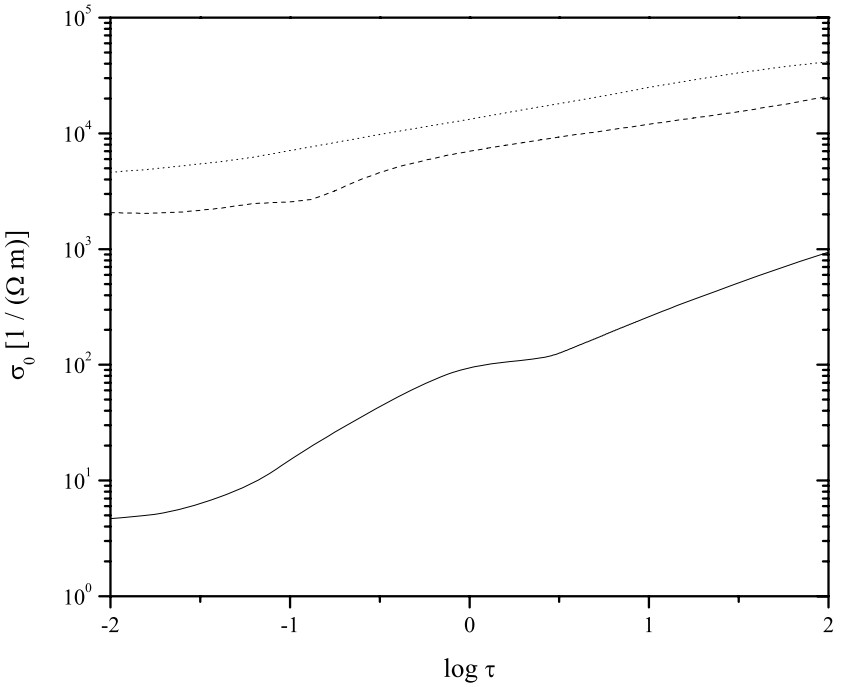

Figure 5. Static electrical conductivity σ_0 as a function of the logarithm of Rosseland opacity τ for DB white dwarf atmosphere models with $\log g = 8$ and $T_{\rm eff} = 12\,000$ K (full curve), $T_{\rm eff} = 20\,000$ K (dashed curve) and $T_{\rm eff} = 30\,000$ K (dotted curve).

Table 2. Static electrical conductivity of helium plasma $\sigma_0[1/(\Omega m)]$

	ρ[g cm^{-3}]								
$T[K]$	5.00E-07	1.00E-06	5.00E-06	1.00E-05	5.00E-05	1.00E-04	5.00E-04	1.00E-03	5.00E-03
8000	6.53E+00	4.69E+00	2.15E+00	1.50E+00	6.90E−01	4.89E−01	2.20E−01	1.53E−01	6.88E−02
9000	4.34E+01	3.16E+01	1.47E+01	1.13E+01	5.12E+00	3.60E+00	1.58E+00	1.19E+00	5.20E−01
10 000	1.69E+02	1.30E+02	6.74E+01	5.02E+01	2.38E+01	1.72E+01	8.12E+00	5.73E+00	2.56E+00
12 000	9.36E+02	8.04E+02	5.09E+02	4.05E+02	2.19E+02	1.66E+02	8.35E+01	6.08E+01	2.92E+01
14 000	2.27E+03	2.08E+03	1.62E+03	1.38E+03	8.87E+02	6.97E+02	3.99E+02	3.00E+02	1.28E+02
16 000	3.64E+03	3.55E+03	3.15E+03	2.87E+03	1.45E+03	1.18E+03	6.85E+02	5.28E+02	2.75E+02
18 000	4.90E+03	4.97E+03	4.76E+03	3.79E+03	2.87E+03	2.46E+03	1.58E+03	1.26E+03	7.07E+02
20 000	6.08E+03	6.22E+03	6.32E+03	5.61E+03	4.99E+03	4.46E+03	3.21E+03	2.53E+03	1.58E+03
25 000			9.95E+03	1.02E+04	9.90E+03	9.90E+03	8.62E+03	7.74E+03	5.95E+03
30 000			1.33E+04	1.40E+04	1.56E+04	1.60E+04	1.57E+04	1.50E+04	1.21E+04
35 000			1.65E+04	1.74E+04	2.02E+04	2.15E+04	2.34E+04	2.35E+04	2.15E+04
40 000			1.97E+04	2.09E+04	2.43E+04	2.61E+04	3.06E+04	3.18E+04	3.22E+04
45 000			2.31E+04	2.45E+04	2.84E+04	3.06E+04	3.69E+04	3.93E+04	4.36E+04
55 000			3.04E+04	3.23E+04	3.70E+04	3.98E+04	4.81E+04	5.26E+04	6.40E+04
65 000			3.81E+04	4.08E+04	4.65E+04	4.98E+04	6.00E+04	6.56E+04	8.20E+04
75 000			4.58E+04	4.93E+04	5.66E+04	6.06E+04	7.26E+04	7.92E+04	9.84E+04

describe other transport characteristics which are important for the study of all mentioned astrophysical objects, such as the electronic thermo-conductivity in the stellar atmosphere layers with large electron density, electrical conductivity in the presence of strong magnetic fields and dynamic (high frequency) electrical conductivity.

ACKNOWLEDGMENTS

This work was supported by the Ministry of Science and Technological Development of Serbia as a part of the projects 'Radiation and Transport Properties of the Non-ideal Laboratory and Ionospheric Plasma' (Project number 141033) and 'Influence of Collisional Processes on Astrophysical Plasma Line Shapes' (Project number 146001).

REFERENCES

Adamyan V. M., Gulyi G., Pushek N. L., Starchik P. D., Tkachenko I. M., S. Shvets I., 1980, High Temp., 18, 186

Adamyan V. M., Djurić Z., Ermolaev A. M., Mihajlov A. A., Tkachenko I. M., 1994a, J. Phys. D, 27, 111

Adamyan V. M., Djurić Z., Ermolaev A. M., Mihajlov A. A., Tkachenko I. M., 1994b, J. Phys. D, 27, 927

Baiko D. A., Yakovlev D. G., 1995, Astron. Lett., 21, 702

Brunger M. J., Buckman S. J., Allen L. J., McCarthy I. E., Ratnavelu K., 1992, J. Phys. B, 25, 1823
Bues I., 1970, A&A, 7, 91
Crompton R. W., Elford M. T., Robertson A. G., 1970, Aust. J. Phys., 23, 667
Djurić Z., Mihajlov A. A., Nastasyuk V. A., Popović M., Tkachenko I. M., 1991, Phys. Lett. A, 155, 415
Esser A., Ropke G., 1998, Phys. Rev. E, 58, 2446
Esser A., Redmer R., Ropke G., 2003, Contr. Plasma Phys., 43, 33
Feldman U., 1993, ApJ, 411, 896
Fon W. C., Barrington K. A., Hibbert A., 1981, J. Phys. B, 14, 307
Fontaine G., Brassard P., Bergeron P., 2001, PASP, 113, 409
Ignjatović L. M., Mihajlov A. A., 1997, Contr. Plasma Phys., 37, 309
Ignjatović L. M., Mihajlov A. A., Sakan N. M., Dimitrijević M. S., Metropoulos A., 2009, MNRAS, 37, 309
Jianke L., Ferrario L., Wickramasinghe D., 1998, ApJ, 503, 151
Kazeminezhad F., Goodman M. L., 2006, ApJS, 166, 613
Koester D., 1980, A&AS, 39, 401
Kopecký M., 1970, Bull. Astron. Inst. Czech., 21, 231
Kopecký M., Kotrč P., 1973, Bull. Astron. Inst. Czech., 24, 39
Kurilenkov Yu. K., Valuev A. A., 1984, Beitr. Plasmaphys., 24, 161
Mazevet S., Challacombe M., Kowalski P. M., 2007, Astophys. Space Sci, 307, 273
Mihajlov A. A., Dimitrijević M. S., 1992, A&A, 256, 305
Mihajlov A. A., Ermolaev A. M., Djurić Z., Ignjatović L. M., 1993, J. Phys. D, 26, 1041
Mihajlov A. A., Dimitrijević M. S., Ignjatović L. M., 1994, A&A, 287, 1026
Mihajlov A. A., Dimitrijević M. S., Ignjatović L. M., Djurić Z., 1995, ApJ, 454, 420
Mihajlov A. A., Ignjatović L. M., Dimitrijević M. S., Djurić Z., 2003, ApJS, 147, 369
Mihajlov A. A., Vitel Y., Ignjatović L. M., 2009, High Temp., 47, 5
Milloy H. B., Crompton R. W., 1977, Phys. Rev. A, 15, 847
Mintsev V. B., Fortov V. E., Gryaznov V. K., 1980, Sov. Phys. JETP, 52, 59
Mott N. F., Massey H. S., 1970, Theory of Atomic Collisions. Oxford University Press, Oxford
Nesbet R. K., 1979, Phys. Rev. A, 20, 58
Nurekenov K. T., Baimbetov F. B., Redmer R., Ropke G., 1997, Contr. Plasma Phys., 6, 473
Potter A. T., Tout C. A., 2010, MNRAS, 402, 1072
Radke R., Gunther K., Popović M. M., Popović S. S., 1976, J. Phys. D, 9, 1139
Register D. F., Trajmer S., Strivastava S. K., 1980, Phys. Rev. A, 21, 1134
Rodriguez-Gil P., Martinez-Pais I. G., Rodriguez J. C., 2009, MNRAS, 395, 973
Ropke G., Redmer R., 1989, Phys. Rev. A, 39, 907
Shilkin N. S., Dudin S. V., Gryaznov V. K., Mintsev V. B., Fortov V. E., 2003, J. Exp. Theor. Phys., 97, 922
Spitzer L., 1962, Physics of Fully Ionized Gases. Wiley, New York
Stancil P. C., Bab J. F., Dalgarno A., 1993, ApJ, 414, 672
Ternovoi V. Ya., Filimonov A. S., Fortov V. E., Kvitov S. V., Nikolaev D. N., Pyalling A. A., 1999, Physica B, 256, 6
Ternovoi V. Ya., Filimonov A. S., Pyalling A. A., Mintsev V. B., Fortov V. E., 2002, in AIP Conf. Proc. 620, Shock Compression of Condensed Matter. Am. Inst. Phys., New York, p. 107
Vitel Y. E. M., Mihajlov A. A., Djurić Z., 2001, Phys. Rev. E, 63, 026408
Zaika E. V., Mulenko I. A., Khomkin A. L., 2000, High Temp., 38, 1
Zhang C. M., Wickramasinghe D. T., Ferrario L., 2009, MNRAS, 397, 2208

This paper has been typeset from a TEX/LATEX file prepared by the author.

Monthly Notices
of the
ROYAL ASTRONOMICAL SOCIETY

Mon. Not. R. Astron. Soc. **417,** 2624–2630 (2011) doi:10.1111/j.1365-2966.2011.19434.x

Quantum Stark broadening data for the C IV, N V, O VI, F VII and Ne VIII resonance doublets

H. Elabidi,[1⋆] S. Sahal-Bréchot,[2] M. S. Dimitrijević,[2,3,4] and N. Ben Nessib[5]

[1]*Groupe de Recherche en Physique Atomique et Astrophysique, Faculté des Sciences de Bizerte, Université de Carthage, Tunisia*
[2]*LERMA, Observatoire de Paris, CNRS UMR 8112, ENS, UPMC, UCP, 5 Place Jules Janssen, 92190 Meudon, France*
[3]*Astronomical Observatory, Volgina 7, 11060 Belgrade 38, Serbia*
[4]*Isaac Newton Institute of Chile, Yugoslavia Branch*
[5]*Groupe de Recherche en Physique Atomique et Astrophysique, INSAT, Université de Carthage, Tunisia*

Accepted 2011 July 11. Received 2011 July 8; in original form 2011 June 8

ABSTRACT

In this paper, we present new Stark electron impact widths of the 2s–2p resonance doublets of the C IV, N V, O VI, F VII and Ne VIII ions, obtained using our quantum mechanical method. The present results are required to develop future spectral analysis using non-local thermodynamic equilibrium model atmospheres, which can make the determination of photospheric properties more accurate. Results are presented for a large range of electron temperatures required for plasma modelling. These are compared to the available theoretical ones. They are also used to check the previously obtained semiclassical perturbation results, and very good agreement is found. The atomic structure and collision data, used for the calculations of line broadening for the five ions studied here, are also calculated and compared to available theoretical results. The agreement found between the two calculations ensures that our line-broadening procedure uses the adequate structure and collision data. Scalings of linewidths with effective charge Z are also studied.

Key words: atomic data – line: profiles – scattering – stars: atmospheres – white dwarfs.

1 INTRODUCTION

The Stark broadening mechanism is important in stellar spectroscopy and the analysis of astrophysical and laboratory plasmas. Its influence should be considered in opacity calculations, the modelling of stellar interiors, the estimation of radiative transfer through stellar plasmas and the determination of chemical abundances of elements. For such investigations, in particular for opacity and radiative transfer calculations, a very large number of lines of different elements and their ions are needed (Dimitrijević 2003). For example, Barstow, Hubeny & Holberg (1998) have shown that the analysis of white dwarf atmospheres, where Stark broadening is dominant in comparison with the thermal Doppler broadening, cannot always be accomplished properly with models that neglect the opacity of heavy elements (Popović, Dimitrijević & Tankosić 1999; Tankosić, Popović & Dimitrijević 2003). Consequently, atomic and line-broadening data for many elements are necessary for stellar plasma research.

Rauch et al. (2007) have stressed that many line-broadening data for many species and their ions have been missed in the literature. Some other data exist but they are absent for the required temperatures and electron densities. It has been necessary to extrapolate these to the temperatures and densities at the line-forming regions, especially the line cores. This procedure can provide inaccurate results, especially in the case of extrapolation to temperatures, because the temperature dependence of linewidths can be very different. This lack of data represents an obstacle for the development of spectral analysis using non-local thermodynamic equilibrium (NLTE) model atmosphere techniques.

Rauch et al. (2007) have reported many problems that they have encountered in their determination of element abundances: the line cores of the S VI resonance doublet appear too deep to match the observation and they are not well suited for an abundance determination. Rauch et al. (2007) attributed this problem to the fact that the line-broadening tables of Dimitrijević & Sahal-Bréchot (1993a) are presented for an insufficient range of temperatures and densities for the calculations of the corresponding element abundances. The same problem has also been encountered for the resonance doublet of N V (the tables of Dimitrijević & Sahal-Bréchot 1992b were used) and O VI (the tables of Dimitrijević & Sahal-Bréchot 1992a were used). There was another problem related to the oxygen; Rauch et al. (2007) reproduced all the oxygen lines in their synthetic spectra except for O V λ1371. The lack of line-broadening data for these species and the lack of accurate results are the origin

⋆E-mail: haykel.elabidi@fsb.rnu.tn

of many discrepancies between the observations and synthetic line profiles in Rauch et al. (2007).

The Stark broadening calculations in this paper are based on a quantum mechanical approach. The quantum mechanical expression for electron impact broadening calculations for intermediate coupling was obtained from Elabidi, Ben Nessib & Sahal-Bréchot (2004). We performed the first applications for the 2s3s–2s3p transitions in Be-like ions from nitrogen to neon (Elabidi et al. 2007, 2008a) and for the 3s–3p transitions in Li-like ions from carbon to phosphor (Elabidi, Ben Nessib & Sahal-Bréchot 2008b; Elabidi, Sahal-Bréchot & Ben Nessib 2009). This approach was also used in Elabidi & Sahal-Bréchot (2011) to check the dependence on the upper-level ionization potential of electron impact widths. Our quantum approach is an *ab initio* method. That is, all the parameters required for the calculations of the line broadening, such as radiative atomic data (energy levels, oscillator strengths, etc.) or collisional data (collision strengths or cross-sections, scattering matrices, etc.) are evaluated during the calculation and are not taken from other data sources. We used the sequence of the UCL atomic codes SST/DW/JAJOM that have been used for many years to provide fine structure wavefunctions, energy levels, wavelengths, radiative probability rates and electron impact collision strengths. Recently, these have been adapted to perform line-broadening calculations (Elabidi et al. 2008a).

In order to provide new line-broadening data at a wide range of temperatures suitable for spectral analysis, and thus useful for a more accurate determination of photospheric properties, in this paper we apply our quantum mechanical method to calculate Stark electron impact widths for the resonant doublets of C IV, N V, O VI, F VII and Ne VIII ions. By providing these quantum results, we hope that we can partially contribute to the removal of some of the above-listed discrepancies between the observations and the synthetic profiles reported in Rauch et al. (2007). Other problems have been reported for some other ions and lines, which will be dealt with in future work.

The results obtained have been used to check the previous semiclassical perturbation (SCP) calculations (Dimitrijević, Sahal-Bréchot & Bommier 1991; Dimitrijević & Sahal-Bréchot 1992a,b, 1994) by comparison with quantum mechanical calculations obtained with a more sophisticated theoretical approach that includes more accurate oscillator strengths. Attention has been paid to the scaling of linewidths with the charge Z 'seen' by the optical electron: $Z = z + 1$ (where z is the ionic charge). There is a difference between the Z-scaling of theoretical and experimental Stark widths for homologous transitions (3s–3p and 2s3s–2s3p within Li-like and Be-like isoelectronic sequences, respectively; Glenzer, Uzelac & Kunze 1992, 1993; Blagojević et al. 1999; Hegazy et al. 2003; Elabidi, Sahal-Bréchot & Ben Nessib 2009). Here, we also study the Z-scaling of the 2s–2p linewidth, and we compare our results with the semiclassical results.

2 OUTLINE OF THE THEORY AND COMPUTATIONAL PROCEDURE

Here, we present an outline of the quantum formalism of electron impact broadening. More details have been given elsewhere (Elabidi, Ben Nessib & Sahal-Bréchot 2004; Elabidi et al. 2008a). The calculations are performed within the frame of the impact approximation. This means that the time interval between collisions is much longer than the duration of a collision. The expression of the full width at half-maximum W obtained in Elabidi et al. (2008a) is

$$W = 2N_{\rm e}\left(\frac{\hbar}{m}\right)^2\left(\frac{2m\pi}{k_{\rm B}T}\right)^{1/2} \times \int_0^\infty \Gamma_w(\varepsilon)\exp\left(-\frac{\varepsilon}{k_{\rm B}T}\right)\,{\rm d}\left(\frac{\varepsilon}{k_{\rm B}T}\right). \quad (1)$$

Here, $k_{\rm B}$ is the Boltzmann constant, $N_{\rm e}$ is the electron density, T is the electron temperature and

$$\Gamma_w(\varepsilon) = \sum_{J_{\rm i}^{\rm T}J_{\rm f}^{\rm T}lK_{\rm i}K_{\rm f}} \frac{\left[K_{\rm i}, K_{\rm f}, J_{\rm i}^{\rm T}, J_{\rm f}^{\rm T}\right]}{2} \times \left\{\begin{array}{ccc} J_{\rm i} & K_{\rm i} & l \\ K_{\rm f} & J_{\rm f} & 1 \end{array}\right\}^2 \left\{\begin{array}{ccc} K_{\rm i} & J_{\rm i}^{\rm T} & s \\ J_{\rm f}^{\rm T} & K_{\rm f} & 1 \end{array}\right\}^2 \times \{1 - [{\rm Re}\,(S_{\rm i}){\rm Re}\,(S_{\rm f}) + {\rm Im}\,(S_{\rm i}){\rm Im}\,(S_{\rm f})]\}, \quad (2)$$

where $L_{\rm i} + S_{\rm i} = J_{\rm i}$, $J_{\rm i} + l = K_{\rm i}$ and $K_{\rm i} + s = J_{\rm i}^{\rm T}$. L and S represent the atomic orbital angular momentum and spin of the target, l is the electron orbital momentum and the superscript 'T' denotes the quantum numbers of the total electron+ion system. $S_{\rm i}$ ($S_{\rm f}$) are the scattering matrix elements for the initial (final) levels, expressed in the intermediate coupling approximation, and Re(S) and Im(S) are the real and imaginary parts, respectively, of the S-matrix element.

$$\left\{\begin{array}{ccc} a & b & c \\ d & e & f \end{array}\right\}$$

represent 6–j symbols, and we adopt the notation $[x, y, \ldots] = (2x + 1)(2y + 1)\ldots$. Both $S_{\rm i}$ and $S_{\rm f}$ are calculated for the same incident electron energy $\varepsilon = mv^2/2$. Equation (1) takes into account fine-structure effects and relativistic corrections resulting from the breakdown of the *LS* coupling approximation for the target.

The calculation starts with the study of the atomic structure in intermediate coupling, which is done using the SUPERSTRUCTURE code (SST; Eissner, Jones & Nussbaumer 1974). The scattering problem in *LS* coupling is carried out by the DISTORTED WAVE (DW) code (Eissner 1998), as in Elabidi et al. (2008a). This weak coupling approximation for the collision part assumed in DW is adequate for highly charged ions colliding with electrons, because the close collisions are of little importance. The JAJOM code (Saraph 1978) is used for the scattering problem in intermediate coupling. $\mathbf{R}$ matrices in intermediate coupling and the real (Re $\mathbf{S}$) and imaginary (Im $\mathbf{S}$) parts of the scattering matrix $\mathbf{S}$ have been calculated using the transformed version of JAJOM (Elabidi & Dubau, unpublished results) and the program RTOS (Dubau, unpublished results), respectively. The evaluation of Re $\mathbf{S}$ and Im $\mathbf{S}$ is carried out according to

$${\rm Re}\,\mathbf{S} = \left(1 - \mathbf{R}^2\right)\left(1 + \mathbf{R}^2\right)^{-1}, \qquad {\rm Im}\,\mathbf{S} = 2\mathbf{R}\left(1 + \mathbf{R}^2\right)^{-1}. \quad (3)$$

The relation $\mathbf{S} = (1 + i\mathbf{R})(1 - i\mathbf{R})^{-1}$ guarantees the unitarity of the $\mathbf{S}$ matrix.

3 RESULTS AND DISCUSSION

3.1 Structure and electron scattering data

We have used the $1s^2\ nl (2 \le n \le 5)$ configurations to study the atomic structure of the five Li-like ions from C IV to Ne VIII. This set of configurations gives rise to 24 fine-structure levels listed in Tables 1 and 2. We have used the SST code (Eissner, Jones &

Table 1. Our present energy levels (in Ry) for C IV, N V and O VI compared to those of NIST (Ralchenko et al. 2011), where *i* labels the 24 levels.

Level designation			C IV		N V		O VI	
i	Conf.	Level	Present	NIST	Present	NIST	Present	NIST
1	$1s^2 2s$	$^2S_{1/2}$	0.00000	0.00000	0.00000	0.00000	0.00000	0.0000
2	$1s^2 2p$	$^2P^o_{1/2}$	0.58723	0.58762	0.73431	0.73324	0.88049	0.8782
3	$1s^2 2p$	$^2P^o_{3/2}$	0.58816	0.58860	0.73660	0.73559	0.88522	0.8831
4	$1s^2 3s$	$^2S_{1/2}$	2.75008	2.75976	4.14688	4.15653	5.82305	5.8325
5	$1s^2 3p$	$^2P^o_{1/2}$	2.90541	2.91651	4.34296	4.35372	6.05983	6.0701
6	$1s^2 3p$	$^2P^o_{3/2}$	2.90568	2.91680	4.34363	4.35442	6.06122	6.0715
7	$1s^2 3d$	$^2D_{3/2}$	2.94672	2.96052	4.40062	4.41422	6.13463	6.1476
8	$1s^2 3d$	$^2D_{5/2}$	2.94680	2.96062	4.40082	4.41442	6.13505	6.1481
9	$1s^2 4s$	$^2S_{1/2}$	3.64512	3.65735	5.51324	5.52546	7.75846	7.7703
10	$1s^2 4p$	$^2P^o_{1/2}$	3.70752	3.72081	5.59245	5.60558	7.85449	7.8673
11	$1s^2 4p$	$^2P^o_{3/2}$	3.70764	3.72092	5.59274	5.60588	7.85508	7.8679
12	$1s^2 4d$	$^2D_{3/2}$	3.72493	3.73926	5.61665	5.63087	7.88581	7.8996
13	$1s^2 4d$	$^2D_{5/2}$	3.72496	3.73929	5.61674	5.63095	7.88599	7.8998
14	$1s^2 4f$	$^2F^o_{5/2}$	3.72545	3.74015	5.61753	5.63217	7.88710	7.9014
15	$1s^2 4f$	$^2F^o_{7/2}$	3.72547	3.74015	5.61757	5.63221	7.88719	7.9015
16	$1s^2 5s$	$^2S_{1/2}$	4.04536	4.05850	6.12777	6.14090	8.63249	8.6451
17	$1s^2 5p$	$^2P^o_{1/2}$	4.07627	4.09028	6.16721	6.18113	8.68047	8.6942
18	$1s^2 5p$	$^2P^o_{3/2}$	4.07633	4.09034	6.16736	6.18128	8.68077	8.6942
19	$1s^2 5d$	$^2D_{3/2}$	4.08517	4.09968	6.17956	6.19400	8.69644	8.7104
20	$1s^2 5d$	$^2D_{5/2}$	4.08518	4.09970	6.17961	6.19404	8.69653	8.7104
21	$1s^2 5f$	$^2F^o_{5/2}$	4.08546	4.10015	6.18005	6.19471	8.69716	8.7115
22	$1s^2 5f$	$^2F^o_{7/2}$	4.08547	4.10015	6.18008	6.19471	8.69721	8.7115
23	$1s^2 5g$	$^2G_{7/2}$	4.08547	4.10023	6.18008	6.19481	8.69722	8.7116
24	$1s^2 5g$	$^2G_{9/2}$	4.08548	4.10023	6.18010	6.19481	8.69724	8.7116

Table 2. Same as in Table 1 but for F VII and Ne VIII.

Level designation			F VII		Ne VIII	
i	Conf.	Level	Present	NIST	Present	NIST
1	$1s^2 2s$	$^2S_{1/2}$	0.00000	0.00000	0.00000	0.00000
2	$1s^2 2p$	$^2P^o_{1/2}$	1.02632	1.02299	1.17210	1.16781
3	$1s^2 2p$	$^2P^o_{3/2}$	1.03503	1.03188	1.18689	1.18284
4	$1s^2 3s$	$^2S_{1/2}$	7.77889	7.78788	10.01479	10.02290
5	$1s^2 3p$	$^2P^o_{1/2}$	8.05640	8.06588	10.33311	10.34142
6	$1s^2 3p$	$^2P^o_{3/2}$	8.05897	8.06849	10.33747	10.34587
7	$1s^2 3d$	$^2D_{3/2}$	8.14910	8.16148	10.44455	10.45540
8	$1s^2 3d$	$^2D_{5/2}$	8.14989	8.16227	10.44589	10.45673
9	$1s^2 4s$	$^2S_{1/2}$	10.38114	10.39238	13.38177	13.39213
10	$1s^2 4p$	$^2P^o_{1/2}$	10.49403	10.50593	13.51157	13.52240
11	$1s^2 4p$	$^2P^o_{3/2}$	10.49511	10.50700	13.51340	13.52427
12	$1s^2 4d$	$^2D_{3/2}$	10.53277	10.54563	13.55808	13.56971
13	$1s^2 4d$	$^2D_{5/2}$	10.53310	10.54596	13.55865	13.57028
14	$1s^2 4f$	$^2F^o_{5/2}$	10.53458	10.54813	13.56049	13.57274
15	$1s^2 4f$	$^2F^o_{7/2}$	10.53474	10.54813	13.56078	13.57302
16	$1s^2 5s$	$^2S_{1/2}$	11.55989	11.57201	14.91051	14.92163
17	$1s^2 5p$	$^2P^o_{1/2}$	11.61644	11.62915	14.97566	14.98728
18	$1s^2 5p$	$^2P^o_{3/2}$	11.61699	11.62974	14.97660	14.98823
19	$1s^2 5d$	$^2D_{3/2}$	11.63618	11.64936	14.99934	15.01128
20	$1s^2 5d$	$^2D_{5/2}$	11.63635	11.64953	14.99963	15.01158
21	$1s^2 5f$	$^2F^o_{5/2}$	11.63718	11.65070	15.00067	15.01295
22	$1s^2 5f$	$^2F^o_{7/2}$	11.63727	11.65070	15.00082	15.01310
23	$1s^2 5g$	$^2G_{7/2}$	11.63728	11.65089	15.00083	15.01322
24	$1s^2 5g$	$^2G_{9/2}$	11.63733	11.65089	15.00092	15.01322

Nussbaumer 1974), where the wavefunctions are determined by diagonalization of the non-relativistic Hamiltonian using orbitals calculated in scaled Thomas–Fermi–Dirac–Amaldi (TFDA) potentials. The scaling parameters λ_l have been obtained by a self-consistent energy minimization procedure, in our case on all term energies of the 14 configurations. Relativistic corrections (spin-orbit, mass, Darwin and one-body) are introduced according to the Breit–Pauli approach (Bethe & Salpeter 1957) in intermediate coupling. In Tables 1 and 2, our level energies are compared to the experimental values compiled by the National Institute of Standards and Technology (NIST; Ralchenko et al. 2011). We find that the agreement between the two results is better than 1 per cent for all the ions studied here.

The oscillator strengths f_{ij} for some allowed transitions are presented in Tables 3 and 4 and are compared to the NIST values. The average agreement between them is about 3 per cent. However, we find for each ion that our oscillator strengths for some transitions are not in good agreement with those from NIST. For example, for the transitions $1s^2 2s\ ^2S_{1/2}$–$1s^2 4p\ ^2P^o_{1/2}$ (1–10), $1s^2 2s\ ^2S_{1/2}$–$1s^2 4p\ ^2P^o_{3/2}$ (1–11), $1s^2 3p\ ^2P^o_{1/2}$–$1s^2 4s\ ^2S_{1/2}$ (5–9) and $1s^2 3p\ ^2P^o_{3/2}$–$1s^2 4s\ ^2S_{1/2}$ (6–9), the agreements with the NIST values are 11, 11, 24 and 25 per cent, respectively. We find the same for the 1–10 and 1–11 transitions in the C IV ion.

Because our calculations are *ab initio*, the accuracy of the atomic structure (especially the oscillator strengths) is a prerequisite for the accuracy of the line-broadening results. From the above comparison, we can conclude that our atomic structure study is sufficiently accurate to be adopted in the scattering problem, and thus in the line-broadening calculations.

The electron scattering calculations in *LS* coupling have been performed in the distorted wave approximation through the DW code (Eissner 1998). Fine-structure collision strengths for low partial wave l of the incoming electron (l up to 29) have been obtained using the JAJOM code (Saraph 1978). This code transforms the transition matrix elements from *LS* coupling into intermediate ones using the term coupling coefficients (TCC)

Table 3. Oscillator strengths of some allowed transitions for C IV, N V and O VI compared to NIST values.

Transition	C IV		N V		O VI	
i–j	Present	NIST	Present	NIST	Present	NIST
1–2	0.0959	0.0953	0.0787	0.0780	0.0667	0.0661
1–3	0.1922	0.1905	0.1580	0.1563	0.1342	0.1327
1–5	0.0696	0.0678	0.0809	0.0794	0.0893	0.0885
1–6	0.1391	0.1355	0.1615	0.1588	0.1782	0.1770
1–10	0.0231	0.0204	0.0250	0.0230	0.0263	0.0247
1–11	0.0462	0.0408	0.0499	0.0459	0.0526	0.0494
2–4	0.0378	0.0375	0.0324	0.0323	0.0289	0.0289
2–7	0.6499	0.6456	0.6551	0.6531	0.6590	0.6576
2–9	0.0073	0.0070	0.0064	0.0062	0.0058	0.0057
3–4	0.0379	0.0377	0.0325	0.0323	0.0290	0.0290
3–7	0.0650	0.0646	0.0656	0.0652	0.0660	0.0656
3–8	0.5852	0.5807	0.5900	0.5874	0.5936	0.5915
3–9	0.0073	0.0070	0.0064	0.0062	0.0058	0.0057
4–5	0.1580	0.1599	0.1302	0.1312	0.1106	0.1114
4–6	0.3166	0.3199	0.2614	0.2630	0.2226	0.2239
4–10	0.0712	0.0678	0.0848	0.0818	0.0946	0.0922
4–11	0.1433	0.1358	0.1692	0.1637	0.1886	0.1849
5–7	0.0589	0.0628	0.0525	0.0552	0.0473	0.0492
5–9	0.0823	0.0815	0.0715	0.0708	0.0644	0.0637
6–7	–	0.0062	0.0052	0.0055	0.0046	0.0048
6–8	0.0528	0.0564	0.0469	0.0492	0.0420	0.0435
6–9	0.0825	0.0815	0.0717	0.0708	0.0647	0.0638
7–10	0.0136	0.0138	0.0131	0.0132	0.0127	0.0127
7–11	0.0027	0.0028	0.0026	0.0026	0.0025	0.0025

Table 4. Same as in Table 3 but for the F VII and Ne VIII transitions.

Transition	F VII		Ne VIII	
i–j	Present	NIST	Present	NIST
1–2	0.0578	0.0558	0.0510	0.0502
1–3	0.1167	0.1125	0.1034	0.1019
1–5	0.0957	0.0955	0.1008	0.1009
1–6	0.1909	0.1910	0.2008	0.2009
1–10	0.0273	0.0242	0.0280	0.0270
1–11	0.0545	0.0483	0.0559	0.0541
2–4	0.0264	0.0240	0.0246	0.0247
2–7	0.6621	0.6652	0.6646	0.6652
2–9	0.0053	0.0047	0.0050	0.0050
3–4	0.0266	0.0239	0.0249	0.0249
3–7	0.0663	0.0667	0.0666	0.0664
3–8	0.5967	0.5983	0.5992	0.5970
3–9	0.0054	0.0047	0.0051	0.0050
4–5	0.0962	0.0955	0.0850	0.0855
4–6	0.1942	0.1927	0.1725	0.1659
4–10	0.1022	0.1074	0.1082	–
4–11	0.2035	0.2143	0.2152	–
5–7	0.0430	0.0439	0.0395	0.0340
5–9	0.0594	0.0449	0.0557	–
6–7	0.0042	0.0043	0.0038	0.0037
6–8	0.0380	0.0388	0.0346	0.0324
6–9	0.0598	0.0448	0.0562	–
7–10	0.0123	–	0.0120	–
7–11	0.0024	–	0.0024	–

provided by SST. It is known that, for highly charged ions, the distorted wave approach is sufficiently accurate and the agreement between DW and more sophisticated methods (e.g. close coupling) is good.

For large l values, the above method becomes cumbersome and inaccurate, but the contributions of these values of l to collision strengths cannot be neglected. For $30 \leq l \leq 50$, we have adopted two different procedures. For allowed transitions, the contribution has been taken into account using the JAJOM–CBE code (Dubau, unpublished results) based upon the Coulomb–Bethe formulation of Burgess & Sheorey (1974) and adapted to the JAJOM approximation. For forbidden transitions, the contribution has been estimated by the SERIE-GEOM code, assuming a geometric series behaviour for high partial wave collision strengths (Chidichimo & Haig 1989; Chidichimo 1992).

We compare our collision strengths with those obtained by Aggarwal & Keenan (2004a,b) and Aggarwal, Keenan & Heeter (2010) using the Dirac atomic R-matrix code (DARC) of Norrington & Grant (private communication). This is a fully relativistic program, taking into account relativistic effects in both the target and the scattering study. This code is based on the *jj* coupling scheme and uses the Dirac–Coulomb Hamiltonian in the R-matrix approach. Table 5 presents collision strengths for C IV and O VI ions for transitions from the ground and the two first excited levels to the 10 first excited levels. In Table 6, we also present the collision strengths for N V, F VII and Ne VIII ions for transitions from the ground level to all the other levels. From Table 5, we find that the average relative difference between the two collision strengths ($\Delta\Omega/\Omega$) is about 36 per cent for C IV and 26 per cent for O VI. Table 6 shows that this difference is about 39 per cent for N V, 26 per cent for F VII and 17 per cent for Ne VIII. These results show clearly that our method is more adequate to highly charged ions. Thus, our results could converge to the more sophisticated R-matrix results for highly ionized atoms. The greatest disagreement between the two calculations is found

Table 5. Collision strengths for some transitions compared to the R-matrix (DARC) calculations: C IV (Aggarwal & Keenan 2004a); O VI (Aggarwal & Keenan 2004b).

Transition	C IV (06 Ry)		O VI (15 Ry)	
i–j	Present	DARC	Present	DARC
1–2	5.1181	4.9960	2.7505	2.8460
1–3	10.4218	9.9880	5.5515	5.6850
1–4	0.2514	0.3909	0.1384	0.1982
1–5	0.0678	0.0808	0.0583	0.0640
1–6	0.1363	0.1613	0.1175	0.1272
1–7	0.2846	0.2760	0.1602	0.1618
1–8	0.4278	0.4139	0.2410	0.2427
1–9	0.0442	0.0796	0.0256	0.0038
1–10	0.0150	0.0297	0.0116	0.0170
2–3	0.4900	0.6494	0.2078	0.2793
2–4	0.0904	0.1057	0.0317	0.0373
2–5	0.3042	0.4366	0.1519	0.2161
2–6	0.0975	0.1055	0.0428	0.0450
2–7	2.1122	2.1040	1.1306	1.1590
2–8	0.1561	0.1664	0.0604	0.0656
2–9	0.0151	0.0292	0.0055	0.0087
2–10	0.0515	0.0916	0.0274	0.0418
3–4	0.1790	0.2118	0.0641	0.0749
3–5	0.0974	0.1057	0.0430	0.0452
3–6	0.7260	0.9789	0.3568	0.0478
3–7	0.5740	1.0340	0.2843	0.3113
3–8	4.0250	3.9250	2.1278	2.1450
3–9	0.0297	0.0584	0.0111	0.0175
3–10	0.0253	0.0402	0.0110	0.0141

Table 6. Same as in Table 5 but for N v, F vii and Ne viii. Comparison is made with the R-matrix results of Aggarwal, Keenan & Heeter (2010).

Transition	N v (10 Ry)		F vii (20 Ry)		Ne viii (40 Ry)	
i–j	Present	DARC	Present	DARC	Present	DARC
1–2	3.6838	3.7070	2.1094	2.2310	1.6683	1.9940
1–3	7.4581	7.4010	4.2512	4.4440	3.3492	3.9660
1–4	0.1846	0.2708	0.1052	0.1502	0.0946	0.1252
1–5	0.0644	0.0723	0.0491	0.0538	0.0638	0.0658
1–6	0.1297	0.1440	0.0989	0.1068	0.1274	0.1304
1–7	0.2101	0.2090	0.1237	0.1260	0.1133	0.1180
1–8	0.3160	0.3135	0.1861	0.1890	0.1705	0.1770
1–9	0.0339	0.0533	0.0194	0.0288	0.0179	0.0240
1–10	0.0132	0.0217	0.0096	0.0134	0.0125	0.0147
1–11	0.0269	0.0432	0.0195	0.0267	0.0253	0.0292
1–12	0.0353	0.0422	0.0197	0.0229	0.0173	0.0196
1–13	0.0531	0.0633	0.0296	0.0343	0.0260	0.0294
1–14	0.0156	0.0185	0.0093	0.0104	0.0078	0.0085
1–15	0.0210	0.0247	0.0125	0.0139	0.0106	0.0113
1–16	0.0127	0.0222	0.0072	0.0116	0.0068	0.0093
1–17	0.0053	0.0116	0.0037	0.0062	0.0047	0.0062
1–18	0.0107	0.0231	0.0075	0.0124	0.0096	0.0123
1–19	0.0125	0.0182	0.0069	0.0092	0.0059	0.0072
1–20	0.0188	0.0273	0.0104	0.0138	0.0089	0.0108
1–21	0.0084	0.0109	0.0049	0.0057	0.0040	0.0043
1–22	0.0112	0.0145	0.0065	0.0077	0.0054	0.0058
1–23	0.0007	0.0011	0.0004	0.0005	0.0003	0.0003
1–24	0.0009	0.0013	0.0005	0.0006	0.0003	0.0004

for the 1–16, 1–17 and 1–18 transitions and also for 1–4 and 1–9 transitions. All these transitions are optically forbidden, except for the two transitions 1–17 and 1–18. We also note that in Aggarwal, Keenan & Heeter (2010), the highest difference between the R-matrix results and those obtained by the fully relativistic distorted wave code (FAC) of Gu (2003) is found for the 1–9, 1–10 and 1–11 transitions.

In general, the two sets of collision strengths agree within 28 per cent for the five ions. We note that besides the comparison of our linewidths with experimental and other theoretical linewidths, the comparison of our scattering parameters with other results can be another tool to ensure that our line-broadening calculations are sufficiently accurate. This is because the scattering problem provides scattering matrices that are used in the line-broadening calculations. A comparison with experimental scattering parameters (cross-sections or collision strengths) should be more efficient for this purpose. Such a comparison can be found in Elabidi, Sahal-Bréchot & Ben Nessib (2011).

3.2 Line-broadening data

Except for the C iv ion, there are no experimental results for the resonance line 2s–2p. In Table 7, we present our C iv linewidths compared to the measured linewidths and to other theoretical data. The present quantum mechanical calculations are always in agreement (within less than 1 per cent) with the semiclassical results (Dimitrijević, Sahal-Bréchot & Bommier 1991), but they are two times higher than the close coupling (CC) results (Seaton 1988). The modified semi-empirical widths (MSEs) are in agreement with the CC results within 23 per cent. If we now compare our widths (W) and the CC widths (W_{CC}) to the experimental values (W_m), we find $(W/W_m)_{av} = 1.71$ and $(W_{CC}/W_m)_{av} = 1.36$. It is perhaps not easy to make a conclusion about this last comparison, and new measurements for the C iv 2s–2p linewidths should be made in order to update the two last experiments (Bogen 1972; El-Farra & Hughes 1983).

Table 7. Present FWHM (in Å) of the C iv 2s ^{2}S–2p ^{2}P^o resonance line compared to the experimental results and to other theoretical results. SCP denotes semiclassical perturbation calculations (Dimitrijević, Sahal-Bréchot & Bommier 1991), MSE denotes modified semi-empirical calculations (Dimitrijević & Konjević 1981) and CC denotes close-coupling calculations (Seaton 1988).

T	W	W_{exp}	W/W_{SCP}	W/W_{CC}	W/W_{MSE}
2.0	1.18E−02	–	1.03	–	–
4.0	8.44E−03	–	–	1.90	2.33
5.0	7.60E−03	–	1.05	–	–
5.3[a]	7.40E−03	3.34E−03	–	1.92	–
6.0[b]	7.00E−03	5.83E−03	–	1.88	–
8.0	6.16E−03	–	1.07	1.96	2.4
10.0	5.61E−03	–	1.08	–	–
15.0	4.78E−03	–	1.11	–	–
20.0	4.30E−03	–	1.13	–	–

[a]El-Farra & Hughes (1983).
[b]Bogen (1972).

In Table 8, some of our results for the N v, O vi, F vii and Ne viii ions are compared to the available semiclassical results (Dimitrijević & Sahal-Bréchot 1992a,b, 1993b, 1994). The agreement between the two calculations is better for N v and O vi (the averaged value of the ratio W/W_{SCP} is about 1.04) than for the F vii and Ne viii cases (W/W_{SCP} is about 0.77). In Tables 9 and 10, we also present the Stark electron impact widths (W) of the C iv, N v, O vi, F vii and Ne viii resonance doublets for a wide range of electron temperatures (10^4–5×10^6 K) and at an electron density of 10^{17} cm^{-3}. Such temperatures are of interest for some hot star atmospheres, such as for PG 1195 stars and DO white dwarfs, subphotospheric layers, soft X-ray lasers and laser-produced plasmas. They are also important for fusion plasmas and stellar interiors. The wavelengths are taken from NIST (Ralchenko et al. 2011).

The results presented for the C iv, N v, O vi, F vii and Ne viii resonance linewidths will be of great interest in the development of spectral analysis using the NLTE model atmosphere techniques because they extend the missing broadening data to a wide range of temperatures and electron densities. For example, Stark broadening parameters for the considered ions are needed for the modelling and theoretical considerations of subphotospheric layers (Seaton 1987) and for the interpretation and modelling of some hot star spectra, such as, for example, PG 1159-type stars (Werner, Heber & Hunger 1991).

3.3 *Z*-scaling of linewidths

Elabidi, Sahal-Bréchot & Ben Nessib (2009) have studied the Z-scaling problem (where Z is the charge 'seen' by the optical electron) for the 3s–3p transitions in 10 Li-like ions from C iv to P xiii. We have found that our calculations give widths that are related to the charge by $W \propto Z^{-1.84}$, and that semiclassical calculations give $W \propto Z^{-1.43}$. This problem has been dealt with in some other experimental works. Blagojević et al. (1999) have found that the measured widths are related to the charge by $W \propto Z^{-0.79}$ for Li-like ions (only C iv, N v and O vi). Glenzer, Uzelac & Kunze (1992, 1993) and Hegazy et al. (2003) found $W \propto Z^{-1.13}$. This shows that there are still discrepancies between the experimental and the theoretical predictions of the Z-scaling of widths. In the present work, we try to look for the same Z-scaling, but for the 2s–2p resonance

Table 8. Present FWHM W (in Å) of the N V, O VI and Ne VIII 2s $^2S_{1/2}$–2p $^2P^o_{3/2}$ lines compared to the semiclassical perturbation results W_{SCP}: N V (Dimitrijević & Sahal-Bréchot 1992b); O VI (Dimitrijević & Sahal-Bréchot 1992a); F VII (Dimitrijević & Sahal-Bréchot 1993b); Ne VIII (Dimitrijević & Sahal-Bréchot 1994). Temperature values are given in 10^5 K and the electron density is 10^{17} cm^{-3}.

	N V		O VI		F VII		Ne VIII	
T	W	W/W_{SCP}	W	W/W_{SCP}	W	W/W_{SCP}	W	W/W_{SCP}
0.5	3.44E−03	0.96	–	–	–	–	–	–
1	2.49E−03	0.98	1.45E−03	0.99	7.20E-04	0.81	–	–
2	1.85E−03	1.01	1.07E−03	1.02	5.21E-04	0.81	3.14E−04	0.72
4	–	–	–	–	–	–	–	–
5	1.30E−03	1.04	7.67E−03	1.11	3.50E-04	0.82	2.07E−04	0.73
8	–	–	6.24E−03	1.09	–	–	–	–
10	–	–	–	–	2.64E-04	0.83	1.55E−04	0.74
20	–	–	–	–	–	–	1.15E−04	0.73

Table 9. Stark electron impact widths (FWHM) in Å of the 2s $^2S_{1/2}$–2p $^2P^o_{3/2}$ line for C IV, N V, O VI, F VII and Ne VIII. Temperature values are given in 10^5 K and the electron density is 10^{17} cm^{-3}.

	C IV	N V	O VI	F VII	Ne VIII
T	1548.19	1238.82	1031.91	883.10	770.41
0.1	1.65E−02	7.54E−03	3.91E−03	2.22E−03	1.35E−03
0.3	9.66E−03	4.39E−03	2.27E−03	1.29E−03	7.81E−04
0.5	7.60E−03	3.44E−03	1.77E−03	1.00E−03	6.08E−04
1.0	5.61E−03	2.49E−03	1.28E−03	7.20E−04	4.35E−04
3.0	3.72E−03	1.58E−03	7.90E−04	4.35E−04	2.60E−04
5.0	3.09E−03	1.30E−03	6.58E−04	3.50E−04	2.07E−04
10.0	2.34E−03	9.92E−04	5.06E−04	2.64E−04	1.55E−04
50.0	9.65E−04	4.38E−04	2.26E−04	1.25E−04	7.46E−05

Table 10. Same as in Table 9 but for the 2s $^2S_{1/2}$–2p $^2P^o_{1/2}$ line.

	C IV	N V	O VI	F VII	Ne VIII
T	1550.77	1242.80	1037.61	890.76	780.32
0.1	1.68E−02	7.68E−03	4.00E−03	2.28E−03	1.40E−03
0.3	9.82E−03	4.47E−03	2.32E−03	1.32E−03	8.09E−04
0.5	7.72E−03	3.50E−03	1.81E−03	1.03E−03	6.30E−04
1.0	5.68E−03	2.53E−03	1.30E−03	7.39E−04	4.50E−04
3.0	3.76E−03	1.60E−03	8.01E−04	4.46E−04	2.69E−04
5.0	3.12E−03	1.32E−03	6.57E−04	3.59E−04	2.14E−04
10.0	2.35E−03	1.00E−03	5.02E−04	2.70E−04	1.60E−04
50.0	9.69E−04	4.42E−04	2.28E−04	1.28E−04	7.68E−05

transitions of Li-like ions. There are not enough experimental widths at the required temperatures for the transitions of ions studied here (except for C IV). Therefore, we cannot perform an experimental Z-scaling for comparison. In Fig. 1, we present the behaviour of $\log_{10}(W)$ and $\log_{10}(W_{SCP})$ as a function of $\log_{10}(Z)$. The widths are expressed in angular frequency units. We find that the dependence of the linewidths with the charge Z can be expressed as $W \propto Z^{-\alpha}$ with $\alpha = 1.67$ for our values and $\alpha_{SCP} = 1.13$ for the semiclassical values. We also note that these values of α can be different for different chosen temperatures. Fig. 2 displays the same Z-scaling of linewidths, but at temperature $T = 2 \times 10^5$ K and for the same electron density as in Fig. 1. We find $\alpha = 1.76$ and $\alpha_{SCP} = 1.11$. To decide about the validity and utility of this scaling, more experimental linewidths are needed for the resonance transitions of the five studied ions.

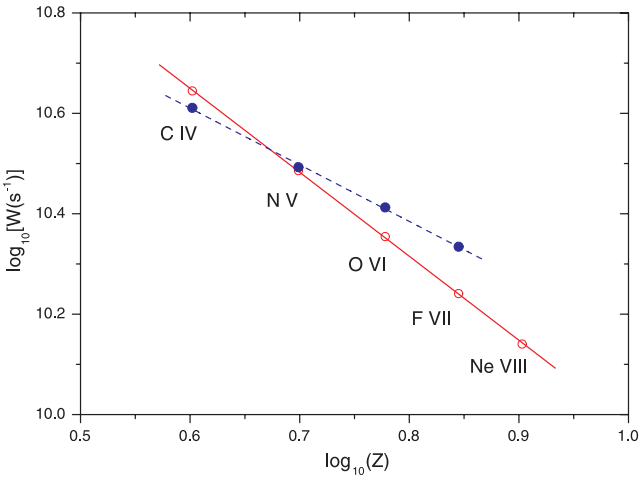

Figure 1. Our Stark width in angular frequency units W (open circles) of the 2s $^2S_{1/2}$–2p $^2P^o_{3/2}$ transition for the C IV, N V, O VI, F VII and Ne VIII ions as a function of Z compared with the semiclassical widths W_{SCP} (solid circles). The solid and dashed lines are the linear fits of the W and W_{SCP} widths, respectively. $T = 10^5$ K and $N_e = 10^{17}$ cm^{-3}.

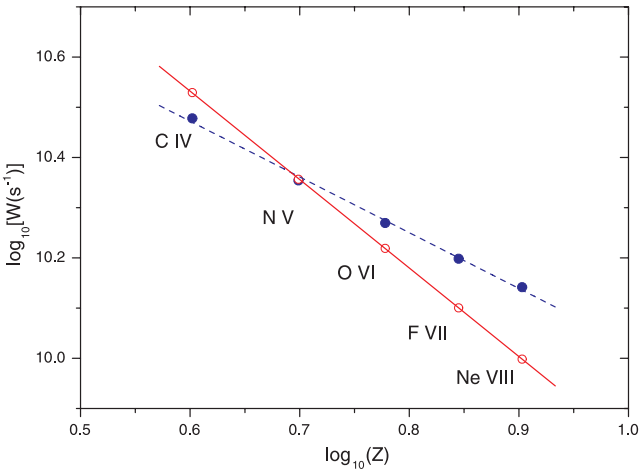

Figure 2. Same as in Fig. 1, but for $T = 2 \times 10^5$ K.

4 SUMMARY OF THE RESULTS AND CONCLUSION

We have performed quantum mechanical calculations of Stark electron impact widths for the resonance doublets of the C IV, N V, O VI,

F VII and Ne VIII ions. Our results are presented within the wide range of temperatures required for the development of spectral analysis using the NLTE model atmospheres. Our calculated data can solve some of the problems that have been encountered and reported by Rauch et al. (2007) when calculating the element abundance by filling in the missing line-broadening data. Thus, it is no longer necessary to extrapolate the existing data, as was done for some cases in Rauch et al. (2007). Our quantum linewidths have also been compared to the SCP results in order to check the previous SCP calculations. A good agreement has been found between them (within 1 per cent).

A confirmation of previous SCP results using more sophisticated quantum mechanical results is important as such data are often used for stellar spectra modelling and interpretation. In some cases (e.g. hot white dwarfs) the Stark broadening is the dominant broadening mechanism, and the accuracy of used data might be important.

Our results are also compared to the only experimental results for C IV lines (El-Farra & Hughes 1983; Bogen 1972). We find that our calculations give linewidths that are 71 per cent higher than those measured. The CC (Seaton 1988) and MSE results (Dimitrijević & Konjević 1981) agree well; regarding the lines investigated here, they exist only for the C IV lines. More measurements of the resonance lines for these ions would be very useful for checking the previous and present calculations.

Part of this work has been dedicated to the Z-scaling of linewidths. As in previous papers (Glenzer, Uzelac & Kunze 1992, 1993; Blagojević et al. 1999; Elabidi, Sahal-Bréchot & Ben Nessib 2009), the scaling with Z is different from one approach to another. We find that widths are related to Z by $W \propto Z^{-\alpha}$ when $\alpha = 1.67$ for our calculations and $\alpha_{\rm SCP} = 1.13$ for the SCP calculations for $T = 10^5$ K. These values of α can change with temperature (e.g. for $T = 2 \times 10^5$ K, we find $\alpha = 1.76$ and $\alpha_{\rm SCP} = 1.11$). Because there are not enough experimental results for these lines, we cannot make any conclusions about this scaling.

We have also calculated the atomic structure and collision data for the five ions. A comparison with the NIST values (Ralchenko et al. 2011) for the atomic structure shows an agreement better than 1 per cent for level energies, and within 3 per cent for the oscillator strengths. Our distorted wave collision strengths have been compared to the R-matrix results (Aggarwal & Keenan 2004a,b; Aggarwal, Keenan & Heeter 2010) at different electron energies. We find an average relative difference (over the five ions) between the two approaches of about 28 per cent. We confirm that the distorted wave method is more adequate for highly charged ions. Because in our line-broadening calculation procedure we use atomic structure (level energies and oscillator strengths) and collision data (collision strengths, scattering matrices), this comparison might be another tool to check our line-broadening results, besides a comparison of widths with those measured.

ACKNOWLEDGMENTS

This work has been supported by the Tunisian research unit 05/UR/12-04, the French UMR 8112 and the bilateral cooperation agreement between the Tunisian DGRS and the French CNRS (project code 09/R 13-03, project No. 22637). This work is also supported by the Ministry of Education and Science of the Republic of Serbia (project 176002). The authors are indebted to J. Dubau and M. Cornille for their invaluable help in the use of the SST/DW/JAJPOLARI/RTOS computer codes and their adaptation to line broadening.

REFERENCES

Aggarwal K. M., Keenan F. P., 2004a, Phys. Scr., 69, 385
Aggarwal K. M., Keenan F. P., 2004b, Phys. Scr., 70, 222
Aggarwal K. M., Keenan F. P., Heeter R. F., 2010, Phys. Scr., 81, 015303
Barstow M. A., Hubeny I., Holberg J. B., 1998, MNRAS, 299, 520
Bethe H. A., Salpeter E. E., 1957, Quantum Mechanics of One-and Two-Electron Atoms. Springer, Berlin
Blagojević B., Popović M. V., Konjević N., Dimitrijević M. S., 1999, J. Quant. Spectrosc. Radiat. Transfer, 61, 361
Bogen P., 1972, Z. Naturf. A, 27, 210
Burgess A., Sheorey V. B., 1974, J. Phys. B: At. Mol. Opt. Phys., 7, 2403
Chidichimo M. C., 1992, Phys. Rev. A, 45, 1690
Chidichimo M. C., Haig S. P., 1989, Phys. Rev. A, 39, 4991
Dimitrijević M. S., 2003, Astronomical and Astrophysical Transactions, 22, 389
Dimitrijević M. S., Konjević K., 1981, in Wende B., de Gruyter W., eds, Spectral Line Broadening by Plasmas. Springer, Berlin, p. 211
Dimitrijević M. S., Sahal-Bréchot S., 1992a, A&AS, 93, 359
Dimitrijević M. S., Sahal-Bréchot S., 1992b, A&AS, 95, 109
Dimitrijević M. S., Sahal-Bréchot S., 1993a, A&AS, 100, 91
Dimitrijević M. S., Sahal-Bréchot S., 1993b, A&AS, 101, 587
Dimitrijević M. S., Sahal-Bréchot S., 1994, A&AS, 107, 349
Dimitrijević M. S., Sahal-Bréchot S., Bommier V., 1991, A&AS, 89, 581
Eissner W., 1998, Comput. Phys. Comm., 114, 295
Eissner W., Jones M., Nussbaumer H., 1974, Comput. Phys. Comm., 8, 270
Elabidi H., Sahal-Bréchot S., 2011, Eur. Phys. J. D, 61, 258
Elabidi H., Ben Nessib N., Sahal-Bréchot S., 2004, J. Phys. B: At. Mol. Opt. Phys., 37, 63
Elabidi H., Sahal-Bréchot S., Ben Nessib N., 2009, Eur. Phys. J. D, 54, 51
Elabidi H., Sahal-Bréchot S., Ben Nessib N., 2011, Baltic Astron., in press
Elabidi H., Ben Nessib N., Cornille M., Dubau J., Sahal-Bréchot S., 2007, in Popović L. Č., Dimitrijević M. S., eds, AIP Conf. Proc. Vol. 938, Spectral Line Shapes in Astrophysics. Am. Inst. Phys., New York, p. 272
Elabidi H., Ben Nessib N., Cornille M., Dubau J., Sahal-Bréchot S., 2008a, J. Phys. B: At. Mol. Opt. Phys., 41, no 025702
Elabidi H., Ben Nessib N., Sahal-Bréchot S., 2008b, in González M. A., Gigosos M. A., eds, AIP Conf. Proc. Vol. 1058, Spectral Line Shapes. Am. Inst. Phys., New York, p. 146
El-Farra M. A., Hughes T. P., 1983, J. Quant. Spectrosc. Radiat. Transfer, 30, 335
Glenzer S., Uzelac N. I., Kunze H. J., 1992, Phys. Rev. A, 45, 8795
Glenzer S., Uzelac N. I., Kunze H. J., 1993, in Stamm R., Talin B., eds, Spectral Line Shapes, Vol. 7. Nova, New York
Gu M. F., 2003, ApJ, 582, 1241
Hegazy H., Seidel S., Wrubel Th., Kunze H. J., 2003, J. Quant. Spectrosc. Radiat. Transfer, 81, 221
Popović L. Č., Dimitrijević M. S., Tankosić D., 1999, A&AS, 139, 617
Ralchenko Yu. V., Kramida A. E., Reader J. and NIST ASD Team (2011), NIST Atomic Spectra Database (version 4.0.1), http://physics.nist.gov
Rauch T., Ziegler M., Werner K., Kruk J. W., Oliveira C. M., Putte D. Vande, Mignani R. P., Kerber F., 2007, A&A, 470, 317
Saraph H. E., 1978, Comput. Phys. Comm., 15, 247
Seaton M. J., 1987, J. Phys. B: At. Mol. Phys., 20, 6363
Seaton M. J., 1988, J. Phys. B: At. Mol. Phys., 21, 3033
Tankosić D., Popović L. Č., Dimitrijević M. S., 2003, A&A, 399, 795
Werner K., Heber U., Hunger K., 1991, A&AS, 244, 437

This paper has been typeset from a TEX/LATEX file prepared by the author.

Monthly Notices
of the
ROYAL ASTRONOMICAL SOCIETY

Mon. Not. R. Astron. Soc. **422,** 610–618 (2012) doi:10.1111/j.1365-2966.2012.20638.x

Stark shifts and transition probabilities within the Kr I spectrum

V. Milosavljević,[1,2,3] Z. Simić,[3,4] S. Daniels[2⋆] and M. S. Dimitrijević[3,4,5]

[1]*Faculty of Physics, University of Belgrade, PO Box 368, Belgrade, Serbia*
[2]*NCPST, Dublin City University, Dublin 9, Ireland*
[3]*Institute Isaac Newton of Chile, Yugoslavia Branch, Belgrade, Serbia*
[4]*Astronomical Observatory, 11060 Belgrade, Volgina 7, Serbia*
[5]*Observatoire de Paris, 92195 Meudon Cedex, France*

Accepted 2012 January 26. Received 2012 January 24; in original form 2011 November 11

ABSTRACT

On the basis of 28 experimentally determined prominent neutral krypton (Kr I) line shapes (in the 5s–5p and 5s–6p transitions), we have obtained electron (d_e) and ion (d_i) contributions to the total Stark shifts (d_t). Stark shifts are also calculated using the semiclassical perturbation formalism (SCPF) for electrons, protons and helium ions as perturbers up to 50 000 K electron temperatures. Transition probabilities of spontaneous emission (Einstein's $A_{k,i}$ values) have been obtained using the relative line-intensity ratio method.

The separate electron (d_e) and ion (d_i) contributions to the total Stark shifts are presented, as well as the ion-broadening parameters, which describe the influence of the ion–dynamical effect on the shift of the line shape, for neutral krypton spectral lines. We made a comparison of our measured and calculated d_e data and compared both of these with other available experimental and theoretical d_e values.

Key words: atomic data – atomic processes – line: profiles – plasmas.

1 INTRODUCTION

Plasma-broadened and shifted spectral line profiles have been used for a number of years as the basis for an important non-interfering plasma diagnostic technique. Numerous theoretical and experimental efforts have been made to provide reliable data for such applications (Hamdi et al. 2008; Lesage 2009; Vennes, Kawka & Neḿeth 2011). This technique became, in some cases, the most sensitive and sometimes even the only possible plasma diagnostic tool, of interest not only for laboratory plasmas but also for astrophysical plasmas.

During investigations of the spectra of planetary nebulae (Dinerstein 2001), it was found that krypton is one of the most abundant elements in the Universe with $Z > 32$. Krypton is an example of the elements produced in asymptotic giant branch (AGB) stars, and quality atomic data like spectral line-broadening parameters or transition probabilities would help to improve surface abundance diagnostics or abundance measurements in planetary nebulae (see e.g. The, El Eid & Meyer 2007; Karakas et al. 2009; Sterling 2011). Moreover, such data are also of interest for diffusion calculations (Hui Bon Hoa et al. 2002). Krypton has been detected in the interstellar medium with the help of the Goddard High-Resolution Spectrograph on the *Hubble Space Telescope* (see e.g. Cardelli, Savage & Ebbets 1991; Cardelli & Meyer 1997; Sonnentrucker at al. 2003; Cartledge et al. 2001, 2008; Cartledge, Meyer & Lauroesch 2003), which renewed interest in its atomic data, particularly for transition probabilities. Cardelli et al. (1991) also underline that 'since the formation of Kr is from a mixture of s- and r-process nucleosynthesis, further observations of this important atom will provide significant insights about nucleosynthesis and interstellar enrichment processes'. Leckrone et al. (1993) emphasize that the material from which young early-type stars are formed also contains krypton, so that good Kr I model atoms and reliable Stark-broadening data are useful for stellar atmosphere calculations, stellar plasma analysis and modelling.

Classical emission laboratory plasma spectroscopy has mainly been applied to optically thin plasmas, where absorption of the emitted radiation is negligible. Investigation of the line profiles of atomic krypton in medium-dense plasmas, at about $1 \times 10^{23}\,\mathrm{m}^{-3}$, is of particular interest to check the predictions of theoretical approximations. Since krypton is a constituent of laboratory and astrophysical plasmas, the Kr I spectral line shapes represent important sources of information about physical conditions in the place of radiation origin (Kennedy et al. 2004; Malcheva et al. 2009; Cowley et al. 2010). Consequently, knowledge of the Stark-broadening parameters of spectral lines is of interest for diagnostics, modelling and consideration of astrophysical, laboratory and technological plasmas (Milosavljević & Djeniže 2002; Elabidi, Ben Nessib & Dimitrijević 2006; Popović at al. 2008; Elabidi et al. 2011). Exhaustive knowledge of Stark broadening and the shift parameters of spectral lines and their dependence on the electron density and temperature enables researchers to determine them using the plasma diagnostics. In the case of krypton, these measurements are

⋆E-mail: stephen.daniels@dcu.ie

important in astrophysics and industry, where krypton plays an important role in lasers and light sources (Eikema at al. 1996).

Various kinetic processes appearing in plasma modelling (Lieberman & Lichtenberg 1994) require reliable knowledge of the $A_{k,i}$ values (Lesage & Fuhr 1999). Furthermore, knowledge of the $A_{k,i}$ values gives us the possibility of determining the ($B_{k,i}$ and $B_{i,k}$) coefficients that characterize the absorption and stimulated emission. These processes are also important in laser physics and astrophysics.

The Stark shift of neutral krypton spectral lines has been studied experimentally several times. The first measurements of the Stark shifts of Kr I lines emitted from a shock-tube plasma have been performed by Klein & Meiners (1977). The broadening and shift of isolated lines are mainly determined by the quadratic Stark effect. The authors have reported emission measurements of the shifts for four Kr I spectral lines with statistical errors. These data have also been reviewed by Konjević, Dimitrijević & Wiese (1984). Vitel et al. (1988) and Valognes et al. (2005) presented experimental results on the broadening and shift of the Kr I 587-nm line emitted by high-electron-density plasma created in linear flash tubes. Also, an experimental study of the Stark broadening and shift for the same Kr I 587-nm line is reported by Uzelac & Konjević (1989). They compared the shifts in previous experimental work with the theoretical results of Dimitrijević & Konjević (1986). As an example, the ratio between the measured and theoretical value is 0.67 for an electron density of 7.6×10^{23} m^{-3} and an electron temperature of 11 900 K.

Due to large uncertainties in the theoretically determined Stark-broadening parameters (e.g. ±30 per cent for the semiclassical method as estimated in Griem 1974), the mutual agreement of experimental values independently obtained in various laboratories permits us to single out some lines as particularly reliable and suitable for diagnostic purposes. Since the dependence of Stark-broadening parameters on temperature is still not known with high accuracy, it is of interest also to have experimental results over a wide temperature range.

Using the semiclassical perturbation formalism (SCPF) (updated several times: Sahal-Bréchot 1969a,b, 1974; Dimitrijević & Sahal-Bréchot 1984, 1985; Dimitrijević, Sahal-Bréchot & Bommier 1991), we have calculated $d_{\rm e}^{\rm Th}$ values for 11 Kr I lines and also Stark-line shifts generated by impacts with protons and helium ions, which are often the main ion perturbers in astrophysical plasmas. Our experimental and theoretical values are compared with other available data. The basic plasma parameters, i.e. electron temperature ($T^{\rm exp}$) and electron density ($N^{\rm exp}$), are measured using independent, well-known, experimental diagnostic techniques (Milosavljević, Djeniže, & Dimitrijević 2003).

Existing measured and calculated Kr I transition-probability values (Einstein's A values) are collected in a number of articles and the most comprehensive data base can be found at the National Institute of Standards and Technology (NIST: Ralchenko et al. 2011). Existing transition-probability values of the spontaneous emission corresponding to the investigated Kr I transitions have also been checked using the known relative line-intensity ratio (RLIR) method described in Djeniže, Milosavljević & Dimitrijević (2002) and Djeniže, Milosavljević & Dimitrijević (2003).

2 EXPERIMENT

A modified version of a linear low-pressure pulsed arc (Djeniže, Milosavljević & Srećković 1998) has been used as a plasma source. A pulsed discharge was driven in a quartz discharge tube of 5 mm inner diameter and effective plasma length of 72 mm (fig. 1 of Djeniže, Milosavljević & Srećković 1998; Milosavljević, Karkari & Ellingboe 2007). The tube has an end-on quartz window. On the opposite side of the electrodes, the glass tube was expanded in order to reduce erosion of the glass wall and also sputtering of the electrode material on to the quartz windows. The working gas was pure krypton at 130 Pa filling pressure in the flowing regime. Spectroscopic observations of isolated spectral lines were made end-on along the axis of the discharge tube. A capacitor of 14 μF was charged up to 1.5 kV and the whole supply unit has been described in Milosavljević et al. (2007). The line profiles were recorded using a shot-by-shot technique with a photomultiplier (EMI 9789 QB and EMI 9659B) and a grating spectrograph (Zeiss PGS–2, reciprocal linear dispersion 0.73 nm mm^{-1} at first order) system. The instrumental full width at half-maximum (FWHM) of 0.008 nm was determined by using the narrow spectral lines emitted by the hollow cathode discharge. The spectrograph exit slit (10 μm) with calibrated photomultiplier was micrometrically traversed along the spectral plane in small wavelength steps (0.0073 nm). More details of experimental set-up, recording technique, plasma reproducibility, deconvolution procedure and plasma diagnostics can be found in Milosavljević et al. (2000), Milosavljević et al. (2003), Milosavljević & Djeniže (2003) and Djeniže et al. (2003). In the works of Milosavljević et al. (2007) and Milosavljević, Popović & Ellingboe (2009), comprehensive electrical investigations of plasma homogeneity are presented. The conclusion of this investigation is that our plasma source is homogeneous within the time limit of local thermodynamic equilibrium (LTE) existence.

The electron temperature decay is obtained by using the Saha equation applied to Kr II and Kr I line-intensity ratios and the electron density decay is obtained using a laser interferometry technique (fig. 2 of Milosavljević et al. 2003). The Saha equation gives a relationship between free particles and those bound in atoms, and it can be used for electron temperature calculations if the plasma is in LTE (Venugopalan 1971). The other option for electron temperature measurement, via spectral line emission, is a Boltzmann plot. For this technique, significant energy difference is required among the upper energy levels of the spectral lines, which is not the case for the selection of krypton spectral lines. The maximum electron temperature (T) is 17 000 K and the electron density (N) is 1.65×10^{23} m^{-3}. The plasma parameters are determined with an error of 11 per cent for T and 7 per cent for N. The errors include reproducibility of the measured parameters: namely, electron density has been determined by a laser interferometry technique and this technique is very dependent on spectroscopic set-up, i.e. geometric factors (distances, size of lens, etc.). Tiny differences in the set-up will give a couple of per cent difference in the results. By repeating the electron density measurement, we found the average electron density is with a maximum error in reproducibility of 7 per cent (in decay). The electron temperature has been calculated and depends mostly on the accuracy of the measured spectral lines. Reproducibility in this case gives an error of 11 per cent for the measurement of electron temperature.

2.1 Stark shift

The total line Stark shift ($d_{\rm t}$) and the corresponding electron ($d_{\rm e}$) and ion ($d_{\rm i}$) contributions are respectively given by

$$d_{\rm t} = d_{\rm e} + d_{\rm i}. \quad (1)$$

In this way we distinguish between $d_{\rm t,\,st}$ and $d_{\rm t,\,s\,+d}$. Here $d_{\rm t,\,st}$ is total 'static' Stark shift (the 'static' refers to semiclassical theory

for the electron-impact contribution and quasistatic theory for the ion contribution (Griem 1964, 1974)) and $d_{\mathrm{t,\,s\,+d}}$ is the total 'static and dynamic' (Kelleher 1981) Stark shift.

Both $d_{\mathrm{t,\,st}}$ and $d_{\mathrm{t,\,s\,+d}}$ can be calculated from the following equations (Griem 1974; Kelleher 1981):

$$\begin{aligned} d_{\mathrm{t,\,st}} &\approx W_{\mathrm{e}}[d_{\mathrm{e}}/W_{\mathrm{e}} \pm 2A(1-0.75R)], \\ d_{\mathrm{t,\,s+d}} &\approx W_{\mathrm{e}}[d_{\mathrm{e}}/W_{\mathrm{e}} \pm 2AE(1-0.75R)], \end{aligned} \tag{2}$$

where

$$R = \sqrt[6]{\frac{36\pi e^6 N}{(kT)^3}} \tag{3}$$

is the so called Debye shielding parameter, i.e. the ratio of the mean ion separation to the Debye radius, where k is the Boltzmann constant and N and T represent the electron density and temperature respectively. In the above equations, W_{e} is the electron-impact full half-width of a spectral line, A the ion-broadening parameter (Griem 1974) and E describes the ion dynamics influence (Kelleher 1981).

The applied deconvolution procedure is extensively described in the literature (Milosavljević & Poparić 2001; Milosavljević, Djeniže, & Dimitrijević 2003; Milosavljević, Ellingboe & Djeniže 2006). It includes an advanced numerical procedure for deconvolution of the theoretical asymmetric convolution integral of a Gaussian and a plasma-broadened spectral line profile $j_{A,R}(\lambda)$. This method gives complete information on the plasma parameters from a single recorded spectral line in the cases when it is applicable. The method determines all broadening ($W_{\mathrm{t}}, W_{\mathrm{e}}, W_{\mathrm{i}}, d_{\mathrm{t}}, d_{\mathrm{e}}, d_{\mathrm{i}}, A, D$ and E) and plasma parameters (N and T) self-consistently and directly from the shape of spectral lines without any assumptions or prior knowledge.

Apart from this approach, it is possible to measure the Stark shifts relative to the unshifted spectral lines emitted by the same plasma using a method established and applied first in Purić & Konjević (1972). According to this method, the Stark shift of a spectral line can be measured experimentally by evaluating the position of the spectral line centre (X_{C}) recorded at different electron density values during the plasma decay. In principle, the method requires recording of the spectral line profile at a higher electron density (N_1), resulting in an appreciable shift, and then later when the electron concentration has dropped to a value (N_2) lower by at least an order of magnitude. The difference of the line centre position in these two cases is ΔX_{C}, so that the shift d_1 at the higher electron density N_1 is

$$d_1 = \frac{N_1 \Delta X_{\mathrm{C}}}{(N_2 - N_1)}. \tag{4}$$

Therefore, equation (2) gives the possibility of calculating the total Stark shift by taking into account electron and ion contributions. On the other hand, equation (4) gives the integral value for the total Stark shift, assuming that the electron contribution is the only one.

2.2 Transition probability

When the plasma remains in LTE, the well-known formula (Griem 1964; Wiese 1968; Djeniže et al. 2003)

$$(I_1/I_2)_{\mathrm{EXPT}} = (A_1 g_1 \lambda_2 / A_2 g_2 \lambda_1) \exp(\Delta E_{21}/kT) \tag{5}$$

can be used for a comparison between measured relative line-intensity ratios and the corresponding calculated values, taking into account the validity of the Boltzmann distribution for the population of excited levels in the emitters. In this expression I denotes the measured (EXPT) relative intensity, λ the wavelength of the transition, A the transition probability of the spontaneous emission, ΔE the difference in excitation energy and g the corresponding statistical weight. T is the electron temperature of the plasma in LTE and k is the Boltzmann constant. With the measured relative line-intensity ratio and electron temperature, from equation (5) one can obtain the ratio of the corresponding transition probabilities or, conversely, the transition probability of a particular transition relative to a selected reference A value. As reference A values, the transition probabilities of the nine (427.397, 436.264, 439.997, 450.235, 587.091, 760.154, 768.525, 810.436 and 826.324) Kr I transitions have been chosen. These lines are the most intense and have the highest reproducibility among the investigated Kr I spectral lines and multiplets.

3 METHOD OF CALCULATION

The description of the calculation procedure is given in detail in Milosavljević et al. (2003), so that only basic information will be repeated here. Calculations have been performed using the semiclassical perturbation formalism (Sahal-Bréchot 1969a,b), updated several times (Sahal-Bréchot 1974; Dimitrijević & Sahal-Bréchot 1984, 1985; Dimitrijević, Sahal-Bréchot & Bommier 1991; Fleurier, Sahal-Bréchot & Chapelle 1977).

Energy levels have been taken from Sugar & Musgrove (1991). Oscillator strengths have been calculated by using the method of Bates & Damgaard (1949) and Oertel & Shomo (1968). For higher levels, the method described in Van Regemorter, Hoang Binh & Prud'homme (1979) has been used.

In addition to the line shifts due to electron collisions, shifts due to collisions with protons and helium ions, the main ionic perturbers in stellar atmospheres, were calculated. Since for the plasma conditions in stellar atmospheres the conditions for the quasistatic approximation are usually not satisfied, the impact approximation is used for ion-shift determination as well.

4 RESULTS AND DISCUSSION

Our experimentally obtained $d_{\mathrm{t}}^{\mathrm{exp}}$, $d_{\mathrm{e}}^{\mathrm{exp}}$ and $d_{\mathrm{i}}^{\mathrm{exp}}$ data are shown in Table 1 together with data of other authors. For comparison between $d_{\mathrm{t}}^{\mathrm{exp}}$ and d_1 we present values for d_1 as well.

As can be seen in Table 1, the d_1 values are higher than the $d_{\mathrm{e}}^{\mathrm{exp}}$ values and lower than $d_{\mathrm{t}}^{\mathrm{exp}}$. This difference is not so significant, since it is within the experimental error bars.

There are no theoretical calculations for these Kr I spectral lines. We calculated Stark-shift values (d^{Th}) generated by electrons, protons and helium ions for 11 Kr I lines in the 5s–5p and 5s–6p transitions using semiclassical perturbation formalism (SCPF), and these are presented in Table 2.

In order to make the comparison between measured and calculated Stark-shift values easier, the theoretical Stark-shift dependence on the electron temperature at an electron density of 10^{22} m^{-3} is presented graphically in Figs 1 and 2. The experimental data of other authors do not belong to calculated neutral krypton wavelengths, thus we could not directly compare them with the theory or our experimental data. Nevertheless, the experimental data from Klein & Meiners (1977) for wavelengths 437.612 and 450.235 nm can be indirectly compared with our theoretical and experimental data for the 436.264- and 431.958-nm Kr I spectral lines, respectively (Fig. 2). Namely, wavelengths 437.612 and 436.264 nm, as well as 450.235 and 431.958 nm, belong to the same multiplets.

Generally, we have obtained very small shift values. Both experimental and measured d values are of the order of pico-meter (pm), within our experimental accuracy (± 0.8 pm at 10^{22} m^{-3}). Our

Table 1. Measured total Stark shifts for Kr I spectral lines: d_t^{exp}, d_e^{exp}, d_i^{exp} and d_1 within 12% accuracy at the measured electron temperature and electron density. Under the 'Ref.' sources of experimental data are listed: Tw – present data; KM – Klein & Meiners (1977); VS – Vitel et al. (1988); UK – Uzelac & Konjević (1989); VB – Valognes et al. (2005). Also, 'exp' denotes experimental data; 't' total, 'i' ion, 'e' electron, 'st' impact electrons and static ions and 's+d' impact electrons and static ions with dynamic correction. The asterisk (*) represents a mean value. The measured electron temperatures T^{exp} are in units of 10^4 K and electron densities N^{exp} in units of 10^{22} m^{-3}.

Transition	Multiplet	λ [nm]	T^{exp}	N^{exp}	E^{exp}	$d_{t,s+d}^{exp}$ [pm]	$d_{t,st}^{exp}$ [pm]	d_e^{exp} [pm]	$d_{i,st}^{exp}$ [pm]	Ref.	d_1 [pm]
5s–5p	$[3/2]_1^o$–$[1/2]_o$	758.741	1.7	16.5	1.69	133.7	128.5	121.0	7.5	Tw	123.1
	$[3/2]_2^o$–$[3/2]_2$	760.154	1.7	16.5	1.80	96.2	91.1	84.7	6.4	Tw	89.8
	$[3/2]_2^o$–$[3/2]_1$	769.454	1.7	16.5	1.98	91.3	86.3	81.2	5.1	Tw	88.7
	$[3/2]_1^o$–$[3/2]_2$	819.005	1.7	16.5	1.85	108.3	102.4	95.5	6.9	Tw	100.3
	$[3/2]_1^o$–$[3/2]_1$	829.811	1.7	16.5	1.91	97.5	91.7	85.2	6.5	Tw	90.1
	$[3/2]_2^o$–$[5/2]_3$	811.290	1.7	16.5	1.84	81.0	75.2	68.3	6.9	Tw	72.4
	$[3/2]_2^o$–$[5/2]_2$	810.436	1.7	16.5	1.74	90.0	84.1	76.1	8.0	Tw	78.2
5s–5p′	$[3/2]_2^o$–$[1/2]_1$	557.029	1.7	16.5	1	104.6	104.6	98.3	6.3	Tw	101.0
			1.03–0.94	5.9–13.0				21.5*		KM	
	$[3/2]_2^o$–$[3/2]_2$	556.222	1.7	16.5	1.47	96.3	93.7	88.2	5.5	Tw	92.6
	$[3/2]_1^o$–$[3/2]_2$	587.091	1.7	16.5	1.51	94.9	92.0	86.3	5.7	Tw	91.3
			1.03–0.93	5.5–12.4				21.8*		KM	
			1.55	76.0				190		VS	
			1.49	92.0				200		VS	
			1.43	97.0				210		VS	
			1.62	123.0				250		VS	
			1.50	124.0				250		VS	
			1.74	158.0				300		VS	
			1.57	162.0				320		VS	
			1.150	45.0				100		UK	
			1.165	64.0				130		UK	
			1.190	76.0				160		UK	
			1.250	87.0				190		UK	
			1.275	102.0				190		UK	
			1.610	133.0				265		VB	
			1.695	177.0				350		VB	
			1.755	228.0				435		VB	
5s′–5p′	$[1/2]_1^o$–$[1/2]_1$	828.105	1.7	16.5	1.88	118.2	112.1	105.3	6.8	Tw	110.2
	$[1/2]_1^o$–$[1/2]_o$	768.525	1.7	16.5	1.82	114.5	109.2	102.8	6.4	Tw	106.2
	$[1/2]_o^o$–$[1/2]_1$	785.482	1.7	16.5	1.84	116.3	111.0	104.6	6.4	Tw	108.4
	$[1/2]_1^o$–$[3/2]_2$	826.324	1.7	16.5	1.87	107.6	101.6	94.7	7.1	Tw	99.9
	$[1/2]_o^o$–$[3/2]_1$	805.95	1.7	16.5	1.96	107.5	102.1	96.4	5.7	Tw	100.5
5s–6p	$[1/2]_0^o$–$[1/2]_1$	564.956	1.7	16.5	1	211.6	211.6	202.4	9.2	Tw	205.7
	$[1/2]_1^o$–$[3/2]_2$	439.997	1.7	16.5	1	198.8	198.8	189.1	9.7	Tw	193.1
	$[1/2]_1^o$–$[3/2]_1$	442.519	1.7	16.5	1	191.4	191.4	181.3	9.9	Tw	184.3
	$[3/2]_2^o$–$[1/2]_1$	436.264	1.7	16.5	1	169.2	169.2	159.2	10.0	Tw	162.0
	$[3/2]_1^o$–$[1/2]_0$	437.612	1.7	16.5	1	174.1	174.1	163.9	9.8	Tw	165.5
			1.04–0.91	4.2–13.5				160*		KM	
	$[3/2]_2^o$–$[3/2]_2$	427.397	1.7	16.5	1	228.0	228.0	213.6	14.4	Tw	218.1
	$[3/2]_2^o$–$[3/2]_1$	428.297	1.7	16.5	1	231.3	231.3	220.0	11.3	Tw	222.2
	$[3/2]_1^o$–$[3/2]_2$	445.392	1.7	16.5	1	222.0	222.0	211.1	10.9	Tw	215.0
	$[3/2]_1^o$–$[3/2]_1$	446.369	1.7	16.5	1	213.7	213.7	203.0	10.7	Tw	205.9
	$[3/2]_2^o$–$[5/2]_3$	431.958	1.7	16.5	1	197.1	197.1	187.0	10.1	Tw	192.3
	$[3/2]_2^o$–$[5/2]_2$	431.855	1.7	16.5	1	203.0	203.0	193.2	10.2	Tw	196.3
	$[3/2]_1^o$–$[5/2]_2$	450.235	1.7	16.5	1	192.2	192.2	181.9	10.3	Tw	184.7
			1.00–0.92	4.5–9.0				135*		KM	
5s′–6p′	$[1/2]_1^o$–$[1/2]_o$	435.136	1.7	16.5	1	245.8	245.8	231.0	14.8	Tw	237.9

measured and calculated d values have the same sign (positive). Positive shift is toward the red.

Measured Stark shifts corresponding to the 5s–5p transition arrays have about 10 per cent lower value than calculated (see Fig. 1). The complexity of the krypton spectrum and missing atomic energy levels lead to a lower accuracy of calculated Stark shifts for transitions from 5p levels and to an even greater extent for transitions involving 6p levels. Therefore our experimental data have very good

Table 2. Calculated Kr I Stark shift (d^{Th} in pm) for (a) electrons, (b) protons and (c) helium ions as perturbers for various temperatures (T) at 10^{22} m^{-3} perturber density.

λ [nm]		T [10^3 K]					
		2.5	5.0	10.0	20.0	30.0	50.0
758.741	a	7.69	9.22	9.18	8.69	7.37	5.98
	b	1.90	2.22	2.55	2.91	3.13	3.44
	c	1.47	1.74	2.02	2.31	2.49	2.73
760.154	a	5.48	6.59	6.64	5.79	4.79	3.86
	b	1.37	1.59	1.82	2.07	2.23	2.44
	c	1.07	1.25	1.44	1.64	1.77	1.94
769.454	a	5.12	6.19	6.00	5.61	4.67	3.72
	b	1.28	1.49	1.70	1.94	2.08	2.28
	c	1.00	1.17	1.35	1.54	1.66	1.82
819.005	a	6.22	7.42	7.49	6.30	5.18	4.22
	b	1.55	1.79	2.06	2.34	2.52	2.75
	c	1.21	1.41	1.63	1.86	2.00	2.19
829.811	a	5.80	6.97	7.03	6.09	5.04	4.11
	b	1.45	1.68	1.92	2.18	2.35	2.57
	c	1.13	1.32	1.52	1.74	1.87	2.05
811.290	a	5.06	5.97	6.02	4.81	3.90	3.19
	b	1.27	1.47	1.68	1.91	2.05	2.24
	c	0.99	1.16	1.33	1.51	1.63	1.79
810.436	a	5.06	5.97	6.02	4.83	3.92	3.21
	b	1.27	1.47	1.68	1.90	2.05	2.24
	c	0.99	1.16	1.33	1.51	1.63	1.79
436.264	a	11.7	13.3	13.2	11.8	10.2	8.29
	b	–	–	3.82	4.45	4.82	5.32
	c	–	–	–	–	3.81	4.22
427.397	a	11.5	13.6	15.2	14.5	12.7	10.6
	b	–	–	3.86	4.49	4.87	5.37
	c	–	–	–	–	–	4.26
446.369	a	12.0	14.2	15.4	15.1	13.1	11.0
	b	–	–	4.01	4.66	5.06	5.58
	c	–	–	–	–	–	4.42
431.958	a	11.5	13.2	13.9	13.1	11.3	9.25
	b	–	–	3.71	4.31	4.67	5.15
	c	–	–	–	–	–	4.09

agreement with the calculated data. There are no other experimental or theoretical data for comparison.

For the atomic krypton spectral lines from 5s–5p′ transition, experimental measurements of other authors also exist (Table 1). For that transition, Milosavljević (2005) mistakenly listed values that are a factor of 2 too small. It should be pointed out that we have not performed calculations of d_{th} values belonging to lines in 5s–5p′, 5s′–5p′ and 5s′–6p′ transitions because of the incompleteness of the set of experimentally determined perturbing energy levels. Since there is no theory, it is only possible to compare experimental data. Nevertheless, Vitel et al. (1988) and Valognes et al. (2005) have a measurement of Stark shifts at electron temperatures of 1.74×10^4 and 1.695×10^4 K, respectively. These electron temperatures are very similar to the electron temperature in our experiment (1.7×10^4 K). Therefore, our Stark-shift value for the 587.091-nm spectral line are about 2.5 times higher than the corresponding values of Vitel et al. (1988) and Valognes et al. (2005) after normalization of Stark-shift data to the same electron density. It is very difficult to make objective conclusions for this wavelength, since there are no theoretical predictions and both works (Vitel et al. 1988; Valognes et al. 2005) were performed with a similar experimental set-up, i.e. a linear flash tube.

In the case of Kr I spectral lines from the 5s′–5p′ and 5s′–6p′ transitions our experimental Stark-shift data are unique, i.e. there are no other experimental or theoretical data for comparison. Therefore we cannot perform any comparison between them.

For the four (436.264, 427.397, 446.369 and 431.958 nm) Kr I spectral lines from the transition 5s–6p, we have Stark-shift calculated values too. For the same transition there are two experimental values of Klein & Meiners (1977) as well (Table 1). In general, our experimental data are about 13 per cent lower than predicted values for those four spectral lines (see Figs 2a–d). Since our electron temperature and the electron temperature from Klein & Meiners (1977) are very different, direct comparison is not possible. We have compared our experimental data and the experimental data from Klein & Meiners (1977) for the Kr I 437.612-nm (Fig. 2e) and 450.235-nm (Fig. 2f) spectral lines with theory. The comparison is done using the fact that there are theoretical values for two other spectral lines from the same multiplets. The experimental value of Klein & Meiners (1977) is more than 30 per cent higher then the calculated value for the Stark shift (Figs 2e and f). Our experimental data, from the same multiplets, are about 13 per cent lower than the calculated value for the Stark shift. We have done the deconvolution procedure and separated ion and electron contributions from the total Stark shift, therefore this could be the reason for the discrepancy between our data and the experimental data of Klein & Meiners (1977).

Our experimental relative A values ($A^{\mathrm{rel}}_{\mathrm{exp}}$) are presented in Table 3 with values from NIST (2011). $A^{\mathrm{rel}}_{\mathrm{exp}}$ represent averaged values obtained during plasma decay during a time interval for which the criterion of the existence of LTE is fulfilled.

We have monitored ratios $(I_1/I_2)_{\mathrm{EXPT}}$ for spectral lines that belong to the same multiplet in a wide region of decaying plasma, up to the moment when the line-intensity maximum drops down to 8 per cent of its maximal value. We have found that these experimental ratios are constant within ±5 per cent during plasma decay. This suggests that the comparison between measured and calculated relative line-intensity ratios can be used as a method for estimation of the transition probabilities relative to the selected reference A values. Namely, we suppose that there exists at least one pair of lines, belonging to the same multiplet, for which measured and calculated relative line-intensity ratios are in agreement (within the accuracy of the measurements) during the whole plasma decay period. If such agreement really exists then one can accept these lines, with the corresponding transition probabilities, as the reference ones. Among the lines we have investigated, such behaviour is found for the 760.154-nm line in the multiplet [3/2]°–[3/2] and the 810.436-nm line in the multiplet [3/2]°–[5/2] from transition 5s–5p, as well the 587.091-nm line in the multiplet [3/2]°–[3/2] from transition 5s–5p′, the 768.525-nm line in the multiplet [1/2]°–[1/2] and 826.324-nm line in the multiplet [1/2]°–[3/2] from transition 5s′–5p′. From transition 5s–6p we find the 439.997-nm line in the multiplet [1/2]°–[3/2], the 436.264-nm line in the multiplet [3/2]°–[1/2], the 427.397-nm line in the multiplet [3/2]°–[3/2] and the 450.235-nm line in the multiplet [3/2]°–[5/2].

Generally, our measured $A^{\mathrm{rel}}_{\mathrm{exp}}$ values are higher for about 11 per cent, except for the 805.95-nm line, where our measured $A^{\mathrm{rel}}_{\mathrm{exp}}$ value is lower by 7 per cent, in comparison with the data provided by NIST (2011). Since some of the measured Kr I spectral lines are single in their own multiplet, we have not measured $A^{\mathrm{rel}}_{\mathrm{exp}}$ data for four such lines (758.741, 557.029, 564.956 and 435.136 nm). For transition probabilities for the 428.297, 431.958 and 431.855-nm Kr I spectral lines, there are no other data in the literature for comparison.

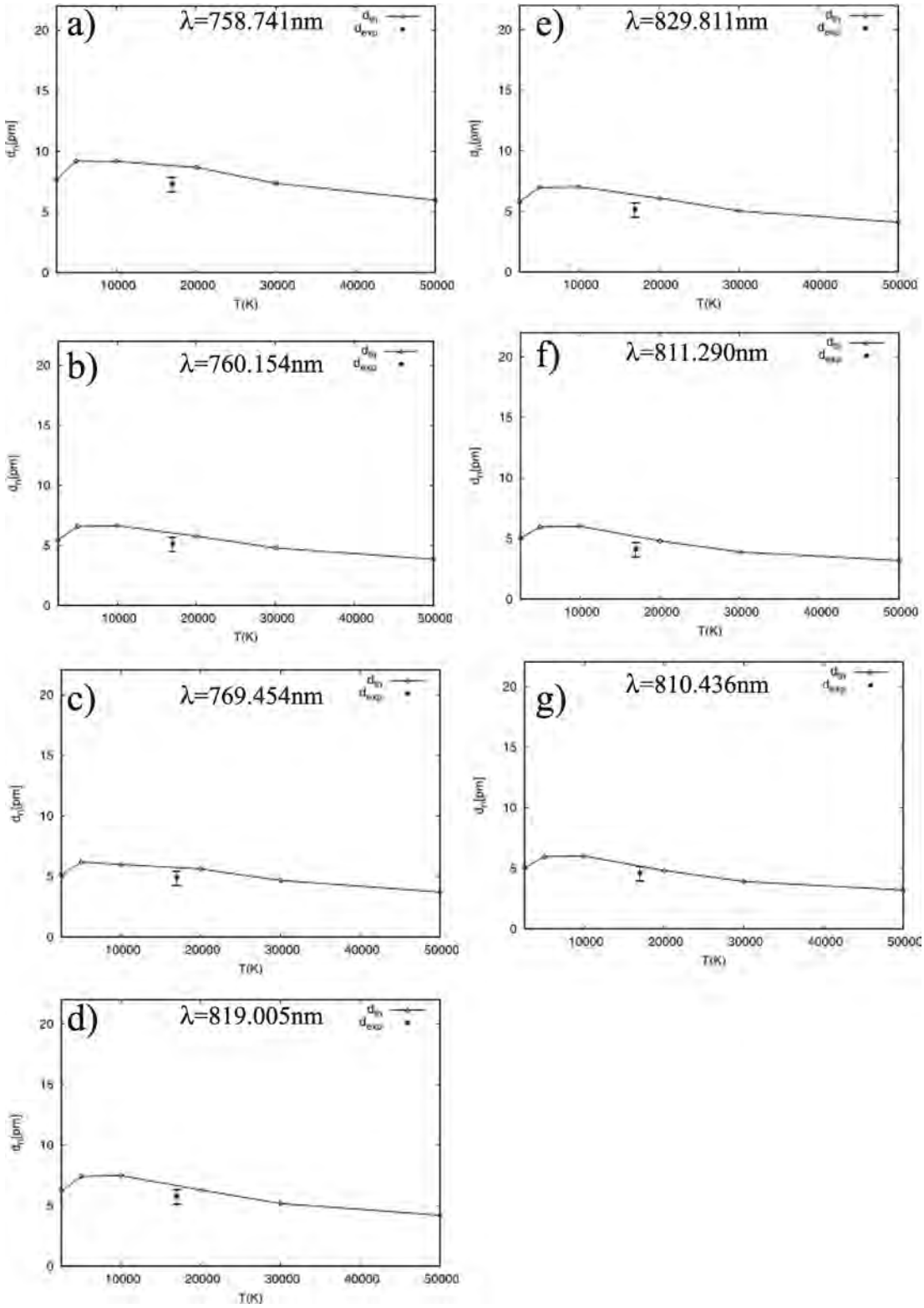

Figure 1. Our experimental electron Stark shift ($d_{\rm exp}$) and the theoretical electron Stark shift ($d_{\rm th}$) versus electron temperature for the Kr I spectral lines from the 5s–5p transition at an electron density of 10^{22} m^{-3}. The experimental value has 12 per cent accuracy, which is due to the reproducibility of the deconvolution procedure.

5 CONCLUSION

We have presented in this work experimental Stark shifts for 28 Kr I spectral lines at an electron temperature of 17 000 K and an electron density of 1.65×10^{23} m^{-3}, as well as calculated Stark-shift values for 11 spectral lines for an electron density of 10^{22} m^{-3} and electron temperatures from 2500 up to 50 000 K. For the 24 Kr I spectral-line Stark shifts and also for all 11 krypton lines considered here

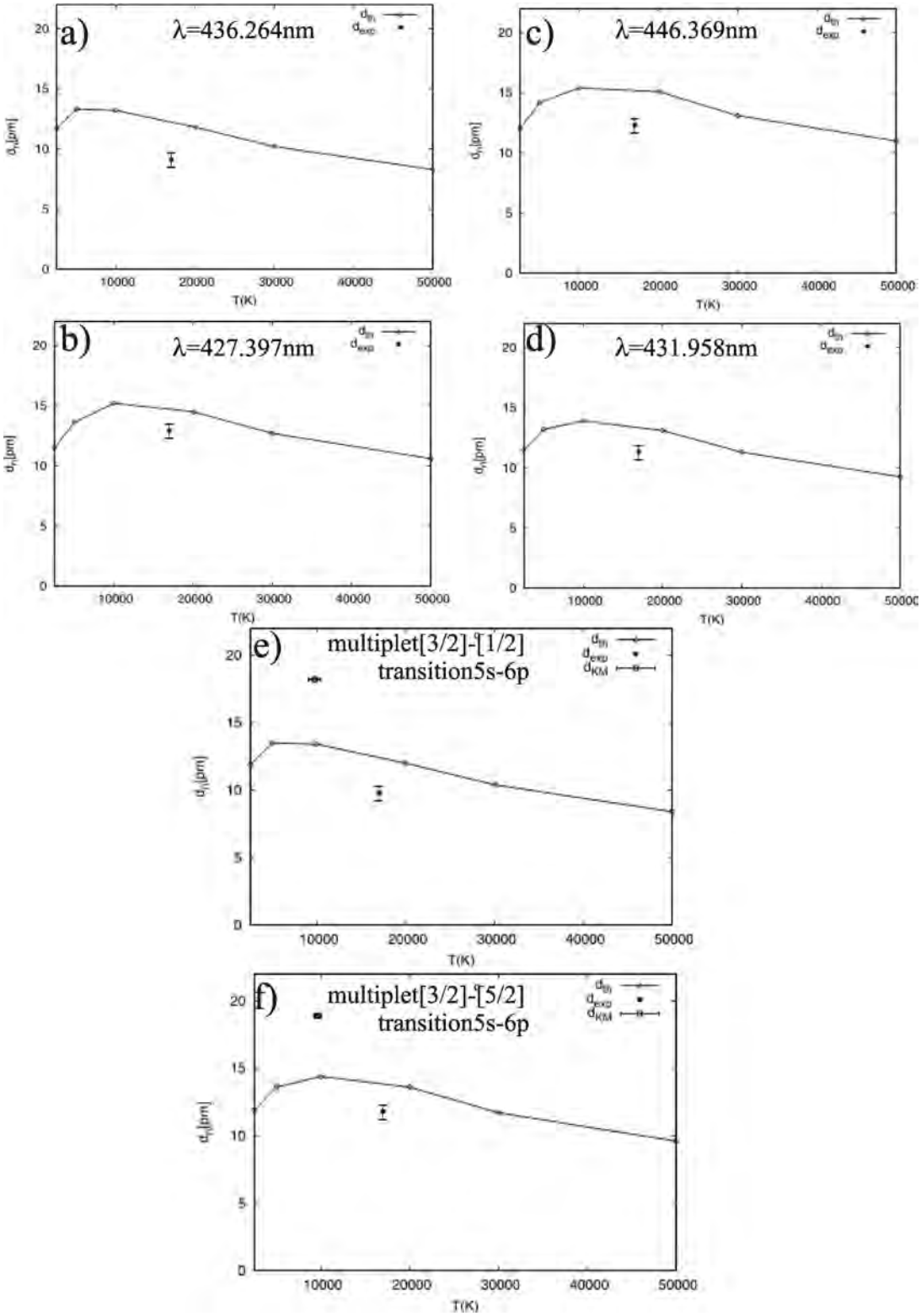

Figure 2. Panels (a)–(d) show our experimental electron Stark shift ($d_{\rm exp}$) and the theoretical electron Stark shift ($d_{\rm th}$) versus electron temperature for the Kr I spectral lines from the 5s–6p transition. Panels (e) and (f) present experiential data and theoretical values within the corresponding multiplet. Here, $d_{\rm KM}$ indicates denoted values from the work of Klein & Meiners (1977). All data are at an electron density of 10^{22} m^{-3}.

theoretically, there are no other data, respectively experimental and theoretical, for comparison. The shift values found are of the order of pm and positive. Using the line-deconvolution procedure, the total spectral-line Stark shift has been separated into ion and electron contributions. We found clear influence of quasistatic ion and ion–dynamical effects on many investigated spectral line shapes. It has been found that the electron contribution to the total Stark shift is about 92 per cent and the krypton ion contribution 8 per cent

Table 3. Transition probability values for Kr I spectral lines. A_{exp} represents our measured transition-probability values and A_N is the transition probability taken from Ralchenko et al. (2011). All transition-probability values are in units of 10^8 s^{-1}.

Transition	Multiplet	λ/nm	E/eV	g	A^{rel}_{exp}	A_N
5s–5p	$[3/2]^o_1$–$[1/2]_o$	758.741	11.66	1	–	0.51
	$[3/2]^o_2$–$[3/2]_2$	760.154	11.55	5	0.31	0.31
	$[3/2]^o_2$–$[3/2]_1$	769.454	11.53	3	0.062	0.0560
	$[3/2]^o_1$–$[3/2]_2$	819.005	11.54	5	0.115	0.11
	$[3/2]^o_1$–$[3/2]_1$	829.811	11.53	3	0.342	0.32
	$[3/2]^o_2$–$[5/2]_3$	811.290	11.44	7	0.386	0.36
	$[3/2]^o_2$–$[5/2]_2$	810.436	11.44	5	0.13	0.13
5s–5p′	$[3/2]^o_2$–$[1/2]_1$	557.029	12.14	3	–	0.021
	$[3/2]^o_2$–$[3/2]_2$	556.222	12.14	5	0.003	0.0028
	$[3/2]^o_1$–$[3/2]_2$	587.091	12.14	5	0.018	0.018
5s′–5p′	$[1/2]^o_1$–$[1/2]_1$	828.105	12.14	3	0.211	0.19
	$[1/2]^o_1$–$[1/2]_o$	768.525	12.26	1	0.49	0.49
	$[1/2]^o_o$–$[1/2]_1$	785.482	12.14	3	0.258	0.23
	$[1/2]^o_1$–$[3/2]_2$	826.324	12.14	5	0.35	0.35
	$[1/2]^o_o$–$[3/2]_1$	805.95	12.10	3	0.177	0.19
5s–6p	$[1/2]^o_0$–$[1/2]_1$	564.956	12.76	3	–	0.0037
	$[1/2]^o_1$–$[3/2]_2$	439.997	13.46	5	0.02	0.02
	$[1/2]^o_1$–$[3/2]_1$	442.519	13.44	3	0.011	0.0097
	$[3/2]^o_2$–$[1/2]_1$	436.264	12.76	3	0.0084	0.0084
	$[3/2]^o_1$–$[1/2]_0$	437.612	12.86	1	0.060	0.056
	$[3/2]^o_2$–$[3/2]_2$	427.397	12.82	5	0.026	0.026
	$[3/2]^o_2$–$[3/2]_1$	428.297	12.81	3	0.004	–
	$[3/2]^o_1$–$[3/2]_2$	445.392	12.82	5	0.009	0.0078
	$[3/2]^o_1$–$[3/2]_1$	446.369	12.81	3	0.024	0.023
	$[3/2]^o_2$–$[5/2]_3$	431.958	12.79	2	0.015	–
	$[3/2]^o_2$–$[5/2]_2$	431.855	12.78	3	0.011	–
	$[3/2]^o_1$–$[5/2]_2$	450.235	12.79	5	0.0092	0.0092
5s′–6p′	$[1/2]^o_1$–$[1/2]_o$	435.136	13.49	1	–	0.032

(on average). Generally our measured electron Stark shifts are smaller than those calculated, by about 11 per cent on average. The common characteristic among calculated d values is a weak dependence on electron temperature from 20 000–50 000 K. Therefore, these can be used for diagnostic purposes as data independent of self-absorption in optically thick astrophysical plasmas.

Our measured A^{rel}_{exp} values, using the RLIR method, are generally higher than those published by NIST. Overestimations are within our experimental accuracy (±10 per cent) and the noticed uncertainties for NIST values (±50 per cent). We note that we could not compare the transition probabilities for three Kr I spectral lines, since there are no other data in the literature. Our A^{rel}_{exp} values provide the possibility of a future comparison with absolute data as well as with data presented in relative form.

ACKNOWLEDGMENTS

This work is part of the project No. 171006 and the project 'Influence of collisions with charged particles on astrophysical spectra (176002)' supported by the Ministry of Education and Science of the Republic of Serbia and a part of the fellowship award funded by the Science Foundation Ireland under Grant No.08/SRC/I1411 and IMPROVE EU project.

REFERENCES

Bates D. R., Damgaard A., 1949, Trans. R. Soc. London Ser. A, 242, 101
Cardelli J. A., Meyer D. M., 1997, ApJ, 477, L57
Cardelli J. A., Savage B. D., Ebbets D. C., 1991, ApJ, 383, L23
Cartledge S. I. B., Meyer D. M., Lauroesch J. T., Sofia U. J., 2001, ApJ, 562, 394
Cartledge S. I. B., Meyer D. M., Lauroesch J. T., 2003, ApJ, 597, 408
Cartledge S. I. B., Lauroesch J. T., Meyer D. M., Sofia U. J., Clayton G. C., 2008, ApJ, 687, 1043
Cowley C. R., Hubrig S., Palmeri P., Quinet P., Biémont É., Wahlgren G. M., Schütz O., González J. F., 2010, MNRAS, 405, 1271
Dimitrijević M. S., Konjević N., 1986, A&A, 163, 297
Dimitrijević M. S., Sahal-Bréchot S., 1984, J. Quant. Spectrosc. Radiative Transfer, 31, 301
Dimitrijević M. S., Sahal-Bréchot S., 1985, Phys. Rev. A, 31, 316
Dimitrijević M. S., Sahal-Bréchot S., Bommier V., 1991, A&AS, 89, 581
Dinerstein H. L., 2001, ApJ, 550, L223
Djeniže S., Milosavljević V., Srećković A., 1998, J. Quant. Spectrosc. Radiative Transfer, 59, 71
Djeniže S., Milosavljević V., Dimitrijević M. S., 2002, A&A, 382, 359
Djeniže S., Milosavljević V., Dimitrijević M. S., 2003, Eur. Phys. J. D, 27, 209
Eikema K. S. E., Ubachs W., Vassen W., Hogervorst W., 1996, Phys. Rev. Lett., 76, 1216
Elabidi H., Ben Nessib N., Dimitrijević S. M., 2006, New Astron., 12, 64
Elabidi H., Sahal-Bréchot S., Dimitrijević S. M., Ben Nessib N., 2006, MNRAS, 417, 2624
Fleurier C., Sahal-Bréchot S., Chapelle J., 1977, J. Quant. Spectrosc. Radiative Transfer, 17, 595
Griem H. R., 1964, Plasma Spectroscopy. McGraw-Hill Book Company, New York
Griem H. R., 1974, Spectral Line Broadening by Plasmas. Academic Press, New York
Hamdi R., Ben Nessib N., Milovanović N., Popović L. Č., Dimitrijević M. S., Sahal-Brećhot S., 2008, MNRAS, 387, 871
Hui Bon Hoa A., LeBlanc F., Hauschildt P. H., Baron E., 2002, A&A, 381, 197
Karakas A. I., van Raai M. A., Lugaro M., Sterling N. C., Dinerstein H. L., 2009, ApJ, 690, 1130
Kelleher D. E., 1981, J. Quant. Spectrosc. Radiat. Transfer, 25, 191
Kennedy T., Costello T. J., Mosnier J.-P., van Kampen P., 2004, Radiation Physics and Chemistry, 70, 291
Klein P., Meiners D., 1977, J. Quant. Spectrosc. Radiative Transfer, 17, 197
Konjević N., Dimitrijević M. S., Wiese W. L., 1984, J. Phys. Chem. Ref. Data, 13, 619
Leckrone D. S., Wahlgren G. M., Johansson S. G., Adelman S. J., 1993, in Dworetsky M. M., Castelli F., Faraggiana R., eds, ASP Conf. Ser. Vol. 44, Peculiar versus Normal Phenomena in A-type and Related Stars. Astron. Soc. Pac., San Francisco, p. 42
Lesage A., 2009, New Astron. Rev., 52, 471
Lesage A., Fuhr J. R., 1999, Bibliography on Atomic Line Shapes and Shifts, April 1992 through June 1999. Observatoire de Paris
Lieberman M., Lichtenberg A., 1994, Principles of Plasma Discharges and Materials Processing. Wiley, New York
Malcheva G. et al., 2009, MNRAS, 395, 1523
Milosavljević V., 2005, Mem. Soc. Astron. It. Suppl., 7, 192
Milosavljević V., Djeniže S., 2002, New Astron., 7, 543
Milosavljević V., Djeniže S., 2003, A&A, 398, 1179
Milosavljević V., Poparić G., 2001, Phys. Rev. E, 63, 36404
Milosavljević V., Djeniže S., Dimitrijević M. S., Popović Č. L., 2000, Phys. Rev. E, 62, 4137
Milosavljević V., Djeniže S., Dimitrijević M. S., 2003, Phys. Rev. E, 68, 16402
Milosavljević V., Ellingboe R. A., Djeniže S., 2006, Spectrochem. Acta B, 61, 81
Milosavljević V., Karkari K. S., Ellingboe R. A., 2007, Plasma Sources Sci. Technol., 16, 304
Milosavljević V., Popopvić D., Ellingboe A. R., 2009, J. Phys. Soc. Jpn, 78, 84501

Oertel G. K., Shomo L. P., 1968, ApJS, 16, 175
Popović L. Č., Dimitrijević S. M., Simić Z., Dačić M., Kovačević A., Sahal-Bréchot S., 2008, New Astron., 13, 85
Purić J., Konjević N., 1972, Zeitschrift für Physik A, 249, 440
Ralchenko Y., Kramida A. E., Reader J., NIST ASD Team, 2011, NIST Atomic Spectra Database (ver. 4.1.0). http://physics.nist.gov/ascl
Sahal-Bréchot S., 1969a, A&A, 1, 91
Sahal-Bréchot S., 1969b, A&A, 2, 322
Sahal-Bréchot S., 1974, A&A, 35, 321
Sonnentrucker P., Friedman S. D., Welty D. E., York D. G., Snow T. P., 2003, ApJ, 596, 350
Sterling N. C., 2011, A&A, 533, A62
Sugar J., Musgrove A., 1991, J. Phys. Chem. Ref. Data, 20, 859
The L.-S., El Eid M. F., Meyer B. S., 2007, ApJ, 655, 1058
Uzelac N. I., Konjević N., 1989, J. Phys. B: Atomic Mol. Opt. Phys., 22, 2517
Valognes J. C., Bardet J. P., Vitel Y., Flih S. A., 2005, J. Quant. Spectrosc. Radiative Transfer, 95, 113
Van Regemorter H., Hoang Binh Dy, Prud'homme M., 1979, J. Phys. B, 12, 1073
Vennes S., Kawka A., Neḿeth P., 2011, MNRAS, 413, 2545
Venugopalan M., ed., 1971, Reactions under plasma conditions. Wiley Interscience, New York
Vitel Y., Skowronek M., Dimitrijević M. S., Popović M. M., 1988, A&A, 200, 285
Wiese W. L., 1968, in Bederson B., Fite W. L., eds, Methods of Experimental Physics, Vol. 7B. Academic Press, New York

This paper has been typeset from a TEX/LATEX file prepared by the author.

Mon. Not. R. Astron. Soc. **423,** 766–773 (2012) doi:10.1111/j.1365-2966.2012.20968.x

Stark-broadening calculations of singly ionized carbon spectral lines

N. Larbi-Terzi,[1] S. Sahal-Bréchot,[2⋆] N. Ben Nessib[1] and M. S. Dimitrijević[2,3,4]

[1]*Groupe de Recherche en Physique Atomique et Astrophysique, Institut National des Sciences Appliquées et de Technologie, University of Carthage, Centre Urbain Nord BP No. 676, 1080 Tunis Cedex, Tunisia*
[2]*Laboratoire d'Étude du Rayonnement et de la Matière en Astrophysique, Observatoire de Paris, UMR CNRS 8112, UPMC, Bâtiment Evry Schatzman, 5 Place Jules Janssen, F-92195 Meudon Cedex, France*
[3]*Astronomical Observatory, Volgina 7, 11060 Belgrade 38, Serbia*
[4]*Isaac Newton Institute of Chile, Yugoslavia Branch, Volgina 7, 11060 Belgrade, Serbia*

Accepted 2012 March 12. Received 2012 January 27

ABSTRACT

Using the semiclassical perturbation approach in the impact approximation, we have obtained Stark-broadening parameters for 148 C II multiplets. Energy levels and oscillator strengths are taken from the TOPbase data base. Results are obtained as a function of temperature for a set of perturber densities of 10^{14}, 10^{17} and 10^{18} cm^{-3}. In addition to electron-impact full half widths and shifts, Stark-broadening parameters due to singly ionized carbon impacts have been calculated. Thus, we have provided Stark-broadening data for the important charged perturbers in the atmospheres of carbon white dwarfs.

Key words: atomic data – atomic processes – line: profiles – white dwarfs.

1 INTRODUCTION

A new type of white dwarf star has recently been discovered by Dufour et al. (2007, 2008). The surface composition of this type of star consists mostly of carbon; there is scarcely either hydrogen or helium in the atmosphere. In order to understand the origin and evolution of this new type of star, the determination of gravity is essential and it is necessary to develop a new generation of accurate models. The astrophysical interpretation of this surprising discovery was hindered by the lack of atomic Stark-broadening data. In fact, the inclusion of accurate spectral line broadening is crucial for modelling this type of white dwarf atmosphere.

At the temperatures and pressures of interest (effective temperatures within 19 000–23 000 K, electron density within 10^{15}–10^{18} cm^{-3}), the dominant ion is C II. There is a contribution of C III for the deepest layers or for very hot models, but it can be neglected. The predominant cause of broadening of C II lines is Stark broadening, i.e. broadening by electron-impact and ion interactions. The colliding ions are C II, and the density number of C II is equal to the density number of electrons. In addition, adequate results for Stark broadening of C II lines are completely missing in the literature, except for a very few calculations by Mahmoudi, Ben Nessib & Sahal-Bréchot (2004). However, results of calculations for 16 multiplets can be found in the book of Griem (1974). We have therefore undertaken to calculate a great number of widths and shifts of C II lines colliding with electrons and C II ions under the conditions of carbon white dwarfs. For this work, we have used the impact semiclassical perturbation (SCP) method and the numerical code of Sahal-Bréchot (1969a,b, 1974) for electron and ion collisions. It includes Feshbach resonances for ion–electron collisions (Fleurier, Sahal-Bréchot & Chapelle 1977) and also quasi-static widths of ionic lines due to ionic interactions (Sahal-Bréchot 1991). This well-proven method gives results with an accuracy of about 20 per cent. The best results are obtained when a sophisticated atomic structure, which enters the Stark-broadening code, is used. We have used the data of The Opacity Project on-line atomic database, TOPbase[1] (**R**-matrix with innovative asymptotic techniques: Cunto et al. 1993). It is suitable for C II and offers a great number of levels and line strengths for the transitions. We have therefore modified the SCP code of Sahal-Bréchot by coupling it to the C II TOPbase data, and a great number (149) of line widths and shifts have been obtained.

In the following, we will recall the basis of the SCP Stark-broadening method and numerical code of Sahal-Bréchot. We will then describe the method of coupling the Stark-broadening code to the C II TOPbase data.

The results are available in an electronic form (see Supporting Information) and will also be implemented in the STARK-B data base (Sahal-Bréchot, Dimitrijević & Moreau 2012).[2] A sample of these results is displayed in the following tables and commented on. A number of systematic trends will be presented and discussed.

2 THEORY

In the derivation by Sahal-Bréchot (1969a,b, 1974) of the expression for Stark-broadening parameters, the optical theorem is used

⋆E-mail: Sylvie.Sahal-Brechot@obspm.fr

[1] http://cdsweb.u-strasbg.fr/topbase/topbase.html
[2] http://stark-b.obspm.fr/

(cf. also Baranger 1958) and the line width can then be expressed in terms of elastic and inelastic collision rates. Thus, experience gained in atomic collision theory can be used as a guide in the choice of impact parameters and strong collision terms. Then, dipole, quadrupole and quadratic (the polarization r^{-4} potential) interactions are taken into account.

For the transition between levels i and f, the total width at half-intensity (FWHM: $W = 2w$) and the shift d can be expressed in the form (Sahal-Bréchot 1969a,b, 1974)

$$W = N \int_0^\infty vf\,(v)\,\mathrm{d}v \left(\sum_{i' \neq i} \sigma_{ii'}\,(v) + \sum_{f' \neq f} \sigma_{ff'}\,(v) + \sigma_{\mathrm{el}} \right), \quad (1)$$

$$d = N \int_0^\infty vf\,(v)\,\mathrm{d}v \int_{R_3}^{R_\mathrm{D}} 2\pi\rho\,\mathrm{d}\rho \sin 2\phi_\mathrm{p}. \quad (2)$$

Here i' and f' are the perturbing levels, N is the density of perturbers, v is the relative velocity and $f(v)$ is the Maxwellian distribution of velocities.

The inelastic cross-section $\sigma_{ii'}(v)$ (resp. $\sigma_{ff'}(v)$) is given by an integration over the impact parameter ρ of the transition probability $P_{ii'}(v, \rho)$ (resp. $P_{ff'}(v, \rho)$) as

$$\sum_{i' \neq i} \sigma_{ii'}\,(v) = \frac{1}{2}\pi R_1^2 + \int_{R_1}^{R_\mathrm{D}} 2\pi\rho\,\mathrm{d}\rho \sum_{i' \neq i} P_{ii'}\,(\rho, v)\,. \quad (3)$$

Table 1. Calculated C II widths and shifts for the $2s^2 3s\ ^2S$–$2s^2 np\ ^2P^o$ series for the electron density $N_\mathrm{e} = 10^{14}$ cm^{-3}. In the first column we give multiplets, wavelengths of the multiplets in Å and C values that give an estimate for the maximum perturber density for which the line may be treated as isolated if it is divided by the corresponding full width. Non-empty cells in Tables 2–6 preceded by an asterisk mean that the impact approximation reaches its limit of validity ($0.1 < NV \leq 0.5$). Empty cells, denoted by an asterisk, mean that the impact approximation is not valid. The energy levels (terms) and wavelengths of the multiplets are those of TOPbase.

Multiplet	T [K]	W_e [Å]	d_e [Å]	$W_{\mathrm{C\,II}}$ [Å]	$d_{\mathrm{C\,II}}$ [Å]
$2s^2 3s\ ^2S$–$2s^2 3p\ ^2P^o$	5000.	0.142E-02	−0.281E-04	0.605E-04	−0.648E-05
	10000.	0.105E-02	−0.334E-04	0.814E-04	−0.105E-04
6741.6 Å	20000.	0.837E-03	−0.287E-04	0.924E-04	−0.146E-04
C= 0.63E+18	30000.	0.784E-03	−0.310E-04	0.989E-04	−0.167E-04
	50000.	0.754E-03	−0.348E-04	0.106E-03	−0.191E-04
	80000.	0.732E-03	−0.308E-04	0.109E-03	−0.214E-04
$2s^2 3s\ ^2S$–$2s^2 4p\ ^2P^o$	5000.	0.330E-03	0.657E-04	0.353E-04	0.664E-05
	10000.	0.261E-03	0.451E-04	0.400E-04	0.883E-05
2195.0 Å	20000.	0.234E-03	0.351E-04	0.443E-04	0.106E-04
C = 0.26E+17	30000.	0.230E-03	0.332E-04	0.456E-04	0.117E-04
	50000.	0.231E-03	0.272E-04	0.471E-04	0.132E-04
	80000.	0.232E-03	0.232E-04	0.474E-04	0.143E-04
$2s^2 3s\ ^2S$–$2s^2 5p\ ^2P^o$	5000.	0.410E-03	0.133E-03	0.663E-04	0.143E-04
	10000.	0.348E-03	0.100E-03	0.735E-04	0.171E-04
1700.8 Å	20000.	0.334E-03	0.804E-04	0.772E-04	0.203E-04
C = 0.72E+16	30000.	0.336E-03	0.704E-04	0.778E-04	0.224E-04
	50000.	0.344E-03	0.577E-04	0.804E-04	0.244E-04
	80000.	0.348E-03	0.497E-04	0.801E-04	0.260E-04
$2s^2 3s\ ^2S\ ^2S$–$2s^2 6p\ ^2P^o$	5000.	0.794E-03	0.424E-03	0.144E-03	0.613E-04
	10000.	0.738E-03	0.355E-03	0.153E-03	0.722E-04
1515.9 Å	20000.	0.734E-03	0.297E-03	0.168E-03	0.831E-04
C = 0.17E+16	30000.	0.763E-03	0.258E-03	0.168E-03	0.890E-04
	50000.	0.796E-03	0.217E-03	0.183E-03	0.101E-03
	80000.	0.810E-03	0.181E-03	0.170E-03	0.108E-03
$2s^2 3s\ ^2S\ ^2S$–$2s^2 7p\ ^2P^o$	5000.	0.133E-02	0.726E-03	0.256E-03	0.117E-03
	10000.	0.128E-02	0.642E-03	0.276E-03	0.136E-03
1434.9 Å	20000.	0.134E-02	0.509E-03	0.292E-03	0.153E-03
C = 0.13E+16	30000.	0.140E-02	0.452E-03	0.291E-03	0.166E-03
	50000.	0.147E-02	0.371E-03	0.292E-03	0.185E-03
	80000.	0.150E-02	0.304E-03	0.298E-03	0.186E-03
$2s^2 3s\ ^2S\ ^2S$–$2s^2 8p\ ^2P^o$	5000.	0.222E-02	−0.466E-07	0.414E-03	−0.161E-03
	10000.	0.225E-02	0.710E-04	0.447E-03	−0.186E-03
1387.1 Å	20000.	0.239E-02	0.843E-04	0.460E-03	−0.208E-03
C = 0.30E+15	30000.	0.249E-02	0.916E-04	0.471E-03	−0.222E-03
	50000.	0.260E-02	0.943E-04	0.499E-03	−0.242E-03
	80000.	0.265E-02	0.740E-04	0.513E-03	−0.289E-03

The elastic contribution to the width or elastic cross-section is given by

$$\sigma_{\rm el} = 2\pi R_2^2 + \int_{R_2}^{R_{\rm D}} 8\pi\rho\, {\rm d}\rho \sin^2\delta + \sigma_{\rm r}, \quad (4)$$

with

$$\delta = \left(\phi_{\rm p}^2 + \phi_{\rm q}^2\right)^{1/2}. \quad (5)$$

The phase shifts $\phi_{\rm p}$ and $\phi_{\rm q}$ are respectively due to the polarization and quadrupolar interactions, described in Sahal-Bréchot (1969a), Sahal-Bréchot (1974) and Bréchot & Van Regemorter (1964). $\sigma_{\rm r}$ is the contribution of Feshbach resonances (Fleurier et al. 1977).

All the cut-offs (R_1, R_2, R_3) as well as the symmetrization procedures in the inelastic cross-sections are described in Sahal-Bréchot (1969b). $R_{\rm D}$ is the upper cut-off allowing for Debye shielding. A description of the semiclassical perturbation formalism used here is given in Sahal-Bréchot (1969a,b).

3 RESULTS AND DISCUSSION

3.1 Results of calculations and comparison with experiments

The results for 149 lines are provided online in electronic form (see Supporting Information) in three tables for electron temperatures within 5000–80 000 K and electron densities 10^{14} (Table S1), 10^{17} (Table S2) and 10^{18} cm^{-3} (Table S3). Atomic data have been taken from the TOPbase data base (Cunto et al. 1993). Values of the parameter C divided by the corresponding full widths give an estimate for the maximum perturber density for which the line may be treated as isolated (see equation 5 in Dimitrijević, Sahal-Bréchot & Bommier 1991). For each value given in the tables, the collision volume V multiplied by the perturber density N is much less than unity and the impact approximation is valid. Values for $NV > 0.5$ are not given but are denoted by an asterisk and values for $0.1 < NV \leq 0.5$ are given but preceded by an asterisk. A number of data that are given for the density 10^{14} cm^{-3} do not appear at 10^{17} and 10^{18} cm^{-3}. This means that the impact approximation is valid neither for electron collisions nor for ionized ion colliders.

We give a sample of our electron-impact full widths and shifts in Tables 1–6.

We present in Table 7 a comparison between our theoretical widths $W_{\rm e}$ and existing experimental ones. For the width of a particular line within a multiplet, we used the following scaling expression (Popović, Milovanović & Dimitrijević 2001):

$$W_{\rm line} = \left(\frac{\lambda}{\lambda}\right)^2 W, \quad (6)$$

Table 2. Same as Table 1, for the $2s^2 3d\ ^2D$–$2s^2 nf\ ^2F^o$ series.

Multiplet	T [K]	$W_{\rm e}$ [Å]	$d_{\rm e}$ [Å]	$W_{\rm C\,II}$ [Å]	$d_{\rm C\,II}$ [Å]
$2s^2 3d\ ^2D$–$2s^2 4f\ ^2F^o$	5000.	0.220E-02	−0.434E-04	0.138E-03	−0.103E-03
	10000.	0.175E-02	−0.212E-04	0.168E-03	−0.123E-03
4299.9 Å	20000.	0.142E-02	−0.121E-04	0.192E-03	−0.144E-03
$C = 0.15$E+17	30000.	0.130E-02	−0.108E-04	0.209E-03	−0.154E-03
	50000.	0.119E-02	−0.123E-04	0.236E-03	−0.178E-03
	80000.	0.110E-02	−0.649E-05	0.241E-03	−0.184E-03
$2s^2 3d\ ^2D$–$2s^2 5f\ ^2F^o$	5000.	0.386E-02	0.151E-03	0.366E-03	0.325E-03
	10000.	0.349E-02	0.194E-03	0.463E-03	0.381E-03
3009.9 Å	20000.	0.316E-02	0.138E-03	0.491E-03	0.419E-03
$C = 0.10$E+16	30000.	0.296E-02	0.112E-03	0.563E-03	0.464E-03
	50000.	0.273E-02	0.110E-03	0.670E-03	0.497E-03
	80000.	0.251E-02	0.960E-04	0.775E-03	0.563E-03
$2s^2 3d\ ^2D$–$2s^2 6f\ ^2F^o$	5000.	0.693E-02	0.531E-03	0.962E-03	0.804E-03
	10000.	0.651E-02	0.502E-03	0.108E-02	0.942E-03
2588.1 Å	20000.	0.605E-02	0.350E-03	0.123E-02	0.114E-02
$C = 0.46$E+15	30000.	0.574E-02	0.313E-03	0.128E-02	0.114E-02
	50000.	0.530E-02	0.285E-03	0.139E-02	0.116E-02
	80000.	0.487E-02	0.202E-03	0.171E-02	0.145E-02
$2s^2 3d\ ^2D$–$2s^2 7f\ ^2F^o$	5000.	0.118E-01	0.146E-02	*0.205E-02	*0.178E-02
	10000.	0.112E-01	0.116E-02	*0.240E-02	*0.196E-02
2386.5 Å	20000.	0.104E-01	0.868E-03	0.252E-02	0.243E-02
$C = 0.25$E+15	30000.	0.990E-02	0.770E-03	0.260E-02	0.228E-02
	50000.	0.920E-02	0.612E-03	0.338E-02	0.274E-02
	80000.	0.847E-02	0.420E-03	0.330E-02	0.285E-02
$2s^2 3d\ ^2D$–$2s^2 8f\ ^2F^o$	5000.	0.221E-01	0.922E-02	*	*
	10000.	0.210E-01	0.720E-02	*	*
2271.8 Å	20000.	0.195E-01	0.547E-02	*0.594E-02	*0.554E-02
$C = 0.16$E+15	30000.	0.183E-01	0.465E-02	*0.780E-02	*0.596E-02
	50000.	0.168E-01	0.362E-02	*0.678E-02	*0.622E-02
	80000.	0.154E-01	0.278E-02	*0.913E-02	*0.554E-02

Table 3. Same as Table 1, for the electron density $N_e = 10^{17}$ cm^{-3}.

Multiplet	T [K]	W_e [Å]	d_e [Å]	$W_{C\,II}$ [Å]	$d_{C\,II}$ [Å]
$2s^23s\ ^2S–2s^23p\ ^2P^o$	5000.	1.42	−0.209E-01	0.583E-01	−0.538E-02
	10000.	1.05	−0.334E-01	0.807E-01	−0.969E-02
6741.6 Å	20000.	0.848	−0.287E-01	0.922E-01	−0.143E-01
$C = 0.63$E+21	30000.	0.791	−0.310E-01	0.988E-01	−0.164E-01
	50000.	0.754	−0.348E-01	0.106	−0.190E-01
	80000.	0.732	−0.309E-01	0.109	−0.214E-01
$2s^23s\ ^2S–2s^24p\ ^2P^o$	5000.	0.330	0.626E-01	*	*
8	10000.	0.261	0.437E-01	*0.387E-01	*0.756E-02
2195.0 Å	20000.	0.234	0.347E-01	*0.440E-01	*0.101E-01
$C = 0.26$E+20	30000.	0.230	0.328E-01	*0.454E-01	*0.114E-01
	50000.	0.231	0.271E-01	*0.471E-01	*0.131E-01
	80000.	0.232	0.233E-01	*0.474E-01	*0.142E-01
$2s^23s\ ^2S–2s^25p\ ^2P^o$	5000.	0.409	0.127	*	*
	10000.	0.348	0.962E-01	*	*
1700.8 Å	20000.	0.334	0.778E-01	*	*
$C = 0.72$E+19	30000.	0.336	0.693E-01	*	*
	50000.	0.344	0.575E-01	*	*
	80000.	0.348	0.495E-01	*	*
$2s^23s\ ^2S–2s^26p\ ^2P^o$	5000.	*0.793	*0.368	*	*
	10000.	0.738	0.317	*	*
1515.9 Å	20000.	0.734	0.275	*	*
$C = 0.17$E+19	30000.	0.763	0.248	*	*
	50000.	0.796	0.215	*	*
	80000.	0.810	0.179	*	*
$2s^23s\ ^2S–2s^27p\ ^2P^o$	5000.	*1.32	*0.574	*	*
	10000.	*1.27	*0.537	*	*
1434.9 Å	20000.	*1.33	*0.449	*	*
$C = 0.13$E+19	30000.	*1.40	*0.422	*	*
	50000.	1.46	0.365	*	*
	80000.	1.50	0.300	*	*
$2s^23s\ ^2S–2s^28p\ ^2P^o$	5000.	*	*	*	*
	10000.	*	*	*	*
1387.1 Å	20000.	*2.29	*0.186	*	*
$C = 0.30$E+18	30000.	*2.41	*0.146	*	*
	50000.	*2.54	*0.104	*	*
	80000.	*2.60	* 0.818E-01	*	*

Table 4. Same as Table 1, for the $2s^23d\ ^2D–2s^2nf\ ^2F^o$ series and for the electron density $N_e = 10^{17}$ cm^{-3}.

Multiplet	T [K]	W_e [Å]	d_e [Å]	$W_{C\,II}$ [Å]	$d_{C\,II}$ [Å]
$2s^23d\ ^2D–2s^24f\ ^2F^o$	5000.	2.20	0.370E-02	*	*
	10000.	1.75	0.114E-01	*0.162	*−0.922E-01
4299.9 Å	20000.	1.42	0.819E-02	*0.192	*−0.134
$C = 0.15$E+20	30000.	1.30	−0.197E-02	*0.213	*−0.147
	50000.	1.19	−0.105E-01	*0.235	*−0.176
	80000.	1.10	−0.477E-02	*0.241	*−0.182
$2s^23d\ ^2D–2s^25f\ ^2F^o$	5000.	*3.50	*−0.127	*	*
	10000.	*3.24	*−0.167E-02	*	*
3009.9 Å	20000.	2.99	0.124E-01	*	*
$C = 0.10$E+19	30000.	2.82	0.411E-01	*	*
	50000.	2.62	0.962E-01	*	*
	80000.	2.42	0.844E-01	*	*
$2s^23d\ ^2D–2s^26f\ ^2F^o$	5000.	*	*	*	*
	10000.	*5.25	*−0.139	*	*
2588.1 Å	20000.	*5.18	*−0.795E-01	*	*
$C = 0.46$E+18	30000.	*5.03	* 0.562E-01	*	*
	50000.	4.76	0.221	*	*
	80000.	4.44	0.151	*	*
$2s^23d\ ^2D–2s^27f\ ^2F^o$	5000.	*	*	*	*
	10000.	*	*	*	*
2386.5 Å	20000.	*	*	*	*
$C = 0.25$E+18	30000.	*7.80	* 0.108	*	*
	50000.	*7.58	* 0.428	*	*
	80000.	*7.19	* 0.270	*	*
$2s^2\ 3d\ ^2D–2s^2\ 8f\ ^2F^o$	5000.	*	*	*	*
	10000.	*	*	*	*
2271.8 Å	20000.	*	*	*	*
$C = 0.16$E+18	30000.	*	*	*	*
	50000.	*	*	*	*
	80000.	*11.6	*2.27	*	*

where W and $\bar{\lambda}$ are respectively the values of the width and the average wavelength of the whole multiplet and W_{line} and λ refer to the line within the multiplet.

We also provide in Table 7 estimates of the uncertainties of the experimental data, with letter codes as used by Konjević et al. (2002):

A = uncertainties within 15 per cent,
B^+ = uncertainties within 23 per cent,
B = uncertainties within 30 per cent,
C^+ = uncertainties within 40 per cent,
C = uncertainties within 50 per cent.

Since we used the same atomic data and Sahal-Bréchot SCP code as Mahmoudi et al. (2004), we should obtain the same results. In fact, this is not exactly the case, because there was a small error in the quadrupolar contribution for C II lines in Mahmoudi et al. (2004). The data corrected by Mahmoudi (private communication) have been implemented in the STARK-B data base (Sahal-Bréchot et al. 2012).

The earliest experiments on C II Stark-broadening parameters are those of Kusch (1967), who used pulsed discharge, and Roberts & Eckerle (1967), who used a T tube; we do not mention these values in Table 7 because the uncertainties are greater than 50 per cent.

To give more accuracy, a few years later Platiša, Popović & Konjević (1978) used a low-pressure pulsed arc, while Goly & Weniger (1982a,b) used a stabilized arc and investigated ultraviolet lines. The visible spectrum was covered by Djeniže et al. (1988) and Perez et al. (1989): both authors used a low-pressure pulsed arc. Sarandaev & Salakhov (1995) used an impulsive capillary discharge, Blagojević et al. (1999) produced plasma with a low-pressure pulsed arc and more recently Srećković et al. (2000) investigated a large spectral range using a linear low-pressure pulsed arc.

We can see from Table 7 that the best agreement between our present theoretical values and the experimental ones is obtained using the results of Blagojević et al. (1999). Moreover, the results of Srećković et al. (2000) for the $2s^23p\ ^2P^o–2s^23d\ ^2D$ multiplet are also in very good agreement with those of Blagojević et al. (1999) and our own, whereas the results of Djeniže et al. (1988) are twice as large as those for our calculations and the two abovementioned experiments. Since the measurements of Djeniže et al. (1988) and Srećković et al. (2000) originate from the same laboratory, we may

Table 5. Same as Table 1, for the electron density $N_e = 10^{18}$ cm^{-3}.

Multiplet	T [K]	W_e [Å]	d_e [Å]	$W_{C\,II}$ [Å]	$d_{C\,II}$ [Å]
$2s^2 3s\ ^2S–2s^2 3p\ ^2P^o$	5000.	14.2	−0.171	*0.386	*−0.339E-01
	10000.	10.5	−0.309	*0.740	*−0.806E-01
6741.6 Å	20000.	8.48	−0.268	*0.891	*−0.127
$C = 0.63E+22$	30000.	7.91	−0.299	*0.977	*−0.154
	50000.	7.54	−0.341	*1.05	*−0.184
	80000.	7.32	−0.306	*1.09	*−0.213
$2s^2 3s\ ^2S–2s^2 4p\ ^2P^o$	5000.	*3.30	*0.578	*	*
8	10000.	2.61	0.407	*	*
2195.0 Å	20000.	2.34	0.321	*	*
$C = 0.26E+21$	30000.	2.30	0.311	*	*
	50000.	2.30	0.264	*	*
	80000.	2.32	0.231	*	*
$2s^2 3s\ ^2S–2s^2 5p\ ^2P^o$	5000.	*4.08	*1.11	*	*
	10000.	*3.48	*0.861	*	*
1700.8 Å	20000.	*3.34	*0.709	*	*
$C = 0.72E+20$	30000.	3.36	0.638	*	*
	50000.	3.44	0.546	*	*
	80000.	3.48	0.473	*	*
$2s^2\ 3s\ ^2S–2s^2\ 6p\ ^2P^o$	5000.	*	*	*	*
	10000.	*	*	*	*
1515.9 Å	20000.	*	*	*	*
$C = 0.17E+20$	30000.	*7.50	*1.98	*	*
	50000.	*7.86	*1.89	*	*
	80000.	*8.02	*1.59	*	*

Table 6. Same as Table 1, for the $2s^2 3d\ ^2D–2s^2 nf\ ^2F^o$ series and for the electron density $N_e = 10^{18}$ cm^{-3}.

Multiplet	T [K]	W_e [Å]	d_e [Å]	$W_{C\,II}$ [Å]	$d_{C\,II}$ [Å]
$2s^2 3d\ ^2D–2s^2 4f\ ^2F^o$	5000.	*21.3	1.33	*	*
	10000.	*17.1	0.939	*	*
4299.9 Å	20000.	13.9	0.677	*	*
$C = 0.15E+21$	30000.	12.9	0.435	*	*
	50000.	11.8	0.128	*	*
	80000.	10.9	0.127	*	*
$2s^2 3d\ ^2D–2s^2 5f\ ^2F^o$	5000.	*	*	*	*
	10000.	*	*	*	*
3009.9 Å	20000.	*23.4	*0.176	*	*
$C = 0.10E+20$	30000.	*23.0	*0.129	*	*
	50000.	*22.2	*0.409	*	*
	80000.	*21.0	*0.425	*	*
$2s^2\ 3d\ ^2D–2s^2\ 6f\ ^2F^o$	5000.	*	*	*	*
	10000.	*	*	*	*
2588.1 Å	20000.	*	*	*	*
$C = 0.46E+19$	30000.	*	*	*	*
	50000.	*	*	*	*
	80000.	*34.9	0.575	*	*

neglect the article of Djeniže et al. (1988). Therefore we may conclude that the experiments of Blagojević et al. (1999) and Srećković et al. (2000) are in excellent agreement with the theoretical results for the $2s^2 3p\ ^2P^o–2s^2 3d\ ^2D$ multiplet. For the $2s^2 3s\ ^2S–2s^2 3p\ ^2P^o$ multiplet, our theoretical results are also in excellent agreement with the experimental data of Blagojević et al. (1999), as well as with those of Sarandaev & Salakhov (1995). They are in very good agreement, better than 30 per cent (which is well within error bars), with the data of Srećković et al. (2000). We will also neglect the old measurements of Djeniže et al. (1988), which disagree with theory and all other experiments by a factor higher than 2. We conclude that for the $2s^2 3s\ ^2S–2s^2 3p\ ^2P^o$ multiplet, theory and recent experiments mutually confirm each other.

If we take into account of the fact that accuracy 'C' denotes experiments with 50 per cent uncertainty, we can see in Table 7 that, for all transitions between terms with a parent term ^1S, the agreement with different experiments is relatively good. The ratio between experimental and calculated widths varies from 0.83–1.49 for Perez et al. (1991). For Goly & Weniger (1982b) it varies from 0.37–1.78 and for Roberts & Eckerle (1967) it varies from 0.97–1.29, always within the estimated uncertainty. For transitions between terms with a parent term $^3P^o$, the agreement is also within the error bars but the experimental data are lower than the theoretical ones. The ratio of experimental to theoretical widths is 0.77 for Djeniže et al. (1993) and from 0.81–1.94 for Srećković et al. (2000). The largest disagreement is for the $2s2p^2\ ^2P–2p^3\ ^2D^o$ and $2s2p^2\ ^2S–2s^2 3p\ ^2P^o$ transitions: it varies from 0.37–1.94. Since most of these experimental results are with accuracies C and C$^+$ and are about 30 years old, except for the data of Srećković et al. (2000), new experimental determination of Stark-broadening parameters would be very welcome.

3.2 Influence of the choice of oscillator strengths on the results of calculations: case of the 3s–*n*p and 3d–*n*f series

Figs 1 and 2 show that the width values achieved using oscillator strengths obtained with the Bates and Damgaard method (W_{BD}) are in good agreement with the values calculated using TOPbase atomic data (W_{TB}). The only exception is for the transition $2s^2 3s\ ^2S–2s^2 8p\ ^2P^o$ (see Fig. 1), where $W_{TB} = 22.141 \times 10^9$ s^{-1}, whereas $W_{BD} = 17.047 \times 10^9$ s^{-1}. This discrepancy is due to the fact that the oscillator strength of the transition between the initial level $2s^2 8p\ ^2P^o$ and the perturbing one $2s2p(^3P^o)3p$ is zero in the Bates and Damgaard method, because an internal electron is excited. If we use the TB oscillator strength for this transition, in the BD calculation we obtain 22.141×10^9 s^{-1}. This TB oscillator strength is equal to 0.1041×10^{-2}: if we neglect the contribution of this transition in the TB calculation, we obtain 15.48×10^9 s^{-1}, which is close to the BD value given above. This shows the limit of validity of the Bates and Damgaard approximation for the calculation of Stark-broadening parameters.

3.3 Systematic trends: variation with principal number *n* along the 3s–*n*p and 3d–*n*f series

Figs 3 and 4 show the asymptotic behaviour of the Stark widths within two series when the principal quantum number n increases. We have fitted the widths with a least-squares fourth-order polynomial fitting:

$$W = a_0 + a_1 n + a_2 n^2 + a_3 n^3 + a_4 n^4.$$

The coefficients of the fitting and the correlation coefficient R^2 are given in Table 8.

As expected from the Coulomb (hydrogenic) behaviour of the dipolar line strengths (n, $l - n$, $l + 1$), the widths increase as n^4 (Sahal-Bréchot, Dimitrijević & Ben Nessib 2011).

Table 7. Comparison between our theoretical electron impact widths W_e and experimental ones W_{exp}. The wavelengths are those of the NIST Atomic Spectra Database (Ralchenko et al. 2011). The electron density N_e is in [10^{17} cm^{-3}]. Ratios W_{exp}/W_e are given. The uncertainties of the experimental data are given in column 'Acc'.

Line	λ [Å]	N_e	T_e [K]	W_e [Å]	W_{exp} [Å]	W_{exp}/W_e	Acc.	Ref.
$2s2p^2\ ^2P_{3/2}–2p^3\ ^2D^o_{5/2}$	2512.06	0.19	12800	0.0647	0.024	0.37	C	Goly & Weniger (1982b)
$2s2p^2\ ^2P_{1/2}–2p^3\ ^2D^o_{3/2}$	2509.13	0.19	12800	0.06455	0.026	0.40	C	Goly & Weniger (1982b)
$2s2p^2\ ^2S_{1/2}–2s^23p\ ^2P^o_{3/2}$	2836.71	0.49	26300	0.06214	0.082	1.32	C^+	Platiša et al. (1978)
		1.96	17800	0.27274	0.530	1.94	B	Srećković et al. (2000)
		0.19	12800	0.02929	0.052	1.78	C	Goly & Weniger (1982b)
$2s2p^2\ ^2S_{1/2}–2s^23p\ ^2P^o_{1/2}$	2837.61	0.49	26300	0.06218	0.083	1.33	C^+	Platiša et al. (1978)
		1.96	17800	0.27294	0.456	1.67	B	Srećković et al. (2000)
		0.19	12800	0.02929	0.052	1.78	C	Goly & Weniger (1982b)
$2s^23p\ ^2P^o_{3/2}–2s^24s\ ^2S_{1/2}$	3920.68	0.19	12800	0.13704	0.15	1.09	C^+	Goly & Weniger (1982b)
		0.95	12800	0.68324	0.95	1.39	C^+	Perez et al. (1991)
$2s^23p\ ^2P^o_{1/2}–2s^24s\ ^2S_{1/2}$	3918.98	0.19	12800	0.13693	0.15	1.09	C^+	Goly & Weniger (1982b)
$2s^23d\ ^2D_{3/2}–2s^25p\ ^2P^o_{5/2}$	3361.05	1.4	30000	1.82	1.76	0.97	C	Roberts & Eckerle (1967)
		1.5	30000	1.95	2.52	1.29	C	–
$2s^23d\ ^2D_{5/2}–2s^24f\ ^2F^o_{5/2}$	4267.26	0.4	12800	0.644	0.96	1.49	C	Perez et al. (1991)
$2s2p(^2P^o)3s\ ^4P^o_{5/2}–2s2p(^2P^o)3p\ ^4P_{3/2}$	5151.08	1.82	18300	0.97706	0.889	0.91	B^+	Srećković et al. (2000)
$2s2p(^2P^o)3s\ ^4P^o_{5/2}–2s2p(^2P^o)3p\ ^4P_{5/2}$	5145.16	1.82	18300	0.97781	0.790	0.81	B^+	Srećković et al. (2000)
$2s2p(^2P^o)3s\ ^4P^o_{3/2}–2s2p(^2P^o)3p\ ^4P_{1/2}$	5143.49	1.82	18300	0.97418	1.194	1.22	B^+	Srećković et al. (2000)
$2s2p(^2P^o)3s\ ^4P^o_{3/2}–2s2p(^2P^o)3p\ ^4S_{3/2}$	5648.07	1.1	20000	0.641	0.53	0.83	C^+	Perez et al. (1991)
$2s^23s\ ^2S_{1/2}–2s^23p\ ^2P^o_{3/2}$	6578.05	1.43	35000	1.10900	1.106	1.00	B	Djeniže et al. (1988)
		1.96	17800	1.70846	2.198	1.29	B^+	Srećković et al. (2000)
		0.31	18800	0.27175	0.265	0.97	B^+	Blagojević et al. (1999)
		2.21	22000	1.83835	1.88	1.02	C	Sarandaev & Salakhov (1995)
$2s^23s\ ^2S_{1/2}–2s^23p\ ^2P^o_{1/2}$	6582.88	1.43	35000	1.11063	1.106	0.99	B	Djeniže et al. (1988)
		1.96	17800	1.71097	2.145	1.25	B^+	Srećković et al. (2000)
		0.31	18800	0.27215	0.265	0.97	B^+	Blagojević et al. (1999)
		2.21	22000	1.84105	1.81	0.98	C	Sarandaev & Salakhov (1995)
$2s2p(^2P^o)3s\ ^4P^o_{5/2}–2s2p(^2P^o)3p\ ^4D_{7/2}$	6783.91	1.61	40000	1.32	1.02	0.77	C	Djeniže et al. (1993)
$2s^23p\ ^2P^o_{3/2}–2s^23d\ ^2D_{5/2}$	7236.42	1.43	35000	1.43976	1.712	1.18	B	Djeniže et al. (1988)
		0.31	18800	0.34594	0.353	1.02	B^+	Blagojević et al. (1999)
		1.96	17800	2.20964	2.034	0.92	B	Srećković et al. (2000)
$2s^23p\ ^2P^o_{3/2}–2s^23d\ ^2D_{3/2}$	7231.33	1.96	17800	2.20653	2.220	1.01	B^+	Srećković et al. (2000)
		0.31	18800	0.34545	0.338	0.98	B^+	Blagojević et al. (1999)

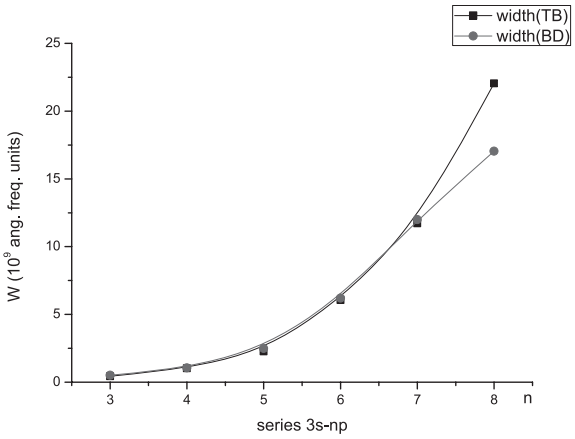

Figure 1. Electron-impact full widths at half-maximum (in 10^{-9} angular frequency units) for the 3s–*n*p series as a function of *n* for $T = 10\,000$ K. The electron density is 10^{14} cm^{-3}. For the calculation of width (TB), energies and oscillator strengths were obtained from the TOPbase data base, while width (BD) was calculated using the TOPbase data base for energy and oscillator strengths were calculated using the method of Bates & Damgaard (1949).

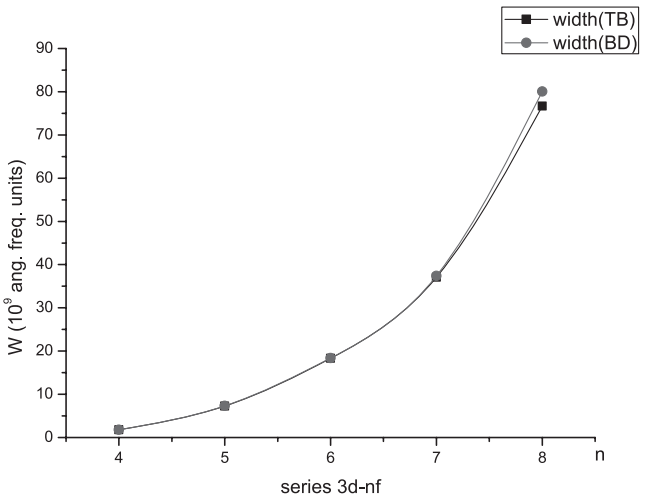

Figure 2. Same as Fig. 1, for the 3d–*n*f series.

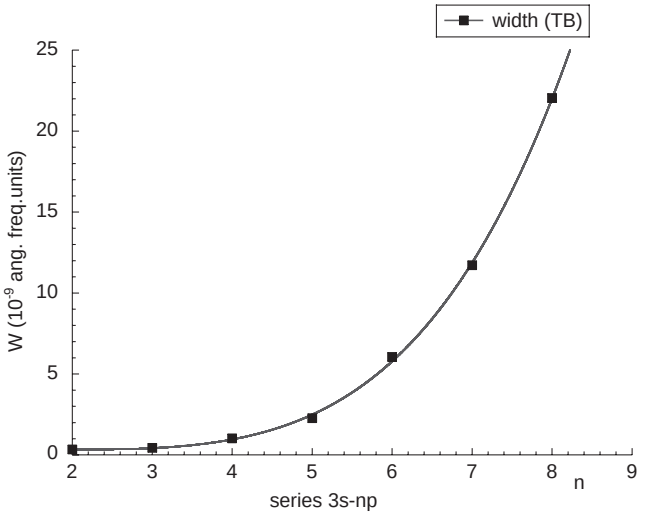

Figure 3. Electron-impact full widths at half-maximum (in 10^{-9} angular frequency units) for the 3s–*n*p series as a function of n for $T = 10\,000$ K and $N = 10^{14}$ cm^{-3}: least-squares fourth-order polynomial fitting of the data showing the n^{-4} asymptotic behaviour. The coefficients of the fitting and the correlation factor R^2 are given in Table 8. The widths (TB) have been calculated using energies and oscillator strengths of TOPbase. Full squares: width calculations; full line: fitting curve.

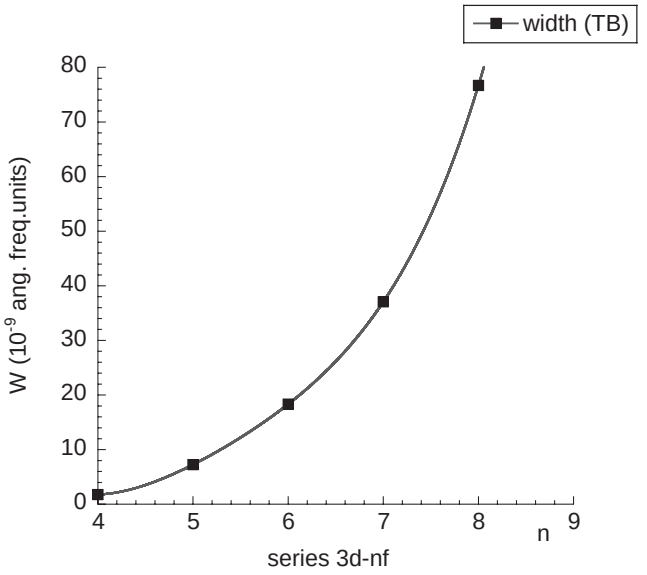

Figure 4. Same as Fig. 3, for the 3d–*n*f series.

Table 8. Coefficients and correlation factor R^2 of the least-squares fourth-order polynomial fitting of the width as a function of the principal quantum number n for the 3s–*n*p and 3d–*n*f series. The electron density is $N_e = 10^{18}$ cm^{-3} and $T = 10\,000$ K.

Series	a_0	a_1	a_2	a_3	a_4	R^2
3s–*n*p	0.71988	−0.39812	0.17792	−0.057296	0.010358	0.99962
3d–*n*f	381.45	−288.27	80.185	−9.8085	0.46181	1

4 CONCLUSIONS

In this work, we have calculated Stark widths and shifts for lines of singly ionized carbon, using the semiclassical perturbation formalism. These data can be used for laboratory and stellar plasma diagnostics, investigation and modelling, in particular for modelling recently discovered carbon white dwarfs.

ACKNOWLEDGMENTS

We thank Patrick Dufour, who encouraged us and followed the development of this work. A part of this work has been supported by the cooperation agreement between Tunisia (DGRS) and France (CNRS) (project code 09/R 13.03, No.22637), by the Programme National de Physique Stellaire (INSU-CNRS), by the Paris Observatory and by the project 176002 of Ministry of Education and Science of Serbia.

REFERENCES

Baranger M., 1958, Phys. Rev., 112, 855
Bates D. R., Damgaard A., 1949, Trans. R. Soc. London Ser. A, 242, 101
Blagojević B., Popović M. V., Konjević N., 1999, Phys. Scr., 59, 374
Bréchot S., Van Regemorter H., 1964, Ann. d'Astrophys., 27, 432
Cunto W., Mendoza C., Ochsenbein F., Zeippen C. J., 1993, A&A, 275, L5
Dimitrijević M. S., Sahal-Bréchot S., Bommier V., 1991, A&A, 89, 581
Djeniže S., Srećković A., Milosavljević V., Labat O., Platiša M., Purić J., 1988, Z. Phys. D, 9, 129
Djeniže S., Popović L. Č., Labat J., Srećković A., Platiša M., 1993, Contrib. Plasma Phys., 33, 103
Dufour P., Liebert J., Fontaine G., Behara N., 2007, Nature Lett., 450, 522
Dufour P., Fontaine G., Liebert J., Schmidt G. D., Behara N., 2008, ApJ, 683, 978
Fleurier C., Sahal-Bréchot S., Chapelle J., 1977, J. Quant. Spectrosc. Radiat. Transfer, 17, 595
Goly A., Weniger S., 1982a, J. Quant. Spectrosc. Radiat. Transfer, 27, 657
Goly A., Weniger S., 1982b, J. Quant. Spectrosc. Radiat. Transfer, 28, 389
Griem H. R., 1974, Spectral Line Broadening by Plasmas. Academic Press Inc., New York
Konjević N., Lesage A., Fuhr J. R., Wiese W. L., 2002, J. Phys. Chem. Ref. Data, 31, 819
Kusch H. J., 1967, Z. Astrophys., 67, 64
Mahmoudi W. F., Ben Nessib N., Sahal-Bréchot S., 2004, Phys. Scr., 70, 142
Perez M. C., de la Rosa M. I., de Frutos A. M., Mar S., 1989, in Szudy J., ed., 9th International Conference on Spectral Line Shapes (ICSLS). Nicholas Copernicus Univ. Press. Poland, p. A9
Perez M. C., de la Rosa M. I., de Frutos A. M., Mar S., 1991, Phys. Rev. A, 44, 6948
Platiša M., Popović M., Konjević N., 1978, J. Quant. Spectrosc. Radiat. Transfer, 20, 477
Popović L. Č., Milovanović N., Dimitrijević M. S., 2001, A&A, 365, 656
Ralchenko Yu., Kramida A. E., Reader J., NIST ASD Team, 2011, NIST Atomic Spectra Database (ver. 4.1.0). National Institute of Standards and Technology, Gaithersburg, MD (Available at http://physics.nist.gov/asd3)
Roberts J. R., Eckerle K. L., 1967, Phys. Rev., 159, 104
Sahal-Bréchot S., 1969a, A&A, 1, 91
Sahal-Bréchot S., 1969b, A&A, 2, 322
Sahal-Bréchot S., 1974, A&A, 35, 319
Sahal-Bréchot S., 1991, A&A, 245, 322
Sahal-Bréchot S., Dimitrijević M. S., Ben Nessib N., 2011, Baltic Astron., 20, 523

Sahal-Bréchot S., Dimitrijević M. S., Moreau N., 2012, Stark-B data base (Available at http://stark-b.obspm.fr)
Sarandaev E. V., Salakhov M. Kh., 1995, J. Quant. Spectrosc. Radiat. Transfer, 54, 827
Strećković A., Drinčić V., Bukvić S., Djeniže S., 2000, J. Phys. B: At. Mol. Opt. Phys., 33, 4873

SUPPORTING INFORMATION

Additional Supporting Information may be found in the online version of this article:

Tables S1– S3. The results for 149 lines for electron temperatures within 5000–80 000 K and electron densities 10^{14} (Table S1), 10^{17} (Table S2) and 10^{18} cm^{-3} (Table S3).

Please note: Wiley-Blackwell are not responsible for the content or functionality of any supporting materials supplied by the authors. Any queries (other than missing material) should be directed to the corresponding author for the article.

This paper has been typeset from a TEX/LATEX file prepared by the author.

Monthly Notices
of the
ROYAL ASTRONOMICAL SOCIETY

MNRAS **431,** 1039–1047 (2013) doi:10.1093/mnras/stt228
Advance Access publication 2013 March 15

Stark broadening of Pb IV spectral lines

Rafik Hamdi,[1⋆] Nabil Ben Nessib,[2,3] Milan S. Dimitrijević[4,5,6] and Sylvie Sahal-Bréchot[5]

[1]*Groupe de Recherche en Physique Atomique et Astrophysique, Faculté des Sciences de Bizerte, Université de Carthage, Tunisia*
[2]*Department of Physics and Astronomy, College of Science, King Saud University. PO Box 2455, Riyadh 11451, Saudi Arabia*
[3]*Groupe de Recherche en Physique Atomique et Astrophysique, INSAT, Université de Carthage, Tunisia*
[4]*Astronomical Observatory, Volgina 7, 11060 Belgrade, Serbia*
[5]*Laboratoire d'Étude du Rayonnement et de la Matière en Astrophysique, Observatoire de Paris, UMR CNRS 8112, UPMC, 5 Place Jules Janssen, 92195 Meudon Cedex, France*
[6]*Institute Isaac Newton of Chile, Yugoslavia Branch, 11060 Belgrade, Serbia*

Accepted 2013 February 5. Received 2013 February 5; in original form 2012 December 12

ABSTRACT

Stark-broadening parameters have been calculated for 114 spectral lines of triply charged lead ion (Pb IV) using semiclassical perturbation approach in the impact approximation. The provided widths and shifts have been obtained for a set of temperatures from 20 000 to 300 000 K and an electron density of 10^{17} cm^{-3}. The studied lines correspond to transitions between the configurations $5d^{10}nl-5d^{10}n'l'$ and $5d^{9}6s^{2}-5d^{10}nl$. Energy levels and oscillator strengths needed for this calculation have been calculated using a Hartree–Fock relativistic (HFR) approach. Comparison has also been made with available theoretical and experimental results. In addition, the regularity in the $5d^{10}6s\,^{2}S_{1/2}-5d^{10}np\,^{2}P^{o}_{1/2}$ spectral series has been studied.

Key words: atomic data – atomic processes – line: profiles.

1 INTRODUCTION

Triply charged lead ion (Pb IV) belongs to the gold isoelectronic sequence, its ground-state configuration is $4f^{14}5d^{10}6s$. This is an interesting isoelectronic sequence with filled 4f and 5d subshells and a single electron in the outer shell. This ion is characterized by a strong resonance line, which is a candidate for spectroscopic detection in hot DA white dwarfs (Vennes, Chayer & Dupuis 2005). O'Toole (2004) reported the discovery of strong photospheric resonance lines of several heavy elements in the ultraviolet (UV) spectra of more than two dozen sdB and sdOB stars at temperatures ranging from 22 000 to 40 000 K. Among these lines, several correspond to Pb IV ones. Pb IV 1313.1 Å resonance line was detected by Proffitt, Sansonetti & Reader (2001) in the main-sequence B star AV 304.

Stark broadening of spectral lines is very important in DA and DB white dwarf atmospheres (Simić, Dimitrijević & Kovačević 2009; Dimitrijević et al. 2011; Dufour et al. 2011; Larbi-Terzi et al. 2012). Hamdi et al. (2008) studied the influence of Stark broadening on Si VI lines in DO white dwarf atmospheres and found that this mechanism is dominant in broad regions. Besides white dwarfs, Stark broadening is the most important pressure-broadening mechanism for A and B stars and this effect must be taken into account for investigation, analysis and modelling of their atmospheres. In Popović et al. (2001), it was shown that Stark broadening can change the spectral line equivalent widths by 10–45 per cent. Hence neglecting this mechanism, significant errors in abundance determinations may be introduced.

Alonso-Medina et al. (2010) carried out semi-empirical (SE) calculations of Stark widths and shifts in the impact approximation for 58 spectral lines of Pb IV using Griem's (1968) formula with a Gaunt factor suggested by Niemann et al. (2003). Atomic data were determined using Hartree–Fock relativistic (HFR) approach (Cowan 1981). They found that their values are for a factor of 2 lower than Dimitrijević & Sahal-Bréchot (1999). The latter ones calculated widths and shifts of the lines within $6s\,^{2}S-6p\,^{2}P^{o}$ and $6s\,^{2}S-7p\,^{2}P^{o}$ multiplets with the impact semiclassical perturbation (SCP) method (Sahal-Bréchot 1969a,b) with Bates and Damgaard (Bates & Damgaard 1949) oscillator strengths. Alonso-Medina et al. (2010) concluded that the Bates and Damgaard oscillator strengths used by Dimitrijević & Sahal-Bréchot (1999) were overestimated because the core-polarization effects were not included.

Due to the interest of SCP and SE methods for Stark-broadening line profiles determination, and since Pb IV lines have been observed in stellar spectra, it is important to clarify the reasons of this discrepancy.

Therefore, we have performed in this paper several SCP calculations of Stark-broadening parameters using different sets of oscillator strengths. First, we have used the oscillator strengths of Alonso-Medina, Colón & Porcher (2011), i.e. the same oscillator strengths as used in the SE work of Alonso-Medina et al. (2010). Secondly, we have calculated oscillator strengths by

⋆ E-mail: Rafik.Hamdi@istls.rnu.tn

using the Cowan code [HFR correction approach (Cowan (1981)]. Thirdly, we have used the oscillator strengths of Safronova & Johnson (2004) obtained using third-order many-body perturbation theory. We have also calculated Stark-broadening parameters using the modified semi-empirical method (MSE; Dimitrijević & Konjević 1980), with the atomic data taken from Alonso-Medina A., Colón & Porcher (2011). Then our obtained results have been compared to the SCP values of Dimitrijević & Sahal-Bréchot (1999) and to the SE results of Alonso-Medina et al. (2010). They have also been compared to the experimental ones of Bukvić et al. (2011). The obtained results are used to clarify the reason for the discrepancy between SE results of Alonso-Medina et al. (2010) and SCP results of Dimitrijević & Sahal-Bréchot (1999).

In addition, we have provided in this work SCP impact Stark widths and shifts for 114 spectral lines between the $5d^{10}nl-5d^{10}n'l'$ and $5d^96s^2-5d^{10}nl$ configurations of Pb IV. The colliding particles are electrons, protons and ionized helium. The energy levels and oscillator strengths have been obtained with the Cowan code with 43 configurations.

Finally, the regularity of behaviour of Stark widths within the $5d^{10}6s\,^2S_{1/2}-5d^{10}np^2P^o_{1/2}$ spectral series has been studied.

2 THE IMPACT SEMICLASSICAL PERTURBATION METHOD

A detailed description of this formalism with all the innovations is given in Sahal-Bréchot (1969a,b, 1974, 1991); Fleurier, Sahal-Bréchot & Chapelle (1977); Dimitrijević, Sahal-Bréchot & Bommier (1991); Dimitrijević & Sahal-Bréchot (1996). The profile $F(\omega)$ is Lorentzian for isolated lines:

$$F(\omega) = \frac{w/\pi}{(\omega - \omega_{if} - d)^2 + w^2}, \tag{1}$$

where

$$\omega_{if} = \frac{E_i - E_f}{\hbar},$$

i and f denote the initial and final states and E_i and E_f their corresponding energies.

The total width at half-maximum ($W = 2w$) and shift (d) (in angular frequency units) of an electron-impact-broadened spectral line can be expressed as

$$W = N \int v f(v) \mathrm{d}v \left(\sum_{i' \neq i} \sigma_{ii'}(v) + \sum_{f' \neq f} \sigma_{ff'}(v) + \sigma_{\mathrm{el}} \right)$$

$$d = N \int v f(v) \mathrm{d}v \int_{R_3}^{R_\mathrm{D}} 2\pi\rho \mathrm{d}\rho \sin(2\varphi_\mathrm{p}), \tag{2}$$

where N is the electron density, $f(v)$ the Maxwellian velocity distribution function for electrons, ρ denotes the impact parameter of the incoming electron, i' (resp. f') denotes the perturbing levels of the initial state i (resp. final state f). The inelastic cross-section $\sigma_{ii'}(v)$ (resp. $\sigma_{ff'}(v)$) can be expressed by an integral over the impact parameter ρ of the transition probability $P_{ii'}(\rho, v)$ (resp. $P_{ff'}(\rho, v)$) as

$$\sum_{i' \neq i} \sigma_{ii'}(v) = \frac{1}{2}\pi R_1^2 + \int_{R_1}^{R_\mathrm{D}} 2\pi\rho \mathrm{d}\rho \sum_{i' \neq i} P_{ii'}(\rho, v), \tag{3}$$

and the elastic cross-section is given by

$$\sigma_{\mathrm{el}} = 2\pi R_2^2 + \int_{R_2}^{R_\mathrm{D}} 2\pi\rho \mathrm{d}\rho \sin^2\delta + \sigma_\mathrm{r},$$

$$\delta = (\varphi_\mathrm{p}^2 + \varphi_\mathrm{q}^2)^{\frac{1}{2}}. \tag{4}$$

The phase shifts φ_p and φ_q due, respectively, to the polarization potential (r^{-4}) and to the quadrupolar potential (r^{-3}), are given in section 3 of chapter 2 in Sahal-Bréchot (1969a) and R_D is the Debye radius. All the cut-offs R_1, R_2 and R_3 are described in section 1 of chapter 3 in Sahal-Bréchot (1969b). σ_r is the contribution of the Feshbach resonances (Fleurier et al. 1977)

The formulae for the ion-impact widths and shifts are analogous to equations (2)– (4), without the Feshbach resonances contribution to the width. For electrons, hyperbolic paths due to the attractive Coulomb force are used, while for perturbing ions the hyperbolic paths are different since the force is repulsive.

The calculations need a relatively complete set of oscillator strengths for transitions starting or ending on energy levels forming the considered line, so that the corresponding oscillator strength sum rules can be satisfied. In our present calculations, energy levels and oscillator strengths have been carried out with the HFR approach using the Cowan code (Cowan 1981). We have adopted an atomic model including 43 configurations: $5d^96s^2$, $5d^96p^2$, $5d^{10}\,n$s ($6 \leq n \leq 11$), $5d^{10}\,n$d ($6 \leq n \leq 11$), $5d^{10}\,n$g ($5 \leq n \leq 11$), $5d^96s7s$, $5d^96s6d$ (even parity) and $5d^{10}\,n$p ($6 \leq n \leq 11$), $5d^{10}\,n$f ($5 \leq n \leq 11$), $5d^{10}\,n$h ($6 \leq n \leq 11$), $5d^96s6p$ (odd parity).

3 COMPARISON BETWEEN DIFFERENT CALCULATIONS

In order to explain the reason of the disagreement found between SE results of Alonso-Medina et al. (2010) and SCP ones of Dimitrijević & Sahal-Bréchot (1999), the present section is devoted to a comparison between different calculations for several lines of Pb IV, using the impact approximation.

The first SCP calculations of Stark-broadening parameters of Pb IV were performed by Dimitrijević & Sahal-Bréchot (1999). Energy levels were taken from Gutmann & Crooker (1973) and oscillator strengths were calculated with the Bates and Damgaard method (Bates & Damgaard 1949). Stark widths were calculated for $6s\,^2S-6p\,^2P^o$ and $6s\,^2S-7p\,^2P^o$ multiplets. The widths of Dimitrijević & Sahal-Bréchot (1999) are denoted here as W_{DS}.

Alonso-Medina et al. (2010) used the SE Griem's formula (Griem 1968) with a Gaunt factor suggested by Niemann et al. (2003). Atomic data, obtained by using HFR approach of Cowan (1981) with 14 configurations, were taken from Alonso-Medina et al. (2011). Yet, it can be noticed that Griem (1974, p. 256) wrote that not much is known about the accuracy of his SE formula (Griem 1968) for multiply charged ions. In fact, this formula was based on the effective Gaunt factor proposed by Van Regemorter (1962) for ions. Furthermore, Dimitrijević & Konjević (1980) showed that the accuracy of SE line widths decreases with the increase of the charge of emitter, and that these SE widths were considerably lower than the results of experiments. Therefore, Alonso-Medina et al. (2010) replaced the Gaunt factor of Van Regemorter (1962) by the Gaunt factor suggested by Niemann et al. (2003). This is another reason to investigate the accuracy of such adaptation of the SE method.

Regarding this work, we have performed three different sets of calculations for the aim of comparison and discussion. SCP calculations using oscillator strengths and energy levels of Alonso-Medina et al. (2011) obtained by Cowan code with 14 configurations (the width is denoted by W_{SC1}) and SCP calculations using oscillator strengths taken from Safronova & Johnson (2004) and energy (the width is denoted by W_{SC2}). Oscillator strengths of Safronova & Johnson (2004) are obtained using third-order many-body

Table 1. Comparison between our electron impact Stark widths (W_{SC1}, W_{SC2}, W_{SC3}), values from Alonso-Medina et al. (2010) (W_{AM}) and values from Dimitrijević & Sahal-Bréchot (1999) (W_{DS}). Present results: W_{SC1} – semiclassical Stark widths obtained using oscillator strengths from Alonso-Medina et al. (2011); W_{SC2} – semiclassical Stark widths obtained using oscillator strengths from Safronova & Johnson (2004); W_{SC3} – semiclassical Stark widths obtained using oscillator strengths calculated with HFR method (Cowan 1981) and the atomic model given in Section 2. W_{SC1}, W_{SC2} and W_{SC3} are obtained using energy levels from Alonso-Medina et al. (2011). Results are given for an electron density of $Ne = 10^{17}$ cm^{-3}.

Transition	T (K)	W_{SC1} (Å)	W_{SC2} (Å)	W_{SC3} (Å)	W_{DS}(Å)	W_{AM} (Å)
$6s\,^2S_{1/2}-6p\,^2P^o_{1/2}$	50 000	0.008 25	0.008 80	0.010 70	0.010 34	0.0051
$\lambda = 1313.1$ Å	200 000	0.004 46	0.004 76	0.005 87	0.005 67	0.0022
$6s\,^2S_{1/2}-6p\,^2P^o_{3/2}$	50 000	0.005 98	0.006 04	0.006 95	0.006 34	0.0051
$\lambda = 1028.6$ Å	200 000	0.003 28	0.003 30	0.003 82	0.003 47	0.0022
$6s\,^2S_{1/2}-7p^2P^o_{1/2}$	50 000	0.002 80	0.003 53	0.003 65	0.003 65	0.0017
$\lambda = 476.7$ Å	200 000	0.001 70	0.002 29	0.002 36	0.002 39	0.0008
$6s\,^2S_{1/2}-7p\,^2P^o_{3/2}$	50 000	0.003 10	0.003 36	0.003 36	0.003 38	0.0030
$\lambda = 459.0$ Å	200 000	0.002 01	0.002 22	0.002 19	0.002 22	0.0014

perturbation theory with the Brueckner-orbital corrections which account for core-polarization effects (Chou & Johnson 1997). In addition, we have performed SCP calculations with oscillator strengths that we have calculated using the Cowan code with 43 configurations (the width is denoted by W_{SC3}).

Furthermore, we have performed another calculation using the MSE approach of Dimitrijević & Konjević (1980) and atomic data of Alonso-Medina et al. (2011). MSE method is valid for singly and multiply charged ions, it uses an effective Gaunt factor and has the advantage that it does not involve a large number of atomic data. The corresponding width is denoted by W_{MSE}. For the details of MSE calculations see Mahmoudi, Ben Nessib & Dimitrijević (2005). We can notice that as a difference from MSE, the complete version of Griem's SE method (Griem 1968) needs the same set of atomic data as the more sophisticated SCP method, so the same effort is needed for simpler (SE) and more advanced (SCP) calculations, if both codes are available.

3.1 Role of oscillator strengths

Table 1 presents the different results for the lines of the $6s\,^2S-6p\,^2P^o$ and $6s\,^2S-7p^2P^o$ multiplets of Pb IV, for two temperatures (50 000 and 200 000 K), and for an electron density of 10^{17} cm^{-3}. Consequently, the use of the set of Bates and Damgaard's oscillator strengths in W_{DS} calculations, which satisfies the corresponding sum rules (Shore & Menzel 1965), cannot explain the large difference between W_{AM} and W_{DS}, for example for 476.7 Å line.

As we can see in Table 1, W_{DS} is always larger than W_{SC1}. The average ratio $\frac{W_{DS}}{W_{SC1}}$ is equal to 1.19 and cannot explain the difference of the factor of 2 (found by Alonso-Medina et al. 2010 in some cases). W_{DS} is also larger than W_{SC2} but the difference is smaller since the average ratio $\frac{W_{DS}}{W_{SC2}}$ is equal to 1.07 only. W_{SC3} are closer to W_{DS} and the average difference is 3 per cent.

A similar conclusion, concerning the use of a set of Bates and Damgaard's oscillator strengths, complete from the point of view of the corresponding sum rules, was obtained by Ben Nessib, Dimitrijević & Sahal-Bréchot (2004) and Hamdi et al. (2007) who calculated line widths and shifts of Si V and Ne V ions. They compared SCP ab initio Stark widths obtained with Bates and Damgaard oscillator strengths and with SUPERSTRUCTURE (Thomas–Fermi–Dirac interaction potential model with relativistic corrections; Eissner, Jones & Nussbaumer 1974) oscillator strengths for Si V and Ne V ions. They found that the difference between the two sets of calculations did not exceed 30 per cent. Thus, the difference in oscillator strengths used in Stark-broadening calculation is not of crucial importance, since the accuracy of the SCP method is about 20 per cent.

One additional reason which could explain the difference between SCP Dimitrijević & Sahal-Bréchot (1999) calculations and SE Alonso-Medina et al. (2010) results, is the eventual existence of a perturbing level close to the initial or final level of the studied transitions, the transition to which is forbidden in Coulomb approximation but becomes allowed if configuration mixing is taken into account. So the corresponding Bates and Damgaard oscillator strength is zero, whereas the Hartree–Fock one can be large. The existence of such levels can increase the width. The influence of a possible close perturbing level will be discussed in Sections 4 and 5.

3.2 Comparison between the three methods: SCP, SE and MSE

By using the same set of atomic levels and oscillator strengths, we compare in Figs 1, 2 and 3 the three methods used in the calculations for the widths: SCP (W_{SC1}), SE (W_{AM}) and MSE (W_{MSE}). The three theoretical widths are also compared with the experimental ones of Bukvić et al. (2011).

Fig. 1 displays electron-impact Stark widths for the $6d\,^2D_{5/2}-7p\,^2P^o_{3/2}$ line as a function of electron temperature for a 10^{17} cm^{-3} electron density. Our SCP and MSE calculations have been obtained with energy levels and oscillator strengths from Alonso-Medina et al. (2011).

As we can see in Fig. 1, W_{SC1} are slightly higher than W_{MSE}. At low temperatures, SE widths of Alonso-Medina et al. (2010) are higher than SCP and MSE ones. At T = 200 000 K, the three methods give the same results. SE results overestimate the experimental line width, our SCP and MSE results underestimate the experimental width, but the SCP value is in the lower limit of experimental error.

Fig. 2 is the same as Fig. 1 but for the $7s\,^2S_{1/2}-7p\,^2P^o_{3/2}$ transition. At low temperatures W_{AM} is higher than W_{SC1} and W_{MSE} and at high temperatures W_{AM} is lower than our SCP and MSE results. Our SCP width is close to the experimental ones, MSE results

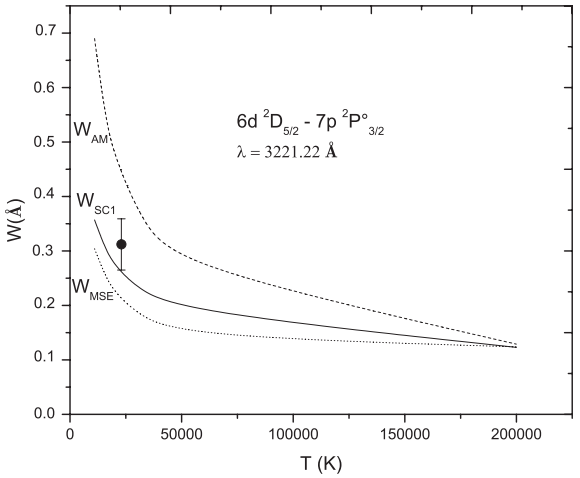

Figure 1. Electron impact Stark widths FWHM for the $6d\,^2D_{5/2}$–$7p\,^2P^o_{3/2}$ ($\lambda = 3221.22$ Å) line as a function of the electron temperature (T) at an electron density of 10^{17} cm^{-3}. Solid line: our Stark widths obtained using SCP approach (Sahal-Bréchot 1969a,b) (W_{SC1}) and oscillator strengths from Alonso-Medina et al. (2011), Dotted line: our Stark widths obtained using modified SE approach (Dimitrijević & Konjević 1980) and oscillator strengths from Alonso-Medina et al. (2011) (W_{MSE}), Dashed line: Stark widths of Alonso-Medina et al. (2010) obtained using SE formula (Griem 1968), with Gaunt factor suggested by Niemann et al. (2003) (W_{AM}), Full circle: experimental Stark width (Bukvić et al. 2011).

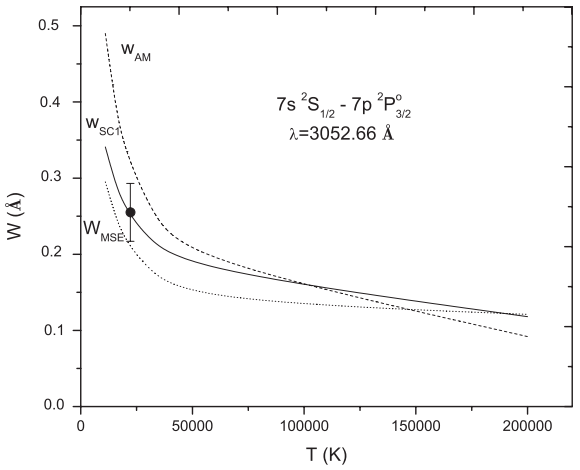

Figure 2. Same as in Fig. 1 but for the $7s\,^2S_{1/2}$–$7p\,^2P^o_{3/2}$ ($\lambda = 3052.66$ Å) transition.

underestimate the experimental width and SE results overestimate the experimental width, but the SCP value is on the lower limit of experimental error.

Fig. 3 is the same as Fig. 1 but for the $5f\,^2F^o_{7/2}$–$5g\,^2G_{9/2}$ transition. W_{AM} is in the higher limit of the experimental error. W_{SC1} and W_{MSE} underestimate the experimental value but W_{MSE} is closer. W_{SC1} is lower than the experimental width by a factor of 3. At low temperatures W_{MSE} is lower than W_{AM} but at high temperatures W_{MSE} is higher than W_{AM}. At T = 100 000 K, SE and MSE approach gives the same width.

One can see that in Figs 1 and 2, the results of three theoretical methods are in much better agreement than in Fig. 3, where there is a large difference. If we look at the partial energy level diagram in Fig. 7, one can see that the structure of perturbing levels is not regular. In particular, MSE theory assumes that the important contribution to the line width proceeds from perturbing levels with the same principal quantum number and that all other perturbing levels are lumped together. But for the $5g\,^2G_{9/2}$ level there is no $5h\,^2H^o$ perturbing term, and the energies of $5f\,^2F^o$ levels are much lower than the $6f\,^2F^o$ and $7f\,^2F^o$ ones. This introduces additional uncertainties in the MSE theoretical approach. Additional experimental results will be of interest for checking and improving theory for such a specific case which is more complicated than the previous two.

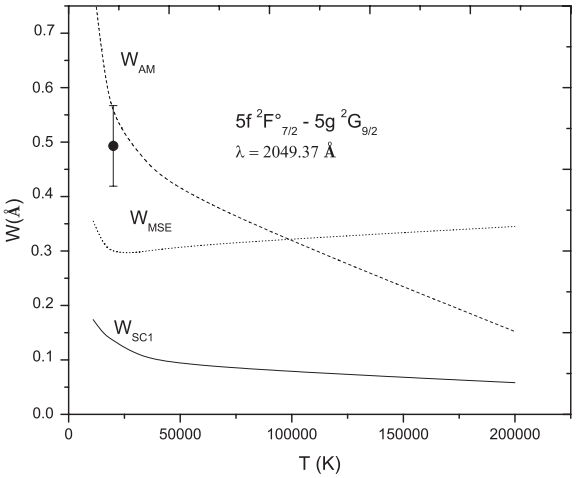

Figure 3. Same as in Fig. 1 but for the $5f\,^2F^o_{7/2}$–$5g\,^2G_{9/2}$ ($\lambda = 2049.37$ Å) transition.

By comparing our new large-scale SCP results for widths, given in Section 5, with those of Alonso-Medina et al. (2010), we see that the SE widths are not always lower than ours (as all values given in Table 1). For many transitions, there is an acceptable agreement between the two calculations. However, for a number of transitions the SE results are greater than ours even by a factor of 2.

In Alonso-Medina & Colón (2011), the overestimation of theoretical widths obtained using SE formula for Sn III lines in some cases when their values are above the existing experimental values is explained by the large number of perturbing levels used for initial and final levels for each transition. From our point of view, the set of atomic data used in the SE and SCP calculation of the width is relatively large but the number of significant perturbing levels involved in the calculation of the width is not large. Adding other perturbing levels will have a negligible effect on the final results for the line width. However, we note that the shift calculations are more sensitive to the number of perturbing levels. This is due to mutual cancellations of contributions with different signs. This is not the case for the widths, where the contributions of different perturbing levels have positive values.

Indeed, in the case of Pb IV the atomic model adopted by Alonso-Medina et al. (2010) is not so large. For example, the 8p and 9p configurations are not included in their atomic model. In fact, these configurations provide levels which significantly perturb the level $8s\,^2S_{1/2}$. For example, for the $7p\,^2P^o_{3/2}$–$8s\,^2S_{1/2}$ transition, our width at T = 20 000 K is equal to 0.374 Å. If we do not take into account the 8p and 9p configurations, the width becomes 0.220 Å.

For the $6s\,^2S$–$6p\,^2P^o$ multiplet, the widths of the fine structure components of Alonso-Medina et al. (2010) are exactly the same. The difference between our widths of the two fine structure components is 46 per cent. It must be noted that the difference between the wavelengths of the two fine structure components is 27 per cent.

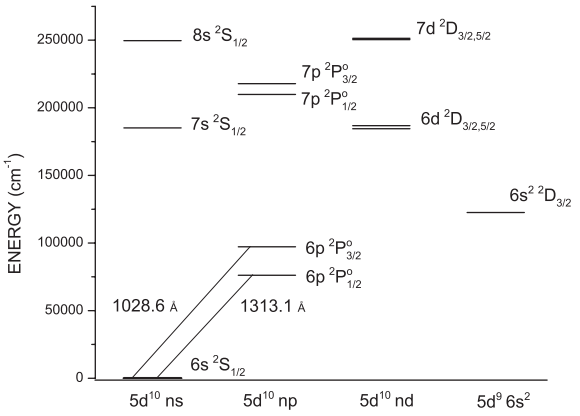

Figure 4. Partial energy level diagram showing the principal perturbing levels for 6s−6p transitions.

This large difference in the widths expressed in Å is only due to the difference in the wavelengths, since in angular frequency units the widths differ only by 6 per cent. The difference between the widths of the two components found by Alonso-Medina et al. (2010) expressed in angular frequency units is 62 per cent. Partial energy level diagram showing the principal perturbing levels for 6s ^{2}S−6p ^{2}P^o multiplet is presented in Fig. 4. This diagram shows that 6s^2 ^{2}D$_{3/2}$ is the nearest level to 6p ^{2}P$^o_{3/2}$ but its contribution is very small. In fact, the value of the oscillator strength given in Alonso-Medina et al. (2011) of the 6p ^{2}P$^o_{3/2}$−6s^2 ^{2}D$_{3/2}$ transition is only 7×10^{-5}. The distances to the perturbing levels 6d ^{2}D, 6s ^{2}S and 7s ^{2}S are much larger than the energy differences between 6p ^{2}P$^o_{3/2}$ and 6p ^{2}P$^o_{1/2}$, so that one expects that the widths of the two fine structure components are close. The large difference found by Alonso-Medina et al. (2010) cannot be explained by the existence of a perturbing level much closer to the upper level of one of the two neighbouring fine structure transitions, which should be consequently more perturbed in this case.

4 COMPARISON WITH EXPERIMENT

Recently, Bukvić et al. (2011) investigated Pb IV and Pb V spectral line shapes in the laboratory helium plasma at electron temperatures around 22 000 K and electron density between 5.1×10^{16} cm^{-3} and 9.1×10^{16} cm^{-3}. In Table 2, our results are compared to these experimental results (W_m) and also to the SE values of Alonso-Medina et al. (2010).

$W_{SC} = W_e + W_i$, where W_e is electron-impact Stark width and W_i is ionic-impact Stark width. Taking into account the experimental conditions, we have taken as ionic perturbers singly charged helium ions. For each value given in Table 2, the collision volume (V) multiplied by perturber density (N) is much less than one and the impact approximation is valid. The greatest value of $N \times V$, equal to 0.25, has been found for the 5g ^{2}G$_{9/2}$−6h ^{2}H^o transition for collisions with ions. For the study of the 5g ^{2}G$_{9/2}$−6h ^{2}H^o transition, the atomic model given in Section 2 has been enriched by the configurations 7i and 8i which give important perturbing levels for 6h ^{2}H^o. In addition, since we have found that magnetic dipole (M1) and electric quadrupole (E2) transitions have no influence on the width, only electric dipole transitions (E1) are considered in our calculations.

A number of levels in Alonso-Medina et al. (2011), used also by Bukvić et al. (2011), belonging to the configuration 5d^9 6s6p are a mixture without a leading term. They are denoted as [1^o], [2^o], ... [27^o]. For some of them, there is a correspondence with energy levels within LS coupling (Moore 1958; Alonso-Medina et al. 2011). Namely 6d^{10} 7p ^{2}P$^o_{1/2}$, 7p ^{2}P$^o_{3/2}$, 5f ^{2}F$^o_{5/2}$ and 5f ^{2}F$^o_{7/2}$ correspond to 5d^9 6s6p [16^o]$_{1/2}$, [22^o]$_{3/2}$, [23^o]$_{5/2}$ and [24^o]$_{7/2}$, respectively. In Table 2, experimental results of Bukvić et al. (2011) are included only for transitions which could be described in LS coupling, since our calculations have been performed only for such Pb IV transitions.

The lines labelled as 4a and 4b in Table 2 correspond to the superposition of two close fine structure components: 6d ^{2}D$_{3/2-}$5f ^{2}F$^o_{5/2}$ (2864.31 Å) and 6d ^{2}D$_{5/2}$−5f ^{2}F$^o_{7/2}$ (2864.55 Å). By assuming local thermodynamical equilibrium and that the lines are optically thin at the temperature $T = 2.38\ 10^4$ K and the density $Ne = 10^{17}$ cm^{-3},

Table 2. Comparison between our Stark widths (FWHM) (W_{SC}) obtained using atomic data calculated using Cowan code (Cowan 1981), experimental values (W_m) of Bukvić et al. (2011) and theoretical values of Alonso-Medina et al. (2010) (W_{AM}). Results are given for an electron density of $Ne = 10^{17}$ cm^{-3}.

Label	Transition	λ (Å)	T (10^4 K)	W_m (pm)	W_{SC} (pm)	W_{AM} (pm)
1	5f ^{2}F$^o_{7/2}$−5g ^{2}G	2049.37	2.00 ± 0.28	49.3 ± 7.4	19.0	54.2
2a	5g ^{2}G$_{9/2}$−6h ^{2}H^o	4534.46	2.33 ± 0.33	301 ± 24	260	300
2b	5g ^{2}G$_{7/2}$−6h ^{2}H^o	4534.93	2.33 ± 0.33			
3	6p ^{2}P$^o_{1/2}$−6s^2 ^{2}D$_{3/2}$	2154.01	2.20 ± 0.30	5.0 ± 1.2	4.08	
4a	6d ^{2}D$_{3/2}$−5f ^{2}F$^o_{5/2}$	2864.31	2.38 ± 0.33	49.4 ± 7.4	40.4	37.3
4b	6d ^{2}D$_{5/2}$−5f ^{2}F$^o_{7/2}$	2864.55	2.38 ± 0.33			
5	6d ^{2}D$_{5/2}$−5f ^{2}F$^o_{5/2}$	3062.43	2.22 ± 0.31	22.5 ± 4.0	21.7	
6	6d ^{2}D$_{3/2}$−7p ^{2}P$^o_{3/2}$	3002.76	2.30 ± 0.32	18.5 ± 3.8	26.6	
7	6d ^{2}D$_{5/2}$−7p ^{2}P$^o_{3/2}$	3221.22	2.30 ± 0.32	31.2 ± 4.7	31.2	43.3
8	6d ^{2}D$_{3/2}$−7p ^{2}P$^o_{1/2}$	3962.49	2.26 ± 0.32	47.0 ± 7.0	48.1	
9	7s ^{2}S$_{1/2}$−7p ^{2}P$^o_{3/2}$	3052.66	2.22 ± 0.31	25.5 ± 3.8	29.4	31.1
10	7s ^{2}S$_{1/2}$−7p ^{2}P$^o_{1/2}$	4049.84	2.38 ± 0.33	61.5 ± 9.2	51.2	
11	7p ^{2}P$^o_{1/2}$−7d ^{2}D$_{3/2}$	2461.51	2.32 ± 0.32	24.9 ± 3.7	31.0	22.0
12	7p ^{2}P$^o_{3/2}$−7d ^{2}D$_{5/2}$	2978.20	2.30 ± 0.32	36.9 ± 5.5	40.0	34.2
13	7p ^{2}P$^o_{3/2}$−7d ^{2}D$_{3/2}$	3071.33	2.26 ± 0.32	43.3 ± 6.5	46.7	
14	7p ^{2}P$^o_{3/2}$−8s ^{2}S$_{1/2}$	3145.47	2.10 ± 0.30	39.2 ± 6.0	42.8	28.4

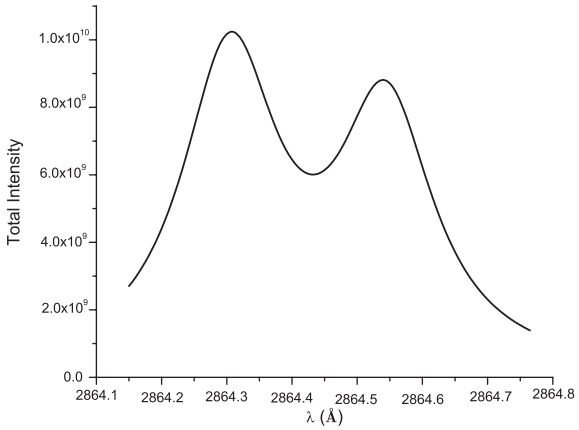

Figure 5. Superposition of $6d\,^2D_{3/2}-5f\,^2F^o_{5/2}$ (2864.31 Å) and $6d\,^2D_{5/2}-5f\,^2F^o_{7/2}$ (2864.55 Å) line profiles.

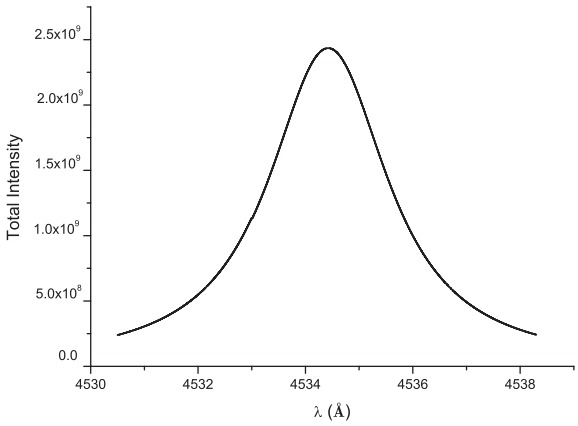

Figure 6. Superposition of $5g\,^2G_{9/2}-6h\,^2H^o$ (4534.46 Å) and $5g\,^2G_{7/2}-6h^2H^o$ (4534.93 Å) line profiles.

we have determined the global profile of this line. Under these conditions the intensities of the lines are additive and the total intensity profile $I_{\rm total}(\lambda)$ is given by the following formula:

$$I_{\rm total}(\lambda) = g_1 A_1 I_1(\lambda) + g_2 A_2 I_2(\lambda), \quad (5)$$

where g_1 (resp. g_2) is the statistical weight of the upper level of the first component of the line (resp. the second component of the line). A_1 (resp. A_2) is the transition probability of spontaneous emission of the first component of the line (resp. the second component of the line). $I_1(\lambda)$ (resp. $I_2(\lambda)$) is the normalized profile of the first component of the line (resp. the second component of the line) with a half-width w_1 and shift d_1 (resp. half-width w_2 and shift d_2). A normalized Lorentzian is given by

$$I(\lambda) = \frac{w}{\pi}\frac{1}{(\lambda-\lambda_{if}-d)^2+w^2}, \quad (6)$$

where $w = W/2$ is the half width at half-maximum and d is the shift. The resulting profile is plotted in Fig. 5. Using this profile, we have found that the full width at half intensity maximum of this global transition is 40.4 pm. The experimental width of this global transition is 49.4 ± 7.4 pm (Bukvić et al. 2011). They found that the composed profile is close to a Lorentz profile and that the width of this composite distribution is less than the width of the broader component. We have found that the composite profile is not Lorentzian (see Fig. 5) and that the width of the composite distribution is much larger than the width of a particular component.

The lines labelled as 2a and 2b in Table 2, are also a superposition of two close transitions: $5g\,^2G_{9/2}-6h^2H^o$ (4534.46 Å) and $5g\,^2G_{7/2}-6h\,^2H^o$ (4534.93 Å). We have calculated the width of the global line using the same method described above. Our calculated width is 260 pm and the measured one is 301 ± 24 pm. Global profile for this line is presented in Fig. 6.

The line labelled as 11 in Table 2, is also a superposition of two close transitions: $7p\,^2P^o{}_{1/2}-7d\,^2D_{3/2}$ and $7p\,^2P^o{}_{3/2}-7d\,^2D_{3/2}$ (2461.51 Å). We have also calculated the width of the global line using the same method described above. Our calculated width is 31.0 pm and the measured one is 24.9 ± 3.7 pm.

We have found a tolerable agrement with measured widths except for one line: $5f\,^2F^o_{7/2}-5g\,^2G$ (2049.37 Å) labelled as 1 in Table 2 for which the experimental width is 49.3 ± 7.4 pm. In Fig. 7, we show a partial energy level diagram for $5f-5g$ transitions. This diagram shows that $5f\,^2F^o_{7/2}-5g\,^2G_{7/2}$ and $5f\,^2F^o_{7/2}-5g\,^2G_{9/2}$ lines have close wavelengths and in fact these are also two superposed

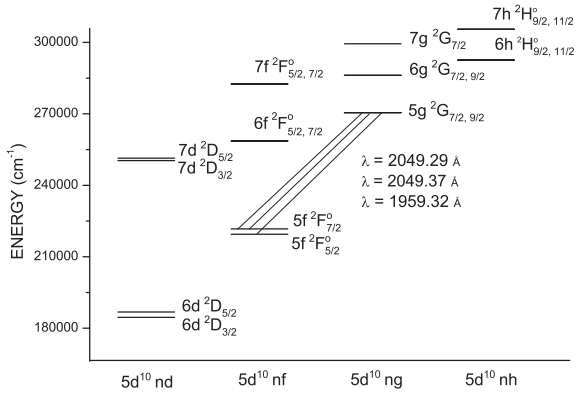

Figure 7. Partial energy level diagram showing the principal perturbing levels for 5f−5g transitions. Wavelengths 2049.37 Å and 1959.32 Å are from Crawford, McLay & Crooker (1937) and λ = 2049.29 Å has been calculated from Pb IV terms in table 1 of Crawford et al. (1937) and scaled to the two previous observed wavelengths.

lines like in the three previous cases, but Alonso-Medina et al. (2010) provided a width only for one component, so that Bukvić et al. (2011) could not calculate the composite distribution. We have also determined the global profile with the same preceding method, and our width of 19.0 pm is still lower than the experimental one by a factor greater than 2. The agreement with experiment for this line can not be improved even we use the atomic data of Alonso-Medina et al. (2011) (see Fig. 3).

5 LARGE-SCALE CALCULATIONS

5.1 SCP calculations for 114 transitions of Pb IV

Our SCP method allows us to study a large number of lines. In fact, a large number of collisional data are needed for deriving precise atmospheric parameters of hot star atmospheres as white dwarfs (Dufour et al. 2011). Accurate and large Stark-broadening tables are of crucial importance for sophisticated spectral analysis by means of non-local thermodynamic equilibrium (NLTE) model atmospheres (Rauch et al. 2007).

Thus, using our SCP code, we have calculated widths and shifts for 114 transitions of Pb IV between the $5d^{10}nl-5d^{10}n'l'$ and $5d^96s^2-5d^{10}nl$ configurations. The results are provided in electronic form in the online journal as additional data (Table S).

Table 3. This table gives electron-, proton- and singly charged helium-impact broadening parameters for Pb IV lines calculated using Cowan code (Cowan 1981) oscillator strengths, for a perturber density of 10^{17} cm^{-3} and temperature of 20 000 to 300 000 K. Calculated wavelength of the transitions (in Å) and parameter C are also given. This parameter when divided with the corresponding Stark width gives an estimate for the maximal pertuber density for which the line may be treated as isolated. W_e: electron-impact full Stark width at half-maximum, d_e: electron-impact Stark shift, W_{H^+}: proton-impact full Stark width at half-maximum, d_{H^+}: proton-impact Stark shift, W_{He^+}: singly charged helium-impact full Stark width at half-maximum, d_{He^+}: singly charged helium-impact Stark shift. This table is available in its entirety for 114 Pb IV spectral lines in machine-readable form in the online journal as additional data. A portion is shown here for guidance regarding its form and content.

Transition	T (K)	W_e (Å)	d_e (Å)	W_{H^+}(Å)	d_{H^+} (Å)	W_{He^+} (Å)	d_{He^+} (Å)
$5f\,^2F^o_{5/2}-7d\,^2D_{3/2}$	20 000	0.462	0.389E−01	0.184E−01	0.126E−01	0.223E−01	0.110E−01
3237.7 Å	30 000	0.399	0.356E−01	0.233E−01	0.160E−01	0.277E−01	0.138E−01
C = 0.50E+20	50 000	0.338	0.336E−01	0.312E−01	0.210E−01	0.320E−01	0.174E−01
	100 000	0.281	0.367E−01	0.380E−01	0.261E−01	0.374E−01	0.211E−01
	200 000	0.239	0.323E−01	0.449E−01	0.310E−01	0.428E−01	0.252E−01
	300 000	0.219	0.306E−01	0.496E−01	0.344E−01	0.455E−01	0.274E−01
$5f\,^2F^o_{5/2}-7g\,^2G_{7/2}$	20 000	0.198	−0.146E−01	*0.191E−01	*−0.117E−01	*0.192E−01	*−0.918E−02
1174.1 Å	30 000	0.178	−0.167E−01	*0.216E−01	*−0.136E−01	*0.214E−01	*−0.110E−01
C = 0.34E+19	50 000	0.161	−0.141E−01	*0.246E−01	*−0.166E−01	*0.237E−01	*−0.133E−01
	100 000	0.140	−0.131E−01	0.289E−01	−0.203E−01	*0.266E−01	*−0.162E−01
	200 000	0.123	−0.120E−01	0.329E−01	−0.231E−01	*0.289E−01	*−0.185E−01
	300 000	0.113	−0.984E−02	0.363E−01	−0.253E−01	*0.301E−01	*−0.198E−01

A sample of the results is only shown in Table 3 for guidance regarding its form and content. The calculations have been made for a perturber density of 10^{17} cm^{-3} and for a set of temperatures from 20 000 to 300 000 K. Stark widths (FWHM) and shifts are given for electron-, proton- and singly ionized helium impact broadening. Energy levels and oscillator strengths needed for this calculation have been determined using Cowan code (Cowan 1981) and the atomic model described above in the end of Section 2 (43 configurations).

All wavelengths given in Tables 3 and S are calculated wavelengths. They have been determined from energy levels obtained with the first three Cowan codes and the fourth part devoted for scaling with experimental energy levels has not been used. So the calculated wavelengths given in Table 3 are not good but the Stark-broadening parameters, which depend on relative and not absolute positions of energy levels are correct in angular frequency units. The relationship between the width expressed in Å and the width expressed in angular frequency units is given by the following formula:

$$W(\mathring{A}) = \frac{\lambda^2}{2\pi c} W(s^{-1}), \tag{7}$$

where c is the speed of light. If we want to introduce a correction to the width due to the difference between calculated and experimental wavelength, one should use the following formula:

$$W_{cor} = \left(\frac{\lambda_{exp}}{\lambda}\right)^2 W. \tag{8}$$

In the above expression, W_{cor} is the corrected width, λ_{exp} is the experimental wavelength, λ is the calculated wavelength and W is the calculated width of Tables 3 and S. A similar formula can be used for the shifts.

We also specify a parameter C (Dimitrijević & Sahal-Bréchot 1984), which gives an estimate for the maximal perturber density for which the line may be treated as isolated, when it is divided by the corresponding full width at half-maximum (FWHM). For each value given in Tables 3 and S, the collision volume V multiplied by the perturber density N is much less than one and the impact approximation is valid (Sahal-Bréchot 1969a,b). For $NV > 0.5$, the impact approximation breaks down and thus the values are not given. For $0.1 < NV \leq 0.5$, the impact approximation reaches his limit of validity and values are preceded by an asterisk. When the impact approximation is not valid, the ion broadening contribution may be estimated by using the quasi-static approach (Griem 1974; Sahal-Bréchot 1991). In the region where none approximation is valid, a unified-type theory should be used. For example, in Barnard, Cooper & Smith (1974) a simple analytical formula is given for such a case.

The difference between the widths of different fine structure components of a multiplet is small except for $5f\,^2F^o-7g\,^2G$ and $6f\,^2F^o-7g^2G$ multiplets for which the ratio of the widths of two components attains 2. This large difference is due to the fact that the upper level $7g\,^2G_{9/2}$ of the considered transition and the closest perturbing level $7h\,^2H^o_{11/2}$ have very close energies ($\Delta E = 240$ cm^{-1}). This is not the case for the $7g\,^2G_{7/2}$, where the closest perturbing level is more distant.

All the data given in the online Table S will be also inserted in the STARK-B data base (Sahal-Bréchot, Dimitrijević & Moreau 2013), which is a part of Virtual Atomic and Molecular Data Center (Dubernet et al. 2010; Rixon et al. 2011), cf. also Sahal-Bréchot (2010). This data base is devoted to diagnostics modelling and investigations of stellar atmospheres and also for fusion and laboratory plasmas. As for diagnostics of stellar plasmas, Stark-broadening parameters are used in the determination of temperature and density of laboratory plasmas. For example, in Hanif, Salik & Baig (2011), spectroscopic emission of laser produced lead plasma was studied and electron number density was determined from Stark-broadened lines.

5.2 Systematic trends: behaviour with the principal quantum number n along the $6s\,^2S_{1/2}-np\,^2P^o_{1/2}$ series

In Fig. 8, electron-impact widths (in angular frequency units) for the series $6s^2S_{1/2}-np^2P^o_{1/2}$ of Pb IV are shown as a function of the principal quantum number of the upper state n, for T = 50 000 K and $Ne = 10^{17}$ cm^{-3}. We can see a gradual increase of Stark width within the considered spectral series. Such regular behaviour of Stark width is the consequence of the gradual change of the energy separation between the initial (upper) level and the principal perturbing levels. As

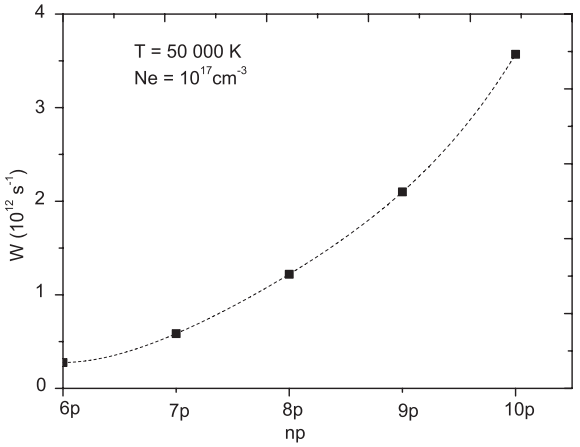

Figure 8. Electron-impact widths (in angular frequency units) for the series $6s\,^2S_{1/2}-np\,^2P^o_{1/2}$ of Pb IV as a function of the principal quantum number of the upper state. Dashed line: least square polynomial fitting (fourth order). The correlation factor $R^2 = 1$.

expected from the Coulomb (hydrogenic) behaviour of the dipolar line strengths, the widths increase as n^4 (Sahal-Bréchot, Dimitrijević & Ben Nessib 2011). The function $W(n)$ has been fitted using the fourth power polynomial:

$$W(n) = an^4 + bn^3 + cn^2 + dn + f, \quad (9)$$

where $W(n)$ is the FWHM expressed in rad s^{-1} per electron and constants are $a = 1.77 \times 10^{10}$, $b = -5.46 \times 10^{11}$, $c = 6.39 \times 10^{12}$, $d = -3.30 \times 10^{13}$ and $f = 6.35 \times 10^{13}$. The correlation factor R^2 is equal to 1.

In Fig. 8, the polynomial function is displayed by a dashed line. Such fitting can be of interest for high n transitions for which atomic data are often insufficient, provided that the line is still isolated.

6 CONCLUSIONS

Our results show an acceptable agreement with the recent experimental results except for one transition. Our atomic model include a large number of configurations. The atomic data used in Alonso-Medina et al. (2010) are obtained after including least square fitting of experimental energy levels and core polarization effect. Our result for the transition for which the disagreement with the experimental width is large has not improved even when we used the atomic data of Alonso-Medina et al. (2011). In conclusion, this work gives an idea of the role of the quality of oscillator strengths for the Stark-broadening calculations. This work also suggests that the disagreement between the results of Alonso-Medina et al. (2010) and those of Dimitrijević & Sahal-Bréchot (1999) is due to the choice of the method of calculation of the Stark width and not due to the choice of the set of atomic data used in the calculation. Finally, we have performed an SCP calculation of Stark-broadening parameters for 114 transitions in Pb IV. Energy levels and oscillator strengths were carried out using Cowan code (Cowan 1981). Stark-broadening parameters are determined for transitions of the type $5d^{10}nl-5d^{10}n'l'$ and $5d^96s^2-5d^{10}nl$.

ACKNOWLEDGEMENTS

This work has been supported by the research unit 05/UR/12-04 and by the bilateral cooperation agreement between the French CNRS and the Tunisian DGRS (project code 09/R 13-03, project No. 22637). This work is also a part of the project 176002 'Influence of collisional processes on astrophysical plasma line shapes' supported by the Ministry of Education, Science and Technological Development of Serbia.

REFERENCES

Alonso-Medina A., Colón C., 2011, MNRAS, 414, 713
Alonso-Medina A., Colón C., Montero J. L., Nation L., 2010, MNRAS, 401, 1080
Alonso-Medina A., Colón C., Porcher P., 2011, At. Data Nucl. Data Tables, 97, 36
Barnard A. J., Cooper J., Smith E. W., 1974, J. Quant. Spectrosc. Radiat. Transfer, 14, 1025
Bates D. R., Damgaard A., 1949, Philos. Trans. R. Soc. Lond. A, 242, 101
Ben Nessib N., Dimitrijević M. S., Sahal-Bréchot S., 2004, A&A, 423, 397
Bukvić S., Djeniže S., Nikolić Z., Srećković A., 2011, A&A, 529, A83
Chou H.-S., Johnson W. R., 1997, Phys. Rev. A, 56, 2424
Cowan R. D., 1981, The Theory of Atomic Structure and Spectra, University of California Press, Berkeley, USA
Crawford M. F., McLay A. B., Crooker A. M., 1937, Proc. R. Soc. Lond. A, 158, 455
Dimitrijević M. S., Konjević N., 1980, J. Quant. Spectrosc. Radiat. Transfer, 24, 451
Dimitrijević M. S., Sahal-Bréchot S., 1984, J. Quant. Spectrosc. Radiat. Transfer, 31, 301
Dimitrijević M. S., Sahal-Bréchot S., 1996, Phys. Scr., 54, 50
Dimitrijević M. S., Sahal-Bréchot S., 1999, J. Appl. Spectrosc., 66, 868
Dimitrijević M. S., Sahal-Bréchot S., Bommier V., 1991, A&AS, 89, 581
Dimitrijević M. S., Kovačević A., Simić Z., Sahal-Bréchot S., 2011, Balt. Astron., 20, 580
Dubernet M. L. et al., 2010, J. Quant. Spectrosc. Radiat. Transfer, 111, 2151, http://www.vamdc.eu
Dufour P., Ben Nessib N., Sahal-Bréchot S., Dimitrijević M. S., 2011, Balt. Astron., 20, 511
Eissner W., Jones M., Nussbaumer H., 1974, Comput. Phys. Commun., 8, 270
Fleurier C., Sahal-Bréchot S., Chapelle J., 1977, J. Quant. Spectrosc. Radiat. Transfer, 17, 595
Griem H. R., 1968, Phys. Rev., 165, 258
Griem H. R., 1974, Spectral line Broadening by Plasmas. McGraw-Hill, New York
Gutmann F., Crooker A. M., 1973, Can. J. Phys., 51, 1823
Hamdi R., Ben Nessib N., Dimitrijević M. S., Sahal-Bréchot S., 2007, ApJS, 170, 243
Hamdi R., Ben Nessib N., Milovanović N., Popović L. Č., Dimitrijević M. S., Sahal-Bréchot S., 2008, MNRAS, 387, 871
Hanif M., Salik M., Baig M. A., 2011, Plasma Sci. Technol., 13, 129
Larbi-Terzi N., Sahal-Bréchot S., Ben Nessib N., Dimitrijević M. S., 2012, MNRAS, 423, 766
Mahmoudi W. F., Ben Nessib N., Dimitrijević M. S., 2005, A&A, 434, 773
Moore C. E., 1958, Atomic Energy Levels, NBS Circ. 467, Vol. III, Washington, DC, p. 213
Niemann C. et al., 2003, J. Phys. D: Appl. Phys., 36, 2102
O'Toole S. J., 2004, A&A, 423, L25
Popović L. Č., Simić S., Milovanović N., Dimitrijević M. S., 2001, ApJS, 135, 109
Proffitt C. R., Sansonetti C. J., Reader J., 2001, ApJ, 557, 320
Rauch T., Ziegler M., Werner K., Kruk J. W., Oliveira C. M., Vande Putte D., Mignani R. P., Kerber F., 2007, A&A, 470, 317
Rixon G. et al., 2011, in Bernotas A., Karazija R., Rudzikas Z., eds, AIP Conf. Ser. Vol. 1344, 7th International Conference on Atomic and Molecular Data and their Applications – ICAMDATA-2010. Am. Inst. Phys., New York, p. 107
Safronova U. I., Johnson W. R., 2004, Phys. Rev. A, 69, 052511
Sahal-Bréchot S., 1969a, A&A, 1, 91

Sahal-Bréchot S., 1969b, A&A, 2, 322
Sahal-Bréchot S., 1974, A&A, 35, 319
Sahal-Bréchot S., 1991, A&A, 245, 322
Sahal-Bréchot S., 2010, J. Phys. Conf. Ser., 257, 012028
Sahal-Bréchot S., Dimitrijević M. S., Ben Nessib N., 2011, Balt. Astron., 20, 523
Sahal-Bréchot S., Dimitrijević M. S., Moreau N., 2013, Stark-B data base, Available at: http://stark-b.obspm.fr . Observatory of Paris, LERMA and Astronomical Observatory of Belgrade
Simić Z., Dimitrijević M. S., Kovačević A., 2009, New Astron. Rev., 53, 246
Shore B. W., Menzel D., 1965, ApJS, 12, 187
Van Regemorter H., 1962, ApJ, 136, 906
Vennes S., Chayer P., Dupuis J., 2005, ApJ, 622, L121

SUPPORTING INFORMATION

Additional Supporting Information may be found in the online version of this article:

Table 3. (http://mnras.oxfordjournals.org/lookup/suppl/doi:10.1093/mnras/stt228/-/DC1).

Please note: Oxford University Press are not responsible for the content or functionality of any supporting materials supplied by the authors. Any queries (other than missing material) should be directed to the corresponding author for the article.

This paper has been typeset from a TEX/LATEX file prepared by the author.

Monthly Notices
of the
ROYAL ASTRONOMICAL SOCIETY

MNRAS **431,** 2960 (2013) doi:10.1093/mnras/stt391
Advance Access publication 2013 March 21

Erratum: Stark-broadening calculations of singly ionized carbon spectral lines

by N. Larbi-Terzi,[1⋆] S. Sahal-Bréchot,[2⋆] N. Ben Nessib[1] and M. S. Dimitrijević[2,3,4]

[1]*Groupe de Recherche en Physique Atomique et Astrophysique, Institut National des Sciences Appliquées et de Technologie, University of Carthage, Centre Urbain Nord BP No. 676, 1080 Tunis Cedex, Tunisia*
[2]*Laboratoire d'Étude du Rayonnement et de la Matière en Astrophysique, Observatoire de Paris, UMR CNRS 8112, UPMC, Bâtiment Evry Schatzman, 5 Place Jules Janssen, F-92195 Meudon Cedex, France*
[3]*Astronomical Observatory, Volgina 7, 11060 Belgrade 38, Serbia*
[4]*Isaac Newton Institute of Chile, Yugoslavia Branch, Volgina 7, 11060 Belgrade, Serbia*

Key words: errata, addenda – atomic data – atomic processes – line: profiles – white dwarfs.

The paper 'Stark-broadening calculations of singly ionized carbon spectral lines' was published in MNRAS, 423, 766 (2012). Due to one unfortunate typing error in one input atomic data necessary for the C II calculations that enters the computer code, some output data in the online tables (S1, S2, S3) are erroneous within a few per cent, and some others are unchanged. This is not the case in tables 1–6 of the paper where there is no error. In addition, there were some typing errors in F and G terms and the parity indicated in the transitions was inadvertently inverted in the online tables, but this has no effect on the numerical results. The new online joined tables are corrected.

SUPPORTING INFORMATION

Additional Supporting Information may be found in the online version of this article:

Tables S1, S2 and S3 (http://mnras.oxfordjournals.org/lookup/suppl/doi:10.1093/mnras/stt391/-/DC1)

Please note: Oxford University Press is not responsible for the content or functionality of any supporting materials supplied by the authors. Any queries (other than missing material) should be directed to the corresponding author for the article.

⋆E-mail: Larbi.terzi.Neila@gnet.tn (NL); sylvie.sahal-brechot@obspm.fr (SS)

This paper has been typeset from a TEX/LATEX file prepared by the author.

Monthly Notices
of the
ROYAL ASTRONOMICAL SOCIETY

MNRAS **431,** 589–599 (2013)
Advance Access publication 2013 February 23

doi:10.1093/mnras/stt187

The non-symmetric ion–atom radiative processes in the stellar atmospheres

A. A. Mihajlov,[1,2] Lj. M. Ignjatović,[1,2] V. A. Srećković,[1,2]★ M. S. Dimitrijević[2,3] and A. Metropoulos[4]

[1]*Institute of Physics, University of Belgrade, PO Box 57, 11001 Belgrade, Serbia*
[2]*Isaac Newton Institute of Chile, Yugoslavia Branch Volgina 7, 11060 Belgrade, Serbia*
[3]*Astronomical Observatory, Volgina 7, 11160 Belgrade 74, Serbia*
[4]*Theoretical and Physical Chemistry Institute, NHRF, 15771 Athens, Greece*

Accepted 2013 January 30. Received 2013 January 30; in original form 2012 November 15

ABSTRACT

The aim of this research is to show that the processes of absorption charge exchange and photoassociation in $A + B^+$ collisions together with the processes of AB^+ photodissociation in the case of strongly non-symmetric ion–atom systems, significantly influence the opacity of stellar atmospheres in ultraviolet (UV) and extreme UV (EUV) region. In this work, the significance of such processes for solar atmosphere is studied. In the case of the solar atmosphere the absorption processes with $A = \mathrm{H}$ and $B = \mathrm{Mg}$ and Si are treated as dominant ones, but the cases $A = \mathrm{H}$ and $B = \mathrm{Al}$ and $A = \mathrm{He}$ and $B = \mathrm{H}$ are also taken into consideration. The choice of just these species is caused by the fact that, of the species relevant for the used solar atmosphere model, it was only for them that we could determine the necessary characteristics of the corresponding molecular ions, i.e. the molecular potential curves and dipole matrix elements. It is shown that the efficiency of the examined non-symmetric processes within the rather wide corresponding quasi-molecular absorption bands in the far-UV and EUV regions is comparable and sometimes even greater than the intensity of the known symmetric ion–atom absorption processes, which are included now in the models of the solar atmosphere. Consequently, the presented results suggest that the non-symmetric ion–atom absorption processes also have to be included *ab initio* in the corresponding models of the stellar atmospheres.

Key words: atomic processes – molecular processes – radiation mechanisms: general – radiative transfer – stars: atmospheres.

1 INTRODUCTION

Significant influence of at least some of the ion–atom radiative processes on the optical characteristics of the solar atmosphere has already been established. Here we mean the following symmetric processes of molecular ion photodissociation/association and radiative charge exchange in ion–atom collisions:

$$\varepsilon_\lambda + \mathrm{H}_2^+ \longleftrightarrow \mathrm{H} + \mathrm{H}^+, \quad (1)$$

$$\varepsilon_\lambda + \mathrm{H}^+ + \mathrm{H} \longleftrightarrow \mathrm{H} + \mathrm{H}^+, \quad (2)$$

which were studied in the context of the atmosphere of the Sun in Mihajlov & Dimitrijević (1986), Mihajlov, Dimitrijević & Ignjatović (1993) and Mihajlov et al. (1994, 2007). Let us note that here $\mathrm{H} = \mathrm{H}(1s)$, H_2^+ is the molecular ion in the ground electronic state, and ε_λ the energy of a photon with wavelength λ. Of course, the results obtained in the mentioned papers are significant and for atmospheres of other solar- or near-solar-type stars.

Only the processes (1) and (2) were taken into account in the mentioned papers, since the contribution of other symmetric ion–atom radiative processes to the solar atmosphere opacity could be completely neglected due to the composition of the atmosphere, while the possible non-symmetric processes were excluded from the consideration because of the orientation of the research, already established in the first paper (Mihajlov & Dimitrijević 1986), towards the visible and near-ultraviolet (UV) and infrared (IR) parts of the electromagnetic (EM) spectrum. However, in Mihajlov et al. (2007) it was demonstrated that the efficiency of the processes (1) and (2) becomes close to the total efficiency of the concurrent electron–ion and electron–atom radiative processes outside of these parts of the EM spectrum, namely in far-UV and extreme UV (EUV) regions.

★ E-mail: vlada@ipb.ac.rs

It is important that just these spectral regions are very significant in the case of the solar atmosphere. This is caused by the fact that the solar emission in far-UV and EUV regions very strongly affects the ionosphere every day, and by extension the whole of the Earth's atmosphere. Therefore the solar EM emission in the mentioned regions has been the object of extensive investigation for a long time (see the classic book: White 1977), which continues up until now (see e.g. Worden, Woods & Bowman 2001; Woods 2008; Woods et al. 2009). It is clear that in this context it becomes necessary to pay attention not only to the symmetrical ion–atom processes (1) and (2), but also to each new process which might affect the mechanisms of EM radiation transfer in far-UV and EUV regions in the solar atmosphere, and consequently the corresponding optical characteristics. These facts suggested that it could be useful to carefully examine also the possible influence of the relevant non-symmetric ion–atom radiative processes on the solar atmosphere opacity, namely

$$\varepsilon_\lambda + AB^+ \longrightarrow A^+ + B, \tag{3}$$

$$\varepsilon_\lambda + A + B^+ \longrightarrow A^+ + B, \tag{4}$$

$$\varepsilon_\lambda + A + B^+ \longrightarrow (AB^+)^*, \tag{5}$$

where B is an atom in the ground state with its ionization potential I_B smaller than the ionization potential I_A of the atom A, while AB^+ and $(AB^+)^*$ are the corresponding molecular ions in the electronic states which are asymptotically correlated with the states of the systems $A + B^+$ and $A^+ + B$, respectively, and the possible partners are determined by the used solar atmosphere models. One can see that the processes (3) and (4) represent the analogues of the processes (1) and (2), while the process (5) does not have a symmetric analogue. In this work the standard non-local thermodynamic equilibrium (LTE) model C for the solar atmosphere from Vernazza, Avrett & Loser (1981) is used. The reason is the fact that as yet all the relevant data needed for our calculations are provided in the tabular form only for this model, and that in Stix (2002) the solar atmosphere model C from Vernazza et al. (1981) is treated as an adequate non-LTE model. In accordance to the chosen model here we take into account the non-symmetric processes (3)–(5) with $A =$ H(1s) and $B =$ Mg, Si, Fe and Al, as well as with $A =$ He($1s^2$) and $B =$ H(1s). For the solar photosphere the behaviour of the densities of the metal Mg^+, Si^+, Fe^+ and Al^+ ions is particularly important. Namely, in accordance with the tables 12, 17 and 19–22 from Vernazza et al. (1981) this behaviour, as well as the behaviour of the temperature T and the ion H^+ density, within the solar photosphere can be illustrated by the Fig. 1, where h is the height of the considered layer with the respect to the chosen referent one. The region of h is chosen here in accordance with the fig. 4 from the previous paper Mihajlov et al. (2007), where the relative efficiencies of the symmetric ion–atom processes (1) and (2) with the respect to the relevant concurrent (electron–atom and electron–ion) radiative processes are presented. This region is slitted in three parts: two denoted with I, which corresponds to the areas where the efficiency of the processes (1) and (2) with $A =$ H is close to the one of the mentioned concurrent processes, and one denoted with II, where their efficiencies can be neglected. From Fig. 1 one can see that in part I the ion H^+ density dominates with the respect to all metal ion B^+ densities, which means that within these parts it is expected that the efficiency of the symmetric processes (1) and (2) is more greater than the one of the non-symmetric processes (3)–(5). However, from the same figure one can see also that

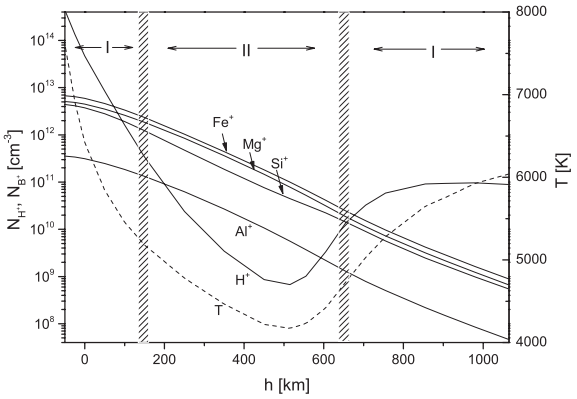

Figure 1. The behaviour of the temperature T and the densities N_{H^+} and N_{B^+} of the ions H^+ and the metal ions B^+ for the non-LTE model C from Vernazza et al. (1981) within the solar atmosphere.

– in the part II, i.e. in the neighbourhood of the temperature minimum, each of the ion B^+ densities is greater than the ion H^+ density;

– the width of the part II is close to the total width of the parts denoted with I.

From here it follows that, in the principle, the contribution of the non-symmetric processes (3)–(5) to the solar atmosphere opacity can be comparable to the one of the symmetric processes (1) and (2), since in the both non-symmetric and symmetric cases as the neutral partner the same atom H appears, and that symmetric and non-symmetric ion–atom radiative processes together could be treated as a serious partner to the above-mentioned concurrent processes in the whole solar photosphere.

In the general case of the partially ionized gaseous plasmas, apart of the absorption processes (3)–(5), it is necessary to consider also the corresponding inverse emission processes, namely the emission charge exchange and photoassociation in $A^+ + B$ collisions, and the photodissociation of the molecular ion $(AB^+)^*$. However, here only the absorption processes (3) and (4) have to be taken into account. Namely, under the conditions from Vernazza et al. (1981) the influence of the emission processes in $A^+ + B$ collisions on the optical characteristics of the considered atmospheres can be neglected in comparison to the other relevant emission processes, since both A^+ and B partners belong to the poorly represented components.

From the beginning of our investigations of ion–atom radiative processes as the final aim we have always the inclusion of the considered processes in the stellar atmospheres models. Here it should be noted that we considered as our task only to provide the relevant data (the corresponding spectral absorption coefficients etc.), which are needed for the stellar atmospheres modelling, without involving into the process of the modelling itself. Consequently, for us it was important only to know whether the processes, which we studied in connection with the considered stellar atmosphere, are included in the corresponding models or not. So during the previous investigations, whose results were published in Mihajlov & Dimitrijević (1986) and Mihajlov et al. (1993, 1994, 2007), we reliably knew that, for example, the processes of the radiative charge exchange (2) generally were not taken into account in connection with the solar atmosphere. Apart of that, it was known that the photodissociation processes (1) were seriously treated only when the atom and ion (H and H^+) densities are close, while our results suggested that the processes (1) and (2) are of the greatest importance for the weakly

ionized stellar layers (ion density/atom density $\lesssim 10^{-3}$). These reasons fully justified the mentioned investigations. It is important that the situation about the symmetric processes (1) and (2) begins to change now in the positive way, since these processes are already included in some solar atmosphere models (Fontenla et al. 2009).

The main aim of this work is to draw attention to the non-symmetric radiative processes (3)–(5) as the factors of the influence on the solar atmosphere opacity in the significant parts of UV and EUV regions and, in accordance with above mentioned, to show that these processes should be included *ab initio* in the solar atmosphere models, as well as in the models of solar- and near-solar-type stars, together with the symmetric processes (1) and (2). In this context we will have to determine here the corresponding spectral absorption coefficients, as the functions of λ, the local temperature T and the relevant particle densities, for the conditions which correspond to the photosphere of the Sun. For that purpose the needed characteristics of the considered ion–atom systems, i.e. the molecular potential curves and dipole matrix elements, are presented in Section 2. Then, the relevant characteristics of these processes themselves, i.e. the mean thermal cross-sections for the photodissociation processes (3), and the spectral rate coefficients for the absorption charge exchange processes (4) and (5), will be presented in Section 3. With the help of these characteristics in Section 4 will be calculated the total spectral absorption coefficients, characterizing (3), (4) and (5) absorption processes as the functions of λ and the position within the solar photosphere. Finally, the values of the parameters which characterize the relative contribution of the non-symmetric processes (3)–(5) with the respect to the total contribution of the symmetric and non-symmetric radiative processes (1)–(5), which are also calculated in Section 4, present the one of the main results of this work. Because of the properties of the considered strongly non-symmetric ion–atom systems only the far-UV and EUV regions of λ are treated here. Let us note that we were able to determine the relevant characteristics of the molecular ions HB^+ for the cases $B =$ Mg, Si and Al, and consequently only these cases are considered within this work.

2 THE PROPERTIES OF THE NON-SYMMETRIC ION–ATOM SYSTEMS

As in the previous papers the ion–atom radiative processes are described here within two basic approximations: the adiabatic approximation for the relative motion of the nucleus of the considered ion–atom systems, and the dipole approximation for the interaction of these systems with the free EM field. Since these approximations are discussed in details in the literature (see e.g. Mihajlov & Popović 1981), the corresponding matter is considered here briefly, with references only to the elements specific just for the non-symmetric processes (3)–(5), which are schematically shown in Fig. 2.

In accordance with Fig. 2 the photodissociation (bound–free) processes (3), charge exchange absorption (free–free) processes (4) and photoassociation (free–bound) processes (5) are caused by the radiative transitions:

$$\begin{aligned}
&|\text{in}; R\rangle|\text{in}, J, v; R\rangle \rightarrow |\text{fin}; R\rangle|\text{fin}, J', E'; R\rangle,\\
&|\text{in}; R\rangle|\text{in}, J, E; R\rangle \rightarrow |\text{fin}; R\rangle|\text{fin}, J', E'; R\rangle,\\
&|\text{in}; R > |\text{in}, J, E; R\rangle \rightarrow |\text{fin}; R\rangle|\text{fin}, J', v'; R\rangle,
\end{aligned} \tag{6}$$

where $|\text{in}; R\rangle\,|\text{in}, J, v; R\rangle$ and $|\text{in}; R\rangle\,|in, J, E; R\rangle$ are initial, and $|\text{fin}; R\rangle\,|\text{fin}, J', E'; R\rangle$, $|\text{fin}; R\rangle\,|\text{fin}, J', E'; R\rangle$ and $|\text{fin}; R\rangle\,|\text{fin}, J', v'; R\rangle$ are final states of considered ion–atom system, determined as the products of the adiabatic electronic states $|\text{in}; R\rangle$ and $|\text{fin}; R\rangle$ and the corresponding states which describe relative nucleus motion, and R denotes the internuclear distance. It is assumed that these transitions are allowed by the dipole selective rules.

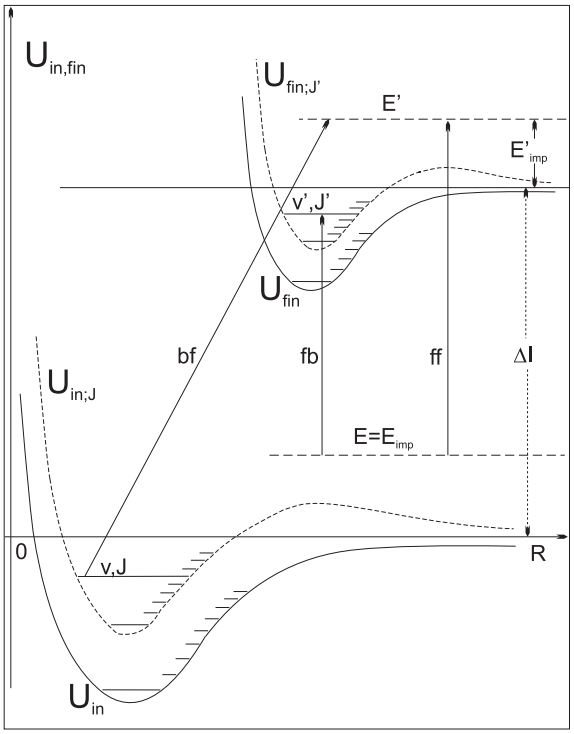

Figure 2. Schematic presentation of the non-symmetric processes (3)–(5) caused by the bf-, ff- and fb-radiative transitions: $\Delta I = I_A - I_B$, where I_A and I_B are ionization potentials of the atoms A and B; $E = E_{\text{imp}}$ and E'_{impa} are the impact energies of the corresponding ion–atom systems; $U_{\text{in};J}(R)$ and $U_{\text{fin};J'}(R)$ are the effective potentials, given by equation (12).

From Fig. 2 one can see that

– $|\text{in}; R\rangle$ and $|\text{fin}; R\rangle$ belongs to the groups (i) and (ii) of the states of the molecular ions AB^+ and $(AB^+)^*$ which are asymptotically correlated with the electronic states of the ion–atom systems $A + B^+$ and $A^+ + B$, respectively;

– $|\text{in}, J, v; R\rangle$ and $|\text{fin}, J', v'; R\rangle$ are the bound rovibrational states of the same molecular ion, defined by the orbital quantum numbers J and J' and vibrational quantum numbers v and v';

– $|\text{in}, J, E; R\rangle$ and $|\text{fin}, J', E'; R\rangle$ are the free states of the same molecular ion defined by the orbital quantum numbers J and J' and the total energies E and E'. Let us note that as zero of energy here is taken the total energy of the immobile atom A and ion B^+ at $R = \infty$.

The states $|\text{in}, J, v; R\rangle$, $|\text{in}, J, E; R\rangle$, $|\text{fin}, J', E'; R\rangle$ and $|\text{fin}, J', v'; R\rangle$ are determined as the solutions of the corresponding Schrodinger equations:

$$\left[-\frac{1}{2\mu}\Delta + U_{\text{in};J}(R)\right]|\text{in}, J, v; R\rangle = \epsilon_{J,v}\,|\text{in}, J, v; R\rangle, \tag{7}$$

$$\left[-\frac{1}{2\mu}\Delta + U_{\text{in};J}(R)\right]|\text{in}, J, E; R\rangle = E\,|\text{in}, J, E; R\rangle, \tag{8}$$

$$\left[-\frac{1}{2\mu}\Delta + U_{\text{fin};J'}(R)\right]|\text{fin}, J', E'; R\rangle = E'_{\text{imp}}\,|\text{fin}, J', E'; R\rangle, \tag{9}$$

$$\left[-\frac{1}{2\mu}\Delta + U_{\mathrm{fin};J'}(R)\right] |\mathrm{fin},\, J',\, E';\, R\rangle = \epsilon'_{J',v'}\, |\mathrm{fin},\, J',\, E';\, R\rangle, \quad (10)$$

where μ is the reduced mass of the considered ion–atom system,

$$E'_{\mathrm{imp}} = E' - (I_A - I_B) \quad (11)$$

and $\epsilon'_{J',v'} < 0$. With $U_{\mathrm{in};J}(R)$ and $U_{\mathrm{fin};J'}(R)$ are defined the effective potential energies given by

$$U_{\mathrm{in};J}(R) = U_{\mathrm{in}}(R) + \frac{\hbar^2 J(J+1)}{2\mu R^2},$$

$$U_{\mathrm{fin};J'}(R) = U_{\mathrm{fin}}(R) + \frac{\hbar^2 J'(J'+1)}{2\mu R^2}, \quad (12)$$

where $U_{\mathrm{in}}(R)$ and $U_{\mathrm{fin}}(R)$ are the adiabatic potential energies of the molecular ions AB^+ and $(AB^+)^*$ in the states $|\mathrm{in};\, R\,\rangle$ and $|\mathrm{fin};\, R\,\rangle$ as the functions of R. In further consideration it is assumed that the radial wave functions which correspond to the considered states satisfy the standard ortho-normalization conditions.

In the case A = He and B = H, as well as in the cases A = H and B = Mg or Al, each of the groups (i) and (ii) of the electronic molecular states contains only one Σ-state: the ground and the first excited electronic state of the considered molecular ion. Because of that in these cases we will denote the states $|\mathrm{in};\, R\,\rangle$ and $|\mathrm{fin};\, R\,\rangle$ with $|1;\, R\,\rangle$ and $|2;\, R\,\rangle$, respectively, and the corresponding potential curves – with $U_1(R)$ and $U_2(R)$. Let $D_{\mathrm{in;fin}}(R)$ be the electronic dipole matrix element which corresponds to the transitions given in equations (6), i.e.

$$D_{\mathrm{in;fin}}(R) = \langle \mathrm{in};\, R|\boldsymbol{D}(R)|\mathrm{fin};\, R\rangle, \quad (13)$$

where $\boldsymbol{D}$ is the operator of the dipole moment of the considered ion–atom system. One can see that in the mentioned cases,

$$D_{\mathrm{in;fin}}(R) = D_{1;2}(R) \equiv \langle 1;\, R|\boldsymbol{D}(R)|2;\, R\rangle. \quad (14)$$

However, in the case A = H and B = Si, the group (i) contains the ground electronic Σ-state and the excited, weekly bounded Π-state, denoted here with $|1a;\, R\,\rangle$ and $|1b;\, R\,\rangle$, respectively, while the group (ii) contains two Σ-states and one Π-state, denoted here with $|2a;\, R\,\rangle$, $|2b;\, R\,\rangle$ and $|2c;\, R\,\rangle$, respectively. In accordance with this, the corresponding potential curves will be denoted by $U_{1a,\,1b}(R)$ and $U_{2a,\,2b,\,2c}(R)$. One can see that, in this case we have the situations when $|\mathrm{in},\, R\,\rangle = |1a;\, R\,\rangle$ and $|\mathrm{fin},\, R\,\rangle = |2a;\, R\,\rangle$ or $|2b;\, R\,\rangle$, and $|\mathrm{in},\, R\,\rangle = |1b;\, R\,\rangle$ and $|\mathrm{fin},\, R\,\rangle = |2c;\, R\,\rangle$. Consequently, the corresponding $D_{\mathrm{in;\,fin}}(R)$ will be defined here by the relations

$$D_{\mathrm{in;fin}}(R) = \begin{cases} D_{1a;2a}(R) \equiv \langle 1a;\, R|\boldsymbol{D}(R)|2a;\, R\rangle, \\ D_{1a;2b}(R) \equiv \langle 1a;\, R|\boldsymbol{D}(R)|2b;\, R\rangle, \\ D_{1b;2c}(R) \equiv \langle 1b;\, R|\boldsymbol{D}(R)|2c;\, R\rangle. \end{cases} \quad (15)$$

For the ions HeH^+ and $(HeH^+)^*$ the potential curves $U_{1,\,2}(R)$ and the values of $D_{1;\,2}(R)$ are taken from Green et al. (1974a,b). For all other considered molecular ions the corresponding potential curves and the values of the dipole matrix elements are calculated within this work. Also, we will introduce the so-called splitting term $U_{\mathrm{in;fin}}(R)$, defined by

$$U_{\mathrm{in;fin}}(R) = U_{\mathrm{fin}}(R) - U_{\mathrm{in}}(R), \quad (16)$$

which is used in the further considerations.

All calculations were done at the multiconfiguration self-consistent field (MCSCF) and multireference configuration interaction (MRCI) levels (with MCSCF orbitals) using the MOLPRO package of programs (Werner & Knowles 2006). The basis sets we employed were the cc-pvqz basis sets of Dunning et al. (Dunning 1989; Kendall, Dunning & Harrison 1992). Initially, test runs were done in the asymptotic region (30 Bohr) at the lowest three to five levels at each selected symmetry to determine the low lying levels corresponding to the H-B^+ and the H^+-B electron distributions and their wave functions (B = Mg, Si, Al). For each level a Mulliken population analysis was done to determine the location of the charges. Since H has the highest ionization potential, the lowest states of a given symmetry correspond to the H-B^+ charge distribution while the H^+-B charge distribution is described by one or more of the excited states. The potential energies of all these states were calculated starting at the asymptotic region and moving inwards. At each point the dipole matrix elements between the H-B^+ and H^+-B states were calculated using the corresponding wave functions. The calculated potential curves are presented in Figs 3–5. Figs 6–8 show the behaviour of $D_{1;\,2}(R)$, $D_{1a;\,2a;\,b}(R)$ and $D_{1b;\,2c}(R)$.

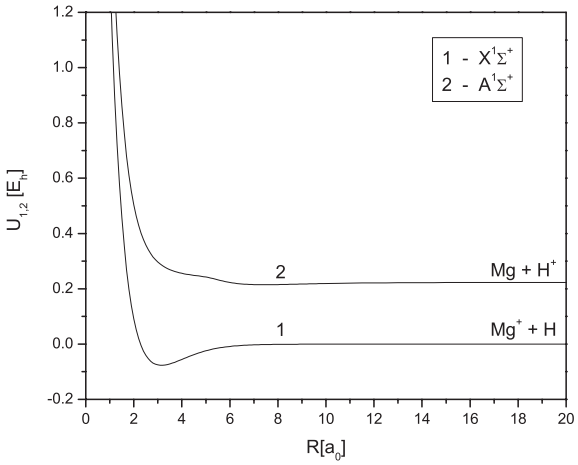

Figure 3. The potential curves of the molecular ion HMg^+.

3 THE RELEVANT SPECTRAL CHARACTERISTICS

In accordance with the aim of this work the considered absorption processes will be characterized by the adequately defined spectral

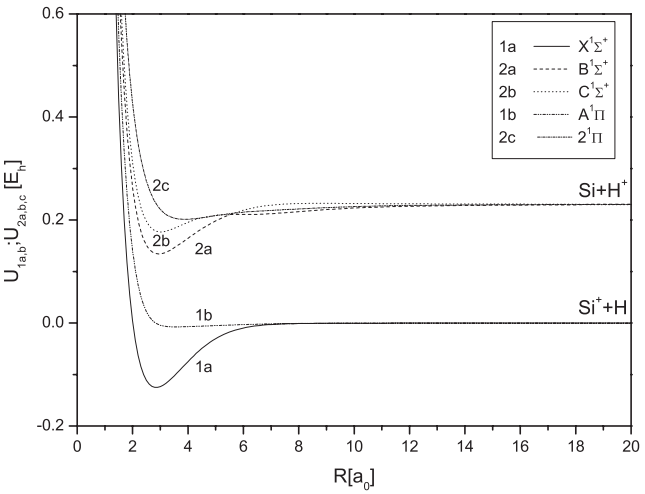

Figure 4. Same as in Fig. 3, but for the molecular ion HSi^+.

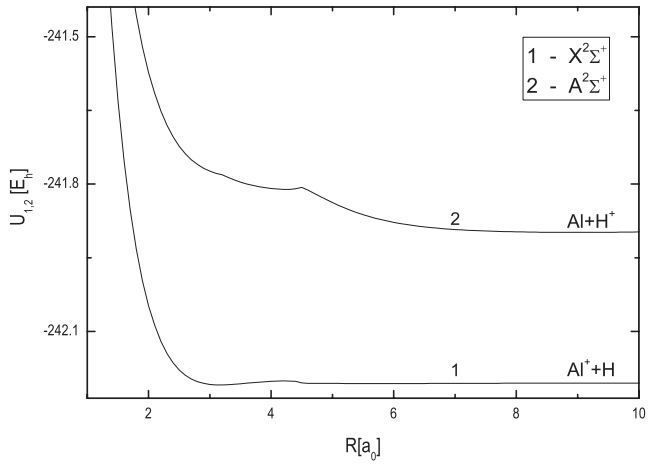

Figure 5. Same as in Fig. 3, but for the molecular ion HAl^+.

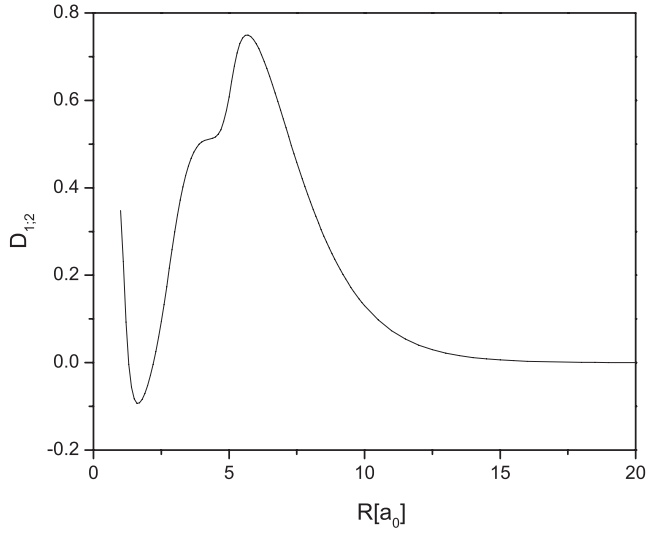

Figure 6. The behaviour of the electronic dipole matrix element $D_{1;\,2}(R)$, given by equations (13) and (14), for the molecular ion HMg^+.

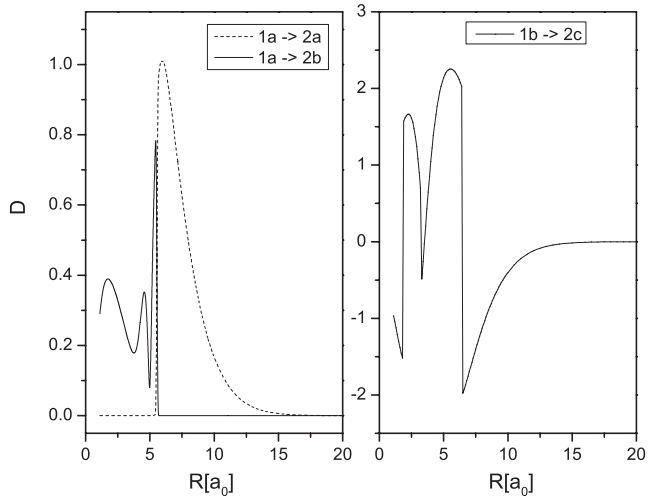

Figure 7. The behaviour of dipole matrix elements $D_{1a;\,2a;\,b}(R)$ and $D_{1b;\,2c}(R)$, given by equations (13) and (15), for the molecular ion HSi^+.

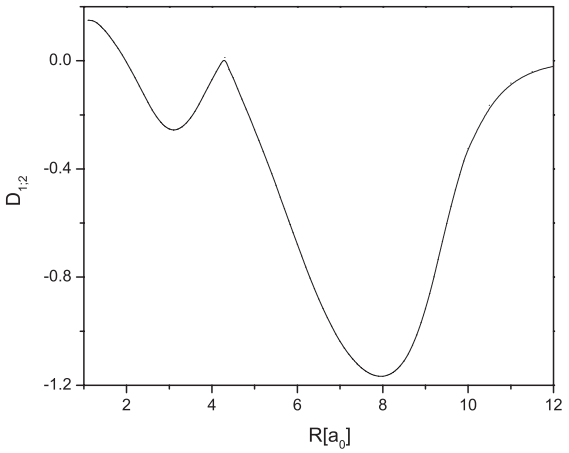

Figure 8. Same as in Fig. 6, but for the molecular ion HAl^+.

absorption coefficients. We will start from the bound–free, free–free and free–bound absorption processes, caused by the radiative transitions given by equations (6), for the given species A and B. In the cases $A = \mathrm{H}$ and $B = \mathrm{Mg}$ and $A = \mathrm{He}$ and $B = \mathrm{H}$ where the transitions given by equations (6) are connected with only one initial and one final Σ-electronic state, the corresponding spectral absorption coefficients are denoted here with $\kappa^{(\mathrm{bf})}_{AB^+}(\lambda, T)$, $\kappa^{(\mathrm{ff})}_{AB^+}(\lambda, T)$ and $\kappa^{(\mathrm{fb})}_{AB^+}(\lambda, T)$, where T is the local plasma temperature in the solar atmosphere.

However, it follows from the above mentioned that in the case $A = \mathrm{H}$ and $B = \mathrm{Si}$ we will have the transitions from two initial Σ- and Π-electronic states to two final Σ- and one final Π-electronic states. Because of that in this case we will have three groups of the spectral absorption coefficients $\kappa^{(\mathrm{bf,ff,fb})}_{AB^+}(\lambda, T; i, f)$, which correspond to these transitions.

3.1 The bound–free processes

In the usual way the spectral absorption coefficients $\kappa_{\mathrm{bf}}(\lambda, T)$ which characterize the efficiency of the photodissociation process (3) are defined by

$$\kappa^{(\mathrm{bf})}_{AB^+}(\lambda, T) = \sigma^{(\mathrm{phd})}_{AB^+}(\lambda, T)\, N_{AB^+}, \tag{17}$$

where $N(AB^+)$ is the local density of the considered molecular ion AB^+, and $\sigma^{(\mathrm{phd})}$ is the corresponding mean thermal photodissociation cross-section, which is given by

$$\sigma^{(\mathrm{phd})}_{AB^+}(\lambda, T) = \frac{\sum_{J,v}(2J+1)\,\mathrm{e}^{\frac{-E_{J,v}}{kT}}\,\sigma_{J,v}(\lambda)}{\sum_{J,v}(2J+1)\,\mathrm{e}^{\frac{-E_{J,v}}{kT}}}, \tag{18}$$

where $\sigma_{J,v}(\lambda)$ is the partial photodissociation cross-section for the rovibrational states with given quantum numbers J and v, and $E_{J,v}$ the energies of these states with the respect to the ground rovibrational states. It means that $E_{J,v} = E_{\mathrm{dis}} + \epsilon_{J,v}$, where E_{dis} is the dissociative energy of the ion AB^+, and the energies $\epsilon_{J,v} < 0$ are determined from equation (7) together with the wave functions of the considered rovibrational states. Within the dipole approximation the partial cross-sections $\sigma_{J,v}(\lambda)$ are given by the expressions

$$\sigma_{J,v}(\lambda) = \frac{8\pi^3}{3\lambda}\left[\frac{J+1}{2J+1}|D_{J,v;J+1,E'_{\mathrm{imp}}}|^2 + \frac{J}{2J+1}|D_{J,v;J-1,E'_{\mathrm{imp}}}|^2\right], \tag{19}$$

$$D_{J,v;J\pm1,E'_{\rm imp}} = \langle {\rm in},\, J,\, v;\, R|D_{\rm in,fin}(R)|{\rm fin},\, J\pm1,\, E'\rangle, \qquad (20)$$

where $E' = \epsilon_{J,\,v} + \varepsilon_\lambda$, $E'_{\rm imp}$ and E' are connected with equation (11), and $D_{\rm in,\,fin}(R)$ is given by equations (13)–(15).

Keeping in mind that the deviations from the LTE of the used model C from Vernazza et al. (1981) are not related to the considered bound–free processes, we will take the photodissociation coefficient $\kappa^{\rm (bf)}_{AB^+}(\lambda, T)$ in an equivalent form, suitable for further considerations, namely

$$\kappa^{\rm (bf)}_{AB^+}(\lambda, T) = K^{\rm (bf)}_{AB^+}(\lambda, T)\, N_A N_{B^+}, \qquad (21)$$

$$K^{\rm (bf)}_{AB^+}(\lambda, T) = \sigma^{\rm (phd)}_{AB^+}(\lambda, T)\, \chi^{-1}(T; AB^+), \qquad (22)$$

$$\chi(T; AB^+) = \left[\frac{N(A)N(B^+)}{N(AB^+)}\right], \qquad (23)$$

where the factor χ is given by the relation

$$\chi(T; AB^+) = \frac{g_A g_{B^+}}{g_{AB^+}} \left(\frac{\mu kT}{2\pi\hbar^2}\right)^{3/2} \frac{1}{\sum_{J,v}(2J+1)\,{\rm e}^{\frac{E_{\rm dis}-E_{J,v}}{kT}}}, \qquad (24)$$

where g_{AB^+}, g_A and g_{B^+} are the electronic statistical weights of the species AB^+, A and B^+, respectively, and $\sigma^{\rm (phd)}_{AB^+}(\lambda, T)$ is given by equations (18)–(20). The behaviour of the photodissociation cross-section $\sigma^{\rm (phd)}_{AB^+}(\lambda, T)$ and the bound–free spectral rate coefficient $K^{\rm (bf)}_{AB^+}(\lambda, T)$ are illustrated in Figs 9 and 10, on the example of the case A = H and B = Mg, for $110 \lesssim \lambda \lesssim 205$ nm and T = 4000, 6000, 8000 and 10 000 K. These figures show that exist a significant difference between temperature dependence of the mean thermal photoionization cross-section and the corresponding spectral rate coefficient.

3.2 The free–free processes

The very fast approaching of the electronic dipole matrix elements $D_{\rm in,\,fin}(R)$ to zero with the increasing of R in the case of the non-symmetric ion–atom systems, which is illustrated by Figs 6–8, makes possible to apply here the complete quantum mechanical treatment not only to the bound–free and free–bound absorption processes (3) and (5), but also to the free–free absorption process (4). Namely, it can be shown (see e.g. Lebedev & Presnyakov 2002) that the free–free spectral absorption coefficients $\kappa^{\rm (ff)}_{AB^+}(\lambda, T)$ can be expressed over the quantities $\sigma^{\rm (ff)}_{AB^+}(\lambda, E) \equiv$

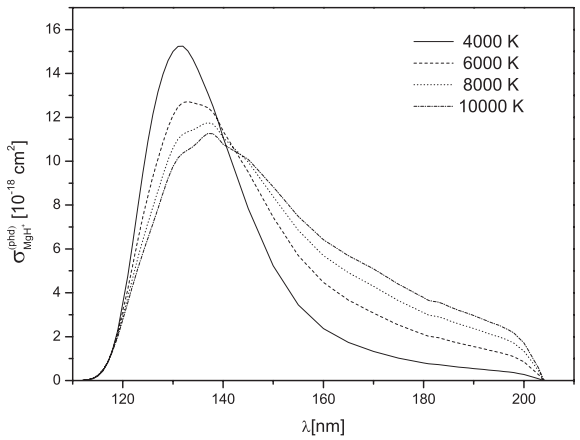

Figure 9. The behaviour of the mean thermal photodissociation cross-section $\sigma^{\rm (phd)}_{\rm HMg^+}(\lambda; T)$ for the molecular ion HMg^+.

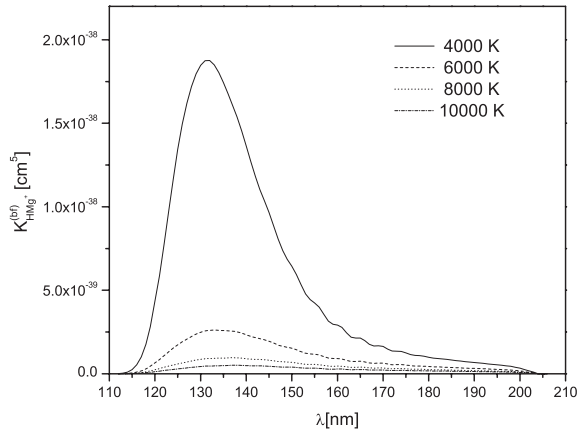

Figure 10. The behaviour of the bound–free (bf) spectral rate coefficient $K^{\rm (bf)}_{\rm HMg^+}(\lambda; T)$ for the molecular ion HMg^+.

$\sigma^{\rm (ff)}_{AB^+}(J, E, \lambda; J\pm1, E'_{\rm imp})$ in the form

$$\kappa^{\rm (ff)}_{AB^+}(\lambda, T) = K^{\rm (ff)}_{AB^+}(\lambda, T)\, N_A N_{B^+},$$

$$K^{\rm (ff)}_{AB^+}(\lambda, T) = \int_0^\infty \left(\frac{2E}{\mu}\right)^{1/2} \sigma^{\rm (ff)}_{AB^+}(\lambda, E) f_T(E)\, {\rm d}E, \qquad (25)$$

where $f_T(E)$ is the Maxwell impact energy distribution function,

$$f_T(E) = \frac{2}{\pi^{1/2}(kT)^{3/2}}\, {\rm e}^{-\frac{E}{k_B T}}\, E^{1/2}\, {\rm d}E, \qquad (26)$$

and $\sigma^{\rm (ff)}_{AB^+}(\lambda, E)$ is given by

$$\sigma^{\rm (ff)}_{AB^+}(\lambda) = \frac{g_{A^+} g_B}{g_A g_{B^+}} \frac{8\pi^4\hbar^2\varepsilon_\lambda}{3c\, 2\mu E} \times \left[(J+1)\,|D_{J,E;J+1,E'_{\rm imp}}|^2 + J\,|D_{J,E;J-1,E'_{\rm imp}}|^2\right], \qquad (27)$$

$$D_{J,E;J\pm1,E'_{\rm imp}} = \langle {\rm in},\, J,\, E;\, R|D_{\rm in,fin}(R)|{\rm fin},\, J\pm1,\, E'\rangle, \qquad (28)$$

where $E'_{\rm imp}$ and $E' = E + \varepsilon_\lambda$ are connected with equation (11), g_{A^+}, g_B, g_A and g_{B^+} are the electronic statistical weights of the species A^+, B, A and B^+, respectively. One can see that the quantity $\sigma^{\rm (ff)}_{AB^+}$ can be treated as the effective cross-section, but is expressed in units cm^4 s, and the rate coefficient $K^{\rm (ff)}_{AB^+}(\lambda, T)$ is equal to the absorption coefficient for the unit densities $N(A)$ and $N(B^+)$.

3.3 The free–bound processes

Similarly to the free–free case the free–bound spectral absorption coefficients $\kappa^{\rm (fb)}_{AB^+}(\lambda, T)$ is taken here as

$$\kappa^{\rm (fb)}_{AB^+}(\lambda, T) = K^{\rm (fb)}_{AB^+}(\lambda, T)\, N_A N_{B^+}, \qquad (29)$$

where the rate coefficient $K^{\rm (fb)}_{AB^+}(\lambda, T)$ can be also expressed over the corresponding free–bound cross-section. In accordance with Mihajlov & Ignjatović (1996) and Ignjatović & Mihajlov (1999) it can be presented in the form

$$K^{\rm (fb)}_{AB^+}(\lambda, T) = \frac{(2\pi)^3}{3\hbar\lambda} \left(\frac{2\pi\hbar^2}{\mu kT}\right)^{3/2} \sum_{J',v'} \left(\frac{\mu}{2E}\right)^{1/2} {\rm e}^{-\frac{E}{kT}}\, C_{J',v'}, \qquad (30)$$

$$C_{J',v'} = \frac{g_{(AB^+)^*}}{g_A g_{B^+}} \left[J'|D_{J'-1,E;J',v'}|^2 + (J'+1)|D_{J'+1,E;J',v'}|^2\right], \qquad (31)$$

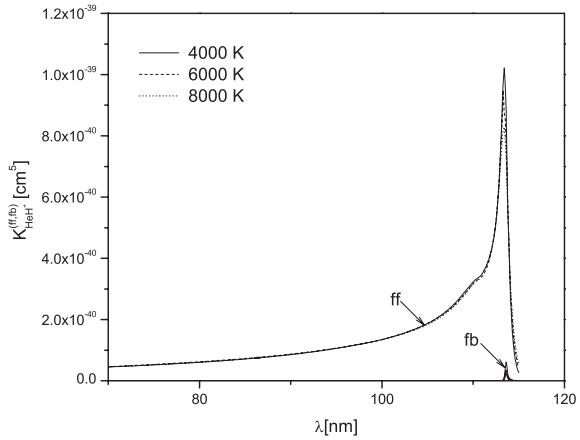

Figure 11. The behaviour of the free–free (ff) and free–bound (fb) spectral rate coefficients $K^{(\mathrm{ff,\,fb})}(\lambda; T)$ for HeH^+.

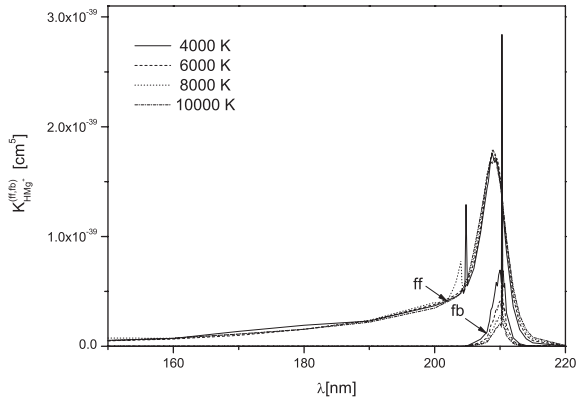

Figure 12. Same as in Fig. 11, but for HMg^+.

$$D_{J'\pm1,E;J',v'} = \langle \mathrm{in},\, J' \pm 1,\, E;\, R|D_{\mathrm{in,fin}}(R)|\mathrm{fin},\, J',\, v'\rangle, \tag{32}$$

where $E = I_A - I_B - \varepsilon_\lambda + \epsilon_{J';v'}$, $g_{(AB^+)^*}$ is the electronic statistical weights of the molecular ion $(AB^+)^*$, $\epsilon_{J';v'} < 0$ the energy of the ion $(AB^+)^*$ in the rovibrational state with the orbital and vibrational quantum numbers J' and v', and summing is performed over all these ro-vibration states. Let us note that within this paper we will neglect everywhere the corrections for stimulated emission as in all the cases considered here the corresponding corrections (given the relevant values of the ratio ε_λ/kT) would be at a level of 0.01 per cent.

The behaviour of the free–free and free–bound spectral rate coefficients $K^{(\mathrm{ff})}_{AB^+}(\lambda, T)$ and $K^{(\mathrm{fb})}_{AB^+}(\lambda, T)$ is illustrated by the Figs 11–13, on the examples:

$A =$ He and $B =$ H for $60 \lesssim \lambda \lesssim 115$ nm and $T = 4000$, 6000 and 8000 K;

$A =$ H and $B =$ Mg for $150 \lesssim \lambda \lesssim 220$ nm and $T = 4000$, 6000, 8000 and 10 000 K;

$A =$ H and $B =$ Si, for the transition $X^1\Sigma^+ \rightarrow B^1\Sigma^+$, for $190 \lesssim \lambda \lesssim 220$ nm and $T = 4000$, 6000, 8000 and 10 000 K.

These figures show that in the general case the absorption processes caused by the free–free and free–bound transitions (6) have to be considered together since their relative efficiency, characterized by $K^{(\mathrm{ff})}_{AB^+}(\lambda, T)$ and $K^{(\mathrm{fb})}_{AB^+}(\lambda, T)$ significantly changes from one to other ion–atom system. Let us note that at least some of the picks, existing in Figs 11–13 which illustrate the shape of the profiles $K^{(\mathrm{ff})}_{AB^+}(\lambda, T)$ and $K^{(\mathrm{fb})}_{AB^+}(\lambda, T)$, can be connected with the

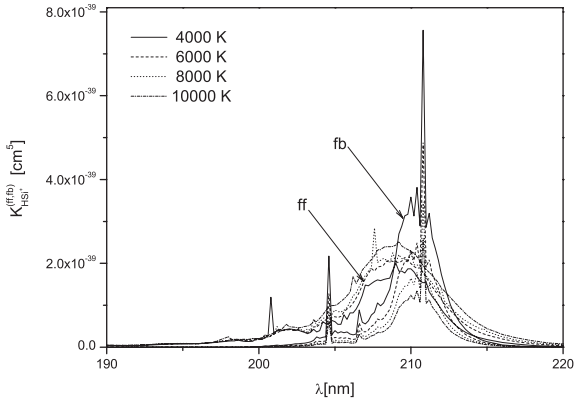

Figure 13. Same as in Fig. 11, but for the transition $X^1\Sigma^+ \rightarrow B^1\Sigma^+$ for HSi^+.

extremums of the corresponding splitting terms. Such phenomena in connection with the ion–atom systems were discussed already in Mihajlov & Popović (1981). Let us note that in the case of non-symmetric atom–atom systems the similar phenomena were also investigated earlier (Veža et al. 1998; Skenderović et al. 2002).

3.4 The partial and total non-symmetric spectral absorption coefficients

The partial absorption coefficients which characterize the individual contribution of the considered ion–atom systems are denoted here with $\kappa_{AB^+}(\lambda) \equiv \kappa_{AB^+}(\lambda, T; N_A, N_{B^+})$. In accordance with the above mentioned we have that

$$\kappa_{AB^+}(\lambda) = \kappa^{(\mathrm{bf})}_{AB^+}(\lambda, T) + \kappa^{(\mathrm{ff})}_{AB^+}(\lambda, T) + \kappa^{(\mathrm{fb})}_{AB^+}(\lambda, T), \tag{33}$$

in the cases $A =$ He and $B =$ H, and $A =$ H and $B =$ Mg and Al, $\kappa_{AB^+}(\lambda)$, and that

$$\kappa_{\mathrm{HSi}^+}(\lambda) = \frac{1}{3}[\kappa_{\mathrm{HSi}^+;1}(\lambda; \Sigma) + \kappa_{\mathrm{HSi}^+;2}(\lambda; \Sigma)] + \frac{2}{3}\kappa_{\mathrm{HSi}^+}(\lambda; \Pi), \tag{34}$$

where $\kappa_{\mathrm{HSi}^+;1}(\lambda; \Sigma)$ and $\kappa_{\mathrm{HSi}^+;2}(\lambda; \Sigma)$ describe the contribution of the radiative transitions $X^1\Sigma^+ \rightarrow B^1\Sigma^+$ and $X^1\Sigma^+ \rightarrow C^1\Sigma^+$, respectively, and $\kappa_{\mathrm{HSi}^+}(\lambda; \Pi)$ the contribution of the transition $A^1\Pi \rightarrow 2^1\Pi$. The spectral absorption coefficients $\kappa^{(\mathrm{bf})}_{AB^+}(\lambda, T)$, $\kappa^{(\mathrm{ff})}_{AB^+}(\lambda, T)$ and $\kappa^{(\mathrm{fb})}_{AB^+}(\lambda, T)$ are defined by equations (17)–(24), (25)–(20) and (29)–(32), respectively.

The total contribution of the mentioned non-symmetric ion–atom absorption processes to the opacity of the considered stellar atmospheres within this work is described by the spectral absorption coefficient $\kappa_{\mathrm{ia;nsim}}(\lambda) \equiv \kappa_{\mathrm{ia;nsim}}(\lambda; T)$ given by

$$\kappa_{\mathrm{ia;nsim}}(\lambda) = \sum \kappa_{AB^+}(\lambda), \tag{35}$$

where the partial coefficients $\kappa_{AB^+}(\lambda; T)$ are given by equations (33) and (34), and summing is performed over all considered pairs of atom and ion species (A, B^+). It is assumed that these coefficients are determined with the plasma temperature T and the atom and ion densities taken from the used model of the considered atmosphere.

4 RESULTS AND DISCUSSION

The absorption coefficients, as functions of the plasma's temperature and the atomic and ionic densities in the solar photosphere,

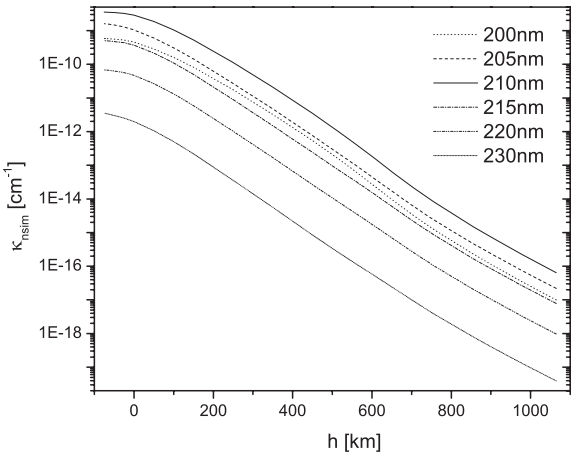

Figure 14. Quiet Sun. Spectral absorption coefficient $\kappa_{\rm nsim}(\lambda, T)$, given by equation (36) for $200 \leq \lambda \leq 230$ nm.

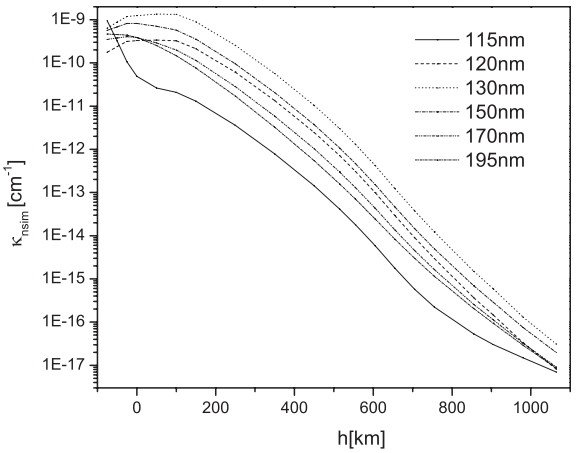

Figure 15. Same as in Fig. 14, but for $115 \leq \lambda \leq 195$ nm.

are determined here based on the non-equilibrium model C from Vernazza et al. (1981), where these parameters are presented as functions of the height (h) of the considered layer with respect to the chosen referent layer. The total non-symmetric spectral absorption coefficient $\kappa_{\rm ia;nsim}(\lambda)$ is taken here, in accordance with equation (35), in the form

$$\kappa_{\rm ia;nsim}(\lambda) = \kappa_{\rm HeH^+}(\lambda) + \kappa_{\rm HMg^+}(\lambda) + \kappa_{\rm HSi^+}(\lambda), \qquad (36)$$

where the partial spectral absorption coefficients $\kappa_{AB^+}(\lambda)$ are determined using the above expressions for the bf, ff and fb rate coefficients. The results of the calculations of $\kappa_{\rm ia;nsim}(\lambda)$ as a function of h, for $-75 \leq h \leq 1100$ km are presented in Figs 14–16 which cover the part of UV and EUV region where $40 \leq \lambda \leq 230$ nm. Consequently, this part covers all regions of λ relevant for the considered ion–atom systems (see Figs 9–13). In accordance with this, Fig. 14 illustrates the common contribution of the HMg^+ and HSi^+ absorption continua, while Fig. 15 refers to the region of exclusive domination of the HMg^+ continuum. Finally, Fig. 16 illustrates the HeH^+ absorption continuum.

As the characteristics of the non-symmetric absorption processes (3)–(5), in the context of their influence on the solar atmosphere

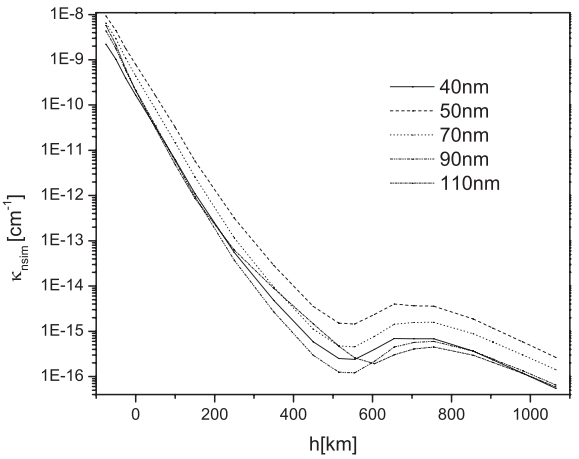

Figure 16. Same as in Fig. 14, but for $40 \leq \lambda \leq 110$ nm.

opacity, here it is used the quantity $G_{\rm tot}^{\rm (nsim)}(\lambda)$ defined by the relations

$$G_{\rm tot}^{\rm (nsim)}(\lambda) = \frac{\kappa_{\rm ia;nsim}(\lambda)}{\kappa_{\rm ia;tot}(\lambda)}, \kappa_{\rm ia;tot}(\lambda) = \kappa_{\rm ia;nsim}(\lambda) + \kappa_{\rm ia;sim}(\lambda), \qquad (37)$$

where $\kappa_{\rm ia;sim}(\lambda)$ characterize the contribution of the symmetric ion–atom absorption processes (1) and (2). In accordance with these relations the quantity $G_{\rm tot}^{\rm (nsim)}(\lambda)$ describes the relative contribution of the non-symmetric processes (3)–(5) to the total absorption caused by all ion–atom absorption processes. Let us note that the use of $\kappa_{\rm ia;sim}(\lambda)$ as a referent quantity is justified as these symmetric processes are now already included in some solar atmosphere models (Fontenla et al. 2009).

It is clear that apart of the quantity $G_{\rm tot}^{\rm (nsim)}(\lambda)$ as the characteristics of the processes (3)–(5) could be used some other quantities, e.g. the ratio $\kappa_{\rm ia;tot}(\lambda)/\kappa_{\rm ia;sim}(\lambda)$, which describes the direct increase of the efficiency of the ion–atom absorption processes caused by the inclusion of the non-symmetric ones. However, in the case of the solar atmosphere it would be very difficult to use this ratio. Namely, in accordance with Vernazza et al. (1981) in the part of the solar atmosphere around its temperature minimum the proton densities $N_{\rm H^+} \ll N_{B+}$, where B = Mg and Si, and consequently the quantity $[\kappa_{\rm ia;nsim}(\lambda) + \kappa_{\rm ia;sim}(\lambda)]/\kappa_{\rm ia;nsim}(\lambda) \gg 1$. Consequently, the behaviour of this quantity can be hardly shown in the whole region of h in the same proportion. Because of that, as the characteristic of the significance of the non-symmetric absorption processes (3)–(5) for the solar atmosphere in UV and EUV region, the quantity $G_{\rm tot}^{\rm (nsim)}(\lambda)$ is used, since from its definition follows that always $0 < G_{\rm tot}^{\rm (nsim)}(\lambda) < 1$. The values of $\kappa_{\rm ia;sim}(\lambda)$, needed for the $G_{\rm tot}^{\rm (nsim)}(\lambda)$ determination, are taken from Mihajlov et al. (2007).

The calculated values of $G_{\rm tot}^{\rm (nsim)}(\lambda)$ as function of h, for the chosen set of λ, are presented in Figs 17–19. From these figures one can see that around the mentioned temperature minimum ($T \lesssim 5000$ K, $150 \lesssim h \lesssim 705$ km) the contribution of non-symmetric processes (3)–(5) is dominant in respect to the symmetric processes (1) and (2). Such region of the non-symmetric processes domination is denoted in these figures as the region 'I'. Apart of that, Figs 17–19 show that within the rest of the considered region of h there are significant parts where the relative contribution of the non-symmetric processes is close to or at least comparable with the contribution of the symmetric ones. In the same figures these parts are denoted as regions 'II'.

In order to additionally show the importance of the considerations in the case of the solar atmosphere of the non-symmetric

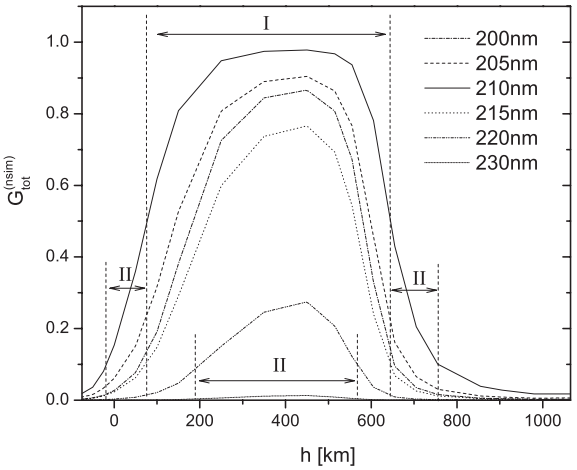

Figure 17. The presented values of $G_{tot}^{(nsim)}(\lambda)$, given by equation (37), as the function of h for the quiet Sun for $200 \leq \lambda \leq 230$ nm; I and II are the regions of h where $0.5 \lesssim G_{tot}^{(nsim)}(\lambda)$ and $0.1 \lesssim G_{tot}^{(nsim)}(\lambda) < 0.5$, respectively.

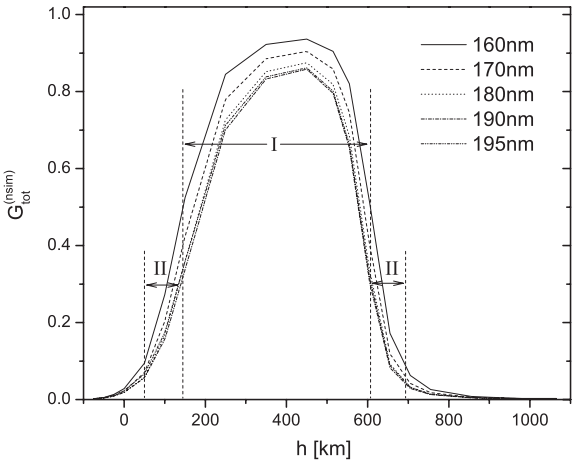

Figure 18. Same as in Fig. 17, but for $160 \leq \lambda \leq 195$ nm.

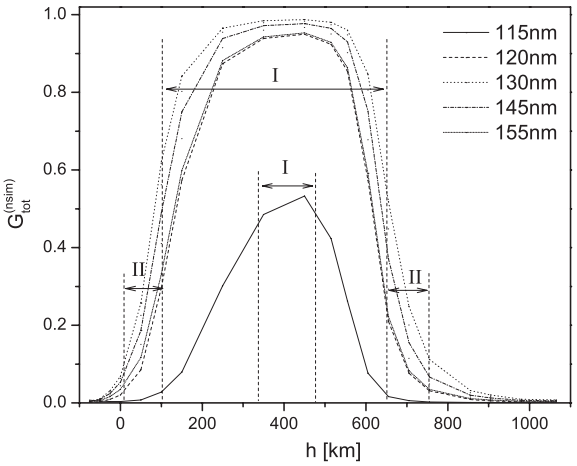

Figure 19. Same as in Fig. 17, but for $115 \leq \lambda \leq 155$ nm.

processes (3)–(5) here, similarly to Mihajlov et al. (2007), it was performed the comparison of the efficiencies of the ion–atom absorption processes and the efficiency of such concurrent processes as the ion H^- photo-detachment and the electron–hydrogen atom inverse 'bremsstrahlung' (H^- continuum). Namely, among relevant concurrent absorption processes just these electron–atom ones can be treated until now as the dominant in the spectral region which was considered in Mihajlov et al. (2007). For that purpose in this work it was compared the behaviour of the quantity

$$F_{ea}^{(sim)}(\lambda) = \frac{\kappa_{ia;sim}(\lambda)}{\kappa_{ea}(\lambda)}, \tag{38}$$

which is similar to the correspond quantity from Mihajlov et al. (2007) and characterize the relative efficiency of the ion–atom symmetric processes and H^- continuum, and the quantity

$$F_{ea}^{(tot)}(\lambda) = \frac{\kappa_{ia;tot}(\lambda)}{\kappa_{ea}(\lambda)}, \tag{39}$$

which characterize the increasing of the total efficiency of the ion–atom radiative processes after the including in the consideration of the non-symmetric processes (3)–(5). In these expressions $\kappa_{ia;tot}(\lambda)$ is given by equation (37), the spectral absorption coefficient $\kappa_{ia;sim}(\lambda)$ characterizes the ion–atom symmetric processes (1) and (2) and is taken from Mihajlov et al. (2007) and the spectral absorption coefficient $\kappa_{ea}(\lambda)$ describes the H^- continuum. In the case of the solar atmosphere $\kappa_{ea}(\lambda)$ is determined based on of Stilley & Callaway (1970), Wishart (1979) and Vernazza et al. (1981). The behaviour of $F_{ea}^{(sim)}(\lambda)$ and $F_{ea}^{(tot)}(\lambda)$, as the functions of h, is presented in Fig. 20. This figure shows that the inclusion in the consideration of the non-symmetric processes (3)–(5) causes the significant increases of the total efficiency of the ion–atom absorption processes, particularly in the neighbourhood of the solar atmosphere temperature minimum, where it become close to the efficiency of the H^- continuum.

In connection with the above mentioned let us note that according to Vernazza et al. (1981) in the neighbourhood of the solar atmosphere temperature minimum ($50 \lesssim h \lesssim 650$ km) the Fe component gives the maximal individual contribution to the electron density in respect to the Mg and Si components. It means that the inclusion in the consideration of the processes (3)–(5) with $A =$ H and $B =$ Fe would surely significantly increase the total contribution of the

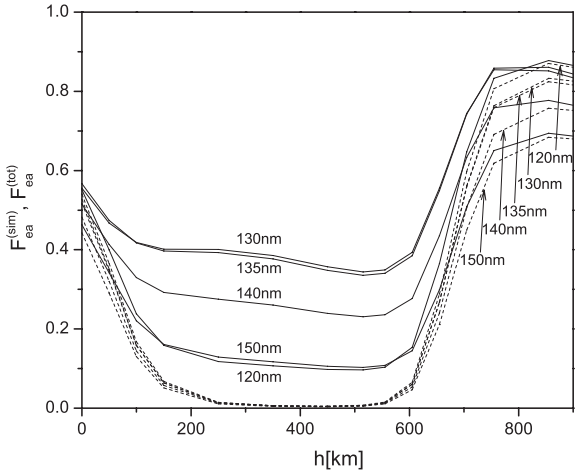

Figure 20. Quantities $F_{ea}^{(sim)}(\lambda)$ (dashed line) and $F_{ea}^{(tot)}(\lambda)$ (full line) defined in equations (38) and (39) as the functions of h for the solar atmosphere for $120 \leq \lambda \leq 150$ nm.

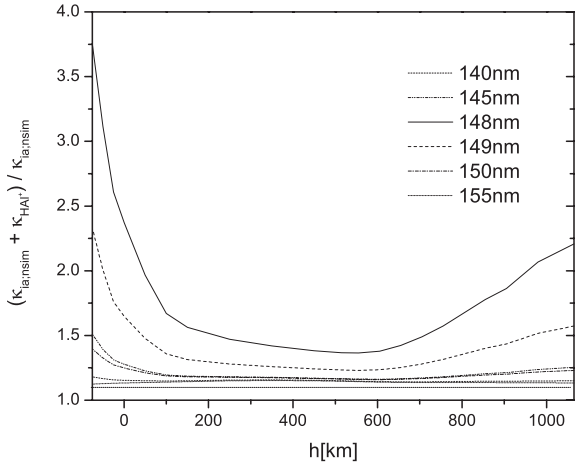

Figure 21. The ratio $(\kappa_{\rm ia;nsim}(\lambda) + \kappa_{\rm AlH^+}(\lambda))/\kappa_{\rm ia;nsim}(\lambda)$, where $\kappa_{\rm ia;nsim}(\lambda)$ is given by equation (36) and $\kappa_{\rm AlH^+}(\lambda)$ by equation (33) for $A =$ H and $B =$ Al, as a function of h for the solar atmosphere for $140 \leq \lambda \leq 155$ nm.

non-symmetric ion–atom absorption processes, perhaps for about 50 per cent. Because of that we have as the task for the nearest future to find the data about the relevant characteristics of the molecular ion HFe^+, since the data from Vernazza et al. (1981) make possible to perform all needed calculations.

Let us note also that, according to the data from Vernazza et al. (1981) and Fontenla et al. (2009), in the solar atmosphere it should be include in the consideration the non-symmetric processes (3)–(5) with $A =$ H, where B is the atom of the one of such components (C, Al etc.), which give visible contribution in narrow regions of h and λ. Now we have only the data needed for the case $A =$ H and $B =$ Al, whose contribution is noticeable in the region $140 \lesssim \lambda \lesssim 155$ nm. Since there is a certain difference between shapes of the lower potential curves for the ion AlH^+, presented in Fig. 5 and the corresponding figure from Guest & Hirst (1981), whose nature by now is not completely clear, the contribution of the processes (3)–(5) with $A =$ H and $B =$ Al was not included in the calculations described above. However, we think that this contribution can serve to estimate the usefulness of the inclusion in the consideration of these processes. For that purpose we presented in Fig. 21 the results of the calculations of the ratios $(\kappa_{\rm ia;nsim}(\lambda) + \kappa_{\rm AlH^+}(\lambda))/\kappa_{\rm ia;nsim}(\lambda)$, as function of h, for $140 \leq \lambda \leq 155$ nm, where $\kappa_{\rm ia;nsim}(\lambda)$ was determined according to equation (36). The behaviour of this ratios presented in above-mentioned figure, in the region $200 < h < 700$ km, is caused by the fast decrees of the corresponding ion species concentration. This figure clearly demonstrates the fact that in the significant parts of the solar photosphere the inclusion in the consideration of the processes (3)–(5) with $A =$ H and $B =$ Al should noticeably increase the total contribution of the non-symmetric ion–atom processes. The above mentioned suggest that the contribution of all metal components which by now were not included in the consideration could significant increase the total efficiency of the ion–atom radiative processes, which is characterized by the quantity $F_{\rm ea}^{\rm (tot)}(\lambda)$ in Fig. 20. The results presented in Figs 17–19 and 20 show that the neglecting of the contribution of the non-symmetric processes (3)–(5) to the opacity of the solar atmosphere, in respect to the contribution of symmetric processes (1) and (2) would caused significant errors. From here it follows that the non-symmetric absorption processes (3)–(5) should be *ab initio* included in the solar atmosphere models.

5 CONCLUSIONS

From the presented material it follows that the considered non-symmetric ion–atom absorption processes cannot be treated only as one channel among many equal channels with influence on the opacity of the solar atmosphere. Namely, these non-symmetric processes around the temperature minimum increase the absorption of the EM radiation, which is caused by all (symmetric and non-symmetric) ion–atom absorption processes, so that this absorption becomes almost uniform in the whole solar photosphere. Moreover, the presented results show that further investigations of these processes promise to demonstrate that they are of similar importance as the known process of photo-detachment of the ion H^-, which was treated until recently as absolutely dominant. Namely, the inclusion of the non-symmetric absorption processes into consideration with $A =$ H and $B =$ Fe, as well as some other similar processes (with $A =$ H and $B =$ Al etc.), would significantly increase the contribution of such processes to the solar atmosphere opacity. All mentioned facts suggest that the considered non-symmetric ion–atom absorption processes should be included *ab initio* in the solar atmosphere models, as well as in the models of solar- and near-solar-type stars.

ACKNOWLEDGEMENTS

The authors wish to thank to Professor V. N. Obridko and A. A. Nusinov for the shown attention to this work. Also, the authors are thankful to the Ministry of Education, Science and Technological Development of the Republic of Serbia for the support of this work within the projects 176002, III4402.

REFERENCES

Dunning T. H., Jr, 1989, J. Chem. Phys., 90, 1007
Fontenla J. M., Curdt W., Haberreiter M., Harder J., Tian H., 2009, ApJ, 707, 482
Green T. A., Michels H. H., Browne J. C., Madsen M. M., 1974a, J. Chem. Phys., 61, 5186
Green T. A., Browne J. C., Michels H. H., Madsen M. M., 1974b, J. Chem. Phys., 61, 5198
Guest M. F., Hirst D. M., 1981, Chem. Phys. Lett., 84, 167
Ignjatović L. M., Mihajlov A. A., 1999, in Vedel F., ed., Proceedings of the 31st EGAS Conference of the European Group for Atomic Spectroscopy. Royal Swedish Academy of Sciences, Stockholm, p. P2
Kendall R. A., Dunning T. H., Jr, Harrison R. J., 1992, J. Chem. Phys., 96, 6796
Lebedev V. S., Presnyakov L. P., 2002, J. Phys. B: At. Mol. Opt. Phys., 35, 4347
Mihajlov A. A., Dimitrijević M. S., 1986, A&A, 155, 319
Mihajlov A. A., Ignjatović L. M., 1996, Dynamique des Ions, des Atomes et des Molecules (DIAM '96) Bourges, France 15–18 Jul 1996, Contrib. Papers, p. 157
Mihajlov A. A., Popović M. P., 1981, Phys. Rev. A, 23, 1679
Mihajlov A. A., Dimitrijević M. S., Ignjatović L. M., 1993, A&A, 276, 187
Mihajlov A. A., Dimitrijević M. S., Ignjatović L. M., Djurić Z., 1994, A&AS, 103, 57
Mihajlov A. A., Ignjatović L. M., Sakan N. M., Dimitrijević M. S., 2007, A&A, 437, 1023
Werner H. J., Knowles P. J., 2006, MOLPRO, a package of programs with contributions from J. Almlof et al. (http://www.molpro.net)
Skenderović H., Beuc R., Ban T., Pichler G., 2002, Eur. Phys. J. D, 19, 49
Stilley J. L., Callaway J., 1970, ApJ, 160, 245

Stix M., 2002, The Sun: An Introduction. Springer, Heidelberg
Vernazza J., Avrett E., Loser R., 1981, ApJS, 45, 635
Veža D., Beuc R., Milošević S., Pichler G., 1998, Eur. Phys. J. D, 2, 45
White O. R., 1977, The Solar Output and its Variation. Colorado Associated University Press, Boulder, CO
Wishart A. W., 1979, MNRAS, 187, 59
Woods T., 2008, Adv. Space Res., 42, 895
Woods T. et al., 2009, Geophys. Res. Lett., 36, L01101
Worden J., Woods T., Bowman K., 2001, ApJ, 560, 1020

This paper has been typeset from a TEX/LATEX file prepared by the author.

Monthly Notices
of the
ROYAL ASTRONOMICAL SOCIETY

MNRAS **432,** 2247–2251 (2013)
Advance Access publication 2013 May 9

doi:10.1093/mnras/stt634

Stark broadening of resonant Cr II $3d^5$–$3d^4 4p$ spectral lines in hot stellar atmospheres

Z. Simić,[1,2]⋆ M. S. Dimitrijević[1,2,3] and S. Sahal-Bréchot[3]

[1]*Astronomical Observatory, Volgina 7, 11060 Belgrade, Serbia*
[2]*Isaac Newton Institute of Chile, Yugoslavia Branch, 11060 Belgrade, Serbia*
[3]*Observatoire de Paris-Meudon, F-92195 Meudon, France*

Accepted 2013 April 3. Received 2013 March 18; in original form 2013 February 13

ABSTRACT

New Stark broadening parameters of interest for the astrophysical, laboratory and technological plasma modelling, investigations and analysis for nine resonant Cr II multiplets have been determined within the semiclassical perturbation approach. In order to demonstrate one possibility for their usage in astrophysical plasma research, obtained results have been applied to the analysis of the Stark broadening influence on stellar spectral line shapes.

Key words: atomic data – line: profiles – stars: atmospheres – white dwarfs.

1 INTRODUCTION

Chromium lines are interesting for astrophysics due to their presence in stellar atmospheres, where they are identified in a large number, so that data on their profiles are obviously of interest for example to determine chromium abundance and investigate chromium stratification in stellar atmospheres (Dimitrijević et al. 2005, 2007) as well as for the diagnostics and modelling of stellar plasma and for analysis and synthesis of stellar spectra. They have been identified in A-type star spectra, such as e.g. in *o* Peg (Adelman 1991), 7 Sex (Adelman & Philip 1996), ϕ Aqu (Caliskan & Adelman 1997) and Przybylski's star (Cowley et al. 2000), which are also chemically peculiar stars. Namely the majority of chemically peculiar stars are of A spectral type. As an example, in the spectrum of ϕ Aqu, Caliskan & Adelman (1997) identified 28 Cr II spectral lines and noted an overabundance of $\log[\mathrm{Cr/H}] = -5.82 \pm 0.27$, in comparison with the Solar value of −6.26. Also for Przybylski's star, Cowley et al. (2000) identified 15 Cr II lines and noted an overabundance with the value $\log[\mathrm{Cr/H}] = -5.92 \pm 0.26$. Cr II spectral lines are before Fe II and Ti II in number and intensity in the Ae/Be Herbig star V380 Ori, where 25 Cr II lines were found (Shevchenko 1994). Since in stellar atmospheres, layers, where the Stark broadening contribution to the line profiles is important, exist (Lanz et al. 1988; Popović, Dimitrijević & Tankosić 1999a; Popović, Dimitrijević & Ryabchikova 1999b; Popović, Milovanović & Dimitrijević 2001; Tankosić, Popović & Dimitrijević 2003; Dimitrijević et al. 2003a, 2004, 2007; Dimitrijević, Jovanović & Simić 2003b; Simić et al. 2005, 2006; Hamdi et al. 2008; Simić, Dimitrijević & Kovačević 2009b), Stark broadening parameters for singly ionized chromium spectral lines are obviously of astrophysical interest.

Dimitrijević et al. (2007) calculated Stark broadening parameters for Cr II spectral lines of seven multiplets belonging to 4s–4p transitions and applied the obtained results to the analysis of Cr II line profiles observed in the spectrum of the Cr-rich star HD 133792. There is only one experimental result on the Stark broadening of Cr II spectral lines, obtained by Rathore et al (1984). The Stark widths and shifts of Cr II 3120.36, 3124.94 and 3132.05 Å of the multiplet 5 ($4s\,^4D - 4p\,^4F^o$) have been measured in a T-tube plasma. These results have been compared with values predicted from established systematic trends and regularities. Using regularities and systematic trends, Lakićević (1983) also made an attempt to estimate Stark broadening parameters of the Cr II 2065.65 Å line. In order to enlarge and complete Stark broadening data for astrophysically interesting Cr II lines, we have determined Stark broadening parameters for nine resonant Cr II $3d^5$–$3d^4$ 4p multiplets in the visible and UV wavelength range (2060–6073 Å). There are no other available theoretical or experimental data for considered multiplets. The obtained results have also been used to analyse the influence of Stark broadening on Cr II spectral lines in a hot A-type star and DB white dwarf atmospheres.

2 THEORETICAL REMARKS

For the determination of Stark broadening parameters the semiclassical perturbation (SCP) formalism (Sahal-Bréchot 1969a,b) has been used. For updates see Fleurier, Sahal-Bréchot & Chapelle (1977), Sahal-Bréchot (1974, 1991), Dimitrijević, Sahal-Bréchot & Bomier (1991), Dimitrijević & Sahal-Bréchot (1996) and the review article of Dimitrijević (1996). The full width at half-maximum intensity (FWHM) ($W = 2w$) and shift (d) of an isolated spectral line broadened by electron impacts can be expressed (in angular frequency units), for an ionized emitter, in terms of cross-sections

⋆ E-mail: zsimic@aob.rs

for elastic and inelastic processes as

$$W = N \int v f(v)\,\mathrm{d}v \left(\sum_{i' \neq i} \sigma_{ii'}(v) + \sum_{f' \neq f} \sigma_{ff'}(v) + \sigma_{\mathrm{el}} \right),$$
$$d = N \int v f(v)\,\mathrm{d}v \int_{R_3}^{R_\mathrm{D}} 2\pi\rho\,\mathrm{d}\rho \sin(2\varphi_\mathrm{p}). \quad (1)$$

In the above equations, N is the electron density, $f(\upsilon)$ the Maxwellian velocity distribution function for electrons, ρ the impact parameter of the incoming electron, i' (respectively, f') denotes the perturbing levels of the initial state i (respectively, final state f), $\sigma_{ii'}(\upsilon)$ [respectively, $\sigma_{ff'}(\upsilon)$] is the inelastic cross-section, and here it is expressed by an integral over the impact parameter ρ of the transition probability $P_{ii'}(\rho, \upsilon)$ [respectively, $P_{ff'}(\rho, \upsilon)$] as

$$\sum_{i' \neq i} \sigma_{ii'}(\upsilon) = \frac{1}{2}\pi R_1^2 + \int_{R_1}^{R_\mathrm{D}} 2\pi\rho\,\mathrm{d}\rho \sum_{i' \neq i} P_{ii'}(\rho, \upsilon). \quad (2)$$

The elastic cross-section is

$$\sigma_{\mathrm{el}} = 2\pi R_2^2 + \int_{R_2}^{R_\mathrm{D}} 2\pi\rho\,\mathrm{d}\rho \sin^2\delta + \sigma_\mathrm{r},$$
$$\delta = (\varphi_\mathrm{p}^2 + \varphi_\mathrm{q}^2)^{\frac{1}{2}}. \quad (3)$$

The phase shifts φ_p and φ_q due, respectively, to the polarization potential (r^{-4}) and to the quadrupolar potential (r^{-3}) are given in section 3 of chapter 2 in Sahal-Bréchot (1969a) and R_D is the Debye radius. The cut-offs R_1, R_2 and R_3 are described in section 1 of chapter 3 in Sahal-Bréchot (1969b). We denote by σ_r the contribution of the Feshbach resonances (Fleurier et al. 1977).

For the determination of the ion-impact widths and shifts, the corresponding equations are analogous to equations (1)–(3), but without the Feshbach resonance contribution to the width. Also, in comparison with electrons different are and hyperbolic paths, since for electrons the Coulomb force is attractive and for perturbing ions repulsive.

3 RESULTS AND DISCUSSION

The atomic energy levels which are needed for the determination of Stark broadening parameters are from Wiese & Musgrove (1989). The needed oscillator strengths have been determined by using the method of Bates & Damgaard (1949) and the tables of Oertel & Shomo (1968), while for higher levels, the calculations have been performed as in van Regemorter, Hoang Binh & Prud'homme (1979). Within the method of Bates and Damgaard, only oscillator strengths for transitions allowed in the LS coupling are different from zero. For simpler spectra it is usually enough to take all perturbing levels with $\Delta n = 0, \pm 1$and ± 2, but for a particular transition we add the perturbing levels until the corresponding sum rules are satisfied.

Concerning the use of a set of Bates and Damgaard's oscillator strengths, which is complete according to the corresponding sum rules, Ben Nessib, Dimitrijević & Sahal-Bréchot (2004) and Hamdi et al. (2007), who calculated line widths and shifts of Si V and Ne V ions, compared SCP ab initio Stark widths obtained with Bates and Damgaard oscillator strengths and with SUPERSTRUCTURE (Thomas–Fermi–Dirac interaction potential model with relativistic corrections; Eissner, Jones & Nussbaumer 1974) oscillator strengths. They obtained that the difference between the two sets of calculations did not exceed 30 per cent. Since the accuracy of the SCP method is about 20 per cent, such a difference, due to different sets of oscillator strengths used in Stark broadening calculation, is not crucial.

Electron-, proton- and helium ion-impact broadening parameters – W (FWHM) and d (shift for five resonant Cr II $3d^5$–$3d^4$4p multiplets) – are shown in Table 1, together with the results of present calculations of helium ion-impact broadening parameters for additional four resonant lines. For these lines in Table 1 are included electron- and proton-impact broadening parameters, previously communicated on a conference and published in the corresponding proceedings (Simić et al. 2009a). This table shows Cr II Stark broadening parameters, for a perturber density of 10^{17} cm^{-3} and temperatures from 5000 to 100 000 K. The quantity C (given in Å cm^{-3}), when divided by the corresponding full width at half-maximum, gives an estimate for the maximum perturber density for which tabulated data may be used. The obtained data could not be compared with experimental results, but in Dimitrijević et al. (2007) the Stark broadening parameters for other Cr II lines, obtained with the same method, have been compared with the experimental results of Rathore et al (1984) and an acceptable agreement has been obtained. Also, they are successfully used in the same article for the synthesis of stellar Cr II lines and their comparison with the observed ones, which indirectly indicates that the present results are also correct.

The largest Stark widths are for resonant Cr II 6073.4, 5279.6 and 4588.2 Å spectral lines, corresponding to transitions with the lower term $3d^5\ {}^4\mathrm{F}$. Fig. 1 shows the full width at half-maximum intensity as a function of the temperature for electron-impact broadening.

In order to show how the obtained results may be used for the investigation of the influence of the Stark broadening mechanism for Cr II spectral lines in stellar plasma conditions, we have compared Doppler and Stark widths for Cr II multiplets $3d^5\ {}^4\mathrm{F}$–$3d^4$4p ${}^4\mathrm{F^o}$ ($\lambda = 5279.6$ Å) and $3d^5\ {}^4\mathrm{F}$–$3d^4$4p ${}^4\mathrm{P^o}$ ($\lambda = 6073.4$ Å) for a Kurucz (1979) A-type star atmosphere model with $T_\mathrm{eff} = 8500$ K and $\log g = 4.0$ (Fig. 2). Due to the characteristics of the Lorentz distribution function describing the Stark broadening contribution and the Gauss distribution function describing the Doppler contribution even when the Stark width is smaller than the Doppler one, Stark broadening will contribute to the line wings, so that it is obvious that layers where the Stark broadening influence is not negligible exist.

To show it more clearly, we synthesized the Cr II 4588.2 Å line profile using the SYNTH code (Piskunov 1992) (Fig. 3) and DIPSO program package for the corresponding equivalent width (EW), for $T_\mathrm{eff} = 8\ 750$ K and $\log g = 4.0$ as a function of the chromium abundance. One can see in Fig. 3 that the influence of Stark broadening increases in line wings with the increase of the chromium abundance as expected. Namely with the increase of the abundance of chromium, an element with much lower ionization potential than hydrogen and helium, the usual main constituents of stellar plasma, the electron density increases due to the increase of the degree of plasma ionization and the corresponding Stark line width also increases.

It is also important to consider the influence of Stark broadening on the EW of chromium, since it is important to see the possible errors in the chromium abundance determination, if this broadening mechanism is neglected. For this reason, Fig. 4 shows (denoted with a dotted line) the ratio of the EW for the Cr II spectral line 4588.2 Å with (EW_2) and without (EW_1) Stark broadening contribution, as a function of the chromium abundance expressed as log[Cr/H]. The full line denotes the ratio of the EW without Stark broadening: with variable chromium abundance (EW_2) and with the

Table 1. Electron-, proton- and He II-impact broadening parameters for Cr II, $3d^5$–$3d^4 4p$ spectral lines, for a perturber density of 10^{17} cm^{-3} and temperatures from 5 000 to 100 000 K. The calculated wavelength of the transitions (in Å) and parameter C are also given. This parameter when divided by the corresponding Stark width gives an estimate for the maximal perturber density for which the line may be treated as isolated. WIDTH is FWHM. We note that for the first four lines, electron- and proton-impact broadening parameters are previously communicated on a conference and published in the corresponding proceedings (Simić et al. 2009a).

Perturber density is 1.E+17 cm^{-3}

Perturbers are:		Electrons		Protons		Helium ions	
Transition	T (K)	Width (Å)	Shift (Å)	Width (Å)	Shift (Å)	Width (Å)	Shift (Å)
	5000	0.514E−01	−0.334E−03	0.148E−02	−0.542E−04	0.219E−02	−0.541E−04
Cr II	10 000	0.382E−01	−0.379E−03	0.268E−02	−0.120E−03	0.335E−02	−0.118E−03
^{6}S−^{6}P^o	20 000	0.282E−01	−0.438E−03	0.382E−02	−0.232E−03	0.433E−02	−0.214E−03
2060.4 Å	30 000	0.238E−01	−0.425E−03	0.431E−02	−0.311E−03	0.468E−02	−0.278E−03
C = 0.15E+21	50 000	0.196E−01	−0.460E−03	0.473E−02	−0.405E−03	0.508E−02	−0.355E−03
	100 000	0.157E−01	−0.515E−03	0.528E−02	−0.547E−03	0.553E−02	−0.446E−03
	5000	0.382	0.718E−01	0.102E−01	0.117E−02	0.147E−01	0.115E−02
Cr II	10 000	0.284	0.491E−01	0.175E−01	0.244E−02	0.218E−01	0.227E−02
^{4}F−^{4}D^o	20 000	0.212	0.378E−01	0.244E−01	0.416E−02	0.269E−01	0.359E−02
4588.2 Å	30 000	0.182	0.319E−01	0.268E−01	0.505E−02	0.290E−01	0.439E−02
C = 0.40E+21	50 000	0.155	0.265E−01	0.295E−01	0.639E−02	0.315E−01	0.522E−02
	100 000	0.133	0.219E−01	0.329E−01	0.770E−02	0.339E−01	0.630E−02
	5000	0.480	0.743E−01	0.120E−01	0.874E−03	0.174E−01	0.868E−03
Cr II	10 000	0.358	0.514E−01	0.209E−01	0.188E−02	0.261E−01	0.180E−02
^{4}F−^{4}F^o	20 000	0.268	0.399E−01	0.293E−01	0.337E−02	0.326E−01	0.304E−02
5279.6 Å	30 000	0.229	0.338E−01	0.325E−01	0.425E−02	0.352E-01	0.370E−02
C = 0.53E+21	50 000	0.194	0.274E−01	0.357E−01	0.546E−02	0.383E−01	0.464E−02
	100 000	0.165	0.229E−01	0.398E−01	0.679E−02	0.414E−01	0.556E−02
	5000	0.793	0.264	0.144E−01	0.411E−02	0.210E−01	0.397E−02
Cr II	10 000	0.577	0.197	0.258E−01	0.806E−02	0.320E−01	0.742E−02
^{4}F−^{4}P^o	20 000	0.425	0.155	0.368E−01	0.127E−01	0.408E−01	0.111E−01
6073.4 Å	30 000	0.357	0.134	0.414E−01	0.156E−01	0.442E−01	0.132E−01
C = 0.70E+21	50 000	0.294	0.110	0.459E−01	0.184E−01	0.483E−01	0.152E−01
	100 000	0.255	0.920E−01	0.521E−01	0.221E−01	0.528E−01	0.182E−01
	5000	0.159	0.646E−02	0.543E−02	0.322E−03	0.781E−02	0.320E−03
Cr II	10 000	0.120	0.399E−02	0.929E−02	0.695E−03	0.116E−01	0.669E−03
^{4}D−^{4}D^o	20 000	0.903E−01	0.383E−02	0.130E−01	0.125E−02	0.143E−01	0.114E−02
3378.0 Å	30 000	0.774E−01	0.355E−02	0.142E−01	0.161E−02	0.154E−01	0.138E−02
C = 0.25E+21	50 000	0.654E−01	0.352E−02	0.156E−01	0.205E−02	0.168E−01	0.176E−02
	100 000	0.547E−01	0.356E−02	0.174E−01	0.257E−02	0.181E−01	0.212E−02
	5000	0.218	0.344E−01	0.585E−02	0.431E−03	0.851E−02	0.429E−03
Cr II	10 000	0.168	0.240E−01	0.103E−01	0.929E−03	0.128E−01	0.891E−03
^{4}D−^{4}F^o	20 000	0.129	0.183E−01	0.144E−01	0.167E−02	0.161E−01	0.151E−02
3738.4 Å	30 000	0.111	0.155E−01	0.160E−01	0.211E−02	0.174E−01	0.183E−02
C = 0.26E+21	50 000	0.951E−01	0.126E−01	0.176E−01	0.270E−02	0.189E−01	0.230E−02
	100 000	0.822E−01	0.106E−01	0.196E−01	0.336E−02	0.204E−01	0.276E−02
	5000	0.309	0.916E−01	0.514E−02	0.245E−02	0.742E−02	0.233E−02
Cr II	10 000	0.229	0.799E−01	0.932E−02	0.463E−02	0.114E−01	0.411E−02
^{4}P−^{4}P^o	20 000	0.168	0.730E−01	0.136E−01	0.701E−02	0.147E−01	0.603E−02
3637.7 Å	30 000	0.141	0.654E−01	0.154E−01	0.836E−02	0.161E−01	0.683E−02
C = 0.32E+21	50 000	0.115	0.592E−01	0.174E−01	0.972E−02	0.177E−01	0.794E−02
	100 000	0.994E−01	0.498E−01	0.201E−01	0.116E−01	0.197E−01	0.945E−02
	5000	0.152	0.363E−01	0.440E−02	0.669E−03	0.633E−02	0.655E−03
Cr II	10 000	0.114	0.253E−01	0.756E−02	0.137E−02	0.942E−02	0.126E−02
^{4}P−^{4}D^o	20 000	0.854E−01	0.195E−01	0.106E−01	0.227E−02	0.116E−01	0.195E−02
3046.9 Å	30 000	0.731E−01	0.164E−01	0.116E−01	0.277E−02	0.126E−01	0.238E−02
C = 0.20E+21	50 000	0.625E−01	0.138E−01	0.128E−01	0.341E−02	0.137E−01	0.278E−02
	100 000	0.539E−01	0.114E−01	0.144E−01	0.409E−02	0.147E−01	0.334E−02
	5000	0.160	0.315E−01	0.424E−02	0.444E−03	0.618E−02	0.439E−03
Cr II	10 000	0.120	0.216E−01	0.745E−02	0.939E−03	0.930E−02	0.886E−03
^{4}G−^{4}F^o	20 000	0.904E−01	0.168E−01	0.105E−01	0.165E−02	0.117E−01	0.144E−02
3197.6 Å	30 000	0.775E−01	0.143E−01	0.117E−01	0.200E−02	0.126E−01	0.176E−02
C = 0.19E+21	50 000	0.657E−01	0.116E−01	0.128E−01	0.258E−02	0.137E−01	0.214E−02
	100 000	0.563E−01	0.968E−02	0.143E−01	0.313E−02	0.149E−01	0.257E−02

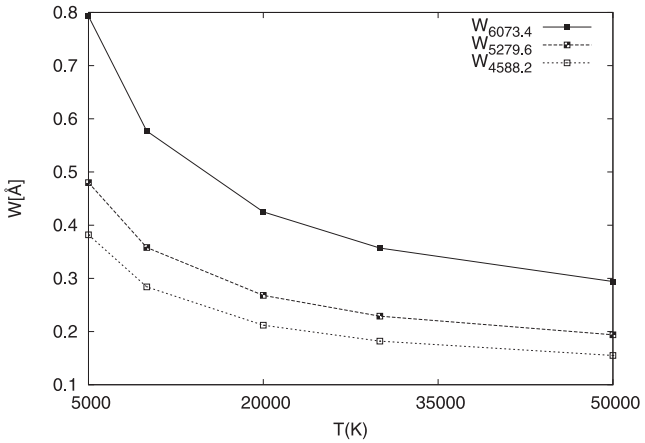

Figure 1. Stark widths for resonant Cr II 4588.2, 5279.6 and 6073.4 Å spectral lines as a function of temperature.

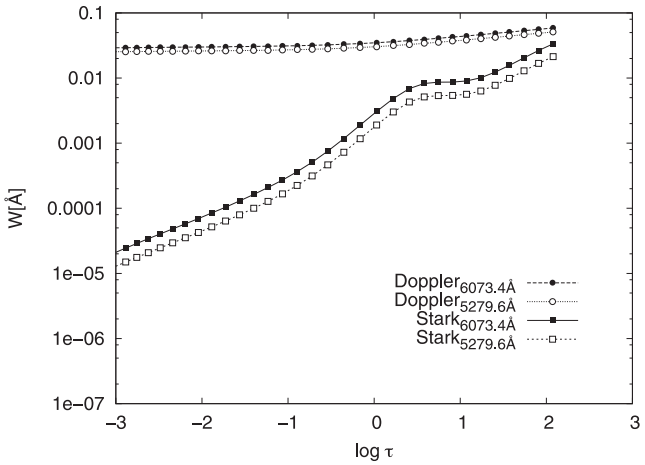

Figure 2. Thermal Doppler and Stark widths for Cr II multiplets $3d^5\ ^4F$–$3d^4 4p\ ^4F^o$ ($\lambda = 5279.6$ Å) and $3d^5\ ^4F$–$3d^4 4p\ ^4P^o$ ($\lambda = 6073.4$ Å), for an A-type star atmosphere model with $T_{\rm eff} = 8500$ K and $\log g = 4.0$, as a function of the Rosseland optical depth.

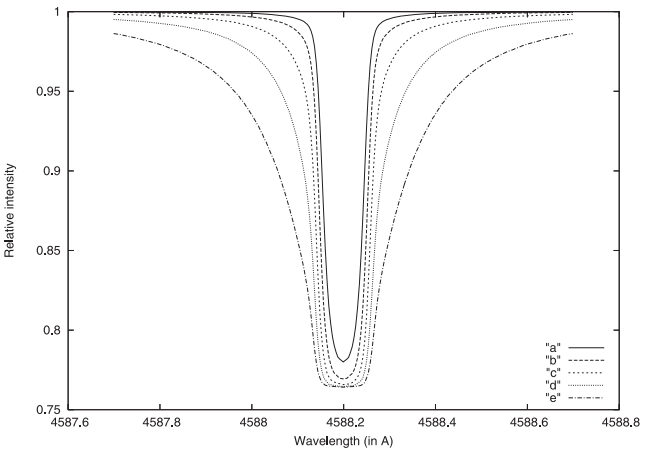

Figure 3. Comparison of the Cr II 4588.2 Å line profile ('a') without the Stark broadening contribution and with this contribution for different Cr abundances log[Cr/H]: 'b' – Solar one; 'c' – (−3.75); 'd' – (−3.25); 'e' – (−2.75); $T_{\rm eff} = 8750$ K, $\log g = 4$. [This figure was preliminary reported in a conference and published in the corresponding proceedings (Simić 2010).]

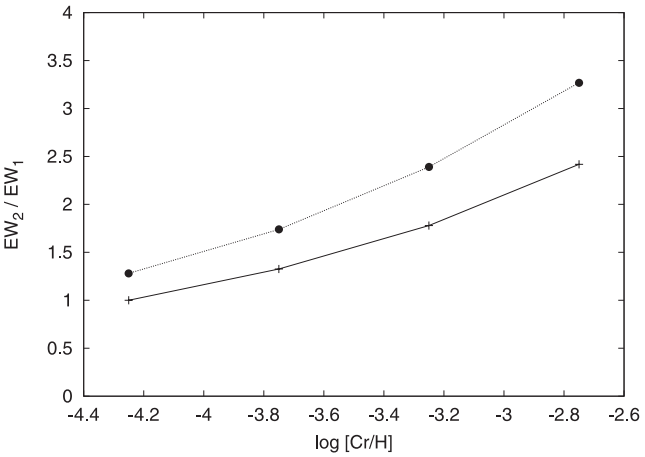

Figure 4. Ratio of EW for Cr II 4588.2 Å as a function of log[Cr/H]. Dotted line – ratio of EW_2 (the EW with Stark broadening included) and EW_1 (without it). Full line – ratio of the EW without Stark broadening contribution: EW_2 denotes the EW with variable chromium abundance and EW_1 the EW with the Solar value of chromium abundance.

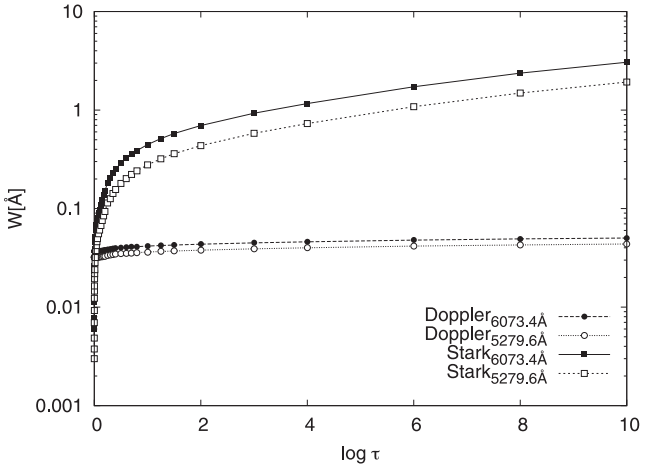

Figure 5. Thermal Doppler and Stark widths for Cr II multiplets $3d^5\ ^4F$–$3d^4 4p\ ^4F^o$ ($\lambda = 5279.6$ Å) and $3d^5\ ^4F$–$3d^4 4p\ ^4P^o$ ($\lambda = 6073.4$ Å), for a DB white dwarfs atmosphere model (Wickramasinghe 1972) with $T_{\rm eff} = 15\,000$ K and $\log g = 8.0$, as a function of the optical depth.

Solar value (EW_1). We can see in Fig. 4 that, in the considered case, the neglecting of Stark broadening will introduce non-negligible errors in abundance determination which increase with the increase of chromium abundance.

The influence of the Stark broadening on Cr II spectral lines for DB white dwarf plasma conditions is investigated here for the multiplets $3d^5\ ^4F$–$3d^4 4p\ ^4F^o$ ($\lambda = 5279.6$ Å) and $3d^5\ ^4F$–$3d^4 4p\ ^4P^o$ ($\lambda = 6073.4$ Å) by using the corresponding model with $T_{\rm eff} = 15\,000$ K and $\log g = 8$ (Wickramasinghe 1972). For the considered model atmosphere of the DB white dwarfs, the pre-chosen optical depth points at the standard wavelength $\lambda_s = 5150$ Å(τ_{5150}) are used in Wickramasinghe (1972) and here as the difference to the A-type star model (Kurucz 1979), where the Rosseland optical depth scale ($\tau_{\rm Ross}$) was taken. As one can see in Fig. 5, for the DB white dwarf atmosphere plasma conditions, thermal Doppler broadening is much less important than in A-type stars, in comparison with the Stark broadening mechanism, which is the most important one here.

We have demonstrated that the Stark broadening of the considered Cr II lines may be non-negligible in A-type star atmospheres, especially in the line wings and when chromium is overabundant. We also note that it is even more important for the modelling of subphotospheric layers. Its neglection, as the present analysis shows, may contribute to errors in chromium abundance determination. The obtained results also show that it is the principal broadening mechanism in DB white dwarf atmospheres. Also, Stark broadening parameters for nine resonant Cr II multiplets are determined.

Cr II Stark broadening parameters given in Table 1 will also be included in the STARK-B data base (Sahal-Bréchot, Dimitrijević & Moreau 2012), a part of Virtual Atomic and Molecular Data Center (Dubernet et al. 2010; Rixon et al. 2011), cf. also Sahal-Bréchot (2010). This data base is devoted to diagnostics modelling and investigations of stellar atmospheres, but also for laboratory, fusion and laser produced plasmas research and modelling.

ACKNOWLEDGEMENTS

This work is a part of the project 176002 'Influence of collisional processes on astrophysical plasma spectra' supported by Ministry of Education and Science of Republic Serbia.

REFERENCES

Adelman J., 1991, MNRAS, 252, 116
Adelman J., Philip A. G., 1996, MNRAS, 282, 1181
Bates D. R., Damgaard A., 1949, Phil. Trans. R. Soc., 242, A101
Ben Nessib N., Dimitrijević M. S., Sahal-Bréchot S., 2004, A&A, 423, 397
Caliskan H., Adelman J., 1997, MNRAS, 288, 501
Cowley C. R., Ryabchikova T., Kupka F., Bord D. J., Mathys G., Bidelman W. P., 2000, MNRAS, 317, 299
Dimitrijević M. S., 1996, Zh. Prikl. Spektrosk., 63, 810
Dimitrijević M. S., Sahal-Bréchot S., 1996, Phys. Scr., 54, 50
Dimitrijević M. S., Sahal-Bréchot S., Bomier V., 1991, A&AS, 89, 581
Dimitrijević M. S., Ryabchikova T., Popović L. Č., Shylyak D., Tsymbal V., 2003a, A&A, 404, 1099
Dimitrijević M. S., Jovanović P., Simić Z., 2003b, A&A, 410, 735
Dimitrijević M. S., Dačić M., Cvetković Z., Simić Z., 2004, A&A, 425, 1147
Dimitrijević M. S., Ryabchikova T., Popović L. Č., Shulyak D., Khan S., 2005, A&A, 435, 1191
Dimitrijević M. S., Ryabchikova T., Simić Z., Popović L. Č., Dačić M., 2007, A&A, 469, 681
Dubernet M. L. et al., 2010, J. Quant. Spectrosc. Radiat. Transf., 111, 2151 (http://www.vamdc.eu)
Eissner W., Jones M., Nussbaumer H., 1974, Comput. Phys. Commun., 8, 270
Fleurier C., Sahal-Bréchot S., Chapelle J., 1977, J. Quant. Spectrosc. Radiat. Transf., 17, 595
Hamdi R., Ben Nessib N., Dimitrijević M. S., Sahal-Bréchot S., 2007, ApJS, 170, 243
Hamdi R., Ben Nessib N., Milovanović N., Popović L. Č., Dimitrijević M. S., Sahal-Bréchot S., 2008, MNRAS, 387, 871
Kurucz R. L., 1979, ApJS, 40, 1
Lakićević I. S., 1983, A&A, 127, 37
Lanz T., Dimitrijević M. S., Artru M. C., 1988, A&A, 192, 249
Oertel G. K., Shomo L. P., 1968, ApJS, 16, 175
Piskunov N., 1992, in Glagolevskij Yu., Romanyuk I., eds, Stellar Magnetism. p. 92
Popović L.Č., Dimitrijević M. S., Tankosić D., 1999a, A&AS, 139, 617
Popović L.Č., Dimitrijević M. S., Ryabchikova T., 1999b, A&A, 350, 719
Popović L. Č., Milovanović N., Dimitrijević M. S., 2001, A&A, 365, 656
Rathore B. A., Lakićević I. S., Ćuk M., Purić J., 1984, Phys. Lett. A, 100, 31
Rixon G. et al., 2011, AIP Conf. Proc. Vol. 1344, Atomic and Molecular Data and their Applications – ICAMDATA-2010. Am. Inst. Phys., New York, p. 107
Sahal-Bréchot S., 1969a, A&A, 1, 91
Sahal-Bréchot S., 1969b, A&A, 2, 322
Sahal-Bréchot S., 1974, A&A, 35, 321
Sahal-Bréchot S., 1991, A&A, 245, 322
Sahal-Bréchot S., 2010, J. Phys. Conf. Ser., 257, 012028
Sahal-Bréchot S., Dimitrijević M. S., Moreau N., 2012, Stark-B data base, Observatory of Paris, LERMA and Astronomical Observatory of Belgrade (http://stark-b.obspm.fr)
Shevchenko V. S., 1994, Astron. Zh., 71, 572
Simić Z., 2010, J. Phys. Conf. Ser., 257, 012037
Simić Z., Dimitrijević M. S., Milovanović N., Sahal-Bréchot S., 2005, A&A, 441, 391
Simić Z., Dimitrijević M. S., Popović L. Č., Dačić M., 2006, New Astron., 12, 187
Simić Z., Dimitrijević M. S., Kovačević A., Dačić M., 2009a, in Dimitrijević M. S., Tsvetkov M., Popović L. Č., Golev V., eds, Proc. 6th Serbian-Bulgarian Astron. Conf., Publ. Astron. Soc. 'Rudjer Bošković', Belgrade, Vol. 9, p. 421
Simić Z., Dimitrijević M. S., Kovačević A., 2009b, New Astron. Rev., 53, 246
Tankosić D., Popović L. Č., Dimitrijević M. S., 2003, A&A, 399, 795
van Regemorter H., Hoang Binh D., Prud'homme M., 1979, J. Phys., B12, 1053
Wickramasinghe D. T., 1972, Mem. R. Astron. Soc., 76, 129
Wiese W. L., Musgrove A., 1989, Atomic Data for Fusion Vol. 6, Spectroscopic Data for Titanium, Chromium and Nickel, Vol. 2, Chromium, Controlled Fusion Atomic Data Center, Oak Ridge National Laboratory, Oak Ridge

This paper has been typeset from a TEX/LATEX file prepared by the author.

Mon. Not. R. Astron. Soc. **374,** 1181–1184 (2007) doi:10.1111/j.1365-2966.2006.11238.x

The flux ratio of the [O III] λλ5007, 4959 lines in AGN: comparison with theoretical calculations

M. S. Dimitrijević,[1⋆] L. Č. Popović,[1⋆] J. Kovačević,[1,2⋆] M. Dačić[1⋆] and D. Ilić[2⋆]

[1]*Astronomical Observatory, Volgina 7, 11160 Belgrade 74, Serbia*
[2]*Department of Astronomy, Faculty of Mathematics, University of Belgrade, Studentski trg 16, 11000 Belgrade, Serbia*

Accepted 2006 October 26. Received 2006 September 29; in original form 2006 July 19

ABSTRACT

By taking into account the relativistic corrections to the magnetic dipole operator, the theoretical [O III] 5006.843/4958.911 line intensity ratio of 2.98 is obtained. In order to check this new value using the active galactic nuclei (AGN) spectra, we present the measurements of the flux ratio of the [O III] λλ4959, 5007 emission lines for a sample of 62 AGN, obtained from the Sloan Digital Sky Survey (SDSS) data base and the published observations. We select only the high signal-to-noise ratio spectra for which the line shapes of the [O III] λλ4959,5007 lines are the same. We obtained an averaged flux ratio of 2.993 ± 0.014, which is in a good agreement with the theoretical one.

Key words: galaxies: active – quasars: emission lines – quasars: general.

1 INTRODUCTION

The forbidden [O III] λ4958.911 Å ($2s^2 2p^2\ ^1D_2 - 2s^2 2p^2\ ^3P_1$) and λ5006.843 Å ($2s^2 2p^2\ ^1D_2 - 2s^2 2p^2\ ^3P_2$) spectral lines are among the most prominent emission lines, not only in the spectra of photoionized nebulae, but also in the spectra of photoionized gas around active galactic nuclei (AGN) due to the relatively high abundance of doubly charged oxygen ions. These lines are typical for AGN and originate from the ionized narrow-line region (NLR) gas surrounding the accreting super massive black hole in the centre (see Osterbrock 1989). It should be emphasized that since they are located in the centre of the visible band they are very often observed in the spectra of H II regions, photoionized nebulae and AGN. Because of observational and physical circumstances this pair of lines are suitable to: (i) test observationally the accuracy of theoretical calculations from atomic theory; (ii) check the linearity of the detectors in use and (iii) eventually test the assumptions on the target physics under extreme circumstances (optical thickness effects).

These two spectral lines are the result of magnetic dipole transitions with a small contribution of electric quadrupole radiation. The elaborate theoretical work of Galavís, Mendoza & Zeippen (1997) provided the [O III] 5006.843/4958.911 intensity ratio of 2.89. Storey & Zeippen (2000) checked this result by using photoionized gaseous nebulae spectra, where these lines can be observed with a very high signal-to-noise ratio (S/N). They found a small, but well-established, difference of 4–9 per cent between observations and theory. Namely Rosa (1985) deduced an intensity ratio of 3.03 ± 0.03, while the measurements of Iye, Ulrich & Peimbert (1987) provided a value of 3.17 ± 0.04, and that of Leisy & Dennefeld (1996) the value of 3.00 ± 0.08.

In order to improve the agreement between observations and theory, Storey & Zeippen (2000) took into account the relativistic corrections to the magnetic dipole operator, demonstrating that they affect the transition probabilities for the [O III] λ5006.843 and λ4958.911 Å lines. They obtained a ratio of the value of 3.01, implying a line intensity ratio of 2.98, which is only two per cent or less different from the values of Rosa (1985) and Leisy & Dennefeld (1996) obtained from gaseous nebulae spectra, and 6 per cent different from the value Iye et al. (1987) obtained from the central region of starburst galaxy Tololo 1924-416 (H II regions). Iye et al. (1987) found a spatial variation of the forbidden line parameters, where the ratio is found to vary from 2.63 ± 0.15 to 3.33 ± 0.07 along the slit (see their table 3 and fig. 10) with a mean value of 3.17 ± 0.04, which significantly deviates from theoretical ratios (Storey & Zeippen 2000). The authors mentioned that such results might be caused by the detector's non-linearity.

Storey & Zeippen (2000) also underlined the necessity to additionally check their theoretical improvement of the line intensity ratio by the corresponding observation in photoionized gaseous nebulae spectra. However, due to instrumentational improvements the accuracy and the resolution of observed spectra have increased to the point where we can now use the AGN spectra for such purposes.

The [O III] λλ4959,5007 lines originate in the NLR of an AGN, the region with conditions which differ from those in photoionized gaseous nebulae are the following: (i) the emission comes from a spatially very extended region, so that one can expect quite different physical and kinematical conditions in different parts of a NLR,[1]

⋆E-mail: mdimitrijevic@aob.bg.ac.yu (MSD); lpopovic@aob.bg.ac.yu (LČP); jkovacevic@aob.bg.ac.yu (JK); mdacic@aob.bg.ac.yu (MD); dilic@matf.bg.ac.yu (DI)

[1] Note here that the [O III] lines observed in AGN very often show a blue asymmetry and substructure in shapes (see e.g. Leipski & Bennert 2006).

(ii) the dust on large spatial scales can result in orientation-dependent effects on NLR line fluxes. However, one can expect that the forbidden line emission is isotropic since self-absorption in narrow lines is negligible. Therefore due to the significance of this pair of lines, it is important to check whether their flux ratio is in agreement with the theory. Only then can it be reliably used for the different checks of theoretical assumptions concerning the physics of the NLR and photoionized gaseous nebulae.

The aim of this paper is to check, with the help of a large sample of AGN spectra, the improved theoretical value of the [O III] 5006.843/4958.911 line intensity ratio (Storey & Zeippen 2000). Additionally, we want to investigate the usability of the AGN [O III] 5006.843/4958.911 emission-line flux ratio for the checks of various theoretical assumptions and the linearity of detectors in use. In order to do so, we will measure the considered flux ratio of the [O III] lines in a large sample of AGN. Moreover, we will derive some explicitly or implicitly given flux ratios of the [O III] λλ5007, 4959 lines in the existing literature (Nazarova, O'Brien & Ward 1996; Bahcall, Steinhardt & Schlegel 2004; Dietrich, Crenshaw & Kraemer 2005), obtained for galaxies and quasars in order to compare them with the Storey & Zeippen (2000) [O III] 5006.843/4958.911 line intensity ratio and our results.

2 THE SAMPLE AND MEASUREMENTS

We selected our AGN sample, choosing the spectra with high S/N, from Data Release Four (DR4) of the SDSS data base and the observations described in the paper of Marziani et al. (2003). The SDSS spectra cover the wavelength region 3800–9200 Å. It was shown that the flux calibration is a few per cent on average, which is impressive for a fibre-fed spectrograph (Tremonti, Heckman & Kauffmann 2004). Tremonti et al. (2004) found that 1σ error in the synthetic colours is 5 per cent in g(4700Å)–r(6200Å). The remaining (small) flux-calibration residuals are coherent on the scales of 500 Å, which has a negligible effect on our flux measurements that are obtained using an interval of less than 100 Å. Consequently, we exclude the effects of non-linearity of the detector on the measured [O III] line ratio.

In our analysis, we first subtracted the continuum by using DIPSO software package. In some spectra the H_β and Fe II emission lines, which contaminate the [O III] λλ4959, 5007, lines, were subtracted.

In order to arrive at a clean sample, we defined the following selection criterion: when scaling the profile of the weaker λ4959 emission line into the stronger λ5007 emission line profile, the line profiles of the two lines in question should differ insignificantly in the given spectrum (Fig. 1). This assures that the measurements of flux ratios and line intensity peak ratios yield identical results. Examples of the maximal difference in the line wings and the central part of the profiles are shown in Figs 2 and 3, respectively. In these examples the observed spectra, the lines without continuum, contaminating Fe II and H_β emission and the profile of λ4959 scaled into the profile of λ5007 are presented. Our initial sample of 62 AGN was selected using the criterion that the shapes of the both lines are same or the difference is negligible as shown in Figs 1–3.

Following the criterion outlined above, from the initial sample of 62 AGN, we selected 56, then 40 and finally 34 spectra, discarding spectra with slightly different [O III] λλ4959, 5007 line shapes (Figs 2 and 3). The final sample of 34 AGN has the best matching of the [O III] λλ 4959, 5007 line profiles (Fig. 1). We measured the

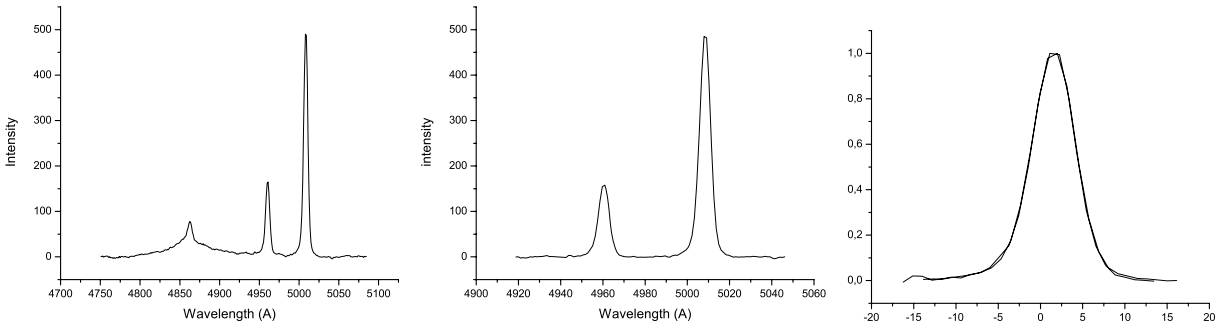

Figure 1. Example of the selected spectrum (SDSS J082308.29+42252000.00) with the same shapes of the [O III] λ 5007 and λ4959 lines. Left-hand panel: observed spectrum, middle panel: lines without continuum and contaminating emission and right-hand panel: the profile of λ4959 line scaled to the profile of λ5007 line.

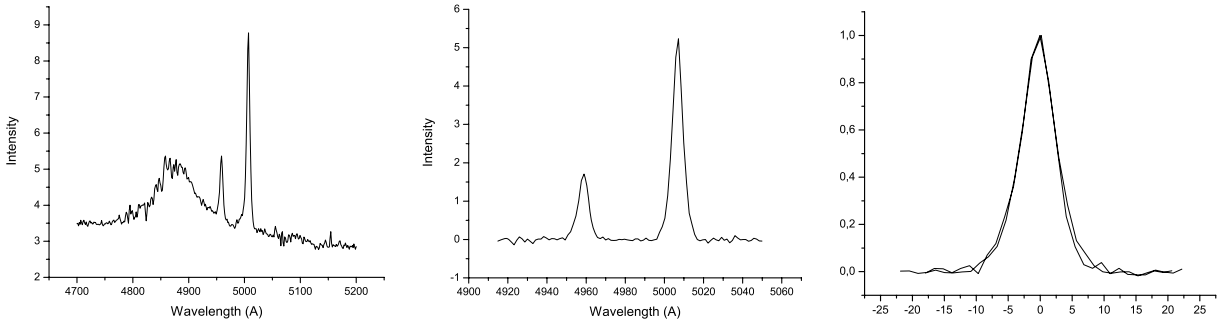

Figure 2. Example of the spectrum (PKS 2135−14) where the line shapes are slightly different in the line wings.

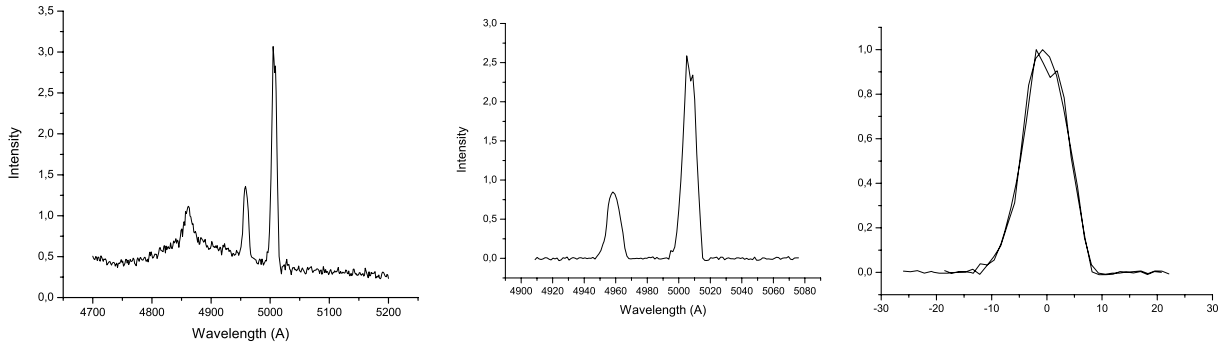

Figure 3. Example of the spectrum (PKS 2300−68) where the line shapes are slightly different in the central part.

flux ratio for each sample and present here the histograms of the flux ratio values of the initial sample of 62 AGN (Fig. 4) and the final sample of 34 AGN (Fig. 5).

3 RESULTS AND DISCUSSION

3.1 The flux ratio of the [O III] λλ 4959, 5007 lines in spectra of active galaxies and quasars

Both the [O III] λ5006.843 and λ4958.911 Å lines originate from the same lower and slightly different upper energy level and have a negligible optical depth since the transitions are strongly forbidden, therefore both may be scaled to exactly the same emission line profile. Moreover, Bahcall et al. (2004) have shown that the effect of differential reddening on the line splitting is of the order of $10^{-8}\ \tau_{5007}$, i.e. negligible. If there are multiple clouds that contribute to the emission, the observed emission line profiles are composed of the same mixture of individual cloud complexes (Bahcall et al. 2004).

Despite the fact that spectra of galaxies and quasars have not been used to explicitly check the theoretical flux ratio of the [O III] λλ5007, 4959 lines, there are examples where such ratios were obtained as a by-product or could be derived from published results (Nazarova et al. 1996; Bahcall et al. 2004; Dietrich et al. 2005).

For example, Nazarova et al. (1996) investigated the Seyfert 1.2 galaxy Mrk 79 with long-slit spectroscopy, using the intensity ratio of the [O III] λλ4959, 5007 lines to check the accuracy of the flux measurements along the slit. Their fig. 2 shows the measured ratios of [O III] λλ4959, 5007 lines plotted against the position along the slit. They report that the ratio is very close to the value of 2.94, but due to the scatter of results and error bars given in their figure, we excluded them from present considerations.

Bahcall et al. (2004) used these [O III] lines of quasars with $0.16 < z < 0.80$, obtained from the SDSS Early Data release, to test whether the fine-structure constant depends on cosmic time. As a by-product, they found that the ratio of transition probabilities corresponding to the [O III] λλ5007, 4959 lines is 2.99 ± 0.02. We note that this result obtained from the spectra of quasars is in agreement with the theoretical value given by Storey & Zeippen (2000). Storey & Zeippen (2000) obtained a theoretical ratio of transition probabilities of 3.01, which is within the given error bars of the observationally derived value.

Dietrich et al. (2005) measured the NLR emission-line flux ratios relative to the flux of the H_β line for 12 narrow-line Seyfert 1 (NLS1) galaxies. Using the [O III] 4959/H_β and [O III] 5007/H_β flux ratios given in Dietrich et al. (2005), we derived the flux ratio of the [O III] λλ5007, 4959 lines for these 12 NLS1 galaxies. The results are given in Table 1. The average value for the ratio of observed fluxes corrected for internal reddening is 2.953 ± 0.014, which also supports the theoretical improvement of Storey & Zeippen (2000).

3.2 Our measurements

The results of our measurements for these three mentioned samples are given in Table 2 and Figs 4 and 5. As one can see from Table 2 and Figs 4 and 5, discarding line profiles with slightly lower quality does not significantly influence the result.

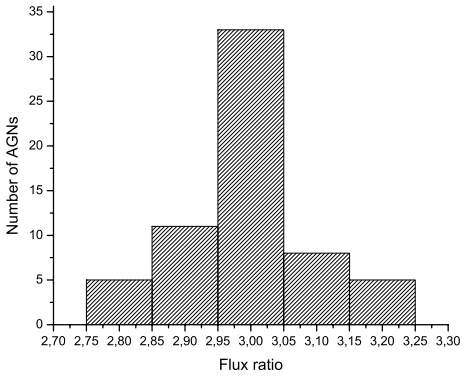

Figure 4. Histogram showing the distribution of the measured flux ratio for the initial 62 AGN sample.

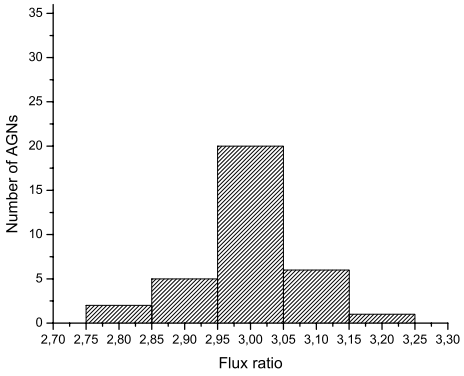

Figure 5. Histogram showing the distribution of the measured flux ratio for the final 34 AGN sample.

Table 1. The flux ratio R of the [O III] λ λ4959, 5007 lines of 12 NLS1 galaxies, derived on the basis of Dietrich et al. (2005).

Object	R
Mrk 705	3.00
Mrk 1239	2.90
Mrk 734	2.92
NGC 4748	2.99
Mrk 783	2.92
IRAS 13224−3809	2.94
CTS J13.12	3.02
IRAS 15091−2107	2.93
Mrk 291	2.95
RXS J20002−5417	2.94
ESO 399−IG 20	3.04
Mrk 896	2.88
The average value	2.953 ± 0.014

Table 2. The flux ratio R of the [O III] λλ5007, 4959 lines of 62 AGN. The initial sample of 62 AGN is successively reduced to 34 by discarding the line profiles of lower quality.

Number of AGN in the sample	R
62	2.992 ± 0.014
56	2.986 ± 0.012
40	2.994 ± 0.014
34	2.993 ± 0.014

The obtained flux ratio of 2.993 ± 0.014 is in agreement with the theoretical improvement of Storey & Zeippen (2000), who obtained the intensity ratio of 2.98. This is better than some of the earlier values derived from photoionized gaseous planetary nebulae and H II region observations, which led to the previously mentioned theoretical reworking (Rosa 1985 – 3.03; Iye et al. 1987 – 3.17; Leisy & Dennefeld 1996 – 3.00). We should note here that the measurements given in Rosa (1985) and Iye et al. (1987) were performed in the 1980s and these differences are probably due to the observational equipment.

4 CONCLUSIONS

In order to check the improved theoretical value of the intensity ratio of the [O III] λλ5007, 4959 lines, we measured the corresponding flux ratio in a sample of 62 AGN with a high-S/N spectra taken from the SDSS data base (DR4) and the observations described in Marziani et al. (2003). Also, from the existing literature we compiled the measurements of the intensity ratio in AGN spectra obtained as a by-product. On the basis of our investigation, we give the following conclusions.

(i) The flux ratio (2.993 ± 0.014) obtained from our measurements is in good agreement with the theoretical improvement obtained by Storey & Zeippen (2000), who derived an intensity ratio of 2.98. Our observational result supports the introduction of theoretical relativistic corrections to the magnetic dipole operator in the calculation of the corresponding line intensity ratio.

(ii) Our measured flux ratio obtained from AGN spectra is in better agreement with the theoretical one compared to the same ratio measured from photoionized gaseous planetary nebulae and H II region spectra. This is probably not caused by different physics, but by technological advances and the better instrumentation used in the observations of AGN spectra.

(iii) Despite the fact that the [O III] lines in spectra of AGN may have very complex line profiles, they can be used to check sophisticated theoretical calculations. Also, we have demonstrated that, with the development of instrumentation, the flux ratio of the [O III] λλ4959, 5007 emission lines in AGN spectra (not only in photoionized gaseous nebulae and H II region spectra) may be used to test observationally the accuracy of theoretical calculations and check the linearity of the detectors.

ACKNOWLEDGMENTS

This work is a part of the projects 146001 ‘Influence of collisional processes on astrophysical plasma line shapes’ and 146002 ‘Astrophysical Spectroscopy of Extragalactic Objects’ supported by the Ministry of Science and Environment Protection of Serbia.

REFERENCES

Bahcall J. N., Steinhardt C. J., Schlegel D., 2004, ApJ, 600, 520
Dietrich M., Crenshaw D. M., Kraemer S. B., 2005, ApJ, 623, 700
Galavís M. E., Mendoza C., Zeippen C. J., 1997, A&AS, 123, 159
Iye M., Ulrich M. H., Peimbert M., 1987, A&A, 186, 84
Leipski C., Bennert N. 2006, A &A, 448, 165
Leisy P., Dennefeld M., 1996, A&AS, 116, 95
Marziani P., Sulentic J. W., Zamanov R., Calvani M., Dultzin-Hacyan D., Bachev R., Zwitter T., 2003, ApJS, 145, 199
Nazarova L. S., O’Brien P. T., Ward M. J., 1996, A&A, 307, 365
Osterbrock D. E., 1989, Astrophysics of Gaseous Nebulae and Active Galactic Nuclei. University Science Books, Mill Valey, CA
Rosa M., 1985, The Messenger, 39, 15
Storey P. J., Zeippen C. J., 2000, MNRAS, 312, 813
Tremonti C. A., Heckman T. M., Kauffmann G. 2004, ApJ, 613, 898

This paper has been typeset from a TEX/LATEX file prepared by the author.